Synthesis of Nitrogen Heterocycles and Chalcones using Multi-Component Reactions: A Spectral and Protein Binding Investigation

This work is submitted in fulfilment of the requirements for the degree of Doctor of Philosophy: Chemistry in the Faculty of Applied Sciences at Durban University of Technology

Arul Murugesan

2018

Supervisor: Professor RM Gengan

DECLARATION

This thesis is being submitted to the Durban University of Technology for the degree of Doctor of Philosophy in Chemistry. I declare that this work is my own and has not been submitted before for any degree or examination to this or any other university or institution for this or any other degree or award.

Student Number: 21452732

Student: [redacted] Date: 28.03.2018

Mr. Arul Murugesan

Supervisor: [redacted] Date: 28.03.2018

Prof RM Gengan

ACKNOWLEDGEMENT

First and foremost, I owe my whole thanks to Lord Almighty for his abundant blessings that has lifted me up to this level. I feel immense pleasure in expressing my deep sense of gratitude and indebtedness to my esteemed Professor ***RM Gengan*** *Department of Chemistry, Durban University of Technology, Durban, for his outstanding guidance, constructive criticism, motivation, valuable advice, untiring support, constant encouragement and inspiration throughout the study holding me strong in all the places I faltered. Further, I also take opportunity to thank Professor* ***K. G. Moodley****, who is a well-wisher and helped me during my tough times. In line I also take an opportunity to thank Professor* ***G. G. Redhi*** *and Professor* ***K. Bisetty, Dr. D.H. Pienaar*** and ***Dr. K. Ramluckan*** *for their timely support. I take a fair opportunity to thank* ***Dr. K. Anand*** *who introduced me to the Durban University of Technology: without him I would not have been registered for a doctoral studies in South Africa. I also express my deep sense of gratitude to Professor* ***M. Ilanchelian*** *of Department of Chemistry, Bharathiar University Coimbatore, India for his fruitful and valuable guidance towards collaboration on my research. I am delighted to extend my profound thanks to Professor* ***Chia-Her Lin, Dr. D. Senthilraja, Mr. M. Vinu, Mr. S. Prabu, Mr. R. Krishnan*** *and* ***Mr. K. Sivasankar*** *of the Chemistry Department, Chung Yuan Christian University, Chung-Li, Taoyuan County, Taiwan for their timely help in crystallographic (single crystals) characterization of my samples and also I thank them for sharing their research thoughts. I extend my thanks to Professor* ***P. S. Mohan****, Head of the Department of Chemistry, Bharathiar University, for his friendly encouragement in my research activity. It is my pride and pleasure to seize the opportunity to record my deep sense of gratitude to* ***Dr. K. J. Rajendra Prasad,*** *former Professor and Head* ***(****UGC-Emeritus Professor),* ***Dr. S. Govindarajan,*** *UGC-Emeritus Professor* ***Dr. S. P. Rajendran*** *Professor (Retd), Department of Chemistry, Bharathiar University and Professor* ***S. Kabilan****, Annamalai University, Chidambaram, for their friendly encouragement and kindness.* ***Dr. R. Selvakumar (****Assistant professor consolidate, Government College of Technology, Coimbatore),* ***Dr. J. Anitha*** *(Post-doctoral researcher, Bharathiar University),* ***Dr. P. Thanigaimalai*** *(AvH-Postdoctoral Fellow, University of Bonn, Germany)****, Dr. A. Selvasharma*** *Post-doctoral researcher Pondicherry University)****, Dr. K. Shanmugaraj*** *(SERB-NPDF The Gandhigram Rural Institute - Deemed University Dindigul)****,*** *for their financial support for travelling to South Africa. In continuation to my acknowledgement, I also express my sincere thanks to* ***Dr. D. Karthick kumar,*** *Associate Professor PSG College Coimbatore,* ***Dr. B. Ravindran*** *Associate Professor Southkorea,* ***Dr.***

Balu Krishnakumar *(Post-doctoral researcher in university of Coimbra) who supported me in my tough times, and encouraged me to write manuscripts in a technical way. I would be doing injustice to myself if I forget to convey my gratitude to my friend* ***Mr. R. Raja Manikandan,*** *who carried out protein binding and molecular docking studies. I extend my thanks to* ***Mr. T. Sasi kumar,*** *(Bharathiar university)* ***Mr. M. Thirupathi, (****National Chung Hsing University)* ***Mr. Chinna (****National Chiao Tung University) and* ***Mr. M. Mathivanan*** *(Bharathiar University) their kind help in characterization of my samples. Sincere thanks to* ***Mr. Dilip Jagjiven*** *from UKZN, Westville Campus, without whom a major part of my thesis would have remained blank, thanks for filling the gap and training me in NMR spectral data acquisition. I am greatly indebted to Professors* ***Dr. M. Veluswamy*** *(Retd) and* ***Ms. V. Lalitha*** *of the Department of Botany, Arraigner Anna Govt. Arts College, Cheyyar, and Tiruvannamalai for their kind help till present. I am greatly indebted to Associate Professor* ***Dr. C. T. Ravichandran****, Head, Department of Chemistry, for his supportive words. Thanks are also extended to Assistant Professors* ***Dr. C. J. Magesh****,* ***Dr. S. Rani****, and* ***Dr. S. Sridevi****, Department of Chemistry, Arraigner Anna Govt. Arts College, Cheyyar, Tiruvannamalai for their kind support. I am greatly indebted towards Professor* ***N. Dharmaraj****, Associate Professor* ***R. Prabhakaran****,* ***Dr. M. V. Kaveri,*** *and* ***Dr. Kannan*** *Department of Chemistry, Bharathiar University, Coimbatore, for their words of encouragement and support during my doctoral studies. I am greatly indebted to Assistant Professors* ***M. Karunananidhi, Mr. P. Senthilrajkapoor*** *Guest Lecture, Department of Chemistry, and Government Arts College – Udumalpet. Tirupur District-Tamilnadu, Assistant Professors,* ***Daniel Raj*** *for their kind help. Acknowledgement will be unsound if I fail to thank my seniors* ***Dr. G. Senthilkumar, Dr. K. Murali, Dr. R. Satheeshkumar, Dr. K. Prabha, Dr. T. Indumathi, Mr. P. Sathiyachandran Dr. P. Manivel, Dr. S. Packiyaraj, Dr. E. Ramachandran, Dr. A. M. Mageshselvakumar, Dr. R. Rajkumar, Dr. K. Saravanamani, Dr. K. Chandra Prakash, Dr. M. Sankaran, Dr. Arasakumar, Dr. S. Anandhakumar, Dr. K. Gayathri*** *and* ***Dr. T. Sathiya Kamatchi*** *for their timely help. I am greatly indebted to* ***Mr. Pannier and Mrs. Rekha*** *their kind help. My thanks go to* ***Mr. Jimmy Chetty*** *Technical Officer and* ***Dr. Thishana Singh****, Asst. Technical Officer and* ***Mr. Rajen*** *other non-teaching staff members of our department for their encouragement and support throughout this study. I also thank my friends* ***Dr. Suresh babu, Mr. Santhosh Kumar*** *and* ***Mr. R. Manikandan*** *Department of Chemistry, University of Madras Chennai for their kind help in carrying out characterization of my samples. I also thank my PG friends* ***Mr. G. Suresh, Mr. M. Surender, Mr. C. Perumal*** *and* ***Mr. B. Ayyanar, Mr. Hariharan****,* ***Ms. P. Sakthi***

Sharmila, *their supportive words and making me strong to carry out my further education. I am greatly indebted to my school and UG friends* ***Mr. B. Lakshmanan, Mr. V. Saranraj, Mr. N. Suresh, Mr. M. Lokesh, Mr. M. Vimal, Mr. T. Sathesish Kumar, Mr. Kumaresan PG Asset government higher secondary school Kikovalaivadu, Ms. K. Vijaya*** *and* ***Ms. E. Deeba*** *their kind help and being with me together till present. I thank to my brothers* ***Mr. M. Elumalai, Mr. M. Arjunan, Mr. Balu, Mr. M. Velu*** *and my uncle* ***Mr. Gnanasekar, Mr. Ethirajanan, Mr. E. Moorthi*** *and Sisters* ***Mrs. E. Ellammal, Mrs. G. Kamalakanni,*** *and* ***Ms. E. Vanathi.*** *Acknowledgement will be rickety if I fail to thank* ***Mr. Talent R. Makhanya, Mr. M. Suresh, Mr. T. Muthu, Mr. A. Vasanthakumar, Dr. Sivanandhan****,* ***Dr. Charlette Tiloke, Ms. N. Rajkoomar, Ms. Thabisile Kaunda*** *and* ***Ms. Sharista Raghunath*** *for their limitless care, precious discussion, unconditional support and encouragement in every stage, to pursue this work. I also thank* ***Mr. A. Nanthakumar, Mr. Hari Ram Chettiar Sivakumar, Mr. Ajay Vasudeo Rane, Dr. Abhishek Guldhe, Dr. Deepak Gusain****,* ***Dr. Adarsh kumar Puri, Dr. Gulshan S****,* ***Mrs. Poonam S, Mr. Timothy Adeliyi*** *and* ***Mr. Bibhuti Ranjan*** *for their valuable support during my stay in Durban University of Technology, which was needed in my tough times. My sincere gratitude also goes to all those who instructed and taught me through the years especially my school teachers, UG and PG faculty members and everybody who has been a part of my life. I owe everything to them. Besides this, several people have knowingly and unknowingly helped me in the successful completion of this project. My sincere gratitude goes to Professor* ***Sibusiso Moyo*** *Deputy Vice-Chancellor: Engagement DUT and* ***Dr. Bloodless Dzwairo*** *Grants Assistant, for my fellowship arrangements for research project and their kind help. I acknowledge the Durban University of Technology and National Research Foundation for financial support. My sincere gratitude goes to Professor* ***Suren Singh*** *Executive Dean,* ***Ms. Gill Shackleford*** *Faculty Officer of the Faculty of Applied Sciences DUT. As you are always with me, I take this golden opportunity to express my heartfelt thanks to my South Africa mother* ***Mrs. Shirley Gengan*** *and sisters* ***Dr. Kerena*** *and* ***Ms. Trinisha Gengan****. As you are always with me, I take this golden opportunity to express my heartfelt thanks to my late parents* ***Mr. A. Muruvan, Mrs. M. Ponnammal****, and my parents* ***Mr. S. Murugesan****,* ***Mrs. M. Amutha****, my Step father* ***Mr. M. Settu,*** *Step Mother* ***Mrs. S. Shebasthi*** *and Brothers* ***Mr. S. Rajnikanth, Mr. S. Sri Ram,*** *for their everlasting love, support and endless help.*

DEDICATED WITH EXTREME AFFECTION AND GRATITUDE TO

Organic Synthesis and Green Chemistry Research Group

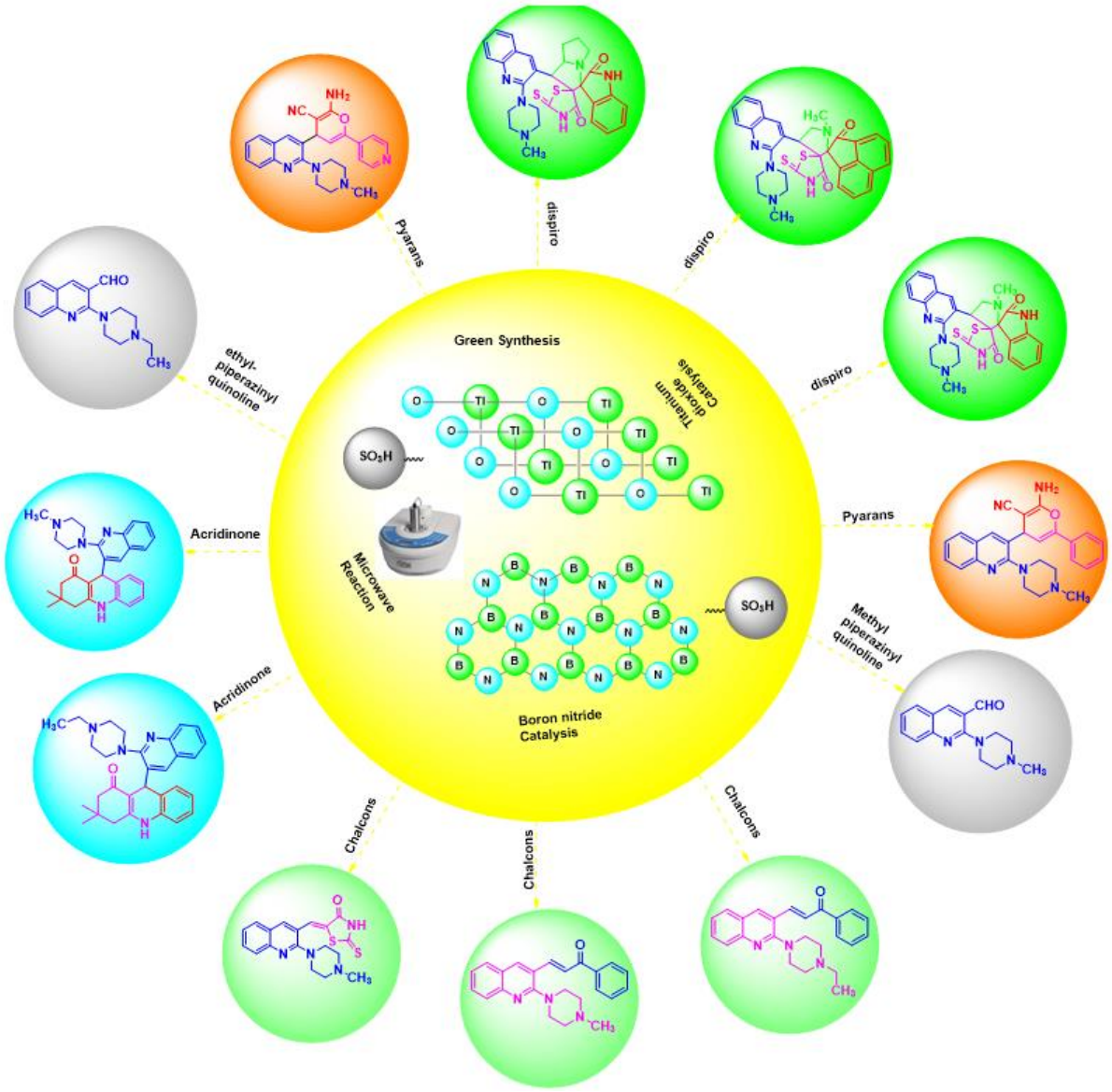

My parents Mr. S. Murugesan, Mrs. M. Amutha and Friends

ABBREVIATIONS

The numbers representing the structure are meant for the particular chapter only. Each chapter contains a separate experimental section. The following abbreviations are used in the text.

aq	- Aqueous
alc	- Alcoholic
dil	- Dilute
concd	- Concentrated
gla	- Glacial
MS	- Mass Spectra
Calcd	- Calculated
mp	- Melting point
mm	- Milli meter
mL	- Milli liter
mmol	- Milli mole
µm	- Micro mole
nm	- Nano meter
h	- Hour (s)
min	- Minutes
TLC	- Thin layer chromatography
KOH	- Potassium hydroxide
EtOAC	- Ethyl acetate
PE	- Petroleum ether
Hex	- Hexane
$CHCl_3$	- Chloroform

CH_2Cl_2	- Dichloromethane
DMF	- Dimethylformamide
MeOH	- Methanol
EtOH	- Ethanol
CH_3CN	- Acetonitrile
Ace	- Acetone
K_2CO_3	- Potassium carbonate
NaOH	- Sodium hydroxide
$NaOCH_3$	- Sodium methoxide
AcOH	- Acetic acid
THF	-Tetrahydrofuran
DMSO	- Dimethyl sulfoxide
H_2SO_4	-Sulfuric acid
H_2O_2	- Hydrogen peroxide
TiO_2	- Titanium dioxide
BN	- Boron nitride
TEM	- Field-emission Scanning Electron Microscopy
HR-TEM	- High Resolution-Transmission Electron Spectroscopy
PXRD	- Powder X-Ray Diffraction
SEM	- Scanning Electron Microscopy
EDXA	- Energy Dispersive X-Ray Analysis
BET	- Brunauer–Emmett–Teller theory
MPBN	- 3-Mercaptopropylboron nitrile
HSA	- Human serum albumin

BSA	- Bovine serum albumin
Trp	- Tryptophan
Tyr	- Tyrosine
DNA	- Deoxyribonucleic acid
FT-IR	- Fourier Transform Infrared
CD	- Circular Dichroism
MRE	- Mean residue ellipticity
NMR	- Nuclear Magnetic Resonance

General Information

Chemicals were purchased from Merck, Sigma Aldrich. The reaction/purity of the product was monitored and accomplished by TLC. FT-IR spectra were recorded in the range of 4000-400 cm^{-1} on a JASCO FT/IR-460 spectrophotometer using KBr pellets. A Bruker D2 PHASER powder diffraction instrument; Cu Kα ray (wavelength λ = 0.154056 nm), was used to measure in a continuous step-scan mode: the minimum width of the stage 0.031°, equilibrium time of 256 seconds, the operating voltage to 30 kV with 10 mA. Scanning electron microscopy (Joel JSM 7600 F) was employed to characterize the morphology. High Resolution-Transmission Electron Spectroscopy was used. The BET gas sorption isotherms were measured 77 K for N_2, H_2, and 273 and 298 K for CO_2 using Micromeritics Auto pore 9500 system. Before recording gas sorption measurements, the sample was initially dehydrated at 423 K for 24 h under vacuum. Raman Spectroscopy was measured using the detector CCD (Triaxle) and the laser (He-Ne laser 632.8 nm). A TOF-MS analyser for accurate mass measurement was used. The melting point (mp) was recorded on a Buchi B-545 apparatus using open capillary tubes.

NMR spectra were recorded in $CDCl_3$ / DMSO-d_6 on a Bruker Advance 400 MHz and 600 MHz instrument using tetramethylsilane as internal standard. In general for all compounds $CDCl_3$ is used as a solvent, where DMSO-d_6 has been used, it is mentioned in the experimental part. The chemical shifts were expressed in ppm. The following abbreviations are used in the NMR spectral data.

s	- Singlet
d	- Doublet
t	- Triplet
q	- Quartet
m	- Multiplet
dd	- doublet of doublet
brs	- broad singlet
J	- Coupling constant

TABLE OF CONTENTS

Chapter One

Introduction, Aim, Objectives and Scope of the Study

Over the years, the development of low molecular weight (less than 900 Dalton) biologically active molecules has increased. These molecules, generally referred to as small molecules, are organic compounds which usually possess pronounced biological activity such as good permeability through cellular membranes, ability to bind at appropriate sites of proteins and exert powerful effect on the function of macromolecules comprising living systems. These small molecules have cemented collaboration between chemists and biologists: the former is responsible for either the synthesis or extraction of new compounds from natural sources, whilst the latter explores their biological properties. The synergy that exists between chemists and biologists is responsible for promoting innovative studies for treating various diseases faced by mankind. In spite of the highly interdisciplinary features of these research fields, synthetic organic chemistry remains the backbone of these types of research. In fact, modern organic synthesis is playing an increasingly prominent role in the life sciences because the production of new small molecules depends entirely on how effectively organic chemistry is managed.

There are several ways in which organic synthesis are contributing to the discovery of biologically active small molecules such as:

- developing new synthetic methodologies
- improving already existing synthetic protocols
- discovering more efficient syntheses or interesting biological compounds
- improving the total synthesis of small natural products

Ultimately, these new methodologies and syntheses contribute to new possibilities in acquiring novel bio-active compounds. This dissertation contributes to the vast area of study on the synthesis of small molecules and an interrogation of their molecular interaction with macromolecules.

The aim of this study is to prepare and characterize new catalysts which can be used for the synthesis of novel nitrogen heterocycles and study their protein and DNA binding ability.

The objectives were to synthesize and characterize:

1. Titanium dioxide-based sulphonic acid catalysts and methyl piperazinyl-quinolinyl pyrans and assess their binding with Hsp90 protein by molecular docking.
2. Boron nitride-based sulphonic acid catalysts and methyl and ethyl piperazinyl-quinolinyl tetrahydroacridinone derivatives and assess their binding with DNA and Hsp90 protein by molecular docking.
3. Titanium dioxide triethylene tetramine-based sulphonic acid and boron nitride-based sulphonic acid catalysts and methyl and ethyl piperazinyl-quinolinyl *(E)*-chalcone derivatives and determine their binding with Human Serum Albumin (HSA) and Bovine Serum Albumin (BSA) protein by molecular docking investigations and
4. Methyl piperazinyl-quinolinyl dispiro heterocyclic derivatives and investigate their binding with HSA.

The outcome of the research study is summarized in **six chapters** as presented below:

Chapter Two presents the literature review which describes and discusses important theories and concepts. These include nitrogen heterocycles and their biological importance, The importance of quinolines and synthetic methods used, the use of multi-component reactions for the synthesis of various classes of nitrogen heterocycles, The synthesis of chalcones, 1,3 dipolar cycloaddition reactions for the formation of spiro compounds, The importance of micro-wave-assisted synthesis and catalysis and protein binding using Molecular docking.

Chapter Three gives a general introduction to the biological importance of pyrans, a comprehensive literature search of pyrans and titanium dioxide-based catalysts, it describes and discusses the synthesis and characterisation of a novel titanium dioxide-based sulphonic acid catalyst and methyl piperazinyl-quinolinyl pyrans. It also outlines the steps taken to optimise the use of the catalyst. Finally, a discussion on the binding potential of two selected pyran derivatives is presented by molecular docking. The scheme for the synthesis of methyl piperazinyl-quinolinyl pyrans is as presented, below.

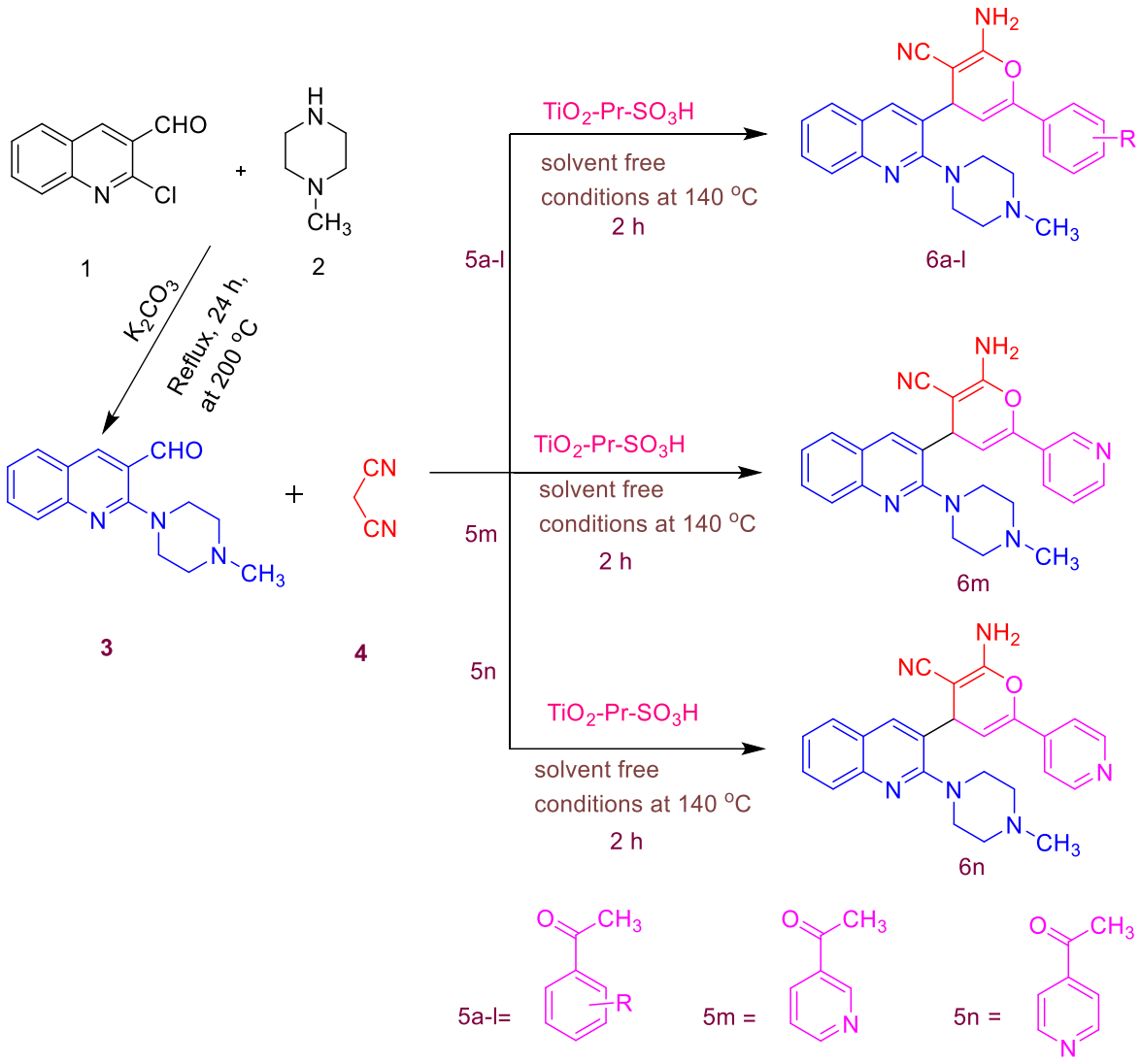

KEY: 6a (R=H); 6b (R=ortho-OH); 6c (R=para OH); 6d (R=4-CH_3); 6e (R=4- NO_2); 6f (R=4-F); 6g (R=4-Cl); 6h (R=4-Br); 6j (R=Ar-H); 6k (R=Ar-H); 6l (R=Ar-H) whilst 6i was obtained from **3** and thioacetophenone

Scheme 3. 3. Synthesis of 2-amino-4-(2-(4-methylpiperazin-1-yl) quinolin-3-yl)-6-phenyl-4H-pyran-3-carbonitrile and 2-amino-4-(2-(4-methylpiperazin-1-yl) quinolin-3-yl)-6-(pyridin-4yl)-4H-pyran-3-carbonitrile derivatives.

Chapter Four was divided into two parts. The discussion therein was focused on using two different boron nitride-based sulphonic acid catalyst for the synthesis of two new starting compounds viz., the methyl and ethyl piperazinyl quinolin-3-carbaldehydes which were used to synthesize 3,3-dimethyl-9-(2-(4-methylpiperazin-1-yl)quinolin-3-yl)-3,4,9,10-tetrahydroacridin-1(2H)-one and 9-(2-(4-ethylpiperazin-1-yl)quinolin-3-yl)-3,3-dimethyl-3,4,9,10-tetrahydroacridin-1(2H)-one derivatives. The morphological properties of the catalyst were determined by XRD, TEM, SEM, BET, and Raman spectroscopy whilst the novel acridinone derivatives were characterized by FT-IR, NMR, MS and Elemental analysis. Thereafter the binding mode of action of the novel compounds with DNA and Hsp90 protein were determined by molecular docking studies.

Part A:

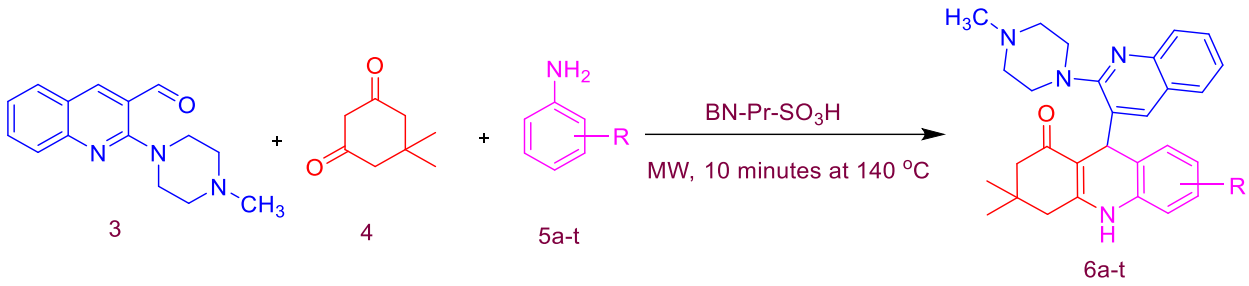

KEY: 6a (R=H); 6b (R=2- NO_2); 6c (R=3-NO_2); 6d (R=4- NO_2); 6e (R=2-F); 6f (R=3-F); 6g (R=4-F); 6h (R=4-Cl); 6i (R= 3,4-Cl); 6j (R= 3-Cl,4-F); 6k (R=4-Br); 6l (R=ortho-CH_3); 6m (R=meta- CH_3); 6n (R=para- CH_3); 6o (R=3,4-CH_3); 6p (R=ortho O-CH_3); 6q (R=para O-CH_3); 6r (R=Ar-H); 6s (R=Ar-H); 6t (R=Ar-H).

Scheme Part 4A. The synthesis of 3,3-dimethyl-9-(2-(4-methylpiperazin-1-yl)quinolin-3-yl)-3,4,9,10 tetrahydroacridin-1(2H)-one derivatives

Part B:

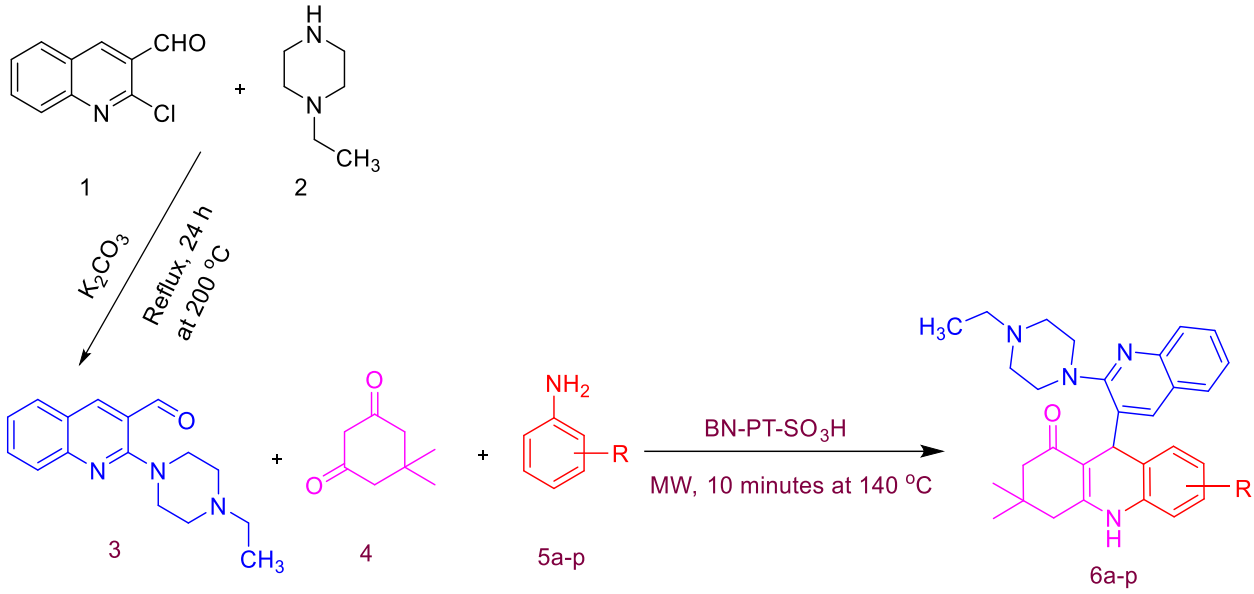

KEY: 6a (R=H); 6b (R=2- NO_2); 6c (R=4- NO_2); 6d (R=4-F); 6e (R=4-Cl); 6f (R= 3,4-Cl); 6g (R=4-Br); 6h (R=ortho-CH_3); 6i (R=meta- CH_3); 6j (R=para-CH_3); 6k (R=3,4-CH_3); 6l (R=ortho O-CH_3); 6m (R=para O-CH_3); 6n (R=Ar-H); 6o (R=Ar-H); 6p (R=Ar-H).

Scheme Part 4B. The synthesis of 9-(2-(4-ethylpiperazin-1-yl) quinolin-3-yl)-3, 3-dimethyl-3, 4, 9, 10-tetrahydroacridin-1(2H)-one derivatives.

Chapter Five was divided into two parts. The discussion therein was focused on the synthesis of one new titanium dioxide triethylene tetramine-based sulphonic acid catalyst, for producing novel molecule, and its characterisation by XRD, TEM, SEM, BET, and Raman spectroscopy. The reported boron nitride based sulphonic acid catalyst and the new catalyst were used to synthesize methyl and ethyl piperazinyl quinoline *(E)*-3-(2-(4-methylpiperazin-1-yl) quinolin-3-yl)-1-phenylprop-2-en-1-one and **(***E*)-3-(2-(4-ethylpiperazin-1-yl)quinolin-3-yl)-1-phenylprop-2-en-1-one chalcone derivatives, respectively. These were fully characterized by FT-IR, NMR, TOF-MS and Elemental analysis. The binding ability of the methyl piperazinyl quinolone-based chalcones and ethyl piperazinyl quinolone-based chalcones with HSA protein and BSA, respectively, are presented and described.

Part A:

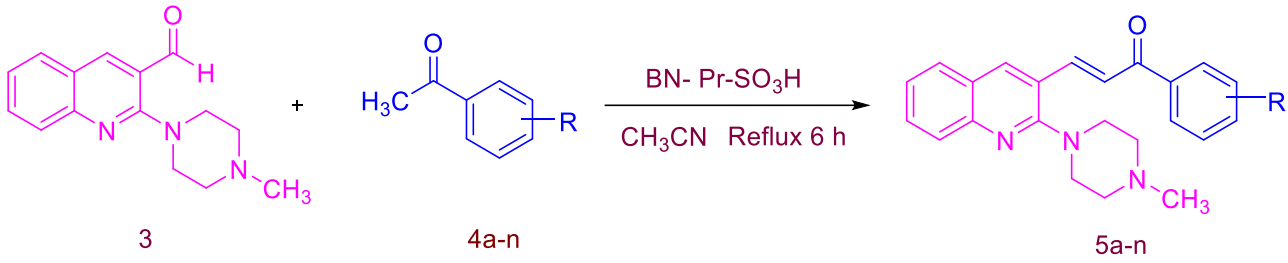

3 4a-n 5a-n

KEY: 5a (R=H); 5b (R=2- OH); 5c (R=4- OH); 5d (R=4-NO_2); 5e (R=para- CH_3); 5f (R=para O-CH_3); 5h (R=4-F); 5i (R=4-Cl); 5j (R=4-Br); 5k (R=meta- NH_2); 5l (R=Ar-H); 5m (R=Ar-H); 5n (R=Ar-H) whilst 5g was obtained from **3** and thioacetophenone.

Scheme Part 5A. The synthesis of phenyl substituted (E)-3-(2-(4-methylpiperazin-1-yl) quinolin-3-yl)-1-phenylprop-2-en-1-ones derivatives.

Part B:

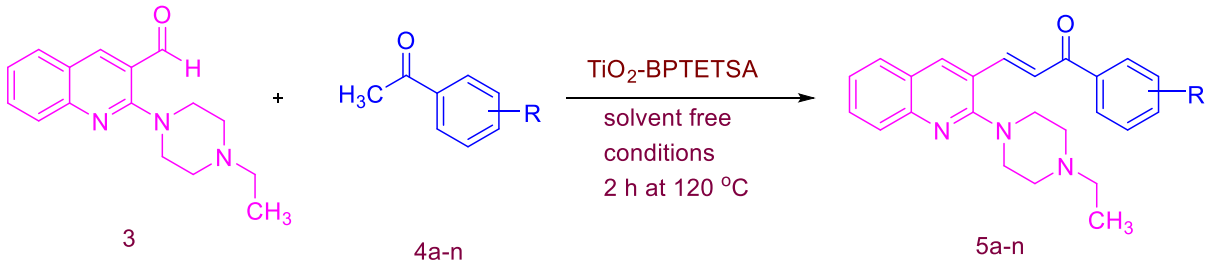

3 4a-n 5a-n

KEY= 5a (R=H); 5b (R=2- OH); 5c (R=4- OH); 5d (R=4- NO_2); 5e (R=para- CH_3); 5f (R=para O-CH_3); 5h (R=4-F);5i (R=4-Cl); 5j (R=4-Br); 5k (R=meta-NH_2); 3l); 5l (R=Ar-H); 5m (R=Ar-H); 5n (R=Ar-H) whilst 5g was obtained from **3** and thioacetophenone

Scheme Part 5B. The synthesis of phenyl substituted (E)-3-(2-(4-ethylpiperazin-1-yl) quinolin-3-yl)-1-phenylprop-2-en-1-ones derivatives.

Chapter six discusses the synthesis and characterisation of novel dispiro heterocyclic systems, containing a piperazinyl-quinolinyl nucleus. The regio and stereochemistry of the synthesized compounds were established by FT-IR, ^{1}H NMR, ^{13}C NMR, 2D NMR and HRMS spectroscopic techniques. A representative compound was studied for its binding with HSA protein using the fluorescence quench titration method. The molecular docking results are discussed.

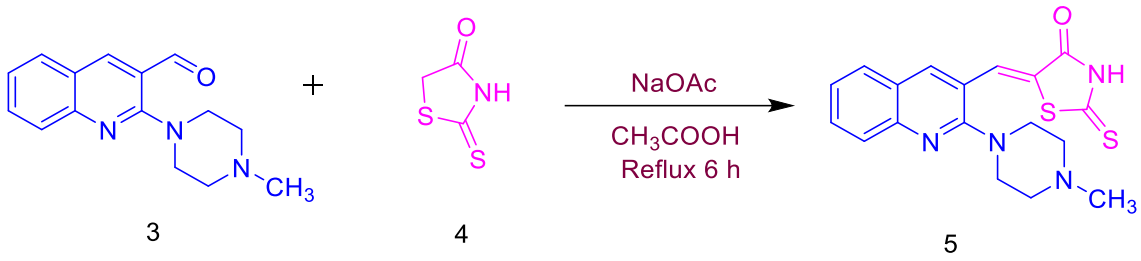

3 4 5

Scheme 6. 1. Synthesis of (Z)-5-((2-(4-methylpiperazin-1-yl)quinolin-3-yl)methylene)-2-thioxothiazolidin-4-one.

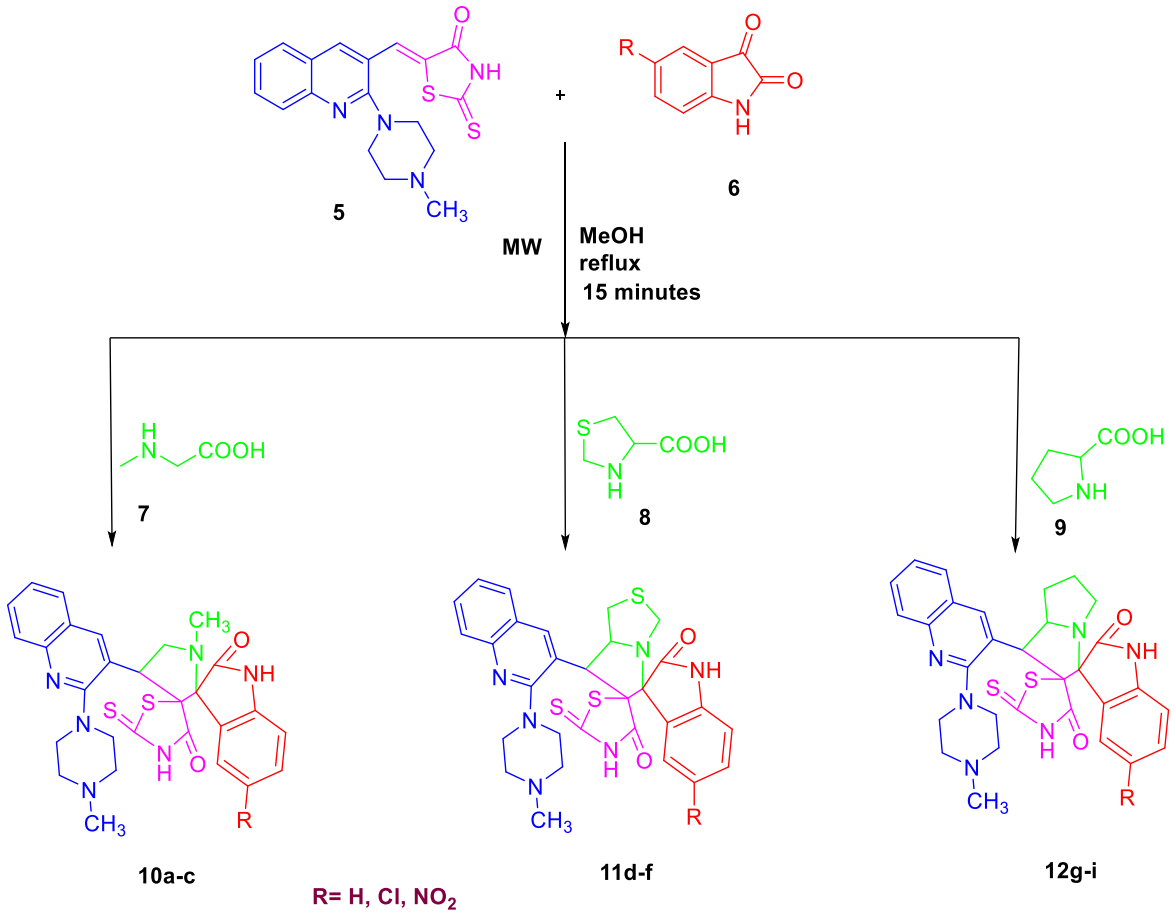

Scheme 6. 2. Synthesis of piperazinyl-quinolinyl dispiro heterocycle isatin derivatives.

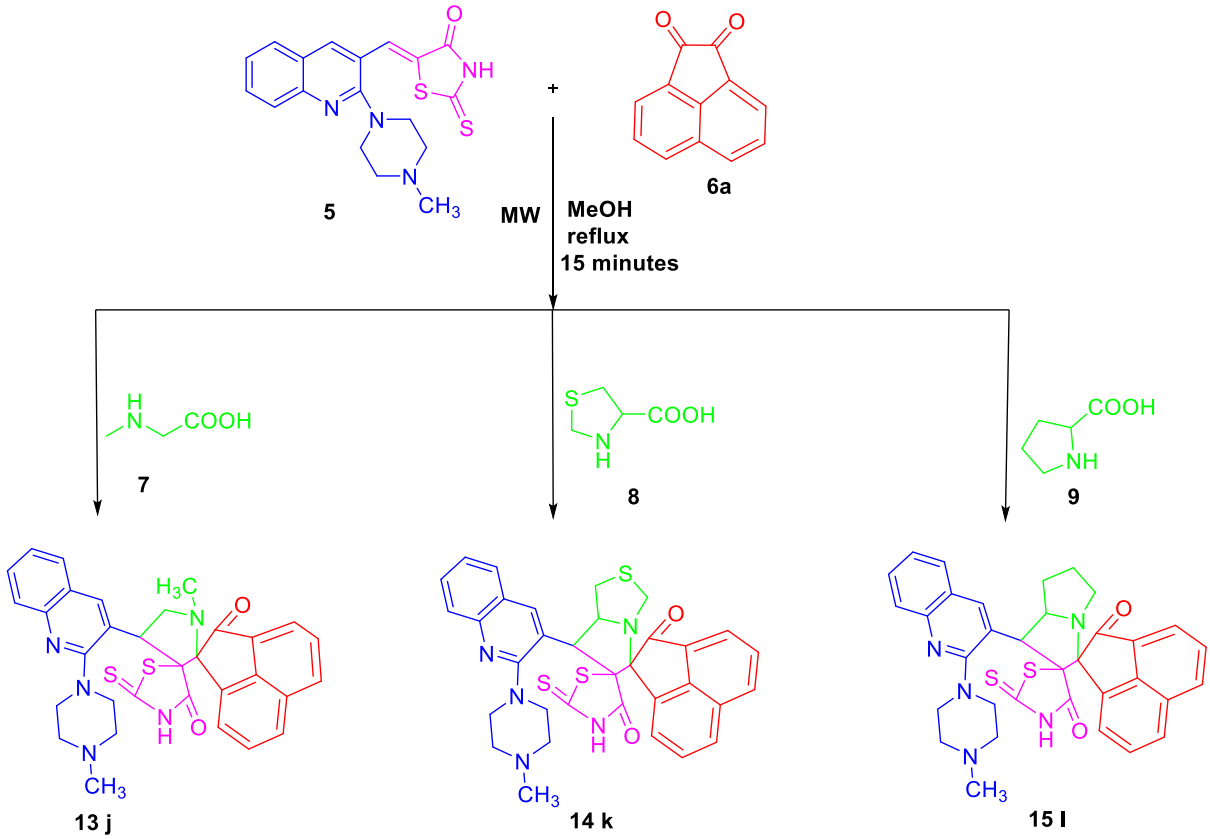

Scheme 6. 3. Synthesis of piperazinyl-quinolinyl dispiro heterocycle acenaphthalene derivatives.

Chapter Two
Literature Review

2. 1. Nitrogen Heterocycles

Nitrogen heterocycles are cyclic carbon compounds in which one or two of the carbons in the ring are replaced by nitrogen atoms. The non-carbon atoms in such rings are referred to as "heteroatoms". Although heterocyclic systems are present in many natural sources, there is a growing trend to synthesize them using well-established synthesis routes in organic chemistry. This interest is motivated by the possibilities that new products made by planned synthesis of novel nitrogen heterocycles may give compounds of value to society and to certain special research areas such as medicinal chemistry. Usually the known structures of nitrogen heterocycles, obtained from natural sources, is used as a target for synthesis. A systematic change to biologically active compounds could result in the discovery of new nitrogen heterocycles with enhanced biological activity. This implies that synthesis must go beyond the stage of mimicking the biologically active products obtained from natural sources. Hence, researchers are engaged in on-going research to design and produce better medicines, pesticides, insecticides, rodenticides, and herbicides by utilizing naturally-occurring heterocycles as starting points.

Nitrogen heterocycles play a major part in biochemical processes. They also exist as part or side groups of natural organic classes such as alkaloids and flavonoids and are important components of active cells. Hence there is much interest in the synthesis of new nitrogen heterocycles because of their potential biological applications (Jenekhe *et al*. 2001:7315).

2. 1. 1. Quinolines

Quinoline and its derivatives have received considerable attention because of their wide spectrum of biological properties (Katritzky Pozharskii 2000:616). Important amongst these are synthetic antimalarials (Klein Favreau 1995) for example chloroquine and primaquine, fungicides such as halacrinate,(Huber-Emden *et al.* 1971) antibacterials such as ciprofloxacin (**1**) and norfloxacin,(Samosorn *et al.* 2006:857) antitumor agents such as streptonigrin (**2**) (Bringmann *et al.* 2004:3539), (Hibino Weinreb 1977:232), luotonin A (**3**) (Wang Ganesan 1998:9097), dynemicin A (Myers *et al.* 1997:6072) and camptothecin (**4**), (Cominutesutes *et al.* 1994:611), (Shen *et al.* 1993:611) the HIV-1 protease inhibitor saquinavir (**5**), (Maignan *et al.*

1998:359) and styrylquinolines (**6**) as potential HIV-1 integrase inhibitors (d'Angelo *et al.* 2001:237), (Zouhiri *et al.* 2001:8189).

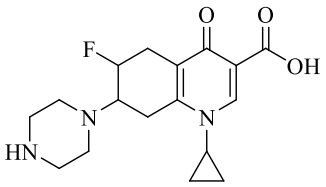

1

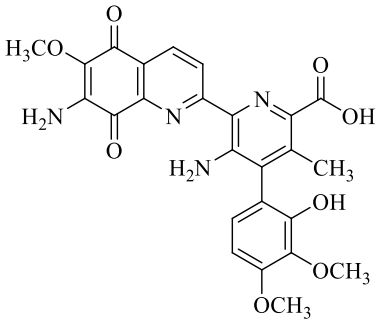

2

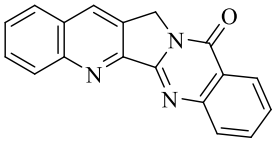

3

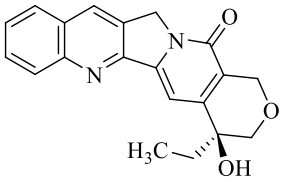

4

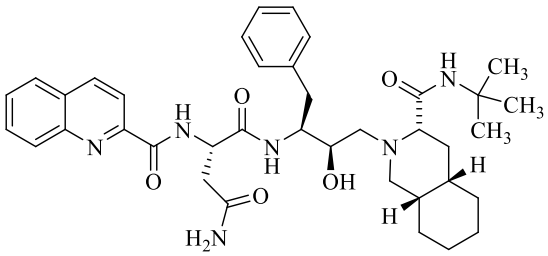

5

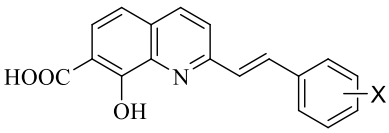

6

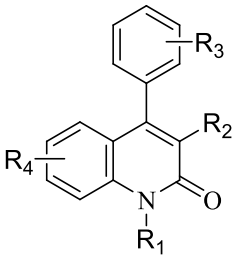

7

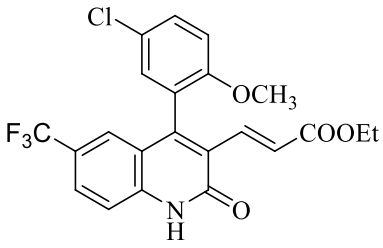

8

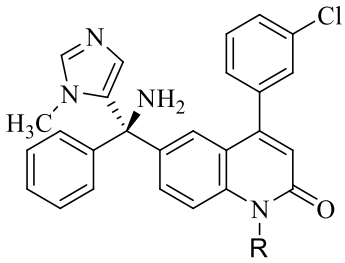

9

The quinoline ring system which is present in natural products, particularly alkaloids (Kametani Kasai 1989:385), (Katritzky *et al.* 1984:511), (Sainsbury Coffey 1978:6929), is a very important moiety for the production of pharmaceuticals, herbicides, dyes, etc (Sundberg *et al.* 995:287). Recently, the synthesis of new functionalized 4-arylquinolin-2(1*H*)-ones (**7**)

and their important biological activities were reported (Hewawasam *et al.* 2002:1779), (Mederski *et al.* 1997:1883).

The importance of 3-(quinolin-3-yl) acrylates derivatives (**8**) and the analogous condensed allylic alcohols were described (Hewawasam *et al.* 2003:2819) as potent maxi-k channel openers valuable for the action of male erectile dysfunction; likewise, the 6-functionalized quinoline derivative (**9)** has emerged as an active antitumor agent (Angibaud *et al.* 2004:479). In the light of the interesting biological activity associated with the quinoline alkaloids and their usefulness as precursors, several synthetic procedures for the synthesis of quinoline derivatives have been reported in the literature as described below.

2. 1. 1. 1. The methods used for the synthesis of selected quinoline derivatives

Curd *et al.* (Curd *et al.* 1947:899) synthesized **13** from 4-hydroxy-2-quinolinone (**10**) and aniline. This compound showed high degree of antimalarial activity against *P.gallinaceum* in chicks.

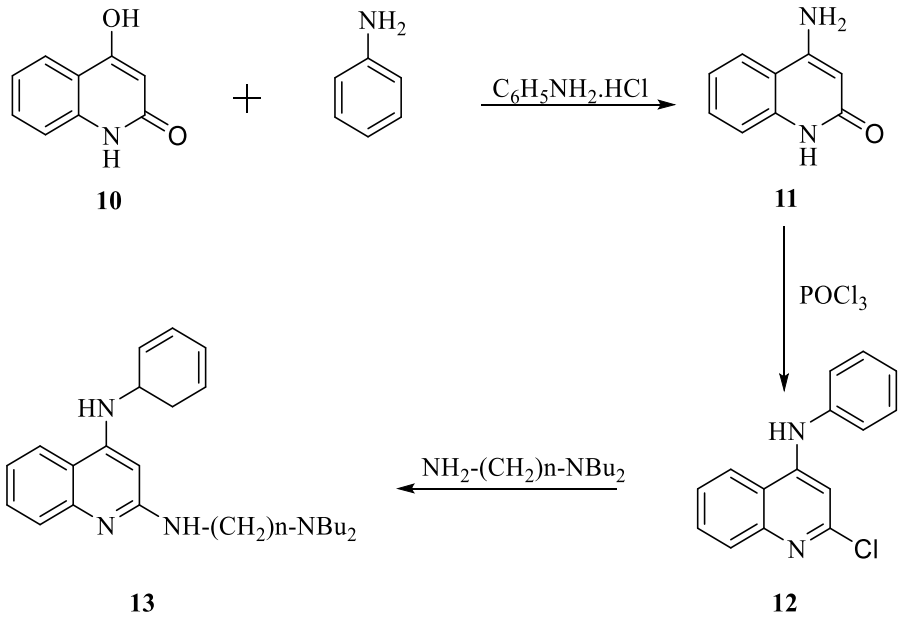

Kermack and Smith (Kermack and Smith 1931:3096) synthesized 2,3-benzo-methyl-γ-carboline (**15**) by reacting 4-chloro-2-methyl quinoline (**14**) and *o*-phenylenediaminutese followed by diazotization and acid catalyzed cyclisation.

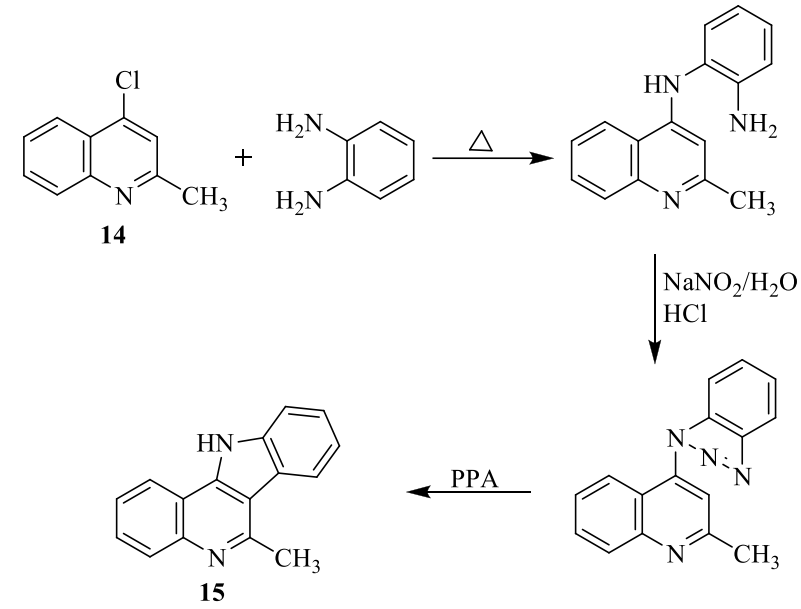

A simple 2-aminutesoquinoline (**18**) was prepared from *o*-nitrobenzaldehyde (**16**) through the intermediate **17** by Compagnone *et al.* (Compagnone *et al.* 997:1631)

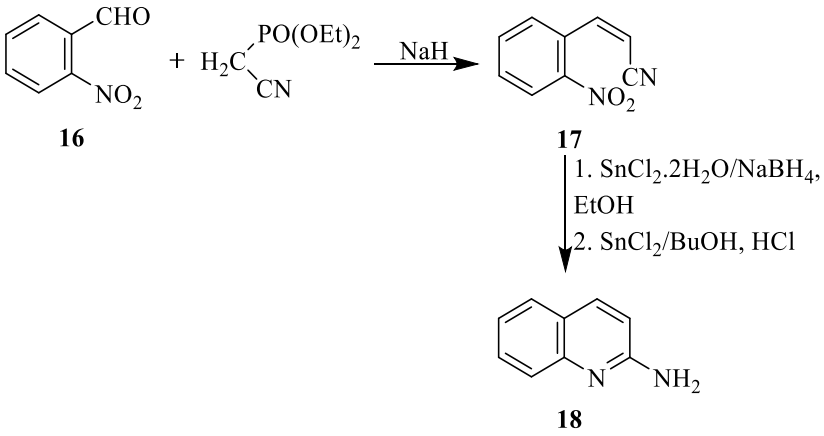

The enaminutese intermediate **19**, synthesized from substituted *o*-aminutesobenzonitrile and phosphine oxide allenes or propargylphosphonium bromide gave the corresponding 4-aminutesoquinolines (**20**) (Kouznetsov *et al*. 2005:141).

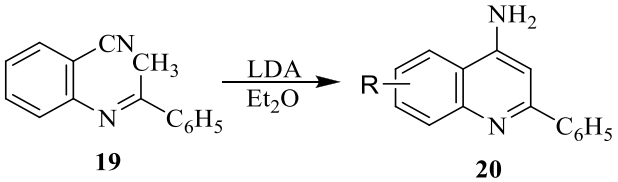

Lin Zhi *et al.* (Zhi *et al.* 1999:1009) synthesized 4-oxo-tetrahydroquinoline (**22**) from aniline (**21**) and 2-butenoic acid with polyphosporic acid (PPA) catalyzing the cyclisation.

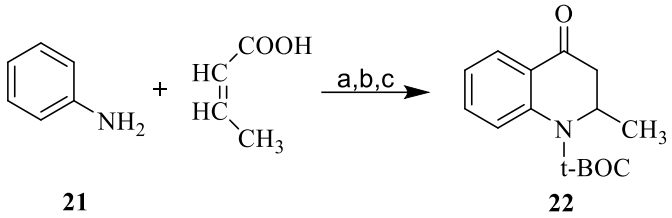

21 **22**

a) Toluene, reflux
b) PPA, 110 ^{o}C
c) t-BOC$_2$O, DMAP, THF, RT

Adams and Hey (Adams and Hey 1950:2354) synthesized 4-anilino-3-phenylquinoline (**25**) from 4-hydroxy-3-phenylquinoline (**23**) with 4-chloro-3-phenylquinoline (**24**) being the intermediate product.

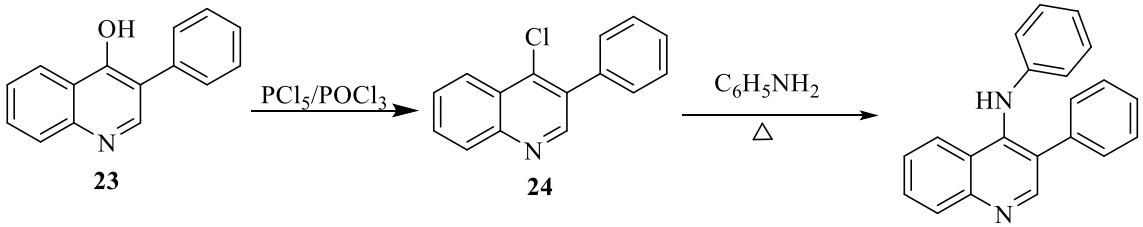

23 **24** **25**

Zhe-Shan Quan *et al.* (Guo *et al.* 2009:954) reported the synthesis of 5-alkoxy-[1, 2, 4] triazolo [4, 3-a] quinolines (**29**) from 4-hydroxyquinolin-2(*1H*)-one (**26**).

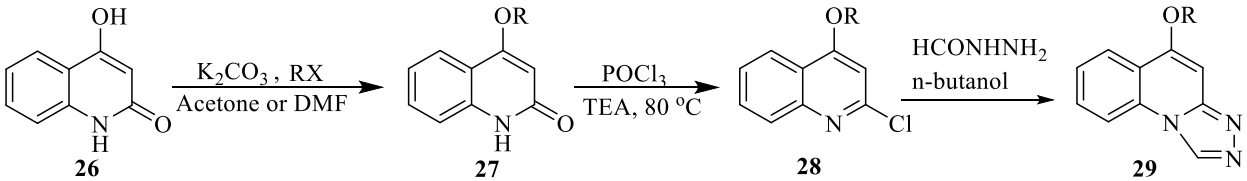

26 **27** **28** **29**

Lee *et al.* (Lee *et al.* 2004:7884) synthesized 2-chloroquinoline (**31**) by the reaction of 2-vinyl-substituted aniline (**30**) with diphosgene, in acetonitrile, via a reactive imidoyl moiety.

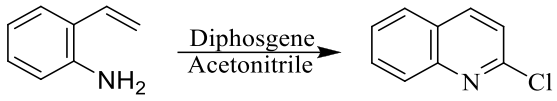

30 **31**

A two-step synthesis was reported by Reddy *et al.* (Reddy *et al.* 2009:32) for 2-alkynyl-4-arylquinolines (**34**) via Pd/C-mediated regioselective C-2 alkynylation of 2,4-dichloroquinoline (**32**) followed by Suzuki coupling of the resulting 4-chloro derivative

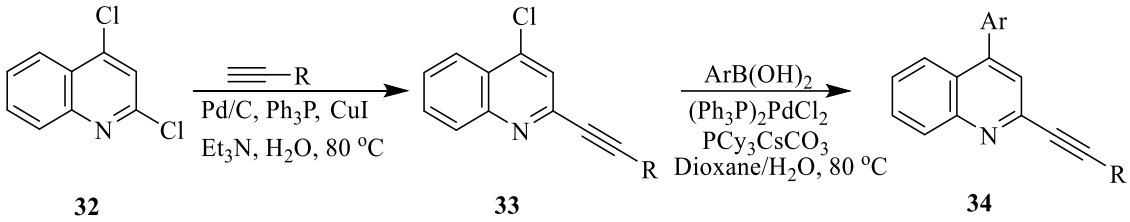

32 **33** **34**

Meth-Cohn *et al* (Meth-Cohn *et al.* 1979:4885) used the Vilsmeier-Haack reagent ($DMF/POCl_3$) for the synthesis of 3-methyl-2-chloroquinoline (**36**) by the cyclization of substituted anilide **(35)**: dechlorination of **36** using zinc and acetic acid produced 3- methyl quinoline **(37)**.

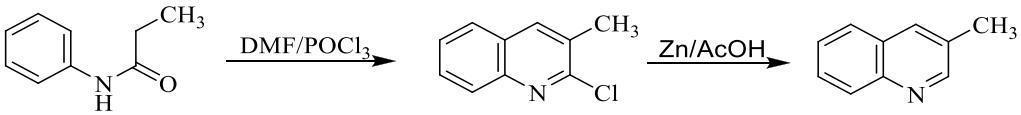

35 **36** **37**

The synthesis of 2,4-dichloroquinoline (**38**) from aniline and malonic acid, in an excess of phosphoryl chloride, was reported by Jones *et al* (Jones *et al.* 2003:4380). It was then treated with sodium methoxide to produce a mixture of 2,4-dimethoxyquinoline (**39**) and 4-chloro-2-methoxyquinoline (**40**).

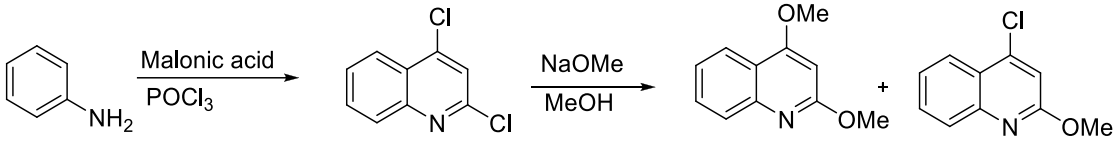

38 **39** **40**

Nasr *et al* (Nasr *et al.* 1988:1347) reported the synthesis of various chloro substituted quinolines (**42-44, 46, 48**) from 3-aminuteso-N,N-dimethylaniline (**41**). The main reagent for the transformation was phosphoryl chloride.

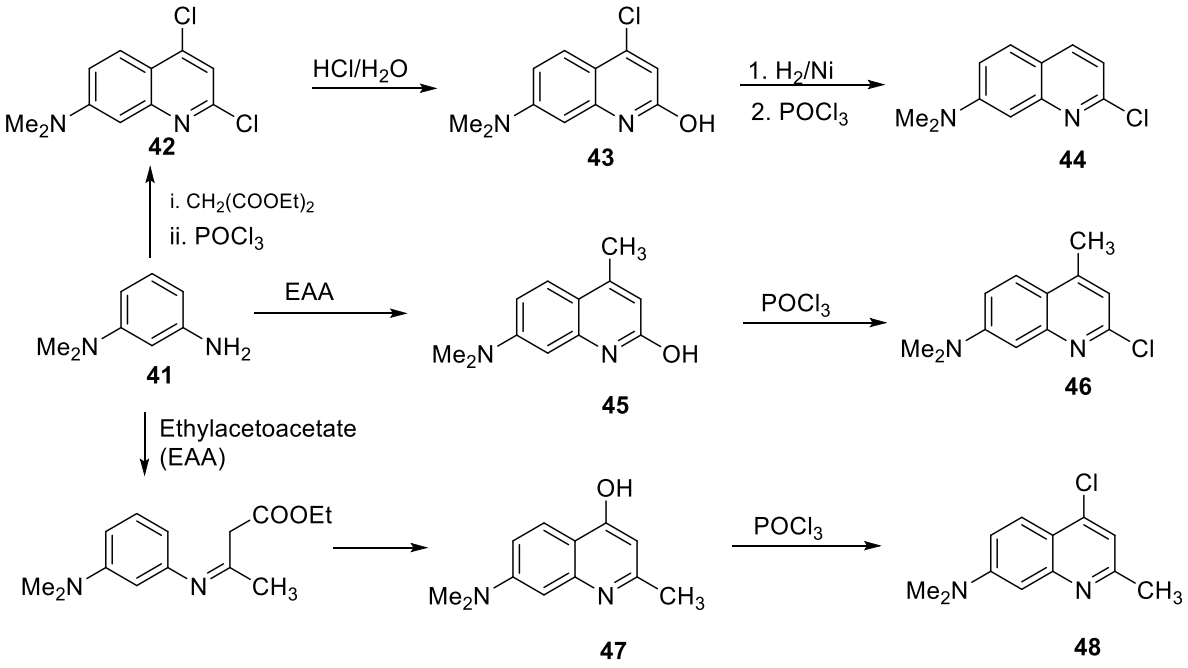

The reaction of *m*-chloroaniline with 3-ethoxyacyloylchloride, in pyridine, followed by acid mediated cyclisation to accomplish two isomeric quinolones (**50** and **51**) was reported by Zaragoza *et al.* (Zaragoza *et al.* 2005:306) Further reaction with excess of phosphoryl chloride afforded the corresponding 2,7-dichloroquinoline (**52**) and 2,5-dichloroquinoline (**53**).

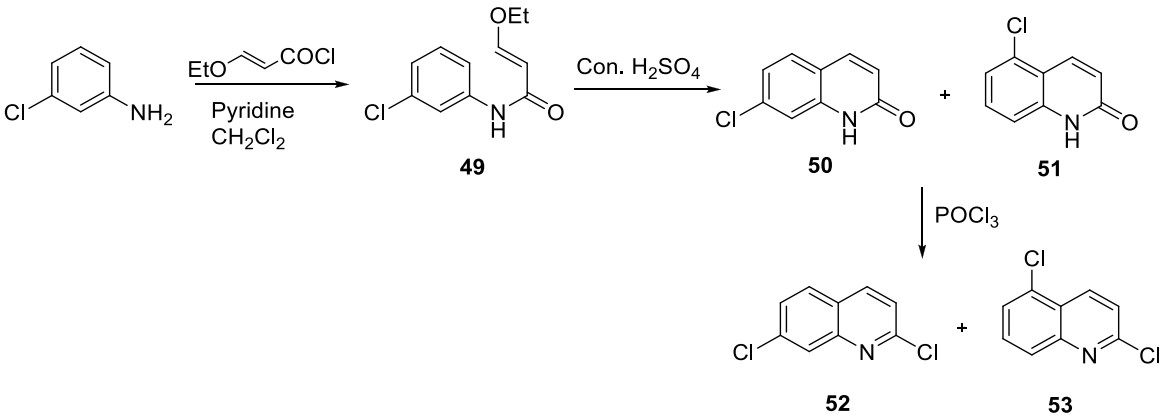

Substituted 2,4-dimethoxyquinolines (**56**) were synthesized by a condensation reaction followed by cyclization: the appropriately substituted aniline (**54**) was reacted with malonic

acid and phosphoryl chloride to give the 2,4-dichloroquinolines (**55**) which underwent a substitution reaction with methoxide ion to produce **56** (Rossiter *et al.* 2005:4086).

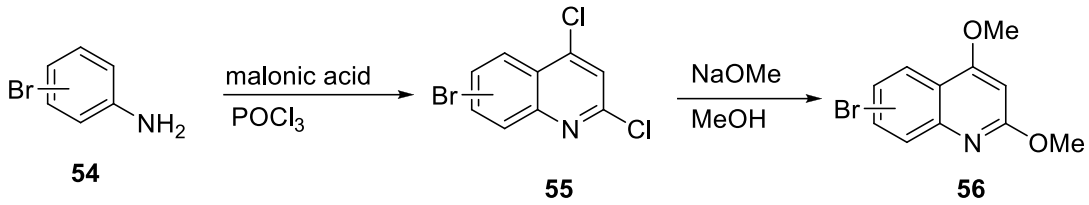

54 **55** **56**

Ethyl-4-chloro-6-methylquinoline-2-carboxylate (**59**) was synthesized by the treatment of *p*-toluidine (**57**) with diethyl acetylene dicarboxylate to give the intermediate **58** which was then chlorinated using phosphoryl chloride (Warner *et al.* 1992:2761).

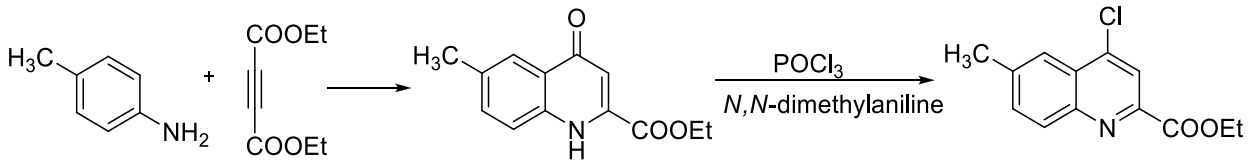

57 **58** **59**

2. 2. Multicomponent reactions

A multicomponent reaction (MCRs) is classified as a reaction in which three or more components are combined together in a single reaction vessel to produce a final product or products displaying features of all starting substrates. MCRs offers greater possibilities for molecular diversity per step with a minutesimum of synthetic time and effort: products from such MCRs result in number of high and atom step economy.

The first reported MCR was Strecker's synthesis of racemic aminuteso acids in the 1850's (Strecker, 1850:27) Strecker's aminuteso acid synthesis combined an aldehyde, hydrogen cyanide and ammonia in a one-pot procedure leading to a range of aminuteso acids. With over 150 years' history and development, MCRs have recently seen a resurgence because of the ease of access to a wide range of diverse and highly functionalized molecules such as the synthesis of compounds with heterocyclic rings of medicinal importance.

The chemistry, reactions and properties of solid acid catalyst has been addressed in a number of excellent review articles in this research area (Hallett and Welton, (Boon *et al.* 1986:480), (Earle *et al.* 1998:2245), (Ellis *et al.* 1999:337), (Earle *et al.* 1999:23), (Calo *et al.* 2000:8973), (Zhang Corey 2000:1097), (Schöfer *et al.* 2001:425) (Dupont *et al.* 2002:3667),

2011:3508). A literature survey on the use of solid acid catalysts and ionic liquids, with a focus on 3- and 4- component MCRs (Bertozzi *et al.* 2002:3147) is presented below.

2. 2. 1. The catalysts used for the synthesis of pyran derivatives

The synthesis of tetrahydrobenzo[b]pyran derivatives (**63**) via a one-pot reaction of malononitrile (**62**), various aldehydes (**61**) and dimedone (**60**) used magnetic core shell titanium dioxide nanoparticles as an efficient catalyst: this was a dominuteso Knoevenagel and Michael condensation reaction (Khazaei *et al.* 2015:14305).

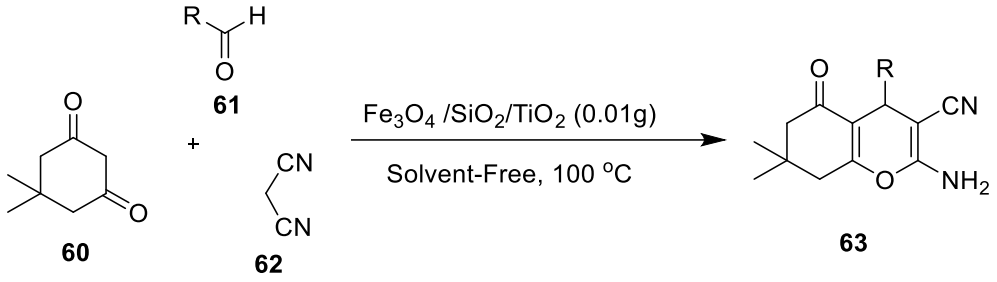

The synthesis of benzylidene malononitrile derivatives **67**, **69** and **71** occurred in the presence of an organo catalyst (Khan *et al.* 2014:3732).

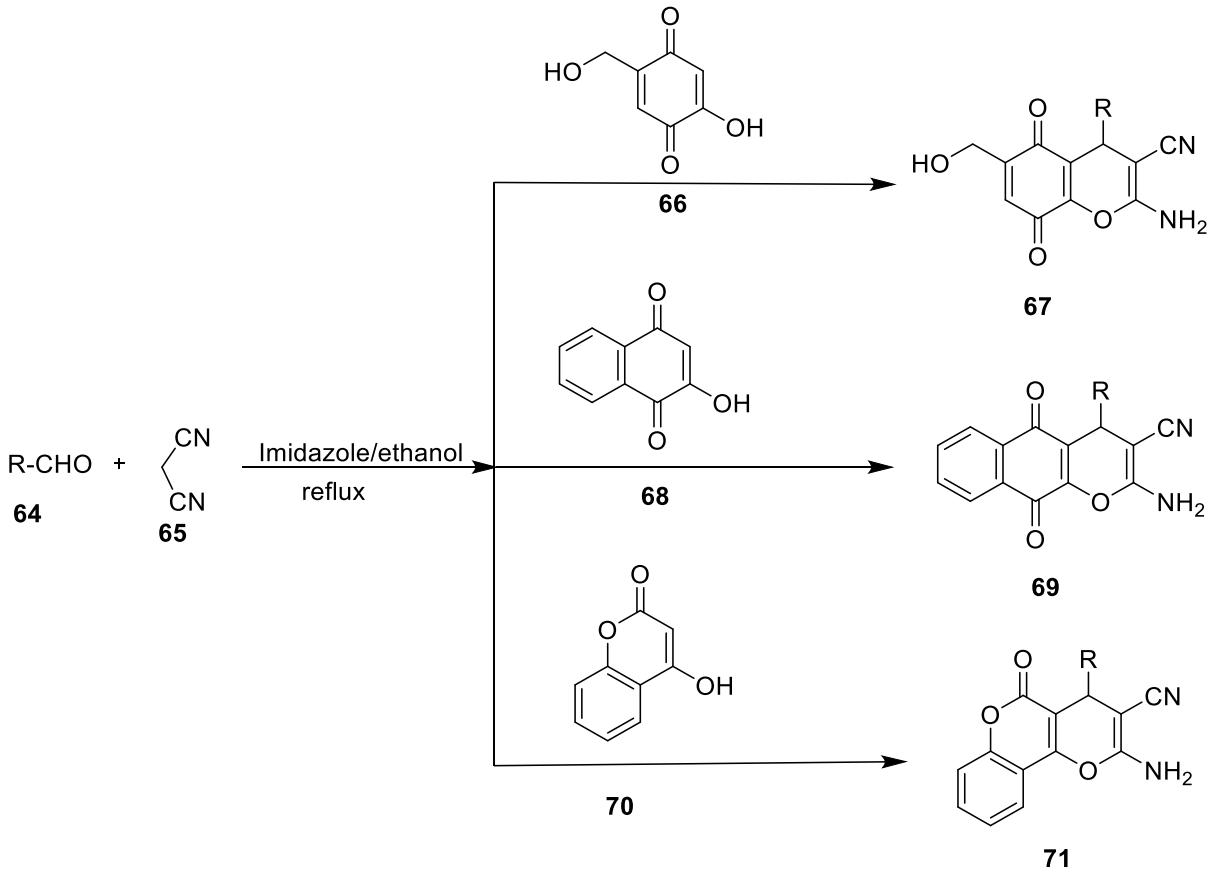

A chitosan-doped calcium hydroxyapatite (CS/CaHAp) catalyst was prepared and then used for the synthesis of 2,6-diaminutesopyran-3,5-dicarbonitrile derivatives (**75**) at room temperature (Maddila *et al.* 2017:247)

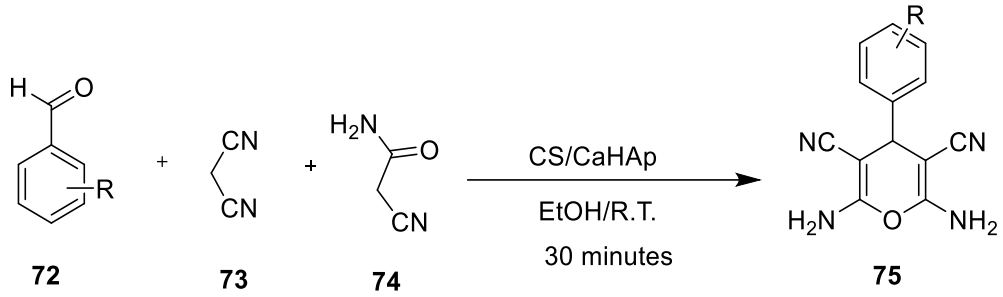

72 **73** **74** **75**

Pyrano pyrimidine dione derivatives (**79**) were synthesized under solvent-free conditions using catalytic amounts of a nano-porous silica sulfonic acid material; **79** displayed urease inhibitory activity (Ziarani *et al.* 2013:3).

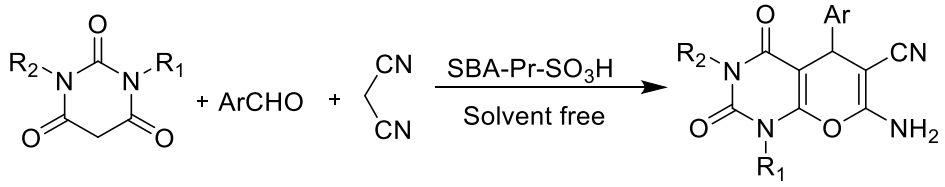

76 **77** **78** **79**

The synthesis of 2-aminuteso-3-cyanopyranochrysin derivatives (**83**) occurred in the presence of piperidine as the catalyst; **83** displayed potential as antimicrobial agents (Ramesh *et al.* 2015: 3696).

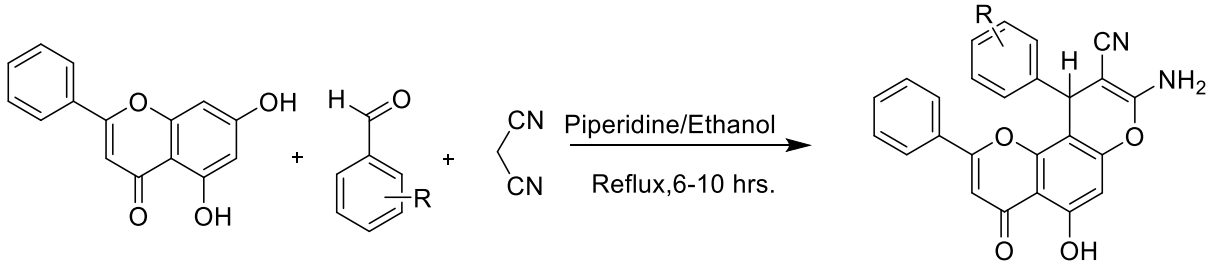

80 **81** **82** **83**

Synthesis of 3-aminuteso-6-(2-oxo-1,2-dihydroquinolin-3-yl)-4-phenyl-4H-pyran-2-carbonitrile derivatives (**87**), under reflux conditions, used piperidine as the catalyst (Sankaran 2012:339).

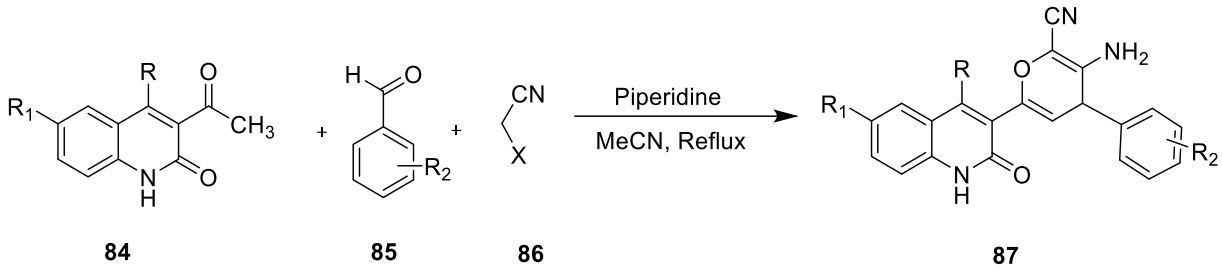

84 **85** **86** **87**

4-(Succinimido)-1-butane sulfonic acid was used as a Bronsted acid catalyst for the synthesis of pyrano [4, 3-*b*] pyran derivatives (**91**) using thermal and ultrasonic irradiation (Khaligh *et al.* 2015:728).

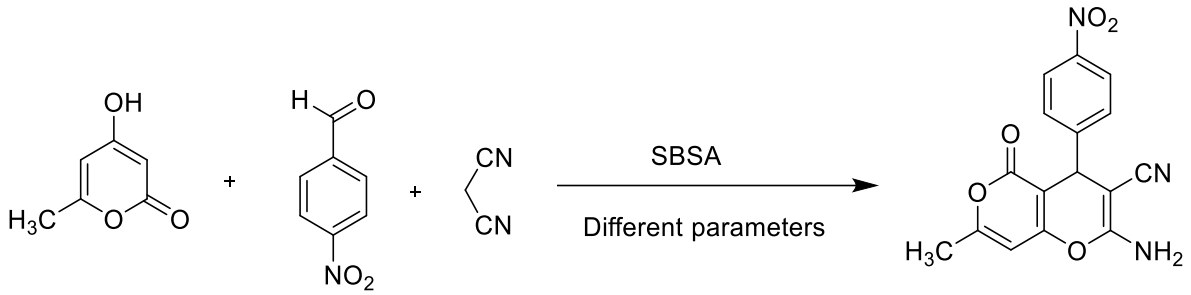

88 **89** **90** **91**

Microwave-assisted synthesis of oxazolo [5, 4-B] quinoline-fused spiro oxindoles derivatives (**95**) occurred under solvent-free conditions (Yuvaraj *et al.* 2015:78).

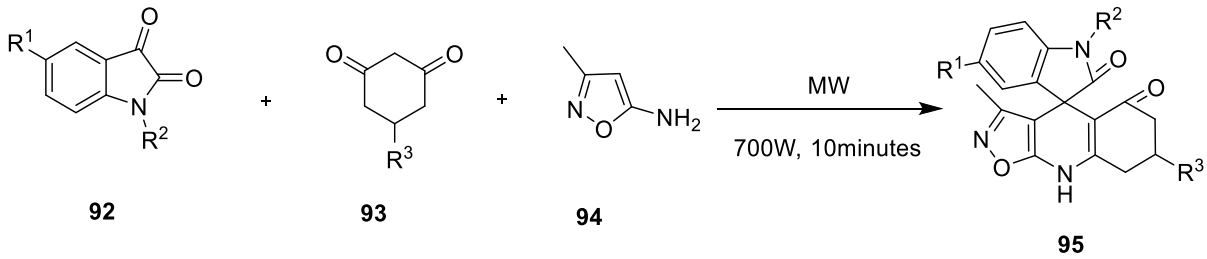

92 **93** **94** **95**

2. 2. 2. Chalcones

Chalcones are α-β unsaturated ketones found in abundance in edible plants and are considered to be precursors of flavonoids and iso-flavonoids. The presence of the double bond in conjugation with a carbonyl functionality is proposed as the functionality that contributes to their important biological activity as compared to their saturated analogues. Chalcones have attracted much attention because of their various biological applications such as anticancer, anti-inflammatory and antihyperglycemic (Xia *et al.* 2000:699), (Hsieh *et al.* 2000:163), (Ko *et al.* 2004:1333), (Satyanarayana *et al.* 2004:883) agents.

2. 2. 2. 1. The synthesis of selected chalcones

The most preferred method for the synthesis of chalcones is by the Claisen-Schmidt condensation of an aldehyde and ketone by either an acid or base catalysed reaction followed by *in situ* dehydration (Anto *et al.* 1995:33). Different heterogeneous catalysts have been used such as Lewis acid (Iranpoor Kazemi 1998:9475), (Narender Reddy 2007:3177), Bronsted acid (Szell Sohar 1969:1254), solid acid, (Drexler Amiridis 2003:136), (Choudary *et al.* 2005:1369) (Saravanamurugan *et al.* 2004:101) and solid base (Daskiewicz *et al.* 1999:7095), (Sebti *et al.* 2002:335), (Wang Cheng 2006:689).

The Claisen-Schmidt condensation reaction is also carried out in common ionic liquids (Yang *et al.* 2007:107), (Dong *et al.* 2008:1924), (Rahman *et al.* 2012:571), (Shen et al. 2008:24) as a green approach (Ql *et al.* 2007:105), (Hua *et al.* 2013:13272). Silica based nano-material solid acid catalyst such as MCM-4, SBA-15, and aminuteso propyl based nano silica were used under solvent-free conditions (Nagendrappa 2002:59), (Romanelli *et al.* 2011:24). Protonated aluminutesate mesoporous silica nano-material was also used for some biologically active compounds (Wang Cheng 2006:689).

Although many chalcones have been synthesized and their biological activity elucidated, new compounds are sought after especially heterocycles which contain a nitrogen atom such as quinolones and quinolines as theses moieties tend to increase the biological activity of compounds. The synthetic methodologies for quinolone-based chalcones are presented below.

The tandem Claisen-Schmidt reaction was used for the synthesis of quinoline and quinolone-based chalcones (**98** and **100**) with NaOH as catalyst at room temperature (Sazegar *et al.* 2016:11023). These compounds displayed DNA gyrase inhibiting properties.

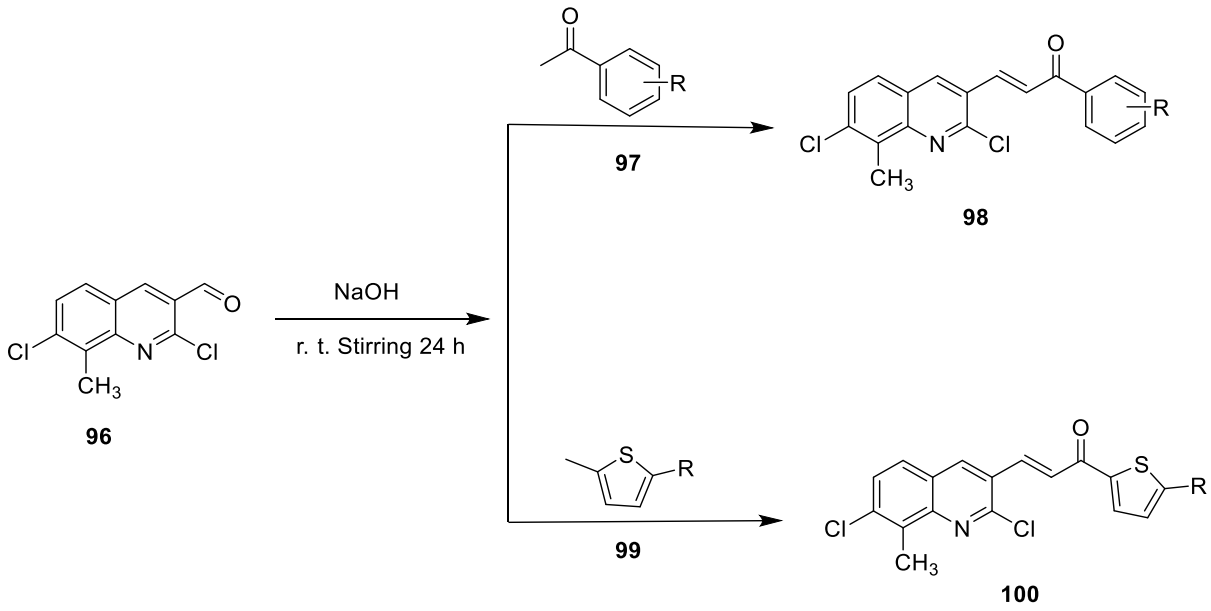

A modified fluorapatite was used as a highly efficient catalyst for the synthesis of chalcones (**103**) via the Claisen–Schmidt condensation reaction (Abdullah *et al.* 2014:31).

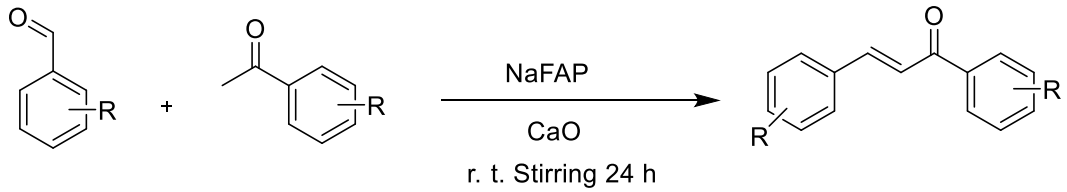

101 **102** **103**

The synthesis of oxoquinoline chalcone (**106**) derivatives, under reflux conditions, utilized catalytic amounts of piperdine (Jioui *et al.* 2016:218).

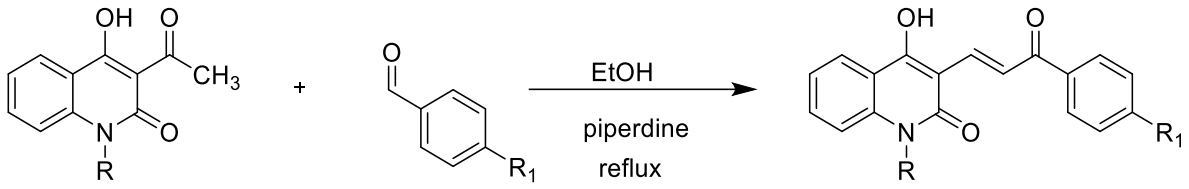

104 **104** **106**

In a similar reaction sequence, the synthesis of oxoquinoline chalcone (**109**) derivatives and (E)-2-((2-methoxyquinolin-3-yl)methylene)-2,3-dihydro-1H-inden-1-onechalcone derivatives (**112** and **114**) was achieved with NaOH and sodium ethanoate, respectively (Munawar *et al.* 2008:288), (Khot *et al.* 2012:70).

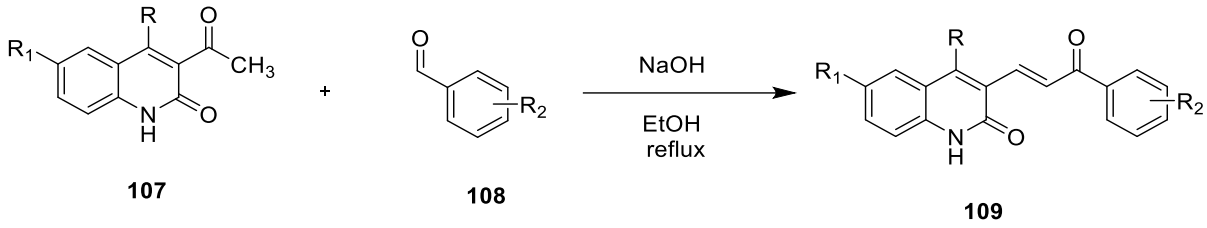

107 **108** **109**

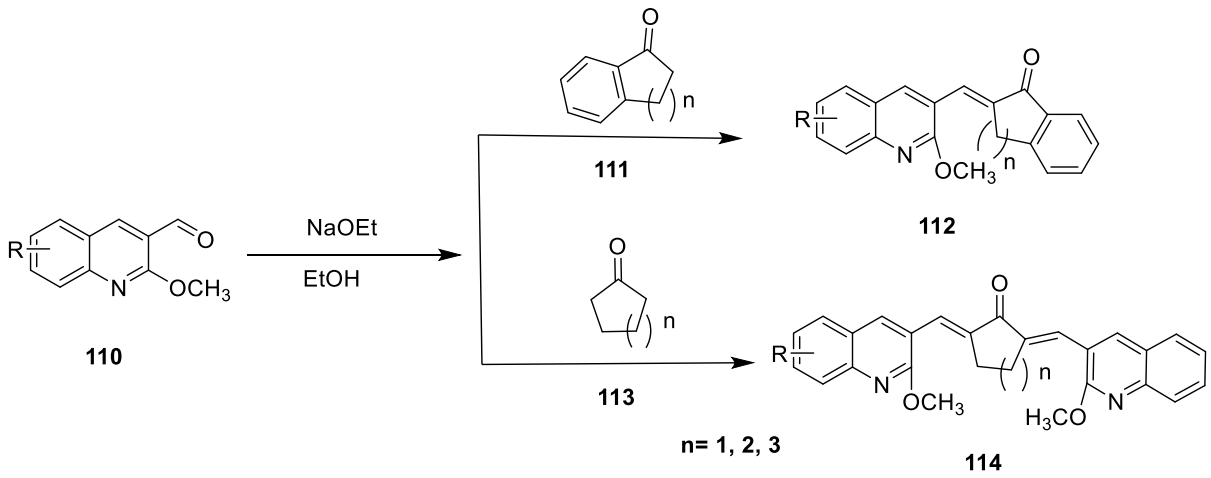

110 **111** **112** **113** **114**

The synthesis of (E)-2-((2-chloroquinolin-3-yl)methylene)-2,3-dihydro-1H-inden-1-one chalcone (**117**) derivatives, at room temperature, was reported; NaOH was the catalyst (Charris *et al.* 2005: 875).

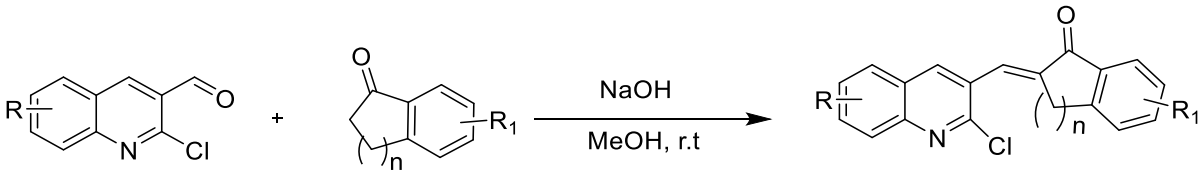

115 **116** **117**

n= 1, 2, 3

The synthesis of (E)-3-(2-chloroquinolin-3-yl)-1-(2-hydroxyphenyl)prop-2-en-1-one (**120**) chalcone derivatives, at room temperature, also used NaOH (Shikha *et al.* 2009:1780).

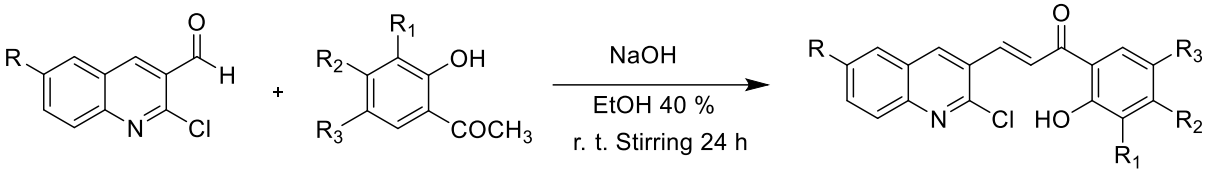

118 **119** **120**

2. 2. 3. The 1,3-dipolar cycloaddition reaction

The 1, 3-Dipolar cycloaddition (1, 3-DC), discovered by Huisgen and coworkers in the early 1950s, is the reaction of a 1, 3-dipole with a multiple bond system. Since the systematic classification of 1,3-DC was made, these reactions have been extensively studied. The 1-substituted-pyridinium-3-olates have been extensively investigated as they behave as 1,3-dipoles and undergo 1,3-DC reactions with a variety of dipolarophile. One of the reasons for the interest in these cycloaddition reactions is that the cycloadducts have a common structural unit, the 8-azabicyclo [3.2.1] octane skeleton, which is a key building block in naturally occurring tropane alkaloids. The tropone derivatives are attractive synthetic targets as they possess potent biological activity: atropine, scopolaminutese and cocaine are some common examples of tropone derivatives. The feasibility of these cycloaddition processes has been interpreted based on the valence bond and frontier molecular orbital (FMO) treatment.

The 1,3-DC reaction (Padwa and Pearson 2003), (Sarotti *et al.* 2012:2556), (Uma *et al.* 2010:7278), (Yavuz *et al.* 2013:1437), (Alcaide *et al.* 2001:1351) is an efficient method for the construction of five-membered heterocycles (Dömling and Ugi 2000:3168), (Balme *et al.*

2003:4101). This methodology allows molecular complexity and diversity to be created by the facile formation of several new covalent bonds in a one-pot transformation quite closely approaching the concept of an ideal synthesis, and it is particularly well adapted for combinatorial synthesis.

2. 2. 3. 1. The synthesis of selected quinolones and quinolines based spirooxindoles by 1,3-Dipolar reactions

The spirooxindole system and its derivatives have become important synthetic targets as these structural frameworks form the core units of pharmaceutical agents and natural alkaloids (Sridhar *et al.* 2007:319), (Kumar *et al.* 2011:3132), (Jiang *et al.* 2006:2105). The 1,3 DC reaction of an azomethine ylide with olefinic and acetylenic dipolarophiles is one of the most effective methods for the regio- and stereo-selective construction of a variety of complex spirooxindole derivatives (Dalpozzo *et al.* 2012:7247).

An efficient synthesis of *(E)*-3-arylidene-2,3-dihydro-8-nitro-4-quinolone spiro heterocycles was reported (Sebahar and Williams 2000:5666). Rane *et al.* (Rane *et al.* 2010:415) reported the synthesis of spiro-oxazino-quinoline derivatives (**123**, **125** and **127**) from **121** with catalytic amounts of zinc chloride.

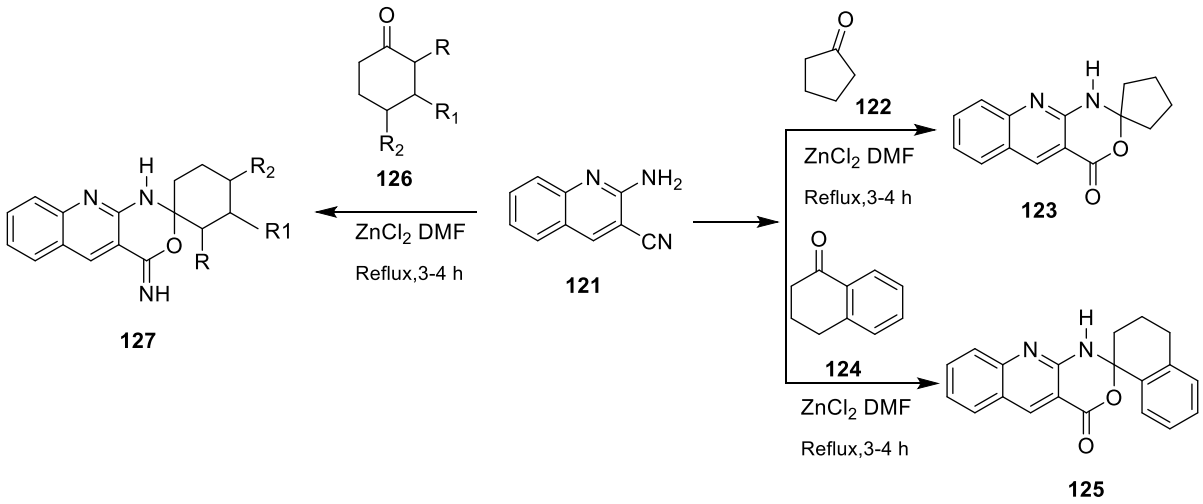

Ghahremanzadeh *et al* (Ghahremanzadeh *et al.* 2008:1617) reported the synthesis of spiro 1H-spiro[pyrimido[4,5-b]quinoline-5,5'-pyrrolo[2,3-d]pyrimidine]-2,2',4,4',6'(1'H,3H,3'H,7'H,10H)-pentaone derivatives (**128)** and 3,6'-bis(methylthio)-3,4-dihydro-2H-spiro[acridine-9,3'-pyrrolo[2,3-b]pyridine]-1,2',4'(1'H,5'H,10H)-trione derivatives (**130**) in an aqueous system with catalytic amounts of *p*-TSA.

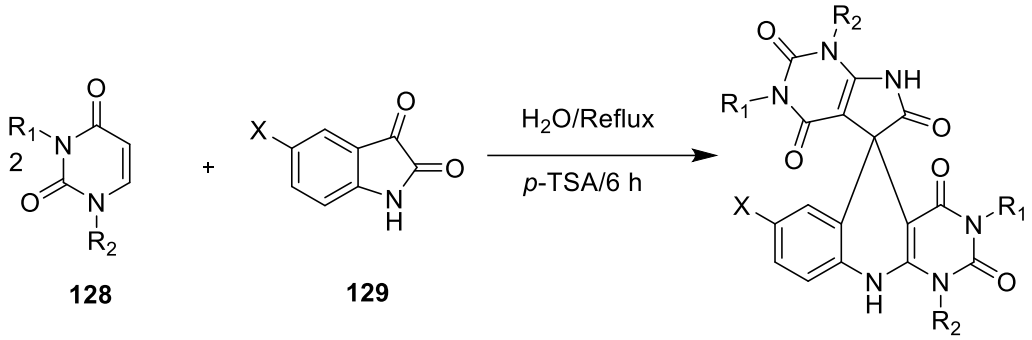

R_1, R_2=H
R_1, R_2=Me
R_1=H, R_2=Me

X=H, Br, NO_2

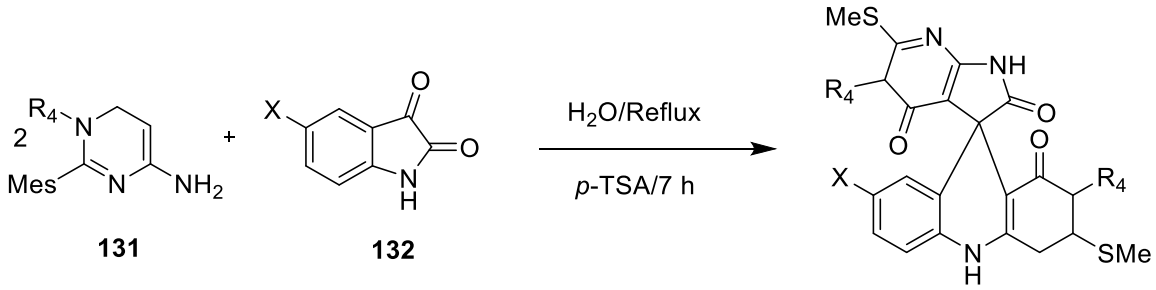

R_4=NH_2

The synthesis of spiro [pyrimido [4,5-b] quinoline-5, pyrrolo [2, 3-d] pyrimidine]-trione (**136**) and spiro [indoline-pyrido [2, 3-d: 6, 5-d] dipyrimidine] (**139**) derivatives, under reflux conditions, using ethanol as solvent and catalytic amounts of *p*-TSA was reported by Khosrow Jadidi *et al* (Jadidi *et al.* 2009:2005).

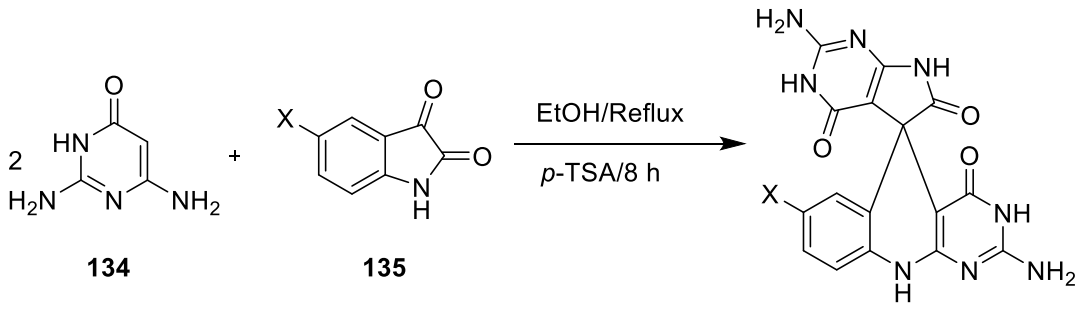

X= H, Br, NO_2, CH_3

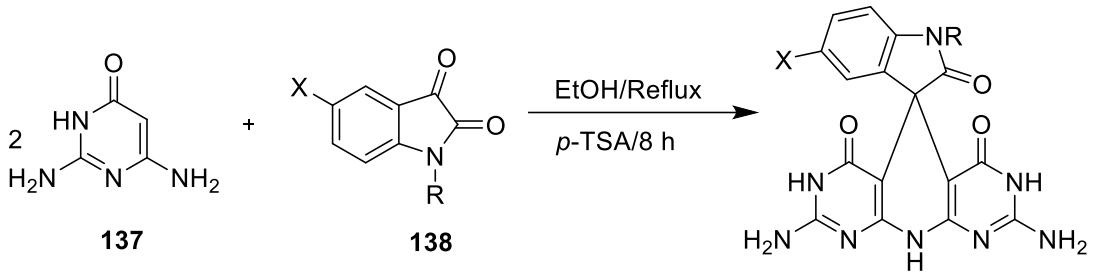

137 **138** **139**

X= H, Br, NO_2, CH_3

R= CH_3, CH_2

The green synthesis of benzo[f] pyrimido [4, 5-b] quinolone derivatives (**143**) was catalyzed by iodine in an aqueous media (Wang *et al.* 2009:3069).

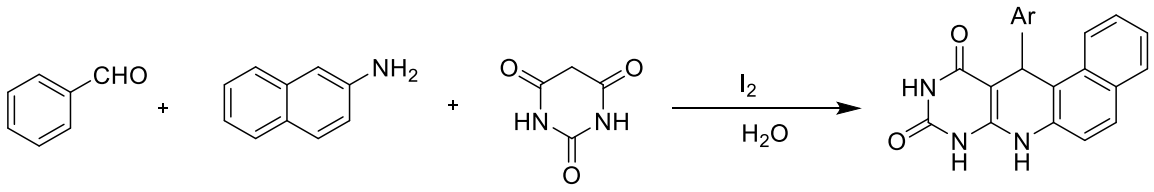

140 **141** **142** **143**

The condensation reaction was used for the synthesis of spiro [benzo[*h*]quinoline-7, 3-indolines] derivatives (**147**) (Rahmati Eskandari-Vashareh 2014:169).

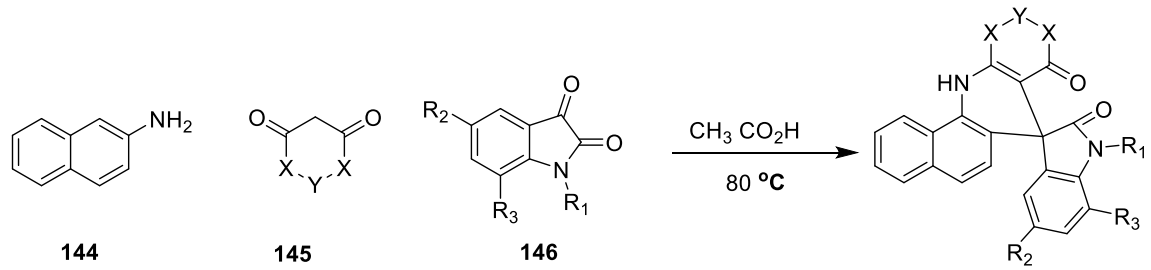

144 **145** **146** **147**

X=NH,HCH_3,CH_2

Y=$C(CH_3)_2$,C=O

X-Y-Z=

A microwave-assisted efficient synthesis of spiro quinoline derivatives (**151** and **155)** occurred via a solvent-free aza-Diels–Alder reaction (Bhuyan *et al.* 2012:6460).

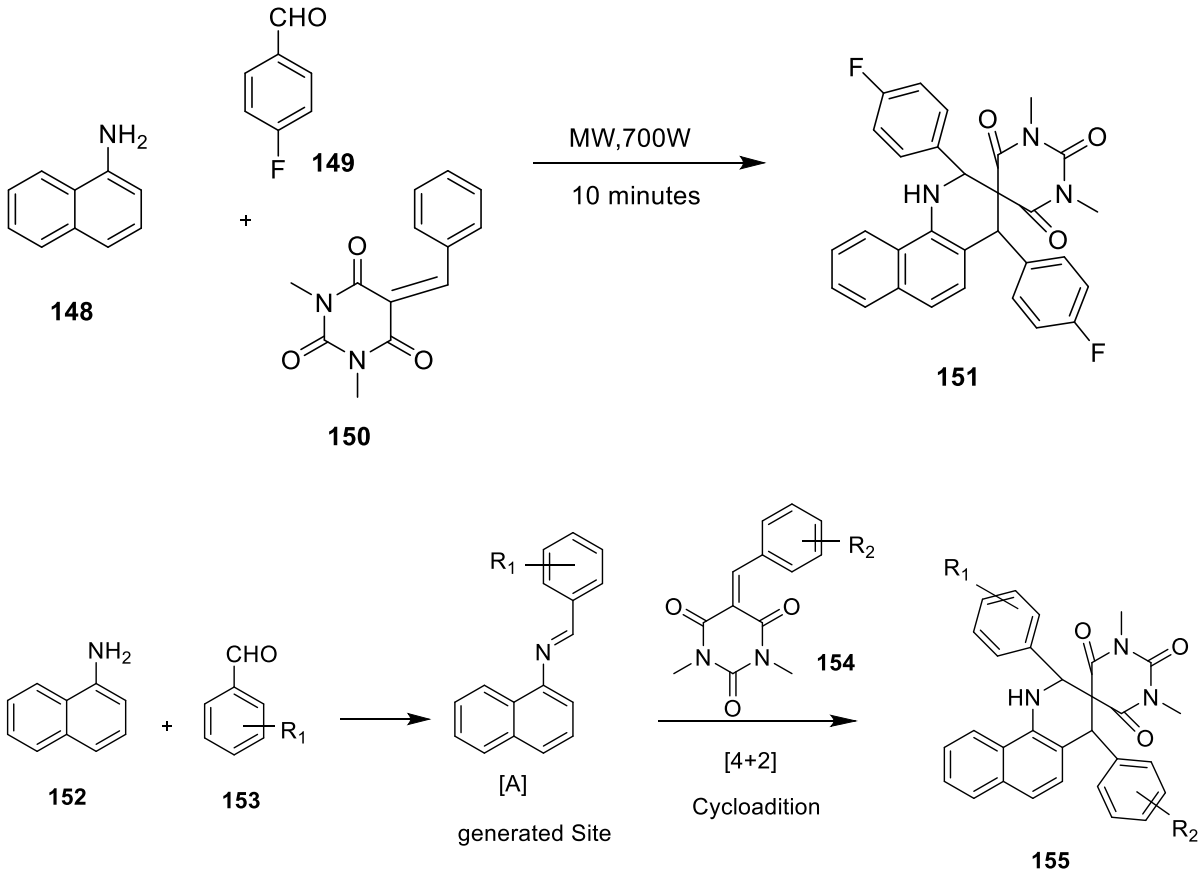

Ultrasound-assisted three-component synthesis of spiro [4H-pyrano [3, 2-c] quinolin-4, 3'-indoline]-2', 5(6H)-dione derivatives (**159** and **163**) occurred in an aqueous system (Gholizadeh and Radmoghadam 2014:1637).

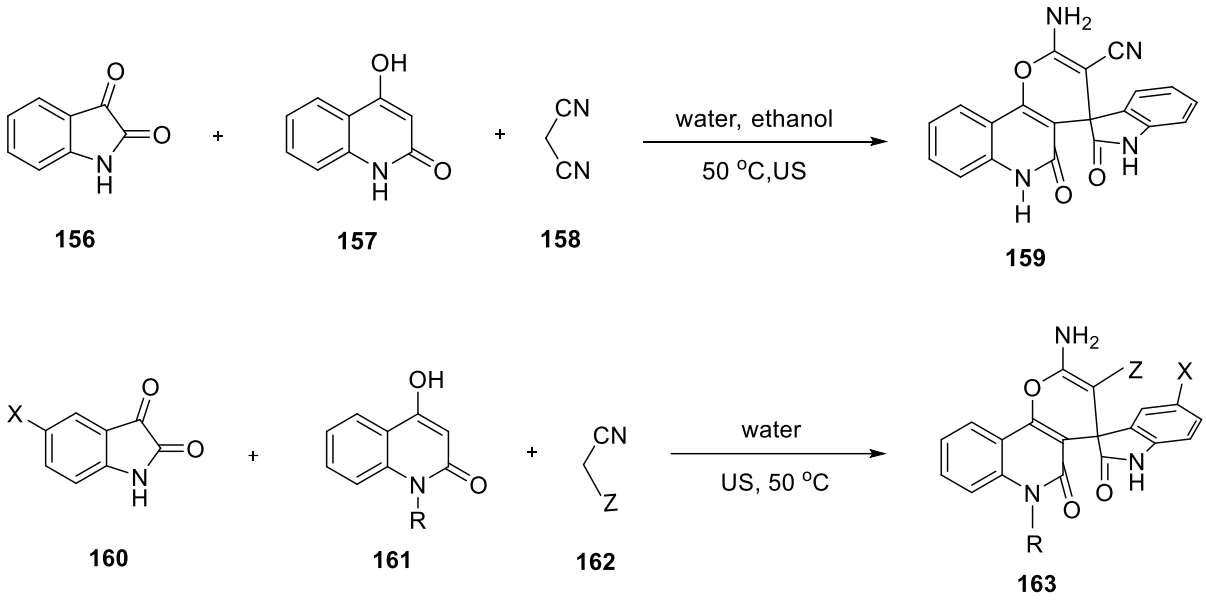

An expedient approach for the synthesis of naphthalene-grafted spiro-oxindolo pyrrolizidines (**167** and **171**) was reported (Saravanan *et al.* 2013:3449) in methanol as the solvent.

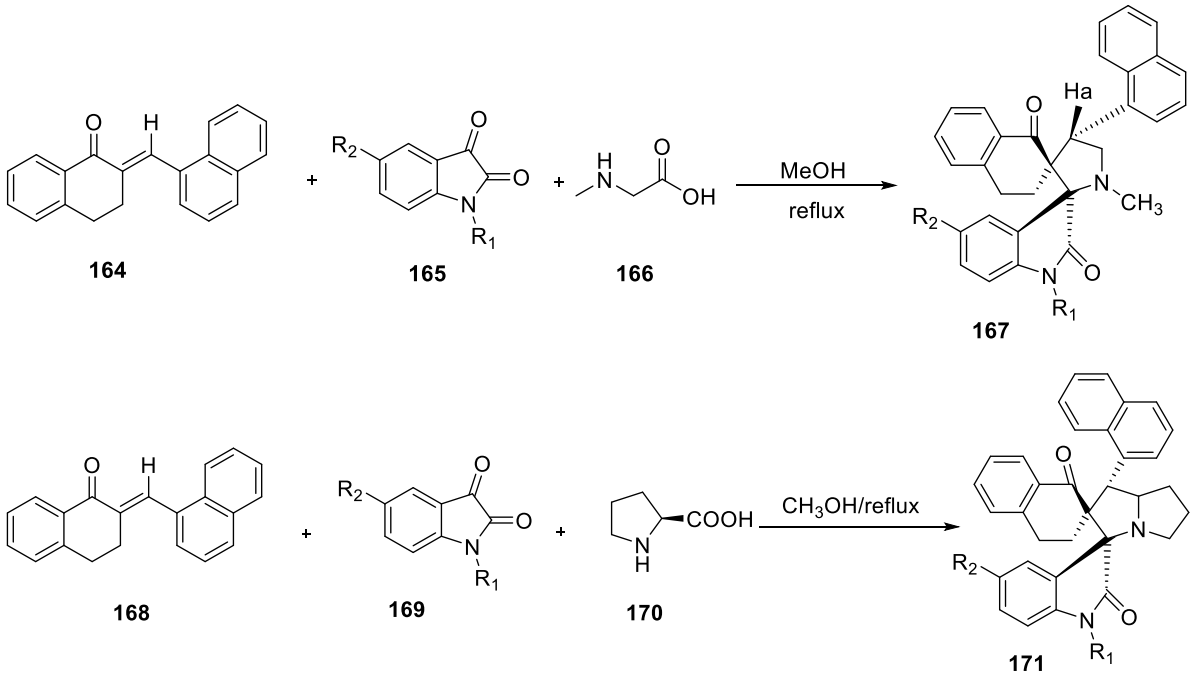

164 165 166 167

168 169 170 171

2. 3. Microwave assisted organic synthesis

In the past few years there has been growing attention to the use of microwave (MW) irradiation in organic synthesis. The first contribution on MW Irradiation was reported by Gedye and Giguere in 1986 (Luo and Zhang 2011:923): since then it is being increasingly used in organic reactions since they are considered clean and easy to operate. MW irradiation has several advantages over conventional technology: remarkable decrease in the reaction time; improved yields of products and sometimes remarkable effects on chemo-regio and stereo-selectivity (Madhav *et al.* 2008:1799). Another advantage is that MWs can promote unfeasible transformations that traditional heating cannot achieve. It appears that MWs have a specific 'microwave effect' that lowers the activation energy of a reaction (Kappe 2004:6250) therefore the organic reactions take place more rapidly, safely, environmentally friendly and with high yields (Polshettiwar and Varma 2008:629). MW synthesis is usually conducted in reflux conditions using different solvent systems such as water, methanol, ethanol, dimethyl form amide, ethyl acetate, acetone, and acetic acid. Microwave chemistry is becominutesg increasingly popular both in industry and in academia (Brinkerhoff *et al.* 2014:49556).

2. 3. 1. The synthesis of selected heterocycles by microwave irradiation

2,2-dimethyl-5-phenyl-7-(thiophen-2-yl)-2,3,5,8-tetrahydroquinolin-4(1H)-one (**174)** and 7-(4-fluorophenyl)-2,2-dimethyl-5-phenyl-2,3,5,8-tetrahydroquinolin-4(1H)-one (**177)** were synthesized by Trivedi *et al* in a one-pot solvent-free MW reaction: these two compounds exhibited good antimicrobial activity (Trivedi *et al.* 2010:6100).

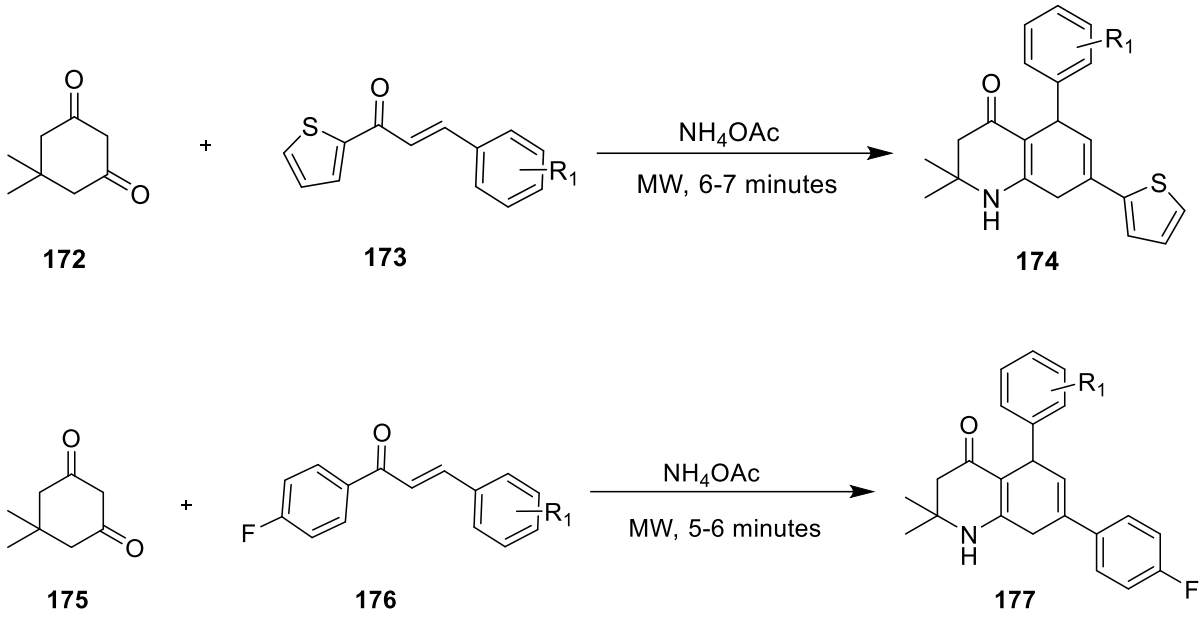

172 173 174

175 176 177

Tu *et al.* (Tu *et al.* 2009:91) synthesized 4-aryl-2-ferrocenyl-7,7-dimethyl-4-phenyl-4,6,7,8-tetrahydroquinolin-5(1H)-one derivatives (**182** and **187**) through MW assisted multicomponent reaction: acetylferrocene (**178**), aromatic aldehydes (**179**) and dimedone (**181**) were used in the presence of ammonium acetate using DMF as reaction media at 100 °C. This new procedure gave excellent yields and no purification steps were necessary.

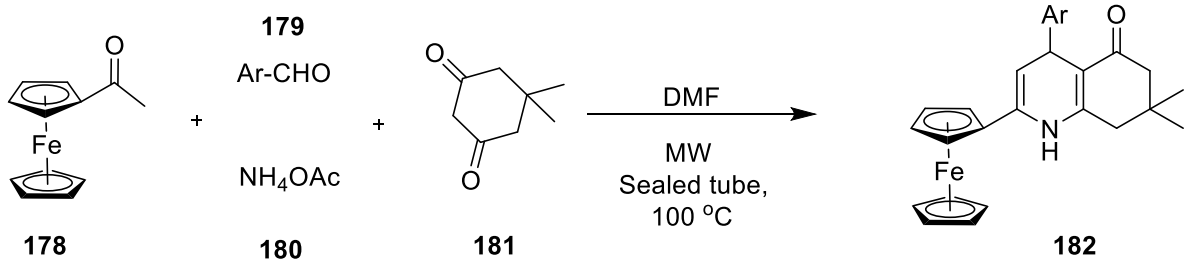

178 180 181 182

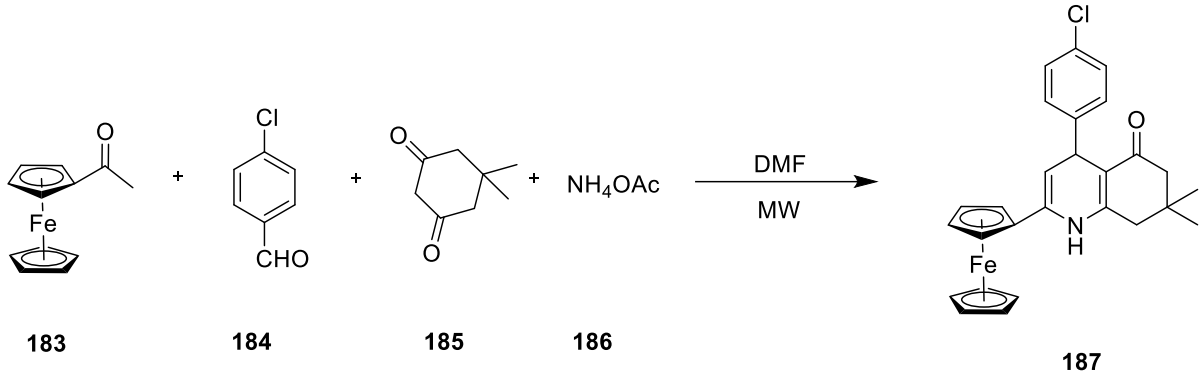

183 **184** **185** **186** **187**

A straightforward MW assisted green synthesis of functionalized spirooxindole-pyrrolothiazole (**191**) *via* a three-component 1,3-DC reaction was also reported (Paneri *et al.* 2016:224).

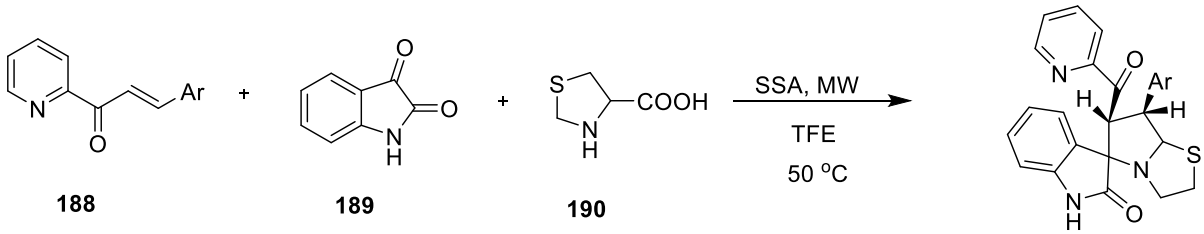

188 **189** **190** **191**

The 1, 2, 3-triazoles derivatives (**195**) were synthesized by the MW assisted one-pot three-component system (Souza *et al.* 2016:1592).

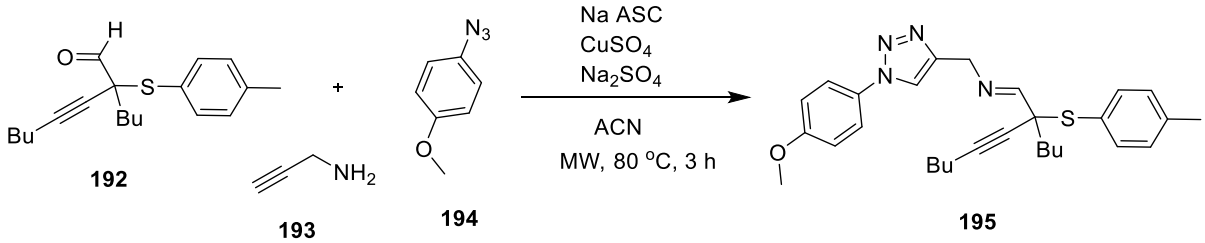

192 **193** **194** **195**

2. 4. Catalyst

The use of catalysts in organic reactions is becominutesg a strategic field of science because it is an alternate way to meet the challenges for difficult synthesis. Scientists are using it in the discovery and the development of new synthetic pathways using alternative reaction conditions and solvents for improved selectivity. Catalysis is sometimes referred to as a "foundational pillar" of green chemistry (Sampaio *et al.* 2013:32), (Rodriguez-Chueca et al. 2014:619), (Carra *et al.* 2014:322), (Ren et al. 2014:064301), (Barreca *et al.* 2015:6219) because it often reduces energy requirements, minutesimizes the quantities of reagents needed and allows for the use of less toxic reagents. New catalytic organic transformations offer several possibilities for improvement in the eco-compatibility of fine

chemical production. Current research activities on new green catalytic systems provide resource-saving synthetic transformations through transition metal catalysed reactions (Yoon *et al.* 2011:666), (Monteagudo *et al.* 2013:210), (Miralles-Cuevas *et al.* 2014:515), (Pouran *et al.* 2014:60), (Xu *et al.* 2015:4593), (Sampaio *et al.* 2015:74), (Sampaio *et al.* 2015:58363), (Pistkova *et al.* 2015:19), (Khalilian *et al.* 2015:239). Recently, the use of recyclable catalysts has evoked great interest in investigating catalytic properties and chemical transformation of substrates to products. They are becominutesg a well-established best choice for many chemical transformations with prominutesence in both heterogeneous and homogeneous processes (Patra *et al.* 2012:5022).

2. 4. 1. Homogeneous and heterogeneous catalysts

Catalyst is divided into two branches, viz., homogeneous and heterogeneous. In a homogeneous catalytic system, the active catalyst sites and the reactants are in the same phase. This system allows for easier interactions between the components, which in turn results in better activity. Homogeneous catalysts have several other advantages, such as high turn-over number and high selectivity (Ortega Liebana *et al.* 2012:316) although these catalysts are widely used in a variety of industries, it is often difficult to isolate and separate the final product from the catalyst after the reaction goes to completion. Even when it is possible to separate the catalyst from the reaction mixture, trace amount of catalyst are likely to remain in the final product. It is necessary to remove the catalyst because metal contaminutesation is highly regulated, especially in the drug and pharmaceutical industry (Herney-Ramirez *et al.* 2010:10), (Punzi *et al.* 2012:30). One efficient way to overcome the problem of isolation and separation with a homogeneous catalyst is the heterogenization of active catalytic molecules, thus creating a heterogeneous catalytic system (Prucek *et al.* 2009:325) Heterogenization is commonly achieved by entrapment or grafting of the active molecules on surface (or) inside the process of a solid support, such as silica, or aluminutesa. However, the active sites in heterogeneous catalyst are not as accessible as in a homogeneous catalyst, and thus the activity of the catalyst is usually reduced.

2. 5. Molecular docking

Molecular Docking is a valuable tool in structural biology and computer-aided drug design. The chief goal of ligand-protein docking is to predict the predominutesant binding modes of a ligand with a protein of known three-dimensional structure. It also predicts the strength of the binding, the energy of the complex; the types of signal produced and the binding affinity between two molecules, using scoring functions, is calculated. Successful docking methods search high-dimensional spaces effectively and use a scoring function that correctly ranks dockings.

Molecular docking is divided into two separate sections.

(i) Search algorithm: the algorithm creates an optimum number of configurations that include the experimentally determinutesed binding modes. The various algorithms used for docking analysis are molecular dynamics, Monte Carlo methods, Gentic algorithms, fragment-based methods, Point complementary methods, Distance geometry methods, and Systematic searches

(ii) Scoring function: these are mathematical methods used to predict the strength of the non-covalent interaction, known as binding affinity, between two molecules after they have been docked. Scoring functions have also been developed to predict the strength of other types of intermolecular interactions, for example between two proteins or between protein and DNA or protein and drug. These configurations are evaluated using scoring functions to distinguish the experimental binding modes from all other modes explored through the searching algorithm.

There are two major methods used for docking:

(i) Lock and key or rigid docking**:** in rigid docking, both the internal geometry of the receptor and ligand are kept fixed and docking is performed**.**

(ii) Induced fit or flexible docking**:** an enumeration on the rotations of one of the molecules (usually smaller one) is performed. For every rotation, the surface cell occupancy and energy is calculated; later the most optimum pose is selected.

The software's available for molecular docking include Schrodinger, Dock, Autodock and iGemdock

2. 5. 1. Selected proteins used in molecular docking

Albuminutes is one of the longest known and probably the most studied of all proteins. Its many properties and functions have attracted the interest of scientists and physicians for generations. Its applications are many, both in clinical medicine and in basic research. Albuminutes is the most abundant soluble protein in the body of all vertebrates and it is the most prominutesent protein in plasma (Peters 1996). The serum albuminutesutes are extensively used in biophysical and biochemical studies as a model system for protein folding aggregation and drug delivery (Peters 1996). They assist in the disposition and transportation of various exogenous and endogenous ligands to specific targets (Peters 1996). Albuminutesutes are the principal bio macromolecules responsible for the maintenance of colloid-blood pressure needed for proper distribution of body fluids between intravascular compartments and body tissues (Kumar and Buranaprapuk 1997:2085), (Singer and Nicolson 1972:720). It also acts as a plasma carrier by nonspecific binding through several hydrophobic steroid hormones across organ-circulatory interfaces such as the liver, intestine, kidney, and brain (Partridge and Am 1987:157), (Banerjee *et al.* 2009:11429) (McLachlan and Walker 1977:543). Some of these albuminutesutes are human serum albuminutes (HSA), bovine serum albuminutes (BSA), equine serum albuminutes (ESA) and rat serum albuminutes (RSA). The molecules and ligands that have been studied include fatty acids, metal ions, pigments and numerous drugs (Feldhoff and Peters 529).

Albuminutesutes are characterized by a low content of tryptophan and methionine and a high content of cysteine and the charged aminuteso acids, aspartic and glutamic acids, lysine and arginine. Glycine and isoleucine contents are lower than in the average protein (Peters 1996) many albuminutesutes have but one tryptophan and avian albuminutesutes reported to date have none (He Carter 1992:209). The high total charge, potentially about 185 ions per molecule at pH 7, aids its solubility and the many disulfide bonds, a feature of most extracellular proteins, contribute to its stability. Structural aspects of HSA and BSA proteins have been reasonably well explored. The primary structure of these proteins has about 580 aminuteso acid residues which assume the solid equilateral triangular shape with sides ~80 Å and depth ~30 Å. The secondary structure of HSA and BSA is constituted of ~67 % helix content with six turns and 17 disulfide bridges (Peters 1985), (Peters 1996). HSA and BSA display approximately 80% sequence homology and a repeating pattern of disulfides that is strictly conserved. The primary structure of HSA consists of 585 aminuteso acids and its aminuteso acid sequences contain 18 tyrosines (Tyr), 6 methionines, 1 tryptophan (Trp-214),

17 disulfide bridges and one free thiol group. The disulfides are positioned in a repeating series of nine loop like structures centered on eight sequential Cys-Cys pairs (figure 2.1). In the case of BSA, the primary structure is composed of 583 aminuteso acid residues consisting of two Trp residues (Trp-134 and Trp-213) (figure 2.1). From the determinutesed crystallographic structure of HSA it was proposed that the single Trp residue (Trp-214) is located in IIA binding site (figure 2.1). In the case of BSA, Trp-213 is located in a similar hydrophobic microenvironment as the single Trp-214 in HSA (sub-domain IIA), whereas, Trp-134 is more exposed to solvent and it is localized in the sub-domain IA (figure 2.1), (Helms *et al.* 1997:67).

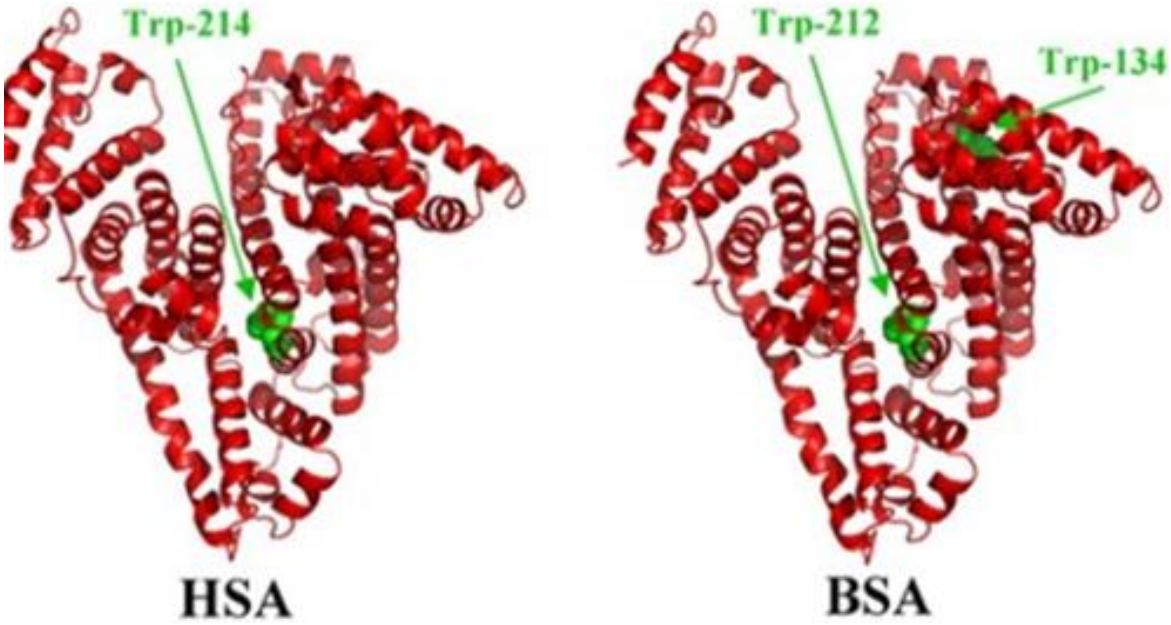

Figure 2. 1. The secondary structure of HSA and BSA (Helms *et al.* 1997:67).

References

Angibaud, P. R., Venet, M. G., Filliers, W., Broeckx, R., Ligny, Y. A., Muller, P., Poncelet, V. S. and End, D.W., 2004. Synthesis routes towards the farnesyl protein transferase inhibitor ZARNESTRATM. European Journal of Organic Chemistry (2004) 479-486.

Adams, W. J. and Hey, D. H., 1950. 634. Some 4-(dialkylaminutesoalkylaminuteso)-3-phenylquinolines. Journal of the Chemical Society (Resumed), pp.3254-3259.

Anto, R. J., Sukumaran, K., Kuttan, G., Rao, M. N. A., Subbaraju, V. and Kuttan, R., 1995. Anticancer and antioxidant activity of synthetic chalcones and related compounds. Cancer letters (97) 33-37.

Abdullah, M. I., Mahmood, A., Madni, M., Masood, S. and Kashif, M., 2014. Synthesis, characterization, theoretical, anti-bacterial and molecular docking studies of quinoline based chalcones as a DNA gyrase inhibitor. Bioorganic chemistry (54) 31-37.

Alcaide, B., Almendros, P., Alonso, J.M. and Aly, M. F., 2001. Rapid and stereocontrolled synthesis of racemic and optically pure highly functionalized pyrrolizidine systems via rearrangement of 1, 3-dipolar cycloadducts derived from 2- azetidinone-tethered azomethine ylides. The Journal of organic chemistry (66) 1351-1358.

Bringmann, G., Reichert, Y., Kane, V. V. 2004. The total synthesis of streptonigrin and related antitumor antibiotic natural products. Tetrahedron (60) 3539-3574.

Boon, J. A., Levisky, J. A., Pflug, J. L. and Wilkes, J. S., 1986. Friedel-Crafts reactions in ambient-temperature molten salts. The Journal of Organic Chemistry (51) 480-483.

Bertozzi, F., Gustafsson, M. and Olsson, R., 2002. A novel metal iodide promoted three-component synthesis of substituted pyrrolidines. Organic letters (4) 3147-3150.

Balme, G., Bossharth, E. and Monteiro, N., 2003. Pd-Assisted Multicomponent Synthesis of Heterocycles. European Journal of Organic Chemistry (2003) 4101-4111.

Bhuyan, D., Sarma, R. and Prajapati, D., 2012. Microwave-assisted efficient synthesis of spiroquinoline derivatives via a catalyst-and solvent-free aza-Diels–Alder reaction. Tetrahedron Letters (53) 6460-6463.

Brinkerhoff, R. C., Tarazona, H. F., de Oliveira, P. M., Flores, D. C., D'Oca, C. D. R. M., Russowsky, D. and D'Oca, M.G.M., 2014. Synthesis of β-ketoesters from renewable resources and Meldrum's acid. RSC Advances, (4).49556-49559.

Banerjee, P., Pramanik, S., Sarkar, A., and Bhattacharya, S. C., 2009. Deciphering the Fluorescence Resonance Energy Transfer Signature of 3-Pyrazolyl 2-Pyrazoline in Transport Proteinous Environment. J. Phys. Chem. B. (113) 11429-11436.

Barreca, D., Carraro, G., Warwick, M. E., A., Kaunisto, K., Gasparotto, A., Gombac, V. S., ada, C., Turner, S., Van Tendeloo, G., Maccato, C., Fornasiero, P., 2015. Fe_2O_3–IO_2 nanosystems by a hybrid PE-CVD/ALD approach: controllable synthesis, growth mechanism, and photocatalytic properties. Cryst Eng Comm (17) 6219-6226.

Cominutesutes, D. L., Hong, H., Saha, J. K., Jianhua, G. A. 1994. Six-Step Synthesis of (. +-.)-Camptothecin. J.Org Chem (59) 5120-5121.

Curd, F. H. S., Raison, C. G. and Rose, F. L., 1947. Synthetic antimalarials. Part XVII. Some aminutesoalkylaminutesoquinoline derivatives. Journal of the Chemical Society (Resumed), (167) 899-909.

Compagnone, R. S., Suárez, A. I., Zambrano, J. L., Piña, I.C. and Domínguez, J. N., 1997. A short and versatile synthesis of 3-substituted 2-aminutesoquinolines. Synthetic communications (27) 1631-1641.

Calo, V., Nacci, A., Lopez, L. and Mannarini, N., 2000. Heck reaction in ionic liquids catalyzed by a Pd–benzothiazole carbene complex. Tetrahedron Letters (41) 8973-8976.

Choudary, B. M., Ranganath, K.V. S., Yadav, J. and Kantam, M. L., 2005. Synthesis of flavanones using nanocrystalline MgO. Tetrahedron Letters (46) 1369-1371.

Charris, J. E., Domínguez, J. N., Gamboa, N., Rodrigues, J. R. and Angel, J. E., 2005. Synthesis and antimalarial activity of E-2-quinolinylbenzocycloalcanones. European Journal of medicinal chemistry (40) 875-881.

Carra, I., Santos-Juanes, L., Acien Fernandez, F. G., Malato, S., Sanchez Perez J. A., 2014. New approach to solar photo-Fenton operation. Raceway ponds as tertiary treatment technology. J Hazard Mater (279) 322-329.

d'Angelo, J., Mouscadet, J. F., Desmele, D., Zouhiri, F., Leh, H. 2001. HIV-1 integrase: the next target for AIDS therapy? L'intégrase du VIH: la prochaine cible de la chimiothérapie du SIDA? Pathol. Biol (49) 237-246.

Dupont, J., de Souza, R. F. and Suarez, P. A., 2002. Ionic liquid (molten salt) phase organometallic catalysis. Chemical reviews (102) 3667-3692.

Drexler, M.T. and Amiridis, M.D., 2003. The effect of solvents on the heterogeneous synthesis of flavanone over MgO. Journal of Catalysis (214) 136-145.

Daskiewicz, J. B., Comte, G., Barron, D., Di Pietro, A. and Thomasson, F., 1999. Organolithium mediated synthesis of prenylchalcones as potential inhibitors of chemoresistance. Tetrahedron letters (40) 7095-7098.

Dong, F., Jian, C., Zhenghao, F., Kai, G. and Zuliang, L., 2008. Synthesis of chalcones via Claisen–Schmidt condensation reaction catalyzed by acyclic acidic ionic liquids. Catalysis Communications, (9) 1924-1927.

Dömling, A. and Ugi, I., 2000. Multicomponent reactions with isocyanides. Angewandte Chemie International Edition (39) 3168-3210.

Dalpozzo, R., Bartoli, G. and Bencivenni, G., 2012. Recent advances in organocatalytic methods for the synthesis of disubstituted 2-and 3-indolinones. Chemical Society Reviews (41) 7247-7290.

Earle, M. J., McCormac, P. B. and Seddon, K. R., 1998. Regioselective alkylation in ionic liquids. Chemical communications (20) 2245-2246.

Ellis, B., Keim, W., Wasserscheid, P. 1999. Linear dimerization of but-1-ene in biphasic mode using buffered chloroaluminutesate ionic liquid. Chem Commun 337-340.

Earle, M. J., McCormac, P. B. and Seddon, K. R., 1999. Diels–Alder reactions in ionic liquids. A safe recyclable alternative to lithium perchlorate–diethyl ether mixtures. Green Chemistry (1) 23-25.

Feldhoff, R.C. and Peters, T., 1976. Determinutesation of the number and relative position of tryptophan residues in various albuminutesutes. Biochemical Journal, (159), 529-533.

Guo, L. J., Wei, C. X., Jia, J. H., Zhao, L. M. and Quan, Z. S., 2009. Design and synthesis of 5-alkoxy-[1, 2, 4] triazolo [4, 3-a] quinoline derivatives with anticonvulsant activity. European journal of medicinal chemistry (44) 954-958.

Ghahremanzadeh, R., Azimi, S. C., Gholami, N. and Bazgir, A., 2008. Clean Synthesis and Antibacterial Activities of Spiro [pyrimido [4, 5-b] quinoline-5, 5′-pyrrolo [2, 3-d] pyrimidine]-pentaones. Chemical and Pharmaceutical Bulletin (56) 1617-1620.

Gholizadeh, S. and Radmoghadam, K., 2014. Ultrasound-assisted the three-component synthesis of spiro [4H-pyrano [3, 2-c] quinolin-4, 3′-indoline]-2′, 5 (6H)-diones in water. Oriental Journal of Chemistry, (29) 1637-1641.

Huber-Emden, H., Hubele, A., Klahre, G., 1971. The Baylis –Hillman approach to quinoline derivatives. Ger. Offen. 3960-3965.

Hibino, S., Weinreb, S, M. 1977. Synthetic approaches to the quinolinequinone system of streptonigrin. J.Org Chem (42) 232-236.

Hewawasam, P., Fan, W., Knipe, J., Moon, S. L., Boissard, C. G., Gribkoff, V. K. and Starrett, J. E., 2002. The synthesis and structure–activity relationships of 4-aryl-3-aminutesoquinolin-2-ones: a new class of calcium-Dependent, large conductance, potassium (maxi-K) channel

openers targeted for post-stroke neuroprotection. Bioorganic & medicinal chemistry letters (12) 1779-1783.

Hewawasam, P., Fan, W., Ding, M., Flint, K., Cook, D., Goggins, G. D., Myers, R. A., Gribkoff, V. K., Boissard, C. G., Dworetzky, S. I. and Starrett, J. E., 2003. 4-Aryl-3-(hydroxyalkyl) quinolin-2-ones: novel maxi-K channel opening relaxants of corpora smooth muscle targeted for erectile dysfunction. Journal of medicinal chemistry (46) 2819-2822.

Hallett, J. P. and Welton, T., 2011. Room-temperature ionic liquids: solvents for synthesis and catalysis. Chemical reviews, (111) 3508-3576.

Hsieh, H. K., Tsao, L.T., Wang, J. P. and LIN, C. N., 2000. Synthesis and Anti-inflammatory Effect of Chalcones. Journal of pharmacy and pharmacology (52) 163-171.

Hua, Q., Ya, W., Dabin, L., 2013. Ultrasound-Accelerated Synthesis of Substituted 2'-Hydroxy chalcones by Reusable Ionic Liquids. Ind. Eng. Chem. Res (52) 13272-13275.

Herney-Ramirez, J., Vicente, M. A., Madeira, L. M., 2010. Heterogeneous photo-Fenton oxidation with pillared clay-based catalysts for wastewater treatment: A review Appl Catal B (98) 10-26.

He, X. M., and Carter, D. C., 1992. Atomic structure and chemistry of human serum albuminutes. Nature (358) 209.

Helms, M. K., Peterson, C. E., Bhagavan, N. V., and Jameson, D. M., 1997. Time-resolved fluorescence studies on site-directed mutants of human serum albuminutes. FEB Lett (408) 67-70. Iranpoor, N. and Kazemi, F., 1998. RuCl 3 catalyses aldol condensations of aldehydes and ketones. Tetrahedron (54) 9475-9480.

Jenekhe, S. A., Lu, L., Alam, M. M. 2001. New Conjugated Polymers with Donor−Acceptor Architectures: Synthesis and Photophysics of Carbazole−Quinoline and Phenothiazine Quinoline Copolymers and Oligomers Exhibiting Large Intramolecular Charge Transfer. Macromolecules (34) 7315-7324.

Jones, K., Roset, X., Rossiter, S. and Whitfield, P., 2003. Demethylation of 2, 4-dimethoxyquinolines: the synthesis of atanine. Organic & biomolecular chemistry, 1(24), 4380-4383.

Jioui, I., Dânoun, K., Solhy, A., Jouiad, M., Zahouily, M., Essaid, B., Len, C. and Fihri, A., 2016. Modified fluorapatite as highly efficient catalyst for the synthesis of chalcones via Claisen–Schmidt condensation reaction. Journal of Industrial and Engineering Chemistry (39) 218-225.

Jiang, T., Kuhen, K. L., Wolff, K., Yin, H., Bieza, K., Caldwell, J., Bursulaya, B., Wu, T.Y. H. and He, Y., 2006. Design, synthesis and biological evaluations of novel oxindoles as HIV-1 non-nucleoside reverse transcriptase inhibitors. Part I. Bioorganic & medicinal chemistry letters (16) 2105-2108.

Jadidi, K., Ghahremanzadeh, R. and Bazgir, A., 2009. Spirooxindoles: reaction of 2, 6-diaminutesopyrimidin-4 (3H)-one and isatins. Tetrahedron, (65) 2005-2009.

Katritzky, A. R., Pozharskii, A. F., 2000. Handbook of Heterocyclic Chemistry, Pergamon, Oxford, 2ndedn 616.

Klein, R. D., Favreau M. A., 1995. The candida species: Biochemistry, molecular Biology, and industrial Applications. VCH Publishers, Inc., New York 297-377.

Kametani, T., Kasai, H., 1989. In Studies in Natural Products Chemistry (3) 385-455.

Katritzky, A. R., Charles, W. R., Meth-Cohn, O. 1984. Comprehensive Heterocyclic Chemistry - The Structure, Reactions, Synthesis and Uses of Heterocyclic Compounds - Volume 1 Part 1 - Introduction, Nomenclature, Review Literature, Biological Aspects, Industrial Uses, Less-common Heteroatoms. Comprehensive Heterocyclic Chemistry (2) pp 511.

Kermack, W.O., and Smith, J. F., 1931. CCCCXXVII-Attempts to find new antimalarials. Part VII. Quinoline compounds having in the 4-position a side chain containing two or more nitrogen atoms. Journal of the Chemical Society (Resumed), 3096-3104.

Kouznetsov, V.V., Méndez, L.Y.V. and Gómez, C. M. M., 2005. Recent progress in the synthesis of quinolines. Current Organic Chemistry (9) 141-161.

Khazaei, A., Gholami, F., Khakyzadeh, V., Moosavi-Zare, A. R. and Afsar, J., 2015. Magnetic core-shell titanium dioxide nanoparticles as an efficient catalyst for dominuteso Knoevenagel–Michael-cyclocondensation reaction of malononitrile, various aldehydes and dimedone. RSC Advances (5) 14305-14310.

Khan, M. N., Pal, S., Karamthulla, S. and Choudhury, L. H., 2014. Imidazole as organ catalyst for multicomponent reactions: diversity oriented synthesis of functionalized hetero-and carbocycles using in situ-generated benzylidenemalononitrile derivatives. RSC Advances (4) 3732-3741.

Khaligh, N. G. and Hamid, S. B. A., 2015. 4-(Succinimido)-1-butane sulfonic acid as a Brönsted acid catalyst for the synthesis of pyrano [4, 3-b] pyran derivatives using thermal and ultrasonic irradiation. Chinese Journal of Catalysis (36) 728-733.

Ko, H. H., Hsieh, H. K., Liu, C.T., Lin, H. C., Teng, C. M. and Lin, C. N., 2004. Structure-activity relationship studies on chalcone derivatives: potent inhibition of platelet aggregation. Journal of pharmacy and pharmacology, 56(10), pp.1333-1337.

Khot, L. R., Sankaran, S., Maja, J. M., Ehsani, R. and Schuster, E.W., 2012. Applications of nanomaterials in agricultural production and crop protection: a review. Crop protection (35) 64-70.

Kumar, R. S., Osman, H., Perumal, S., Menéndez, J. C., Ali, M. A., Ismail, R. and Choon, T. S., 2011. A facile three-component [3+ 2]-cycloaddition/annulation dominuteso protocol for the regio-and diastereoselective synthesis of novel penta-and hexacyclic cage systems, involving the generation of two heterocyclic rings and five contiguous stereocenters. Tetrahedron (67) 3132-3139.

Kappe, C.O., 2004. Controlled microwave heating in modern organic synthesis. Angewandte Chemie International Edition, (43) 6250-6284.

Khalilian, H., Behpour, M., Atouf, V., Hosseini, S. N., 2015. Immobilization of S, N-codoped TiO_2 nanoparticles on glass beads for photocatalytic degradation of methyl orange by fixed bed photoreactor under visible and sunlight irradiation. Sol Energy (112) 239-245.

Kumar C.V., and Buranaprapuk, A. S., 1997. Site-Specific Photocleavage of proteins. Angew Chem Int Ed Engl (36) 2085-2087.

Lee, B. S., Lee, J. H. and Chi, D.Y., 2002. Novel synthesis of 2-chloroquinolines from 2-vinylanilines in nitrile solvent. The Journal of organic chemistry (67) 7884-7886.

Luo, J. and Zhang, Q., 2011. A one-pot multicomponent reaction for synthesis of 1-amidoalkyl-2-naphthols catalyzed by PEG-based dicationic acidic ionic liquids under solvent-free conditions. Monatshefte für Chemie-Chemical Monthly, (142) 923.

Myers, A. G., Tom, N. J., Fraley, M. E., Cohen, S. B., Madar, D. J. 1997. A convergent synthetic route to (+)-dynemicin A and analogs of wide structural variability. J. Am. Chem (119) 6072-6094.

Maignan, S., Guilloteau, J., Zhou-Liu, Q., Clement-Mella, C., Mikol, V. 1998. Crystal structures of the catalytic domain of HIV-1 integrase free and complexed with its metal cofactor: high level of similarity of the active site with other viral integrases. J. Mol.Biol. (282) 359-368.

Mederski, W.W., Osswald, M., Dorsch, D., Christadler, M., Schmitges, C. J. and Wilm, C., 1997. 1, 4-Diaryl-2-oxo-1, 2-dihydro-quinoline-3-carboxylic acids as endothelin receptor antagonists. Bioorganic & Medicinal Chemistry Letters (7) 1883-1886.

Meth-Cohn, O., Rhouati, S. and Tarnowski, B., 1979. A versatile new synthesis of quinolines and related fused pyridines. Part III. Tetrahedron Letters (20) 4885-4886.

Maddila, S., Gangu, K. K., Maddila, S. N. and Jonnalagadda, S. B., 2017. A facile, efficient, and sustainable chitosan/CaHAp catalyst and one-pot synthesis of novel 2, 6-diaminuteso-pyran-3, 5-dicarbonitriles. Molecular diversity (21) 247-255.

Munawar, M., Azad, M., Athar, M. and Groundwater, P., 2008. Synthesis and antimicrobial activity of quinoline-based 2-pyrazolines. Chemical Papers (62) 288-293.

Madhav, J.V., Kumar, V.N. and Rajitha, B., 2008. Sulfamic Acid–Catalyzed One-Pot Synthesis of 3-(4, 6-Dimethyl-oxazolo [4, 5-c] quinolin-2-yl)-chromen-2-ones using the Conventional Method and Microwave Irradiation. Synthetic Communications, (38) 1799-1807.

Monteagudo, J. M., Durán, A., Culebradas, R., San Martín, I., Carnicer, A., 2013. Optimization of pharmaceutical wastewater treatment by solar/ferrioxalate photo-catalysis. J Environ Manage (128) 210-219.

Miralles-Cuevas, S., Audino, F., Oller, I., Sanchez-Moreno, R., Sanchez Perez, J. A., Malato S., 2014 Pharmaceuticals removal from natural water by nanofiltration combined with advanced tertiary treatments (Solar photo-Fenton, photo-Fenton-like Fe (III)–EDDS complex and ozonation). Sep Purif Technol (122) 515-522.

McLachlan A. D., and Walker, J. E., 1977. Evolution of serum albuminutes. J Mol Bio (112) 543-558

Nasr, M., Drach, J. C., Smith, S. H., Shipman Jr, C. and Burckhalter, J. H., 1988. 7-Aminutesoquinolines. A novel class of agents active against herpes viruses. Journal of medicinal chemistry (31) 1347-1351.

Narender, T. and Reddy, K. P., 2007. A simple and highly efficient method for the synthesis of chalcones by using borontrifluoride-etherate. Tetrahedron Letters (48) 3177-3180.
Nagendrappa, G., 2002. Organic synthesis under solvent-free condition: an environmentally benign procedure–I. Resonance, 7(10), pp.59-68.

Ortega Liebana M. C., SanchezLopez, E., HidalgoCarrillo, J., Marinas, A., Marinas, J. M., Urbano, F., 2012. A comparative study of photocatalytic degradation of 3-chloropyridine under UV and solar light by homogeneous (photo-Fenton) and heterogeneous (TiO_2) photocatalysis. J Appl Catal B (127) 316-322.

Padwa, A. and Pearson, W.H. eds., 2003. The Chemistry of Heterocyclic Compounds, Synthetic Applications of 1, 3-Dipolar Cycloaddition Chemistry toward Heterocycles and Natural Products (59) John Wiley & Sons.

Polshettiwar, V. and Varma, R. S., 2008. Microwave-assisted organic synthesis and transformations using benign reaction media. Accounts of Chemical Research, (41) 629-639.

Paneri, M., Joshi, A. and Khan, S., 2016. A straightforward Microwave assisted green synthesis of Functionalized Spirooxindole-Pyrrolothiazole Derivatives via Three-Component 1, 3-Dipolar Cycloaddition Reactions. Chemistry & Biology Interface, (6) 224-233.

Pouran, H. M., Banwart, S. A., Romero-Gonzalez, M., 2014. Coating a polystyrene well-plate surface with synthetic hematite, goethite and aluminutesium hydroxide for cell minuteseral adhesion studies in a controlled environment. Appl Geochem (42) 60-68.

Pistkova, V., Tasbihi, M., Vavrova, M., Stangar, U. L., 2015. Photocatalytic degradation of β-blockers by using immobilized titania/silica on glass slides. J Photochem. Photobiol A (305) 19-28.

Patra, A. K., Dutta, A., Bhaumik, A., 2012. Highly ordered mesoporous TiO_2–Fe_2O_3 mixed oxide synthesized by sol-gel pathway: an efficient and reusable heterogeneous catalyst for dehalogenation reaction. ACS Appl Mater Interfaces (4) 5022-5028.

Punzi, M., Mattiasson, B., Jonstrup, M., 2012. Treatment of synthetic textile wastewater by homogeneous and heterogeneous photo-Fenton oxidation J Photochem. Photobiol A (248) 30-35.

Prucek, R., Hermanek, M., Zboril, R., 2009. An effect of iron (III) oxides crystallinity on their catalytic efficiency and applicability in phenol degradation competition between homogeneous and heterogeneous catalysis. Appl Catal A (366) 325-332.

Peters, T., 1996. Genetics and Medicinal Applications. Academic Press San Diego CA. 133. Partridge, W. M. Am. J. Physiol. 1987, Differential effect of vasopressin on angiotensin and norepinephrine pressor action in rats 252, 157.

Peters, T. Jr., Advances in protein Chemistry, Academic press, New York, 1985.

Peters, T. Jr., All about albuminutes, Academic press, Inc, San Diego, California, 1996.

Ql, X., Cheng, G.B., Lu, C. and Qian, D., 2007. Nitration of Toluene and Chlorobenzene with HNO_3/Ac_2O Catalyzed by Caprolactam-based Bronsted Acidic Ionic Liquids. Central European Journal of Energetic Materials (4) 105-113.

Reddy, E. A., Islam, A., Mukkanti, K., Bandameedi, V., Bhowmik, D. R. and Pal, M., 2009. Regioselective alkynylation followed by Suzuki coupling of 2, 4-dichloroquinoline: Synthesis of 2-alkynyl-4-arylquinolines. Beilstein journal of organic chemistry (5), 32.

Rossiter, S., Peron, J-M., Whitified, P. J., Jones, K., 2005. Synthesis and anthelminutestic properties of arylquinolines with activity against drug-resistant nematodes. Bioorg Med Chem Lett (15) 4086-4088.

Ramesh, P., Reddy, C. S., Babu, K. S., Reddy, P. M., Rao, V. S. and Parthasarathy, T., 2015. Synthesis, characterization and molecular docking studies of novel 2-aminuteso 3-cyano pyrano [2, 3H] chrysin derivatives as potential antimicrobial agents. Medicinal Chemistry Research (24) 3696-3709.

Rahman, A. F. M., Ali, R., Jahng, Y. and Kadi, A. A., 2012. A Facile Solvent Free Claisen-Schmidt Reaction: Synthesis of α, α′-bis-(Substituted-benzylidene) cycloalkanones and α, α′-bis-(Substituted-alkylidene) cycloalkanones. Molecules (17) 571-583.

Romanelli, G., Pasquale, G., Sathicq, A., Thomas, H., Autino, J. and Vázquez, P., 2011. Synthesis of chalcones catalyzed by aminutesopropylated silica sol–gel under solvent-free conditions. Journal of Molecular Catalysis A: Chemical (340) 24-32.

Rane, B. S., Kazi, M. A., Bagul, S. M., Shelar, D. P., Toche, R. B. and Jachak, M. N., 2010. Synthesis of novel spiro-oxazino-quinoline derivatives and study of their photophysical properties. Journal of fluorescence (20) 415-420.

Rahmati, A. and Eskandari-Vashareh, M., 2014. Synthesis of spiro [benzo [h] quinoline-7, 3′-indolines] via a three-component condensation reaction. Journal of Chemical Sciences, (126) 169-176.

Rodriguez-Chueca, J., Polo-Lopez, M. I., Mosteo, R., Ormad, M. P., Fernandez-Ibanez, P., 2014. Disinfection of real and simulated urban wastewater effluents using a mild solar photo-Fenton Appl. Catal. (B. 150-151) 619-629.

Ren, S. T., Fan, G. H., Liang, M. L., Wang, Q., Zhao, G. L., 2014. Zhao Electrodeposition of hierarchical ZnO/Cu_2O nanorod films for highly efficient visible-light-driven photocatalytic applications. J Appl Phys (115) 064301.

Samosorn, S., Bremner, J. B., Ball, A., Lewis, K. 2006. Synthesis of functionalised 2-aryl-5-nitro-1H-indoles and their activity as bacterial Nor A efflux pump inhibitors. Bioorg. Med. Chem (14) 857-865.

Shen, W., Coburn, C. A., Bornmann, W. G., Danishefsky, S. J. 1993. Concise total syntheses of dl-camptothecin and related anticancer drugs. J. Org. Chem (58) 611-617.

Sainsbury, M., Coffey, S. 1978. Synthesis of substituted benzoquinolines by the irradiation of 3-aminuteso-2-alkene iminuteses Chemistry of Carbon Compounds (54) 6929-6938.

Sundberg, R. L., Duff, J.W., Gruninger, J. H., Bernstein, L. S., Matthew, M.W., Adler-Golden, S. M., Robertson, D. C., Sharma, R. D., Brown, J. H. and Healey, R. J., 1995. SHARC, a Model for Calculating Atmospheric Infrared Radiation under Non-Equilibrium Conditions. The upper mesosphere and lower thermosphere: A review of experiment and theory, 287-295.

Strecker, A., 1850. Ueber die künstliche Bildung der Milchsäure und einen neuen, dem Glycocoll homologen Körper. European Journal of Organic Chemistry (75) 27-45.

Schöfer, S. H., Kaftzik, N., Wasserscheid, P. and Kragl, U., 2001. Enzyme catalysis in ionic liquids: lipase catalysed kinetic resolution of 1-phenylethanol with improved enantioselectivity. Chemical Communications (2001) 425-426.

Sankaran, M., 2012. Protective effect of Solanum nigrum fruit extract on the functional status of liver and kidney against ethanol induced toxicity. Journal of Biochemical Technology (3) 339-343.

Satyanarayana, M., Tiwari, P., Tripathi, B. K., Srivastava, A.K. and Pratap, R., 2004. Synthesis and antihyperglycemic activity of chalcone based aryloxypropanolaminuteses. Bioorganic & medicinal chemistry (12) 883-889.

Szell, T. and Sohar, I., 1969. New nitrochalcones. IX. Canadian Journal of Chemistry (47) 1254-1258.

Saravanamurugan, S., Palanichamy, M., Arabindoo, B. and Murugesan, V., 2004. Liquid phase reaction of 2′-hydroxyacetophenone and benzaldehyde over ZSM-5 catalysts. Journal of Molecular Catalysis A: Chemical (218) 101-106.

Sebti, S., Solhy, A., Smahi, A., Kossir, A. and Oumimoun, H., 2002. Dramatic activity enhancement of natural phosphate catalyst by lithium nitrate. An efficient synthesis of chalcones. Catalysis Communications (3) 335-339.

Shen, J., Wang, H., Liu, H., Sun, Y. and Liu, Z., 2008. Brønsted acidic ionic liquids as dual catalyst and solvent for environmentally friendly synthesis of chalcone. Journal of Molecular Catalysis A: Chemical (280) 24-28.

Sazegar, M. R., Mahmoudian, S., Mahmoudi, A., Triwahyono, S., Jalil, A. A., Mukti, R.R., Kamarudin, N.H.N. and Ghoreishi, M.K., 2016. Catalyzed Claisen–Schmidt reaction by protonated aluminutesate mesoporous silica nanomaterial focused on the (E)-chalcone synthesis as a biologically active compound. RSC Advances, 6(13), pp.11023-11031.

Shikha, S. D., Ajay, M. G., Anjali, M. R., Mukund, S. C., Chavoun, P. M. S., Kumkum, S. 2009. Synthesis of Bioactive Nitrogen Heterocycles and Functionalized Nanomaterials for Biological and Catalytic Applications. ind. J .chem. (48) 1780.

Sarotti, A. M., Spanevello, R. A., Suárez, A. G., Echeverría, G. A. and Piro, O. E., 2012. 1, 3-Dipolar Cycloaddition Reactions of Azomethine Ylides with a Cellulose-Derived Chiral Enone. A Novel Route for Organocatalysts Development. Organic letters (14) 2556-2559.

Sridhar, G., Gunasundari, T. and Raghunathan, R., 2007. A greener approach for the synthesis of 1-N-methyl-(spiro [2.3′] oxindolespiro [3.2 ″]/spiro [2.3′] indan-1, 3-dionespiro [2.2 ″]) cyclopentanone-4-aryl pyrrolidines. Tetrahedron letters (48) 319-322.

Sebahar, P.R. and Williams, R. M., 2000. The asymmetric total synthesis of (+)-and (−)-spirotryprostatin B. Journal of the American Chemical Society (122) 5666-5667

.

Saravanan, P., Pushparaj, S. and Raghunathan, R., 2013. An expedient approach for the synthesis of naphthyl dispiro pyrrolidine/pyrrolizidine through 1, 3-dipolar cycloaddition reaction. Tetrahedron Letters (54) 3449-3452.

Souza, F. B., Pimenta, D. C. and Stefani, H. A., 2016. Microwave-assisted one-pot three-component synthesis of iminutese 1, 2, 3-triazoles. Tetrahedron Letters, (57) 1592-1596.

Sampaio, M. J., Silva, C. G., Silva, A. M. T., Vilar, V. J. P., Boaventura, R. A. R., Faria, J. L., 2013. Photocatalytic activity of TiO_2-coated glass raschig rings on the degradation of phenolic derivatives under simulated solar light irradiation. Chem Eng J (224) 32-38.

Sampaio, M. J., Silva, C. G., Silva, A. M. T., Pastrana-Martínez, L. M., Han, C., Morales-Torres, S., .Figueiredo, J. L., Dionysiou, D. D., Faria, J. L., 2015. Carbon-based TiO_2 materials for the degradation of Microcystin-LA. Appl Catal B (170-171) 74-82.

Sampaio, M. J., PastranaMartinez, L. M., Silva, A. M. T., Buijnsters, J. G., Han, C., Silva, C. G., Carabineiro, S. A. C., Dionysiou, D. D., Faria, J. L., 2015. Nanodiamond-TiO_2 composites for photocatalytic degradation of microcystin-LA in aqueous solutions under simulated solar light. RSC Adv (5) 58363-58370.

Singer, S. J., and Nicolson, G. L., 1972. A fluid lipid-globular protein mosaic model of membrane structure. Science (175) 720.

Trivedi, A. R., Bhuva, V. R., Dholariya, B. H., Dodiya, D. K., Kataria, V. B. and Shah, V. H., 2010. Novel dihydropyrimidines as a potential new class of antitubercular agents. Bioorganic & medicinal chemistry letters, (20) 6100-6102.

Tu, S. J., Yan, S., Cao, X.D., Wu, S. S., Zhang, X. H., Hao, W. J., Han, Z. G. and Shi, F., 2009. A facile and expeditious microwave-assisted synthesis of 4-aryl-2-ferrocenyl-quinoline derivatives via multi-component reaction. Journal of Organometallic Chemistry, (694).91-96.

Uma Maheswari, S., Balamurugan, K., Perumal, S., Yogeeswari, P., Sriram, D., 2010. A facile 1,3-dipolar cycloaddition of azomethine ylides to 2-arylidene-1,3- indanediones Synthesis of dispiro-oxindolylpyrrolothiazoles and their antimycobacterial evaluation. Bioorg & Med Chem Lett (20) 7278-7282.

Wang, H., and Ganesan, A., 1998. Total synthesis of the cytotoxic alkaloid luotonin A. Tetrahedron letters, (39) 9097-9098.

Warner, P., Barker, A. J., Jackman, A. L., Burrows, K. D., Roberts, N., Bishop, J. A., O'Connor, B. M. and Hughes, L. R., 1992. Quinoline antifolate thymidylate synthase inhibitors: variation of the C2-and C4-substituents. Journal of medicinal chemistry (35) 2761-2768.

Wang, X. and Cheng, S., 2006. Solvent-free synthesis of flavanones over aminutesopropyl-functionalized SBA-15. Catalysis Communications (7) 689-695.

Wang, X. and Cheng, S., 2006. Solvent-free synthesis of flavanones over aminutesopropyl-functionalized SBA-15. Catalysis Communications (7) 689-695.

Wang, X. S., Li, Q., Wu, J. R. and Zhang, M. M., 2009. Green method for the synthesis of benzo [f] pyrimido [4, 5-b] quinoline derivatives catalyzed by iodine in aqueous media. Synthetic Communications® (39) 3069-3080.

Xia, Y., Yang, Z.Y., Xia, P., Bastow, K. F., Nakanishi, Y. and Lee, K. H., 2000. Antitumor agents. Part 202: novel 2′-aminuteso chalcones: design, synthesis and biological evaluation. Bioorganic & medicinal chemistry letters (10) 699-701.

Xu, Z., Huang, C., Wang, L., Pan, X., Qin, L., Guo, X., Zhang, G., 2015. Sulfate functionalized Fe_2O_3 nanoparticles on TiO_2 nanotube as efficient visible light-active photo-Fenton catalyst. Ind Eng Chem Res (54) 4593-4602.

Yuvaraj, P., Manivannan, K. and Reddy, B. S., 2015. Microwave-assisted efficient and highly chemoselective synthesis of oxazolo [5, 4-B] quinoline-fused spirooxindoles via catalyst-and solvent-free three-component tandem Knoevenagel/Michael addition reaction.Tetrahedron Letters (56) 78-81.

Yang, S. D., Wu, L.Y., Yan, Z.Y., Pan, Z. L. and Liang, Y. M., 2007. A novel ionic liquid supported organocatalyst of pyrrolidine amide: Synthesis and catalyzed Claisen–Schmidt reaction. Journal of Molecular Catalysis A: Chemical (268) 107-111.

Yavuz, S., Özkan, H., Tok, G. and Dişli, A., 2013. Facile Method for 1, 3-Dipolar Cycloaddition Reaction of Azomethine Ylides: Highly Stereoselective Synthesis of Substituted Pyrrolidine Derivatives. Journal of Heterocyclic Chemistry (50) 1437-1440.

Yoon, T. H., Hong, L. Y., Kim D. P., 2011. Photocatalytic reaction using novel inorganic polymer derived packed bed microreactor with modified TiO_2 microbeads. Chem Eng J (167) 666-670.

Zouhiri, F., Desmaele, D., d'Angelo, J., Ourevitch, M., Mouscadet, J. F., Leh, H., Bret, M. L. 2001. HIV-1 replication inhibitors of the styrylquinoline class: incorporation of a masked diketo acid pharmacophore. Tetrahedron Letter (42) 8189-8192.

Zhi, L., Tegley, C. M., Marschke, K. B. and Jones, T. K., 1999. Switching androgen receptor antagonists to agonists by modifying C-ring substituents on piperidino [3, 2-g] quinolinone. Bioorganic & medicinal chemistry letters (9) 1009-1012.

Zaragoza, F., Stephensen, H., Peschke, B. and Rimvall, K., 2005. 2-(4-Alkylpiperazin-1-yl) quinolines as a new class of imidazole-free histaminutese H3 receptor antagonists. Journal of medicinal chemistry (48) 306-311.

Zhang, F.Y. and Corey, E. J., 2000. Highly enantioselective Michael reactions catalyzed by a chiral quaternary ammonium salt. Illustration by asymmetric syntheses of (S)-ornithine and chiral 2-cyclohexenones. Organic letters (2) 1097-1100.

Ziarani, G. M., Faramarzi, S., Asadi, S., Badiei, A., Bazl, R. and Amanlou, M., 2013. Three-component synthesis of pyrano [2, 3-d]-pyrimidine dione derivatives facilitated by sulfonic acid nanoporous silica (SBA-Pr-SO 3 H) and their docking and urease inhibitory activity. DARU Journal of Pharmaceutical Sciences (21) 3.

Chapter Three

[1]A nanocrystalline titanium-based sulfonic acid catalyst for the synthesis of new quinoline bearing pyrans and molecular docking studies

3. 1. Abstract

A nanocrystalline titanium-based sulfonic acid (TiO_2-Pr-SO_3H) material was prepared, characterized and used as an effective and efficient catalyst for the synthesis of 2-amino-4-(2-(4-methylpiperazin-1-yl) quinolin-3-yl)-6-phenyl-4H-pyran-3-carbonitriles and 2-amino-4-(2-(4-methylpiperazin-1-yl) quinolin-3-yl)-6-(pyridin-4-yl)-4H-pyran-3-carbonitrile derivatives under solvent-free conditions. The compound was fully characterized by FT-IR, ^{1}H NMR, ^{13}C NMR, TOF-MS and elemental analysis. This simple three component one-pot synthesis resulted in high yield products within two hours via conventional heating protocols. The catalyst was characterized by XRD, TEM, SEM, BET and Raman spectroscopy. The catalyst was recycled five times and recorded a decrease of 10 % in catalytic activity making it cost effective for large scale production. Computational docking analysis of two selected derivatives with heat shock protein 90 (Hsp 90) indicated that binding occurred inside the binding pocket located in subdomain II A of Hsp 90 and in the locality of the Trp-214 amino acid residue.

3. 2. Introduction

Heterocyclic compounds such as pyrans and pyranopyrans are important scaffolds as they increase the bioactivity of compounds. The biological activity of these classes is further enhanced when a quinoline scaffold is present since the latter displays high activity alone. A wealth of information is reported on their wide spectrum of pharmacological activities such as insecticidal (Perez-Perez *et al.* 1995:1115), anti-viral (Dailly *et al.* 2004:767), anti-tumor (Taylor *et al.* 1995:798), inhibition of influenza virus (Evidente *et al.* 2005:568) and phytotoxic activities (Li *et al*. 2011:2202), (Reddy *et al.* 2010:5677), (Sagar *et al.* 2009:2171), (Pałasz *et al.* 2007:481), (Philipp Jirkovsky 1980:1372), (Woods 1962:696).

[1]***Arul Murugesan, Robert M Gengan and Anand Krishnan*** *"Green approach: nanocrystalline titania-based sulfonic acid catalyst for the synthesis of piperazinyl-quinolinyl pyran derivatives" Advanced Materials Letters,* ***2017, 8, 128-135***

Due to the biological properties displayed by pyran-based compounds, there was a renewed interest in developing a general, versatile and more efficient method for their synthesis. Several synthetic approaches to pyrans were documented (Rahmati 2010:2967) (Rahmati and Alizadeh-Kouzehrash 2011:2373). The synthesis of 2-amino-4-aryl-3-cyano-4H-pyrans by the cyclization of arylidene malononitrile and other active methylene compounds, in the presence of organic bases such as piperidine (Martin *et al* 1987:2811), pyridine (Harb *et al.* 1989:585) and trimethylamine (Zayed *et al.* 1991:2175), (Elnagdi *et al.* 1987:1677) have been reported. However most of the methods utilise volatile solvents and require long reaction time (~ 12 h) whilst catalyst recovery is also sometimes problematic. Recently, a one-pot synthesis using Mg/La mixed oxide and MgO as a basic catalyst was reported (Seshu Babu *et al.* 2008:2730), (Kumar *et al.* 2007:3093). Multi-component synthesis of 2-amino-4H-pyran derivatives in aqueous medium (Kumar *et al.* 2009:3805) (Moshtaghi *et al.* 2012:91) and a new Brönsted acid, i.e., 4-(succinimido)-1-butane sulfonic acid (SBSA) was used for the synthesis of dihydropyrano [4, 3-b] pyran derivatives (Khaligh, Nader Ghaffari, 2015:26).

There is a global shift towards application of green chemistry principles. One of which is the utility of catalysts because it avoids the use of stoichiometric amounts of reagents: this increases selectivity, minimizes waste, reduces reaction times and energy demands. Over the decades the development and application of catalyst has made great strides however in recent years advances in the catalysis of organic reactions by solid acid catalysts had been witnessed. They increase the yield of desired products and can be recovered and easily recycled from reaction mixtures. Titanium oxide (TiO_2) is a widely studied catalyst and is used in many systems because of its strong oxidizing ability, good facilitation of the decomposition of organic pollutants and properties such as super hydrophilicity, chemical stability, long durability, non-toxicity, low cost and transparency to visible light. For example, the photocatalytic property of TiO_2 is due to the formation of photo generated charge carriers (hole and electron) which are formed upon the absorption of ultraviolet (UV) light corresponding to the band gap. The photo generated holes in the valence band diffuses through the TiO_2 surface and react with adsorbed water molecules, forming hydroxyl radicals ($^{\bullet}OH$). The photo generated holes and the hydroxyl radicals oxidize organic molecules on the TiO_2 surface in the vicinity. The development of new materials, however, is strongly required to provide enhanced performances with respect to the photocatalytic properties and to find new uses for TiO_2 photo catalysis. The dimension of the structure of a TiO_2 material can affect its properties and functions, including its photocatalytic performance (Kazuya Akira 2012:169). Recently a sulfonic acid derivative and titanium oxide viz., TiO_2-Pr-SO_3H was synthesized, characterized

then applied to the synthesis of quinoxalines (Atghia Beigbaghlou 2013:3) and coumarins (Atghia Beigbaghlou 2014:1155) and facilitated the N-Boc protection of amines (Atghia Beigbaghlou 2013:14).

3. 3. Results and discussion

A one-pot multicomponent synthesis of piperazinyl-quinolinyl pyran derivatives under solvent free conditions, using the TiO_2-Pr-SO_3H catalyst, is presented. The catalyst was selected because it is a new entry in the catalytic field and is highly efficient (Kazuya Akira 2012:169) (Atghia and Beigbaghlou 2013:3). Briefly, the catalyst was synthesized in two stages: a mixture of TiO_2 and (3-mercaptopropyl) trimethoxysilane were refluxed for 24 h and after the work-up of the reaction, the product was oxidised with H_2O_2 in an acidic medium (Scheme 3. 1). The catalyst was characterized completely by several techniques.

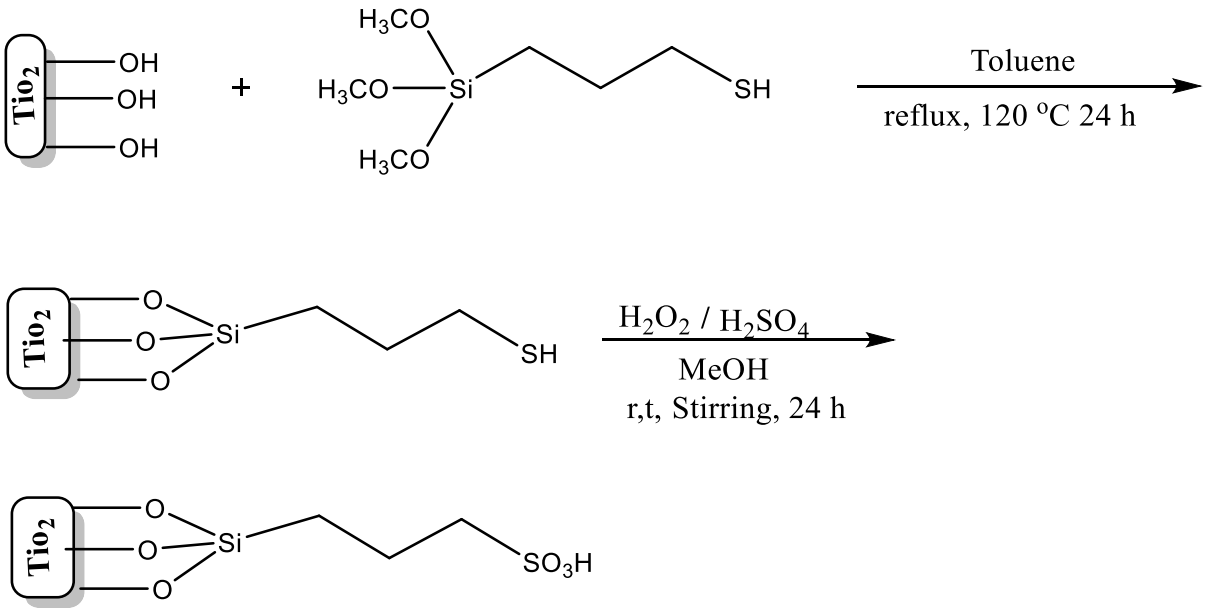

Scheme 3. 1. The reaction scheme for the synthesis of TiO_2-Pr-SO_3H.

Analysis of the FT-IR spectra of TiO_2 and TiO_2-Pr-SO_3H reveals the following information: TiO_2 - the absorption at 958, 1414, 2351 and 1645 cm^{-1} corresponds to the -OH bending and stretching vibrations of adsorbed water. The spectrum of TiO_2-Pr-SO_3H is similar to TiO_2. However the absorption at 3243 cm^{-1} is flattened which can be attributed to the modification of TiO_2. Also, the CH stretching vibrations of silylating agent was observed at 2954 cm^{-1} and the absorption at 1211 cm^{-1} was due to the Si-O stretching vibration.

Furthermore, the absorptions at 1163 and 1141 cm^{-1} was due to the stretching mode of S=O in SO_3H.

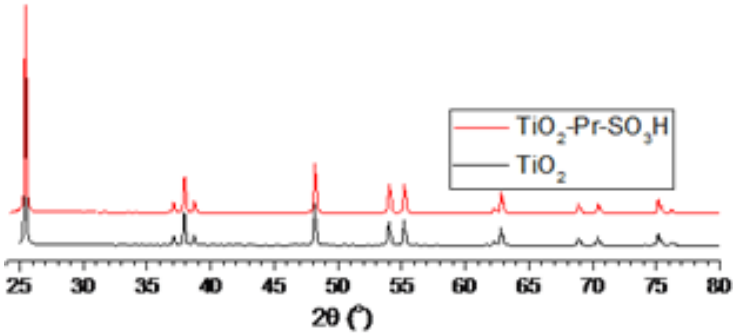

Figure 3. 1. Comparison of PXRD pattern of TiO_2 and TiO_2-Pr-SO_3H.

The XRD pattern of TiO_2 and TiO_2-Pr-SO_3H (Figure 3. 1) clearly showed the anatase lines. It seems that the peak intensities of TiO_2-Pr-SO_3H are almost the same as those of TiO_2 thereby supporting information that the sulphate modification does not change the phase of TiO_2.

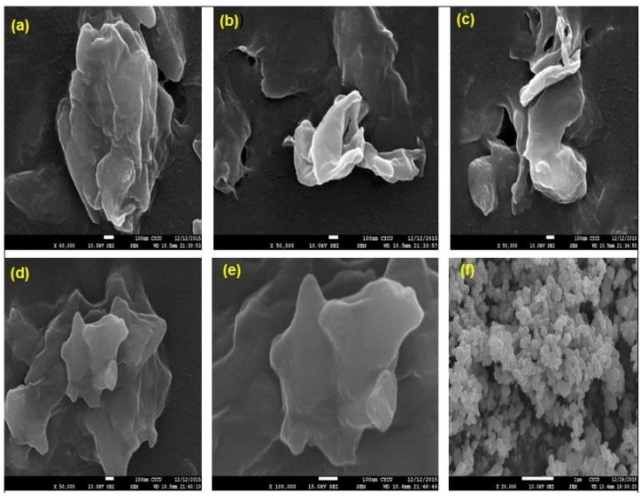

Figure 3. 2. The SEM image of TiO_2 (a, b and c) and TiO_2-Pr-SO_3H (d, e and f).

The representative SEM images of TiO_2 (Figure 3. 2 (a-c)) exhibit an aggregation of cloud-like structures of small spherical-shaped particles. The SEM micrographs of TiO_2-Pr-SO_3H showed a slight change on its surface however the cloud-like structure and small spherical-shaped particles still existed.

The EDS analysis for TiO_2 and TiO_2-Pr-SO_3H (Figure 3. 3) confirms the presence of all the elements and the actual weight % is presented in Table 3. 1.

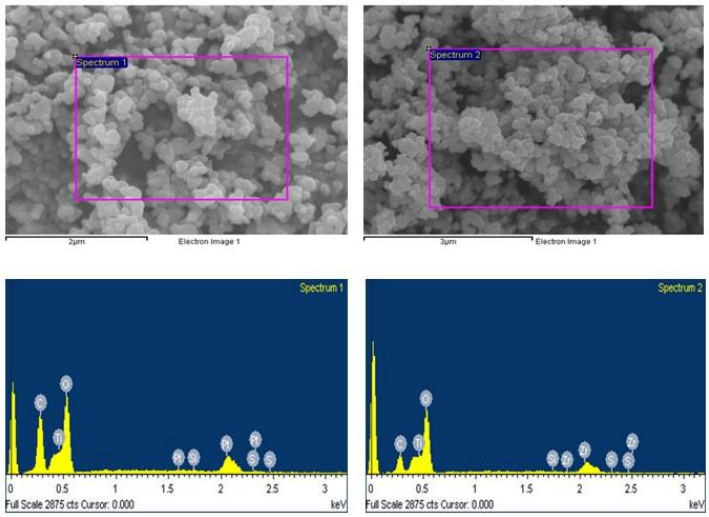

Figure 3. 3. The EDS pattern for TiO_2 (image 1) and TiO_2-Pr-SO_3H (image 2).

Table 3. 1. The weight (%) analysis for TiO_2 and TiO_2-Pr-SO_3H.

	TiO_2		TiO_2-Pr-SO_3H	
Element	Weight (%)	Atomic (%)	Weight (%)	Atomic (%)
Ti	35.95	16.67	40.09	19.21
O	36.20	50.25	43.22	62.0
C	17.24	31.88	8.71	16.64
S	-	-	0.30	0.22

Field-emission scanning electron microscopy was employed to characterize the morphology. The TEM image (Figure 3. 4) captured at different positions of the sample (a-1000 nm, b-200 nm, c-500 nm, d-100 nm, e-200 nm, and f-200 nm) shows the crystalline size of TiO_2-Pr-SO_3H. A mesoporous structure observed thereby suggesting a good surface for catalytic activity. The porous properties of TiO_2 and TiO_2-Pr-SO_3H, analysed by N_2 gas sorption measurements at 273 K (Figure 3. 5), shows TiO_2 as a type-I adsorption isotherm which is characteristic of microporous material. The BET and Langmuir surface area of TiO_2 were calculated as 7 and 11 m^2/g respectively. The N_2 adsorption isotherm of TiO_2-Pr-SO_3H also indicated a type-I adsorption isotherm whilst the BET and Langmuir surface area were calculated as 16 and 37 m^2/g respectively.

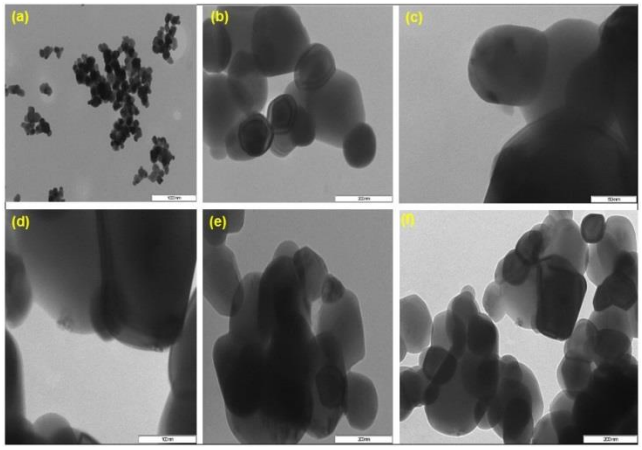

Figure 3. 4. The TEM image of TiO_2-Pr-SO_3H at different positions (a, b, c, d, e, f).

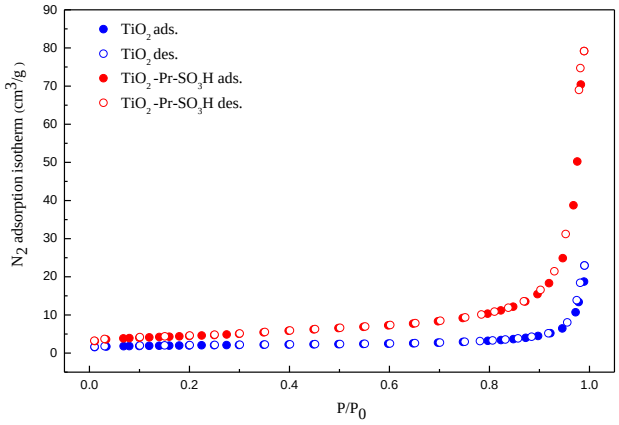

Figure 3. 5. Adsorption and desorption isotherms of TiO_2 and TiO_2-Pr-SO_3H at 273 K.

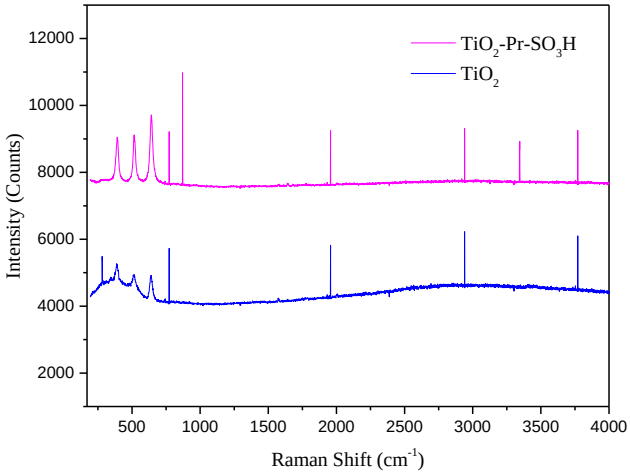

Figure 3. 6. Raman Shift of TiO_2 and TiO_2-Pr-SO_3H.

Further investigation of the structure of TiO_2 and TiO_2-Pr-SO_3H was conducted by Raman spectroscopy (Figure 3. 6). Absorption signals were at 450, 470, 500, 570, 600, 2000, 3000 and 3650 cm^{-1} for TiO_2. Absorption signals at 470, 500, 650, 800, 900, 2000, 3000, 3650 cm^{-1} were observed for TiO_2-Pr-SO_3H, with an additional signal at 3450 cm^{-1} indicating the hydroxyl acidic functional group.

To synthesize new piperazinyl-quinolinyl pyran derivatives, a new starting compound viz., 2-(4-methylpiperazin-1-yl) quinoline-3-carbaldehyde (**3**) was required. This was a two-step reaction. In the first step, the Vilsmeier-Haack reaction was used to prepare 2-chloroquinoline-3-carbaldehyde (**1**) from acetanilide (Cohn *et. al* 1981:1520). This reaction was well established in our laboratory. The second step was achieved by refluxing a mixture of **1** and 1-methylpiperazine (**2**) in a basic medium for 24 h (Scheme 3. 2). A yellow powder of 90 % yield (m.p 180 ˚C) was obtained.

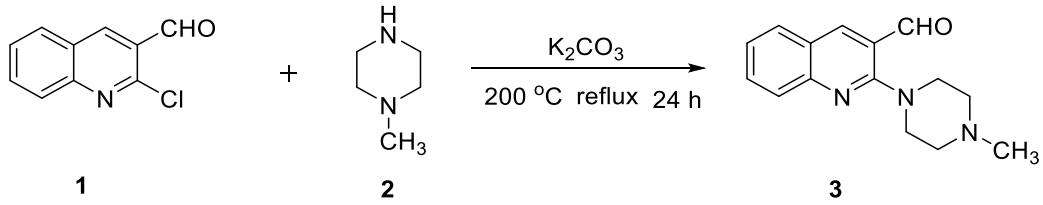

1 **2** **3**

Scheme 3. 2. Synthesis of 2-(4-methylpiperazin-1-yl) quinoline-3-carbaldehyde.

This compound was fully characterized by FT-IR, ^1H NMR, ^{13}C NMR, TOF-MS and elemental analysis.

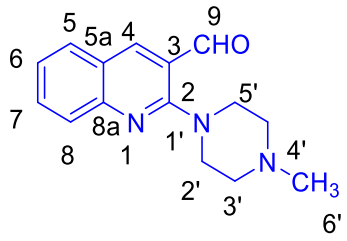

Figure 3. 7. 2-(4-methylpiperazin-1-yl) quinoline-3-carbaldehyde.

The FT-IR spectrum of **3** shows CHO stretching hydrogen bonding -OH at 3624 cm^{-1}, for C-H of CHO overtone stretching at 2850 and 2750 cm^{-1} and C=O (CHO-group carbonyl) stretching at 1693 cm^{-1}, C=C stretching at 1615 and 1421 cm^{-1} and C=N quinoline stretching at 2358 cm^{-1}. The ^1H NMR spectrum of the two singlet proton at δ 8.4 quinoline (Ar-H) and 10.09 (CHO) were identified as C_4-H and C_9-H respectively. Two doublet quinoline proton at δ 7.7 (Ar-H) and 7.76 (Ar-H) was identified as C_5-H and C_8-H respectively. Two triplet

quinoline protons at δ 7.31 (Ar-H) and 7.62 (Ar-H) was identified as C_6-H and C_7-H respectively. The piperazinyl ring -CH_2 protons of $C_{2'}$ and $C_{5'}$ appeared at δ 2.6 (4H) as a triplet whilst the -CH_2 protons of $C_{3'}$ and $C_{4'}$ occurred at δ 3.47 (4H) as a triplet and piperazinyl ring –CH_3 singlet protons of $C_{6'}$ appeared at δ 2.3 (3H).

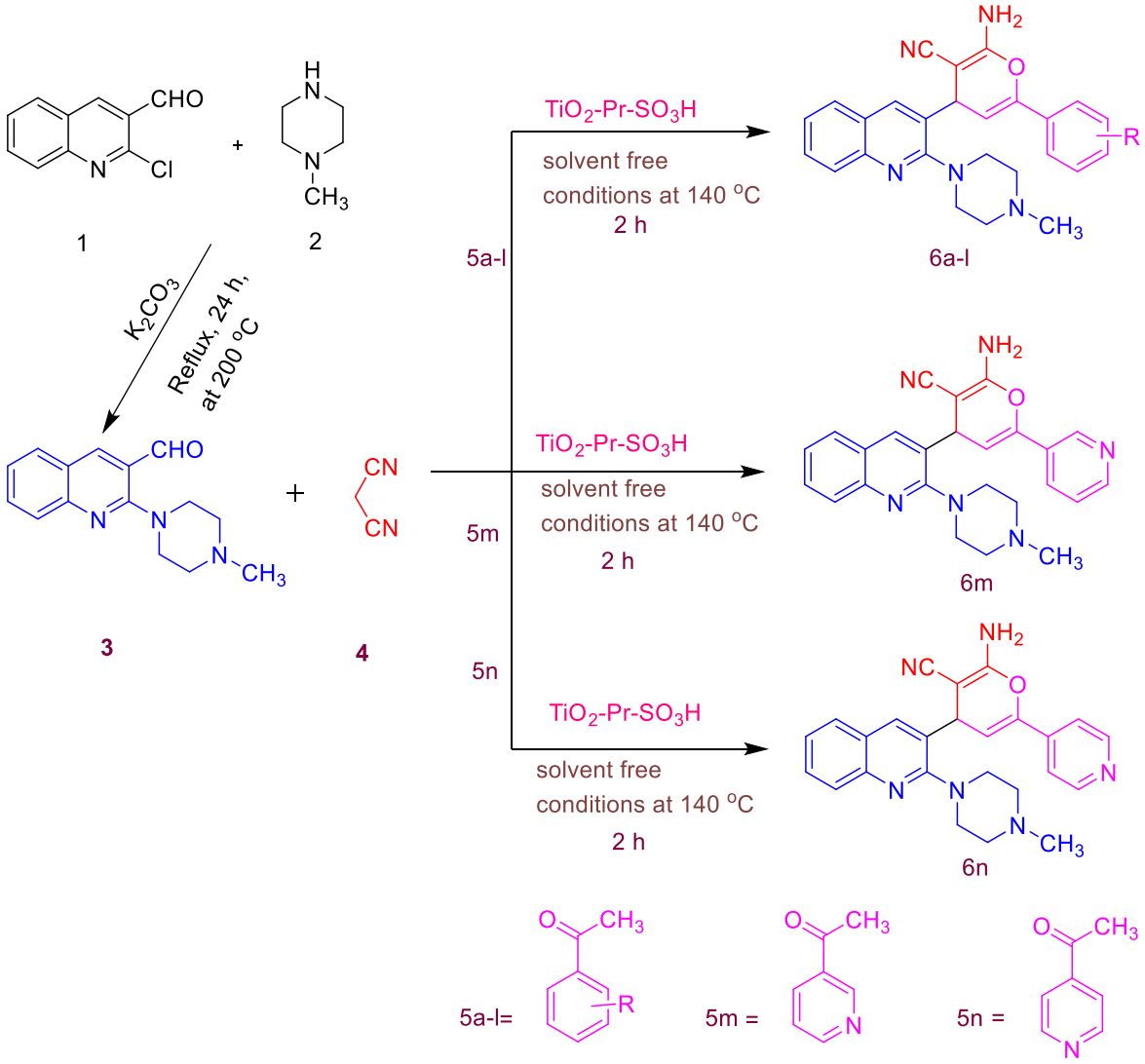

KEY: 6a (R=H); 6b (R=ortho-OH); 6c (R=para OH); 6d (R=4-CH_3); 6e (R=4- NO_2); 6f (R=4-F); 6g (R=4-Cl); 6h (R=4-Br); 6j (R=Ar-H); 6k (R=Ar-H); 6l (R=Ar-H) whilst 6i was obtained from **3** and thioacetophenone

Scheme 3. 3. Synthesis of 2-amino-4-(2-(4-methylpiperazin-1-yl) quinolin-3-yl)-6-phenyl-4H-pyran-3-carbonitrile and 2-amino-4-(2-(4-methylpiperazin-1-yl) quinolin-3-yl)-6-(pyridin-4yl)-4H-pyran-3-carbonitrile derivatives.

The ^{13}C NMR spectrum showed the presence of one carbonyl carbon (CHO) at δ 190, -CH_2 carbon at δ 50, 54 and –CH_3 carbon at δ 45 and all aromatic carbon signals appeared at δ 122,

123, 124, 127, 129, 132, 142, 149, 158 . The TOF MS ES+ Calcd mass was 256.1450; Found: 256.1449 Anal. Calcd. For $C_{15}H_{17}N_3O$: C, 70.56; H, 6.71; N, 16.46; Found: C, 70.58; H, 6.72; N, 16.43.

Having synthesized and characterized the starting material **3**, the one pot multi-component reaction to synthesize the desired target compounds was investigated. Briefly, for this reaction, a mixture of **3**, malononitrile and selected aromatic ketone was refluxed and after the usual work-up and purification, the desired compound was obtained (Scheme 3. 3).

In a preliminary investigation to synthesize **6a**, as a model reaction, a solvent-free system was compared against a system containing ethanol. Better yield of the product was obtained with a solvent-free system. The structure of **6a** was identified by FT-IR, ^{1}H-NMR, ^{13}C-NMR, TOF-MS and elemental analysis (a characterisations is presented in the chapter).

To determine the optimum quantity of TiO_2-Pr-SO_3H required for the reaction, different amounts of catalyst ie, 0.02, 0.05, 0.07 g in a solvent-free condition were investigated. It was found that 0.05 g of the catalyst gave the highest yield of **6a** and this quantity was used in all subsequent reactions. Having established the feasibility of the reaction and the optimum quantity of the catalyst required, an investigation on different solvent systems was undertaken as shown in (Table 3. 2).

Table 3. 2. A comparison of the reaction of a solvent/solvent-free system using TiO_2-Pr-SO_3H for the synthesis of **6a**.

Entry	Catalyst	Solvent	Temp (°C)	Time(h)	Isolated Yield (%)
1	TiO_2- Pr-SO_3H	EtOH	Reflux	6	60
2	TiO_2- Pr-SO_3H	MeOH	Reflux	6	50
3	TiO_2- Pr-SO_3H	CH_3CN	Reflux	3	80
4	TiO_2- Pr-SO_3H	EtOH	Reflux	3	65
5	TiO_2- Pr-SO_3H	MeOH	Reflux	3	58
6	TiO_2- Pr-SO_3H	Neat	140	2	90

It was observed that the use of a solvent needed a longer reaction time whilst the yield of **6a** was lower than a solvent-free reaction. Also, it was observed that if the solvent-free reaction was conducted at a higher temperature, viz., 140 °C, some additional spots were observed on the TLC plate thereby suggesting formation of by-products. Also, a shorter reaction time showed the presence of starting materials thereby indicating an incomplete reaction. A maximum yield of 90 % was obtained under a solvent free condition after heating for 2 h.

Table 3. 3. The synthesis of 2-amino-4-(2-(4-methylpiperazin-1-yl) quinoline-3-yl)-6-phenyl-4H-pyran-3-carbonitriles and 2-amino-4-(2-(4-methylpiperazin-1-yl) quinolin-3-yl)-6-(pyridin-4-yl)-4H-pyran-3-carbonitrile in the presence of TiO_2-Pr-SO_3H.

Entry	Substrate (5a-n)	Product (6a-n)	Time (h)	Yield (%)	M. p. (°C)
1	$C_6H_5COCH_3$	6a	2	90	260-262
2	$HOC_6H_4COCH_3$	6b	2	85	280-283
3	$HOC_6H_4COCH_3$	6c	2	90	285-287
4	$CH_3C_6H_4COCH_3$	6d	3	78	278-280
5	$O_2NC_6H_4COCH_3$	6e	2	75	275-278
6	$FC_6H_4COCH_3$	6f	2	70	277-279
7	$ClC_6H_4COCH_3$	6g	2	90	297-300
8	$BrC_6H_4COCH_3$	6h	2	87	290-292
9	C_6H_6OS	6i	3	83	280-283
10	$C_{10}H_7COCH_3$	6j	2	90	288-290
11	$HOC_{10}H_6COCH_3$	6k	2	90	285-287
12	$C_{16}H_{12}O$	6l	2	75	267-269
13	C_7H_7NO	6m	2	88	270-272
14	C_7H_7NO	6n	2	90	285-287

2-(4-methylpiperazin-1-yl) quinoline-3-carbaldehyde (1mmol), acetophenone (1mmol) and malononitrile (1mmol) catalyst 0.07 g under solvent-free conditions at 140 °C

The re-usability potential of TiO_2-Pr-SO_3H was also investigated in the model reaction to synthesize **6a**: briefly, the solid was rinsed with acetonitrile followed by methanol and heated at 100 °C, cooled to room temperature and then used for subsequent reactions. It was found that the catalyst could be re-used five times within 10 % loss of catalytic activity (Table 3. 4**)**. These results indicated that this catalyst is feasible if commercial application is required. Having

optimised the reaction conditions, synthesis of the functionalised piperazinyl-quinolinyl pyran derivatives **6a-6n**, using TiO_2-Pr-SO_3H, were undertaken in a solvent-free system for a reaction time of 2 h at 140 ˚C (Table 3. 3). The yield of the products **(**Table 3. 4**)** ranged from 70 % to 90 %. All compounds **6a-6n** were characterized by FT-IR, ^{1}H NMR, ^{13}C NMR and MS-TOF whilst **6c, 6k** and **6n** included DEPT-90 and DEPT-135. Compound **6n** was selected as the template for characterisation therefore 2D NMR spectroscopy was included in its characterisation. The analysis of **6n** was extrapolated to all the other derivatives which were easily identified from their spectroscopic data.

Table 3. 4. The yield (%) of product **6a** versus the number of times the catalyst was re-used.

Entry	Time (h)	Yield (%)
1	2	90
2	2	88
3	2	85
4	2	82
5	2	80

The FT-IR spectrum of **6n** showed NH_2 stretching at 3449 cm^{-1} and carbonitrile C-N stretching at 2189, 2157 cm^{-1}. The ^{1}H NMR spectrum of the compound showed two singlets at δ 8.30 and 7.06 identified as C_4-H and N-$H_{8'}$ respectively. Two doublets at δ 7.70 and 7.72 was identified as $C_{4'}$-H and $C_{5'}$-H respectively. The -CH_2 protons of C_{10} and C_{14} appeared at δ 2.26 (4H) as a doublet whilst the -CH_2 protons of C11 and C13 occurred at δ 2.42 (4H) as a doublet. The ^{13}C NMR spectrum showed the presence of one carbonitrile group at δ 116.43. The HMBC correlation of compound **6n** is shown in Figure 3. 8.

The C, H-COSY (HSQC) correlation assigned the carbon signals at δ 21.06, 45.56, 48.63, 54.02, 90.50, 122.92, 123.96, 125.76, 126.49, 128.09, 130.29, 139.74, 149.93 and 150. 43, to $C_{4'}$, C_{15}, (C_{10}, C_{14}), (C_{11}, C_{13}), $C_{5'}$, $C_{5''}$, $C_{3''}$, C_6, C_8, C_5, C_7, C_4, $C_{2''}$ and $C_{6''}$ respectively. The carbon signal at δ 139.74, was due to the quinolinyl C_4-carbon. The COSY spectrum of the compound revealed the singlet at δ 8.30 which confirmed one hydrogen. The long range HMBC correlation is given in Figure 3.9. The characteristic C_4-H proton was correlated to the quinolinyl carbon C_3 at δ 122. 18, C_5 at δ 128. 09, $C_{6'}$ at δ 145. 12 and C_{8a} at δ 157. 35. The $C_{8'}$-NH_2 protons were correlated to the quinolinyl carbon $C_{2'}$ at δ 158. 86, $C_{6'}$ at δ 145. 12, $C_{5'}$ at δ 90. 50, $C_{7'}$ at δ 116. 43 and $C_{5''}$ at δ 122 92. Also, the C_5-H proton was correlated to the

quinolinyl carbon C_4 at δ 139.74, C_6 at δ 125.76 and C_7 at δ 130. 29, the C_6-H proton was correlated to the quinolinyl carbon C_{5a} at δ 124.14 and $C_{4'}$-H proton was correlated to the quinolinyl carbon C_3 at δ 121. 18.

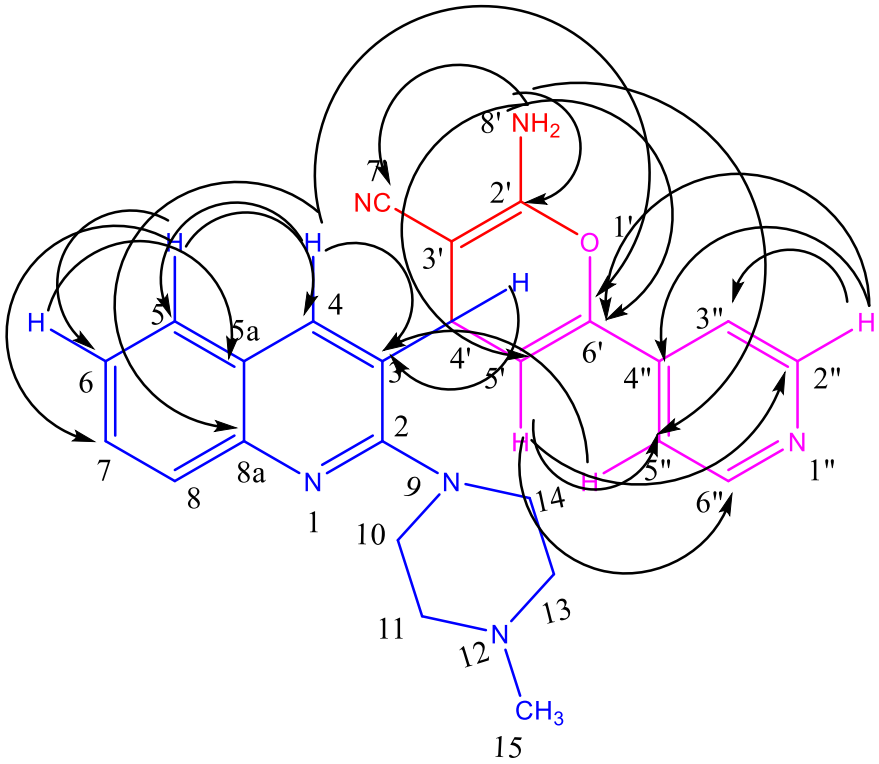

Figure 3. 8. Selected HMBC correlations of compound **6n**.

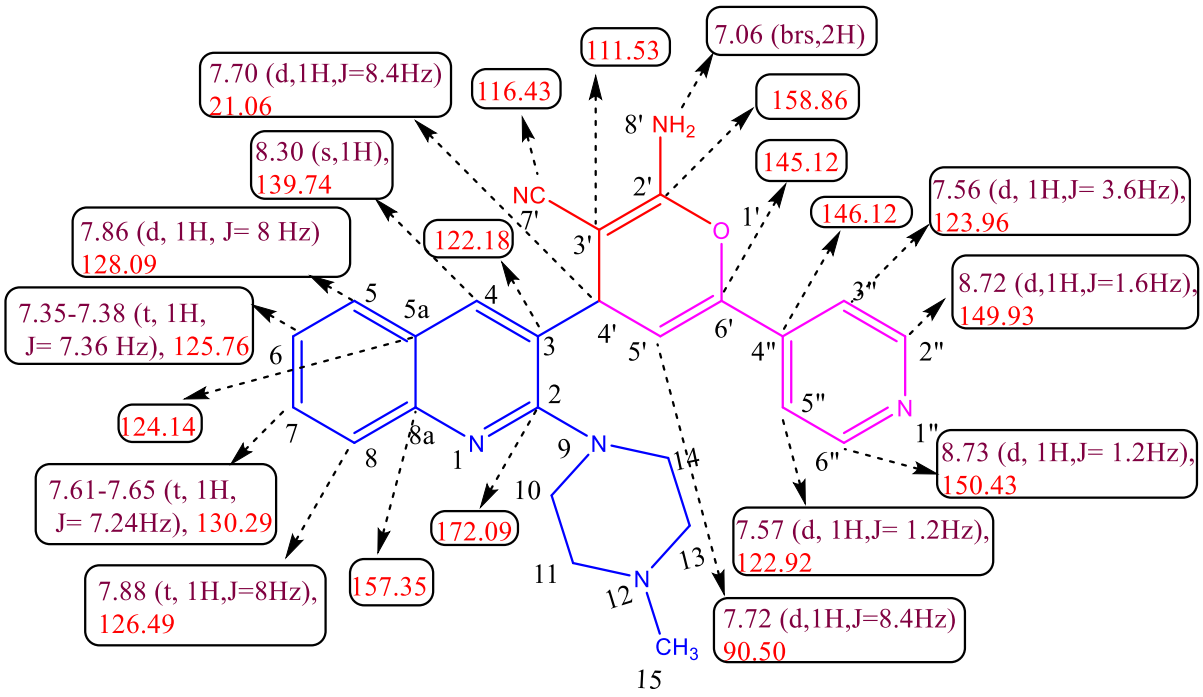

Figure 3. 9. Selected (^{1}H) NMR and (^{13}C) NMR and HMBC chemical shifts of **6n**

The $C_{5'}$-H proton was correlated to the pyridinyl carbon, $C_{6''}$ at δ 150. 43, $C_{2''}$ at δ 149.93, $C_{4''}$ at δ 146.40 and $C_{5''}$ at δ 122 92, The $C_{2''}$-H pyridine proton was correlated to the pyridinyl carbon, $C_{4''}$ at δ 146.40, $C_{3''}$ at δ 123.96 and correlated to pyran carbon $C_{6'}$ at δ 145.12, the $C_{5''}$-H pyridine proton was correlated to the quinolinyl carbon C_3 at δ 122. 18. The ^{1}H NMR, ^{13}C NMR and HMBC chemical shifts of **6n** are presented in Table 3. 5. Based on the above spectral details, TOF MS ES+ Calcd mass 424.20, Found: 424.31 and its elemental analysis Calcd. For $C_{25}H_{24}N_6O$: C 70.73, H 5.70, N 19.80; Found: C 70.75, H 5.72, N 19.81, the structure was confirmed as 2-amino-4-(2-(4-methylpiperazin-1-yl) quinolin-3-yl)-6-(pyridin-4-yl)-4H-pyran-3-carbonitrile **6n**.

Table 3. 5. Selected HMBC correlations of compound **6n**

S.NO	Proton	Correlated Carbons
1	C_4-H (s,1H) at δ. 8.30	C_3 at δ. (122.18), C_5 at δ. (128.09), $C_{6'}$ at δ. (150.43) C_{8a} at δ. (157.35)
2	C_8'-H (brs, 1H) at δ. 7.06	$C_{2'}$ at δ. (158.86), $C_{6'}$ at δ. (145.12), $C_{5'}$ at δ. (90.50), $C_{7''}$ at δ. (116.43), $C_{5''}$ at δ. (122.92),
3	C_5-H (d, 1H, J=8Hz) at δ. 7.86	C_6 at δ. (125.76), C_7 at δ. (130.29), C_4 at δ. (139.74)
4	C_6-H (t, 1H, J=7.36Hz) at δ. 7.35-7.38	C_{5a} at δ. (124.14)
5	C_4'-H (d, 1H, J= 8.4Hz) at δ. 7.70	C_3 at δ. (122.18)
6	C_5'-H (d, 1H, J=8.4Hz) at δ. 7.72	$C_{5''}$ at δ. (122.92), $C_{4''}$ at δ. (146.40), $C_{6''}$ at δ. (150.43), $C_{2''}$ (at δ. 149.93)
7	C_5''-H (d, 1H, J=1.6Hz) at δ. 7.57	C_3 at δ. (122.18)
8	C_2''-H (d, 1H, J=1.6Hz) at δ. 8.72	$C_{3''}$ at δ. (123.96), $C_{4''}$ at δ. (146.40), $C_{6'}$ at δ. (145.12)

Thus, the one pot multi-component synthesis of the new methyl piperazinyl-quinolinyl pyran derivatives, using TiO_2-Pr-SO_3H as a catalyst, was a very neat and efficient reaction which is selective for the formation of the sought after molecule.

A mechanism for this multicomponent reaction is as proposed in Scheme 3. 4. In the first step, the catalyst activates the aldehyde carbonyl functionality thereby enabling malononitrile to form a new covalent bond with loss of water as indicated by a Knoevenagel condensation

reaction to produce an intermediate **I**. In the next step, the catalyst activates the nitrogen of intermediate **I** thereby facilitating a Michael addition to give intermediate **II**. This is followed by a simple intramolecular condensation reaction to produce intermediate **III** which subsequently undergoes a proton transfer reaction to produce **6a**.

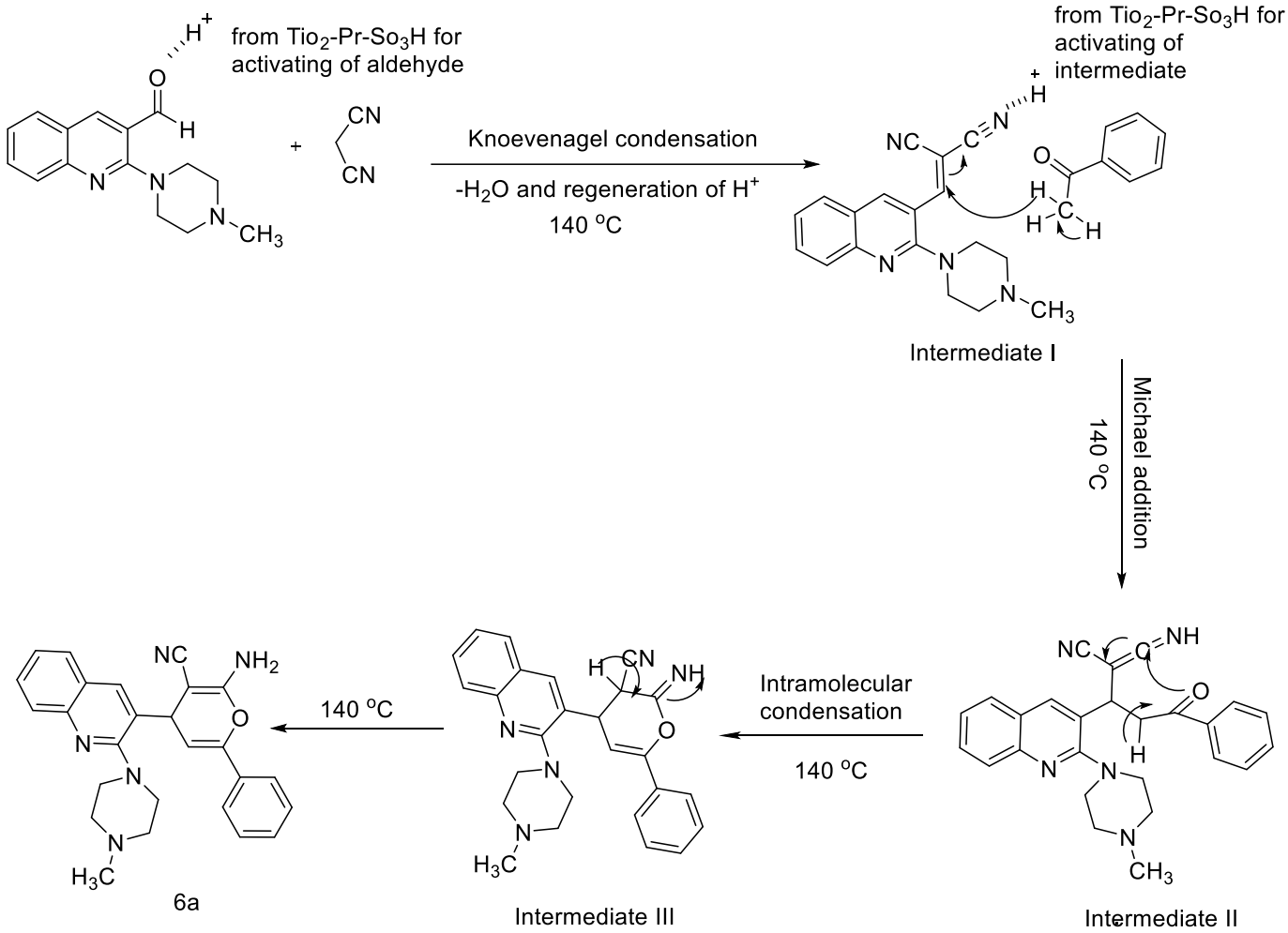

Scheme 3. 4. Proposed mechanism for the synthesis of 2-amino-4-(2-(4-methylpiperazin-1-yl) quinolin-3-yl)-6-phenyl-4H-pyran-3-carbonitrile **6a** at 140 °C.

Computational docking of **6a & 6n** were undertaken with Heat shock protein 90 (Hsp 90). This protein contains two sub domains (IA and B, IIA and B, IIIA and B) which possess common structural motifs. The Sudlow site I and Sudlow site II which are subdomains IIA and IIIA, respectively are usually the most probable binding site for ligands. The energetically most feasible Hsp 90 complex formed with **6a & 6n** which is presented in Figure 3. 10. (a-b). The docking results indicated that both **6a & 6n** binds inside the binding pocket located in subdomain II A of Hsp 90. Also, **6a & 6n** is located adjacent to the amino acid residues Leu-

42, Agp-40, Ser-36, Leu-89, Asn-91, Arg-32, Lys-98, Ala-213, Phe-120, Ser-99, Lys-44, Gln-119, Gly-116, Gly-121 and Thr-101 of subdomain IIA of Hsp 90. The carbonitrile and amine group of **6a &6n** form a hydrogen bond LYS-98 with bond length 1.9 Å. It was found that **6a & 6n** is in the locality of Trp-214 amino acid residue of Hsp 90. These observations only provided the probable geometry of the complexes; however the binding mode can only be determined experimentally.

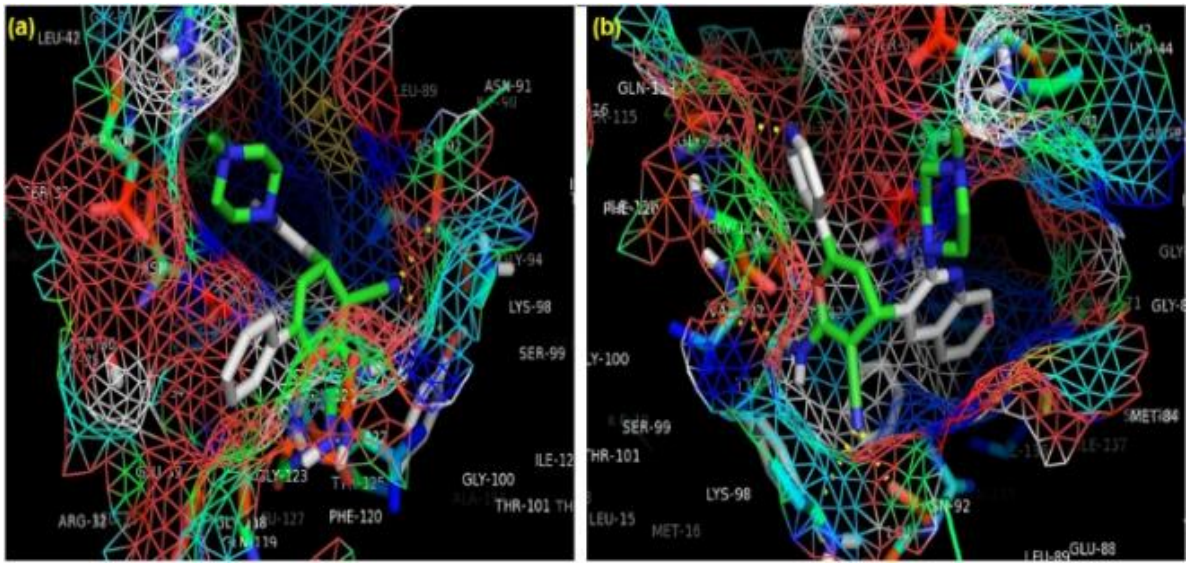

Figure 3. 10. (a-b). (a) Molecular docking of the Hsp90-compound 6a and (b) Hsp90-compound **6n** complex selected amino acid residues are represented by stick and cartoon models. Hydrogen bond is shown in pink dotted line.

3. 4. Conclusion

Titanium based sulfonic acid catalyst was used for the synthesis of 2-amino-4-(2-(4-methylpiperazin-1-yl) quinolin-3-yl)-6-phenyl-4H-pyran-3-carbonitriles and 2-amino-4-(2-(4-methylpiperazin-1-yl) quinolin-3-yl)-6-(pyridin-4-yl)-4H-pyran-3-carbonitrile derivatives under solvent-free conditions. The preparation of the catalyst was simple, safe and can be recovered easily and displayed high activity for the multicomponent reaction. Furthermore, this one pot reaction created a new type of piperazinyl-quinolinyl pyran derivatives which have suitable functionality for a host of possible biochemical applications.

3. 5. Experimental

3. 5. 1. Preparation of the catalyst

3. 5. 1. 1. The synthesis of 3-mercaptopropyltitania

The synthesis of 3-mercaptopropyltitania (MPT) was achieved by following a known protocol (Atghia and Beigbaghlou, 2014, 1155). Briefly, TiO_2 and 3-mercaptopropyl trimethoxysilane were added to dry toluene and the reaction mixture was refluxed for 24 h. After this period, the mixture was filtered, washed with acetone and dried: the yield of the product was 95 %.

3. 5. 1. 2. The oxidation of MPT to nanocrystalline titanium-based sulfonic acid catalyst

MPT was oxidized as follows: an aliquot of 10 mL of 30 % H_2O_2 and 30 mL methanol was added to MPT followed by two drops of conc. H_2SO_4. The reaction mixture was stirred for 24 h at room temperature, filtered and washed with distilled water and acetone: the yield of the solid acid catalyst was 97 % (Scheme 3. 1).

3. 5. 2. The general procedure for the synthesis of substituted 2-(4-methylpiperazin-1-yl) quinoline-3-carbaldehyde (**3**)

The starting compound 2-chloroquinoline-3-carbaldehyde (**1**) was prepared from acetanilide, DMF and $POCl_3$ by the Vilsmeier-Haack reaction (Cohn *et al* 1981:1520). Thereafter an aliquot of (**1**) (0.001 mol) and potassium carbonate (0.002 mol) was transferred into a round bottom flask followed by the addition of an excess of 1-methylpiperazine. The mixture was refluxed for 24 h at 200 ˚C; the reaction was monitored by TLC. After completion of the reaction, the content was cooled to room temperature and poured into water. It was then filtered, washed with water and dried. The crude product was purified by column chromatography using silica gel mesh and a mobile phase consisting of acetone: hexane (70:30) to produce a yellow powder of 90 % yield (m.p 180 ˚C). FT-IR (neat, cm^{-1}): 3464, 2979, 2934, 2643, 2901, 2358, 2333, 1693, 1615, 1593, 1421, 1372, 1239, 952, 765, 512, 482 cm^{-1}. ^1H NMR ($CDCl_3$, 400 MHz) : δ 10.09 (1H, brs, CHO), 8.4 (1H, brs, Ar-H), 7.76 (1H, d, Ar-H, *J* = 8.48 Hz), 7.7 (1H, d, Ar-H, *J*= 7.36 Hz), 7.62 (1H, t, Ar-H, *J*=1.44 Hz), 7.31(1H, t, Ar-H, *J*= 0.84Hz), 3.47 (4H, t, CH_2, *J*=5.4Hz), 2.6 (4H, t, CH_2, *J*= 4.84 Hz), 2.3 (3H, s, CH_3).^{13}C NMR ($CDCl_3$, 100 MHz): δ 190, 158, 149, 142, 132, 129, 127, 124, 123, 122, 54, 50, 45. TOF MS ES+ Calc. mass 256.1450, Found: 256.1449Anal. Calc. For $C_{15}H_{17}N_3O$: C, 70.56; H, 6.71; N, 16.46; Found: C, 70.58; H, 6.72; N, 16.43.

3. 5. 3. The general procedure for the synthesis of 2-amino-4-(2-(4-methylpiperazin-1-yl) quinolin-3-yl)-6-phenyl-4H-pyran-3carbonitrile derivatives (6a-l)

To a mixture containing acetophenone derivative (**5a-l**) (1.0 mmol), 2-(4-methylpiperazin-1-yl) quinoline-3-carbaldehyde (1.0 mmol) and malononitrile (1.0 mmol) was added TiO_2-Pr-SO_3H (0.07 g). The resulting mixture was heated at 140 °C under solvent-free conditions. Upon completion of the reaction, monitored by TLC, 10 mL ethanol was added and the mixture was filtered. The filter-cake was washed with warm ethanol (5 mL × 3) to clean the catalyst. The filtrates were subsequently combined, the solvent evaporated *in vacuo* and the crude mixture was purified by column chromatography using silica gel mesh and a mobile phase of acetone: hexane (70: 30). The recovered catalyst was dried and re-used in subsequent runs when assessing its recyclability potential.

3. 5. 4. The general procedure for the synthesis of 2-amino-4-(2-(4-methylpiperazin-1-yl) quinolin-3-yl)-6-(pyridin-4yl)-4H-pyran-3- carbonitrile derivatives (6m&6n)

To a mixture of acetyl pyridine derivatives (**5m-n**) (1.0 mmol), 2-(4-methylpiperazin-1-yl) quinoline-3-carbaldehyde (1.0 mmol) and malononitrile (1.0 mmol), TiO_2-Pr-SO_3H (0.07 g) was added. The resulting mixture was heated at 140 °C under solvent-free conditions. Upon reaction completion, monitored by TLC, 10 mL ethanol was added and the resultant mixture was filtered. The filter-cake was washed with warm ethanol (5 mL × 3) to effectively clean the catalyst. The filtrates were subsequently combined, the solvent evaporated *in vacuo* and the crude mixture was purified by column chromatography using silica gel and a mobile phase of acetone: hexane (70: 30). The recovered catalyst was dried and re-used in the subsequent runs.

3. 5. 5. The spectroscopic analysis of 6a-n

3. 5. 5. 1. 2-amino-4-(2-(4-methylpiperazin-1-yl)quinolin-3-yl)-6-phenyl-4H-pyran-3 carbonitrile (6a).

Yellow colour solid; yield 90 %: FT-IR (neat, cm^{-1}): 3413 (NH_2), 3054 (CH), 2989 (CH), 2717, 2636, 2141, 2186 (C-N), 1654 (C=C), 1528, 1398, 1236, 767, 708. ^{1}H NMR (400 MHz, $DMSOd_6$): δ 2.5 (s, 3H CH_3), 2.8 (t, 4H, CH_2), 3.27 (t, 4H, CH_2,), 6.99 (brs, 2H, NH_2), 7.40(t, Ar, 3H, J =7.52Hz), 7.52 (d, Ar, 2H, J =6 Hz), 7.60 (dd, Ar, 1H, J = 5.52 Hz), 7.67 (t, Ar, 2H, J = 7.6 Hz), 7.72 (d, 2H, CH, J = 8.24 Hz), 7.87 (d, Ar, 2H, J = 7.92), 8.4 (brs, Ar, 1H). ^{13}C NMR (100 MHz, $DMSOd_6$): δ 30.62, 42.56, 45.6, 52.20, 91.97, 112.31, 116.82, 122.75, 124.24, 125.31, 126.36, 128.05, 128.48, 128.57, 129.34, 130.51, 137.30, 140.50, 146.05, 155.43, 155.64, 158.75, 161.65. TOF MS ES+ Calcd mass 423.21, Found: 424.3441 Anal. Calcd. For $C_{26}H_{26}N_5O$: C 73.74, H 5.95, N 16.54; Found: C 73.76, H 5.97, N 16.58.

3. 5. 5. 2. 2-amino-6-(2-hydroxyphenyl)-4-(2-(4-methylpiperazin-1-yl)quinolin-3-yl)-4H-pyran-3-carbonitrile (**6b**).

Yellow colour solid; yield 85 %: FT-IR (neat, cm^{-1}): 3469, 3102, 3070, 2797, 2211, 1624, 1595, 1568, 1455, 1430, 1353, 1262, 1199, 1145, 1000, 759, 624. ^{1}H NMR (400 MHz, $DMSOd_6$): δ 1.9 (s, 3H, CH_3), 2.26 (t, 4H, CH_2), 2.80 (t, 4H, CH_2), 6.89 (dd, Ar, 2H, *J* = 8.6 Hz), 6.96 (brs, 2H, NH_2), 7.37 (t, Ar, 1H, *J* =0.92Hz), 7.47 (t, Ar, 2H, *J* =4.84 Hz), 7.65 (t, Ar, 1H, *J* = 6.96 Hz), 7.72 (d, 2H, CH, *J* = 8.24 Hz), 7.87 (d, Ar, 2H, *J* = 7.64 Hz), 8.38 (brs, Ar, 1H), 9.93 (brs, 1H, OH). ^{13}C NMR (100 MHz, $DMSOd_6$): δ 42.66, 45.72, 52.26, 91.53, 111.99, 115.33, 115.69,117.21, 122.87, 124.15, 124.25, 125.52, 126.35, 127.78, 128.03, 130.07, 130.41, 140.34,146.04, 130.51, 137.30, 140.50, 146.05, 155.23, 155.72, 158.59, 158.64, 161.86. For $C_{26}H_{25}N_5O_2$: C 71.05, H 5.73, N 15.93; Found: C 71.08, H 5.74, N 15.92.

3. 5. 5. 3. 2-amino-6-(4-hydroxyphenyl)-4-(2-(4methylpiperazin-1-yl)quinolin-3-yl)-4H-pyran-3-carbonitrile (**6c**).

Yellow colour solid; yield 90 %: FT-IR (neat, cm^{-1}): 3426, 3043, 2765, 2194, 2153, 1614, 1591, 1560, 1529, 1514, 1457, 1405, 1361, 1282, 1251, 1166, 1018, 981, 834, 770. ^{1}H NMR (400 MHz, $DMSOd_6$): δ 1.9 (s, 3H, CH_3), 2.26 (t, 4H, CH_2), 2.80 (t, 4H, CH_2), 6.89 (d, Ar, 2H, *J* = 8.6 Hz), 6.96 (brs, 2H, NH_2), 7.37(t, Ar, 1H, *J* =0.92Hz), 7.47 (d, Ar, 2H, *J* =4.84 Hz), 7.65 (t, Ar, 1H, *J* = 6.96 Hz), 7.72 (d, 2H, CH, *J* = 8.24 Hz), 7.87 (d, Ar, 2H, *J* = 7.64 Hz), 8.38 (brs, Ar, 1H), 9.93 (brs, 1H, OH). ^{13}C NMR (100 MHz, $DMSOd_6$): δ 42.66, 45.72, 52.26, 91.53, 111.99, 115.33, 115.69,117.21, 122.87, 124.15, 124.25, 125.52, 126.35, 127.78, 128.03, 130.07, 130.41, 140.34,146.04, 130.51, 137.30, 140.50, 146.05, 155.23, 155.72, 158.59, 158.64, 161.86. Calcd. For $C_{26}H_{25}N_5O_2$: C 71.05, H 5.73, N 15.93; Found: C 71.08, H 5.76, N 15.92.

3. 5. 5. 4. 2-amino-4-(2-(4-methylpiperazin-1-yl)quinolin-3-yl)-6-(p-tolyl)-4H-pyran-3-carbonitrile (**6d**).

Yellow colour solid; yield 78 %: FT-IR (neat, cm^{-1}): 3450, 3419, 2999, 2719, 2636, 2472, 2198, 2182, 2144, 1610, 1596, 1566, 1524, 1436, 1406, 1236, 1208, 980, 821, 767.617. ^{1}H NMR (400 MHz, $DMSOd_6$): δ 2.38 (s, 6H, $2CH_3$), 2.47 (t, 4H, CH_2), 2.75 (t, 4H, CH_2), 6.97 (brs, 2H, NH_2), 7.33(d, Ar, 2H, *J* =7.96Hz), 7.35 (t, Ar, 1H, *J* =6.76 Hz), 7.52 (d, Ar, 2H, *J* = 8.08 Hz), 7.64 (t, Ar, 1H, *J* = 7.32 Hz), 7.72 (d, 2H, CH, *J* = 8.08 Hz), 7.88 (d, Ar, 2H, *J* = 7.84 Hz), 8.4 (brs, Ar, 1H). ^{13}C NMR (100 MHz, $DMSOd_6$): δ 20.82, 40.04, 42.51, 45.60, 52.16,

91.70, 112.13, 113.67, 116.92, 124.17, 124.26, 125.38, 126.36, 128.06, 128.44, 128.70, 129.12, 129.45 130.47, 134.46, 139.02, 140.48, 146.06, 155.36, 155.63, 158.69, 161.73. Calcd. For $C_{27}H_{27}N_5O$: C 74.12, H 6.22, N 16.01; Found C 74.13, H 6.24, N 16.04.

3. 5. 5. 5. 2-amino-4-(2-(4-methylpiperazin-1-yl) quinolin-3-yl)-6-(4 nitrophenyl)-4H-pyran-3-carbonitrile (**6e**).

Yellow colour solid; yield 75 %: FT-IR (neat, cm^{-1}): 34941, 3127, 2849, 2713, 2204, 2185, 2148, 1713, 1616, 1598, 1530, 1406, 1345, 1289, 1206, 1015, 849, 774, 698. ^{1}H NMR (400 MHz, $DMSOd_6$): δ 2.07 (s, 3H, CH_3), 2.5 (t, 4H, CH_2), 2.85 (t, 4H, CH_2), 7.05 (brs, 2H, NH_2), 7.38(d, Ar, 2H, *J* =8.28Hz), 7.64 (t, Ar, 1H, *J* =0.64 Hz), 7.73 (d, 2H, CH, *J* = 8.28 Hz), 7.88 (d, Ar, 4H, *J* = 8.72 Hz), 8.37 (d, Ar, 2H, *J* = 8.8 Hz), 8.41 (brs, Ar, 1H). ^{13}C NMR (100 MHz, $DMSOd_6$): δ 30.64, 40.61, 42.47, 45.65, 52.18, 91.23, 112.02, 116.41, 123.65, 124.25, 124.32, 125.10, 126.41, 128.09, 130.13, 130.62, 140.63, 143.81, 146.10, 147.85, 153.39, 155.63, 158.97, 161.58. Anal. Calcd. For $C_{26}H_{24}N_6O_3$: C 66.65, H 5.16, N 17.94; Found: C 66.63, H 5.18, N 17.96.

3. 5. 5. 6. 2-amino-6-(4-fluorophenyl)-4-(2-(4-methylpiperazin-1-yl) quinolin-3-yl)-4H-pyran-3-carbonitrile (**6f**).

Yellow colour solid; yield 70 %: FT-IR (neat, cm^{-1}): 3529, 3390, 3057, 2996, 2715, 2628, 2481, 2204, 2187, 2155, 1616, 1528, 1438, 1238, 1161, 980, 835, 771, 570, 517. ^{1}H NMR (400 MHz, $DMSOd_6$): δ 2.08 (s, 3H, CH_3), 2.5 (t, 4H, CH_2), 2.80 (t, 4H, CH_2), 6.99 (brs, 2H, NH_2), 7.38(d, Ar, 4H, *J* =9.04Hz), 7.64 (t, Ar, 2H, *J* =3.44 Hz), 7.73 (d, 2H, CH, *J* = 8.32 Hz), 7.84 (d, Ar, 2H, *J* = 7.92 Hz), 8.4 (brs, Ar, 1H). ^{13}C NMR (100 MHz, $DMSOd_6$): δ 42.26, 42.83, 45.94, 52.36, 91.62, 112.18, 113.68, 115.41, 115.62,116.79, 122.58, 124.15, 124.24, 125.36, 126.38, 128.06, 130.45, 130.81, 130.89, 133.77, 140.43, 146.11, 154.25, 137.30, 155.80, 158.76, 161.45, 161.72. ^{19}F NMR (400 MHz, $DMSOd_6$): δ -111.19. Calcd. For $C_{26}H_{24}FN_5O$: C 70.73, H 5.48, N 15.86; Found: C 70.70, H 5.49, N 15.88.

3. 5. 5. 7. 2-amino-6-(4-chlorophenyl)-4-(2-(4-methylpiperazin-1-yl) quinolin-3-yl)-4H-pyran-3-carbonitrile (**6g**).

Yellow colour solid; yield 90 %: FT-IR (neat, cm^{-1}): 3373, 3246, 2939, 2746, 2358, 2204, 2185, 2152, 1595, 1618, 1526, 1409, 1491, 1240, 1090, 831, 758, 621, 556, 483. ^{1}H NMR (400 MHz, $DMSOd_6$): δ 2.38 (s, 3H, CH_3), 2.47 (t, 4H, CH_2), 2.75 (t, 4H, CH_2), 6.97 (brs, 2H, NH_2), 7.33 (d, 2H, *J* =7.96Hz), 7.35 (t, Ar, 1H, *J* =6.76 Hz), 7.52 (d, Ar, 2H, *J* = 8.08

Hz), 7.64 (t, Ar, 1H, *J* = 7.32 Hz), 7.72 (d, 2H, CH, *J* = 8.08 Hz), 7.88 (d, Ar, 2H, *J* = 7.84 Hz), 8.4 (brs, Ar, 1H). ^{13}C NMR (100 MHz, DMSOd_6): δ 45.18, 48.21, 53.74, 69.73, 91.16, 111.89, 116.79, 122.45, 123.96, 124.13, 124.39, 125.11, 125.82, 126.45, 126.64, 128.03, 128.63, 128.89, 130.16, 130.29, 130.43, 130.62, 131.55, 131.64, 134.09, 136.30, 139.76, 146.32, 153.43, 157.14, 157.47, 158.66, 162.04. Calcd. For $C_{26}H_{24}ClN_5O$: C 68.19, H 5.28, N 15.29; Found C 68.21, H 5.30, N 15.27.

3. 5. 5. 8. 2-amino-6-(4-bromophenyl)-4-(2-(4-methylpiperazin-1-yl) quinolin-3-yl)-4H-pyran-3-carbonitrile (**6h**).

Yellow colour solid; yield 87 %: FT-IR (neat, cm^{-1}): 3376, 2927, 2952, 2224, 2186, 2148, 1729, 1629, 1560, 1449, 1588, 1382, 1276, 1123, 778, 751, 572, 525. ^{1}H NMR (400 MHz, DMSOd_6): δ 2.07 (s, 3H, CH_3), 2.5 (t, 4H, CH_2), 2.85 (t, 4H, CH_2), 7.05 (brs, 2H, NH_2), 7.38(d, Ar, 2H, *J* =8.28Hz), 7.64 (t, Ar, 1H, *J* =0.64 Hz), 7.73 (d, 2H, CH, *J* = 8.28 Hz), 7.88 (d, Ar, 4H, *J* = 8.72 Hz), 8.37 (d, Ar, 2H, *J* = 8.8 Hz), 8.41 (brs, Ar, 1H). ^{13}C NMR (100 MHz, DMSOd_6): δ 42.42, 43.41, 47.69, 52.55, 96.19, 107.54, 116.97, 122.23, 123.99, 124.55, 127.25, 131.14, 142.27, 146.18, 151.54, 157.55, 160.30. Calcd. For $C_{26}H_{24}BrN_5O$: C 62.16, H 4.82, N 13.94; Found: C 62.19, H 4.81, N 13.96.

3. 5. 5. 9. 2-amino-4-(2-(4-methylpiperazin-1-yl) quinolin-3-yl)-6-(thiophen-2-yl)-4H-pyran-3-carbonitrile (**6i**).

Yellow colour solid; yield 83 %: FT-IR (neat, cm^{-1}): 3460, 3424, 3105, 3063, 2982, 2710, 2637, 2479, 2207, 2185, 2143, 1613, 1596, 1527, 1397, 1245, 1215, 772, 718, 618. ^{1}H NMR (400 MHz, DMSOd_6): δ 2.9 (s, 3H, CH_3), 2.7 (t, 4H, CH_2), 3.1 (t, 4H, CH_2), 7.16 (brs, 2H, NH_2), 7.26(t, Ar, 1H, *J* =3.96Hz), 7.4 (t, Ar, 1H, *J* =7.2 Hz), 7.68 (t, Ar, 1H, *J* = 6.96 Hz), 7.74 (d, 2H, CH, *J* = 9.68 Hz), 7.82 (d, Ar, 2H, *J* = 4.68 Hz), 7.9 (d, Ar, 2H, *J* = 7.84 Hz), 8.4 (s, Ar, 1H), ^{13}C NMR (100 MHz, DMSOd_6): δ 42.47, 45.65, 52.18, 91.23, 112.02, 116.45, 123.65, 124.32, 125.10, 126.41, 128.09,130.13, 130.62, 140.63, 143.81, 146.10, 147.85, 153.39, 158.97, 161.58. Calcd. For $C_{24}H_{23}N_5OS$: C 67.11, H 5.40, N 16.30; Found: C 67.14, H 5.43, N 16.31.

3. 5. 5. 10. 2-amino-4-(2-(4-methylpiperazin-1-yl)quinolin-3-yl)-6-(naphthalen-1-yl)-4H-pyran-3-carbonitrile (**6j**).

Yellow colour solid; yield 90 %: FT-IR (neat, cm^{-1}): 3464, 3409, 3067, 2342, 2204, 2187, 2161, 1634, 1596, 1554, 1521, 1410, 1360, 1234, 1158, 1017, 786, 479. ^{1}H NMR (400 MHz, $DMSOd_6$): δ 2.5 (s, 3H, CH_3), 2.7 (t, 4H, CH_2), 3.1 (t, 4H, CH_2), 7.16 (brs, 2H, NH_2), 7.26(t, Ar, 1H, *J* =3.96Hz), 7.4 (t, Ar, 1H, *J* =7.2 Hz), 7.68 (t, Ar, 1H, *J* = 6.96 Hz), 7.74 (d, 2H, CH, *J* = 9.68 Hz), 7.82 (d, Ar, 2H, *J* = 4.68 Hz), 7.9 (d, Ar, 2H, *J* = 7.84 Hz), 8.1 (brs, Ar, 1H),8.4 (brs, Ar, 1H), ^{13}C NMR (100 MHz, $DMSOd_6$): δ 42.47, 45.65, 52.18, 91.23, 112.02, 116.45, 123.65, 124.32, 125.10, 126.41, 128.09, 130.13, 130.62, 140.63, 143.81, 146.10, 147.85, 153.39, 158.97, 161.58.Calcd. For $C_{30}H_{27}N_5O$: C 76.09, H 5.75, N 14.79; Found: C 76.12, H 5.74, N 14.81.

3. 5. 5. 11. 2-amino-6-(1-hydroxynaphthalen-2-yl)-4-(2-(4-methylpiperazin-1-yl) quinolin-3-yl)-4H-pyran-3-carbonitrile (**6k)**.

Yellow colour solid; yield 90 %: FT-IR (neat, cm^{-1}): 3291, 3159, 2366, 2208, 1639, 1611, 1592, 1367, 1419, 1008, 1262, 1196, 951, 803, 748. ^{1}H NMR (400 MHz, $DMSOd_6$): δ 2.0 (s, 3H CH_3), 2.35 (t, 4H, CH_2), 3.2 (t, 4H, CH_2), 7.38(dd, Ar, 2H, *J* =6.92Hz), 7.57 (brs, 2H, NH_2), 7.65(d, 2H, CH, *J* =7.12Hz), 7.76 (t, Ar, 2H, *J* =4.12 Hz), 7.96 (d, Ar, 2H, *J* = 2.64 Hz), 8.08 (d, Ar, 1H, *J* = 3.64 Hz), 8.24 (d, Ar, 2H, *J*= 2.92Hz). 8.49 (d, Ar, 1H, *J*= 4.6Hz) 8.4 (brs, Ar, 1H), 10.22 (brs, 1H, OH). ^{13}C NMR (100 MHz, $DMSOd_6$): δ 45.58, 48.71, 54.14, 112.45, 121.50, 123.05, 124, 126.49, 127.82, 128.24, 129.01, 135.02, 146.63, 148.05, 156, 157.54. Calcd. For $C_{30}H_{27}N_5O_2$: C 73.60, H 5.56, N 14.31; Found: C 73.62, H 5.58, N 14.32.

3. 5. 5. 12. 2-amino-6-(anthracen-9-yl)-4-(2-(4-methylpiperazin-1-yl) quinolin-3-yl)-4H-pyran-3-carbonitrile (**6l**).

Yellow colour solid; yield 75 %: FT-IR (neat, cm^{-1}): 3456, 2857, 2727, 2506, 2223, 2185, 2150, 1654, 1589, 1561, 1493, 1458, 1281, 1215, 1129, 1060, 1025, 987, 786, 752, 609. ^{1}H NMR (400 MHz, $DMSOd_6$): δ 2.07 (s, 3H, CH_3), 2.73 (t, 4H, CH_2), 3.1 (t, 4H, CH_2), 7.03 (brs, 2H, NH_2), 7.48(t, Ar, 3H, *J* =0.76Hz), 7.74 (t, Ar, 3H, *J* =5.84 Hz), 7.8 (d, Ar,4H, *J* = 8.24 Hz), 7.93 (d, Ar,4H, *J* = 7.84 Hz), 8.28 (brs, Ar, 2H). ^{13}C NMR (100 MHz, DMSO-d_6): δ 40.05, 42.81, 43.65, 45.63, 52.49, 80, 84.78, 116.53, 116.64, 122.39, 123.95, 124.74, 126.77, 128.12, 130.99, 140.47, 146.66, 155.74, 156.83, 158.86, 158.64, 162.96. Calcd. For $C_{34}H_{29}N_5O$: C 77.99, H 5.58, N 13.37; Found: C 77.96, H 5.50, N 13.38.

3. 5. 5. 13. 2-amino-4-(2-(4-methylpiperazin-1-yl)quinolin-3-yl)-6-(pyridin-4yl)-4H-pyran-3-carbonitrile (**6m**).

Yellow colour solid; yield 88 %: FT-IR (neat, cm^{-1}): 3467, 3334, 2952, 2210, 2185, 2148, 1618, 1592, 1528, 1437, 1239, 1145, 760, 712, 621. ^{1}H NMR (400 MHz, DMSO-d_6): δ 1.9 (s, 3H, CH_3), 2.26 (t, 4H, CH_2), 3.2 (t, 4H, CH_2), 7.0 (brs, 2H, NH_2), 7.38(t, Ar,1H, *J* =7.68Hz), 7.56 (t, Ar, 1H, *J* =2.8 Hz), 7.65 (t, Ar, 1H, *J* = 0.8 Hz), 7.72 (d, 2H, CH, *J* = 8.32 Hz), 7.8 (d, Ar, 2H , *J* = 8.04 Hz), 8.0 (d, Ar, 1H, *J* = 6.2 Hz), 8.32 (brs, Ar, 1H), 8.68 (d, Ar, 2H, *J* = 3.28Hz), 8.77 (brs, Ar, 1H). ^{13}C NMR (100 MHz, DMSOd_6): δ 45.16, 48.22, 53.80, 91.21, 112.01, 116.73, 122.29, 123.51, 123.95, 124.16, 125.79, 126.48, 128.06, 130.27, 133.42, 136.01, 139.83, 146.36, 148.47, 150.11, 151.39, 157.13, 158.81, 162.03. Calcd. For $C_{26}H_{24}N_6O_3$: C 66.65, H 5.16, N 17.94; Found: C 66.63, H 5.18, N 17.96.

3. 5. 5. 14. 2-amino-4-(2-(4-methylpiperazin-1-yl)quinolin-3-yl)-6-(pyridin-4yl)-4H-pyran-3-carbonitrile (**6n**).

Yellow colour solid; yield 90 %: FT-IR (neat, cm^{-1}): 3449, 3054, 2994, 2948, 2726, 2496, 2366, 2201, 2189, 2157, 1596, 1551, 1524, 1400, 1243, 981, 823, 770. ^{1}H NMR (400 MHz, DMSOd_6): δ 1.9 (s, 3H, CH_3), 2.26 (t, 4H, CH_2), 2.42 (t, 4H, CH_2), 7.06 (brs, 2H, NH_2), 7.35-7.38 (t, Ar, 1H, *J* =7.36Hz), 7.56 (d, 1H, *J* =3.6 Hz), 7.57 (d, 1H, *J* =1.2 Hz), 7.61-7.65 (m, Ar, 1H, *J* = 0.84 Hz), 7.70 (d, 1H, CH, *J* = 8.4 Hz), 7.72 (d, 1H, CH, *J* = 8.4 Hz), 7.86 (d, Ar, 1H, *J* = 8 Hz), 7.88 (d, Ar, 1H, *J* = 8 Hz), 8.30 (brs, Ar, 1H), 8.72 (d, Ar, 2H, *J* = 1.6 Hz), 8.73 (d, Ar, 2H, *J* = 1.2 Hz). ^{13}C NMR (100 MHz, DMSOd_6): δ 21.06, 40.7, 45.55, 48.62, 54.01, 90.49, 111.52, 116.42, 122.17, 122.92, 123.95, 124.13, 125.75, 126.49, 128.08, 130.29, 139.73, 143.92, 145.11, 146.40, 149.93, 150.43, 152, 157.34, 158.85, 162.03, 172.08. TOF MS ES+ Calcd mass 424.20, Found: 424.31 Calcd. For $C_{25}H_{24}N_6O$: C 70.73, H 5.70, N 19.80; Found: C 70.75, H 5.72, N 19.81.

3. 6. Molecular Docking Studies

The Auto Dock 4.2 program which operates the Lamarckian Genetic Algorithm (LGA) was used to dock compound **6a** and **6n** with the 3D structure of Hsp 90. The crystal structure of Hsp 90 (PDB id: 1AO6) was obtained from the Protein Data Bank and all water molecules were eliminated with successive addition of hydrogen atoms, followed by the computation of Gasteiger charges as required for LGA molecular docking procedure. The grid size along the x-, y-, z-axes and grid space were set to 60 Å, 60 Å and 60 Å and 0.403 Å for Hsp90. To include the whole subdomain IIA of Hsp90 during the docking process, the grid centre along the x-, y-, z-axes was set as 34.016 Å, 42.121 Å, and 50.644 Å. The following docking parameters were used: Genetic Algorithm (GA) population=150; maximum number of energy evaluations=250,000 and GA crossover mode of two points. For each docking simulation, 20 different conformers were generated and PyMOL package software was used for visualization of the interaction of the docked protein−ligand complex. The conformation with the lowest binding free energy was used for further analysis.

References

Atghia, S. V., Beigbaghlou, S. S., 2013. Nanocrystalline titania-based sulfonic acid (TiO_2-Pr-SO_3H) as a new, highly efficient, and recyclable solid acid catalyst for preparation of quinoxaline derivatives. Journal of Nanostructure Chemistry (3) 3-38.

Atghia, S. V., Beigbaghlou, S. S. C., 2014. Use of a highly efficient and recyclable solid-phase catalyst based on nanocrystalline titania for the Pechmann condensation. Chimie (17) 1155-1159.

Atghia, S. V., Beigbaghlou, S., 2013. Surface Modification Approach to TiO_2 Nanofluids with High Particle Concentration, Low Viscosity, and Electrochemical Activity. J. Organomet. Chem. (37) 42-49.

Cohn, O. M., Narine, B., Tarnowski, B., 1981. A versatile new synthesis of quinolines and related fused pyridines, Part 5. The synthesis of 2-chloroquinoline-3-carbaldehydes. J. Chem Soc. Perkin Trans. (1) 1520- 1530.

Dailly, E., Chenu, F., Renard, C. E., Bourin, M., 2004. Evidence for involvement of the monoaminergic system in antidepressant-like activity of an ethanol extract of Boerhaavia diffusa and its isolated constituent, punarnavine, in mice. Arch Pharm (18)767-774.

Evidente, A., Andolfi, A., Maddau, L., Franceschini, A., Biscopyran, M. F., 2005. Biscopyran, a Phytotoxic Hexasubstituted Pyranopyran Produced by Biscogniauxia mediterranea, a Fungus Pathogen of Cork Oak. Jornal of Natural Products (68) 568-571.

Elnagdi, M. H., Adbel-Motaleb, R. M., Mustafa, M., 1987. Studies on heterocyclic enamines: New syntheses of 4H-pyranes, pyranopyrazoles and pyranopyrimidines. J. Heterocycl. Chem. (24) 1677- 1681.

Harb, A. F., Hesien, A. M., Metwally, S. A., Elnagdi Liebigs, M. H., 1989. The use of some activated nitriles in heterocyclic syntheses. Ann. Chem. (26) 585-588.

Kumar, D., Reddy, V. B., Mishra, B. G., Rana, R. K., Nadagouda, M. N., Varma, R. S., 2007. Nanosized magnesium oxide as catalyst for the rapid and green synthesis of substituted 2-amino-2-chromenes. Tetrahedron (63) 3093-3097.

Kumar, D., Reddy, V. B., Sharad, S. H., Dube, U., Kapur, S., 2009. A facile one-pot green synthesis and antibacterial activity of 2-amino-4H-pyrans and 2-amino-5-oxo-5,6,7,8-tetrahydro-4H-chromenes. Eur. J. Med. Chem. (44) 3805- 3809.

Khaligh, N.G., 2015. 4-(Succinimido)-1-butane sulfonic acid as a Brönsted acid catalyst for synthesis of pyrano [4, 3-b] pyran derivatives under solvent-free conditions. Chinese Chemical Letters, (26) 26-30.

Kazuya, N., AkIRa, F., 2012. TiO_2 photocatalysis: Design and applications. Journal of Photochemistry and Photobiology C: Photochemistry (13) 169-189.

Li, W, L., Wu, L, Q., Yan, F, L., 2011. Alum-catalyzed one-pot synthesis of dihydropyrano [3,2-b]chromenediones. Journal of the Brazilian Chemical Society (22) 2202-2205.

Martin, N., Pascual, C., Seoane, C., Soto, J, L., 1987. The use of some activated nitriles in heterocyclic syntheses. Heterocycles (26) 2811-2816.

Moshtaghi, Z. A., Eskandari, I., Moghani, D., 2012. Acceleration of Multicomponent Reactions in Aqueous Medium: Multicomponent Synthesis of a 4H-pyran Library. Chem. Sci. Trans. (1) 91-102.

Perez-Perez, M., Balzarini, J., Rusenski, J., De-Clereq, E., Herdewijn, P., 1995.Synthesis and antivIRal activity of phosphonate derivatives of enantiomeric dihydro-pyranyl nucleosides. Bioorg. Med. Chem. Lett. (5) 1115-1118.

Pałasz, A., Jelska, K., Ożog, M., Serda, P., 2007. 5-Arylidene Derivatives of Meldrum's Acid as Synthons in Pyrano [4, 3-b] pyran Synthesis. Monatsch Chem (138) 481-488.

Philipp, A., JIRkovsky, I. and Martel, R. R., 1980. Synthesis and antiallergic properties of some 4H, 5H-pyrano [3, 2-c][1] benzopyran-4-one, 4H, 5H-[1] benzothiopyrano [4, 3-b] pyran-4-

one, and 1, 4-dihydro-5H-[1] benzothiopyrano [4, 3-b] pyridin-4-one derivatives. Journal of medicinal chemistry, 23(12), 1372-1376.

Reddy, B. V. S., Reddy, M. R., Narasimhulu, G., Yadav, J. S., 2010. $InCl_3$-catalyzed three-component reaction: a novel synthesis of dihydropyrano [3,2-b]chromenediones under solvent-free conditions. Tetrahedron Lett. (51) 5677- 5679.

Rahmati, A., 2010. Synthesis of 4-aryl-3-methyl-6-oxo-4,5,6,7-tetrahydro-2H-pyrazolo[3,4-b]pyridine-5-carbonitrile via a one-pot, three-component reaction.Tetrahedron Lett. (51) 2967-2970.

Rahmati, A., Alizadeh- Kouzehrash, M., 2011. Microwave-induced Stereoselectivity in Synthesis of trans-4-Aryl-3-methyl-6-oxo-4, 5, 6,7-tetrahydro-2H-pyrazolo [3, 4-b]pyridine-5-carbonitriles. Chin J Chem. (29) 2373-2378.

Sagar, R., Park, J., Koh, M., Park, S. B., 2009. Diastereoselective Synthesis of Polycyclic Acetal-Fused Pyrano [3,2-c]pyran-5(2H)-one Derivatives. J. Org Chem. (74) 2171-2174.

Seshu Babu, N., Pasha, N., Venkateswara Roa, K. T., Sai Prasad, P, S., Lingaiah, N., 2008. A heterogeneous strong basic Mg/La mixed oxide catalyst for efficient synthesis of polyfunctionalized pyrans. Tet. Lett. (49) 2730-2733.

Taylor, R. N., Cleasby, A., Singh, O., Sharzynski, T., 1995. Utility of β-diketones in heterocyclic synthesis: Synthesis of new tetrahydro-pyrimidinethione, pyrazole, thiophene, dihydropyridine, dihydropyrane, pyridazine derivatives and investigation of theIR antimicrobial activity. J. Med. Chem. (41) 798-807.

Woods, L. L., 1962. The Reactions of Pyrones with Carboxylic Acids, Esters, and Chloromethyl Ether. J. Org. Chem. (27) 696-698.

Zayed, S. E., Abou Elmaged, E. I., Metwally, S. A., Elnagd, M. H., 1991. Reactions of six-membered heterocyclic β-enaminonitriles with electrophilic reagents. Collect Czech. Chem.Commun. (56) 2175-2182.

APPENDIX

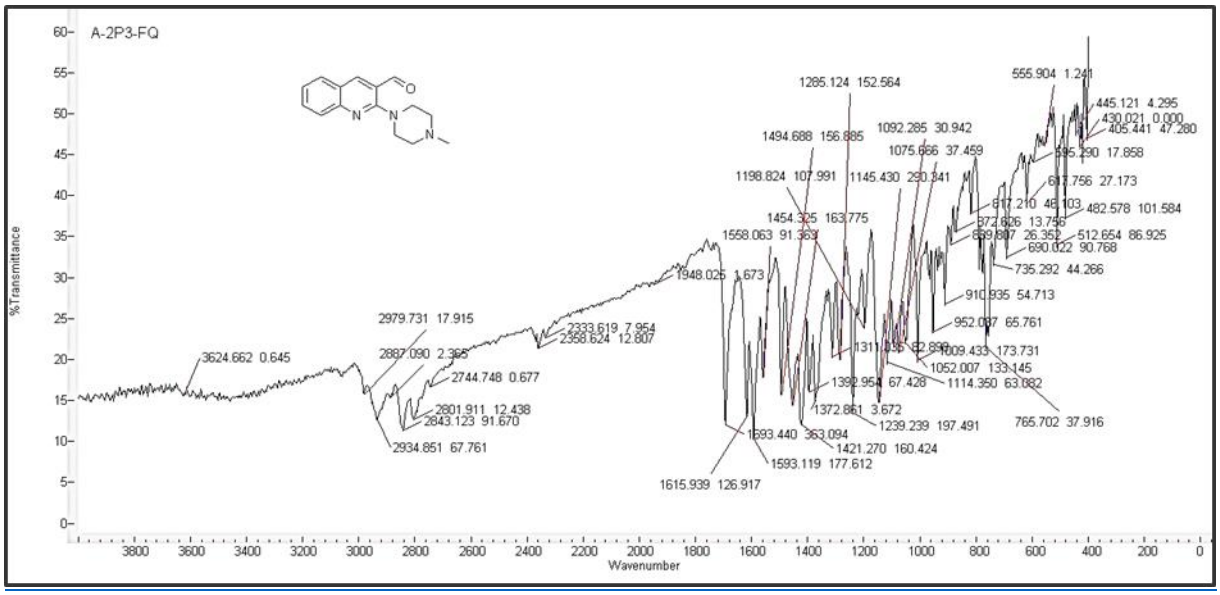

Figure 3. S. 1. The Infra-Red Spectrum of compound 3

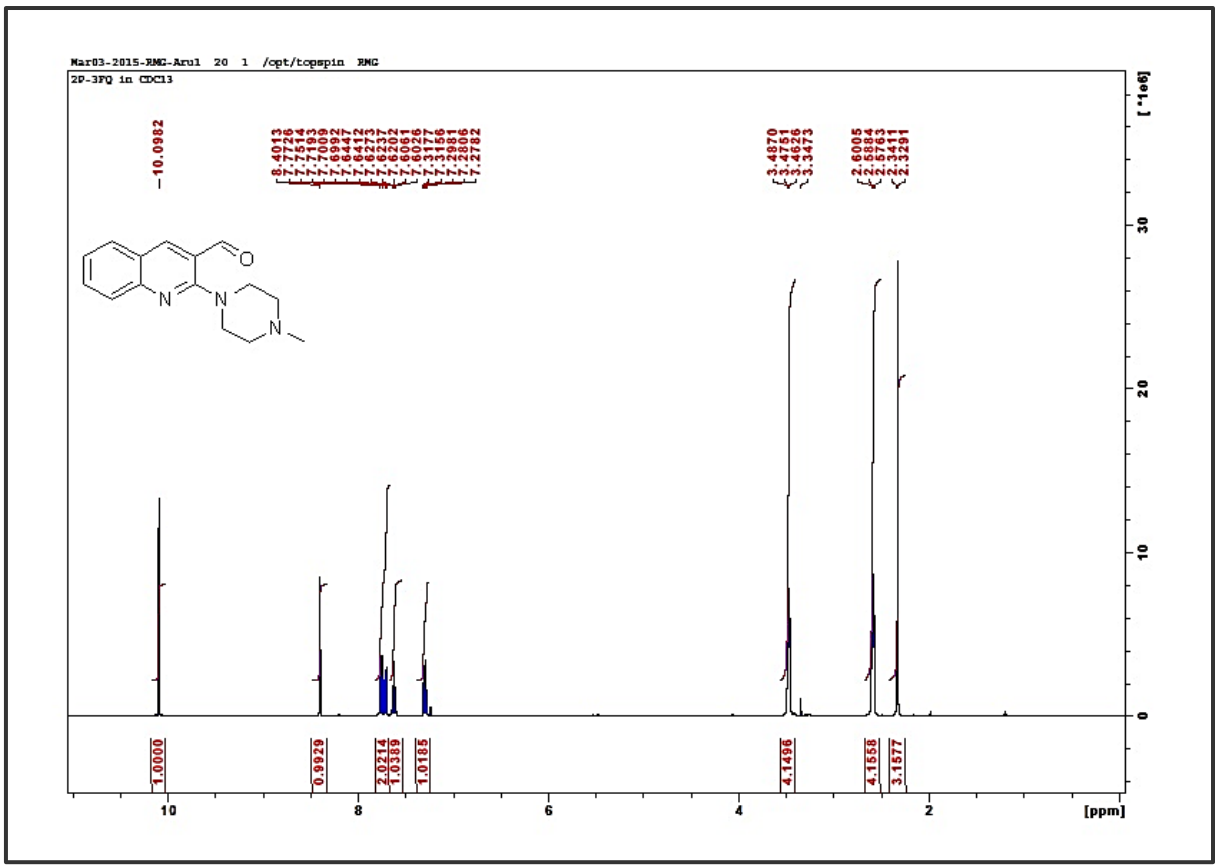

Figure 3. S. 2. The ^{1}H NMR of compound 3

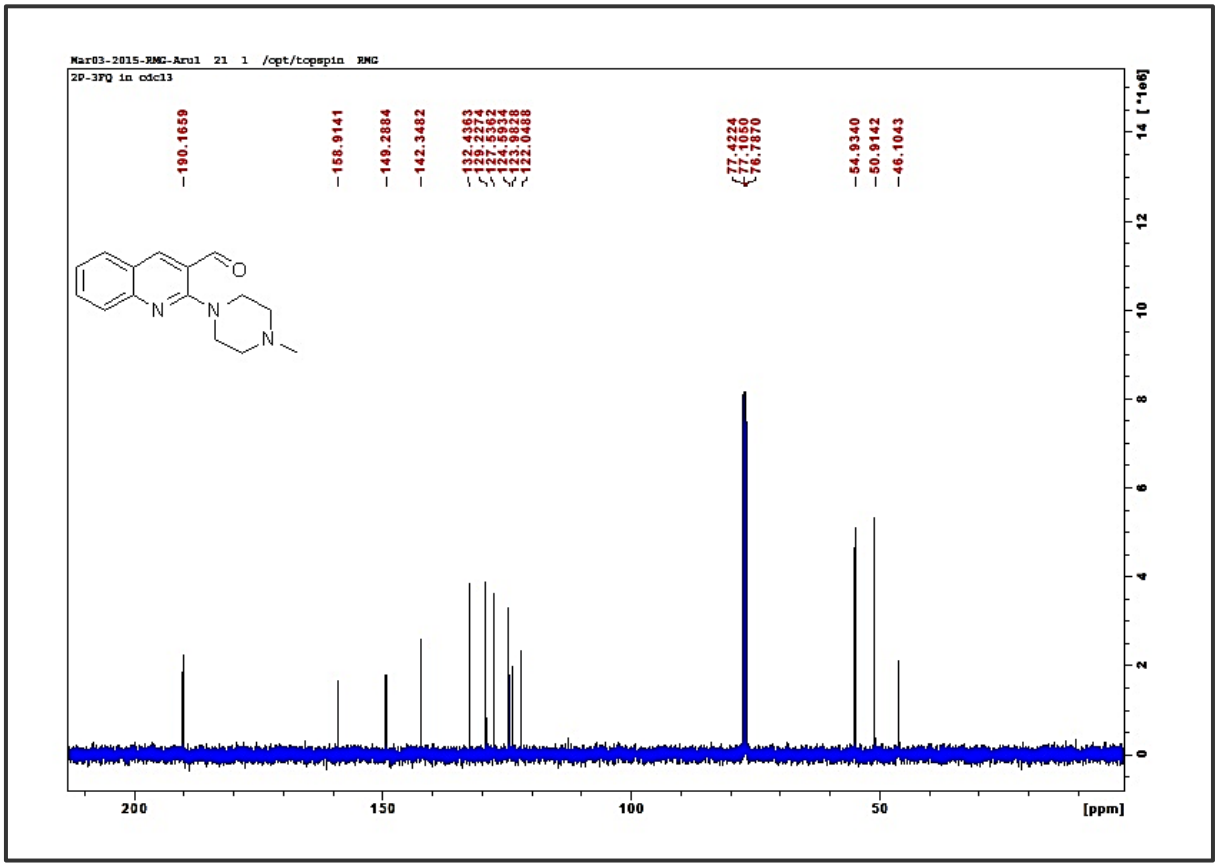

Figure 3. S. 3. The ^{13}C NMR of compound 3

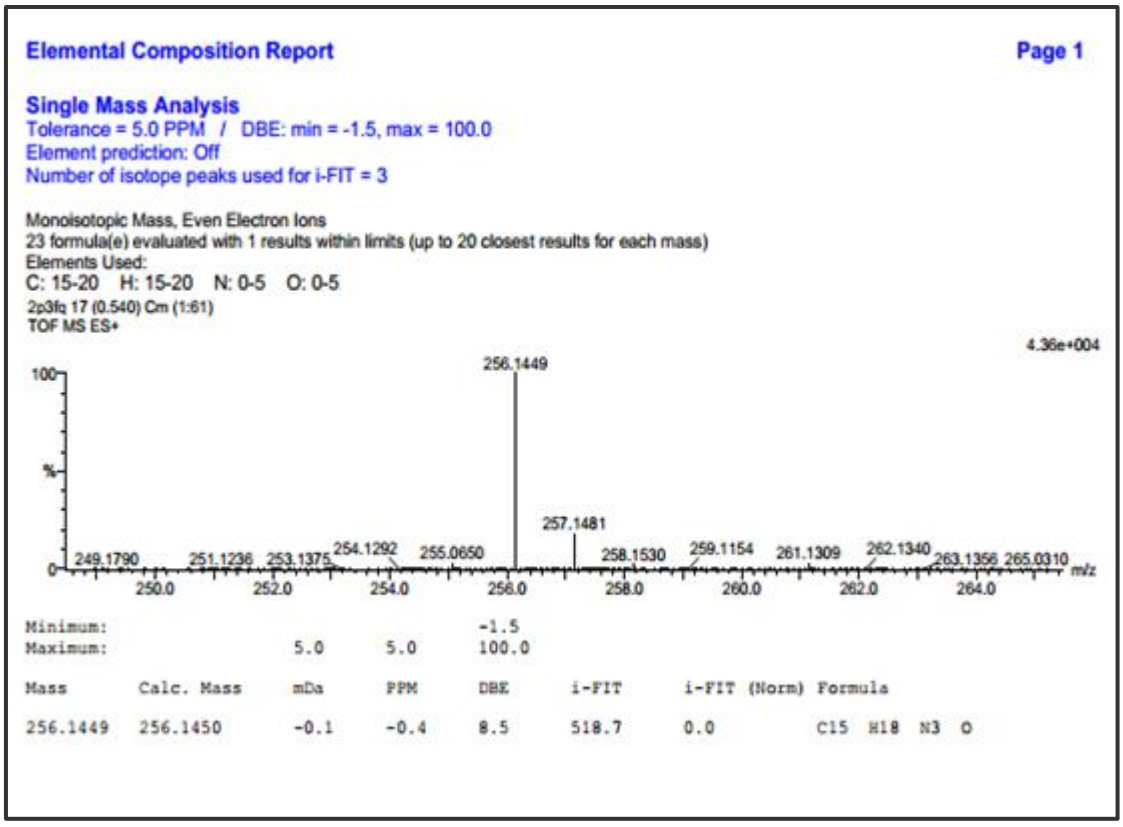

Figure 3. S. 4. The HRMS of compound 3

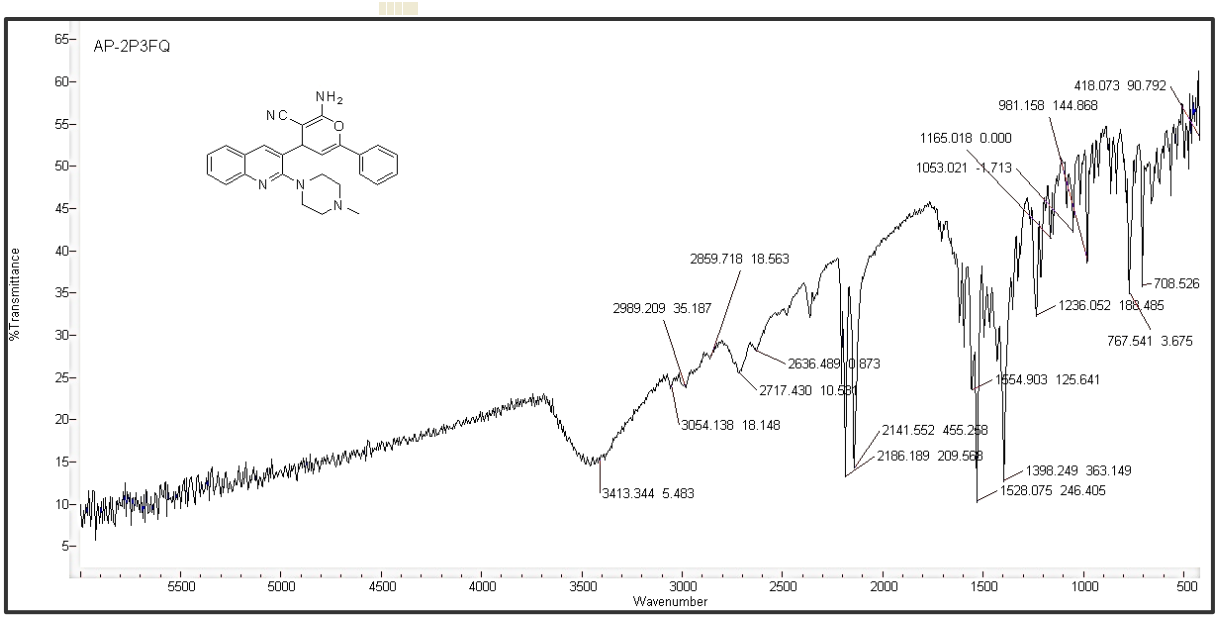

Figure 3. S. 5. The Infra-Red Spectrum spectra of compound 6a

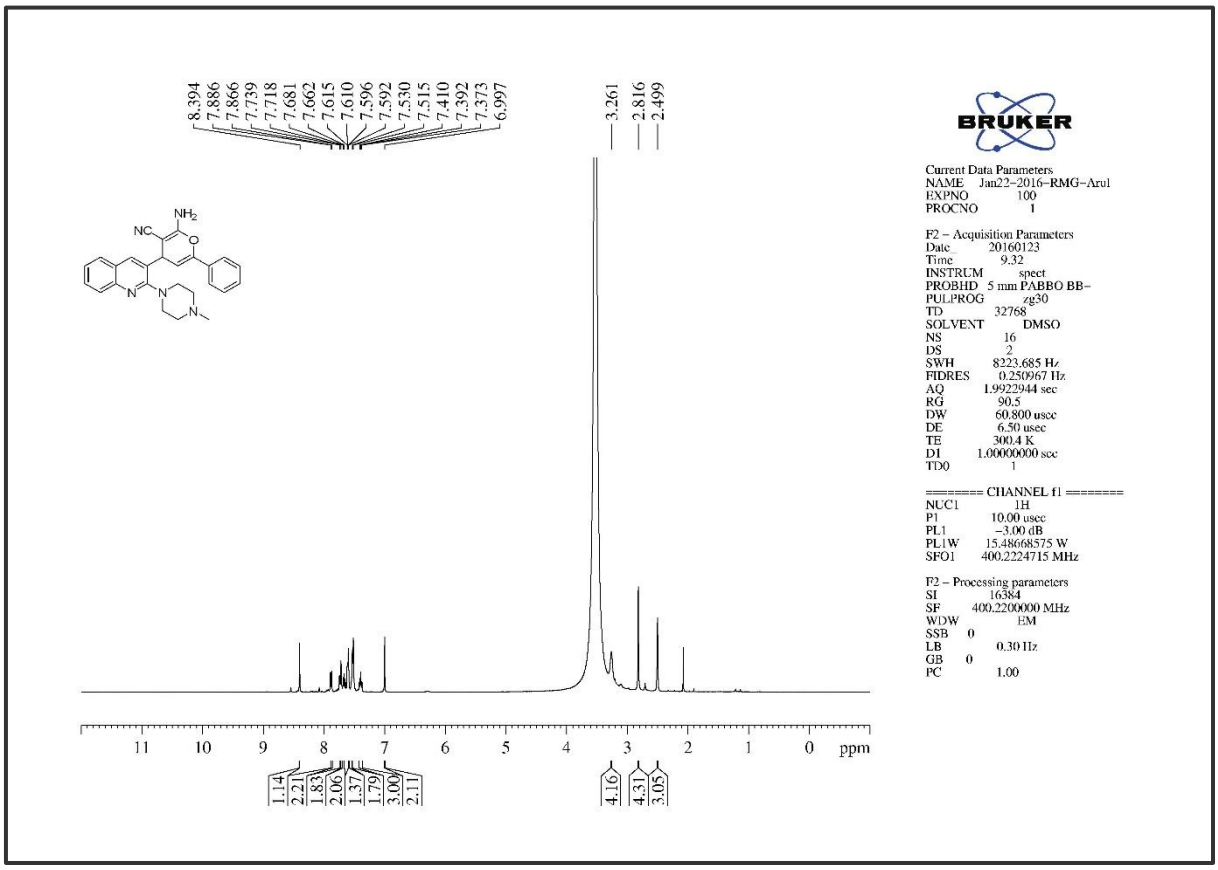

Figure 3. S. 6. The ^{1}H NMR of compound 6a

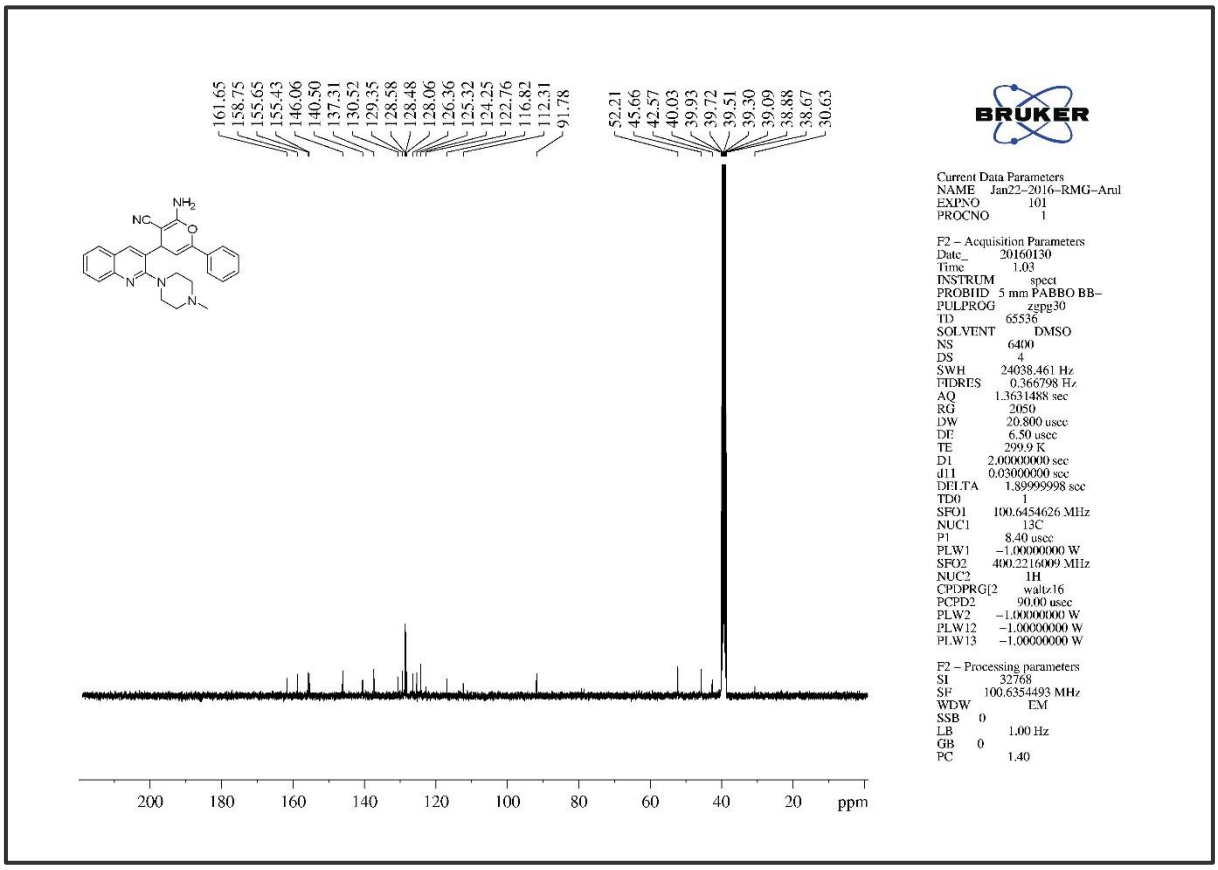

Figure 3. S. 7. The ^{13}C NMR of compound 6a

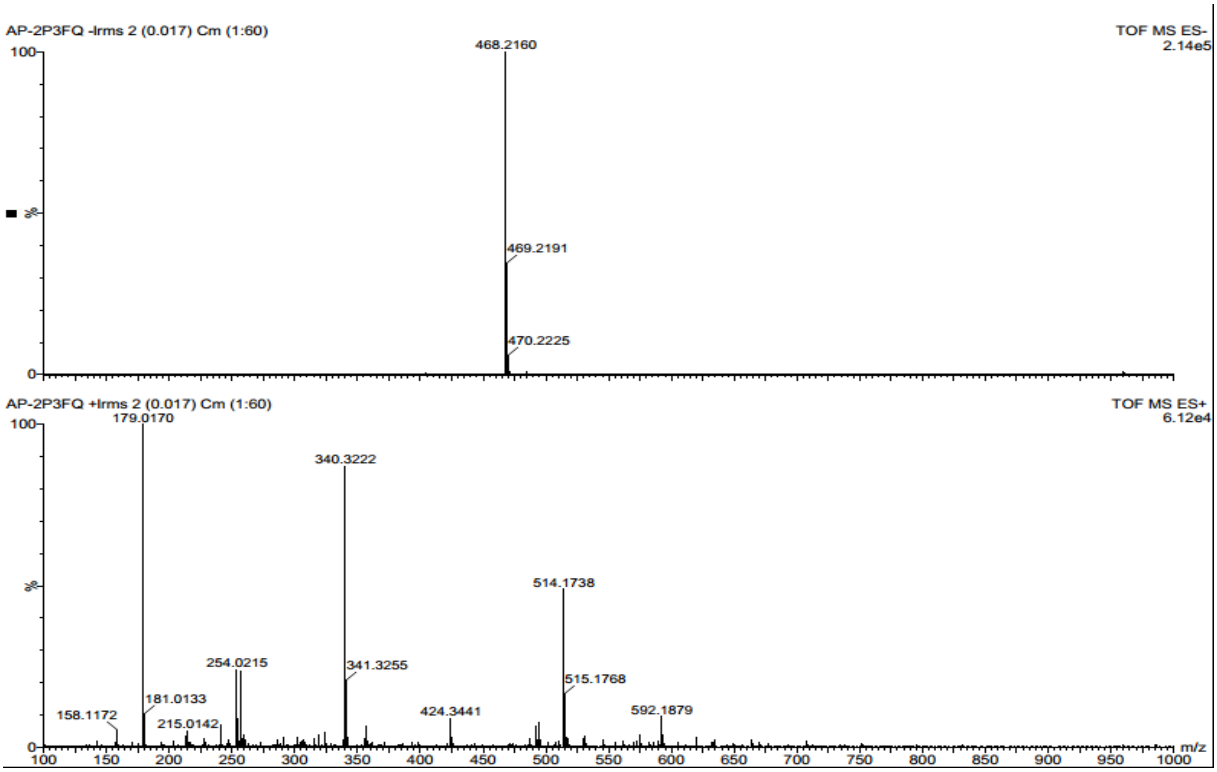

Figure 3. S. 8. The HRMS of compound 6a

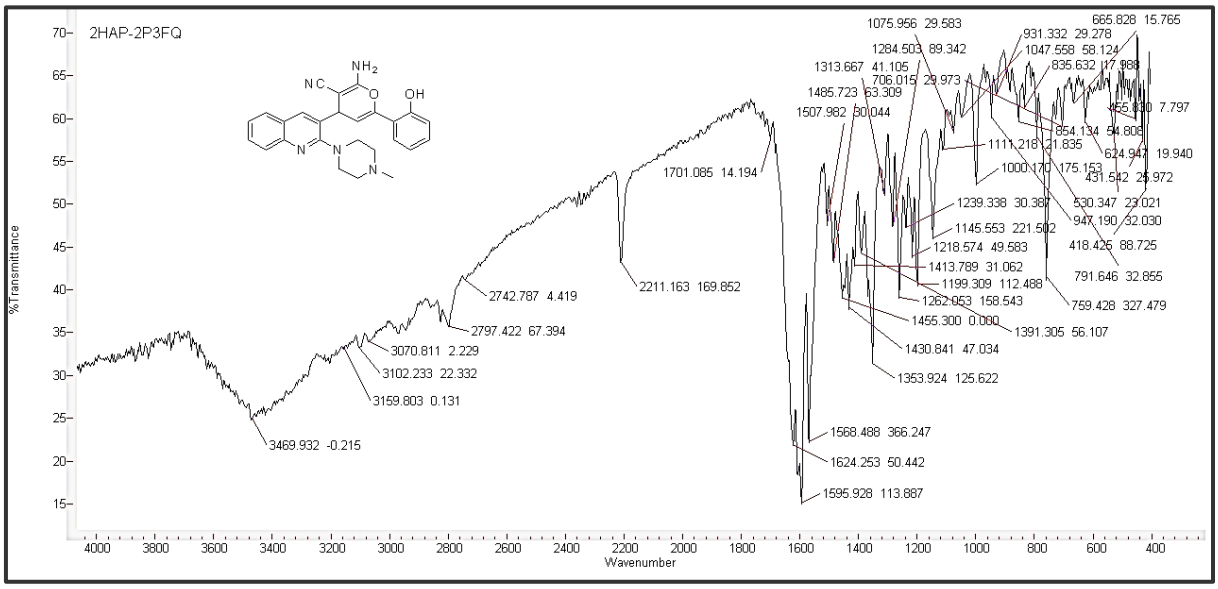

Figure 3. S. 9. The Infra-Red Spectrum of compound 6b

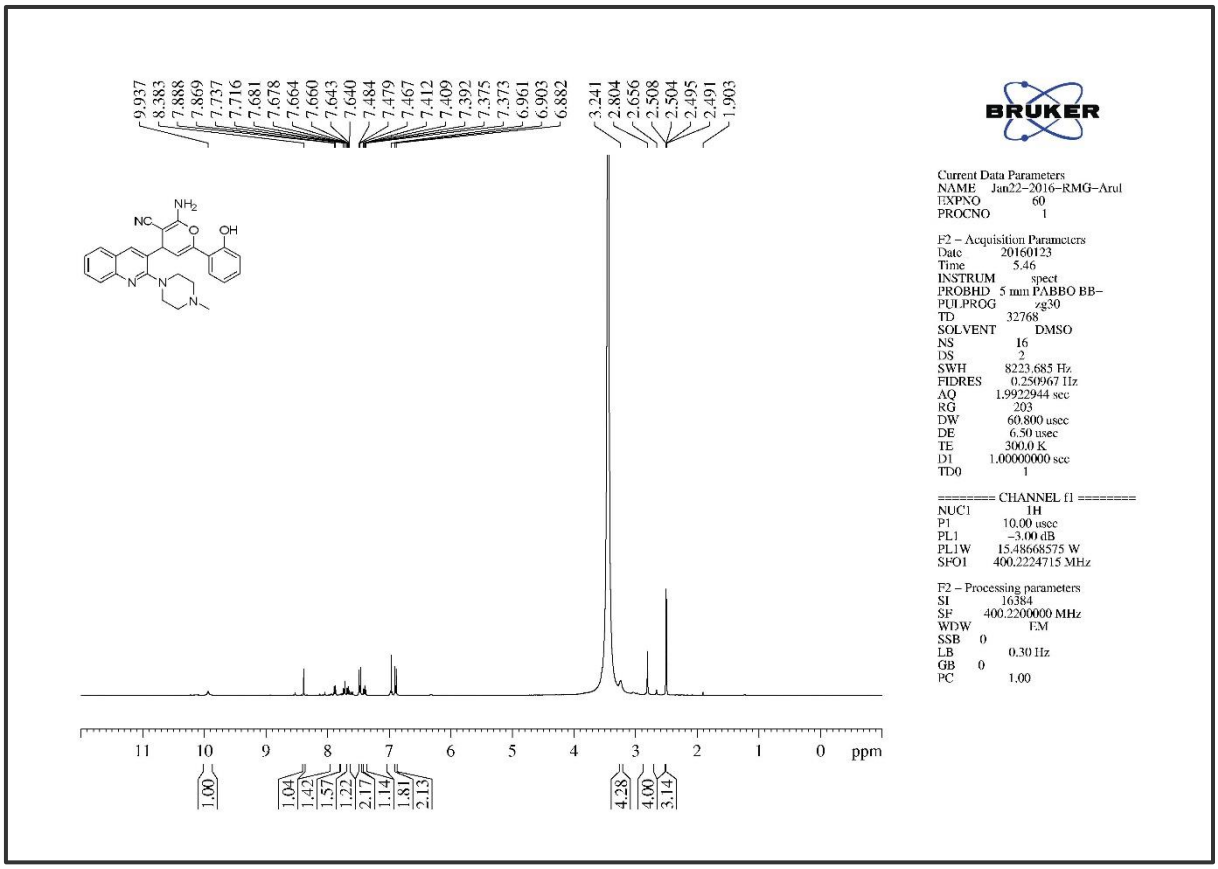

Figure 3. S. 10. The ^{1}H NMR of compound 6b

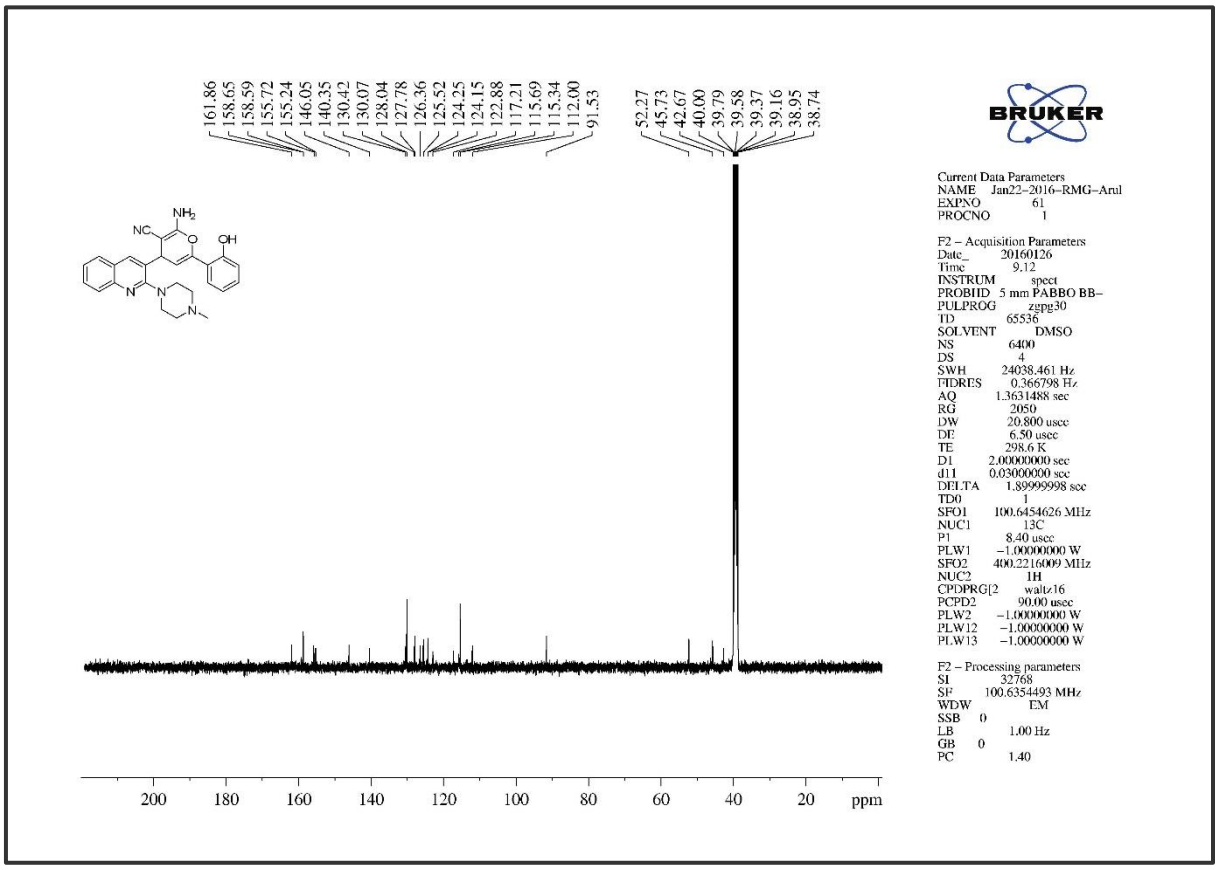

Figure 3. S. 11. The ^{13}C NMR of compound 6b

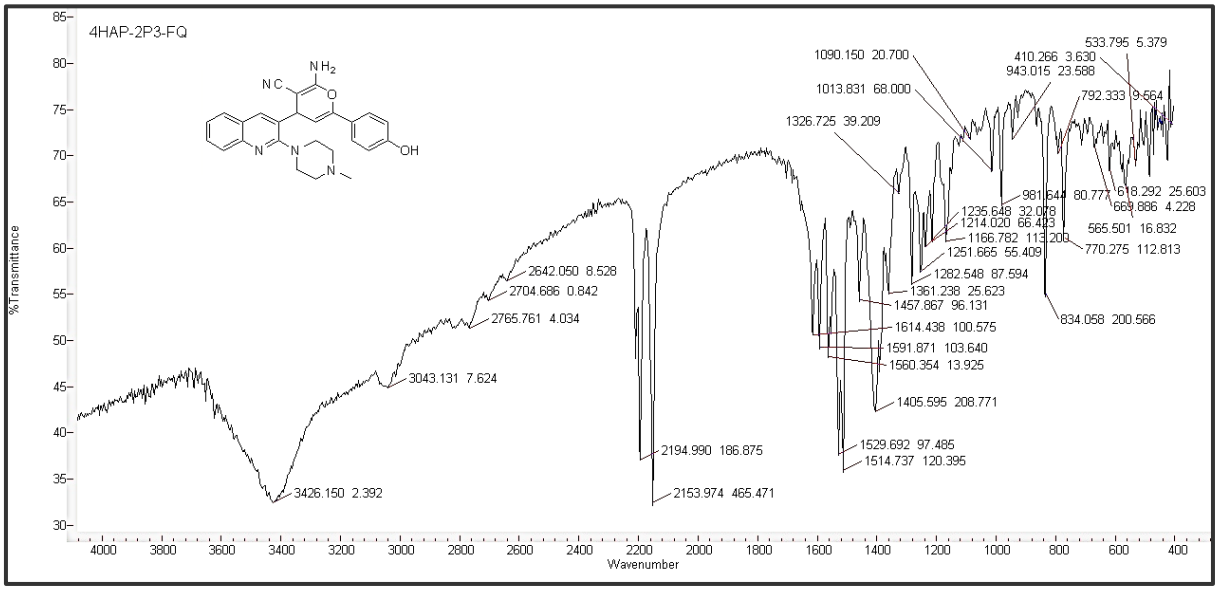

Figure 3. S. 12. The Infra-Red Spectrum of compound 6c

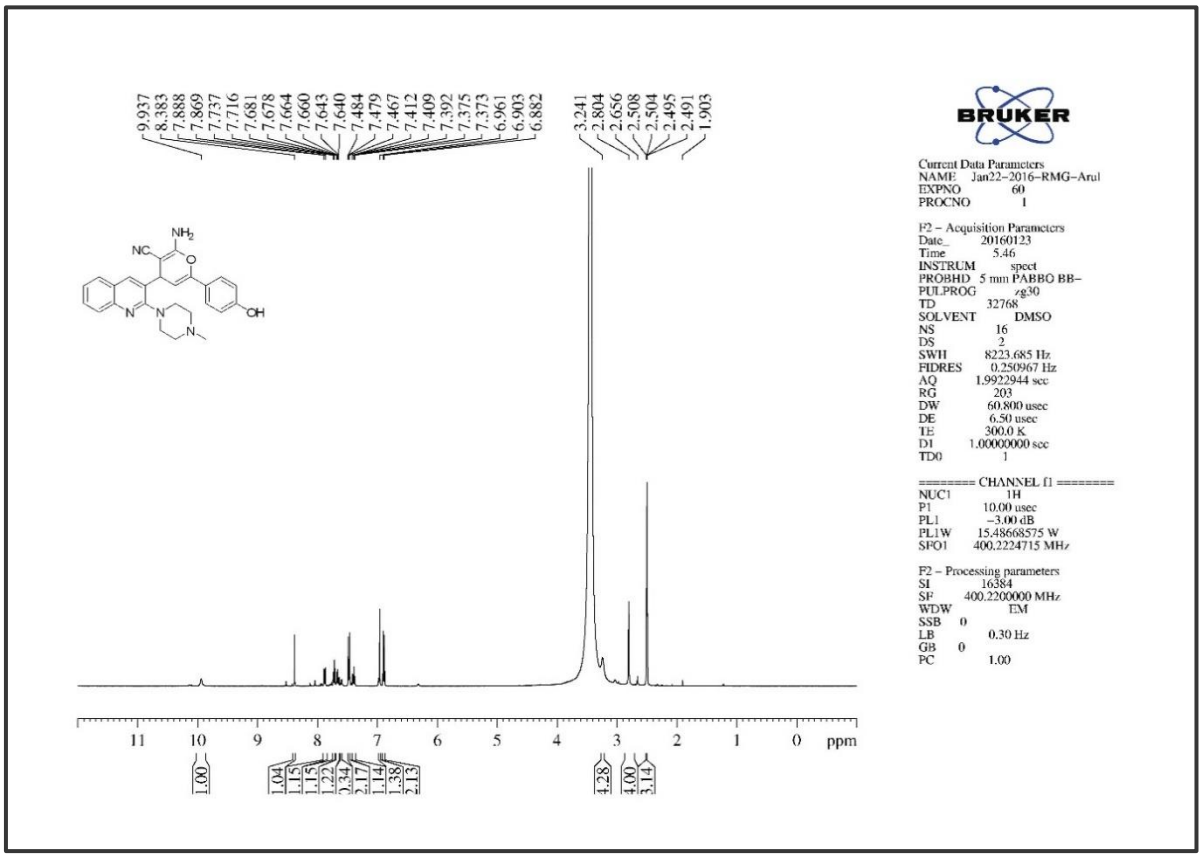

Figure 3. S. 13. The ^{1}H NMR of compound 6c

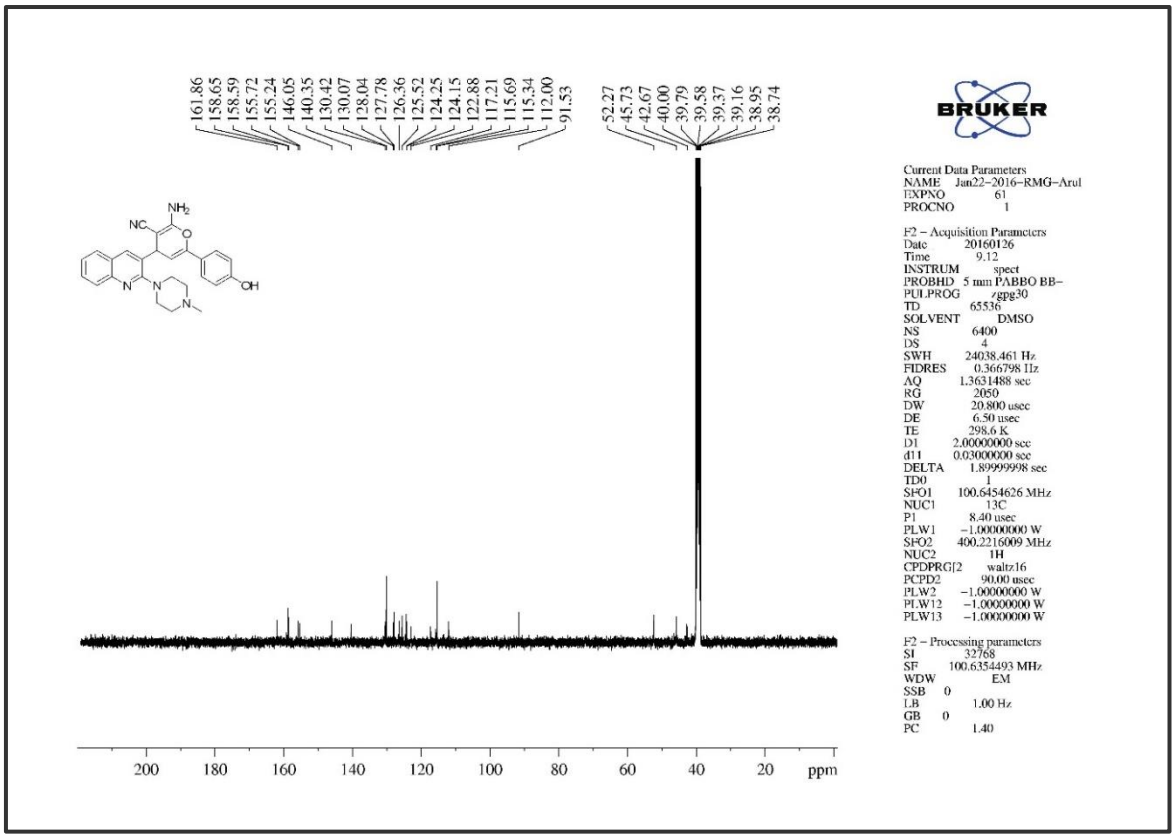

Figure 3. S. 14. The ^{13}C NMR of compound 6c

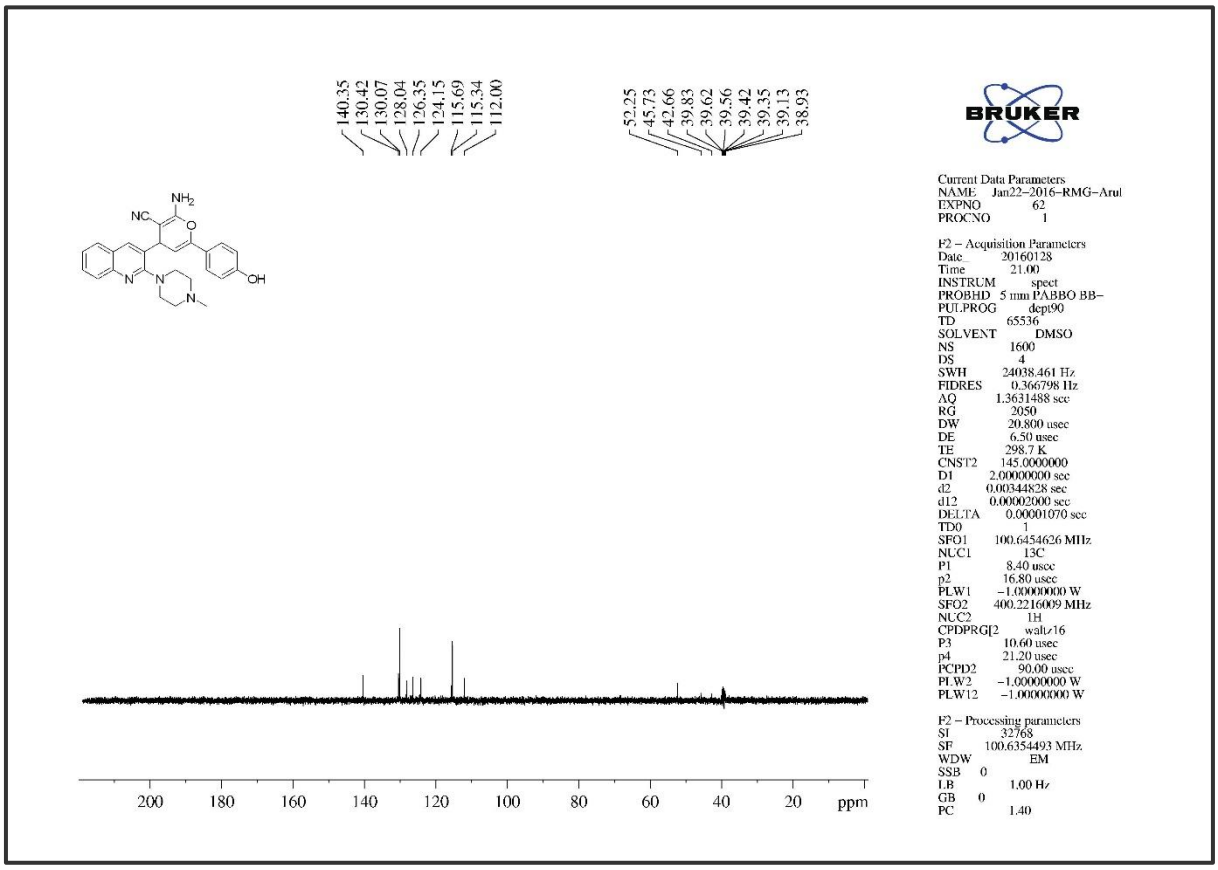

Figure 3. S. 15. The DEPT-90 NMR of compound 6c

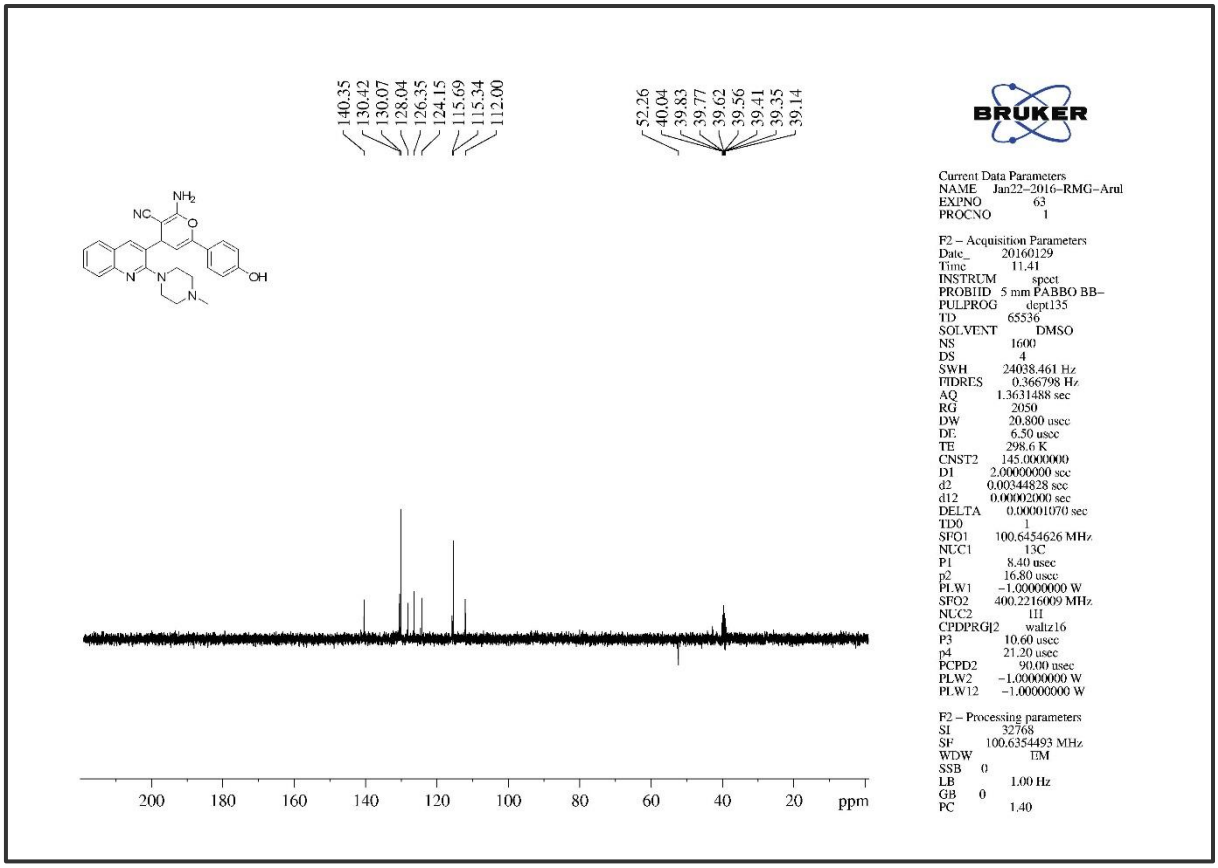

Figure 3. S. 16. The DEPT-135 NMR of compound 6c

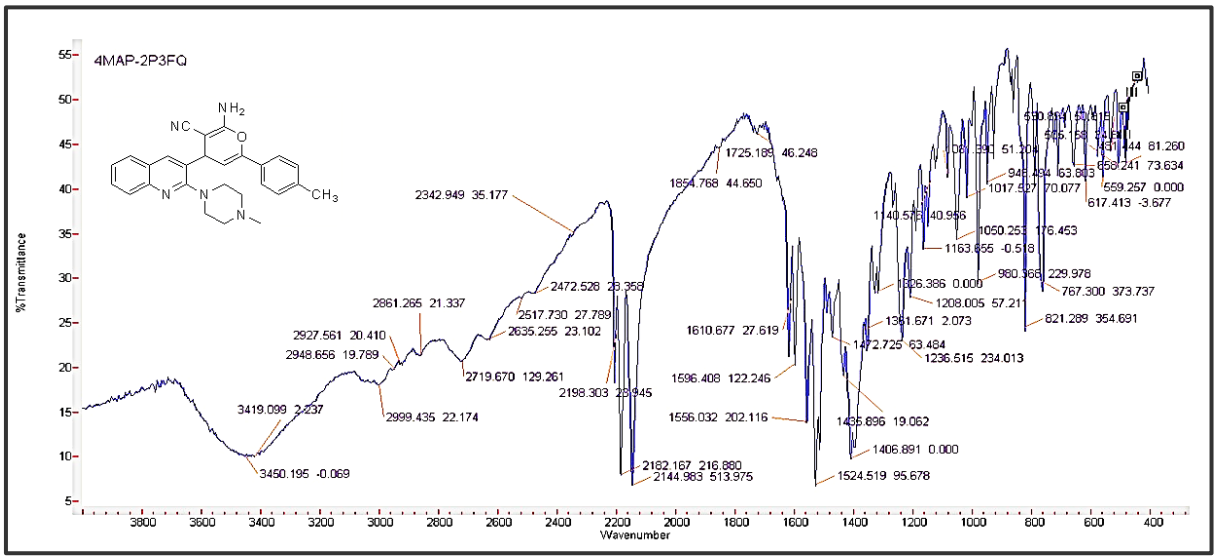

Figure 3. S. 17. The Infra-Red Spectrum of compound 6d

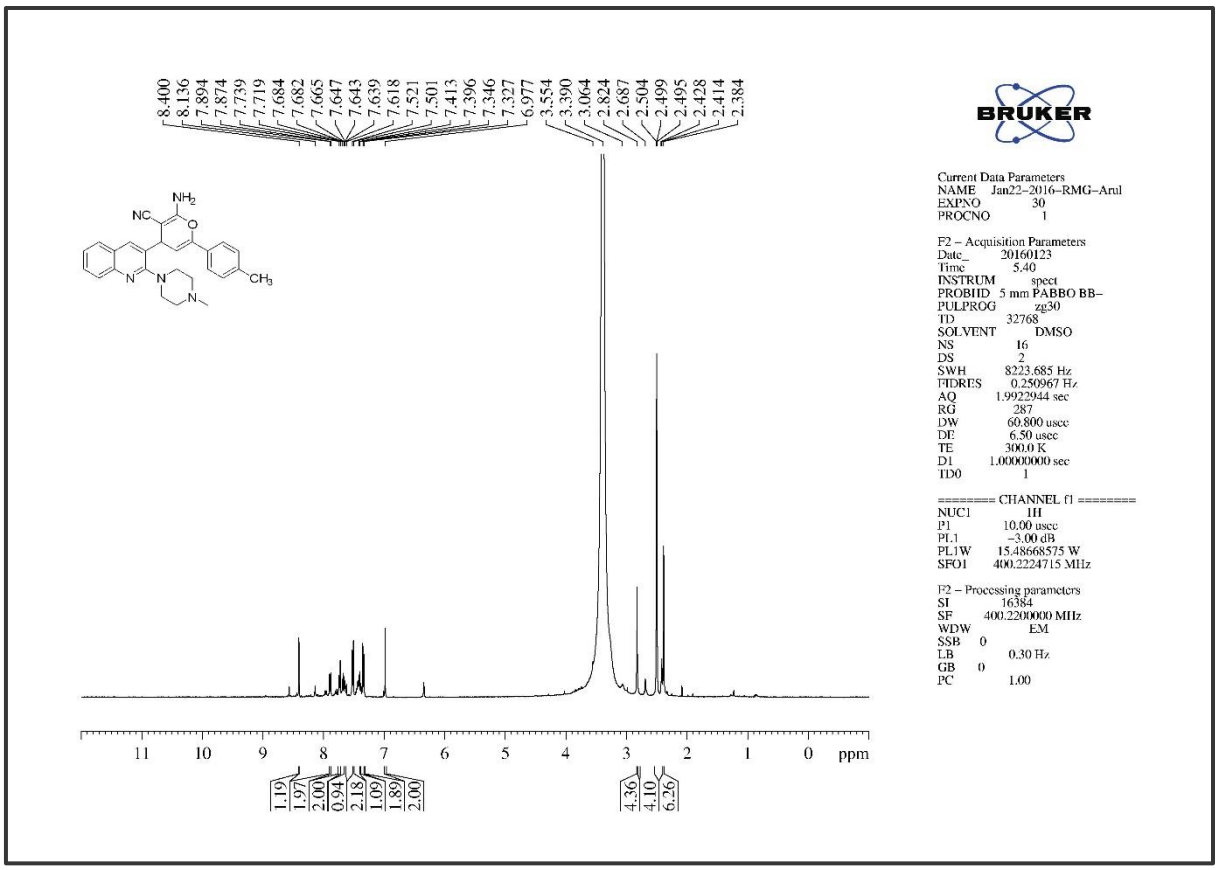

Figure 3. S. 18. The ^{1}H NMR of compound 6d

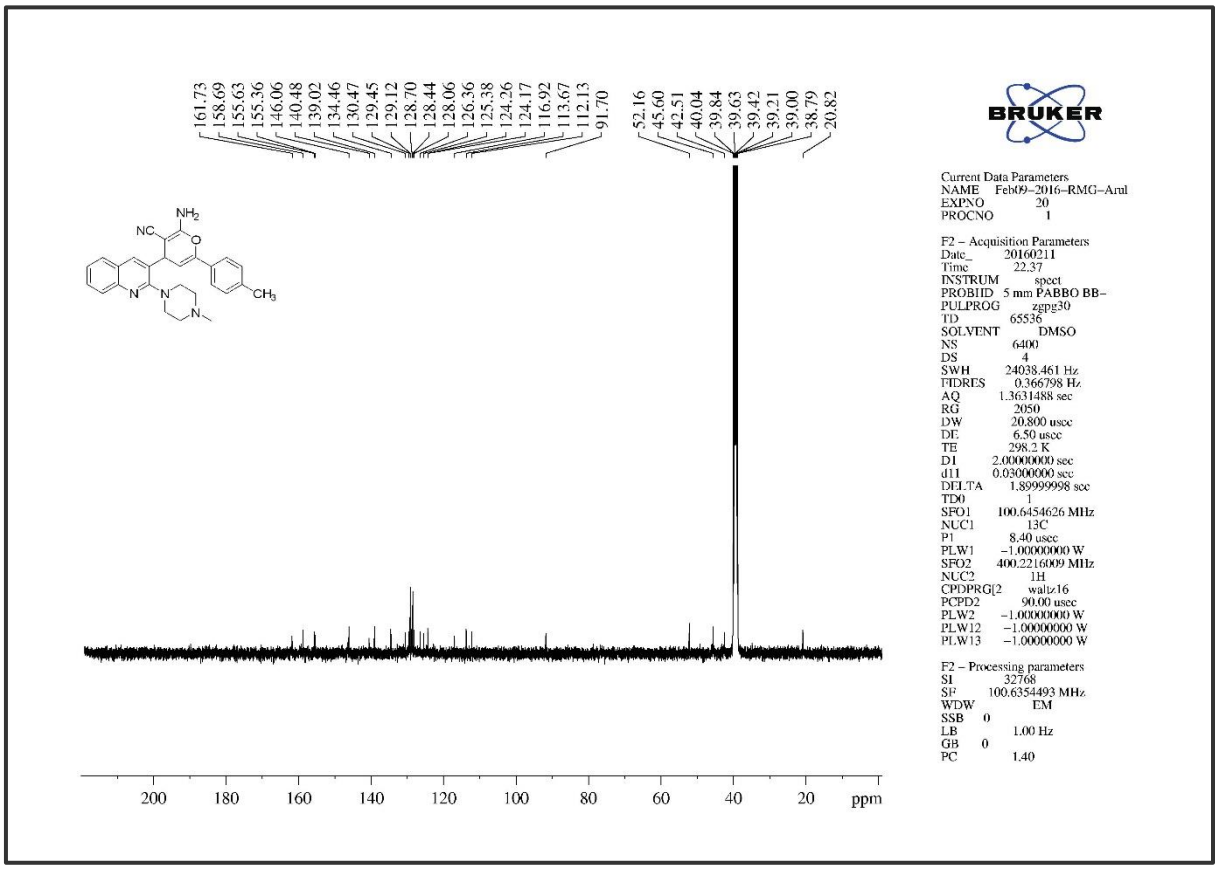

Figure 3. S. 19. The ^{13}C NMR of compound 6d

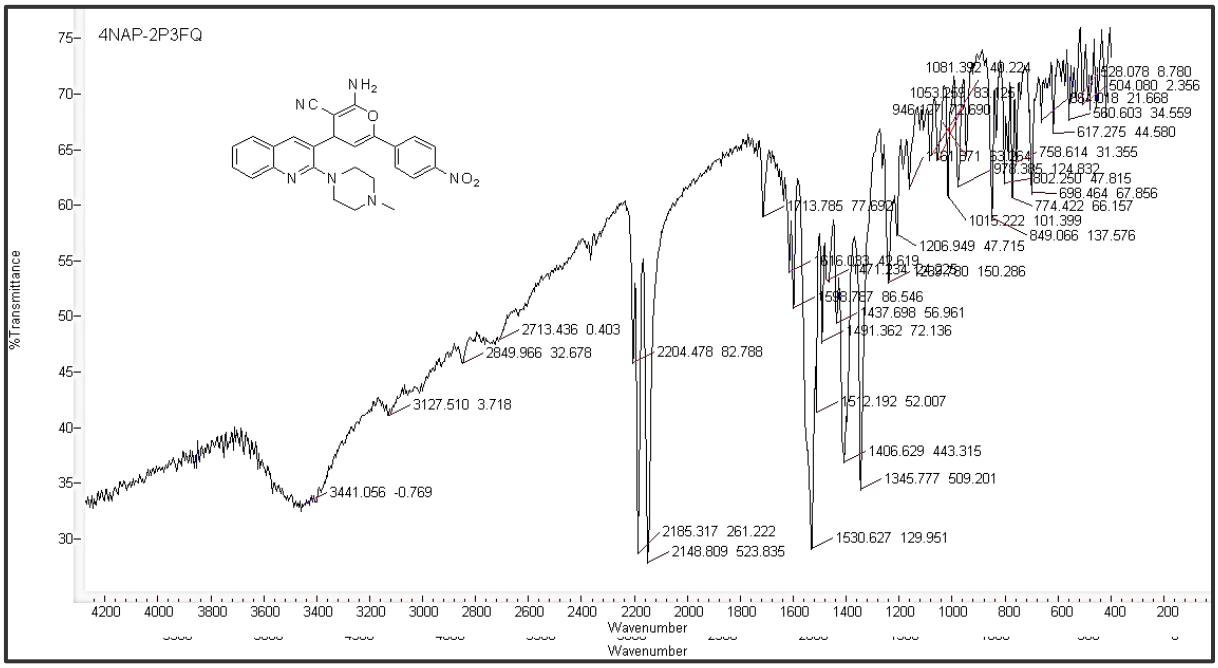

Figure 3. S. 20. The Infra-Red Spectrum of compound 6e

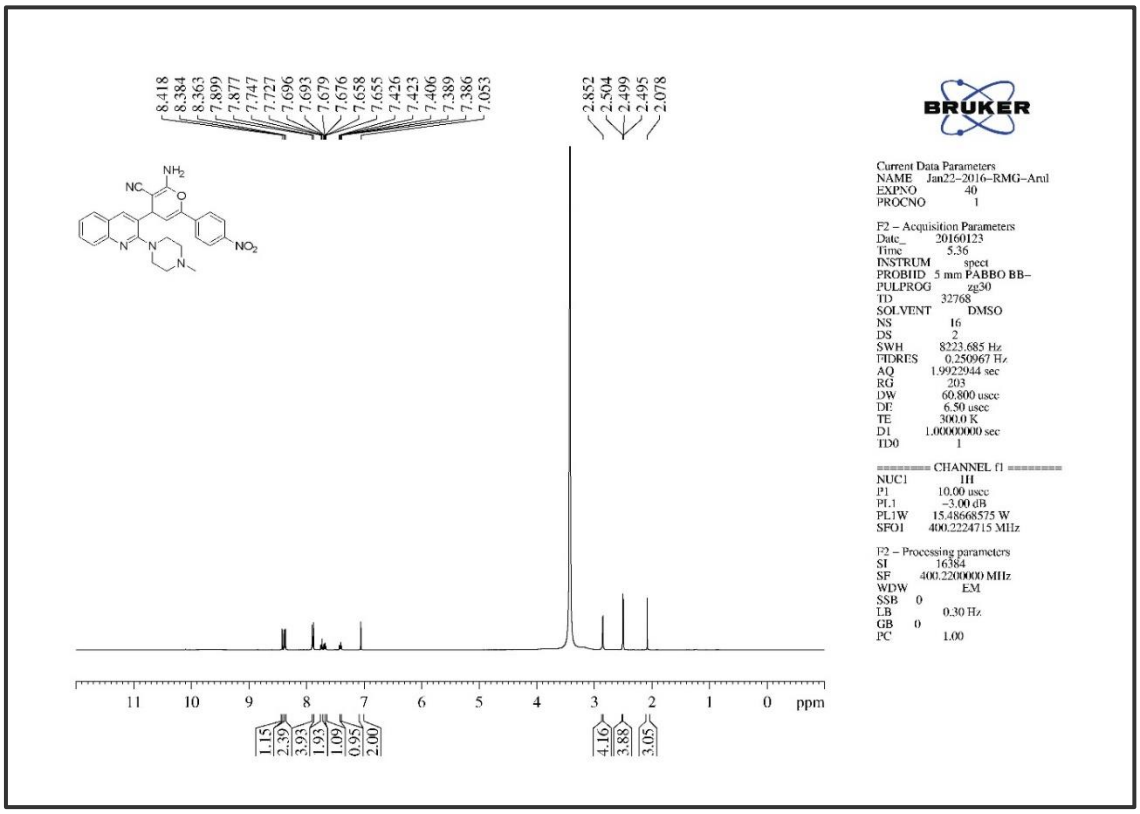

Figure 3. S. 21. The ^{1}H NMR of compound 6e

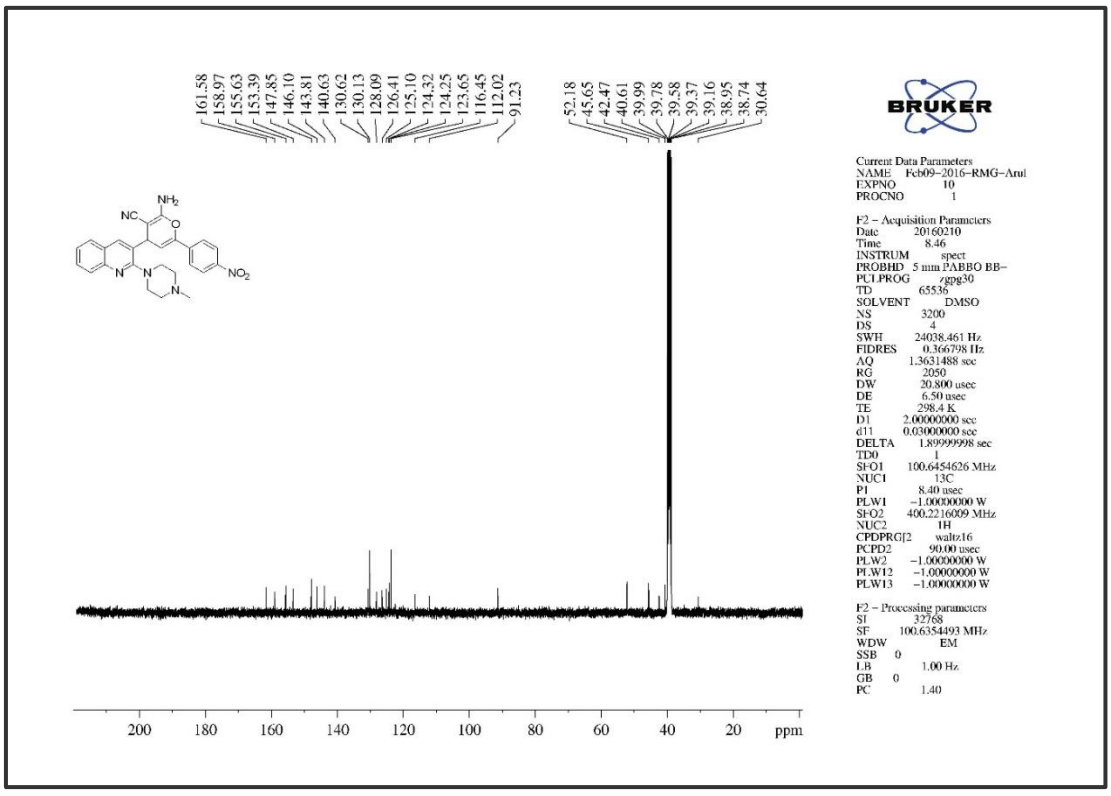

Figure 3. S. 22. The ^{13}C NMR of compound 6e

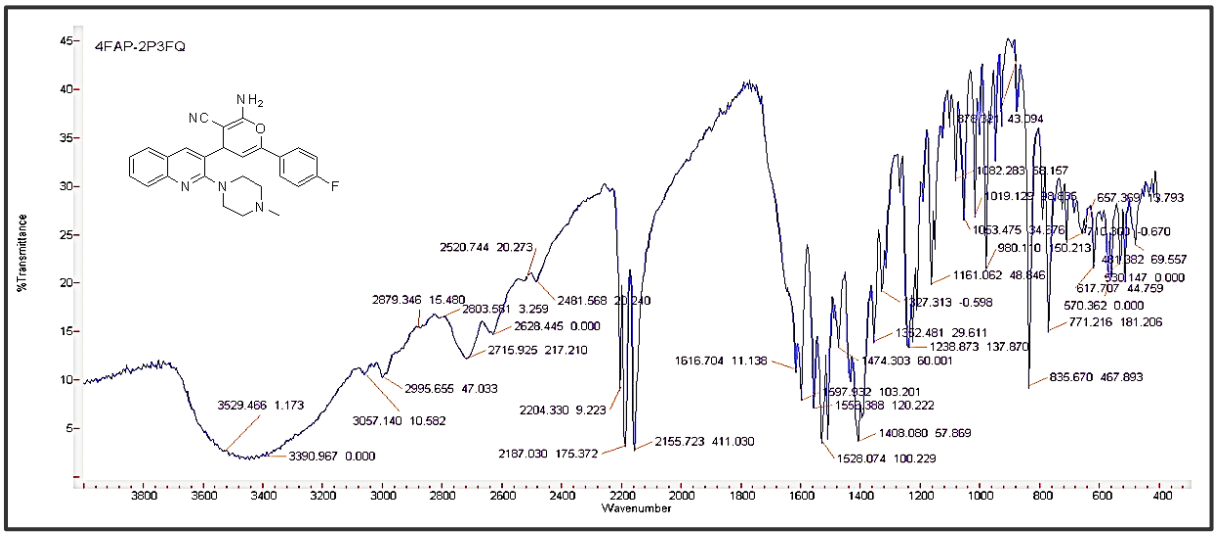

Figure 3. S. 23. The Infra-Red Spectrum of compound 6f

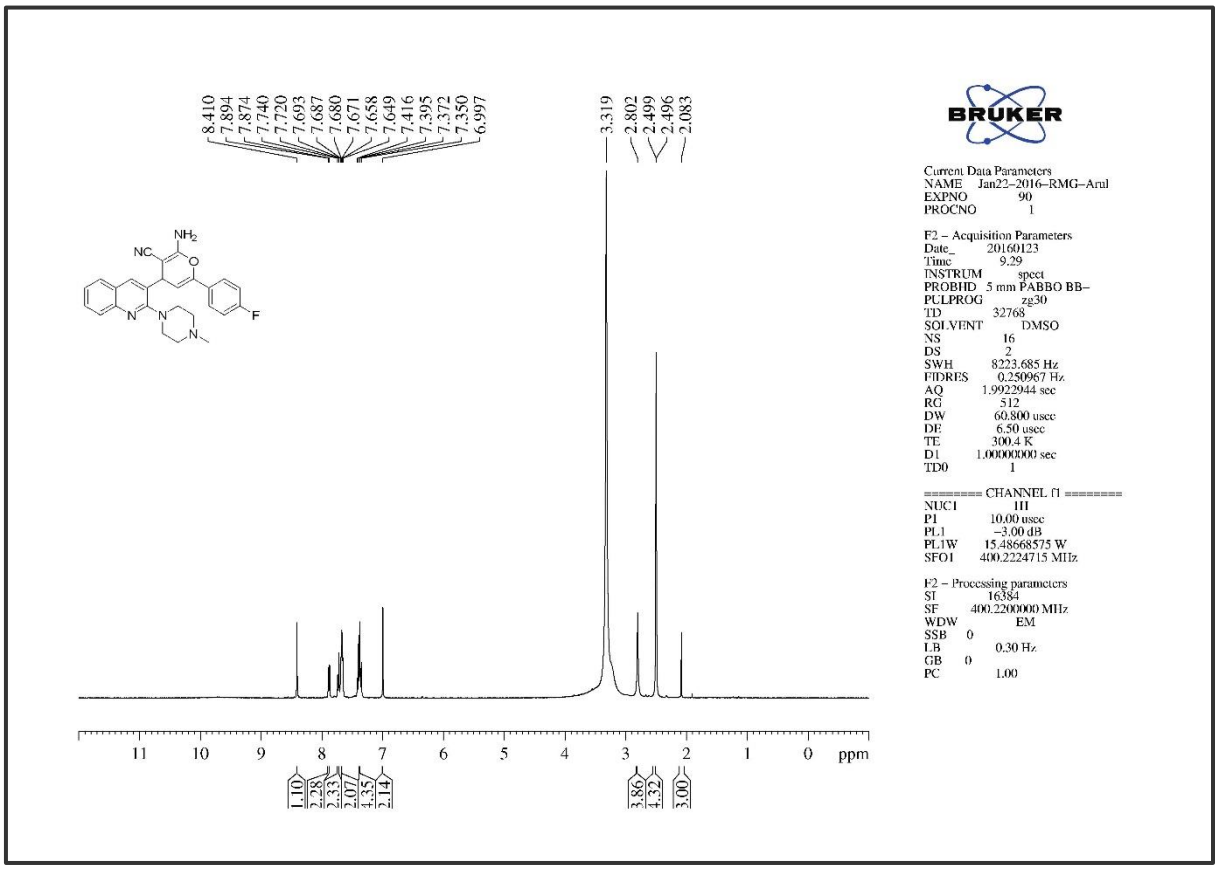

Figure 3. S. 24. The ^{1}H NMR of compound 6f

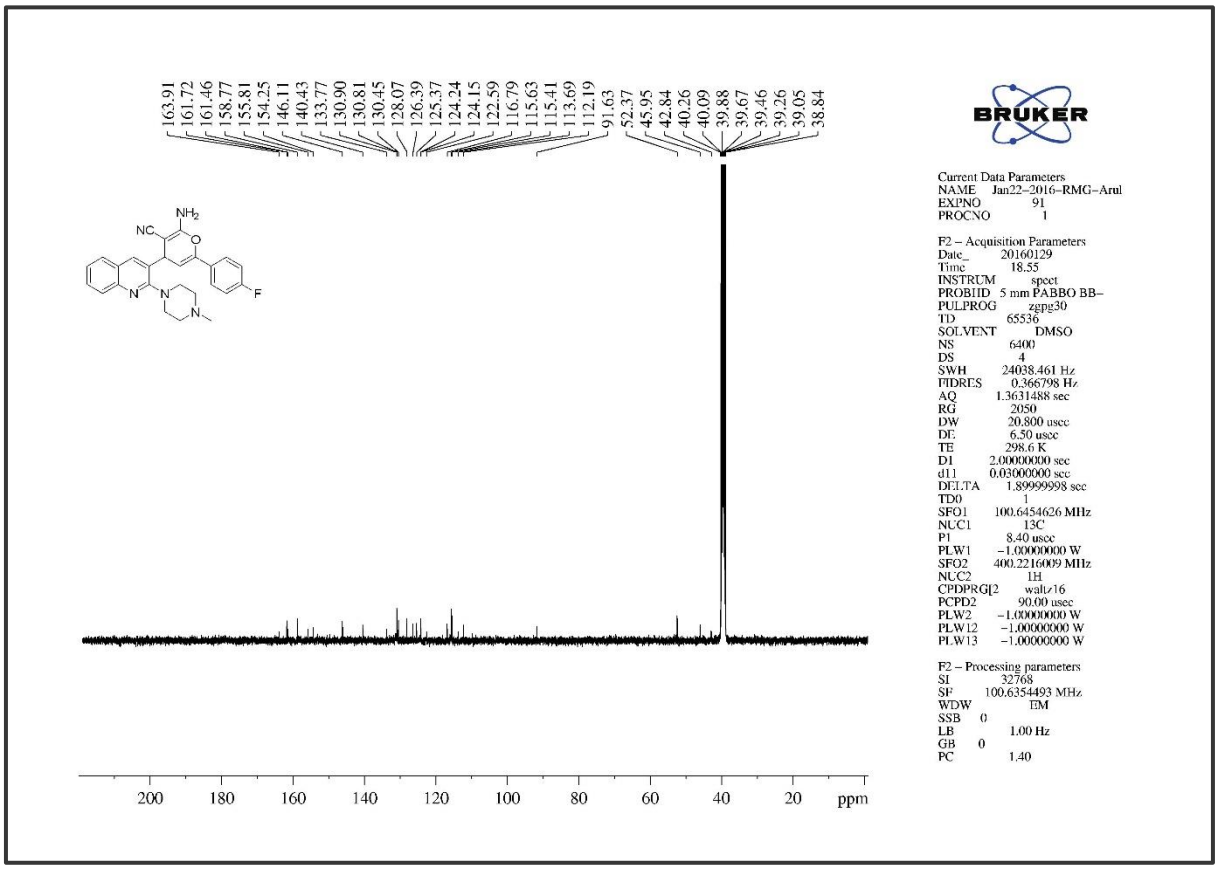

Figure 3. S. 25. The ^{13}C NMR of compound 6f

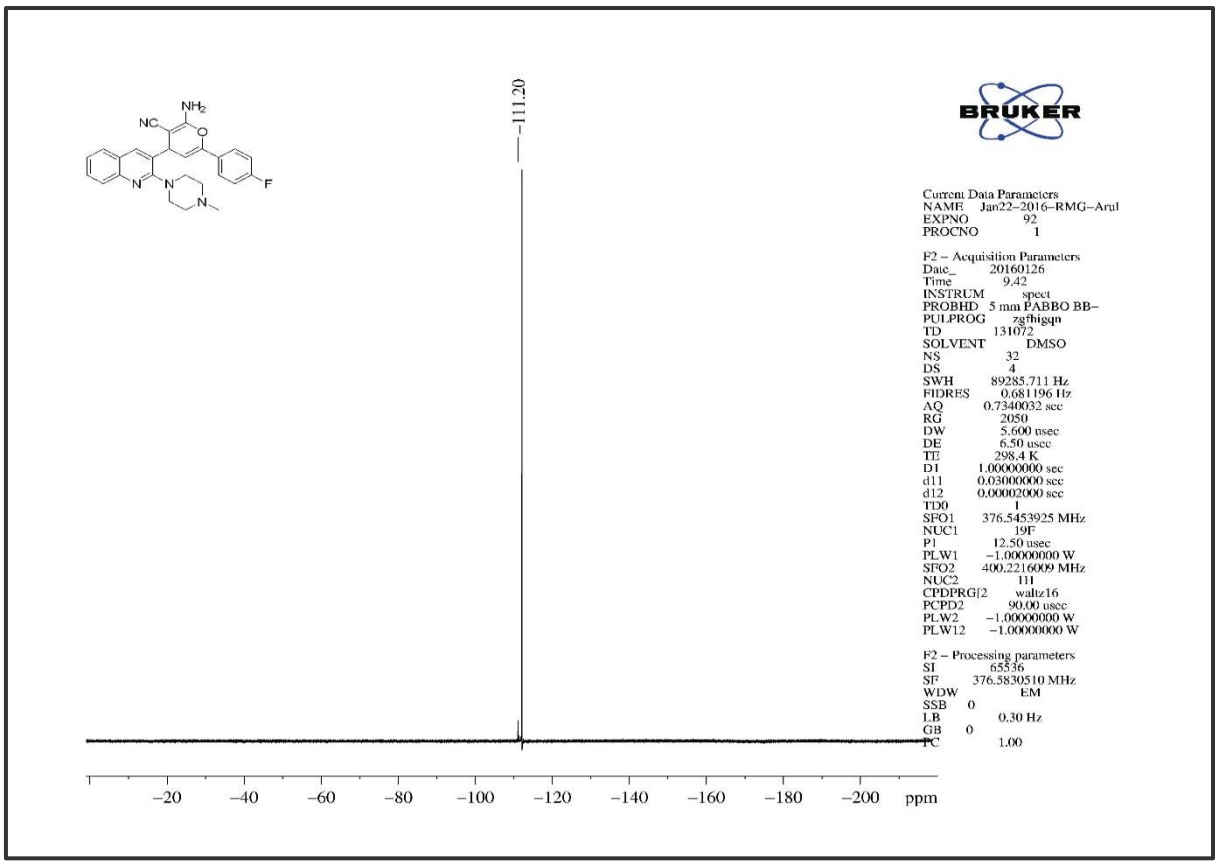

Figure 3. S. 26. The ^{19}F NMR of compound 6f

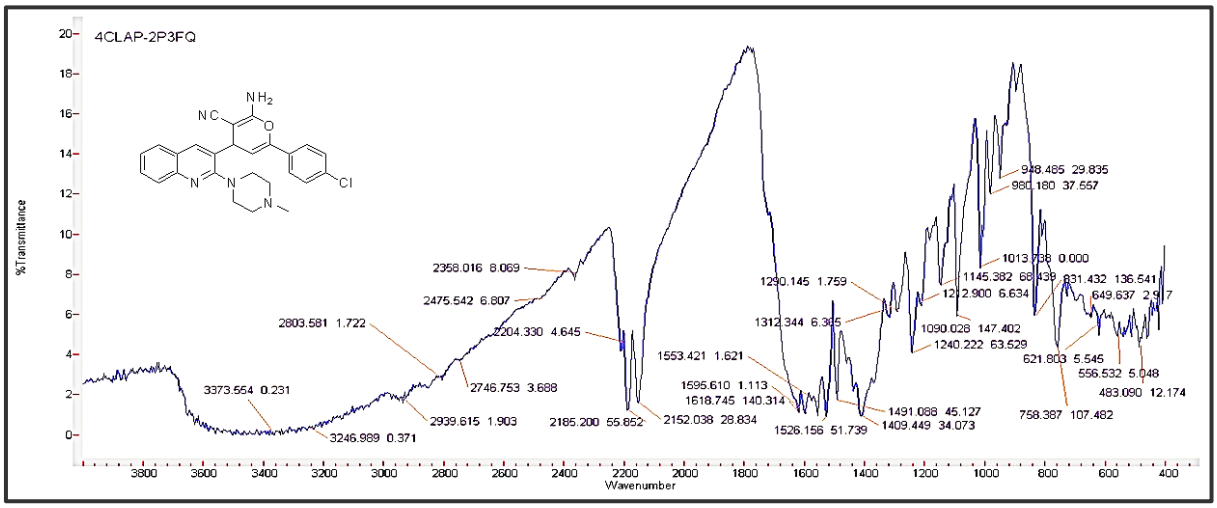

Figure 3. S. 27. The Infra-Red Spectrum of compound 6g

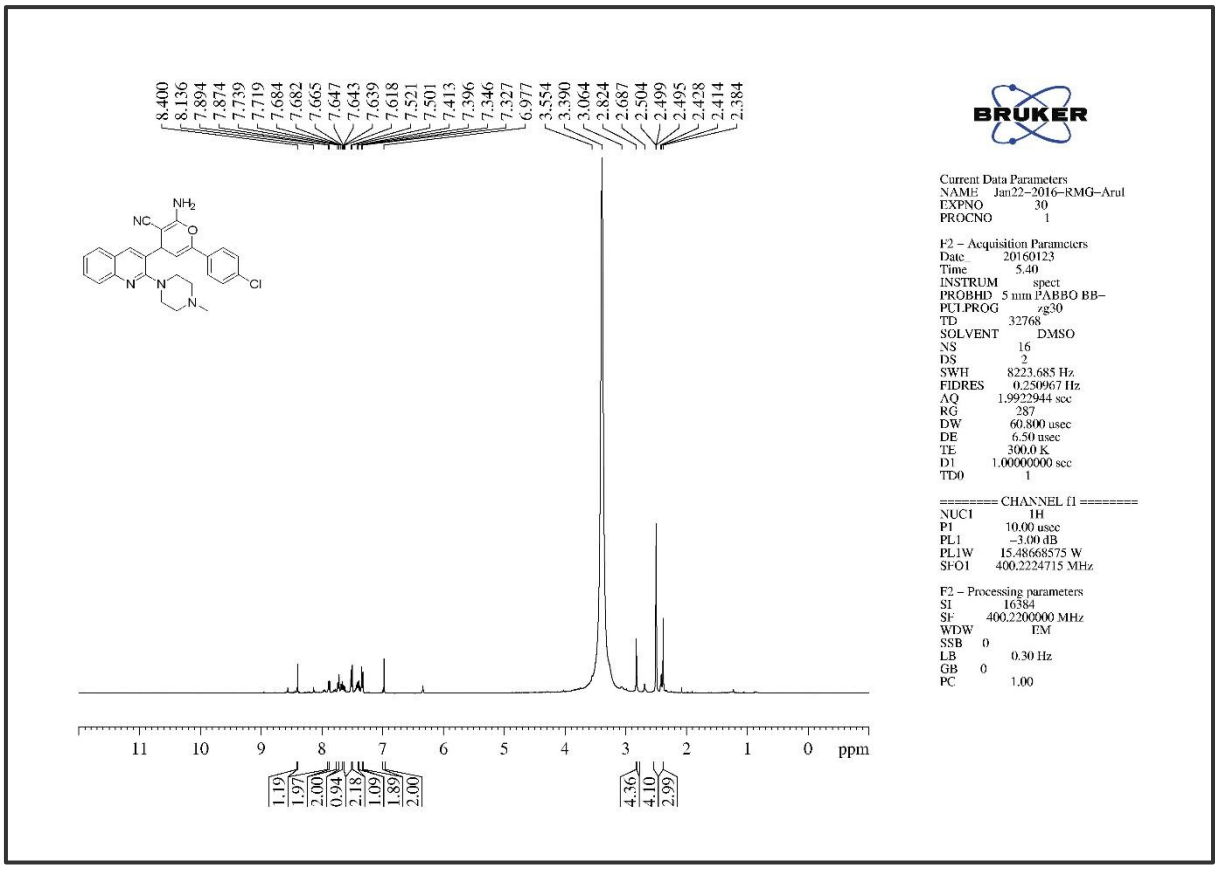

Figure 3. S. 28. The ^{1}H NMR of compound 6g

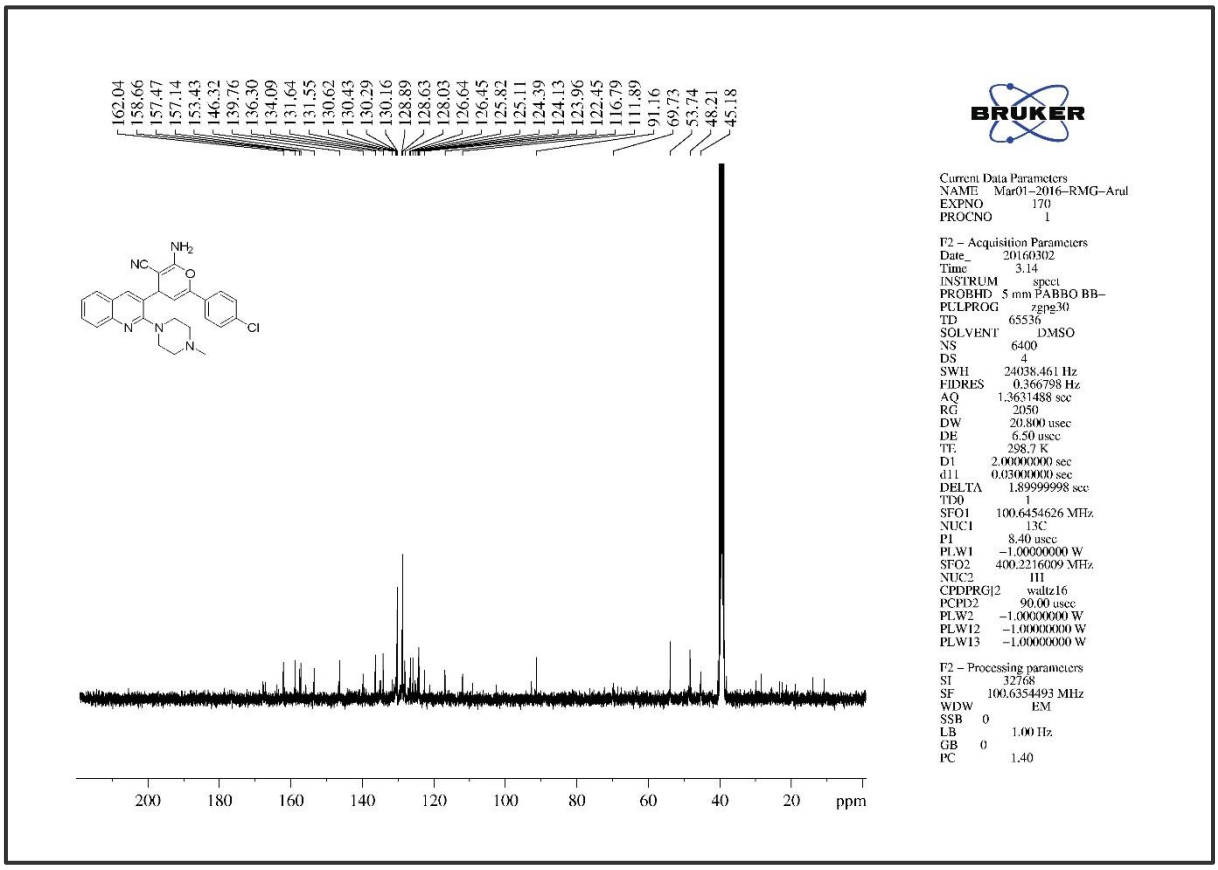

Figure 3. S. 29. The ^{13}C NMR of compound 6g

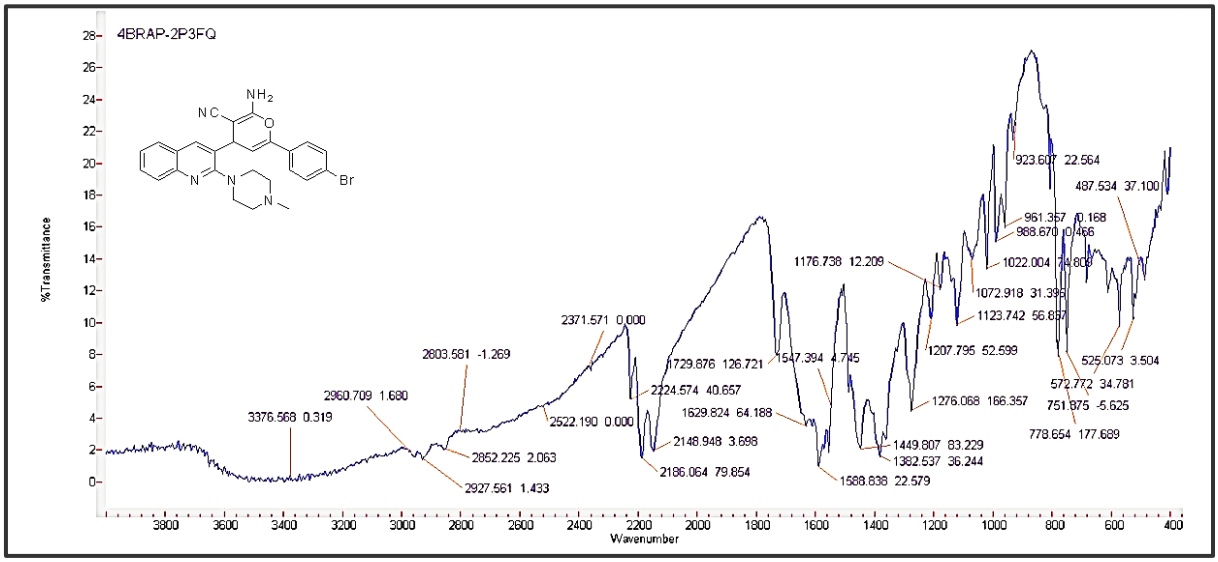

Figure 3. S. 30. The Infra-Red Spectrum of compound 6h

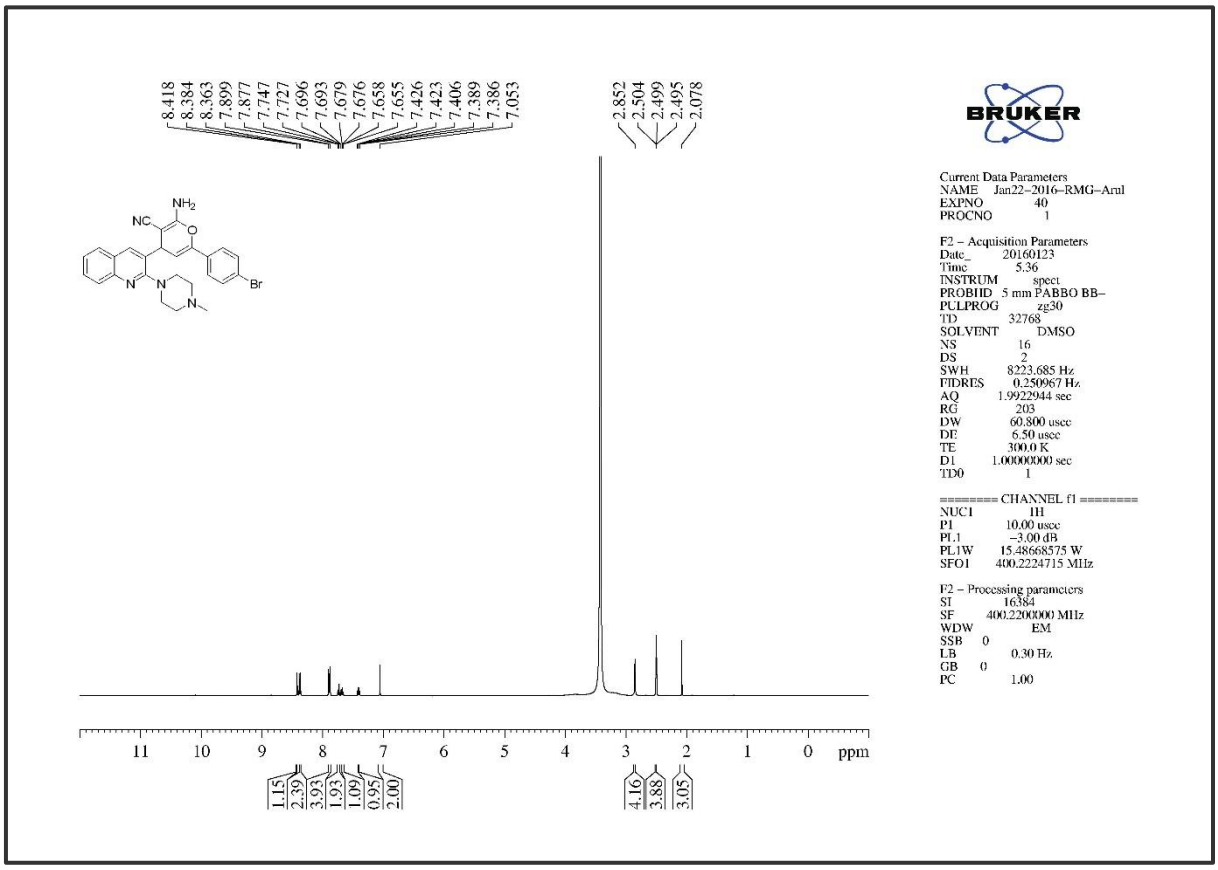

Figure 3. S. 31. The ^{1}H NMR of compound 6h

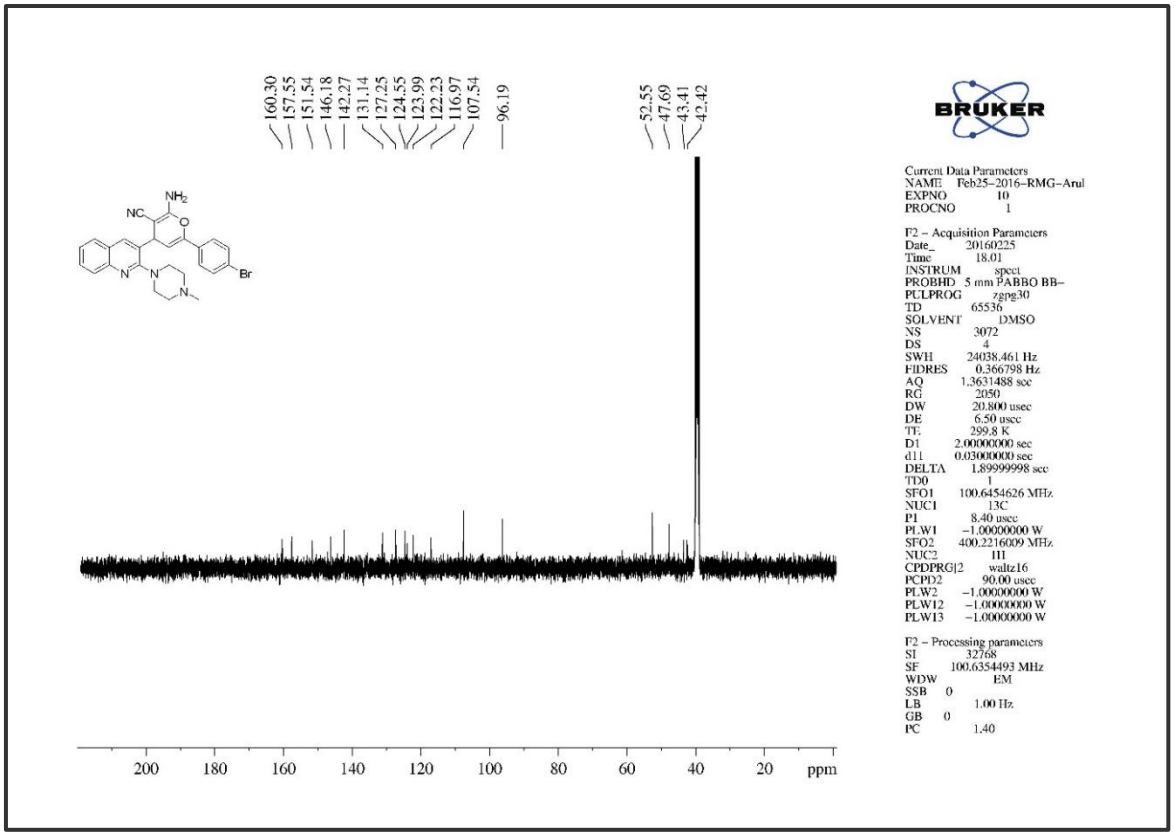

Figure 3. S. 32. The ^{13}C NMR of compound 6h

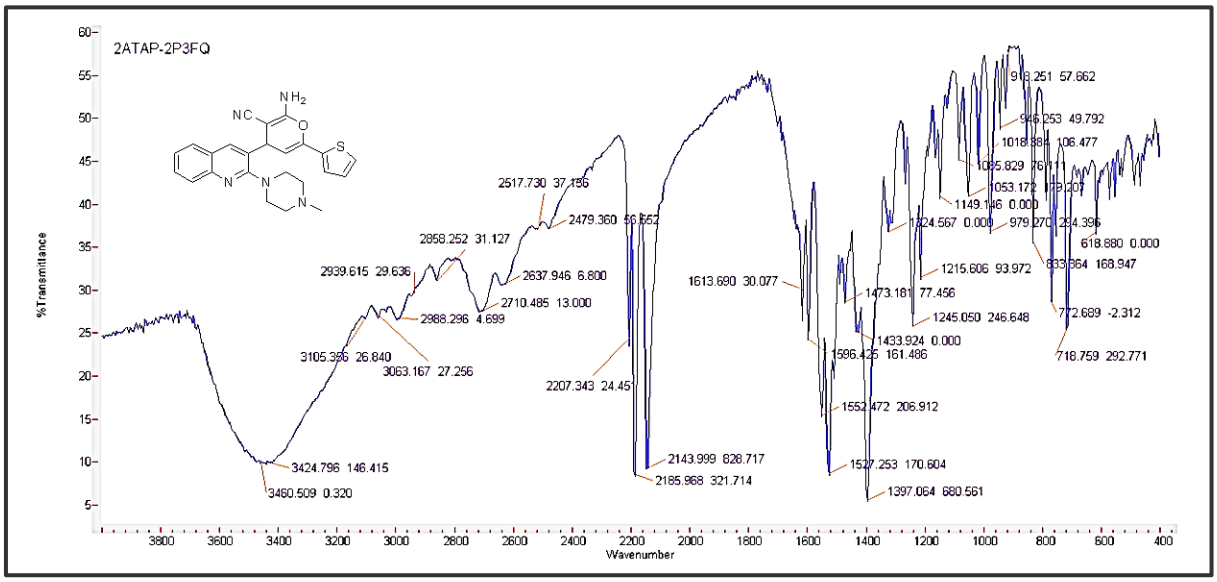

Figure 3. S. 33. The Infra-Red Spectrum of compound 6i

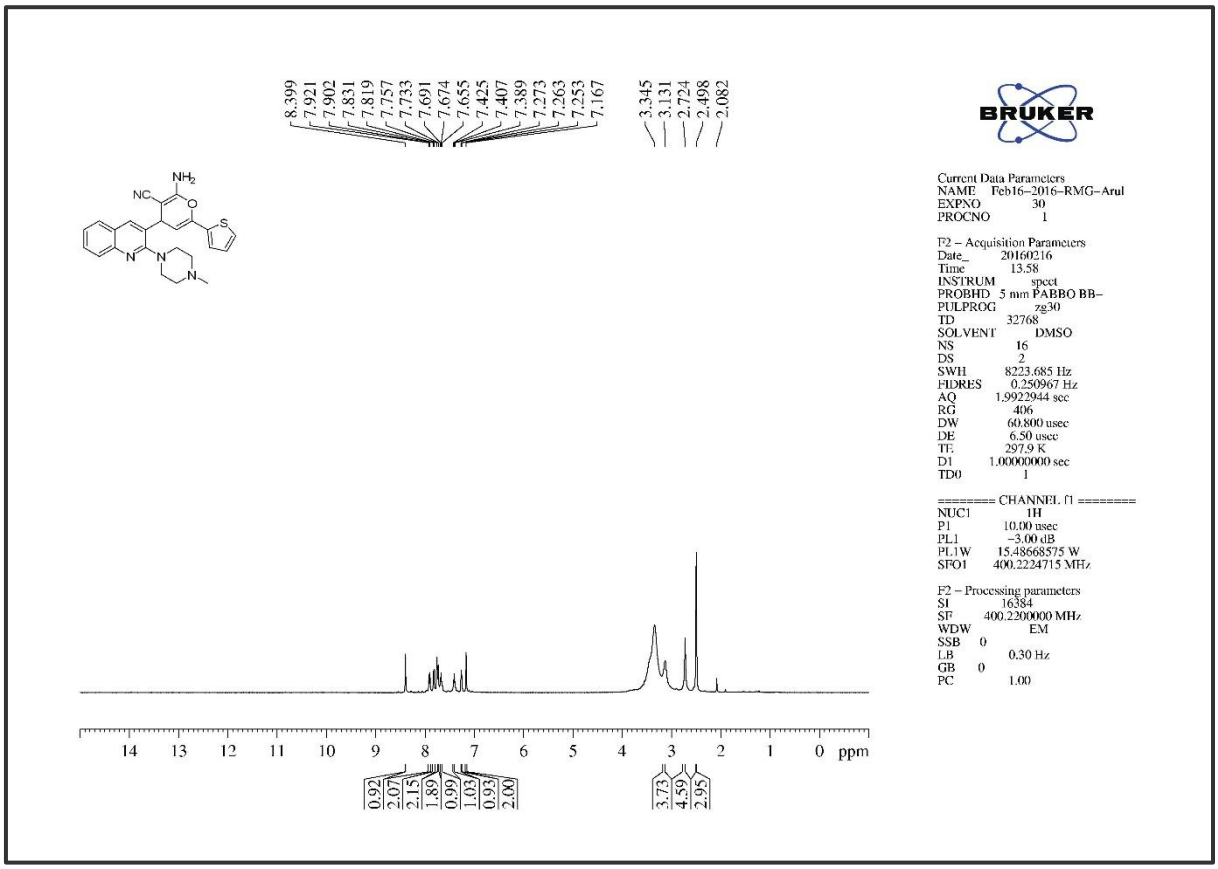

Figure 3. S. 34. The ^{1}H NMR of compound 6i

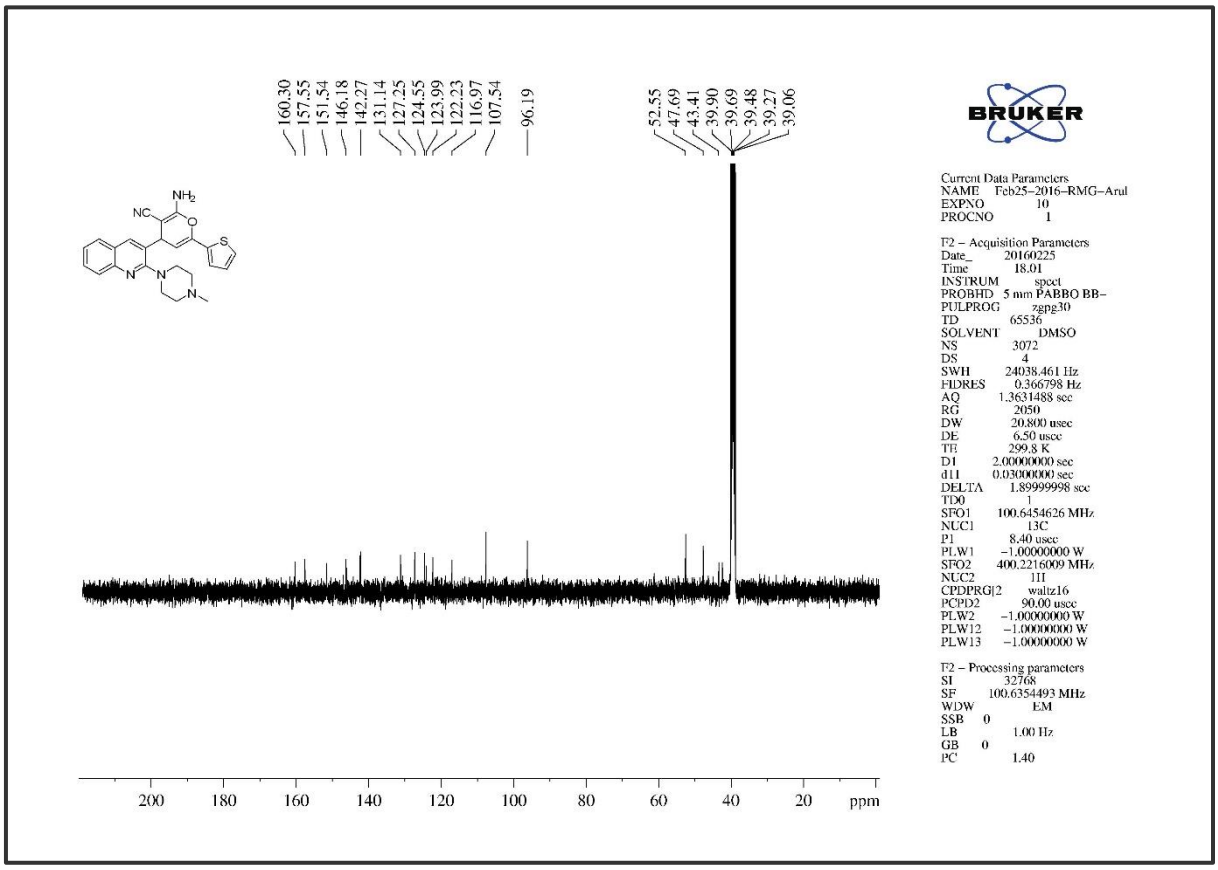

Figure 3. S. 35. The ^{13}C NMR of compound 6i

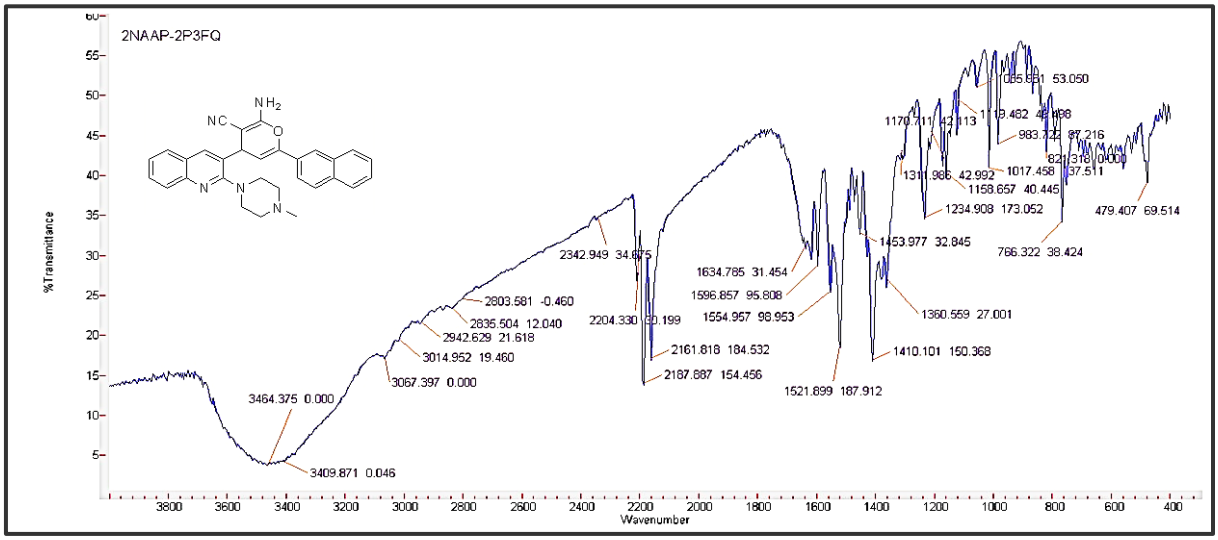

Figure 3. S. 36. The Infra-Red Spectrum of compound 6j

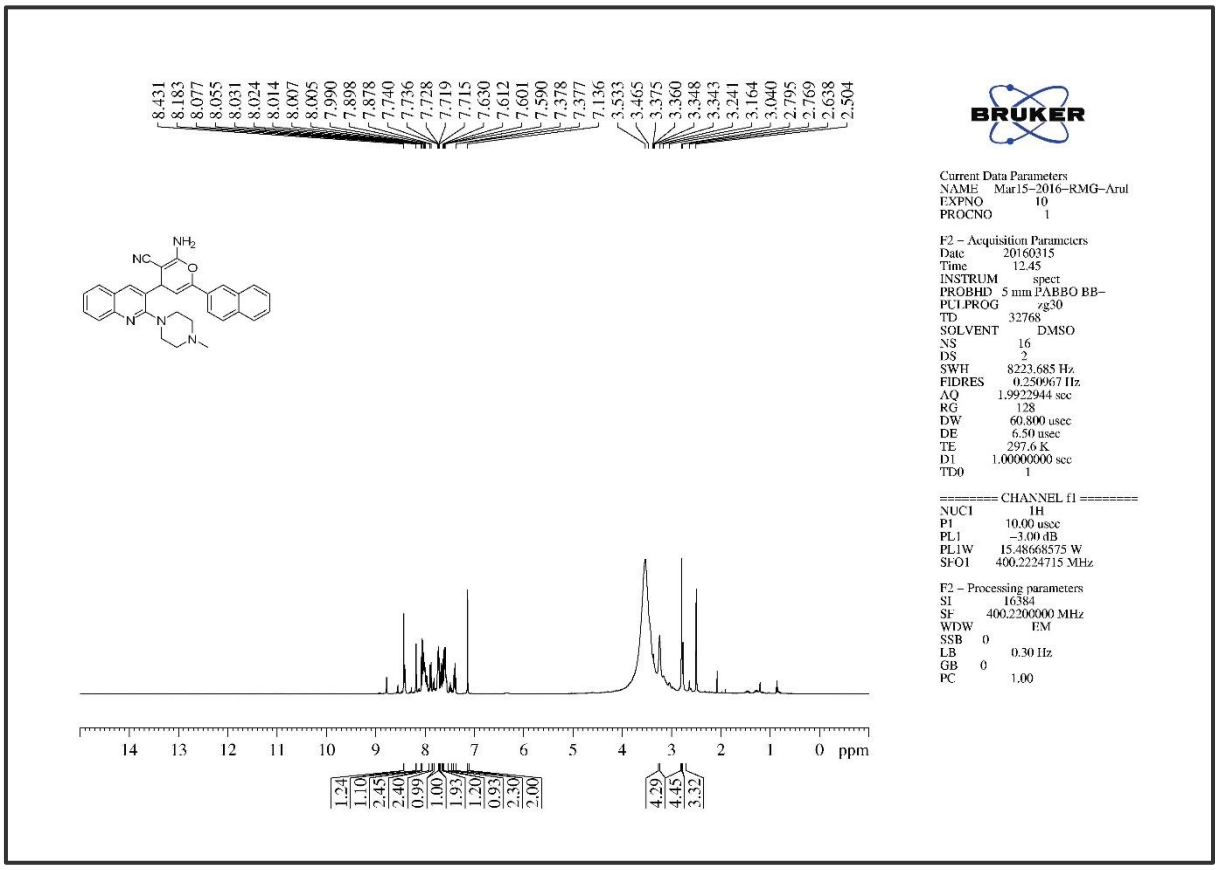

Figure 3. S. 37. The ^{1}H NMR of compound 6j

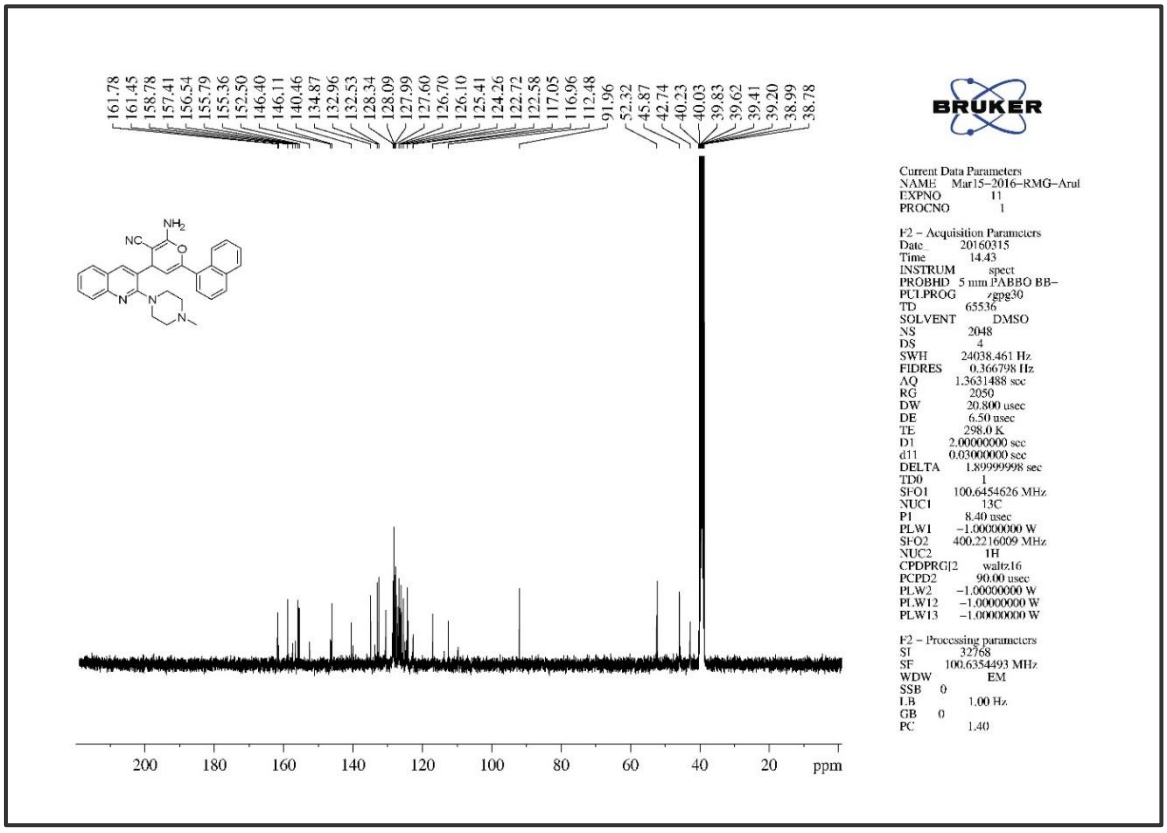

Figure 3. S. 38. The ^{13}C NMR of compound 6j

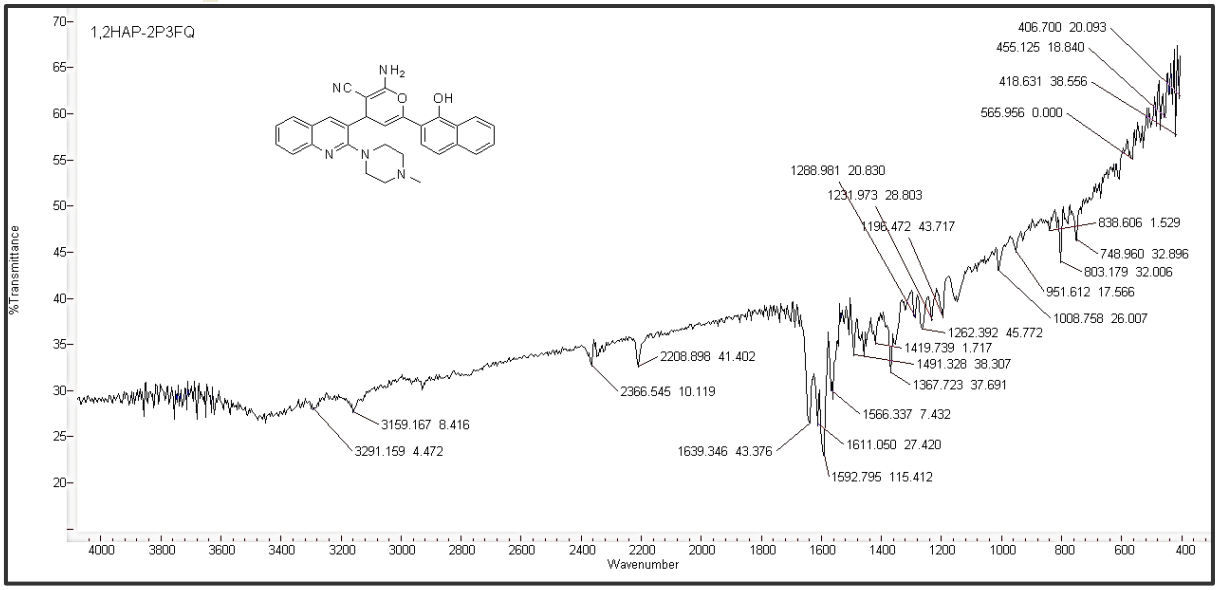

Figure 3. S. 39. The Infra-Red Spectrum of compound 6k

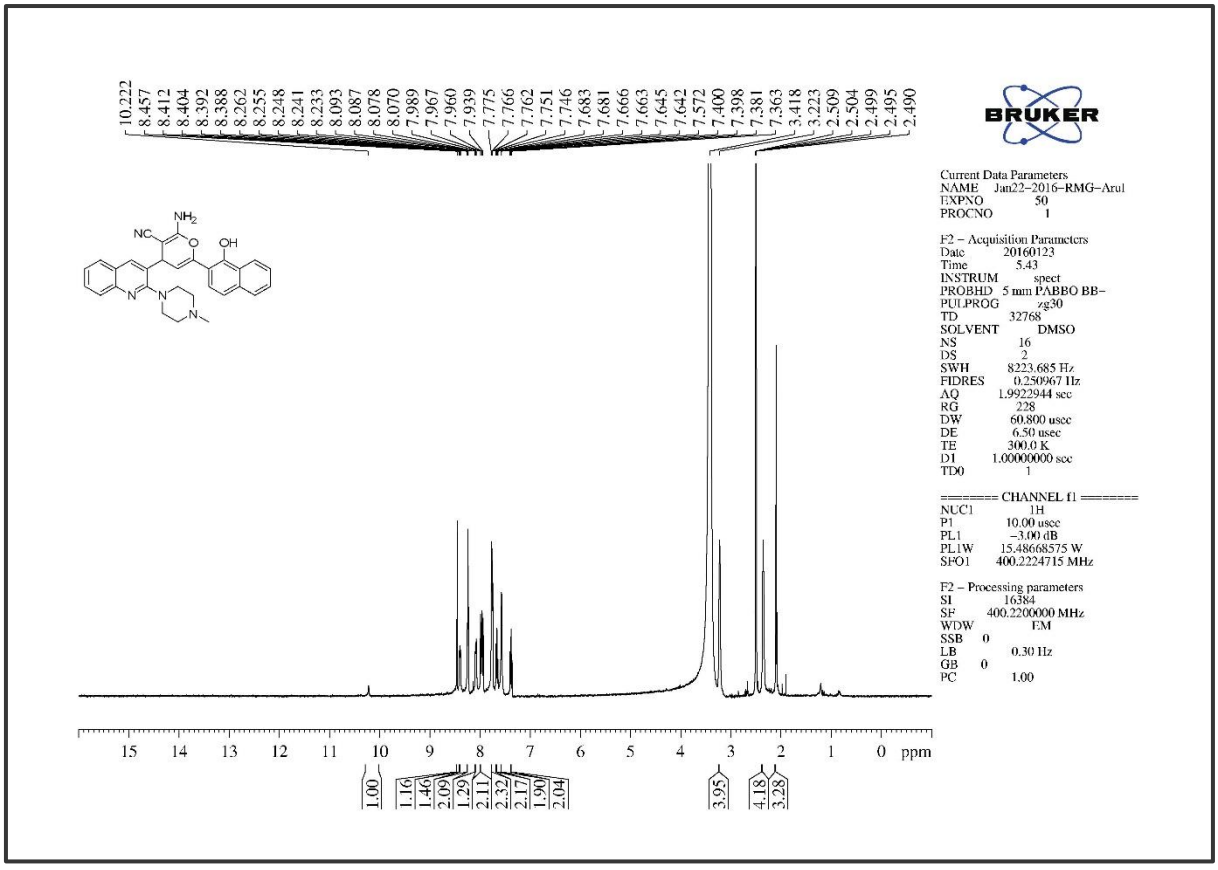

Figure 3. S. 40. The ^{1}H NMR of compound 6k

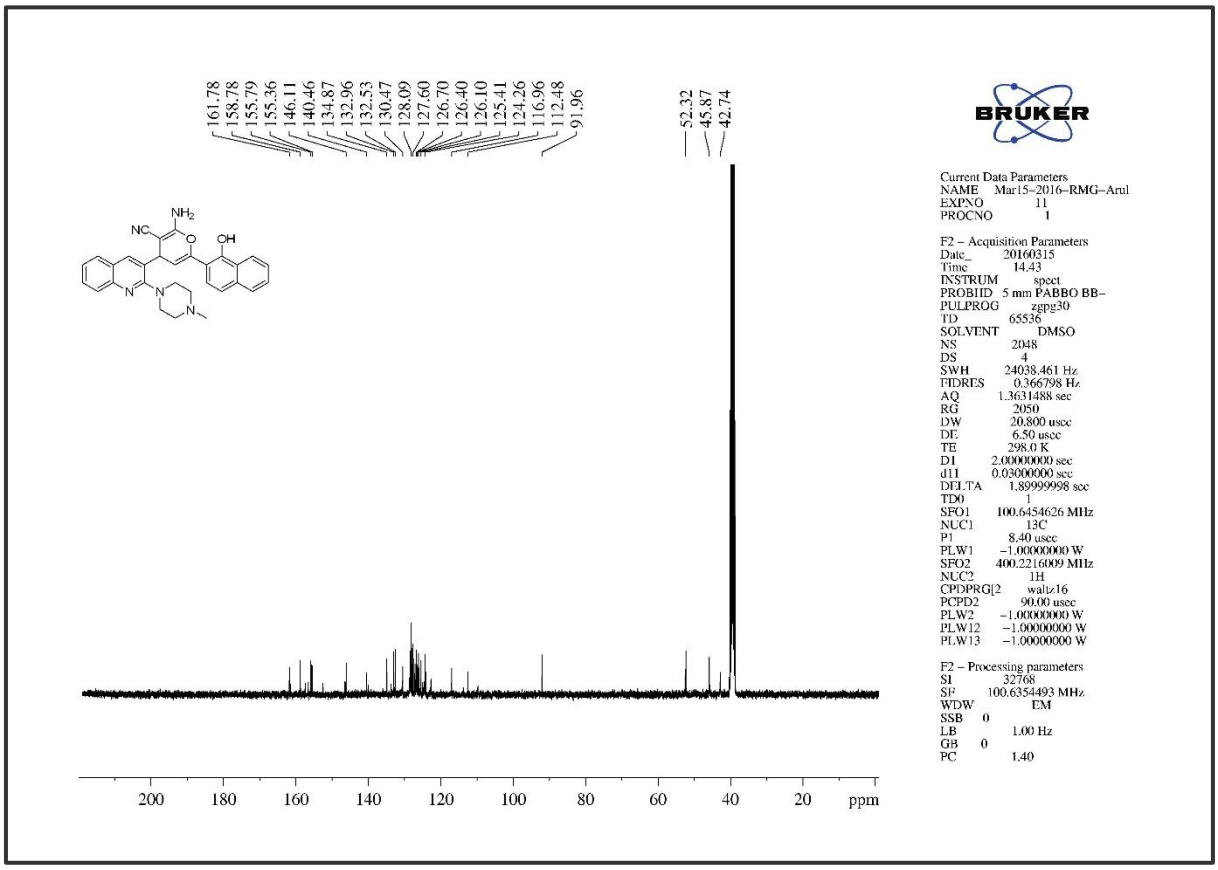

Figure 3. S. 41. The ^{13}C NMR of compound 6k

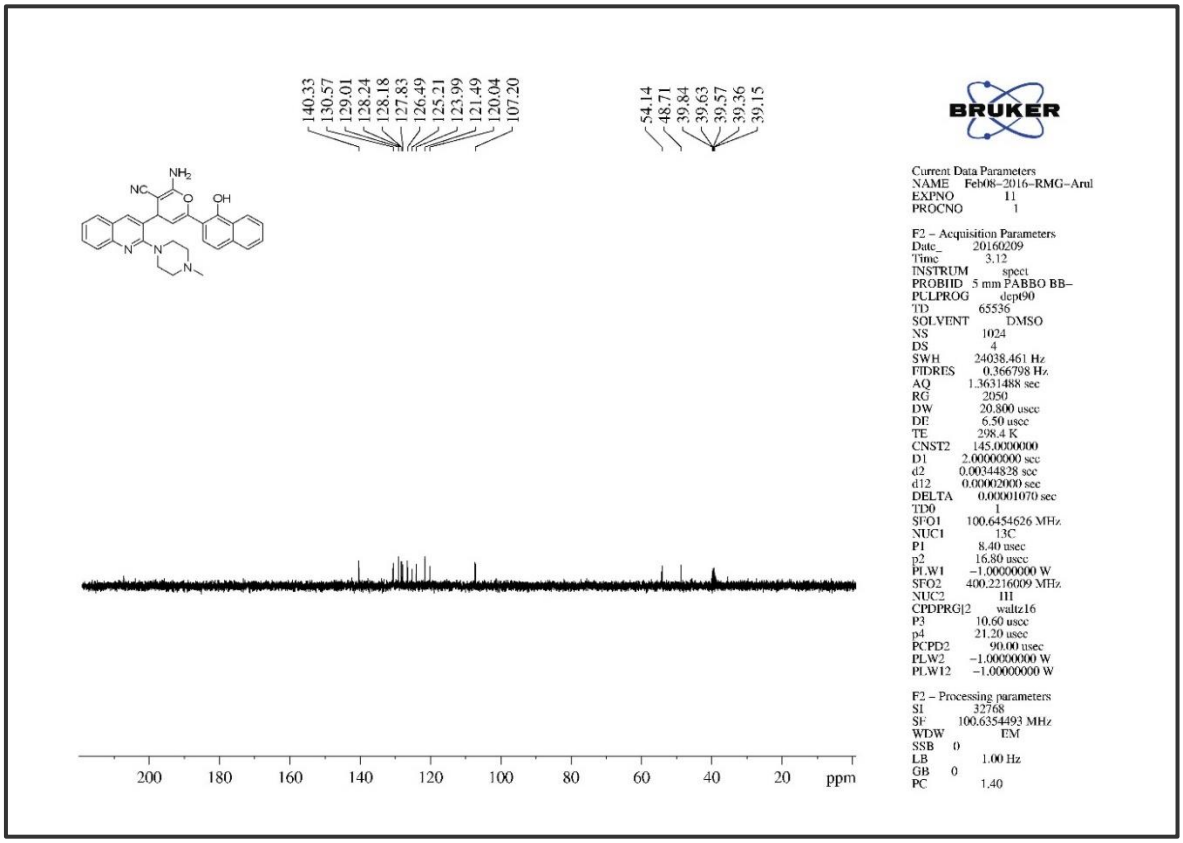

Figure 3. S. 42. DEPT-90 NMR of compound 6k

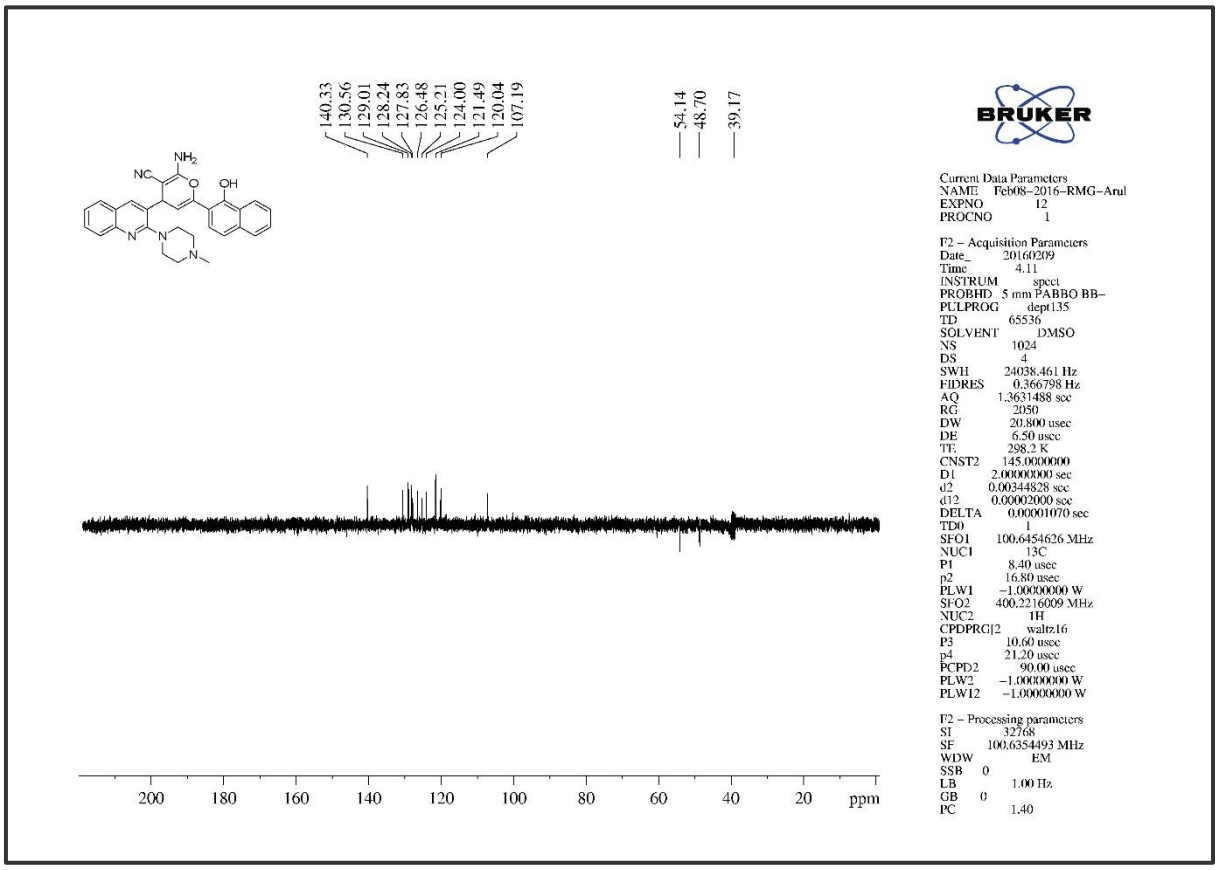

Figure 3. S. 43. DEPT-135 NMR of compound 6k

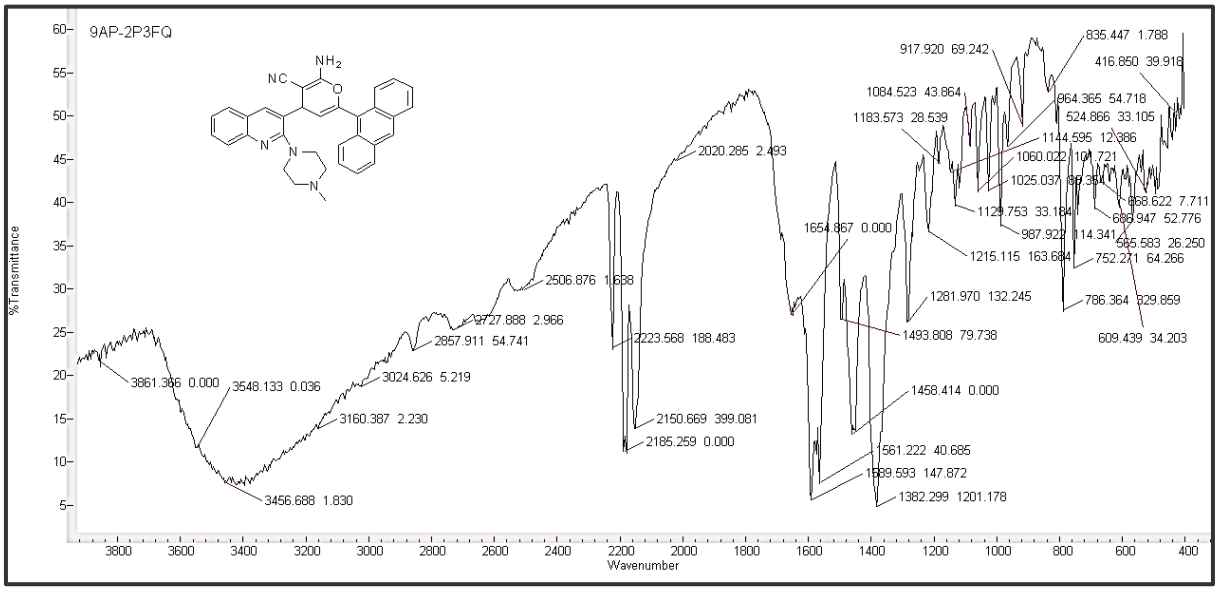

Figure 3. S. 44. The Infra-Red Spectrum of compound 6l

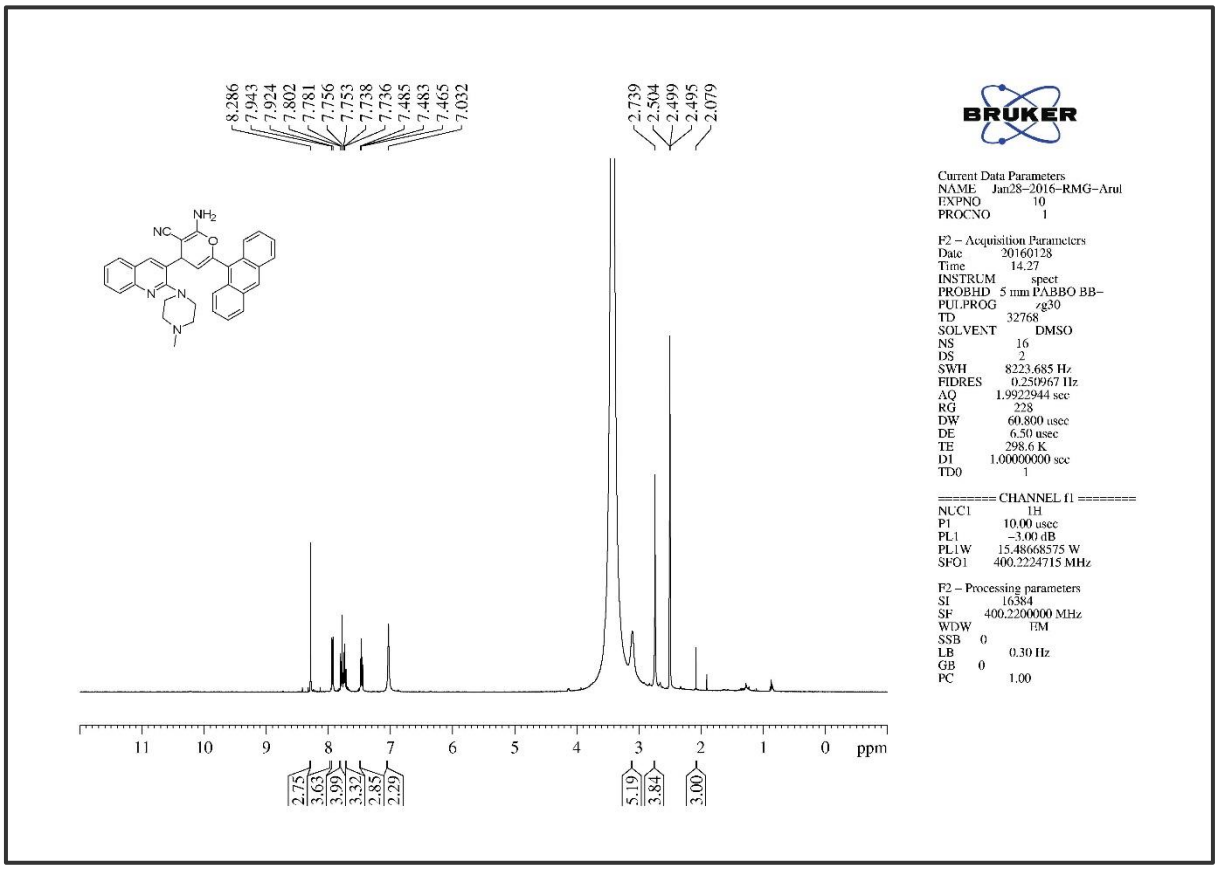

Figure 3. S. 45. The ^{1}H NMR of compound 6l

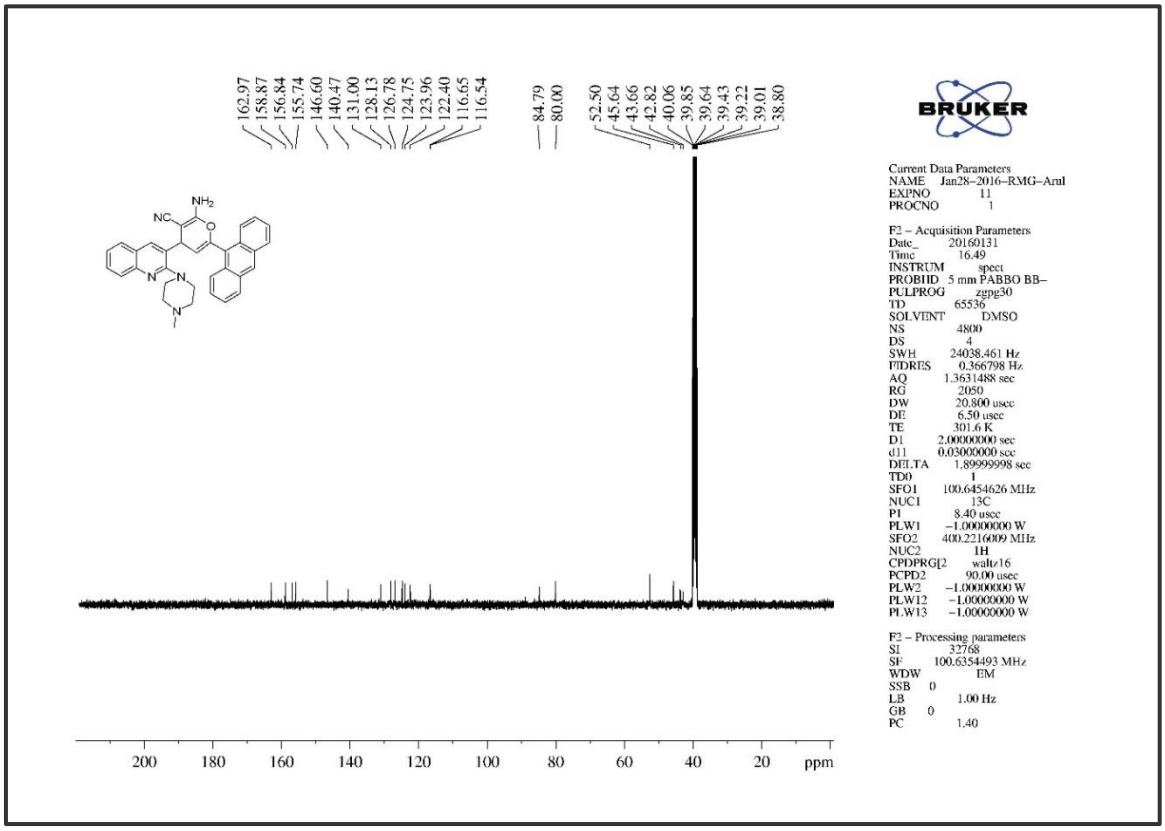

Figure 3. S. 46. The ^{13}C NMR of compound 6l

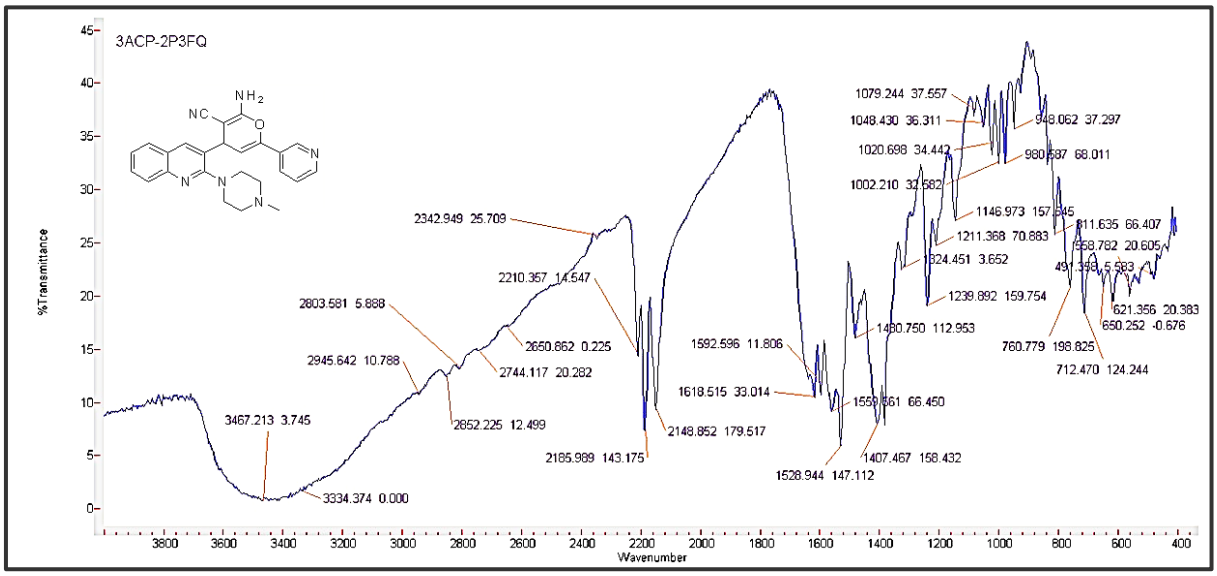

Figure 3. S. 47. The Infra-Red Spectrum of compound 6m

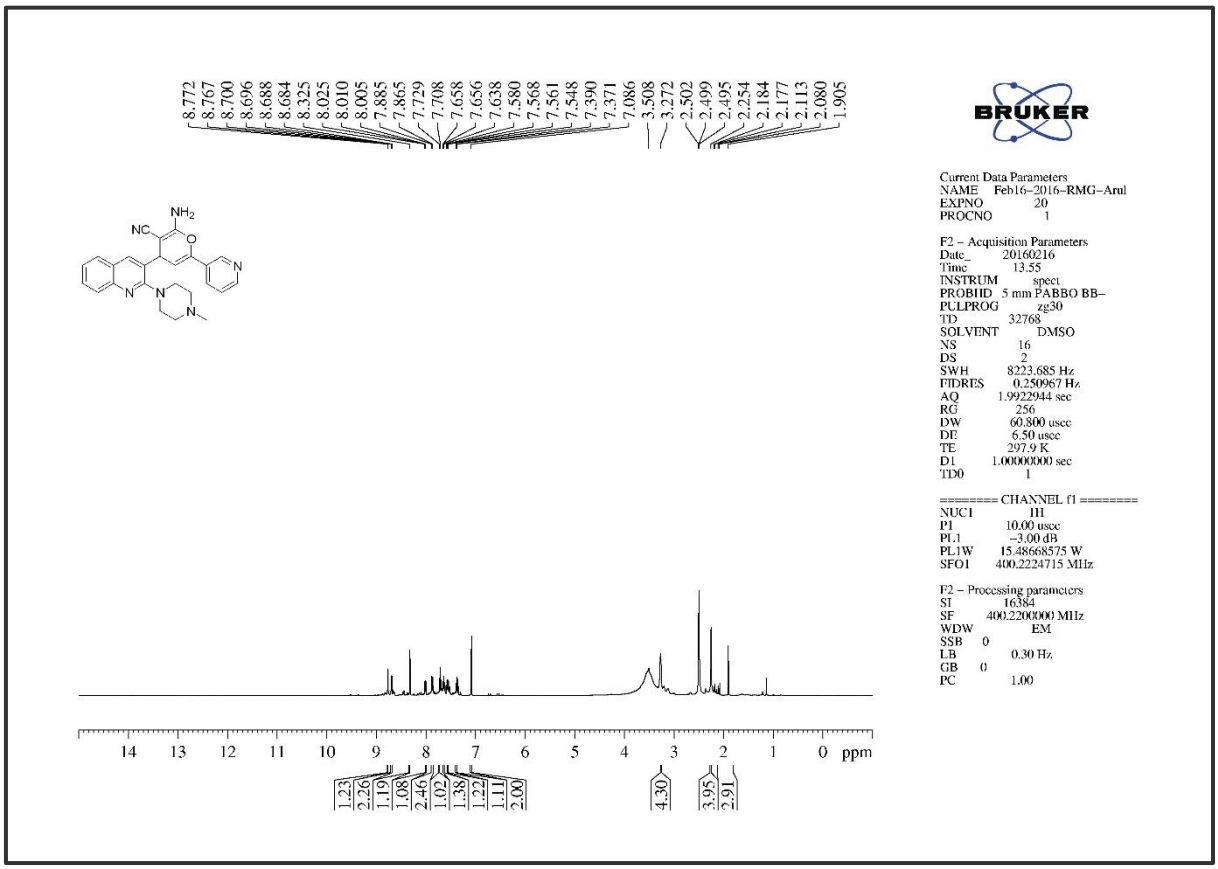

Figure 3. S. 48. The ^{1}H NMR of compound 6m

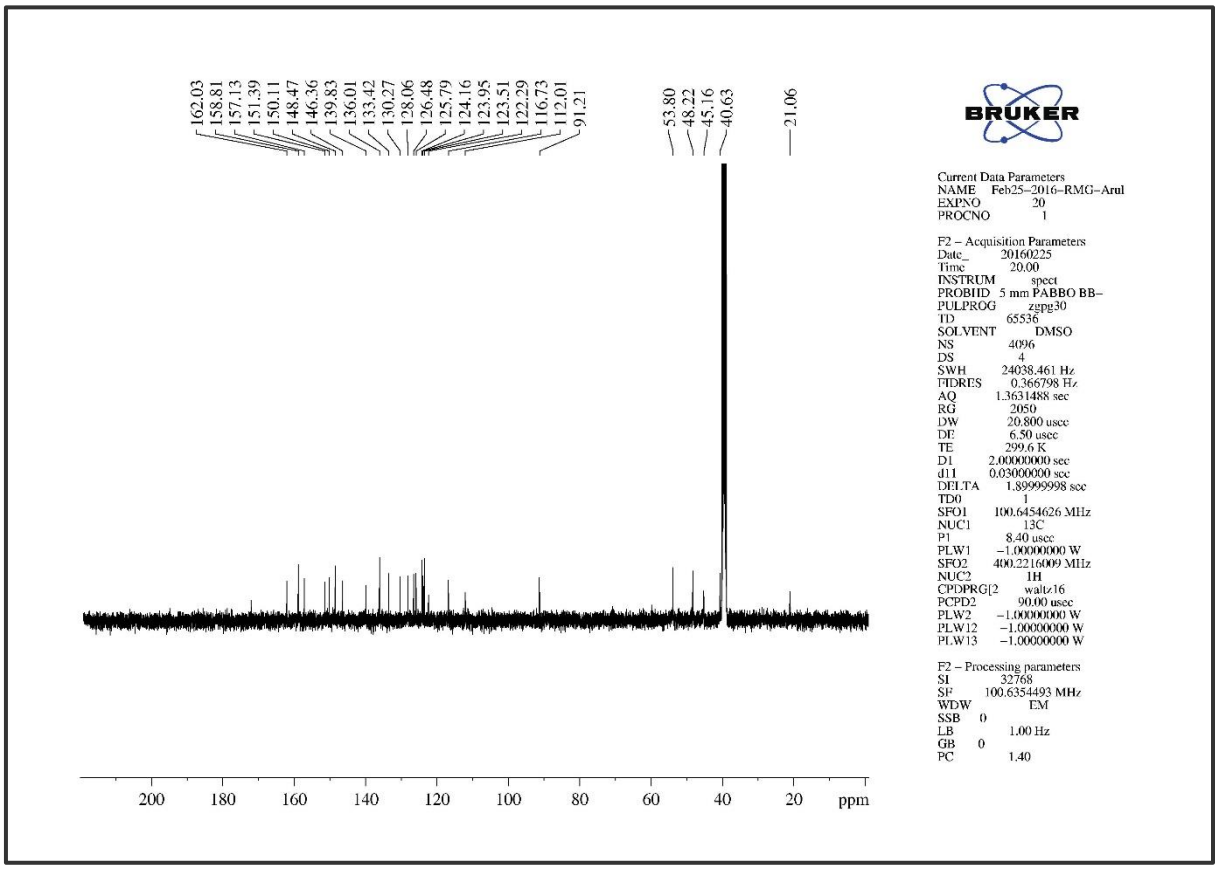

Figure 3. S. 49. The ^{13}C NMR of compound 6m

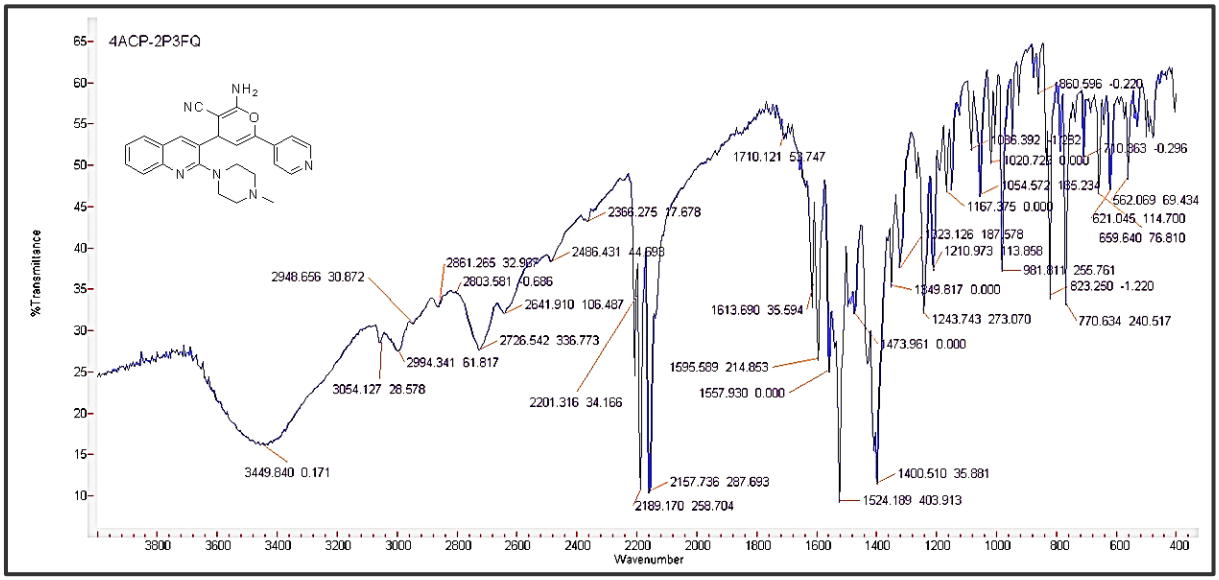

Figure 3. S. 50. The Infra-Red Spectrum of compound 6n

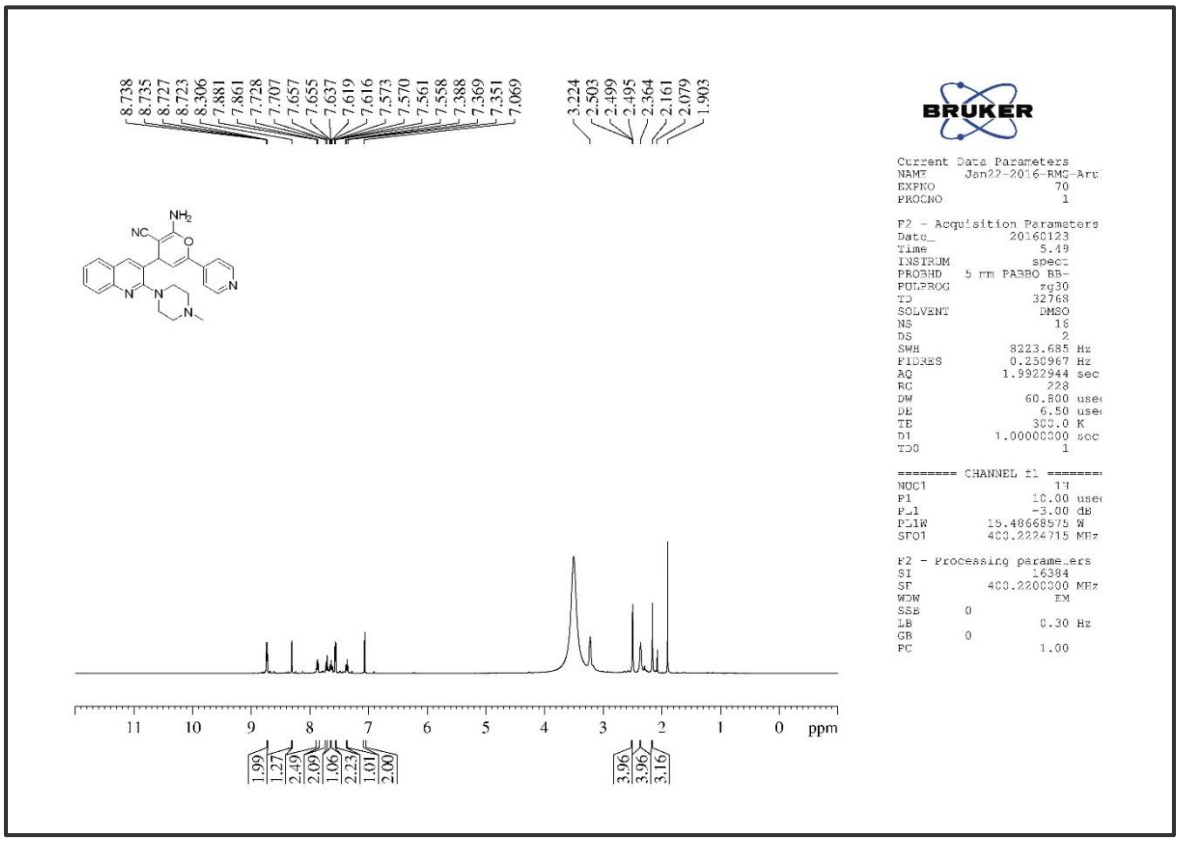

Figure 3. S. 51. The ^{1}H NMR of compound 6n

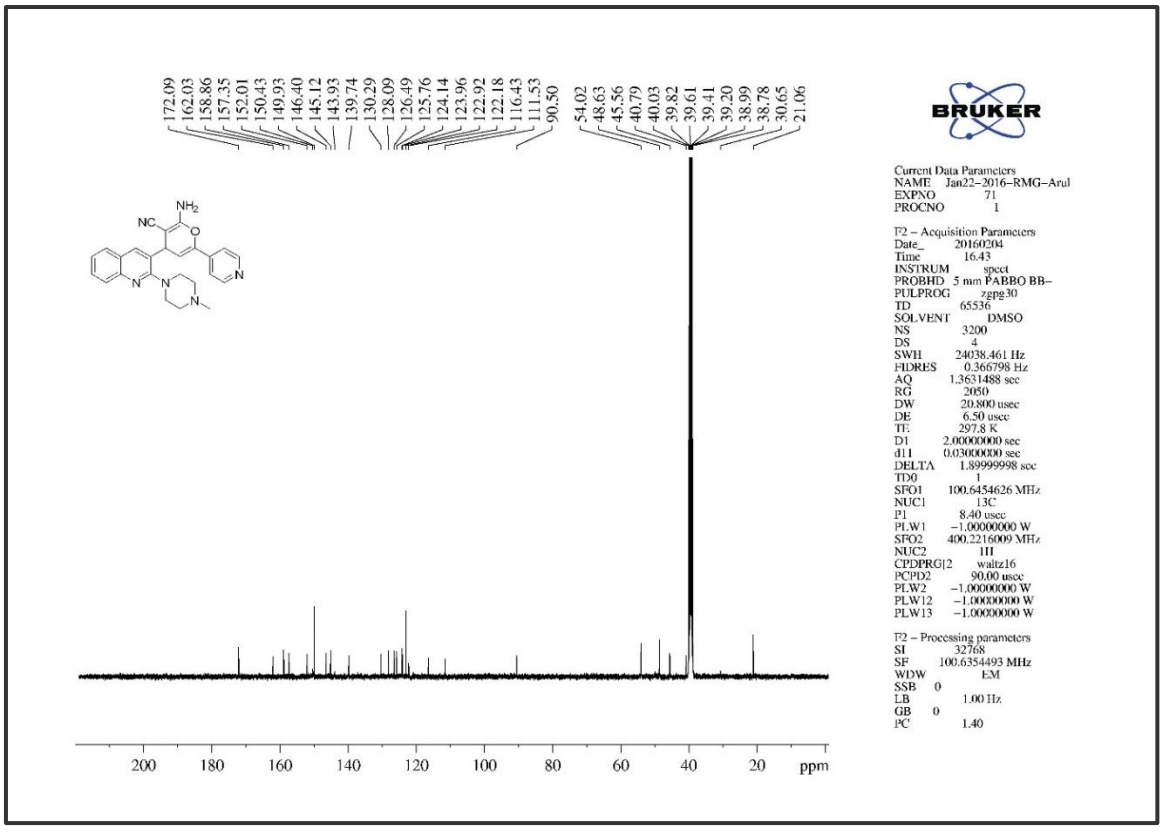

Figure 3. S. 52. The ^{13}C NMR of compound 6n

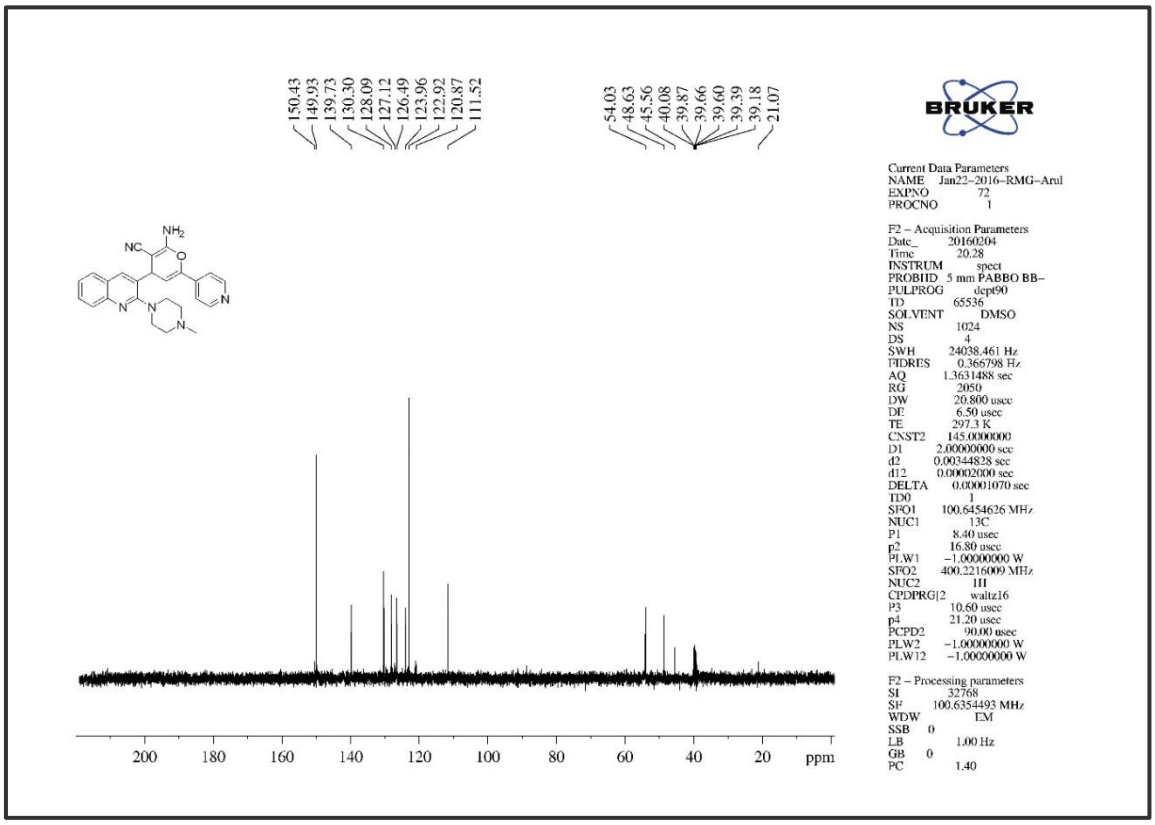

Figure 3. S. 53. The DEPT-90 NMR of compound 6n

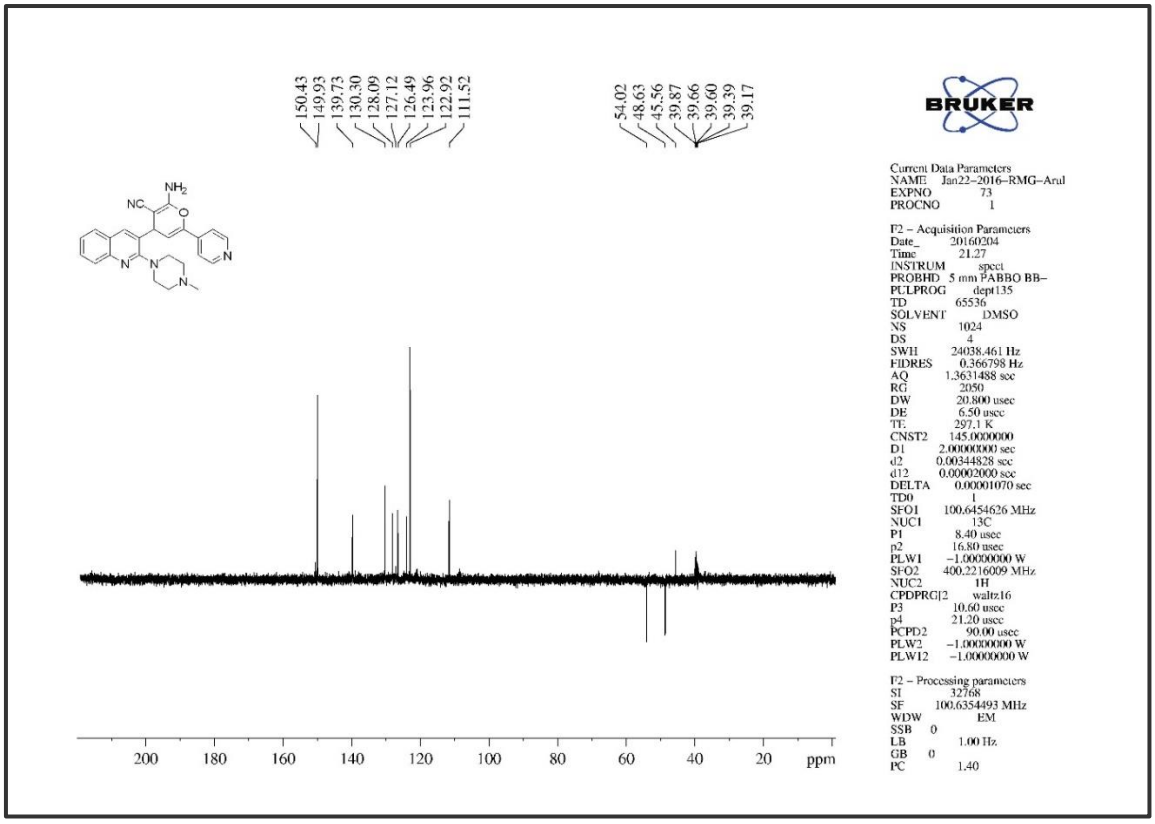

Figure 3. S. 54. The DEPT-135 NMR of compound 6n

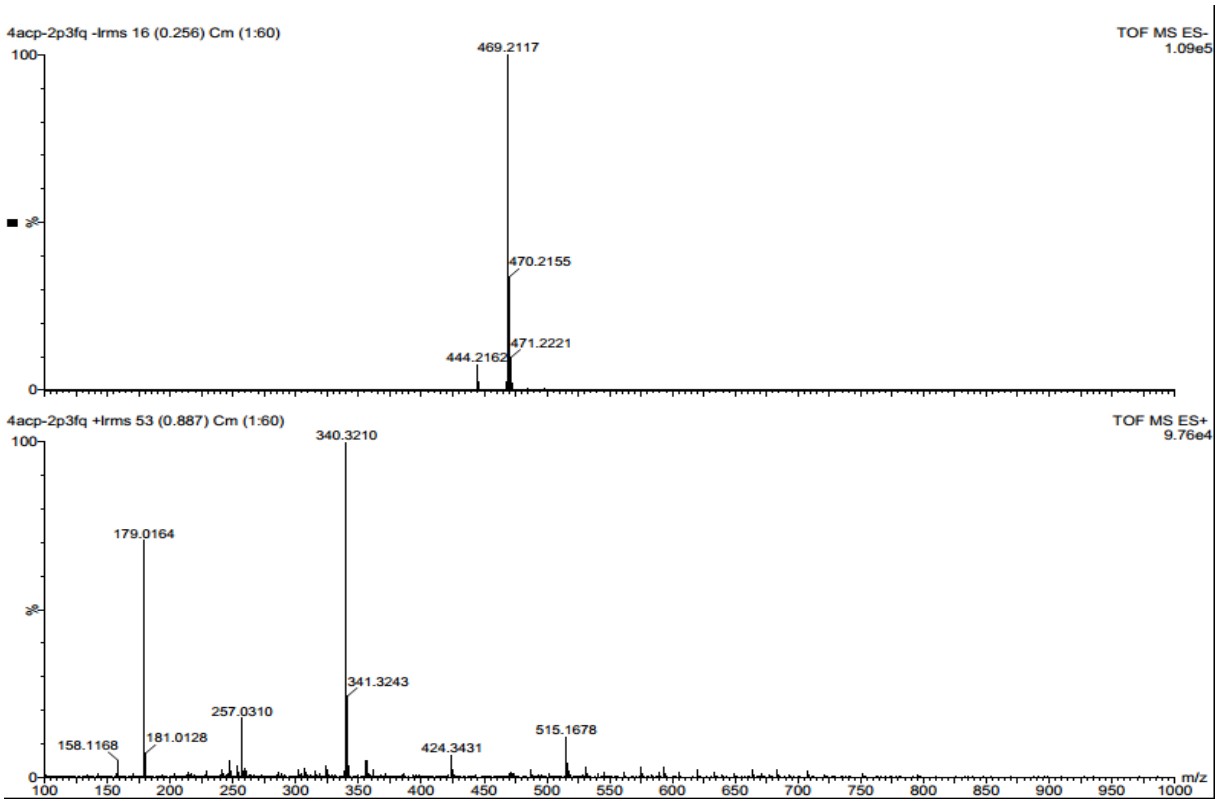

Figure 3. S. 55. The HRMS of compound 6n

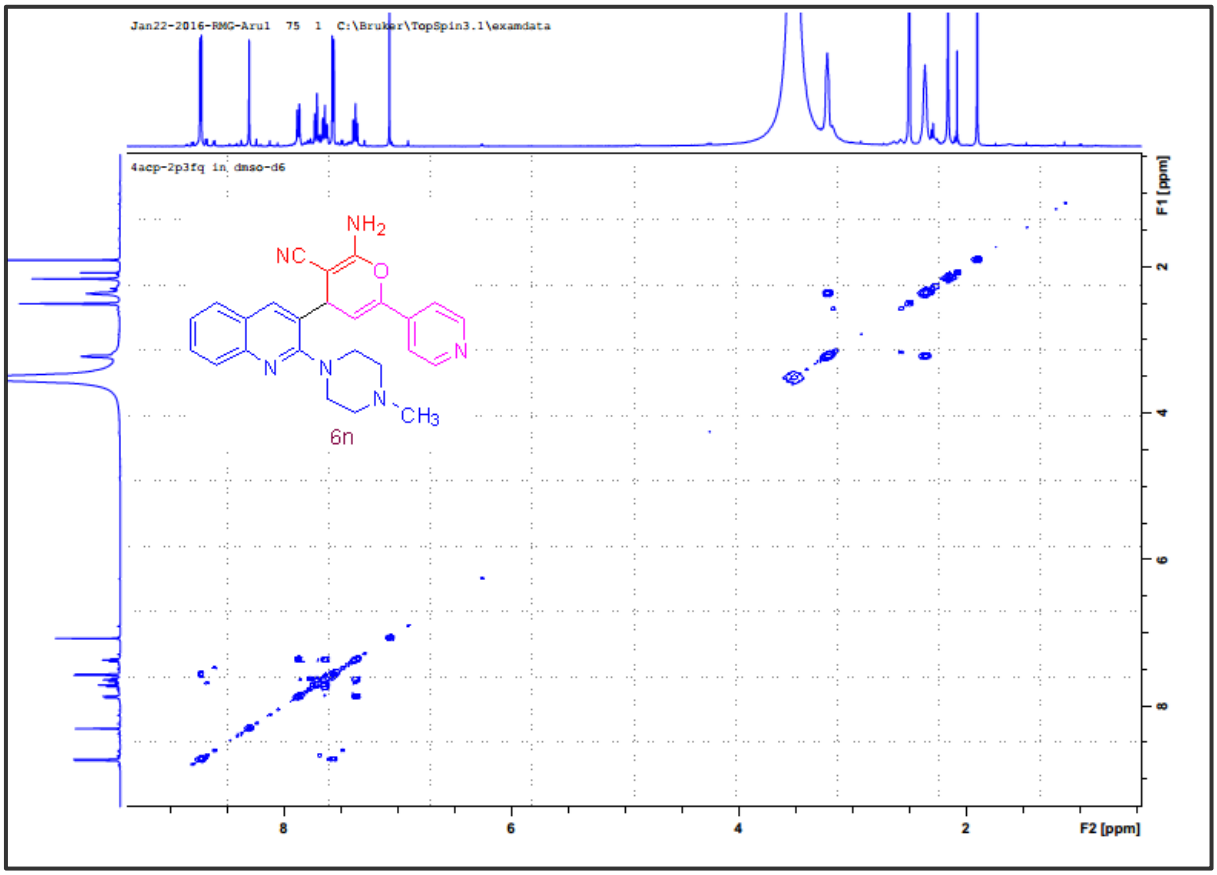

Figure 3. S. 56. The COSY NMR of compound 6n

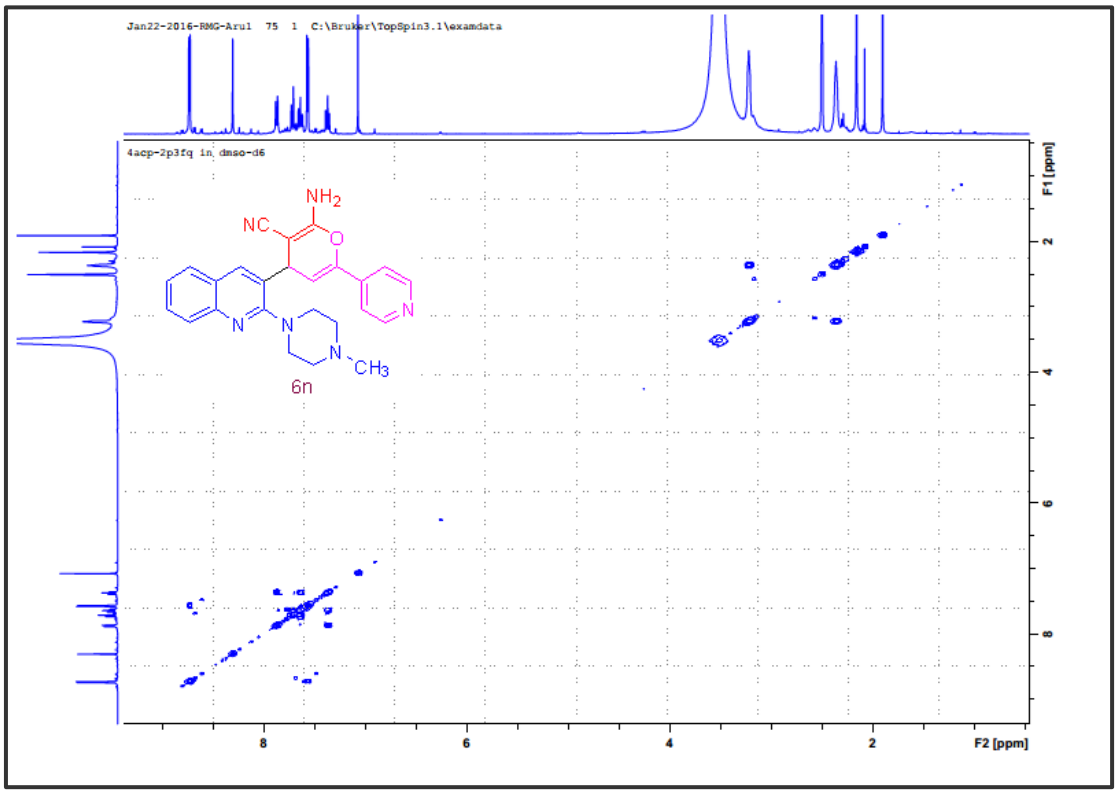

Figure 3. S. 57. The NOESY NMR of compound 6n

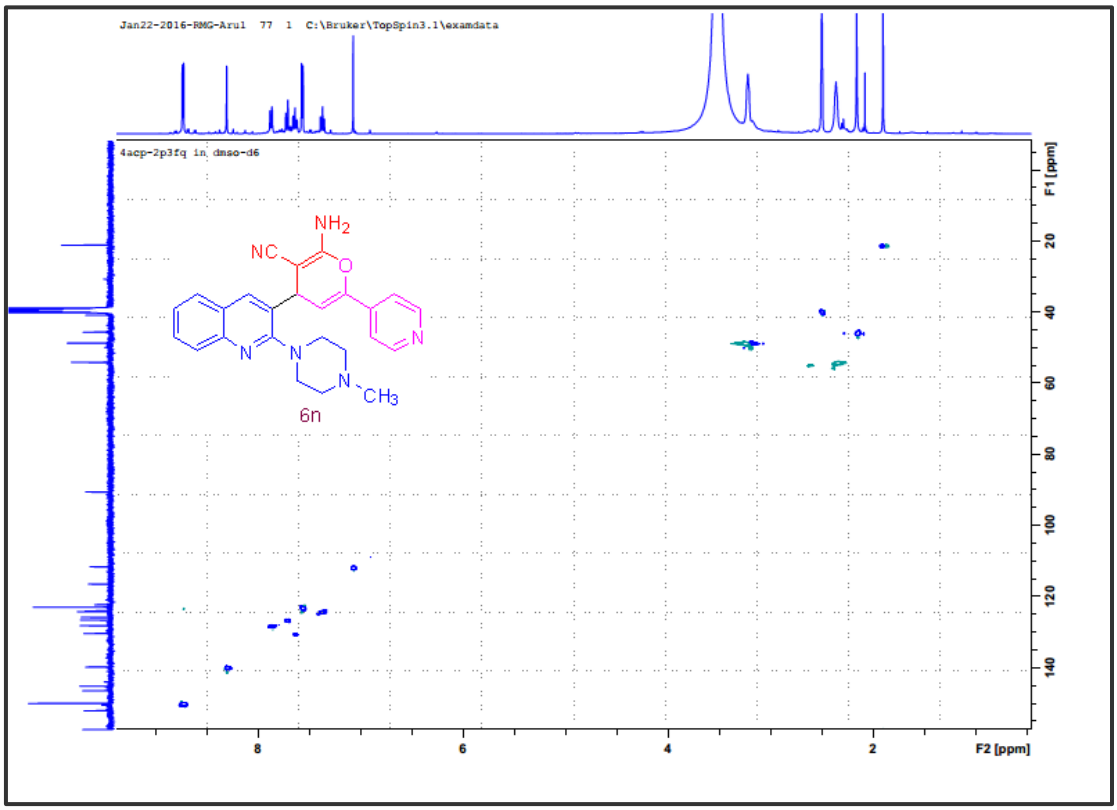

Figure 3. S. 58. The HSQCE NMR of compound 6n

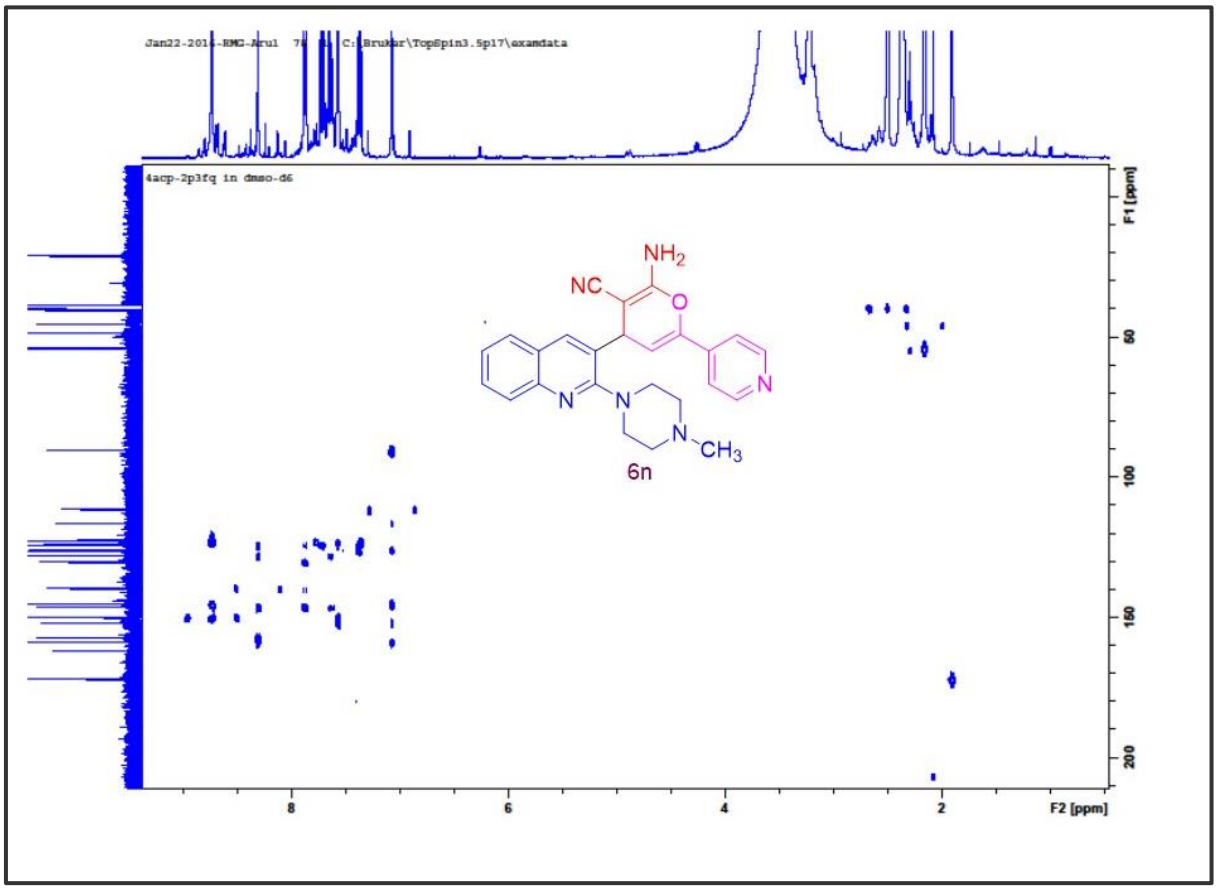

Figure 3. S. 59. The HMBC NMR of compound 6n

Chapter Four

Part A: [1]Boron nitride based sulfonic acid catalyst and its microwave assisted one-pot synthesis of methyl piperazinyl-quinolinyl tetrahydroacridinones

4A. 1. Abstract

A simple and safe method was used to prepare a new boron nitride-based sulfonic acid catalyst (BN-Pr-SO_3H) by activating boron nitride with nitric acid followed by its reaction with (3-mercaptopropyl) trimethoxysilane. This catalyst was used for a microwave-assisted one pot synthesis of novel 3,3-dimethyl-9-(2-(4-methylpiperazin-1-yl)quinolin-3-yl)-3,4,9,10-tetrahydroacridin-1(2H)-ones (DMPQAs) in a Knoevenagel and Michael type reaction. The morphological properties of BN-Pr-SO_3H were determined by XRD, TEM, SEM, BET and Raman spectroscopy whilst DMPQAs were characterized by FT-FT-IR, NMR, MS and Elemental analysis. The method developed in this study has advantages of producing good yields and simplicity coupled with safety and short reaction time. Most importantly it was found that the catalyst could be recycled at least five times with only 5 % loss of its catalytic activity. In order to determine the binding mode of action of the novel compounds with DNA, molecular docking analysis was performed with **6a, 6g** and **6t:** tricyclic system intercalated between the base pairs of DNA. Also, the benzo[c]acridine group was oriented into the minor groove. In all of the cases analysed, the benzo ring was stacked in between thymine bases DT-619 and DT-620, with the exception of **6a** which was stacked in between adenine bases DA-616 and DA-617. The guanine base pairs DG-512 and DG-514 and cytosine base pairs DC-512 and DC-514 showed that the complex binds to DNA towards the guanine base pairs G-C rich region due to Van der Waals interaction and hydrophobic contacts with the functional groups of DNA.

[1]***Murugesan, A., Gengan, R.M. and Krishnan, A., 2017.*** *Sulfonic acid functionalized boron nitride nano materials as a microwave-assisted efficient and highly biologically active one-pot synthesis of piperazinyl-quinolinyl fused Benzo [c] acridine derivatives. Materials Chemistry and Physics* ***(188) 154-167.***

4A. 2. Introduction

The acridines are an important class of heterocycles because of their valuable chemical and biological properties. The benzo acridine derivatives are used as antibacterial **(**Antonini *et al.* 1999:2535), cytotoxic (McCarthy *et al.* 1992:1664), anti-fungal (Spalding *et al.* 1954:357) and antimalarial agents. Recently the acridone and acridine scaffolds have gained increased attention towards developing new anti-cancer drugs (Charmantray Martelli 2001:1703). In addition, they are being exploited for their anti-melanoma (Filloux and Galy 2001:1137) and DNA binding abilities (Antonini *et al.* 2003:399).

The acridines are relatively easy to synthesize by using multi-component reactions (MCRs). The benzo[*c*]acridine derivatives have been synthesized by MCRs using naphthylamines, dimedone and aldehydes, as starting substrates, under various reaction conditions. In these reactions, catalysts such as triethylbenzylammonium chloride ionic liquids (Zang *et al.* 2010:495) have been used whilst microwave irradiation (MWI), (Bahrami *et al.* 2011:389), (Van *et al.* 1998:317), (Karimi and Zareyee 2008:3989), (Kureshy *et al.* 2009:572) and ultrasound irradiation (USI) (Das *et al.* 2006: 107) are examples of green protocols. The more acidic ILs [DISM][CCl_3COO] and [DSIM][CF_3COO] have been efficiently utilized as recyclable catalysts for the preparation of 14*H*-dibenzo[*a*,*j*]xanthene and 1,8-dioxo-decahydroacridine derivatives in short times under solvent-free conditions at 80-100 °C with excellent yields. The above two ILs were also effectively utilized as catalysts for the synthesis of 1,8-dioxo-decahydroacridine in water.

The use of heterogeneous catalysts has recently received considerable attention in various organic syntheses. Catalysts such as the SBA-15, nano-porous silica, which has a hexagonal structure, large pore size, high surface area and good thermal constancy, are very effective because of their thick aperture walls and higher aperture size (Van Rhijn *et al.* 1998:317). However, there are only a few reports of the applications of SBA propyl-based sulphonic acids for important chemical transformations (Karimi Zareyee 2008:3989), (Kureshy *et al.* 2009:572) (Valentini *et al.* 2006:2196).

Research based on altering the surface chemistry of boron nitride nanotubes (BNNTs) is still in its early stages, and effective surface functionalization remains a challenging task. The 3-aminopropyltriethoxysilane (APTES) molecule is used as a silanizing agent for BNNT surface. APTES is an important aminosilane which has wide applications in many fields. (Kathi and Rhee 2008:33) Reports on multi-walled carbon nanotubes functionalized with APTES showed improved compatibility with other polymers for the application in nanotube-based polymer matrix composites (Ciofani *et al.* 2012:308). It was reported that, after oxidation of

BNNT with concentrated nitric acid, the APTES molecules were linked to the nanotube walls thereby producing functionalized BNNTs (f-BNNTs) with free amino groups on their surfaces. The f-BNNTs were characterized by SEM and TEM, Z-potential analysis, EDS and XPS. Biocompatibility tests were performed for f-BNNTs. Thereafter the possibility of covalently binding molecules on their surface was assessed by labelling f-BNNTs with a fluorescent dye. Fluorescent f-BNNTs were finally used for *in-vitro* experiments, demonstrating their internalization by NIH/3T3 fibroblasts (Dutta *et al.* 2014: 41287).

4A. 3. Results and discussion

The boron nitride-based sulfonic acid catalyst (BN-Pr-SO_3H) was synthesized in three stages: firstly, a mixture of boron nitrile (BN) and 65 % nitric acid was reflux for 24 h; the purpose of this step was to introduce hydroxyl groups on the surface of BN by an oxidation process that may be described by Eq. (1). Thereafter (3-mercaptopropyl) trimethoxysilane was added and the mixture refluxed. Under these conditions, trimethoxy groups were easily hydrolysed by the hydroxyl groups on the surface on the nanocrystalline surface produced through oxidation. After the work-up of the reaction, the final step was an oxidation reaction with H_2O_2 in an acidic medium (Scheme 4A. 1). The catalyst was characterized completely by microscopic and spectroscopic techniques.

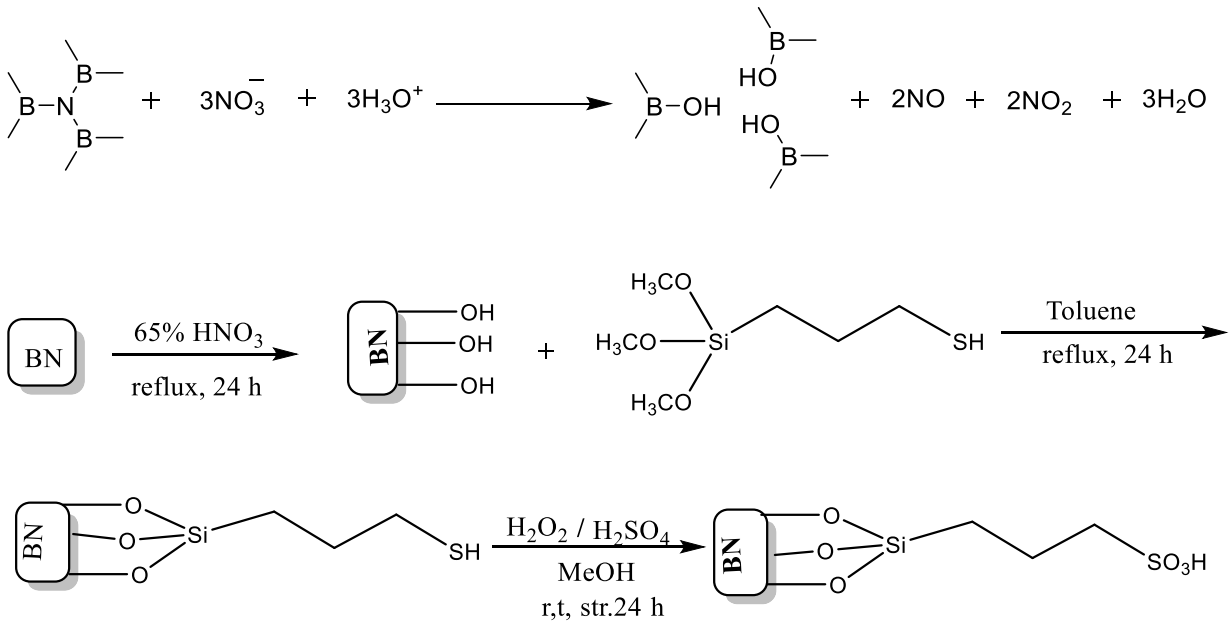

Scheme 4A. 1. The reaction scheme for the synthesis of BN-Pr-SO_3H.

The FT-IR spectrum of BN and BN-Pr-SO_3H (Figure 4A. 1-2, Appendix X-Y**)** revealed the following information: in the case of BN, peaks were observed at 815, 1494, 1569 and 3310 cm^{-1} due to B-N, BN-O bonding, attribution to hexagonal BN and B-OH bonding, respectively. The spectrum of BN-Pr-SO_3H showed the absorption of C-H stretching at 2954 cm^{-1} and the absorption at 1211 cm^{-1} was due to Si-O stretching. The absorptions at 1163 and 1141 cm^{-1} was due to the stretching mode of S=O.

The crystallinity and morphology of BN and BN-Pr-SO_3H were confirmed by PXRD and SEM images. The PXRD pattern of BN-Pr-SO_3H was almost identical to that of BN; this was taken as an indication that the sulphate modification might not have a drastic change on BN (Figure 4A. 1).

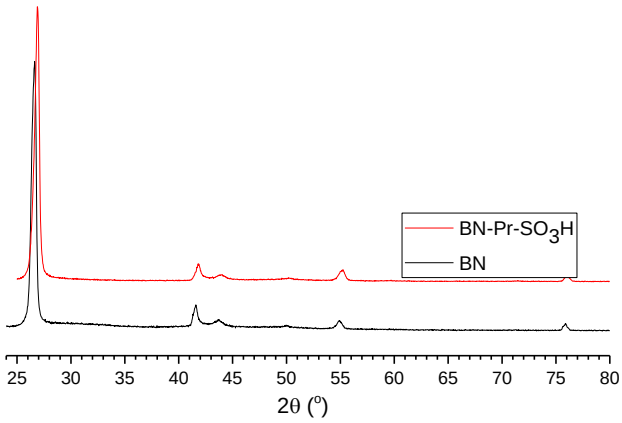

Figure 4A. 1. PXRD pattern of BN and BN-Pr-SO_3H

The representative SEM images of BN and BN-Pr-SO_3H (Figure 4A. 2) exhibits an aggregation of cloud-like structures of small spherical-shaped particles. The SEM micrographs of BN-Pr-SO_3H showed some modifications, with respect to BN, such that the primary surface structure had changed, however the cloud-like structure and small spherical-shaped particles still existed. TEM images of BN and BN-Pr-SO_3H (Figure 4A. 4) shaped at different places BN (A-1 µm, B-200 and C-500 nm); BN-Pr-SO_3H (D-1 µm, E-100 and F-500 nm) showed the crystalline nature whilst 1 µm showed a mesoporous structure which provides a good surface for catalytic activity.

Energy-dispersive X-ray spectroscopy (EDS) confirmed the presence of all the elements (Figure 4A. 3) and the actual weight % is presented in Table 4A. 1.

The porous nature of BN and BN-Pr-SO_3H, analysed by N_2 gas adsorption measurements at 273K (Figure 4A. 5**)**, showed BN as a type-I adsorption isotherm as a characteristic of microporous material and the BET and Langmuir surface areas of BN were calculated as 18

and 46 m^2/g respectively. The N_2 adsorption isotherm of BN-Pr-SO_3H also indicated a type-I adsorption isotherm. However, the BET and Langmuir surface area were calculated as 6 and 9 m^2/g respectively. This smaller value indicated that the catalyst has a biggest surface area and will therefore possess better catalytic property.

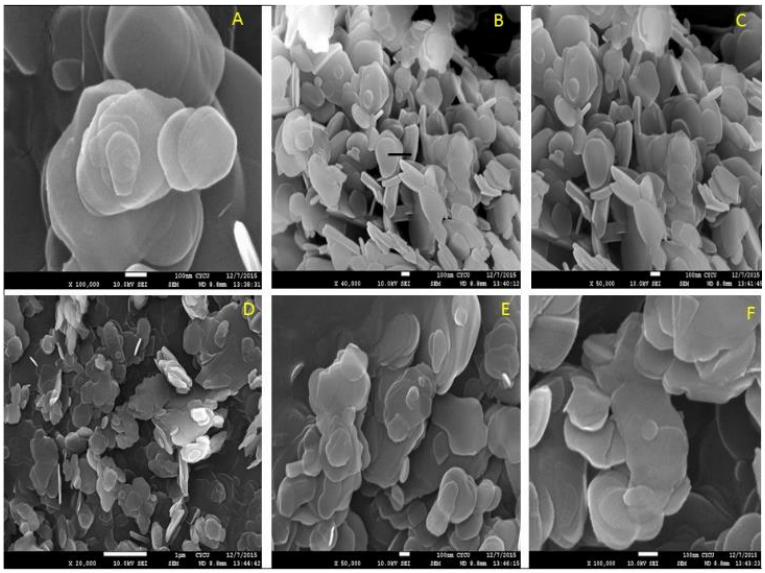

Figure 4A. 2. SEM image of BN (A, B, C) and BN-Pr-SO_3H (D, E, F)

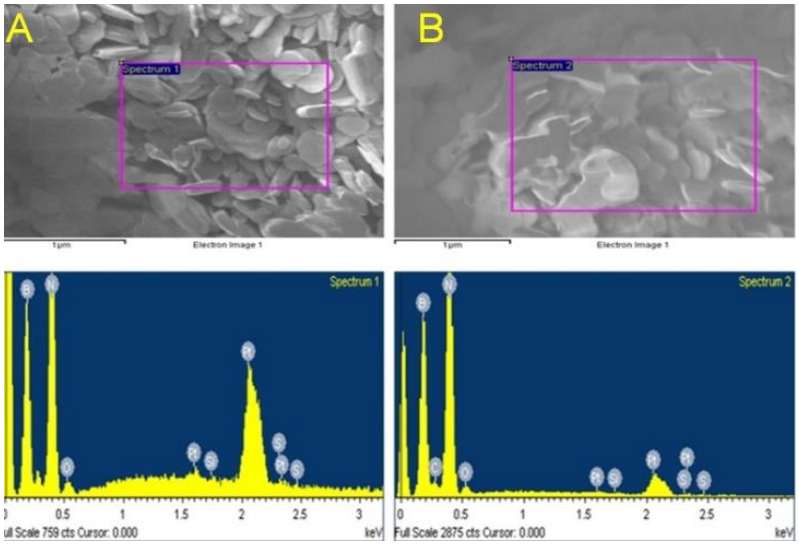

Figure 4A. 3. EDS analysis for BN (A) and BN-Pr-SO_3H (B)

The Raman spectra (Figure 4A. 6) shows absorption signals at 600, 1480, 2000, 3000, and 3750 cm^{-1} for BN whereas BN-Pr-SO_3H shows absorptions signals at 600, 2000, 3000, 3750 cm^{-1} with an additional signal at 3250 cm^{-1} most probably due to the acidic functional group.

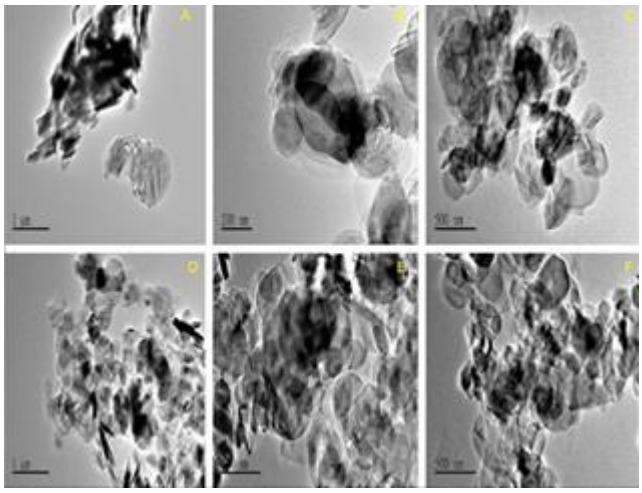

Figure 4A. 4. TEM image of BN (A, B, C) and BN-Pr-SO_3H (D, E, F)

Table 4A. 1. The weight (%) analysis for BN and BN-Pr-SO_3H.

	BN		BN-Pr-SO_3H	
Element	Weight (%)	Atomic (%)	Weight (%)	Atomic (%)
B	38.60	52.95	41.56	49.10
N	41.75	44.14	49.10	44.77
O	1.69	1.56	1.28	1.02
C	-	-	4.56	4.58
S	-	-	0.08	0.03
pt	17.90	1.36	3.41	0.22

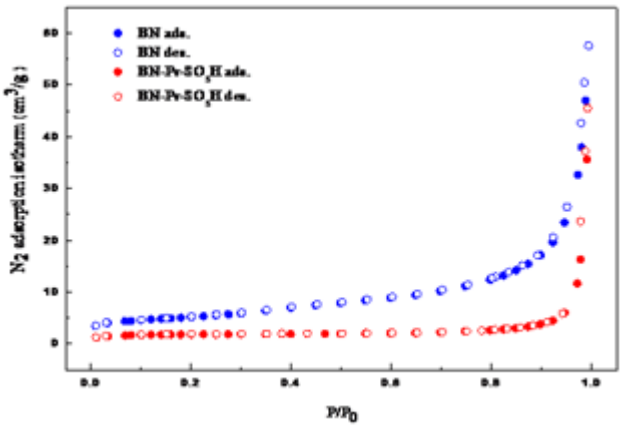

Figure 4A. 5. Adsorption and desorption isotherms of BN and BN-Pr-SO_3H at 273K.

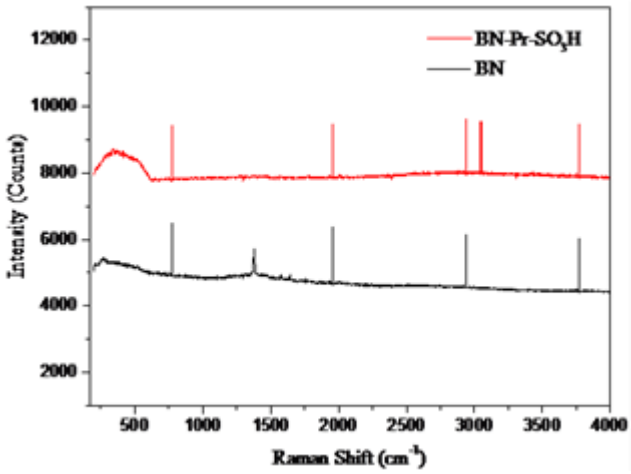

Figure 4A. 6. Raman Shift of BN and BN-Pr-SO_3H

To synthesize new piperazinyl-quinolinyl benzo[*c*]acridinones, a new starting compound viz., 2-(4-methylpiperazin-1-yl)quinoline-3-carbaldehyde (**3**) was used: this was discussed in Chapter 3. Briefly, the Vilsmeier-Haack reaction was used to prepare 2-chloroquinoline-3-carbaldehyde (**1**) from acetanilide followed by its reaction with 1-methylpiperazine. The reaction scheme for the multicomponent reaction is presented in Scheme 4A. 2. In this reaction, the condensation of compound (**3**), dimedone (**4**) and aniline derivatives (**5a-t**) was easily achieved to produce the acridinones of choice.

The reaction to form **6a** was chosen as a template reaction. In a preliminary study, a solvent-free system was compared against ethanol in the presence of 0.07 g of the catalyst. It was found that better yield of **6a** was obtained in a solvent-free system. To determine the optimum quantity of catalyst required, different amounts of catalyst were investigated, viz., 0.02, 0.05, 0.07 g. It was found that increasing the quantity of the catalyst beyond 0.05 g did not increase the yield noticeably hence 0.06 g was selected as optimum for all subsequent reactions. Thereafter solvents such as methanol and acetonitrile were tested for their effect on the yield of **6a**. It was found that a microwave-assisted reaction in a solvent-free system produced the best yield (95 %) (Table 4A. 2: entry 6). Moderate yields were observed when ethanol, methanol or acetonitrile were used under different reflux conditions at 24 h (Table 4A. 2 entries 3-5). The yield decreased and longer reaction time was required to proceed the reaction with ethanol and methanol (Table 4A. 2 entries 1-2). Whilst investigating the microwave reaction, it was observed that a 10 minutes reaction at a temperature greater than140 $^{\circ}$C produced additional spots on the TLC plate which was taken as evidence for the formation

of by-products. Also a shorter reaction time showed the presence of starting materials as an indication of incomplete reaction.

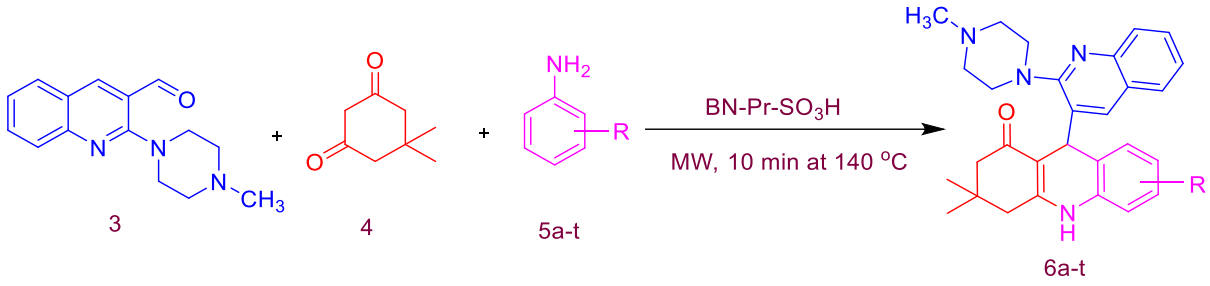

KEY: 6a (R=H); 6b (R=2- NO_2); 6c (R=3- NO_2); 6d (R=4- NO_2); 6e (R=2-F); 6f (R=3-F); 6g (R=4-F); 6h (R=4-Cl); 6i (R= 3,4-Cl); 6j (R= 3-Cl,4-F); 6k (R=4-Br); 6l (R=ortho-CH_3); 6m (R=meta- CH_3); 6n (R=para- CH_3); 6o (R=3,4- CH_3); 6p (R=ortho O-CH_3); 6q (R=para O-CH_3); 6r (R=Ar-H); 6s (R=Ar-H); 6t (R=Ar-H).

Scheme 4A. 2. The synthesis of 3,3-dimethyl-9-(2-(4-methylpiperazin-1-yl)quinolin-3-yl)-3,4,9,10 tetrahydroacridin-1(2H)-one derivatives.

Table 4A. 2. Optimization of the synthesis of **6a** under MW irradiation using BN-Pr-SO_3H

Entry	Catalyst	Solvent	Temp (°C)	Time(h/min)	Isolated Yield (%)
1	BN- Pr-SO_3H	EtOH	r.t	24	60
2	BN- Pr-SO_3H	MeOH	r.t	24	50
3	BN- Pr-SO_3H	CH_3CN	Reflux	24	80
4	BN- Pr-SO_3H	EtOH	Reflux	24	65
5	BN- Pr-SO_3H	MeOH	Reflux	24	58
6	BN- Pr-SO_3H	Neat	140	10 (min)	95

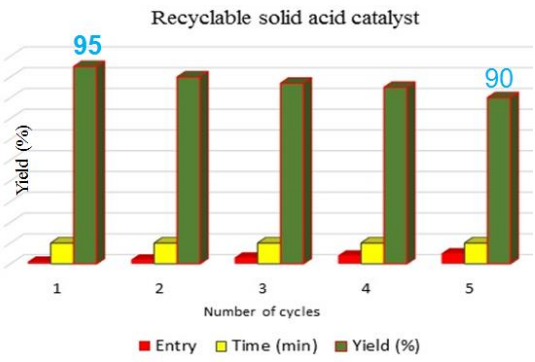

Figure 4A. 7. Reusability of catalyst

The re-usability potential of BN-Pr-SO_3H was also investigated in the model reaction to synthesize **6a**: briefly, the solid was rinsed with acetonitrile followed by methanol and heated at 100 °C, cooled and then used for subsequent reactions. It was found that BN-Pr-SO_3H could be re-used five times with only 5 % loss of catalytic activity (Figure 4A.7) and it was concluded that this catalyst might benefit industry if commercial application is required.

Table 4A. 3. The synthesis of piperazinyl-quinolinyl-fused benzo[*c*]acridinone derivatives in the presence of BN-Pr-SO_3H.

Entry	Substrate (5a-t)	Product (6a-t)	Time (min)	Isolated Yield (%)	M. p. (°C)
1	$C_6H_{6n}H_2$	6a	10	95	252-255
2	2-$O_2NC_6H_4NH_2$	6b	10	90	>300
3	3-$O_2NC_6H_4NH_2$	6c	10	85	290-292
4	4-$O_2NC_6H_4NH_2$	6d	10	87	>300
5	2-$FC_6H_4NH_2$	6e	10	90	>300
6	3-$FC_6H_4NH_2$	6f	10	88	280-283
7	4-$FC_6H_4NH_2$	6g	10	95	275-278
8	4-$ClC_6H_4NH_2$	6h	10	90	>300
9	$Cl_2C_6H_3NH_2$	6i	10	85	290-292
10	$ClC_6H_3(F)NH_2$	6j	10	90	270-272
11	4-$BrC_6H_4NH_2$	6k	10	85	>300
12	o-$CH_3C_6H_4NH_2$	6l	10	80	>300
13	m-$CH_3C_6H_4NH_2$	6m	10	85	270-272
14	p-$CH_3C_6H_4NH_2$	6n	10	83	>300
15	$(CH3)_2C_6H_4NH_2$	6o	10	90	280-282
16	o-C_6H_9NO	6p	10	80	>300
17	p-C_6H_9NO	6q	10	75	>300
18	$C_6H_6N_2$	6r	15	90	>300
19	$C_6H_8N_2$	6s	15	90	>300
20	$C_{10}H_7NH_2$	6t	15	85	>300

After optimising the reaction conditions, all the other products **5a-t** were synthesized using the appropriate starting materials (Scheme 4A. 3). Compounds **6a-6t** was characterized by FT-IR, ^{1}H NMR, ^{13}C NMR and MS-TOF whilst **6a** included 2D NMR, DEPT-90 and DEPT-135 (Appendix). Compound **6a** was chosen as the template structure for unambiguous

characterisation. The FT-IR spectrum showed stretching at 1681 and 3495 cm^{-1} for carbonyl and NH groups respectively. The ^{1}H NMR spectrum showed three singlets at δ 12.35, 8.24 and 4.85 for N_{19}-H, C_4-H and C_{16}-H respectively. The C_{22}-CH_2 proton was assigned at δ 2.48 (J = 13.04 Hz) as a doublet and C_{24}-CH_2 at δ 2.23 (J = 16.32 Hz,) as a doublet. The ^{13}C NMR spectrum showed the presence of one carbonyl group at δ 197.17. The structure was further confirmed on the basis of 2D NMR spectral studies. The selected HMBC correlation of compound **6a** is shown in Figure 4A. 8.

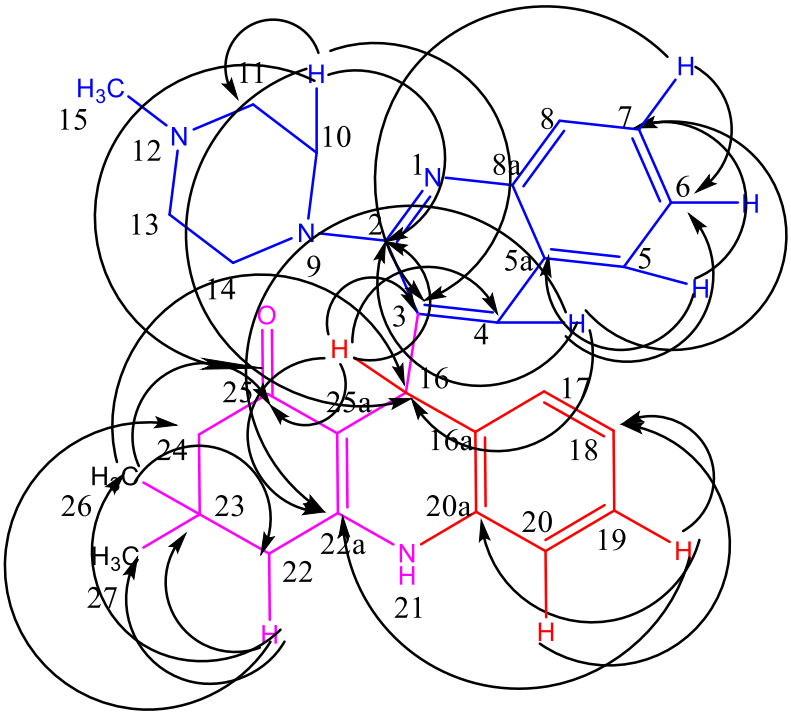

Figure 4A. 8. Selected HMBC correlation of compound **5a**.

The C, H-COSY (HSQC) correlation at δ 27.18, 29.24, 31.12, 40.92, 50.85, 111.24, 115.54, 123.41, 129.23, 128.77 and 142.96 are assigned to $C_{26, 27}$, C_{16}, C_{15}, $C_{22, 14, 10}$, $C_{24, 11, 13}$, C_{20}, C_{18}, C_7, C_{19}, C_5 and C_4 respectively. The carbon signal at δ 142.96, was due to the quinolinyl C_4-carbon. The H, HCOSY spectrum revealed the singlet at δ 4.85 which confirmed only one nearby hydrogen to C_4. The long range HMBC correlation is presented in Figure 4A. 8. The characteristic C_4-H correlated with quinolinyl and C-H carbon C_{16} at δ (29.24), C_6 at δ (123.41), C_7 at δ (129.23) C_{22}a at δ (130.43) and C_2 at δ (162.92), whilst the C_{16}-H correlated with quinolinyl carbon C_3 at δ (120.91), C_4 at δ (142.92) C_2 at δ (162.92), dimedone carbon C_{22}a at δ (130.43), C_{25} at δ (197.19). Similarly, correlation of C_5-H with quinolinyl carbon C_7 at δ (129.23), C_5a at δ (136.98), C_{19}-H proton correlated with amine carbon C_{18} at δ. (115.54),

at *δ.* C_{22}a at *δ.* (130.43), C_{20}a at *δ.* (136.98), whilst C_7-H correlated with quinolinyl carbon C_3 at *δ.* (120.91), C_6 at *δ.* (123.41), whilst C20-H correlated with amine carbon C_{18} at *δ.* (115.54), C_{10}-H correlated with quinolinyl carbon C_2 at *δ.* (164.92), C_3 at *δ.* (120.91), C_{16} C-H carbon at *δ.* (29.24), dimedone carbon C_{11} at *δ.* (50.85), C_{25} at *δ.* (197.19). Whilst C_{22}-H correlated with dimedone carbon C_{24} at *δ.* (50.85), $C_{26,\ 27}$ at *δ.* (27.18), C_{23} at *δ.* (32.20) and C_{26}-H correlated with C-H carbon C_{16} at *δ.* (29.91), dimedone carbon C_{22}a at *δ.* (130.43), C_{24} at *δ.* (50.85) C_2 at *δ.* (197.19) Figure 4A. 9. Selected ^{1}H NMR and ^{13}C NMR and HMBC chemical shifts of **6a** are as presented in Table 4A. 4. Based on the above spectral details, mass and elemental analysis TOFMS ES *m/z* (rel. int.): 455.37[M]$^+$. Anal. Calc. for $C_{29}H_{32}N_4O$: C, 76.96; H, 7.13; N, 12.38 %. Found: C, 76.98; H, 7.11; N, 12.36 %, the structure was confirmed as of 3,3-dimethyl-9-(2-(4-methylpiperazin-1-yl)quinolin-3-yl)-3,4,9,10-tetrahydroacridin-1(2H)-one **6a**. Thus, the one pot multi-component synthesis of the new piperazinyl-quinolinyl benzo-acridinone derivatives using the less studied BN-Pr-SO_3H was a neat and efficient reaction which is selective for the formation of the sought after molecule.

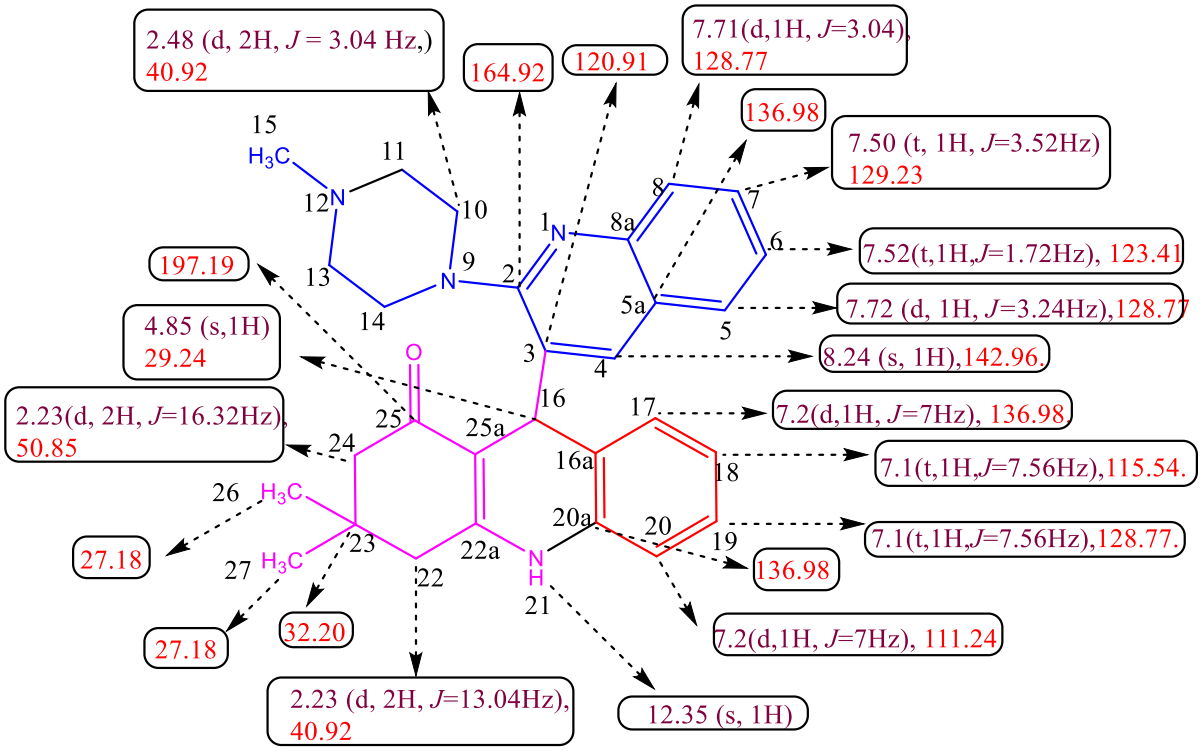

Figure 4A. 9. Selected (^{1}H) NMR and (^{13}C) NMR and HMBC chemical shifts of **5a**.

Table 4A. 4. Selected HMBC correlations of compound **6a**

S.NO	Proton	Correlated Carbons
1	C_4-H (s, 1H) at *δ.* 8.24	C_{16} at *δ.* (29.24), C_6 at *δ.* (123.41), C_7 at *δ.* (129.23) C_{22}a at *δ.* (130.43) C_2 at *δ.* (162.92).
2	C_{16}-H (s,1H) at *δ.* 4.85	C_3 at *δ.* (120.91), C_{22}a at *δ.* (130.43), C_4 at *δ.* (142.92) C_2 at *δ.* (162.92) C_{25} at *δ.* (197.19).
3	C_5-H (d, 1H, *J*=3.24Hz) at *δ.* 7.72	C_7 at *δ.* (129.23), C_5a at *δ.* (136.98)
4	C_{19}-H (t, 1H, *J*=7.56Hz) at *δ.* 7.1	C_{18} at *δ.* (115.54), at *δ.* C_{22}a at *δ.* (130.43), C_{20}a at *δ.* (136.98)
5	C_7-H (t, 1H, *J*=3.52Hz) at *δ.* 7.50	C_3 at *δ.* (120.91), C_6 at *δ.* (123.41)
6	C_{20}-H (d, 1H, *J*= 7Hz) at *δ.* 7.2	C_{18} at *δ.* (115.54)
7	C_{10}-H CH_2 (d, 2H, *J*=3.04Hz) at *δ.* 2.48	C_2 at *δ.* (164.92), C_3 at *δ.* (120.91), C_{16} at *δ.* (29.24) C_{11} at *δ.* (50.85), C_{25} at *δ.* (197.19).
8	C_{22}-H CH_2 (d, 2H, *J*=13.04Hz) at *δ.* 2.23	C_{24} at *δ.* (50.85), $C_{26, 27}$ at *δ.* (27.18), C_{23} at *δ.* (32.20)
9	C_{26}-H CH_3 (s, 3H) at *δ.* 0.95	C_{16} at *δ.* (29.91), C_{22}a at *δ.* (130.43), C_{24} at *δ.* (50.85) C_2 at *δ.* (197.19)

Since this is a new reaction, a proposed mechanism as presented in the scheme 4A.3. In the first step, the acidic catalyst activated the aldehyde carbonyl functionality thereby enabling dimedone to form a new covalent bond with loss of water as in the Knoevenagel condensation to produce intermediate **I**. In the next step, the catalyst activated the intermediate **I** thereby facilitating a Michael addition to give intermediate **II**. This was followed by a simple

intramolecular condensation reaction to produce intermediate **III** which subsequently underwent a proton transfer reaction and subsequent water loss to produce **6a**.

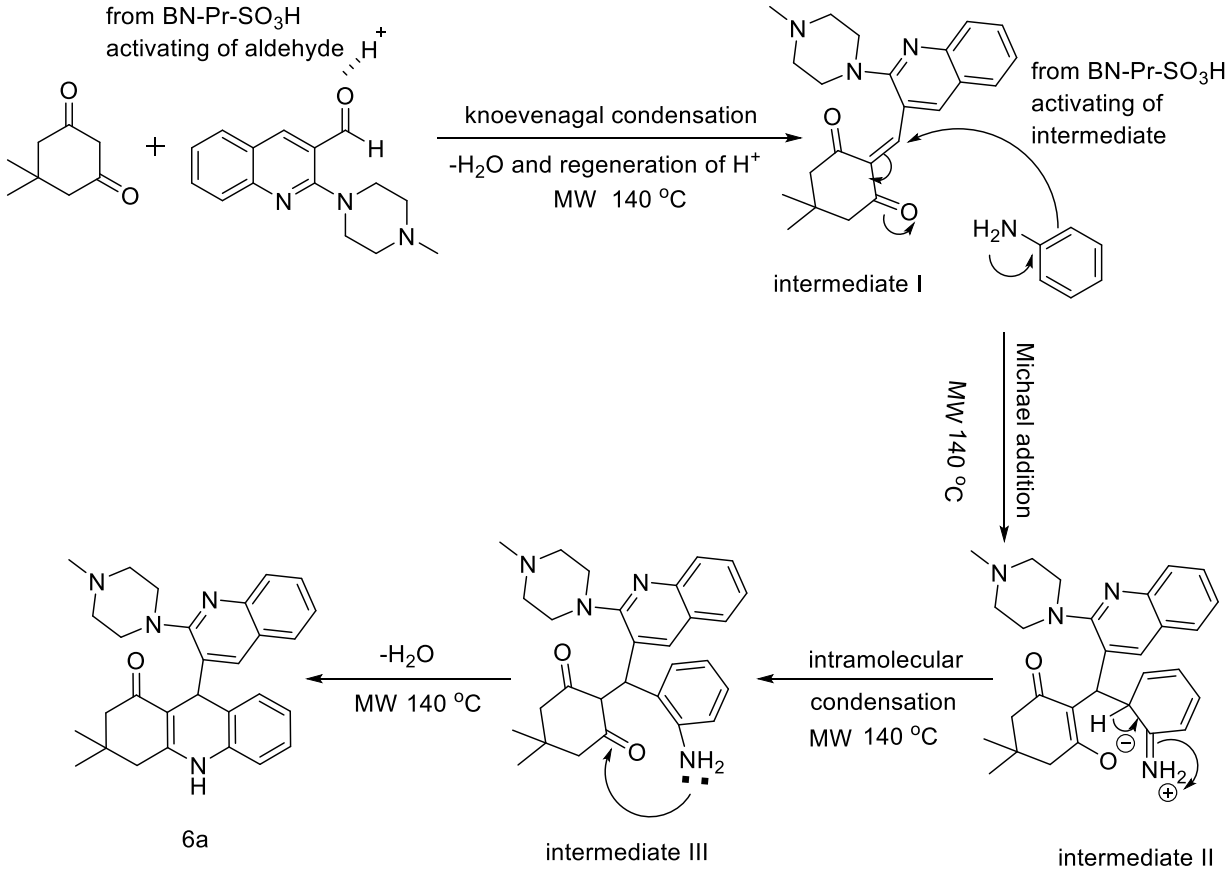

Scheme 4A. 3. A proposed mechanism for the synthesis of 3,3-dimethyl-9-(2-(4-methylpiperazin-1-yl) quinolin-3-yl)-3,4, 9,10-tetrahydroacridin-1(2H)-one

In order to determine the binding mode of action of the novel compounds, rigid/flexible molecular docking analyses were performed using an Auto Dock 4.2 program. Investigations with DNA and **6a, 6g** and **6t** complex crystals (Malinina *et al.* 2002) were performed. The binding activity of DNA-intercalates was generally associated with strong DNA-binding and long drug residence times at individual sites. The tricyclic system was intercalated between the base pairs of DNA, and the benzo-acridine group was always oriented into the minor groove. In all of the cases analysed, the benzo ring was stacked in between thymine bases (DT-619 and DT-620), with the exception of **6a** which was stacked in between adenine bases DA-616 and DA-617. The guanine base pairs DG-512 and DG-514 and cytosine base pairs DC-512 and DC-514 indicated that the complex binds to DNA towards the guanine

base pairs G-C rich region due to Van der Waals interaction and hydrophobic contacts with the functional groups of DNA as shown in Figure 4A. 10.

The tricyclic system intercalated between the base pairs of DNA, and the fluorobenzo-acridine **6g** group always oriented into the minor groove. In all of the cases analysed, the fluorobenzo-acridine ring was stacked in between adenine base pairs DA-618 and DA-619, with the exception of compounds **6g** in which it was stacked in between thymine bases DT-619 and DT-620. The guanine base pairs DG-519 and DG-520 and cytosine base pairs DC-415 and DC-416 indicated that the complex bind to DNA towards the guanine base pairs G-C rich region due to Van der Waals interaction and hydrophobic contacts with the functional groups of DNA. The principal interactions observed for the compounds were π–π stacking, hydrogen bonding and salt bridge formation. A salt bridge was consistently formed between the tertiary amino groups shown in (Figure 4A. 11).

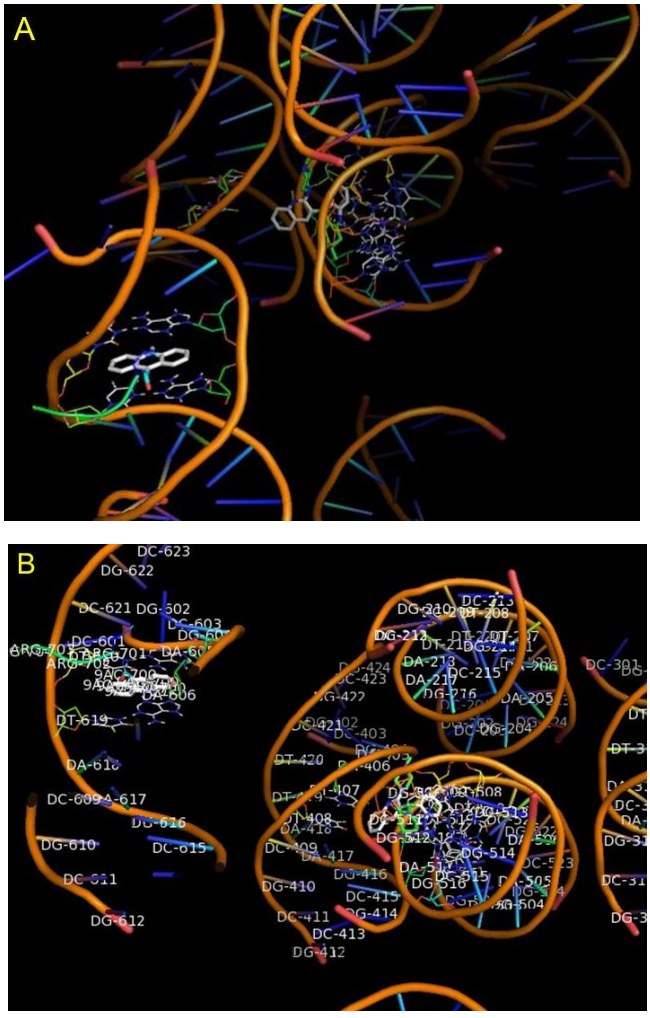

Figure 4A. 10. (A-B). (A) Molecular docking of the DNA-compound **6a** complex. (B) Binding site of DNA-compound **6a** and selected base pairs residues are represented by stick and cartoon models. Hydrogen bonds are shown in pink dotted line.

The orientation adopted by the tricyclic system of **6t** in the docked complex showed optimum overlap with the DNA base pairs; the naphthalene benzo-acridine group always oriented into the minor groove. **6t** was stacked in between guanine bases DG-602 and DG-604 and cytosine bases DC-603 and DC-604. From the analysis of the docked complexes, compounds bearing the benzo-acridine group were predicted to dock into DNA with a better overlap of the piperazinyl quinoline nucleus and the DNA base pairs; whereas the compounds without this substituent were shifted towards the thymine ring, thus decreasing their overlap (Figure 4A . 12).

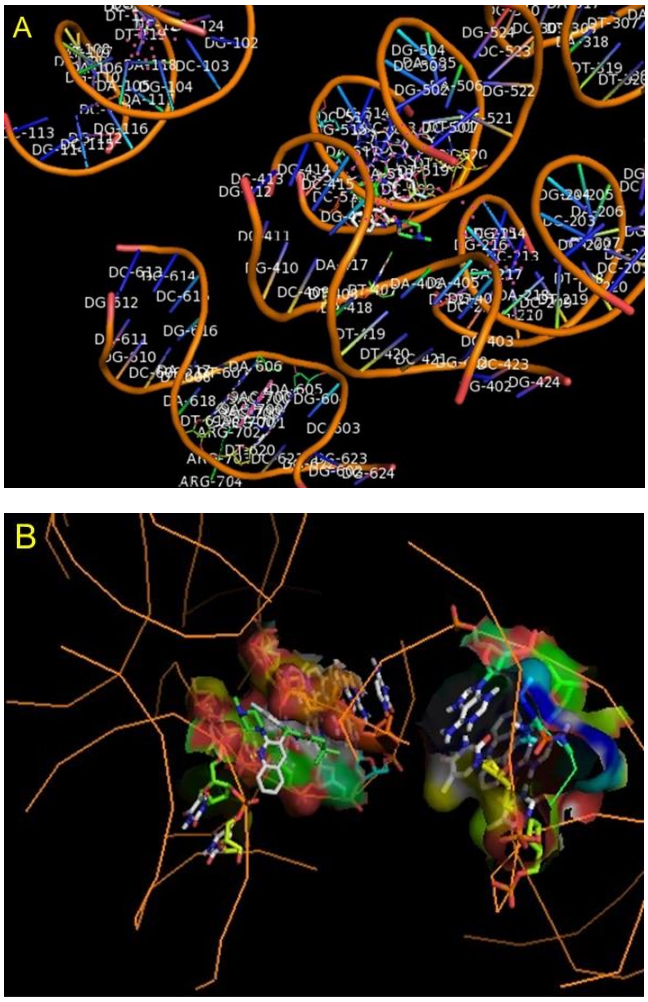

Figure 4A. 11. (A-B). (A) Binding site of DNA-compound **6g** and selected base pairs residues are represented by stick and cartoon models. Hydrogen bonds are shown in pink dotted line. (B) Molecular docking of the DNA-compound **6g** complex.

Formation of a charge transfer complex of **6a, 6g** and **6t** through π–π interactions is known to play a major role in the stability of DNA-intercalated complexes, and such electronic

interaction depends on a good overlap. This observation can explain why the presence of a benzo-acridine group at position two led to a reduction of the number of sites occupied by these derivatives in the DNA (QMAX) which relates with the ability of the compound to displace ethidium bromide from specific DNA sites, and hence this cannot be directly correlated with the theoretical calculations presented here. These obtained values just provide the probable geometry of the complexes; however the binding has been established experimentally.

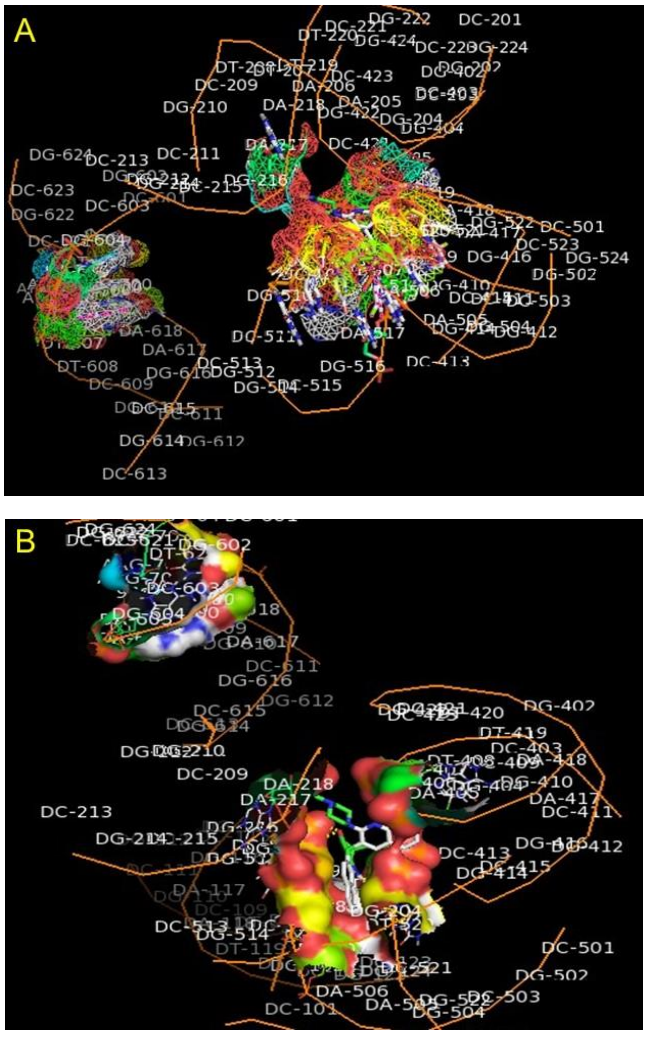

Figure 4A. 12. (A-B). (A) Molecular docking of the DNA-compound **6t** complex. (B) Binding site of DNA-compound **6t** and selected base pairs residues are represented by stick and cartoon models. Hydrogen bonds are shown in pink dotted line

4A. 4. Conclusion

A new boron nitride based sulphonic acid catalyst was prepared and fully characterized. It was used in a one-pot reaction for the synthesis of functionalised methyl piperazinyl-quinolinyl benzo-acridinone derivatives. This reaction under microwave conditions is fast, safe, and environmentally friendly and produces compounds in high yield. Furthermore, the catalyst was recycled five times and showed only 5 % loss in catalytic activity thereby making it cost-effective for possible industrial application. Molecular docking analysis with DNA and **6a, 6g** and **6t** showed the tricyclic system intercalated between the base pairs of DNA, whilst the benzo-acridinone group was always oriented into the minor groove.

4A. 5. Experimental

4A. 5. 1. Preparation of the boron nitride based sulphonic acid catalyst

A mixture containing BN and 65 % nitric acid was refluxed for 24h. Thereafter, BN (10 g) and (3-mercaptopropyl) trimethoxysilane (15 mL) were added to dry toluene (30 mL), in a round bottom flask, and the reaction mixture was refluxed for 24 h. After this period, the mixture was filtered and the solid was washed with acetone and dried. To 5 g of the solid, 30 % H_2O_2 (10 mL) and methanol (30 mL) was added followed by two drops of conc. H_2SO_4. The reaction mixture was stirred for 24 h at room temperature. The mixture were filtered and washed with distilled water followed by acetone and air dried to give BN-Pr-SO_3H.

4A. 5. 2. General Procedure for the synthesis of substituted 2-(4-methylpiperazin-1-yl) quinoline-3-carbaldehyde (3)

The procedure and spectroscopic data are presented in **Chapter 3. 5. 2**

4A. 5. 3. General Procedure for the synthesis of 3, 3-dimethyl-9-(2-(4-methylpiperazin-1-yl) quinolin-3-yl)-3, 4, 9, 10-tetrahydroacridin-1(2H)-one derivatives (6a-t).

An aliquot of BN-Pr-SO_3H (0.07g) was activated in vacuum at 100 °C, cooled to room temperature and added to a mixture containing 2-(4-methylpiperazin-1-yl)quinoline-3-carbaldehyde (1.0 mmol), dimedone (1.0 mmol) and aniline (1.0 mmol). The mixture was heated at 140 °C in a microwave set at 200 W. The reaction was monitored by TLC. After completion of the reaction, the mixture was dissolved in ethanol and filtered. The filtrate was collected and purified by chromatography using silica gel in a mobile phase of hexane: acetone of 85:15. The catalyst was washed subsequently with dilute hydrochloric acid, distilled water

and acetone, sequentially. The catalyst was dried under vacuum and re-used. The spectral data of **6a-t** is presented below.

4A. 5. 3. 1. 3, 3-dimethyl-9-(2-(4-methylpiperazin-1-yl)quinolin-3-yl)-3,4,9,10 tetrahydroacridin-1(2H)-one (6a).

White colour solid: yield 95 %: FT-IR (KBr): 3495, 3236, 3159, 2961, 2259, 1681, 1630, 1568, 1434, 1358, 1196, 1135, 999, 764, 571 cm^{-1}. ^{1}H NMR ($CDCl_3$, 400 MHz): δ 12.35 (1H, s, N-H), 8.24 (1H, s, Ar-H), 7.72 (1H, d, *J* = 3.24 Hz, Ar-H), 7.71 (1H, d, *J* = 3.04 Hz, Ar-H), 7.52 (1H, t, *J* = 1.12 Hz, Ar-H), 7.50 (1H, t, *J* = 3.52 Hz, Ar-H), 7.35 (2H, d, *J* = 8.36 Hz, Ar-H), 7.26 (2H, t, *J* = 3.76 Hz, Ar-H), 4.85 (1H, s, CH), 2.48 (4H, d, *J* = 3.04 Hz, CH_2), 2.23 (4H, d, *J* = 16.32 Hz, CH_2), 2.17 (4H, d, *J* = 16.32 Hz, CH_2), 1.08 (3H, s, CH_3), 0.95 (6H, s, CH_3). ^{13}C NMR ($CDCl_3$, 100 MHz): δ 197.1, 164.9, 162.3, 142.9, 136.9, 130.4, 129.2, 128.7, 123.4, 120.9, 115.5, 111.2, 50.8, 40.9, 32.2, 31.1, 29.2, 27.1. TOFMS ES *m/z* (rel. int.): 455.37$[M]^{+}$. Anal. Calc. for $C_{29}H_{32}N_4O$: C, 76.96; H, 7.13; N, 12.38 %. Found: C, 76.98; H, 7.11; N, 12.36 %.

4A. 5. 3. 2. 3, 3-dimethyl-9-(2-(4-methylpiperazin-1-yl)quinolin-3-yl)-5-nitro-3,4,9,10 tetrahydroacridin-1(2H)-one (6b).

White colour solid: yield 90 %: FT-IR (KBr): 3319, 3164, 3106, 3066, 2963, 2306, 1968, 1812, 1680, 1636, 1568, 1480, 1487, 1194, 1136, 999, 929, 764 cm^{-1}. ^{1}H NMR ($CDCl_3$, 400 MHz): δ 12.72 (1H, s, N-H), 8.05 (1H, s, Ar-H), 7.58 (2H, d, *J* = 7.48 Hz, Ar-H), 7.38 (1H, t, *J* = 7.16 Hz, Ar-H), 7.23 (2H, d, *J* = 8.12 Hz, Ar-H), 7.1 (2H, t, *J* = 7.56 Hz, Ar-H), 4.74 (1H, s, CH), 2.3 (4H, CH_2), 2.1 (8H, CH_2), 0.98 (3H, s, CH_3), 0.82 (6H, s, CH_3). ^{13}C NMR ($CDCl_3$, 100 MHz): δ 197.1, 164.8, 163.1, 141.4, 138, 130.1, 129.5, 128.6, 122.2, 120.4, 115, 111.5, 50.8, 41, 32.1, 31.2, 29.3, 27.3. Anal. Calc. for $C_{29}H_{31}N_5O_3$: C, 70.00; H, 6.28; N, 14.07 %. Found: C, 70.2; H, 6.26; N, 14.10 %.

4A. 5. 3. 3. 3,3-dimethyl-9-(2-(4-methylpiperazin-1-yl)quinolin-3-yl)-6-nitro-3,4,9,10 tetrahydroacridin-1(2H)-one (6c).

White colour solid: yield 85 %: FT-IR (KBr): 3466, 3306, 3162, 3057, 2962, 2367, 1969, 1811, 1676, 1664, 1663, 1583, 1434, 1358, 1197, 1165, 1136, 999, 765 cm^{-1}. ^{1}H NMR ($CDCl_3$, 400 MHz): δ 12.74 (1H, s, N-H), 8.13 (1H, s, Ar-H), 7.67 (1H, d, *J* = 7.6 Hz, Ar-H), 7.47 (1H, s, Ar-H), 7.45 (2H, d, *J* = 0.76 Hz, Ar-H), 7.32 (1H, d, *J* = 8.12 Hz, Ar-H), 7.22 (2H, t, *J* = 7.56 Hz, Ar-H), 4.83 (1H, s, CH), 2.47(4H, s, CH_2), 2.24 (4H, d, CH_2), 2.16(4H, d, CH_2), 1.06

(3H, s, CH_3), 0.90 (6H, s, CH_3). ^{13}C NMR ($CDCl_3$, 100 MHz): δ 197.1, 164.8, 163.1, 141.4, 138, 130.1, 129.5, 128.6, 122.2, 120.4, 115, 111.5, 50.8, 41, 32.1, 31.2, 29.3, 27.3. Anal. Calc. for $C_{29}H_{31}N_5O_3$: C, 70.00; H, 6.28; N, 14.07 %. Found: C, 70.08; H, 6.30; N, 14.08 %.

4A. 5. 3. 4. 3,3-dimethyl-9-(2-(4-methylpiperazin-1-yl)quinolin-3-yl)-7-nitro-3,4,9,10 tetrahydroacridin-1(2H)-one (6d).

White colour solid: yield 87 %: FT-IR (KBr): 3496, 3236, 3159, 2961, 2259, 1968, 1811, 1681, 1630, 1568, 1434, 1358, 1196, 1135, 999, 929, 764, 571 cm^{-1}. ^1H NMR ($CDCl_3$, 400 MHz): δ 12.52 (1H, s, N-H), 8.06 (1H, s, Ar-H), 7.6 (1H, s, Ar-H), 7.59 (1H, d, J = 7.52 Hz, Ar-H), 7.41 (1H, d, J = 1.2 Hz, Ar-H), 7.37 (1H, d, J = 7.2 Hz, Ar-H), 7.22 (1H, d, J = 8.12 Hz, Ar-H), 7.12 (2H, t, J = 7.16 Hz, Ar-H), 4.74 (1H, s, CH), 2.43(4H, s, CH_2), 2.15 (4H, d, CH_2), 2.07(4H, d, CH_2), 0.9 (3H, s, CH_3), 0.82 (6H, s, CH_3). ^{13}C NMR ($CDCl_3$, 100 MHz): δ 197.1, 164.7, 141.5, 129.6, 128.6, 122.3, 120.4, 115, 111.5, 50.9, 41, 32.1, 31.2, 29.3, 27. Anal. Calc. for $C_{29}H_{31}N_5O_3$: C, 70.00; H, 6.28; N, 14.07 %. Found: C, 70.05; H, 6.25; N, 14.04 %.

4A. 5. 3. 5. 5-fluoro-3,3-dimethyl-9-(2-(4-methylpiperazin-1-yl)quinolin-3-yl)-3,4,9,10 tetrahydroacridin-1(2H)-one (6e).

White colour solid: yield 90 %: FT-IR (KBr): 3496, 3163, 3108, 3063, 2961, 2921, 2364, 1969, 1812, 1664, 1625, 1568, 1488, 1466, 1434, 1408, 1360, 1196, 1136, 999, 765, 628, 572 cm^{-1}. ^1H NMR ($CDCl_3$, 400 MHz): δ 12.75 (1H, s, N-H), 8.12 (1H, s, Ar-H), 7.67 (1H, d, J = 7.6 Hz, Ar-H), 7.47 (1H, t, J = 7.36 Hz, Ar-H), 7.45 (2H, d, J = 0.76 Hz, Ar-H), 7.32 (1H, d, J = 8.16 Hz, Ar-H), 7.22 (2H, t, J = 7.28 Hz, Ar-H), 4.82 (1H, s, CH), 2.47(4H, s, CH_2), 2.23 (4H, d, CH_2), 2.15(4H, d, CH_2), 1.0 (3H, s, CH_3), 0.9 (6H, s, CH_3). ^{13}C NMR ($CDCl_3$, 100 MHz): δ 197.1, 164.7, 163.1, 141.3, 138, 130.1, 129.5, 128.5 122.2, 120.4, 114.9, 111.5, 50.8, 41, 32.1, 31.2, 29.3, 27. ^{19}F NMR ($CDCl_3$, 400 MHz): δ -105.8, -109.8, -110.2, -110.7, -110.8, -111.5, -115.8. Anal. Calc. for $C_{29}H_{31}FN_4O$: C, 74.02; H, 6.64; N, 11.91 %. Found: C, 74.05; H, 6.66; N, 11.98 %.

4A. 5. 3. 6. 6-fluoro-3,3-dimethyl-9-(2-(4-methylpiperazin-1-yl)quinolin-3-yl)-3,4,9,10 tetrahydroacridin-1(2H)-one (6f).

White colour solid: yield 88 %: FT-IR (KBr): 3309, 3160, 3108, 3063, 2961, 2918, 2358, 1966, 1942, 1812, 1664, 1662, 1568, 1434, 1360, 1197, 1165, 1136, 765, 999, 952, 571, 514 cm^{-1}. ^1H NMR ($CDCl_3$, 400 MHz): δ 12.73 (1H, s, N-H), 8.13 (1H, s, Ar-H), 7.67 (1H, d, J = 7.6 Hz, Ar-H), 7.49 (1H, d, J = 0.96 Hz, Ar-H), 7.47 (1H, s, Ar-H), 7.45 (1H, d, J = 0.76 Hz,

Ar-H), 7.32 (1H, d, *J* = 8.16 Hz, Ar-H), 7.15 (2H, t, *J* = 7.28 Hz, Ar-H), 4.82 (1H, s, CH), 2.47(4H, s, CH_2), 2.23 (4H, d, CH_2), 2.15 (4H, d, CH_2), 1.06 (3H, s, CH_3), 0.9 (6H, s, CH_3). ^{13}C NMR ($CDCl_3$, 100 MHz): δ 197.1, 164.7, 163, 141.4, 138, 130.1, 129.5, 128.6, 122.3, 120.4, 115, 111.5, 50.8, 41, 32.1, 31.2, 29.3, 27. ^{19}F NMR ($CDCl_3$, 400 MHz): δ -105.8, -109.8, -110.2, -110.7, -110.8, -111.5, -115.8. Anal. Calc. for $C_{29}H_{31}FN_4O$: C, 74.02; H, 6.64; N, 11.91 %. Found: C, 74.08; H, 6.62; N, 11.96 %.

4A. 5. 3. 7. 7-fluoro-3,3-dimethyl-9-(2-(4-methylpiperazin-1-yl)quinolin-3-yl)-3,4,9,10 tetrahydroacridin-1(2H)-one (6g).

White colour solid: yield 95 %: FT-IR (KBr): 3456, 3307, 3159, 3108, 3060, 2961, 2915, 2361, 1966, 1811, 1664, 1663, 1589, 1466, 1434, 1366, 1197, 1165, 1136, 999, 765, 571 cm^{-1}. ^{1}H NMR ($CDCl_3$, 400 MHz): δ 12.66 (1H, s, N-H), 8.14 (1H, s, Ar-H), 7.66 (1H, d, *J* = 7.6 Hz, Ar-H), 7.49 (1H, d, *J* = 0.96 Hz, Ar-H), 7.47 (1H, s, Ar-H), 7.45 (1H, d, *J* = 0.76 Hz, Ar-H), 7.32 (1H, d, *J* = 8.16 Hz, Ar-H), 7.18 (2H, t, *J* = 7.28 Hz, Ar-H), 4.83 (1H, s, CH), 2.47 (4H, s, CH_2), 2.23 (4H, d, CH_2), 2.15 (4H, d, CH_2), 1.07 (3H, s, CH_3), 0.9 (6H, s, CH_3). ^{13}C NMR ($CDCl_3$, 100 MHz): δ 197.1, 164.7, 163, 141.4, 137.9, 130.1, 129.5, 128.6, 122.3, 120.4, 115, 111.5, 50.8, 41.9, 32.1, 31.1, 29.2, 27. ^{19}F NMR ($CDCl_3$, 400 MHz): δ -105.8, -109.8, -110.2, -110.7, -110.8, -111.5, -115.8. Anal. Calc. for $C_{29}H_{31}FN_4O$: C, 74.02; H, 6.64; N, 11.91 %. Found: C, 74.04; H, 6.67; N, 11.93 %.

4A. 5. 3. 8. 7-chloro-3,3-dimethyl-9-(2-(4-methylpiperazin-1-yl)quinolin-3-yl)-3,4,9,10 tetrahydroacridin-1(2H)-one (6h).

White colour solid: yield 90 %: FT-IR (KBr): 3474, 3306, 3161, 3108, 3062, 2961, 2918, 2367, 1969, 1811, 1661, 1568, 1434, 1359, 1197, 1165, 1135, 765, 572 cm^{-1}. ^{1}H NMR ($CDCl_3$, 400 MHz): δ 12.57 (1H, s, N-H); 8.14 (1H, s, Ar-H), 7.67 (1H, d, *J* = 7.6 Hz, Ar-H), 7.5 (2H, d, *J* = 7.2 Hz, Ar-H), 7.45 (1H, s, Ar-H), 7.32 (1H, d, *J* = 8.16 Hz, Ar-H), 7.22 (2H, t, *J* = 7.6 Hz, Ar-H), 4.83 (1H, s, CH), 2.47 (4H, s, CH_2), 2.24 (4H, d, CH_2), 2.16 (4H, d, CH_2), 1.07 (3H, s, CH_3), 0.91 (6H, s, CH_3). ^{13}C NMR ($CDCl_3$, 100 MHz): δ 197.1, 164.8, 162.8, 137.6, 129.8, 128.6, 122.6, 120.5, 115.1, 111.4, 50.8, 40.9, 32.1, 31.1, 29.2, 27. Anal. Calc. for $C_{29}H_{31}ClN_4O$: C, 71.52; H, 6.42; N, 11.50 %. Found: C, 71.56; H, 6.40; N, 11.53 %.

4A. 5. 3. 9. 7,8-dichloro-3,3-dimethyl-9-(2-(4-methylpiperazin-1-yl)quinolin-3-yl)-3,4,9,10 tetrahydroacridin-1(2H)-one (6i).

White colour solid: yield 85 %: FT-IR (KBr): 3308, 3105, 3161, 3067, 2961, 2915, 2364, 2327, 1969, 1812, 1667, 1664, 1568, 1434, 1408, 1360, 1197, 1135, 999, 765, 571, 514 cm^{-1}. ^1H NMR ($CDCl_3$, 400 MHz): δ 12.41 (1H, s, N-H), 8.14 (1H, s, Ar-H), 7.67 (1H, d, *J* = 7.6 Hz, Ar-H), 7.49 (1H, d, *J* = 0.88 Hz, Ar-H), 7.45 (1H, d, *J* = 7.2 Hz, Ar-H), 7.3 (1H, d, *J* = 8.16 Hz, Ar-H), 7.25 (2H, t, *J* = 7.68 Hz, Ar-H), 4.83 (1H, s, CH), 2.47 (4H, s, CH_2), 2.24 (4H, d, CH_2), 2.16 (4H, d, CH_2), 1.07 (3H, s, CH_3), 0.92 (6H, s, CH_3). ^{13}C NMR ($CDCl_3$, 100 MHz): δ 197.1, 164.8, 141.9, 137.6, 129.8, 128.6, 122.7, 120.6, 115.1, 111.4, 50.8, 40.9, 32.1, 31.1, 29.2, 27. Anal. Calc. for $C_{29}H_{30}Cl_2N_4O$: C, 66.79; H, 5.80; N, 10.74 %. Found: C, 66.76; H, 5.82; N, 10.76 %.

4A. 5. 3. 10. 8-chloro-7-fluoro-3,3-dimethyl-9(2(4methylpiperazin1yl)quinolin3yl)3,4,9,10 tetrahydroacridin-1(2H)-one (6j).

White colour solid: yield 90 %: FT-IR (KBr): 3307, 3161, 3105, 2961, 2397, 1968, 1811, 1646, 1466, 14078, 1368, 1196, 1135, 999, 765, 577, 574 cm^{-1}. ^1H NMR ($CDCl_3$, 400 MHz): δ 12.76 (1H, s, N-H), 8.05 (1H, s, Ar-H), 7.59 (1H, d, *J*=7.6 Hz, Ar-H), 7.45 (2H, d, *J* = 7.2 Hz, Ar-H), 7.37 (1H, d, *J* = 0.8 Hz, Ar-H), 7.12 (2H, t, *J* = 7.6 Hz, Ar-H), 4.74 (1H, s, CH), 2.39 (4H, s, CH_2), 2.15 (4H, d, CH_2), 2.07 (4H, d, CH_2), 0.98 (3H, s, CH_3), 0.82 (6H, s, CH_3). ^{13}C NMR ($CDCl_3$, 100 MHz): δ 197.1, 164.7, 163.1, 141.3, 138, 130.1, 129.5, 128.6, 122.2, 120.4, 115, 111.5, 50.8, 41, 32.1, 31.2, 29.3, 27. ^{19}F NMR ($CDCl_3$, 400 MHz): δ -109.8, -110.2, -110.7, -110.8, -111.5. Anal. Calc. for $C_{29}H_{30}ClFN_4O$: C, 68.97; H, 5.99; N, 11.09 %. Found: C, 68.95; H, 5.97; N, 11.12 %.

4A. 5. 3. 11. 7-bromo-3,3-dimethyl-9-(2-(4-methylpiperazin-1-yl)quinolin-3-yl)-3,4,9,10 tetrahydroacridin-1(2H)-one (6k).

White colour solid: yield 85 %: FT-IR (KBr): 3308, 3162, 3108, 3037, 2961, 2306, 1968, 1812, 1625, 1568, 1487, 1437, 1434, 1408, 1356, 1198, 1136, 999, 764, 571 cm^{-1}. ^1H NMR ($CDCl_3$, 400 MHz): δ 12.64 (1H, s, N-H), 8.14 (1H, s, Ar-H), 7.67 (1H, d, *J* = 7.76 Hz, Ar-H), 7.5 (2H, d, *J* = 7.2 Hz, Ar-H), 7.48 (1H, s, Ar-H), 7.32 (1H, d, *J* = 8.16 Hz, Ar-H), 7.25 (2H, t, *J* = 7.52 Hz, Ar-H), 4.83 (1H, s, CH), 2.47 (4H, s, CH_2), 2.24 (4H, d, CH_2), 2.16 (4H, d, CH_2), 1.07 (3H, s, CH_3), 0.91 (6H, s, CH_3). ^{13}C NMR ($CDCl_3$, 100 MHz): δ 197.1, 164.8, 141.5, 137.8, 129.7, 128.6, 122.5, 120.5, 115.1, 111.5, 50.8, 41, 32.1, 31.1, 29.2, 27. Anal. Calc. for $C_{29}H_{31}BrN_4O$: C, 65.54; H, 5.88; N, 10.54 %. Found: C, 65.56; H, 5.86; N, 10.57 %.

4A. 5. 3. 12. 3,3,5-trimethyl-9-(2-(4-methylpiperazin-1-yl)quinolin-3-yl) 3,4,9,10 tetrahydroacridin-1(2H)-one (6l).

White colour solid: 80 %: FT-IR (KBr): 3474, 3309, 3159, 3111, 3066, 2962, 2376, 1972, 1812, 1664, 1626, 1565, 1434, 1360, 1197, 1165, 1135, 999, 929, 765, 571, 467 cm^{-1}. ^{1}H NMR ($CDCl_3$, 400 MHz): δ 12.85 (1H, s, N-H); 8.13 (1H, s, Ar-H), 7.66 (1H, d, *J* = 0.56 Hz, Ar-H), 7.48 (1H, t, *J* = 1.16 Hz, Ar-H), 7.45 (2H,d t, *J* = 0.96 Hz, Ar-H), 7.32 (1H, d, *J* = 8.12 Hz, Ar-H), 7.18 (2H, t, *J* = 0.72 Hz, Ar-H), 4.82 (1H, s, CH), 2.47 (4H, s, CH_2), 2.23 (4H, d, CH_2), 2.15 (4H, d, CH_2), 1.06 (6H, s, CH_3), 0.9 (6H, s, CH_3). ^{13}C NMR ($CDCl_3$, 100 MHz): δ 197.1, 164.7, 163, 141.5, 137.9, 130, 129.6, 128.6, 122.3, 120.4, 115, 111.4, 50.8, 41, 32.1, 31.2, 29.3, 27. Anal. Calc. for $C_{30}H_{34}N_4O$: C, 77.22; H, 7.34; N, 12.01 %. Found: C, 77.24; H, 7.36; N, 12.05 %.

4A. 5. 3. 13. 3,3,6-trimethyl-9-(2-(4-methylpiperazin-1-yl)quinolin-3-yl)-3,4,9,10 tetrahydroacridin-1(2H)-one (6m).

White colour solid: yield 85 %: FT-IR (KBr): 3507, 3306, 3160, 2961, 2315, 1969, 1812, 1668, 1646, 1568, 1434, 1197, 1135, 999, 929, 764, 571 cm^{-1}. ^{1}H NMR ($CDCl_3$, 400 MHz): δ 12.5 (1H, s, N-H); 8.1 (1H, s, Ar-H), 7.68 (1H, d, *J* = 7.4 Hz, Ar-H), 7.5 (1H, d, *J* = 0.96 Hz, Ar-H), 7.48 (1H, s, Ar-H), 7.45 (1H, d, *J* = 1.16 Hz, Ar-H), 7.32 (1H, d, *J* = 8.37 Hz, Ar-H), 7.23 (2H, t, *J* = 7.4 Hz, Ar-H), 4.83 (1H, s, CH), 2.48 (4H, s, CH_2), 2.24 (4H, d, CH_2), 2.16 (4H, d, CH_2), 1.07 (6H, s, CH_3), 0.92 (6H, s, CH_3). ^{13}C NMR ($CDCl_3$, 100 MHz): δ 197.1, 164.7, 163, 141.5, 137.9, 130, 129.6, 128.6, 122.3, 120.4, 115, 111.4, 50.8, 41, 32.1, 31.2, 29.3, 27. Anal. Calc. for $C_{30}H_{34}N_4O$: C, 77.22; H, 7.34; N, 12.01 %. Found: C, 77.26; H, 7.35; N, 12.04 %.

4A. 5. 3. 14. 3,3,7-trimethyl-9-(2-(4-methylpiperazin-1-yl)quinolin-3-yl)-3,4,9,10 tetrahydroacridin-1(2H)-one (6n).

White colour solid: yield 83 %: FT-IR (KBr): 3307, 3158, 3114, 3066, 2961, 2918, 2860, 2367, 1963, 1939, 1812, 1664, 1568, 1434, 1360, 1197, 1135, 1166, 999, 764, 571 cm^{-1}. ^{1}H NMR ($CDCl_3$, 400 MHz): δ 12.43 (1H, s, N-H), 8.15 (1H, s, Ar-H), 7.68 (1H, d, *J* = 7.4 Hz, Ar-H), 7.5 (1H, d, *J* = 0.96 Hz, Ar-H), 7.48 (1H, s, Ar-H), 7.45 (1H, d , *J* = 1.16 Hz, Ar-H), 7.32 (1H, d, *J* = 8.37 Hz, Ar-H), 7.23 (2H, t, *J* = 7.4 Hz, Ar-H), 4.83 (1H, s, CH), 2.47 (4H, s, CH_2), 2.24 (4H, d, CH_2), 2.16 (4H, d, CH_2), 1.07 (6H, s, CH_3), 0.92 (6H, s, CH_3). ^{13}C NMR ($CDCl_3$, 100 MHz): δ 197.1, 164.8, 162.8, 137.6, 129.8, 128.6, 122.6, 120.5, 115.1, 111.4, 50.8,

40.9, 32.1, 31.1, 29.2, 27. Anal. Calc. for $C_{30}H_{34}N_4O$: C, 77.22; H, 7.34; N, 12.01 %. Found: C, 77.23; H, 7.32; N, 12.00 %.

4A. 5. 3. 15. 3,3,5,7-tetramethyl-9-(2-(4-methylpiperazin-1-yl)quinolin-3-yl)-3,4,9,10 tetrahydroacridin-1(2H)-one (6o).

White colour solid: 90 %: FT-IR (KBr): 3615, 3304, 3158, 3111, 3063, 2962, 2367, 1968, 1812, 1638, 1568, 1434, 1360, 1197, 1135, 999, 764, 572, 514 cm^{-1}. ^1H NMR ($CDCl_3$, 400 MHz): δ 12.62 (1H, s, N-H), 8.13 (1H, s, Ar-H), 7.67 (1H, d, J = 7.6 Hz, Ar-H), 7.5 (1H, s, Ar-H), 7.47 (1H, s, Ar-H), 7.3 (1H, d, J = 8.16 Hz, Ar-H), 7.25 (2H, t, J = 7.68 Hz, Ar-H), 4.83 (1H, s, CH), 2.47 (4H, s, CH_2), 2.24 (4H, d, CH_2), 2.16 (4H, d, CH_2), 1.07 (6H, s, CH_3), 0.91 (9H, s, CH_3). ^{13}C NMR ($CDCl_3$, 100 MHz): δ 197.1, 164.8, 162.9, 141.6, 137.8, 129.9, 129.6, 128.6, 122.4, 120.5, 115.1, 111.4, 50.8, 40.9, 32.1, 31.2, 29.2, 27. Anal. Calc. for $C_{31}H_{36}N_4O$: C, 77.47; H, 7.55; N, 11.66 %. Found: C, 77.50; H, 7.58; N, 11.64 %.

4A. 5. 3. 16. 5-methoxy-3,3-dimethyl-9-(2-(4-methylpiperazin-1-yl)quinolin-3-yl)-3,4,9,10 tetrahydroacridin-1(2H)-one (6p).

White colour solid: yield 80 %: FT-IR (KBr): 3307, 3159, 3111, 3063, 2960, 2315, 1969, 1812, 1664, 1663, 1568, 1434, 1197, 1136, 765, 572, 514 cm^{-1}. ^1H NMR ($CDCl_3$, 400 MHz): δ 12.66 (1H, s, N-H), 8.06 (1H, s, Ar-H), 7.59 (1H, d, J = 7.48 Hz, Ar-H), 7.41(1H, t, J = 7.16 Hz, Ar-H), 7.39 (2H, dt, J = 7.16 Hz, Ar-H), 7.24 (1H, d, J = 8.12Hz, Ar-H), 7.12 (2H, t, J = 7.76 Hz, Ar-H), 4.75 (1H, s, CH), 2.4 (4H, s, CH_2), 2.16 (4H, d, CH_2), 2.1 (4H, d, CH_2), 0.9 (6H, s, CH_3), 0.83 (6H, s, CH_3). ^{13}C NMR ($CDCl_3$, 100 MHz): δ 197.1, 164.8, 141.9, 137.7, 129.8, 128.6, 122.6, 120.5, 115.2, 111.4, 50.8, 40.9, 32.1, 31.2, 29.2, 27. Anal. Calc. for $C_{30}H_{34}N_4O_2$: C, 74.66; H, 7.10; N, 11.61 %. Found: C, 74.68; H, 7.13; N, 11.63 %.

4A. 5. 3. 17. 7-methoxy-3,3-dimethyl-9-(2-(4-methylpiperazin-1-yl)quinolin-3-yl)-3,4,9,10 tetrahydroacridin-1(2H)-one (6q).

White colour solid: yield 75 %: FT-IR (KBr): 3319, 3165, 3102, 3069, 2963, 2364, 1968, 1811, 1677, 1664, 1627, 1568, 1498, 1434, 1362, 1200, 1136, 999, 929, 765, 572, 514 cm^{-1}. ^1H NMR ($CDCl_3$, 400 MHz): δ 12.60 (1H, s, N-H), 8.15 (1H, s, Ar-H), 7.68 (1H, d, J = 7.72 Hz, Ar-H), 7.5 (1H, d, J = 7.24 Hz, Ar-H), 7.46 (1H, d, J = 0.92 Hz, Ar-H), 7.48(1H, s, Ar-H), 7.31 (1H, d, J = 8.12Hz, Ar-H), 7.23 (2H, t, J = 7.52 Hz, Ar-H), 4.83 (1H, s, CH), 2.47 (4H, s, CH_2), 2.24 (4H, d, CH_2), 2.16 (4H, d, CH_2), 1.07 (6H, s, CH_3), 0.91 (6H, s, CH_3). ^{13}C NMR ($CDCl_3$, 100 MHz): δ 197.1, 164.8, 141.9, 137.7, 129.8, 122.6, 120.5, 115.2, 111.4, 50.8, 40.9,

32.1, 31.2, 29.2, 27. Anal. Calc. for $C_{30}H_{34}N_4O_2$: C, 74.66; H, 7.10; N, 11.61 %. Found: C, 74.65; H, 7.12; N, 11.62 %.

4A. 5. 3. 18. 8,8-dimethyl-5-(2-(4-methylpiperazin-1-yl)quinolin-3-yl)-5,8,9,10 tetrahydrobenzo[b][1,8]naphthyridin-6(7H)-one (6r).

White colour solid: yield 90 %: FT-IR (KBr): 3309, 3157, 3114, 3063, 2962, 2312, 1968, 1811, 1677, 1640, 1568, 1487, 1434, 1368, 1134, 962, 764, 522, 514 cm^{-1}. ^1H NMR ($CDCl_3$, 400 MHz): δ 12.5 (1H, s, N-H), 8.15 (1H, s, Ar-H), 7.68 (1H, d, J = 7.6 Hz, Ar-H), 7.49 (1H, t, J = 7.12 Hz, Ar-H), 7.46 (2H, d t, J = 7.12 Hz, Ar-H), 7.3 (1H, d, J = 8.16 Hz, Ar-H), 7.2 (2H, t, J = 7.68 Hz, Ar-H), 4.83 (1H, s, CH), 2.47 (4H, s, CH_2), 2.24 (4H, d, CH_2), 2.16 (4H, d, CH_2), 1.07 (3H, s, CH_3), 0.9 (6H, s, CH_3). ^{13}C NMR ($CDCl_3$, 100 MHz): δ 197.1, 164.8, 162.9, 141.6, 137.8, 129.9, 129.6, 128.6, 122.4, 120.5, 115.1, 111.4, 50.8, 40.9, 32.1, 31.2, 29.2, 27. Anal. Calc. for $C_{28}H_{31}N_5O$: C, 74.14; H, 6.89; N, 15.44 %. Found: C, 74.16; H, 6.88; N, 15.46 %.

4A. 5. 3. 19. 4,8,8-trimethyl-5-(2-(4-methylpiperazin-1-yl)quinolin-3-yl)-5,8,9,10 tetrahydrobenzo[b][1,8]naphthyridin-6(7H)-one (6s).

White colour solid: yield 90 %: FT-IR (KBr): 3481, 3319, 3160, 3066, 1664, 1360, 1568, 1434, 1197, 1135, 1165, 999, 764, 571, 514 cm^{-1}. ^1H NMR ($CDCl_3$, 400 MHz): δ 12.66 (1H, s, N-H), 8.14 (1H, s, Ar-H), 7.68 (1H, d, J = 7.6 Hz, Ar-H), 7.48 (1H, d, J = 0.96 Hz, Ar-H), 7.46 (2H,d , J = 1.16 Hz, Ar-H), 7.3 (1H, d, J = 8.16 Hz, Ar-H), 7.2 (2H, t, J = 7.12 Hz, Ar-H), 4.83 (1H, s, CH), 2.47 (4H, s, CH_2), 2.24 (4H, d, CH_2), 2.16 (4H, d, CH_2), 1.07 (6H, s, CH_3), 0.9 (6H, s, CH_3). ^{13}C NMR ($CDCl_3$, 100 MHz): δ 197.1, 164.8, 162.9, 141.6, 137.8, 129.9, 129.6, 128.6, 122.4, 120.5, 115.1, 111.4, 50.8, 40.9, 32.1, 31.2, 29.2, 27. Anal. Calc. for $C_{29}H_{33}N_5O$: C, 74.49; H, 7.11; N, 14.98 %. Found: C, 74.51; H, 7.15; N, 14.96 %.

4A. 5. 3. 20. 10,10-dimethyl-7-(2-(4-methylpiperazin-1-yl)quinolin-3-yl)-7,10,11,12 tetrahydrobenzo[c]acridin-8(9H)-one (6t).

White colour solid: yield 85 %: FT-IR (KBr): 3306, 3163, 3108, 2961, 2921, 2358, 2336, 2297, 1811, 1667, 1664, 1625, 1568, 1487, 1434, 1360, 1197, 1135, 1165, 764 cm^{-1}. ^1H NMR ($CDCl_3$, 400 MHz): δ 12.62 (1H, s, N-H), 8.14 (1H, s, Ar-H), 7.67 (3H, d, J = 7.84 Hz, Ar-H), 7.46 (2H,t , J = 7.68 Hz, Ar-H), 7.32 (3H, d, J = 8.12 Hz, Ar-H), 7.15 (2H, t, J = 7.36 Hz, ArH), 4.82 (1H, s, CH), 2.47 (4H, s, CH_2), 2.23 (4H, d, CH_2), 2.16 (4H, d, CH_2), 1.06 (3H, s, CH_3), 0.91 (6H, s, CH_3). ^{13}C NMR ($CDCl_3$, 100 MHz): δ 197.1, 164.8, 163.1, 141.4, 138, 130.1,

129.5, 128.6, 122.2, 120.4, 115, 111.5, 50.8, 41, 32.1, 31.2, 29.3, 27. Anal. Calc. for $C_{33}H_{34}N_4O$: C, 78.85; H, 6.82; N, 11.15 %. Found: C, 78.87; H, 6.85; N, 11.16 %.

4A. 6. Molecular Docking Studies

The crystal structure of a benzo-acridine in complex with a DNA dodecamer was downloaded from Protein Data Bank (PDB ID: 1G3X) (Malinina et al., 2002) and edited using PyMOL v.1.4.1 software (http: //www. pymol.org). After editing, the structure was minimised with WHAT IF: A molecular modelling and drug design program (http://swift.cmbi.ru.nl/whatif/) (Vriend, 1990). All docking studies were performed with Auto Dock 4.2. Software (Morris *et al.* 1996, 1998) employing the Lamarckian Genetic Algorithm, generating 20 independent docking poses for each compound. In all the cases the population size was set to 150 and the maximal number of evaluations was set to 5,000,000. The position of the docking grid was centred at the position of the original co-crystallized ligand which was removed. The dimension of the grid was 100 Å × 100 Å × 100 Å points with spacing of 0.375 between the grid points. The DNA was considered as a rigid molecule, while the ligands were considered as flexible molecules. The best binding mode was selected based on the lowest binding free energy and the largest cluster size ligands equilibrium geometries. All calculations were performed with SPARTAN'08® software (2008, WAVEFUNCTION, Inc., Irvine, CA). Molecules were built by assembling standard fragments and the resulting geometries were optimized by molecular mechanics. Conformational analysis of the compounds by Systematic Search protocol around rotatable bonds was performed using the MMFF94 force field. The most frequent conformer for each compound was selected and geometry optimization was carried out with the semi empirical AM1 method. Due to the basic properties of the tertiary amino side chain at 2-position, the protonated form of the compounds with this substituent was used in the docking studies and neutral form was also used.

Part B: [2]Boron nitride nano material based sulfonic acid catalyst for the synthesis of ethyl piperazinyl-quinolinyl fused acridine derivatives

4B. 1. Abstract

Boron nitride nanomaterial-based solid acid catalyst was prepared by mixing boron nitride and 3-amino-4-methoxybenzenesulfonic acid. The morphological properties of the catalyst were determined by using FT-IR, XRD, TEM, SEM, BET and Raman spectroscopy. It was found to be an efficient and reusable sulfonic acid catalyst for the synthesis of one-pot Knoevenagel and Michael type reactions. Novel 9-(2-(4-ethylpiperazin-1-yl)quinolin-3-yl)-3,3-dimethyl-3,4,9,10-tetrahydroacridin-1(2H)-ones, under microwave irradiation conditions, were synthesized. The compounds were characterized by FT-IR ^{1}H NMR, ^{13}C NMR, 2D NMR and HRMS spectroscopic techniques The method developed in this study has the advantages of producing good yield, simplicity coupled with safety and short reaction time. Most importantly it was found that the solid acid catalyst can be recycled without loss of activity. Furthermore, the newly-synthesized compounds were used for molecular docking with Hsp 90 protein. Two compounds **6a** and **6d** showed good binding located in the subdomain IIA mapped at Asp 93 and Lys 58 residues.

4B. 2. Results and discussion

A one-pot multicomponent synthesis of highly functionalised ethyl piperazinyl-quinolinyl acridine derivatives under microwave conditions, using nanocrystalline boron nitride-based sulfonic acid catalyst, was achieved. The catalyst was synthesized in two stages: a mixture of BN and 65 % nitric acid was refluxed for 24h. This preliminary step aimed at introducing -OH groups on the surface of BN through an oxidation process (Scheme 4B. 1). Thereafter, 3-amino-4-methoxybenzenesulfonic acid was added and the mixture refluxed. In this process, the methoxy group was hydrolysed by the -OH group on the nanocrystals surface. After the work-up of the reaction, the product was filtered and washed with distilled water and acetone to obtain the solid acid catalyst (Scheme 4B. 1). The catalyst was characterized completely by FT-IR, XRD, TEM, SEM, BET and Raman spectroscopy.

[2]***Murugesan, A., Gengan, R.M., Moodley, K.G. and Gericke, G., 2017.*** *Microwave-assisted: Boron nitride nano materials based sulfonic acid catalyst for the synthesis of biologically active ethyl piperazinyl-quinolinyl fused acridine derivatives. Advanced Materials Letters* ***(8) 773-782.***

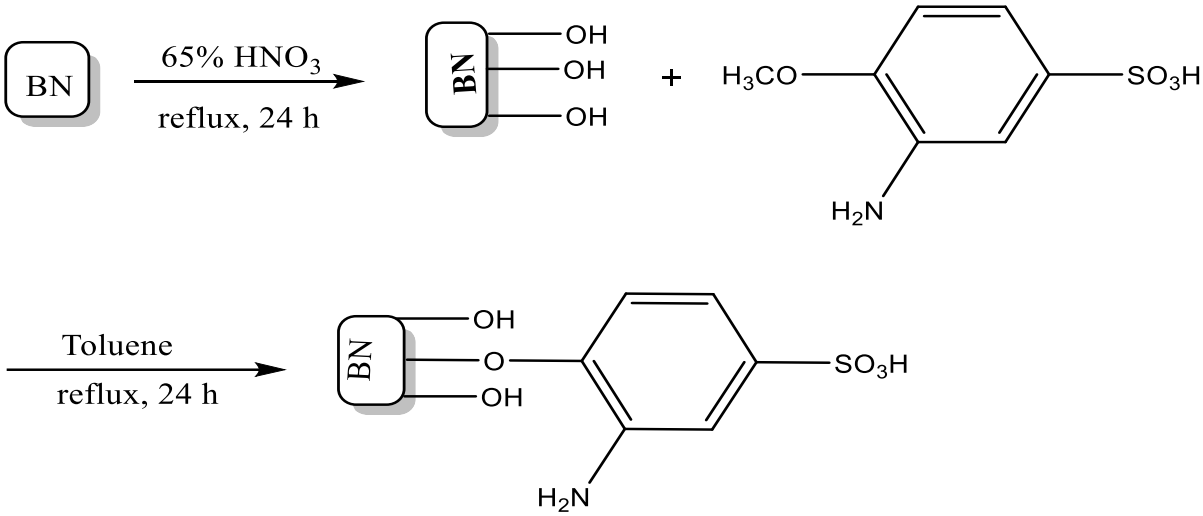

Scheme 4B. 1. The reaction scheme for the synthesis of BN-PT-SO_3H.

The FT-IR spectra for pure BN and BN-PT-SO_3H revealed the following information: in the case of BN, peaks were observed at 815, 1494, 1569 and 3310 cm^{-1} due to B-N, BN-O bonding, attribution to hexagonal BN and B-OH bonding, respectively. The spectrum of BN-PT-SO_3H showed the -NH_2 absorption at 3243 cm^{-1} was flattened due to the modification of BN. Also, the C-H stretching vibrations was observed at 2954 cm^{-1} and the absorption at 1211 cm^{-1} was due to the C=C stretching. The absorptions at 1163 and 1141 cm^{-1} was due to the stretching mode of S=O.

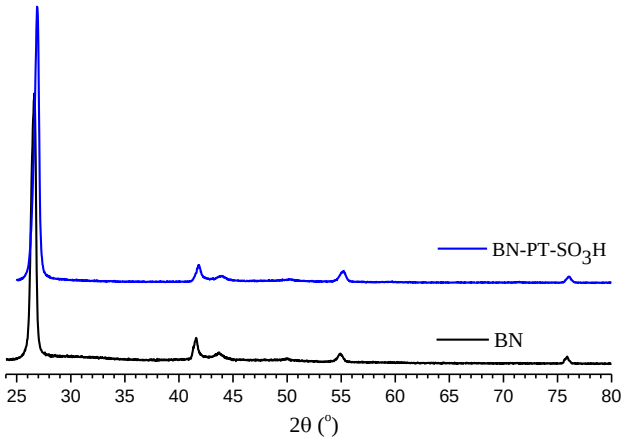

Figure 4B. 1. PXRD pattern of BN and BN-PT-SO_3H.

The XRD patterns of BN and BN-PT-SO_3H (Figure 4B. 1**)** clearly showed the crystallinity. The peak intensities of BN-PT-SO_3H were almost the same as those of BN which was taken as indication that the sulphate modification does not change the phase of BN.

The representative SEM images of BN (Figure 4B. 2**)** exhibited an aggregation of cloud-like structures of small spherical-shaped particles. The SEM micrographs of BN-PT-SO_3H showed some modifications with respect to BN as the primary surface structure was changed, however the cloud-like structure and small spherical-shaped particles still existed.

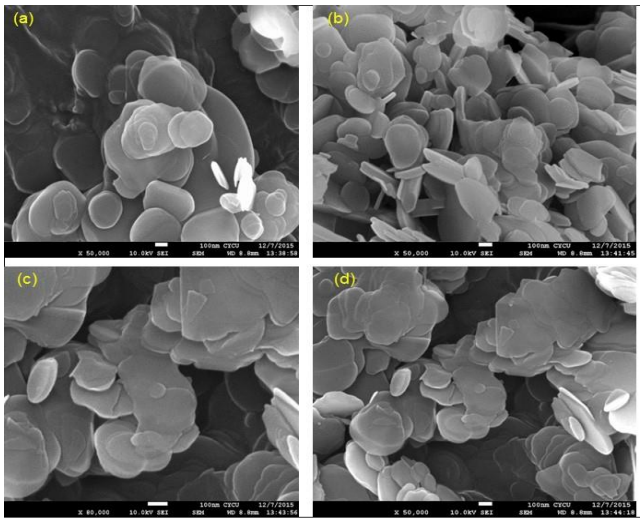

Figure 4B. 2. SEM image of BN (a and b) and BN-PT-SO_3H (c and d).

The EDS analysis for BN and BN-PT-SO_3H (Figure 4B. 3**)** confirmed the presence of all elements and the actual weight % that was present in BN Element B, N, O, C, S, weight % 45.10, 50.35, 4.65, 0, 0, Atomic (%) 52.32, 44.14, 3.54, 0, 0, The catalyst BN-PT-SO_3H Element B, N, O, C, S, weight % 41.23, 49.10, 3.23, 5.36, 0.08, Atomic (%) 48.10, 44.75, 3.52, 5.58, 0.05, respectively (Table 4B. 1).

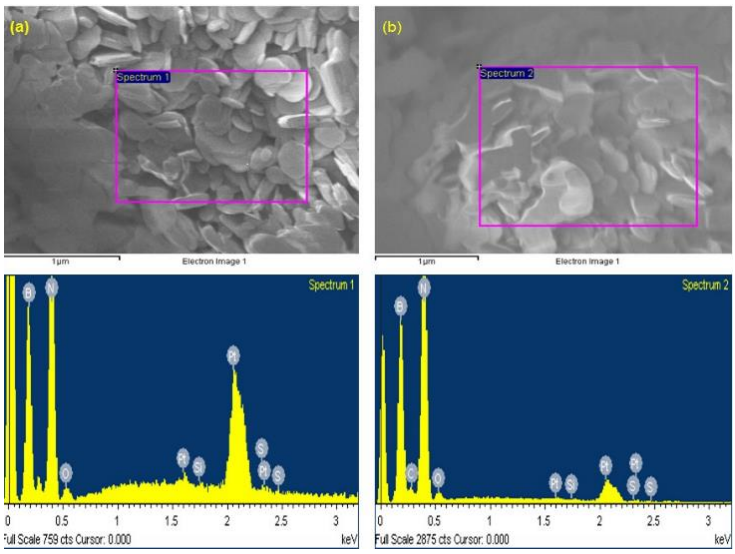

Figure 4B. 3. EDS pattern for BN (image a) and BN-PT-SO_3H (image b).

TEM was employed to determine the morphology. TEM image for different orientations was performed to obtain the average crystalline size of BN-PT-SO_3H. TEM images of BN and BN-PT-SO_3H are shown in Figure 4B.4 which was captured at different orientations of BN scale bars (a-1 µm and b-200 nm) and BN-Pr-SO_3H (c-1 µm, d-100). The figure 4B.4 which indicated the crystallinity size of BN-PT-SO_3H with size of 1 µm and good mesoporous structures suggesting a good surface for catalytic activity.

Table 4B. 1 The weight (%) analysis for BN and BN-PT-SO_3H.

	BN		BN-PT-SO_3H	
Element	Weight (%)	Atomic (%)	Weight (%)	Atomic (%)
B	45.10	52.32	41.23	48.10
N	50.35	44.14	49.10	44.75
O	4.65	3.54	3.23	3.52
C	-	-	5.36	5.58
S	-	-	0.08	0.05

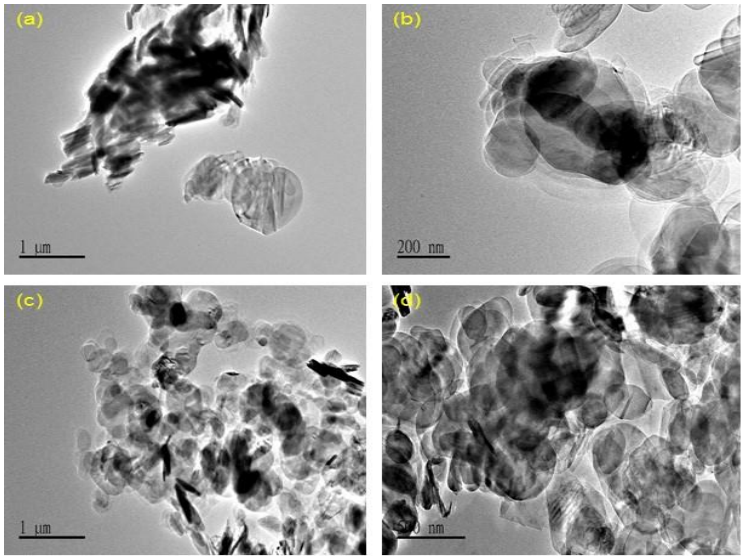

Figure 4B. 4. TEM image of BN (a and b) and BN-PT-SO_3H (c and d).

The porous properties of BN and BN-PT-SO_3H (Figure 4B. 5), analysed by N_2 gas sorption measurements at 273 K, showed BN as a type-I adsorption isotherm which is a

characteristic of microporous material. The BET and Langmuir surface area of BN were calculated as 20 and 48 m^2/g respectively. The N_2 adsorption isotherm of BN-PT-SO_3H also indicated a type-I adsorption isotherm whilst the BET and Langmuir surface area were calculated as 7 and 10 m^2/g respectively.

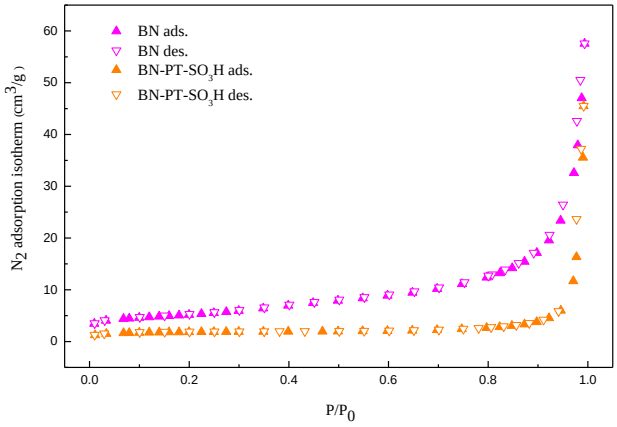

Figure 4B. 5. Adsorption and desorption isotherms of BN and BN-PT-SO_3H at 273 K.

Further investigation of the structure of BN and BN-PT-SO_3H were conducted by Raman spectroscopy (Figure 4B. 6) which showed absorption signals at 600, 1480, 2000, 3000, and 3750 cm^{-1} for BN. The absorption signal of BN-PT-SO_3H showed absorptions at 600, 2000, 3000, 3750 cm^{-1} with an additional signal at 3250 cm^{-1} indicating the acidic functional group.

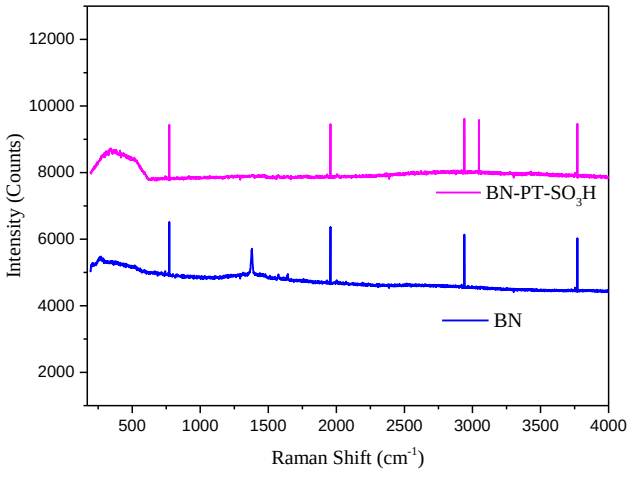

Figure 4B. 6. Raman Shift of BN and BN-PT-SO_3H.

To synthesize new ethyl piperazinyl-quinolinyl acridine derivatives, a new starting compound viz., 2-(4-ethylpiperazin-1-yl)quinoline-3-carbaldehyde (**3**) was required. It was

synthesized using the Vilsmeier-Haack reaction to prepare 2-chloroquinoline-3-carbaldehyde (**1**) from acetanilide (Meth-Cohn *et al.* 1981:1520). Thereafter a mixture of **1** and 1-ethylpiperazine (**2**) was refluxed in a basic medium to obtain **3** after 24 h. This compound was fully characterized by FT-IR, ^{1}H NMR, ^{13}C NMR, TOF-MS and elemental analysis.

Description of the structure of compound 3

The molecular structure of compound **3** is shown in Figure 4B.7

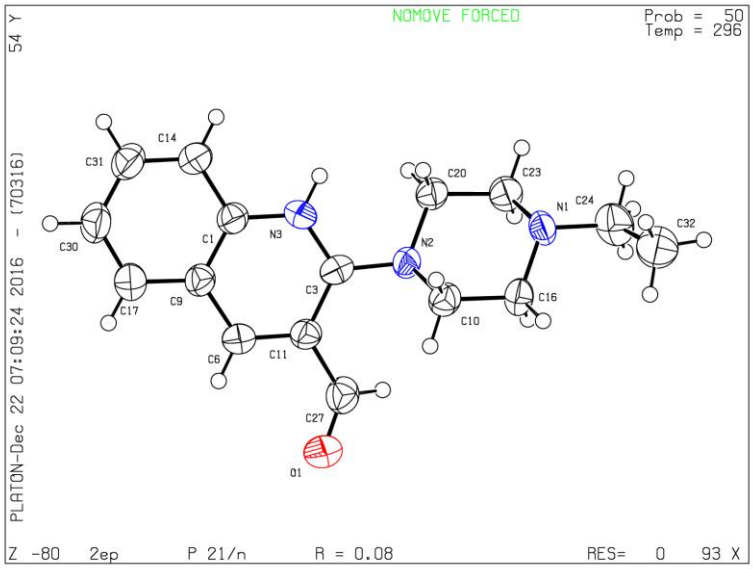

Crystal structure of compound, **3** (**CCDCNo. 1524433)**

Figure 4B. 7. The molecular structure of compound **3** showing the atom labelling. Oxygen, nitrogen atom labels and hydrogen atoms have been omitted for clarity. Displacement ellipsoids are drawn at the 50 % probability level.

The carbonyl carbon had a distorted trigonal-planar geometry and was flanked by the two sterically bulky groups in the presence of a bulky N ethyl-piperazinyl group in the ortho position of the heterocycle. The ethyl-piperazinyl ring was in a half-chair conformation having approximate sp^3 hybridization. The dihedral angle between the mean planes of the six piperazinyl and ethyl ring atoms and through the quinoline ring system is 111.1 (3). The ethyl-piperazinyl group containing carbon atoms such as C23, C16, C24 and C10 are essentially bisected by the plane of the ethyl-piperazinyl ring to which they are attached, subtending dihedral angle (C23/N1/C24) 111.8(3), (C3/N3/C1)120.7 (4), (C9/C1/C14) 119.5 (4) and (C11/C6/C9) 120.4 (4), relative to the carbon atoms C1, C9, and C6 while the quinoline groups containing C9 and C17 deviated significantly from this bisected geometry with dihedral angle

117.4 (4) and 119.8(4), (C10/N2/C16) and 110.8(3). The formyl group O 1- C27-C11 had a bond length of 123.2 (4) A°. The crystal packing of the compound suggested weak intermolecular interactions. Crystal data, data collection and structure refinement details are summarized in Table 4B S1 in the appendix.

All H atoms were positioned with idealized geometry using a riding model with C-H = 0.93-0.97 A. All H atoms refined with isotropic displacement parameters (set to 1.2 times of the Ueq of the parent C atom). (All experimental data are in the Appendix).

In a preliminary study to synthesize **6a** (Scheme 4B. 2), compound **3,** dimedone (**4**) and aniline (**5a**) were used in a solvent-free system followed by a reaction in ethanol to obtain the best yield. It was observed that better yield was obtained in a solvent free condition: **6a** was subsequently characterized by FT-IR, ^{1}H NMR, ^{13}C NMR, TOF-MS and elemental analysis.

To determine the optimum quantity of BN-PT-SO_3H, different amounts of catalyst such as 0.02, 0.05, 0.07 g were investigated. It was found that increasing the quantity of the catalyst beyond 0.05 g did not increase the yield noticeably hence this quantity was selected as optimum for all subsequent reactions. The choice of an appropriate reaction medium is crucial for successful synthesis. To accelerate the Knoevenagel reactions, various solvents such as ethanol, methanol and acetonitrile were examined and showed a significant impact on the yield. The desired product was obtained with fairly good yields of up to 97 % when the reaction was carried out with catalyst BN-PT-SO_3H in a solvent-free condition under MW conditions at 10 min (Table 4B. 2 entry 6). Moderate yields were observed when ethanol, methanol or acetonitrile were used under reflux conditions at 24 h **(**Table 4B. 2 entries 3-5). The yield decreased and a longer reaction time was required to proceed the reaction with either ethanol or methanol, (Table 4B. 2 entries 1-2). Consequently, BN-PT-SO_3H catalyst was used without solvent. With the optimized reaction conditions, the Knoevenagel reactions of **3**, **4** and **6a-p** were carried out**.** Whilst optimising the reaction conditions (Table 4B. 2), it was observed that the use of a solvent needed a longer reaction time whilst the yield of **6a** was lower. Herein, the reaction was observed that if we conducted the MW for 10 minutes at a higher temperature, viz., 140 $^{\circ}$C, some additional spots were observed on the TLC plate which was taken as indication of the formation of by-products. Also, a shorter reaction time showed the presence of starting materials as indication of incomplete reaction. The maximum yield of **6a** (97 %) was obtained under a MW condition after heating for 10 minutes.

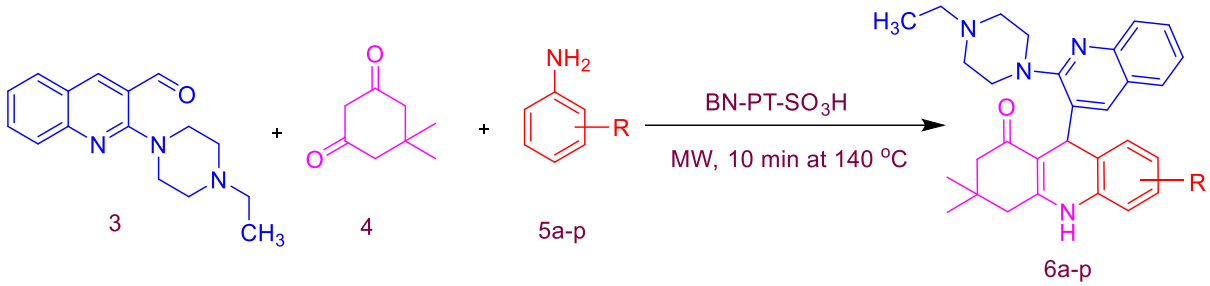

KEY: 6a (R=H); 6b (R=2- NO_2); 6c (R=4- NO_2); 6d (R=4-F); 6e (R=4-Cl); 6f (R= 3,4-Cl); 6g (R=4-Br); 6h (R=ortho-CH_3); 6i (R=meta-CH_3); 6j (R=para-CH_3); 6k (R=3,4-CH_3); 6l (R=ortho O-CH_3); 6m (R=para O-CH_3); 6n (R=Ar-H); 6o (R=Ar-H); 6p (R=Ar-H).

Scheme 4B. 2. The synthesis of 9-(2-(4-ethylpiperazin-1-yl) quinolin-3-yl)-3, 3-dimethyl-3, 4, 9, 10-tetrahydroacridin-1(2H)-one derivatives.

Table 4B. 2. Optimization of the synthesis of **6a** under MW irradiation system using BN-PT-SO_3H.

Entry	Catalyst	Solvent	Temp (°C)	Time (h)	Yield (%)
1	BN- PT-SO_3H	EtOH	r.t	24	60
2	BN- PT-SO_3H	MeOH	r.t	24	50
3	BN- PT-SO_3H	CH_3CN	110	24	80
4	BN- PT-SO_3H	EtOH	100	24	65
5	BN- PT-SO_3H	MeOH	100	24	58
6	BN- PT-SO_3H	Neat	140	10 (min)	97

The re-usability potential of the catalyst was also investigated in the model reaction to synthesize **6a.** Briefly, the solid was rinsed with acetonitrile and methanol, heated at 100 °C and used for subsequent reactions. It was found that the catalyst could be re-used five times without any significant loss of catalytic activity. It can be beneficial for commercial application if required.

The synthesis **(**Scheme 4B. 2) of the functionalised ethyl piperazinyl-quinolinyl benzo acridine derivatives **6a-6p** using the monocrystalline boron nitride-based sulfonic acid catalyst were undertaken in a MW system for a reaction time of 10 min at 140 °C. The product yield ranged from 75 to 97 %. Compounds **6a-6p** was characterized by FT-IR, ^{1}H NMR, ^{13}C NMR and MS-TOF whilst **6a** included 2D-NMR, DEPT-90 and DEPT-135.

Table 4B. 3. The synthesis of 9-(2-(4-ethylpiperazin-1-yl)quinolin-3-yl)-3,3-dimethyl-3,4,9,10-tetrahydroacridin-1(2H)-one in the presence of BN-PT-SO_3H

Entry	Substrate (6a-p)	Product (6a-p)	Time (min)	Isolated Yield (%)	M. p. (°C)
1	$C_6H_{6n}H_2$	6a	10	97	254-256
2	2-$O_2NC_6H_4NH_2$	6b	10	85	>300
3	4-$O_2NC_6H_4NH_2$	6c	10	90	>300
4	4-$FC_6H_4NH_2$	6d	10	95	275-277
5	4-$ClC_6H_4NH_2$	6e	10	80	>300
6	$Cl_2C_6H_3NH_2$	6f	10	87	290-292
7	4-$BrC_6H_4NH_2$	6g	10	90	270-272
8	o-$CH_3C_6H_4NH_2$	6h	10	87	>300
9	m-$CH_3C_6H_4NH_2$	6i	10	83	>300
10	p-$CH_3C_6H_4NH_2$	6j	10	90	270-272
11	$(CH3)_2C_6H_4NH_2$	6k	10	90	280-282
12	o-C_6H_9NO	6l	10	78	>300
13	p-C_6H_9NO	6m	10	85	>300
14	$C_6H_6N_2$	6n	20	90	>300
15	$C_6H_8N_2$	6o	20	95	>300
16	$C_{10}H_7NH_2$	6p	20	75	>300

To assess the suitability of the MW method, the product was also prepared by a conventional method (thermal method). The physical properties of the product made by the conventional method are shown below: The % yield, melting point, and total reaction time (Table 4B.4) for product **6a, 6b, 6c, 6d, 6e, 6f, 6g, 6h, 6i, 6j, 6k, 6l, 6m, 6n, 6o**, and **6p** were yield (%) for conventional method (thermal) 90, 80, 85, 87, 77, 80, 83, 78, 75, 87, 80, 70, 75, 80, 85 and 65 % for reaction time 30 mins, 1 h, 2 h, 30 mins, 46 mins, 30, 30, 1 h, 1 h, 36 mins, 46 mins, 30 mins, 1 h, 1 h, 1 h, 1 h, respectively. The reaction time for 13 compounds was 10 mins whilst **6n, 6o, 6p** was 20 mins. For all syntheses 120W was used except for **6n, 6o, 6p** for which 200W was used as shown in Table 4B.4.

Table 4B. 4. The synthesis of 9-(2-(4-ethylpiperazin-1-yl)quinolin-3-yl)-3,3-dimethyl-3,4,9,10-tetrahydroacridin-1(2H)-one in the presence of BN-PT-SO_3H with conventional method (thermal)

Entry	Substrate (6a-p)	Product (6a-p)	Time (min/h)	Isolated Yield (%)	M. p. (°C)
1	$C_6H_{6n}H_2$	6a	30	90	254-256
2	2-$O_2NC_6H_4NH_2$	6b	1h	80	>300
3	4-$O_2NC_6H_4NH_2$	6c	2h	85	>300
4	4-$FC_6H_4NH_2$	6d	30	87	275-277
5	4-$ClC_6H_4NH_2$	6e	45	77	>300
6	$Cl_2C_6H_3NH_2$	6f	30	80	290-292
7	4-$BrC_6H_4NH_2$	6g	30	83	270-272
8	o-$CH_3C_6H_4NH_2$	6h	1h	78	>300
9	m-$CH_3C_6H_4NH_2$	6i	1h	75	>300
10	p-$CH_3C_6H_4NH_2$	6j	35	87	270-272
11	$(CH3)_2C_6H_4NH_2$	6k	45	80	280-282
12	o-C_6H_9NO	6l	30	70	>300
13	p-C_6H_9NO	6m	1h	75	>300
14	$C_6H_6N_2$	6n	1h	80	>300
15	$C_6H_8N_2$	6o	1h	85	>300
16	$C_{10}H_7NH_2$	6p	1h	65	>300

Compound **6a** was used as a template structure for characterisation. The FT-IR spectrum of **6a** showed stretching vibrations at 3495 and 1681 cm^{-1} for N-H and carbonyl groups respectively. The ^1H NMR spectrum showed three singlets at δ, 12.98, 8.10, and 4.82 for C_{14}-H, C_4-H and N_{19}-H respectively. The C_{20}-CH_2 protons was found at δ, 2.47, d (J = 13.04 Hz) as a doublet and C_{22}-CH_2 protons at δ, 2.47 d, (J = 16.32 Hz,) as doublets. The ^{13}C NMR spectrum showed the presence of one carbonyl group at δ 197.17.

The selected HMBC correlation of **6a** is shown in Figure 4B. 8. The C, H-COSY (HSQC) correlation at δ 26.95, 29.32, 31.16, 41, 50.88, 111.58, 115.01, 119.70, 129.41, 130.32 and 141.10 are assigned to $C_{24, 25}$, C_{14}, C_{13a}, C_{22}, C_{15}, C_{18}, C_7, C_6, and C_4 respectively. The carbon signal at δ 141.10, was due to the quinolinyl C_4-carbon. The H, HCOSY spectrum showed a singlet at δ 4.82 which confirmed one nearby hydrogen to C_4.

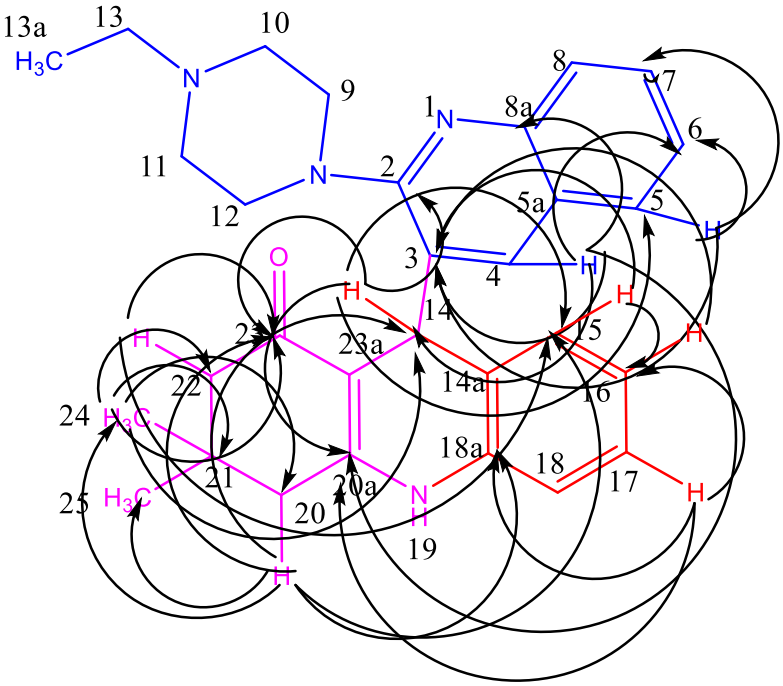

Figure 4B. 8. Selected HMBC correlations of compound **6a**.

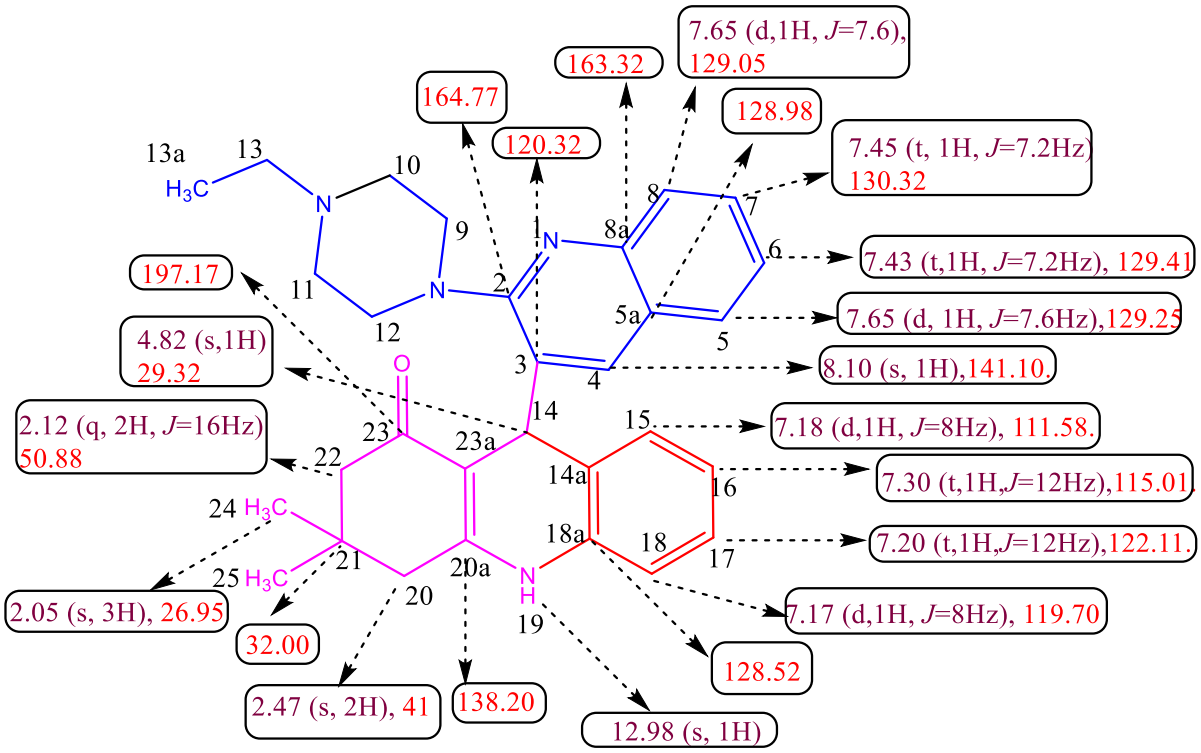

Figure 4B. 9. Selected (^{1}H) NMR and (^{13}C) NMR and HMBC chemical shifts of **6a**.

The long range HMBC correlation showed C_{14}-H correlated with quinolinyl carbon C_5 at *δ.* (129.25), C_2 at *δ.* (164.77), amine carbon C_{15} at *δ.* (111.58), C_{20a} at *δ.* (138.20) and dimedone carbonyl carbon C_{23} at *δ.* (197.17). C_4-H correlated with quinolinyl carbon C_3 at *δ.* (120.32), C_5 at *δ.* (129.25), C_6 at *δ.* (129.41), C_{8a} at *δ.* (163.32), C-H carbon C_{14} at *δ.* (29.32) amine carbon C_{20a} at *δ.* (138.20), respectively. Similarly, C_5-H correlated with quinolinyl carbon C_3 at *δ.* (120.32), C_6 at *δ.* (129.41), C_7 at *δ.* (130.32), C_{17}-H correlates with amine carbon C_{16} at *δ.* (115.01), at *δ.* C_{18}a at *δ.* (128.52), C_{20}a at *δ.* (138.20), C_{16}-H correlated with quinolinyl carbon C_3 at *δ.* (120.32), C_{20}-H correlates with dimedone methyl carbon $C_{24, 25}$ at *δ.* (26.95), C-H carbon C_{14} at *δ.* (29.32), amine carbon C_{15} at *δ.* (111.58) C_{18}a at *δ.* (128.52) and dimedone carbonyl carbon C_{23} at *δ.* (197.17), C_{22}-H correlated with amine carbon C_{15} at *δ.* (111.58), and dimedone carbonyl carbon C_{23} at *δ.* (197.17) and C_{24}-H correlated with dimedone ethylene carbon C_{22} at *δ.* (50.88), C_{20} at *δ.* (41), C_{21} at *δ.* (32), and dimedone carbonyl carbon C_{23} at *δ.* (197.17).

Based on the above spectral details and its elemental analysis, the structure was confirmed as 9-(2-(4-ethylpiperazin-1-yl)quinolin-3-yl)-3,3-dimethyl-3,4,9,10-tetrahydroacridin-1(2H)-one **6a** (Figure 4B. 9. Selected ^{1}H NMR and ^{13}C NMR and HMBC chemical shifts of **5a** are as presented in Table 4A. 4.

Thus, the one pot multi-component synthesis of new ethyl piperazinyl-quinolinyl acridinone derivatives using the BN-PT-SO_3H was a neat and efficient reaction which is selective for the formation of the sought after molecule. This multicomponent reaction is similar to the one discussed in Chapter 4A except that the starting substrate was different hence leading to new acridinone derivatives. Also, the catalyst that was used in these reactions was different.

A molecular docking of 16 derivatives with Hsp 90 was undertaken however, only two compounds, namely, **6a** and **6d** showed good binding activity. The hit compounds retrieved (74 Maybridge and 1076 Scaffold) from the databases which satisfied drug-like properties were docked in the active site of Hsp 90 using a Ligand Fit programme. In order to support the experimental results, computational docking analysis was performed to create a model for Hsp 90 with compound **6a** and **6d** as a complex. It had been stated earlier, that each domain of the protein contains two sub domains (IA and B, IIA and B, IIIA and B) which possess common structural motifs. Sudlow site I and Sudlow site II (subdomains IIA and IIIA respectively) are the most probable binding sites of the ligands. Molecular docking analysis was performed using

the Auto Dock 4.2 program and the energetically most feasible Hsp 90-compound **6a** and **6d** complexes are displayed in Figure 4B .10 (a-b).

Table 4A. 4. Selected HMBC correlations of compound **5a**

S.NO	Proton	Correlated Carbons
1	C_{14}-H (s,1H) at *δ.* 4.82	C_{15} at *δ.* (111.58), C_5 at *δ.* (129.25), C_{20a} at *δ.* (138.20) C_2 at *δ.* (164.77), C_{23} at *δ.* (197.17).
2	C_4-H (s, 1H) at *δ.* 8.10	C_{14} at *δ.* (29.32), C_3 at *δ.* (120.32), C_5 at *δ.* (129.25), C_6 at *δ.* (129.41), C_{20a} at *δ.* (138.20), C_{8a} at *δ.* (163.32).
3	C_5-H (d, 1H, *J*=7.6Hz) at *δ.* 7.65	C_3 at *δ.* (120.32), C_6 at *δ.* (129.41), C_7 at *δ.* (130.32)
4	C_{17}-H (t, 1H, *J*=12Hz) at *δ.* 7.20	C_{16} at *δ.* (115.01), at *δ.* C_{18}a at *δ.* (128.52), C_{20}a at *δ.* (138.20)
5	C_{16}-H (t, 1H, *J*=12Hz) at *δ.* 7.30	C_3 at *δ.* (120.32)
6	C_{15}-H (d, 1H, *J*= 7.6Hz) at *δ.* 7.17	C_{16} at *δ.* (115.01), C_3 at *δ.* (120.32)
7	C_{20}-H CH_2 (s , 2H,) at *δ.* 2.47	$C_{24, 25}$ at *δ.* (26.95), C_{14} at *δ.* (29.32), C_{15} at *δ.* (111.58) C_{18}a at *δ.* (128.52), C_{23} at *δ.* (197.17).
8	C_{22}-H CH_2 (q, 2H, *J*= 16Hz) at *δ.* 2.12	C_{15} at *δ.* (111.58), C_{23} at *δ.* (197.17).
9	C_{24}-H CH_3 (s, 3H) at *δ.* 1.05	C_{22} at *δ.* (50.88), C_{20} at *δ.* (41), C_{21} at *δ.* (32), C_{23} at *δ.* (197.17).

Docking results clearly pointed out that **6a** and **6d** bind inside the binding pocket located in subdomain IIA of Hsp 90. It can be seen from figure **4B. 10 (a-b)**, **6a** an**d 6d** are located adjacent to the amino acid residues mapped as Asp-93 and Lys-58 residues. **6a** and **6d** showed hydrogen bonds and hydrophobic interactions with Asp-93, Asn-51, Ala-55, Lys-58, Glu-97,

Met-98 and Ser-99. Figure 4B .10 a-b represents the binding orientation of the hit compounds and also shows how well the compounds fit into hydrogen bonding. The compounds were further sorted based on the consensus scoring function. The training set compounds showed the dock score greater than 80 and the maximum fit value of 10. All of the hit compounds possessed the maximum fit value of 11 and the dock score of more than 85. Some of the active compounds in the training set showed hydrogen bonding and hydrophobic interaction with the two active site residues at Asp-93, Lys-58 with few hydrophobic residues Asn-51, Ala-55, Lys-58, Met-98, and Ser-99 which are considered to be crucial for inhibitory activity.

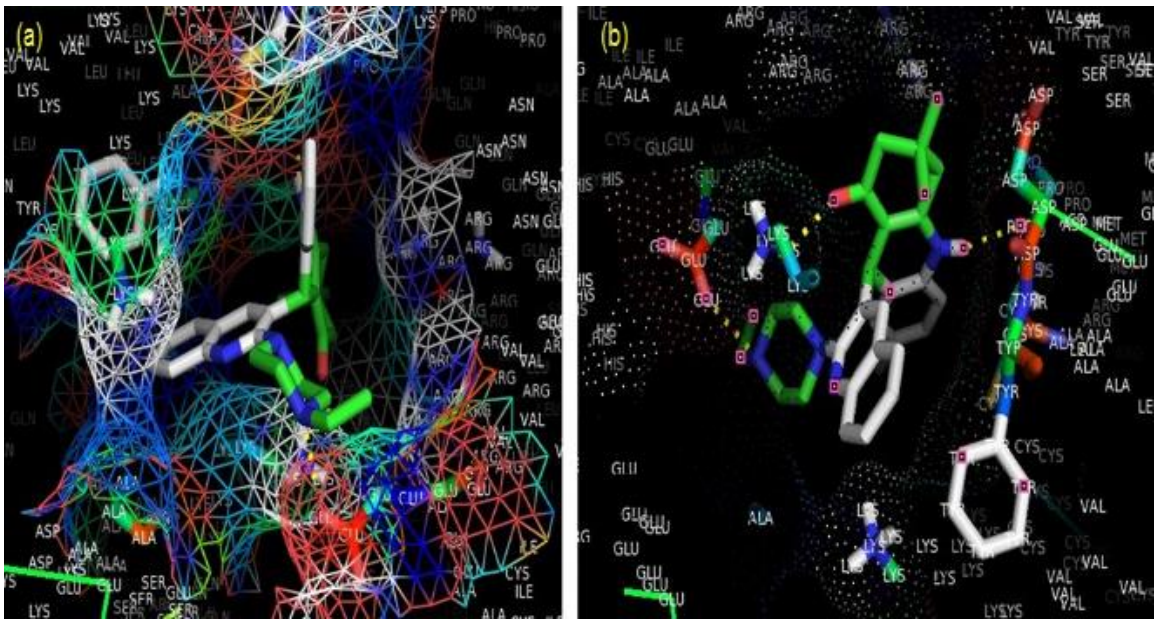

Figure 4B. 10. (a-b). (a) Molecular docking of the Hsp 90-compound **6a** and (b) Hsp 90-compound **6d** complex selected amino acid residues are represented by stick and cartoon models. Hydrogen bond is shown in yellow dotted line.

The hit compounds showed very good interactions with the critical residues of Asp-93 and Lys-58. It is imperative to note from the computational observations that compound **6a** and **6d** are in the locality of Lys-58 amino acid residue of Hsp 90.

4B. 3. Conclusion

The preparation of the catalyst was simple and safe whilst demonstrating only 10 % loss in catalytic activity after five cycles of re-use thereby making it cost-effective for possible industrial application. The synthesized acid catalyst was successfully used in a new one pot reaction for the synthesis of ethyl piperazinyl-quinolinyl acridinone derivatives. This reaction, under MW conditions, was relatively fast, safe, and environmentally friendly and produces high yield molecule. Furthermore, the one pot reaction used in this study gives rise to new types of ethyl piperazinyl-quinolinyl acridinone derivatives which have suitable functionalities for a host of possible biological applications such as Hsp 90 protein binding.

4B. 4. Experimental

4B. 4. 1. Catalyst preparation

A mixture of BN and 65 % nitric acid was refluxed for 24 h; to add –OH groups to the surface of BN. To 10 g of BN and 15 g of 3-amino-4-methoxybenzenesulfonic acid, 30 mL dry toluene was added and the reaction mixture was refluxed for 24 h. After this period, the mixture was filtered and washed with distilled water and acetone to obtain solid acid catalyst BN-PT-SO_3H in 96 % yield (Scheme 4B .1).

4B. 4. 2. General Procedure for the synthesis of substituted 2-(4-ethylpiperazin-1 yl)quinoline-3-carbaldehyde (3)

The starting compound 2-chloroquinoline-3-carbaldehyde (**1**) was prepared from acetanilide, DMF and $POCl_3$ by the Vilsmeier Haack reaction. An aliquot (0.001 mol) of (**1**) and potassium carbonate (0.002 mol) was added to a round bottom flask with excess of 1-ethylpiperazine. The mixture was refluxed for 24 h at 200 $^{\circ}$C; the reaction was monitored by TLC. After completion, the reaction mass was cooled to room temperature and poured into water. It was then filtered, washed with water and dried. The crude product was purified by column chromatography using silica gel mesh and a mobile phase of acetone and hexane (70:30) to produce a yellow powder of 95 % yield (m.p 220-222 $^{\circ}$C). FT-IR (KBr): 2979, 2934, 2643, 2901, 2358, 2333, 1693, 1615, 1593, 1421, 1372, 1239, 952, 765, 512, 482 cm^{-1}. ^1H NMR ($CDCl_3$, 400 MHz): δ 10.16 (1H, brs, CHO), 8.47 (1H, brs, Ar-H), 7.82 (1H, d, J = 8.4 Hz, Ar-H), 7.76-7.79 (1H, dd, J = 1 Hz, Ar-H), 7.66-7.70 (1H, m, J =1.52 Hz, Ar-H), 7.34-7.38 (1H, m, J =1.04 Hz, Ar-H), 3.53-3.55 (4H, t, J= 4.84 Hz, CH_2), 2.66-2.69 (4H, t, J=4.92

Hz, CH_2), 2.49-2.54 (2H, q, *J*=7.28 Hz, CH_2), 1.13-1.16 (3H, t, CH_3). ^{13}C NMR ($CDCl_3$, 100 MHz): δ 190.27, 159, 149.35, 142.18, 132.41, 129.24, 127.56, 124.55, 123.98, 122.06, 52.70, 52.38, 51.04, 11.97. TOF MS ES+ Calc. mass 270.16, Found: 270.15 Anal. Calc. For $C_{16}H_{19}N_3O$: C, 71.35; H, 7.11; N, 15.60 %. Found: C, 71.37; H, 7.12; N, 15.62 %. This compound was fully characterized by FT-IR, ^1H-NMR, ^{13}C-NMR, TOF-MS and elemental analysis.

4B. 4. 3. General Procedure for the synthesis of 9-(2-(4-ethylpiperazin-1-yl)quinolin-3-yl)-3,3-dimethyl-3,4,9,10-tetrahydroacridin-1(2H)-one derivatives (6a-p).

The sulfonic acid functionalized BN-PT-SO_3H solid acid catalyst (0.07 g) was activated in vacuum at 100 °C and following cooling to room temperature, 2-(4-ethylpiperazin-1-yl) quinoline-3-carbaldehyde (1.0 mmol), dimedone (1.0 mmol), and aniline (1.0 mmol) were added. The mixture was heated at 140 °C in MW, conditions at 120W for an appropriate time as shown in Table 4B. 4. The reaction was monitored by TLC. After completion, the mixture was dissolved in ethanol in order to separate the catalyst. The filtrate was cooled and the mixture was purified by column chromatography with acetone: hexane (70:30) to produce a pure product of white colour solid. The catalyst was washed subsequently with dilute acid solution, distilled water and then acetone, dried under vacuum and recycled several times. The spectral (^1H NMR, ^{13}C NMR, MS, elemental analysis and FT-IR) data for new compounds are given below.

4B. 4. 3. 1. 9-(2-(4-ethylpiperazin-1-yl)quinolin-3-yl)-3,3-dimethyl-3,4,9,10 tetrahydroacridin1(2H)-one (6a).

White colour solid: yield 97 %: FT-IR (KBr): 3495, 3236, 3159, 2961, 2259, 1681, 1630, 1568, 1434, 1358, 1196, 1135, 999, 764, 571 cm^{-1}. ^1H NMR ($CDCl_3$, 400 MHz): δ 12.98 (1H, s, N-H), 8.10 (1H, s, Ar-H), 7.65 (2H, d, *J* = 7.6 Hz, Ar-H), 7.43-7.45 (2H, t, *J* = 7.2 Hz, Ar-H), 7.20-730 (2H, t, *J* = 12 Hz, Ar-H), 7.17 (2H, d, *J* = 7.6 Hz, Ar-H), 4.82 (1H, s, CH), 2.47 (6H, m, CH_2), 2.12-2.25 (8H, q, CH_2), 1.05 (6H, s, CH_3), 0.88 (3H, s, CH_3). ^{13}C NMR ($CDCl_3$, 100 MHz): δ 197.17, 164.77, 163.32, 141.10, 138.20, 130.32, 129.41, 129.25, 129.05, 128.98, 128.52, 122.11, 120.32, 119.70, 115.01, 111.58, 52.88, 52.04, 50.88, 41, 32.18, 32, 31.16, 30.92, 29.32, 26.95. TOFMS ES *m/z* (rel. int.): 457.12 $[M]^+$. Anal. Calc. for $C_{30}H_{34}N_4O$: C, 77.22; H, 7.34; N, 12.01 %. Found: C, 77.24; H, 7.36; N, 12.12 %.

4B. 4. 3. 2. 9-(2-(4-ethylpiperazin-1-yl)quinolin-3-yl)-3,3-dimethyl-5-nitro-3,4,9,10 tetrahydroacridin-1(2H)-one (6b).

White colour solid: yield 85 %: FT-IR (KBr): 3319, 3164, 3106, 3066, 2963, 2306, 1968, 1812, 1680, 1636, 1568, 1480, 1487, 1194, 1136, 999, 929, 764 cm^{-1}. ^{1}H NMR ($CDCl_3$, 400 MHz): δ 11.84 (1H, s, N-H), 8.01 (1H, s, Ar-H), 7.76 (1H, d, *J* = 8.4 Hz, Ar-H), 7.57 (2H, d, *J* = 7.6 Hz, Ar-H), 7.34-7.38 (3H, t, *J* = 7.8 Hz, Ar-H), 4.73 (1H, s, CH), 3.49-3.88 (4H, m, CH_2), 2.39 (4H, m, CH_2), 2.05-2.17 (6H, q, CH_2), 1.18 (3H, s, CH_3), 0.99 (3H, s, CH_3), 0.84 (3H, s, CH_3). ^{13}C NMR ($CDCl_3$, 100 MHz): δ 197.16, 164.74, 162.81, 141.15, 137.96, 130.88, 130.44, 129.52, 128.80, 128.57, 127.65, 122.22, 120.32, 114.82, 50.89, 49.79, 40.97, 38.73, 32.18, 31.11, 29.69, 29.32, 28.92, 27.02, 22.98. Anal. Calc. for $C_{30}H_{33}N_5O_3$: C, 70.43; H, 6.50; N, 13.69 %. Found: C, 70.42; H, 6.52; N, 13.67 %.

4B. 4. 3. 3. 9-(2-(4-ethylpiperazin-1-yl)quinolin-3-yl)-3,3-dimethyl-7-nitro-3,4,9,10 tetrahydroacridin-1(2H)-one (6c).

White colour solid: yield 90 %: FT-IR (KBr): 3496, 3236, 3159, 2961, 2259, 1968, 1811, 1681, 1630, 1568, 1434, 1358, 1196, 1135, 999, 929, 764, 571 cm^{-1}. ^{1}H NMR ($CDCl_3$, 400 MHz): δ 12.99 (1H, s, N-H), 8.12 (1H, s, Ar-H), 7.66 (2H, d, *J* = 7.6 Hz, Ar-H), 7.44-7.49 (2H, dd, *J* = 6.8 Hz, Ar-H), 7.32(2H, d, *J* = 8.4 Hz, Ar-H), 7.18 (1H, s, Ar-H), 4.82 (1H, s, CH), 2.47 (6H, m, CH_2), 2.13-2.25 (8H, q, CH_2), 1.06 (6H, s, CH_3), 0.89 (3H, s, CH_3). ^{13}C NMR ($CDCl_3$, 100 MHz): δ 197.16, 164.79, 163.26, 141.25, 138.14, 130.19, 129.46, 128.58, 122.18, 120.38, 115.82, 111.54, 50.89, 41.01, 32.19, 31.21, 29.32, 26.98. Anal. Calc. for $C_{30}H_{33}N_5O_3$: C, 70.43; H, 6.50; N, 13.69 %. Found: C, 70.44; H, 6.53; N, 13.67 %.

4B. 4. 3. 4. 9-(2-(4-ethylpiperazin-1-yl)quinolin-3-yl)-7-fluoro-3,3-dimethyl-3,4,9,10 tetrahydroacridin-1(2H)-one (6d).

White colour solid: yield 95 %: FT-IR (KBr): 3456, 3307, 3159, 3108, 3060, 2961, 2915, 2361, 1966, 1811, 1664, 1663, 1589, 1466, 1434, 1366, 1197, 1165, 1136, 999, 765, 571 cm^{-1}. ^{1}H NMR ($CDCl_3$, 400 MHz): δ 12.87 (1H, s, N-H), 8.11 (1H, s, Ar-H), 7.66 (2H, d, *J* = 8 Hz, Ar-H), 7.44-7.48 (2H, t, *J* = 7.6 Hz, Ar-H), 7.32 (2H, d, *J* = 8.4 Hz, Ar-H), 7.17 (1H, s, Ar-H), 4.82 (1H, s, CH), 2.47 (6H, m, CH_2), 2.13-2.21 (8H, t, CH_2), 1.06 (6H, s, CH_3), 0.89 (3H, s, CH_3). ^{13}C NMR ($CDCl_3$, 100 MHz): δ 197.18, 164.77, 163.22, 141.14, 138.17, 130.30, 129.43, 128.56, 122.14, 120.34, 114.97, 111.58, 50.89, 41.01, 32.19, 32.01, 31.18, 29.32, 26.98. ^{19}F NMR ($CDCl_3$, 400 MHz): δ -120.68, -115.81, -113.31. Anal. Calc. for $C_{30}H_{33}FN_4O$: C, 74.35; H, 6.86; N, 11.56 %. Found: C, 74.37; H, 6.87; N, 11.58 %.

4B. 4. 3. 5. 7-chloro-9-(2-(4-ethylpiperazin-1-yl)quinolin-3-yl)-3,3-dimethyl-3,4,9,10 tetrahydroacridin-1(2H)-one (6e).

White colour solid: yield 80 %: FT-IR (KBr): 3474, 3306, 3161, 3108, 3062, 2961, 2918, 2367, 1969, 1811, 1661, 1568, 1434, 1359, 1197, 1165, 1135, 765, 572 cm^{-1}. ^{1}H NMR ($CDCl_3$, 400 MHz): δ 12.31 (1H, s, N-H), 8.16 (1H, s, Ar-H), 7.68 (3H, d, J = 8 Hz, Ar-H), 7.56 (1H, d, J = 7.6 Hz, Ar-H), 7.31-7.48 (3H, t, J = 7.6 Hz, Ar-H), 7.29 (1H, s, Ar-H), 4.83 (1H, s, CH), 2.48 (6H, m, CH_2), 2.14-2.26 (8H, q, CH_2), 1.07 (6H, s, CH_3), 0.93 (3H, s, CH_3). ^{13}C NMR ($CDCl_3$, 100 MHz): δ 197.17, 164.83, 162.68, 141.91, 137.64, 129.85, 128.68, 122.66, 120.57, 115.11, 111.41, 50.88, 40.97, 32.19, 32.20, 29.29, 27.07. Anal. Calc. for $C_{30}H_{33}ClN_4O$: C, 71.91; H, 6.64; N, 11.18 %. Found: C, 71.89; H, 6.66; N, 11.16 %.

4B. 4. 3. 6. 7,8-dichloro-9-(2-(4-ethylpiperazin-1-yl)quinolin-3-yl)-3,3-dimethyl-3,4,9,10 tetrahydroacridin-1(2H)-one (6f).

White colour solid: yield 87 %: FT-IR (KBr): 3308, 3105, 3161, 3067, 2961, 2915, 2364, 2327, 1969, 1812, 1667, 1664, 1568, 1434, 1408, 1360, 1197, 1135, 999, 765, 571, 514 cm^{-1}. ^{1}H NMR ($CDCl_3$, 400 MHz): δ 12.16 (1H, s, N-H), 8.12 (1H, s, Ar-H), 7.64 (2H, d, J = 8 Hz, Ar-H), 7.47 (1H, d, J = 7.6 Hz, Ar-H), 7.45 (2H, d, J = 7.8 Hz, Ar-H), 7.19 (1H, d, J = 7.4 Hz, Ar-H), 4.83 (1H, s, CH), 3.76-3.90 (2H, t, CH_2), 2.48 (4H, m, CH_2), 2.14-2.26 (6H, q, CH_2), 1.07 (6H, s, CH_3), 0.92 (3H, s, CH_3). ^{13}C NMR ($CDCl_3$, 100 MHz): δ 197.17, 164.78, 162.72, 141.41, 137.83, 130.27, 129.65, 128.61, 122.40, 120.43, 114.92, 111.55, 50.89, 40.97, 32.19, 31.11, 30.93, 29.30, 27.05. Anal. Calc. for $C_{30}H_{32}Cl_2N_4O$: C, 67.29; H, 6.02; N, 10.46 %. Found: C, 67.32; H, 6.05; N, 10.45 %.

4B. 4. 3. 7. 7-bromo-9-(2-(4-ethylpiperazin-1-yl)quinolin-3-yl)-3,3-dimethyl-3,4,9,10 tetrahydroacridin-1(2H)-one (6g).

White colour solid: yield 90 %: FT-IR (KBr): 3308, 3162, 3108, 3037, 2961, 2306, 1968, 1812, 1625, 1568, 1487, 1437, 1434, 1408, 1356, 1198, 1136, 999, 764, 571 cm^{-1}. ^{1}H NMR ($CDCl_3$, 400 MHz): δ 12.42 (1H, s, N-H), 8.14 (1H, s, Ar-H), 7.64 (2H, d, J = 8 Hz, Ar-H), 7.49 (1H, s, Ar-H), 7.31-7.47 (2H, t, J = 7.2 Hz, Ar-H), 7.28 (2H, d, J = 7.8 Hz, Ar-H), 4.83 (1H, s, CH), 2.48 (6H, m, CH_2), 2.14-2.26 (8H, q, CH_2), 1.07 (6H, s, CH_3), 0.92 (3H, s, CH_3). ^{13}C NMR ($CDCl_3$, 100 MHz): δ 197.17, 164.80, 162.88, 141.54, 137.87, 130.06, 129.64, 128.64, 122.41, 120.47, 115.01, 111.48, 50.89, 40.99, 32.19, 31.20, 29.30, 27.03. Anal. Calc. for $C_{30}H_{33}BrN_4O$: C, 66.05; H, 6.10; N, 10.27 %. Found: C, 66.08; H, 6.13; N, 10.28 %.

4B. 4. 3. 8. 9-(2-(4-ethylpiperazin-1-yl)quinolin-3-yl)-3,3,5-trimethyl-3,4,9,10 tetrahydroacridin-1(2H)-one (6h).

White colour solid: yield 87 %: FT-IR (KBr): 3474, 3309, 3159, 3111, 3066, 2962, 2376, 1972, 1812, 1664, 1626, 1565, 1434, 1360, 1197, 1165, 1135, 999, 929, 765, 571, 467 cm^{-1}. ^{1}H NMR ($CDCl_3$, 400 MHz): δ 12.69 (1H, s, N-H), 8.13 (1H, s, Ar-H), 7.67 (1H, d, *J* = 7.6 Hz, Ar-H), 7.47-7.49 (3H, t, *J* = 7.4 Hz, Ar-H), 7.45(1H, d, *J* = 1.2 Hz, Ar-H), 7.32 (2H, t, *J* = 8.2 Hz, Ar-H), 4.82 (1H, s, CH), 2.47 (6H, m, CH_2), 2.13-2.26 (8H, q, CH_2), 1.06 (6H, s, CH_3), 0.96 (6H, s, CH_3). ^{13}C NMR ($CDCl_3$, 100 MHz): δ 197.17, 164.80, 163.06, 141.43, 137.98, 130.11, 129.57, 128.62, 122.33, 120.44, 115.02, 111.50, 50.89, 40.99, 32.19, 31.21, 29.31, 27.01. Anal. Calc. for $C_{31}H_{36}N_4O$: C, 77.47; H, 7.55; N, 11.66 %. Found: C, 77.49; H, 7.57; N, 11.68 %.

4B. 4. 3. 9. 9-(2-(4-ethylpiperazin-1-yl)quinolin-3-yl)-3,3,6-trimethyl-3,4,9,10 tetrahydroacridin-1(2H)-one (6i).

White colour solid: yield 83 %: FT-IR (KBr): 3507, 3306, 3160, 2961, 2315, 1969, 1812, 1668, 1646, 1568, 1434, 1197, 1135, 999, 929, 764, 571 cm^{-1}. ^{1}H NMR ($CDCl_3$, 400 MHz): δ 12.69 (1H, s, N-H), 8.13 (1H, s, Ar-H), 7.67 (2H, d, *J* = 7.6 Hz, Ar-H), 7.45-7.49 (2H, dd, *J* = 7.2 Hz, Ar-H), 7.32 (2H, d, *J* = 8.4 Hz, Ar-H), 7.18 (1H, s, Ar-H), 4.83 (1H, s, CH), 2.47 (6H, m, CH_2), 2.13-2.26 (8H, q, CH_2), 1.06 (6H, s, CH_3), 0.96 (6H, s, CH_3). ^{13}C NMR ($CDCl_3$, 100 MHz): δ 197.17, 164.80, 163.09, 141.42, 138.01, 130.11, 129.56, 128.62, 122.30, 120.43, 115.02, 111.51, 50.89, 41, 32.19, 31.21, 29.31, 27.01. Anal. Calc. for $C_{31}H_{36}N_4O$: C, 77.47; H, 7.55; N, 11.66 %. Found: C, 77.45; H, 7.57; N, 11.64 %.

4B. 4. 3. 10. 9-(2-(4-ethylpiperazin-1-yl)quinolin-3-yl)-3,3,7-trimethyl-3,4,9,10 tetrahydroacridin1(2H)-one (6j).

White colour solid: yield 90 %: FT-IR (KBr): 3307, 3158, 3114, 3066, 2961, 2918, 2860, 2367, 1963, 1939, 1812, 1664, 1568, 1434, 1360, 1197, 1135, 1166, 999, 764, 571 cm^{-1}. ^{1}H NMR ($CDCl_3$, 400 MHz): δ 12.74 (1H, s, N-H), 8.13 (1H, s, Ar-H), 7.67 (2H, d, *J* = 7.8 Hz, Ar-H), 7.45-7.49 (2H, dd, *J* = 7.4 Hz, Ar-H), 7.32 (2H, d, *J* = 8.2 Hz, Ar-H), 7.18 (1H, s, Ar-H), 4.82 (1H, s, CH), 2.47 (6H, m, CH_2), 2.13-2.26 (8H, q, CH_2), 1.06 (6H, s, CH_3), 0.90 (6H, s, CH_3). ^{13}C NMR ($CDCl_3$, 100 MHz): δ 197.17, 164.79, 163.15, 141.35, 138.06, 130.14, 129.52, 128.61, 122.26, 120.41, 115.01, 111.52, 50.89, 41, 32.19, 31.19, 31.21, 29.31, 27. Anal. Calc. for $C_{31}H_{36}N_4O$: C, 77.47; H, 7.55; N, 11.66 %. Found: C, 77.48; H, 7.57; N, 11.67 %.

4B. 4. 3. 11. 9-(2-(4-ethylpiperazin-1-yl)quinolin-3-yl)-3,3,5,7-tetramethyl-3,4,9,10 tetrahydroacridin-1(2H)-one (6k).

White colour solid: yield 90 %: FT-IR (KBr): 3615, 3304, 3158, 3111, 3063, 2962, 2367, 1968, 1812, 1638, 1568, 1434, 1360, 1197, 1135, 999, 764, 572, 514 cm^{-1}. ^{1}H NMR ($CDCl_3$, 400 MHz): δ 12.72 (1H, s, N-H), 8.11 (1H, s, Ar-H), 7.65-7.67 (1H, t, J = 0.8 Hz, Ar-H), 7.46-7.48 (2H, t, J = 7.2 Hz, Ar-H), 7.44 (1H, d, J = 0.8 Hz, Ar-H), 7.32 (2H, d, J = 8 Hz, Ar-H), 4.82 (1H, s, CH), 3.90 (2H, d, CH_2), 2.47 (4H, m, CH_2), 2.13-2.25 (8H, q, CH_2), 1.06 (6H, s, CH_3), 0.89 (9H, s, CH_3). ^{13}C NMR ($CDCl_3$, 100 MHz): δ 197.17, 164.76, 163.15, 141.16, 138.15, 130.28, 129.43, 128.57, 122.14, 120.34, 114.94, 111.56, 50.89, 41, 32.19, 31.20, 29.31, 26.99. Anal. Calc. for $C_{32}H_{38}N_4O$: C, 77.70; H, 7.74; N, 11.33 %. Found: C, 77.72; H, 7.76; N, 11.36 %.

4B. 4. 3. 12. 9-(2-(4-ethylpiperazin-1-yl)quinolin-3-yl)-5-methoxy-3,3-dimethyl-3,4,9,10 tetrahydroacridin-1(2H)-one (6l).

White colour solid: yield 78 %: FT-IR (KBr): 3307, 3159, 3111, 3063, 2960, 2315, 1969, 1812, 1664, 1663, 1568, 1434, 1197, 1136, 765, 572, 514 cm^{-1}. ^{1}H NMR ($CDCl_3$, 400 MHz): δ 12.68 (1H, s, N-H), 8.13 (1H, s, Ar-H), 7.67 (1H, d, J = 7.6 Hz, Ar-H), 7.47-7.49 (2H, dd, J = 7.4 Hz, Ar-H), 7.32 (1H, d, J = 8 Hz, Ar-H), 7.19-7.23 (3H, t, J = 7.2 Hz, Ar-H), 4.83 (1H, s, CH), 2.47 (6H, m, CH_2), 2.13-2.26 (8H, q, CH_2), 1.05 (6H, s, CH_3), 0.91 (6H, s, CH_3). ^{13}C NMR ($CDCl_3$, 100 MHz): δ 197.16, 164.74, 162.81, 141.15, 137.96, 130.88, 130.44, 129.52, 128.80, 128.57, 127.65, 122.22, 120.32, 114.82, 68.16, 50.89, 49.79, 40.97, 38.73, 32.18, 31.11, 29.69, 29.32, 28.92, 27.02, 22.98. Anal. Calc. for $C_{31}H_{36}N_4O_2$: C, 74.97; H, 7.31; N, 11.28 %. Found: C, 74.95; H, 7.33; N, 11.27 %.

4B. 4. 3. 13. 9-(2-(4-ethylpiperazin-1-yl)quinolin-3-yl)-7-methoxy-3,3-dimethyl-3,4,9,10 tetrahydroacridin-1(2H)-one (6m).

White colour solid: yield 85 %: FT-IR (KBr): 3319, 3165, 3102, 3069, 2963, 2364, 1968, 1811, 1677, 1664, 1627, 1568, 1498, 1434, 1362, 1200, 1136, 999, 929, 765, 572, 514 cm^{-1}. ^{1}H NMR ($CDCl_3$, 400 MHz): δ 11.73 (1H, s, N-H), 8.11 (1H, s, Ar-H), 7.62 (2H, d, J = 7.6 Hz, Ar-H), 7.43-7.47 (1H, t, J = 7.2 Hz, Ar-H), 7.25 (2H, t, J = 16.4 Hz, Ar-H), 7.19 (2H, d, J = 7.8 Hz, Ar-H), 4.82 (1H, s, CH), 3.72-3.94 (2H, m, CH_2), 2.48 (4H, m, CH_2), 2.14-2.26 (6H, q, CH_2), 1.73 (2H, s, CH_2), 1.09 (6H, s, CH_3), 0.91 (6H, s, CH_3). ^{13}C NMR ($CDCl_3$, 100 MHz): δ 197.16, 164.74, 162.81, 141.15, 137.96, 130.88, 130.44, 129.52, 128.80, 128.57, 127.65, 122.22, 120.32, 114.82, 68.16, 50.89, 49.79, 40.97, 38.73, 32.18, 31.11, 29.69, 29.32, 28.92,

27.02, 22.98. Anal. Calc. for $C_{31}H_{36}N_4O_2$: C, 74.97; H, 7.31; N, 11.28 %. Found: C, 74.96; H, 7.33; N, 11.30 %.

4B. 4. 3. 14. 5-(2-(4-ethylpiperazin-1-yl)quinolin-3-yl)-8,8-dimethyl-5,8,9,10 tetrahydrobenzo[b][1,8]naphthyridin-6(7H)-one (6n).

White colour solid: yield 90 %: FT-IR (KBr): 3309, 3157, 3114, 3063, 2962, 2312, 1968, 1811, 1677, 1640, 1568, 1487, 1434, 1368, 1134, 962, 764, 522, 514 cm^{-1}. ^1H NMR ($CDCl_3$, 400 MHz): δ 12.24 (1H, s, N-H), 8.15 (1H, s, Ar-H), 7.68 (2H, d, J = 7.6 Hz, Ar-H), 7.46-7.49 (2H, t, J = 7.2 Hz, Ar-H), 7.24-7.30 (3H, t, J = 7.84 Hz, Ar-H), 4.83 (1H, s, CH), 2.48 (6H, m, CH_2), 2.07-2.26 (8H, m, CH_2), 1.07 (6H, s, CH_3), 0.93 (3H, s, CH_3). ^{13}C NMR ($CDCl_3$, 100 MHz): δ 197.17, 164.76, 163.15, 141.16, 138.15, 130.28, 129.43, 128.57, 122.14, 120.34, 114.94, 111.56, 50.89, 41, 32.19, 31.20, 29.31, 26.99. Anal. Calc. for $C_{29}H_{33}N_5O$: C, 74.49; H, 7.11; N, 14.98 %. Found: C, 74.50; H, 7.13; N, 15 %.

4B. 4. 3. 15. 5-(2-(4-ethylpiperazin-1-yl)quinolin-3-yl)-4,8,8-trimethyl-5,8,9,10 tetrahydrobenzo[b][1,8]naphthyridin-6(7H)-one (6o).

White colour solid: yield 95 %: FT-IR (KBr): 3481, 3319, 3160, 3066, 1664, 1360, 1568, 1434, 1197, 1135, 1165, 999, 764, 571, 514 cm^{-1}. ^1H NMR ($CDCl_3$, 400 MHz): δ 12.70 (1H, s, N-H), 8.13 (1H, s, Ar-H), 7.67 (2H, d, J = 7.6 Hz, Ar-H), 7.45-7.49 (1H, dd, J = 7.2 Hz, Ar-H), 7.32 (2H, d, J = 7.86 Hz, Ar-H), 7.15 (1H, t, J = 12.6 Hz, Ar-H), 4.82 (1H, s, CH), 2.47 (6H, m, CH_2), 2.13-2.26 (8H, q, CH_2), 1.07 (6H, s, CH_3), 0.90 (6H, s, CH_3). ^{13}C NMR ($CDCl_3$, 100 MHz): δ 197.17, 164.79, 163.06, 141.42, 137.99, 130.11, 129.56, 128.62, 122.31, 120.43, 115.02, 111.50, 50.89, 41, 32.19, 31.21, 29.31, 27.01. Anal. Calc. for $C_{30}H_{36}N_5O$: C, 74.81; H, 7.32; N, 14.54 %. Found C, 74.83; H, 7.35; N, 14.56 %.

4B. 4. 3. 16. 7-(2-(4-ethylpiperazin-1-yl)quinolin-3-yl)-10,10-dimethyl-7,10,11,12 tetrahydrobenzo[c]acridin-8(9H)-one (6p).

White colour solid: yield 75 %: FT-IR (KBr): 3306, 3163, 3108, 2961, 2921, 2358, 2336, 2297, 1811, 1667, 1664, 1625, 1568, 1487, 1434, 1360, 1197, 1135, 1165, 764 cm^{-1}. ^1H NMR ($CDCl_3$, 400 MHz): δ 12.72 (1H, s, N-H), 8.11 (1H, s, Ar-H), 7.65-7.67 (2H, t, J = 7.68 Hz, Ar-H), 7.44-7.48 (4H, dd, J = 8.4 Hz, Ar-H), 7.31 (2H, d, J = 7.4 Hz, Ar-H), 7.18 (2H, d, J = 6.8 Hz, Ar-H), 7.17 (2H, d, J = 7.6 Hz, Ar-H), 4.82 (1H, s, CH), 2.47 (6H, m, CH_2), 2.13-2.25 (8H, q, CH_2), 1.06 (6H, s, CH_3), 0.89 (3H, s, CH_3). ^{13}C NMR ($CDCl_3$, 100 MHz): δ 197.16, 164.74, 162.81, 141.15, 137.96, 130.88, 130.44, 129.52, 128.80, 128.57, 127.65, 122.22,

120.32, 114.82, 50.89, 49.79, 40.97, 38.73, 32.18, 31.11, 29.69, 29.32, 28.92, 27.02, 22.98. Anal. Calc. for $C_{34}H_{36}N_4O$: C, 79.04; H, 7.02; N, 10.84 %. Found: C, 79.06; H, 7.04; N, 10.86 %.

4B. 5. Molecular Docking Studies

Molecular docking was executed for accurate docking of ligands into protein active sites using Ligand Fit module in DS. The protein complexes were selected from a protein databank (PDB, www.rcsb.org). To date, many Hsp 90 complexes have been reported. From them PDB ID: 3EKO was selected, based on the resolution of the complex and the size of the co-crystal. For docking study, the protein was prepared by removing all water compounds. Force field was applied using Receptor–Ligand Interactions tool in DS. Two methods were applied to define the binding site for a protein: (i) Firstly, binding sites were identified based on the shape of the receptor using "eraser" algorithm and (ii) Secondly, by the volume occupied by the known ligand already in an active site. The binding site was defined using the second method and the critical amino acids were identified by analysing the protein–ligand interactions from 40 Hsp 90 co-crystal structures which were deposited in PDB.

References

Antonini, I., Polucci, P., Kelland, L. R., Menta, E., Pescalli, N. and Martelli, S., 1999. 2, 3-Dihydro-1 H, 7 H-pyrimido [5, 6, 1-de] acridine-1, 3, 7-trione Derivatives, a Class of Cytotoxic Agents Active on Multidrug-Resistant Cell Lines: Synthesis, Biological Evaluation, and Structure− Activity Relationships. Journal of medicinal chemistry (42) 2535-2541.

Antonini, I., Polucci, P., Magnano, A., Cacciamani, D., Konieczny, M. T., Paradziej-Łukowicz, J. and Martelli, S., 2003. Rational design, synthesis and biological evaluation of hiadiazinoacridines: A new class of antitumor agents. Bioorganic & medicinal chemistry (11) 399-405.

Bahrami, K., Khodaei, M. M. and Fattahpour, P., 2011. SBA-15-Pr–SO_3 H as nanoreactor catalyzed oxidation of sulfides into sulfoxides. Catalysis Science & Technology (1) 389-393.
Charmantray, F. and Martelli, A., 2001. Interest of acridine derivatives in the anticancer chemotherapy. Current pharmaceutical design (7) 1703-1724.

Ciofani, G., Genchi, G. G., Liakos, I., Athanassiou, A., Dinucci, D., Chiellini, F. and Mattoli, V., 2012. A simple approach to covalent functionalization of boron nitride nanotubes. Journal of colloid and interface science (374) 308-314.

Das, B., Venkateswarlu, K., Holla, H. and Krishnaiah, M., 2006. Sulfonic acid functionalized silica: A remarkably efficient heterogeneous reusable catalyst for α-monobromination of carbonyl compounds using N-bromosuccinimide. Journal of Molecular Catalysis A: Chemical (253) 107-111.

Dutta, A.K., Gogoi, P. and Borah, R., 2014. Synthesis of dibenzoxanthene and acridine derivatives catalyzed by 1, 3-disulfonic acid imidazolium carboxylate ionic liquids. RSC Advances (4) 41287-41291.

Filloux, N. and Galy, J. P., 2001. New polyacridine compounds: synthesis of acridine dimers and tetramers. Synlett (2001) 1137-1139.

Karimi, B. and Zareyee, D., 2008. Design of a highly efficient and water-tolerant sulfonic acid nanoreactor based on tunable ordered porous silica for the von Pechmann reaction. Organic letters (10) 3989-3992.

Kureshy, R. I., Ahmad, I., Pathak, K., Khan, N. H., Abdi, S. H. and Jasra, R. V., 2009. Sulfonic acid functionalized mesoporous SBA-15 as an efficient and recyclable catalyst for the synthesis of chromenes from chromanols. Catalysis Communications (10) 572-575.

Karimi, B. and Zareyee, D., 2008. Design of a highly efficient and water-tolerant sulfonic acid nanoreactor based on tunable ordered porous silica for the von Pechmann reaction. Organic letters (10) 3989-3992.

Kureshy, R. I., Ahmad, I., Pathak, K., Khan, N. H., Abdi, S. H. and Jasra, R.V., 2009. Sulfonic acid functionalized mesoporous SBA-15 as an efficient and recyclable catalyst for the synthesis of chromenes from chromanols. Catalysis Communications (10) 572-575.

Kathi, J. and Rhee, K.Y., 2008. Surface modification of multi-walled carbon nanotubes using 3-aminopropyltriethoxysilane. Journal of materials science (43) 33-37.

McCarthy, P. J., Pitts, T. P., Gunawardana, G. P., Kelly-Borges, M. and Pomponi, S. A., 1992. Antifungal activity of meridine, a natural product from the marine sponge Corticium sp. Journal of natural products (55) 1664-1668.

Meth-Cohn, O., Narine, B. and Tarnowski, B., 1981. A versatile new synthesis of quinolines and related fused pyridines, Part 5. The synthesis of 2-chloroquinoline-3-carbaldehydes. Journal of the Chemical Society, Perkin Transactions (1) 1520-1530.

Spalding, D. P., Chapin, E. C. and Mosher, H. S., 1954. Heterocyclic Basic Compounds XV Benzoacridine derivatives The Journal of Organic Chemistry (19) 357-364.

Van Rhijn, W., De Vos, D., Sels, B. and Bossaert, W., 1998. Sulfonic acid functionalised ordered mesoporous materials as catalysts for condensation and esterification reactions. Chemical communications (3) 317-318.

Van Rhijn, W., De Vos, D., Sels, B. and Bossaert, W., 1998. Sulfonic acid functionalised ordered mesoporous materials as catalysts for condensation and esterification reactions. Chemical communications (3) 317-318.

Valentini, L., Macan, J., Armentano, I., Mengoni, F. and Kenny, J. M., 2006. Modification of fluorinated single-walled carbon nanotubes with aminosilane molecules. Carbon (44) 2196-2201.

Zang, H., Zhang, Y., Zang, Y. and Cheng, B.W., 2010. An efficient ultrasound-promoted method for the one-pot synthesis of 7, 10, 11, 12-tetrahydrobenzo [c] acridin-8 (9H)-one derivatives. Ultrasonics sonochemistry (17) 495-499.

Chapter Four

Part A

Appendix

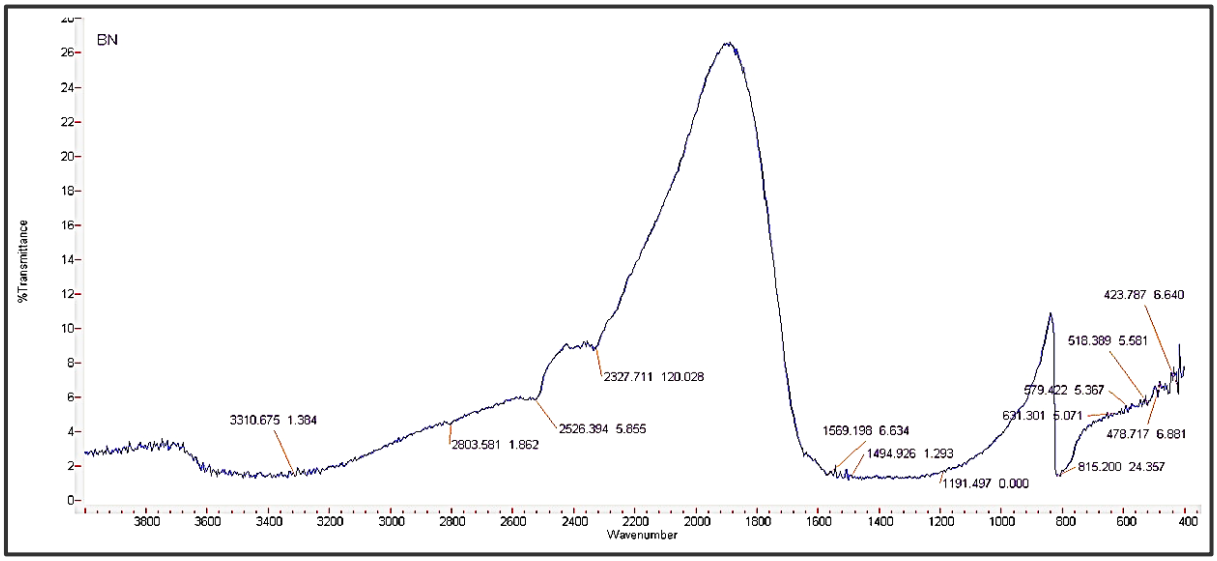

Figure 4A. S. 1. The Infra-Red Spectrum of boron nitride

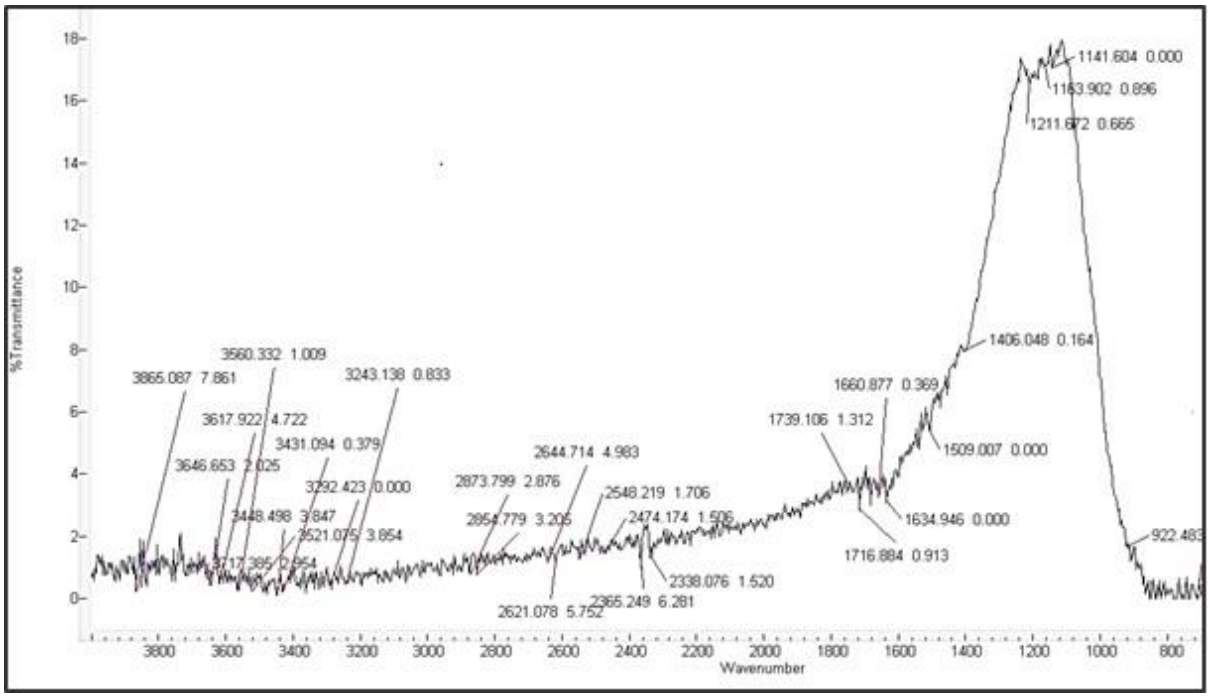

Figure 4A. S. 2. The Infra-Red Spectrum of the catalyst BN-Pr-SO_3H

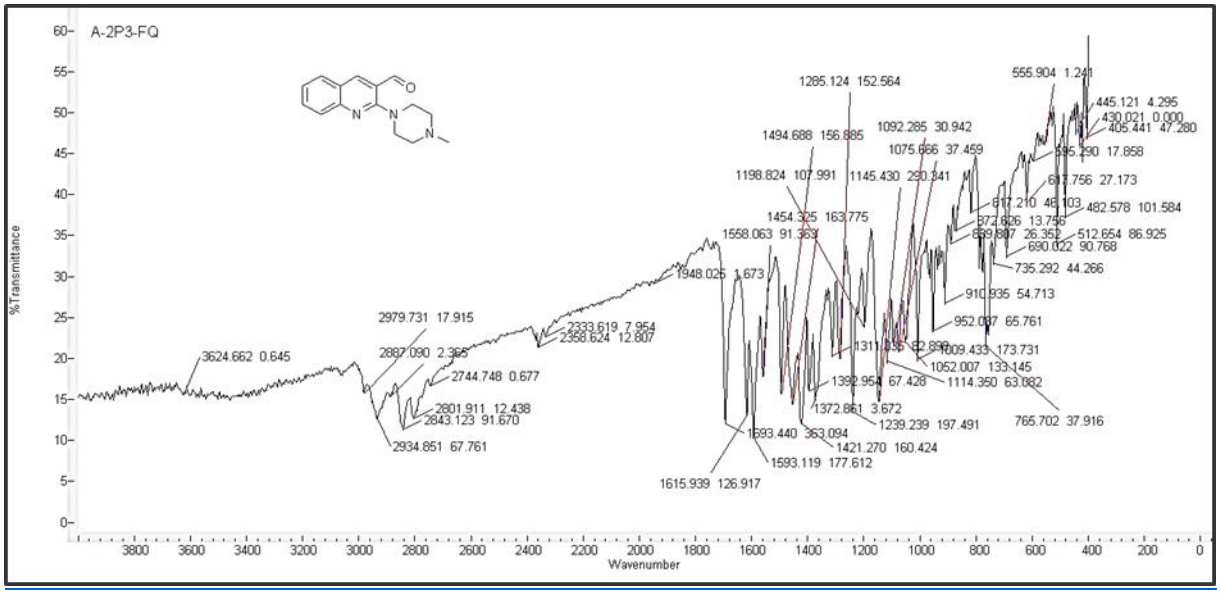

Figure 4A. S. 3. The Infra-Red Spectrum of compound 3

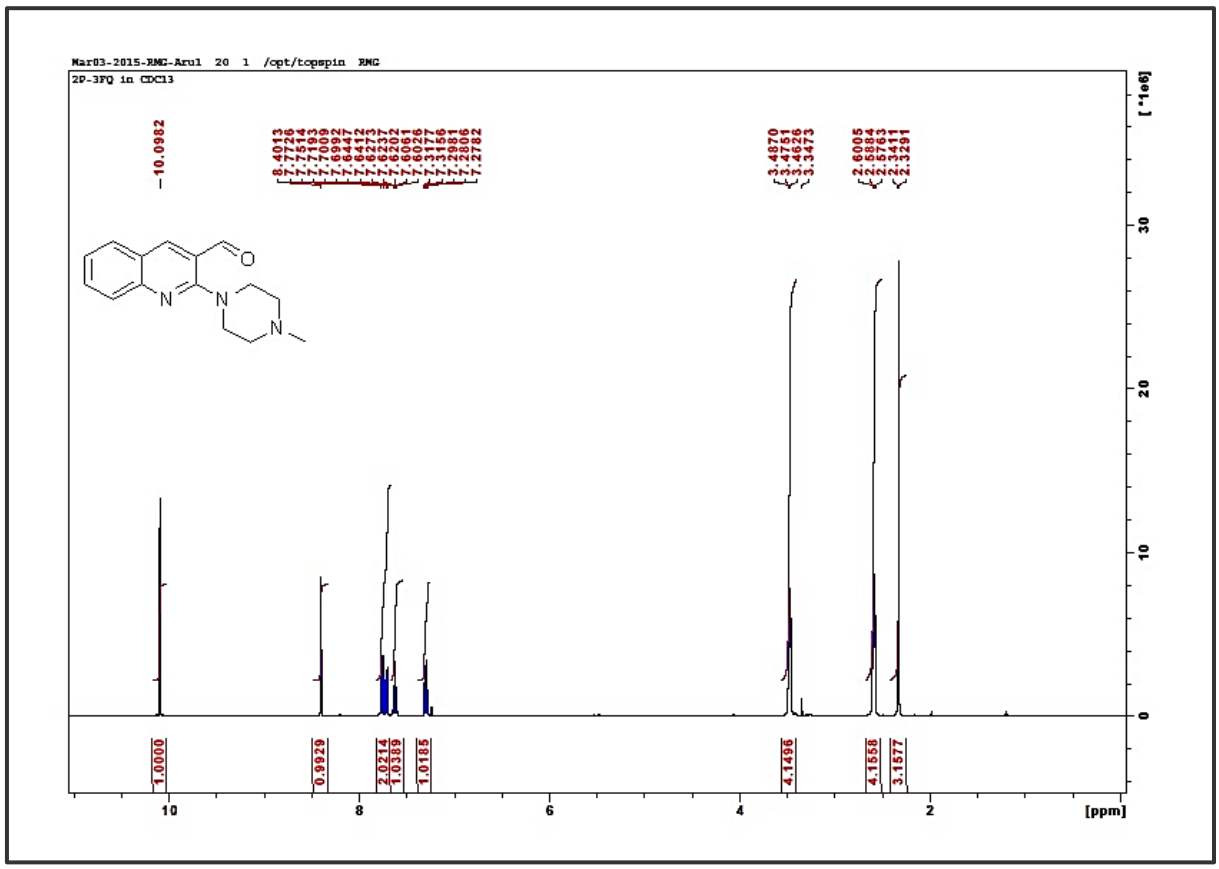

Figure 4A. S. 4. The ^{1}H NMR of compound 3

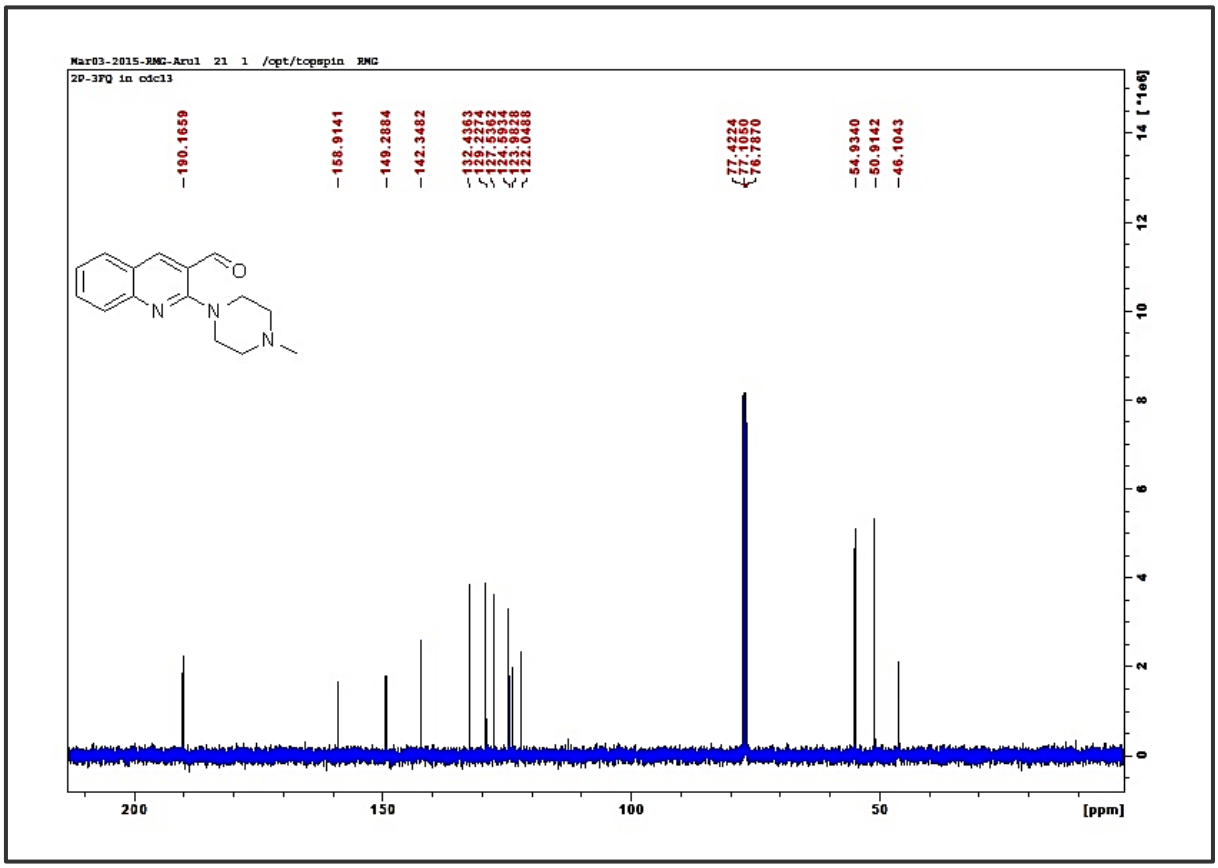

Figure 4A. S. 5. The ^{13}C NMR of compound 3

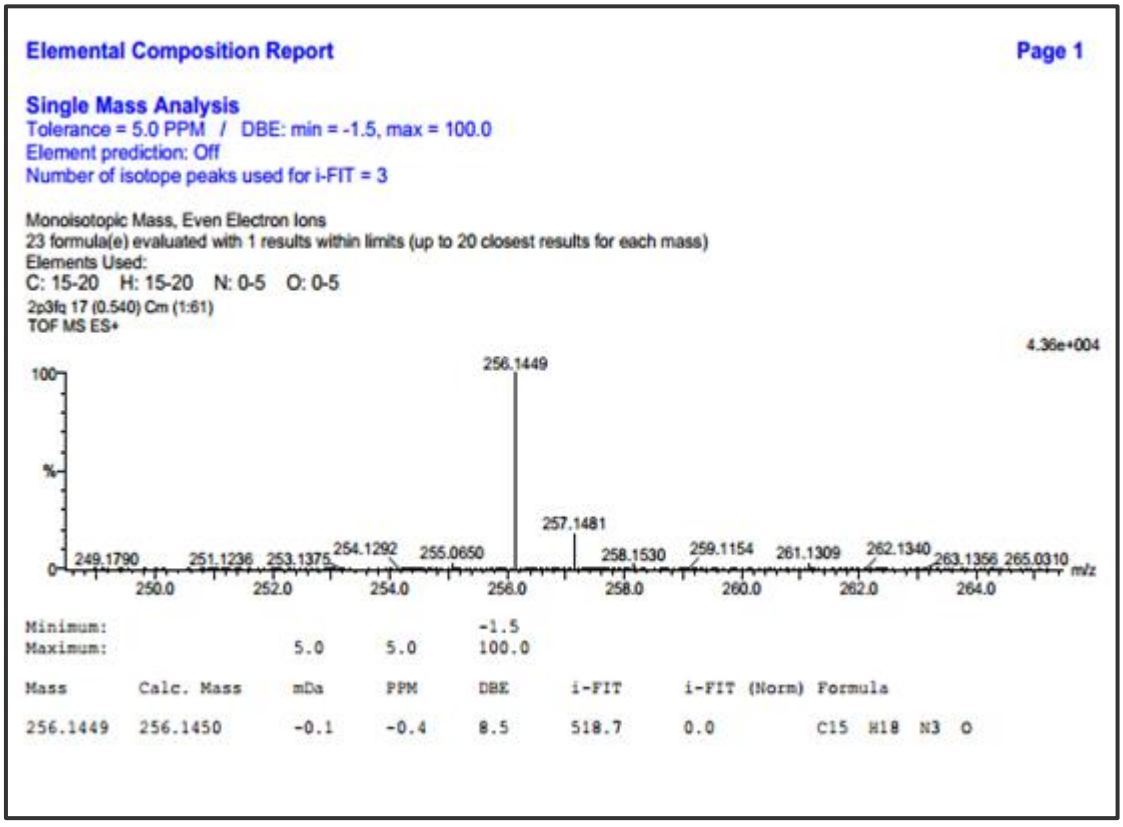

Figure 4A. S. 6. The HRMS of compound 3

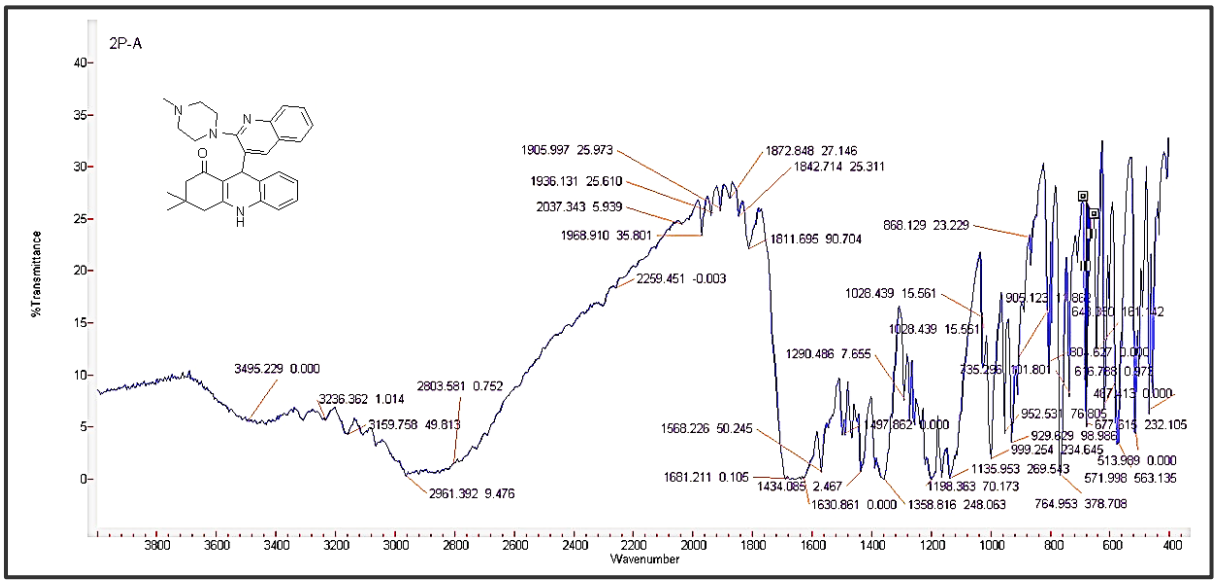

Figure 4A. S. 7. The Infra-Red Spectrum of compound 6a

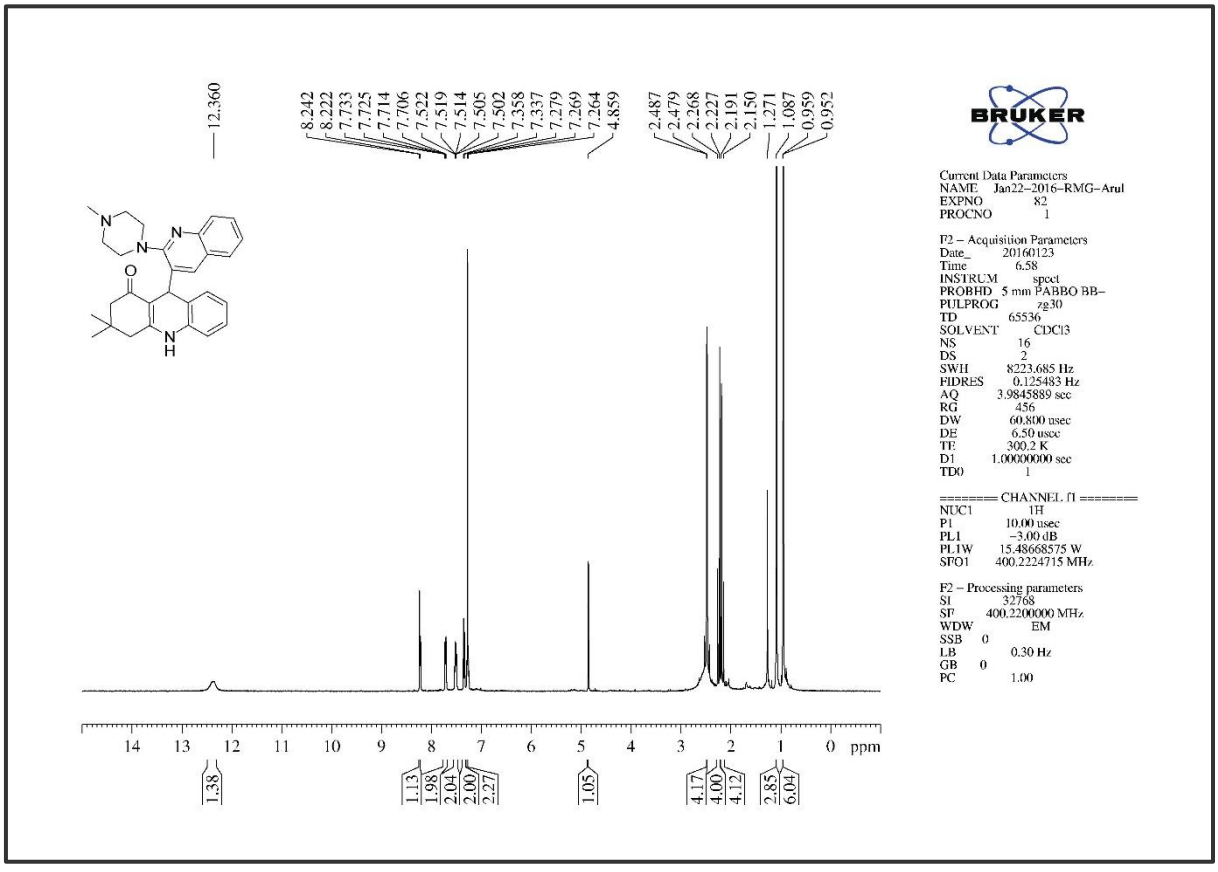

Figure 4A. S. 8. The ^{1}H NMR of compound 6a

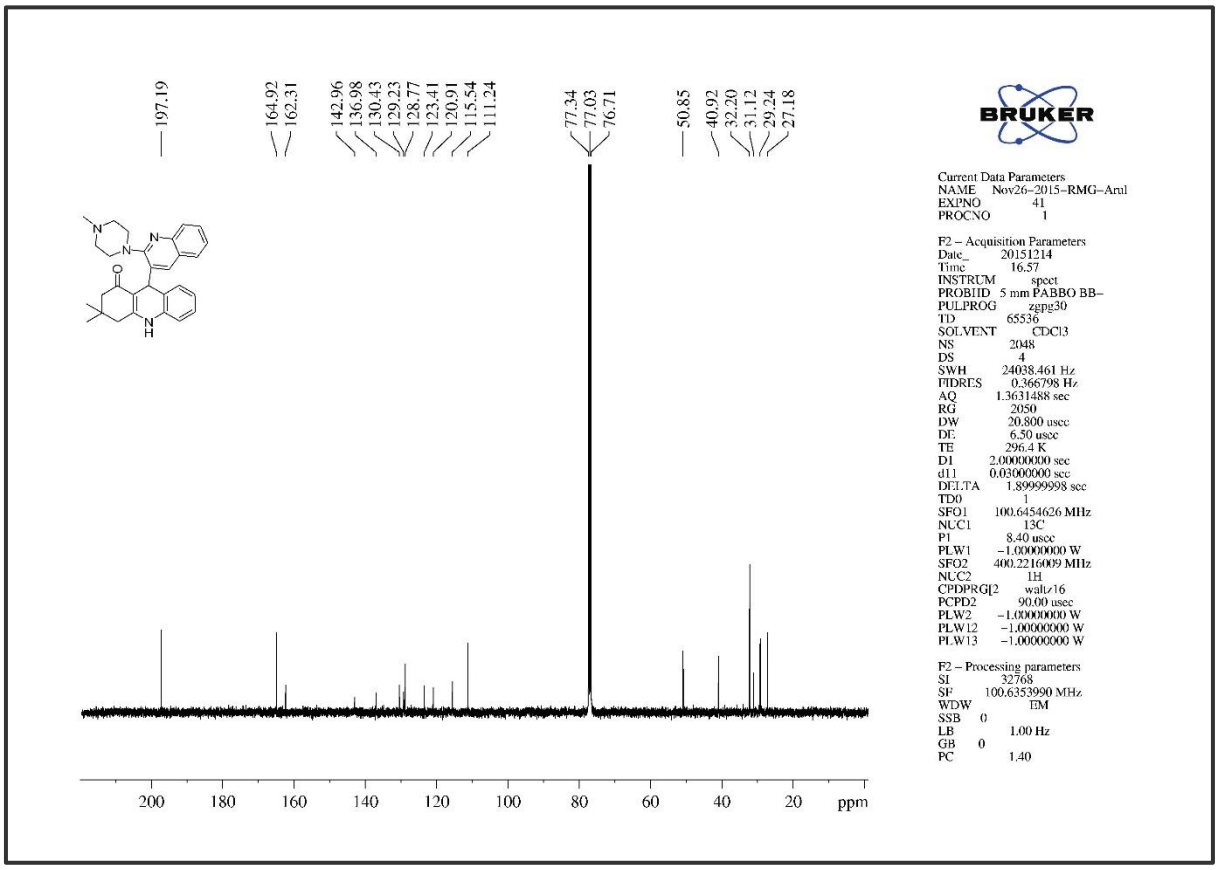

Figure 4A. S. 9. The ^{13}C NMR of compound 6a

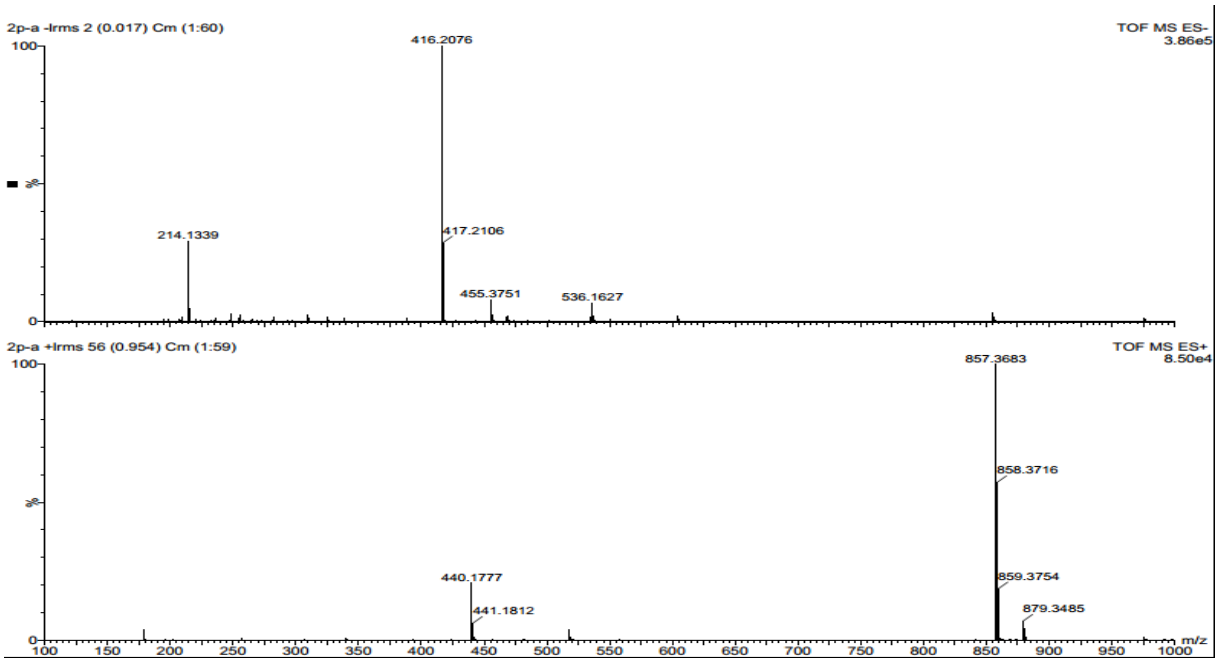

Figure 4A. S. 10. The HRMS of compound 6a

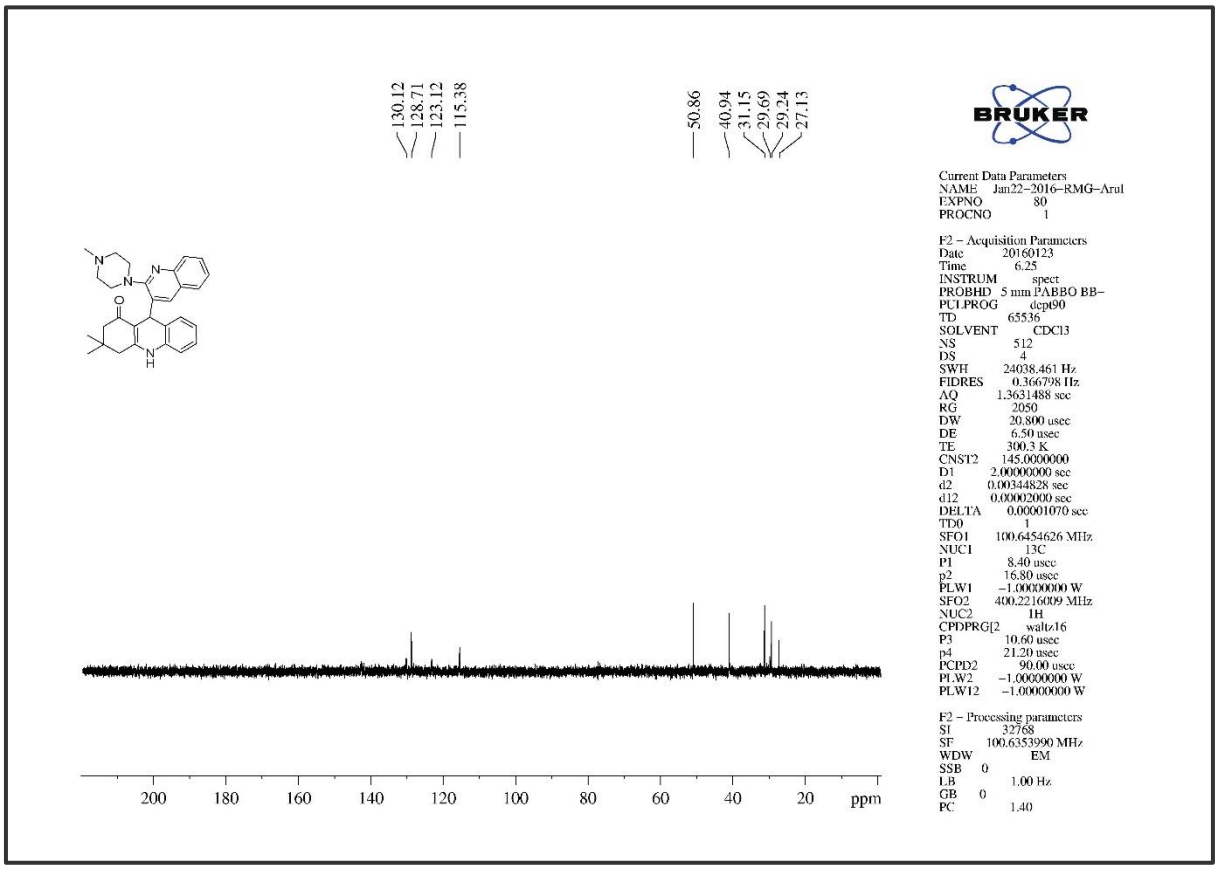

Figure 4A. S. 11. The DEPT-90 NMR of compound 6a

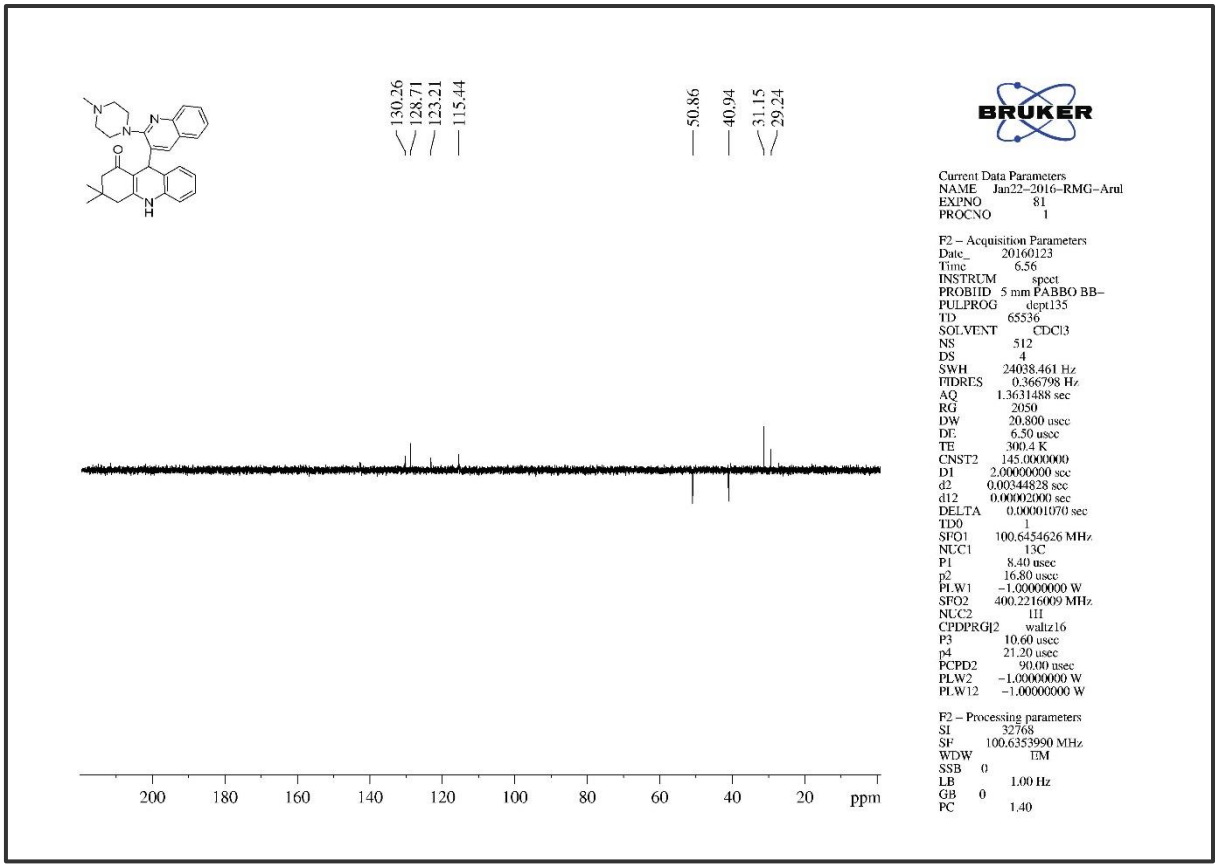

Figure 4A. S. 12. DEPT-135 NMR of compound 6a

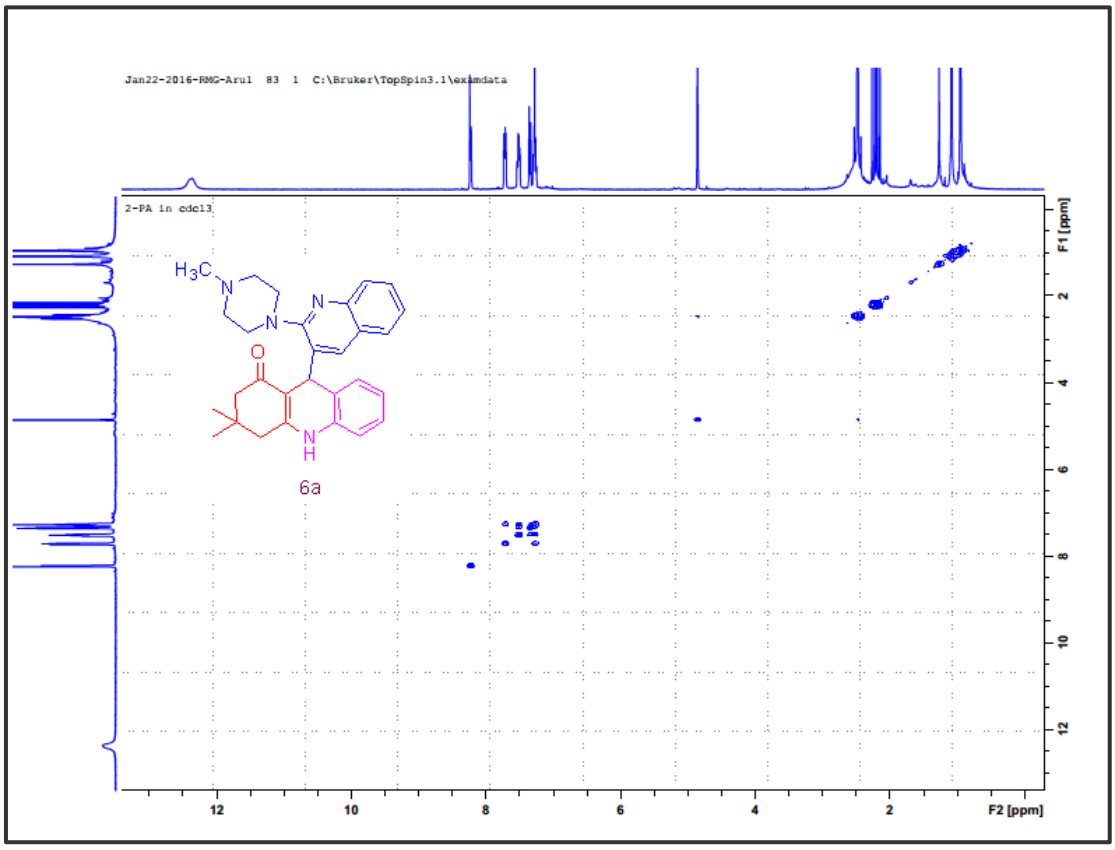

Figure 4A. S. 13. COSY NMR of compound 6a

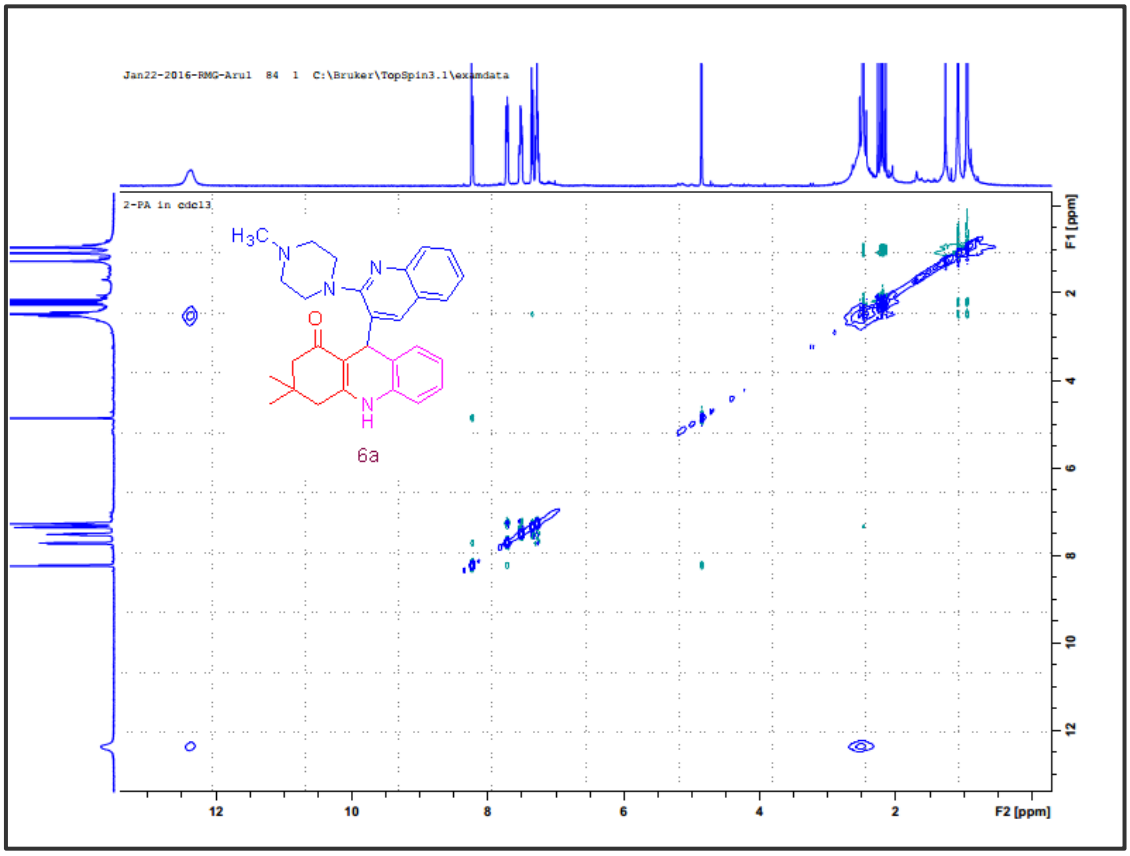

Figure 4A. S. 14. NOESY NMR of compound 6a

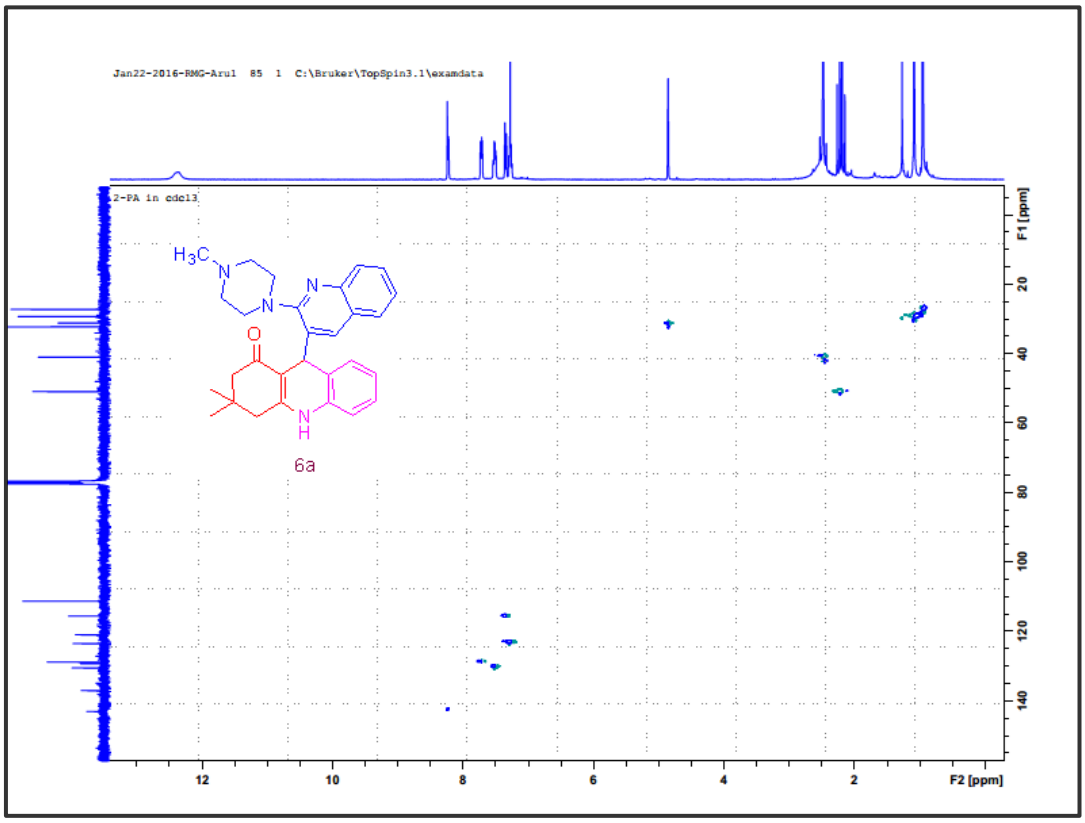

Figure 4A. S. 15. HSQCE NMR of compound 6a

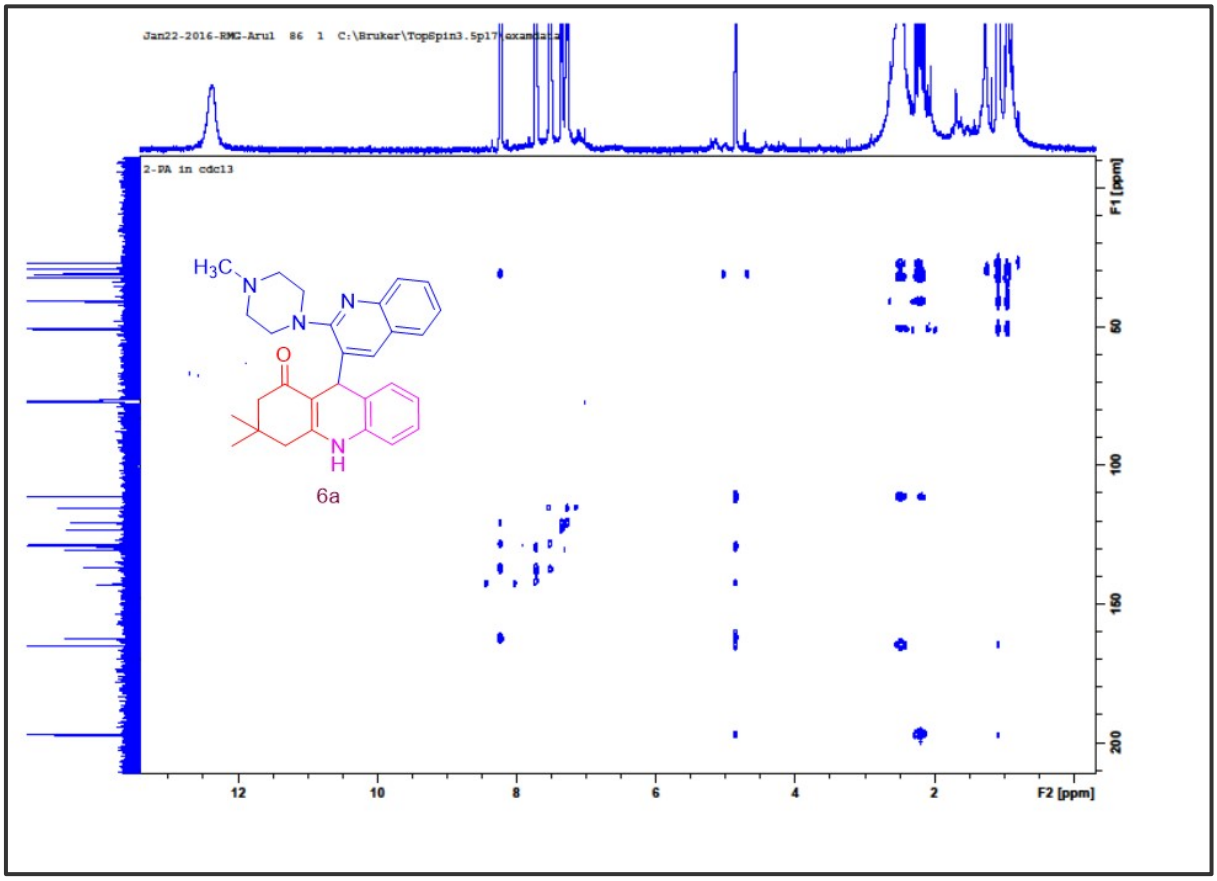

Figure 4A. S. 16. HMBC NMR of compound 6a

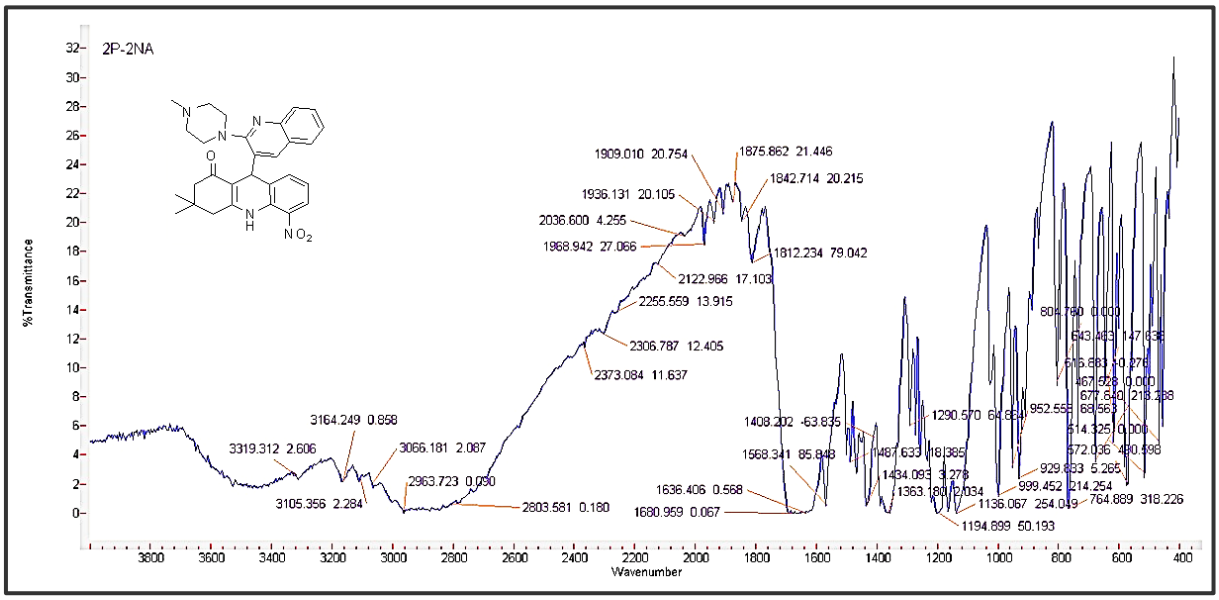

Figure 4A. S. 17. The Infra-Red Spectrum of compound 6b

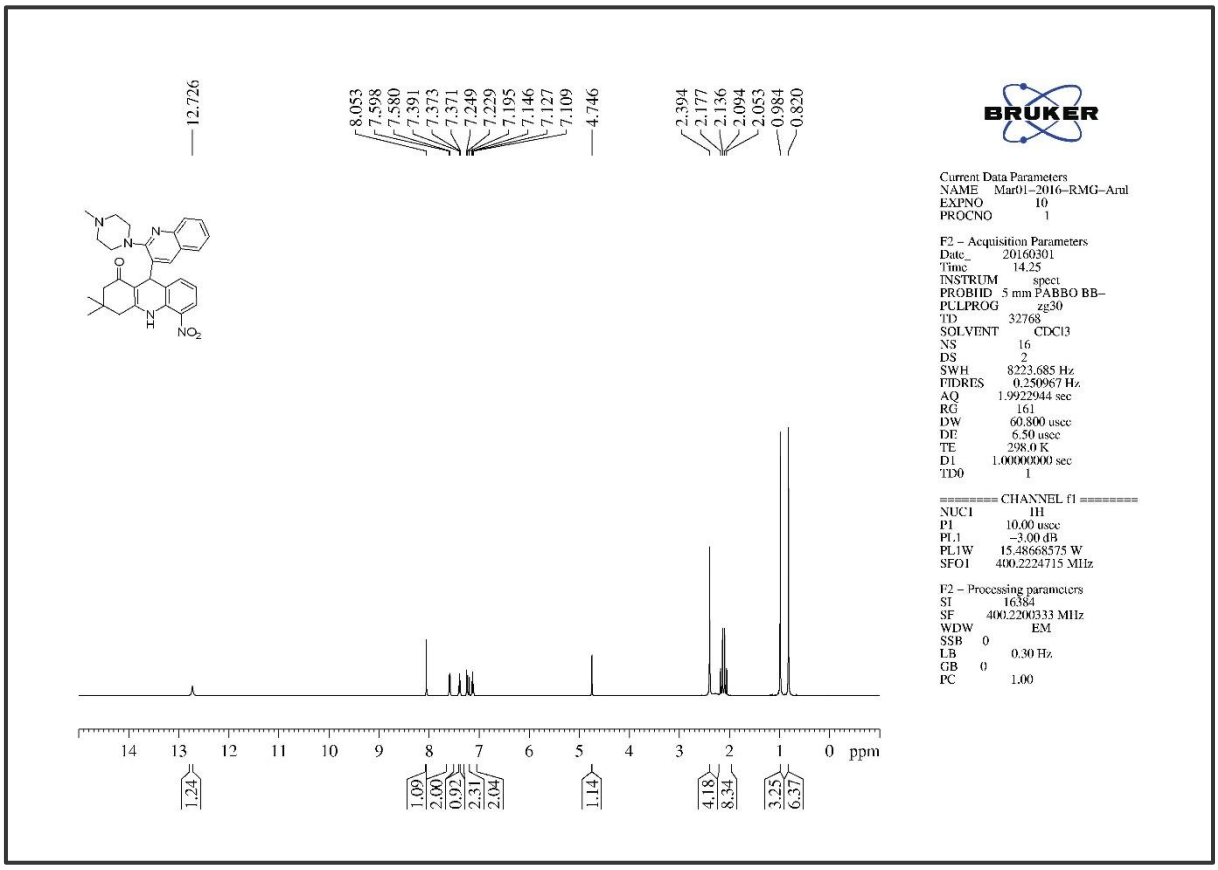

Figure 4A. S. 18. The ^{1}H NMR of compound 6b

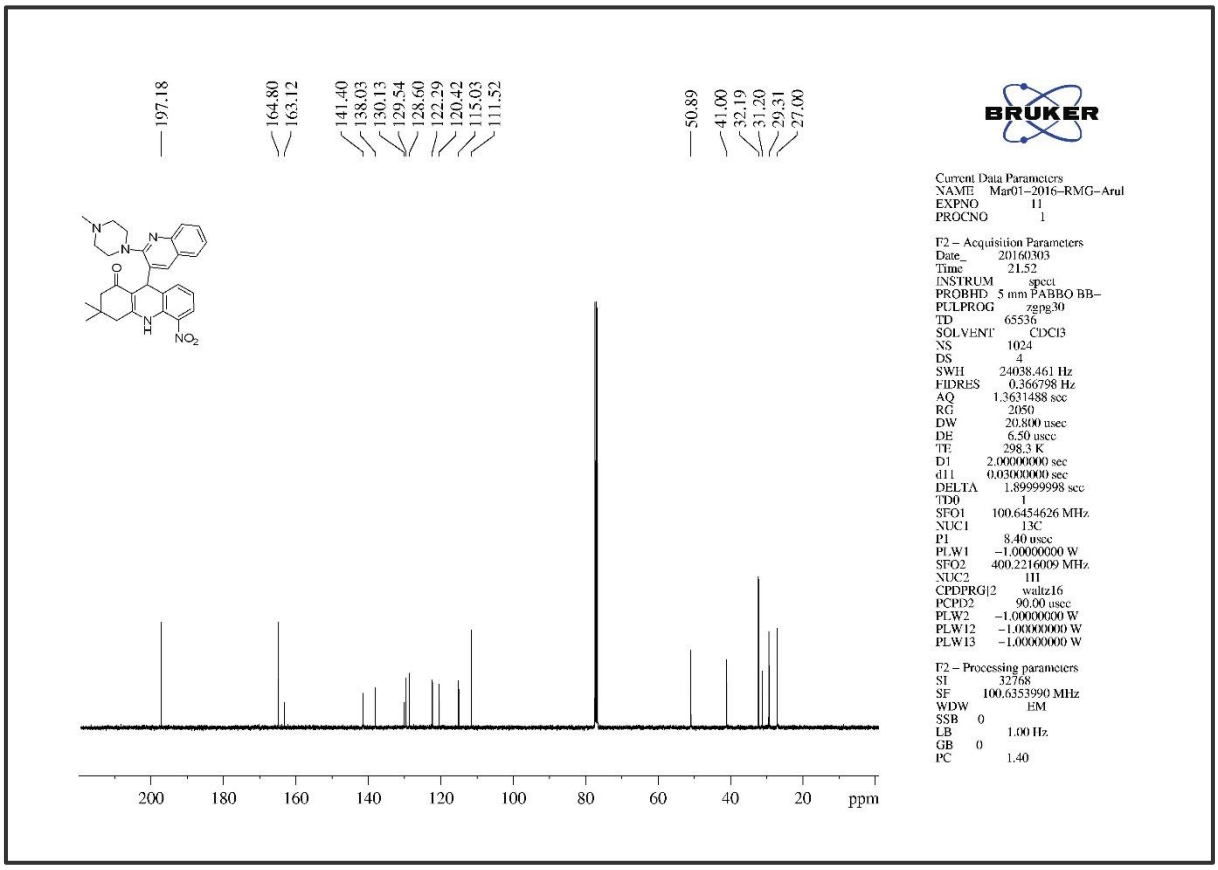

Figure 4A. S. 19. The ^{13}C NMR of compound 6b

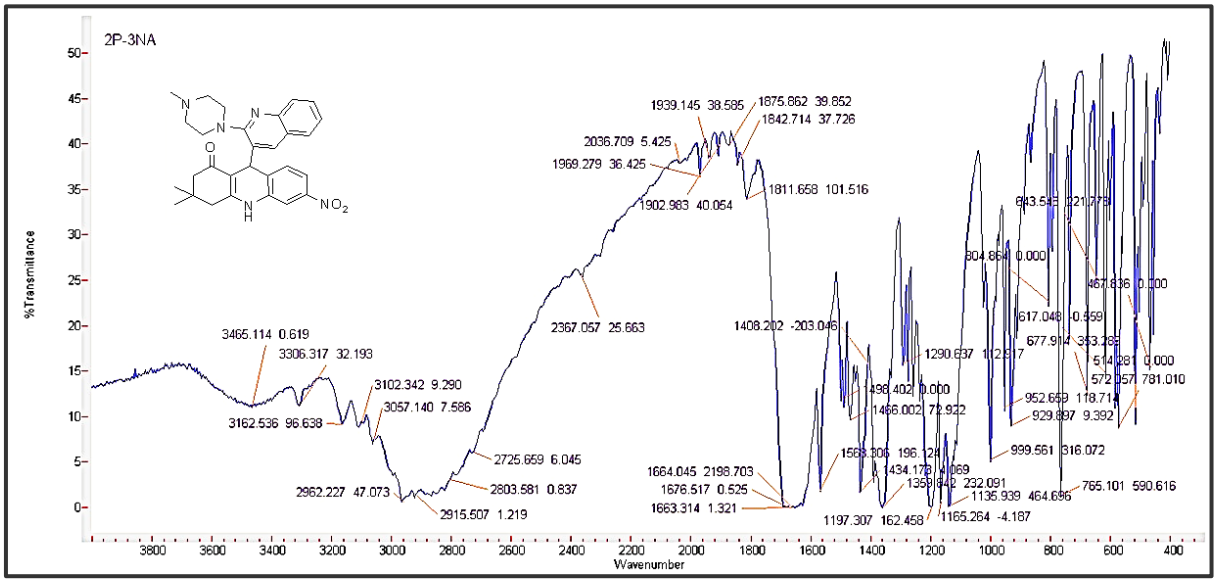

Figure 4A. S. 20. The Infra-Red Spectrum of compound 6c

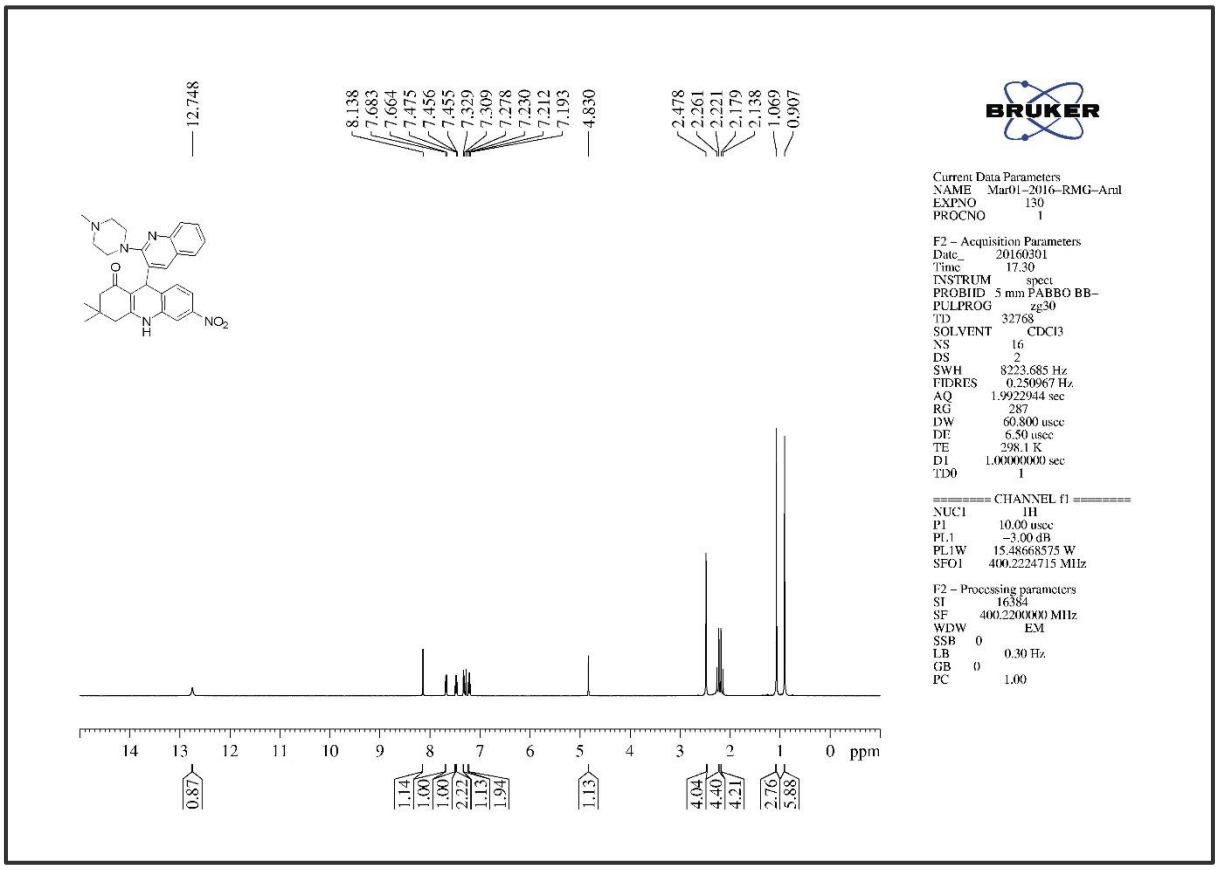

Figure 4A. S. 21. The ^{1}H NMR of compound 6c

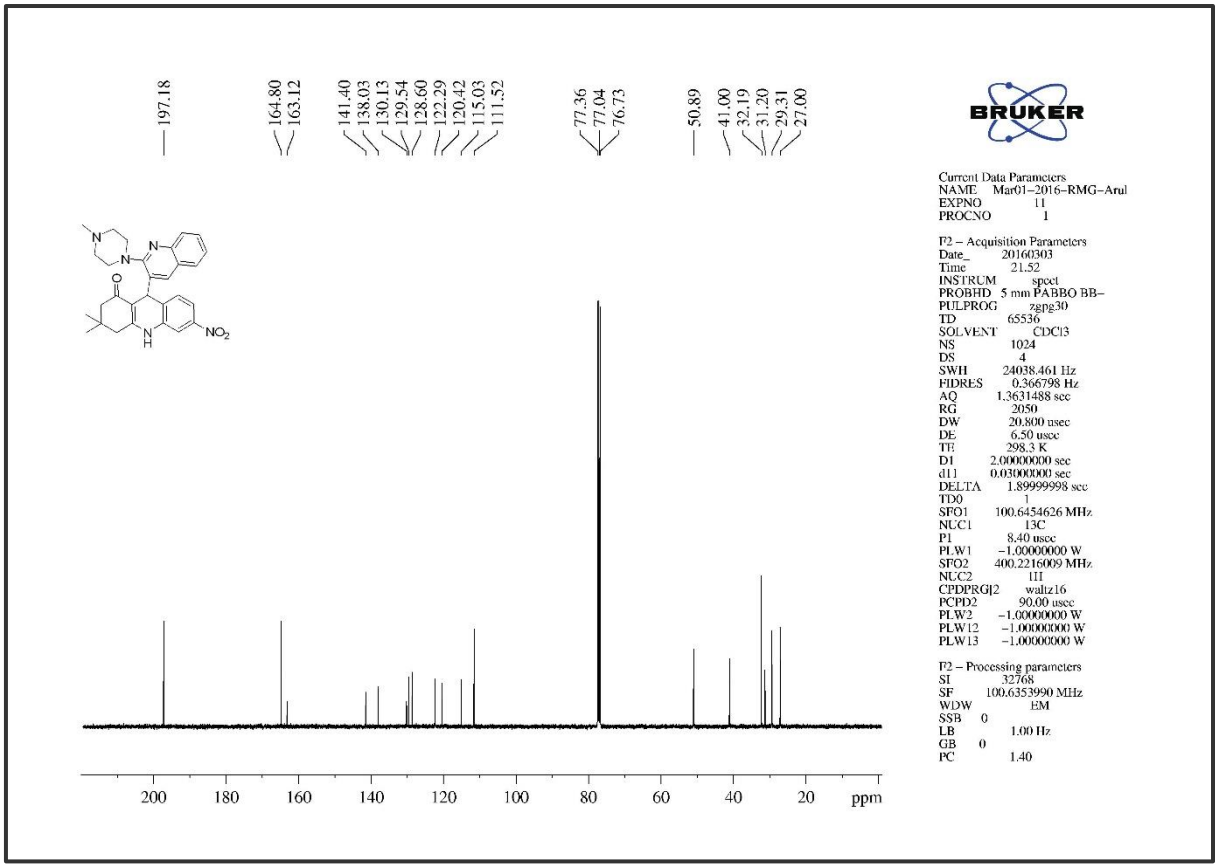

Figure 4A. S. 22. The ^{13}C NMR of compound 6c

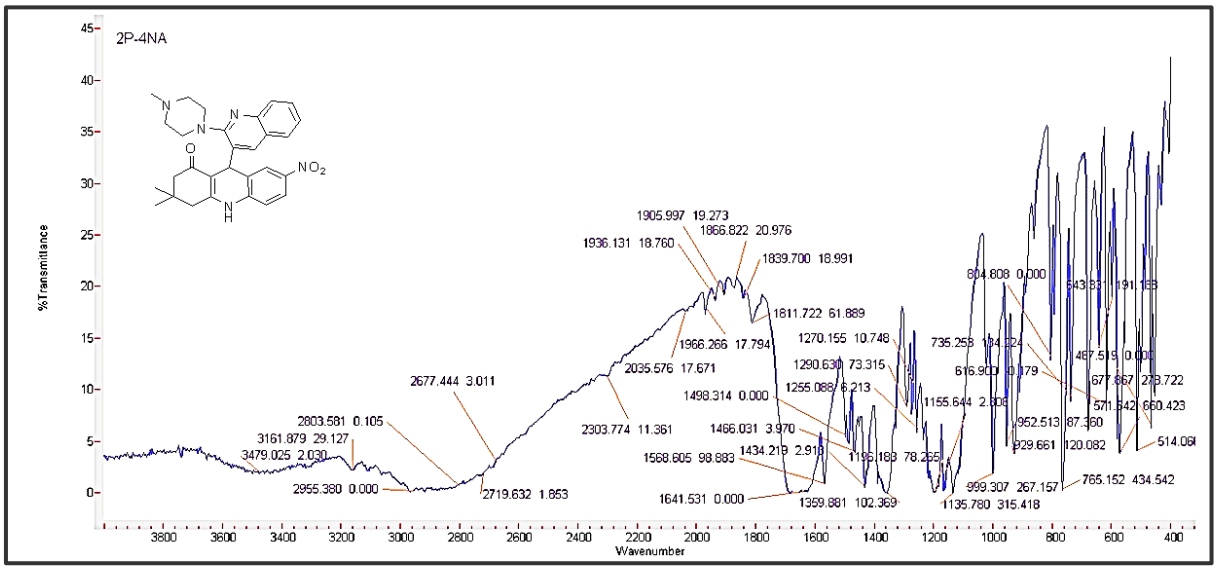

Figure 4A. S. 23. The Infra-Red Spectrum of compound 6d

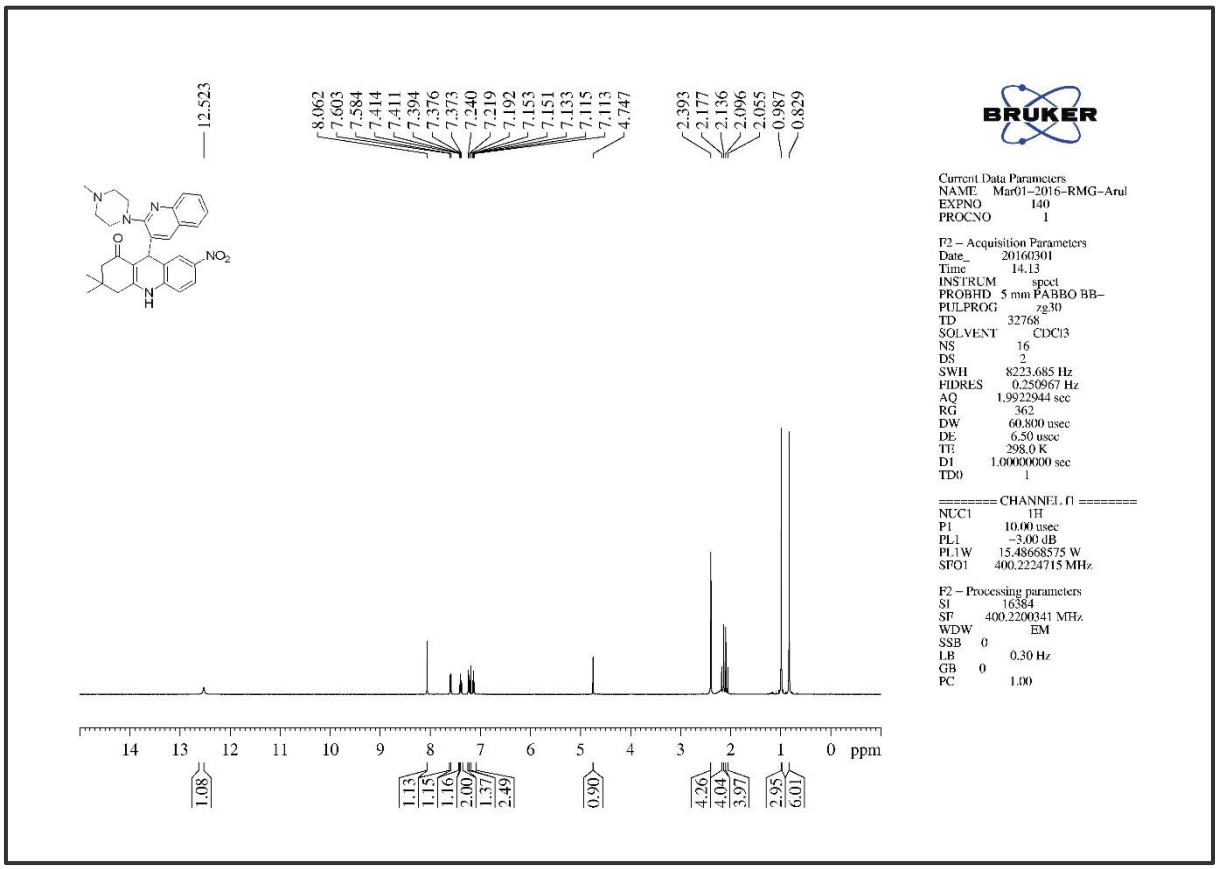

Figure 4A. S. 24. The ^{1}H NMR of compound 6d

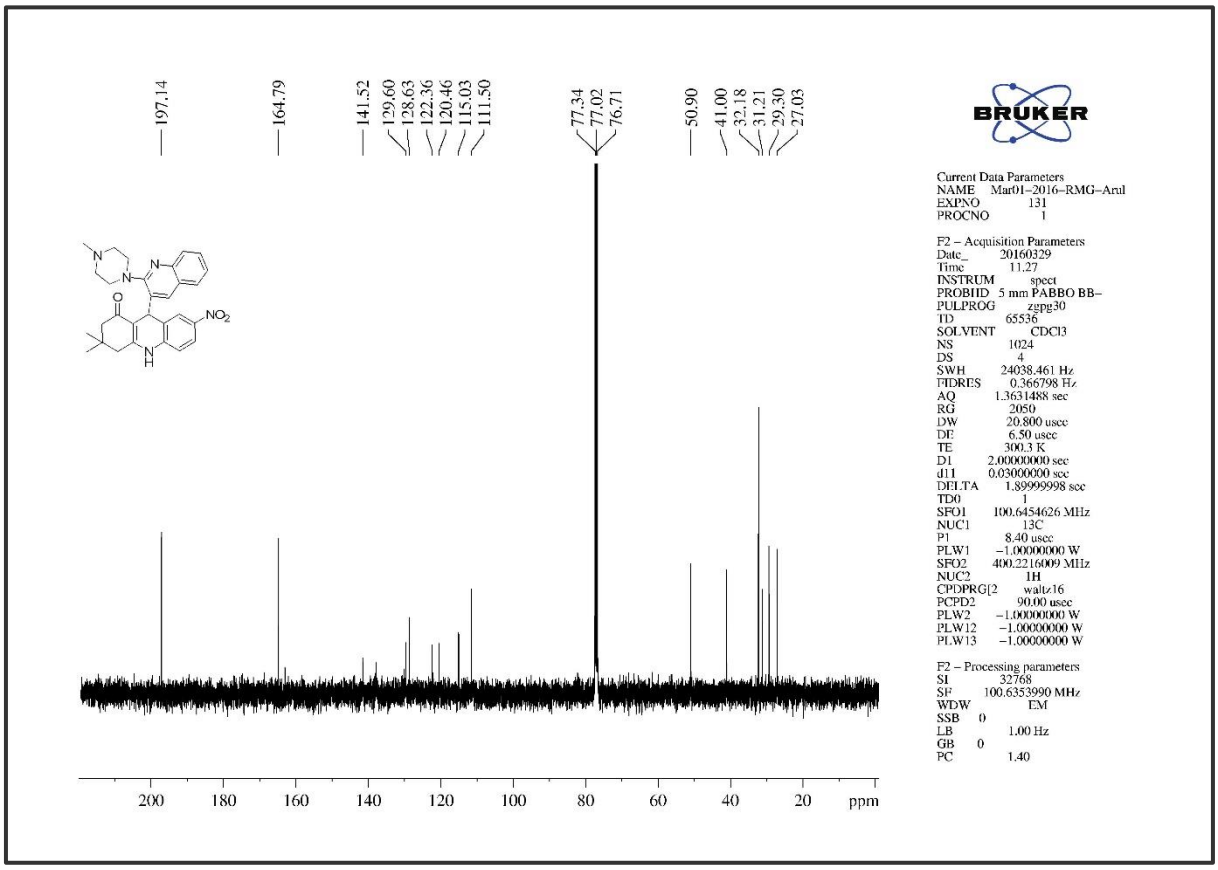

Figure 4A. S. 25. The ^{13}C NMR of compound 6d

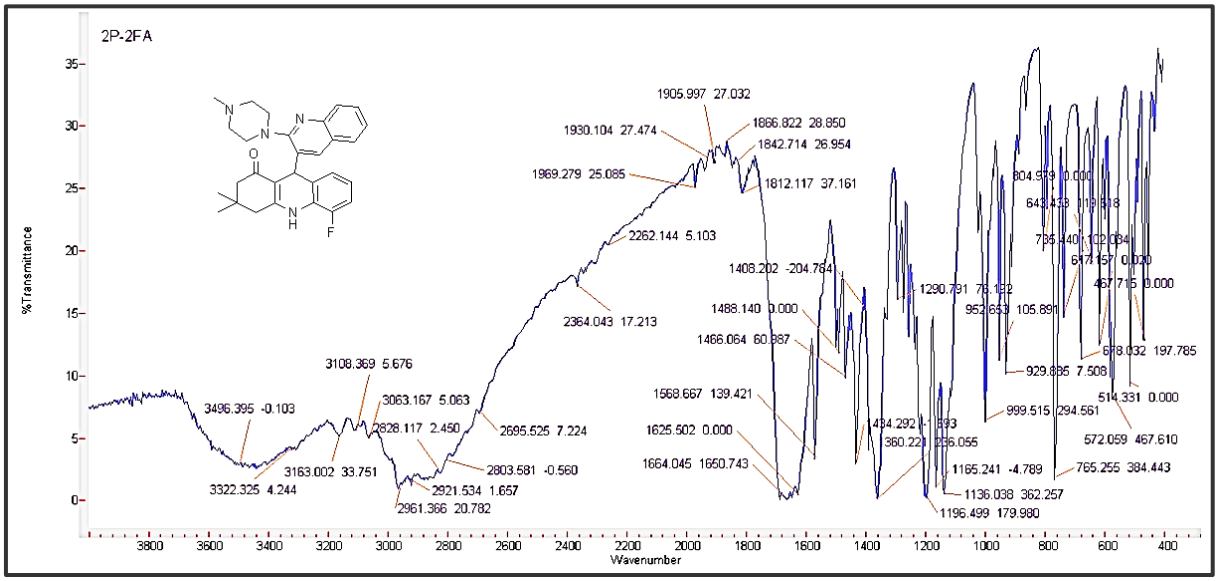

Figure 4A. S. 26. The Infra-Red Spectrum of compound 6e

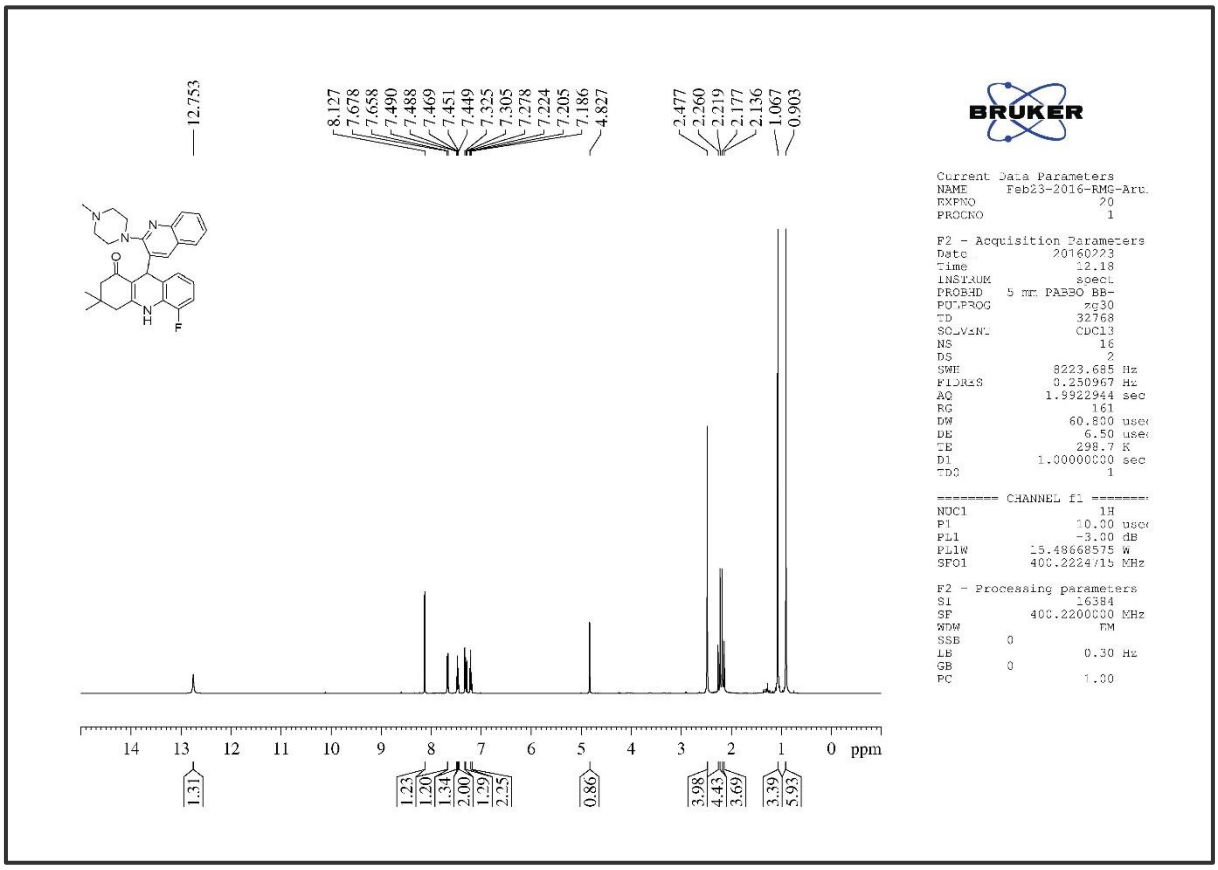

Figure 4A. S. 27. The ^{1}H NMR of compound 6e

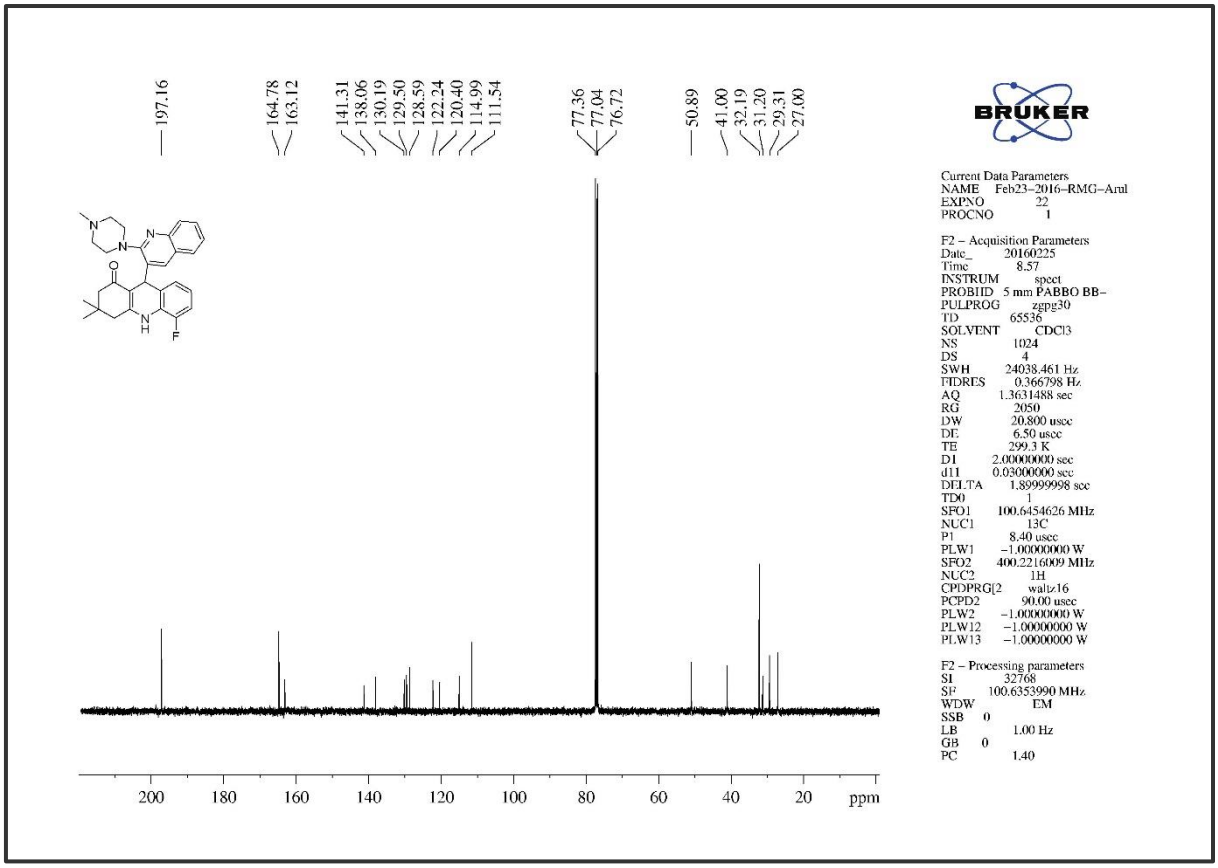

Figure 4A. S. 28. The ^{13}C NMR of compound 6e

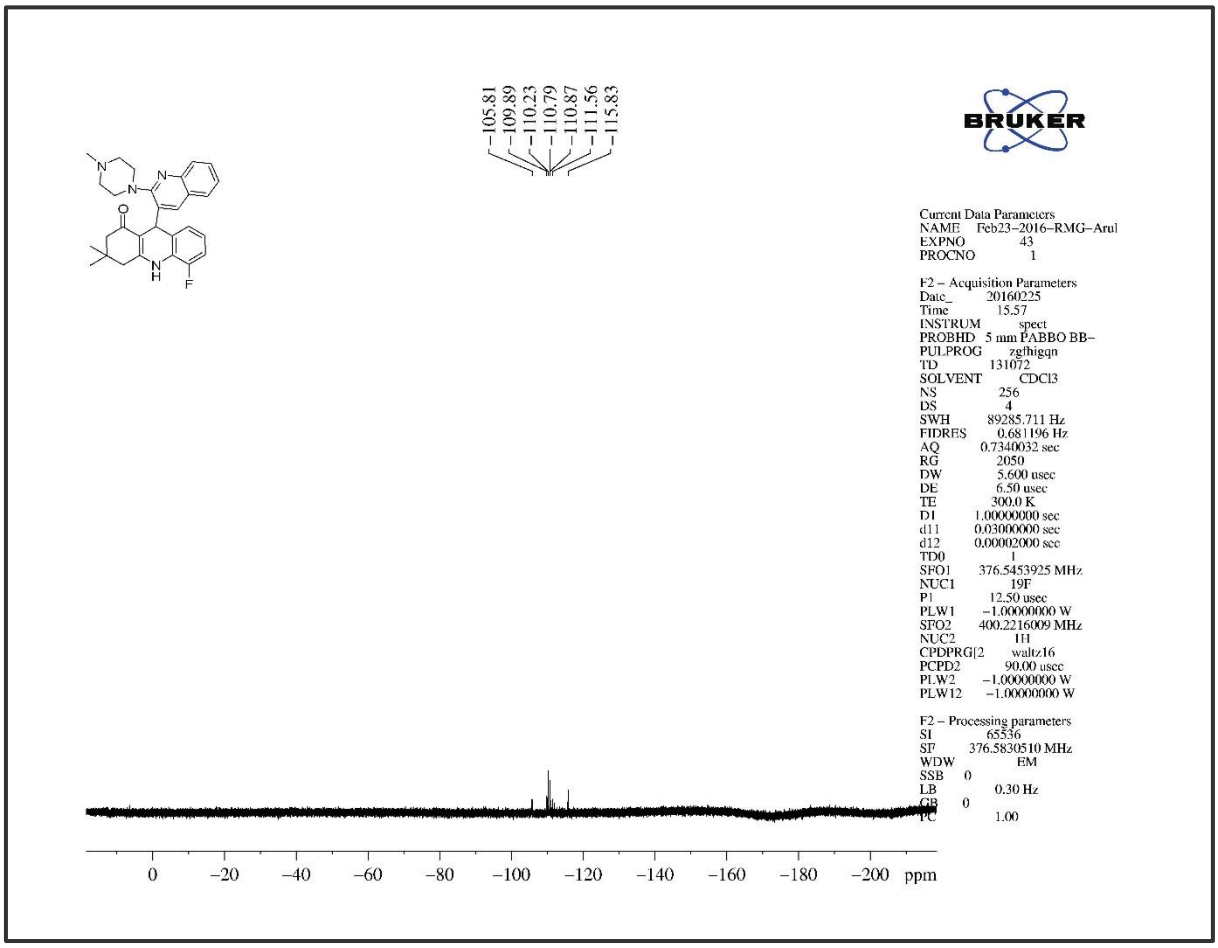

Figure 4A. S. 29. The ^{19}F NMR of compound 6e

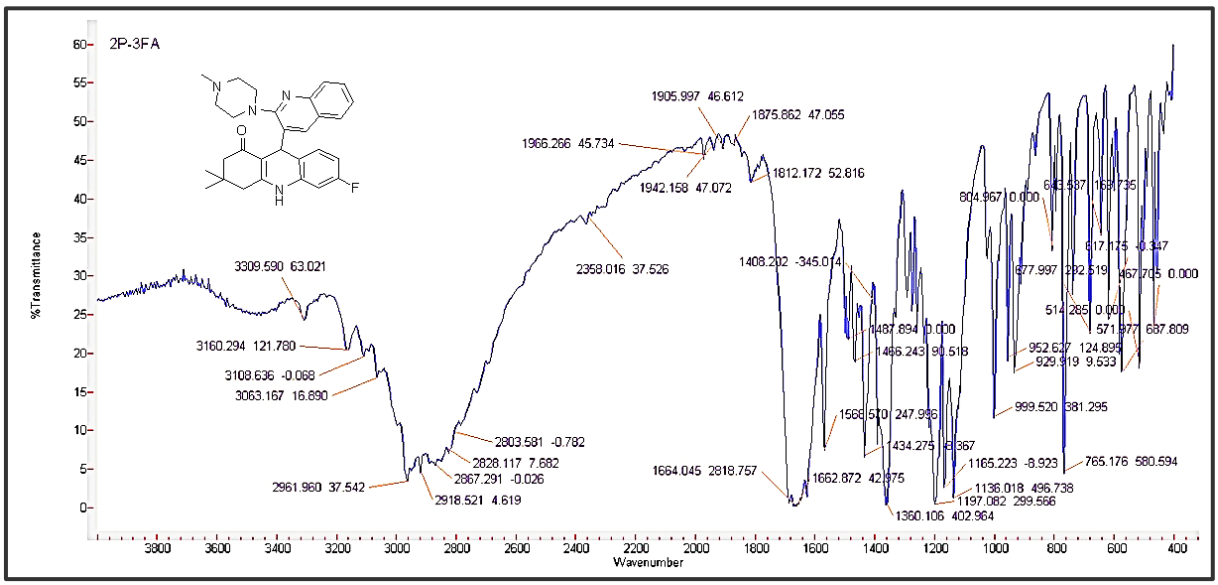

Figure 4A. S. 30. The Infra-Red Spectrum of compound 6f

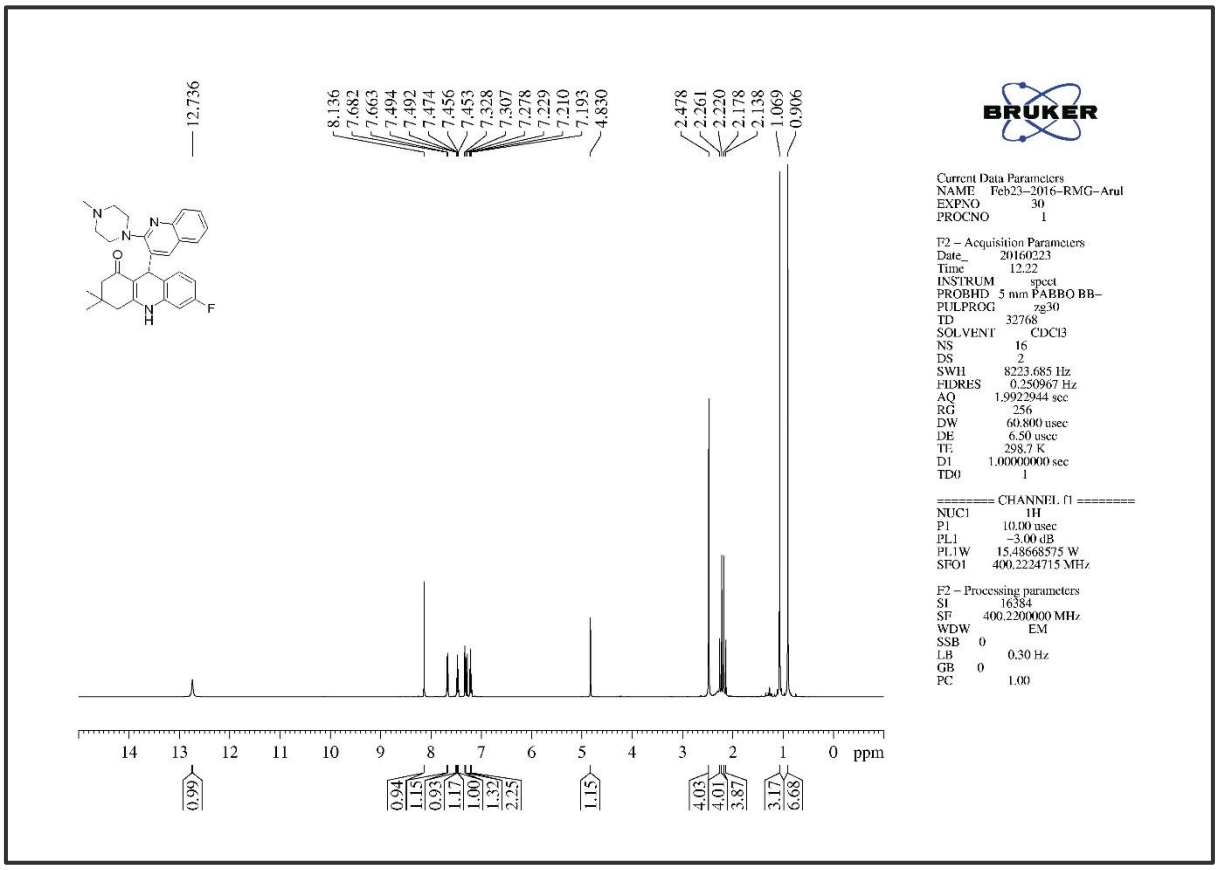

Figure 4A. S. 31. The ^{1}H NMR of compound 6f

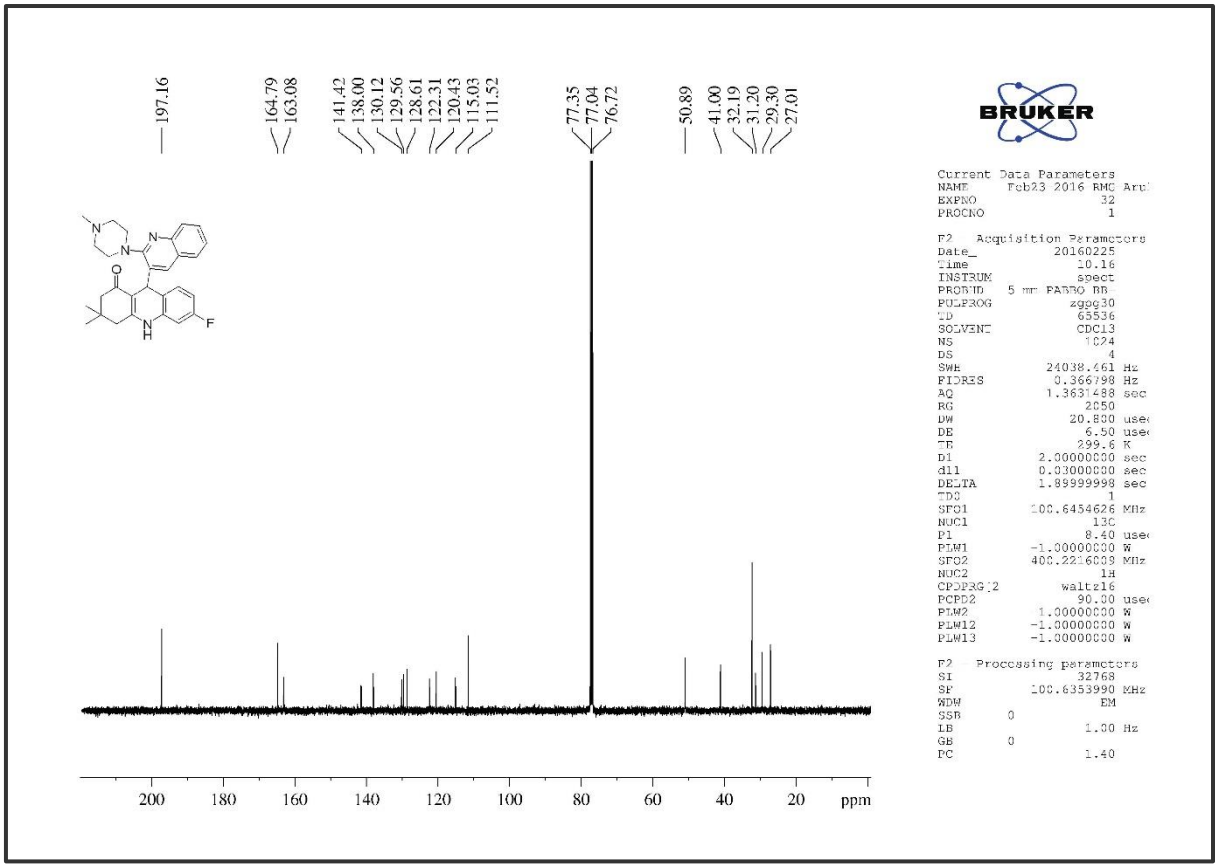

Figure 4A. S. 32. The ^{13}C NMR of compound 6f

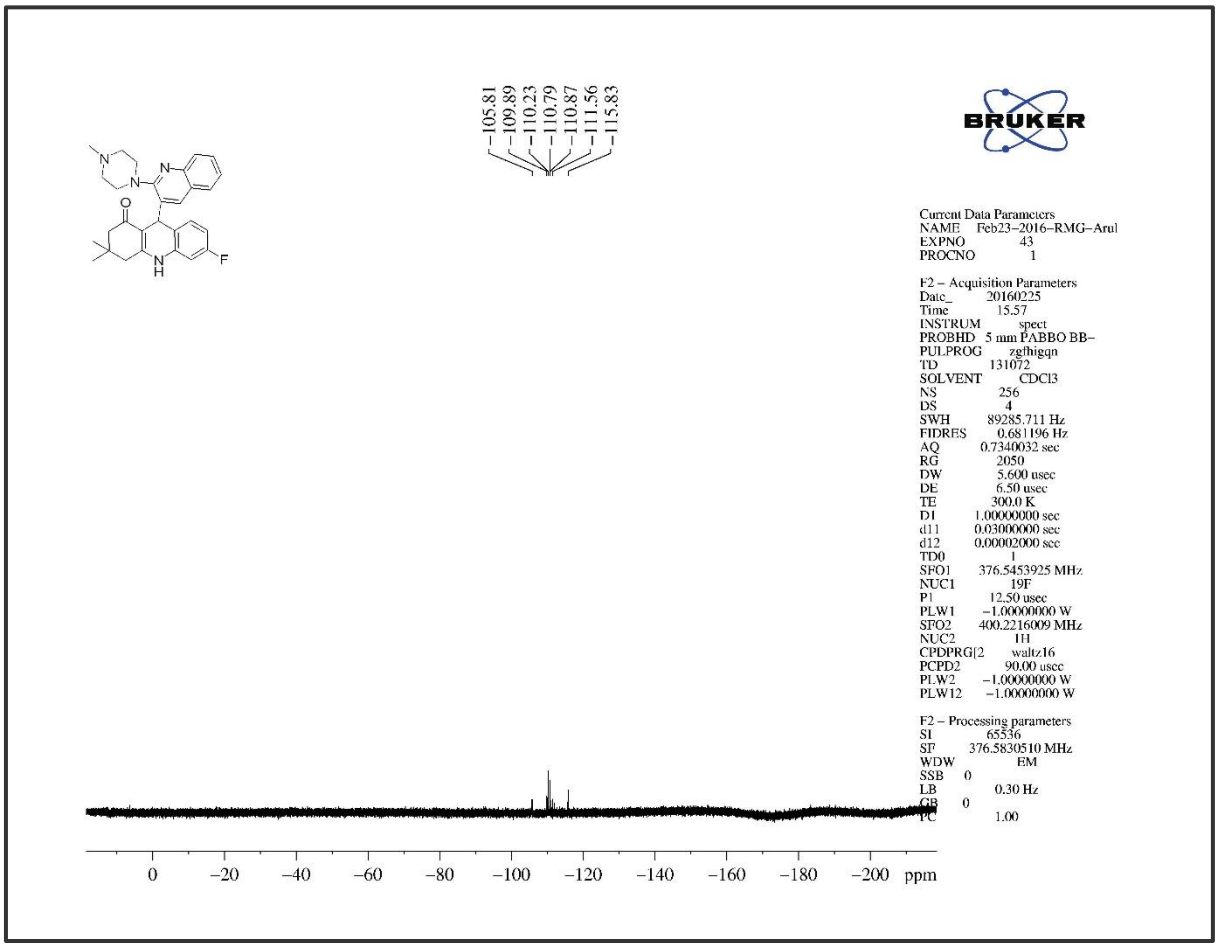

Figure 4A. S. 33. The ^{19}F NMR of compound 6f

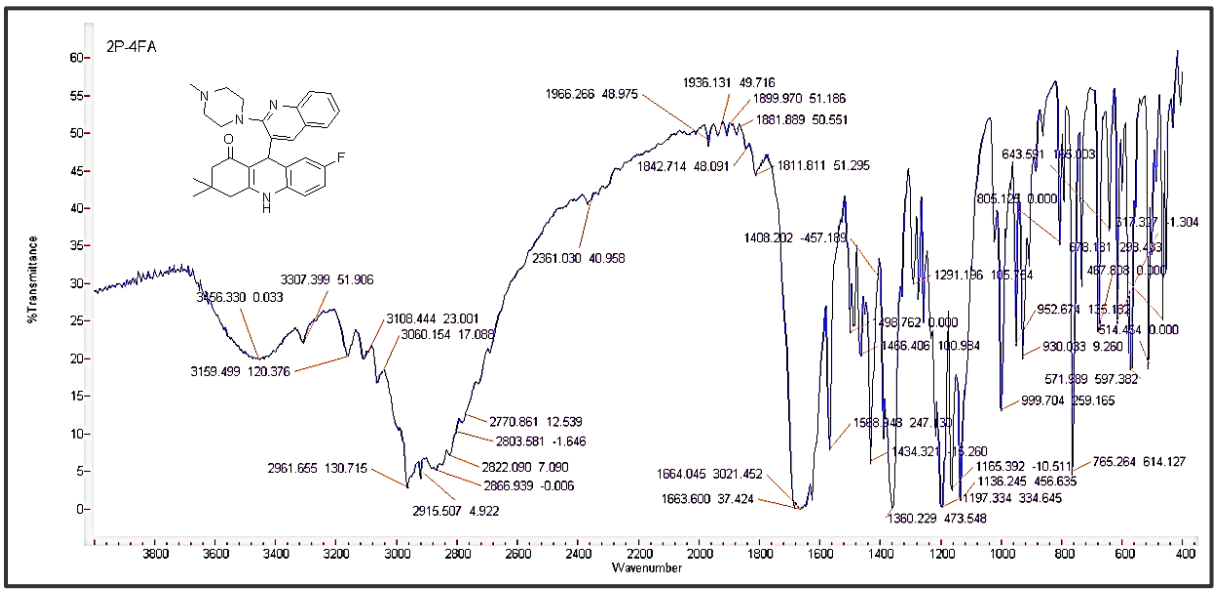

Figure 4A. S. 34. The Infra-Red Spectrum of compound 6g

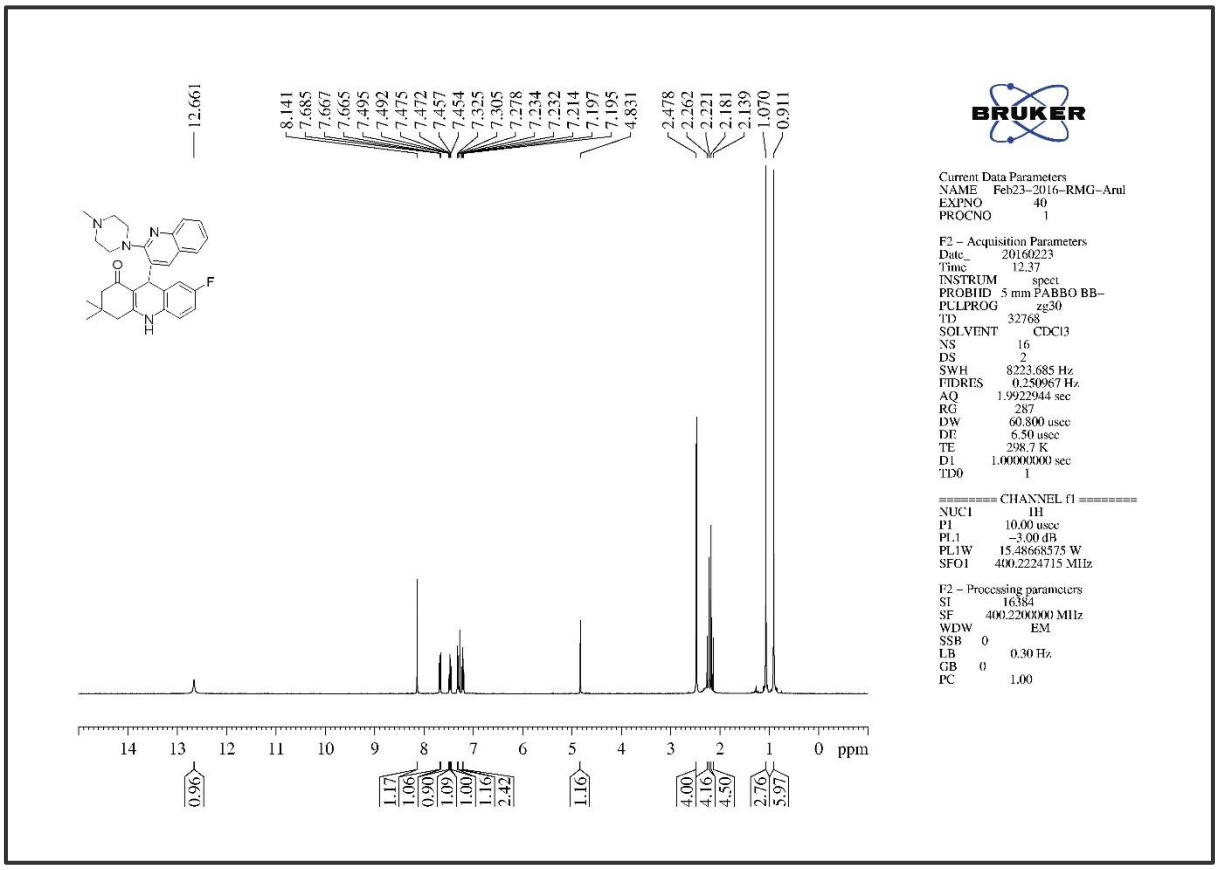

Figure 4A. S. 35. The ^{1}H NMR of compound 6g

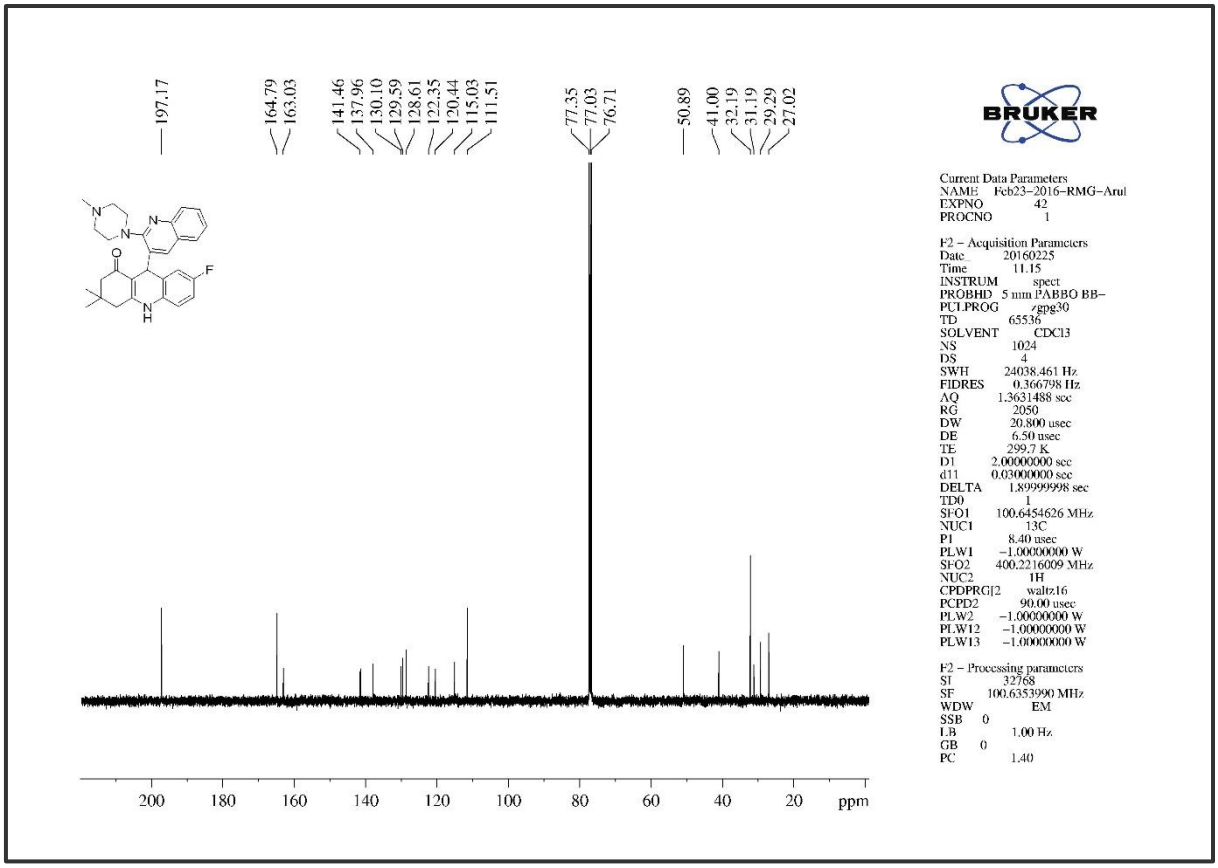

Figure 4A. S. 36. The ^{13}C NMR of compound 6g

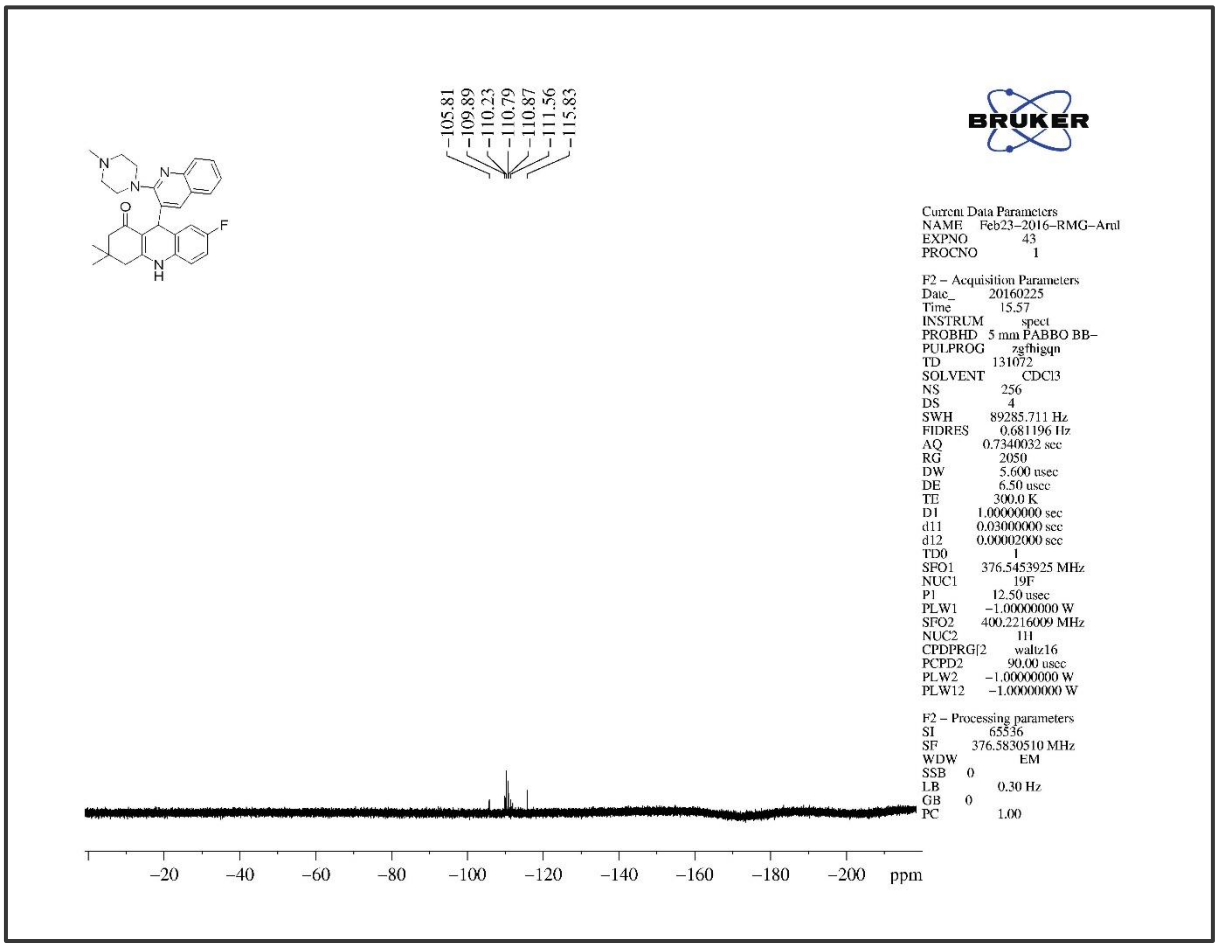

Figure 4A. S. 37. The ^{19}F NMR of compound 6g

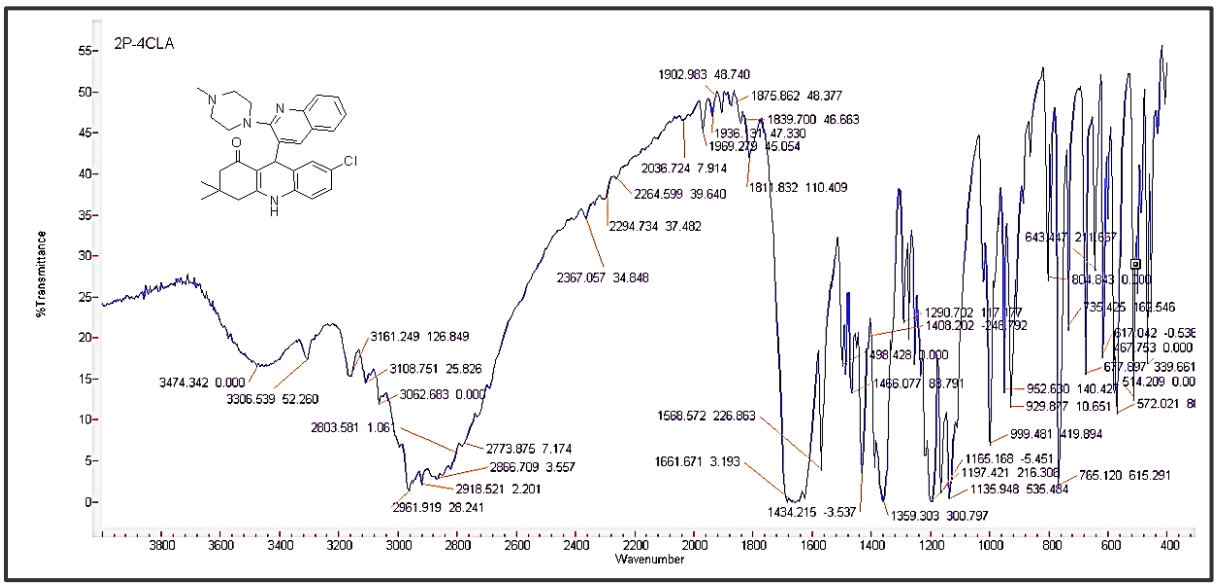

Figure 4A. S. 38. The Infra-Red Spectrum of compound 6h

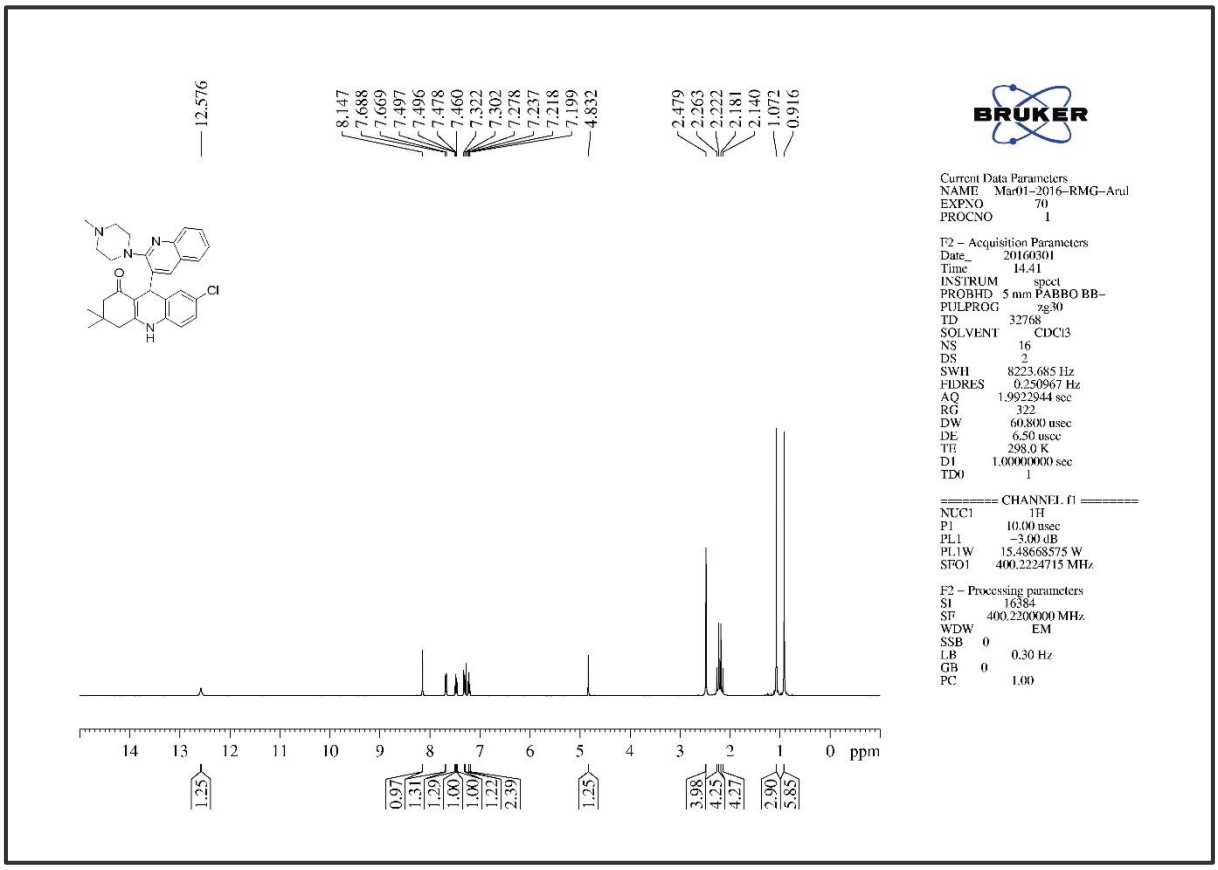

Figure 4A. S. 39. The ^{1}H NMR of compound 6h

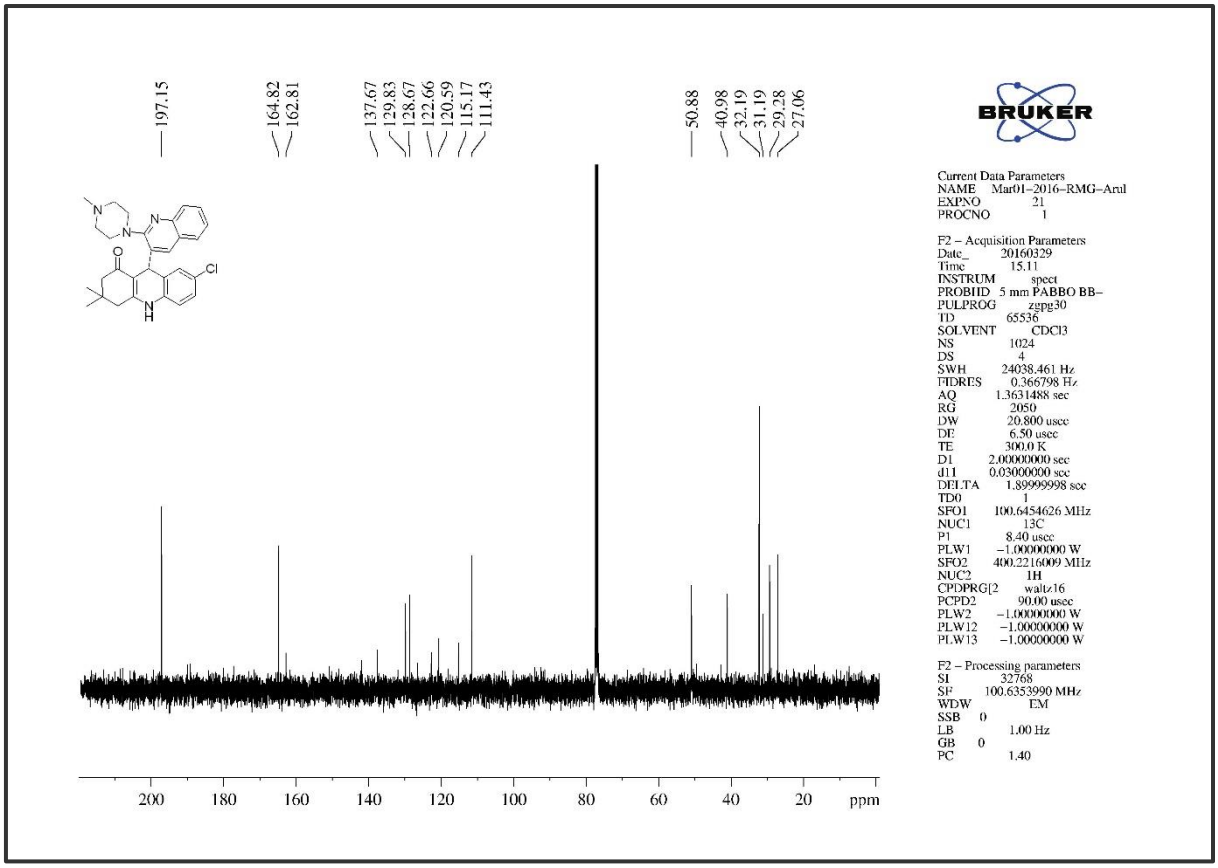

Figure 4A. S. 40. The ^{13}C NMR of compound 6h

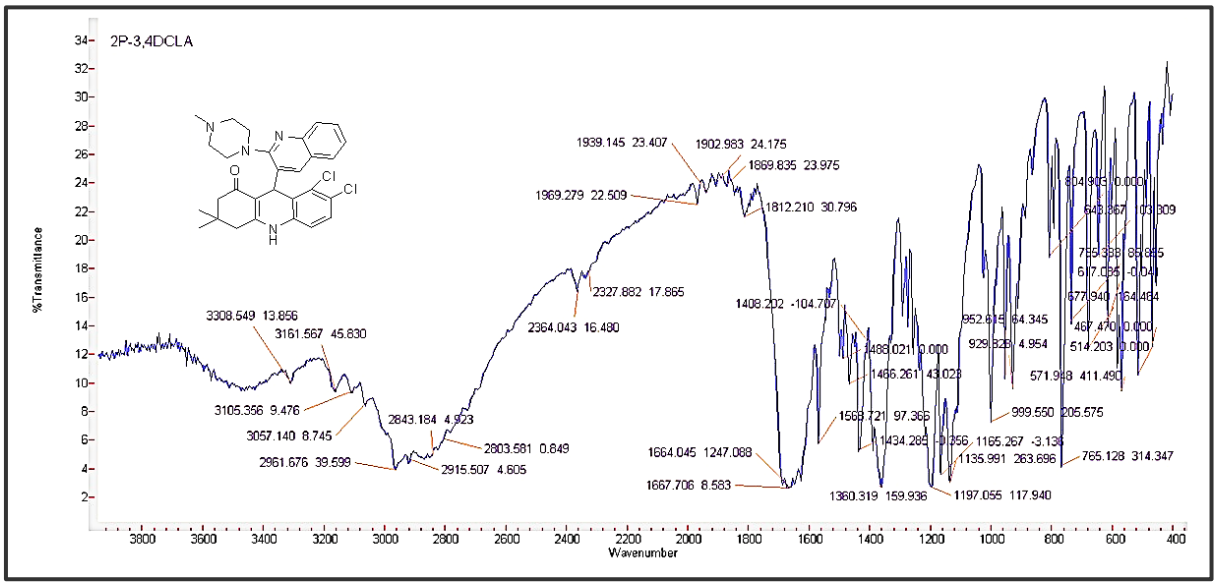

Figure 4A. S. 41. The Infra-Red Spectrum of compound 6i

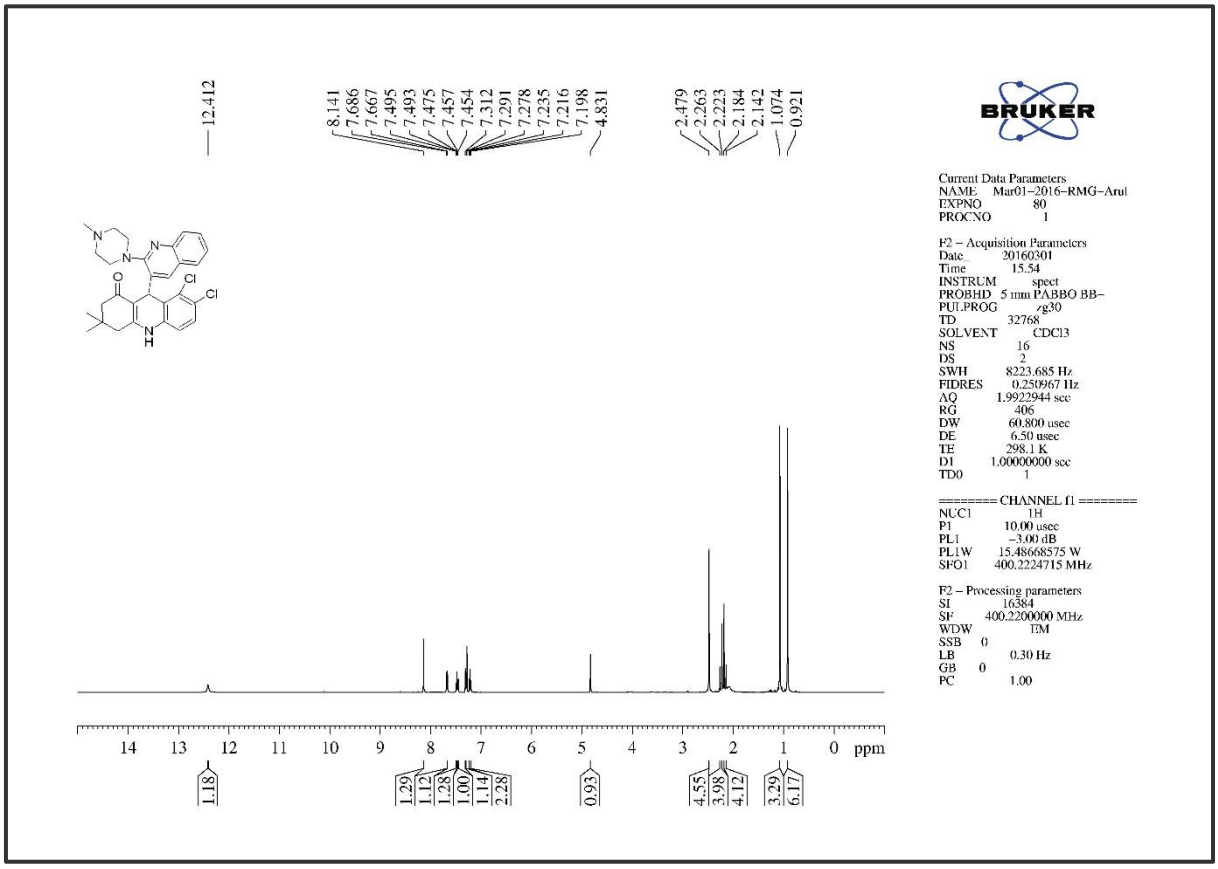

Figure 4A. S. 42. The ^{1}H NMR of compound 6i

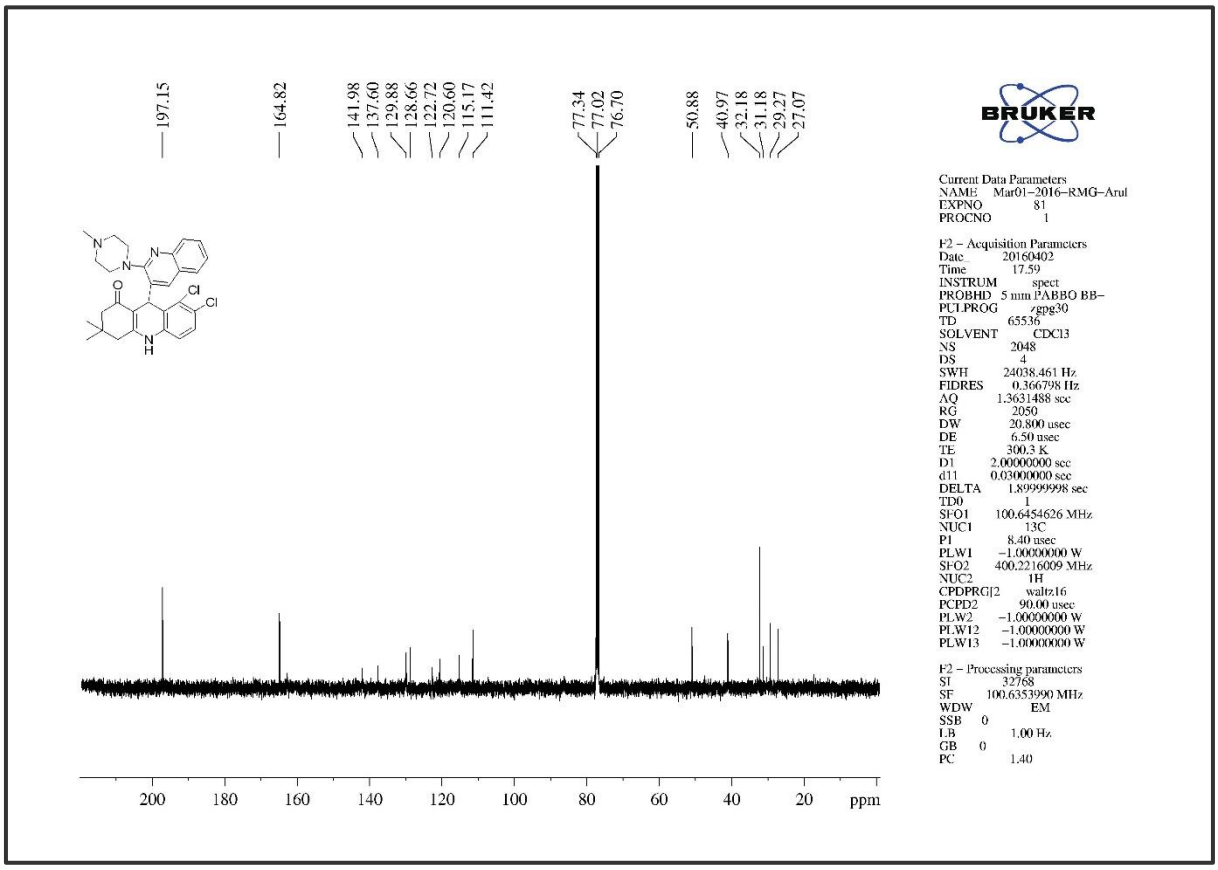

Figure 4A. S. 43. The ^{13}C NMR of compound 6i

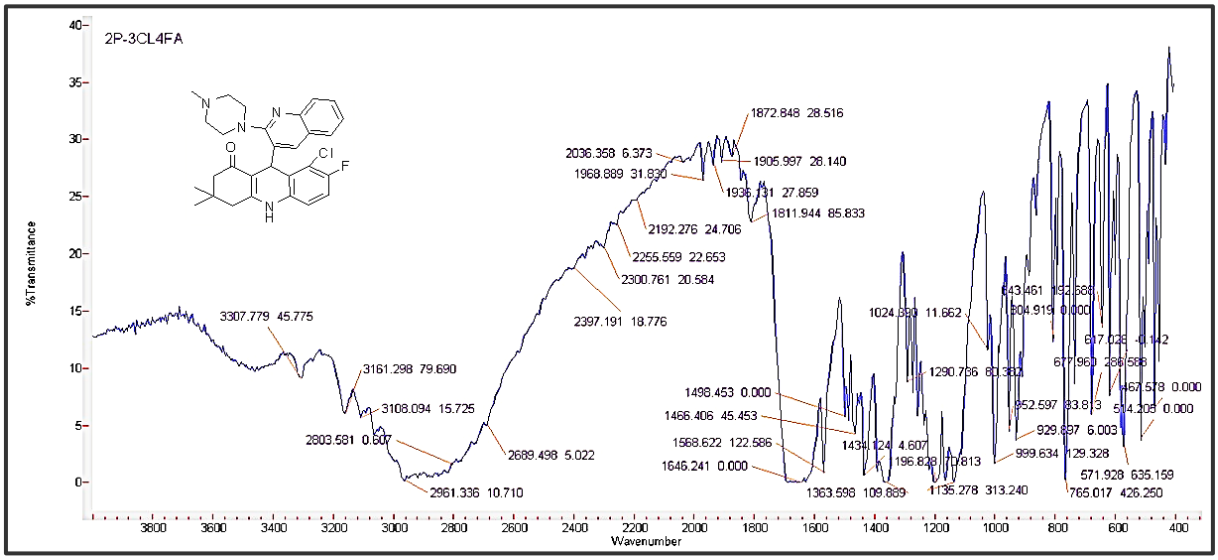

Figure 4A. S. 44. The Infra-Red Spectrum of compound 6j

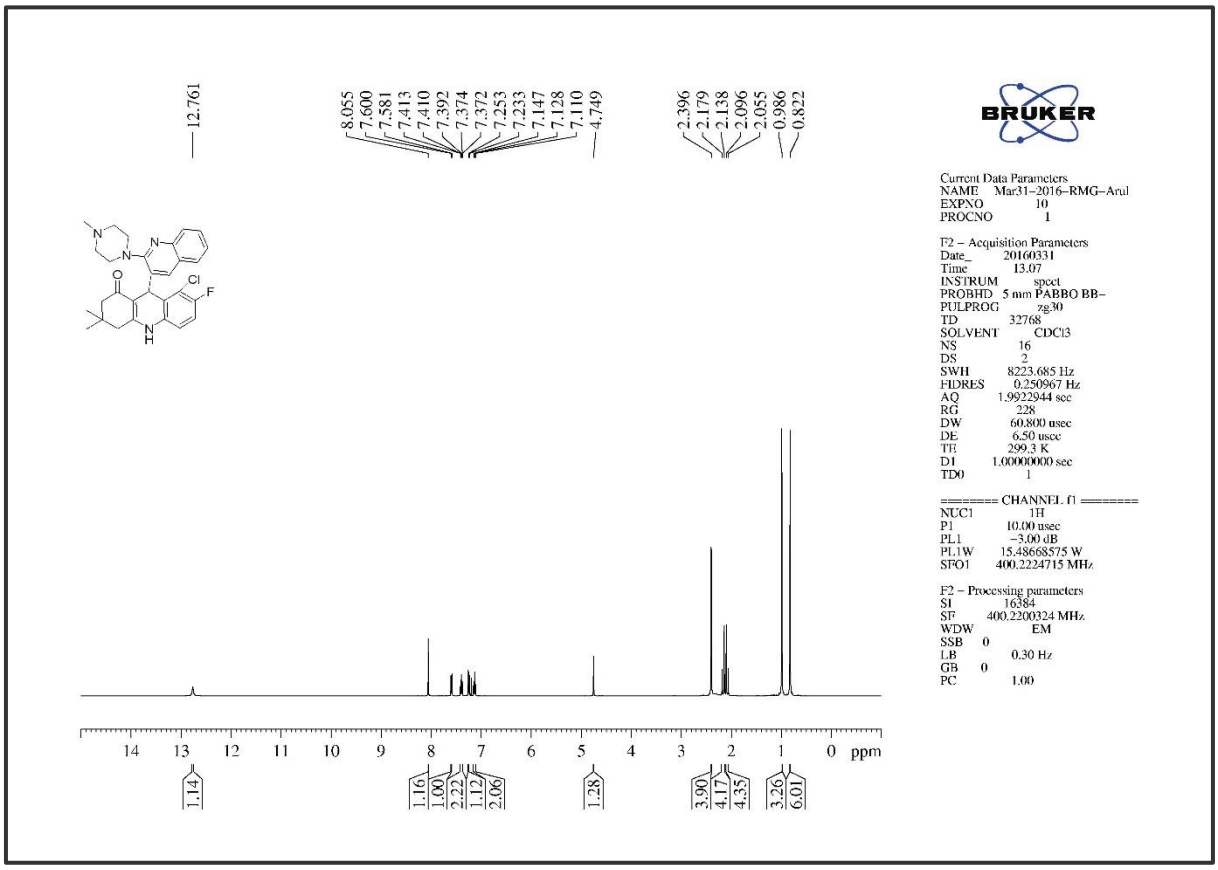

Figure 4A. S. 45. The ^{1}H NMR of compound 6j

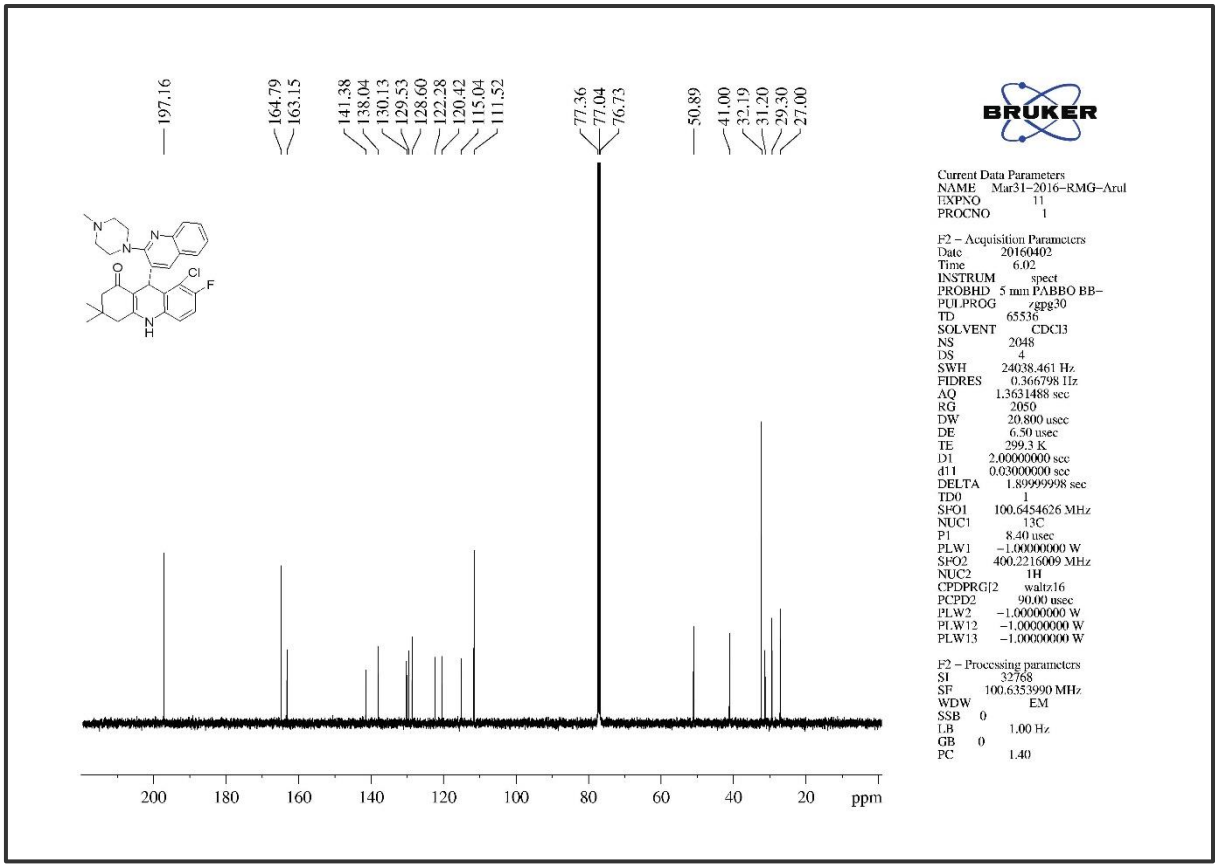

Figure 4A. S. 46. The ^{13}C NMR of compound 6j

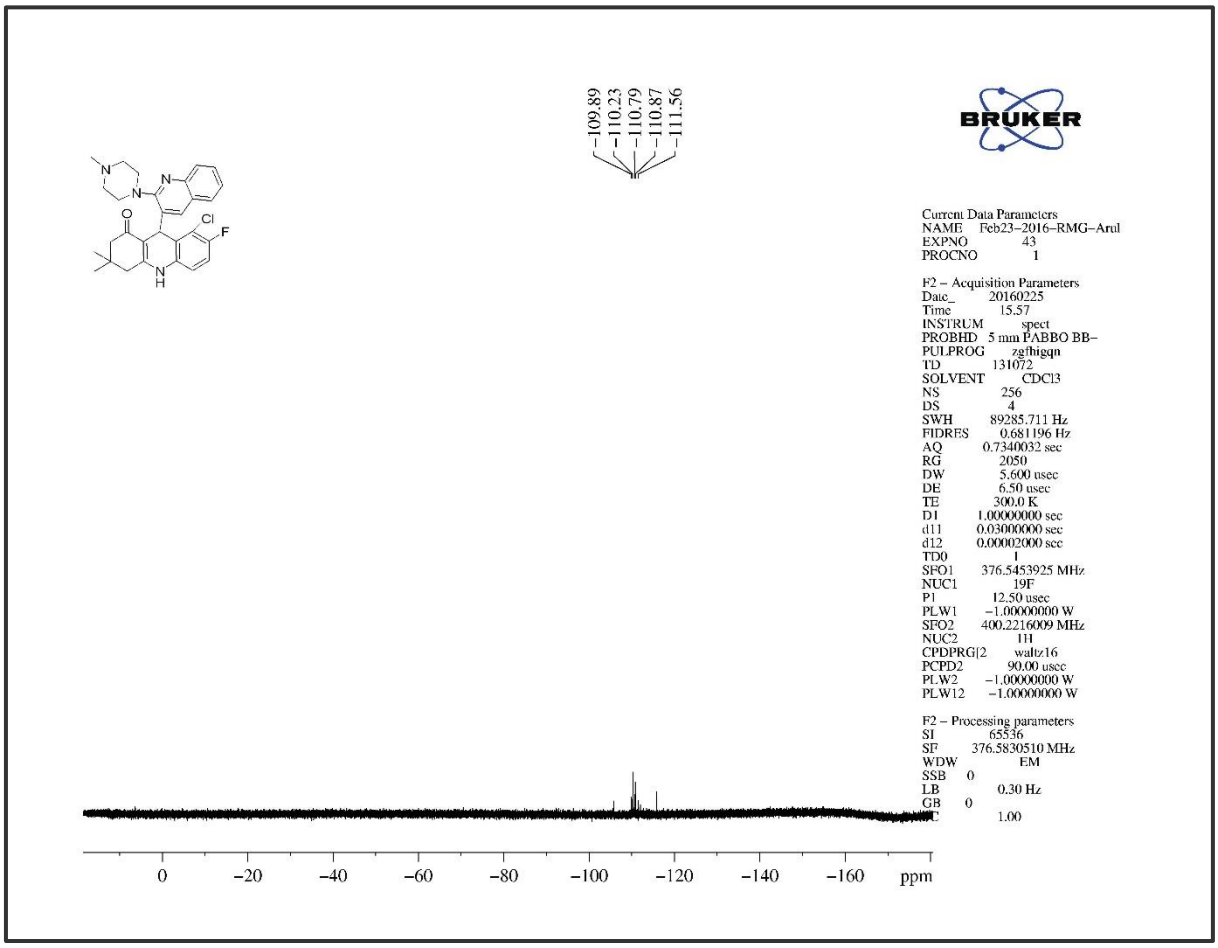

Figure 4A. S. 47. The ^{19}F NMR of compound 6j

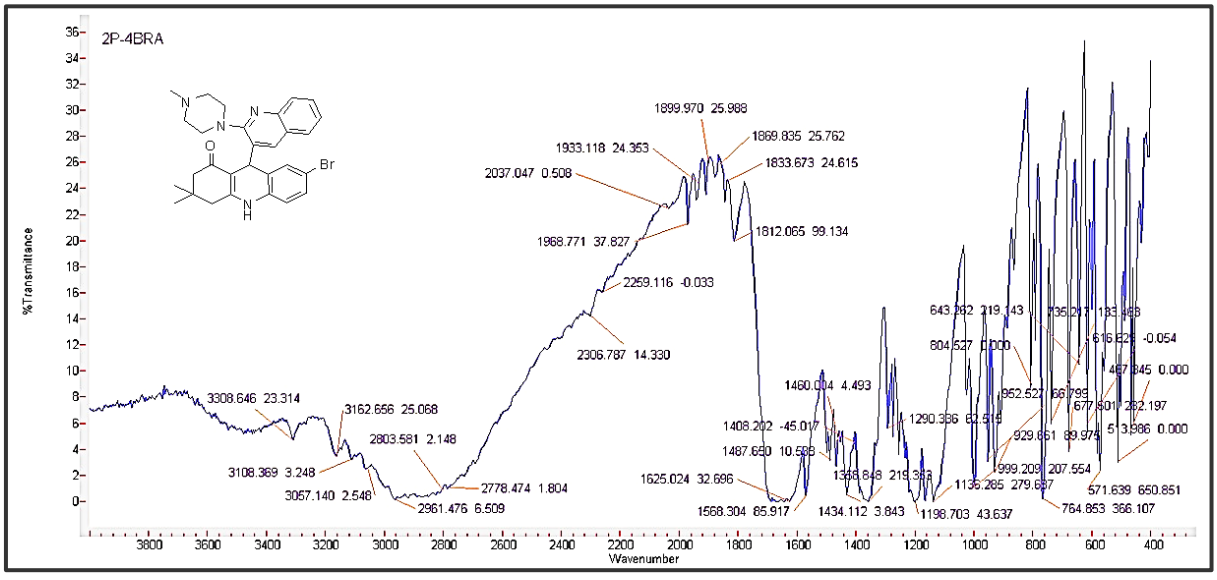

Figure 4A. S. 48. The Infra-Red Spectrum of compound 6k

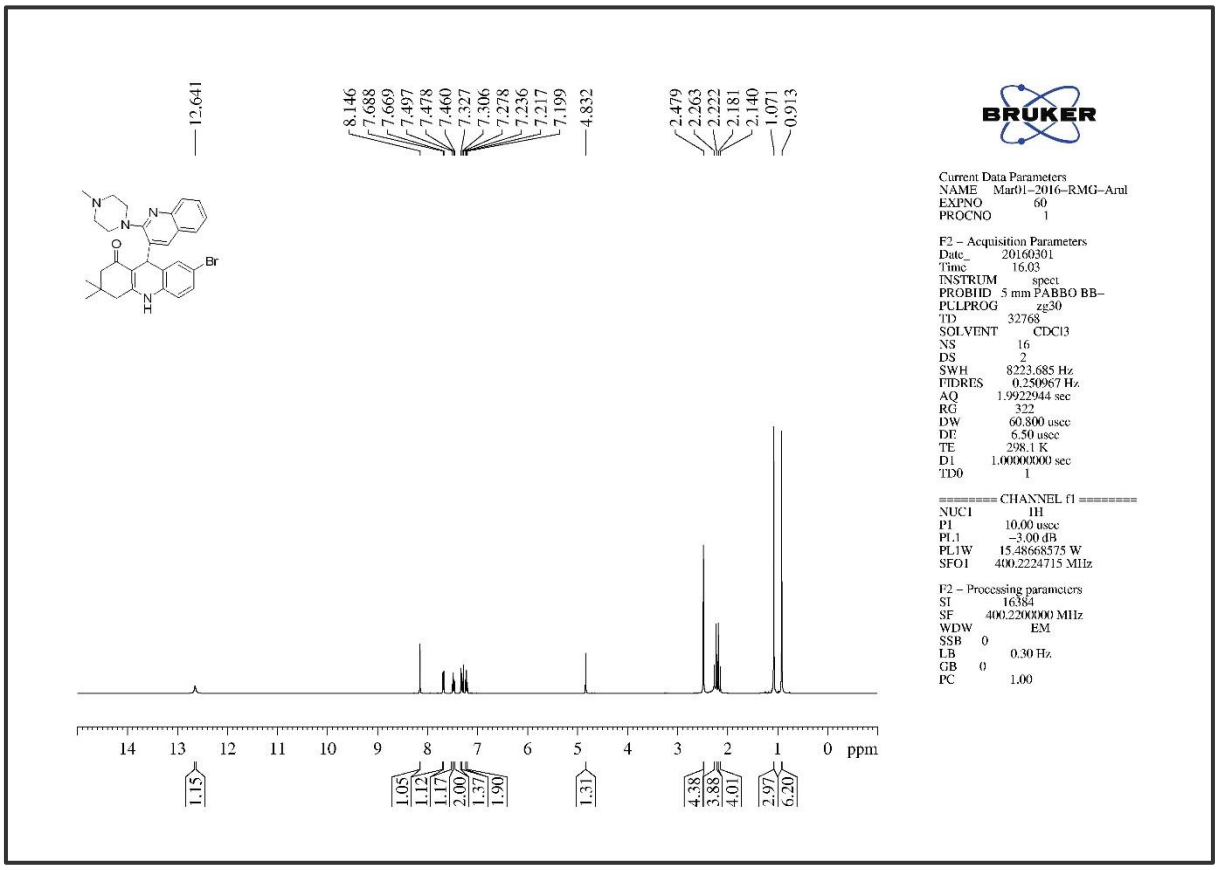

Figure 4A. S. 49. The ^{1}H NMR of compound 6k

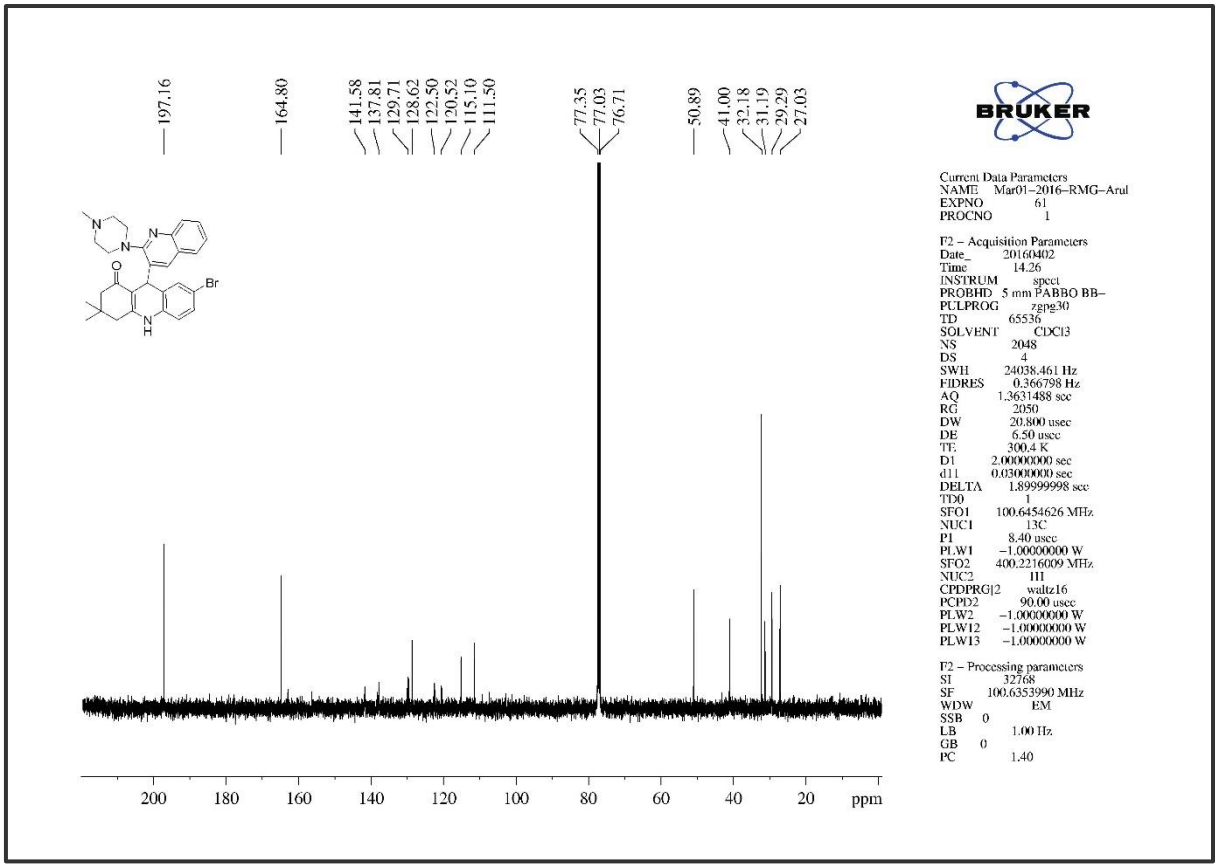

Figure 4A. S. 50. The ^{13}C NMR of compound 6k

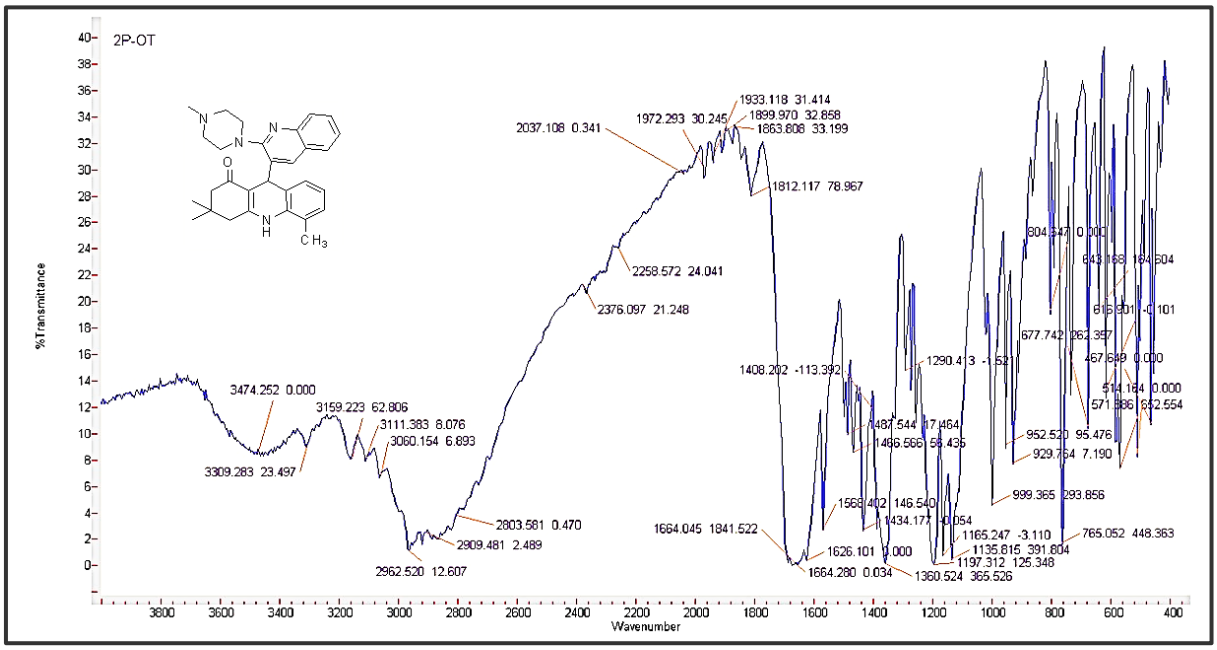

Figure 4A. S. 51. The Infra-Red Spectrum of compound 6l

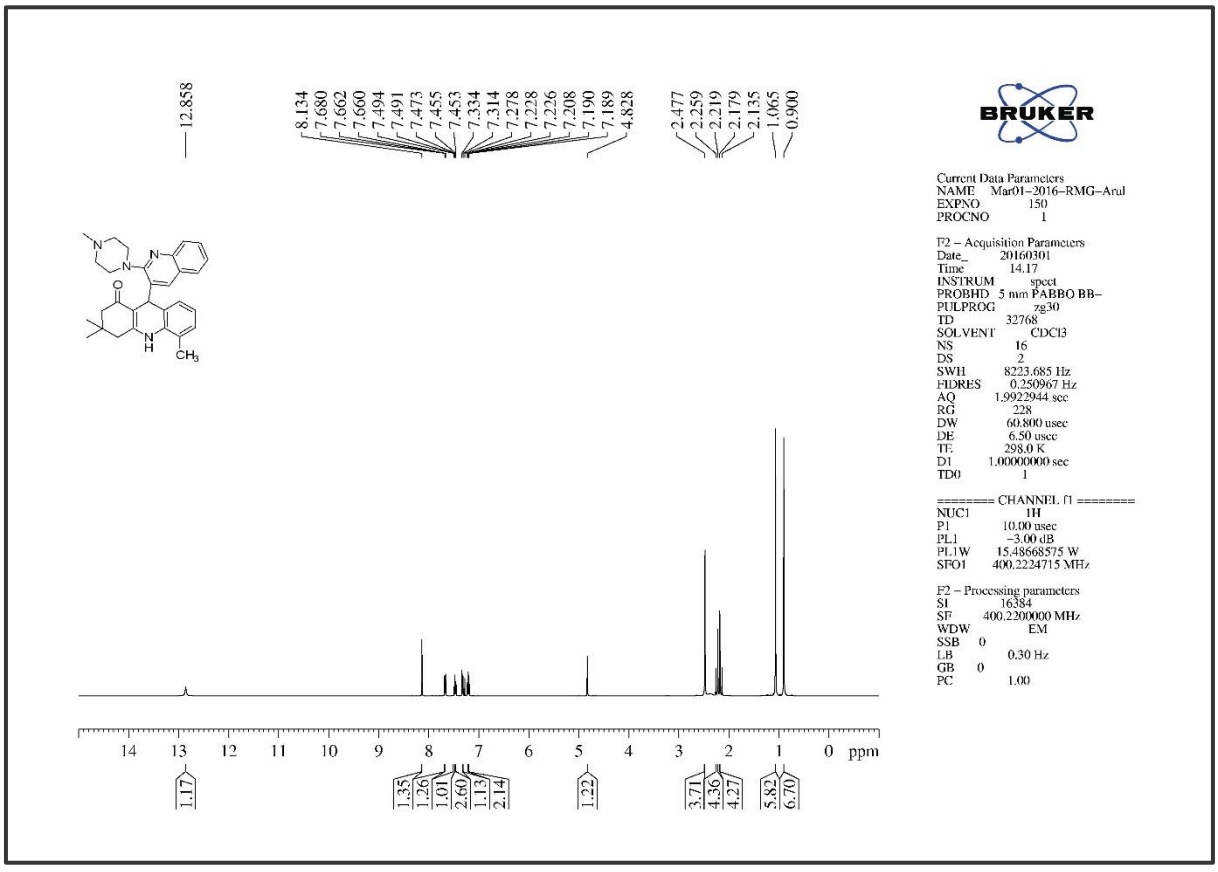

Figure 4A. S. 52. The ^{1}H NMR of compound 6l

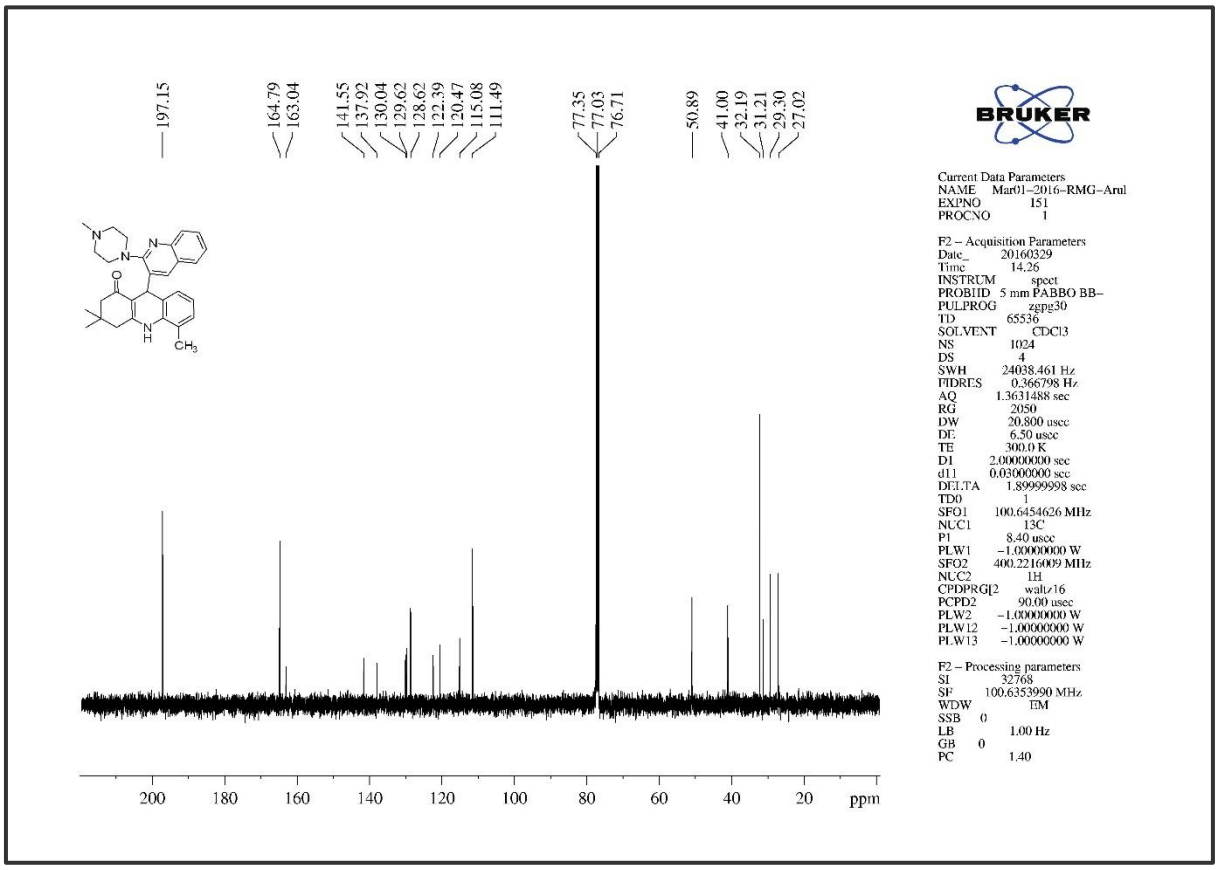

Figure 4A. S. 53. The ^{13}C NMR of compound 6l

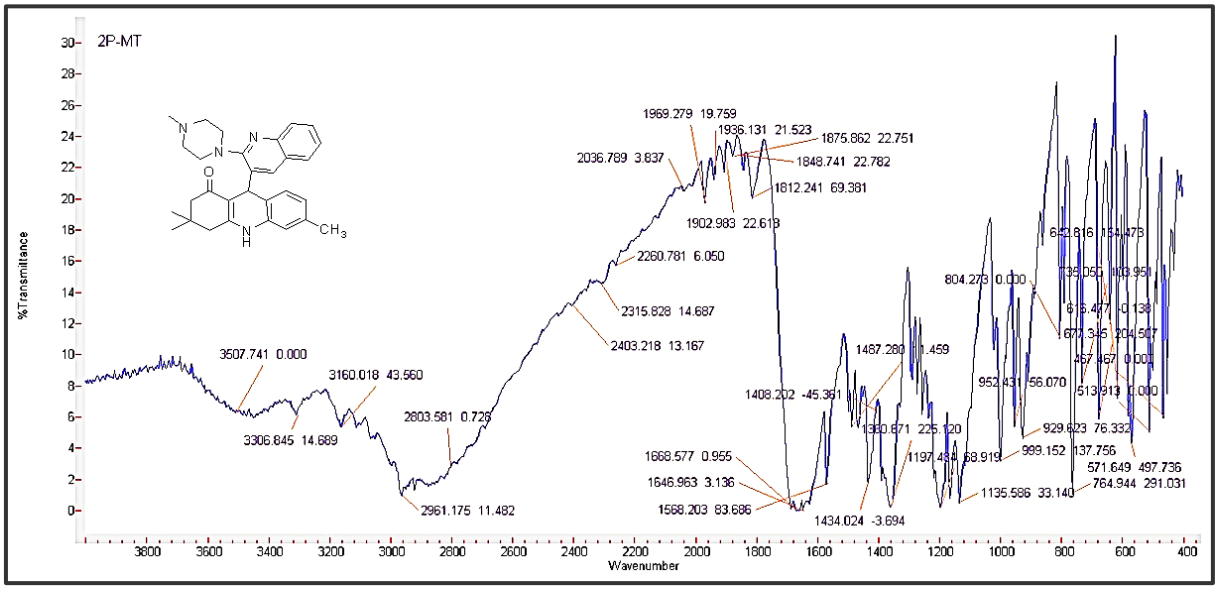

Figure 4A. S. 54. The Infra-Red Spectrum of compound 6m

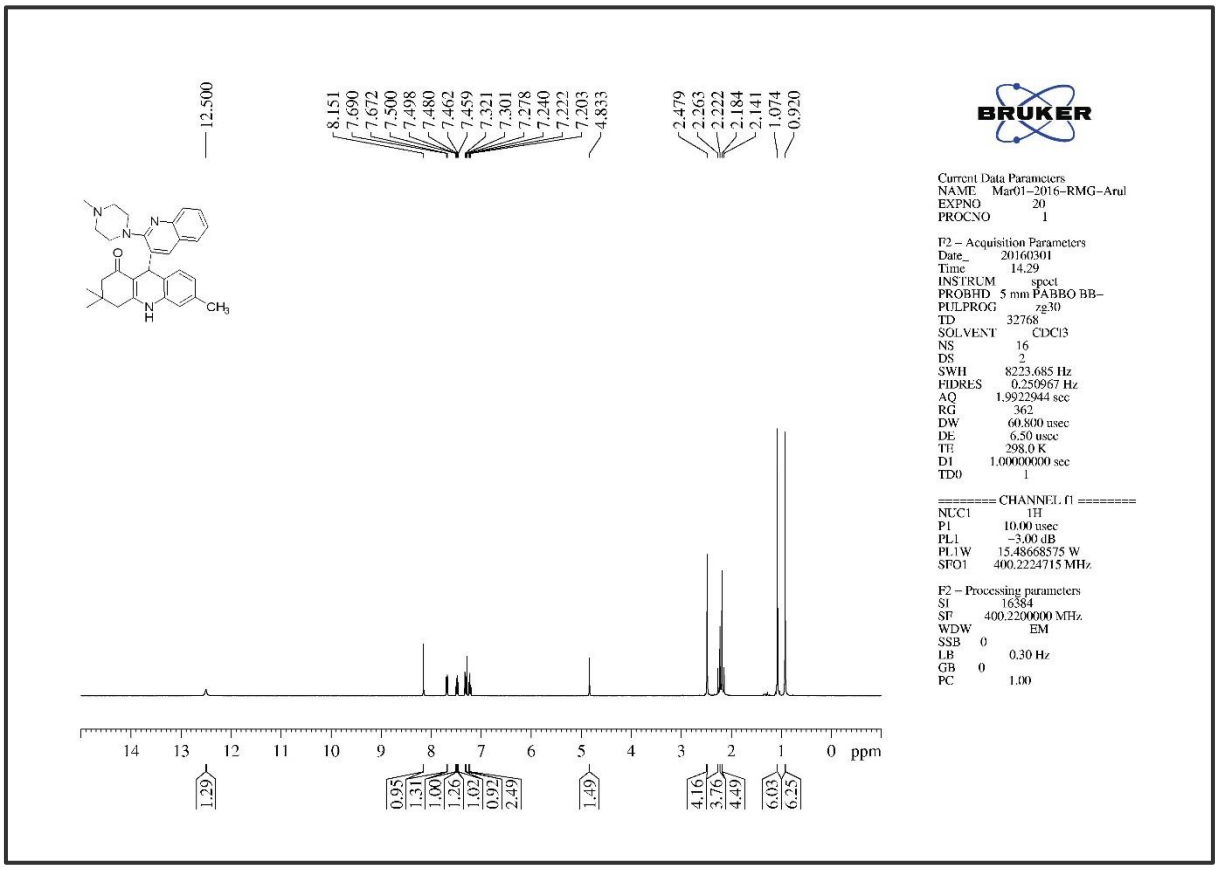

Figure 4A. S. 55. The ^{1}H NMR of compound 6m

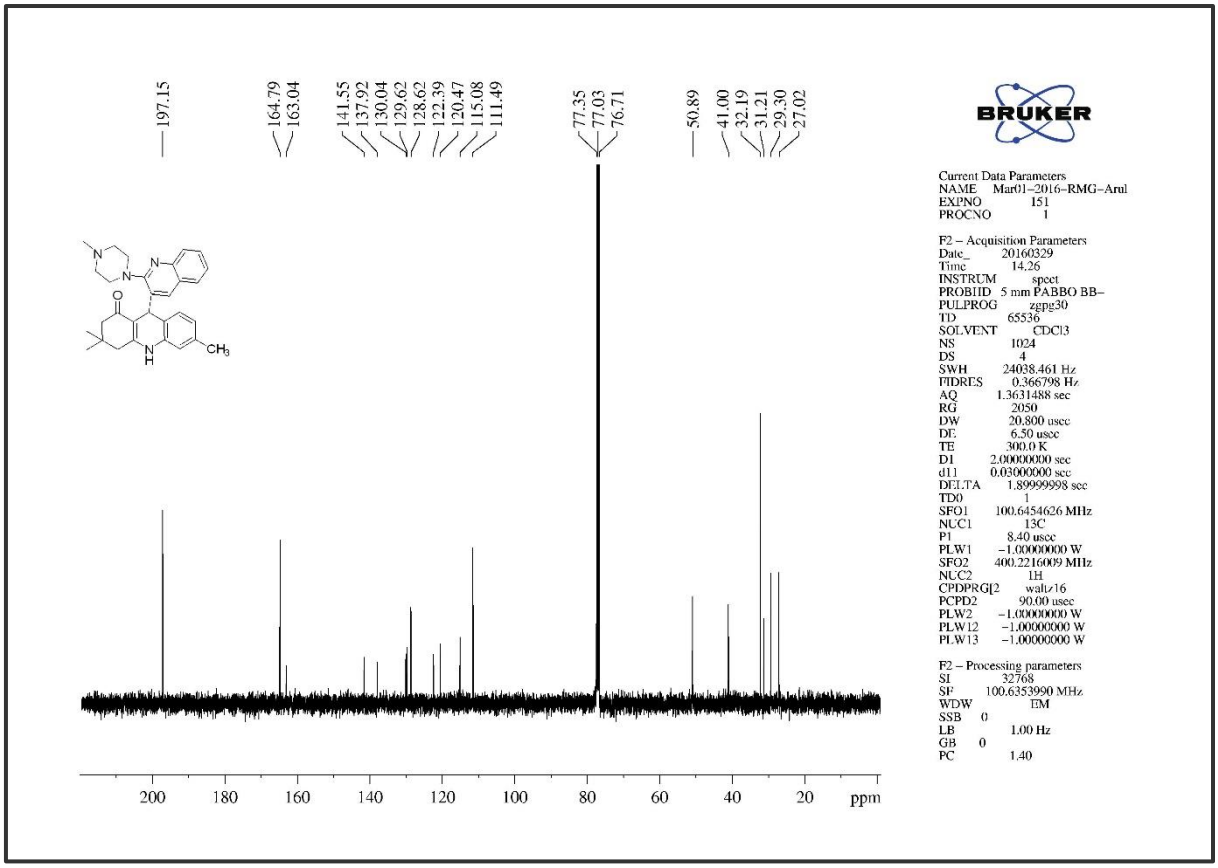

Figure 4A. S. 56. The ^{13}C NMR of compound 6m

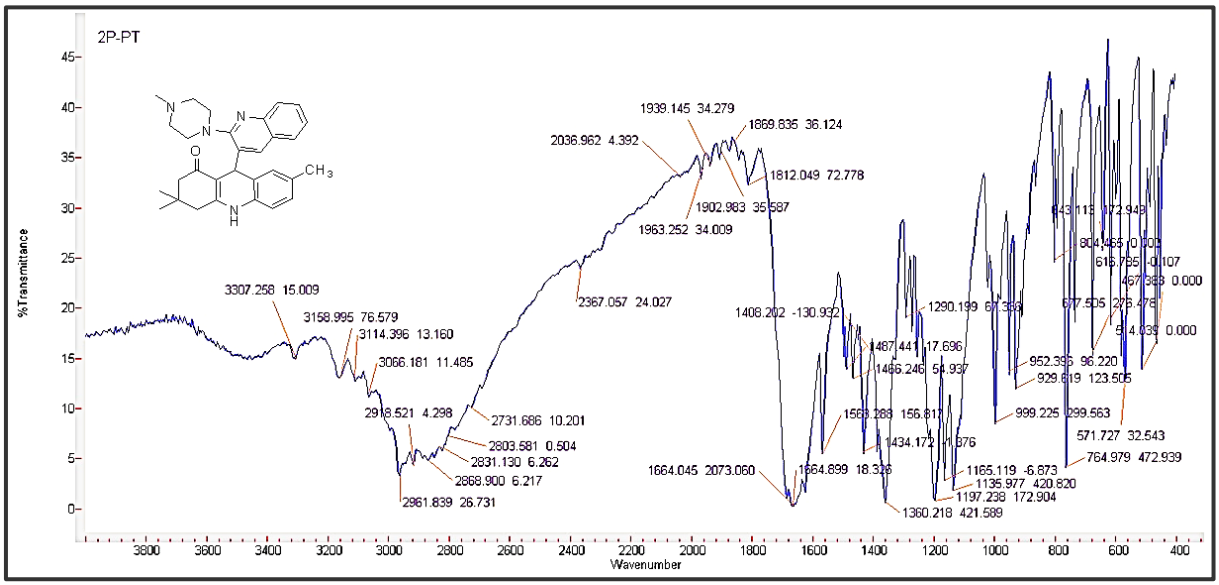

Figure 4A. S. 57. The Infra-Red Spectrum of compound 6n

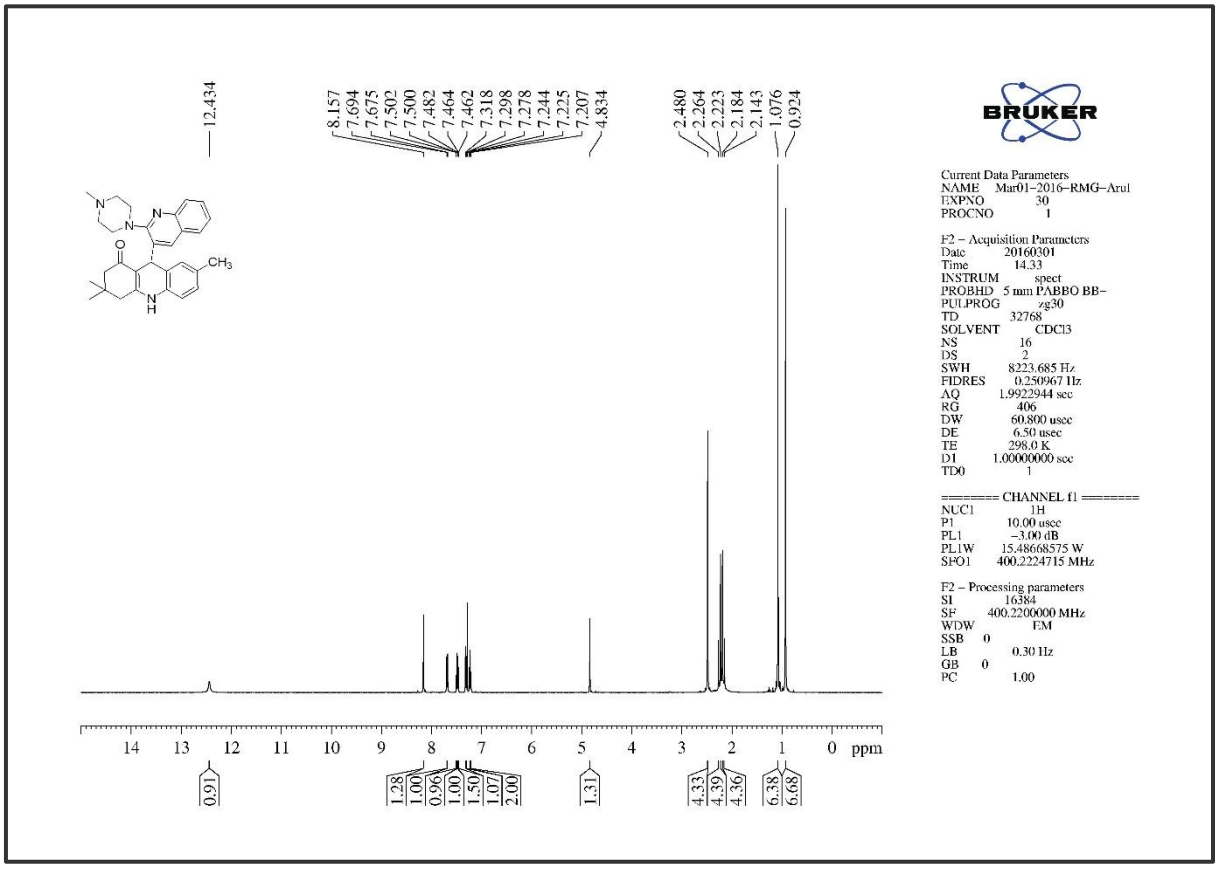

Figure 4A. S. 58. The ^{1}H NMR of compound 6n

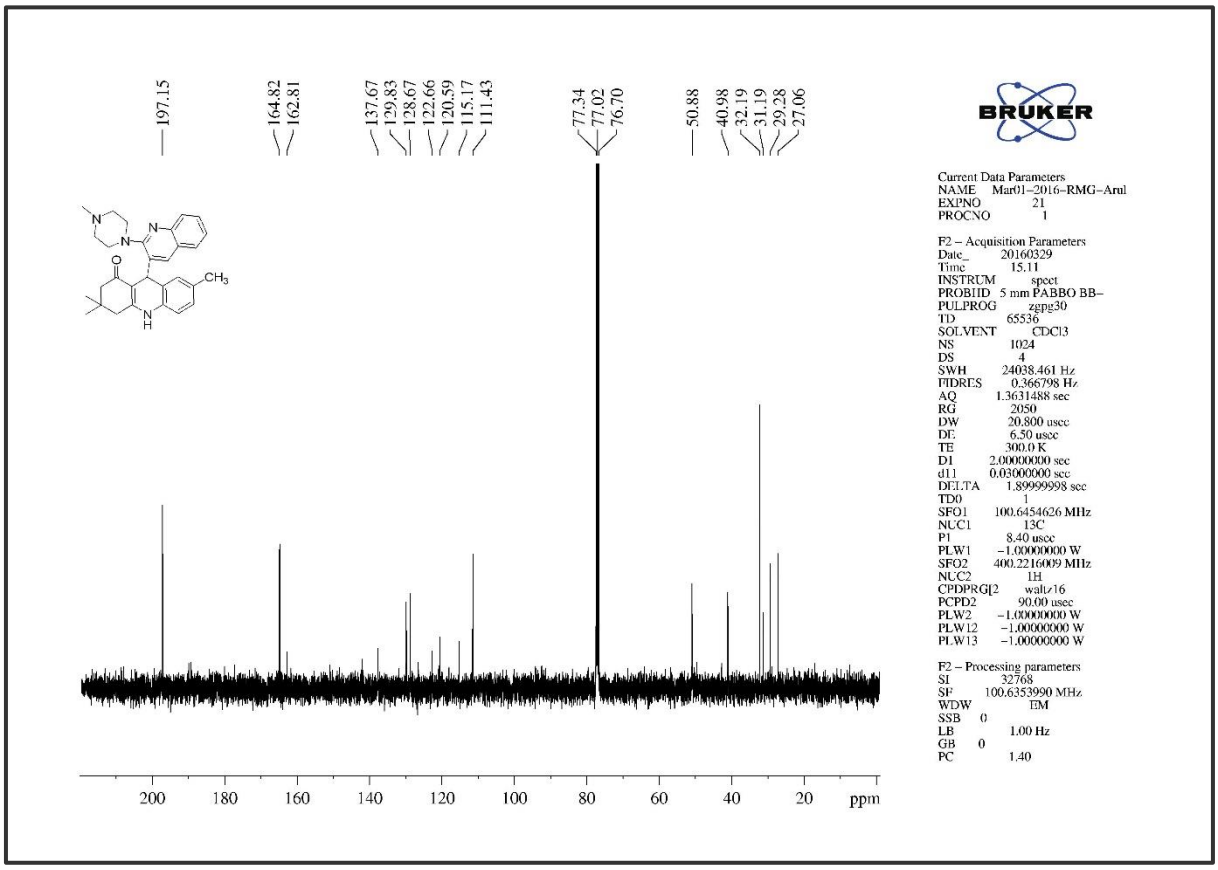

Figure 4A. S. 59. The ^{13}C NMR of compound 6n

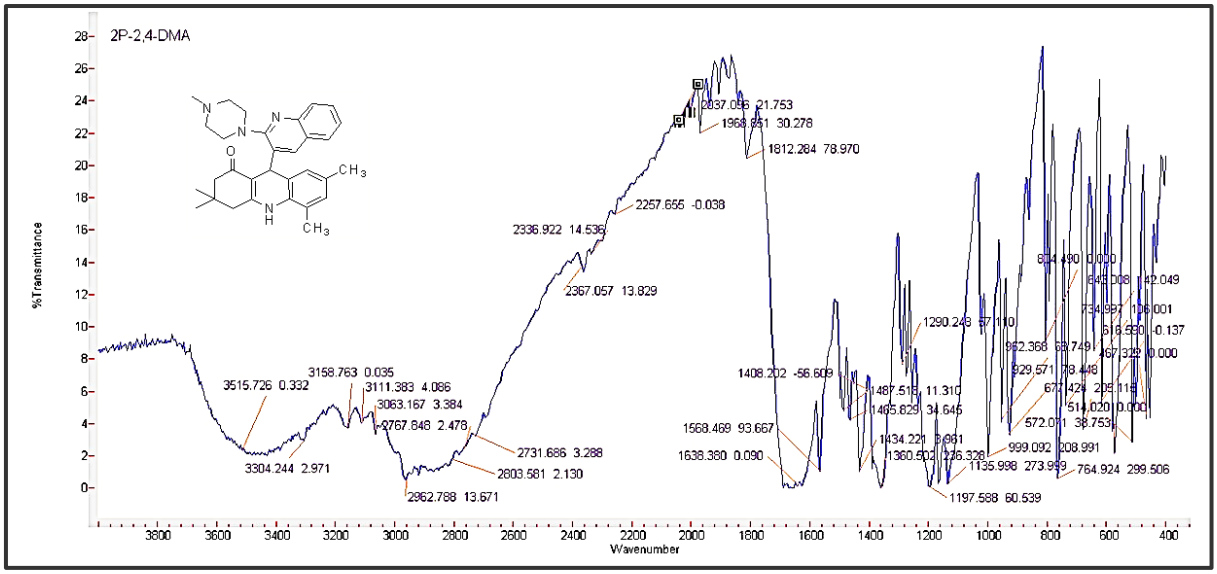

Figure 4A. S. 60. The Infra-Red Spectrum of compound 6o

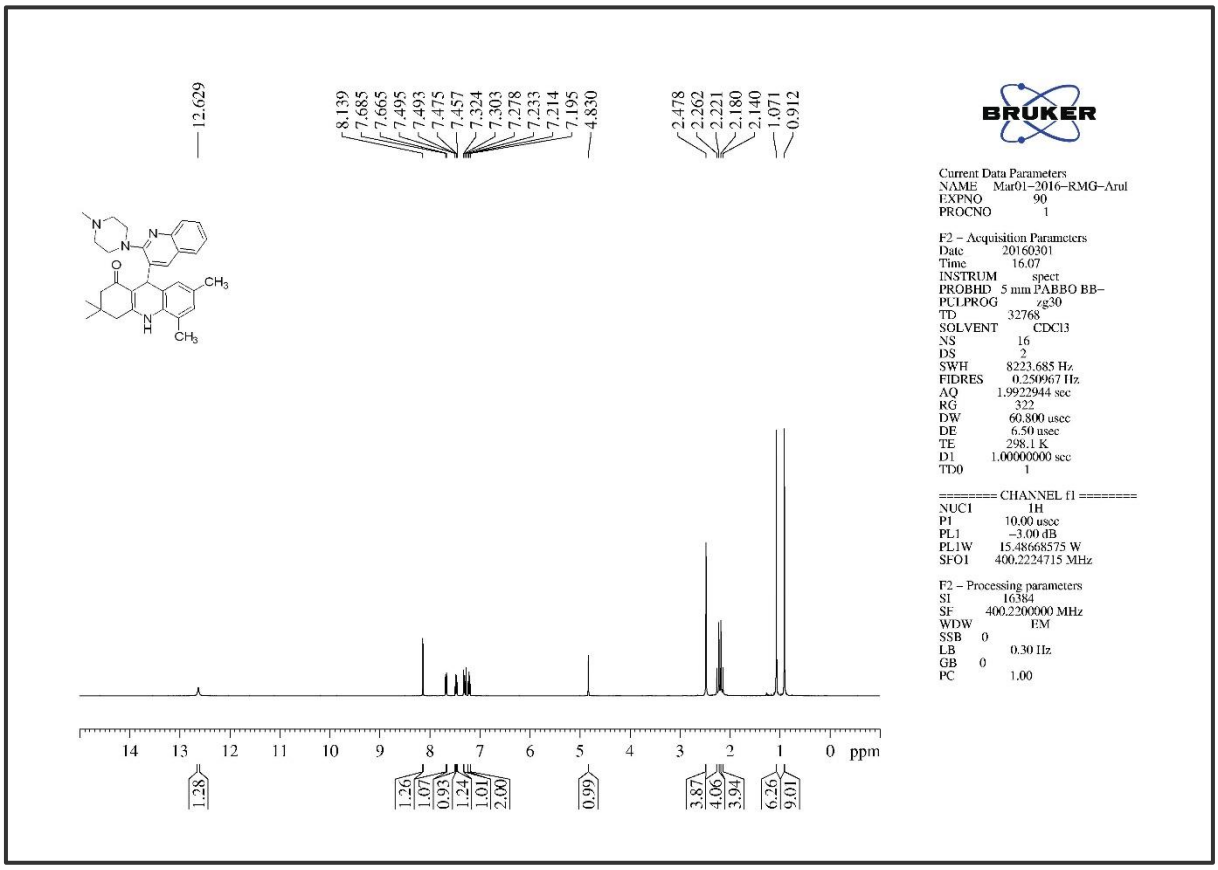

Figure 4A. S. 61. The ^{1}H NMR of compound 6o

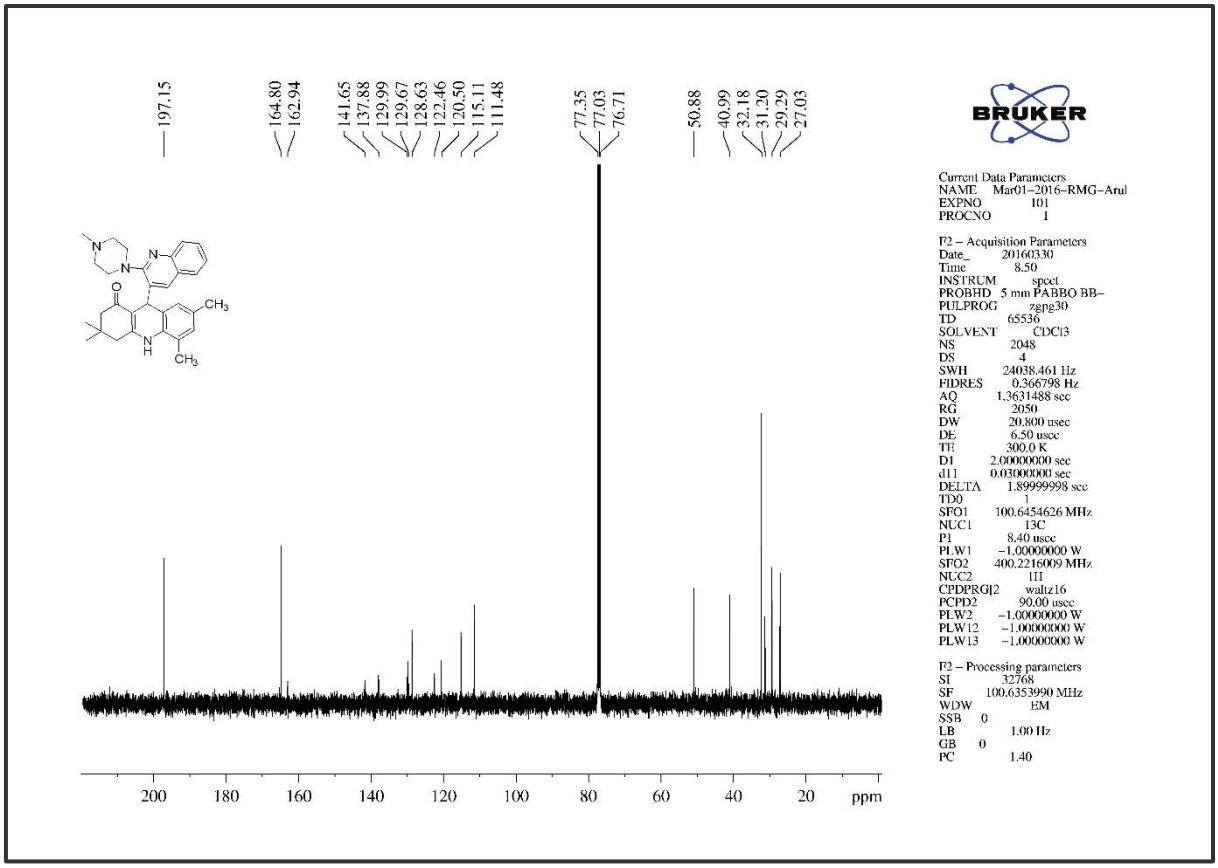

Figure 4A. S. 62. The ^{13}C NMR of compound 6o

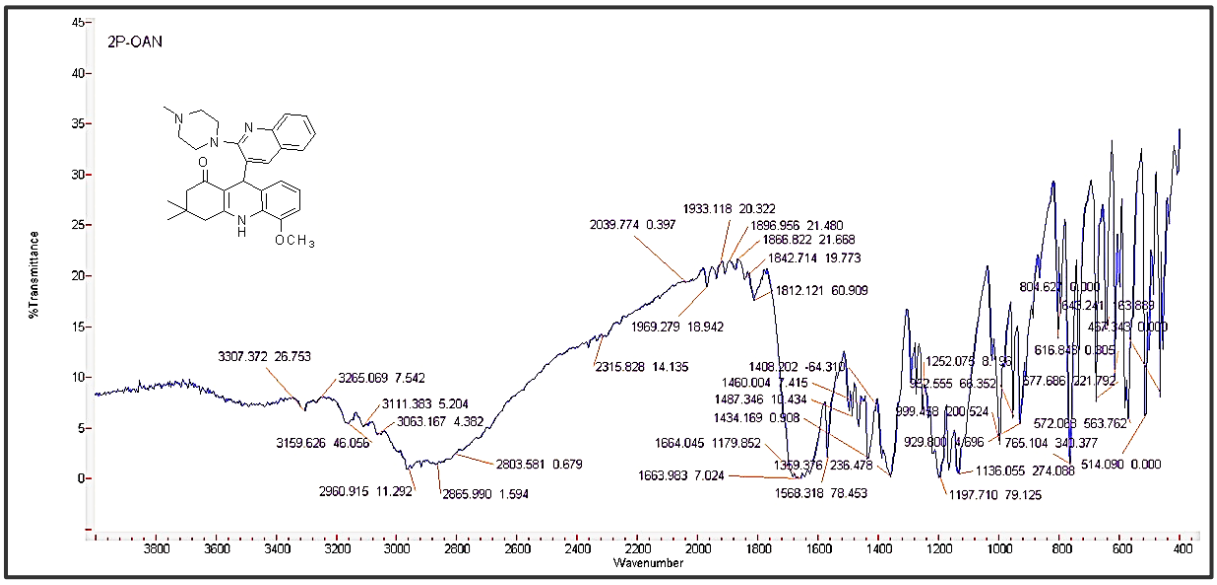

Figure 4A. S. 63. The Infra-Red Spectrum of compound 6p

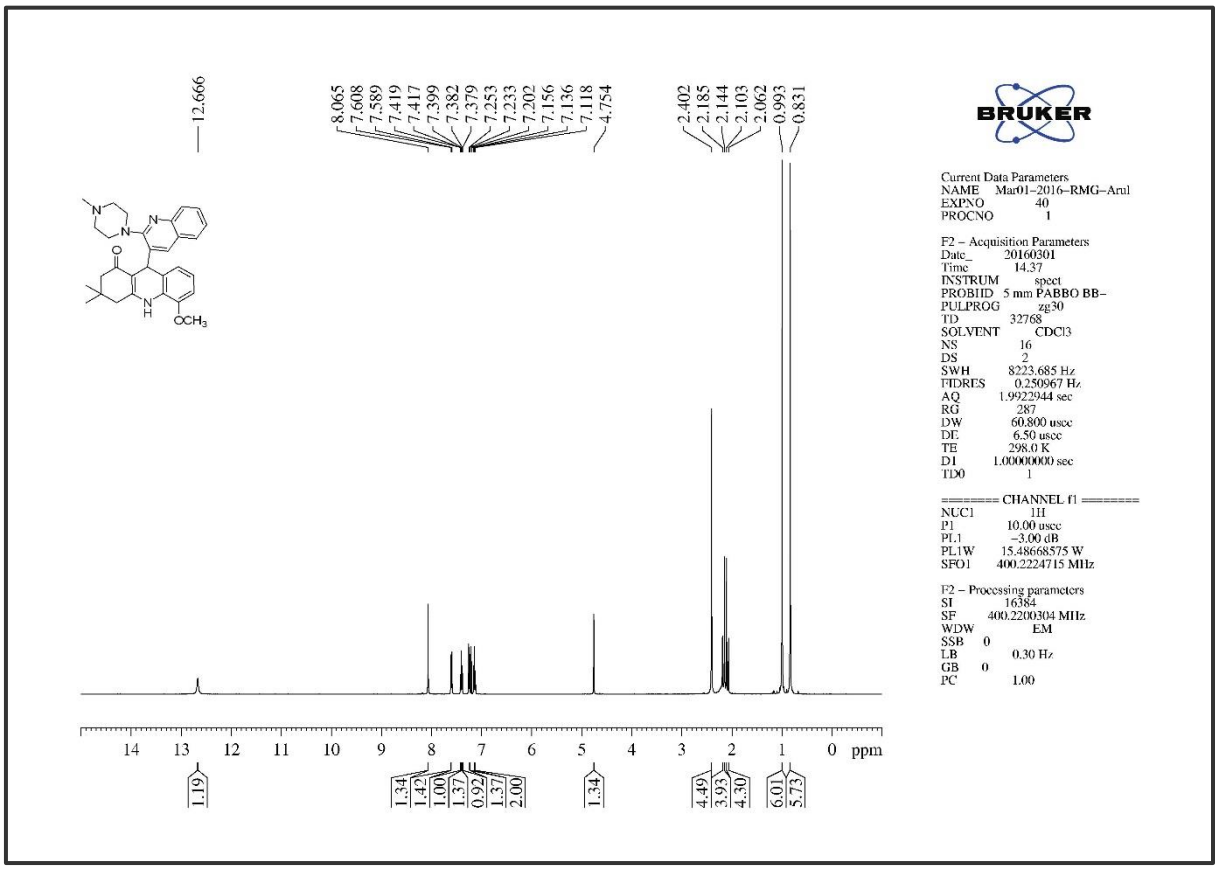

Figure 4A. S. 64. The ^{1}H NMR of compound 6p

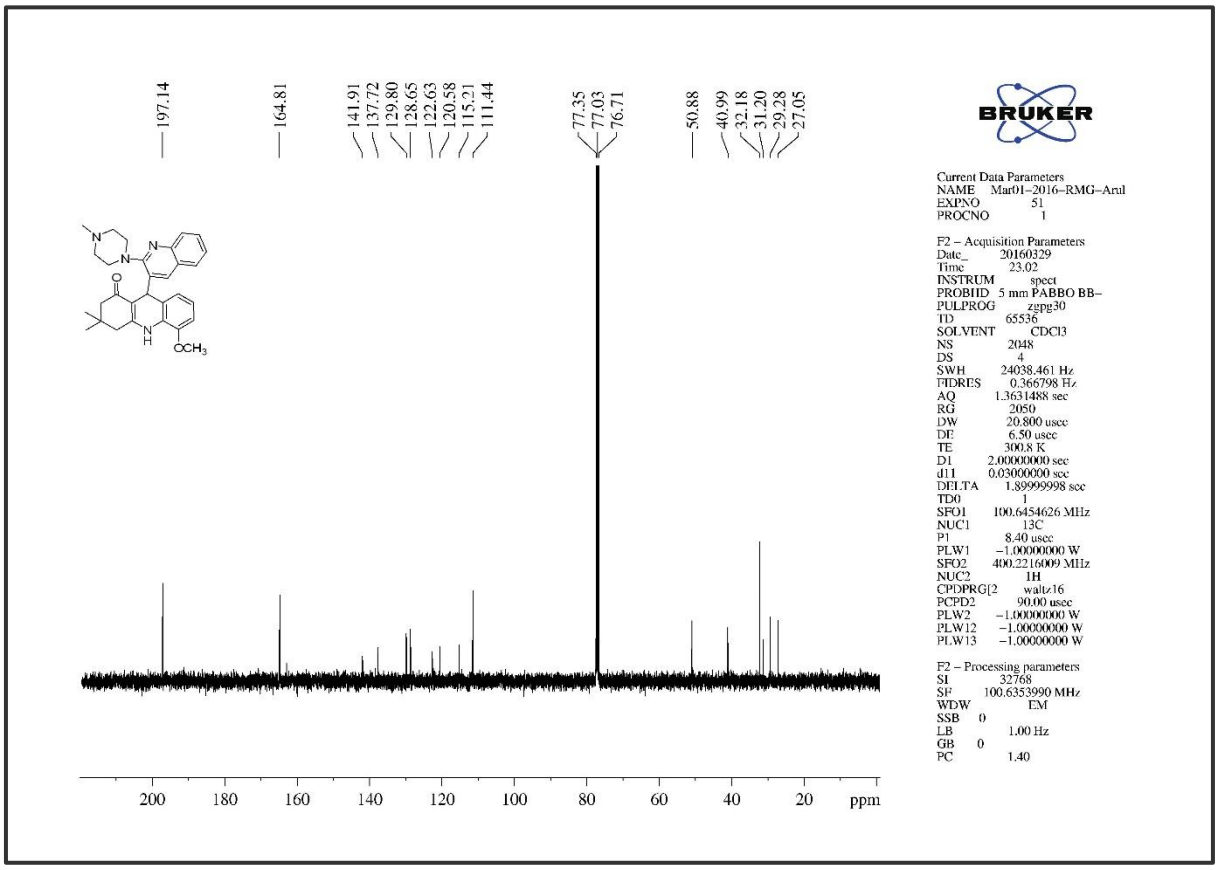

Figure 4A. S. 65. The ^{13}C NMR of compound 6p

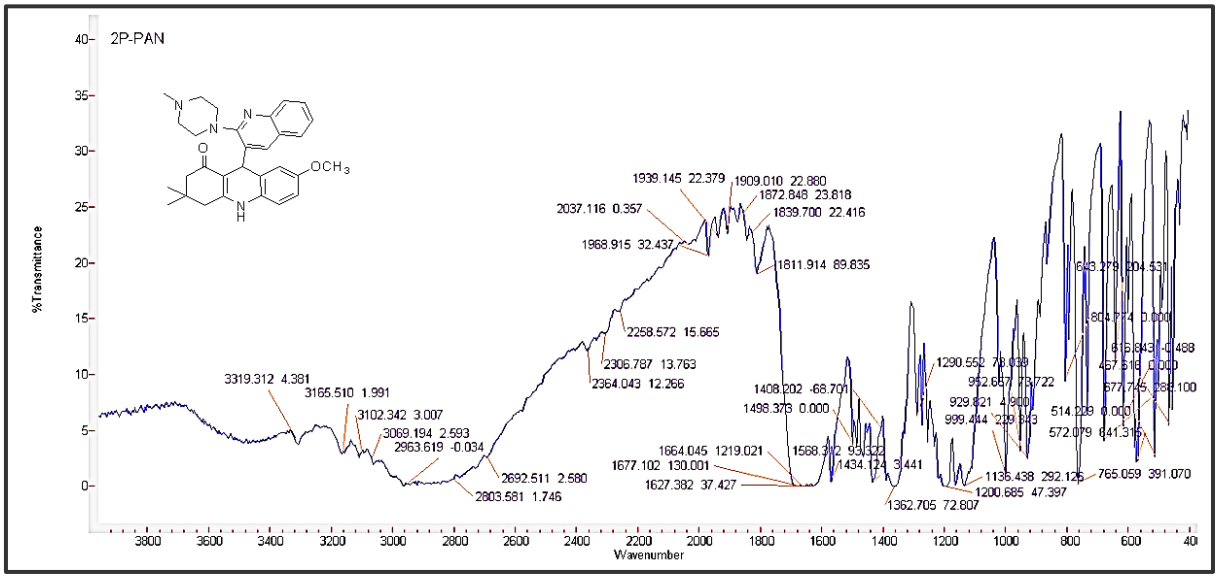

Figure 4A. S. 66. The Infra-Red Spectrum of compound 6q

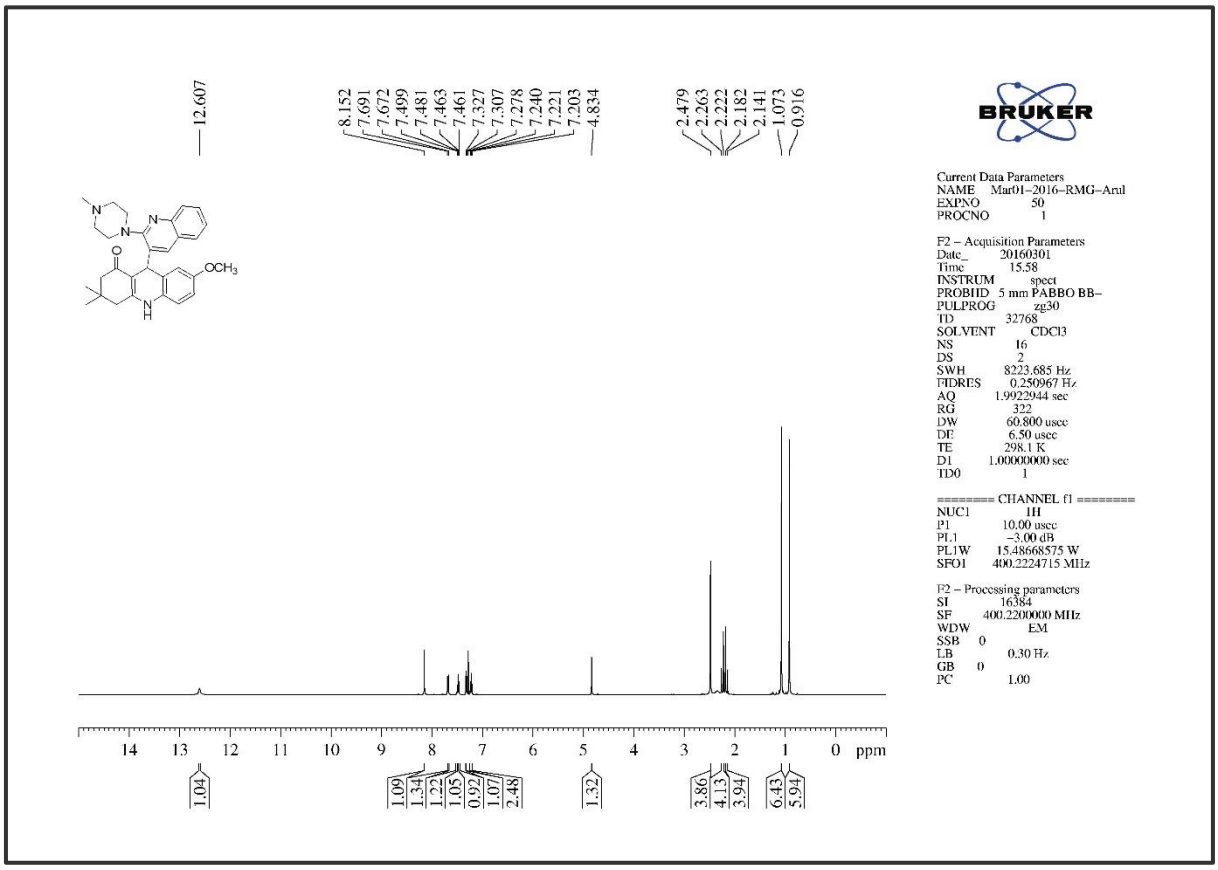

Figure 4A. S. 67. The ^{1}H NMR of compound 6q

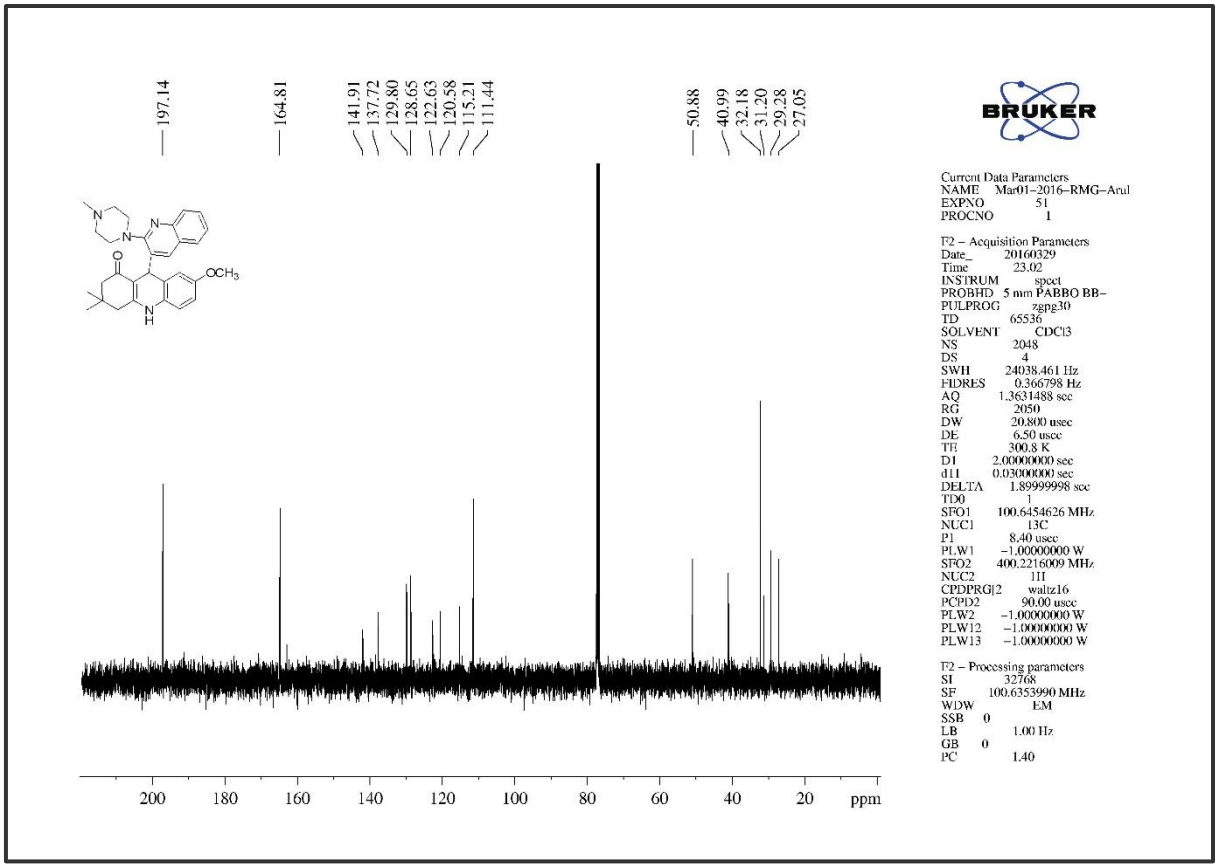

Figure 4A. S. 68. The ^{13}C NMR of compound 6q

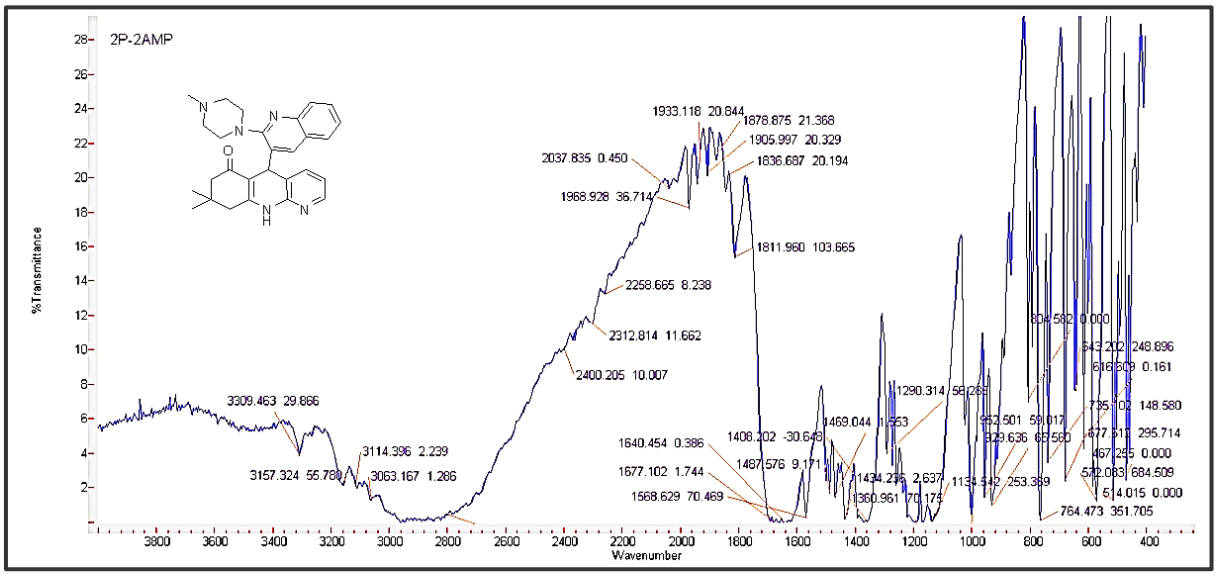

Figure 4A. S. 69. The Infra-Red Spectrum of compound 6r

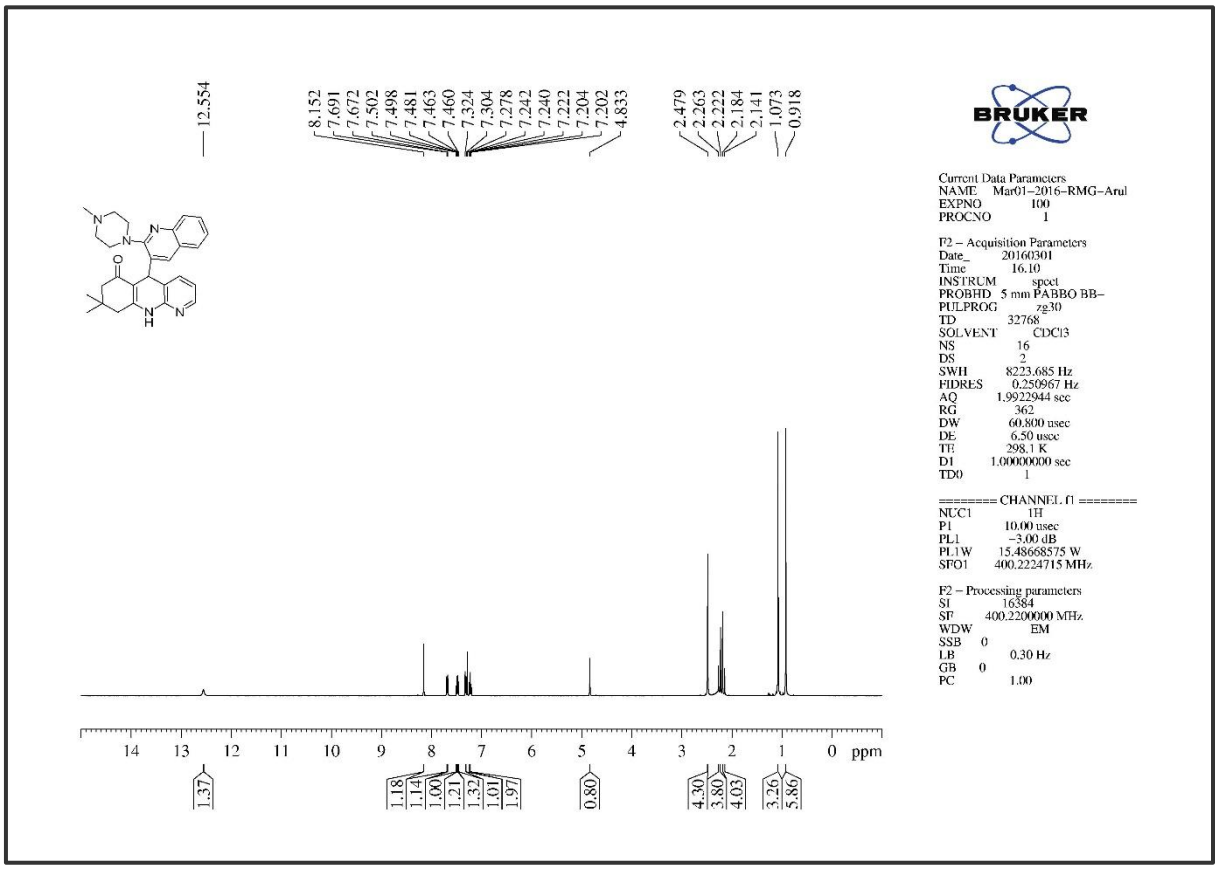

Figure 4A. S. 70. The ^{1}H NMR of compound 6r

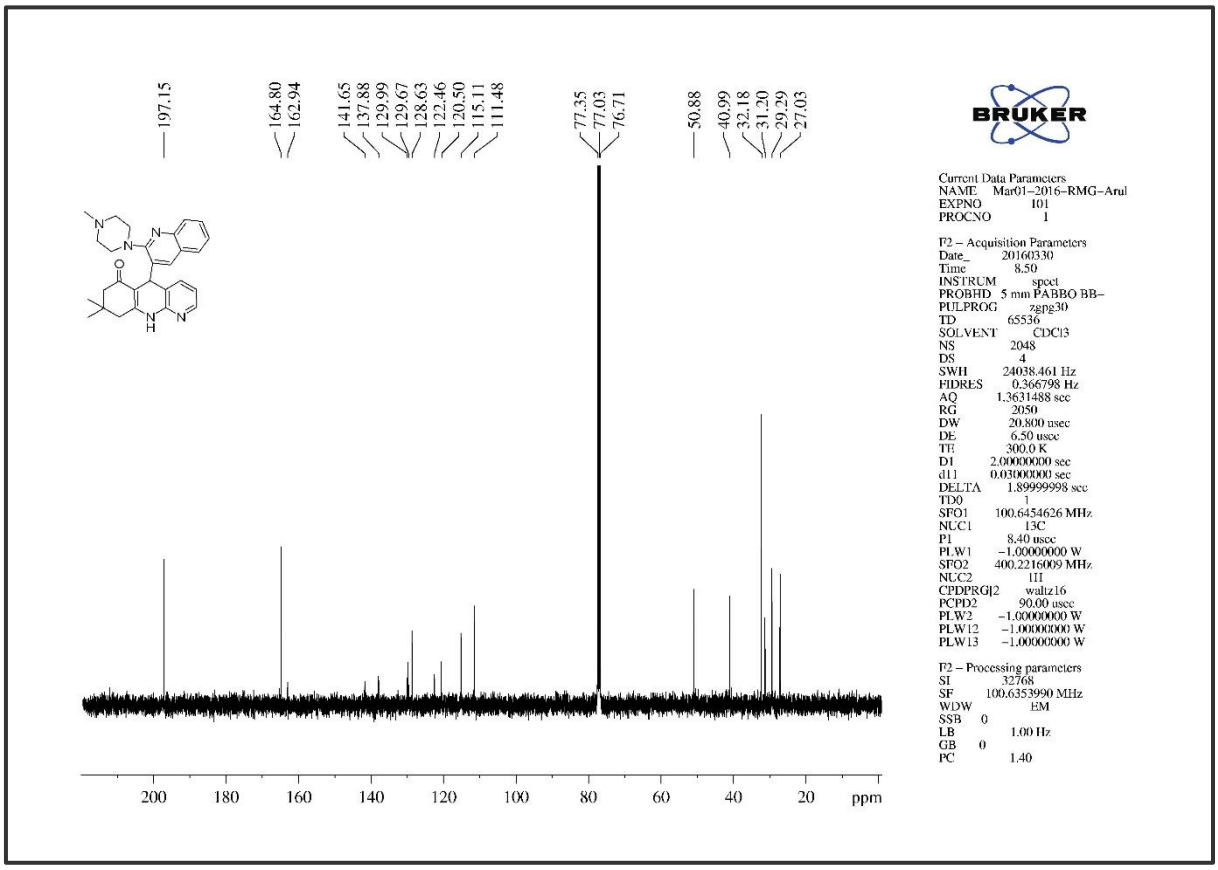

Figure 4A. S. 71. The ^{13}C NMR of compound 6r

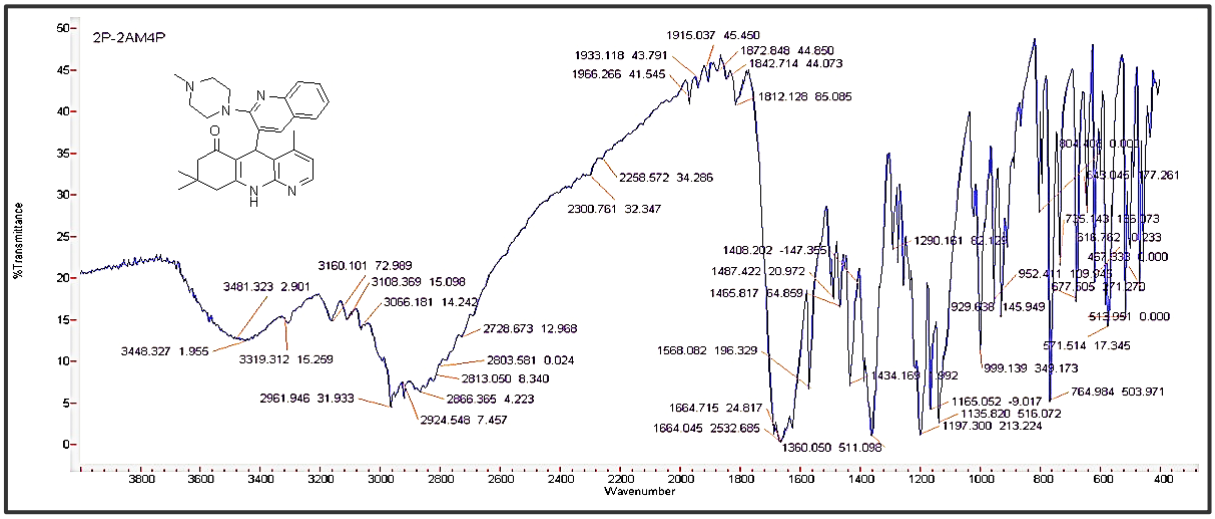

Figure 4A. S. 72. The Infra-Red Spectrum of compound 6s

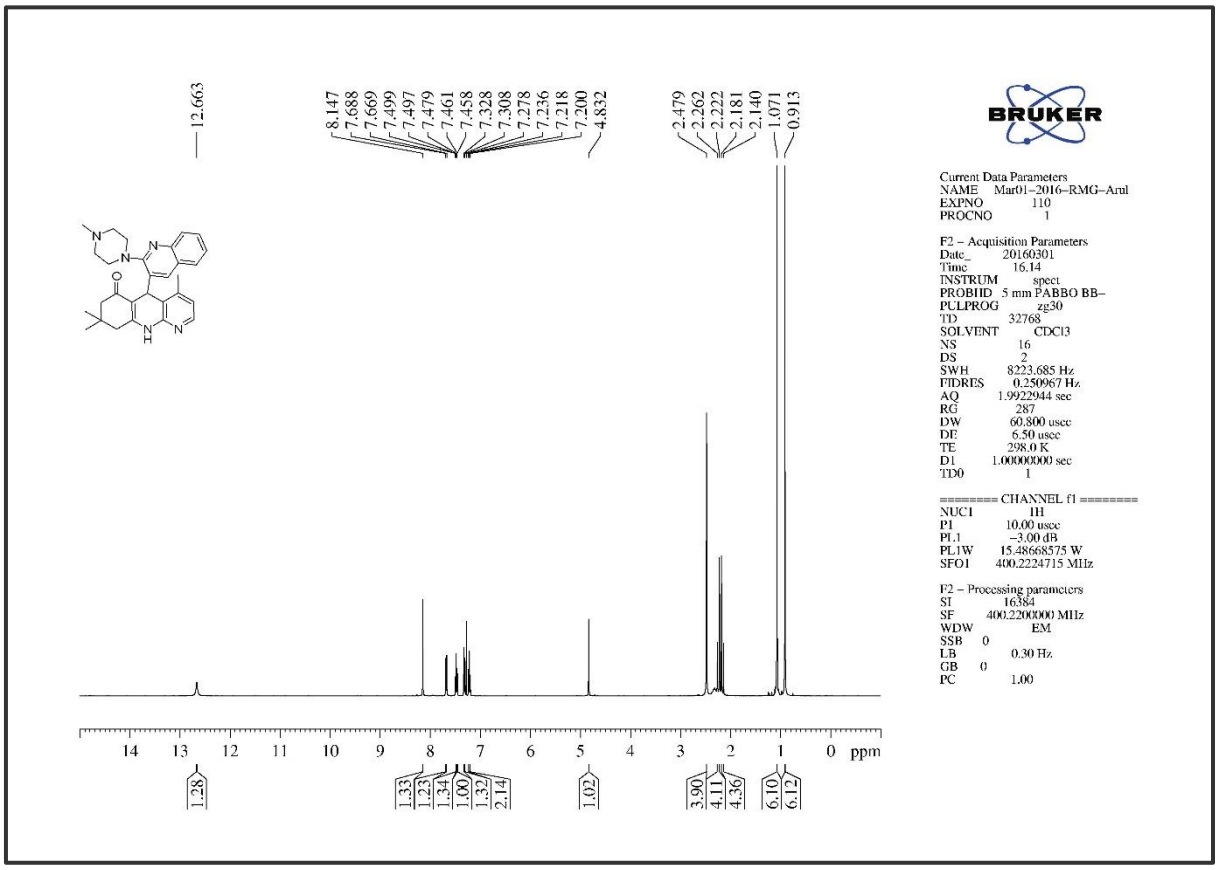

Figure 4A. S.73. The ^{1}H NMR of compound 6s

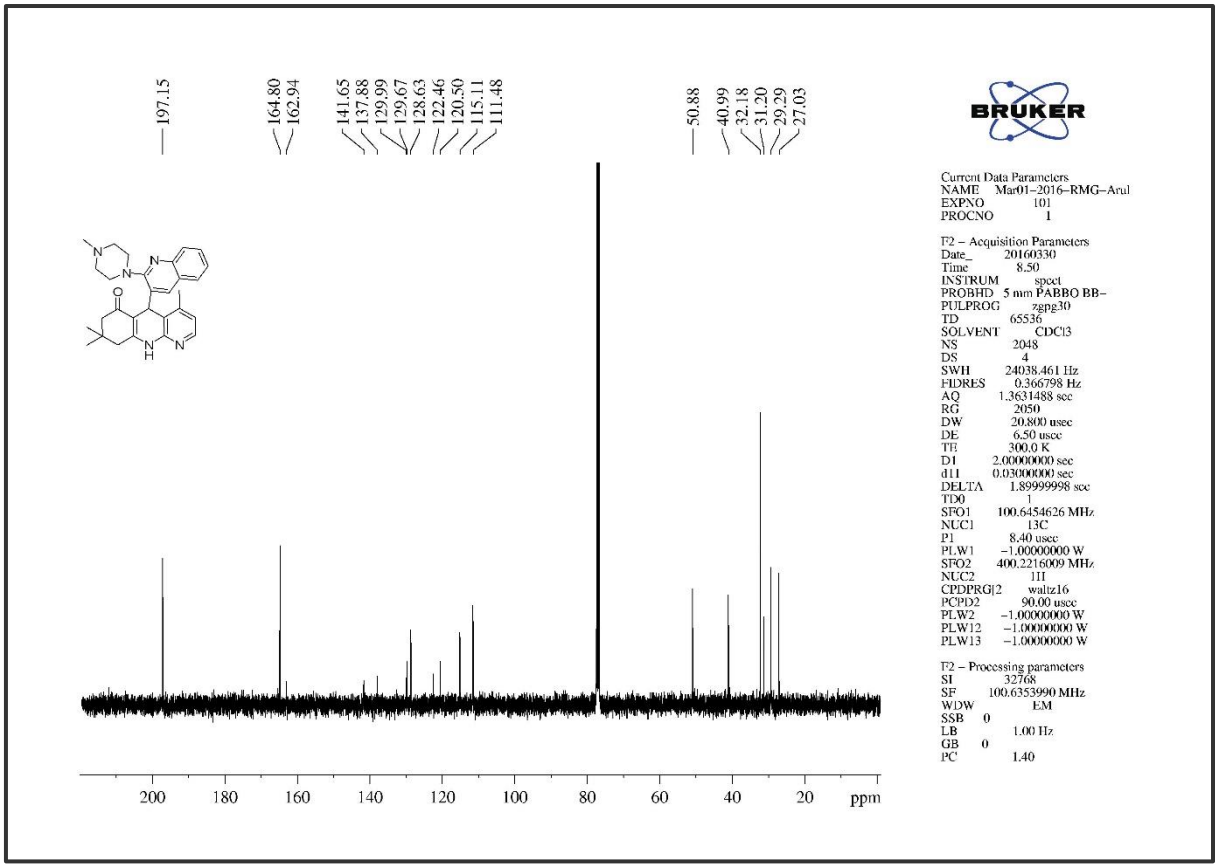

Figure 4A. S.74. The ^{13}C NMR of compound 6s

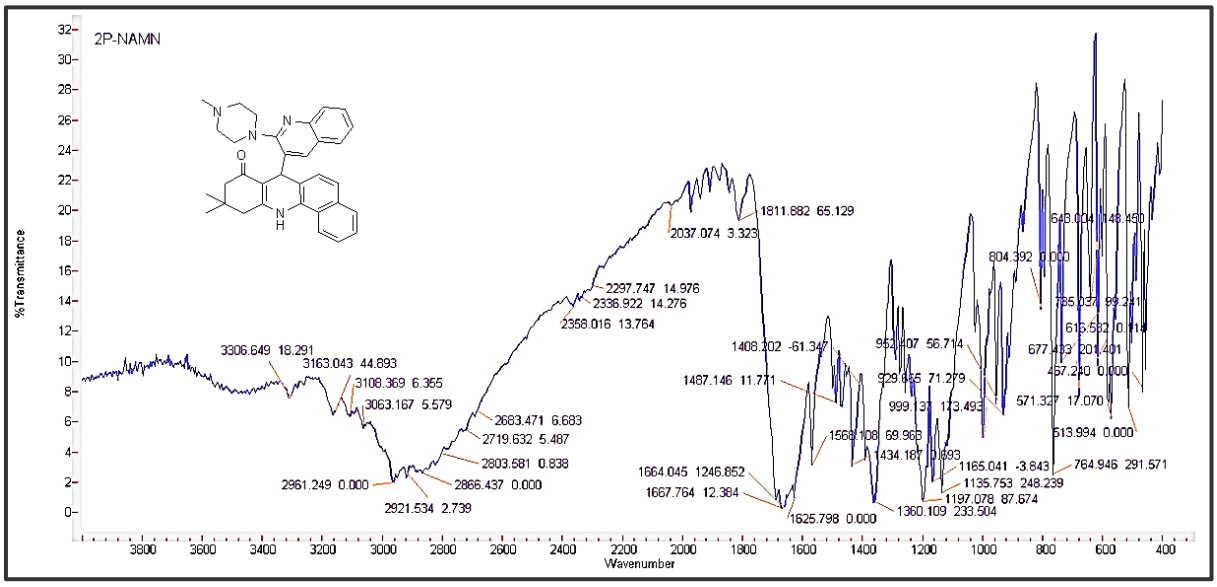

Figure 4A. S. 75. The Infra-Red Spectrum of compound 6t

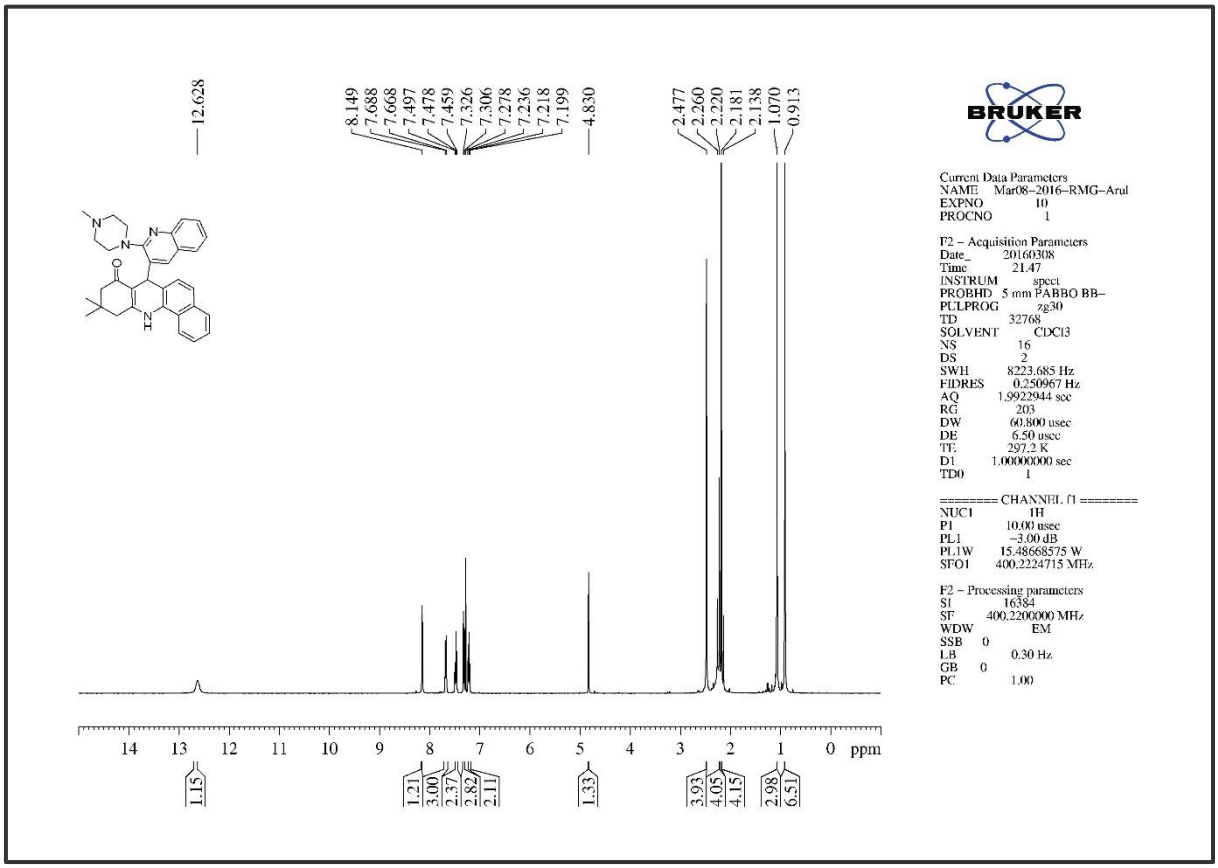

Figure 4A. S. 76. The ^{1}H NMR of compound 6t

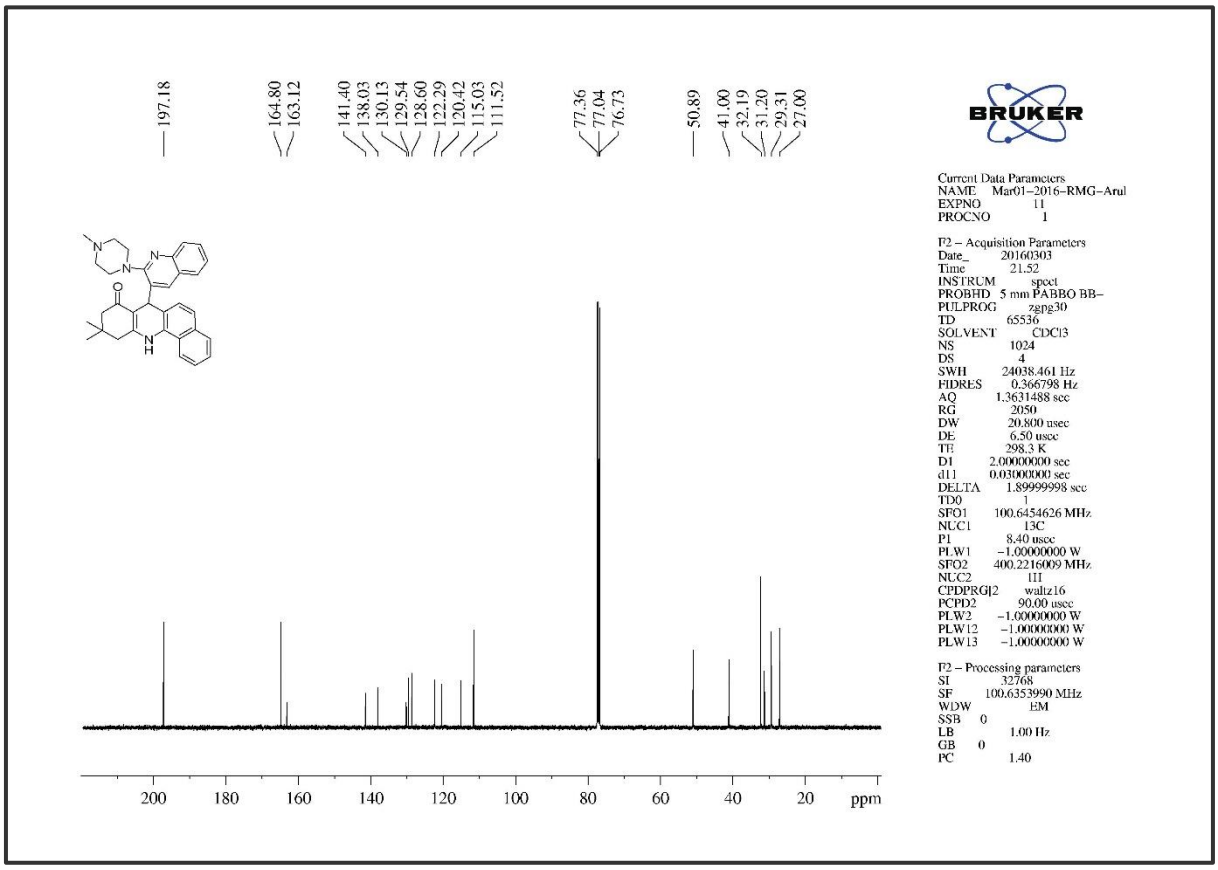

Figure 4A. S. 77. The ^{13}C NMR of compound 6t

Chapter Four

Part B

Appendix

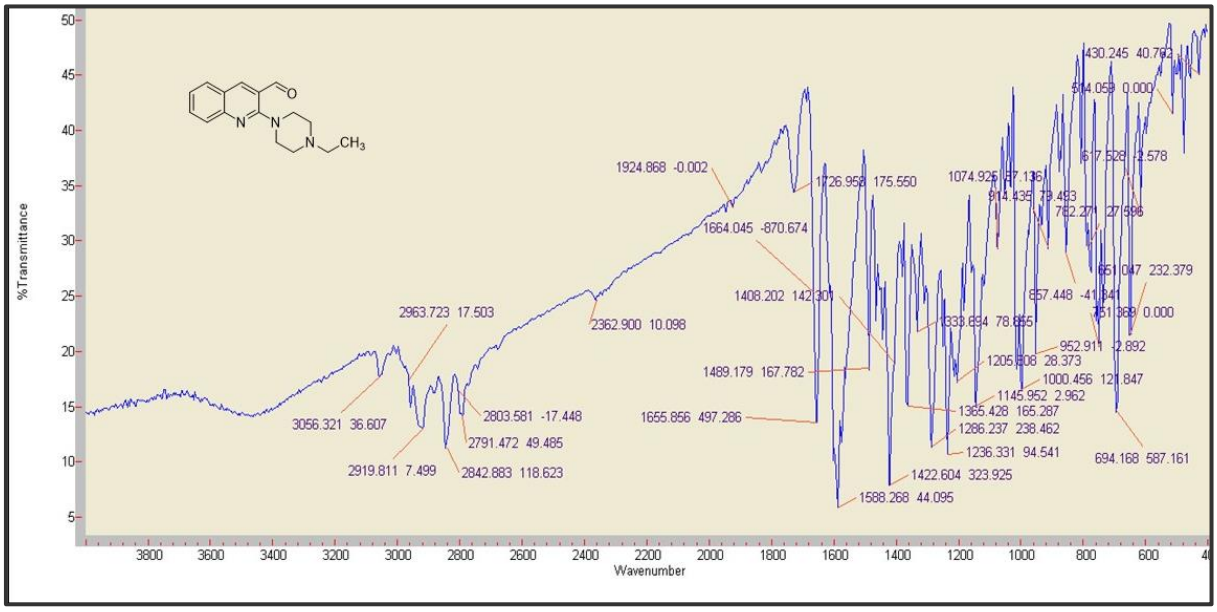

Figure 4B. S. 1. The Infra-Red Spectrum of compound 3

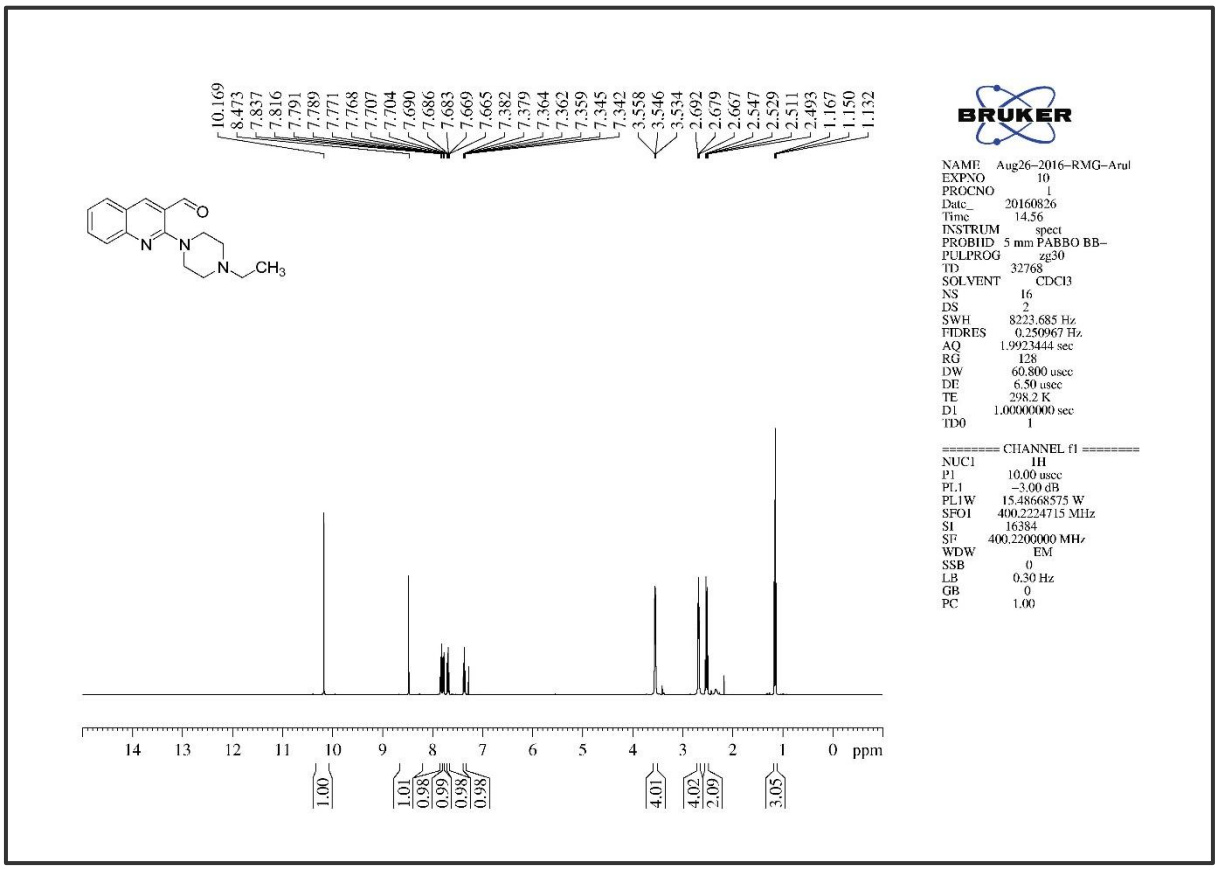

Figure 4B. S. 2. The ^{1}H NMR of compound 3

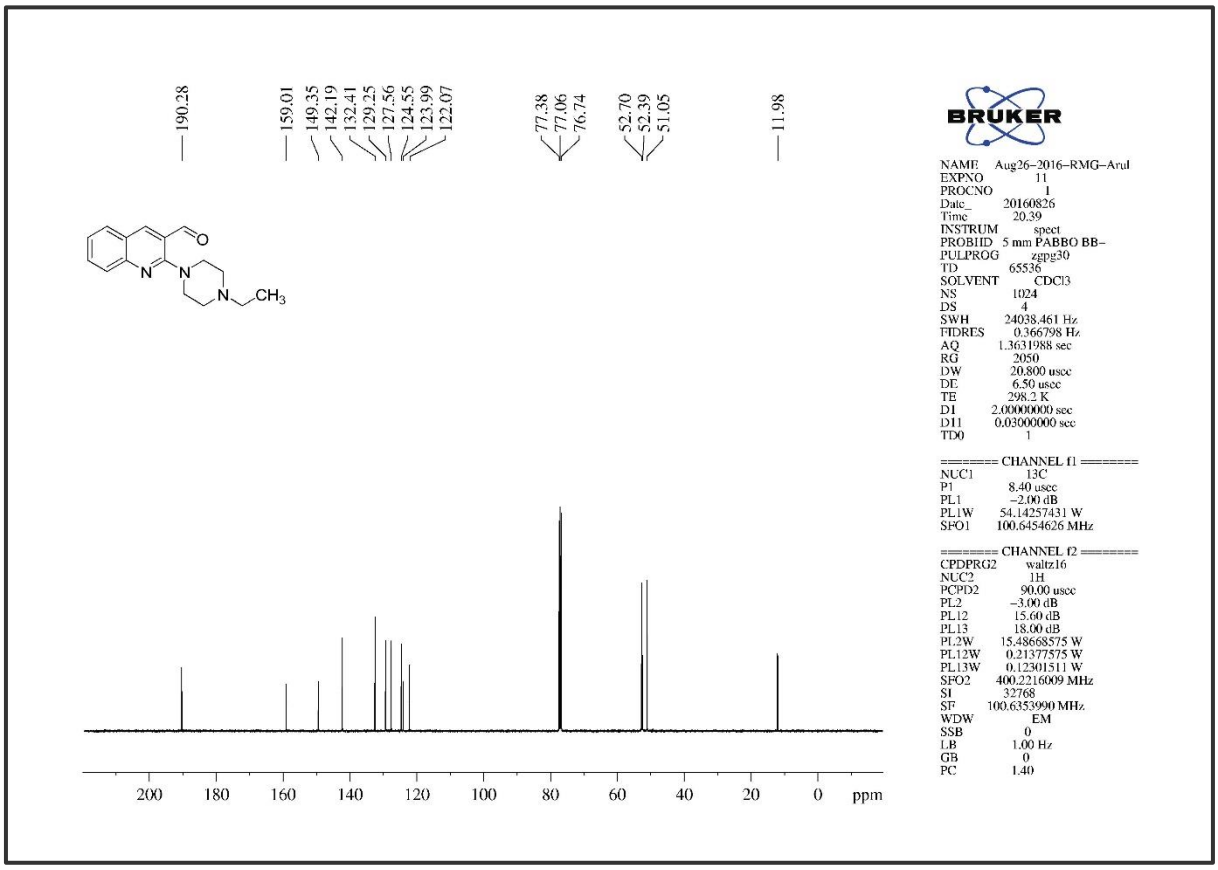

Figure 4B. S. 3. The ^{13}C NMR of compound 3

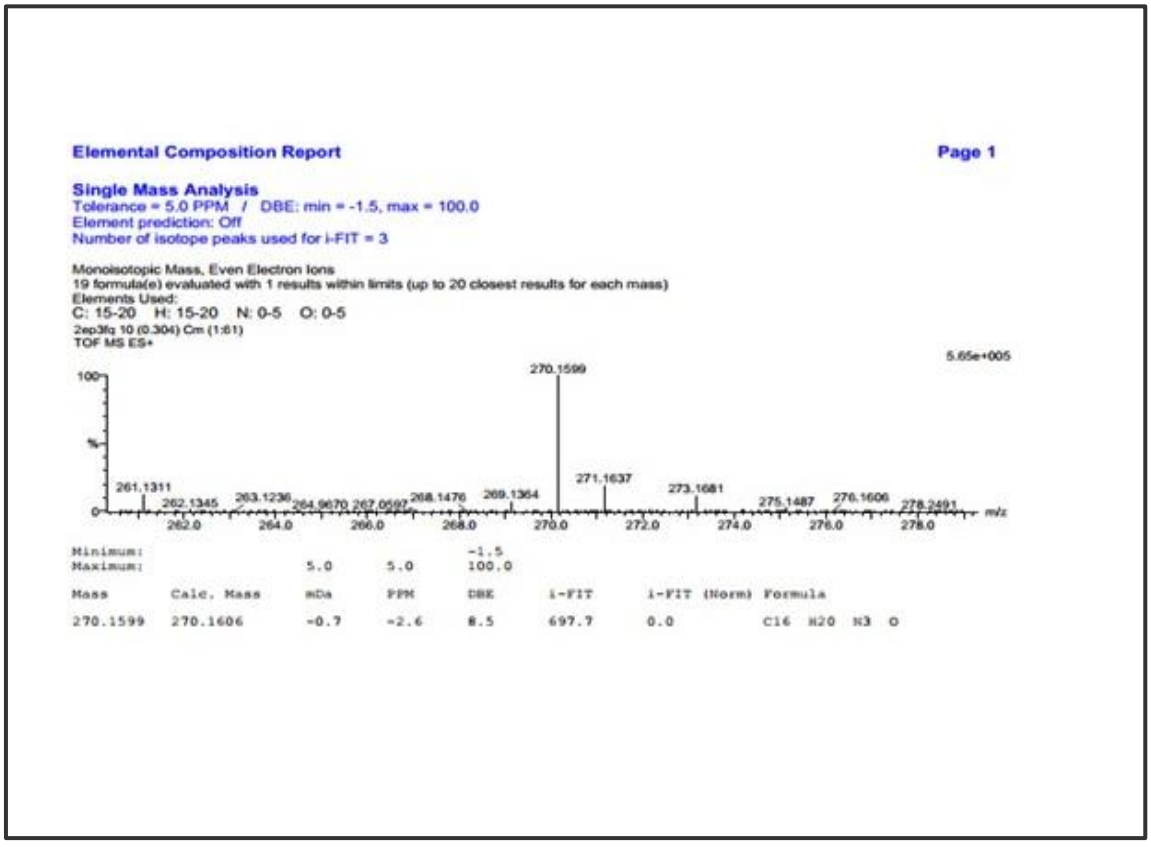

Figure 4B. S. 4. The HRMS of compound 3

Crystal structure of 2-(4-ethylpiperazin-1-yl)quinoline-3-carbaldehyde 1

Computing details

Data collection: *APEX2* (Bruker, 2008); cell refinement: *SAINT* (Bruker, 2008); data reduction: *SAINT*; program (s) used to solve structure: *SHELXS97* (Sheldrick, 2008); program (s) used to solve structure: *SHELXS97* (Sheldrick, 2008); molecular graphics: *ORTEP-3 for windows* (Farrugia, 2012) and Mercury (Macrae et al., 2008); software used to prepare materials for publication: *SHELXL97* and *PLATON* (Spek, 2009).

2-(4-ethylpiperazin-1-yl)quinoline-3-carbaldehyde **1**

Crystal data and structure refinement
Table 4B. S1. Experimental details.

Crystal data		
EmpFT-IRical formula	C_{16} H_{21} N_3 O	
Formula weight	271.36	
Temperature	296(2) K	
Wavelength	0.71073 Å	
Crystal system	Monoclinic	
Space group	P 21/n	
Unit cell dimensions	a = 14.1176(16) Å	□= 90°.
	b = 6.1388(8) Å	□= 106.689(7) °.
	c = 17.509(2) Å	□ = 90°.
Volume	1453.5(3) $Å^3$	
Z	4	
Density (calculated)	1.240 Mg/m^3	
Absorption coefficient	0.079 mm^{-1}	
F (000)	584	
Crystal size	0.20 x 0.18 x 0.08 mm^3	
Theta range for data collection	2.19 to 28.29°.	
Index ranges	-18<=h<=14, -8<=k<=5, -19<=l<=23	
Reflections collected	13445	
Independent reflections	3590 [R (int) = 0.1730]	
Completeness to theta = 28.29°	99.3 %	
Absorption correction	Semi-empFT-IRical from equivalents	
Max. And min. transmission	0.987 and 0.968	
Refinement method	Full-matrix least-squares on F^2	
Data / restraints / parameters	3590 / 0 / 177	
Goodness-of-fit on F^2	0.872	

Final R indices [I>2sigma (I)]	R1 = 0.0766, wR2 = 0.1301
R indices (all data)	R1 = 0.3488, wR2 = 0.1994
Extinction coefficient	N/A
Largest diff. peak and whole	0.190 and -0.372 e.Å^{-3}

Geometry. All esds (except the esds in the dihedral angle between two 1.s, planes) are estimated using the full covariance matrix. The cell esds were taken into account individually in the estimation of esds in distances, angles and torsion angles. Correlations between esds in cell parameters were only used when they are defined by crystal symmetry. An approximate (isotropic) treatment of cell esds was used for estimating esds involving 1.s, planes.

Fractional atomic coordinates and equivalent isotropic displacement parameters (Å^2)

	x	y	z	U (eq)
O (1)	-573(2)	-3920(6)	3683(2)	72(1)
N (1)	1274(2)	2432(6)	1694(2)	44(1)
N (2)	951(2)	1340(5)	3192(2)	40(1)
N (3)	1816(2)	1669(5)	4538(2)	49(1)
C (1)	2088(3)	952(8)	5309(2)	43(1)
C (3)	1149(3)	603(7)	3979(2)	41(1)
C (6)	945(3)	-2021(7)	4933(2)	46(1)
C (9)	1697(3)	-958(8)	5527(2)	42(1)
C (10)	1097(3)	-337(6)	2637(2)	45(1)
C (11)	649(3)	-1224(7)	4175(2)	41(1)
C (14)	2791(3)	2143(7)	5891(3)	56(1)
C (16)	754(3)	462(7)	1792(2)	46(1)
C (17)	2038(3)	-1719(7)	6323(2)	57(1)
C (20)	1447(3)	3348(6)	3077(2)	46(1)
C (23)	1087(3)	4074(7)	2225(2)	49(1)
C (24)	992(3)	3165(7)	873(2)	62(1)
C (27)	-246(3)	-2144(9)	3604(2)	52(1)
C (30)	2743(3)	-552(9)	6873(2)	59(1)
C (31)	3108(3)	1374(8)	6654(2)	58(1)
C (32)	1315(3)	1770(7)	298(2)	72(2)

Geometric parameters (Å, °)

O (1)-C (27)	1.207(5)
N (1)-C (23)	1.445(4)
N (1)-C (24)	1.448(4)
N (1)-C (16)	1.450(4)
N (2)-C (3)	1.400(4)
N (2)-C (20)	1.459(4)
N (2)-C (10)	1.471(4)
N (3)-C (3)	1.320(4)
N (3)-C (1)	1.367(4)
N (3)-H (3A)	0.8596
C (1)-C (9)	1.394(5)
C (1)-C (14)	1.406(5)
C (3)-C (11)	1.419(5)
C (6)-C (11)	1.363(5)
C (6)-C (9)	1.414(5)
C (6)-H (6B)	0.9300
C (9)-C (17)	1.417(5)
C (10)-C (16)	1.500(4)
C (10)-H (10A)	0.9700
C (10)-H (10B)	0.9700
C (11)-C (27)	1.480(5)
C (14)-C (31)	1.366(5)
C (14)-H (14A)	0.9300
C (16)-H (16A)	0.9700
C (16)-H (16B)	0.9700
C (17)-C (30)	1.372(5)
C (17)-H (17A)	0.9300
C (20)-C (23)	1.500(4)
C (20)-H (20A)	0.9700
C (20)-H (20B)	0.9700
C (23)-H (23A)	0.9700
C (23)-H (23B)	0.9700
C (24)-C (32)	1.490(5)
C (24)-H (24A)	0.9303
C (24)-H (26a)	0.9468
C (24)-H (26b)	0.9629

C (27)-H (27A)	0.9300
C (30)-C (31)	1.387(5)
C (30)-H (30A)	0.9300
C (31)-H (31A)	0.9300
C (32)-H (32A)	0.9600
C (32)-H (32B)	0.9600
C (32)-H (32C)	0.9600

C (23)-N (1)-C (24)	111.8(3)
C (23)-N (1)-C (16)	108.3(3)
C (24)-N (1)-C (16)	111.9(3)
C (3)-N (2)-C (20)	116.1(3)
C (3)-N (2)-C (10)	113.5(3)
C (20)-N (2)-C (10)	109.7(3)
C (3)-N (3)-C (1)	120.7(4)
C (3)-N (3)-H (3A)	119.9
C (1)-N (3)-H (3A)	119.4
N (3)-C (1)-C (9)	121.3(4)
N (3)-C (1)-C (14)	119.2(4)
C (9)-C (1)-C (14)	119.5(4)
N (3)-C (3)-N (2)	117.9(4)
N (3)-C (3)-C (11)	120.7(4)
N (2)-C (3)-C (11)	121.4(4)
C (11)-C (6)-C (9)	120.4(4)
C (11)-C (6)-H (6B)	119.8
C (9)-C (6)-H (6B)	119.8
C (1)-C (9)-C (6)	117.4(4)
C (1)-C (9)-C (17)	119.8(4)
C (6)-C (9)-C (17)	122.8(4)
N (2)-C (10)-C (16)	110.8(3)
N (2)-C (10)-H (10A)	109.5
C (16)-C (10)-H (10A)	109.5
N (2)-C (10)-H (10B)	109.5
C (16)-C (10)-H (10B)	109.5
H (10A)-C (10)-H (10B)	108.1
C (6)-C (11)-C (3)	119.0(4)
C (6)-C (11)-C (27)	118.9(4)
C (3)-C (11)-C (27)	121.8(4)

C (31)-C (14)-C (1)	119.6(4)
C (31)-C (14)-H (14A)	120.2
C (1)-C (14)-H (14A)	120.2
N (1)-C (16)-C (10)	111.0(3)
N (1)-C (16)-H (16A)	109.4
C (10)-C (16)-H (16A)	109.4
N (1)-C (16)-H (16B)	109.4
C (10)-C (16)-H (16B)	109.4
H (16A)-C (16)-H (16B)	108.0
C (30)-C (17)-C (9)	119.4(4)
C (30)-C (17)-H (17A)	120.3
C (9)-C (17)-H (17A)	120.3
N (2)-C (20)-C (23)	110.5(3)
N (2)-C (20)-H (20A)	109.6
C (23)-C (20)-H (20A)	109.6
N (2)-C (20)-H (20B)	109.6
C (23)-C (20)-H (20B)	109.6
H (20A)-C (20)-H (20B)	108.1
N (1)-C (23)-C (20)	111.1(3)
N (1)-C (23)-H (23A)	109.4
C (20)-C (23)-H (23A)	109.4
N (1)-C (23)-H (23B)	109.4
C (20)-C (23)-H (23B)	109.4
H (23A)-C (23)-H (23B)	108.0
N (1)-C (24)-C (32)	116.2(3)
N (1)-C (24)-H (24A)	121.6
C (32)-C (24)-H (24A)	122.2
N (1)-C (24)-H (26a)	108.1
C (32)-C (24)-H (26a)	107.6
H (24A)-C (24)-H (26a)	54.7
N (1)-C (24)-H (26b)	108.1
C (32)-C (24)-H (26b)	106.5
H (24A)-C (24)-H (26b)	55.6
H (26a)-C (24)-H (26b)	110.3
O (1)-C (27)-C (11)	123.2(4)
O (1)-C (27)-H (27A)	118.4
C (11)-C (27)-H (27A)	118.4
C (17)-C (30)-C (31)	120.3(4)

C (17)-C (30)-H (30A)	119.9
C (31)-C (30)-H (30A)	119.9
C (14)-C (31)-C (30)	121.4(4)
C (14)-C (31)-H (31A)	119.3
C (30)-C (31)-H (31A)	119.3
C (24)-C (32)-H (32A)	109.5
C (24)-C (32)-H (32B)	109.5
H (32A)-C (32)-H (32B)	109.5
C (24)-C (32)-H (32C)	109.5
H (32A)-C (32)-H (32C)	109.5
H (32B)-C (32)-H (32C)	109.5

Symmetry transformations used to generate equivalent atoms:

Anisotropic displacement parameters ($Å^2$)

	U^{11}	U^{22}	U^{33}	U^{23}	U^{13}	U^{12}
O (1)	72(2)	75(3)	60(2)	1(2)	4(2)	-31(2)
N (1)	62(2)	38(2)	34(2)	7(2)	17(2)	1(2)
N (2)	54(2)	35(2)	31(2)	-2(2)	12(2)	-2(2)
N (3)	60(3)	44(2)	46(2)	0(2)	19(2)	-18(2)
C (1)	41(3)	51(3)	39(3)	-6(3)	15(2)	-7(3)
C (3)	36(3)	41(3)	44(3)	-9(2)	10(2)	-3(2)
C (6)	44(3)	47(3)	46(3)	-1(2)	10(2)	-8(2)
C (9)	39(3)	52(3)	37(3)	-2(2)	12(2)	-4(2)
C (10)	52(3)	43(3)	41(3)	-4(2)	12(2)	1(2)
C (11)	36(3)	46(3)	40(3)	-3(2)	12(2)	-5(2)
C (14)	61(3)	64(3)	44(3)	-9(3)	15(3)	-22(3)
C (16)	55(3)	48(3)	34(3)	0(2)	12(2)	7(3)
C (17)	60(3)	67(3)	44(3)	5(3)	13(3)	-7(3)
C (20)	64(3)	34(3)	40(3)	-5(2)	13(2)	-2(2)
C (23)	63(3)	40(3)	46(3)	-3(2)	19(2)	2(2)
C (24)	75(3)	45(3)	66(3)	10(3)	21(3)	18(3)
C (27)	48(3)	66(4)	44(3)	-2(3)	16(2)	-2(3)
C (30)	52(3)	83(4)	38(3)	8(3)	5(3)	-3(3)
C (31)	47(3)	85(4)	42(3)	-9(3)	11(2)	-16(3)

Hydrogen coordinates (x 10^4) and isotropic displacement parameters (Å^{2}x 10^3

		z	U (eq)	
H (3A)	2089	2819	4416	59
H (6B)	651	-3271	5060	56
H (10A)	730	-1638	2689	54
H (10B)	1792	-717	2770	54
H (14A)	3039	3447	5757	67
H (16A)	868	-658	1438	55
H (16B)	49	751	1648	55
H (17A)	1785	-2999	6471	69
H (20A)	2155	3107	3222	56
H (20B)	1317	4478	3421	56
H (23A)	383	4367	2087	59
H (23B)	1420	5415	2159	59
H (24A)	630	4437	717	75
H (26a)	293	3254	694	75
H (26b)	1280	4579	858	75
H (27A)	-574	-1314	3163	62
H (30A)	2978	-1054	7394	71
H (31A)	3579	2159	7036	70
H (32A)	1134	2453	-217	108
H (32B)	1000	373	261	108
H (32C)	2019	1586	480	108

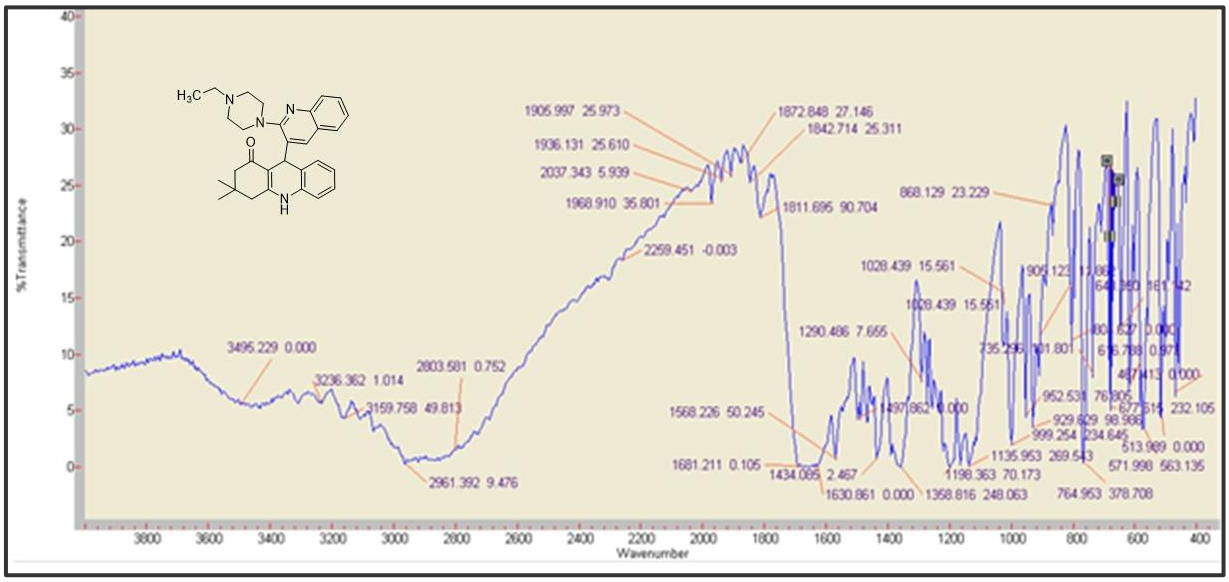

Figure 4B. S. 5. The Infra-Red Spectrum of compound 6a

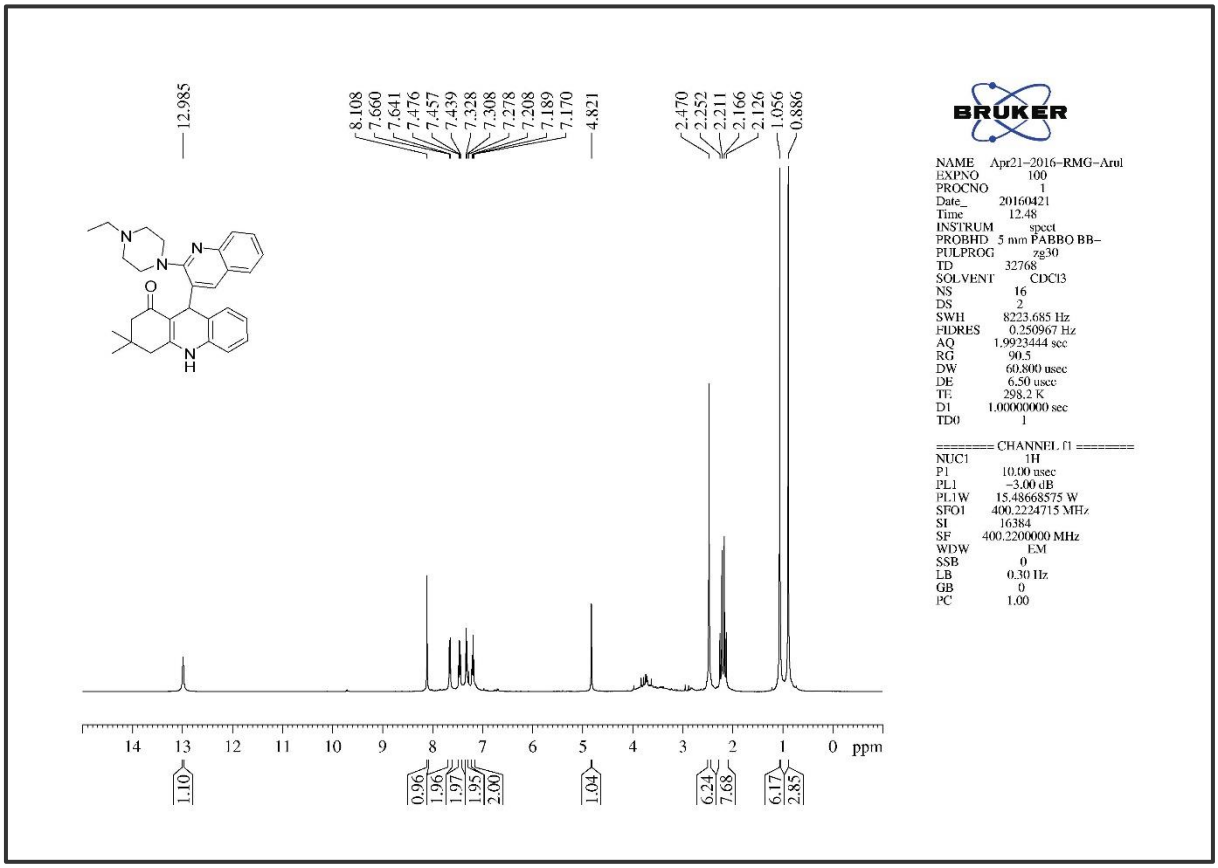

Figure 4B. S. 6. The ^{1}H NMR of compound 6a

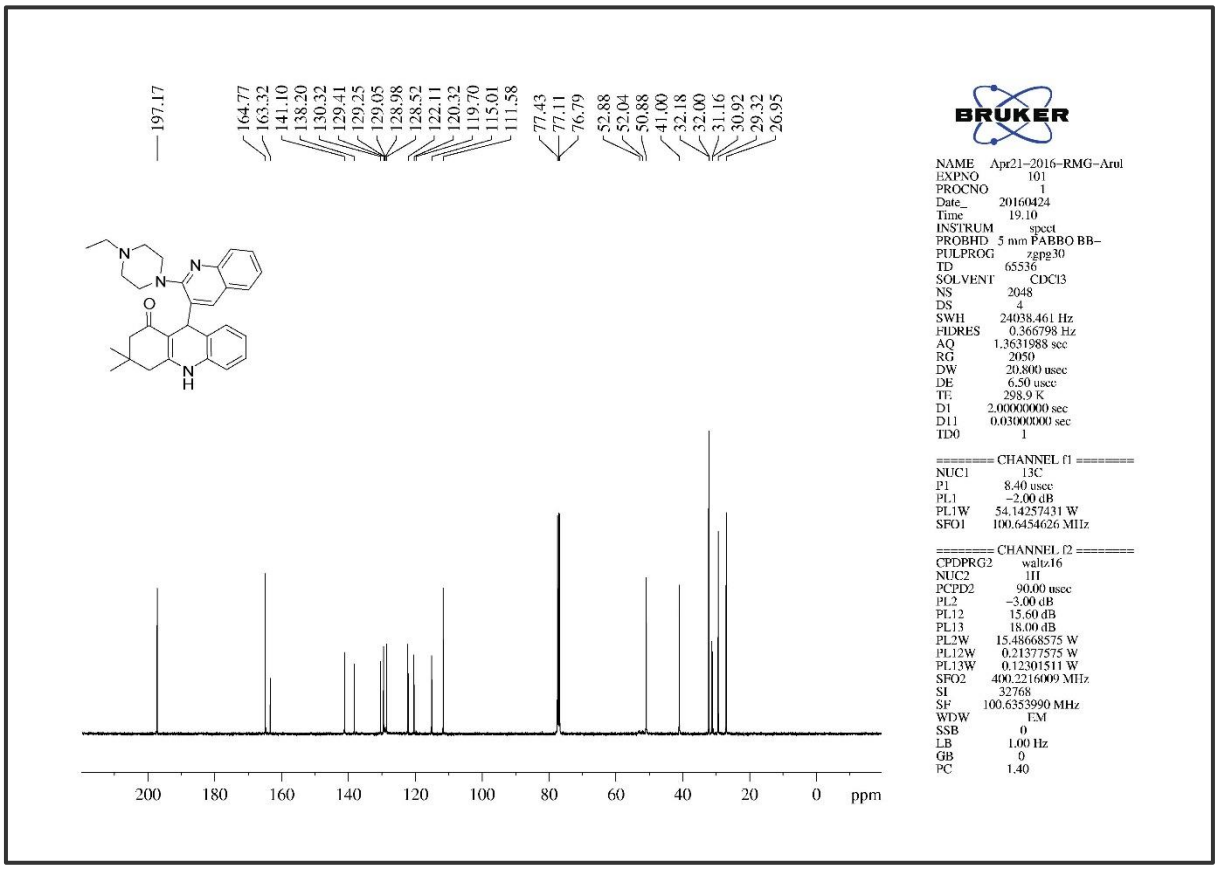

Figure 4B. S. 7. The ^{13}C NMR of compound 6a

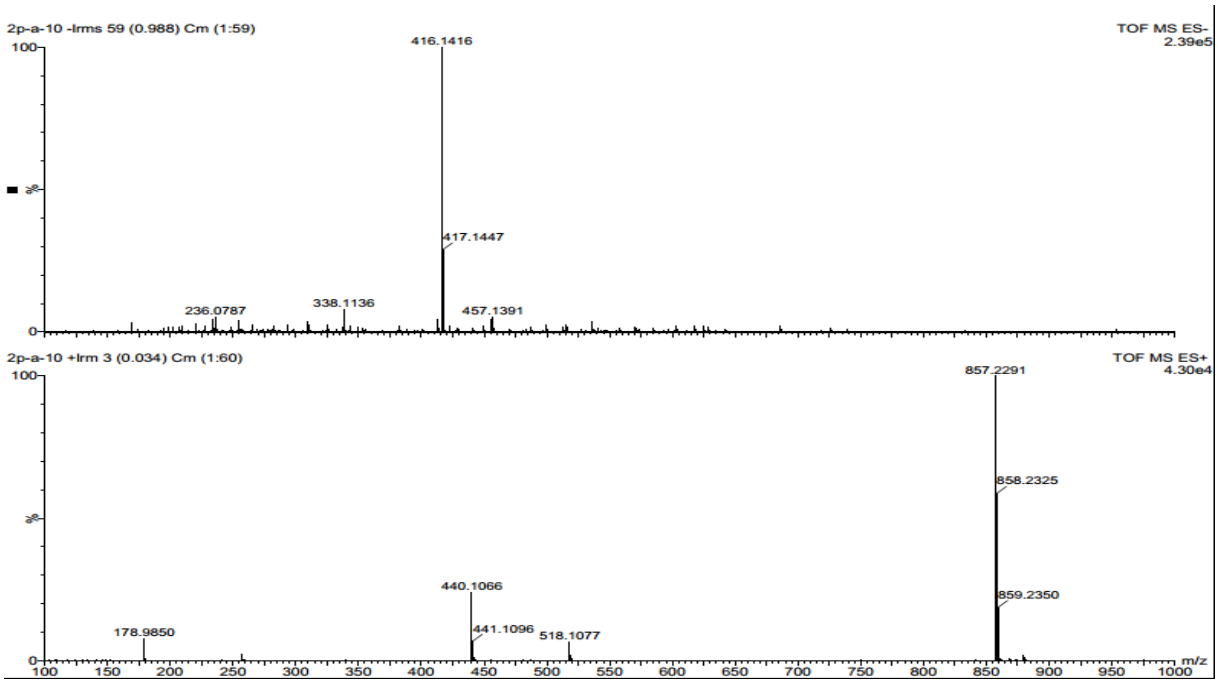

Figure 4B. S. 8. The HRMS of compound 6a

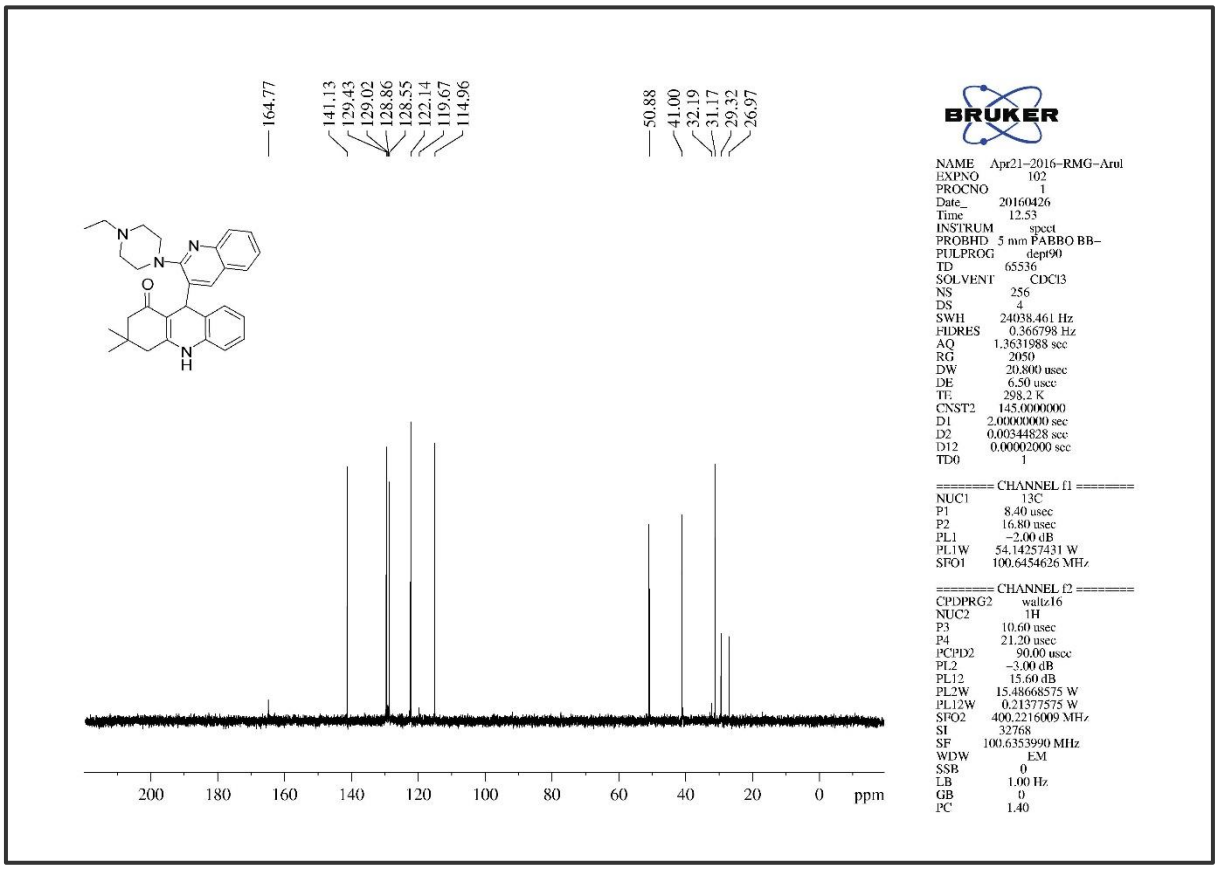

Figure 4B. S. 9. The DEPT-90 NMR of compound 6a

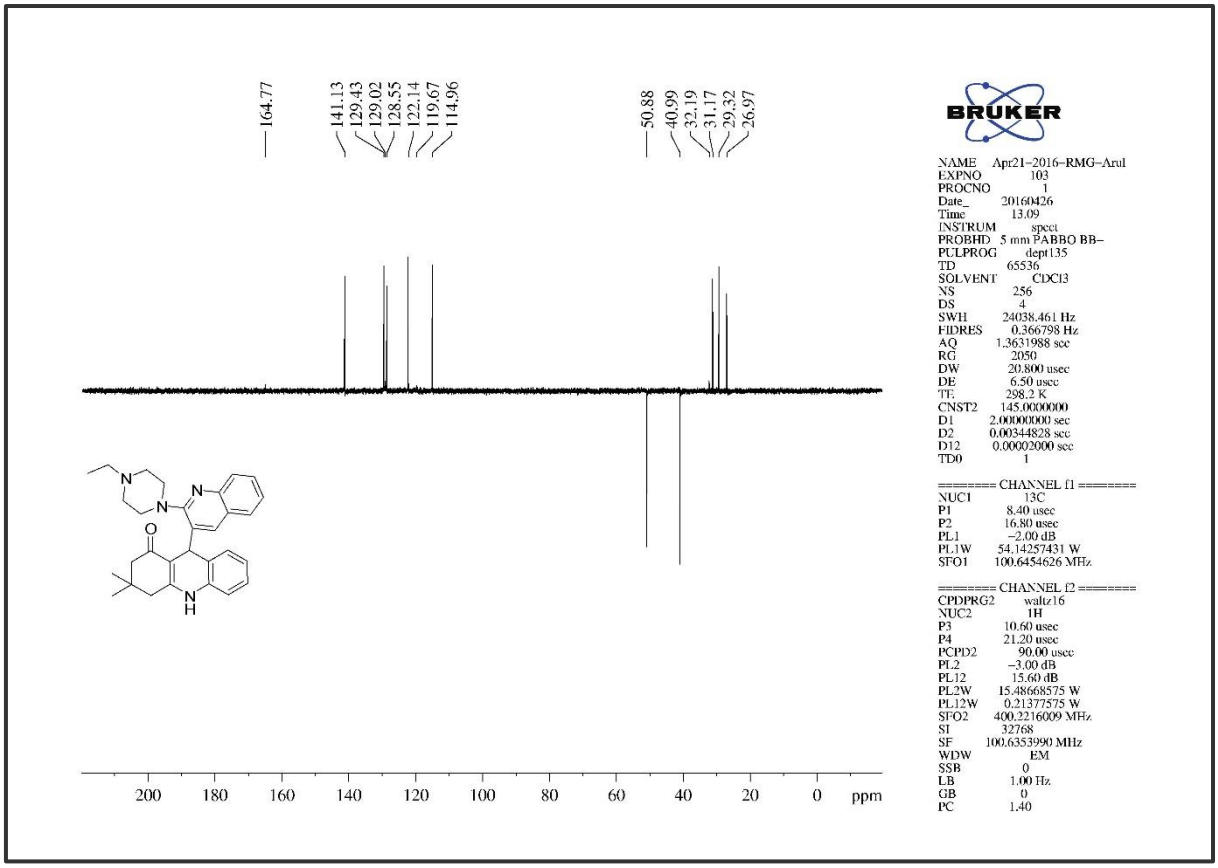

Figure 4B. S. 10. DEPT-135 NMR of compound 6a

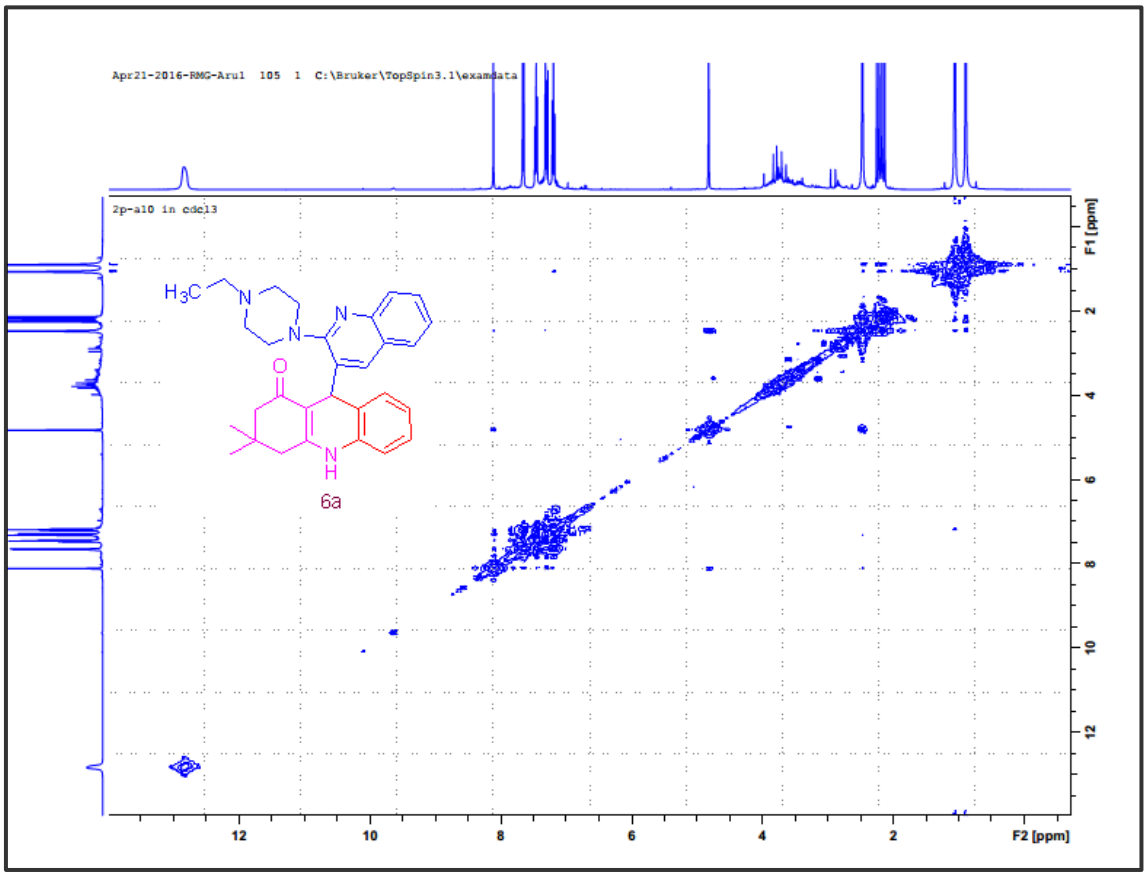

Figure 4B. S. 11. COSY NMR of compound 6a

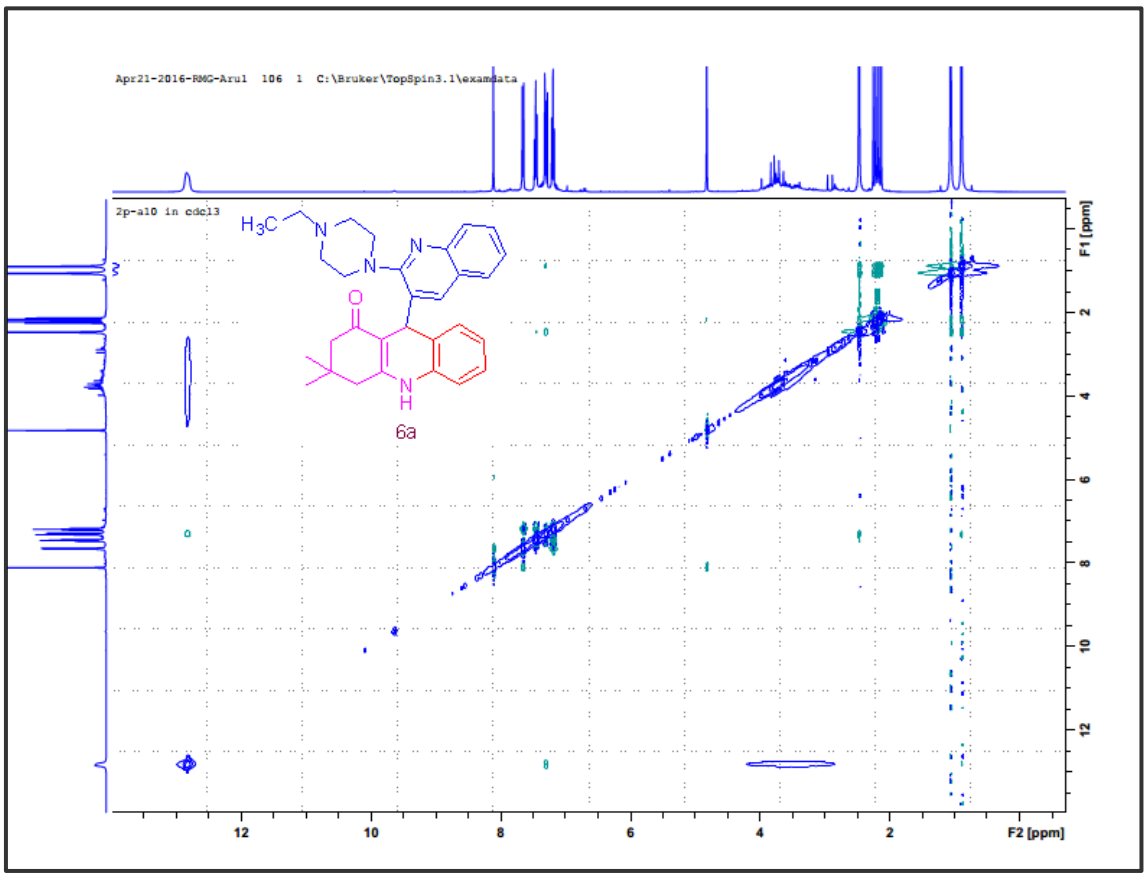

Figure 4B. S. 12. NOESY NMR of compound 6a

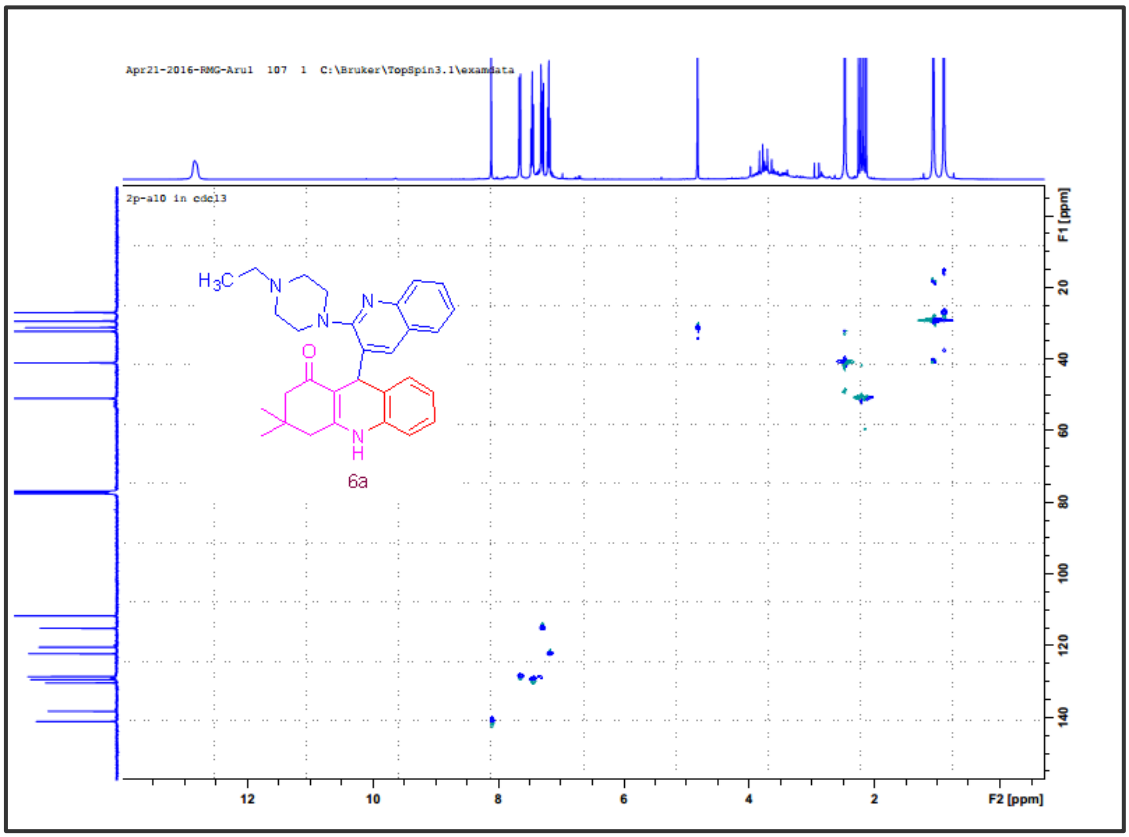

Figure 4B. S. 13. HSQCE NMR of compound 6a

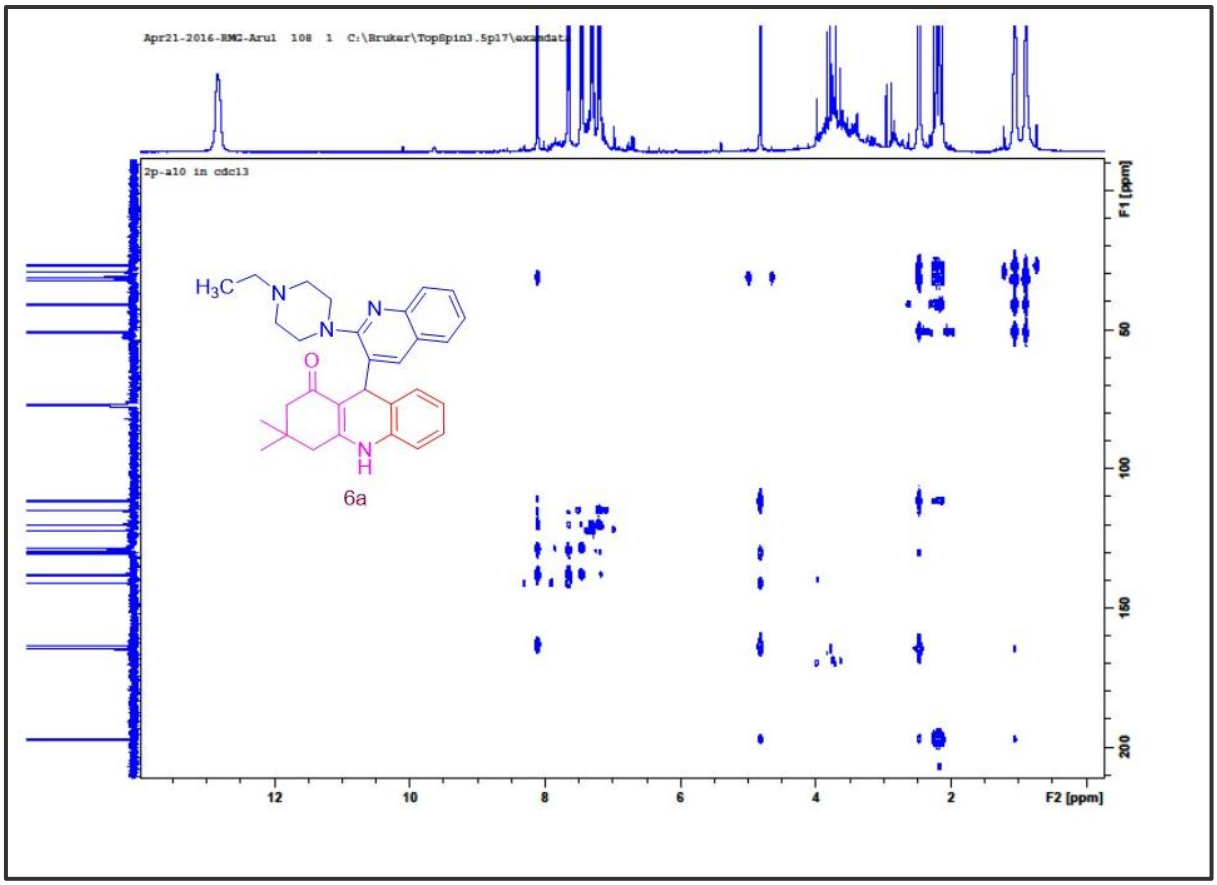

Figure 4B. S. 14. HMBC NMR of compound 6a

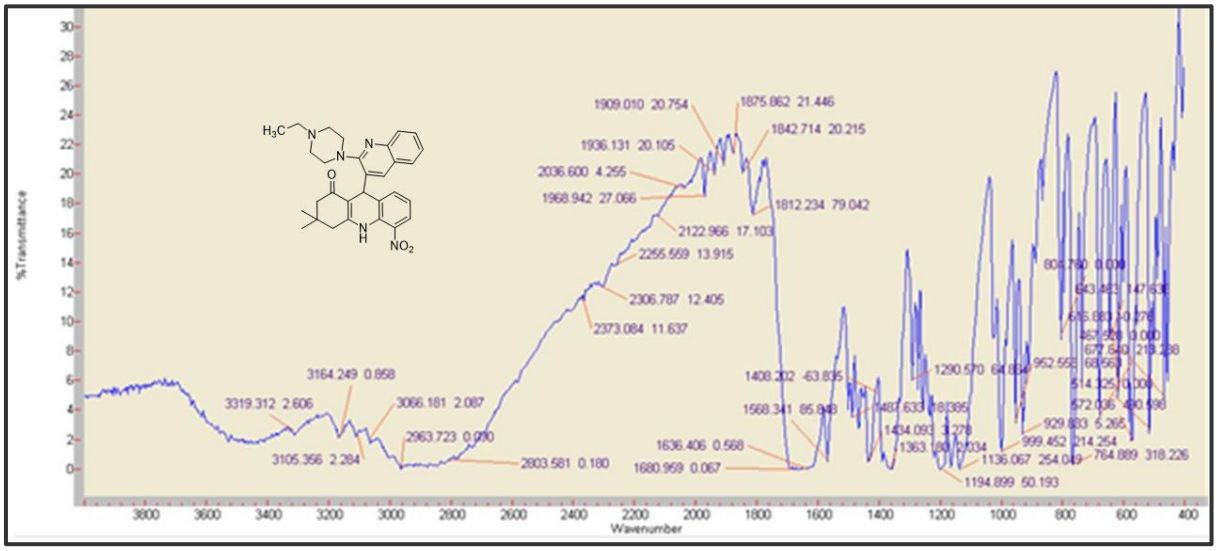

Figure 4B. S. 15. The Infra-Red Spectrum of compound 6b

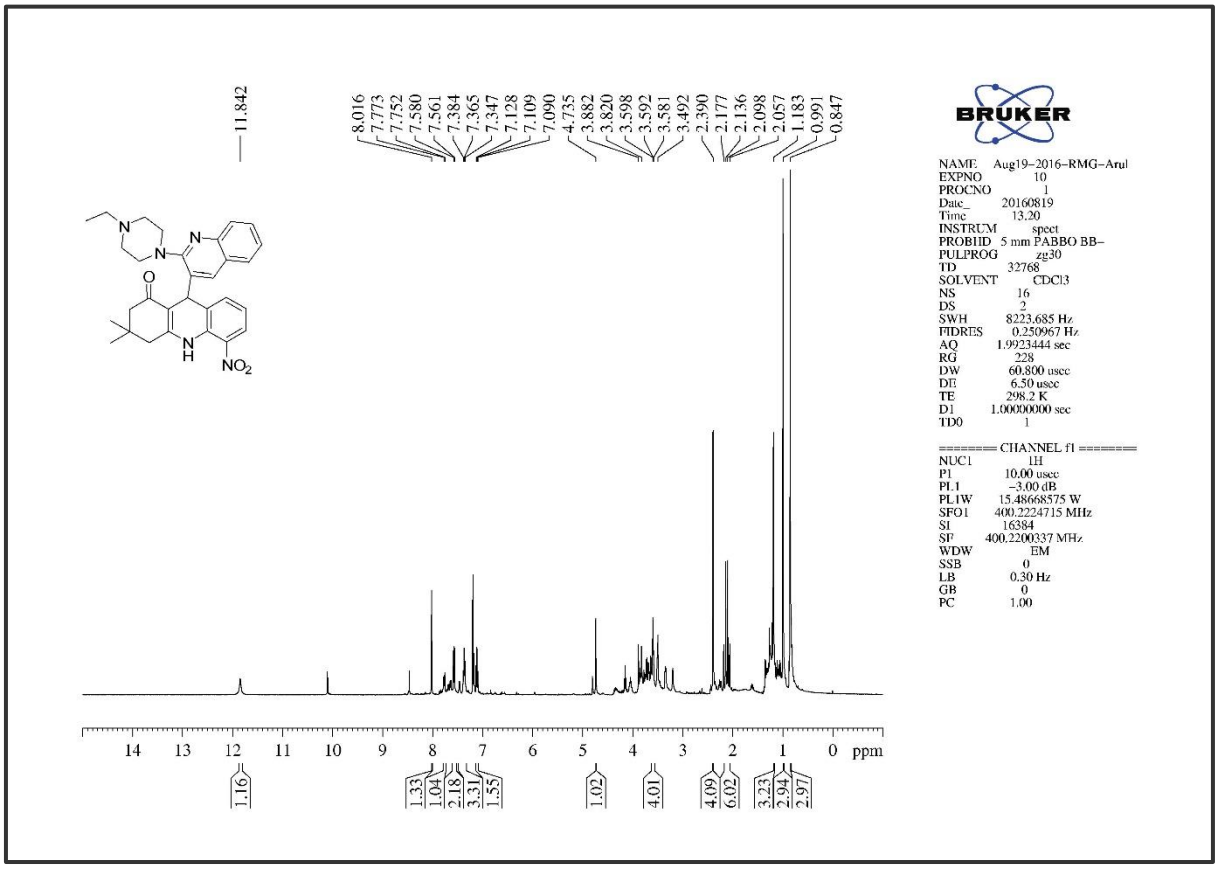

Figure 4B. S. 16. The ^{1}H NMR of compound 6b

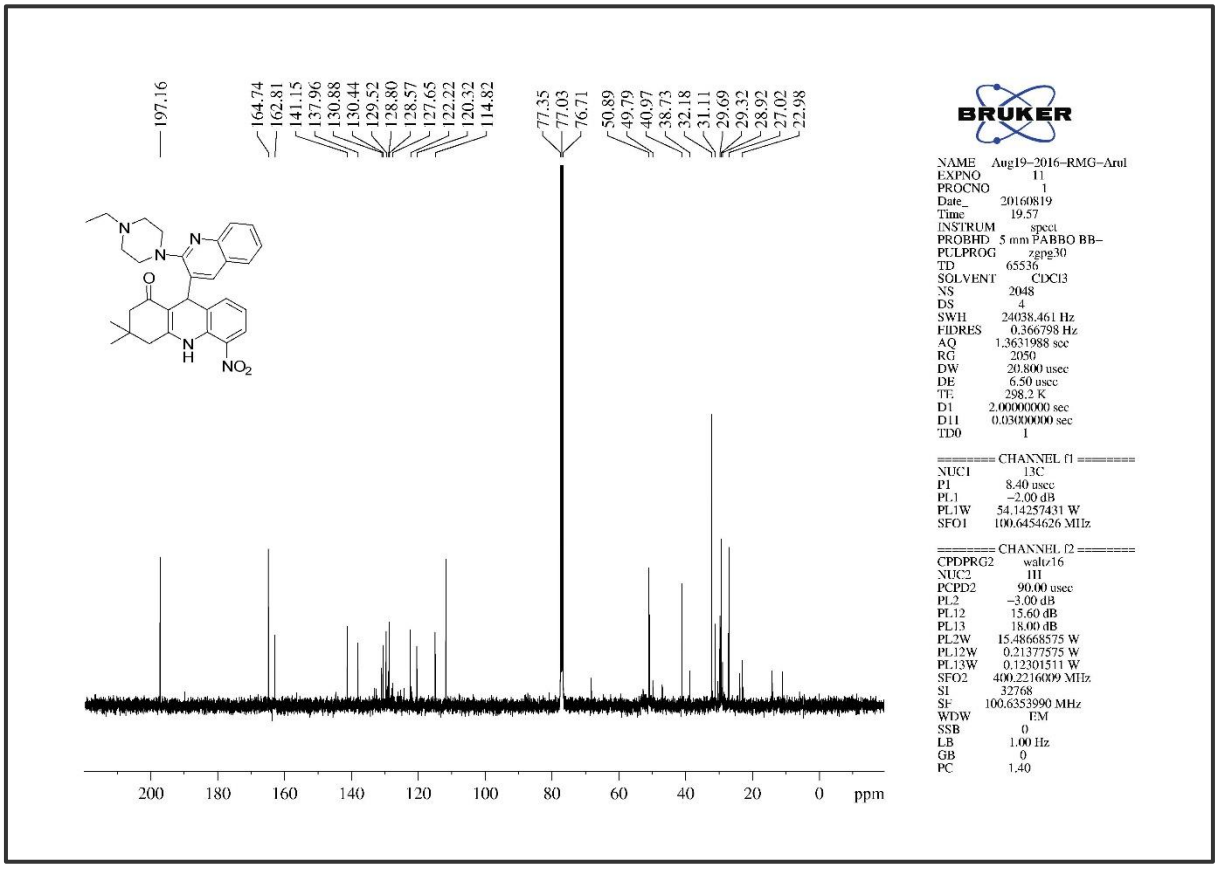

Figure 4B. S. 17. The ^{13}C NMR of compound 6b

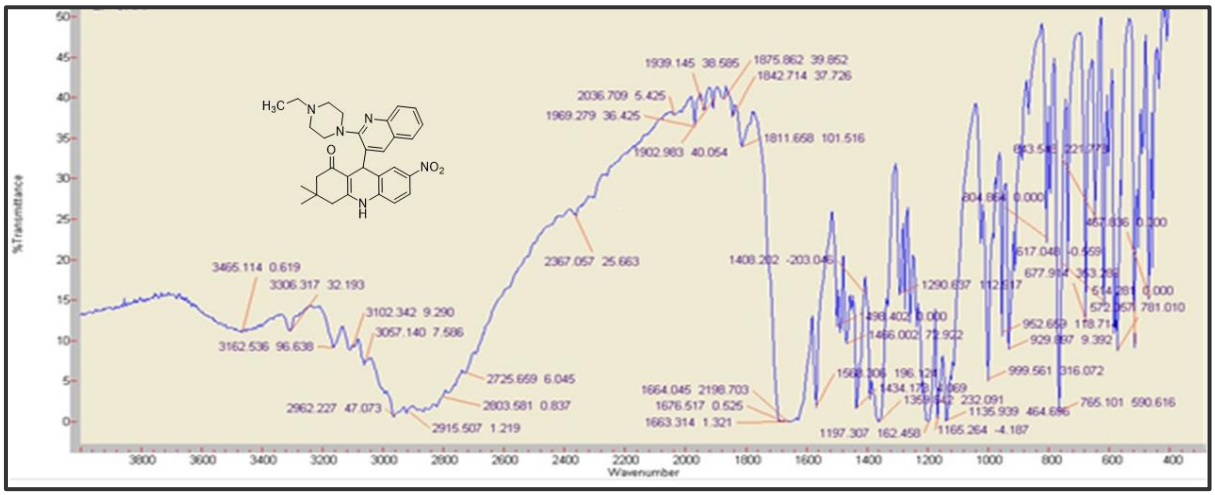

Figure 4B. S. 18. The Infra-Red Spectrum of compound 6c

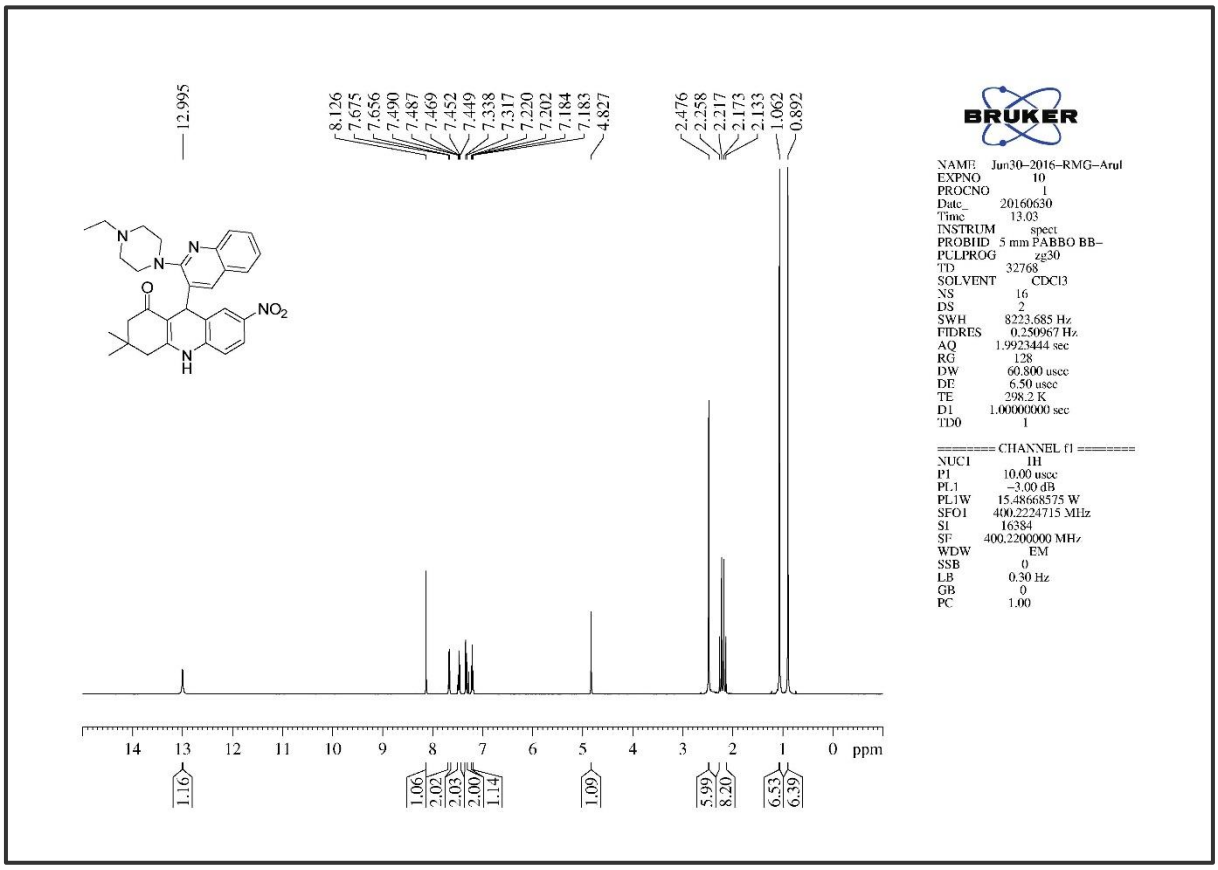

Figure 4B. S. 19. The ^{1}H NMR of compound 6c

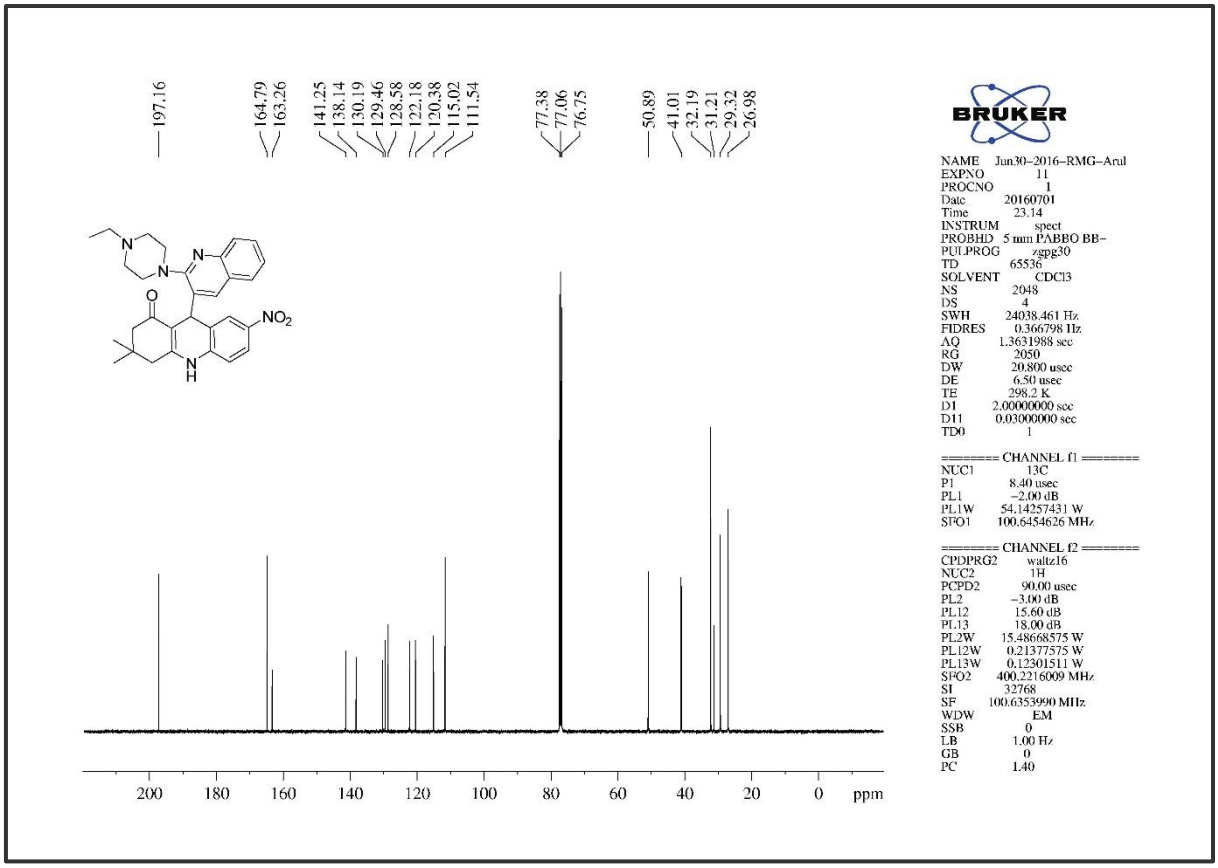

Figure 4B. S. 20. The ^{13}C NMR of compound 6c

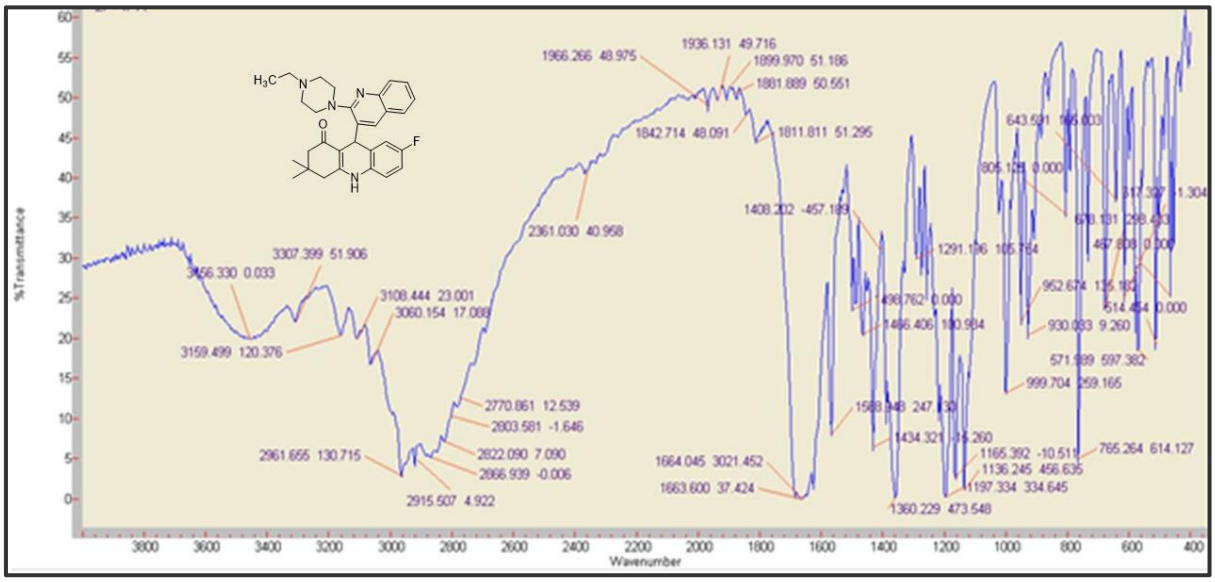

Figure 4B. S. 21. The Infra-Red Spectrum of compound 6d

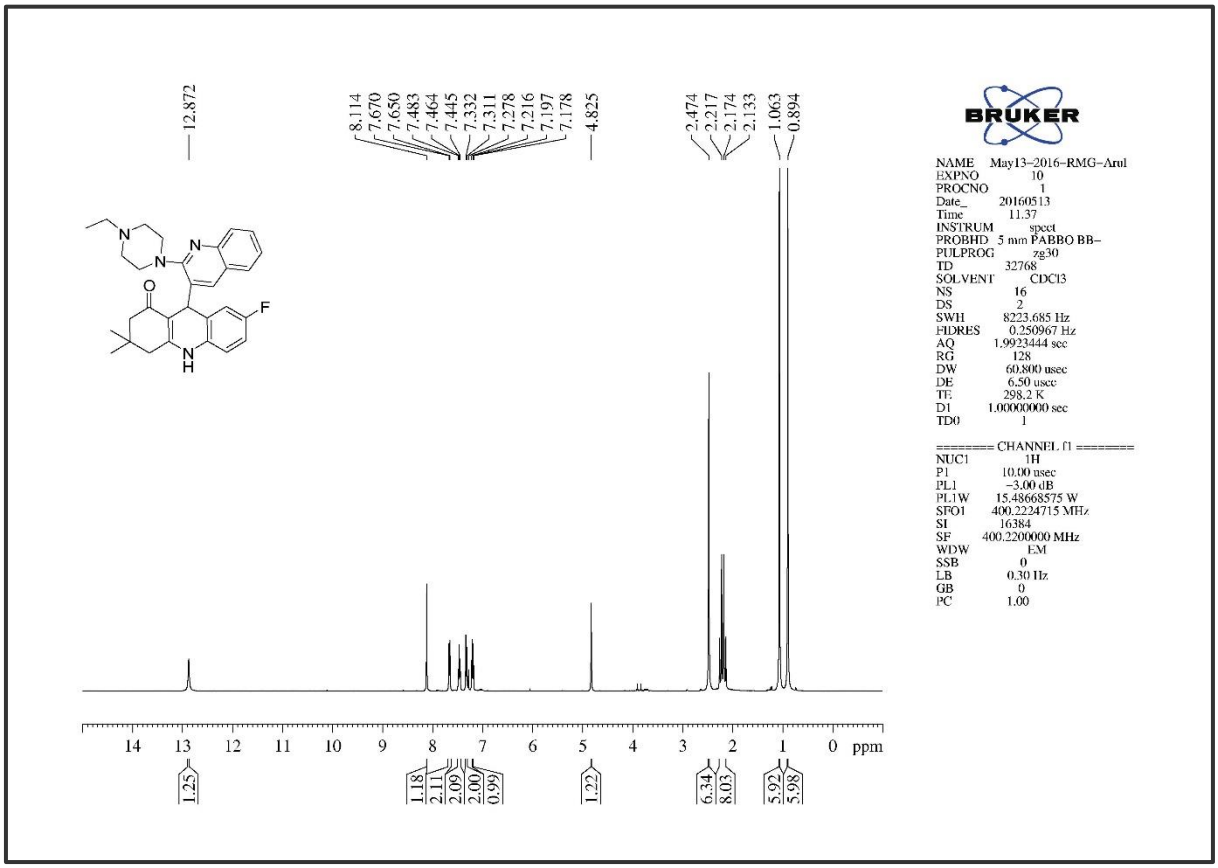

Figure 4B. S. 22. The ^{1}H NMR of compound 6d

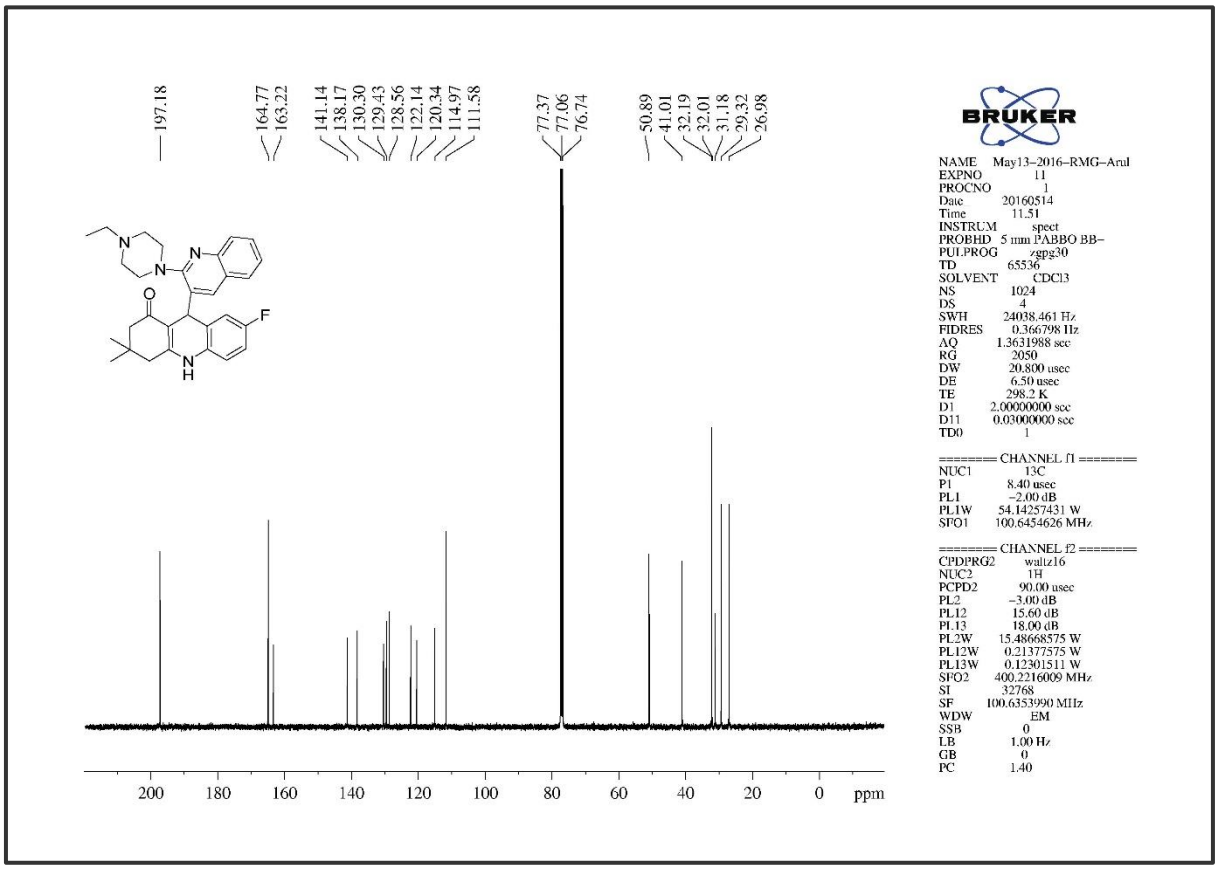

Figure 4B. S. 23. The ^{13}C NMR of compound 6d

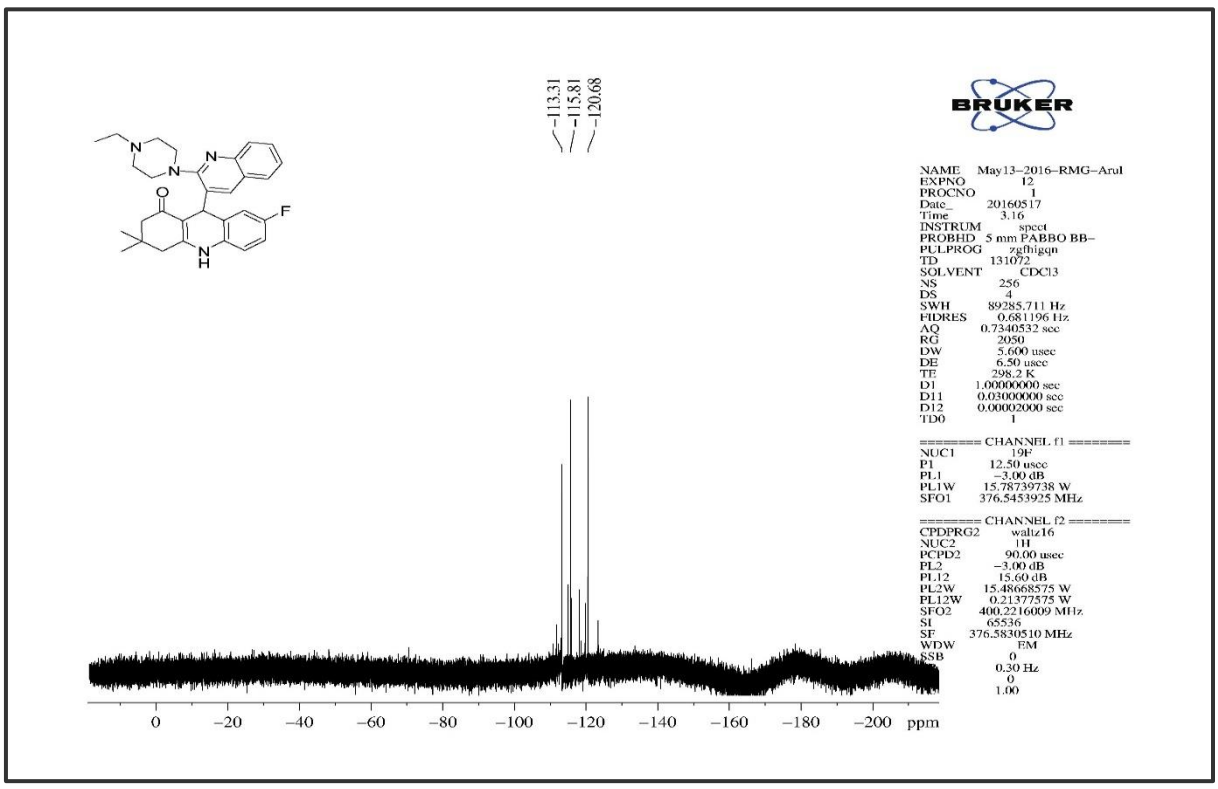

Figure 4B. S. 24. The ^{19}F NMR of compound 6d

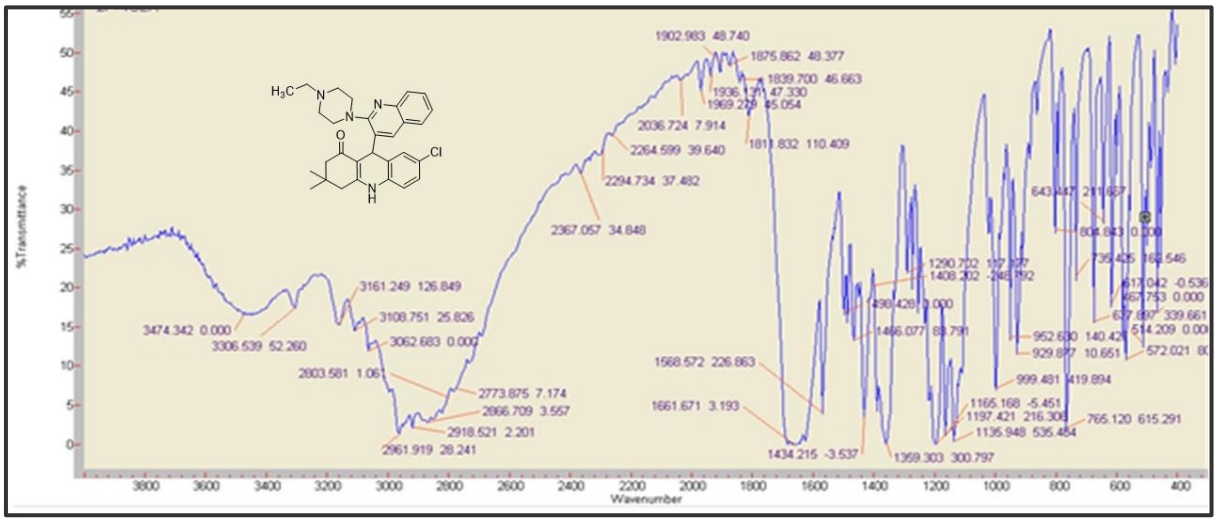

Figure 4B. S. 25. The Infra-Red Spectrum of compound 6e

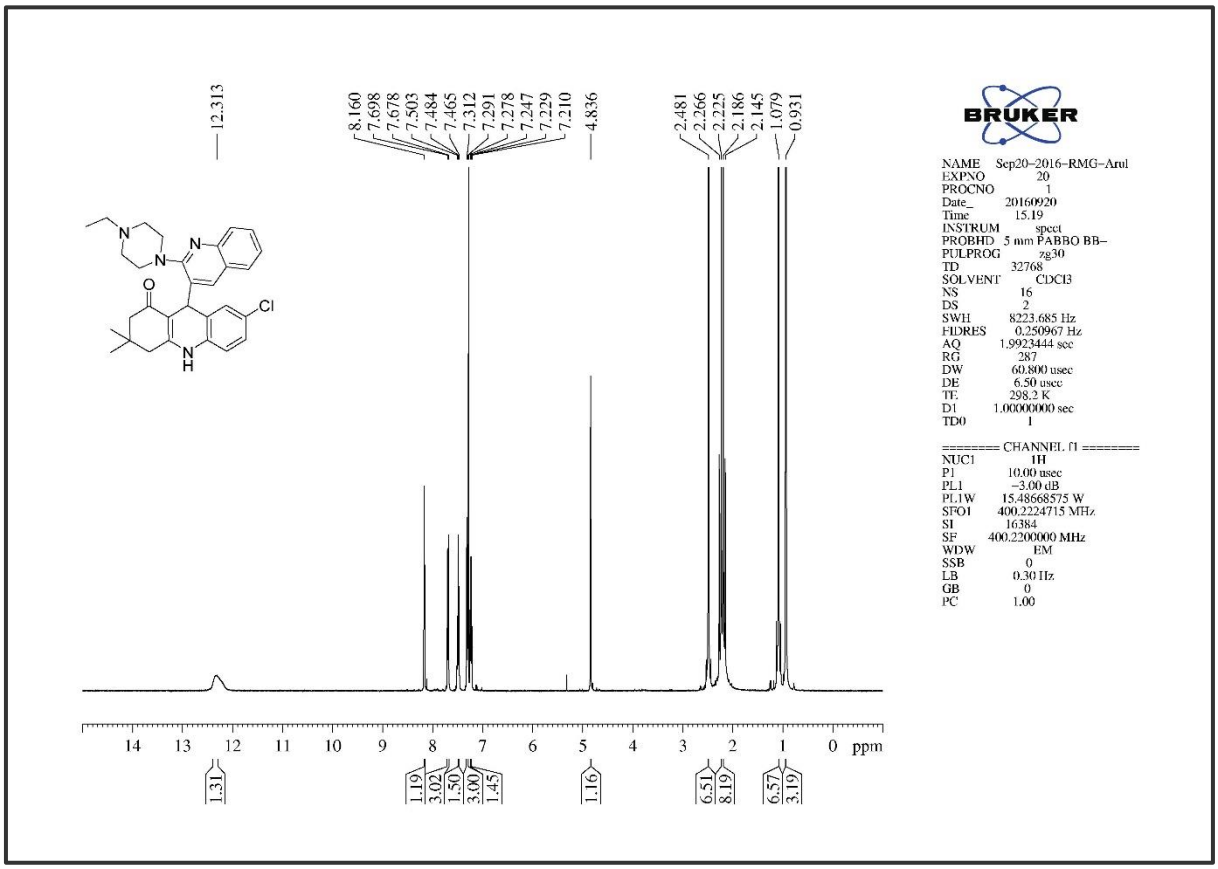

Figure 4B. S. 26. The ^{1}H NMR of compound 6e

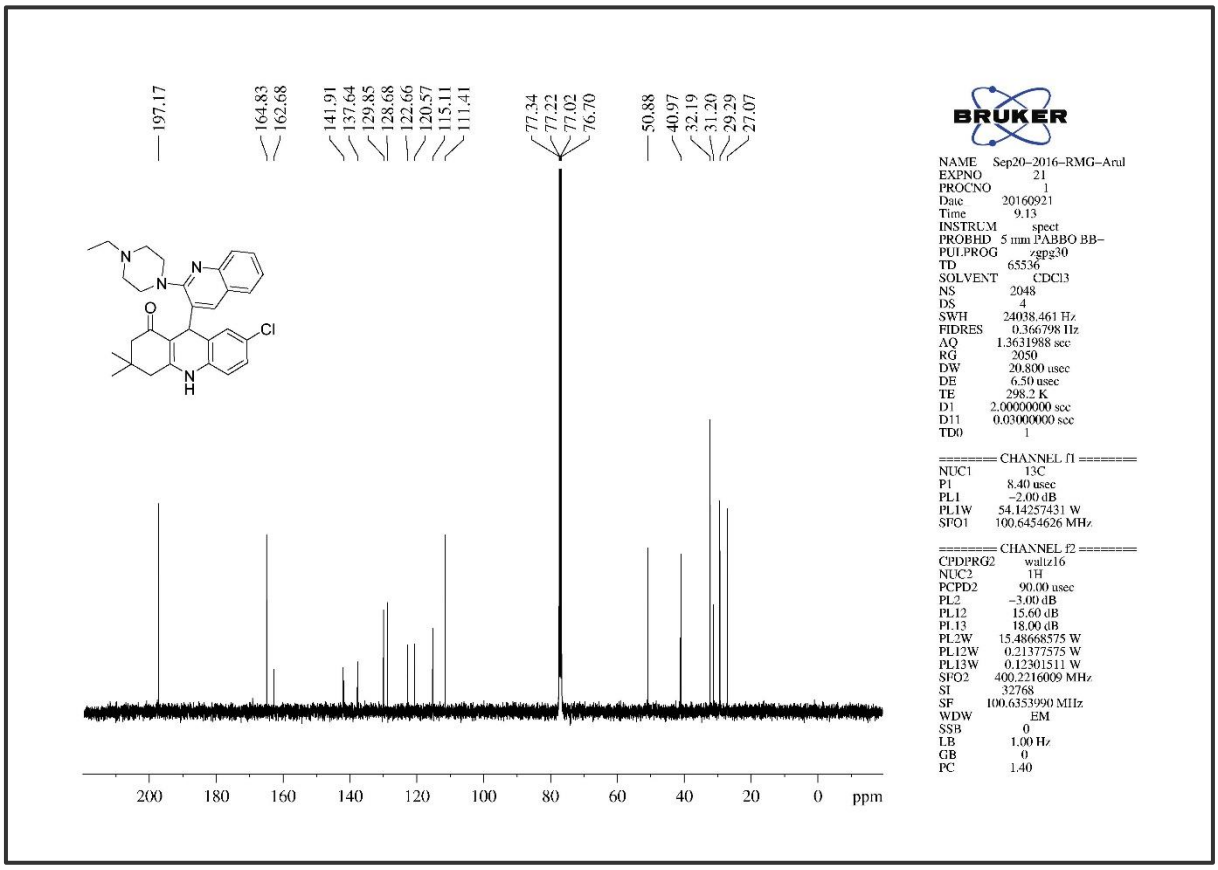

Figure 4B. S. 27. The ^{13}C NMR of compound 6e

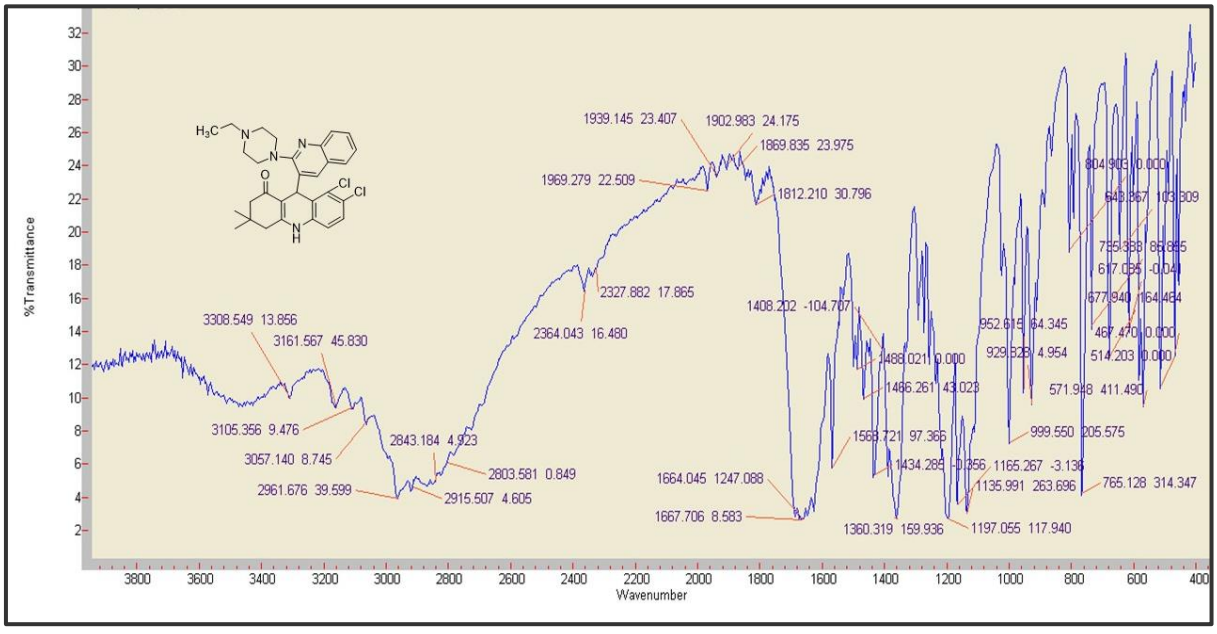

Figure 4B. S. 28. The Infra-Red Spectrum of compound 6f

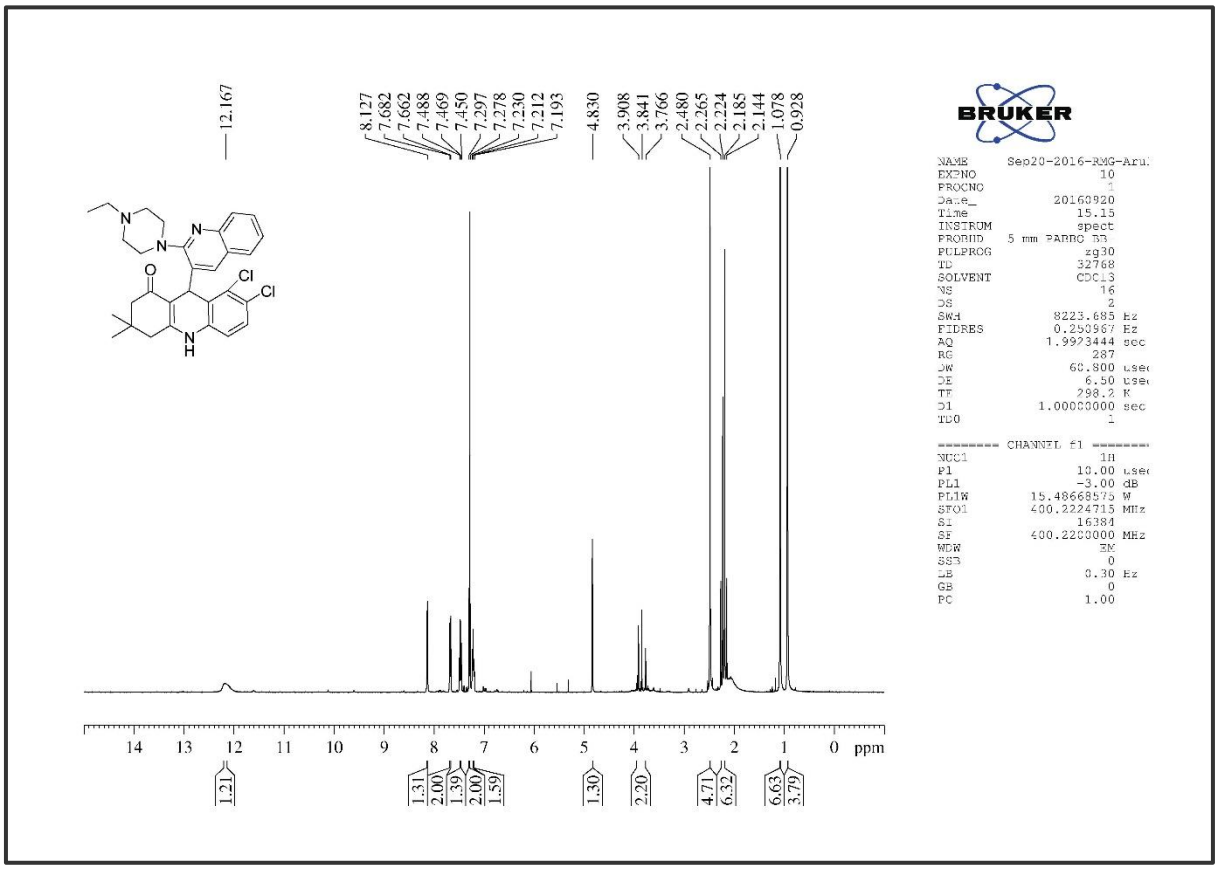

Figure 4B. S. 29. The ^{1}H NMR of compound 6f

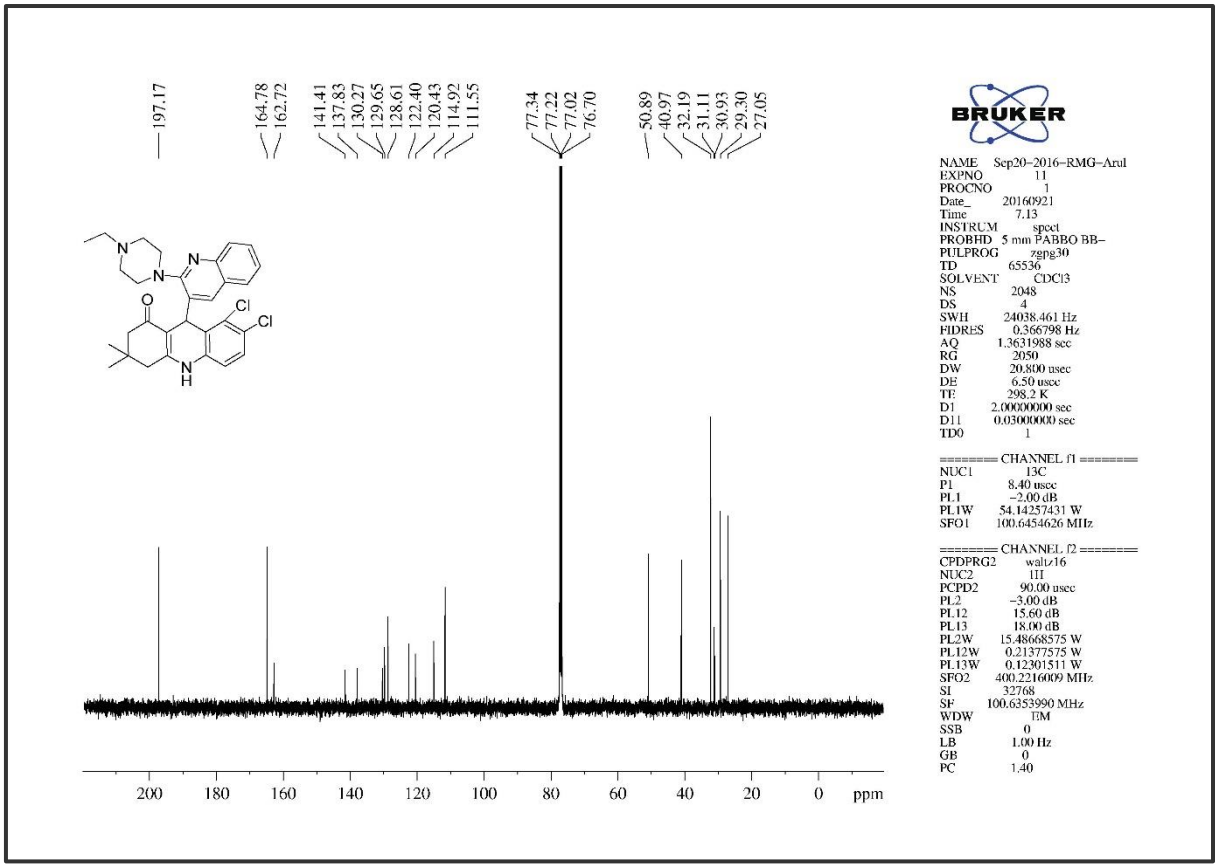

Figure 4B. S. 30. The ^{13}C NMR of compound 6f

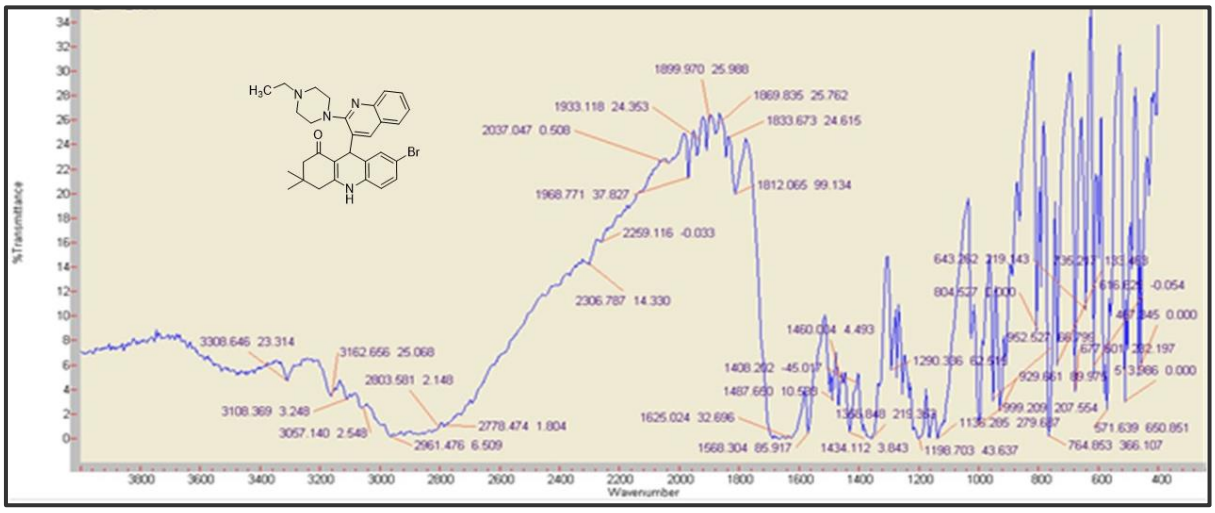

Figure 4B. S. 31. The Infra-Red Spectrum of compound 6g

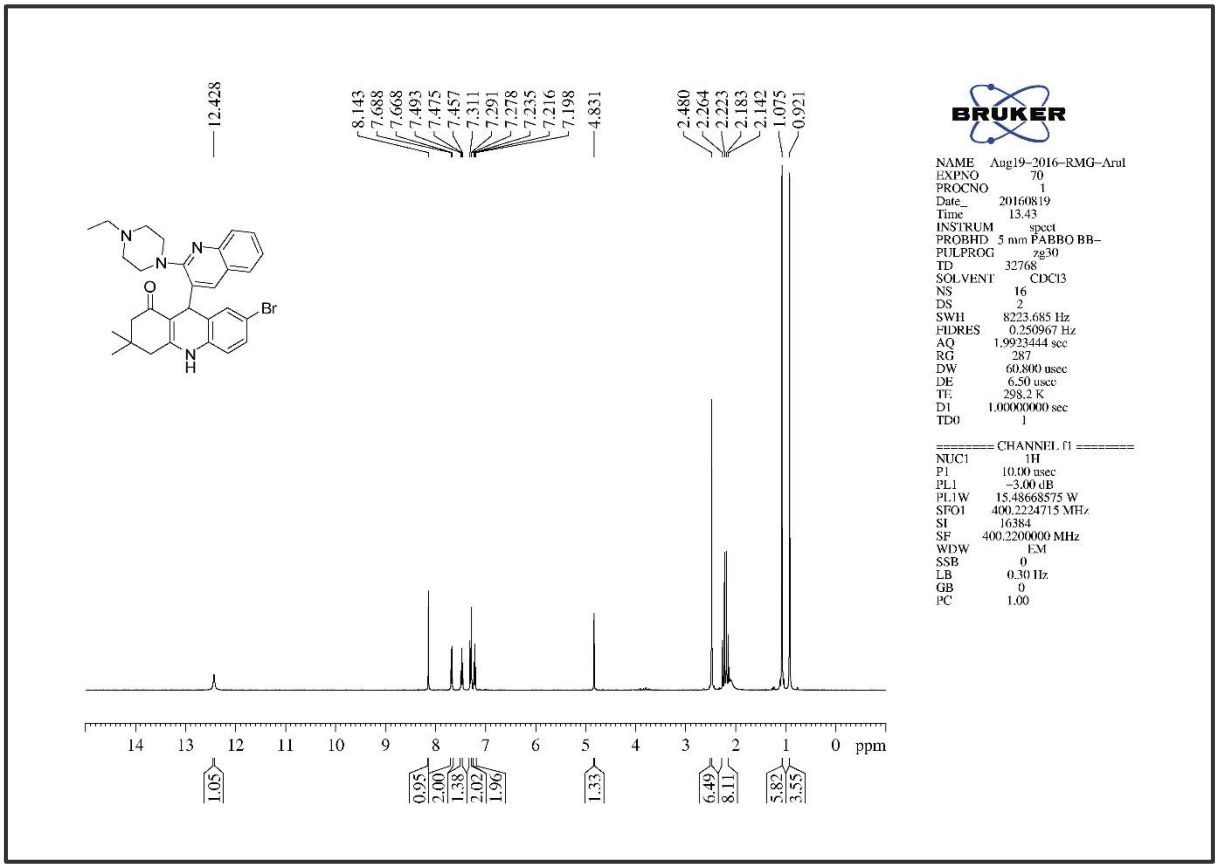

Figure 4B. S. 32. The ^{1}H NMR of compound 6g

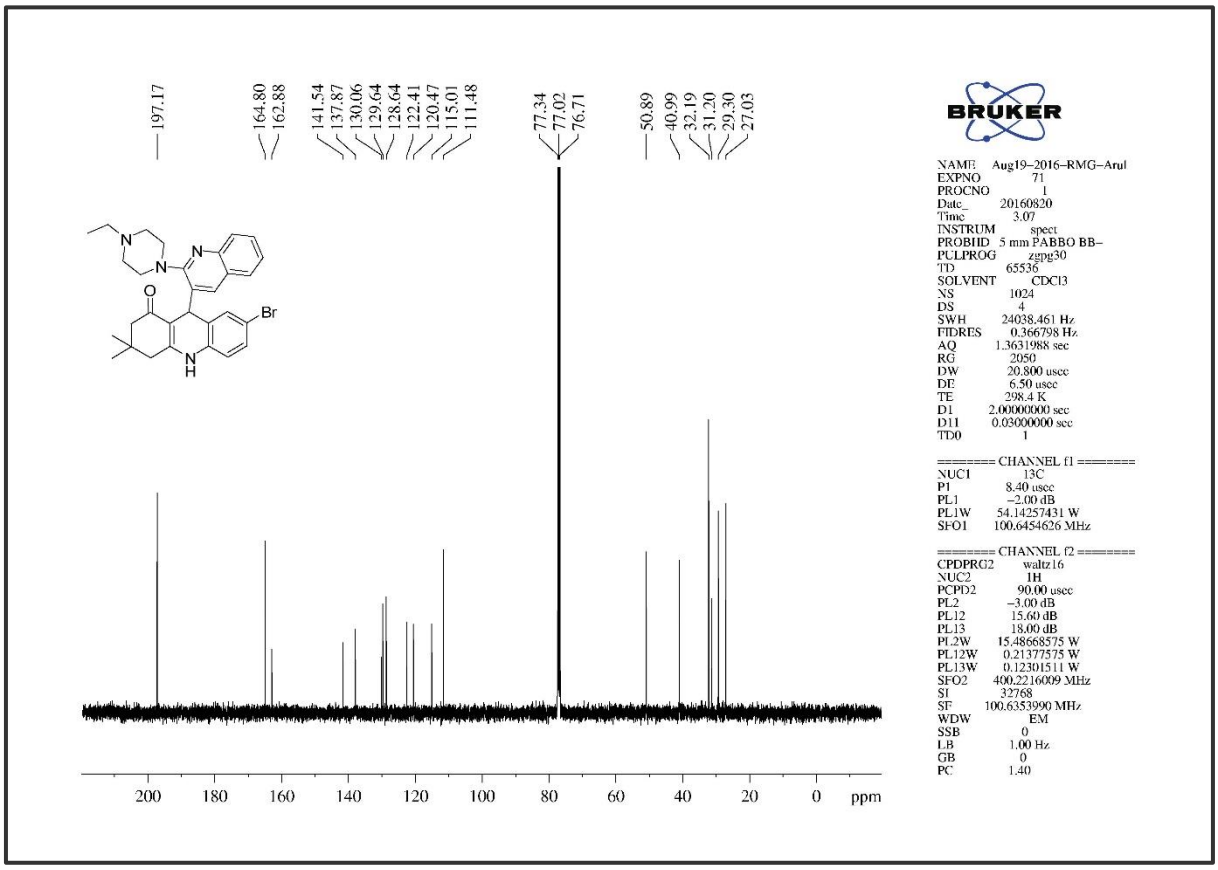

Figure 4B. S. 33. The ^{13}C NMR of compound 6g

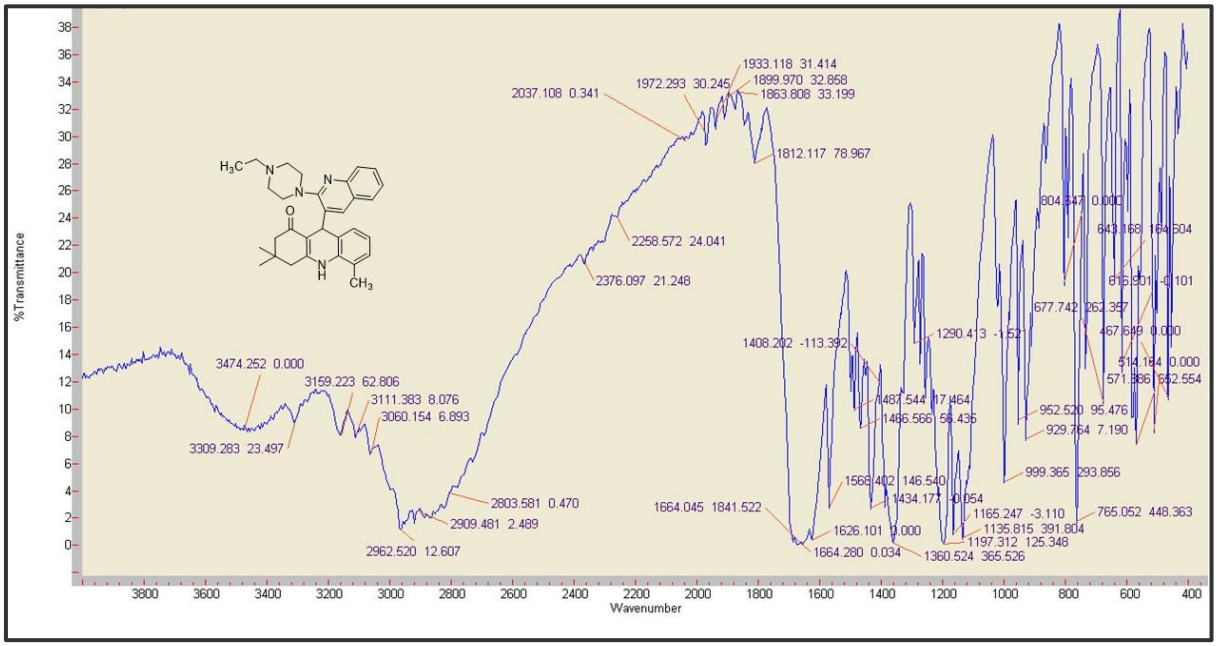

Figure 4B. S. 34. The Infra-Red Spectrum of compound 6h

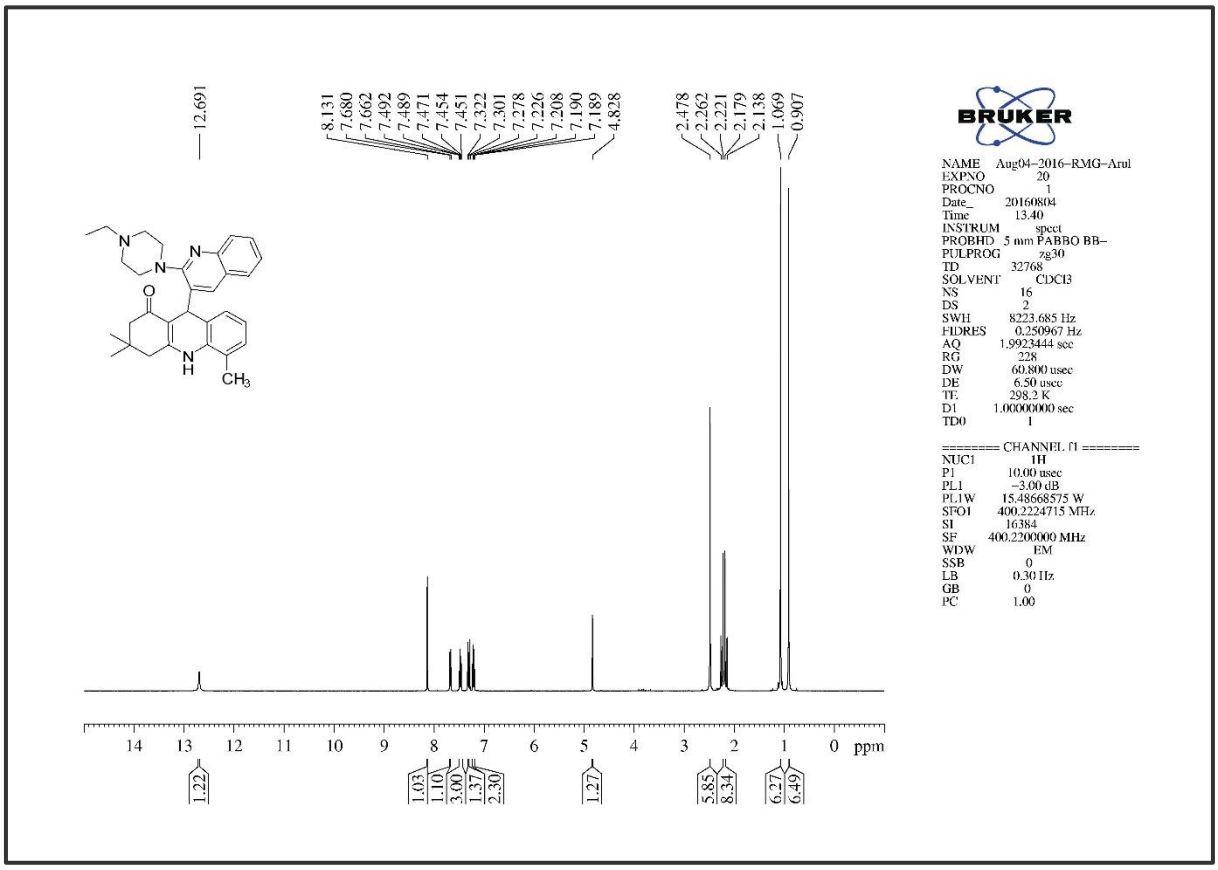

Figure 4B. S. 35. The ^{1}H NMR of compound 6h

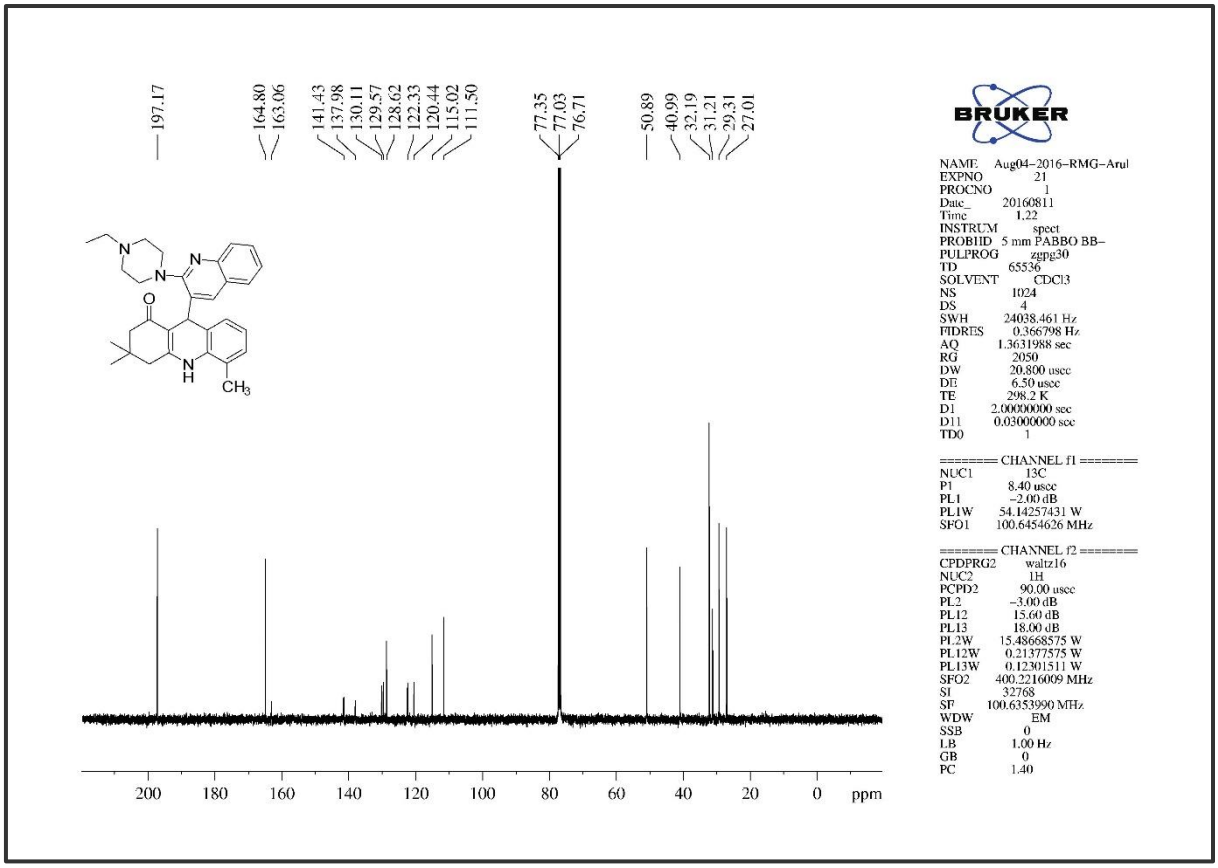

Figure 4B. S. 36. The ^{13}C NMR of compound 6h

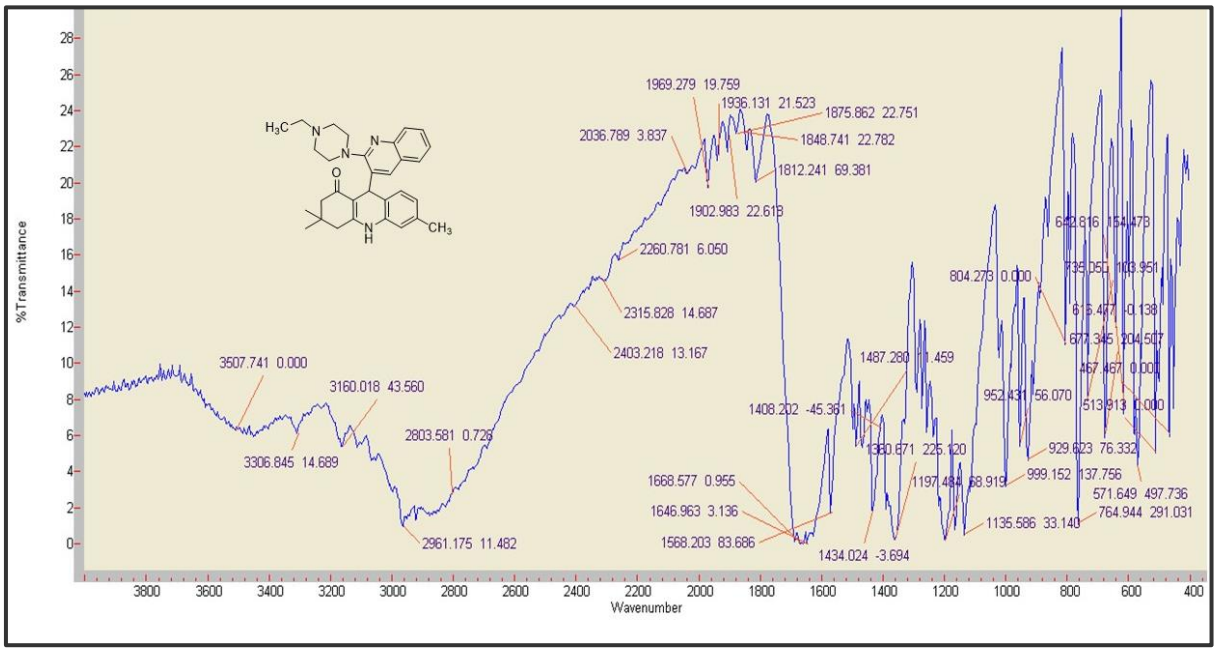

Figure 4B. S. 37. The Infra-Red Spectrum of compound 6i

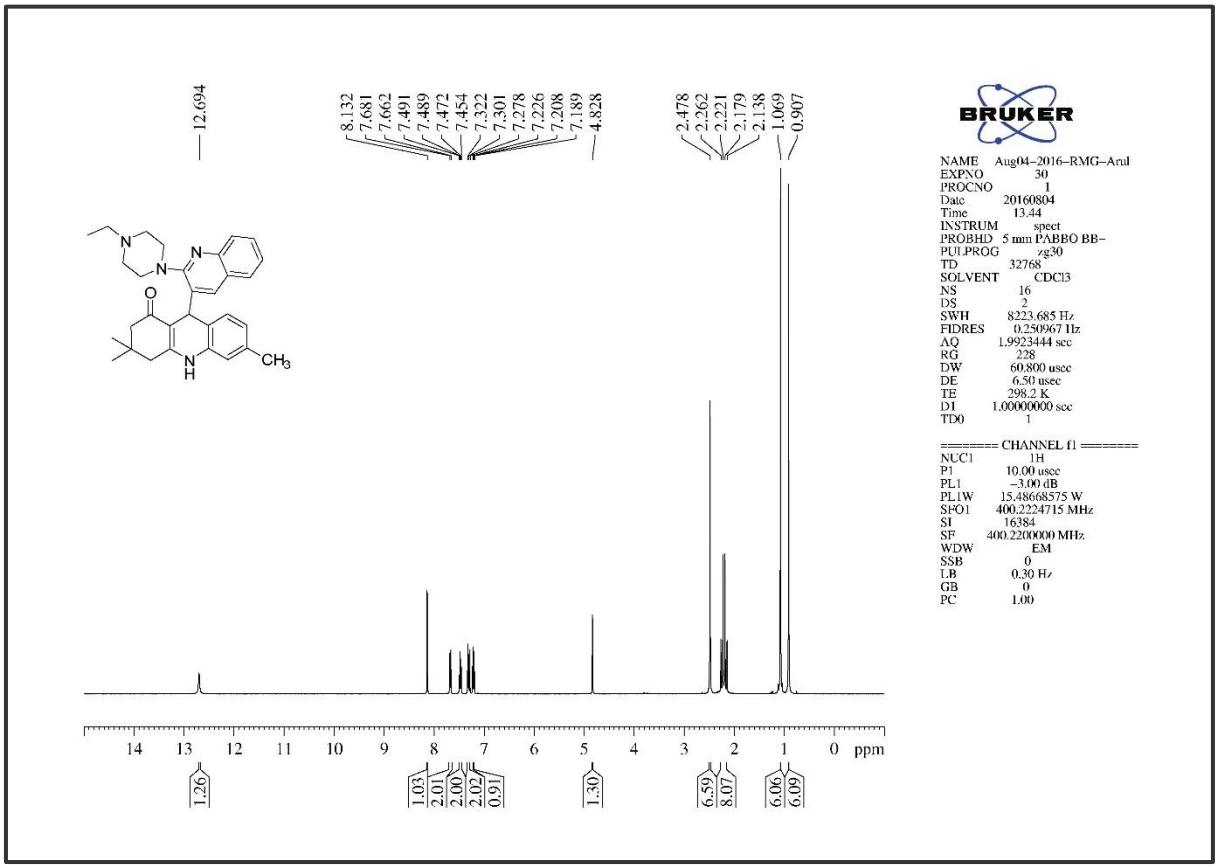

Figure 4B. S. 38. The ^{1}H NMR of compound 6i

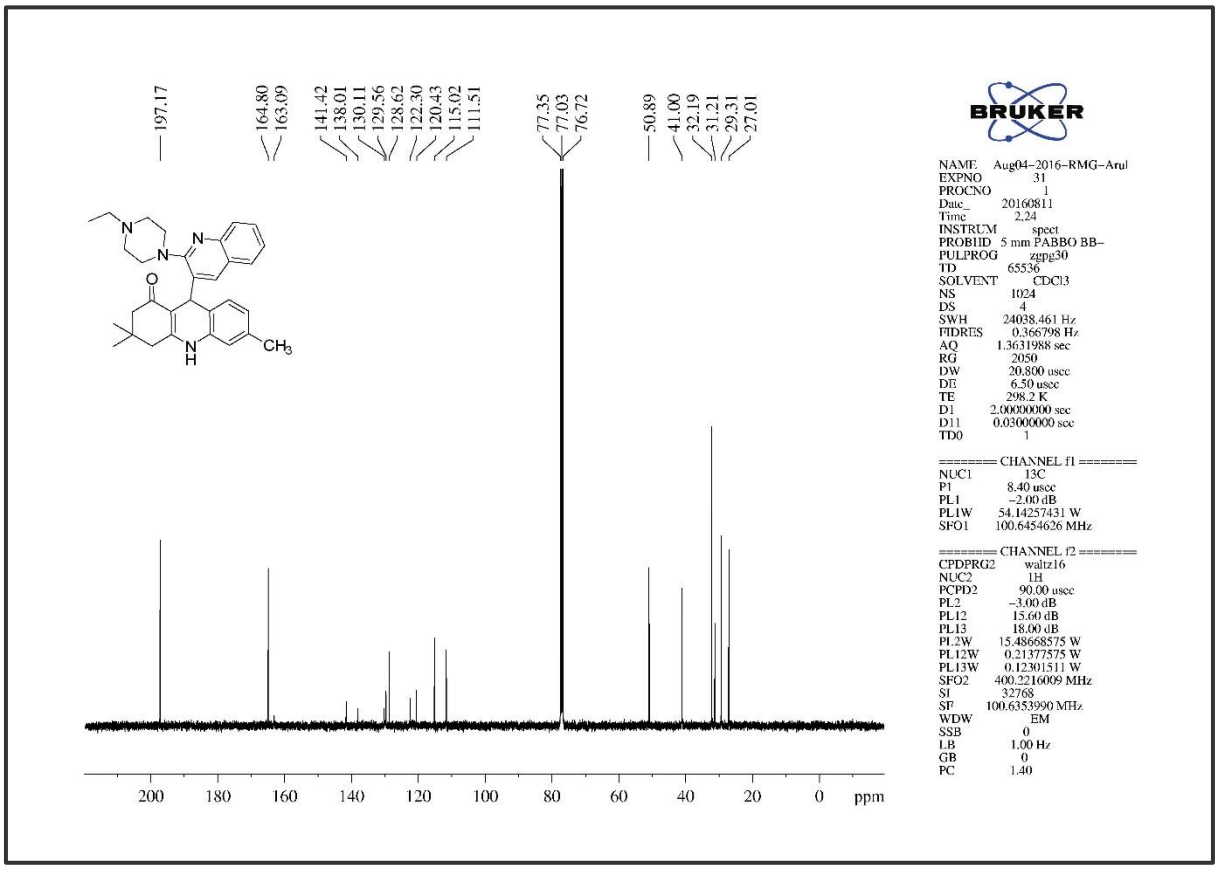

Figure 4B. S. 39. The ^{13}C NMR of compound 6i

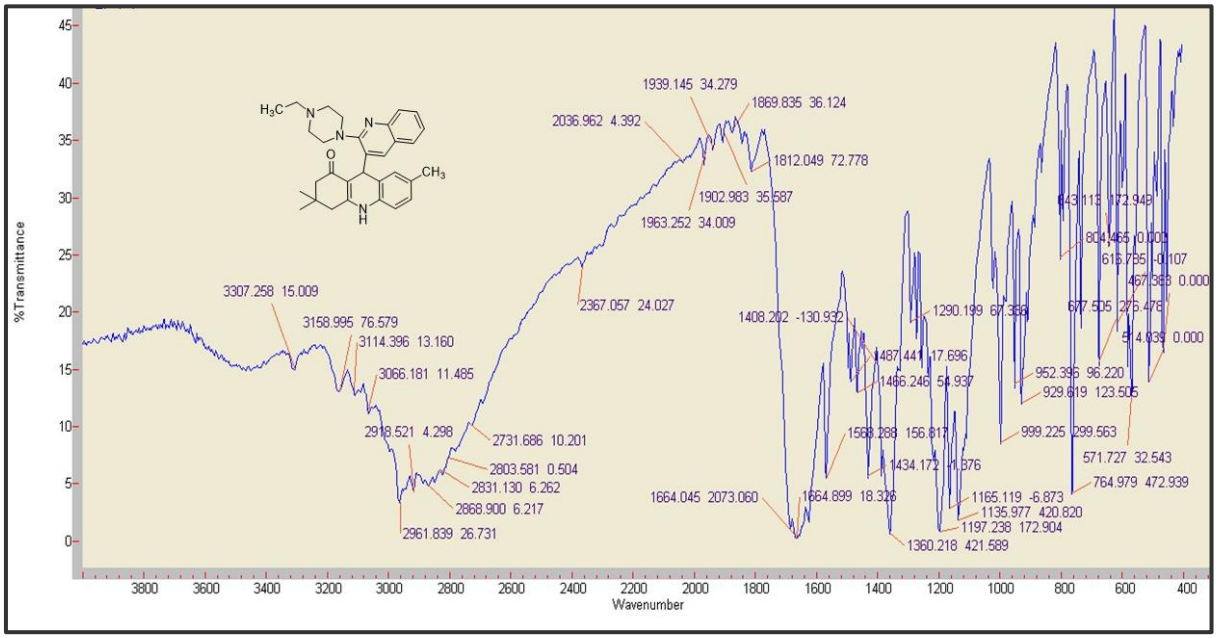

Figure 4B. S. 40. The Infra-Red Spectrum of compound 6j

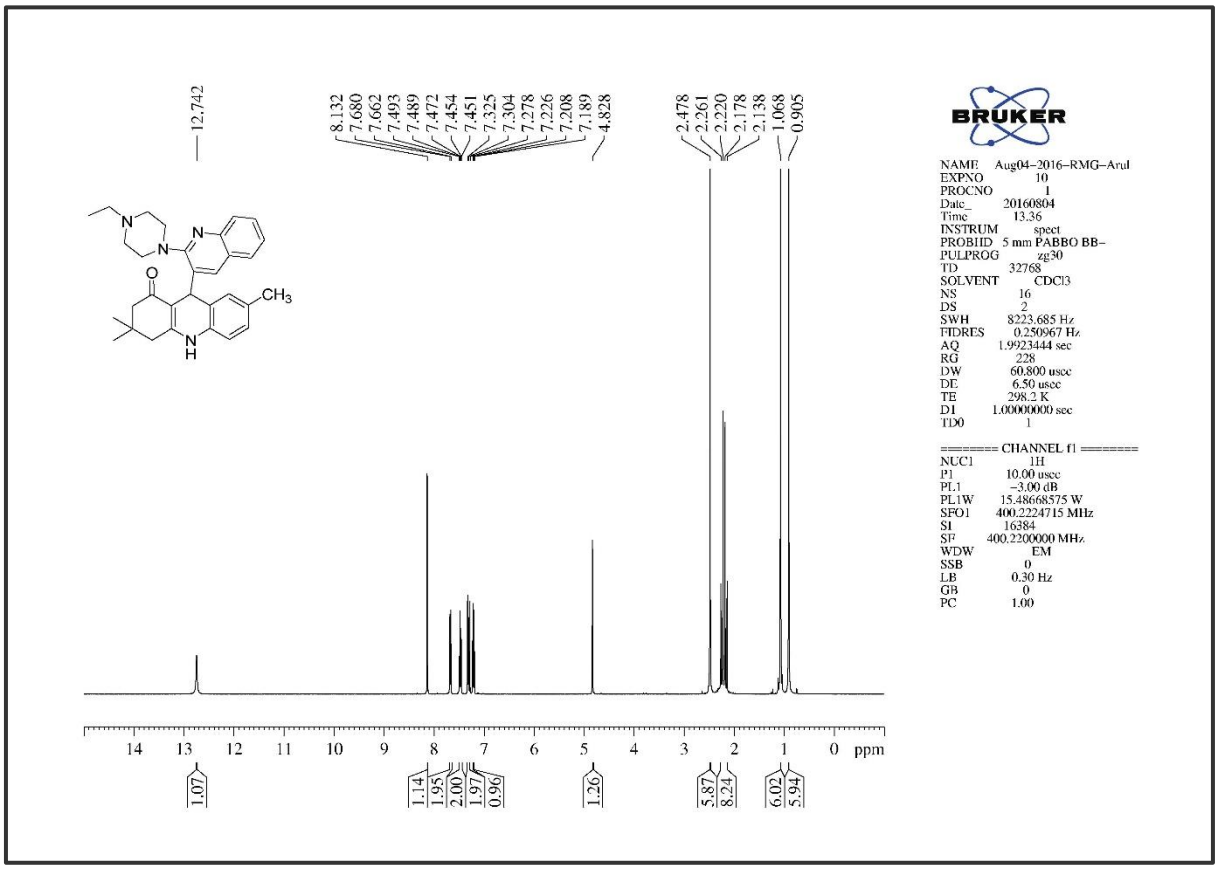

Figure 4B. S. 41. The ^{1}H NMR of compound 6j

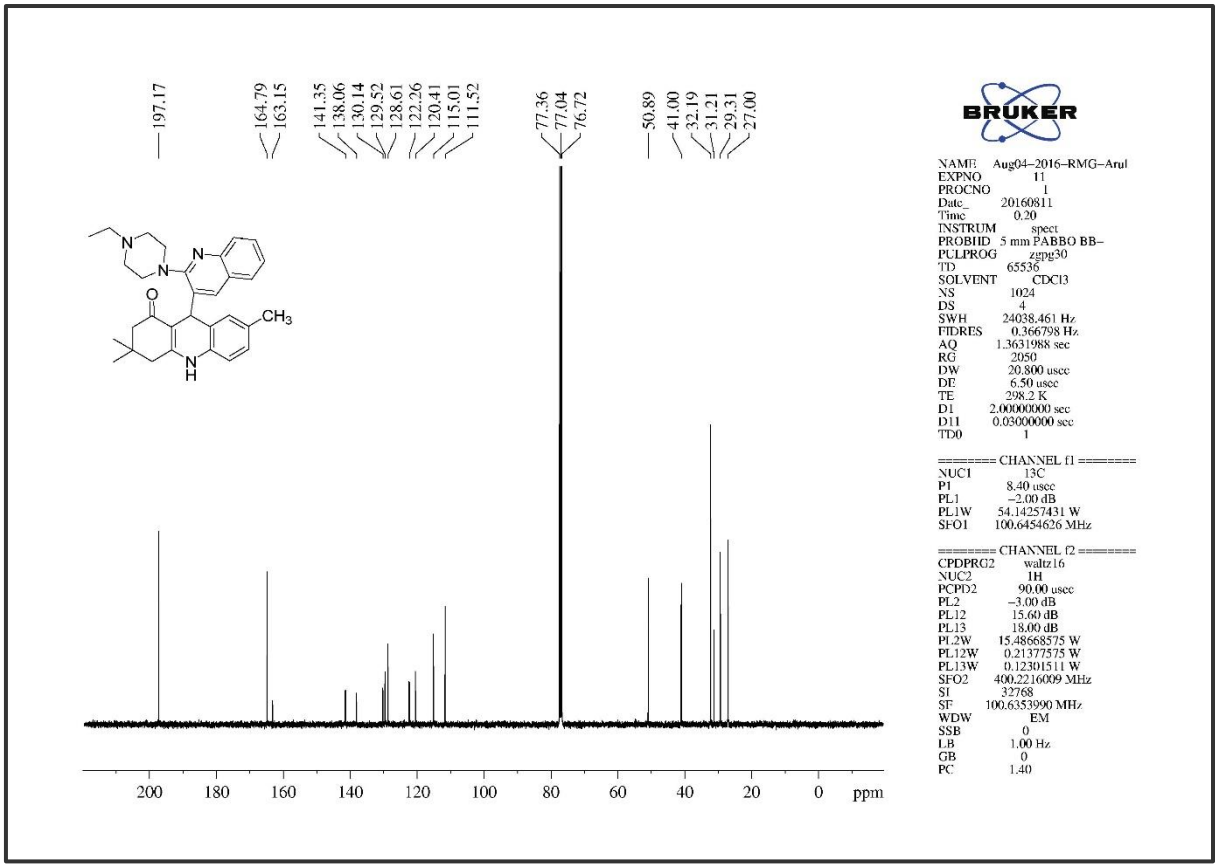

Figure 4B. S. 42. The ^{13}C NMR of compound 6j

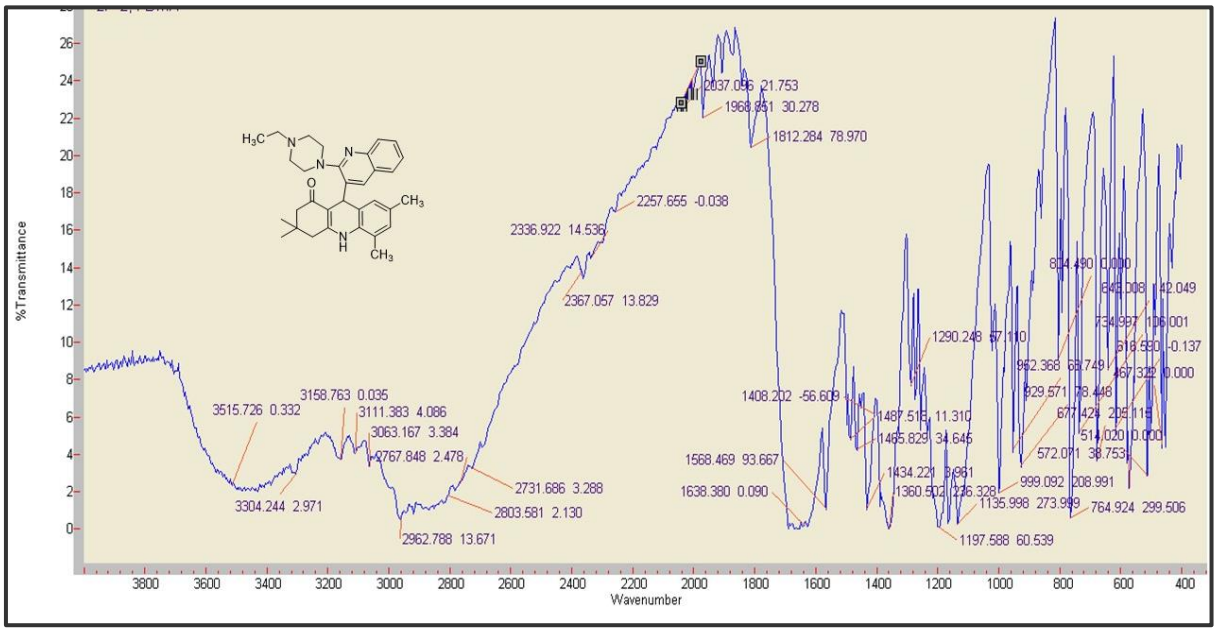

Figure 4B. S. 43. The Infra-Red Spectrum of compound 6k

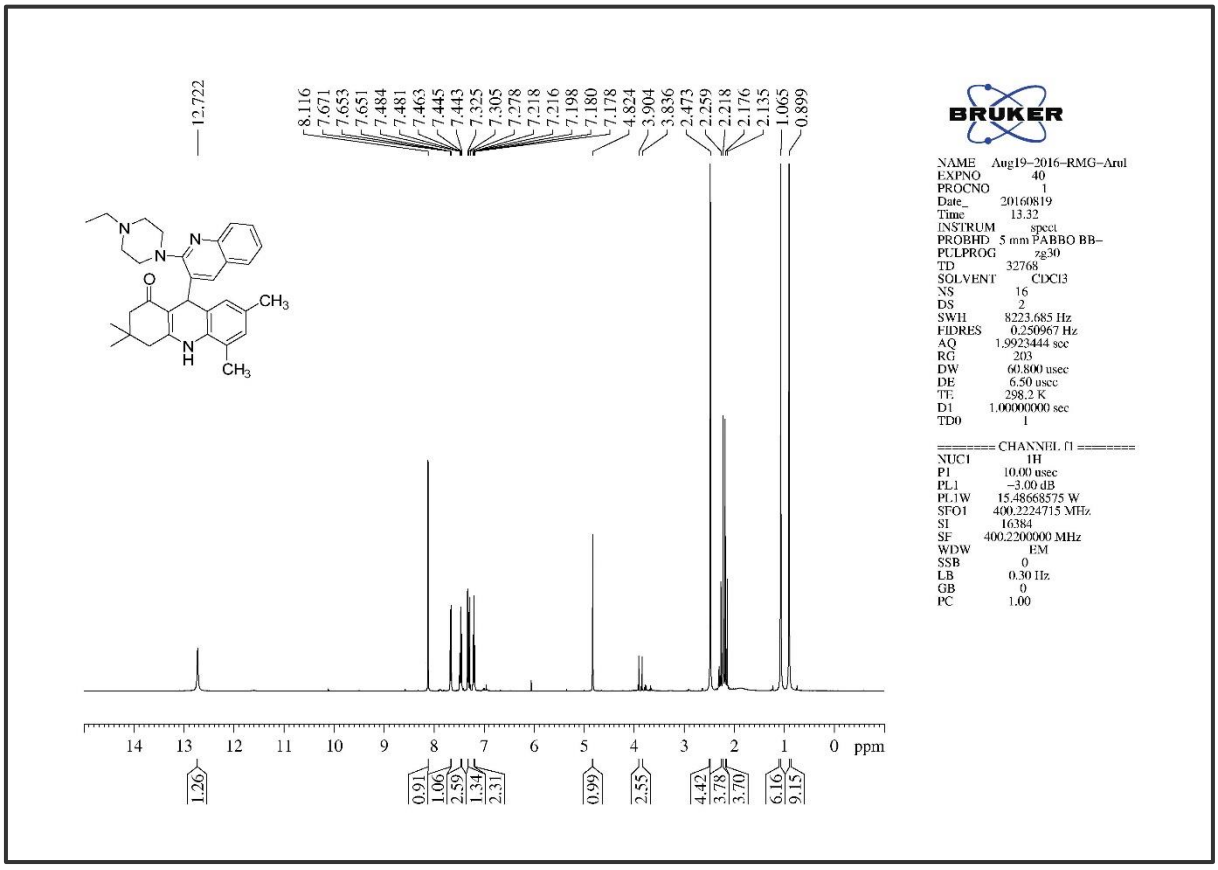

Figure 4B. S. 44. The ^{1}H NMR of compound 6k

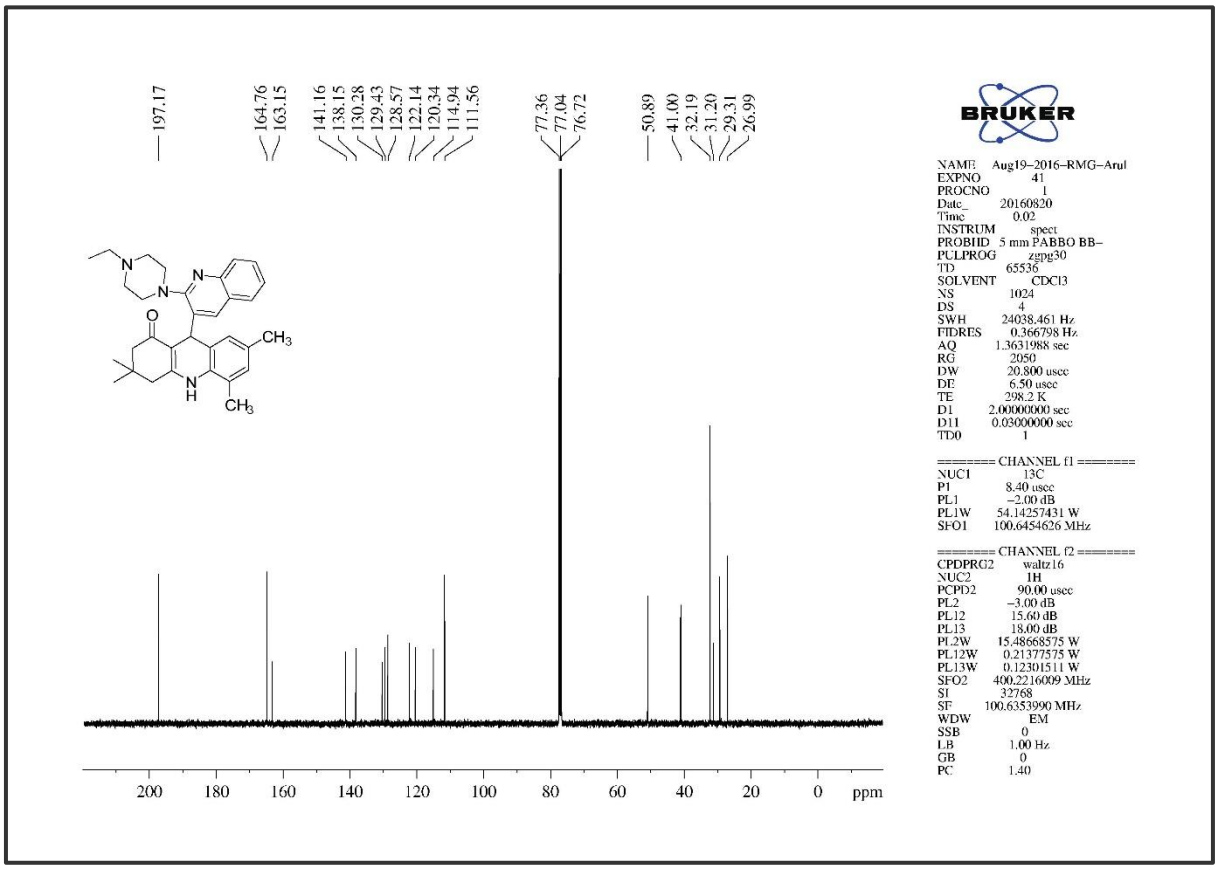

Figure 4B. S. 45. The ^{13}C NMR of compound 6k

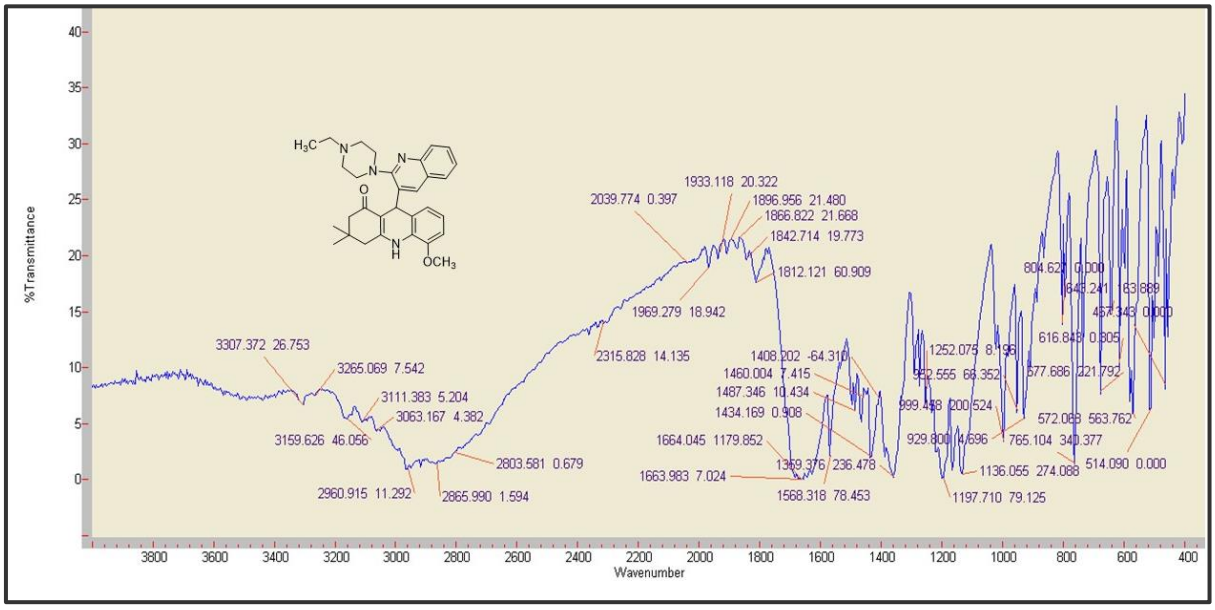

Figure 4B. S. 46. The Infra-Red Spectrum of compound 6l

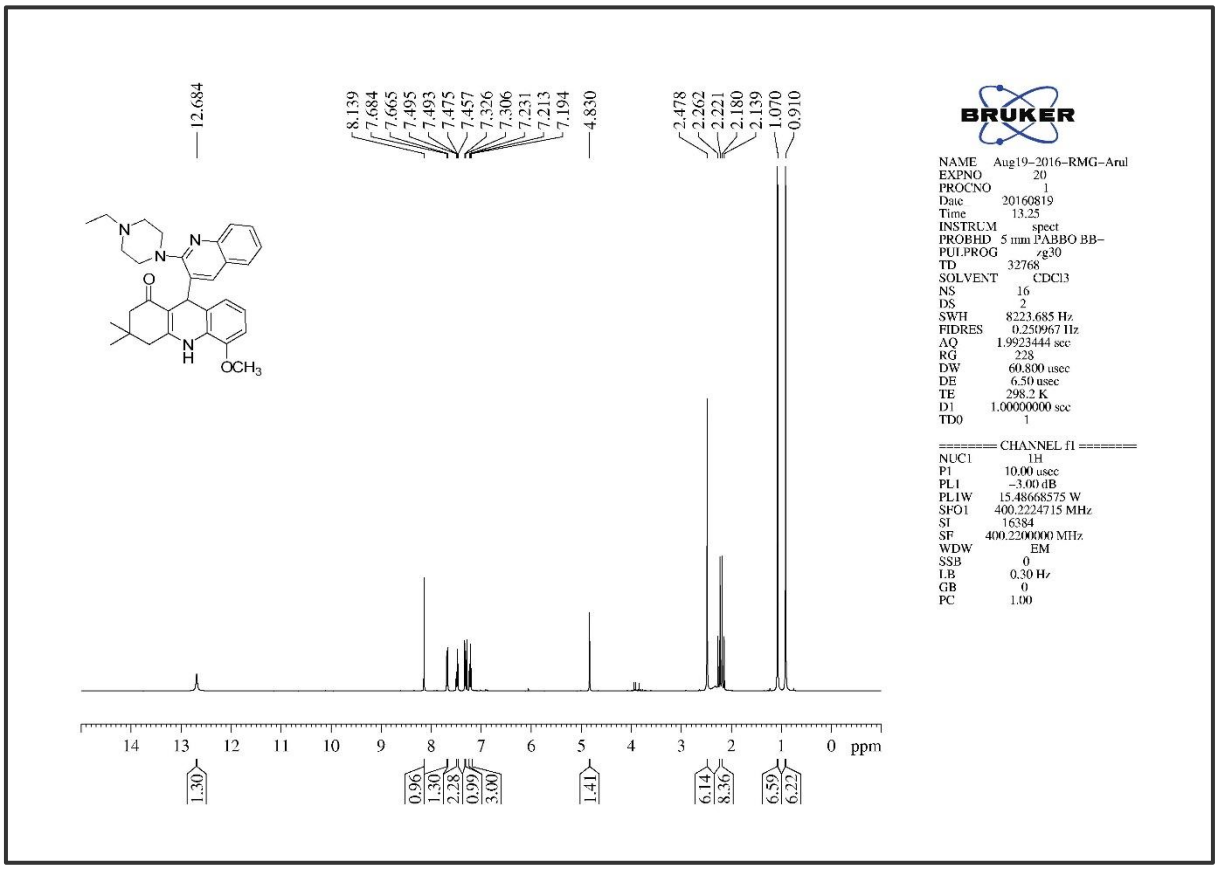

Figure 4B. S. 47. The ^{1}H NMR of compound 6l

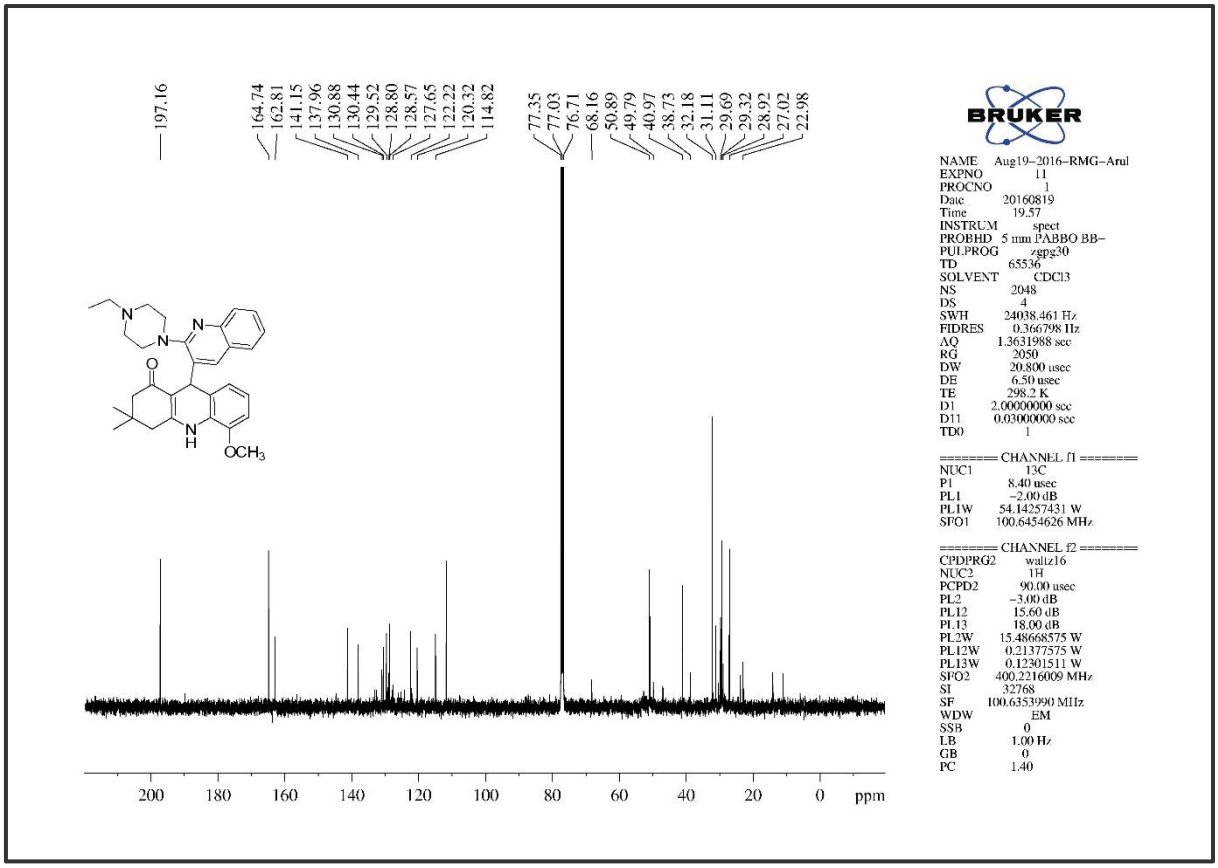

Figure 4B. S. 48. The ^{13}C NMR of compound 6l

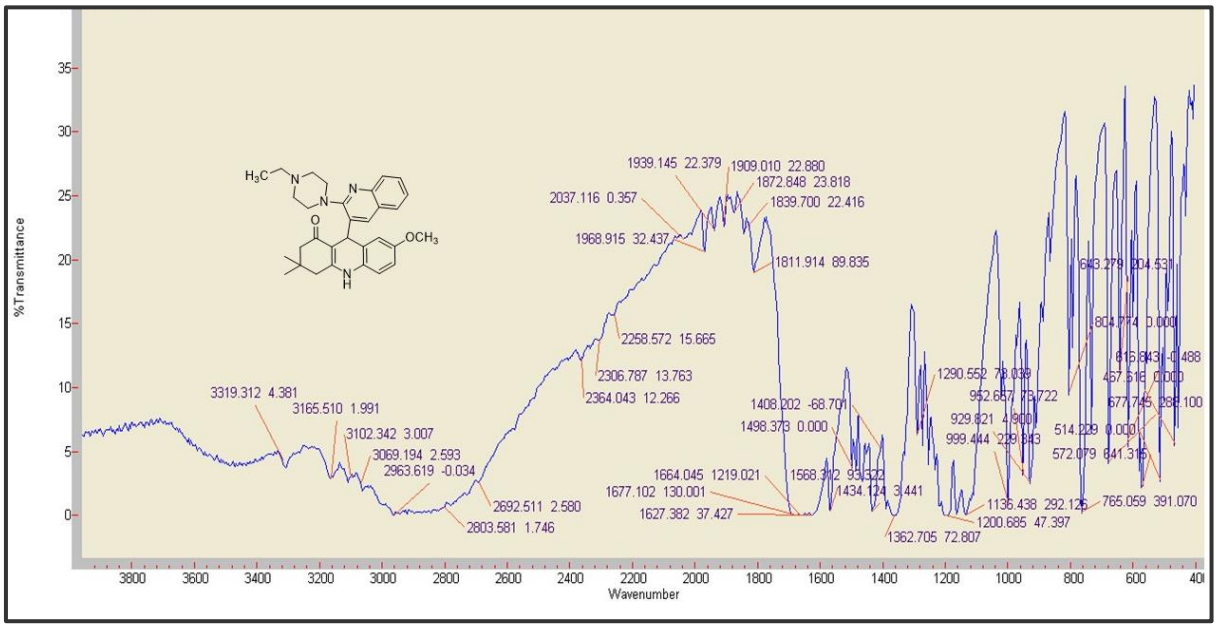

Figure 4B. S. 49. The Infra-Red Spectrum of compound 6m

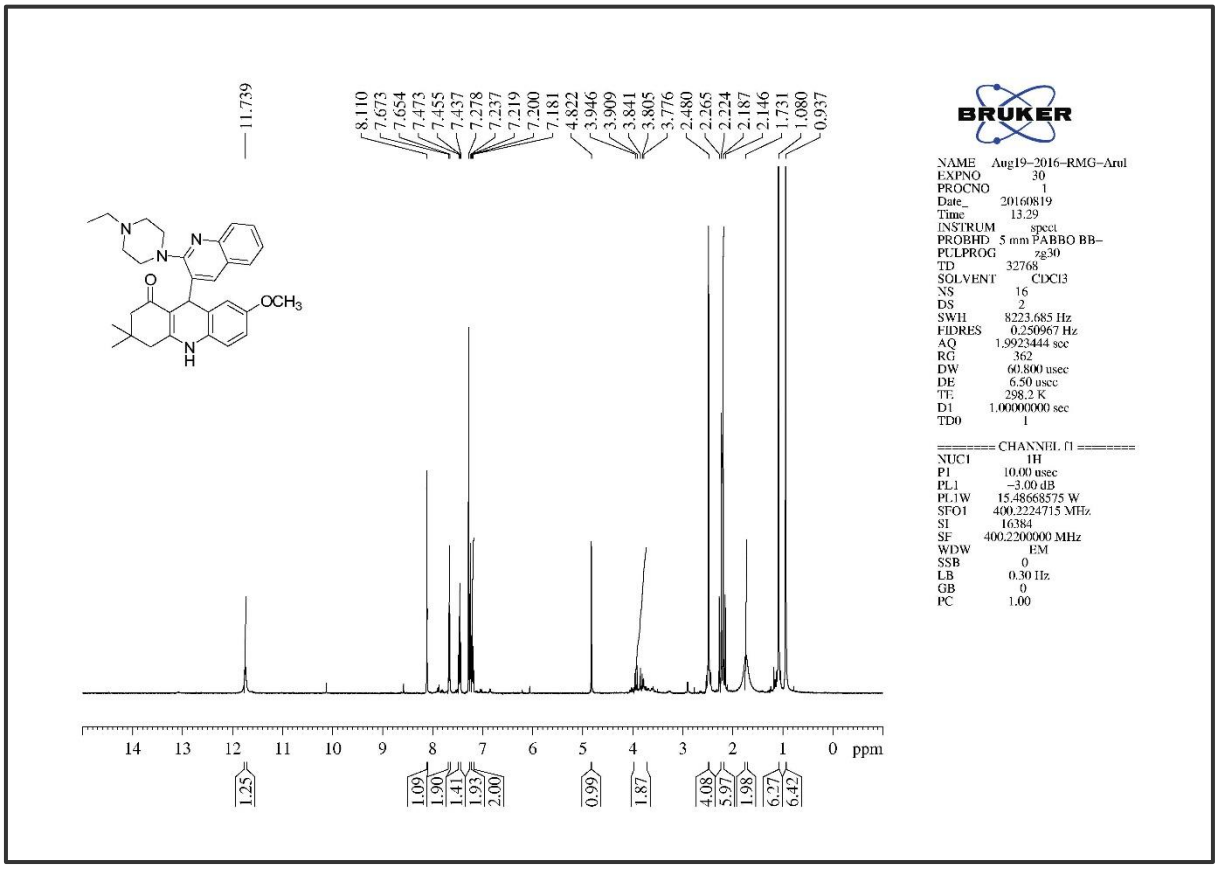

Figure 4B. S. 50. The ^{1}H NMR of compound 6m

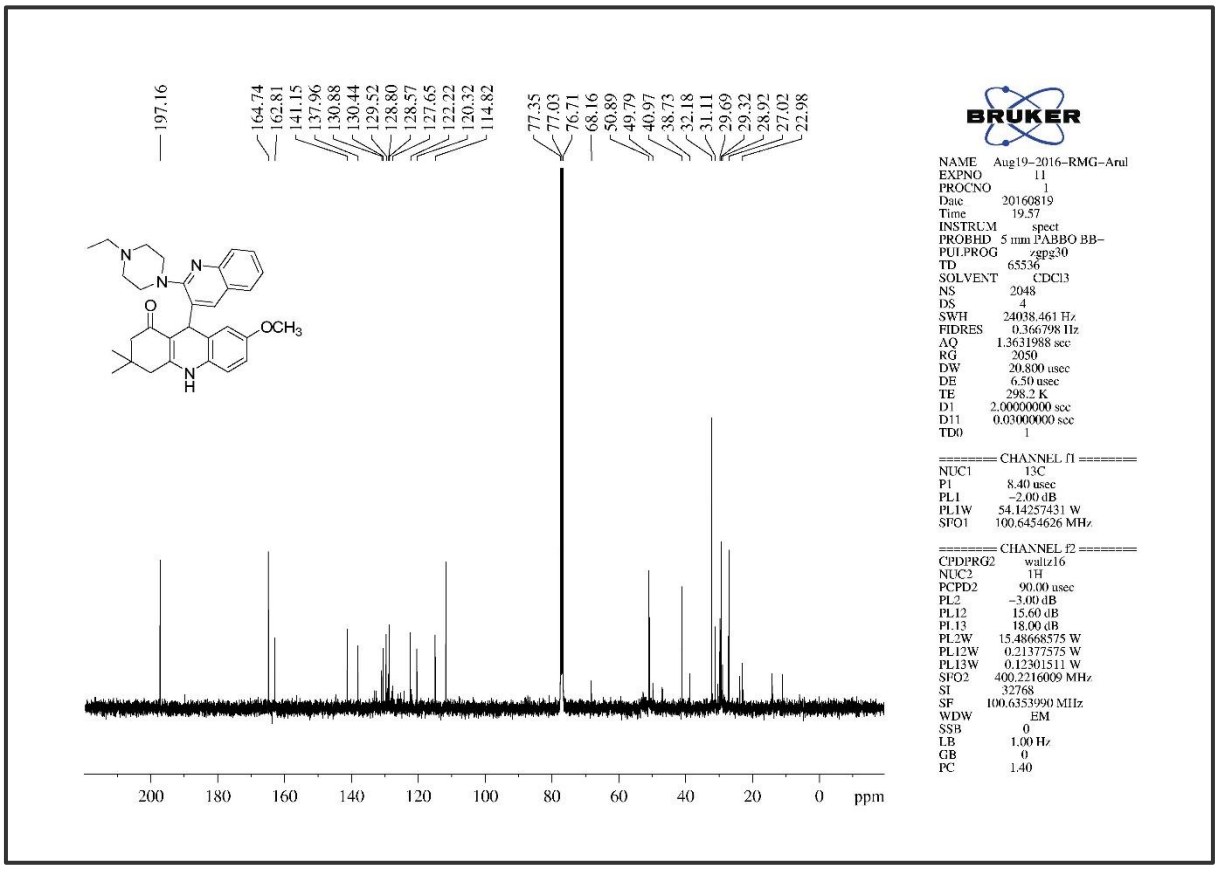

Figure 4B. S. 51. The ^{13}C NMR of compound 6m

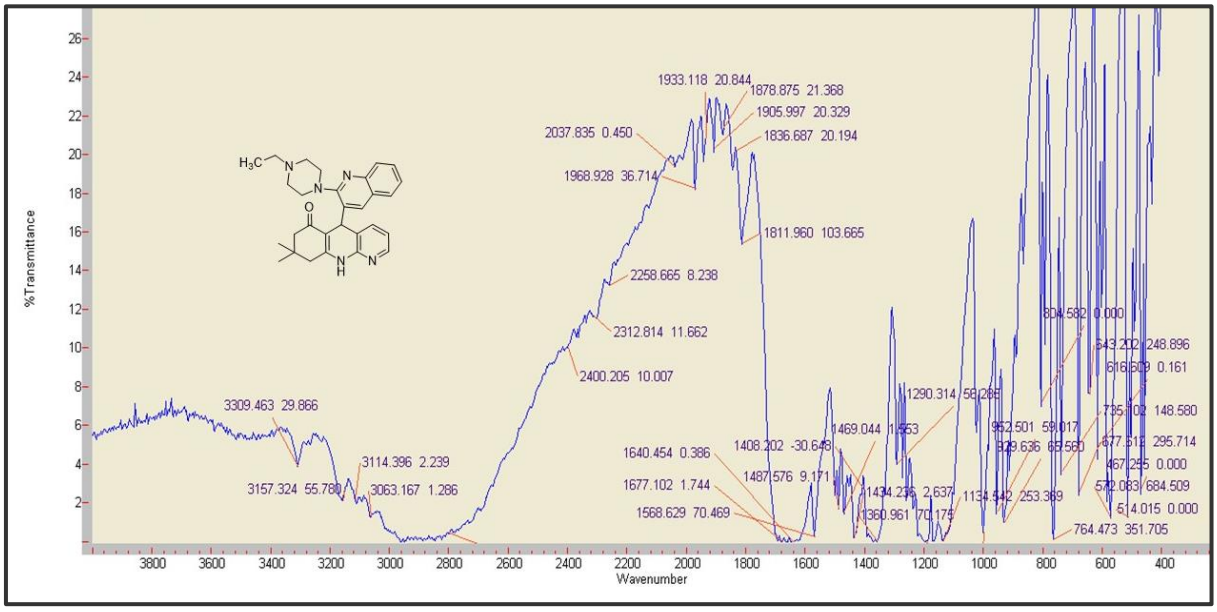

Figure 4B. S. 52. The Infra-Red Spectrum of compound 6n

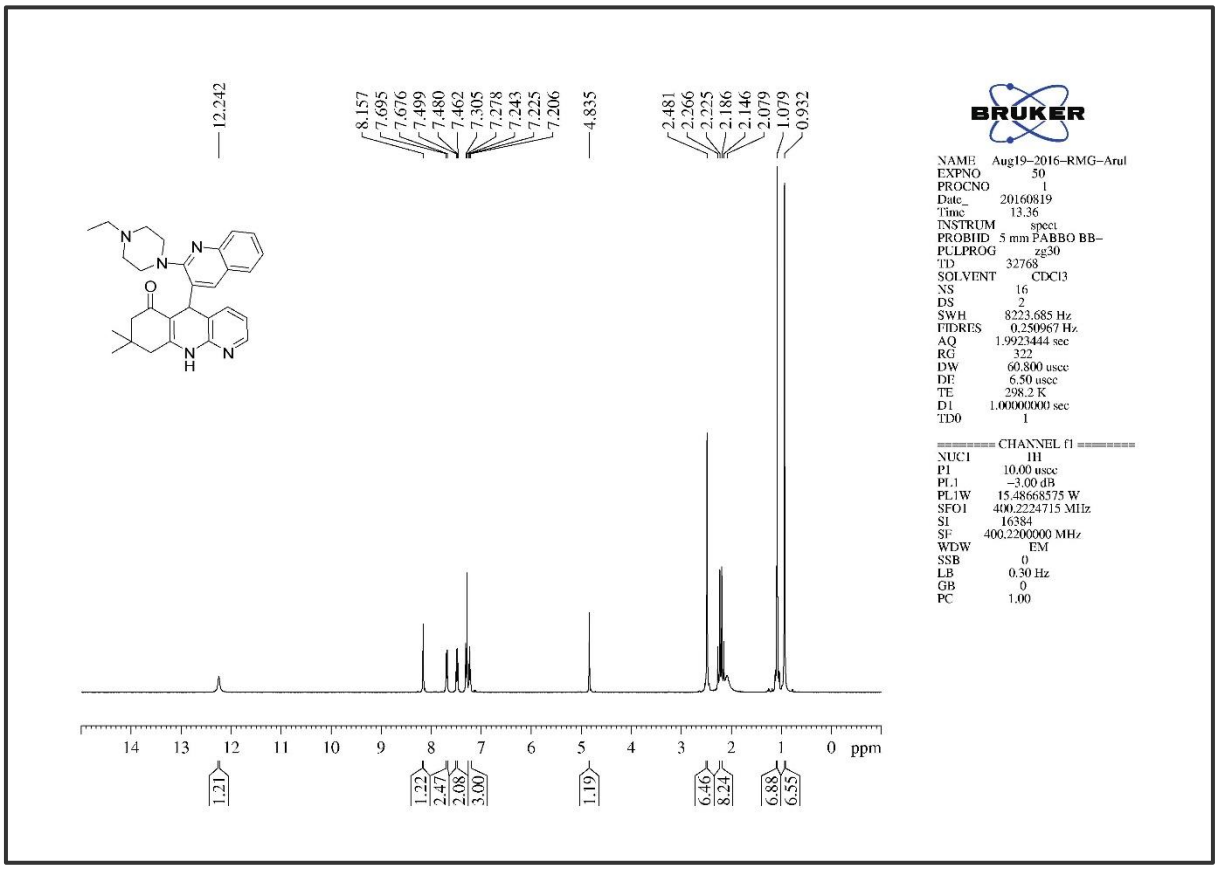

Figure 4B. S. 53. The ^{1}H NMR of compound 6n

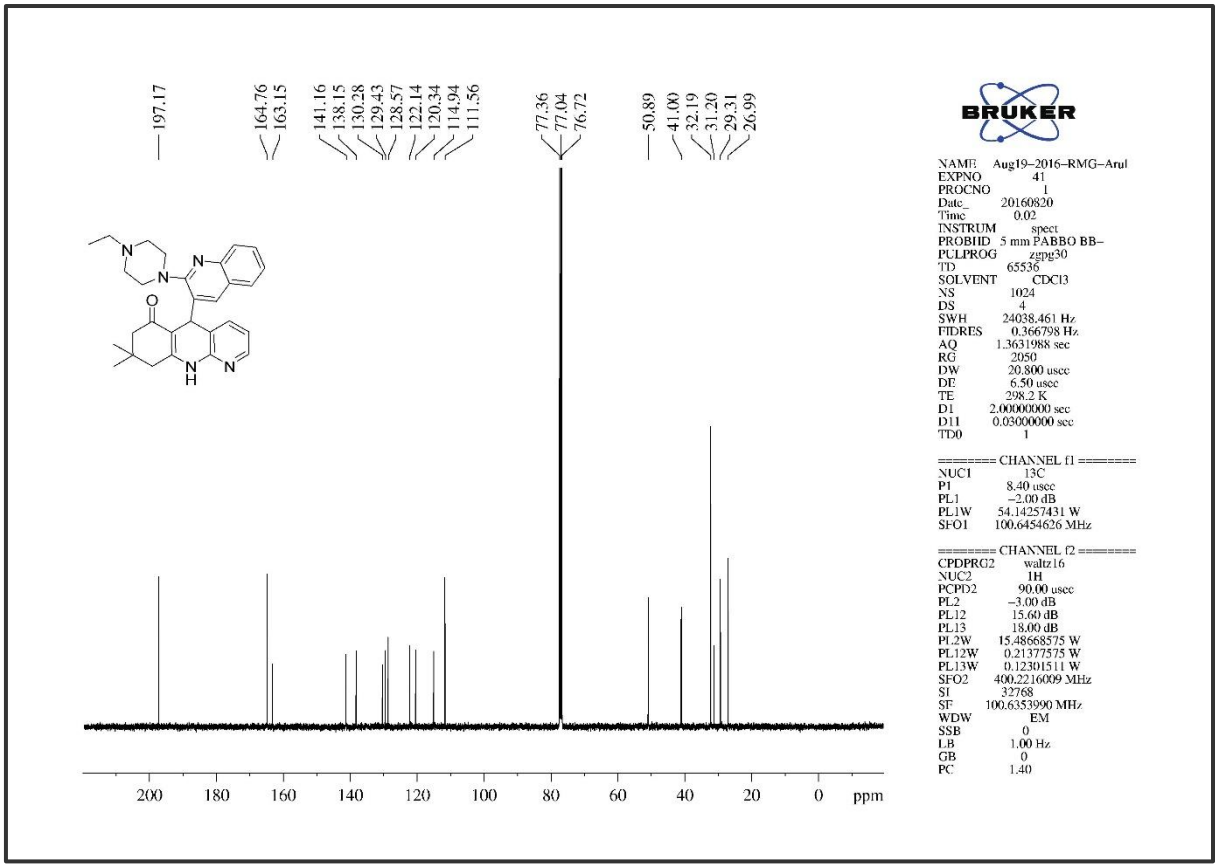

Figure 4B. S. 54. The ^{13}C NMR of compound 6n

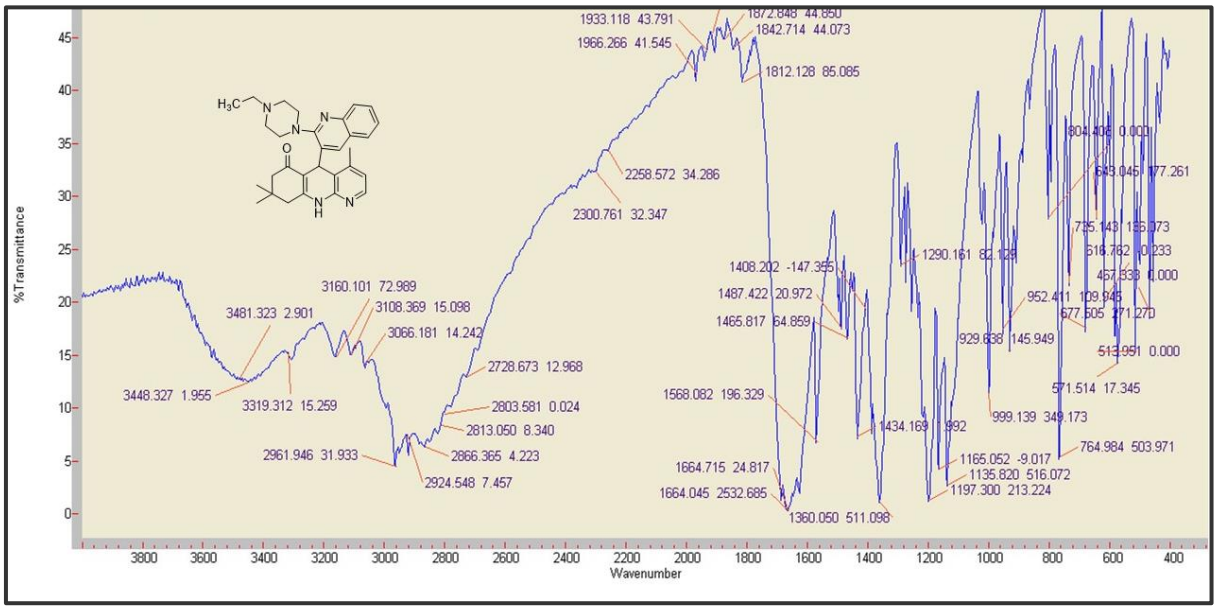

Figure 4B. S. 55. The Infra-Red Spectrum of compound 6o

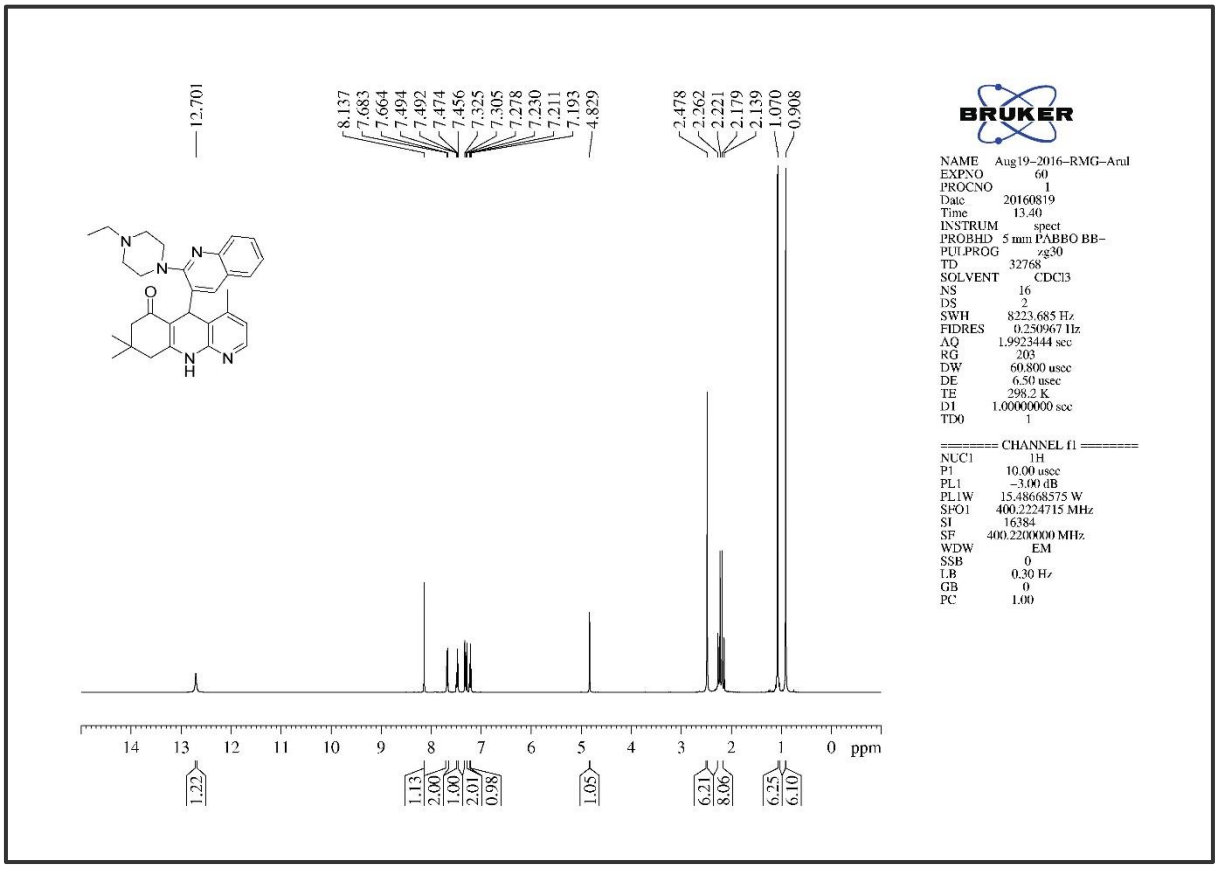

Figure 4B. S. 56. The ^{1}H NMR of compound 6o

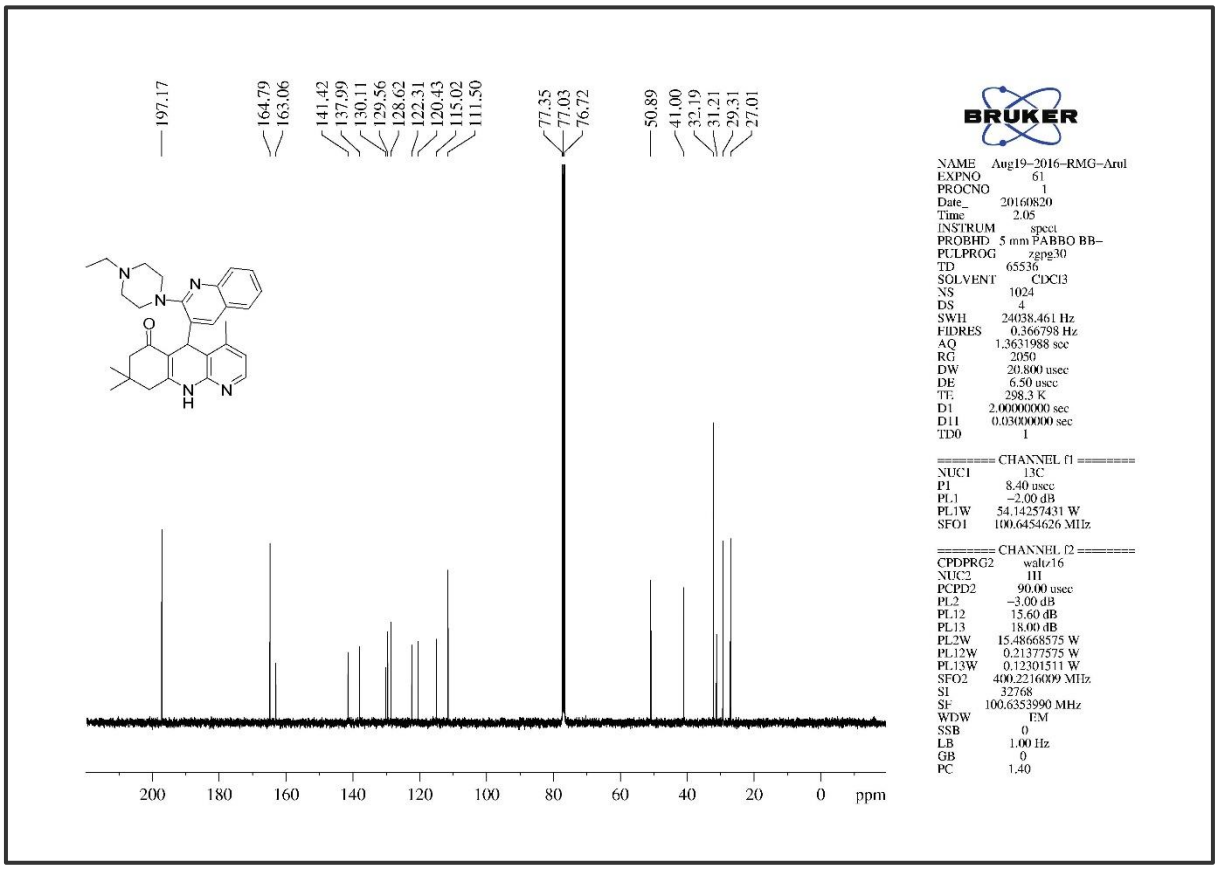

Figure 4B. S. 57. The ^{13}C NMR of compound 6o

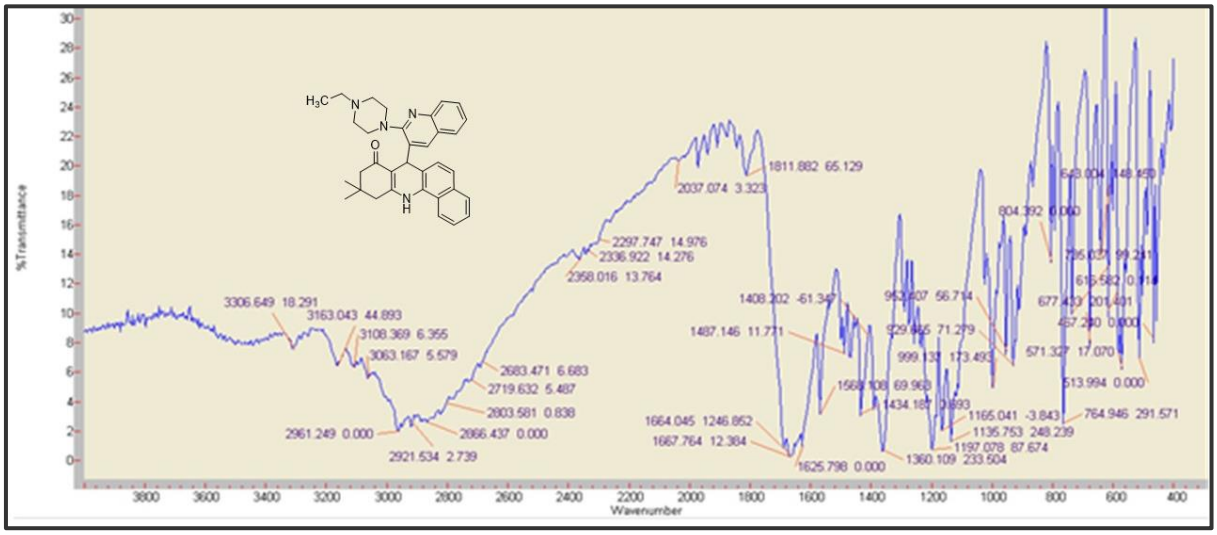

Figure 4B. S. 58. The Infra-Red Spectrum of compound 6p

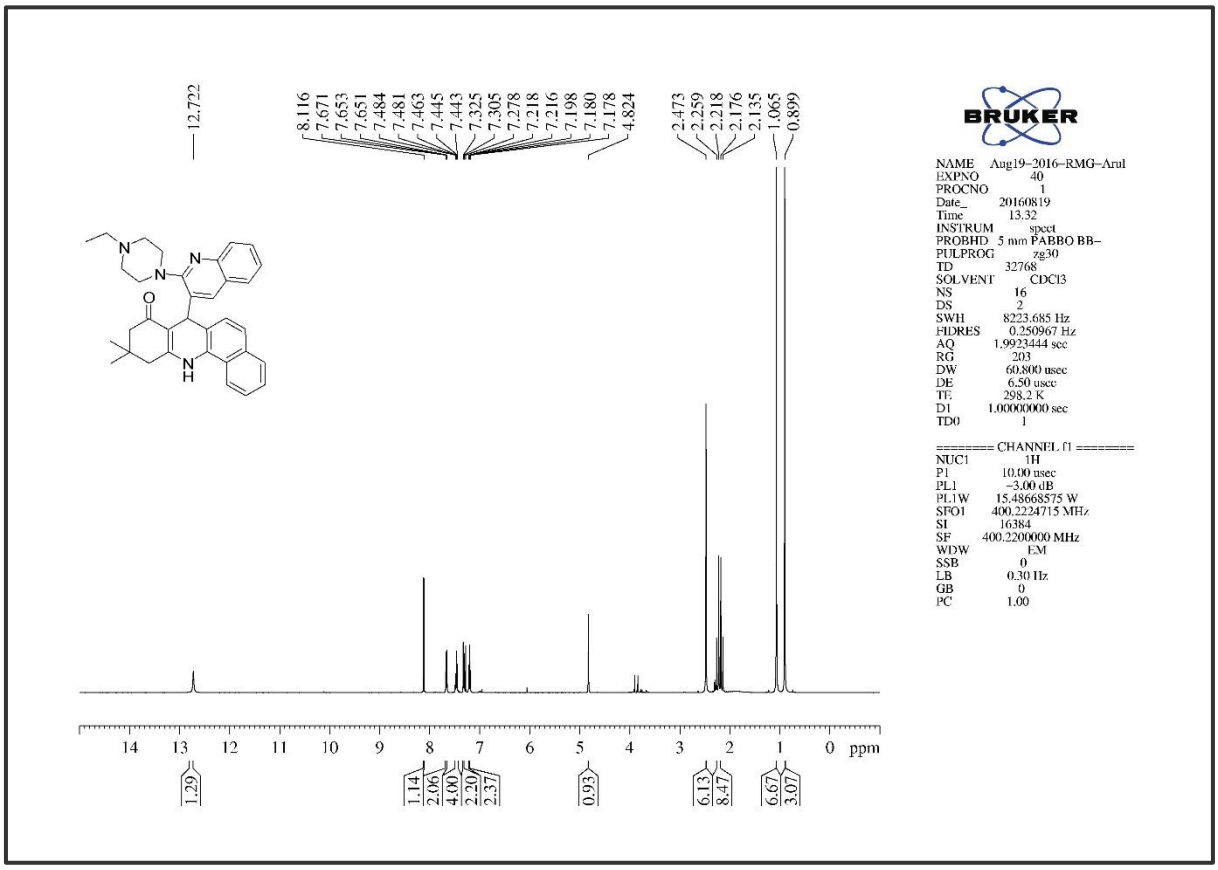

Figure 4B. S. 59. The ^{1}H NMR of compound 6p

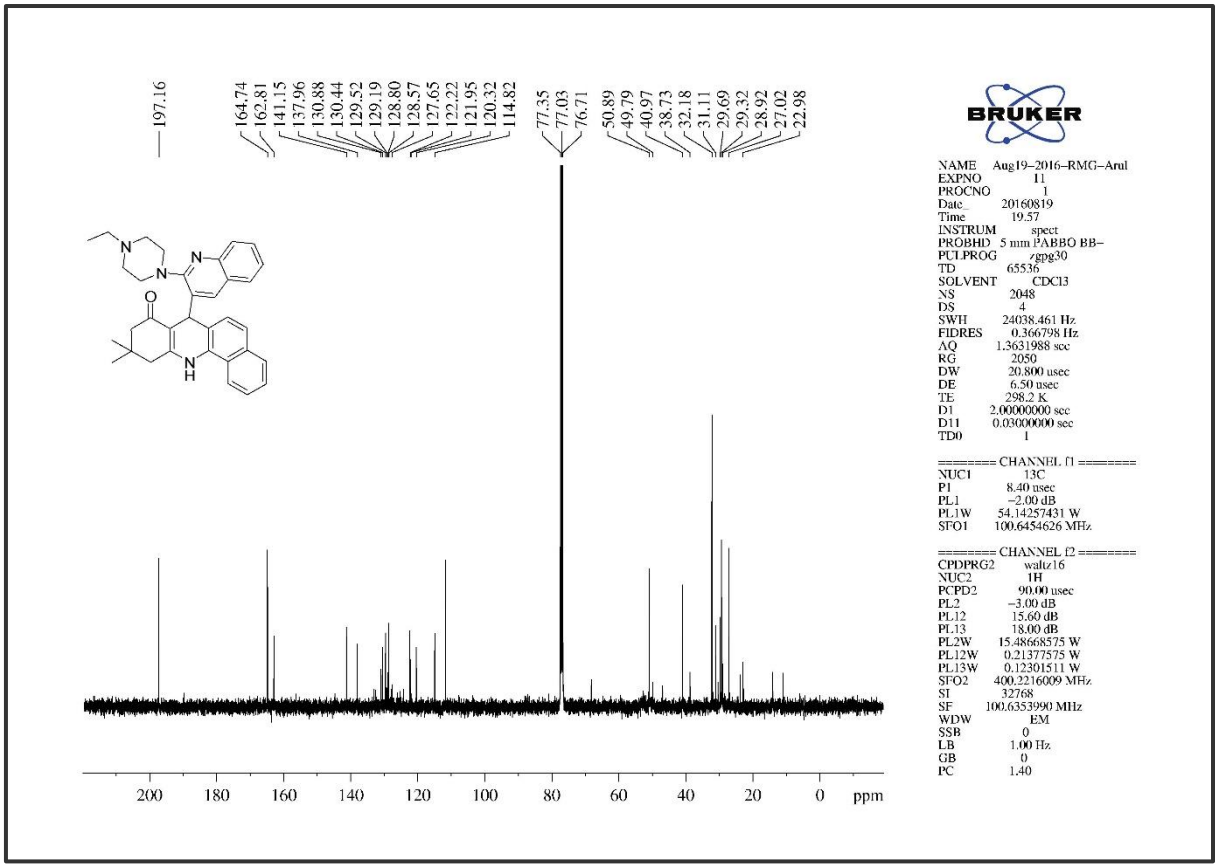

Figure 4B. S. 60. The ^{13}C NMR of compound 6p

Chapter Five

[1]Part A: One-pot synthesis of methyl piperazinyl-quinolinyl chalcones and their protein binding and molecular docking interactions

5A. 1. Abstract

A one-pot multicomponent method was used to synthesize (E)-3-(2-(4-methylpiperazin-1-yl) quinolin-3-yl)-1-phenylprop-2-en-1-one chalcones with the aid of a boron nitride based sulphonic acid catalyst. The new chalcones were characterized by FT-IR, ^{1}H NMR, ^{13}C NMR, TOF-MS and elemental analysis whilst X-ray crystallography was used to elucidate the structure of (*E*)-1-(anthracen-9-yl)-3-(2-(4-methylpiperazin-1-yl)quinolin-3-yl)prop-2-en-1-one **(5n)**. Thereafter, the fluorescence quench titration method was used to assess the binding ability of the chalcones with human serum albumin (HSA) protein whilst molecular docking was performed to determine their interaction at the binding site. It was observed that the addition of chalcones to HSA caused a red shift in the emission spectra and slight fluorescence quenching occurred. The bi-molecular quenching constant was estimated as 7.00×10^{12} dm^3 mol^{-1} s^{-1} whereas the maximum scatter collision quenching constant with the biopolymer was 2.00×10^{10} dm^3 mol^{-1} s^{-1}. Also, the free energy change for the complex was evaluated as -29.98 kJ mol^{-1}. This indicated a spontaneous and highly favourable reaction. Furthermore, molecular docking analyses showed the free energy change was -21.54 kJ mol^{-1}. This is comparable with the experimental value obtained from emission data at room temperature. These observations supported Trp-214 as the moiety for binding between HSA and the compound.

5A. 2. Introduction

Chalcones are α-β unsaturated ketones found in abundance in edible plants and are considered to be precursors to flavonoids and iso-flavonoids. The presence of the double bond in conjugation with carbonyl functionality is proposed as one of the functionalities that contribute to their important biological activity as compared to their saturated analogues.

[1]Murugesan, A., Gengan, R.M., Rajamanikandan, R., Ilanchelian, M. and Lin, C.H., *2017. One-pot synthesis of Claisen–Schmidt reaction through (E)-chalcone derivatives: Spectral studies in human serum albumin protein binding and molecular docking investigation. Synthetic Communications,* ***47(20), pp.1884-1904.***

The study of chalcones have attracted much attention because of their various biological applications such as anti-cancer, anti-inflammatory and anti-hyperglycaemic (Xia *et al.* 2000:699), (Ko *et al.* 2004:1333), (Satyanarayana *et al.* 2004:883) agents.

The most preferred method for the synthesis of chalcones is by the Claisen-Schmidt condensation of an aldehyde and ketone catalysed by either an acid or base followed by *in situ* dehydration (Anto *et al.* 1995:33). Different heterogeneous catalysts have been used such as Lewis acids (Iranpoor Kazemi 1998: 9475), (Narender Reddy 2007:3177), Brønsted acids (Szell Sohar 1969:1254), solid acids (Drexler and Amiridis 2003:136), (Chandrasekhar *et al.* 2005:6991), (Saravanamurugan *et al.* 2004:101) and solid bases (Daskiewicz *et al.* 1999:7095) (Sashidhara *et al.* 2009:2288) (Wang and Cheng 2006:689). The Claisen-Schmidt condensation reaction is also carried out in common ionic liquids (Yang *et al.* 2007:107), (Dong *et al.* 2008:1924), (Jahng *et al.* 2012:571), (Li *et al.* 2009:825). The reaction ensures C-C bond formation between two carbonyl derivatives and is a modification of the well-known aldol condensation (Dean *et al.* 2007:1308), (Rodriguez *et al.* 2007:2213) which also provides the synthesis of various important molecules promoted under acidic and basic (Khalilzadeh *et al.* 2007:535), (Baigrie *et al.* 1985:3640), (Xu *et al.* 2008:1579) catalytic conditions. Recently an ionic liquid catalyst was used for the aldol condensation (Kang *et al.* 2014:337), (Sarda *et al.* 2009:481) for C-C bond formation in an acid medium and further extended to the synthesis of chalcone derivatives via Claisen-Schmidt condensation (Tiecco *et al.* 2016:43740). Also, new ionic liquid catalysts were used as a green approach (Qian *et al.* 2010:1146), (Qian *et al.* 2013:13272) for new chalcones. Silica based nanomaterial solid acid catalysts such as MCM-4, SBA-15 and amino propyl based nanosilica were used under solvent free conditions (Nagendrappa 2002:64), (Romanelli *et al.* 2011:24), (Wang and Cheng 2006:689). Protonated aluminate mesoporous silica nanomaterial was also used for synthesising some biologically active chalcones (Mohammad *et al.* 2016:11023).

Although 1000's of chalcones have been synthesized and their biological activity assessed, new compounds are sought after especially for those possessing a heterocycle portion. In particular, nitrogen containing atoms such as quinolones and quinolines, and other classes which have the correct scaffold to increase the biological activity of compounds. Concurrent with the investigation of new biologically potent chalcones, new catalytic systems are sought after to increase the efficiency of the Claisen-Schmidt reaction and improve the final yield of chalcones.

5A. 3. Results and discussion

In the present study, a one-pot synthesis of functionalised piperazinyl-quinolinyl chalcone derivatives using nanocrystalline boron nitride-based propyl sulfonic acid catalyst (BN-Pr-SO_3H) is presented. The synthesis and characterisation of BN-Pr-SO_3H was presented in Chapter 4A whilst the starting compound 2-(4-methylpiperazin-1-yl)quinoline-3-carbaldehyde (**3**) was described in Chapter 3.

In order to synthesize new piperazinyl-quinolinyl chalcones (Scheme 5A.1), a preliminary study was undertaken to synthesize **5a** (Scheme 5A. 1), as a model reaction, with BN-Pr-SO_3H. Herein a mixture of **3** and **4a** were refluxed in acetonitrile for 6 h. To determine the optimum quantity of BN-Pr-SO_3H required, the reaction was carried out with different quantity of BN-Pr-SO_3H: 0.02, 0.05 and 0.07 g. The usual work-up of the reaction content provided impure **5a** which was subsequently purified and characterized by FT-IR, ^{1}H NMR, ^{13}C NMR, TOF-MS and elemental analysis. It was found that increasing the quantity of BN-Pr-SO_3H beyond 0.05 g did not increase the yield noticeably hence this quantity was selected as optimum for all subsequent reactions. Thereafter, various solvents such as methanol, ethanol, acetonitrile, and base catalyst such as NaOH, KOH, piperidine, piperizine and pyrrolidines were investigated. It was found that these reagents have an impact on the yield of **5a**. The best yield (95%) was obtained with acetonitrile (Table 5A. 2 entry 12) which was the main solvent chosen initially. Moderate yields of **5a** were obtained when pyrrolidines with solvents such as ethanol and methanol were refluxed for 6 h (Table 5A. 2 entries 9-11).

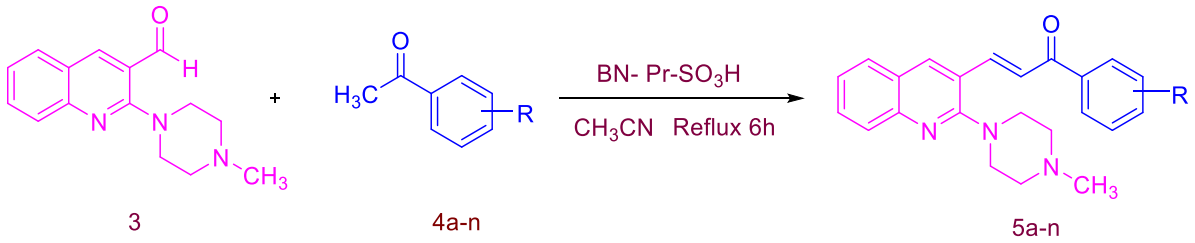

KEY: 5a (R=H); 5b (R=2- OH); 5c (R=4- OH); 5d (R=4- NO_2); 5e (R=para- CH_3); 5f (R=para O-CH_3); 5h (R=4-F);5i (R=4-Cl); 5j (R=4-Br); 5k (R=meta- NH_2); 5l (R=Ar-H); 5m (R=Ar-H); 5n (R=Ar-H) whilst 5g was obtained from **3** and thioacetophenone.

Scheme 5A. 1. The synthesis of phenyl substituted (E)-3-(2-(4-methylpiperazin-1-yl) quinolin-3-yl)-1-phenylprop-2-en-1-ones derivatives.

The yield decreased and a longer reaction time was required with NaOH, KOH, piperidine and piperazine (Table 5A. 2 entries 1-8). Consequently, BN-Pr-SO_3H and acetonitrile were used for the synthesis of **5a-n** (Table 5A. 2).

The re-usability potential of BN-Pr-SO_3H was also investigated in the model reaction. Briefly, after the one-pot reaction, the content was filtered and the solid was rinsed with acetonitrile, dried in an oven at 105 °C and re-used. It was found that BN-Pr-SO_3H could be re-used five times with an overall loss of only 10 % catalytic activity. This was an important advantage if commercial application is required in the future.

Table 5A. 2. Optimization of the reaction to synthesize **5a**: the effect of solvent and catalyst

Entry	Catalyst	Solvent	Temp (°C)	Time(h)	Isolated Yield (%)
1	NaOH	EtOH	r.t	24	80
2	KOH	MeOH	r.t	24	85
3	piperidine	CH_3CN	Reflux	24	80
4	piperidine	EtOH	Reflux	24	65
5	piperidine	MeOH	Reflux	24	58
6	piperazine	CH_3CN	Reflux	24	75
7	piperazine	EtOH	Reflux	24	70
8	piperazine	MeOH	Reflux	24	60
9	pyrrolidine	CH_3CN	Reflux	6	90
10	pyrrolidines	EtOH	Reflux	6	80
11	pyrrolidines	MeOH	Reflux	6	75
12	BN- Pr-SO_3H	CH_3CN	Reflux	6	95

The synthesis of piperazinyl-quinolinyl chalcone derivatives **5a-5n** (Scheme 5A. 1), using BN-Pr-SO_3H, were undertaken in CH_3CN for 6 h reflux. The yield of the products (Table 5A. 3) ranged from 75 to 95 %. Chalcones which contained electron withdrawing groups such as NO_2, F, Cl and Br produced yields of 87 %, 90 %, 87 %, and 85 % respectively (Table 5A.3 entry 4, 8, 9 and 10). Chalcones which contained electron donating groups CH_3, OCH_3, and

NH_2 gave yields of 80 %, 85 %, and 87 % (Table 5A. 3 entry 5, 6, and 11). The functional group usually has an effect on electrophilic aromatic substitution. However the reaction under study was a condensation reaction and hence electronic effects may not be involved in the synthetic process.

Table 5A. 3. The synthesis of E)-3-(2-(4-methylpiperazin-1Yl) quinolin-3-yl)-1-phenylprop-2-en-1-one derivatives in the presence of BN-Pr-SO_3H.

Entry	Substrate (4a-n)	Product (5a-n)	Time (h)	Isolated Yield (%)	M. p. (°C)
1	$C_6H_5COCH_3$	5a	6	95	135-137
2	2-$HOC_6H_4COCH_3$	5b	6	92	138-140
3	4-$HOC_6H_4COCH_3$	5c	6	90	163-162
4	$O_2NC_6H_4COCH_3$	5d	6	87	175-178
5	$CH_3C_6H_4COCH_3$	5e	6	80	135-136
6	$OCH_3C_6H_4COCH_3$	5f	6	85	165-167
7	C_6H_6OS	5g	6	90	140-143
8	$FC_6H_4COCH_3$	5h	6	90	150-152
9	$ClC_6H_4COCH_3$	5i	6	87	160-163
10	$BrC_6H_4COCH_3$	5j	6	85	155-157
11	$C_6H_6NCOCH_3$	5k	6	87	130-132
12	$C_{10}H_7COCH_3$	5l	6	90	136-138
13	$HOC_{10}H_6COCH_3$	5m	6	92	170-173
14	$C_{16}H_{12}O$	5n	6	90	145-147

Compounds **5a-5n** were characterized by FT-IR, ^{1}H NMR, ^{13}C NMR, MS-TOF whilst **5m** included DEPT-90 and DEPT-135, COSY, NOSEY, HSQCE, HMBC (Characterisation data are presented in Appendix). To elucidate the structure of the chalcones, **5m** was selected as a template. Characterisation of the remaining chalcones was relatively simple since only one functional group was changed on the aromatic ring. The FT-IR spectrum of **5m** showed stretching at 3403, 2918 and 1724 cm^{-1} for the OH, C-H and carbonyl groups respectively. The ^{1}H NMR spectrum showed two singlets at δ 14.88 and 8.30 which was assigned to C_{19}-OH and C_4-H respectively. The C_9-H protons appears at δ 8.18 (J = 9.48 Hz) as a doublet and C_{10}-H at δ 7.80 (J =8.96 Hz) also as a doublet. The ^{13}C NMR spectrum showed the presence of one

carbonyl group at δ 192.9 and 2D NMR spectral studies were undertaken to confirm the structure. The selected HMBC correlation of **5m** is presented in Figure 5A. 1.

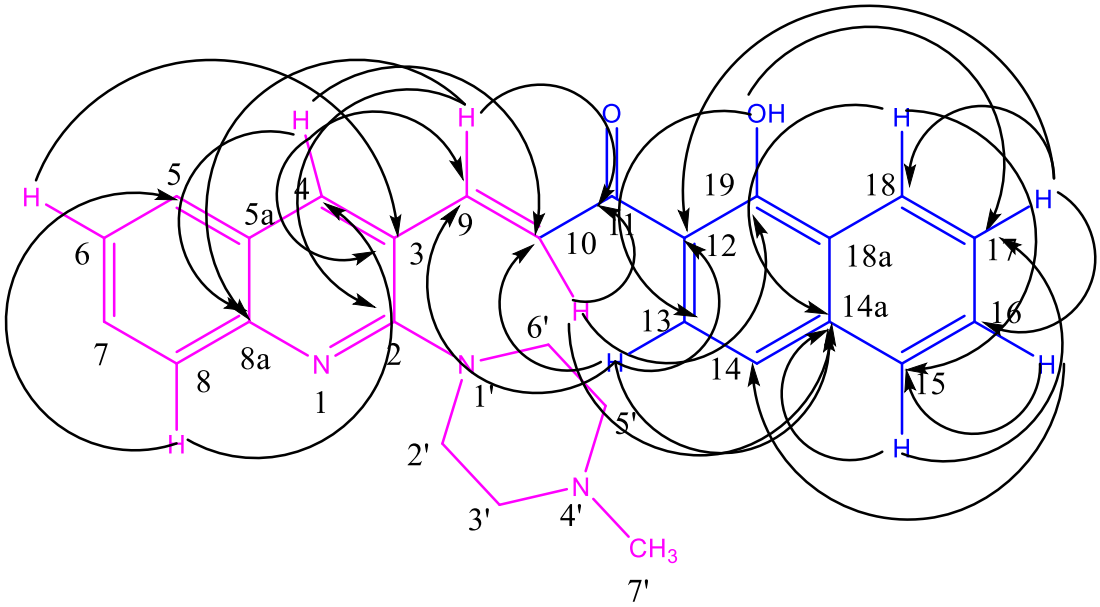

Figure 5A. 1. Selected HMBC correlations of compound 5m.

The C, H-COSY correlation assigned the carbon signals at δ 45.93, 50.13, 54.90, 142.28, 126.04, 130.56, 127.88, 124.73, 122.60, 113.39, 118.37, 121.36, 130.36, 127.44, 124.87 and 159. 48 to $C_{7'}$, $C_{2'}$and $C_{6'}$, $C_{3'}$ and $C_{5'}$, C_9, C_{10}, C_4, C_5, C_6, C_7, C_8, C_{13}, C_{14}, C_{15}, C_{16}, C_{17}, C_{18} and C_{19} respectively. The carbon signal at δ 137.56 was due to the quinolinyl C_4-carbon. The H, H-COSY spectrum showed singlets at δ 8.30 and 14.88 which indicated only one nearby hydrogen to C_4 and hydroxyl group at C_{19}. The long range HMBC correlation showed Similarly, C_{19}-H correlated with hydroxynaphthalen carbon C_{13} at δ (113.39), C_{17} at δ (127.44), C_{15}-H correlated with hydroxynaphthalen carbon C_{14} at δ (124.87), C_{18} at δ (124.73), C_4-H with quinolinyl carbon C_3 at δ (123.82), C_{8a} at δ (147.82) and C-H carbon C_{10} at δ (126.04), C_9 at δ (142.28), whilst C_{10}-H correlated with quinolinyl carbon C_3 at δ (123.82), hydroxyl carbon C_{19} at δ (159.48) and hydroxynaphthalen carbonyl carbon C_{11} at δ (192.98), C_9-H correlated with quinolinyl carbon C_2 at δ (164.4), C_{8a} at δ (147.82), hydroxynaphthalen carbonyl carbon C_{11} at δ (192.98), C_{18}-H correlated with hydroxynaphthalen carbon C_{15} at δ (127.88), C_{14a} at δ (137.46), C_{13}-H correlated with hydroxynaphthalen carbon C_{12} at δ (125.52), C_{14a} at δ (137.46) and C-H carbon C_9 at δ (142.28), C_{10} at δ (126.04), whilst C_{17}-H correlated with hydroxynaphthalen carbon C_{12} at δ (125.52), C_{18} at δ (124.87), C_{16} at δ (130.36), C_{16}-H correlated hydroxynaphthalen carbon C_{15} at δ (127.88), C_{14} at δ (118.37), whilst C_8-H

correlated with quinolinyl carbon C_5 at δ (127.88), C_4 at δ (137.56), C_6-H correlated with quinolinyl carbon C_3 at δ (123.82) showed in (Figure 5A. 2)

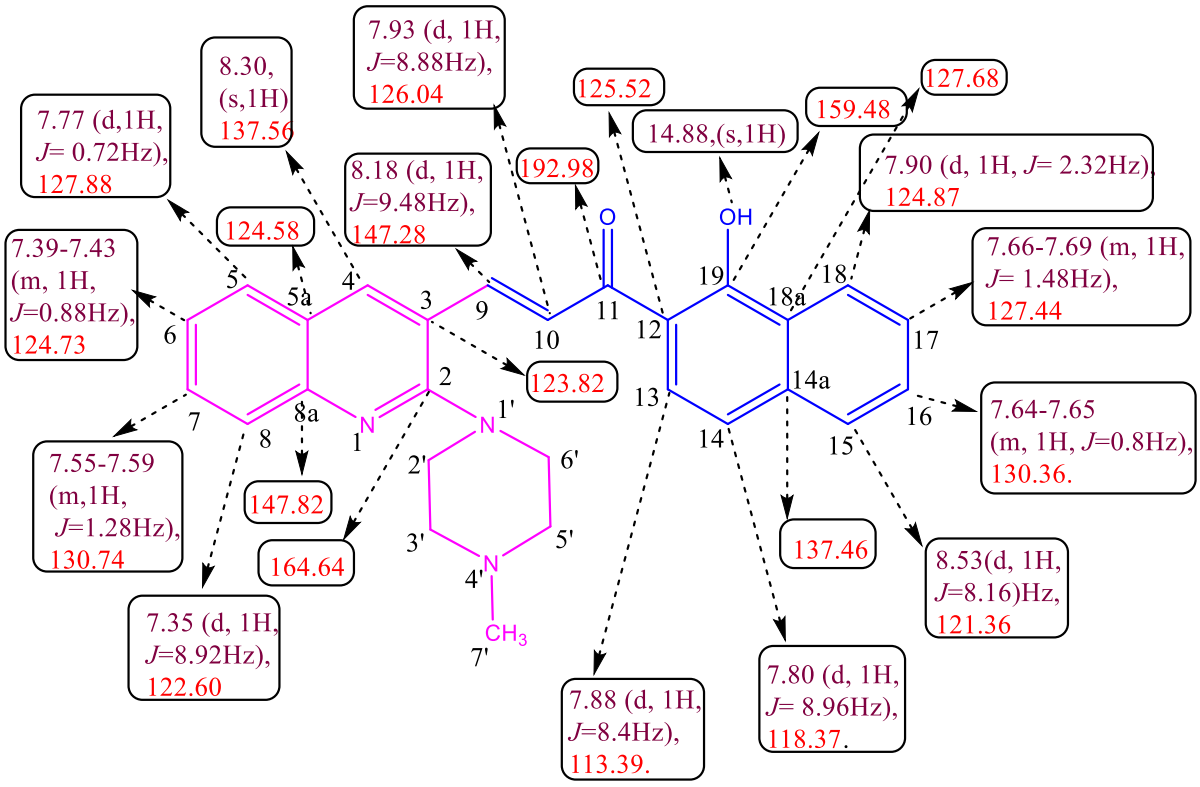

Figure 5A. 2. Selected (^{1}H) and (^{13}C) NMR and HMBC chemical shifts of 5m.

Selected ^{1}H NMR and ^{13}C NMR and HMBC chemical shifts of **5m** are as presented in Table 5A. 4. Based on the above spectral details, mass spectra and elemental analysis: TOFMS ES *m/z* (rel. int.): m/z: 423. 19 $[M]^+$. Anal. Calc. for $C_{27}H_{25}N_3O_2$: C, 76.57; H, 5.95; N, 9.92 %. Found: C, 76.59; H, 5.96; N, 9.93 %, the structure was confirmed as (E)-1-(1-hydroxynaphthalen-2-yl)-3-(2-(4-methylpiperazin-1-yl)quinolin-3-yl)prop-2-en-1-one (Figure 5A. 2).

A proposed mechanism was described to support the formation of **5A. 2** In the first step, the catalyst activated the ketone carbonyl functionality thereby enabling acetophenone to form a new covalent bond with intermediate **I** as in the Claisen Schmidt reaction to produce loss of proton to an intermediate **II**. In the next step, again intermediate **II** lost a proton resulting in intermediate **III** as an enolate ion. This attacked the carbonyl group of 2-(4-methylpiperazin-1-yl) quinoline-3-carbaldehyde resulting in intermediate **IV**. The addition of a proton to intermediate **IV** resulted in intermediate **V** being formed and finally the loss of a water molecule formed product **5a**.

Table 5A. 4. Selected HMBC correlations of compound **5m**

S.NO	Proton	Correlated Carbons
1	C_{19}-H (s, 1H) at *δ.* 14.88	C_{13} at *δ* (113.39), C_{17} at *δ* (127.44),
2	C_{15}-H (d, 1H, *J*= 8.16Hz) at *δ.* 8.16	C_{14} at *δ* (124.87), C_{18} at *δ* (124.73)
3	C_4-H (d,1H, *J*= 8.4Hz) at *δ.* 7.88	C_3 at *δ* (123.82), C_{10} at *δ* (126.04), C_9 at *δ* (142.28), C_{8a} at *δ* (147.82)
4	C_{10}-H (d, 1H, *J*= 8.96Hz) at *δ.* 7.93	C_3 at *δ* (123.82), C_{19} at *δ* (159.48), C_{11} at *δ* (192.98),
5	C_9-H (d, 1H, *J*= 9.48Hz) at *δ.* 8.18	C_2 at *δ* (164.4), C_{8a} at *δ* (147.82), C_{11} at *δ* (192.98),
6	C_{18}-H (d, 1H, *J*= 2.32Hz) at *δ.* 7.90	C_{15} at *δ* (127.88), C_{14a} at *δ* (137.46),
7	C_{13}-H (d, 1H, *J*= 8.4Hz) at *δ.* 7.88	C_{12} at *δ* (125.52), C_{10} at *δ* (126.04), C_9 at *δ* (142.28), C_{14a} *δ* (137.46)
8	C_{17}-H (m, 1H, *J*= 1.48Hz) at *δ.* 7.66-7.69	C_{12} at *δ* (125.52), C_{18} at *δ* (124.87), C_{16} at *δ* (130.36),
9	C_{16}-H (m, 1H, *J*= 0.8Hz) at *δ.* 7.64-7.65	C_{15} at *δ* (127.88), C_{14} at *δ* (118.37),
10	C_8-H (d,1H, *J*= 8.92Hz) at *δ.* 7.35	C_5 at *δ* (127.88), C_4 at *δ* (137.56),
11	C_6-H (m,1H, *J*= 0.88Hz) at *δ.* 7.39-7.43	C_3 at *δ* (123.82),

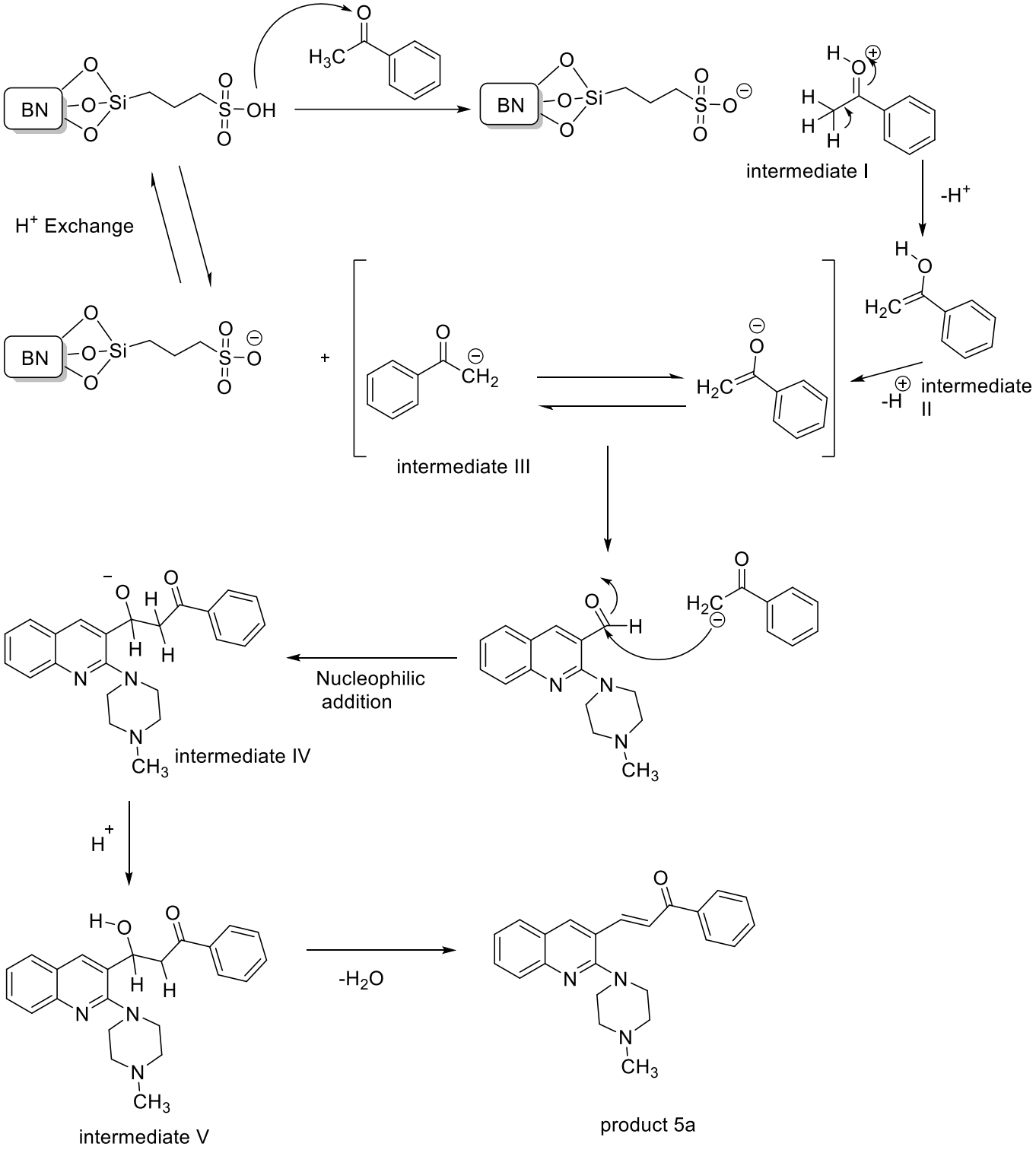

Scheme 5A. 2. Proposed mechanism for the synthesis of E-3-(2-(4-methylpiperazin-1yl) quinolin-3-yl)-1-phenylprop-2-en-1-one

Whilst synthesising the derivatives, **5n** was obtained as a single crystal. Hence it was analysed by x-ray crystallography. It was observed that the carbonyl carbon had a distorted trigonal-planar geometry and was flanked by a bulky N piperazinyl group in the ortho position of the heterocycle. The piperazinyl ring was in a half-chair conformation having approximate sp^3 hybridisation. The dihedral angle between the mean planes of the six piperazinyl ring atoms and through the quinoline ring system was 119.2 (4).

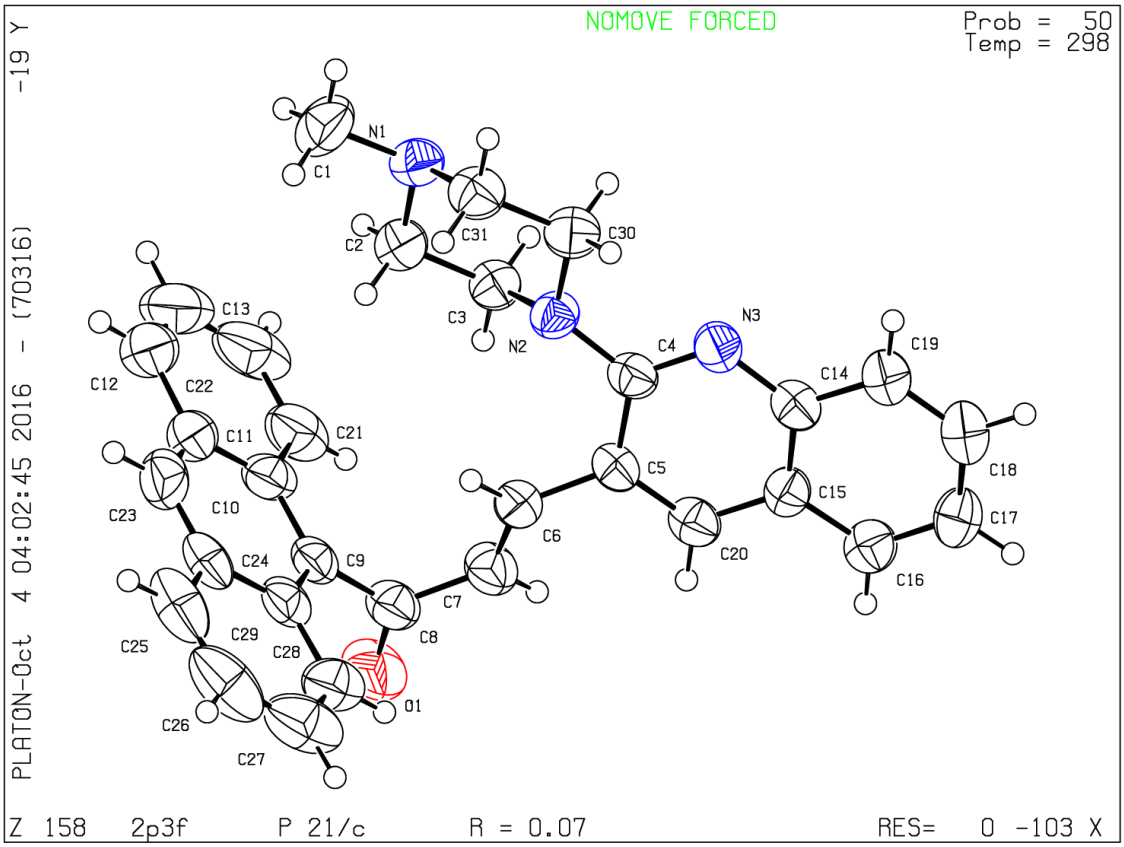

Crystal structure of compound, 5n (**CCDCNo. 1509962)**

Figure 5A. 3. The molecular structure of compound **5n** showing the atom labelling. Oxygen, nitrogen atom labels and hydrogen atom labels have been omitted for clarity. Displacement ellipsoids are drawn at the 50 % probability level**.**

The anthracene group containing C9, C10 and C21 was essentially bisected by the plane of the benzene ring to which they were attached, subtending dihedral angle 122.2(4), (C9/C10/C11) 118.9 (4) and (C10/C9/C8) 119.0(4), relative to the carbon atoms C8, C7, C6 and C5 while the quinoline groups containing C5 and C20 significantly deviated from this bisected geometry with dihedral angle 120.9(4), (C4/N2/C30) and 117.1(3). The C6-C7 had a

bond length of 1.332 (5) A°. In the crystal packing of the compound there was evidence of weak intermolecular interactions.

Crystal data, data collection and structure refinement details were summarized in All H atoms which were positioned with idealized geometry using a riding model with C-H = 0.93-0.97 A. All H atoms were refined with isotropic displacement parameters (set to 1.2 times of the Ueq of the parent C atom). (All data and experimental information are presented in Appendices).

Steady state emission spectral studies of HSA with **5m** were also undertaken. It was reported that tryptophan, tyrosine, and phenylalanine are the three aromatic fluorophores that are used in fluorescence spectroscopy for studying structural alterations on drug binding. However, among them, the contribution for intrinsic emission behaviour of tryptophan is at maximum (Zhang *et al.* 2013:14018), (Zaidi *et al.* 2013:2595).

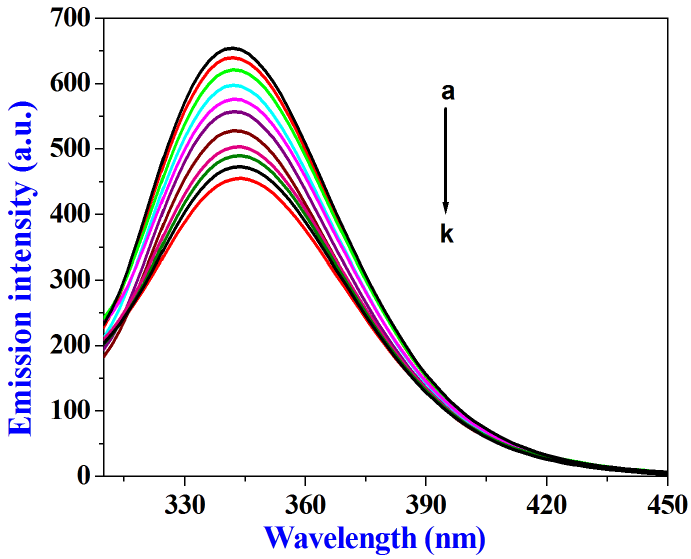

Figure 5A. 4. Emission spectra of HSA (4.00×10^{-6} mol dm^{-3}) at various concentrations of compound. [compound]: [a] 0.00, [b] 1.00×10^{-6}, [c] 2.00×10^{-6}, [d] 3.00×10^{-6}, [e] 4.00×10^{-6}, [f] 5.00×10^{-6}, [g] 6.00×10^{-6}, [h] 7.00×10^{-6}, [i] 8.00×10^{-6}, [j] 9.00×10^{-6} and [k] 10.00×10^{-6} mol dm^{-3}; pH 7.40.

The emission spectrum of HSA (Figure 5A. 4**)** in the absence of **5m** demonstrated an emission maximum at 346 nm, when excited at 295 nm. Upon the regular addition of increasing concentration of **5m**, the emission intensity of HSA decreased and a large red shift in the maximum emission wavelength 346-349 nm occurred. Previously, similar behaviour was reported in the case of HSA with other organic moieties (Sharma *et al.* 2014:206),

(Bhattacharya *et al.* 2009:2143), (Zhang *et al.* 2013:14018), (Khan *et al.* 2011:617). This red shift are indication of binding between **5m** and an amino acid moiety present in HSA. The emission spectra monitored for HSA with increasing concentrations of **5m** is as presented in Figure 5A.4.

To determine a quenching mechanism of **5m**, the emission quenching data was analysed by the conventional Stern-Volmer equation (Lakowicz *et al.* 2003:435) (Eq. (5.1)).

$$\frac{F_0}{F} = 1 + K_{SV}[Q] = 1 + k_q\,\tau_0[Q] \ldots\ldots\ldots(5.1)$$

F_0 and F are emission intensities in the absence and presence of **5m** respectively. K_{SV} is the Stern-Volmer quenching constant, which was computed by linear plot of F_0/F against [compound], k_q is the bimolecular quenching rate constant, τ_0 is the average lifetime of the biomolecule without quencher ($\tau_0 = 10^{-8}$ s)[3] and [Q] is the concentration of quencher. Figure 5A. 5 **s**hows the Stern-Volmer plot for the quenching of HSA with **5m**.

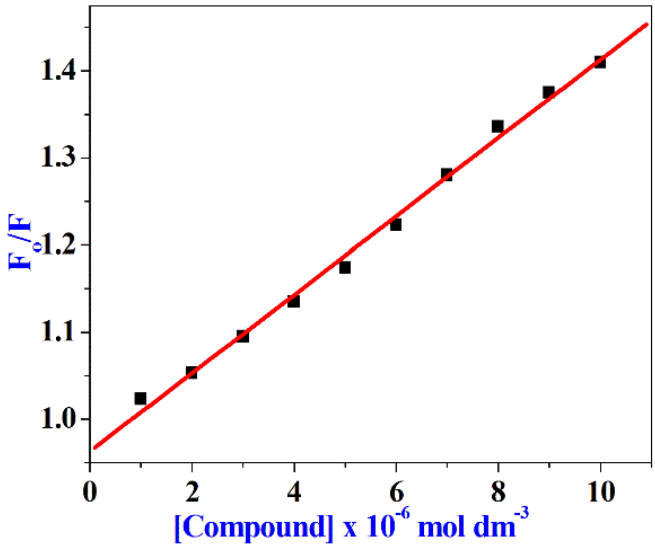

Figure 5A. 5. Stern-Volmer plot of HSA by various ratio of compound. [HSA] = 4 × 10^{-6} mol dm^{-3}; [compound] = (1.00 to 10.00 × 10^{-6} mol dm^{-3}); pH 7.40

The Stern-Volmer plot (Figure 5A. 5) demonstrated a good linear relationship with the experimental concentrations of the quencher. The K_{SV} value was determined from the slope of the linear plot and is tabulated in Table 5A. 5.

The bimolecular quenching constant K_q was calculated from the relation $K_q = K_{SV}/\tau_0$ and it was estimated as 7.00×10^{12} dm^3 mol^{-1} s^{-1}. However, the maximum scatter collision quenching constant, K_q of various quenchers with the biopolymer was 2.00×10^{10} dm^3 mol^{-1} s^{-1} (Hu *et al.* 2004: 915), (Shanmugaraj *et al.* 2014:43). Thus, the rate constant calculated by protein quenching procedure is greater than K_q of scatter procedure which means that the quenching process is static quenching.

Table 5A. 5. Binding parameters of HSA with synthesized compound system

Binding Parameters	K_{sv} (dm^3 mol^{-1})	K_q ($dm^3 mol^{-1} s^{-1}$)	K_b (dm^3 mol^{-1})	n
HSA -compound	4.70×10^4	4.70×10^{12}	2.67×10^5	1.13

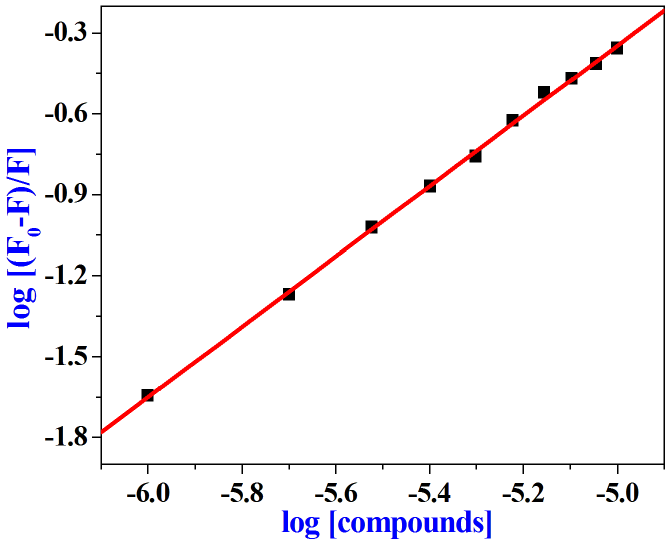

Figure 5A. 6. Plot of log [(F_0-F)/F] *vs* log [compound] for the HSA-compound system; pH 7.40.

The data obtained from emission spectral studies were used to determine the binding constant (K_b) and number of binding sites (n.) The emission quenching of HSA by **5m** was exploited to obtain binding parameters. K_b and n were calculated using the double-logarithmic equation (Anand *et al.* 2010:15839), (Sharma *et al.* 2014:206), (Shanmugaraj *et al.* 2014:43). (Eq. (5. 2).

$$\log\left[\frac{F_0-F}{F}\right] = \log K_b + n \log [Q] \ldots\ldots\ldots (5.\ 2)$$

F_0, F and [Q] are the same as in Eq. 5. 1. According to Eq. (5. 2), the plot of log [(F_0-F)/F] *vs* log [compound] is represented in Figure 5A. 6.

As illustrated in Figure 5A. 6, the double-logarithmic plot yielded a straight line with a slope value of approximately close to 1 and the analogous results are presented in **Table 5A.6.** The value of binding sites close to unity indicated that there is only one independent class of binding site on HSA for **5m**. The correlation coefficients are closer to 0.9996 which showed that the interaction between HSA and **5m** is in good accordance with the binding site model and obeyed Eq. (5. 2). In order to elucidate the complexation between **5m** and HSA, the free energy change (ΔG) was calculated by using the equation (Sharma *et al.* 2014:206), (Shanmugaraj *et al.* 2014:43), (Anand *et al.* 2010:15839).

$$\Delta G = -2.303\ RT \log K$$

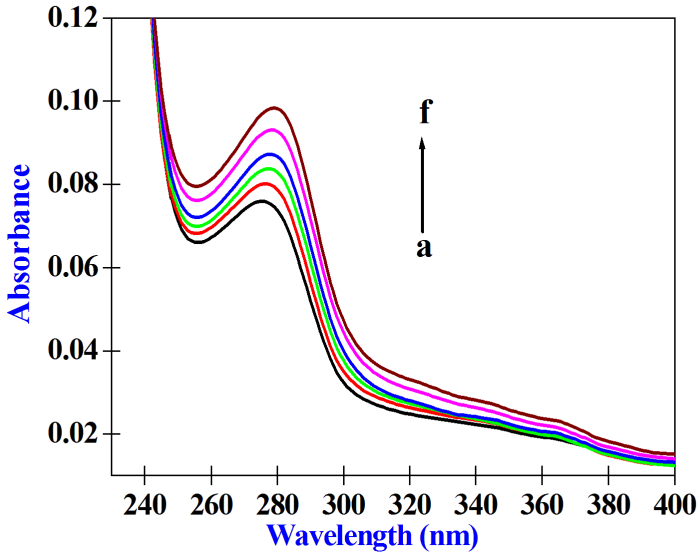

Figure 5A. 7. Absorption spectra of HSA (2.80×10^{-6} mol dm^{-3}) at various concentrations for compound 5m. [compound 5m]: [a] 0.00, [b] 2.00×10^{-6}, [c] 4.00×10^{-6}, [d] 6.00×10^{-6}, [e] 8.00×10^{-6} and [f] 10.00×10^{-6} mol dm^{-3}; pH 7.40

where, ΔG is free energy change, R is universal gas constant and T is room temperature (298 K) and K is analogous to the binding constant value obtained from double logarithmic equation. The free energy (ΔG) change for the complexation process of **5m** and HSA is

evaluated as -29.98 kJ mol^{-1}. The observed negative free energy change value indicated that the complexation process of **5m** with HSA was spontaneous and highly favourable.

To explore the structural changes of HSA and establish the quenching mechanism, UV-visible absorption spectra of HSA in different ratios of **5m** to HSA were measured (Figure 5A. 7). It was observed that in the absence of **5m,** HSA exhibited a strong absorption band at 279 nm which mainly arises from aromatic amino acid residues and disulphide bonds in the protein. Upon the successive addition of increasing concentrations of **5m** to HSA, the absorption intensity of the peak at 279 nm increased with a small red shift from 279 nm to 276 nm. Thus, the changes in absorption spectra of HSA suggested that small structural changes are due to an increased hydrophobicity of the Trip environment upon interaction of **5m** (Khan *et al.* 2011:617).

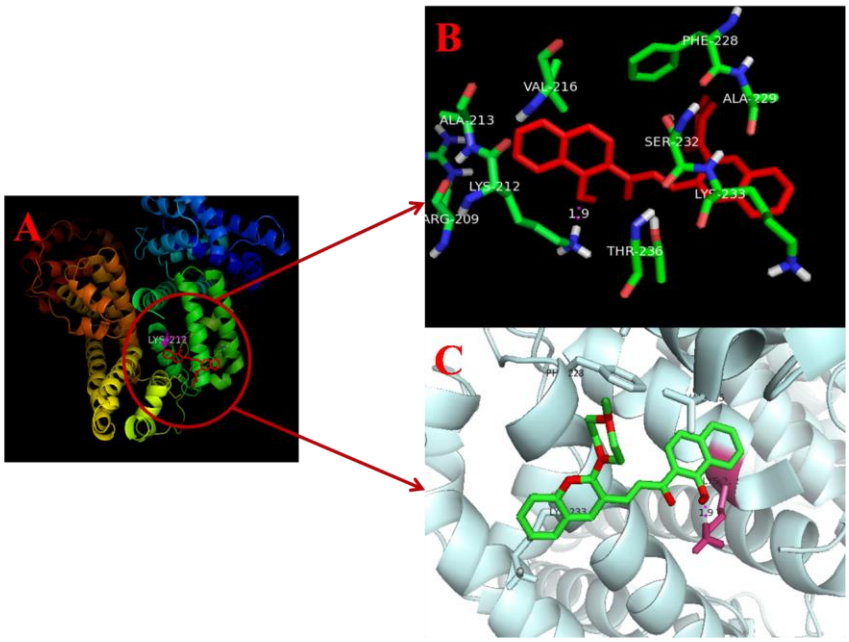

Figure 5A. 8. (A-C). (A) Molecular docking of the HSA-compound 5m complex. (B and C) Binding site of compound 5m on HSA-compound **5m** and selected amino acid residues are represented by stick and cartoon models. Hydrogen bond is shown in pink dotted line

In order to support the experimental results, computational docking analysis was performed to create a model for HSA-compound **5m** complex. It has been stated earlier that each domain of HSA protein contains two sub domains (IA and B, IIA and B, IIIA and B) that possess common structural motifs. Sudlow site I and Sudlow site II (subdomains IIA and IIIA respectively) are the most probable binding sites of the ligands. Molecular docking analysis

was performed using Auto Dock 4.2 program and the energetically most feasible HSA-compound **5m** complex is displayed in Figure 5A. 8 (A-C).

Docking results clearly pointed out that **5m** binds inside the binding pocket located in subdomain II A of HSA. It can be seen from Figure (A-C), **5m** is located adjacent to the amino acid residues Arg-209, Lys-212, Ala-213, Val-216, Phe-226, Ala-229, Ser-232, Lys-233 and Thr-239 of subdomain IIA of HSA. Furthermore, carbonyl group containing O atom of **5m** formed a hydrogen bond with Lys-212 with bond length of 1.9 Å. It is imperative to note from the computational observations that **5m** is in the locality of Trp-214 amino acid residue of HSA. From docking analyses, the free energy changes acquired for HSA binding is -21.54 kJ mol^{-1}. This is analogous with the experimental value obtained from emission data -29.98 kJ mol^{-1} at room temperature. Therefore, molecular docking study supports the emission spectral results regarding intrinsic emission quenching of Trp-214 for binding interaction between HSA and **5m**.

5A. 3. Conclusion

A boron nitride-based propyl sulphonic acid catalyst was employed for a one pot reaction for the synthesis of new functionalised methyl piperazinyl-quinolinyl chalcone derivatives. The reaction was effective in solvent conditions with a relatively short reaction time. However the catalytic activity was most effective in acetonitrile. Furthermore, this reaction creates new types of piperazinyl-quinolinyl chalcone derivatives which have suitable functionality for a host of possible biological applications. The chalcones could bind to HSA and causes a red shift in the emission spectra and slight fluorescence quenching occurred. The bi-molecular quenching constant, maximum scatter collision quenching constant and the free energy change for the complex were evaluated. Furthermore, molecular docking analyses showed that the free energy change was -21.54 kJ mol-1 and Trp-214 was the moiety of HSA that binds the chalcones.

5A. 4. Experimental

5A. 4. 1. Preparation of boron nitride based sulphonic acid (BN-Pr-SO_3H) catalyst

The preparation of BN-Pr-SO_3H was described in Chapter 4.4.2

5A. 4. 2. The procedure for the synthesis of substituted 2-(4-methylpiperazin-1-yl) quinoline-3-carbaldehyde (**3**)

The synthetic method was described in Chapter 3.4.3.

5A. 4. 3. General Procedure for the synthesis of (E)-3-(2-(4-methylpiperazin-1-yl) quinolin-3-yl)-1-phenylprop-2-en-1-one derivative (5a-n)

Firstly, BN-Pr-SO_3H (0.07 g) was activated in vacuum at 100 °C and subsequently cooled to room temperature. 2-(4-methylpiperazin-1-yl) quinoline-3-carbaldehyde (1.0 mmol), acetophenone (1.0 mmol) and acetonitrile (20 ml) were added. The mixture was heated at reflux in an oil bath: the condition for an appropriate time is shown in Table 5A. 3. The reaction profile was monitored by TLC. Thereafter the mixture was cooled and poured into ethanol in order to separate the catalyst. It was then filtered and the filtrate was cooled and the solvent removed *in vacuo*. Column chromatography using silica gel mesh was used to purify the compound with a solvent system of acetone and hexane. The catalyst was subsequently washed with dilute acid, distilled water and then acetone, dried under vacuum and recycled several times without loss of significant activity. The spectral (^{1}H NMR, ^{13}C NMR, MS, elemental analysis and FT-IR) data for the new compounds are presented below:

5A. 4. 3. 1. (E)-3-(2-(4-methylpiperazin-1-yl) quinolin-3-yl)-1-phenylprop-2-en-1-one (5a)

Yellow colour solid: yield 95 %: FT-IR (KBr): 3059, 2936, 2838, 2787, 1673, 1586, 1423, 1212, 1010, 759 cm^{-1}. ^{1}H NMR ($CDCl_3$, 400 MHz): δ 8.27 (1H, s, Ar-H), 8.08 (1H, dd, *J* = 5.32 Hz, Ar-H), 8.04 (2H, d, *J* = 15.92 Hz, Ar-H), 7.86 (1H, d, *J* = 8.44 Hz, Ar-H), 7.75 (1H, t, *J* = 8 Hz, Ar-H), 7.68 (1H, t, *J* = 7.52 Hz, Ar-H), 7.61-7.67 (2H, m, *J* = 1.84 Hz, Ar-H), 7.53-7.57 (2H, m, *J* = 6.64 Hz, Ar-H), 7.37-7.41 (1H, m, *J* = 7 Hz, Ar-H), 3.52 (4H, t, *J* = 4.32 Hz, CH_2), 2.75 (4H, d, *J* = 4.16 Hz, CH_2), 2.44(3H, s, CH_3). ^{13}C NMR ($CDCl_3$, 100 MHz): δ 190.1, 159.4, 147.7, 142, 137.9, 137.1, 133, 130.5, 127.8, 127.6, 124.8, 124.6, 122.8, 122.7, 54.8, 50, 45.8. TOFMS ES *m/z* (rel. int.): m/z: 358.19 $[M]^+$. Anal. Calc. for $C_{23}H_{23}N_3O$: C, 77.28; H, 6.49; N, 11.76 %. Found: C, 77.30; H, 6.48; N, 11.75 %.

5A. 4. 3. 2. (E)-1-(2-hydroxyphenyl)-3-(2-(4-methylpiperazin-1-yl) quinolin-3-yl) prop-2-en-1-one (5b)

Yellow colour solid: yield 92 %: FT-IR (KBr): 3453, 3356, 3025, 2970, 1739, 1366, 1217, 459 cm^{-1}. ^{1}H NMR ($CDCl_3$, 400 MHz): δ 12.76 (1H, s, Ar-OH), 8.13 (1H, s, Ar-H), 8 (1H, d, *J* = 15.48 Hz, Ar-H), 7.88 (1H, dd, *J* = 6.68 Hz, Ar-H), 7.75 (2H, t, *J* = 8.4 Hz, Ar-H), 7.63 (1H, d, *J* = 8 Hz, Ar-H), 7.56-7.51 (1H, dt, *J* = 1.48 Hz, Ar-H), 7.40-7.44 (1H, m, *J* = 1.48 Hz, Ar-H), 7.29-7.25 (1H, dt, *J* = 0.68 Hz, Ar-H), 6.96-6.94 (1H, dd, *J* = 0.76 Hz, Ar-H), 6.89-6.85

(1H, dt, *J* = 7.12 Hz, Ar-H), 3.35 (4H, t, *J* = 4.2 Hz, CH_2), 2.58 (4H, d, *J* = 4.48 Hz, CH_2), 2.30 (3H, s, CH_3). ^{13}C NMR ($CDCl_3$, 100 MHz): δ 193.5, 163.7, 159.6, 147.8, 142.8, 137.4, 136.5, 130.7, 129.6, 127.8, 127.6, 124.7, 124.6, 122.4, 120.8, 119.9, 118.9, 55, 50.4, 46.1. Anal. Calc. for $C_{23}H_{23}N_3O_2$: C, 73.97; H, 6.21; N, 11.25 %. Found: C, 73.95; H, 6.23; N, 11.27 %.

5A. 4. 3. 3. (E)-1-(4-hydroxyphenyl)-3-(2-(4-methylpiperazin-1-yl) quinolin-3-yl) prop-2-en-1-one (5c)

Yellow colour solid: yield 90 %: FT-IR (KBr): 3286, 3027, 2971, 1739, 1366, 1217, 732 cm^{-1}. ^{1}H NMR ($DMSOd_6$, 400 MHz): δ 10.50 (1H, s, Ar-OH), 8.79(1H, s, Ar-H), 8.11-8.08 (2H, dd, *J* = 5.44 Hz, Ar-H), 8.03 (1H, d, *J* = 15.6 Hz, Ar-H), 7.87 (1H, d, *J* = 7.96 Hz, Ar-H), 7.77(2H, t, *J* = 5.08Hz, Ar-H), 7.68-7.64 (1H, dt, *J* = 1.36 Hz, Ar-H), 7.44 (1H, dt, *J* = 6.84 Hz, Ar-H), 6.92 (2H, d, *J* = 8.72 Hz, Ar-H), 3.30 (4H, d, *J* = 17.52 Hz, CH_2), 2.50 (4H, m, *J* = 1.72 Hz, CH_2), 2.26 (3H, s, CH_3). ^{13}C NMR ($DMSOd_6$, 100 MHz): δ 206.4, 186.9, 162.3, 159.5, 146.78, 138.96, 137.14, 131.20, 130.4, 128.8, 128, 126, 124.7, 124.5, 123.1, 122.3, 115.4, 54.5, 50.1, 45.7, 40.1, 30.6. Anal. Calc. for $C_{23}H_{23}N_3O_2$: C, 73.97; H, 6.21; N, 11.25 %. Found: C, 73.95; H, 6.23; N, 11.26 %.

5A. 4. 3. 4. (E)-3-(2-(4-methylpiperazin-1-yl) quinolin-3-yl)-1-(4-nitrophenyl) prop-2-en-1-one (5d)

Yellow colour solid: yield 87 %: FT-IR (KBr): 2937, 2833, 2792, 1669, 1522, 1423, 1344, 1006, 706 cm^{-1}. ^{1}H NMR ($CDCl_3$, 400 MHz): δ 8.42 (1H, s, Ar-H), 8.90-8.36 (1H, dd, *J* = 1.96Hz, Ar-H), 8.34 (1H, d, *J* = 4.52 Hz, Ar-H), 8.30 (1H, d, *J* = 6.12 Hz, Ar-H), 8.22-8.17 (2H, dd, *J* = 8.76 Hz, Ar-H), 8.10 (1H, d, *J* = 15.68 Hz, Ar-H), 7.87-7.81(1H, dd, *J* = 5.72 Hz, Ar-H), 7.67 (1H, t, *J* = 6.92 Hz, Ar-H), 7.63-7.58 (1H, dt, *J* = 7.12 Hz, Ar-H), 7.76 (1H, dt, *J* = 7.08 Hz, Ar-H), 3.96 (1H, dd, *J* = 5.04 Hz, CH_2), 3.70 (2H, dd, *J* = 2.96Hz, CH_2), 3.45 (2H, dd, *J* = 10.52 Hz, CH_2), 3.02 (1H, s, CH) 2.69 (1H, s, CH), 2.50 (1H, s, CH), 2.20 (3H, s, CH_3). ^{13}C NMR ($CDCl_3$, 100 MHz): δ 188.6, 159.5, 150.8, 150.4, 148, 146.5, 144, 142.7, 141.4, 140.9, 139.6, 137.5, 130.9, 129.6, 129.6, 129.4, 129.2, 127.9, 127.7, 127.7, 126.9, 124.8, 124.8, 124.7, 124.1, 124, 123.9, 122, 121.7, 120.9, 54, 50.3, 48.9, 36.3, 35.2, 34.3. Anal. Calc. for $C_{23}H_{22}N_4O_3$: C, 68.64; H, 5.51; N, 13.92 %. Found: C, 68.66; H, 5.53; N, 13.90 %.

5A. 4. 3. 5. (E)-3-(2-(4-methylpiperazin-1-yl) quinolin-3-yl)-1-(p-tolyl) prop-2-en-1-one (5e)

Yellow colour solid: yield 80 %: FT-IR (KBr): 2953, 2838, 2792, 1677, 1663, 1602, 1426, 1279, 759 cm^{-1}. ^{1}H NMR ($CDCl_3$, 400 MHz): δ 7.93 (3H, d, J = 8.2 Hz, Ar-H), 7.89 (1H, s, Ar-H), 7.86 (1H, d, J = 8.4Hz, Ar-H), 7.64 (1H, d, J = 7.92 Hz, Ar-H), 7.54-7.58 (1H, td, J = 7.08 Hz, Ar-H), 7.34-7.38 (1H, td, J = 7.12 Hz, Ar-H), 7.28 (3H, d, J = 8.04 Hz, Ar-H), 4.51 (1H, t, J = 7.04 Hz, CH_2), 3.2-3.47 (7H, m, J = 7Hz, CH_2), 2.42 (3H, s, CH_3), 2.34 (3H, s, CH_3). ^{13}C NMR ($CDCl_3$, 100 MHz): δ 198.2, 160.9, 146, 144, 134.3, 134, 132.5, 129.3, 128.7, 128.4, 127.7, 126.9, 126, 124.7, 54.9, 50.7, 46, 44.2, 32, 30.9, 21.6. Anal. Calc. for $C_{24}H_{25}N_3O$: C, 77.60; H, 6.78; N, 11.31 %. Found: C, 77.62; H, 6.76; N, 11.33 %.

5A. 4. 3. 6. (E)-1-(4-methoxyphenyl)-3-(2-(4-methylpiperazin-1-yl) quinolin-3-yl) prop-2-en-1-one (5f)

Yellow colour solid: yield 85 %: FT-IR (KBr): 2940, 2837, 2791, 1659, 1587, 1421, 1171, 1005, 834, 760 cm^{-1}. ^{1}H NMR ($CDCl_3$, 400 MHz): δ 8.23 (1H, s, Ar-H), 8.19 (2H, d, J = 8.8 Hz, Ar-H), 8.0 (1H, d, J = 15.68 Hz, Ar-H), 7.84 (1H, d, J = 8.4 Hz, Ar-H), 7.72 (2H, d, J = 5.96 Hz, Ar-H), 7.60-7.64 (1H, m, J = 1.12 Hz, Ar-H), 7.38 (1H, t, J = 7.12 Hz, Ar-H), 7.01 (2H, d, J = 7.04 Hz, Ar-H), 3.90 (3H, s, OCH_3), 3.46 (4H, s, CH_2), 32.68 (4H, t, J = 4.36Hz, CH_2), 2.39 (3H, s, CH_3). ^{13}C NMR ($CDCl_3$, 100 MHz): δ 188.2, 163.6, 159.6, 147.6, 141.3, 136.9, 130.8, 130.3, 127.7, 127.5, 124.8, 124.4, 122.9, 122.5, 113.9, 55.5, 55, 50.2, 46.1. Anal. Calc. for $C_{24}H_{25}N_3O_2$: C, 74.39; H, 6.50; N, 10.84 %. Found: C, 74.41; H, 6.52; N, 10.82 %.

5A. 4. 3. 7. (E)-3-(2-(4-methylpiperazin-1-yl) quinolin-3-yl)-1-(thiophen-2-yl) prop-2-en-1-one (5g)

Yellow colour solid: yield 90 %: FT-IR (KBr): 3059, 2936, 2838, 2787, 1673, 1586, 1423, 1212, 759 cm^{-1}. ^{1}H NMR ($CDCl_3$, 400 MHz): δ 8.13 (1H, s, Ar-H), 7.94 (1H, d, J = 15.64 Hz, Ar-H), 7.84-7.83 (1H, dd, J = 3.08 Hz, Ar-H), 7.75 (1H, d, J = 8.44 Hz, Ar-H), 7.63 (2H, dd, J = 3.92 Hz, Ar-H), 7.55-7.51 (2H, dt, J = 1.4 Hz, Ar-H), 7.29-7.25 (1H, m, J = 0.84 Hz, Ar-H), 7.13-7.11 (1H, dd, J = 4 Hz, Ar-H), 3.36 (4H, t, J = 3.96Hz, CH_2), 2.58 (4H, t, J = 4.52Hz, CH_2), 2.30 (3H, s, CH_3). ^{13}C NMR ($CDCl_3$, 100 MHz): δ 181.8, 159.6, 147.7, 145.4, 141.4, 137.2, 134.1, 131.9, 130.5, 128.3, 127.8, 127.6, 124.7, 124.5, 122.5, 122.3, 55, 50.3, 46.1. .Anal. Calc. for $C_{21}H_{21}N_3OS$: C, 69.39; H, 5.82; N, 11.56 %. Found: C, 69.42; H, 5.84; N, 11.58%.

5A. 4. 3. 8. (E)-1-(4-fluorophenyl)-3-(2-(4-methylpiperazin-1-yl) quinolin-3-yl) prop-2-en-1-one (5h)

Yellow colour solid: yield 90 %: FT-IR (KBr): 2944, 2838, 2787, 1675, 1583, 1425, 1009, 759 cm^{-1}. ^{1}H NMR ($CDCl_3$, 400 MHz): δ 8.08 (1H, s, Ar-H), 8.05 (1H, d, *J* = 1.72Hz, Ar-H), 8.02 (1H, d, *J* = 8.88 Hz, Ar-H), 7.90 (1H, d, *J* = 1.76 Hz, Ar-H), 7.87 (1H, d, *J* = 8.4 Hz, Ar-H), 7.70 (1H, d, *J* = 8.28 Hz, Ar-H), 7.56-7.59 (1H, m, *J* = 1.6 Hz, Ar-H), 7.17 (1H, d, *J* = 2.48 Hz, Ar-H), 7.15 (1H, d, *J* = 2.64 Hz, Ar-H), 7.13 (1H, d, *J* = 2.68 Hz, Ar-H), 6.95 (1H, d, *J* = 8.92 Hz, Ar-H), 3.95 (2H, d, *J* = 13.4 Hz, CH_2), 3.44 (2H, d, *J* = 7.2 Hz, CH_2), 3.26-3.37 (4H, m, *J* = 6.8 Hz, CH_2), 2.34 (3H, s, CH_3). ^{13}C NMR ($CDCl_3$, 100 MHz): δ 196.8, 163.7, 160.8, 146, 134.1, 133.1, 132.3, 132.1, 131, 130.5, 129.7, 128.9, 128.8, 127.8, 127.7, 126.9, 126, 124.9, 124.8, 115.9, 113.8, 55.6, 55, 50.8, 44.2, 31.8. ^{19}F NMR ($CDCl_3$, 400 MHz): δ -104.78. Anal. Calc. for $C_{23}H_{22}FN_3O$: C, 73.58; H, 5.91; N, 11.19 %. Found: C, 73.60; H, 5.95; N, 11.17 %.

5A. 4. 3. 9. (E)-1-(4-chlorophenyl)-3-(2-(4-methylpiperazin-1-yl) quinolin-3-yl)prop-2-en-1-one (5i)

Yellow colour solid: yield 87 %: FT-IR (KBr): 2926, 2838, 2788, 1644, 1583, 1519, 1421, 1008, 759 cm^{-1}. ^{1}H NMR ($CDCl_3$, 400 MHz): δ 7.97 (3H, d, *J* = 8.52Hz, Ar-H), 7.88 (1H, s, Ar-H), 7.86 (1H, d, *J* = 9.76Hz, Ar-H), 7.64 (1H, d, *J* = 7.96 Hz, Ar-H), 7.55-7.59 (1H, td, *J* = 7.2 Hz, Ar-H), 7.46 (3H, d, *J* = 8.48 Hz, Ar-H), 7.36 (1H, t, *J* = 7.52 Hz, Ar-H), 4.50 (1H, t, *J* = 7.28 Hz, CH), 3.48 (1H, d, *J* = 7.28 Hz, CH), 3.44 (1H, d, *J* = 7.2 Hz, CH), 3.34 (1H, d, *J* =6.72 Hz, CH), 3.30 (1H, d, *J* = 6.72 Hz, CH_2), 3.24 (3H, t, *J* = 4.32Hz, CH_2), 2.33 (3H, s, CH_3). ^{13}C NMR ($CDCl_3$, 100 MHz): δ 197.2, 160.7, 146, 139.8, 134.9, 134.2, 131.9, 129.7, 129, 128.9, 127.8, 126.9, 125.9, 124.9, 55, 50.9, 46, 44.3, 31.7, 30.9. Anal. Calc. for $C_{23}H_{22}ClN_3O$: C, 70.49; H, 5.66; N, 10.72 %. Found: C, 70.51; H, 5.68; N, 10.75 %.

5A. 4. 3. 10. (E)-1-(4-bromophenyl)-3-(2-(4-methylpiperazin-1-yl) quinolin-3-yl) prop-2-en-1-one (5j)

Yellow colour solid: yield 85 %: FT-IR (KBr): 3058, 2929, 3846, 2791, 1676, 1595, 1421, 1156, 835, 759 cm^{-1}. ^{1}H NMR ($CDCl_3$, 400 MHz): δ 8.18 (1H, s, Ar-H), 7.95 (1H, d, *J* = 15.92 Hz, Ar-H), 7.87 (1H, d, *J* = 8.52 Hz, Ar-H), 7.80 (2H, t, *J* = 8.44 Hz, Ar-H), 7.66 (1H, d, *J* = 7.36 Hz, Ar-H), 7.60 (3H, d, *J* = 8.68 Hz, Ar-H), 7.55 (2H, t, *J* = 6.08 Hz, Ar-H), 3.40 (4H, d, *J* = 4.16 Hz, CH_2), 3.24 (2H, d, *J* = 6.88 Hz, CH_2), 2.63 (2H, t, *J* = 4.04 Hz, CH_2), 2.34 (3H, s, CH_3). ^{13}C NMR ($CDCl_3$, 100 MHz): δ 197.4, 160.7, 146, 135.3, 134.2, 132, 131.9, 129.8,

129, 128.6, 127.8, 126.9, 125.9, 124.9, 55, 50.9, 46.1, 44.3, 31.6, 29.7. Anal. Calc. for $C_{23}H_{22}BrN_3O$: C, 63.31; H, 5.08; N, 9.63 %. Found: C, 63.34; H, 5.10; N, 9.65 %.

5A. 4. 3. 11. (E)-1-(3-aminophenyl)-3-(2-(4-methylpiperazin-1-yl) quinolin-3-yl) prop-2-en-1-one (5k)

Yellow colour solid: yield 87 %: FT-IR (KBr): 3467, 3014, 2971, 2937, 2838, 1739, 1566, 1365, 749 cm^{-1}. ^1H NMR ($CDCl_3$, 400 MHz): δ 8.20 (1H, s, Ar-H), 7.96 (1H, d, *J* = 15.72 Hz, Ar-H), 7.84 (1H, d, *J* = 8.4Hz, Ar-H), 7.72 (1H, d, *J* = 7.96 Hz, Ar-H), 7.60-7.64 (2H, dt, *J* = 8.48 Hz, Ar-H), 7.43 (1H, d, *J* = 7.64 Hz, Ar-H), 7.36 (1H, m, *J* = 2.08 Hz, Ar-H), 7.34 (1H, s, Ar-H), 7.36 (1H, t, *J* = 7.8 Hz, Ar-H), 6.89-6.92 (1H, dd, *J* = 2.04 Hz, Ar-H), 3.92 (2H, s, NH_2), 3.44 (4H, s, CH_2), 2.65 (4H, d, *J* = 3.84 Hz, CH_2), 2.31 (3H, s, CH_3). ^{13}C NMR ($CDCl_3$, 100 MHz): δ 190.3, 159.6, 147.6, 147, 141.7, 139, 137, 130.4, 129.5, 127.8, 127.5, 124.8, 124.5, 122.9, 122.7, 119.6, 118.7, 114.3, 55, 50.2, 46.1. Anal. Calc. for $C_{23}H_{24}N_4O$: C, 74.17; H, 6.49; N, 15.04 %. Found: C, 74.20; H, 6.50; N, 15.08 %.

5A. 4. 3. 12. (E)-3-(2-(4-methylpiperazin-1-yl) quinolin-3-yl)-1-(naphthalen-2-yl) prop-2-en-1-one (5l)

Yellow colour solid: yield 90 %: FT-IR (KBr): 3050, 2953, 2935, 2283, 2789, 1673, 1586, 1423, 759 cm^{-1}. ^1H NMR ($CDCl_3$, 400 MHz): δ 8.61 (1H, s, Ar-H), 8.32 (1H, s, Ar-H), 8.15-8.17 (1H, dd, *J* = 1.48Hz, Ar-H), 8.03-8.11 (2H, d, *J* = 15.68 Hz, Ar-H), 7.98 (1H, d, *J* = 8.64 Hz, Ar-H), 7.94 (1H, t, *J* = 2.84 Hz, Ar-H), 7.86-7.90 (2H, dd, *J* = 5.24 Hz, Ar-H), 7.77 (1H, d, *J* = 7.96 Hz, Ar-H), 7.67 (1H, d, *J* = 1.24 Hz, Ar-H), 7.66 (1H, d, *J* = 2.84 Hz, Ar-H), 7.61-7.63 (1H, m, *J* = 1.48 Hz, Ar-H), 7.40 (1H, t, *J* = 7.32 Hz, Ar-H), 3.45 (4H, d, *J* = 6.24 Hz, CH_2), 2.71 (4H, d, *J* = 4.2 Hz, CH_2), 2.40 (3H, s, CH_3). ^{13}C NMR ($CDCl_3$, 100 MHz): δ 189.8, 159.6, 147.7, 142, 137.2, 135.5, 135.3, 132.5, 130.5, 130, 129.5, 128.7, 128.5, 127.8, 127.6, 124.8, 124.6, 124.4, 122.8, 122.7, 54.9, 50.2, 46. TOFMS ES *m/z* (rel. int.): m/z: 407.20 $[M]^+$. Anal. Calc. for $C_{27}H_{25}N_3O$: C, 79.58; H, 6.18; N, 10.31 %. Found: C, 79.60; H, 6.21; N, 10.33 %.

5A. 4. 3. 13. (E)-1-(1-hydroxynaphthalen-2-yl)-3-(2-(4-methylpiperazin-1-yl) quinolin-3-yl) prop-2-en-1-one (5m)

Yellow colour solid: yield 92 %: FT-IR (KBr): 3467, 3014, 2971, 2937, 2838, 1739, 1566, 1365, 749 cm^{-1}. ^1H NMR ($CDCl_3$, 400 MHz): δ 14.88 (1H, s, Ar-OH), 8.53 (1H, d, *J* = 8.16 Hz, Ar-H), 8.30 (1H, s, Ar-H), 8.18 (1H, d, *J* = 9.48 Hz, Ar-H), 7.93 (1H, d, *J* = 8.88 Hz, Ar-

H), 7.90 (1H, d, *J* =2.32 Hz, Ar-H), 7.88 (1H, d, *J* =8.4 Hz, Ar-H), 7.80 (1H, d, *J* =8.96 Hz, Ar-H), 7.77 (1H, d, *J* =0.72 Hz, Ar-H), 7.66-7.69 (1H, m, *J* = 1.48 Hz, Ar-H), 7.64-7.65 (1H, m, *J* = 0.8 Hz, Ar-H), 7.55-7.59 (1H, m, *J* = 1.28 Hz, Ar-H), 7.39-7.43 (1H, m, *J* = 0.88 Hz, Ar-H), 7.35 (1H, d, *J* = 8.92 Hz, Ar-H), 3.54 (4H, s, CH_2), 2.78 (4H, d, *J* = 4.08 Hz, CH_2), 1.27 (3H, s, CH_3). ^{13}C NMR ($CDCl_3$, 100 MHz): δ 192.9, 164.6, 159.4, 147.8, 142.2, 137.5, 137.4, 130.7, 130.3, 127.8, 127.6, 127.4, 126, 125.5, 124.8, 124.7, 124.5, 123.8, 122.6, 121.3, 118.3, 113.3, 54.90, 50.12, 45.9. TOFMS ES *m/z* (rel. int.): m/z: 423.19 $[M]^+$. Anal. Calc. for $C_{27}H_{25}N_3O_2$: C, 76.57; H, 5.95; N, 9.92 %. Found: C, 76.59; H, 5.96; N, 9.93 %.

5A. 4. 3. 14. (E)-1-(anthracen-9-yl)-3-(2-(4-methylpiperazin-1-yl) quinolin-3-yl) prop-2-en-1-one (5n)

Yellow colour solid: yield 90 %: FT-IR (KBr): 3466, 3067, 2931, 2850, 1706, 1652, 1404, 704 cm^{-1}. ^{1}H NMR ($CDCl_3$, 400 MHz): δ 8.56 (1H, s, Ar-H), 8.25 (1H, s, Ar-H), 8.07 (2H, t, *J* = 7.16 Hz, Ar-H), 7.92 (2H, t, *J* = 7.28 Hz, Ar-H), 7.74 (1H, d, *J* = 8.4 Hz, Ar-H), 7.70 (1H, d, *J* = 7.92 Hz, Ar-H), 7.55-7.59 (1H, m, *J* = 0.96 Hz, Ar-H), 7.46-7.50 (4H, m, *J* = 3.12 Hz, Ar-H), 7.35 (1H, d, *J* = 16.36 Hz, Ar-H), 7.34 (1H, t, *J* = 7.12 Hz, Ar-H), 7.11 (1H, d, *J* = 16.44 Hz, Ar-H), 3 (4H, t, *J* = 4.4 Hz, CH_2), 2 (3H, s, CH_3) 1.67 (4H, s, CH_2). ^{13}C NMR ($CDCl_3$, 100 MHz): δ 201, 159, 147.9, 146.5, 136.9, 134, 131.2, 130.7, 130.1, 128.8, 128.5, 128.3, 128, 127.5, 126.7, 125.6, 125, 124.6, 121.6, 54.3, 50.1, 45.7. Anal. Calc. for $C_{31}H_{27}N_3O$: C, 81.37; H, 5.95; N, 9.18 %. Found: C, 81.35; H, 5.97; N, 9.17 %.

5A. 5. Absorption and emission spectral measurements

Absorption and emission spectral measurements were made by using JASCO V-630 UV-visible spectrophotometer and JASCO FP-6600 Spectrofluorometer equipped with a quartz cuvette of path length 1 cm. All the emission titration experiments were carried out by adding appropriate amount of compound **5m** to 1 ml of HSA solution in a 5 ml standard flask in sequence with addition of phosphate buffer solution (PBS). The solution was allowed to equilibrate for 15 min before recording the spectra. The homogeneous solution systems were in a quartz (1 cm) cuvette. The stock solution of HSA was prepared by using PBS of pH= 7.40. The concentration of HSA was spectrophotometrically measured using a reported procedure (Hu *et al.* 2004: 915). All experimentation was carried out at an ambient temperature (25 °C).

5A. 6. Molecular Docking Studies

The Auto Dock 4.2 program which operates the Lamarckian genetic algorithm (LGA) was used to dock compound **5m** with the 3D structure of HSA. The crystal structure of HSA (PDB id: 1AO6) was obtained from the protein data bank and all water molecules were eliminated with successive addition of hydrogen atoms, followed by the computation of Gasteiger charges as required for LGA molecular docking procedure. The grid size along the x-, y- z- axes and grid space were set to 60 Å, 60 Å and 60 Å and 0.403 Å, respectively for HSA. To include the whole subdomain IIA of HSA during the docking process, the grid centre along the x-, y- z- axes was set at 34.016 Å, 42.121 Å, and 50.644 Å. The following docking parameters were used: Genetic Algorithm (GA) population=150; maximum number of energy evaluations=250,000 and GA crossover mode of two points. For each docking simulation, 20 different conformers were generated and the PyMOL package software was used for visualization of the interaction of the docked protein−ligand complex. The conformation with the lowest binding free energy was used for further analysis (Hu *et al.* 2004: 915).

[2]Part B: Synthesis of ethyl-piperazinyl quinolinyl-(*E*)-chalcone derivatives by using a novel titanium nanomaterial based sulfonic acid catalyst

5B. 1. Abstract

A new rutile titanium dioxide nanomaterial-based sulfonic acid catalyst (TiO_2-BPTETSA) was synthesized and characterized by FT-IR, XRD, TEM, SEM, BET and Raman spectroscopy. It exhibited efficient catalytic activity for the synthesis of (*E*)-3-(2-(4-ethylpiperazin-1-yl) quinolin-3-yl)-1phenylprop-2-en-1-one derivatives under solvent free conditions. Briefly the catalyst was synthesized by refluxing a mixture of nitric acid activated titanium dioxide, 3-mercaptochloropropyl and triethylene tetramine. This was a facile and environmentally benign method for the preparation of catalyst. The starting substrate 2-(4-ethylpiperazin-1-yl) quinoline-3-carbaldehyde (**1**) was synthesized from 2-chloroquinoline-3-carbaldehyde and an excess of 1-ethylpiperazine. The one-pot reaction of **1** and acetophenone derivatives produced chalcone derivatives **5a-n** of yield 85-97 %. The chalcones were characterized by FT-IR, ^{1}H NMR, ^{13}C NMR and MS-TOF whilst **5m** included DEPT-90, DEPT-135, COSY, NOSEY, HSQCE and HMBC. High yield, simple methodology and short reaction time were some of the advantages of this methodology whilst a decrease of a mere 10 % in catalytic activity, in five cycles, makes it cost effective for any possible large scale production. Furthermore **(***E*)-1-(1-hydroxynaphthalen-2-yl)-3-(2-(4-ethylpiperazin-1 yl)quinolin-3-yl) prop-2-en-1-one was used in molecular docking studies with bovine serum albumin (BSA) protein: binding was located in subdomain II A of BSA containing the amino acid residues Arg-209, Lys-212, Ala-213, Val-216, Phe-226, Ala-229, Ser-232, Lys-233 and Thr-239.

5B. 2. Results and discussion

A one-pot synthesis of functionalised ethyl-piperazinyl quinolinyl chalcone derivatives, under solvent-free conditions, using a new titanium dioxide nanomaterial based sulfonic acid catalyst (TiO_2-BPTETSA) is presented in this study. The catalyst was synthesized in three stages. Briefly, a mixture of TiO_2 and 65 % nitric acid was refluxed for 24 h; this preliminary step aimed at introducing –OH groups on the surface of TiO_2 through an oxidation process.

[2]***Murugesan, A., Gengan, R.M. and Lin, C.H., 2017.*** *Efficient synthesis of ethyl–piperazinyl quinolinyl-(E)-chalcone derivatives via Claisen–Schmidt reaction by using TiO2-BPTETSA catalyst. Journal of the Taiwan Institute of Chemical Engineers,* ***80, pp.852-866.***

Thereafter (3-mercaptochloropropyl) trimethoxysilane was added and the reaction mixture was refluxed for 24 h. A solution of triethylenetetramine was subsequently added and the resulting mixture was refluxed for 24 h. The reaction mixture was then cooled to room temperature and filtered: the filter-cake was washed with xylene and ethanol and dried under vacuum overnight. To the product 3-TETANPTiO$_2$, chlorosulfonic acid was added and the mixture was stirred for a further 3 h, filtered, washed with ethanol and dried at room temperature to produce TiO$_2$-BPTETSA as a cream powder (Scheme 5B. 1).

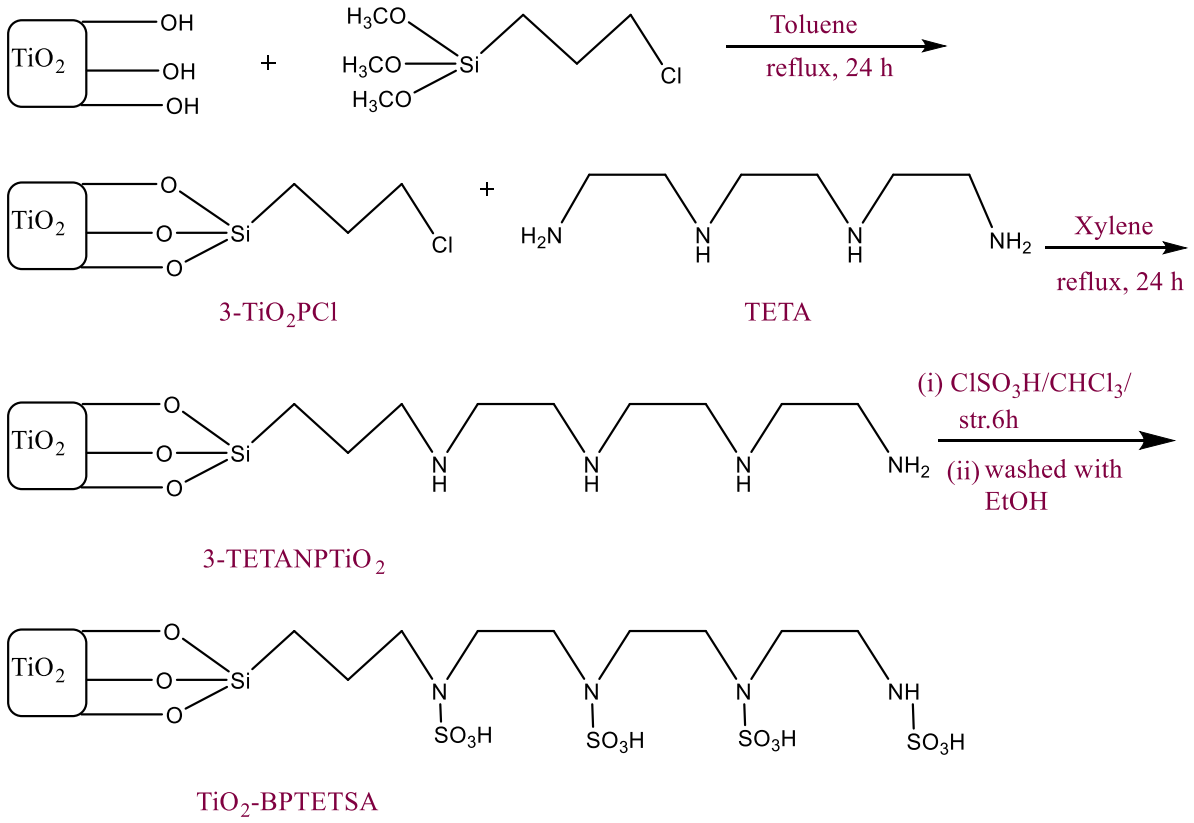

Scheme 5B. 1. The reaction scheme for the synthesis of TiO$_2$-BPTETSA

TiO$_2$-BPTETSA was characterized by FT-IR, XRD, TEM, SEM, BET and Raman spectroscopy. The FT-IR spectrum of pure TiO$_2$ and TiO$_2$-BPTETSA were analysed. In the case of TiO$_2$, the absorption at 868 cm^{-1} is Ti-O stretch and 1414 cm^{-1} is the Ti-O-Ti stretch. The spectrum of TiO$_2$-BPTETSA was similar to TiO$_2$. However the N-H stretch was observed at 3243 cm^{-1}. Also, the C-H stretch at 2954 cm^{-1} and Si-O stretch at 1211 cm^{-1} was observed. The absorptions at 1163 and 1141 cm^{-1} was assigned to the S=O stretch (Appendix Figure 5B.S1 and 5B. S2).

The crystallinity and morphology of TiO_2 and TiO_2-BPTETSA were obtained by using XRD and SEM techniques, respectively. The XRD patterns of TiO_2-BPTETSA are almost the same as those of TiO_2 which suggested that the sulphate modification does not alter TiO_2 (Figure 5B. 1).

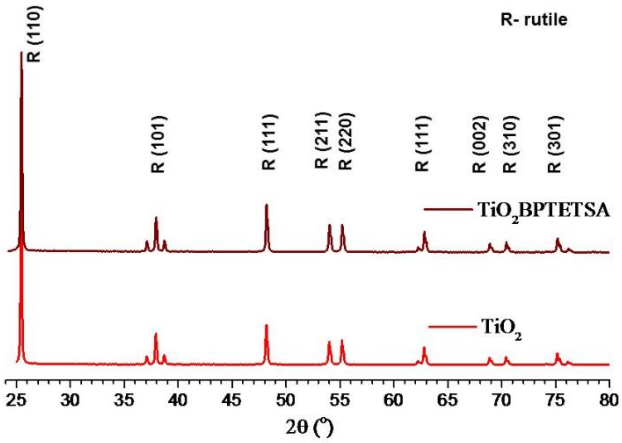

Figure 5B. 1. PXRD pattern of TiO_2 and TiO_2-BPTETSA

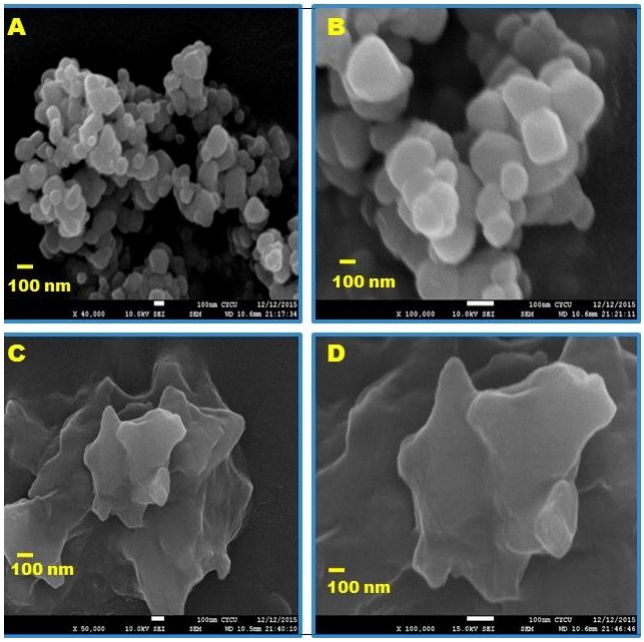

Figure 5B. 2. Scanning electron micrograph images of TiO_2 (A, B) and TiO_2-BPTETSA (C, D)

SEM was used to determine the morphology and microstructure of TiO_2 and TiO_2-BPTETSA (Figure 5B. 2: A, B, and C, D**).** Aggregates of spherically shaped particles were observed. The particles are tightly packed.

The identity of TiO_2 and TiO_2-BPTETSA were confirmed by EDS analysis for Ti, O, C, and S elements (Figure 5B. 3). The actual weight % in TiO_2 elements for Ti, O, C, S and Pt

were weight % 36, 36.80, 17.28, 0, 9.92, whilst the atomic (%) were 17, 50.40, 31.76, 0, 0.84, respectively. The carbon content in TiO_2 may be due to carbon tape that was used. The EDS of the catalyst TiO_2-BPTETSA displayed elements Ti, O, C, S, Pt, of weight % 39.09, 42.22, 8.73, 0.58, 9.38 whilst the atomic (%) were 19.25, 61.0, 16.60, 0.42, 2.73, respectively (Table 5B.1).

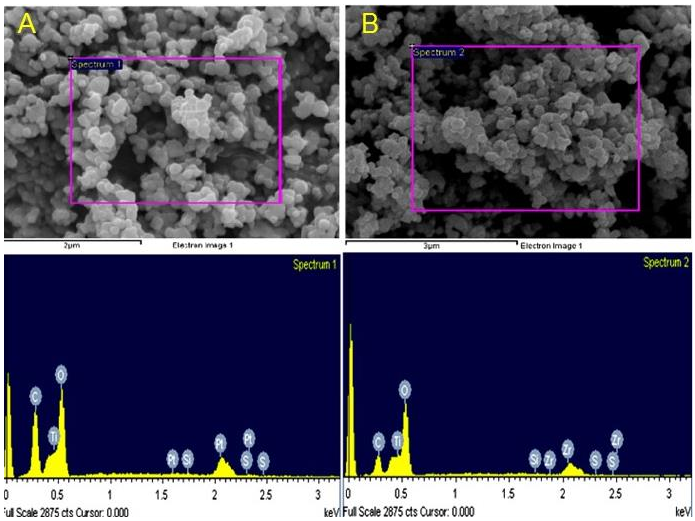

Figure 5B. 3. Energy-dispersive X-ray spectroscopy (EDS) analysis for TiO_2 (A) and TiO_2-BPTETSA (B)

Table 5B. 1. The weight (%) analysis for TiO_2 and TiO_2-BPTETSA.

	TiO_2		TiO_2-BPTETSA	
Element	Weight (%)	Atomic (%)	Weight (%)	Atomic (%)
Ti	36	17	39.09	19.25
O	36.80	50.40	42.22	61.0
C	17.28	31.76	8.73	16.60
S	-	-	0.58	0.42
Pt	9.92	0.84	9.38	2.73

The morphology and microstructure of the catalyst were characterized with TEM. The TEM image for different orientations was done to get the average crystallite size of TiO_2-BPTETSA (Figure 5B. 4). The dimensions of TiO_2-BPTETSA at 200 nm indicated good mesoporous structures as evidence of good surface for catalytic activity.

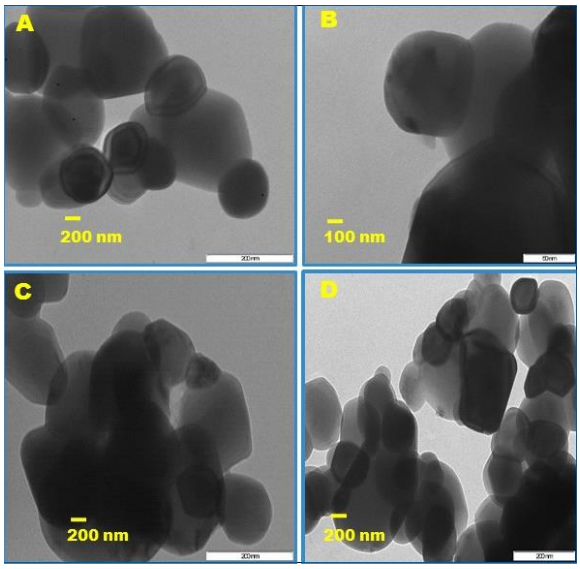

Figure 5B. 4. Transmission electron microscopy (TEM) micrographs image of TiO_2 (A, B) and TiO_2-BPTETSA (C, D)

The porous property of TiO_2 and TiO_2-BPTETSA is as shown by N_2 gas adsorption measurements at 273 K. Figure 5B. 5 shows TiO_2 as a type-I adsorption isotherm which is characteristic of microporous material and the BET and Langmuir surface area of TiO_2 were calculated as 8 and 12 m^2/g respectively. The N_2 adsorption isotherm of TiO_2-BPTETSA also indicated a type-I adsorption isotherm however the BET and Langmuir surface area were calculated as 17 and 38 m^2/g respectively.

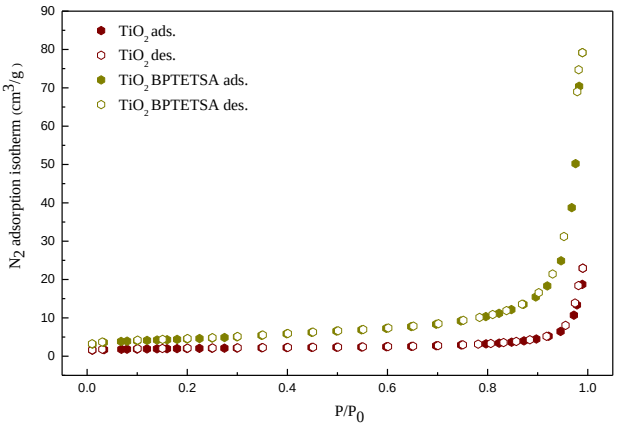

Figure 5B. 5. Adsorption and desorption isotherms of TiO_2 and TiO_2-BPTETSA at 273 K.

The structure of TiO_2 and TiO_2-BPTETSA were also investigated by Raman spectroscopy (Figure 5B. 6). The spectrum shows absorption signals at 450, 470, 500, 570, 600, 2000, 3000 and 3650 cm^{-1} for TiO_2. The absorption signal of TiO_2-BPTETSA showed

absorptions signals at 470, 500, 650, 800, 900, 2000, 3000, 3650 cm^{-1} with an additional signal at 3450 cm^{-1} indicating the acidic functional groups.

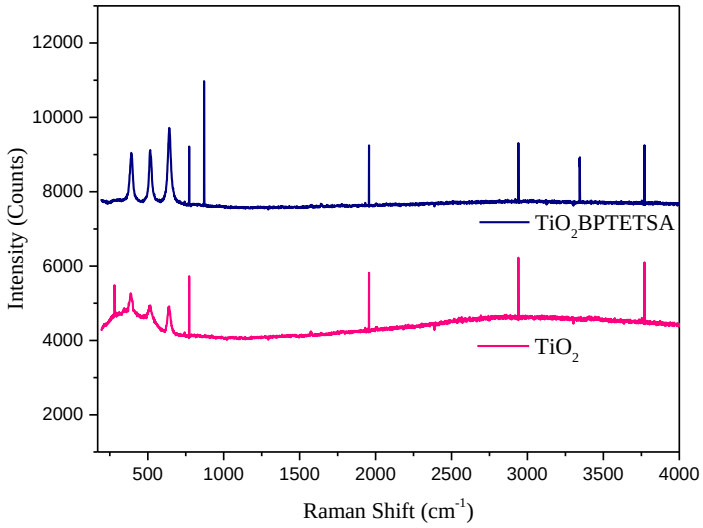

Figure 5B. 6. Raman Shift of TiO_2 and TiO_2-BPTETSA

In order to synthesize new ethyl-piperazinyl quinolinyl (*E*)-3-(2-(4-ethylpiperazin-1-yl)quinolin-3-yl)-1-phenylprop-2-en-1-one chalcone derivatives (**5a-n**), compound **1** and various acetophenone (**4a-n**) derivatives, in the presence of TiO_2-BPTETSA catalyst, were investigated (Scheme 5B. 2).

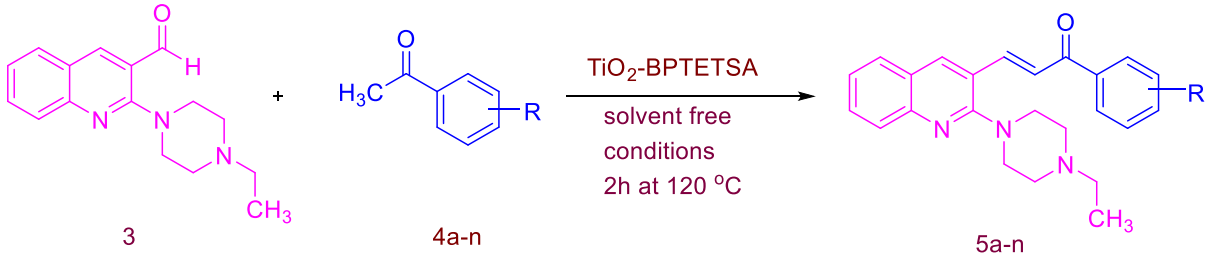

KEY= 5a (R=H); 5b (R=2- OH); 5c (R=4- OH); 5d (R=4- NO_2); 5e (R=para- CH_3); 5f (R=para O-CH_3); 5g (R= S); 5h (R=4-F); 5i (R=4-Cl); 5j (R=4-Br); 5k (R=meta- NH_2); 5l (R=Ar-H); 5m (R=Ar-H); 5n (R=Ar-H) whilst 5g was obtained from **3** and thioacetophenone.

Scheme 5B. 2. The synthesis of **(***E*)-3-(2-(4-ethylpiperazin-1-yl) quinolin-3-yl)-1-phenylprop-2-en-1-one derivatives in the presence of TiO_2-BPTETSA catalyst under solvent free conditions.

The synthesis and characterisation of **3** was discussed in Chapter 4B. This was the main starting compound that was required to follow our research plan.

In a preliminary study to synthesize compound **5a** (Scheme 5B.2) ethanol was used as the solvent. To determine the optimum quantity of TiO_2-BPTETSA, different amounts of catalyst such as 0.02, 0.05, 0.07 g were used to produce compound **5a** which was subsequently characterized by FT-IR, ^{1}H-NMR, ^{13}C-NMR, TOF-MS and elemental analysis. It was found that increasing the quantity of the catalyst beyond 0.05 g did not increase the yield noticeably hence this quantity was selected as optimum for all subsequent reactions. To accelerate the Claisen–Schmidt reaction, various solvents and base catalyst, such as ethanol, methanol, acetonitrile, NaOH, KOH, piperidine, piperazine, and pyrrolidines were investigated and showed significant impact on the yield of **5a**. The desired product had fairly good yields when the reaction was carried out with TiO_2-BPTETSA and solvent acetonitrile under reflux conditions at 6 h (Table 5B. 2 entry 12). Moderate yields were observed when base pyrrolidines and solvent ethanol, methanol, acetonitrile were used (Table 5B. 2 entries 9-11). The yield decreased and a longer reaction time was required with base catalyst NaOH, KOH, piperidine, piperazine, and solvent ethanol, methanol, acetonitrile (Table 5B. 2 entries 1-8). Whilst optimising the reaction conditions (Table 5B. 3), monitored by TLC, we observed that the use of a solvent needed a longer reaction time compared to a solvent-free reaction whilst at a higher temperature of 120 $^{\circ}$C some additional spots were observed on the TLC plate which was taken as evidence for the formation of by-products. Also, a shorter reaction time showed the presence of starting materials thereby indicating an incomplete reaction. The maximum yield of **5a** (97 %) was obtained under solvent-free conditions after heating for 2 h. Consequently TiO_2-BPTETSA was used in solvent-free conditions for the Claisen–Schmidt reaction with starting compound **3** and **5a-n.**

The re-usability potential of TiO_2-BPTETSA was also investigated in the model reaction to synthesize compound **5a**. We found that the catalyst could be re-used five times with only 10% loss of catalytic activity: this was important evidence if commercial application is required.

After optimisation, the synthesis of **5a-n** (Scheme 5B. 2) in the presence of TiO_2-BPTETSA, in a solvent-free system for a reaction time of 2 h at 120 $^{\circ}$C, was conducted. Briefly, the catalyst was activated in vacuum at 100 °C, cooled to room temperature, then 2-(4-ethylpiperazin-1-yl) quinoline-3-carbaldehyde and acetophenone derivatives were added. The mixture was heated in an oil bath under solvent free conditions. The product yield (Table 5B. 3) ranged from 75 to 97 %. The presence of electron withdrawing groups NO_2, F, Cl, and Br

gave product yields of 87, 90, 87 and 85 % respectively (Table 5B. 3, entry 4, 8, 9, and 10). The presence of electron donating group and the -OH group in ortho and para positions gave higher yields of 92 and 90 %, respectively (Table 5B. 3, entry 2 and 3). The CH_3, OCH_3 and NH_2 groups gave yields of 80, 85 and 87 % respectively (Table 5B. 3, entry 5, 6, and 11). Compounds **5a-n** were characterized by FT-IR, ^{1}H NMR, ^{13}C NMR, MS-TOF whilst **5m** included DEPT-90 and DEPT-135, COSY, NOSEY, HSQCE and HMBC (All characterisation data are presented in the Appendix).

Table 5B. 2. Optimization of the reaction with solvent and catalyst for the synthesis of compound **5a**.

Entry	Catalyst	Solvent	Temp (°C)	Time(h)	Isolated Yield (%)
1	NaOH	EtOH	r.t	24	80
2	KOH	MeOH	r.t	24	85
3	piperidine	CH_3CN	Reflux	24	80
4	piperidine	EtOH	Reflux	24	65
5	piperidine	MeOH	Reflux	24	58
6	piperazine	CH_3CN	Reflux	24	75
7	piperazine	EtOH	Reflux	24	70
8	piperazine	MeOH	Reflux	24	60
9	pyrrolidine	CH_3CN	Reflux	6	90
10	pyrrolidines	EtOH	Reflux	6	80
11	pyrrolidines	MeOH	Reflux	6	75
12	TiO_2BPTETSA	Neat	120	2	97

The FT-IR spectrum of **5m** showed the OH stretching at 3403 cm^{-1}, C-H stretching at 2918 cm^{-1} and 1724 cm^{-1} for the carbonyl groups. The ^{1}H NMR spectrum of **5m** showed two singlets at δ 14.88 and at δ 8.30, assigned to C_{19}-H and C_4-H, respectively. The C_9-CH protons were found at δ 8.18 (J=15.48 Hz) as a doublet and C_{10}-CH δ 7.80 (J =8.96 Hz) as a doublet. The ^{13}C NMR spectrum showed the presence of one carbonyl group at δ 192.9 and the structure

was further confirmed based on the above spectral details and its elemental analysis Anal. Calc. for $C_{28}H_{27}N_3O_2$: C, 76.86; H, 6.22; N, 9.60 %. Found: C, 76.88; H, 6.25; N, 9.62 %. The structure was confirmed as (*E*)-1-(1-hydroxynaphthalen-2-yl)-3-(2-(4-ethylpiperazin-1-yl)quinolin-3-yl)prop-2-en-1-one **5m**. Thus, the one pot multi-component synthesis of the new ethyl-piperazinyl quinolinyl chalcone derivatives, by using the TiO_2-BPTETSA, was a neat and efficient reaction which was taken as evidence for the formation of the sought after target molecule.

Table 5B. 3. The synthesis of E)-3-(2-(4-ethylpiperazin-1Yl) quinolin-3-yl)-1-phenylprop-2-en-1-one derivatives in the presence of TiO_2-BPTETSA

Entry	Substrate (**4a-n**)	Product (**5a-n**)	Time (h)	Isolated Yield (%)	M. p. (°C)
1	$C_6H_5COCH_3$	3a	2	97	137-139
2	2-$HOC_6H_4COCH_3$	3b	2	90	130-142
3	4-$HOC_6H_4COCH_3$	3c	2	92	165-167
4	$O_2NC_6H_4COCH_3$	3d	2	85	177-179
5	$CH_3C_6H_4COCH_3$	3e	2	80	137-139
6	$OCH_3C_6H_4COCH_3$	3f	2	87	167-169
7	C_6H_6OS	3g	2	90	142-144
8	$FC_6H_4COCH_3$	3h	2	90	152-154
9	$ClC_6H_4COCH_3$	3i	2	87	162-164
10	$BrC_6H_4COCH_3$	3j	2	85	157-159
11	$C_6H_6NCOCH_3$	3k	2	87	132-134
12	$C_{10}H_7COCH_3$	3l	3	90	138-140
13	$HOC_{10}H_6COCH_3$	3m	3	92	172-175
14	$C_{16}H_{12}O$	3n	3	90	147-149

Computational docking analysis was conducted to create a model for BSA protein and **5m** complex. Each domain of BSA contains two sub domains (IA and B, IIA and B, IIIA and B) that possess common structural motifs. Sudlow site I and Sudlow site II as subdomains IIA and IIIA respectively, are the most probable binding sites of the ligands. Molecular docking analysis was performed using Auto Dock 4.2 program and the energetically most feasible BSA and compound **5m** complex is displayed in Figure 5B. 10 (A-B)

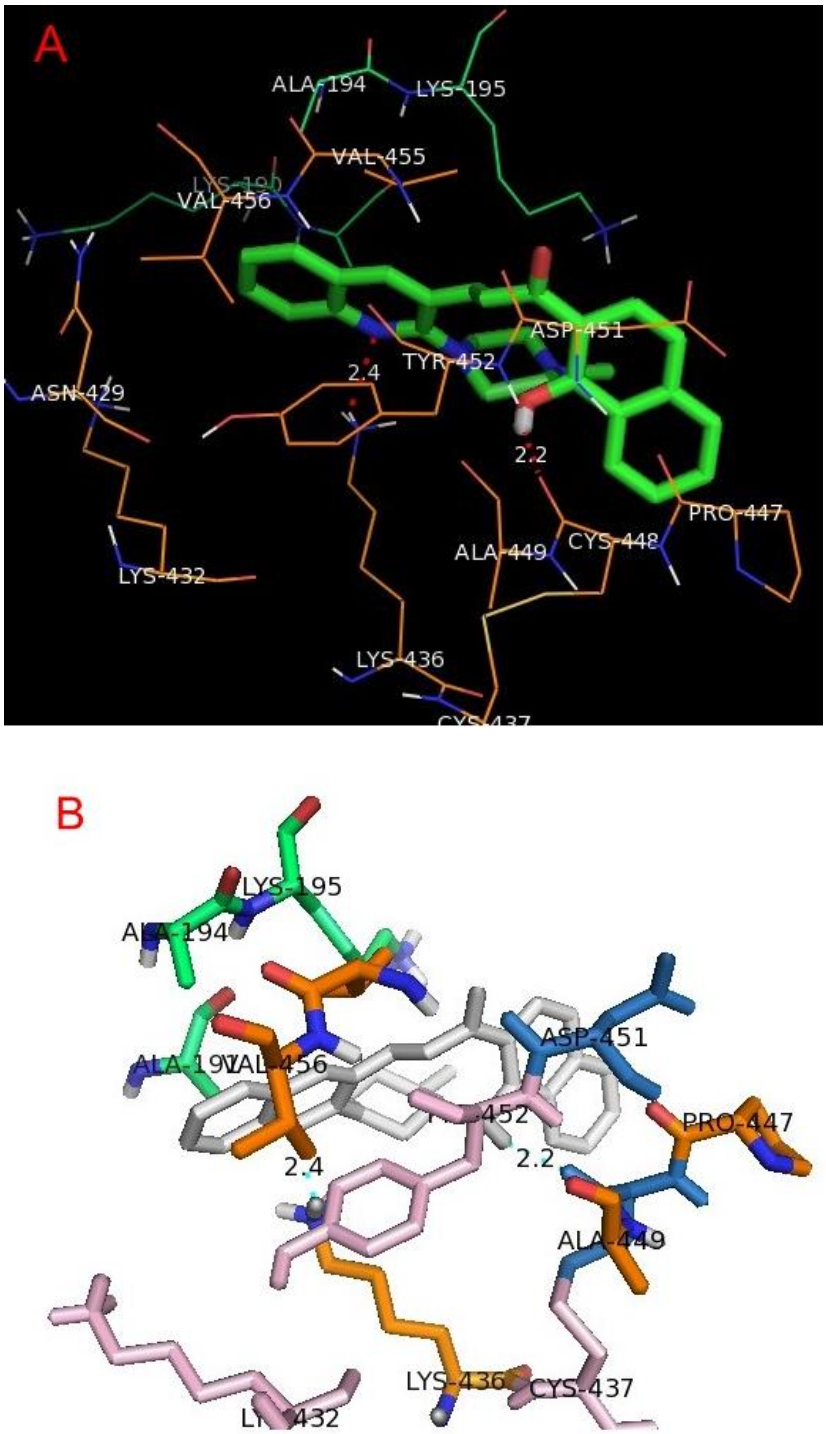

Figure 5B. 10. (A-B) Molecular docking of BSA-compound **5m** complex and the binding site of compound **5m** on BSA together with selected amino acid residues are represented by stick and cartoon models. Hydrogen bond is shown in pink dotted line

Docking results clearly pointed out that **5m** binds inside the binding pocket located in subdomain II A. It can be seen in Figure 5B.10 (A-B), **5m** is located adjacent to the amino acid residues Arg-209, Lys-212, Ala-213, Val-216, Phe-226, Ala-229, Ser-232, Lys-233 and Thr-

239 of subdomain IIA of BSA. Furthermore, carbonyl group containing O atom of compound **5m** forms a hydrogen bond to Lys-212 with bond length of 1.9 Å. It is imperative to note from the computational observations that **5m** is in the locality of the Trp-214 amino acid residue of BSA. From docking analyses, the free energy changes acquired for BSA binding was -19.34 kJ mol^{-1} which is analogous with the experimental value obtained from emission data of -27.58 kJ mol^{-1} at room temperature. Therefore, molecular docking study supports the emission spectral results regarding intrinsic emission quenching of Trp-214 for binding interaction between BSA and **5m**. These values obtained just provide the probable geometry of the complexes; however the binding has been established experimentally.

5B. 3. Conclusion

In conclusion, a novel titanium dioxide nanomaterial-based sulfonic acid catalyst was prepared and subsequently used in a one pot reaction for the synthesis of highly functionalised ethyl-piperazinyl quinolinyl chalcone derivatives. The reaction was effective under solvent-based conditions in a relatively short reaction time however, the catalytic activity is most effective in a solvent-free system. Furthermore, this new reaction creates new types of ethyl-piperazinyl quinolinyl chalcone derivatives which have suitable functionality for a host of possible biological activity studies such as protein and DNA binding. The preparation of the catalyst was simple and safe whilst demonstrating only 10 % loss in catalytic activity after five cycles of re-used thereby making it cost-effective for possible industrial applications.

5B. 4. Experimental

5B. 4. 1. Synthesis of catalyst

The catalyst was synthesized in three stages. A mixture of TiO_2 and 65 % nitric acid was reflux at 24 h; this preliminary step was aimed at introducing –OH groups on the surface of TiO_2 through an oxidation process. Briefly, the nanocrystalline surface was produced through oxidation. After that TiO_2 and (3-mercaptochloropropyl) trimethoxysilane were refluxed for 24 h. To a mixture of chloropropyl titanium dioxide (15 g) in anhydrous xylene (150 ml), an excess of triethylenetetramine (20 ml) was added. The resulting mixture was refluxed with stirring for 24 h. The reaction mixture was then cooled to room temperature and filtered through a vacuum glass filter. The filter-cake was washed sequentially with xylene and a large excess of ethanol and dried under vacuum overnight at 80 °C to give the desired product

3-TETANPTiO$_2$ (14 g). To a magnetically stirred mixture of 3-TETANPTiO$_2$ (14 g) in CHCl$_3$ (30 ml), chlorosulfonic acid (20 ml) in a drop-wise manner was added at 0°C over a period of 3 h. Upon completion of the reaction, the mixture was stirred for a further 3 h and then filtered. The filter-cake was washed with ethanol (50 ml) and dried at room temperature to afford the desired product, TiO$_2$-BPTETSA, as a cream powder (15 g) (Scheme 5B. 1).

5B. 4. 2. General Procedure for the synthesis of substituted 2-(4-ethylpiperazin-1 yl)quinoline-3-carbaldehyde (3) in chapter 4- 4B. 6. 3**.**

5B. 4. 3. General Procedure for the synthesis of (E)-3-(2-(4-ethylpiperazin-1-yl)quinolin-3-yl)-1-phenylprop-2-en-1-one (3a-n):

The sulfonic acid functionalized TiO$_2$-BPTETSA solid acid catalyst (0.07g) was activated in vacuum at 100 °C for 15 min then cooled to room temperature. Thereafter, it was added to a mixture containing 2-(4-ethylpiperazin-1-yl)quinoline-3-carbaldehyde (1.0 mmol) and acetophenone (1.0 mmol). The mixture was heated on an oil bath under solvent-free conditions for an appropriate time as shown in Table 5B. 3. The reaction was monitored by TLC. After completion of the reaction, the solid was dissolved in minimal ethanol, filtered and the filtrate was purified by column chromatography with acetone and hexane 80: 20. The catalyst was subsequently washed with diluted acid solution, distilled water and then acetone, dried under vacuum and reused. The spectral data obtained from ^{1}H NMR, ^{13}C NMR, elemental analysis and FT-IR is presented below:

5B. 5. 1. (E)-3-(2-(4-ethylpiperazin-1-yl) quinolin-3-yl)-1-phenylprop-2-en-1-one (5a)

Yellow colour solid: yield 97 %: FT-IR (KBr): 3059, 2936, 2838, 2787, 1673, 1586, 1423, 1212, 1010, 759 cm^{-1}. ^{1}H NMR (CDCl$_3$, 400 MHz): δ 8.27 (1H, s, Ar-H), 8.08 (1H, dd, J = 5.32 Hz, Ar-H), 8.04 (2H, d, J = 15.92 Hz, Ar-H), 7.86 (1H, d, J = 8.44 Hz, Ar-H), 7.75 (1H, t, J = 8 Hz, Ar-H), 7.68 (1H, t, J = 7.52 Hz, Ar-H), 7.61-7.67 (2H, m, J = 1.84 Hz, Ar-H), 7.53-7.57 (2H, m, J = 6.64 Hz, Ar-H), 7.37-7.41 (1H, m, J = 7 Hz, Ar-H), 3.52 (4H, t, J = 4.32 Hz, CH$_2$), 2.75 (6H, d, J = 4.16 Hz, CH$_2$), 2.44(3H, s, CH$_3$). ^{13}C NMR (CDCl$_3$, 100 MHz): δ 190.1, 159.4, 147.7, 142, 137.9, 137.1, 133, 130.5, 127.8, 127.6, 124.8, 124.6, 122.8, 122.7, 54.8, 50, 45.8. Anal. Calc. for C$_{24}$H$_{25}$N$_3$O: C, 77.60; H, 6.48; N, 11.75 %. Found: C, 77.62; H, 6.49; N, 11.77 %.

5B. 5. 2. (E)-1-(2-hydroxyphenyl)-3-(2-(4-ethylpiperazin-1-yl) quinolin-3-yl) prop-2-en-1-one (5b)

Yellow colour solid: yield 90 %: FT-IR (KBr): 3453, 3356, 3025, 2970, 1739, 1366, 1217, 459 cm^{-1}. ^{1}H NMR ($CDCl_3$, 400 MHz): δ 12.76 (1H, s, Ar-OH), 8.13 (1H, s, Ar-H), 8 (1H, d, *J* = 15.48 Hz, Ar-H), 7.88 (1H, dd, *J* = 6.68 Hz, Ar-H), 7.75 (2H, t, *J* = 8.4 Hz, Ar-H), 7.63 (1H, d, *J* = 8 Hz, Ar-H), 7.56-7.51 (1H, dt, *J* = 1.48 Hz, Ar-H), 7.40-7.44 (1H, m, *J* = 1.48 Hz, Ar-H), 7.29-7.25 (1H, dt, *J* = 0.68 Hz, Ar-H), 6.96-6.94 (1H, dd, *J* = 0.76 Hz, Ar-H), 6.89-6.85 (1H, dt, *J* = 7.12 Hz, Ar-H), 3.35 (4H, t, *J* = 4.2 Hz, CH_2), 2.58 (6H, d, *J* = 4.48 Hz, CH_2), 2.30 (3H, s, CH_3). ^{13}C NMR ($CDCl_3$, 100 MHz): δ 193.5, 163.7, 159.6, 147.8, 142.8, 137.4, 136.5, 130.7, 129.6, 127.8, 127.6, 124.7, 124.6, 122.4, 120.8, 119.9, 118.9, 55, 50.4, 46.1. Anal. Calc. for $C_{24}H_{25}N_3O_2$: C, 74.39; H, 6.50; N, 10.84 %. Found: C, 74.41; H, 6.51; N, 10.85 %.

5B. 5. 3. (E)-1-(4-hydroxyphenyl)-3-(2-(4-ethylpiperazin-1-yl) quinolin-3-yl) prop-2-en-1-one (5c)

Yellow colour solid: yield 92 %: FT-IR (KBr): 3286, 3027, 2971, 1739, 1366, 1217, 732 cm^{-1}. ^{1}H NMR ($DMSOd_6$, 400 MHz): δ 8.10 (1H, s, Ar-OH), 8.79 (1H, s, Ar-H), 8.11-8.08 (2H, dd, *J* = 5.44 Hz, Ar-H), 8.03 (1H, d, *J* = 15.6 Hz, Ar-H), 7.87 (1H, d, *J* = 7.96 Hz, Ar-H), 7.77 (2H, t, *J* = 5.08Hz, Ar-H), 7.68-7.64 (1H, dt, *J* = 1.36 Hz, Ar-H), 7.44 (1H, dt, *J* = 6.84 Hz, Ar-H), 6.92 (2H, d, *J* = 8.72 Hz, Ar-H), 3.30 (4H, d, *J* = 17.52 Hz, CH_2), 2.50 (6H, m, *J* = 1.72 Hz, CH_2), 2.26 (3H, s, CH_3). ^{13}C NMR ($DMSOd_6$, 100 MHz): δ 206.4, 186.9, 162.3, 159.5, 146.78, 138.96, 137.14, 131.20, 130.4, 128.8, 128, 126, 124.7, 124.5, 123.1, 122.3, 115.4, 54.5, 50.1, 45.7, 40.1, 30.6. Anal. Calc. for $C_{24}H_{25}N_3O_2$: C, 74.39; H, 6.50; N, 10.84 %. Found: C, 74.40; H, 6.52; N, 10.86 %.

5B. 5. 4. (E)-3-(2-(4-ethylpiperazin-1-yl) quinolin-3-yl)-1-(4-nitrophenyl) prop-2-en-1-one (5d)

Yellow colour solid: yield 85 %: FT-IR (KBr): 2937, 2833, 2792, 1669, 1522, 1423, 1344, 1006, 706 cm^{-1}. ^{1}H NMR ($CDCl_3$, 400 MHz): δ 8.42 (1H, s, Ar-H), 8.90-8.36 (1H, dd, *J* = 1.96Hz, Ar-H), 8.34 (1H, d, *J* = 4.52 Hz, Ar-H), 8.30 (1H, d, *J* = 6.12 Hz, Ar-H), 8.22-8.17 (2H, dd, *J* = 8.76 Hz, Ar-H), 8.10 (1H, d, *J* = 15.68 Hz, Ar-H), 7.87-7.81 (1H, dd, *J* = 5.72 Hz, Ar-H), 7.67 (1H, t, *J* = 6.92 Hz, Ar-H), 7.63-7.58 (1H, dt, *J* = 7.12 Hz, Ar-H), 7.76 (1H, dt, *J* = 7.08 Hz, Ar-H), 4.10 (1H, dd, *J* = 5.06 Hz, CH_2), 3.96 (1H, dd, *J* = 5.04 Hz, CH_2), 3.70 (1H, dd, *J* = 2.96Hz, CH_2), 3.45 (3H, dd, *J* = 10.52 Hz, CH_2), 3.02 (1H, s, CH) 2.69 (1H, s, CH), 2.50 (3H, s, CH_2), 2.20 (3H, s, CH_3). ^{13}C NMR ($CDCl_3$, 100 MHz): δ 188.6, 159.5, 150.8,

150.4, 148, 146.5, 144, 142.7, 141.4, 140.9, 139.6, 137.5, 130.9, 129.6, 129.6, 129.4, 129.2, 127.9, 127.7, 127.7, 126.9, 124.8, 124.8, 124.7, 124.1, 124, 123.9, 122, 121.7, 120.9, 54, 50.3, 48.9, 36.3, 35.2, 34.3. Anal. Calc. for $C_{24}H_{24}N_4O_3$: C, 69.21; H, 5.81; N, 13.45 %. Found: C, 69.23; H, 5.83; N, 13.47 %.

5B. 5. 5. (E)-3-(2-(4-ethylpiperazin-1-yl) quinolin-3-yl)-1-(p-tolyl) prop-2-en-1-one (5e)

Yellow colour solid: yield 80 %: FT-IR (KBr): 2953, 2838, 2792, 1677, 1663, 1602, 1426, 1279, 759 cm^{-1}. ^1H NMR ($CDCl_3$, 400 MHz): δ 7.93 (3H, d, J = 8.2 Hz, Ar-H), 7.89 (1H, s, Ar-H), 7.86 (1H, d, J = 8.4Hz, Ar-H), 7.64 (1H, d, J = 7.92 Hz, Ar-H), 7.54-7.58 (1H, td, J = 7.08 Hz, Ar-H), 7.34-7.38 (1H, td, J = 7.12 Hz, Ar-H), 7.28 (3H, d, J = 8.04 Hz, Ar-H), 4.51 (1H, t, J = 7.04 Hz, CH_2), 3.2-3.47 (9H, m, J = 7Hz, CH_2), 2.42 (3H, s, CH_3), 2.34 (3H, s, CH_3). ^{13}C NMR ($CDCl_3$, 100 MHz): δ 198.2, 160.9, 146, 144, 134.3, 134, 132.5, 129.3, 128.7, 128.4, 127.7, 126.9, 126, 124.7, 54.9, 50.7, 46, 44.2, 32, 30.9, 21.6. Anal. Calc. for $C_{25}H_{27}N_3O$: C, 77.89; H, 7.06; N, 10.90 %. Found: C, 77.91; H, 7.08; N, 10.88 %.

5B. 5. 6. (E)-1-(4-ethoxyphenyl)-3-(2-(4-methylpiperazin-1-yl) quinolin-3-yl) prop-2-en-1-one (5f)

Yellow colour solid: yield 87 %: FT-IR (KBr): 2940, 2837, 2791, 1659, 1587, 1421, 1171, 1005, 834, 760 cm^{-1}. ^1H NMR ($CDCl_3$, 400 MHz): δ 8.23 (1H, s, Ar-H), 8.19 (2H, d, J = 8.8 Hz, Ar-H), 8.0 (1H, d, J = 15.68 Hz, Ar-H), 7.84 (1H, d, J = 8.4 Hz, Ar-H), 7.72 (2H, d, J = 5.96 Hz, Ar-H), 7.60-7.64 (1H, m, J = 1.12 Hz, Ar-H), 7.38 (1H, t, J = 7.12 Hz, Ar-H), 7.01 (2H, d, J = 7.04 Hz, Ar-H), 3.90 (3H, s, OCH_3), 3.46 (4H, s, CH_2), 3.26 (6H, t, J = 4.36Hz, CH_2), 2.39 (3H, s, CH_3). ^{13}C NMR ($CDCl_3$, 100 MHz): δ 188.2, 163.6, 159.6, 147.6, 141.3, 136.9, 130.8, 130.3, 127.7, 127.5, 124.8, 124.4, 122.9, 122.5, 113.9, 55.5, 55, 50.2, 46.1. Anal. Calc. for $C_{25}H_{27}N_3O_2$: C, 74.79; H, 6.78; N, 10.47 %. Found: C, 74.80; H, 6.80; N, 10.49 %.

5B. 5. 7. (E)-3-(2-(4-ethylpiperazin-1-yl) quinolin-3-yl)-1-(thiophen-2-yl) prop-2-en-1-one (5g)

Yellow colour solid: yield 90 %: FT-IR (KBr): 3059, 2936, 2838, 2787, 1673, 1586, 1423, 1212, 759 cm^{-1}. ^1H NMR ($CDCl_3$, 400 MHz): δ 8.13 (1H, s, Ar-H), 7.94 (1H, d, J = 15.64 Hz, Ar-H), 7.84-7.83 (1H, dd, J = 3.08 Hz, Ar-H), 7.75 (1H, d, J = 8.44 Hz, Ar-H), 7.63 (2H, dd, J = 3.92 Hz, Ar-H), 7.55-7.51 (2H, dt, J = 1.4 Hz, Ar-H), 7.29-7.25 (1H, m, J = 0.84 Hz, Ar-H), 7.13-7.11 (1H, dd, J = 4 Hz, Ar-H), 3.36 (4H, t, J = 3.96Hz, CH_2), 2.58 (6H, t, J = 4.52Hz, CH_2), 2.30 (3H, s, CH_3). ^{13}C NMR ($CDCl_3$, 100 MHz): δ 181.8, 159.6, 147.7, 145.4, 141.4,

137.2, 134.1, 131.9, 130.5, 128.3, 127.8, 127.6, 124.7, 124.5, 122.5, 122.3, 55, 50.3, 46.1. .Anal. Calc. for $C_{22}H_{23}N_3OS$: C, 70.00; H, 5.84; N, 11.58 %. Found: C, 70.2; H, 5.85; N, 11.60 %.

5B. 5. 8. (E)-1-(4-fluorophenyl)-3-(2-(4-ethylpiperazin-1-yl) quinolin-3-yl) prop-2-en-1-one (5h)

Yellow colour solid: yield 90 %: FT-IR (KBr): 2944, 2838, 2787, 1675, 1583, 1425, 1009, 759 cm^{-1}. ^1H NMR ($CDCl_3$, 400 MHz): δ 8.08 (1H, s, Ar-H), 8.05 (1H, d, *J* = 1.72Hz, Ar-H), 8.02 (1H, d, *J* = 8.88 Hz, Ar-H), 7.90 (1H, d, *J* = 1.76 Hz, Ar-H), 7.87 (1H, d, *J* = 8.4 Hz, Ar-H), 7.70 (1H, d, *J* = 8.28 Hz, Ar-H), 7.56-7.59(1H, m, *J* = 1.6 Hz, Ar-H), 7.17 (1H, d, *J* = 2.48 Hz, Ar-H), 7.15 (1H, d, *J* = 2.64 Hz, Ar-H), 7.13 (1H, d, *J* = 2.68 Hz, Ar-H), 6.95 (1H, d, *J* = 8.92 Hz, Ar-H), 3.95 (2H, d, *J* = 13.4 Hz, CH_2), 3.44 (2H, d, *J* = 7.2 Hz, CH_2), 3.26-3.37 (6H, m, *J* = 6.8 Hz, CH_2), 2.34 (3H, s, CH_3). ^{13}C NMR ($CDCl_3$, 100 MHz): δ 196.8, 163.7, 160.8, 146, 134.1, 133.1, 132.3, 132.1, 131, 130.5, 129.7, 128.9, 128.8, 127.8, 127.7, 126.9, 126, 124.9, 124.8, 115.9, 113.8, 55.6, 55, 50.8, 44.2, 31.8. ^{19}F NMR ($CDCl_3$, 400 MHz): δ -104.78. Anal. Calc. for $C_{24}H_{24}FN_3O$: C, 74.60; H, 5.95; N, 11.17 %. Found: C, 74.62; H, 5.97; N, 11.19 %.

5B. 5. 9. (E)-1-(4-chlorophenyl)-3-(2-(4-ethylpiperazin-1-yl) quinolin-3-yl)prop-2-en-1-one (5i)

Yellow colour solid: yield 87 %: FT-IR (KBr): 2926, 2838, 2788, 1644, 1583, 1519, 1421, 1008, 759 cm^{-1}. ^1H NMR ($CDCl_3$, 400 MHz): δ 7.97 (3H, d, *J* = 8.52Hz, Ar-H), 7.88 (1H, s, Ar-H), 7.86 (1H, d, *J* = 9.76Hz, Ar-H), 7.64 (1H, d, *J* = 7.96 Hz, Ar-H), 7.55-7.59 (1H, td, *J* = 7.2 Hz, Ar-H), 7.46 (3H, d, *J* = 8.48 Hz, Ar-H), 7.36 (1H, t, *J* = 7.52 Hz, Ar-H), 4.50 (1H, t, *J* = 7.28 Hz, CH), 3.48-3.3 (3H, m, *J* = 7.28 Hz, CH_2), 3.24 (6H, t, *J* = 4.32Hz, CH_2), 2.33 (3H, s, CH_3). ^{13}C NMR ($CDCl_3$, 100 MHz): δ 197.2, 160.7, 146, 139.8, 134.9, 134.2, 131.9, 129.7, 129, 128.9, 127.8, 126.9, 125.9, 124.9, 55, 50.9, 46, 44.3, 31.7, 30.9. Anal. Calc. for $C_{24}H_{24}ClN_3O$: C, 71.01; H, 5.96; N, 10.35 %. Found: C, 71.03; H, 5.95; N, 10.37 %.

5B. 5. 10. (E)-1-(4-bromophenyl)-3-(2-(4-ethylpiperazin-1-yl) quinolin-3-yl) prop-2-en-1-one (5j)

Yellow colour solid: yield 85 %: FT-IR (KBr): 3058, 2929, 3846, 2791, 1676, 1595, 1421, 1156, 835, 759 cm^{-1}. ^1H NMR ($CDCl_3$, 400 MHz): δ 8.18 (1H, s, Ar-H), 7.95 (1H, d, *J* = 15.92 Hz, Ar-H), 7.87 (1H, d, *J* = 8.52 Hz, Ar-H), 7.80 (2H, t, *J* = 8.44 Hz, Ar-H), 7.66 (1H, d, *J* =

7.36 Hz, Ar-H), 7.60 (3H, d, *J* = 8.68 Hz, Ar-H), 7.55 (2H, t, *J* = 6.08 Hz, Ar-H), 3.40 (4H, d, *J* = 4.16 Hz, CH_2), 3.24 (2H, d, *J* = 6.88 Hz, CH_2), 2.63-2.61 (4H, t, *J* = 4.04 Hz, CH_2), 2.34 (3H, s, CH_3). ^{13}C NMR ($CDCl_3$, 100 MHz): δ 197.4, 160.7, 146, 135.3, 134.2, 132, 131.9, 129.8, 129, 128.6, 127.8, 126.9, 125.9, 124.9, 55, 50.9, 46.1, 44.3, 31.6, 29.7. Anal. Calc. for $C_{24}H_{24}BrN_3O$: C, 64.00; H, 5.37; N, 9.33 %. Found: C, 64.10; H, 5.39; N, 9.35 %.

5B. 5. 11. (E)-1-(3-aminophenyl)-3-(2-(4-ethylpiperazin-1-yl) quinolin-3-yl) prop-2-en-1-one (5k)

Yellow colour solid: yield 87 %: FT-IR (KBr): 3467, 3014, 2971, 2937, 2838, 1739, 1566, 1365, 749 cm^{-1}. ^{1}H NMR ($CDCl_3$, 400 MHz): δ 8.20 (1H, s, Ar-H), 7.96 (1H, d, *J* = 15.72 Hz, Ar-H), 7.84 (1H, d, *J* = 8.4Hz, Ar-H), 7.72 (1H, d, *J* = 7.96 Hz, Ar-H), 7.60-7.64 (2H, dt, *J* = 8.48 Hz, Ar-H), 7.43 (1H, d, *J* = 7.64 Hz, Ar-H), 7.36 (1H, m, *J* = 2.08 Hz, Ar-H), 7.34 (1H, s, Ar-H), 7.36 (1H, t, *J* = 7.8 Hz, Ar-H), 6.89-6.92 (1H, dd, *J* = 2.04 Hz, Ar-H), 3.92 (2H, s, NH_2), 3.44 (4H, s, CH_2), 2.65 (6H, d, *J* = 3.84 Hz, CH_2), 2.31 (3H, s, CH_3). ^{13}C NMR ($CDCl_3$, 100 MHz): δ 190.3, 159.6, 147.6, 147, 141.7, 139, 137, 130.4, 129.5, 127.8, 127.5, 124.8, 124.5, 122.9, 122.7, 119.6, 118.7, 114.3, 55, 50.2, 46.1. Anal. Calc. for $C_{24}H_{26}N_4O$: C, 74.58; H, 6.78; N, 14.50 %. Found: C, 74.60; H, 6.80; N, 14.52 %.

5B. 5. 12. (E)-3-(2-(4-ethylpiperazin-1-yl) quinolin-3-yl)-1-(naphthalen-2-yl) prop-2-en-1-one (5l)

Yellow colour solid: yield 90 %: FT-IR (KBr): 3050, 2953, 2935, 2283, 2789, 1673, 1586, 1423, 759 cm^{-1}. ^{1}H NMR ($CDCl_3$, 400 MHz): δ 8.61 (1H, s, Ar-H), 8.32 (1H, s, Ar-H), 8.15-8.17 (1H, dd, *J* = 1.48Hz, Ar-H), 8.03-8.11 (2H, d, *J* = 15.68 Hz, Ar-H), 7.98 (1H, d, *J* = 8.64 Hz, Ar-H), 7.94 (1H, t, *J* = 2.84 Hz, Ar-H), 7.86-7.90 (2H, dd, *J* = 5.24 Hz, Ar-H), 7.77 (1H, d, *J* = 7.96 Hz, Ar-H), 7.67 (1H, d, *J* = 1.24 Hz, Ar-H), 7.66 (1H, d, *J* = 2.84 Hz, Ar-H), 7.61-7.63 (1H, m, *J* = 1.48 Hz, Ar-H), 7.40 (1H, t, *J* = 7.32 Hz, Ar-H), 3.45 (4H, d, *J* = 6.24 Hz, CH_2), 2.71 (6H, d, *J* = 4.2 Hz, CH_2), 2.40 (3H, s, CH_3). ^{13}C NMR ($CDCl_3$, 100 MHz): δ 189.8, 159.6, 147.7, 142, 137.2, 135.5, 135.3, 132.5, 130.5, 130, 129.5, 128.7, 128.5, 127.8, 127.6, 124.8, 124.6, 124.4, 122.8, 122.7, 54.9, 50.2, 46. Anal. Calc. for $C_{28}H_{27}N_3O$: C, 79.78; H, 6.46; N, 9.97 %. Found: C, 79.80; H, 6.47; N, 9.95 %.

5B. 5. 13. (E)-1-(1-hydroxynaphthalen-2-yl)-3-(2-(4-ethylpiperazin-1-yl) quinolin-3-yl) prop-2-en-1-one (5m)

Yellow colour solid: yield 92 %: FT-IR (KBr): 3467, 3014, 2971, 2937, 2838, 1739, 1566, 1365, 749 cm^{-1}. ^{1}H NMR ($CDCl_3$, 400 MHz): δ 14.88 (1H, s, Ar-OH), 8.53 (1H, d, *J* = 8.16 Hz, Ar-H), 8.30 (1H, s, Ar-H), 8.18 (1H, d, *J* = 15.48 Hz, Ar-H), 7.93 (1H, d, *J* = 8.88 Hz, Ar-H), 7.90 (1H, d, *J* =2.32 Hz, Ar-H), 7.88 (1H, d, *J* =8.4 Hz, Ar-H), 7.80 (1H, d, *J* =8.96 Hz, Ar-H), 7.77 (1H, d, *J* =0.72 Hz, Ar-H), 7.66-7.69 (1H, m, *J* = 1.48 Hz, Ar-H), 7.64-7.65 (1H, m, *J* = 0.8 Hz, Ar-H), 7.55-7.59 (1H, m, *J* = 1.28 Hz, Ar-H), 7.39-7.43 (1H, m, *J* = 0.88 Hz, Ar-H), 7.35 (1H, d, *J* = 8.92 Hz, Ar-H), 3.54 (4H, s, CH_2), 2.78 (4H, d, *J* = 4.08 Hz, CH_2), 2.47 (2H, s, CH_2), 1.27 (3H, s, CH_3). ^{13}C NMR ($CDCl_3$, 100 MHz): δ 192.9, 164.6, 159.4, 147.8, 142.2, 137.5, 137.4, 130.7, 130.3, 127.8, 127.6, 127.4, 126, 125.5, 124.8, 124.7, 124.5, 123.8, 122.6, 121.3, 118.3, 113.3, 54.90, 50.12, 45.9, 29.7 Anal. Calc. for $C_{28}H_{27}N_3O_2$: C, 76.86; H, 6.22; N, 9.60 %. Found: C, 76.88; H, 6.25; N, 9.62 %.

5B. 5. 14. (E)-1-(anthracen-9-yl)-3-(2-(4-ethylpiperazin-1-yl) quinolin-3-yl) prop-2-en-1-one (5n)

Yellow colour solid: yield 90 %: FT-IR (KBr): 3466, 3067, 2931, 2850, 1706, 1652, 1404, 704 cm^{-1}. ^{1}H NMR ($CDCl_3$, 400 MHz): δ 8.56 (1H, s, Ar-H), 8.25 (1H, s, Ar-H), 8.07 (2H, t, *J* = 7.16 Hz, Ar-H), 7.92 (2H, t, *J* = 7.28 Hz, Ar-H), 7.74 (1H, d, *J* = 8.4 Hz, Ar-H), 7.70 (1H, d, *J* = 7.92 Hz, Ar-H), 7.55-7.59 (1H, m, *J* = 0.96 Hz, Ar-H), 7.46-7.50 (4H, m, *J* = 3.12 Hz, Ar-H), 7.35 (1H, d, *J* = 16.36 Hz, Ar-H), 7.34 (1H, t, *J* = 7.12 Hz, Ar-H), 7.11 (1H, d, *J* = 16.44 Hz, Ar-H), 3 (4H, t, *J* = 4.4 Hz, CH_2), 2 (3H, s, CH_3), 1.67 (6H, s, CH_2). ^{13}C NMR ($CDCl_3$, 100 MHz): δ 201, 159, 147.9, 146.5, 136.9, 134, 131.2, 130.7, 130.1, 128.8, 128.5, 128.3, 128, 127.5, 126.7, 125.6, 125, 124.6, 121.6, 54.3, 50.1, 45.7. Anal. Calc. for $C_{32}H_{29}N_3O$: C, 81.50; H, 6.20; N, 8.91 %. Found: C, 81.52; H, 6.23; N, 8.92 %.

5B. 4. 4. Molecular Docking Studies

Auto Dock 4.2 program which operates the Lamarckian Genetic Algorithm (LGA) was used to dock compound (*E*)-1-(1-hydroxynaphthalen-2-yl)-3-(2-(4-ethylpiperazin-1-yl) quinolin-3-yl) prop-2-en-1-one **(5m)** with the 3D structure of BSA. The crystal structure of BSA (PDB id: 1AO6) was obtained from the Protein Data Bank and all water molecules were eliminated with successive addition of hydrogen atoms, followed by the computation of Gasteiger charges as required for LGA molecular docking procedure. The grid size along the x-, y-, z-axes and grid space were set to 60 Å, 60 Å and 60 Å and 0.403 Å respectively for BSA. To include the whole subdomain IIA of BSA during the docking process, the grid centre along the x-, y-, z-axes was set as 34.016 Å, 42.121 Å, and 50.644 Å, respectively. The following docking parameters were used, Genetic Algorithm (GA) population=150; maximum number of energy evaluations=250,000 and GA crossover mode of two points. For each docking simulation, 20 different conformers were generated and PyMOL package software was used for visualization of the interaction of docked protein−ligand complex. The conformation with the lowest binding free energy was used for further analysis.

Reference

Anto, R. J., Sukumaran, K., Kuttan, G., Rao, M. N. A., Subbaraju, V. and Kuttan, R., 1995. Anticancer and antioxidant activity of synthetic chalcones and related compounds. Cancer letters (97) 33-37.

Anand, U., Jash, C. and Mukherjee, S., 2010. Spectroscopic probing of the microenvironment in a protein− surfactant assembly. The Journal of Physical Chemistry B (114) 15839-15845.

Baigrie, L. M., Cox, R. A., Slebocka-Tilk, H., Tencer, M. and Tidwell, T. T., 1985. Acid-catalyzed enolization and aldol condensation of acetaldehyde. Journal of the American Chemical Society (107) 3640-3645.

Bhattacharya, B., Nakka, S., Guruprasad, L. and Samanta, A., 2009. Interaction of bovine serum albumin with dipolar molecules: fluorescence and molecular docking studies. The Journal of Physical Chemistry B (113) 2143-2150.

Chandrasekhar, S., Vijeender, K. and Reddy, K.V., 2005. New synthesis of flavanones catalyzed by L-proline. Tetrahedron letters (46) 6991-6993.

Drexler, M.T. and Amiridis, M.D., 2003. The effect of solvents on the heterogeneous synthesis of flavanone over MgO. Journal of Catalysis (214) 136-145.

Daskiewicz J. B., Comte G., Barron D., Pietro A. D., Thomasson F., 1999.Organolithium mediated Synthesis of prenylchalcones as potential inhibitors of chemoresistance. Tetrahedron Lett (40) 7095-7098.

Dong, F., Jian, C., Hao, F. Z., Kai, G., Liang, L. Z., 2008. Synthesis of chalcones via Claisen-Schmidt Condensation reaction catalyzed by acyclic acidic ionic liquids. Catal Commun (9) 1924-1927.

Dean, S. M., Greenberg, W. A. and Wong, C. H., 2007. Recent advances in aldolase- catalyzed asymmetric synthesis. Advanced Synthesis & Catalysis (349) 1308-1320.

Hu, Y. J., Liu, Y., Wang, J. B., Xiao, X. H. and Qu, S. S., 2004. Study of the interaction between monoammonium glycyrrhizinate and bovine serum albumin. Journal of Pharmaceutical and Biomedical Analysis (36) 915-919.

Iranpoor, N. and Kazemi, F., 1998. $RuCl_3$ catalyses aldol condensations of aldehydes and ketones. Tetrahedron (54) 9475-9480.

Jahng, Y., Rahman, A. M., Ali, R. and Kadi, A. A., 2012. A Facile Solvent Free Claisen-Schmidt Reaction&58; Synthesis of α, α′-bis-(Substituted-benzylidene) cycloalkanones and α, α′-bis-(Substituted-alkylidene) cycloalkanones. Molecules (17) 571-583.

Ko, H. H., Hsieh, H. K., Liu, C.T., Lin, H. C., Teng, C. M. and Lin, C. N., 2004. Structure-activity relationship studies on chalcone derivatives: potent inhibition of platelet aggregation. Journal of pharmacy and pharmacology, (56) 1333-1337.

Khalilzadeh, M. A., Hosseini, A. and Tajbakhsh, M., 2007. Synthesis of tacrine derivatives under solvent less conditions. Journal of heterocyclic chemistry (44) 535-538.

Kang, L. Q., Cai, Y. Q., Wang, H. and Li, L. H., 2014. Solvent-free catalytic preparation of 2, 6-dibenzylidenecycloalkanones using 2-hydroxyethylammonium acetate ionic liquid as catalyst. Monatshefte für Chemie-Chemical Monthly (145) 337-340.

Khan, M. K., Rakotomanomana, N., Dufour, C. and Dangles, O., 2011. Binding of citrus flavanones and their glucuronides and chalcones to human serum albumin. Food & function (2) 617-626.

Li, D., Wang, Z., Wang, L., Qu, C. and Zhang, H., 2009. Separation and determination of amino acids by ce using 1-butyl-3-methylimidazolium-based ionic liquid as background electrolyte. Chromatographia (70) 825-830.

Lakowicz, J. R., Malicka, J., Gryczynski, I. and Gryczynski, Z., 2003. Directional surface plasmon-coupled emission: a new method for high sensitivity detection. Biochemical and biophysical research communications (307) 435-439.

Mohammad, R. S., Shaya, M., Ali, M., Sugeng, T., Aishah, A. J., Mukti, R., Nur, H., Nazirah K., Ghoreishi, M. K., 2016. Catalyzed Claisen–Schmidt reaction by protonated aluminate mesoporous silica nanomaterial focused on the (E)-chalcone synthesis as a biologically active compound. RSC Adv (6) 11023.

Narender, T. and Reddy, K. P., 2007. A simple and highly efficient method for the synthesis of chalcones by using borontrifluoride-etherate. Tetrahedron Letters (48) 3177-3180.
Nagendrappa, G., Organic synthesis using clay catalyst 2002. Resonance (7) 64-67.

Qian, H., Liu, D. and Lv, C., 2010. Synthesis of chalcones via Claisen-Schmidt reaction catalyzed by sulfonic acid-functional ionic liquids. Industrial & Engineering Chemistry Research (50) 1146-1149.

Qian, H., Wang, Y. and Liu, D., 2013. Ultrasound-accelerated synthesis of substituted 2′-hydroxychalcones by reusable ionic liquids. Industrial & Engineering Chemistry Research (52) 13272-13275.

Rodriguez, B., Bruckmann, A., Rantanen, T. and Bolm, C., 2007. Solvent-Free Carbon-Carbon Bond Formations in Ball Mills. Advanced Synthesis & Catalysis (349) 2213-2233.

Romanelli, G., Pasquale, G., Sathicq, A., Thomas, H., Autino, J. and Vázquez, P., 2011. Synthesis of chalcones catalyzed by aminopropylated silica sol–gel under solvent-free conditions. Journal of Molecular Catalysis A: Chemical (34) 24-32.

Satyanarayana, M., Tiwari, P., Tripathi, B. K., Srivastava, A. K. and Pratap, R., 2004. Synthesis and antihyperglycemic activity of chalcone based aryloxypropanolamines. Bioorganic & medicinal chemistry (12) 883-889.

Szell, T. and Sohar, I., 1969. New nitrochalcones. IX. Canadian Journal of Chemistry (47) 1254-1258.

Saravanamurugan, S., Palanichamy, M., Arabindoo, B. and Murugesan, V., 2004. Liquid phase reaction of 2′-hydroxyacetophenone and benzaldehyde over ZSM-5 catalysts. Journal of Molecular Catalysis A: Chemical (218) 101-106.

Sashidhara, K.V., Rosaiah, J. N. and Kumar, A., 2009. Iodine-catalyzed mild and efficient method for the synthesis of chalcones. Synthetic Communications (39) 2288-2296.

Sarda, S. R., Jadhav, W. N., Tekale, S. U., Jadhav, G. V., Patil, B. R., Suryawanshi, G. S. and Pawar, R. P., 2009. Phosphonium ionic liquid catalyzed an efficient synthesis of chalcones. Letters in Organic Chemistry (6) 481-484.

Sharma, A. S., Anandakumar, S. and Ilanchelian, M., 2014. A combined spectroscopic and molecular docking study on site selective binding interaction of Toluidine blue O with Human and Bovine serum albumins. Journal of Luminescence (151) 206-218.

Shanmugaraj, K., Anandakumar, S. and Ilanchelian, M., 2014. Exploring the biophysical aspects and binding mechanism of thionine with bovine hemoglobin by optical spectroscopic and molecular docking methods. Journal of Photochemistry and Photobiology B: Biology (131) 43-52.

Tiecco, M., Germani, R. and Cardellini, F., 2016. Carbon–carbon bond formation in acid deep eutectic solvent: chalcones synthesis via Claisen–Schmidt reaction. RSC Advances (6) 43740-43747.

Wang, X. and Cheng, S., 2006. Solvent-free synthesis of flavanones over aminopropyl-functionalized SBA-15. Catalysis Communications (7) 689-695.

Wang, X. and Cheng, S., 2006. Solvent-free synthesis of flavanones over aminopropyl-functionalized SBA-15. Catalysis Communications (7) 689-695.

Xia, Y., Yang, Z.Y., Xia, P., Bastow, K.F., Nakanishi, Y. and Lee, K. H., 2000. Antitumor agents. Part 202: novel 2′-amino chalcones: design, synthesis and biological evaluation. Bioorganic & medicinal chemistry letters (10) 699-701.

Xu, Q., Yang, Z., Yin, D. and Zhang, F., 2008. Synthesis of chalcones catalyzed by a novel solid sulfonic acid from bamboo. Catalysis Communications (9) 1579-1582.

Yang, S. D., Wu, L.Y., Yan, Z.Y., Pan, Z. L. and Liang, Y. M., 2007. A novel ionic liquid supported organ catalyst of pyrrolidine amide: Synthesis and catalysed Claisen–Schmidt reaction. Journal of Molecular Catalysis A: Chemical (268) 107-111.

Zhang, J., Tian, Z., Liang, L., Subirade, M. and Chen, L., 2013. Binding interactions of β-conglycinin and glycinin with vitamin B12. The Journal of Physical Chemistry B (117) 14018-14028.

Zaidi, N., Ahmad, E., Rehan, M., Rabbani, G., Ajmal, M. R., Zaidi, Y., Subbarao, N. and Khan, R. H., 2013. Biophysical insight into furosemide binding to human serum albumin: a study to unveil its impaired albumin binding in uremia. The Journal of Physical Chemistry B (117) 2595-2604.

Chapter Five

Part A

APPENDIX

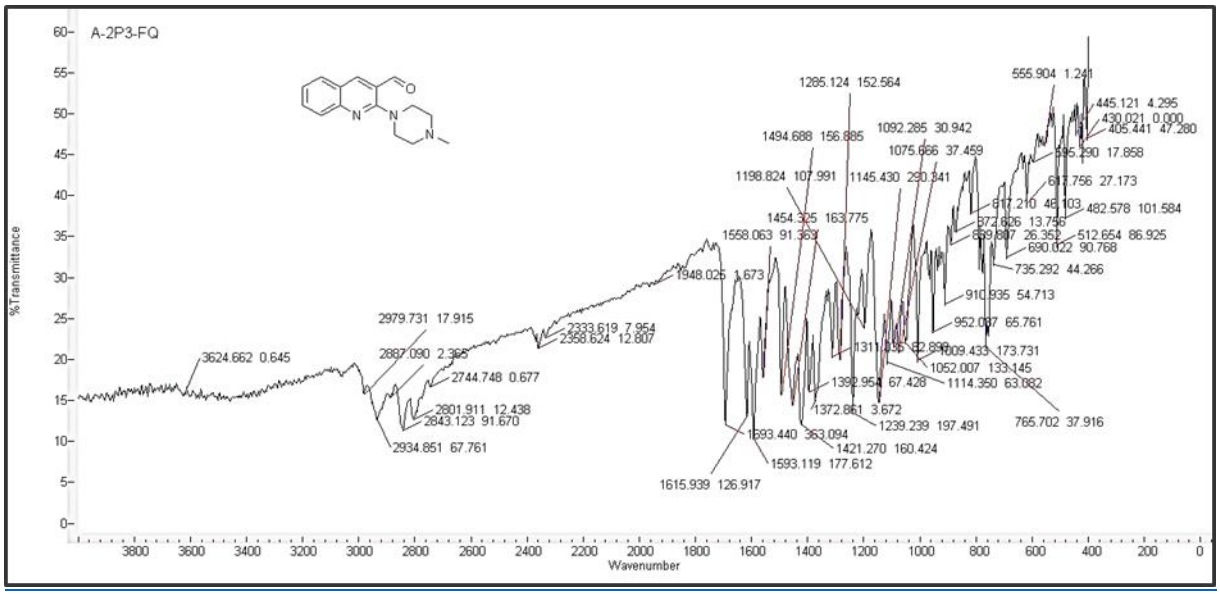

Figure 5A. S. 1. The Infra-Red Spectrum of compound 3

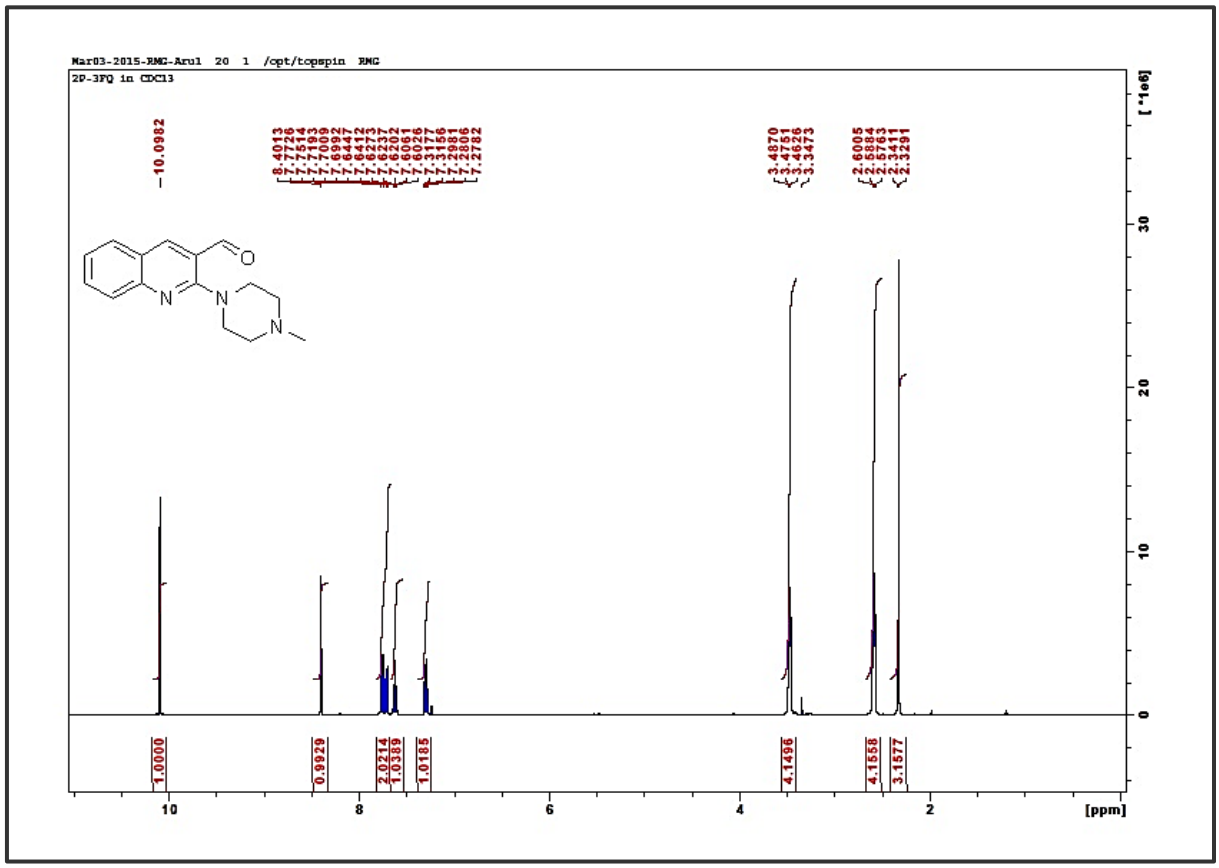

Figure 5A. S. 2. The ^{1}H NMR of compound 3

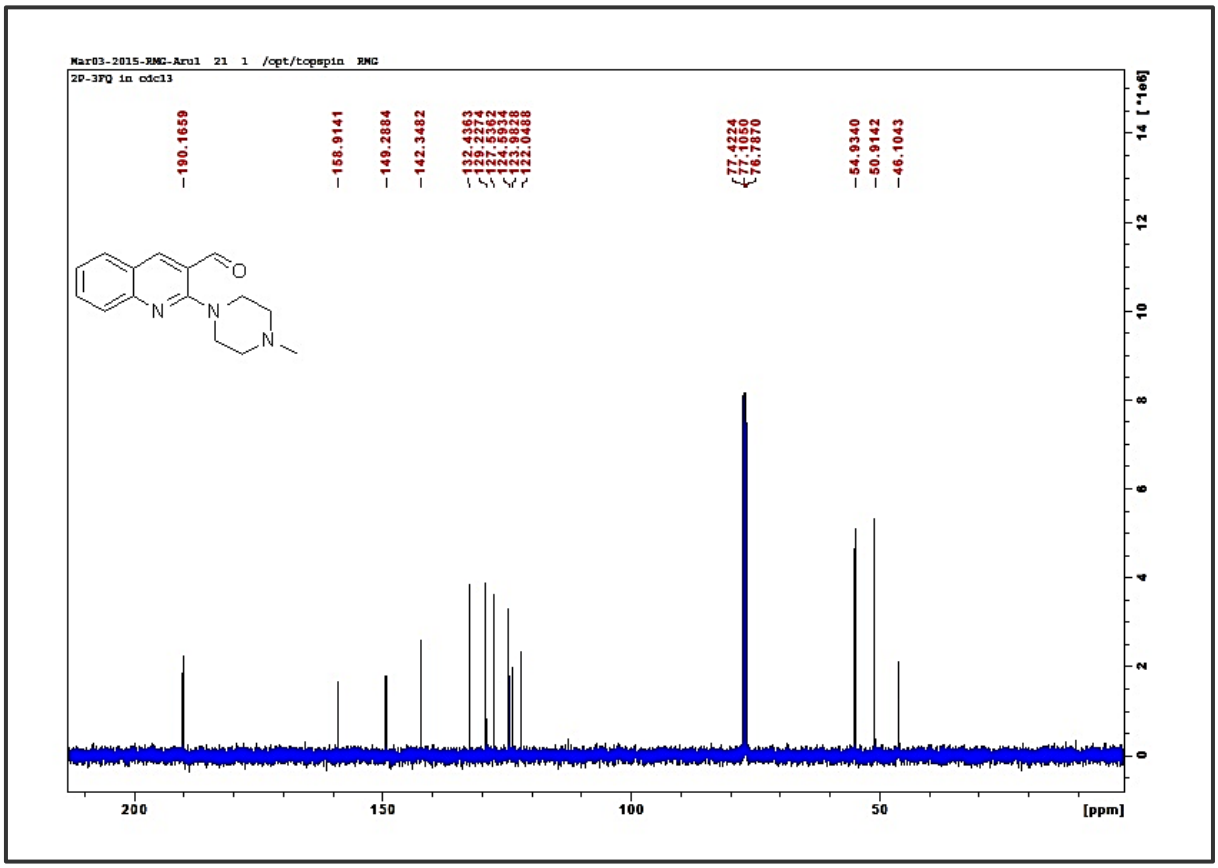

Figure 5A. S. 3. The ^{13}C NMR of compound 3

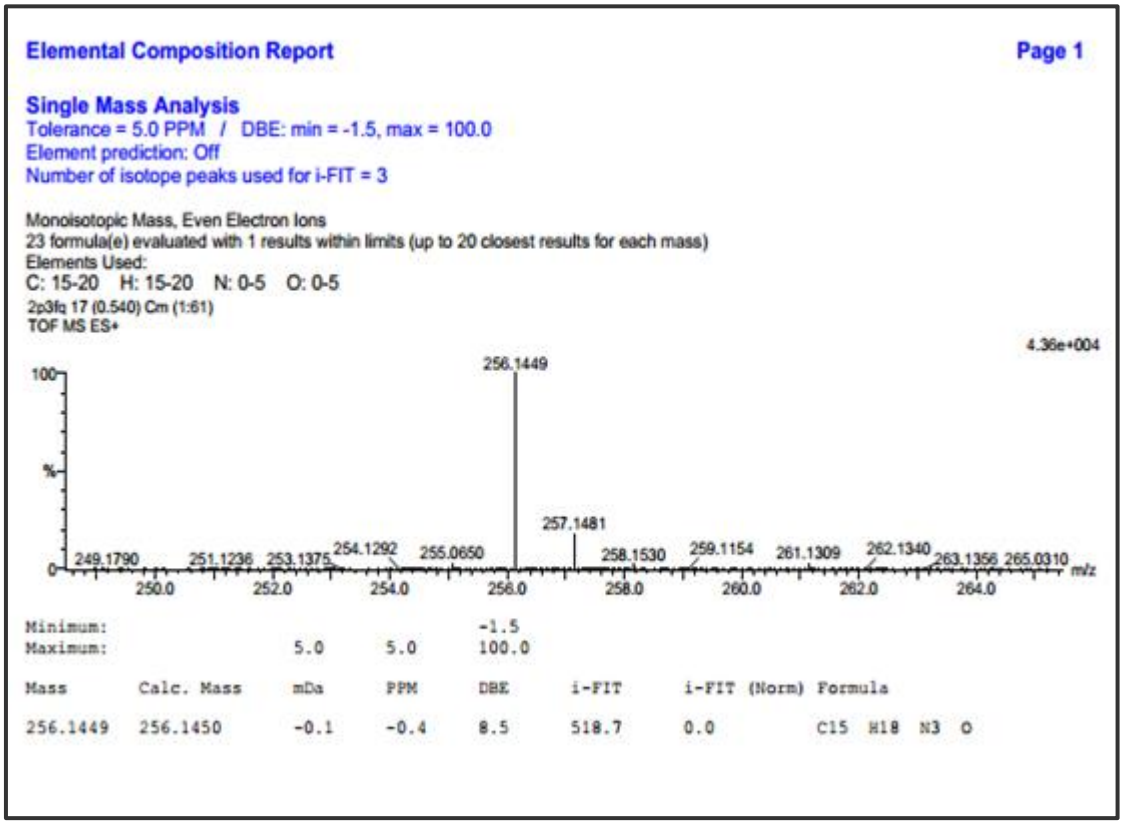

Figure 5A. S. 4. The HRMS of compound 3

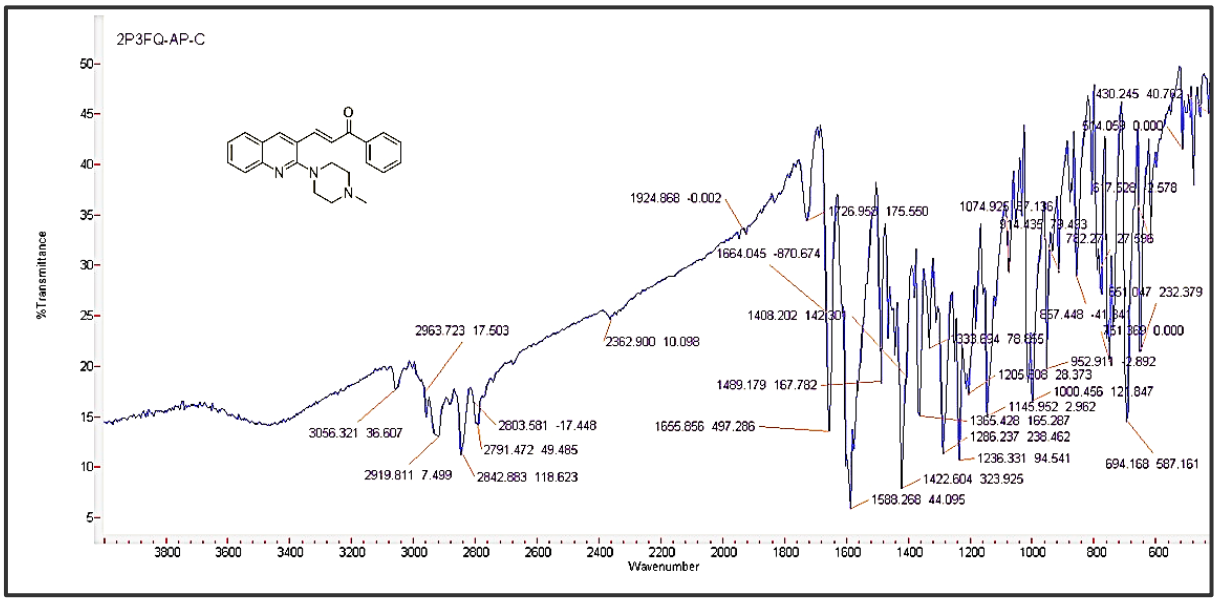

Figure 5A. S. 5. The Infra-Red Spectrum of compound 5a

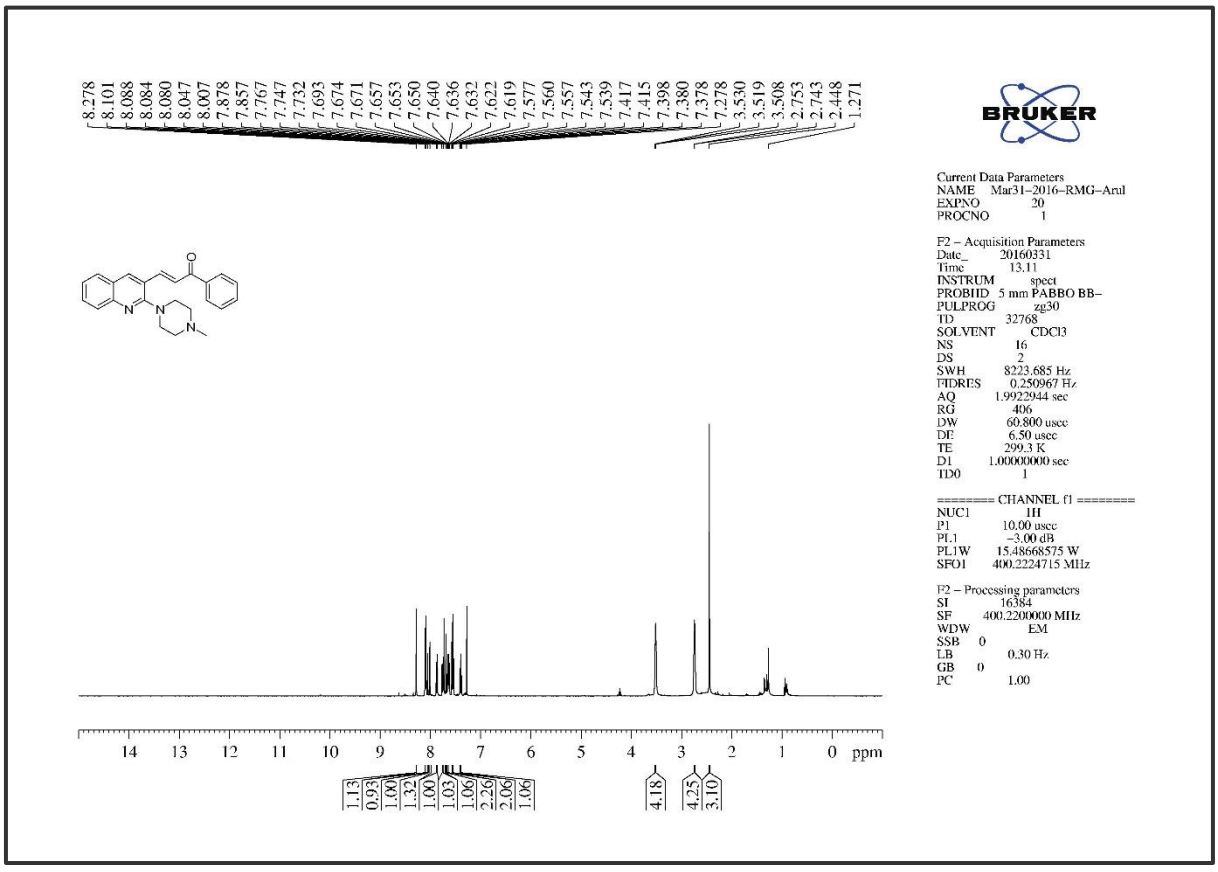

Figure 5A .S. 6. The ^{1}H NMR of compound 5a

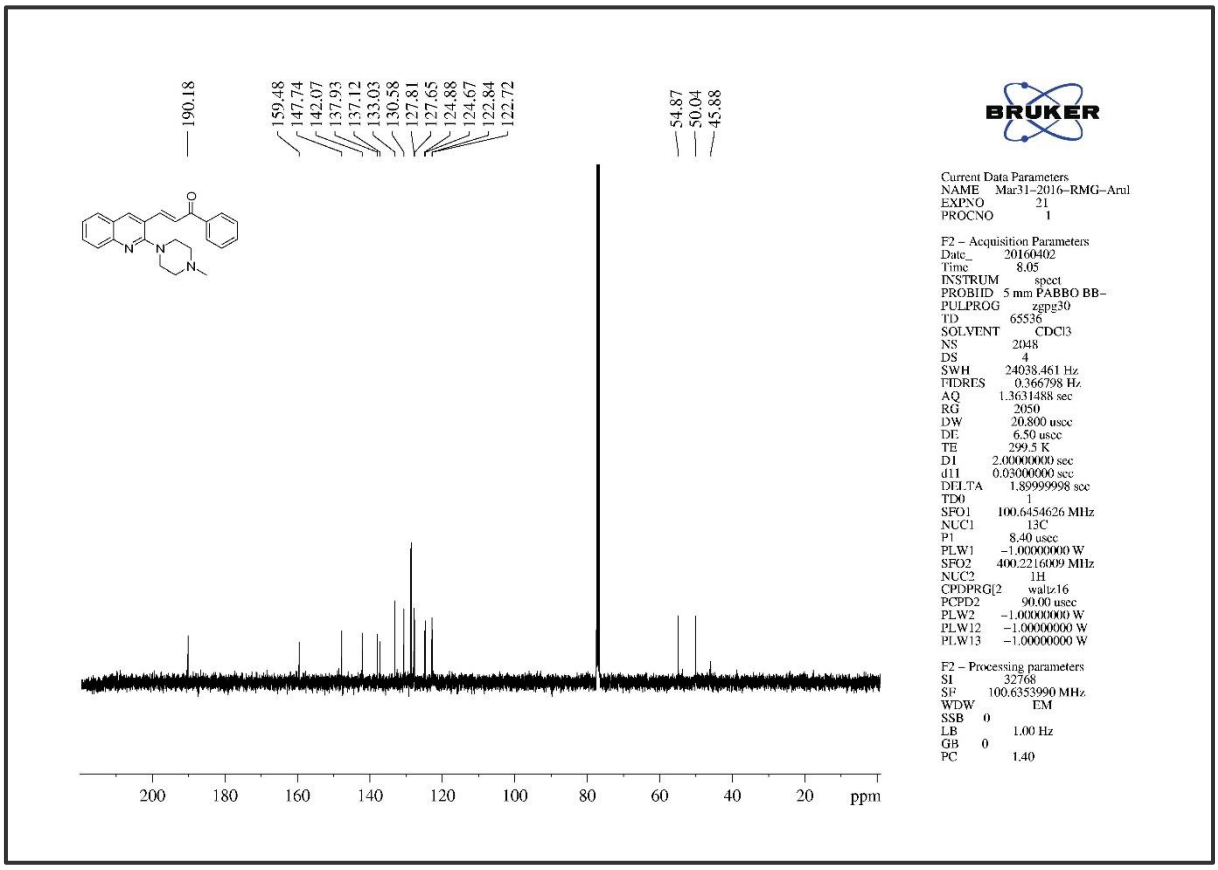

Figure 5A. S. 7. The ^{13}C NMR of compound 5a

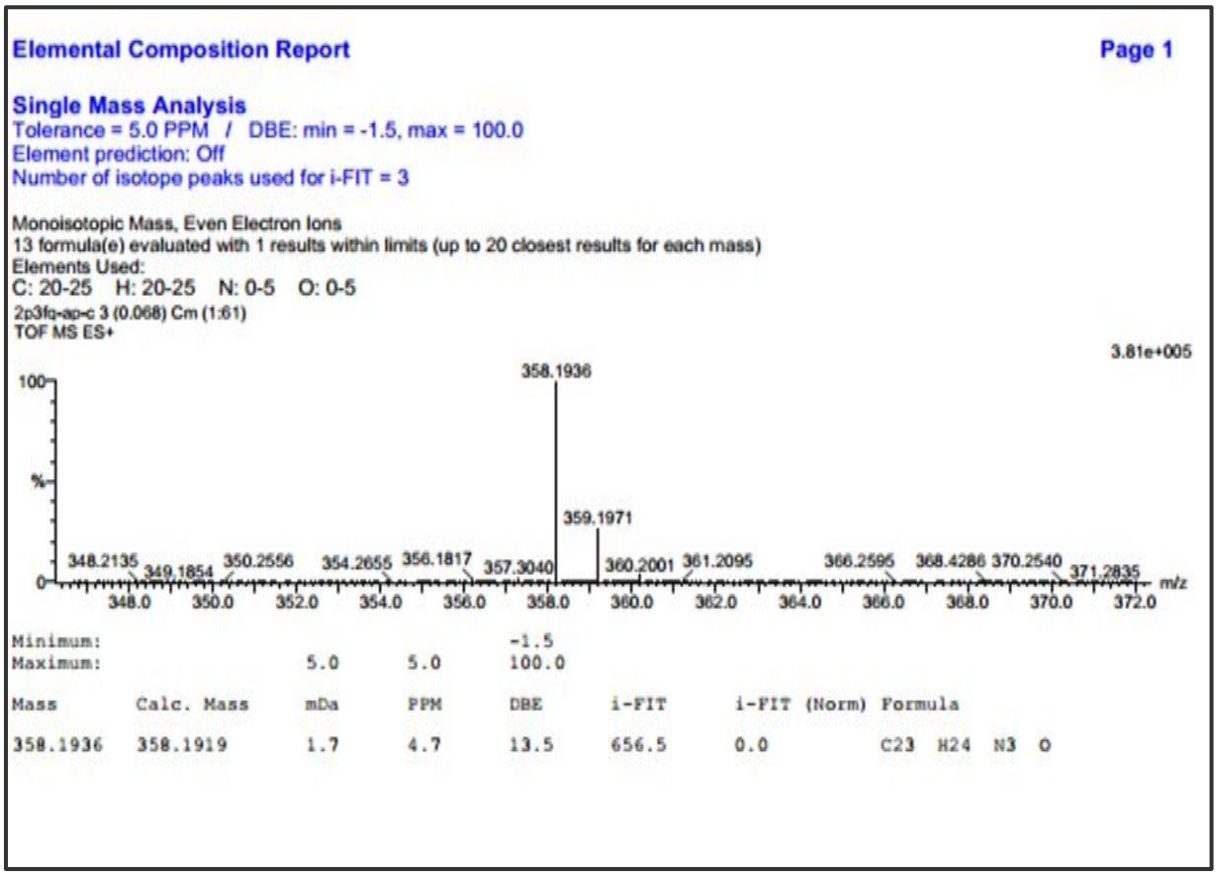

Figure 5A. S. 8. The HRMS of compound 5a

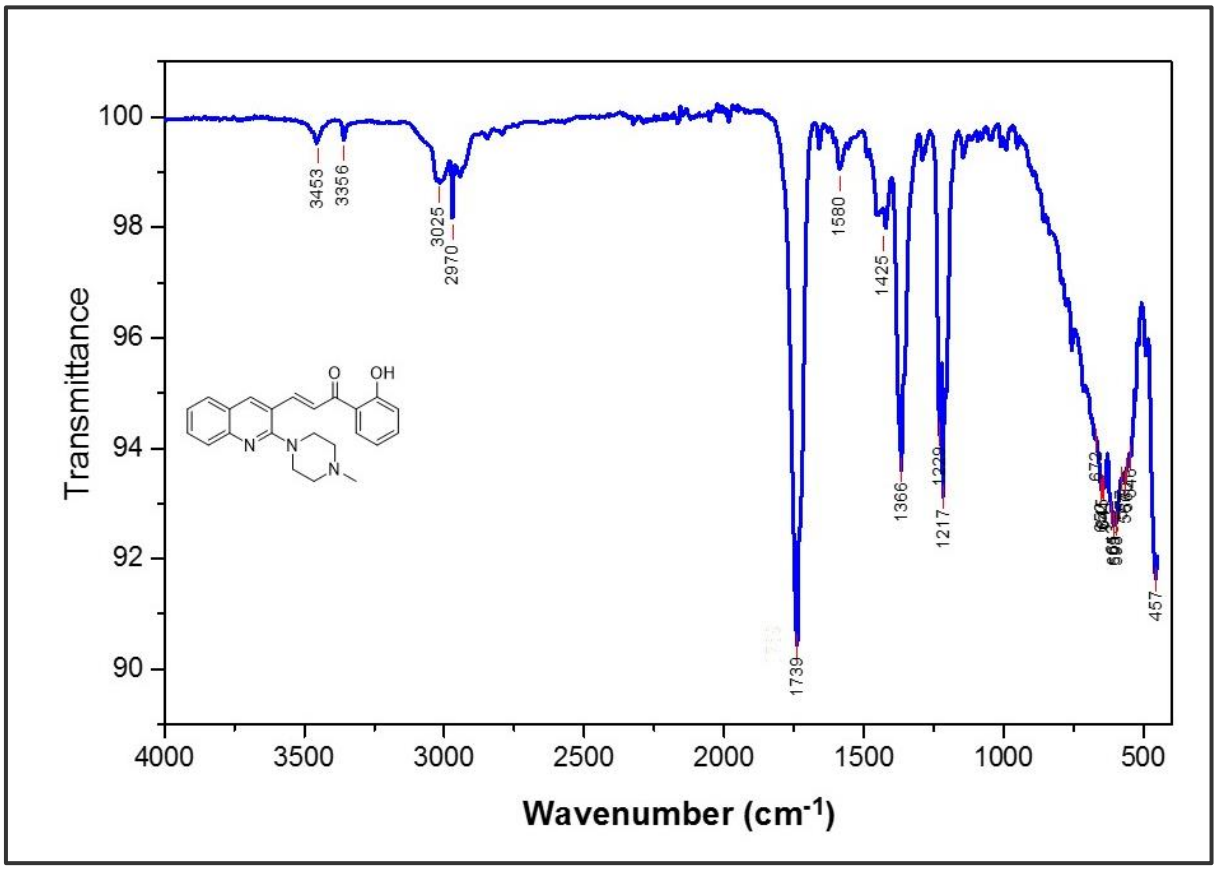

Figure 5A. S. 9. The Infra-Red Spectrum of compound 5b

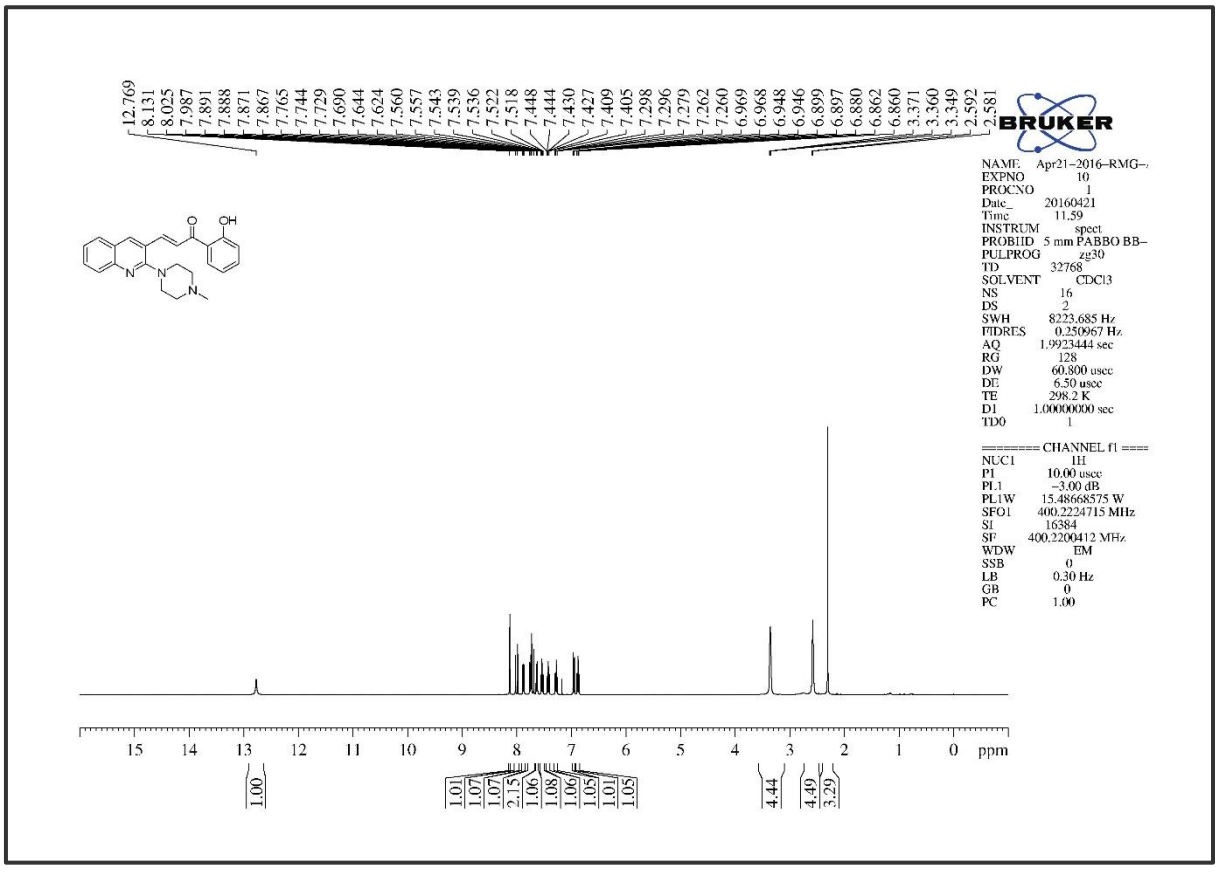

Figure 5A. S. 10. The ^{1}H NMR of compound 5b

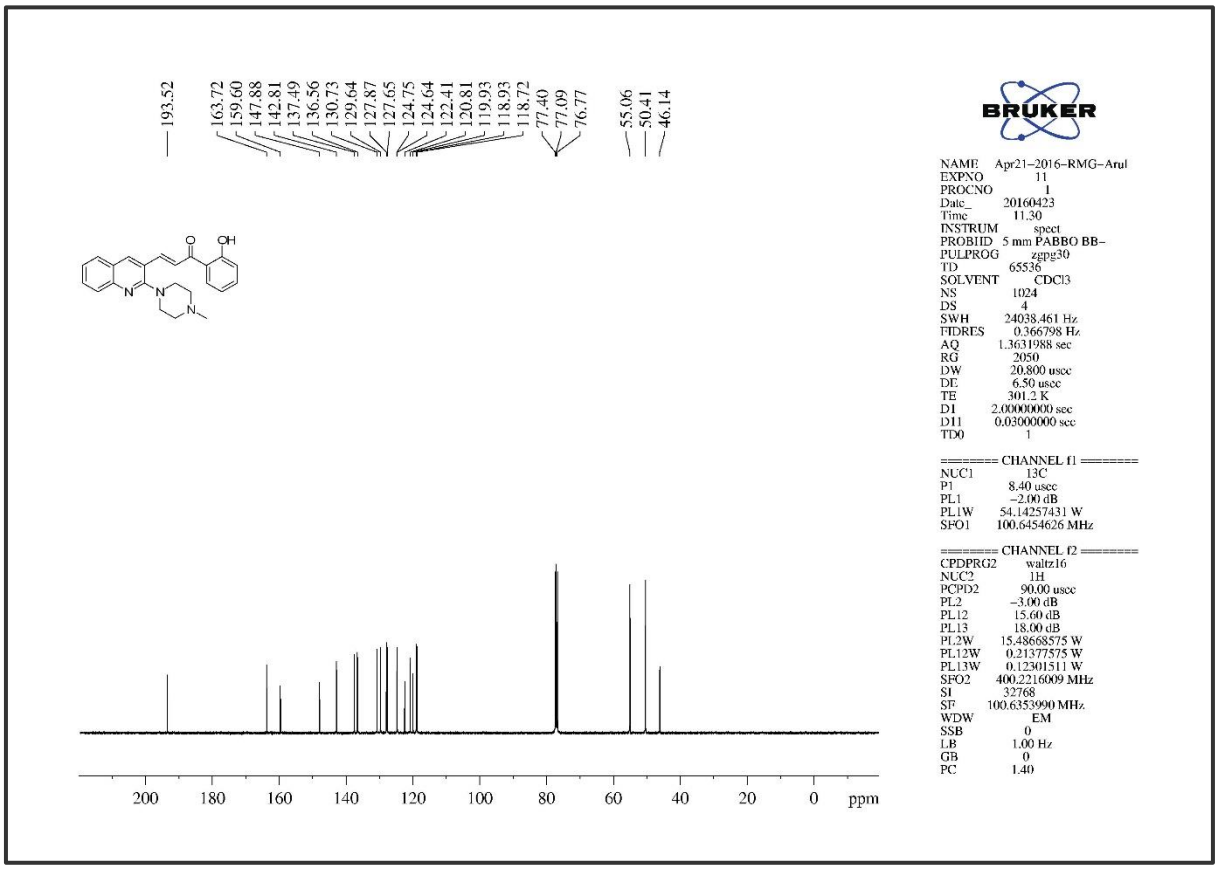

Figure 5A. S. 11. The ^{13}C NMR of compound 5b

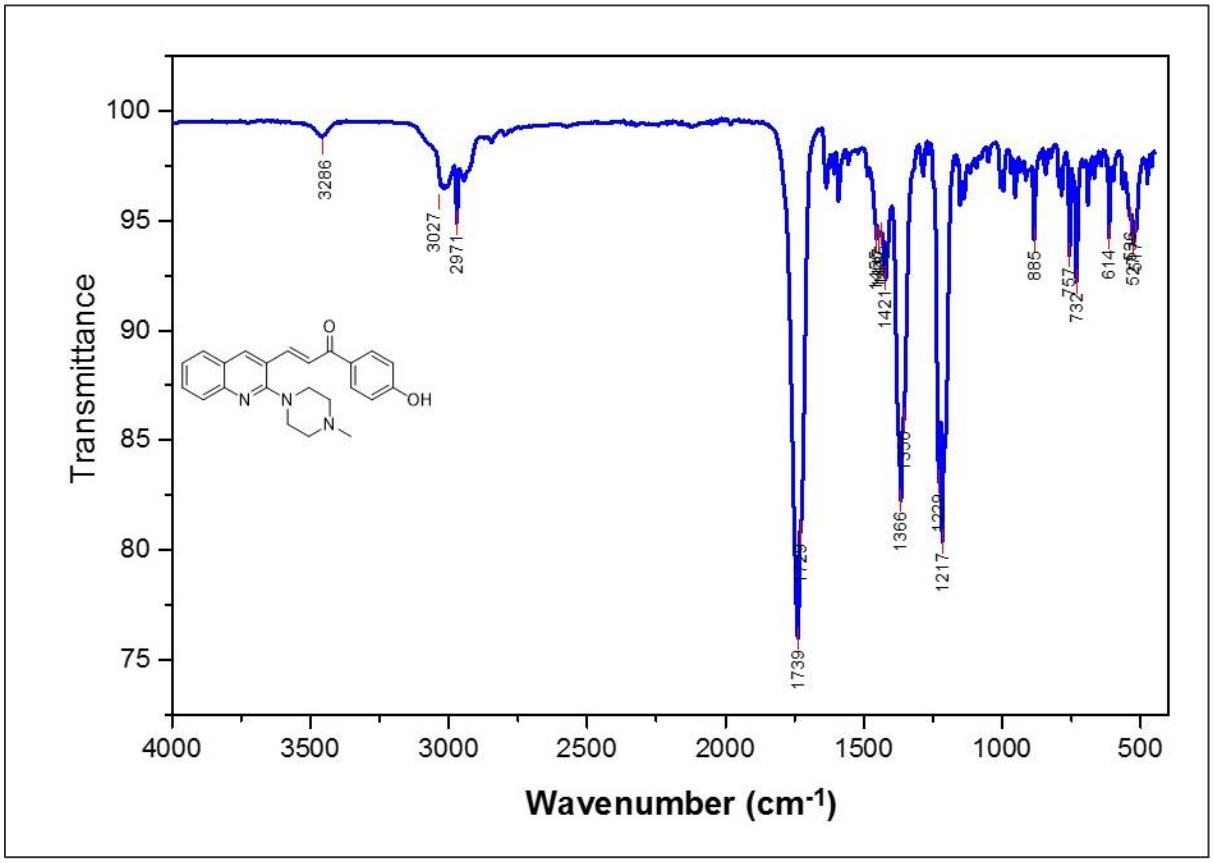

Figure 5A. S. 12. The Infra-Red Spectrum of compound 5c

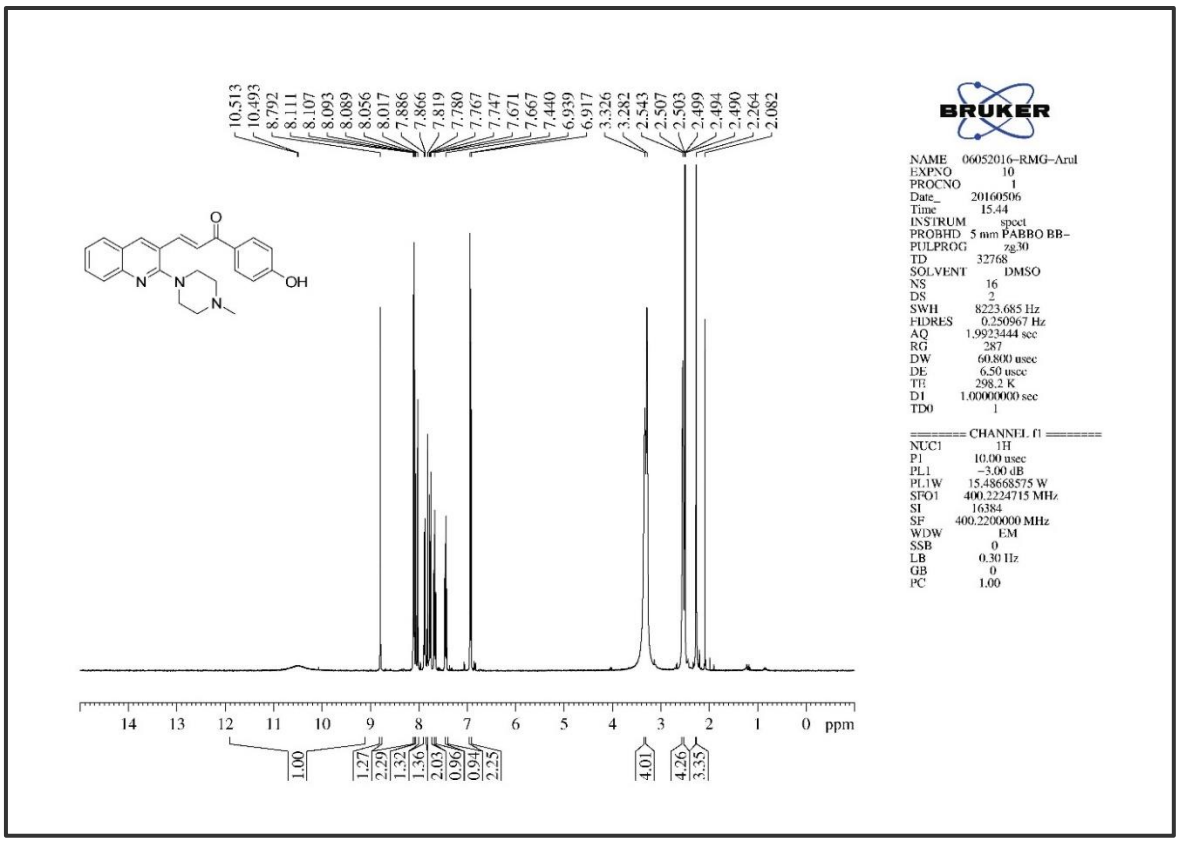

Figure 5A. S. 13. The ^{1}H NMR of compound 5c

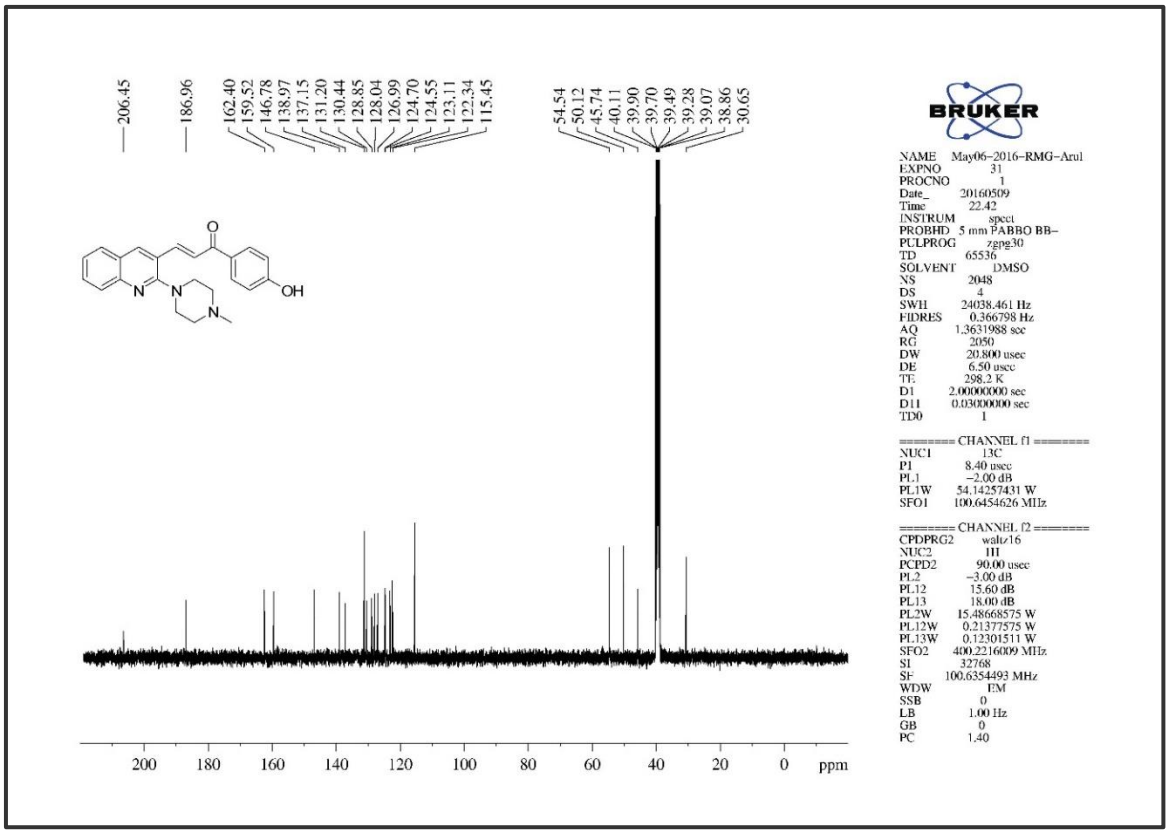

Figure 5A. S. 14. The ^{13}C NMR of compound 5c

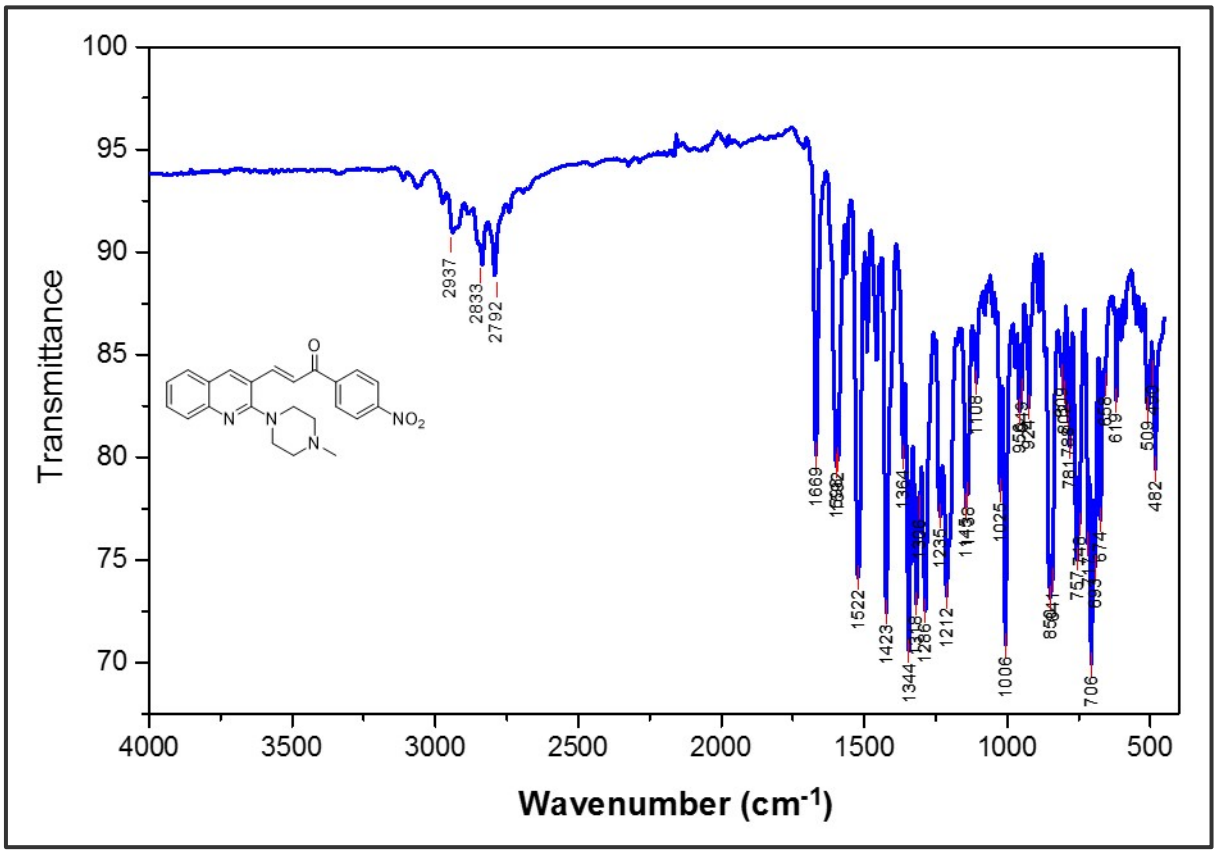

Figure 5A. S. 15. The Infra-Red Spectrum of compound 5d

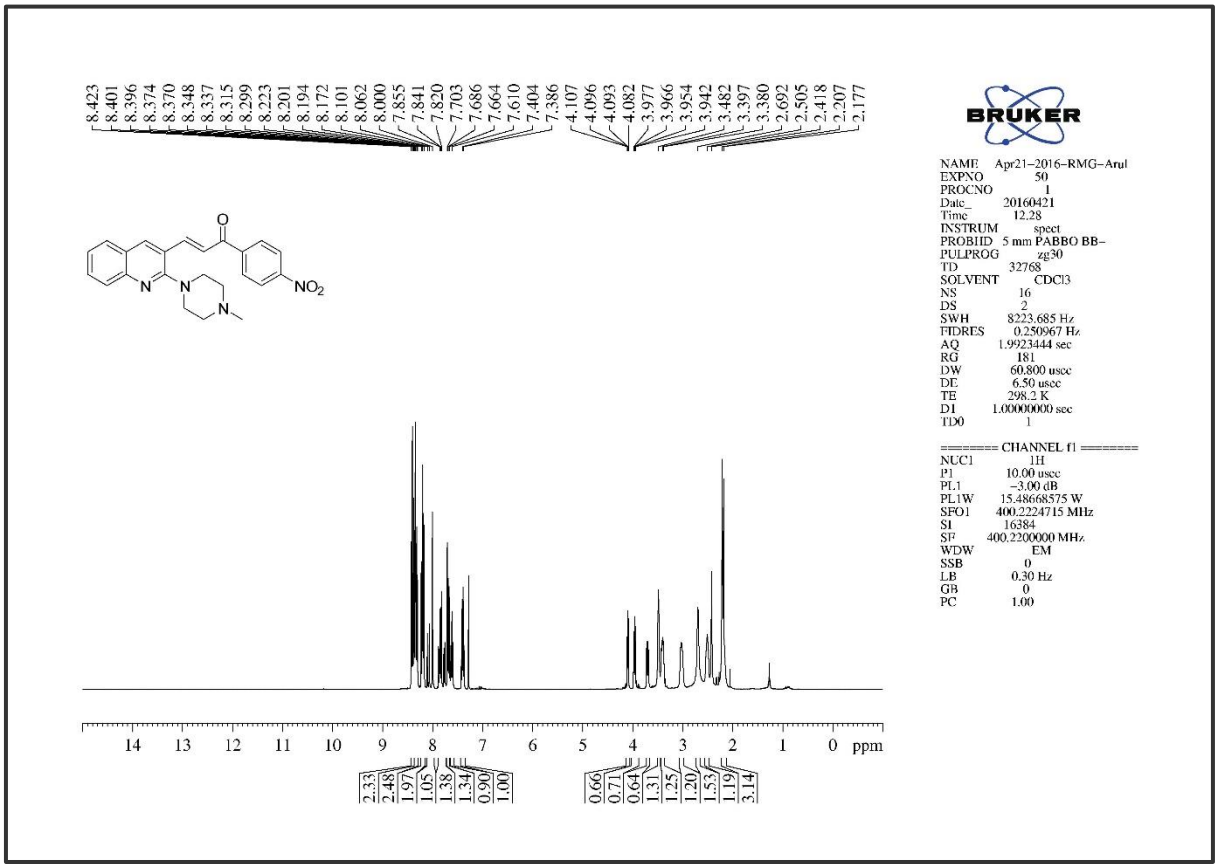

Figure 5A. S. 16. The ^{1}H NMR of compound 5d

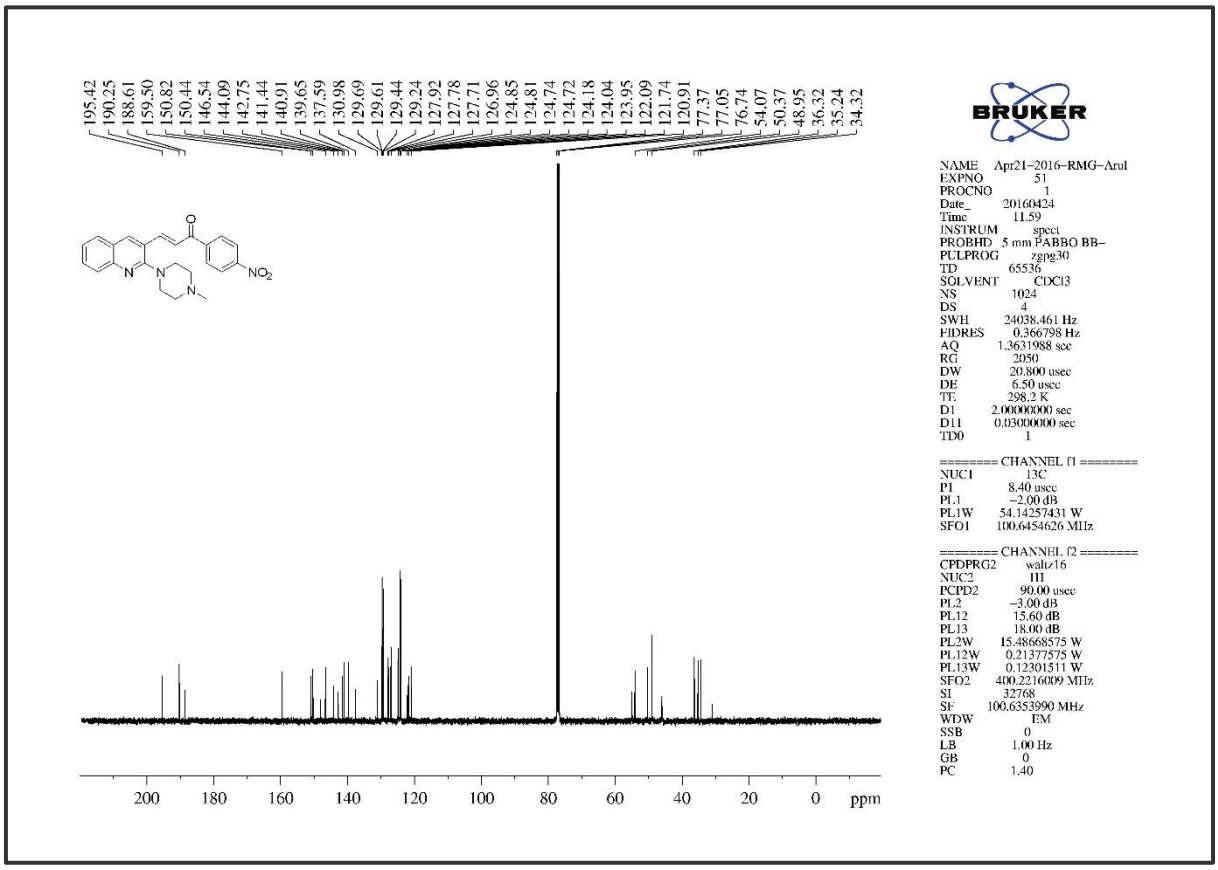

Figure 5A. S. 17. The ^{13}C NMR of compound 5d

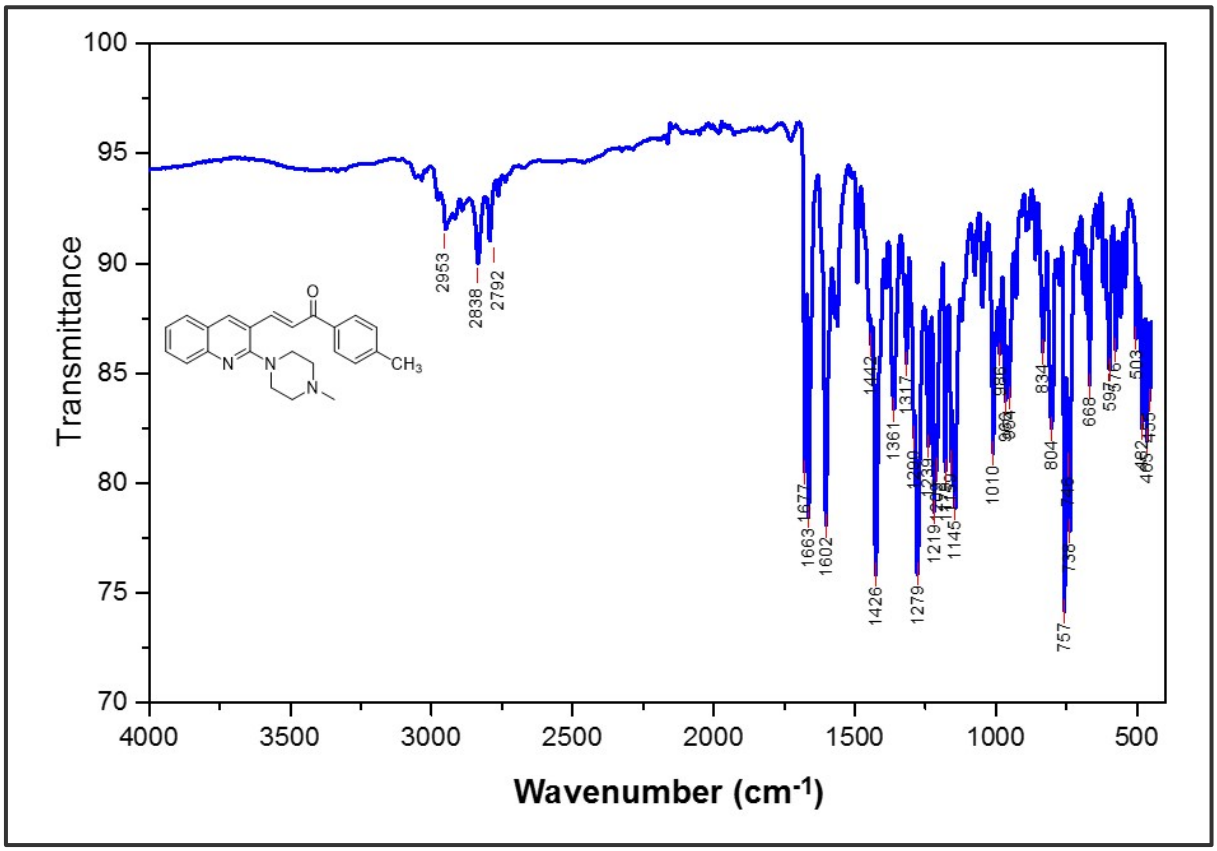

Figure 5A. S. 18. The Infra-Red Spectrum of compound 5e

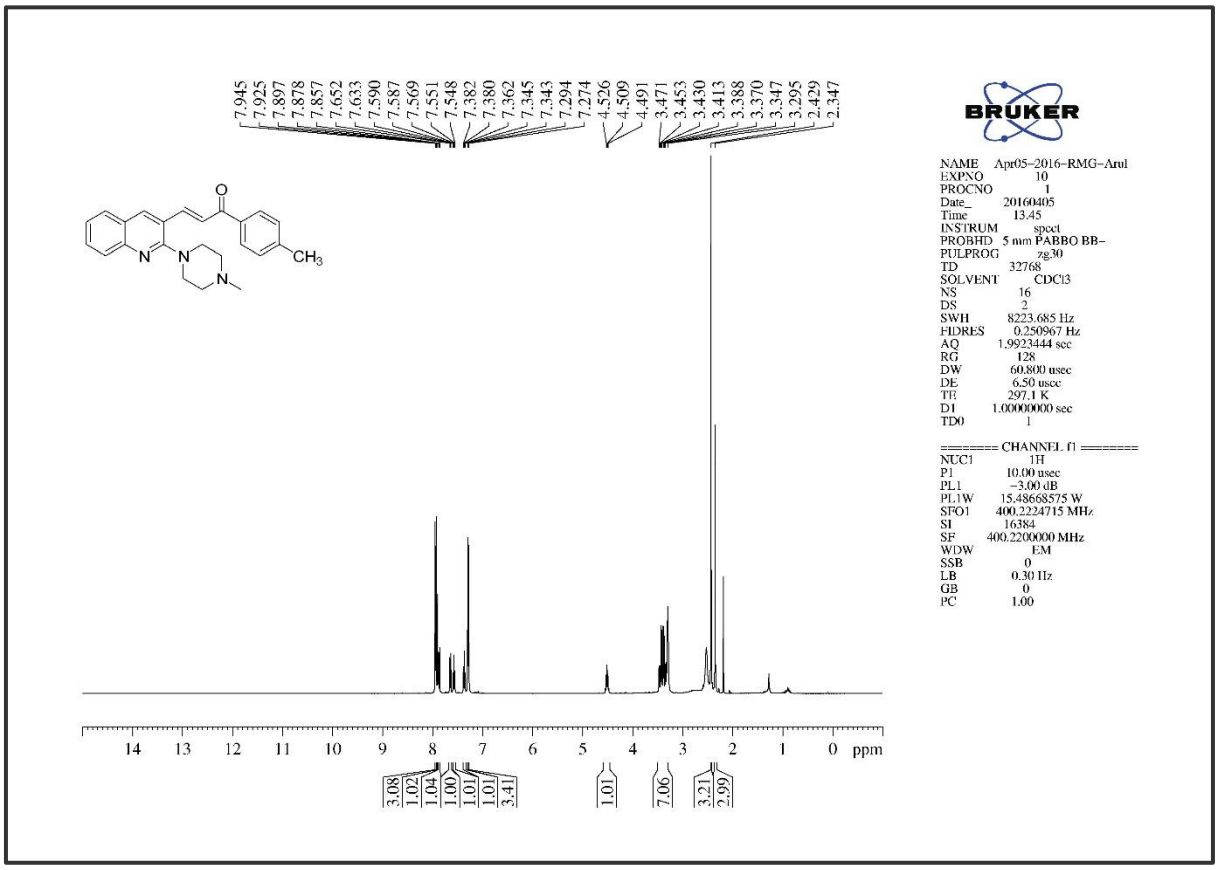

Figure 5A. S. 19. The ^{1}H NMR of compound 5e

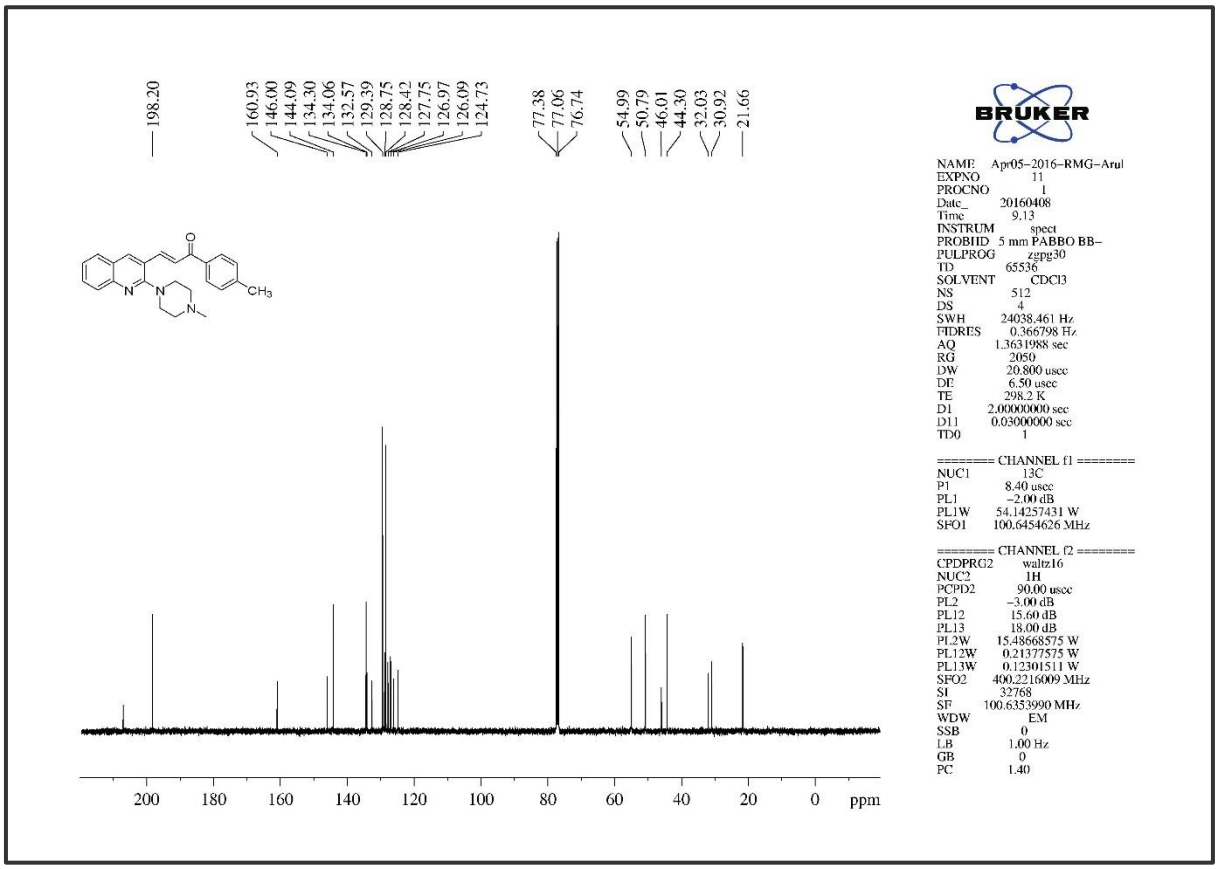

Figure 5A. S. 20. The ^{13}C NMR of compound 5e

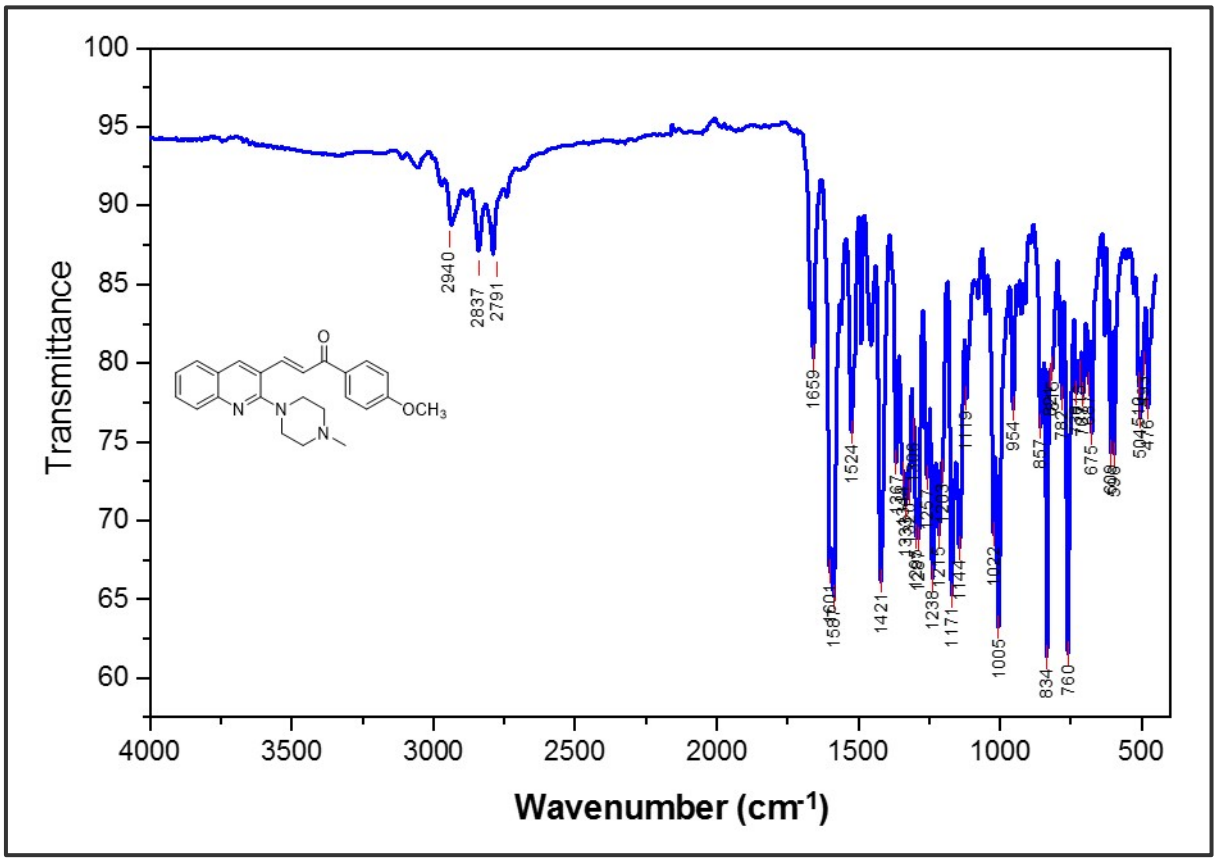

Figure 5A. S. 21. The Infra-Red Spectrum of compound 5f

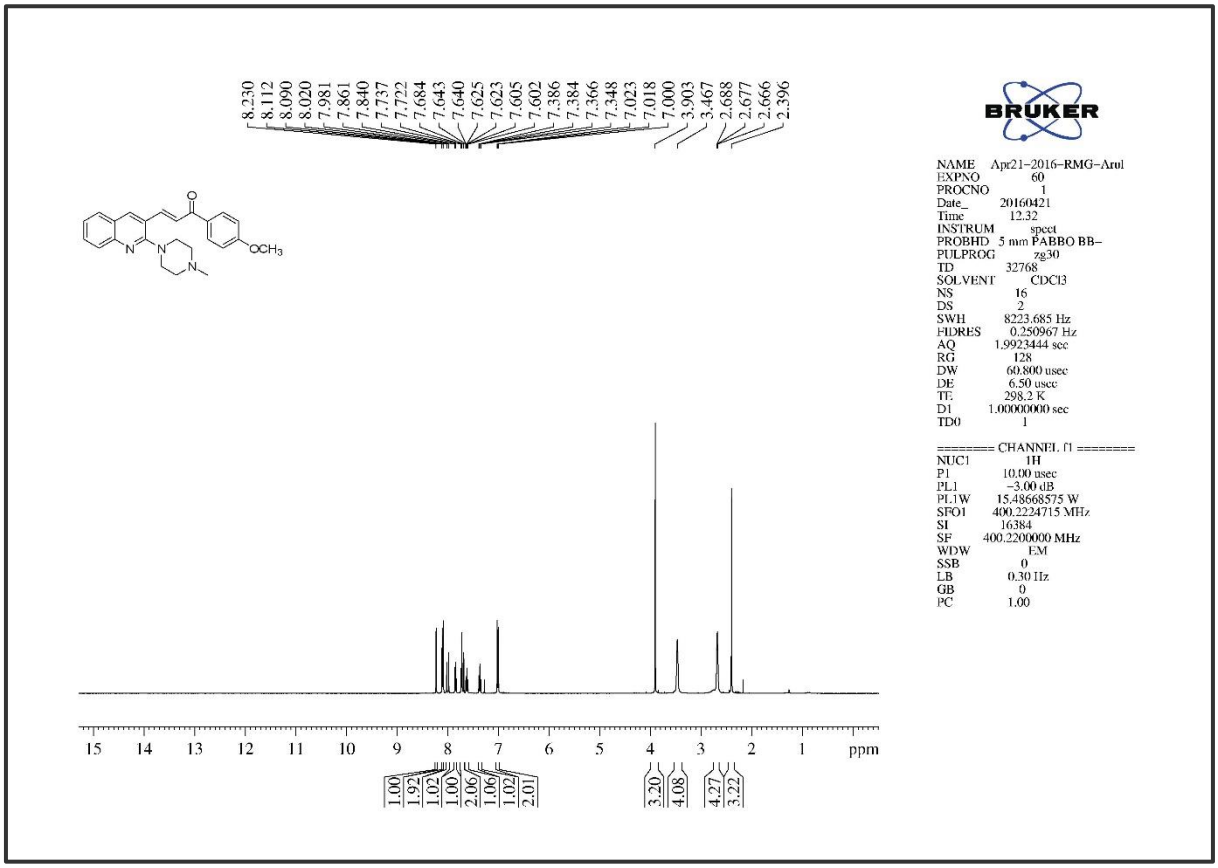

Figure 5A. S. 22. The ^{1}H NMR of compound 5f

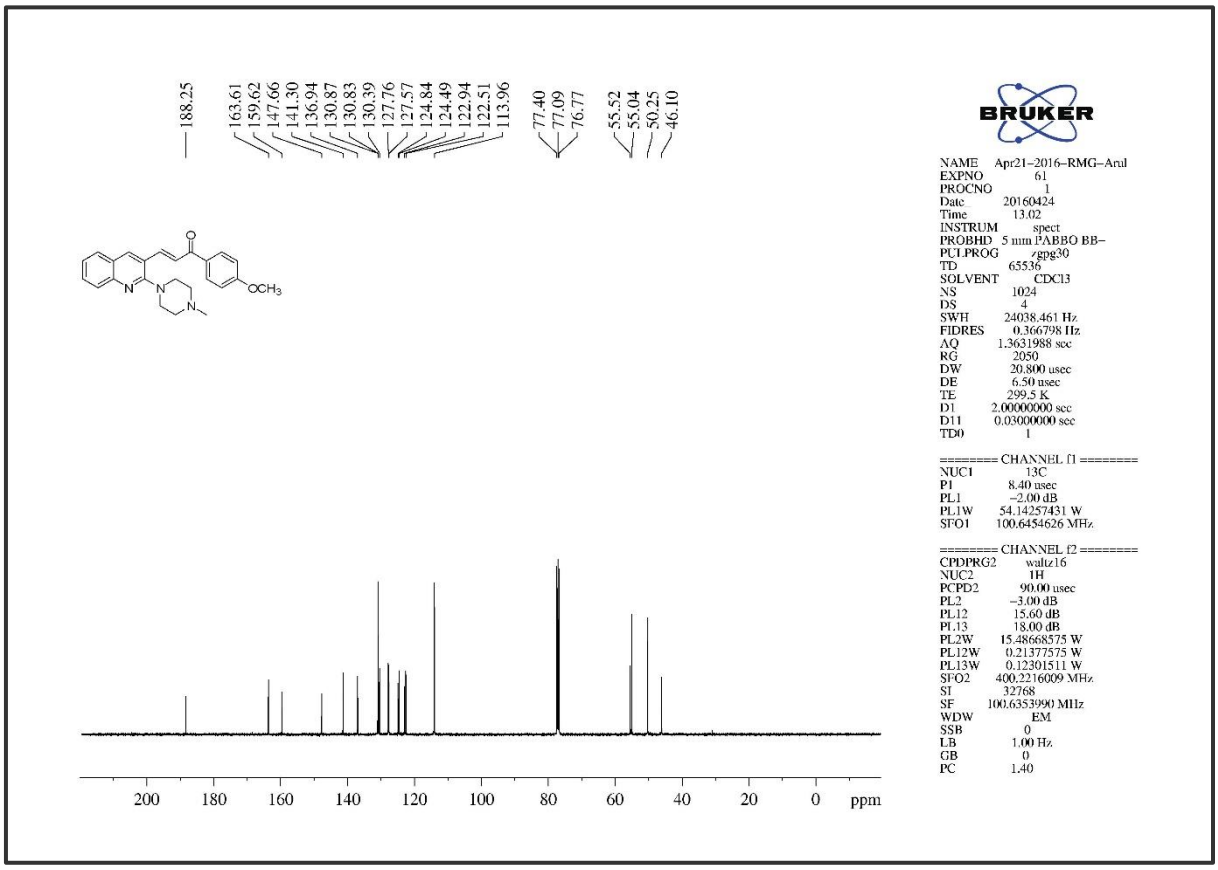

Figure 5A. S. 23. The ^{13}C NMR of compound 5f

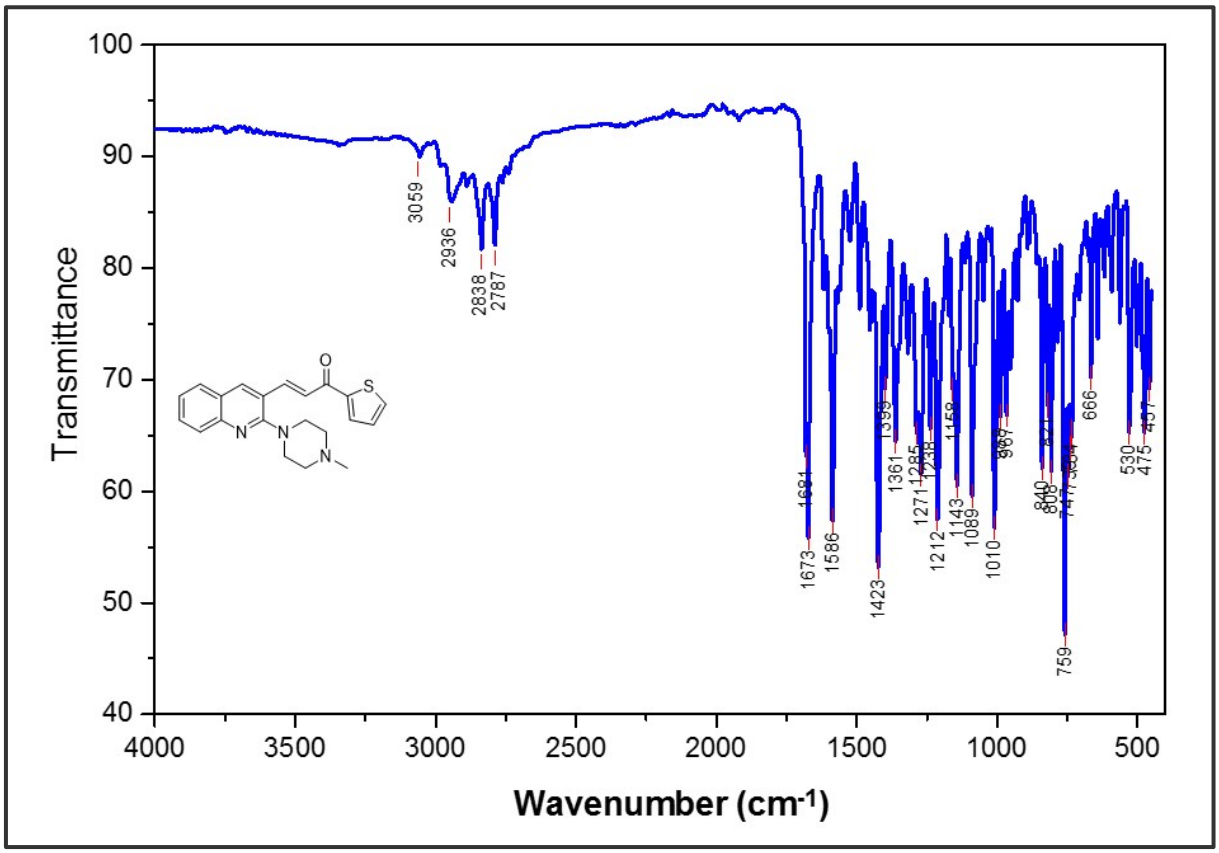

Figure 5A. S. 24. The Infra-Red Spectrum of compound 5g

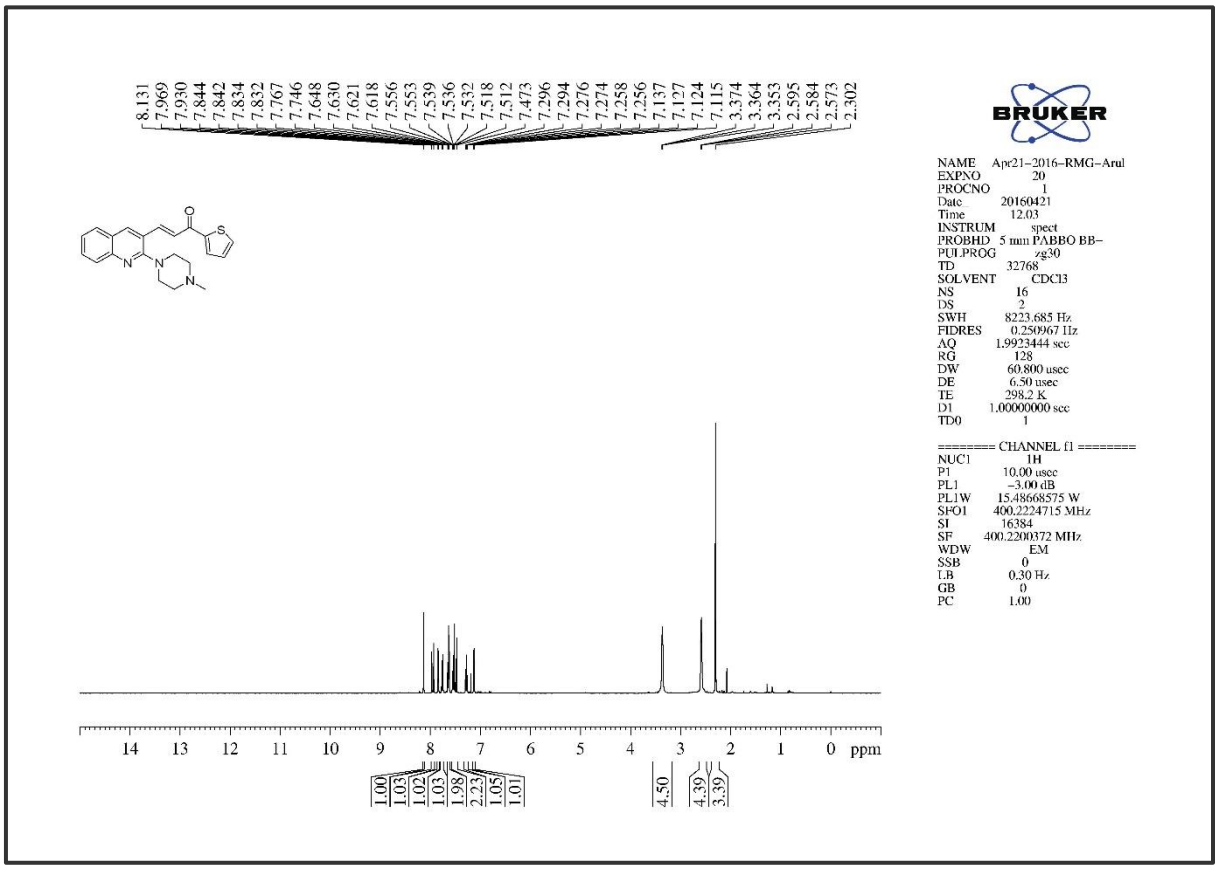

Figure 5A. S. 25. The ^{1}H NMR of compound 5g

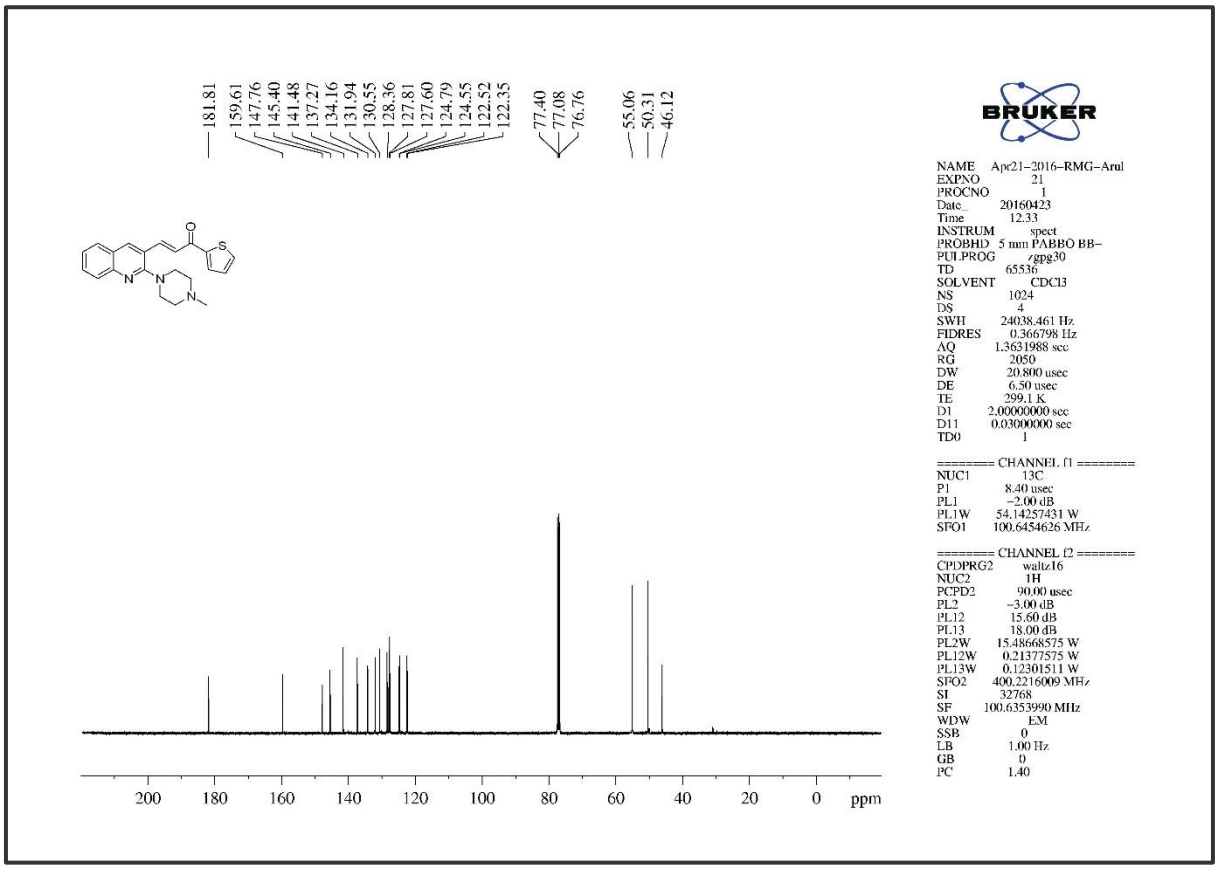

Figure 5A. S. 26. The ^{13}C NMR of compound 5g

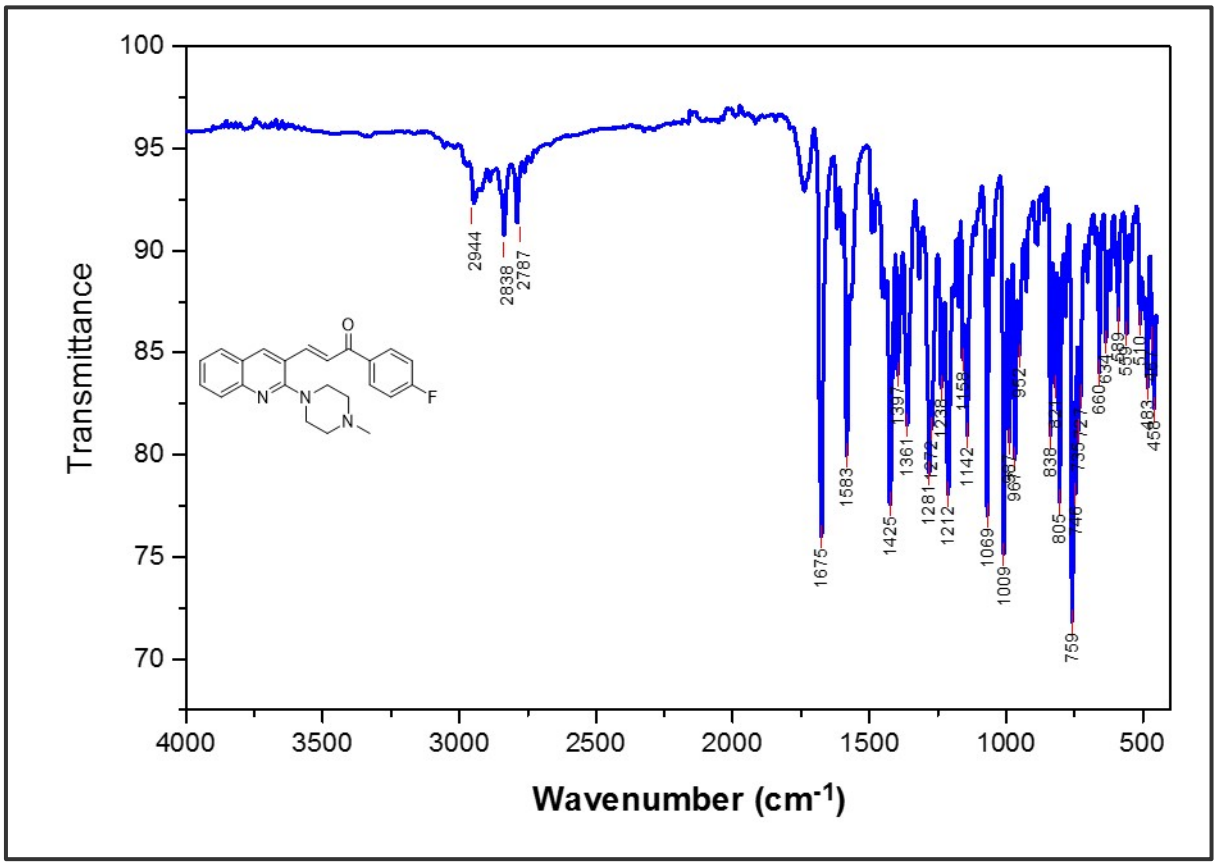

Figure 5A. S. 27. The Infra-Red Spectrum of compound 5h

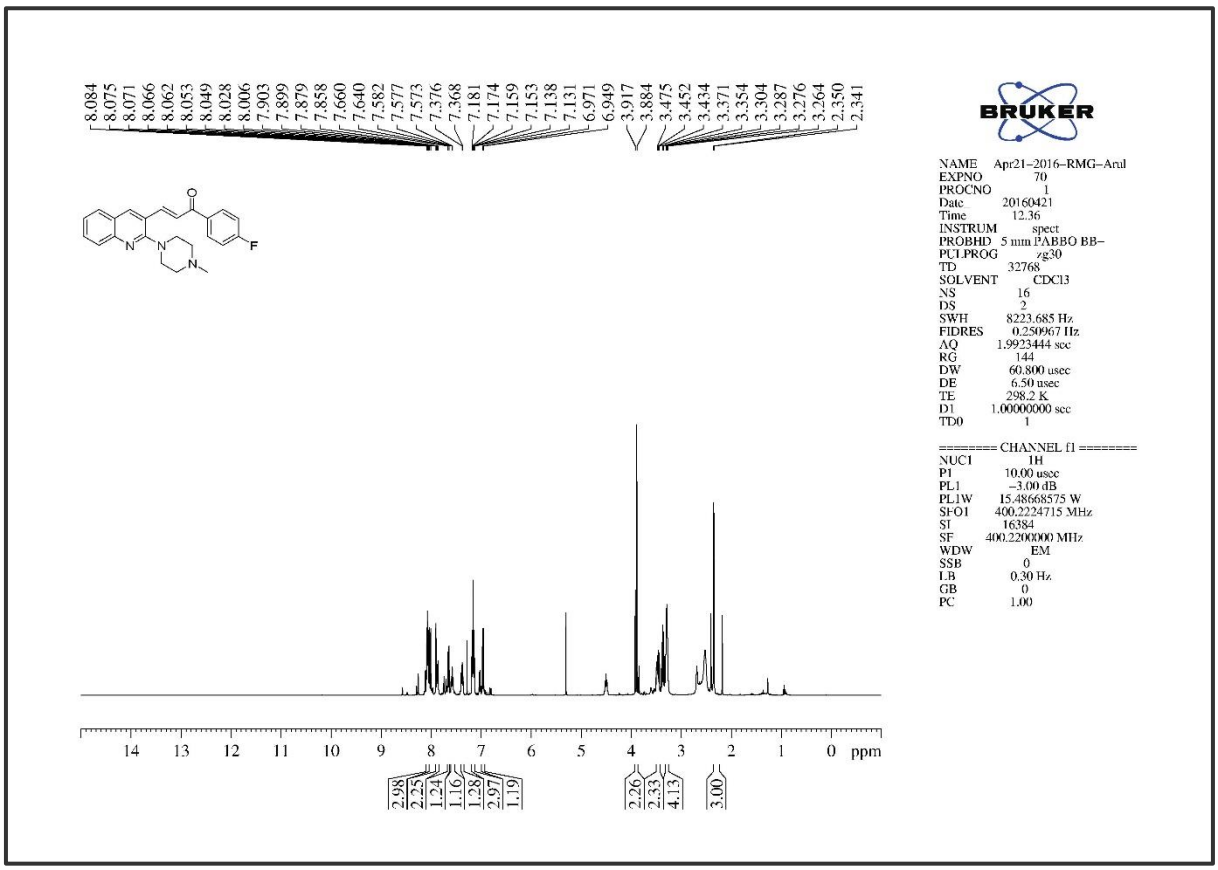

Figure 5A. S. 28. The ^{1}H NMR of compound 5h

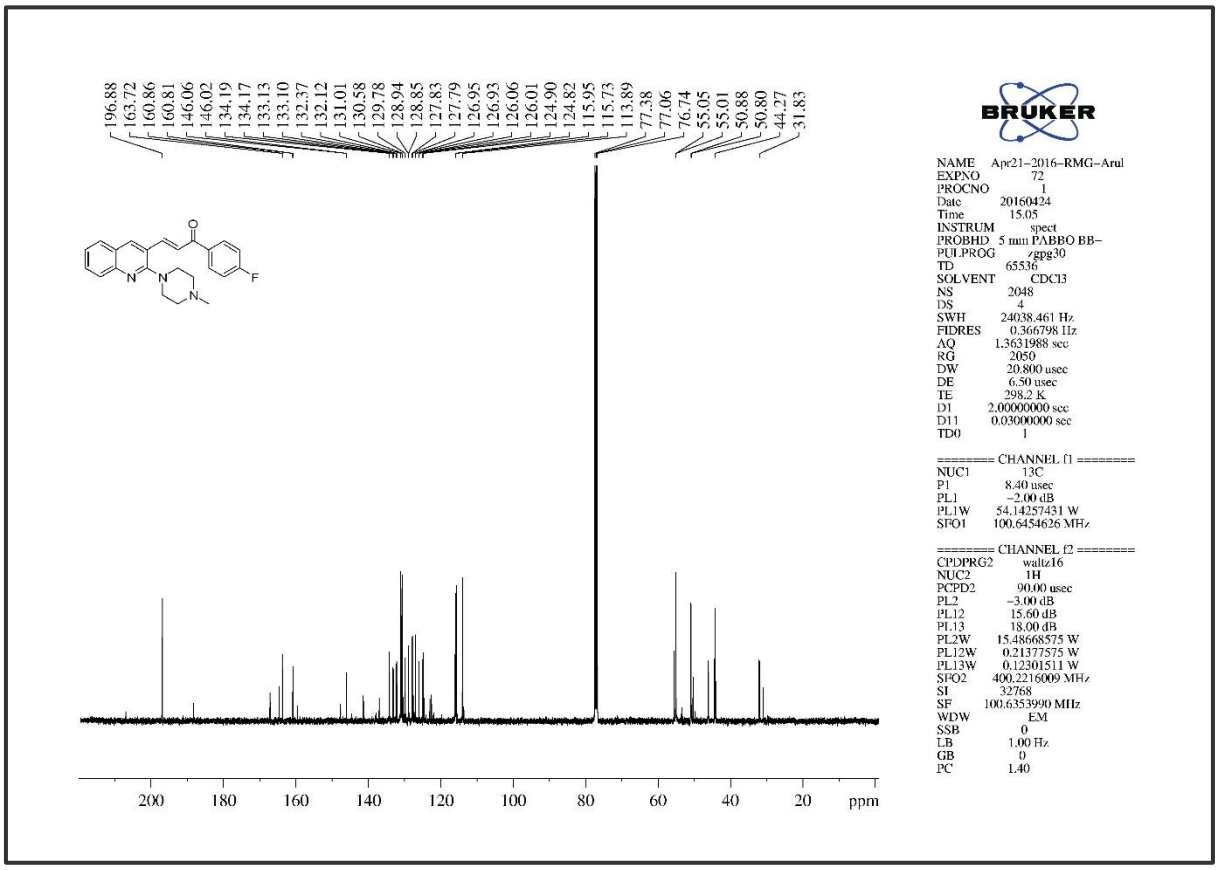

Figure 5A. S. 29. The ^{13}C NMR of compound 5h

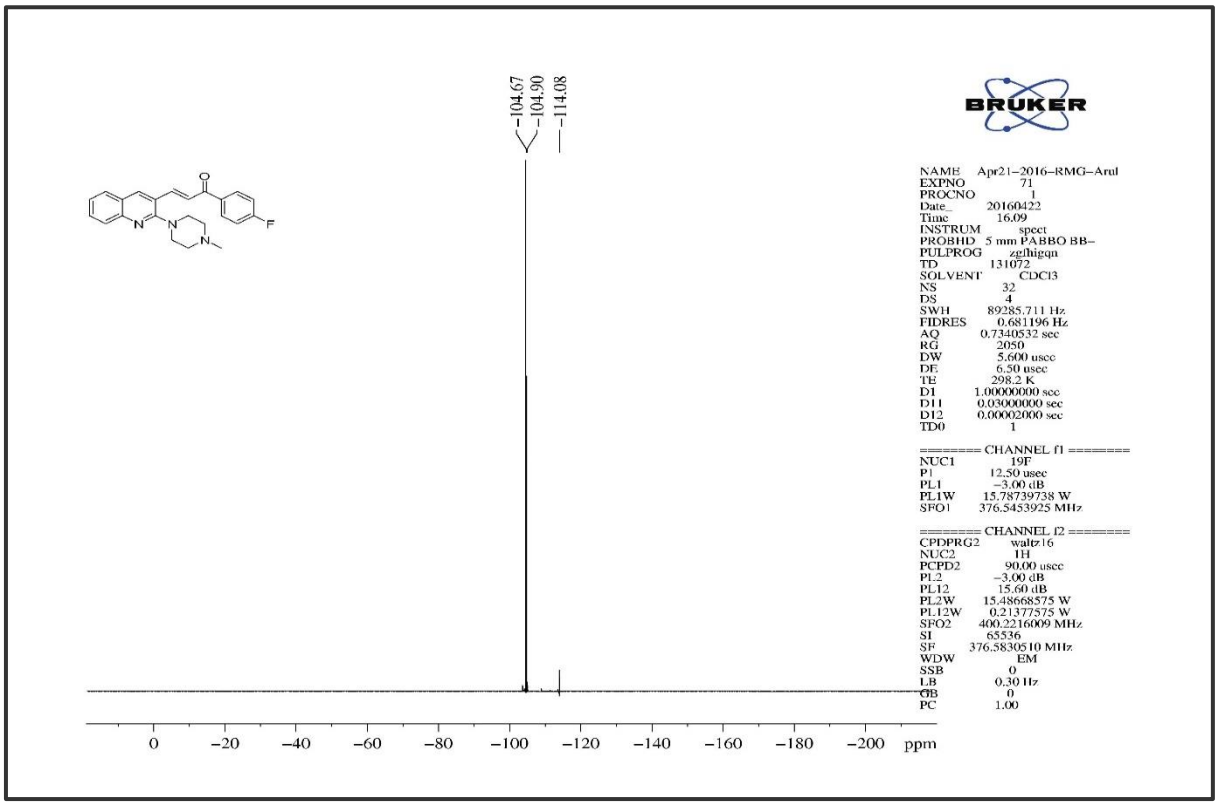

Figure 5A. S. 30. The ^{19}F NMR of compound 5h

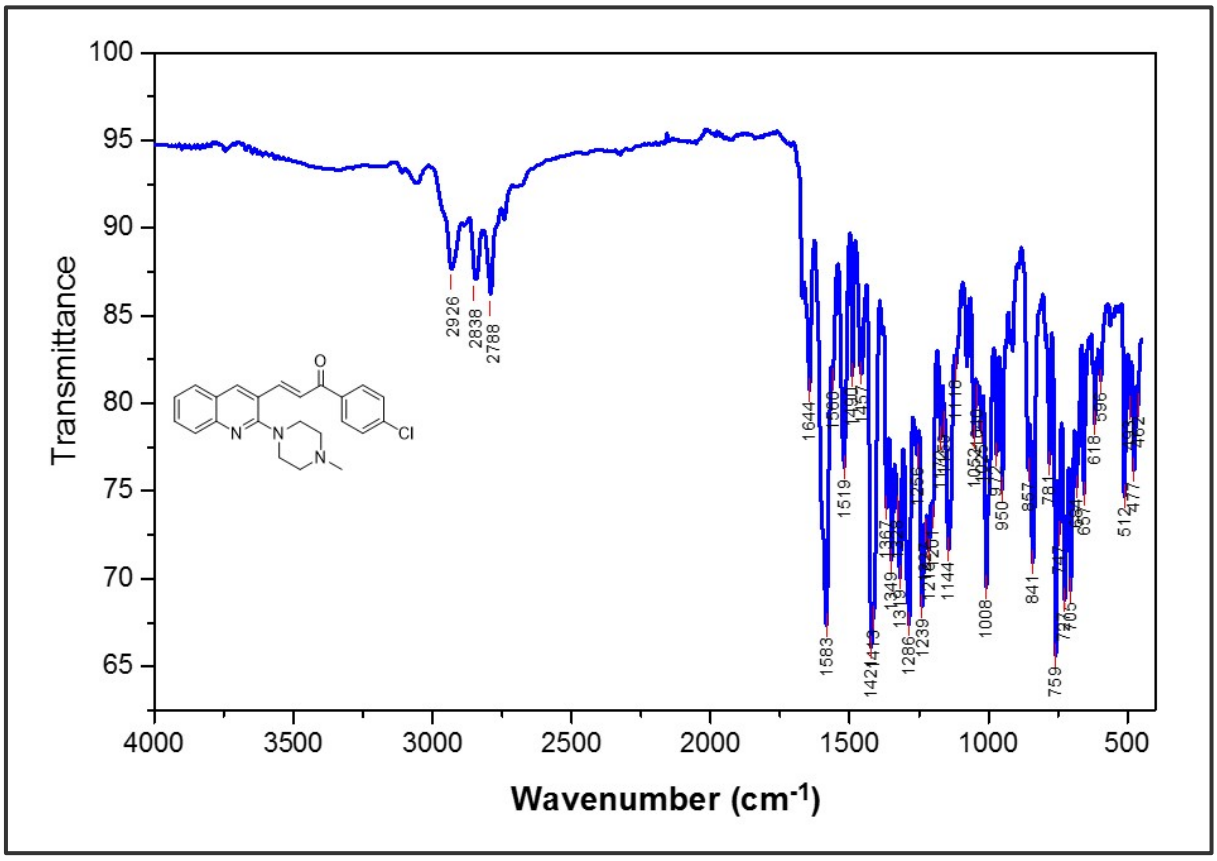

Figure 5A. S. 31. The Infra-Red Spectrum of compound 5i

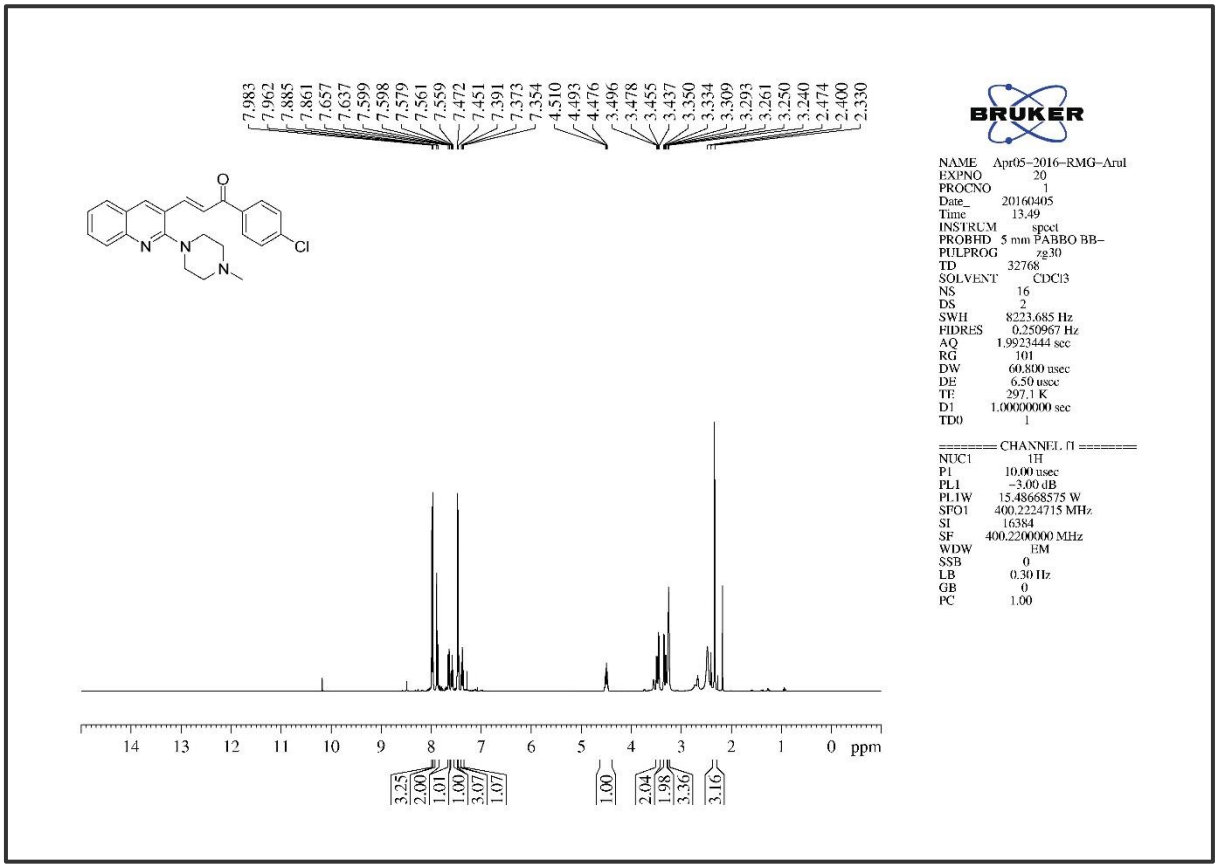

Figure 5A. S. 32. The ^{1}H NMR of compound 5i

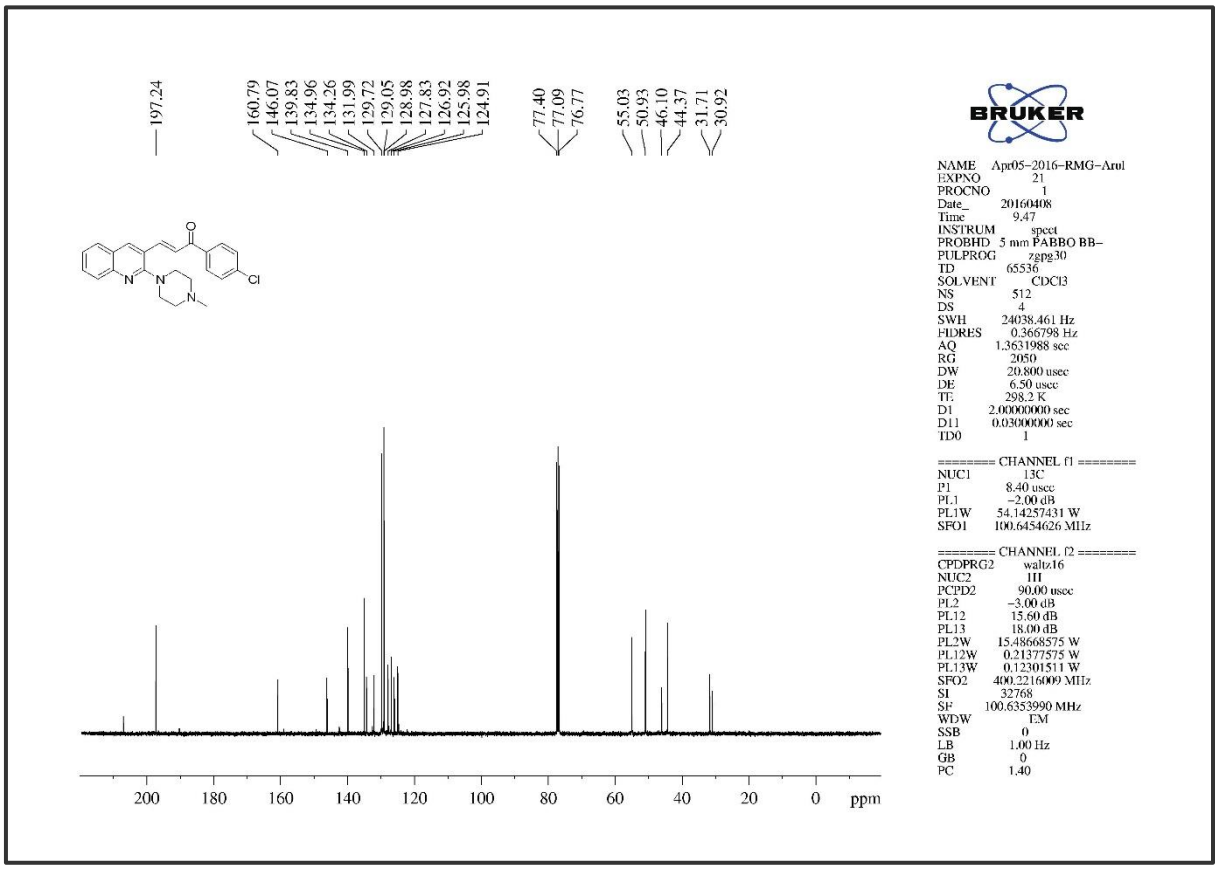

Figure 5A. S. 33. The ^{13}C NMR of compound 5i

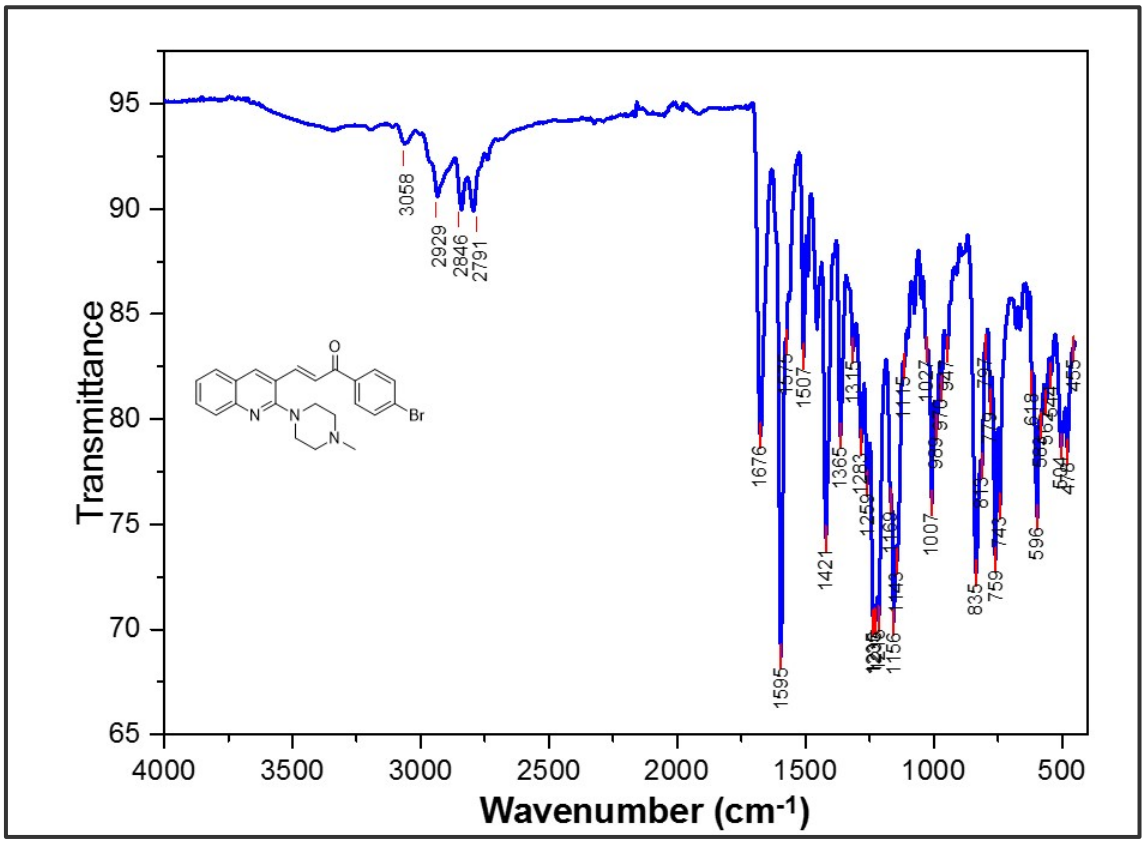

Figure 5A. S. 34. The Infra-Red Spectrum of compound 5j

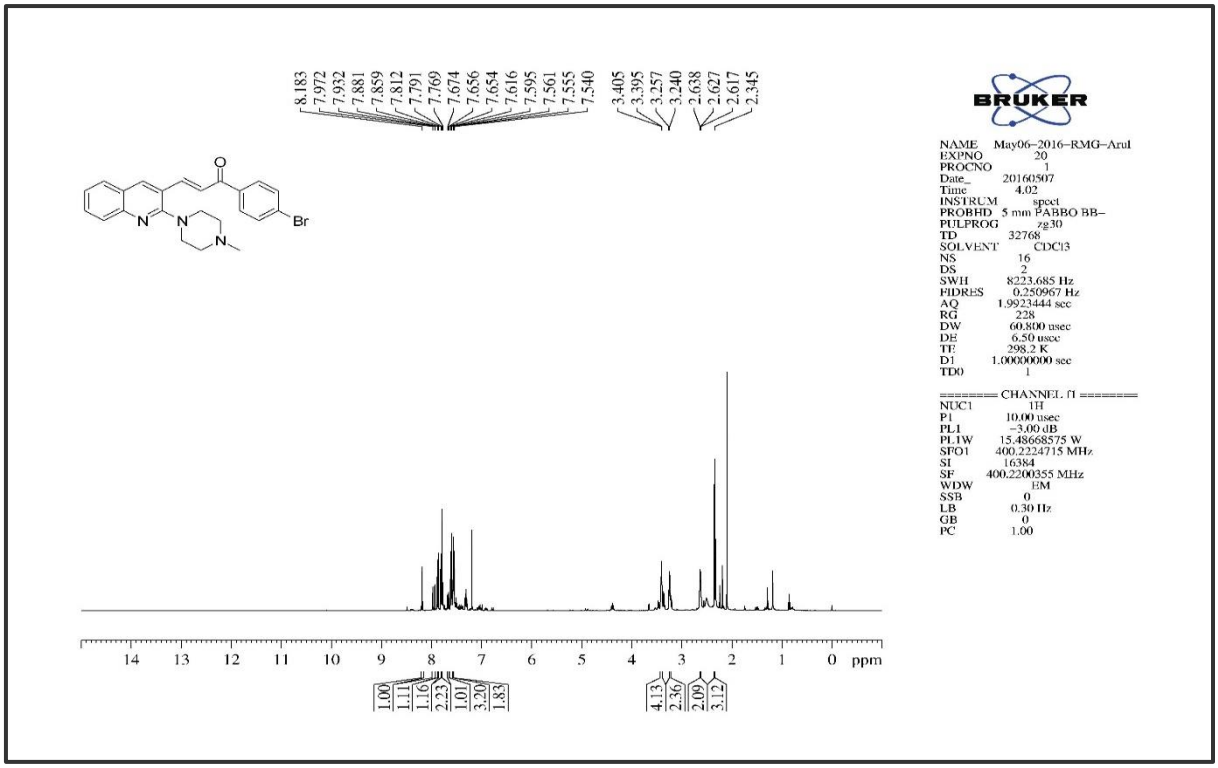

Figure 5A. S. 35. The ^{1}H NMR of compound 5j

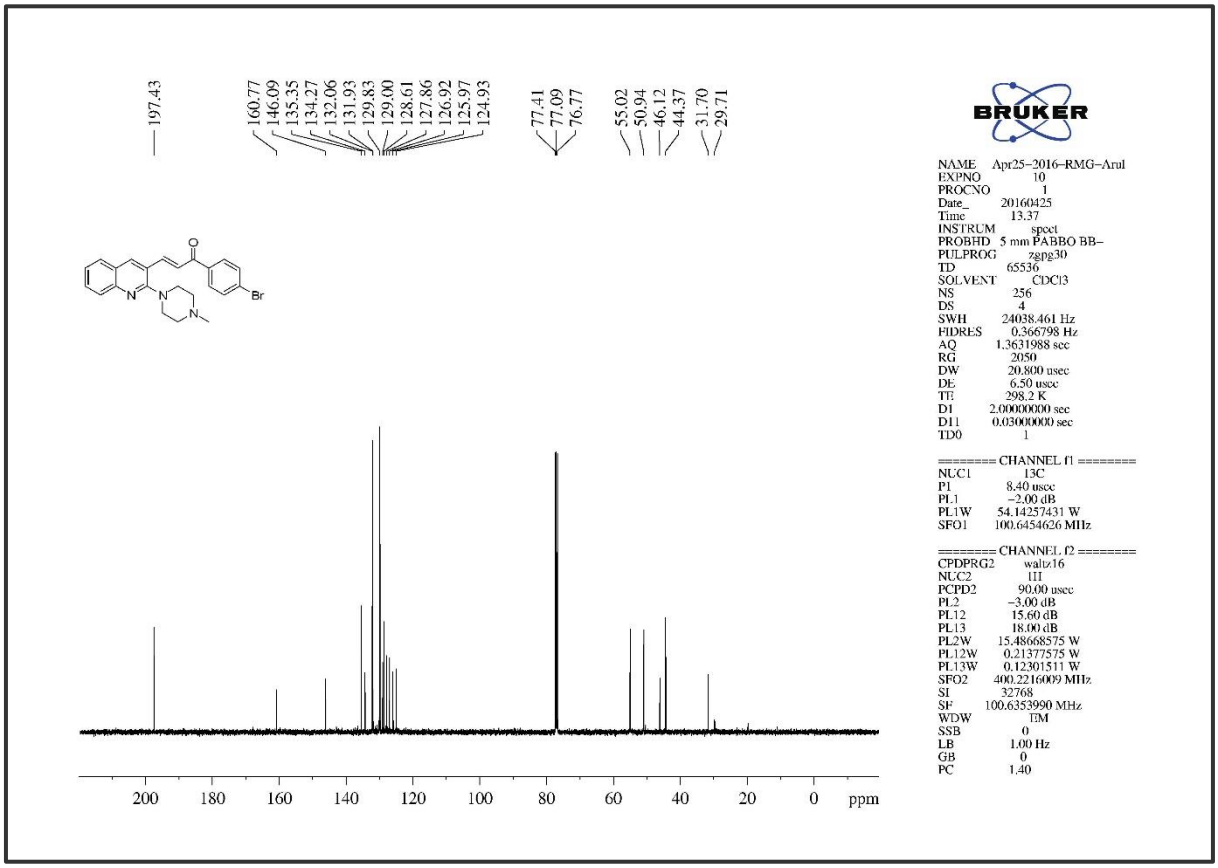

Figure 5A. S. 36. The ^{13}C NMR of compound 5j

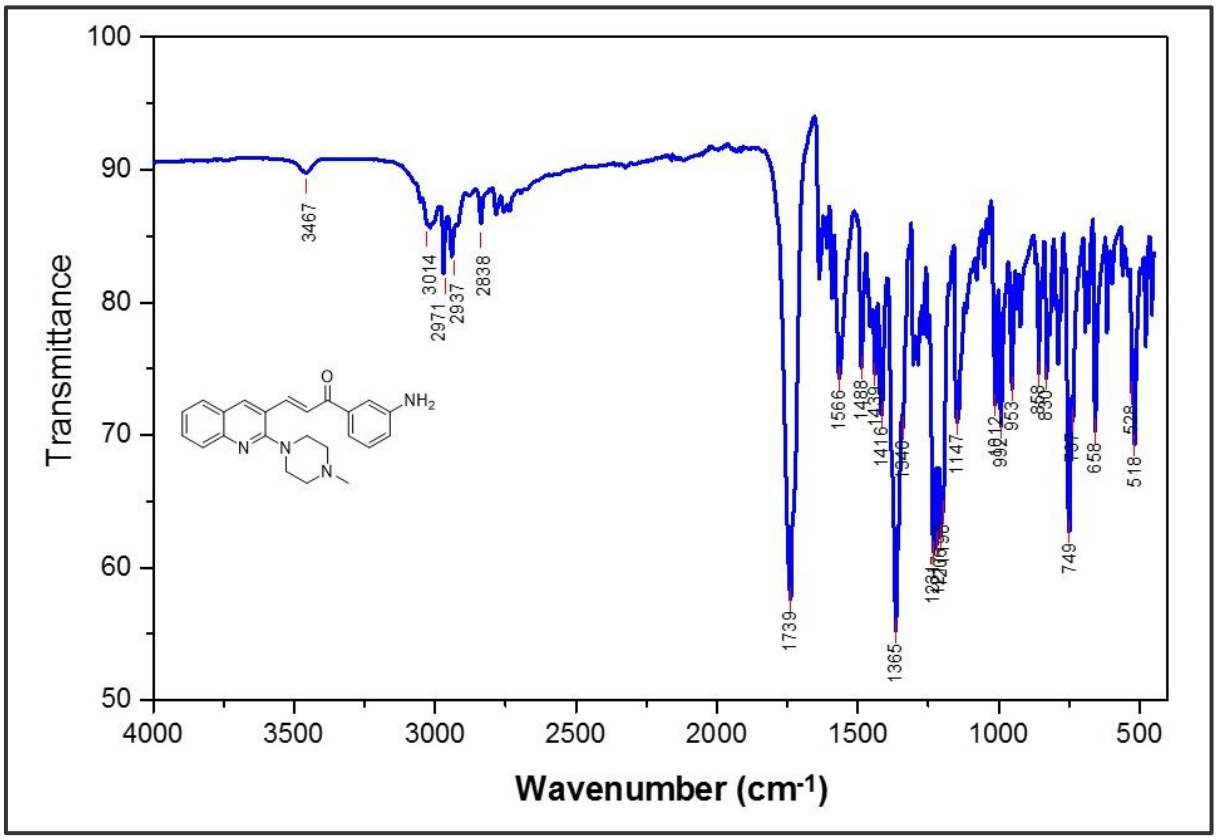

Figure 5A. S. 37. The Infra-Red Spectrum of compound 5k

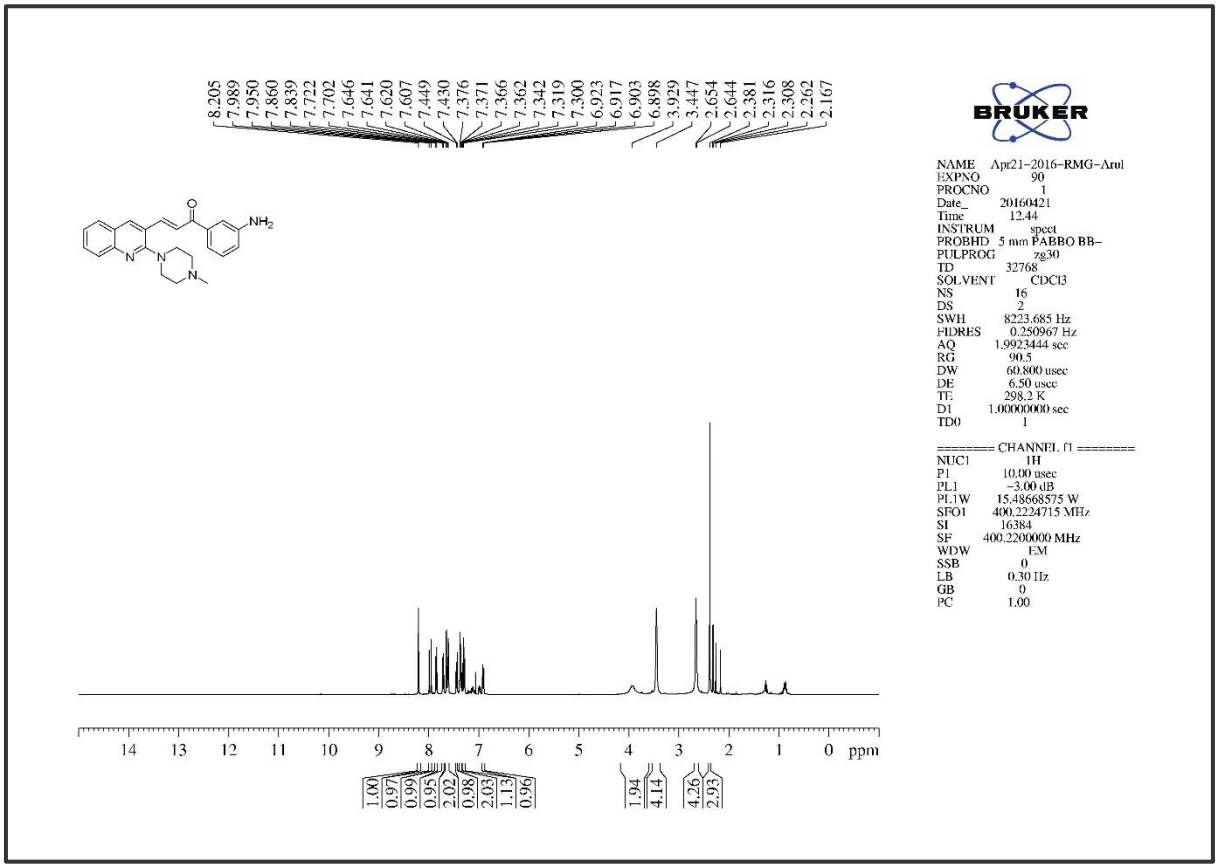

Figure 5A. S. 38. The ^{1}H NMR of compound 5k

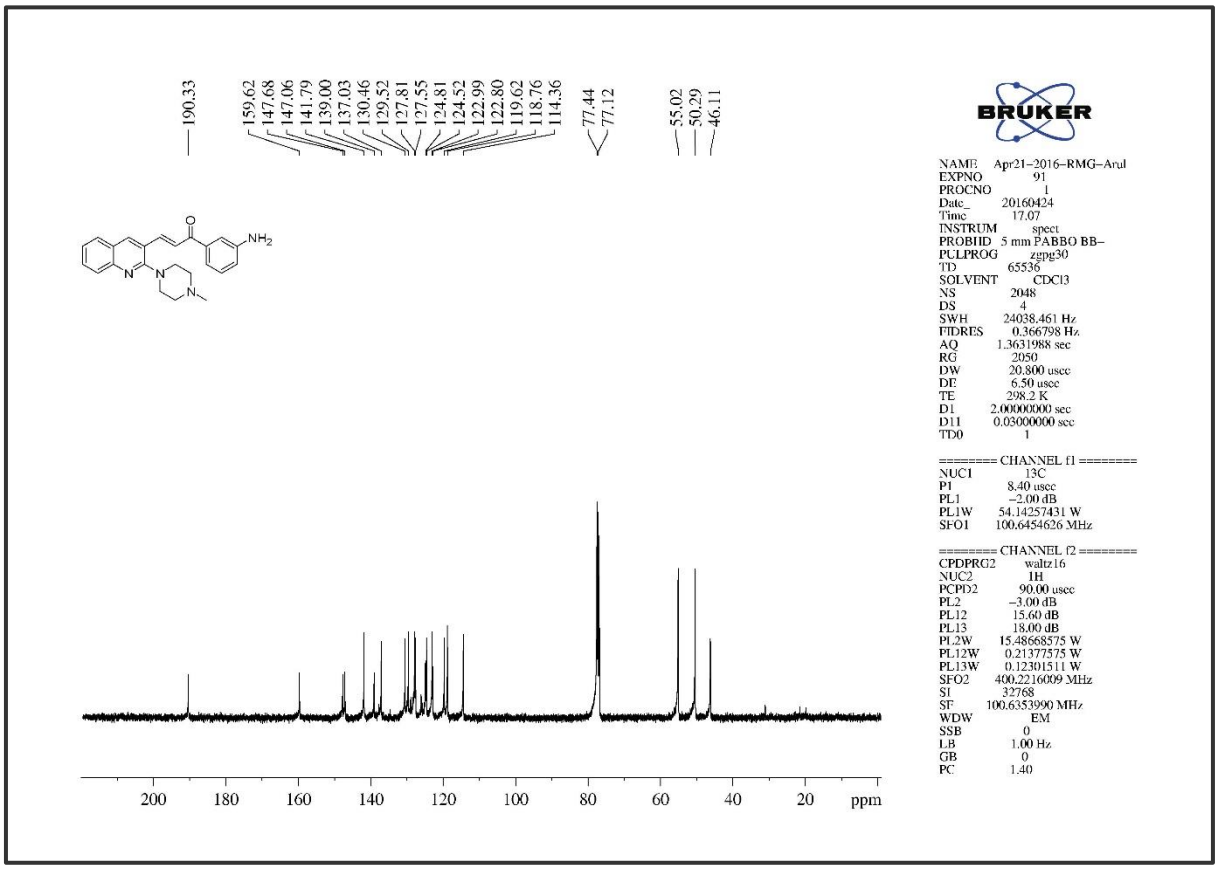

Figure 5A. S. 39. The ^{13}C NMR of compound 5k

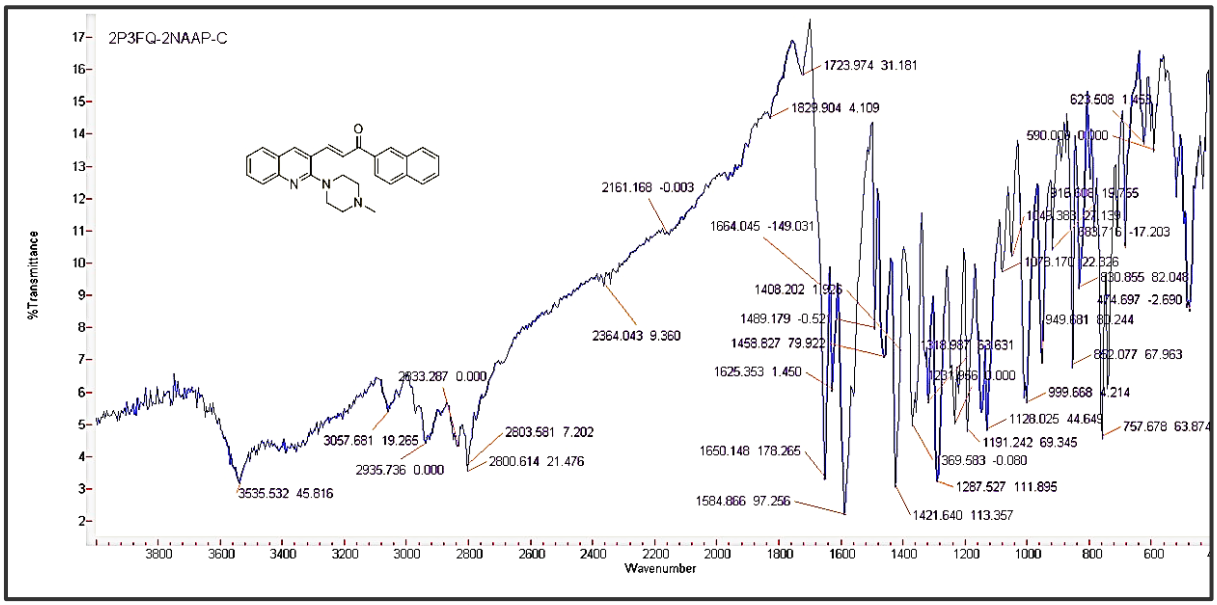

Figure 5A. S. 40. The Infra-Red Spectrum of compound 5l

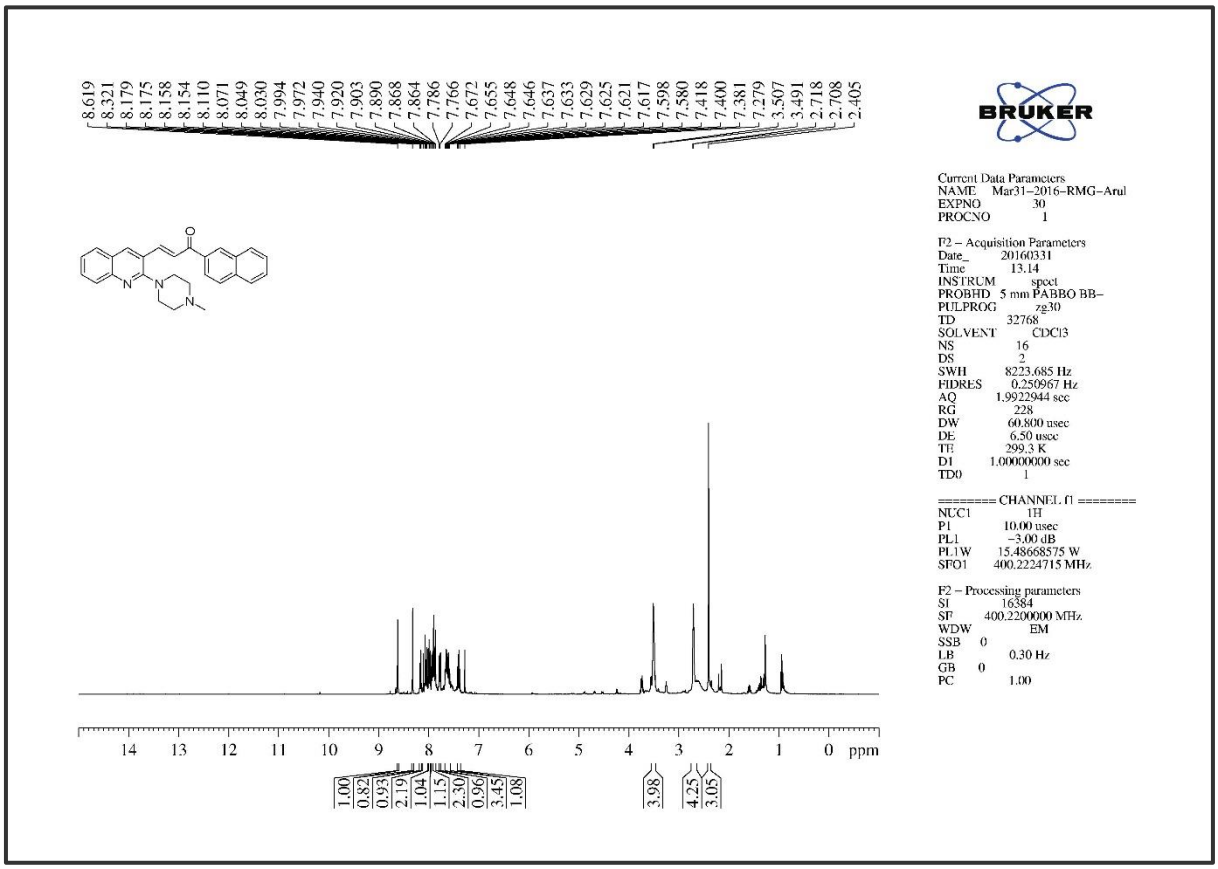

Figure 5A. S. 41. The ^{1}H NMR of compound 5l

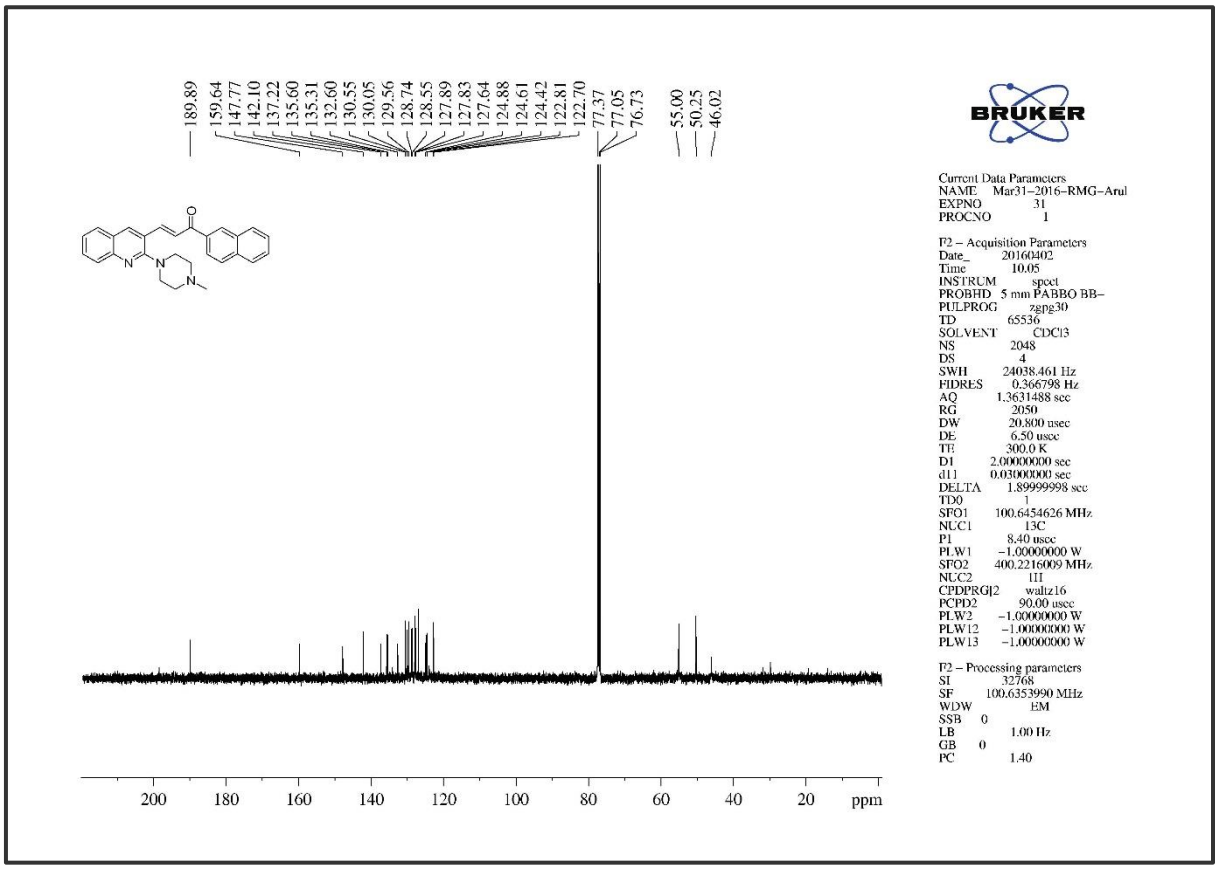

Figure 5A. S. 42. The ^{13}C NMR of compound 5l

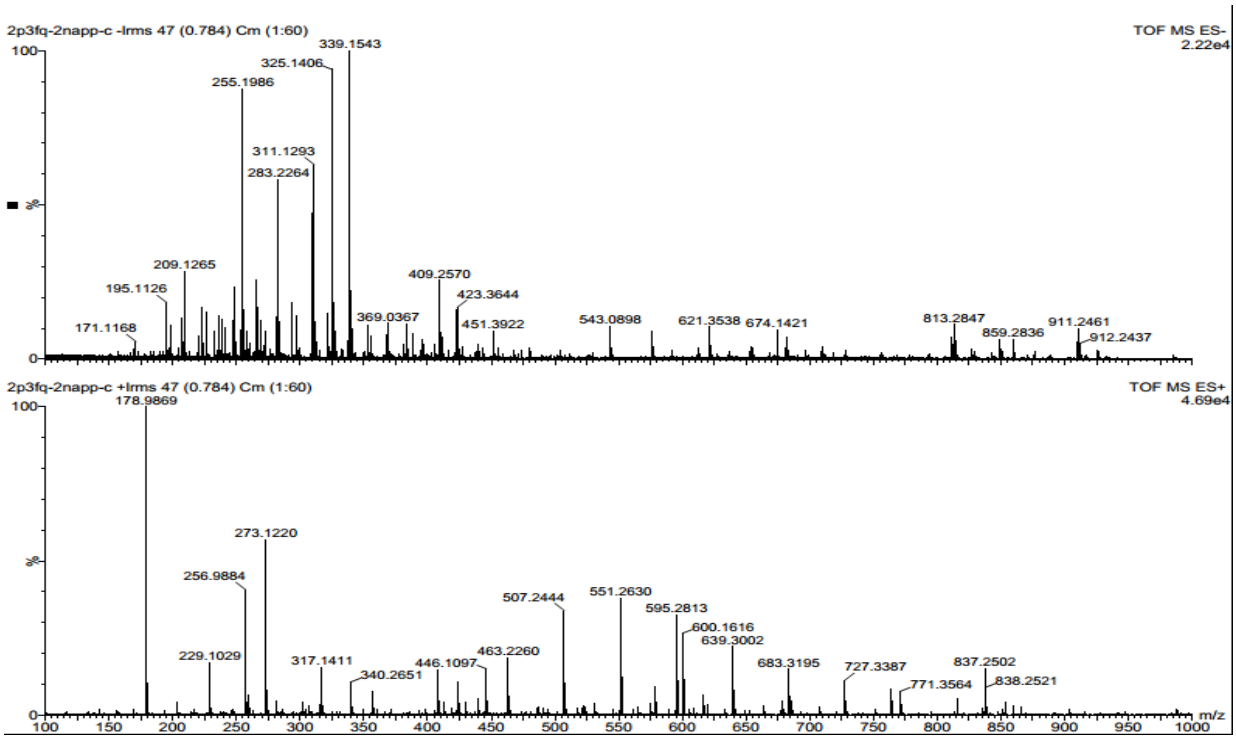

Figure 5A. S. 43. The HRMS of compound 5l

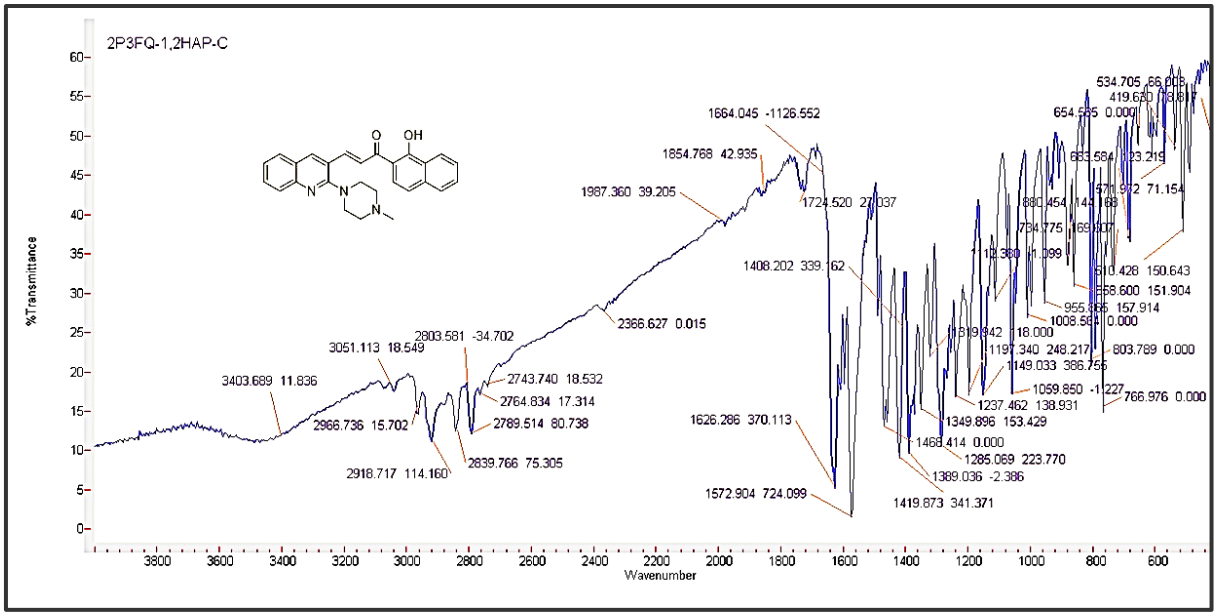

Figure 5A. S. 44. The Infra-Red Spectrum of compound 5m

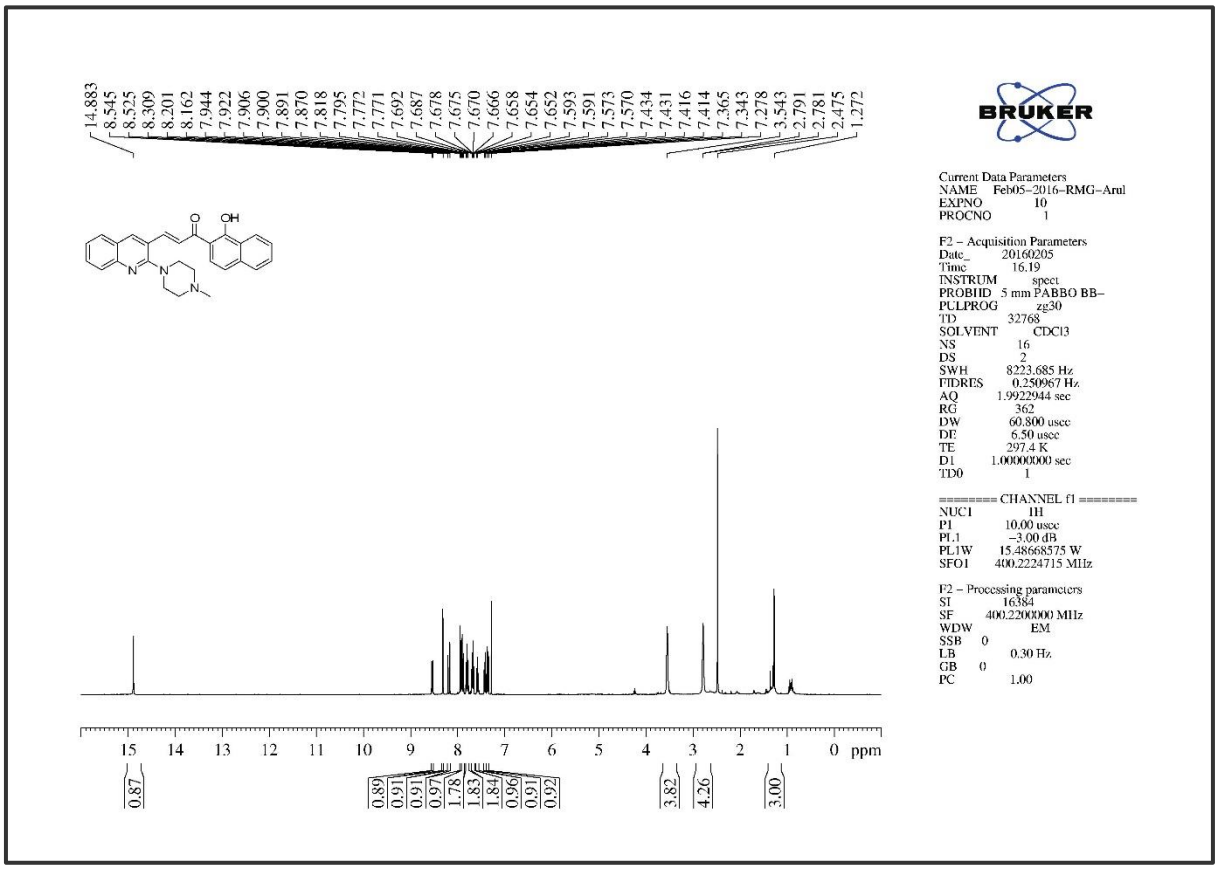

Figure 5A. S. 45. The ^{1}H NMR of compound 5m

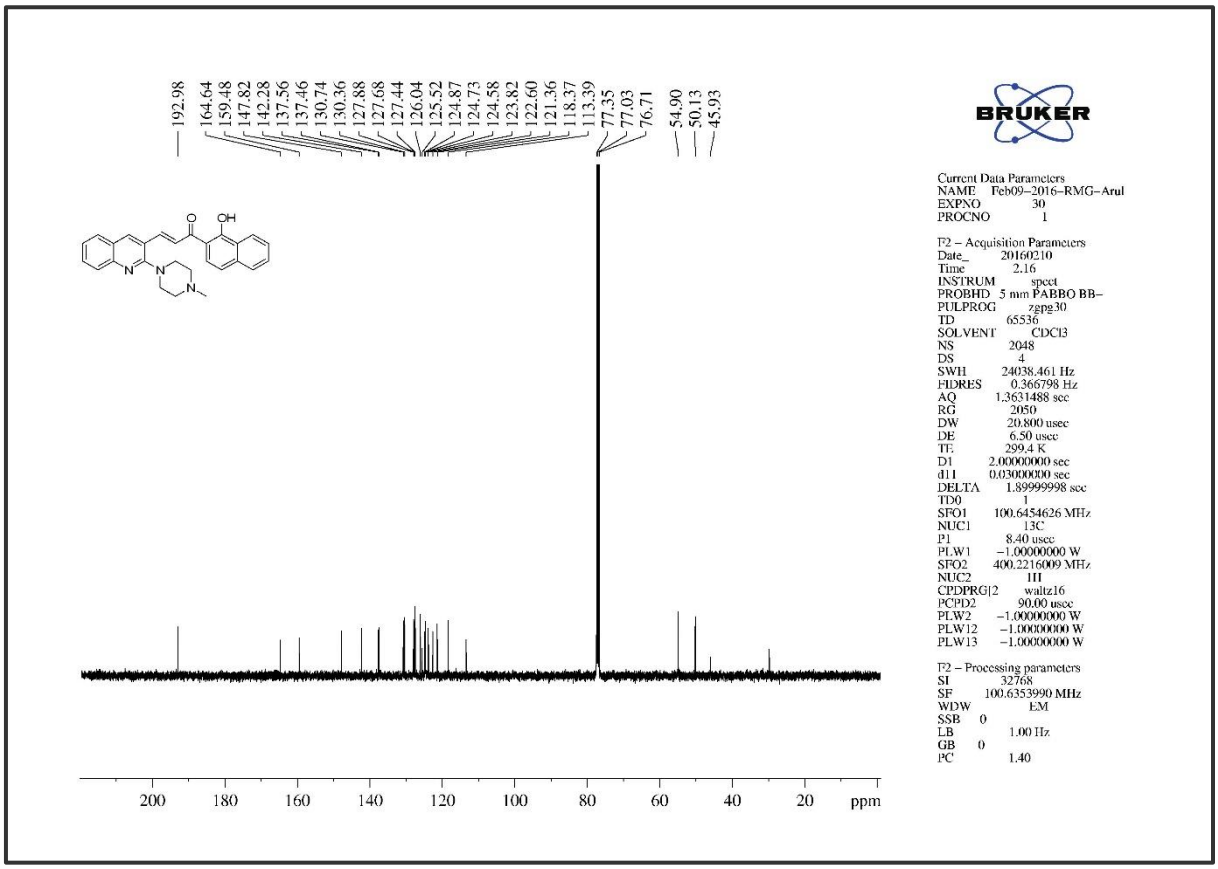

Figure 5A. S. 46. The ^{13}C NMR of compound 5m

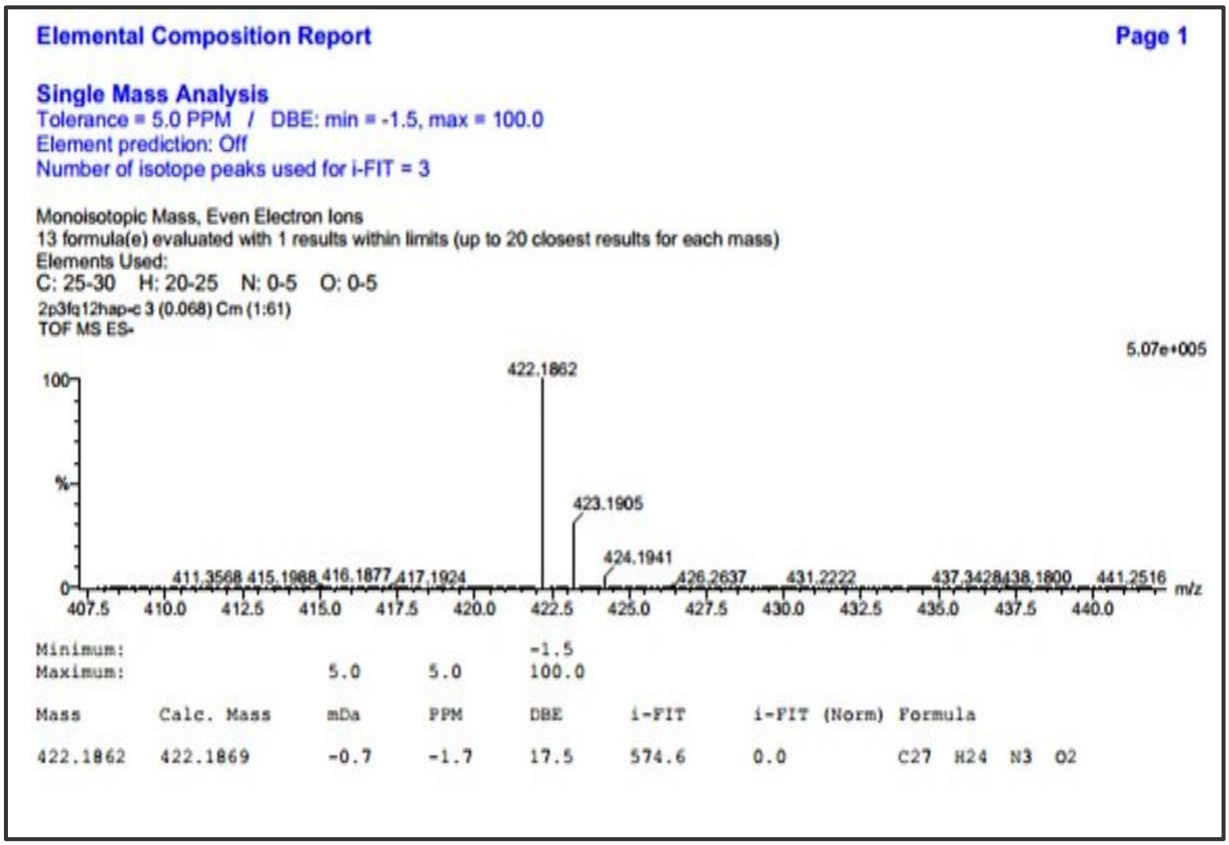

Figure 5A. S. 47. The HRMS of compound 5m

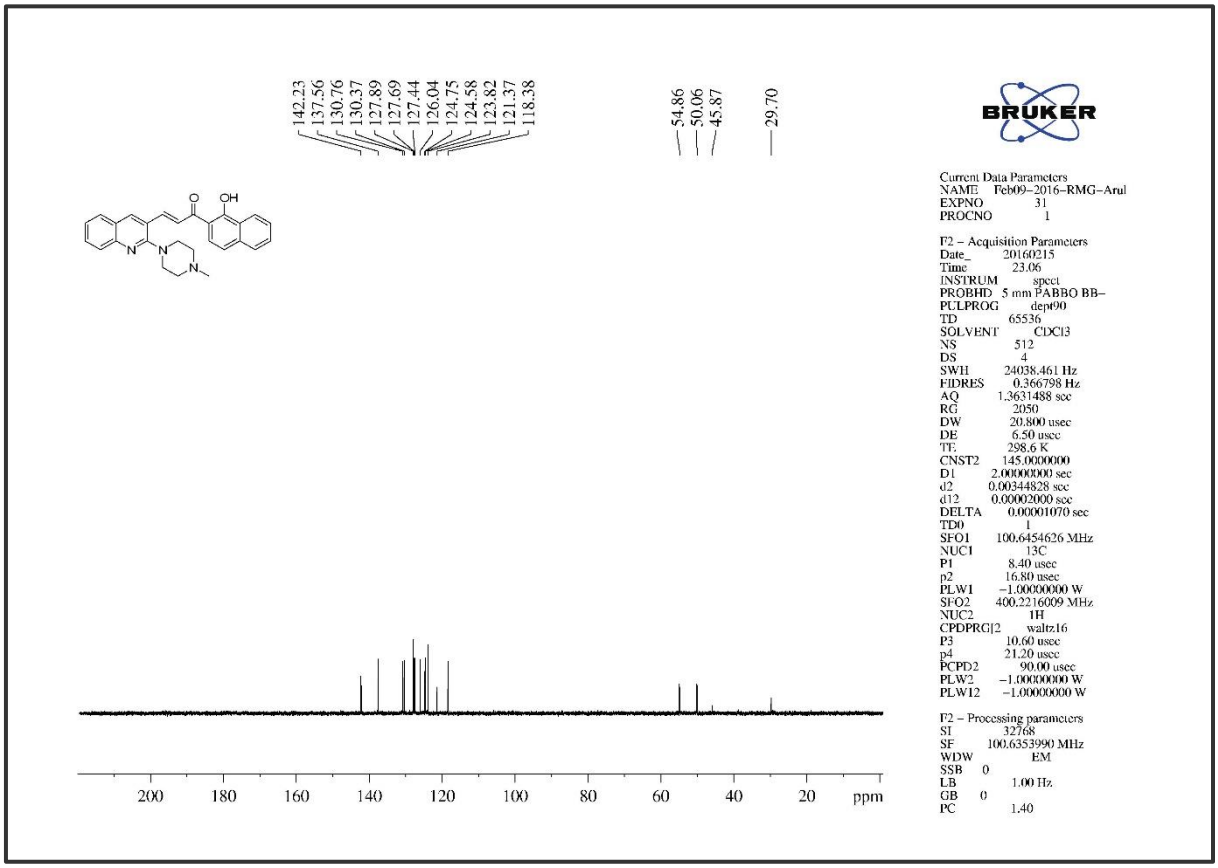

Figure 5A. S. 48. The DEPT-90 NMR of compound 5m

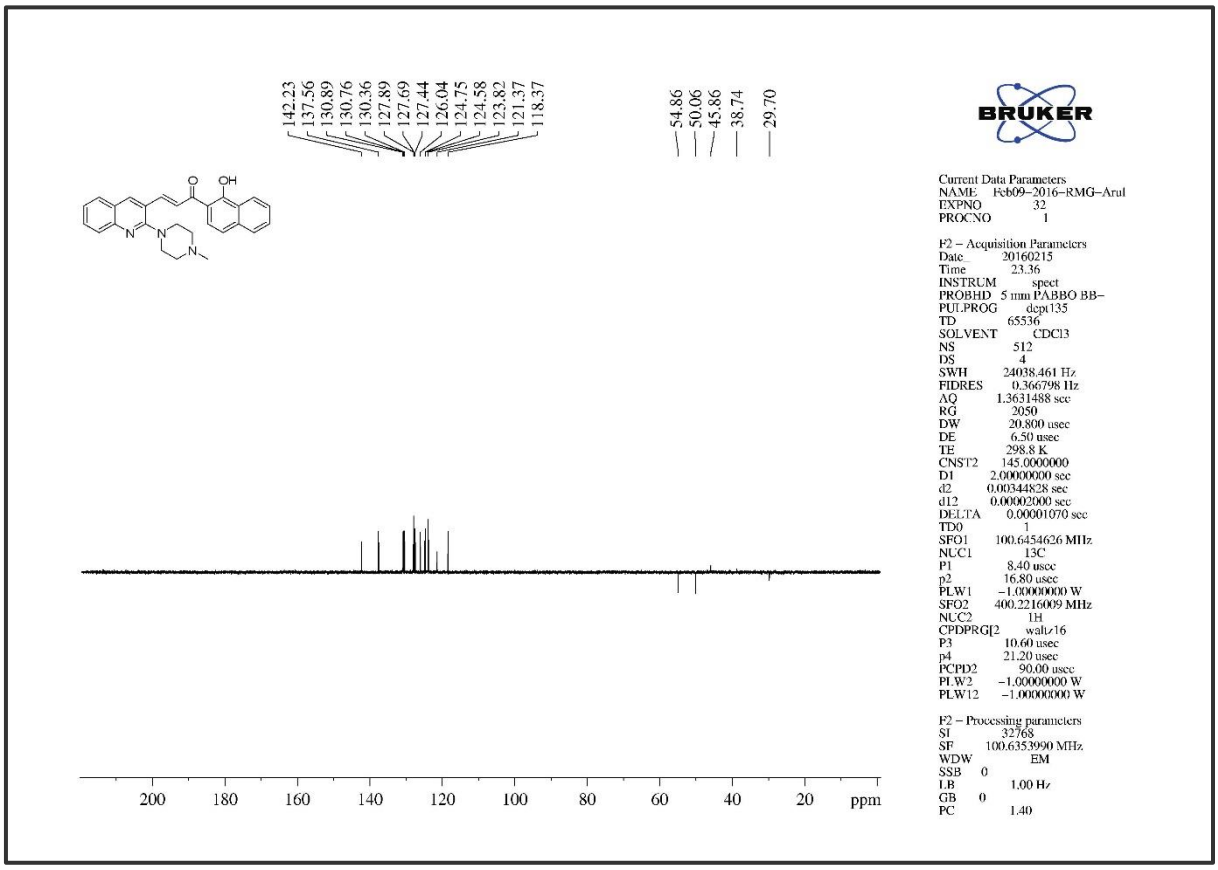

Figure 5A. S. 49. DEPT-135 NMR of compound 5m

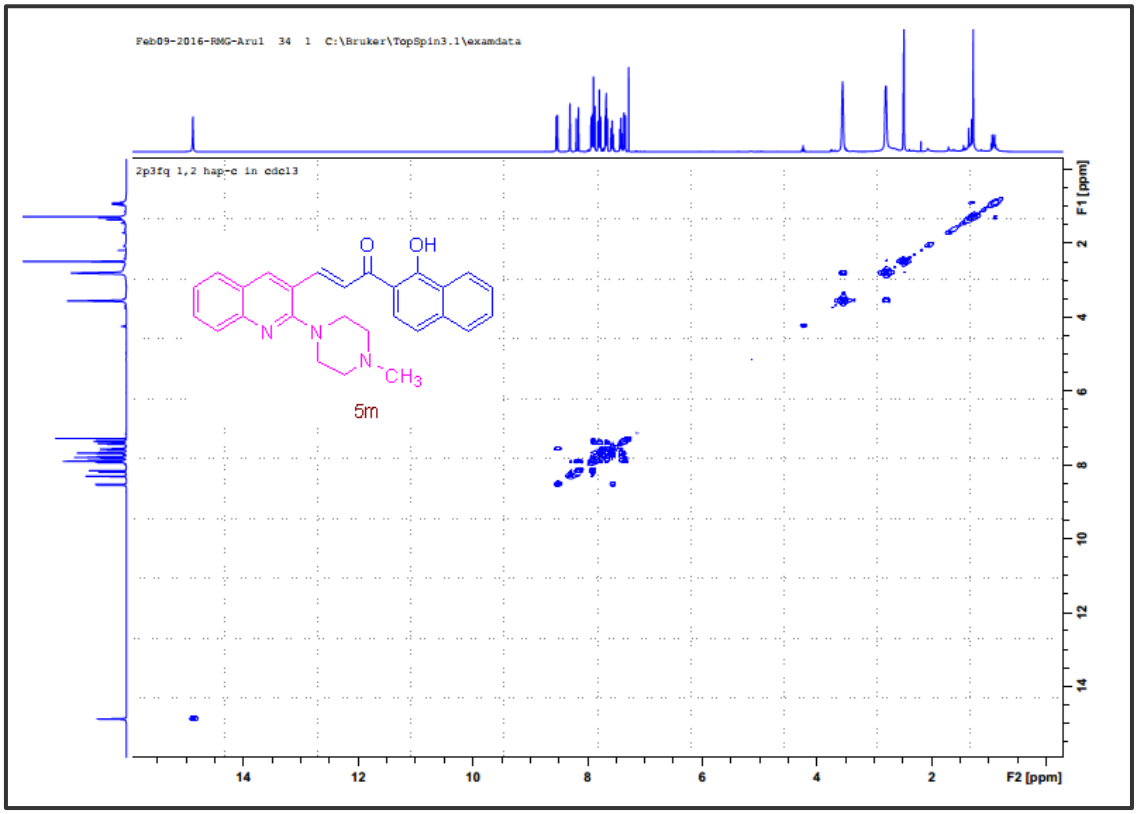

Figure 5A. S. 50. COSY NMR of compound 5m

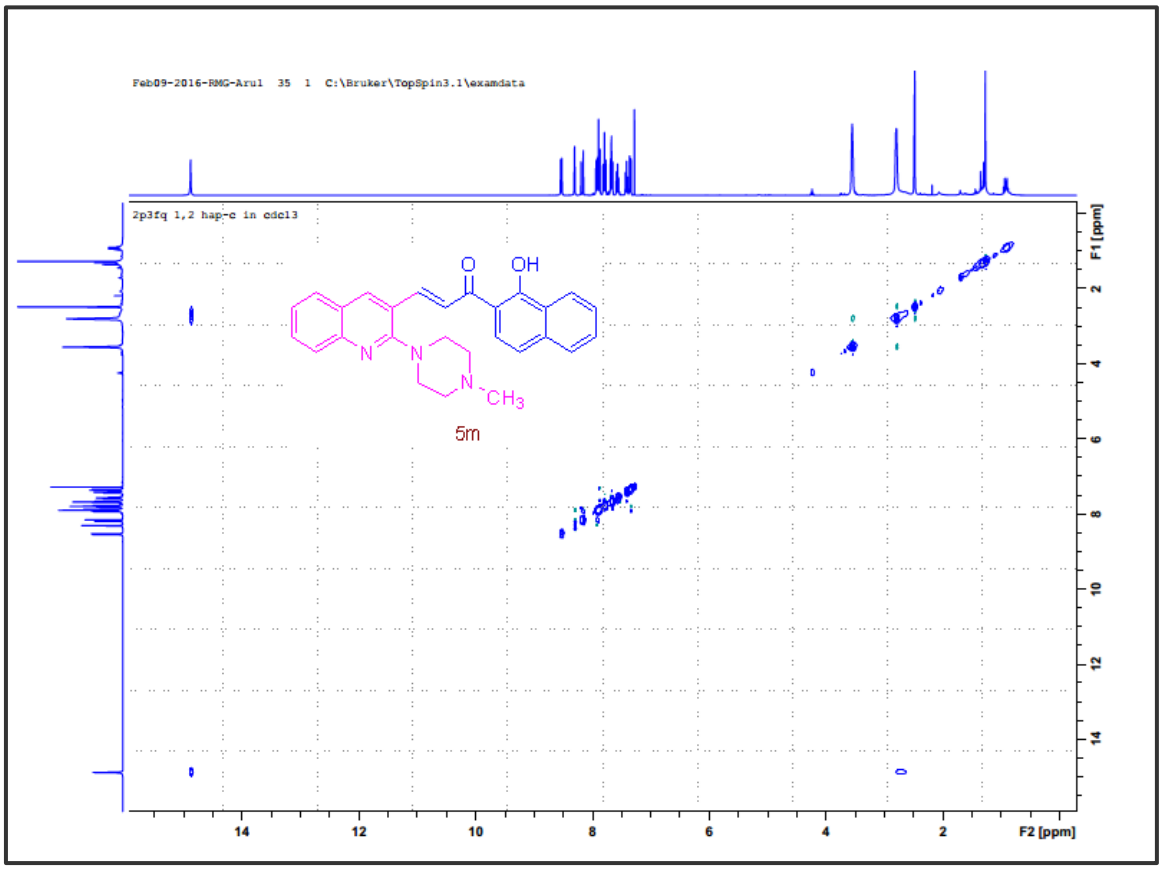

Figure 5A. S. 51. NOESY NMR of compound 5m

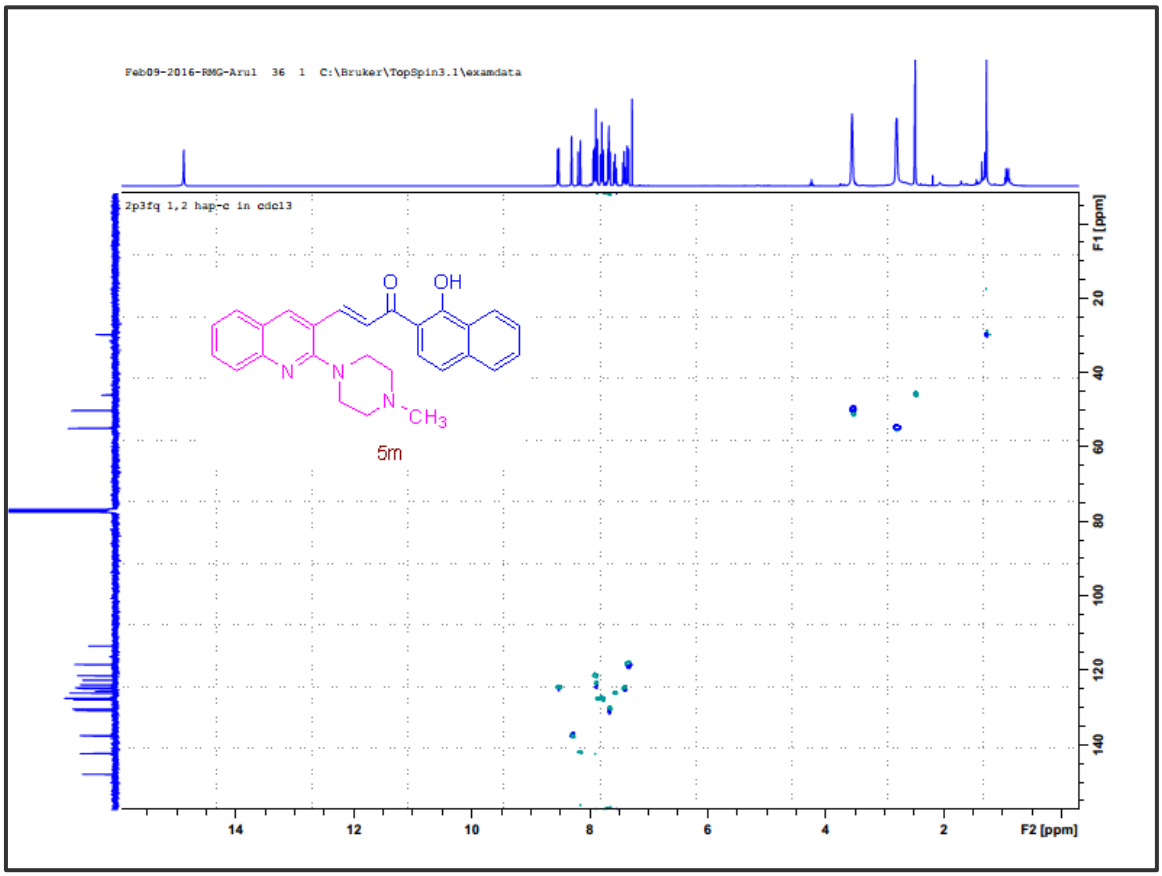

Figure 5A. S. 52. HSQCE NMR of compound 5m

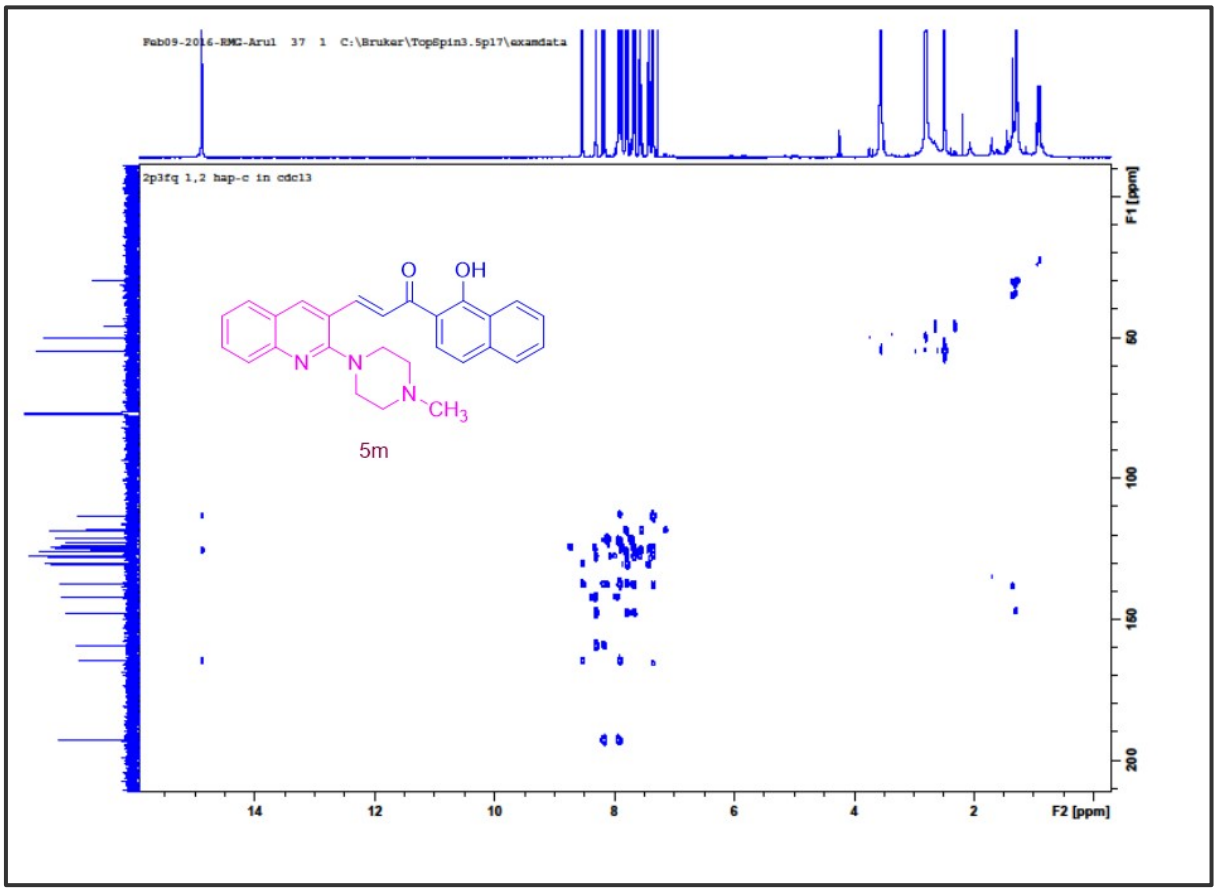

Figure 5A. S. 53. HMBC NMR of compound 5m

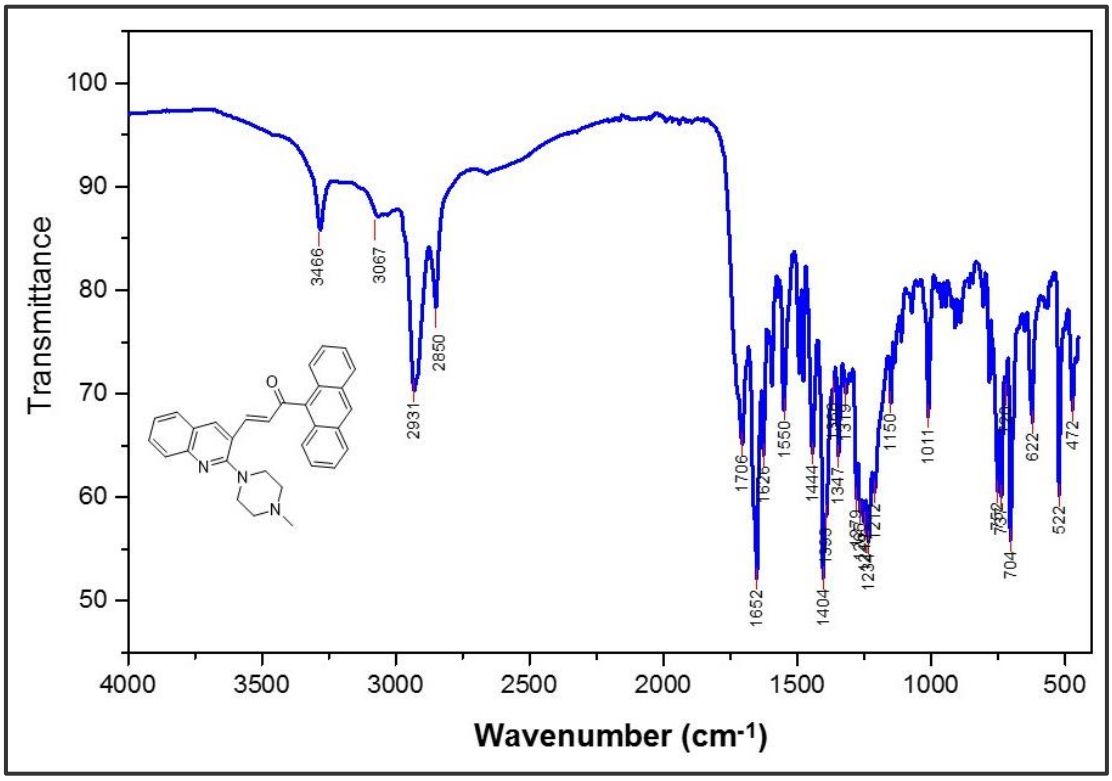

Figure 5A. S. 54. The Infra-Red Spectrum of compound 5n

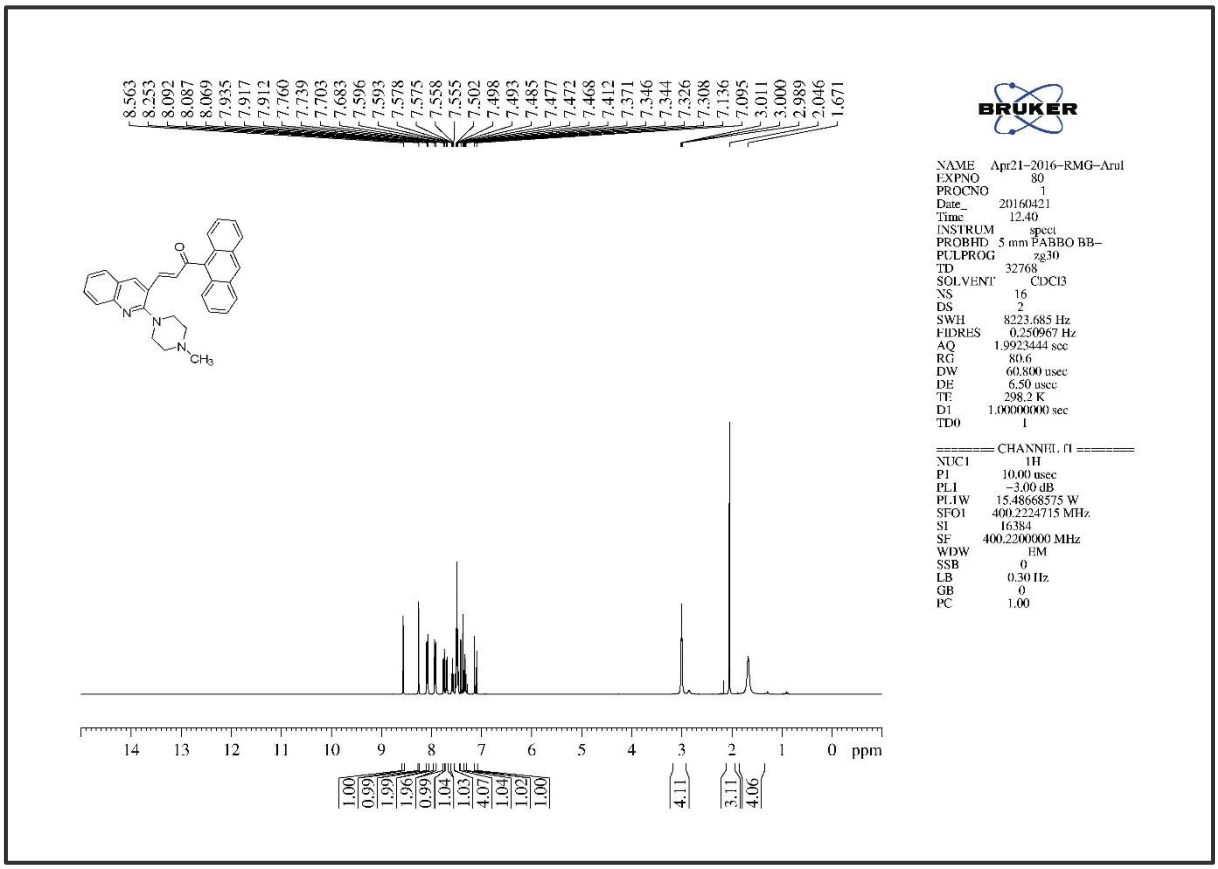

Figure 5A. S. 55. The ^{1}H NMR of compound 5n

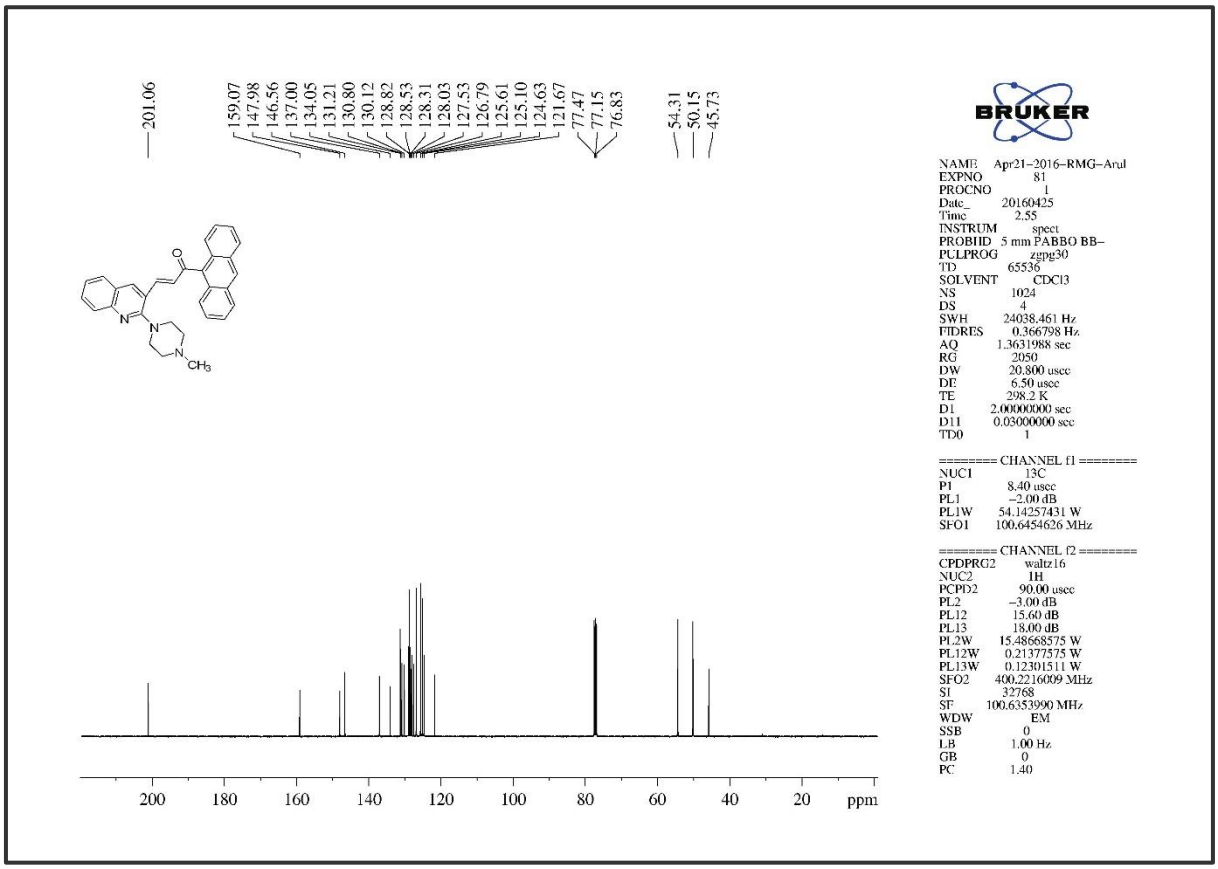

Figure 5A. S. 56. The ^{13}C NMR of compound 5n

Crystal structure of (E)-1-(anthracen-9-yl)-3-(2-(4-methylpiperazin-1-yl)quinolin-3-yl)prop-2-en-1-one **5n**

Computing details

Data collection: *APEX2* (Bruker, 2008); cell refinement: *SAINT* (Bruker, 2008); data reduction: *SAINT*; program (s) used to solve structure: *SHELXS97* (Sheldrick, 2008); program (s) used to solve structure: *SHELXS97* (Sheldrick, 2008); molecular graphics: *ORTEP-3 for windows* (Farrugia, 2012) and Mercury (Macrae et al., 2008); software used to prepare materials for publication: *SHELXL97* and *PLATON* (Spek, 2009).

(E)-1-(anthracen-9-yl)-3-(2-(4-methylpiperazin-1-yl)quinolin-3-yl)prop-2-en-1-one

Crystal data and structure refinement

Empirical formula	C_{31} H_{27} N_3 O
Formula weight	457.55
Temperature	298(2) K
Wavelength	0.71073 Å
Crystal system	Monoclinic
Space group	$P2_1/c$
Unit cell dimensions	a = 15.5664(16) Å □= 9 b = 9.2342(9) Å □= 91.6 c = 17.3360(15) Å □ = 9
Volume	2490.9(4) $Å^3$
Z	4
Density (calculated)	1.220 Mg/m^3
Absorption coefficient	0.075 mm^{-1}
F (000)	968
Crystal size	0.250 x 0.150 x 0.120 mm^3
Theta range for data collection	1.309 to 28.382°.
Index ranges	-20<=h<=11, -12<=k<=12, -23<=l<=22
Reflections collected	23761
Independent reflections	6207 [R (int) = 0.1417]
Completeness to theta = 25.242°	100.0 %
Absorption correction	Semi-empirical from equivalents
Max. And min. transmission	0.9143 and 0.8258
Refinement method	Full-matrix least-squares on F^2
Data / restraints / parameters	6207 / 0 / 317
Goodness-of-fit on F^2	0.890

Final R indices [I>2sigma (I)]	R1 = 0.0664, wR2 = 0.1282
R indices (all data)	R1 = 0.2869, wR2 = 0.2195
Extinction coefficient	N/A
Largest diff. peak and whole	0.204 and -0.237 e.Å^{-3}

Geometry. All esds (except the esd in the dihedral angle between two 1.s planes) are estimated using the full covariance matrix. The cell esds are taken into account individually in the estimation of esds in distances, angles and torsion angles; correlations between esds in cell parameters are only used when they are defined by crystal symmetry. An approximate (isotropic) treatment of cell esds is used for estimating esds involving 1.s, planes.

Fractional atomic coordinates and equivalent isotropic displacement parameters (Å^2)

	x	y	z	U (eq)
O (1)	8817(2)	1594(3)	-712(2)	88(1)
N (1)	6293(2)	5073(3)	2588(2)	53(1)
N (2)	5713(2)	3868(3)	1140(2)	47(1)
N (3)	4494(2)	3034(3)	484(2)	53(1)
C (1)	6800(3)	6148(5)	3026(2)	79(1)
C (2)	6852(3)	4189(4)	2118(2)	57(1)
C (3)	6337(2)	3125(4)	1645(2)	50(1)
C (4)	5336(3)	3089(4)	527(2)	48(1)
C (5)	5879(2)	2453(4)	-40(2)	47(1)
C (6)	6796(2)	2782(4)	-52(2)	50(1)
C (7)	7399(3)	1953(4)	-356(2)	60(1)
C (8)	8305(3)	2354(5)	-373(2)	58(1)
C (9)	8609(2)	3673(4)	55(2)	49(1)
C (10)	8822(2)	3557(5)	845(2)	58(1)
C (11)	9139(3)	4806(6)	1247(3)	67(1)
C (12)	9331(3)	4656(8)	2053(3)	96(2)
C (13)	9237(4)	3415(10)	2432(3)	119(3)
C (14)	4109(2)	2269(4)	-112(2)	52(1)
C (15)	4593(2)	1481(4)	-647(2)	45(1)
C (16)	4156(3)	689(4)	-1228(2)	55(1)
C (17)	3284(3)	672(4)	-1281(2)	61(1)
C (18)	2811(3)	1485(5)	-758(3)	67(1)

C (19)	3210(2)	2255(4)	-183(2)	61(1)
C (20)	5489(3)	1623(4)	-601(2)	50(1)
C (21)	8738(3)	2232(5)	1257(3)	77(1)
C (22)	8942(3)	2167(8)	2026(4)	105(2)
C (23)	9237(2)	6092(6)	852(3)	71(1)
C (24)	9029(2)	6225(5)	78(3)	61(1)
C (25)	9123(3)	7553(5)	-333(4)	84(2)
C (26)	8890(3)	7644(7)	-1085(4)	99(2)
C (27)	8555(3)	6447(7)	-1486(3)	93(2)
C (28)	8459(3)	5156(5)	-1128(3)	69(1)
C (29)	8696(2)	4993(5)	-332(2)	54(1)
C (30)	5141(2)	4745(4)	1605(2)	57(1)
C (31)	5672(3)	5805(4)	2078(2)	59(1)

Geometric parameters (Å, °)

O (1)-C (8)	1.224(4)
N (1)-C (31)	1.457(4)
N (1)-C (2)	1.460(4)
N (1)-C (1)	1.467(4)
N (2)-C (4)	1.398(4)
N (2)-C (3)	1.460(4)
N (2)-C (30)	1.463(4)
N (3)-C (4)	1.312(4)
N (3)-C (14)	1.375(4)
C (1)-H (1)	0.9600
C (1)-H (3)	0.9600
C (1)-H (27)	0.9600
C (2)-C (3)	1.498(5)
C (2)-H (25)	0.9700
C (2)-H (26)	0.9700
C (3)-H (4)	0.9700
C (3)-H (5)	0.9700
C (4)-C (5)	1.440(5)
C (5)-C (20)	1.366(5)
C (5)-C (6)	1.460(5)
C (6)-C (7)	1.332(5)

C (6)-H (20)	0.9300
C (7)-C (8)	1.460(5)
C (7)-H (11)	0.9300
C (8)-C (9)	1.496(5)
C (9)-C (29)	1.401(5)
C (9)-C (10)	1.404(5)
C (10)-C (21)	1.425(5)
C (10)-C (11)	1.428(6)
C (11)-C (23)	1.382(6)
C (11)-C (12)	1.427(6)
C (12)-C (13)	1.331(8)
C (12)-H (13)	0.9300
C (13)-C (22)	1.419(8)
C (13)-H (2)	0.9300
C (14)-C (19)	1.400(5)
C (14)-C (15)	1.413(5)
C (15)-C (20)	1.401(5)
C (15)-C (16)	1.406(5)
C (16)-C (17)	1.358(5)
C (16)-H (9)	0.9300
C (17)-C (18)	1.402(5)
C (17)-H (6)	0.9300
C (18)-C (19)	1.360(5)
C (18)-H (8)	0.9300
C (19)-H (7)	0.9300
C (20)-H (10)	0.9300
C (21)-C (22)	1.363(6)
C (21)-H (19)	0.9300
C (22)-H (12)	0.9300
C (23)-C (24)	1.378(5)
C (23)-H (14)	0.9300
C (24)-C (25)	1.427(6)
C (24)-C (29)	1.431(5)
C (25)-C (26)	1.345(7)
C (25)-H (18)	0.9300
C (26)-C (27)	1.399(7)
C (26)-H (15)	0.9300
C (27)-C (28)	1.354(6)

C (27)-H (16)	0.9300
C (28)-C (29)	1.425(5)
C (28)-H (17)	0.9300
C (30)-C (31)	1.508(5)
C (30)-H (21)	0.9700
C (30)-H (24)	0.9700
C (31)-H (22)	0.9700
C (31)-H (23)	0.9700

C (31)-N (1)-C (2)	108.4(3)
C (31)-N (1)-C (1)	109.8(3)
C (2)-N (1)-C (1)	110.3(3)
C (4)-N (2)-C (3)	118.1(3)
C (4)-N (2)-C (30)	117.1(3)
C (3)-N (2)-C (30)	109.5(3)
C (4)-N (3)-C (14)	118.4(3)
N (1)-C (1)-H (1)	109.5
N (1)-C (1)-H (3)	109.5
H (1)-C (1)-H (3)	109.5
N (1)-C (1)-H (27)	109.5
H (1)-C (1)-H (27)	109.5
H (3)-C (1)-H (27)	109.5
N (1)-C (2)-C (3)	110.7(3)
N (1)-C (2)-H (25)	109.5
C (3)-C (2)-H (25)	109.5
N (1)-C (2)-H (26)	109.5
C (3)-C (2)-H (26)	109.5
H (25)-C (2)-H (26)	108.1
N (2)-C (3)-C (2)	110.9(3)
N (2)-C (3)-H (4)	109.5
C (2)-C (3)-H (4)	109.5
N (2)-C (3)-H (5)	109.5
C (2)-C (3)-H (5)	109.5
H (4)-C (3)-H (5)	108.0
N (3)-C (4)-N (2)	117.4(3)
N (3)-C (4)-C (5)	123.4(4)
N (2)-C (4)-C (5)	119.2(4)
C (20)-C (5)-C (4)	117.3(4)

C (20)-C (5)-C (6)	121.4(3)
C (4)-C (5)-C (6)	121.1(4)
C (7)-C (6)-C (5)	125.9(4)
C (7)-C (6)-H (20)	117.0
C (5)-C (6)-H (20)	117.0
C (6)-C (7)-C (8)	123.7(4)
C (6)-C (7)-H (11)	118.2
C (8)-C (7)-H (11)	118.2
O (1)-C (8)-C (7)	120.5(4)
O (1)-C (8)-C (9)	120.2(4)
C (7)-C (8)-C (9)	119.3(4)
C (29)-C (9)-C (10)	120.7(4)
C (29)-C (9)-C (8)	120.3(4)
C (10)-C (9)-C (8)	119.0(4)
C (9)-C (10)-C (21)	122.2(4)
C (9)-C (10)-C (11)	118.9(4)
C (21)-C (10)-C (11)	119.0(4)
C (23)-C (11)-C (10)	119.6(4)
C (23)-C (11)-C (12)	123.0(5)
C (10)-C (11)-C (12)	117.3(5)
C (13)-C (12)-C (11)	122.9(6)
C (13)-C (12)-H (13)	118.5
C (11)-C (12)-H (13)	118.5
C (12)-C (13)-C (22)	119.6(6)
C (12)-C (13)-H (2)	120.2
C (22)-C (13)-H (2)	120.2
N (3)-C (14)-C (19)	119.0(4)
N (3)-C (14)-C (15)	121.9(4)
C (19)-C (14)-C (15)	119.2(4)
C (20)-C (15)-C (16)	123.4(4)
C (20)-C (15)-C (14)	117.6(4)
C (16)-C (15)-C (14)	118.8(4)
C (17)-C (16)-C (15)	121.2(4)
C (17)-C (16)-H (9)	119.4
C (15)-C (16)-H (9)	119.4
C (16)-C (17)-C (18)	119.4(4)
C (16)-C (17)-H (6)	120.3
C (18)-C (17)-H (6)	120.3

C (19)-C (18)-C (17)	121.1(4)
C (19)-C (18)-H (8)	119.4
C (17)-C (18)-H (8)	119.4
C (18)-C (19)-C (14)	120.2(4)
C (18)-C (19)-H (7)	119.9
C (14)-C (19)-H (7)	119.9
C (5)-C (20)-C (15)	120.9(4)
C (5)-C (20)-H (10)	119.5
C (15)-C (20)-H (10)	119.5
C (22)-C (21)-C (10)	120.4(5)
C (22)-C (21)-H (19)	119.8
C (10)-C (21)-H (19)	119.8
C (21)-C (22)-C (13)	120.8(6)
C (21)-C (22)-H (12)	119.6
C (13)-C (22)-H (12)	119.6
C (24)-C (23)-C (11)	122.2(4)
C (24)-C (23)-H (14)	118.9
C (11)-C (23)-H (14)	118.9
C (23)-C (24)-C (25)	122.5(5)
C (23)-C (24)-C (29)	119.0(4)
C (25)-C (24)-C (29)	118.4(5)
C (26)-C (25)-C (24)	120.5(5)
C (26)-C (25)-H (18)	119.7
C (24)-C (25)-H (18)	119.7
C (25)-C (26)-C (27)	121.3(6)
C (25)-C (26)-H (15)	119.4
C (27)-C (26)-H (15)	119.4
C (28)-C (27)-C (26)	120.7(5)
C (28)-C (27)-H (16)	119.6
C (26)-C (27)-H (16)	119.6
C (27)-C (28)-C (29)	120.5(5)
C (27)-C (28)-H (17)	119.7
C (29)-C (28)-H (17)	119.7
C (9)-C (29)-C (28)	122.0(4)
C (9)-C (29)-C (24)	119.5(4)
C (28)-C (29)-C (24)	118.5(4)
N (2)-C (30)-C (31)	109.0(3)
N (2)-C (30)-H (21)	109.9

C (31)-C (30)-H (21)	109.9
N (2)-C (30)-H (24)	109.9
C (31)-C (30)-H (24)	109.9
H (21)-C (30)-H (24)	108.3
N (1)-C (31)-C (30)	111.9(3)
N (1)-C (31)-H (22)	109.2
C (30)-C (31)-H (22)	109.2
N (1)-C (31)-H (23)	109.2
C (30)-C (31)-H (23)	109.2
H (22)-C (31)-H (23)	107.9

Symmetry transformations used to generate equivalent atoms:

Anisotropic displacement parameters ($Å^2$)

	U^{11}	U^{22}	U^{33}	U^{23}	U^{13}	U^{12}
O (1)	66(2)	94(2)	106(2)	-32(2)	31(2)	8(2)
N (1)	63(2)	50(2)	47(2)	-2(2)	6(2)	-1(2)
N (2)	47(2)	49(2)	46(2)	-7(2)	0(2)	5(2)
N (3)	46(2)	56(2)	57(2)	-6(2)	5(2)	-4(2)
C (1)	96(4)	74(3)	65(3)	-17(3)	-11(3)	-14(3)
C (2)	58(3)	60(3)	54(3)	-2(2)	1(2)	0(2)
C (3)	53(2)	44(2)	54(2)	-5(2)	4(2)	3(2)
C (4)	50(3)	48(2)	47(3)	2(2)	9(2)	-3(2)
C (5)	43(2)	47(2)	52(2)	3(2)	8(2)	-4(2)
C (6)	50(3)	53(3)	48(2)	0(2)	4(2)	-6(2)
C (7)	54(3)	58(3)	68(3)	-11(2)	13(2)	-2(2)
C (8)	52(3)	63(3)	59(3)	-2(2)	13(2)	1(2)
C (9)	35(2)	59(3)	54(3)	1(2)	10(2)	0(2)
C (10)	46(2)	80(3)	49(3)	7(3)	10(2)	8(2)
C (11)	42(3)	100(4)	58(3)	-13(3)	3(2)	5(3)
C (12)	55(3)	169(7)	64(4)	-19(4)	1(3)	4(4)
C (13)	68(4)	236(10)	53(4)	9(5)	8(3)	26(5)
C (14)	48(3)	52(3)	57(3)	2(2)	8(2)	-3(2)
C (15)	51(3)	39(2)	46(2)	6(2)	-3(2)	-6(2)
C (16)	62(3)	47(2)	57(3)	0(2)	1(2)	-3(2)
C (17)	62(3)	51(3)	69(3)	-6(2)	-7(2)	-11(2)

C (18)	50(3)	71(3)	81(3)	1(3)	-5(3)	-9(2)
C (19)	48(3)	69(3)	65(3)	-3(2)	1(2)	-5(2)
C (20)	54(3)	41(2)	57(3)	-1(2)	12(2)	-2(2)
C (21)	61(3)	99(4)	71(3)	27(3)	12(2)	5(3)
C (22)	69(4)	171(7)	76(4)	54(4)	21(3)	30(4)
C (23)	44(3)	87(4)	83(4)	-23(3)	2(2)	-1(3)
C (24)	35(2)	67(3)	82(3)	2(3)	18(2)	0(2)
C (25)	51(3)	64(4)	137(5)	4(4)	23(3)	-1(3)
C (26)	64(4)	92(5)	143(6)	48(5)	33(4)	20(3)
C (27)	78(4)	116(5)	86(4)	38(4)	26(3)	34(4)
C (28)	64(3)	83(4)	61(3)	9(3)	10(2)	13(3)
C (29)	34(2)	66(3)	63(3)	0(3)	12(2)	5(2)
C (30)	58(3)	54(3)	61(3)	-13(2)	8(2)	9(2)
C (31)	65(3)	49(3)	63(3)	-8(2)	9(2)	3(2)

Chapter Five

Part B

APPENDIX

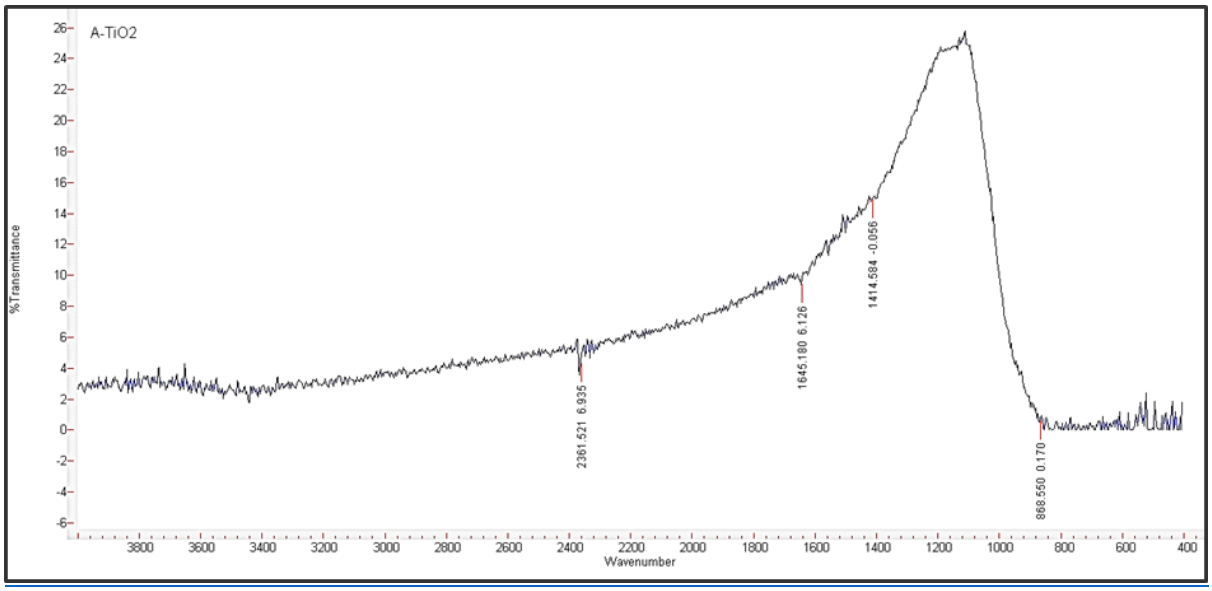

Figure 5B. S. 1. The Infra-Red Spectrum of TiO_2

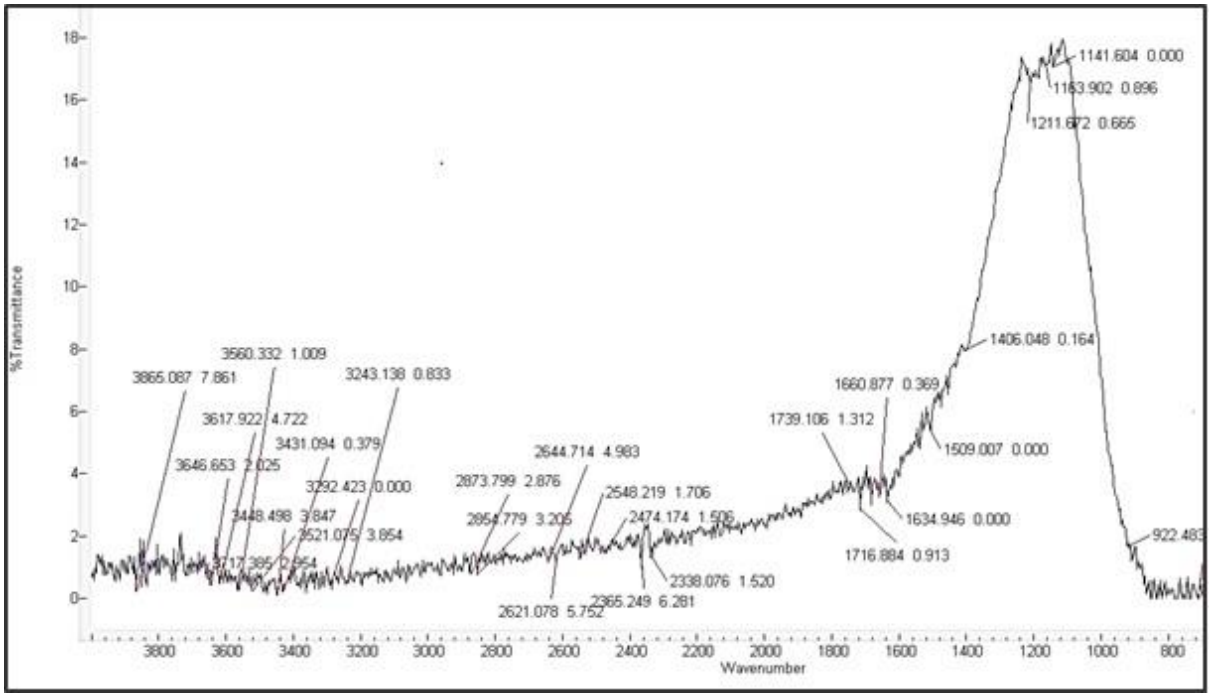

Figure 5B. S. 2. The Infra-Red Spectrum of the catalyst TiO_2-BPTETSA

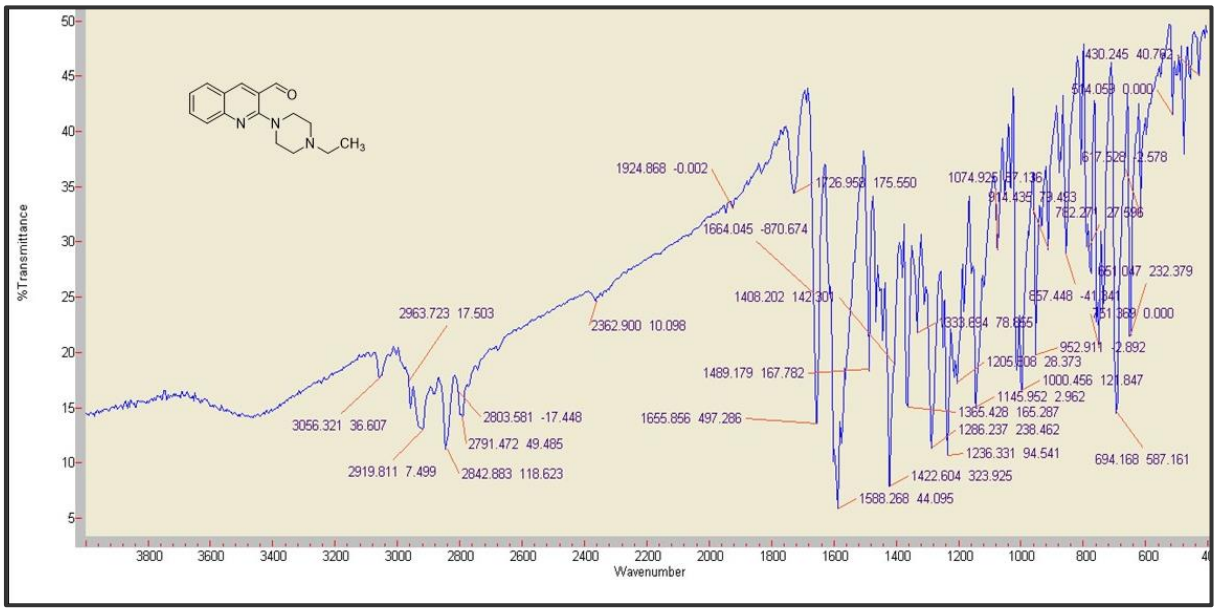

Figure 5B. S. 3. The Infra-Red Spectrum of compound 3

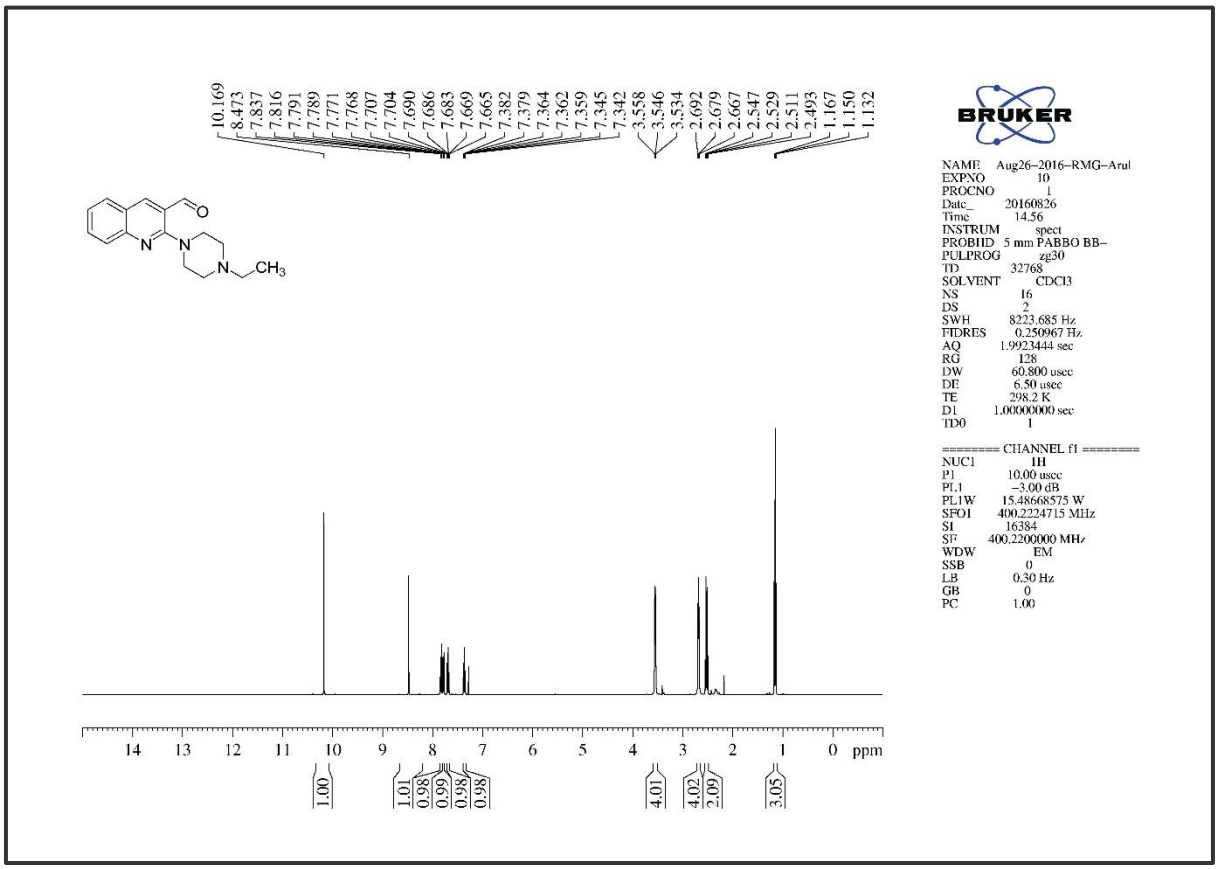

Figure 5B. S. 4. The ^{1}H NMR of compound 3

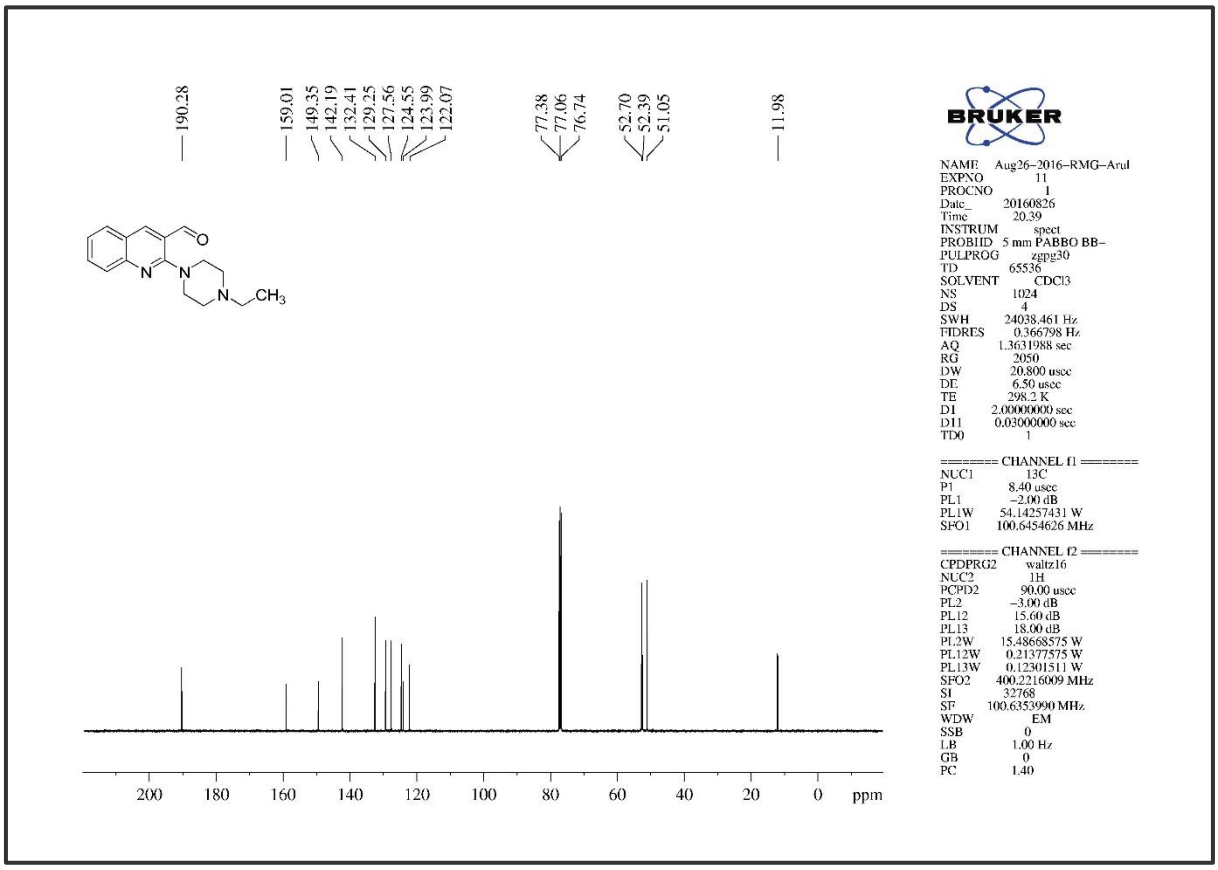

Figure 5B. S. 5. The ^{13}C NMR of compound 3

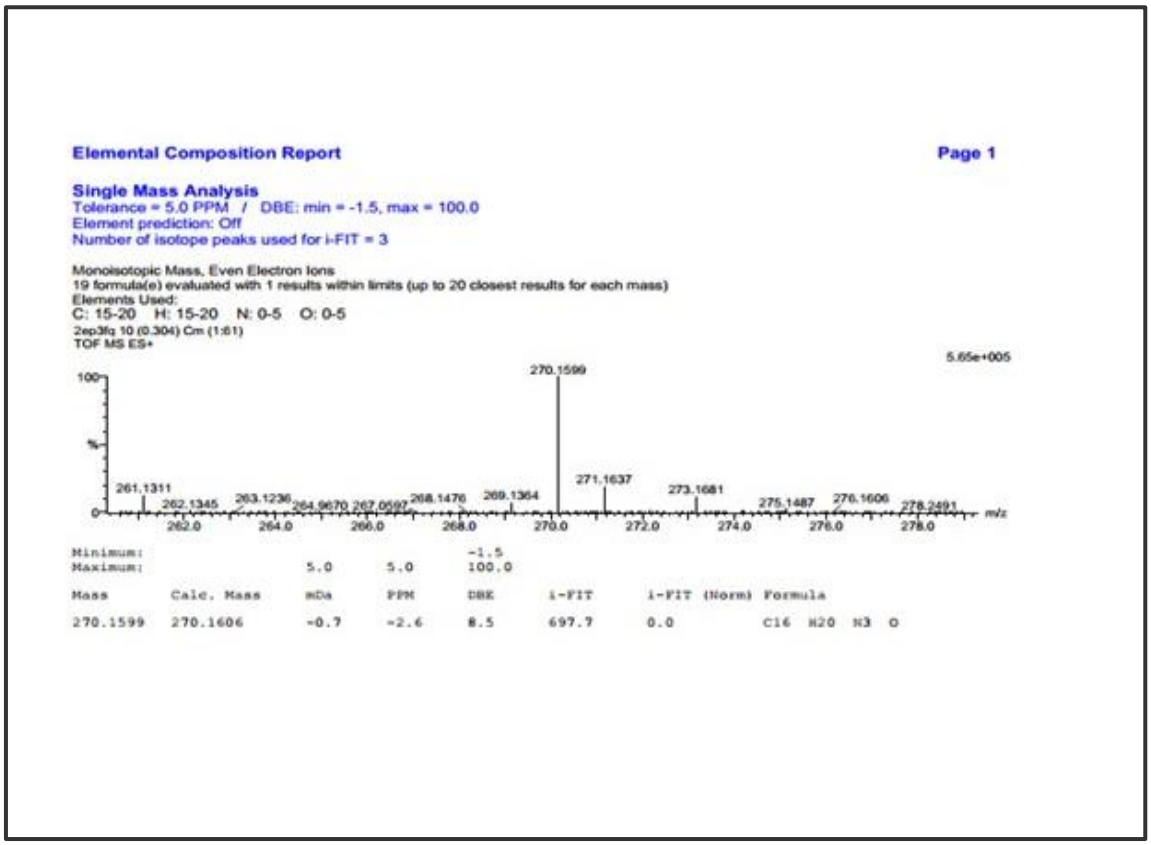

Figure 5B. S. 6. The HRMS of compound 3

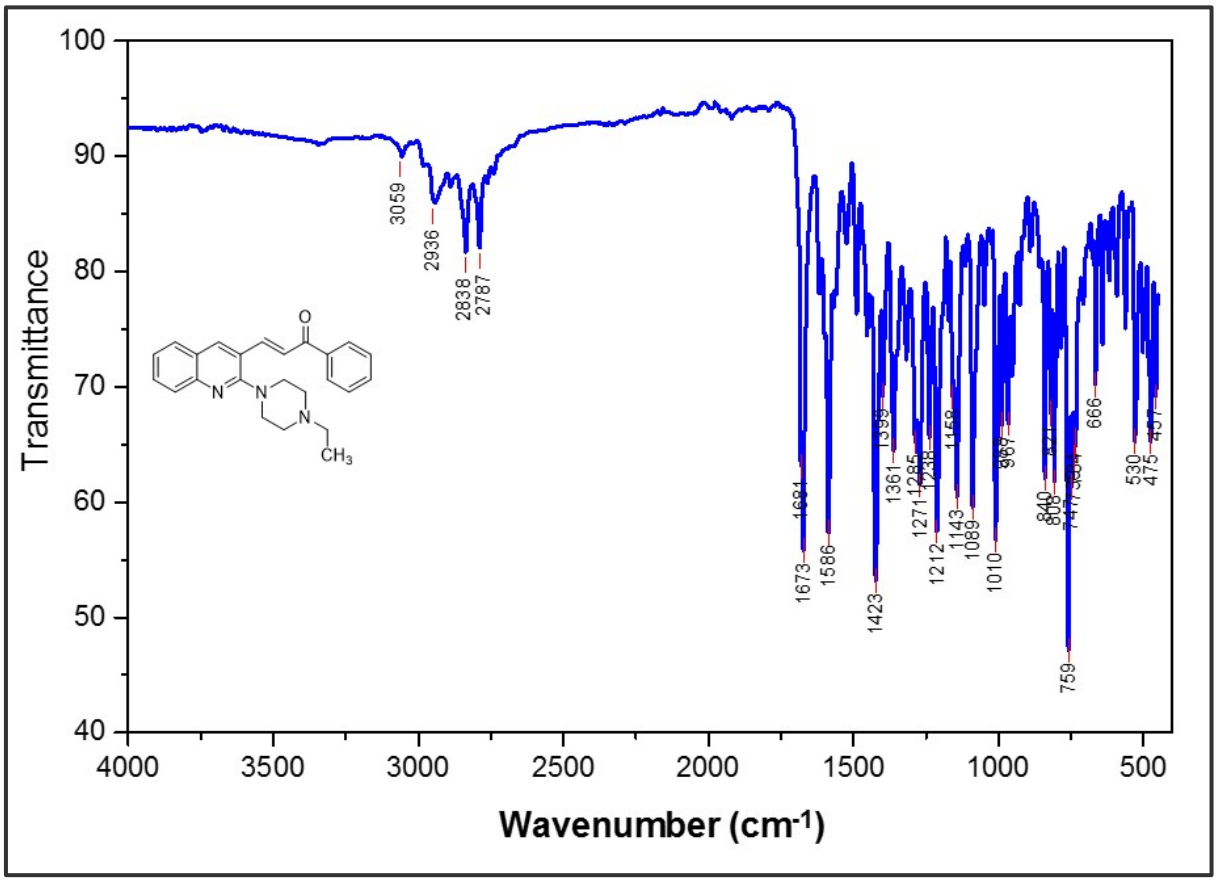

Figure 5B. S. 7. The Infra-Red Spectrum of compound 5a

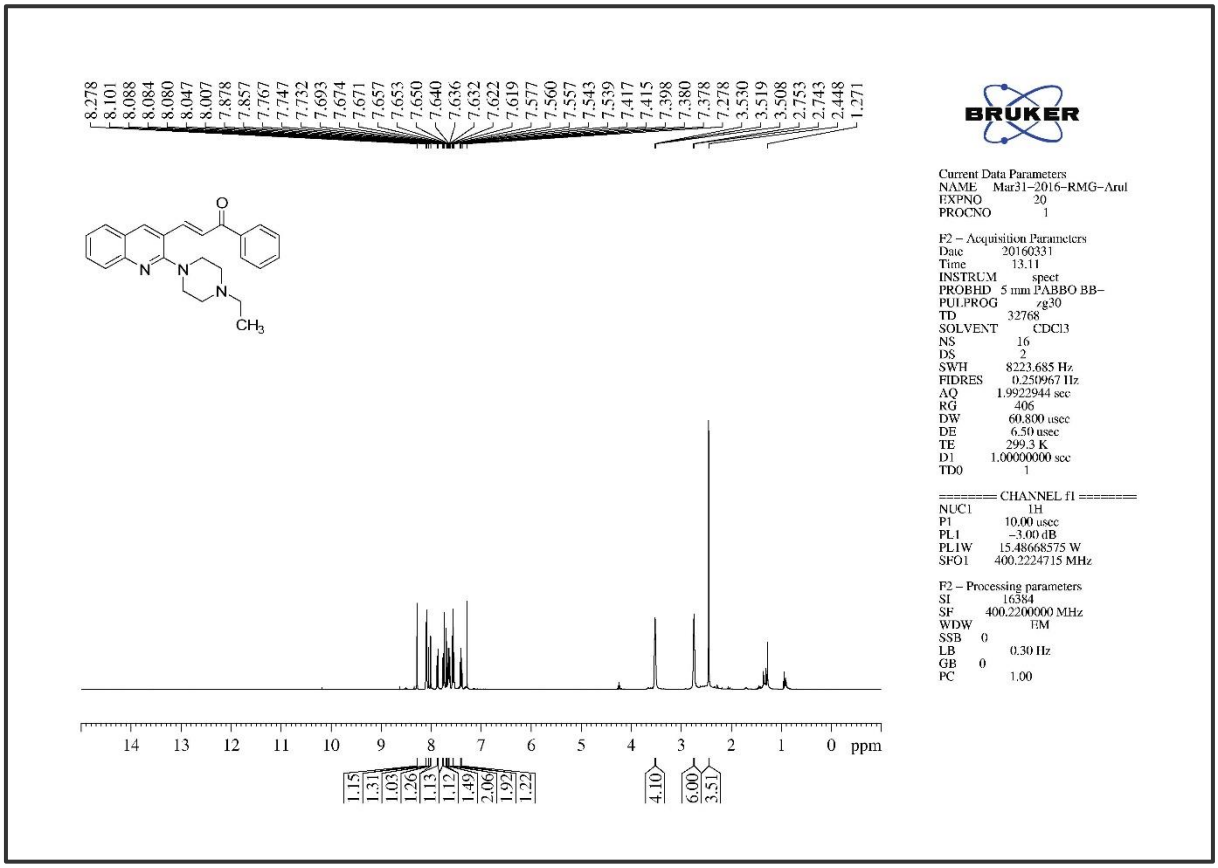

Figure 5B. S. 8. The ^{1}H NMR of compound 5a

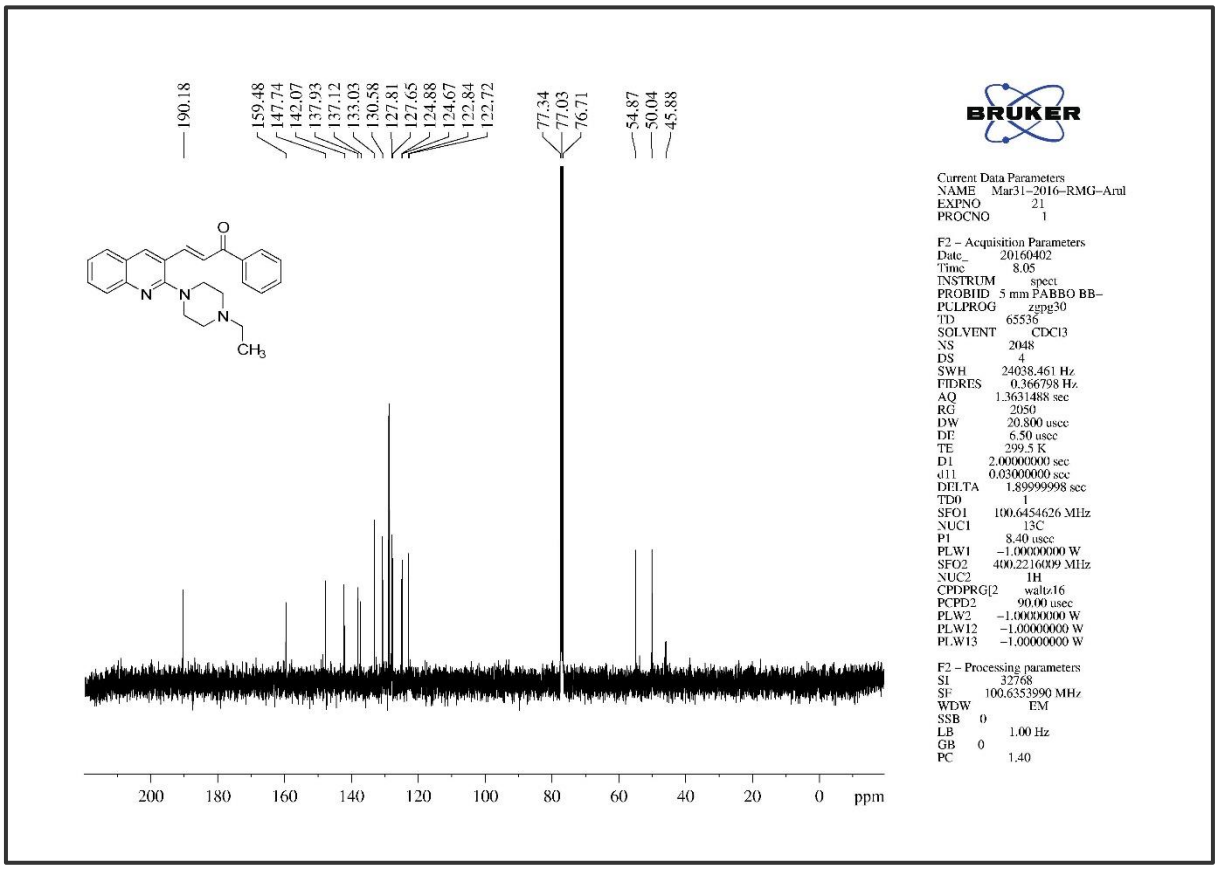

Figure 5B. S. 9. The ^{13}C NMR of compound 5a

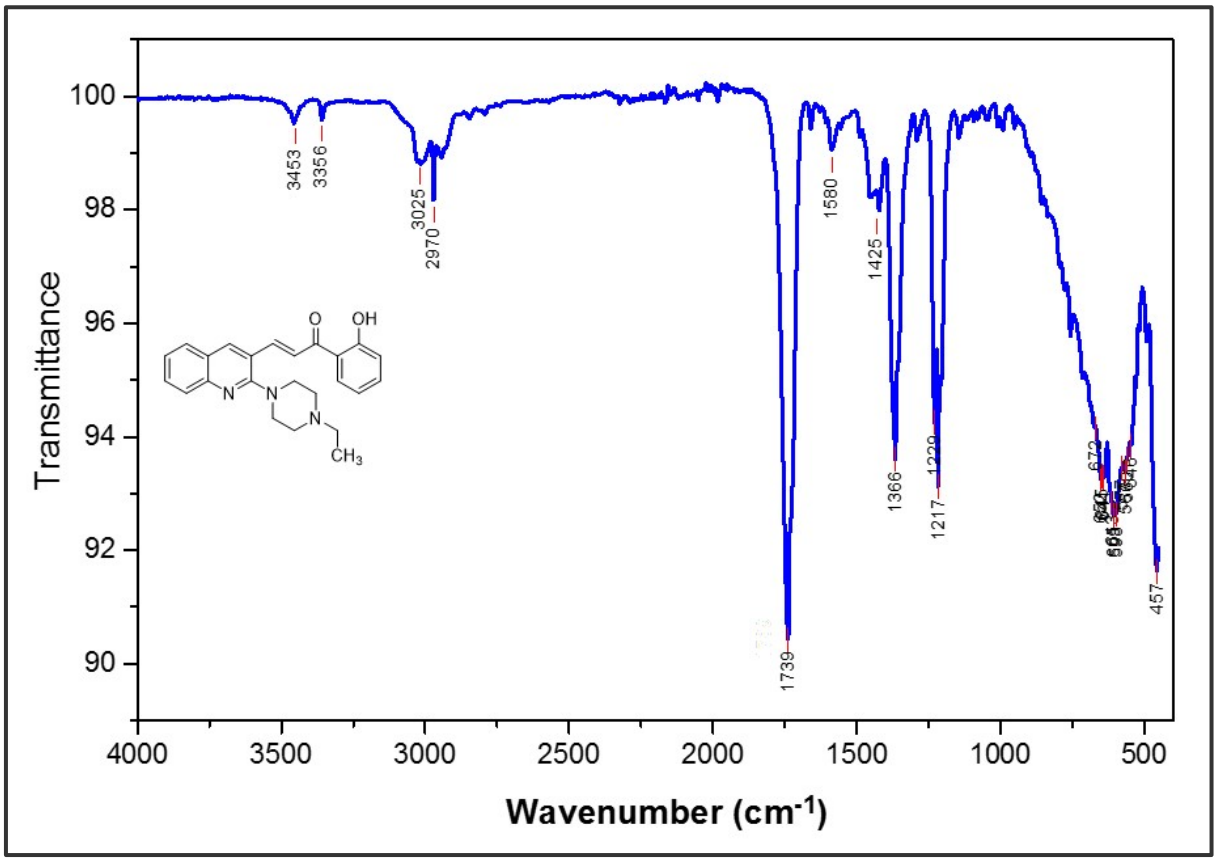

Figure 5B. S. 10. The Infra-Red Spectrum of compound 5b

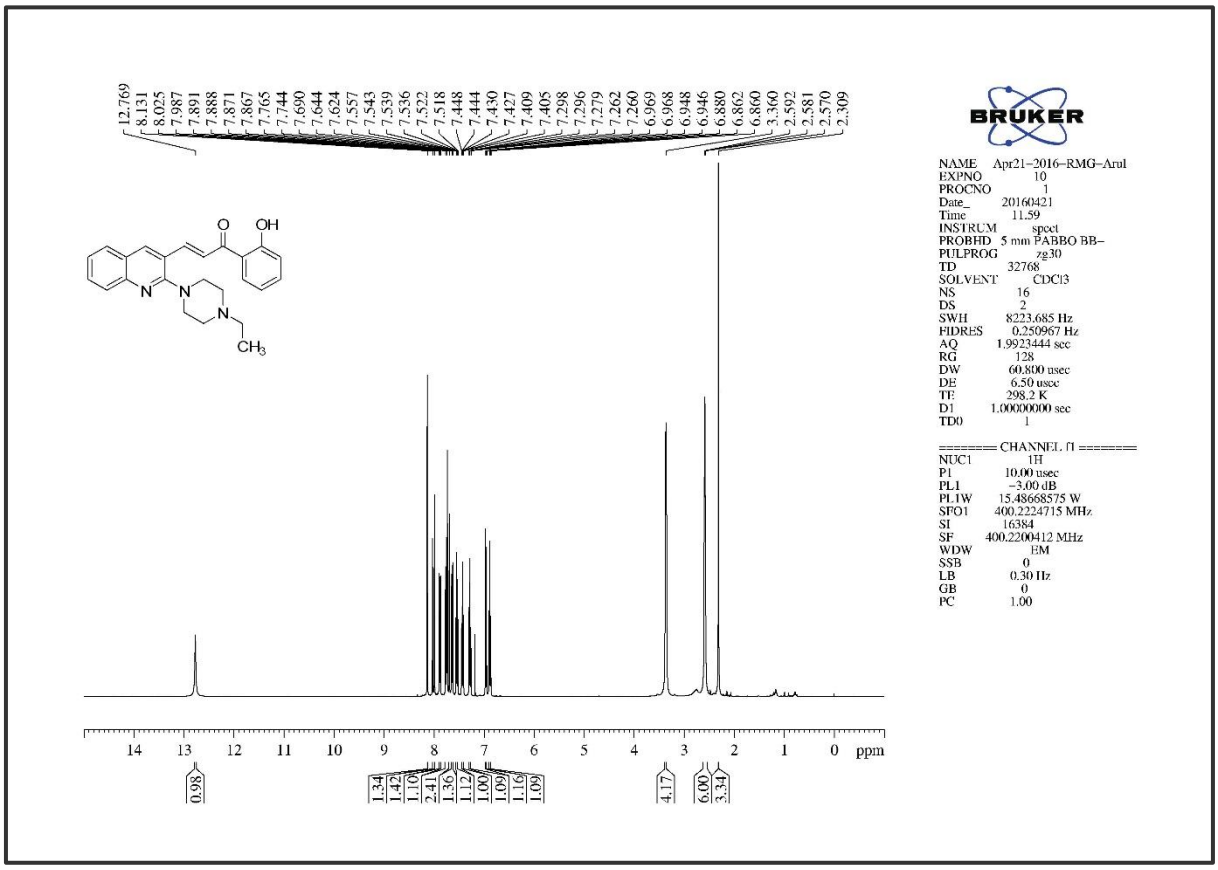

Figure 5B. S. 11. The ^{1}H NMR of compound 5b

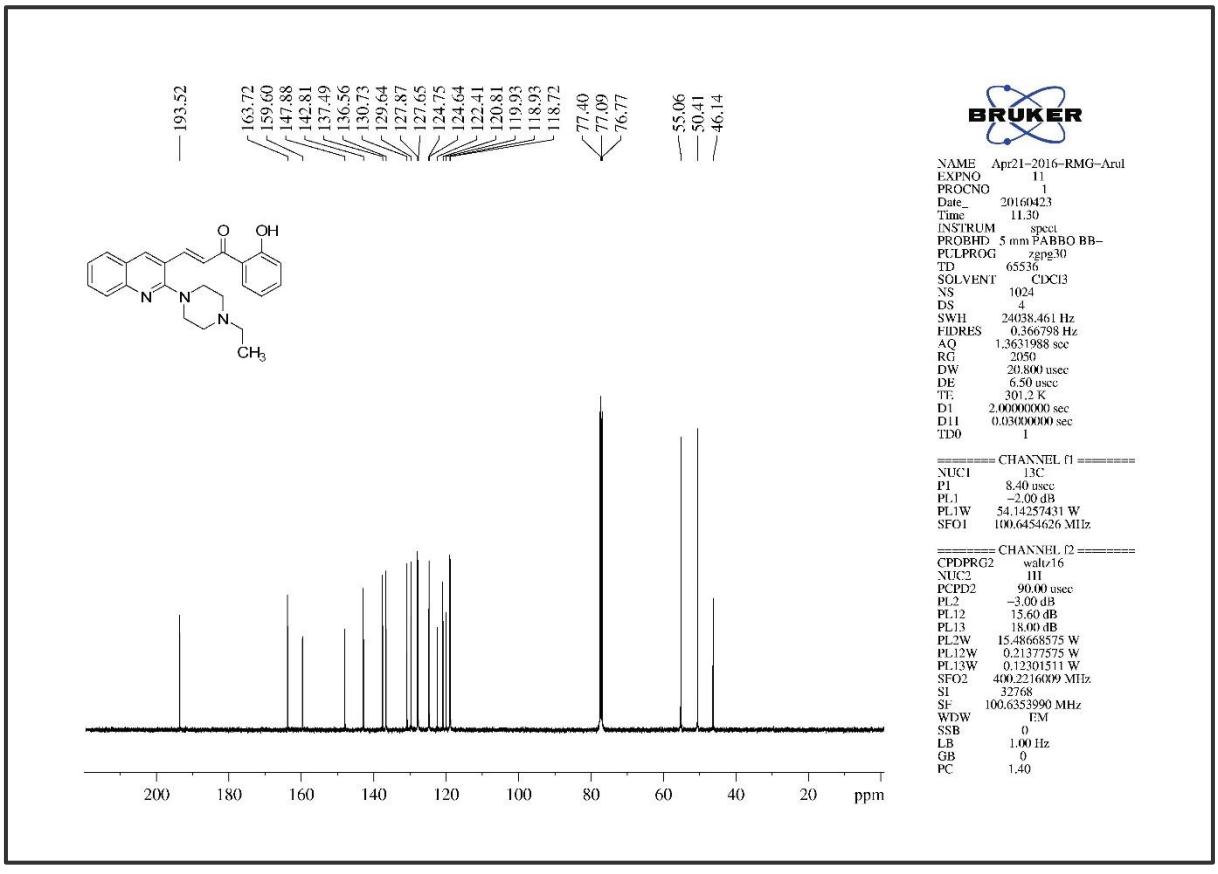

Figure 5B. S. 12. The ^{13}C NMR of compound 5b

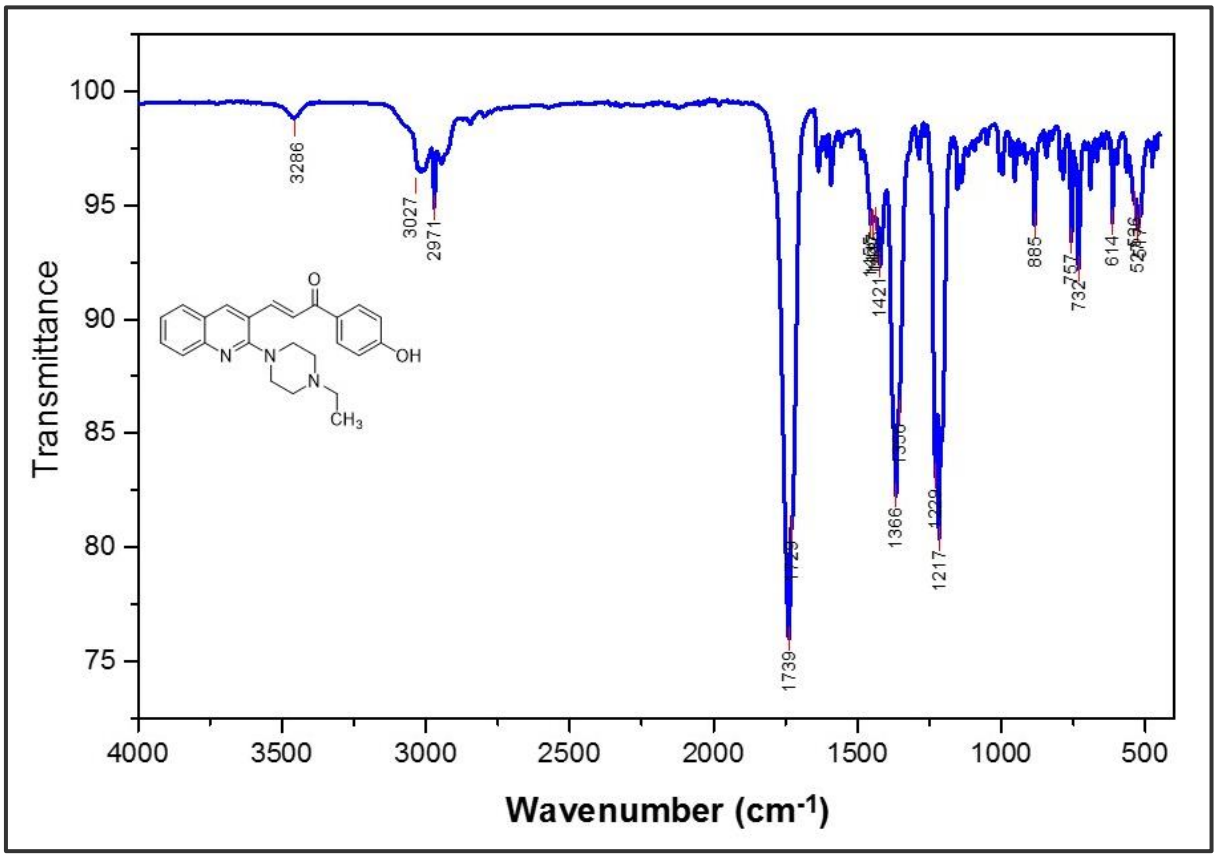

Figure 5B. S. 13. The Infra-Red Spectrum of compound 5c

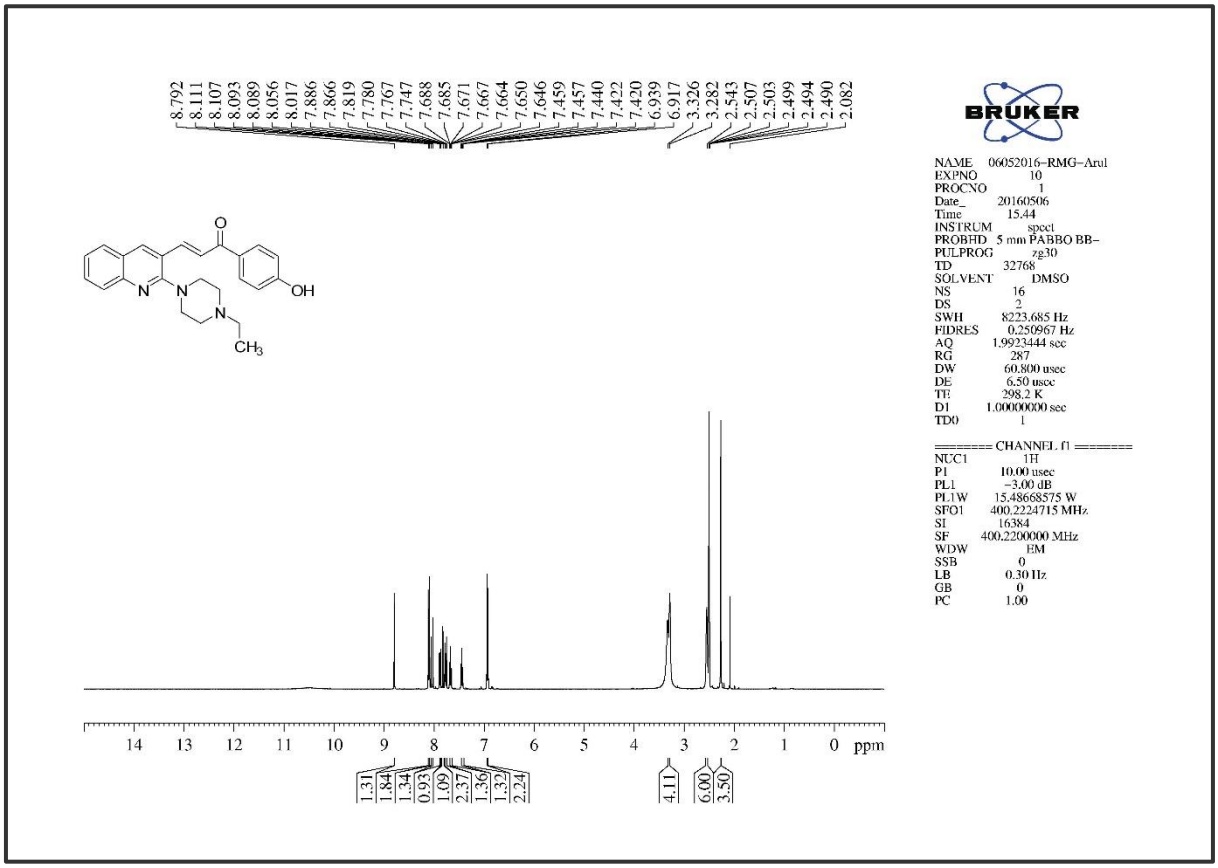

Figure 5B. S. 14. The ^{1}H NMR of compound 5c

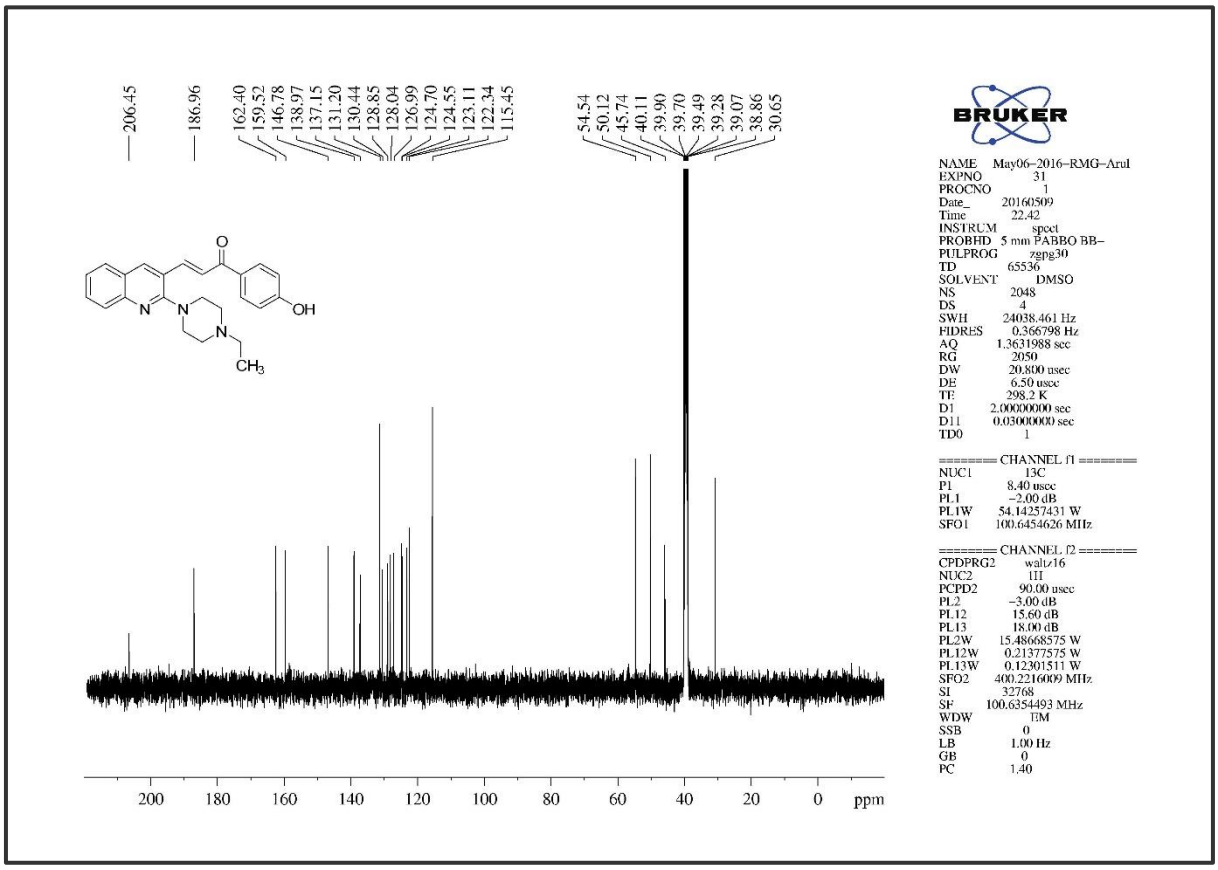

Figure 5B. S. 15. The ^{13}C NMR of compound 5c

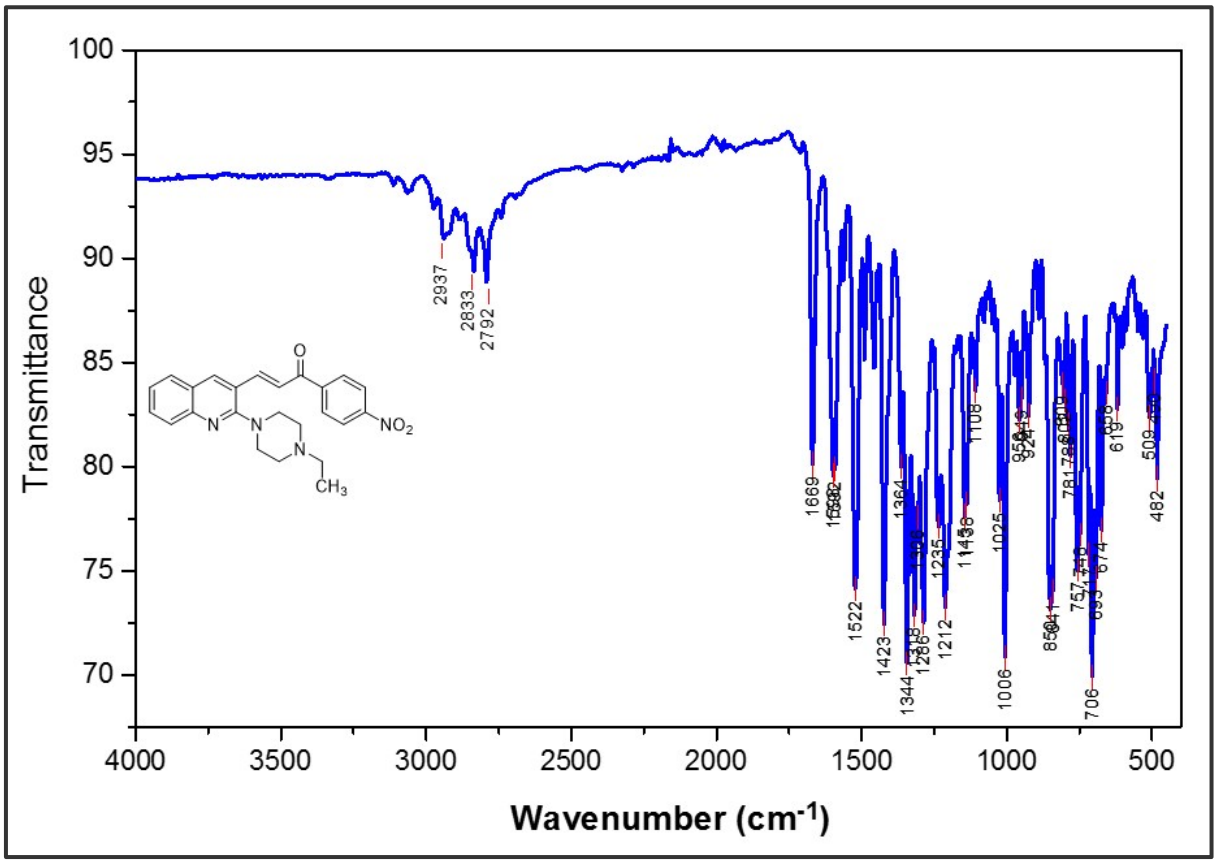

Figure 5B. S. 16. The Infra-Red Spectrum of compound 5d

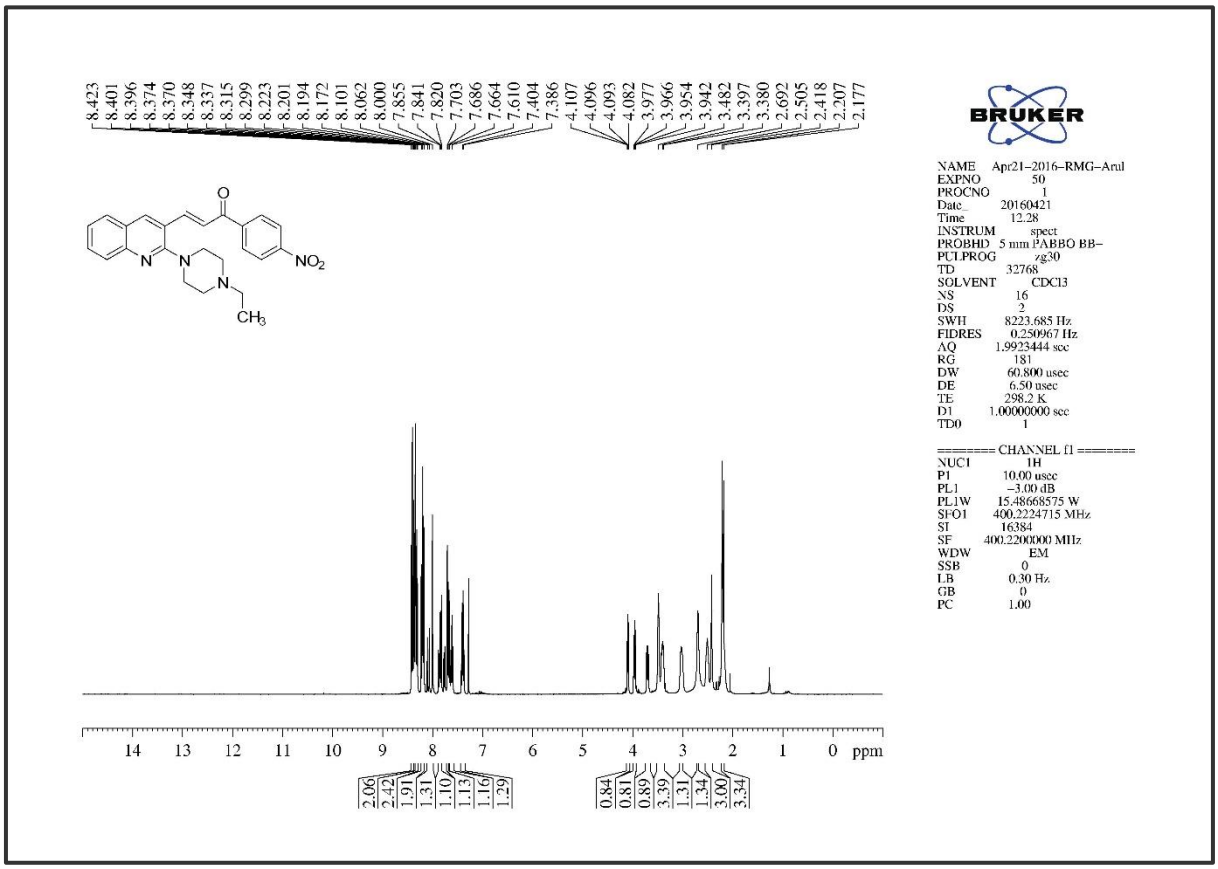

Figure 5B. S. 17. The ^{1}H NMR of compound 5d

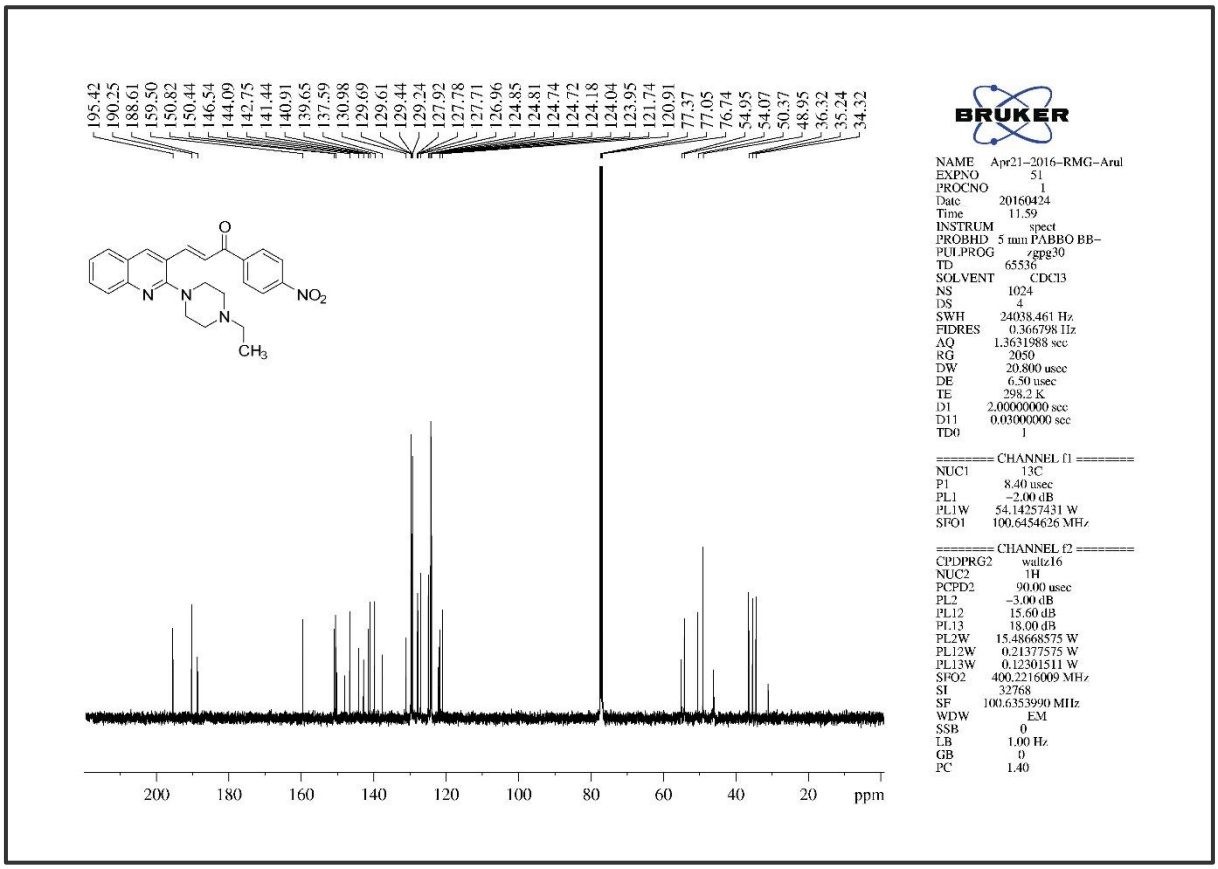

Figure 5B. S. 18. The ^{13}C NMR of compound 5d

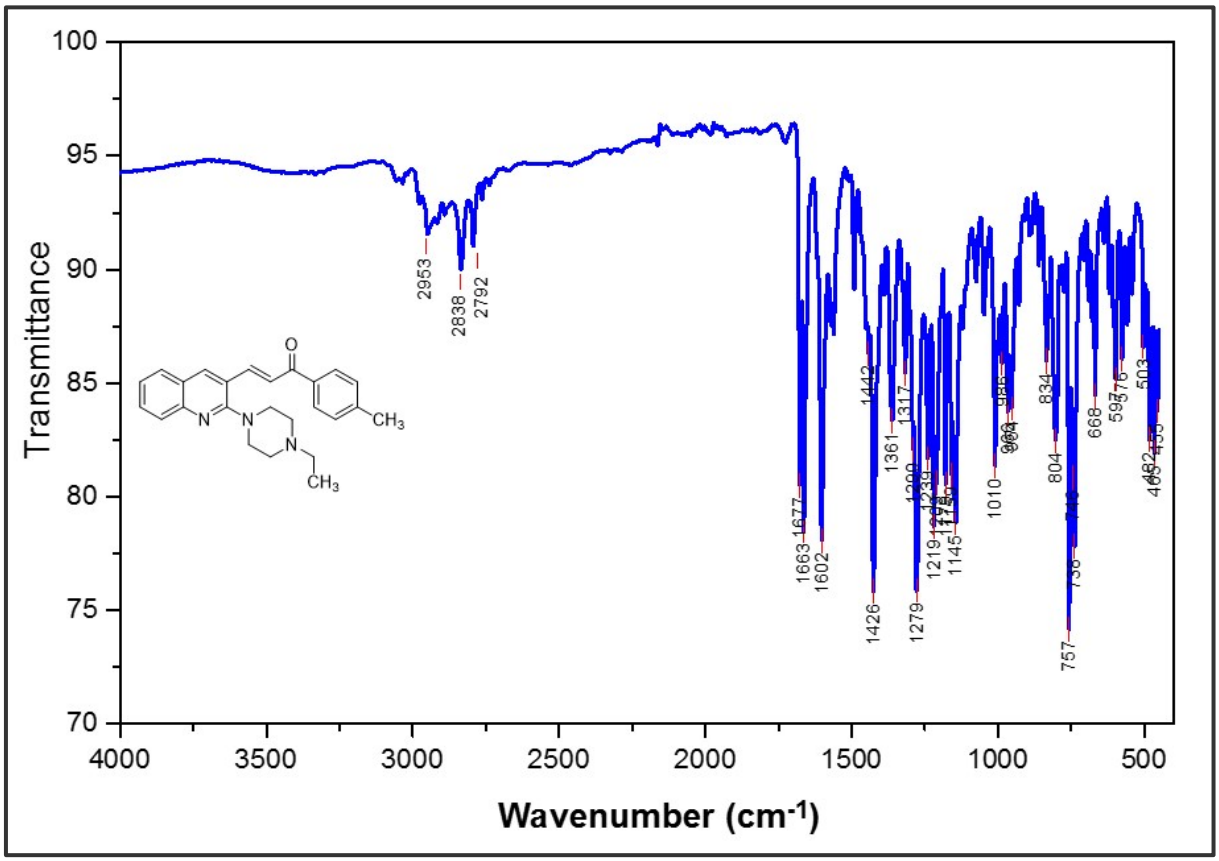

Figure 5B. S. 19. The Infra-Red Spectrum of compound 5e

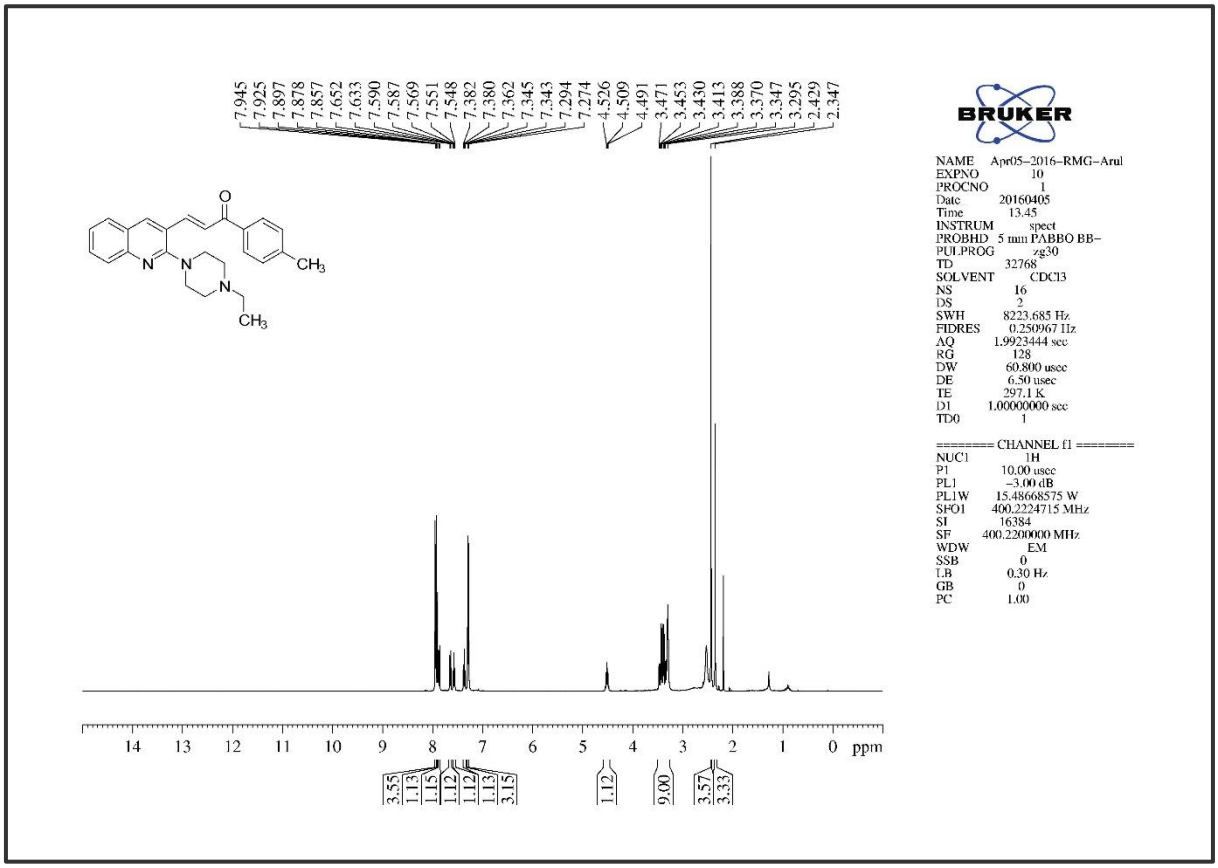

Figure 5B. S. 20. The ^{1}H NMR of compound 5e

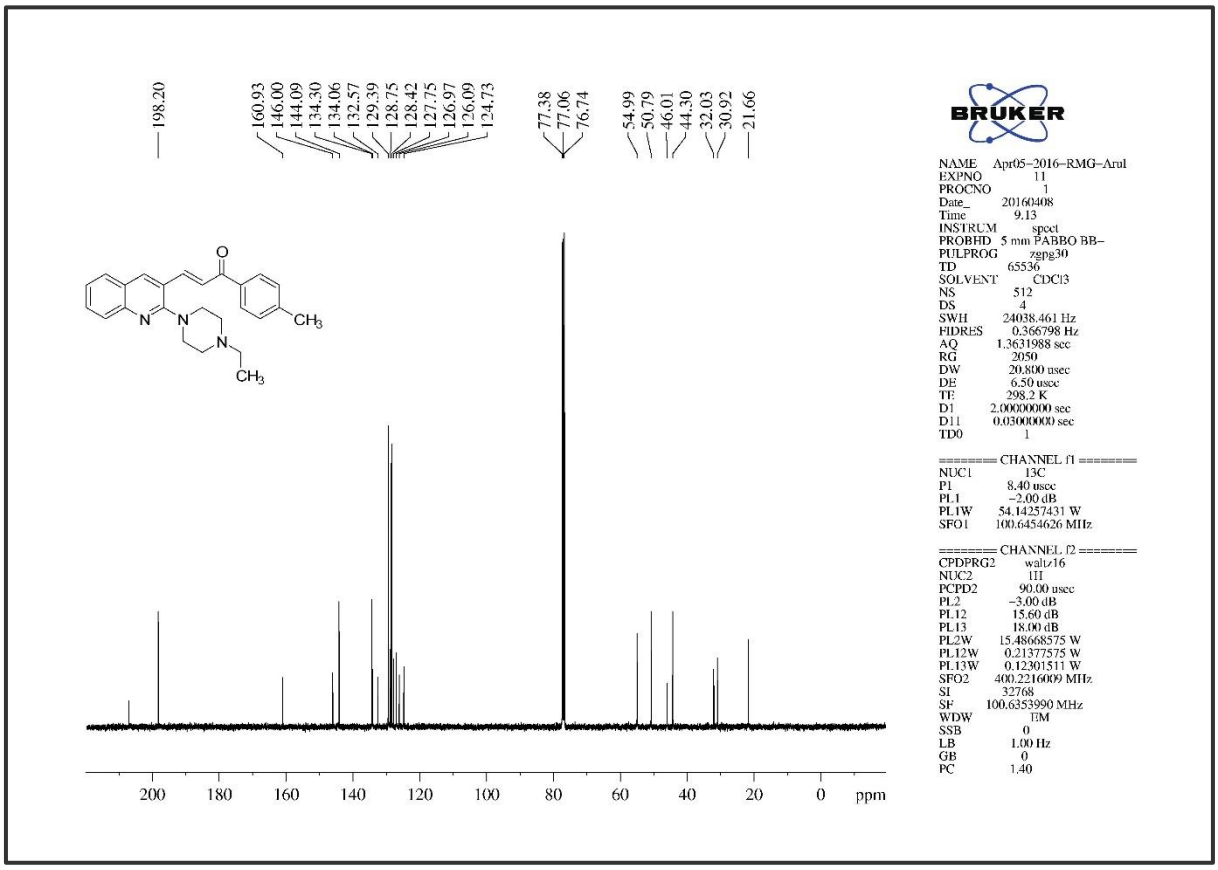

Figure 5B. S. 21. The ^{13}C NMR of compound 5e

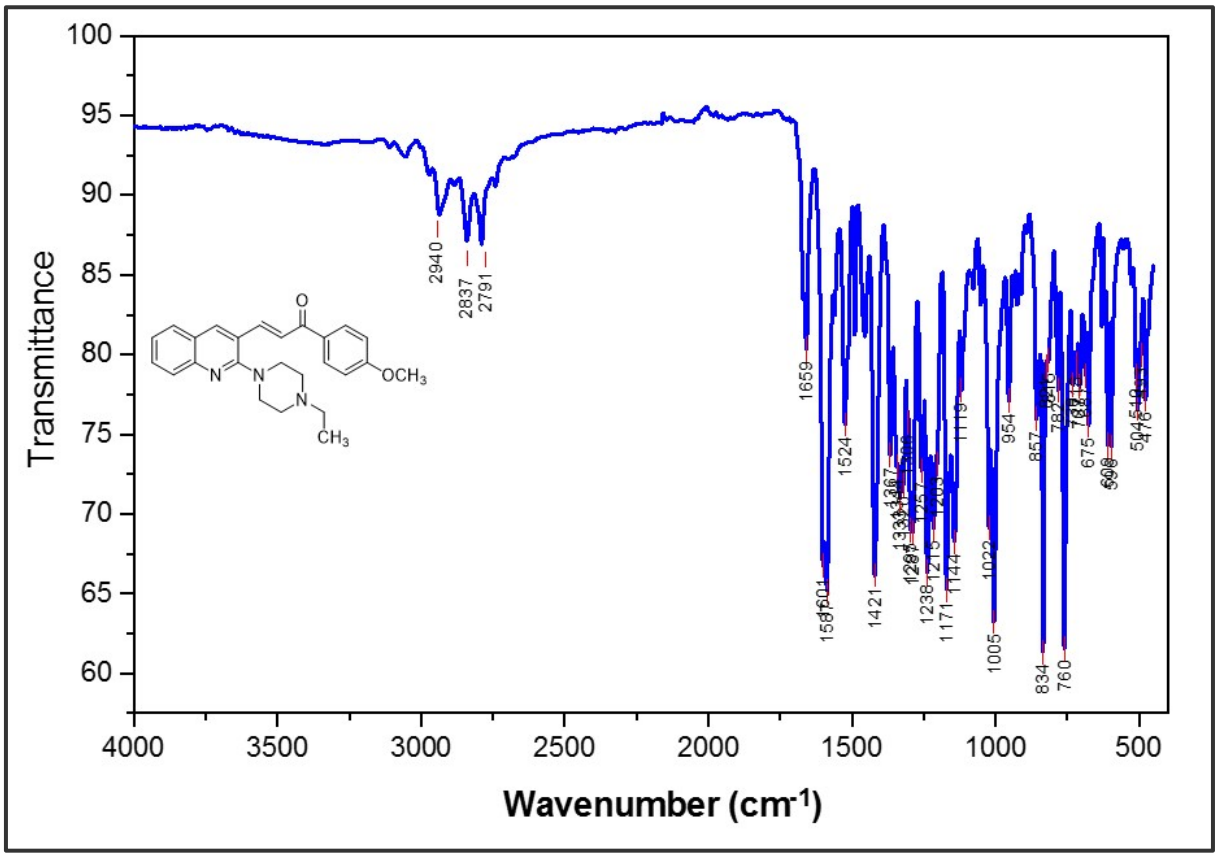

Figure 5B. S. 22. The Infra-Red Spectrum of compound 5f

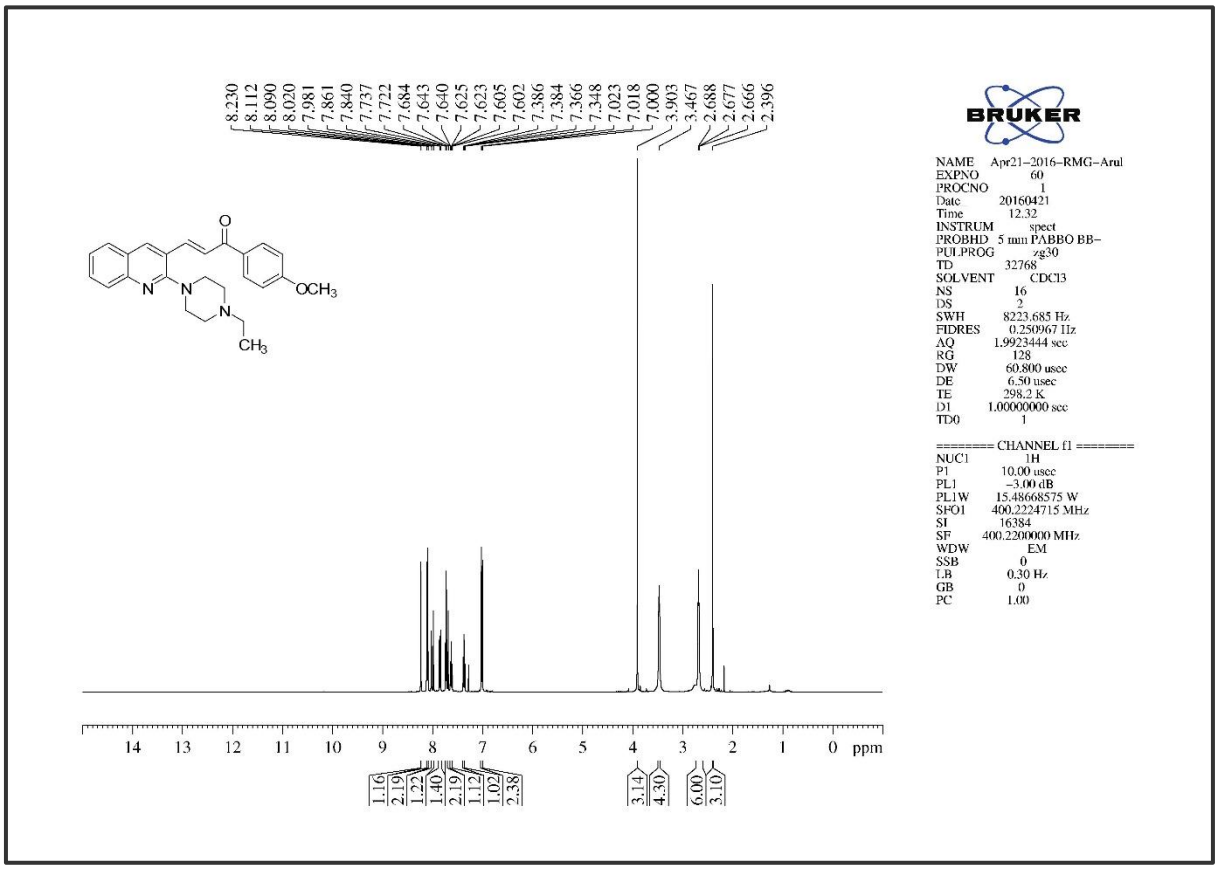

Figure 5B. S. 23. The ^{1}H NMR of compound 5f

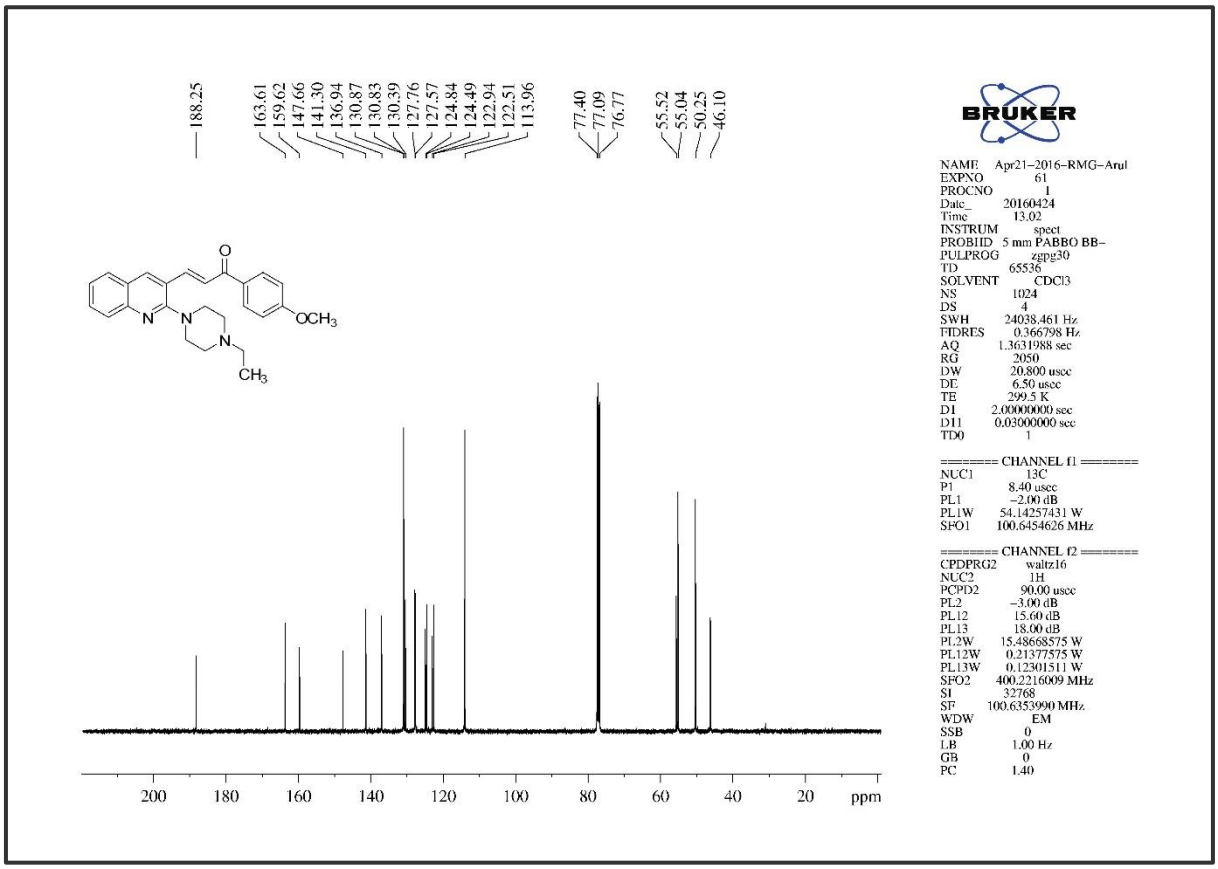

Figure 5B. S. 24**.** The ^{13}C NMR of compound 5f

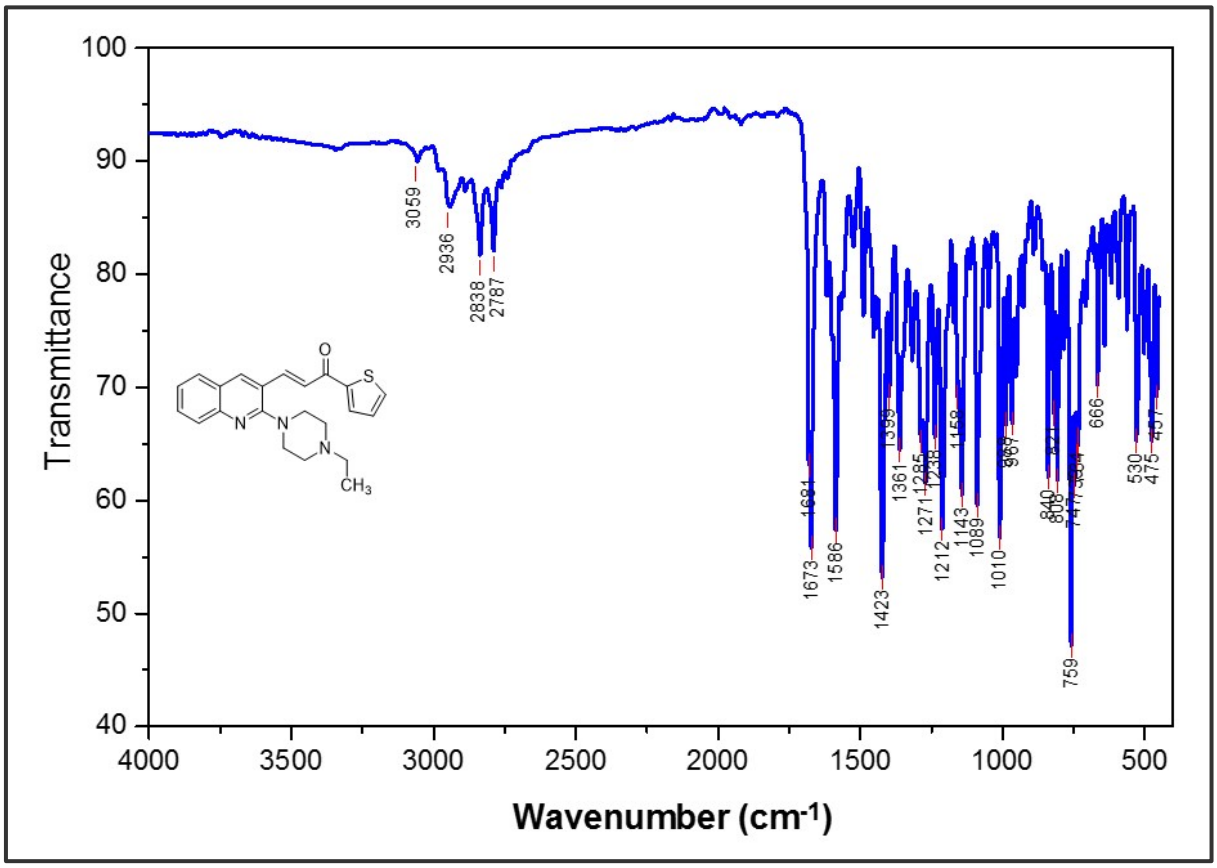

Figure 5B. S. 25. The Infra-Red Spectrum of compound 5g

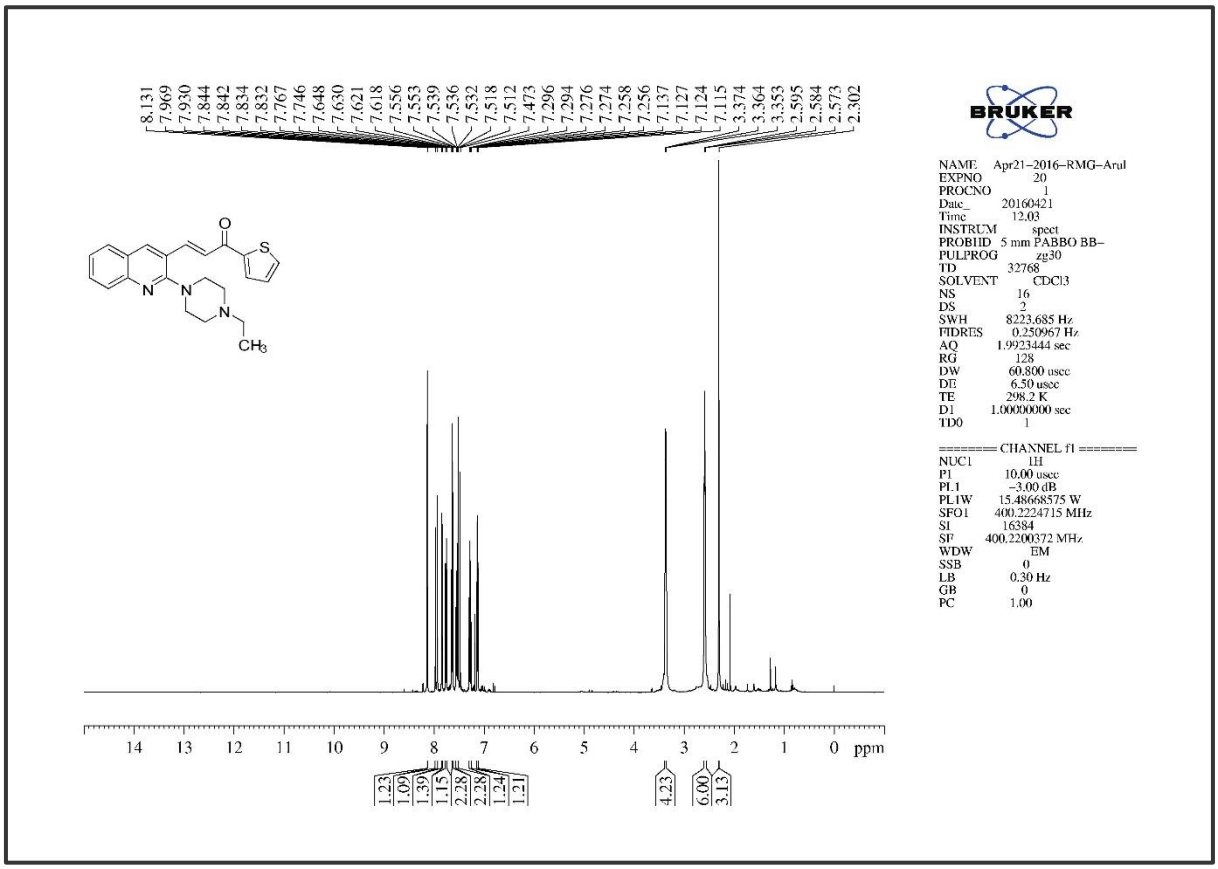

Figure 5B. S. 26. The ^{1}H NMR of compound 5g

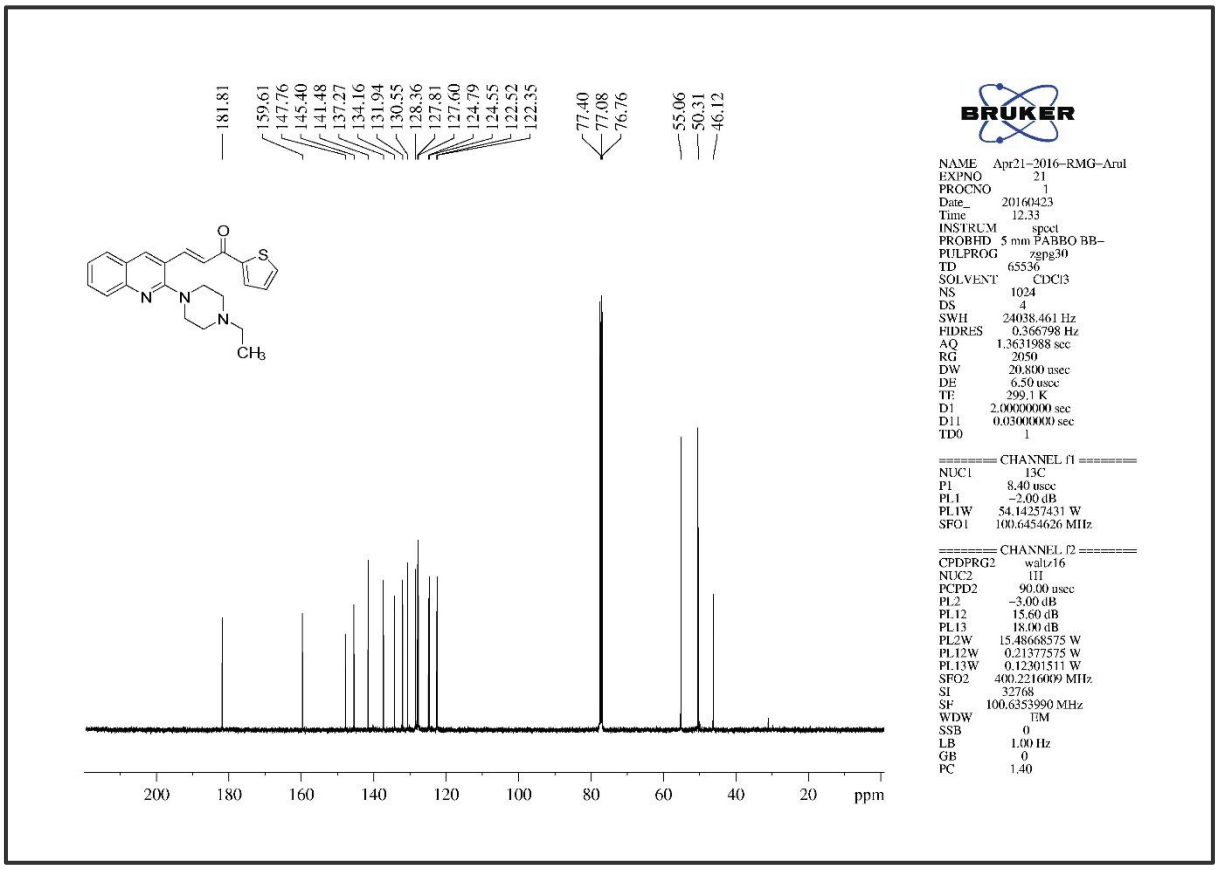

Figure 5B. S. 27. The ^{13}C NMR of compound 5g

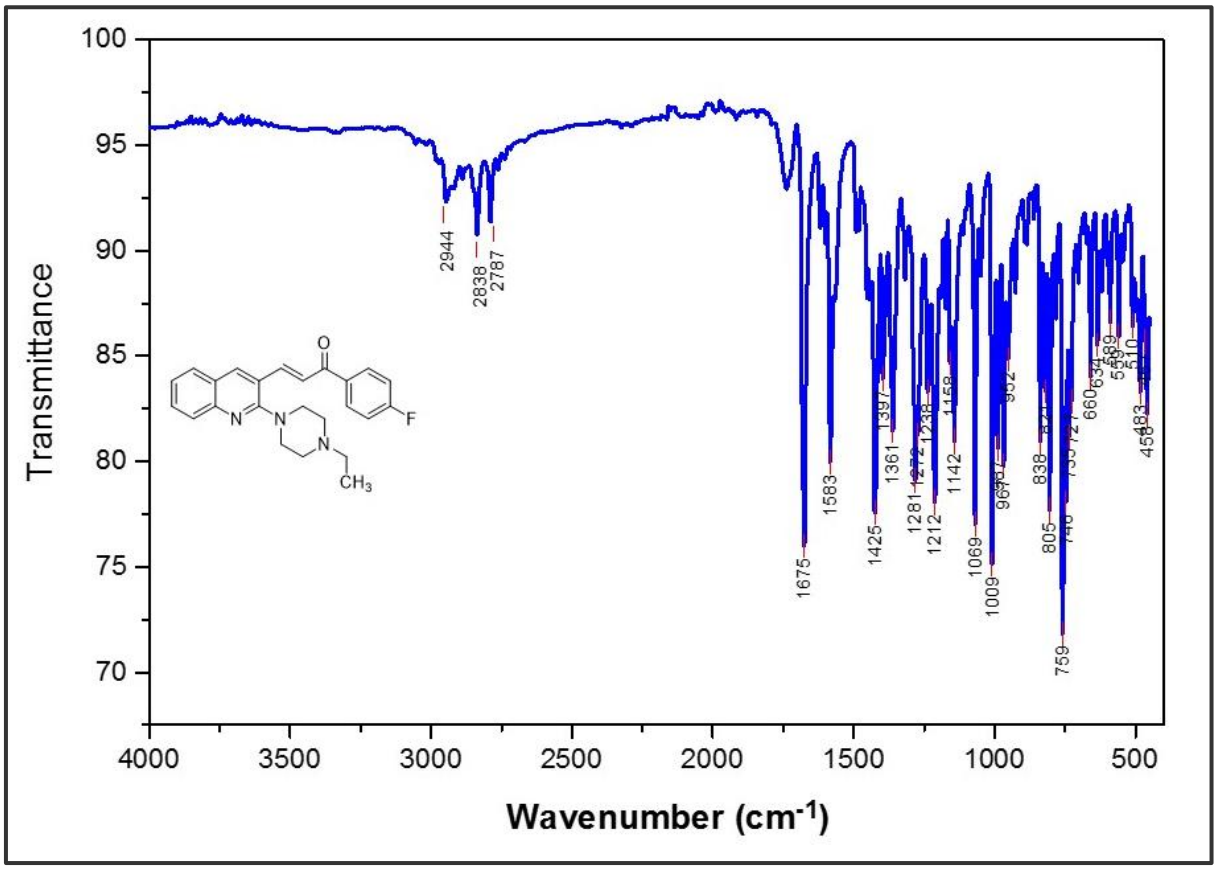

Figure 5B. S. 28. The Infra-Red Spectrum of compound 5h

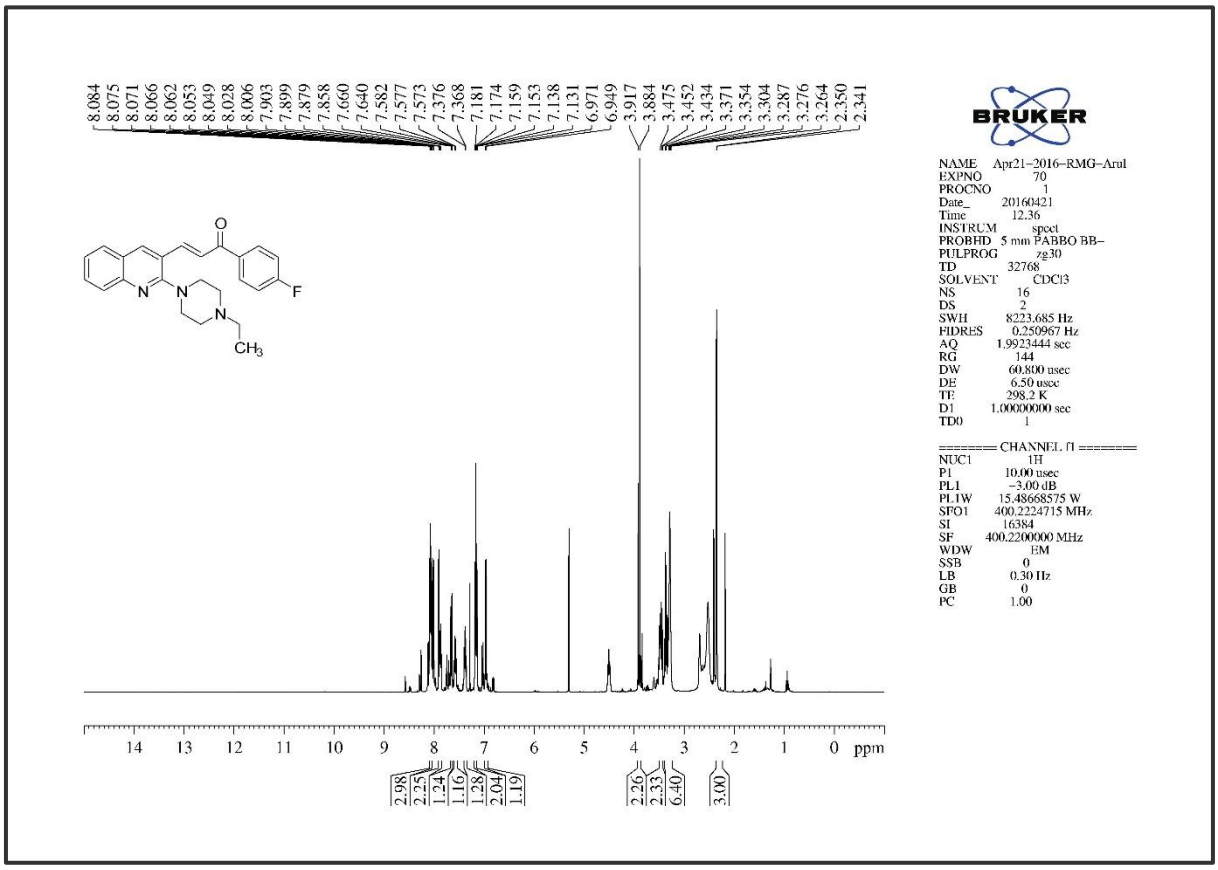

Figure 5B. S. 29. The ^{1}H NMR of compound 5h

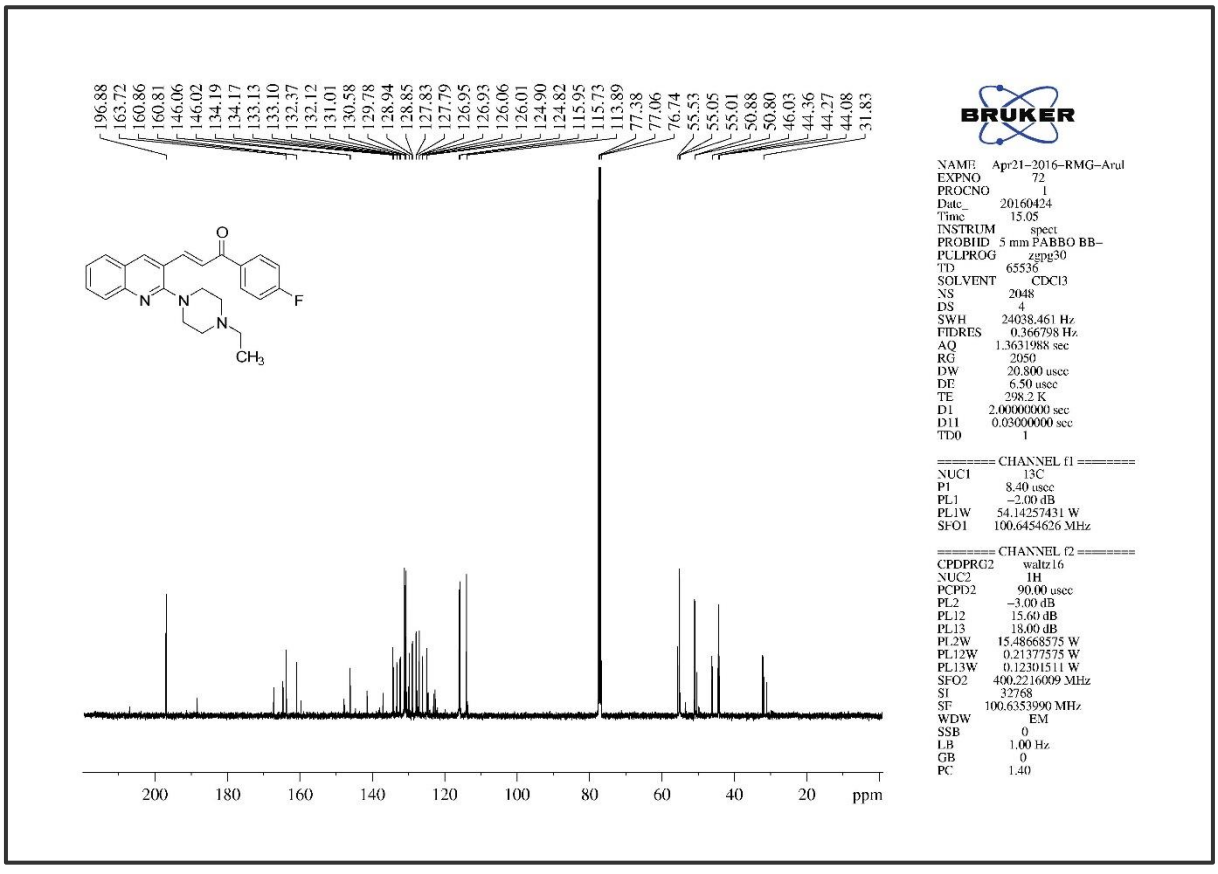

Figure 5B. S. 30. The ^{13}C NMR of compound 5h

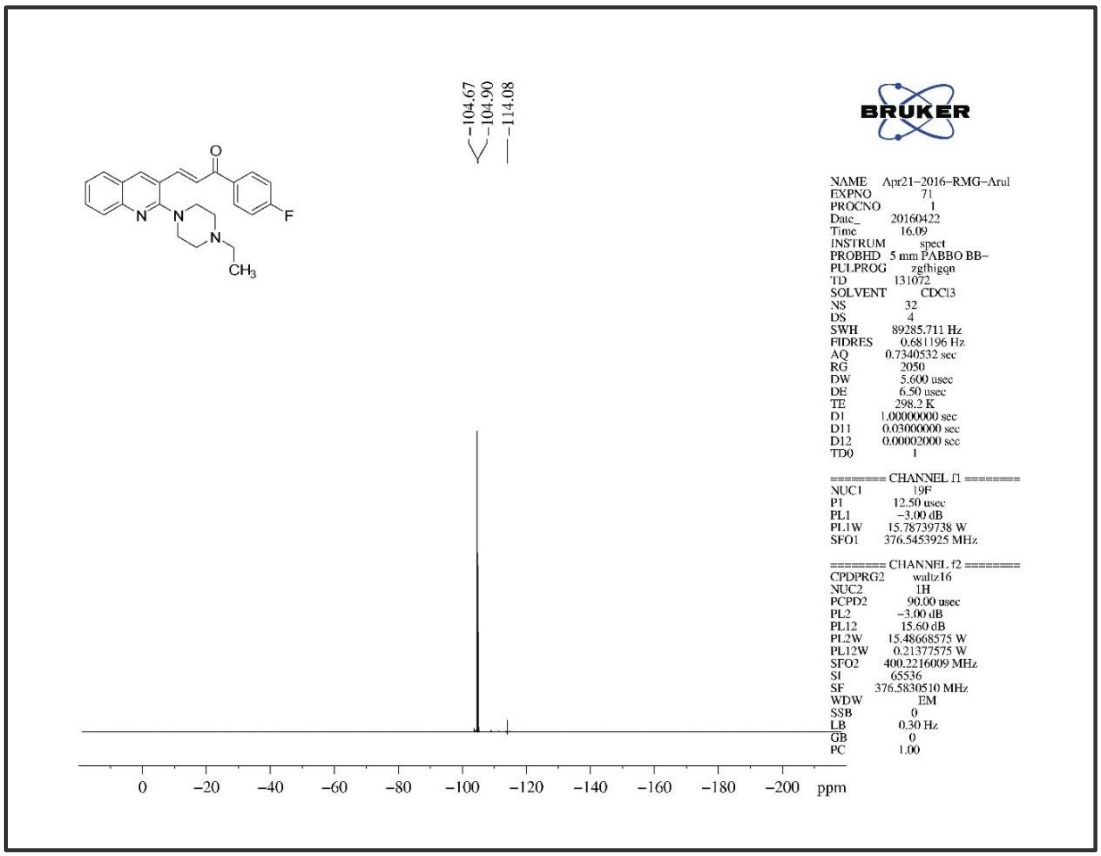

Figure 5B. S. 31. The ^{19}F NMR of compound 5h

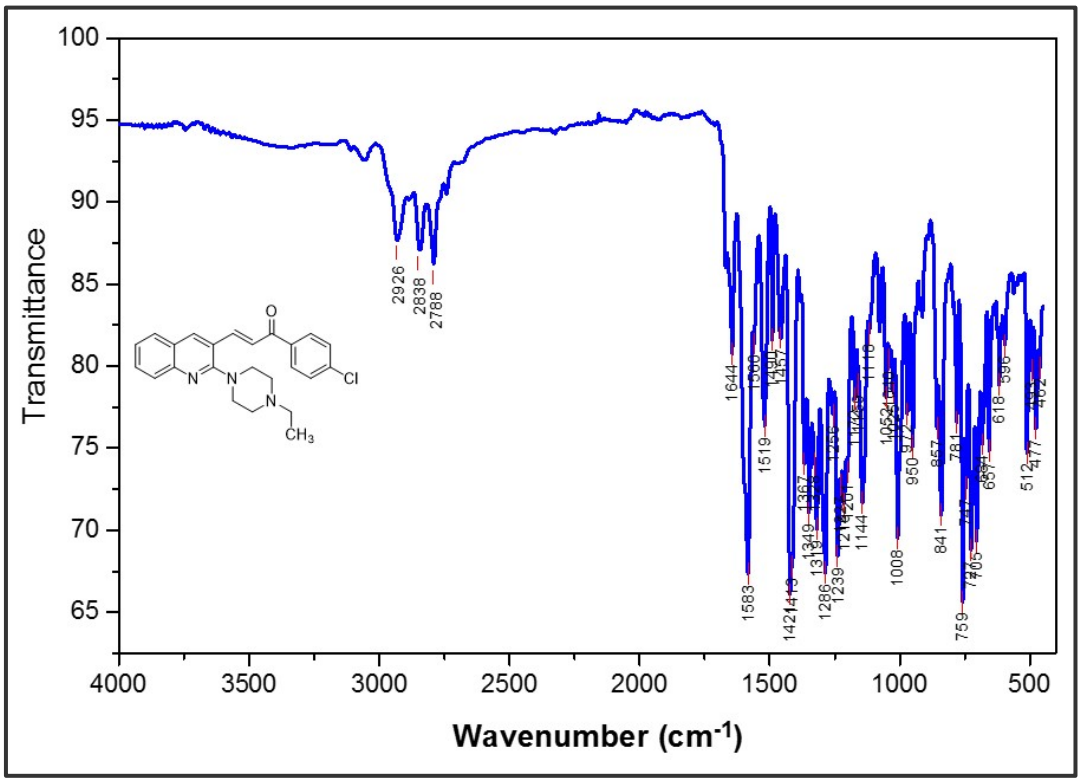

Figure 5B. S. 32. The Infra-Red Spectrum of compound 5i

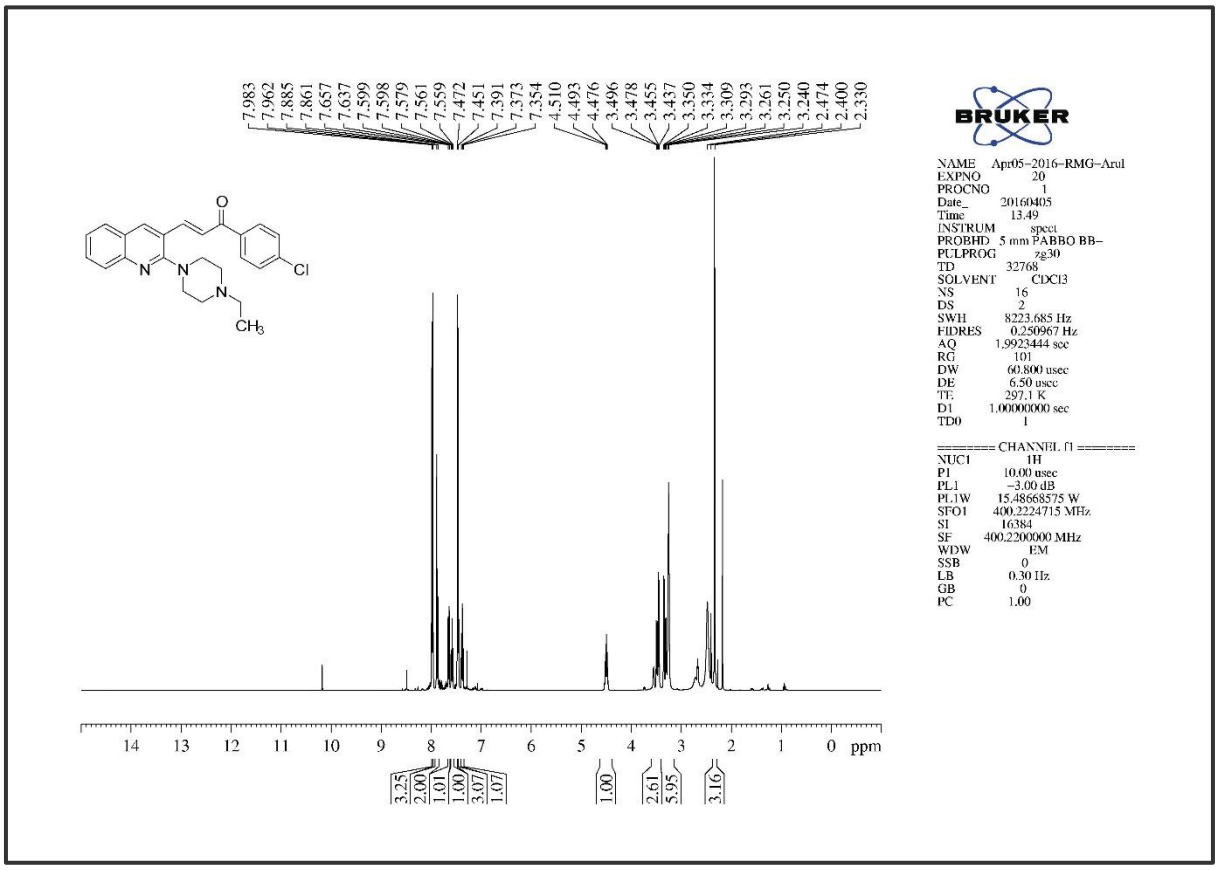

Figure 5B. S. 33. The ^{1}H NMR of compound 5i

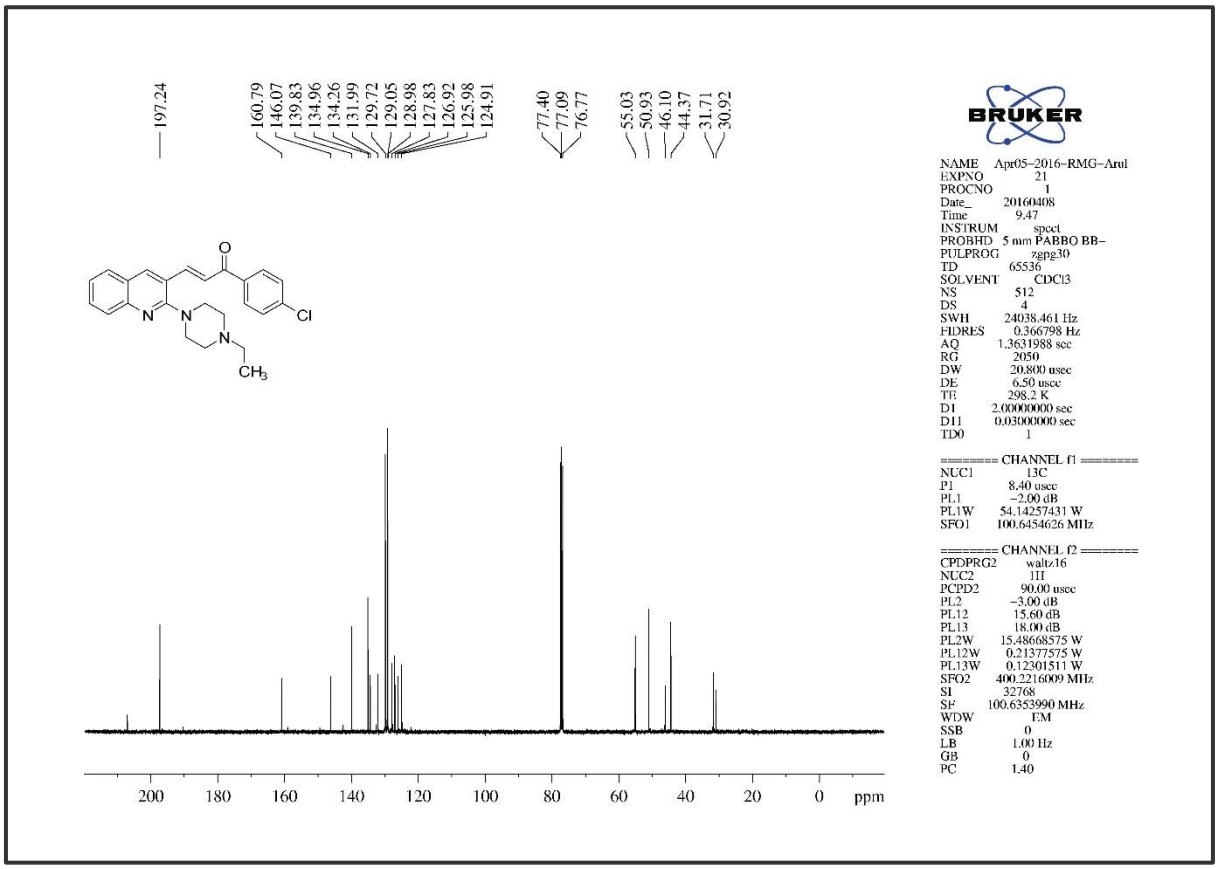

Figure 5B. S. 34. The ^{13}C NMR of compound 5i

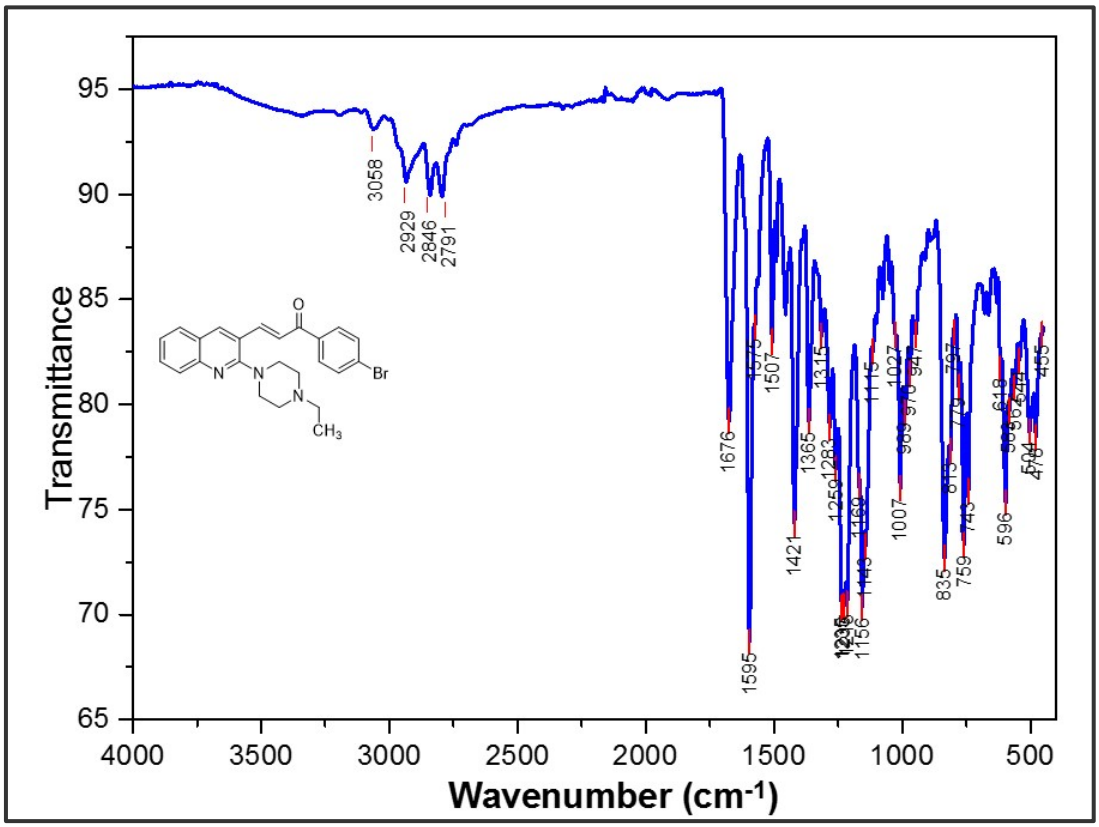

Figure 5B. S. 35. The Infra-Red Spectrum of compound 5j

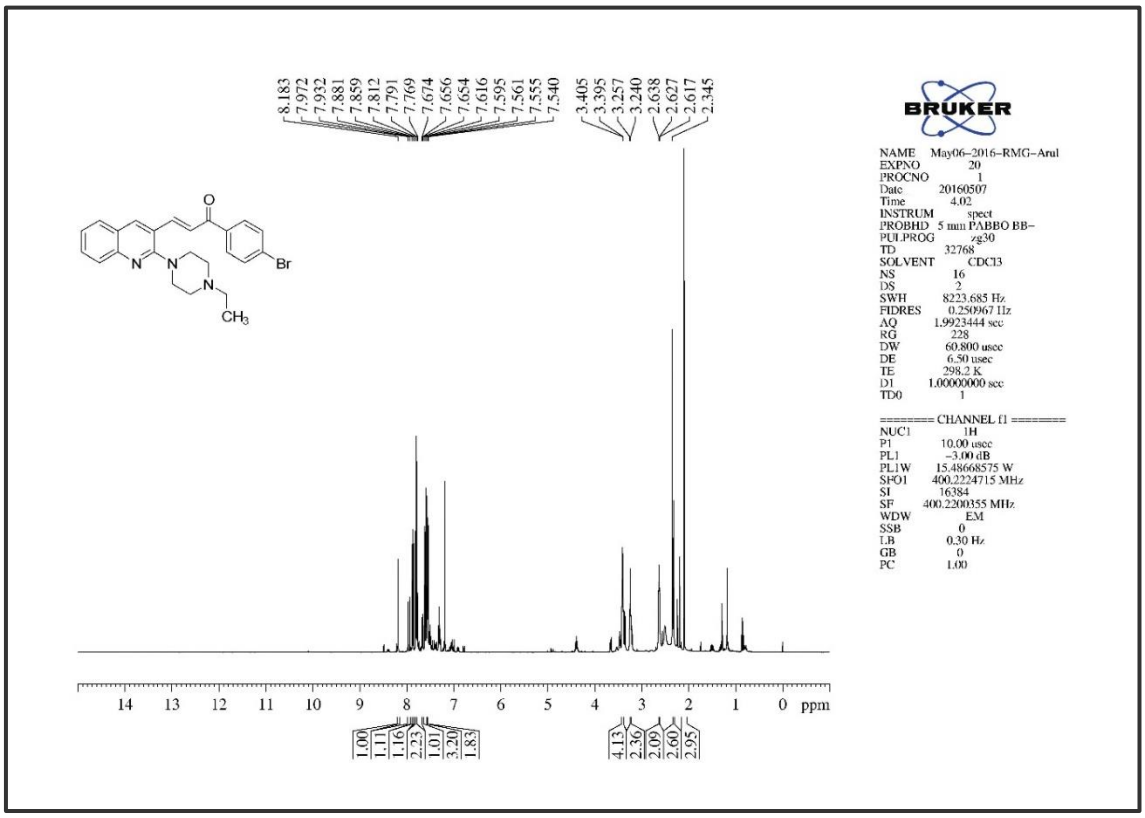

Figure 5B. S. 36. The ^{1}H NMR of compound 5j

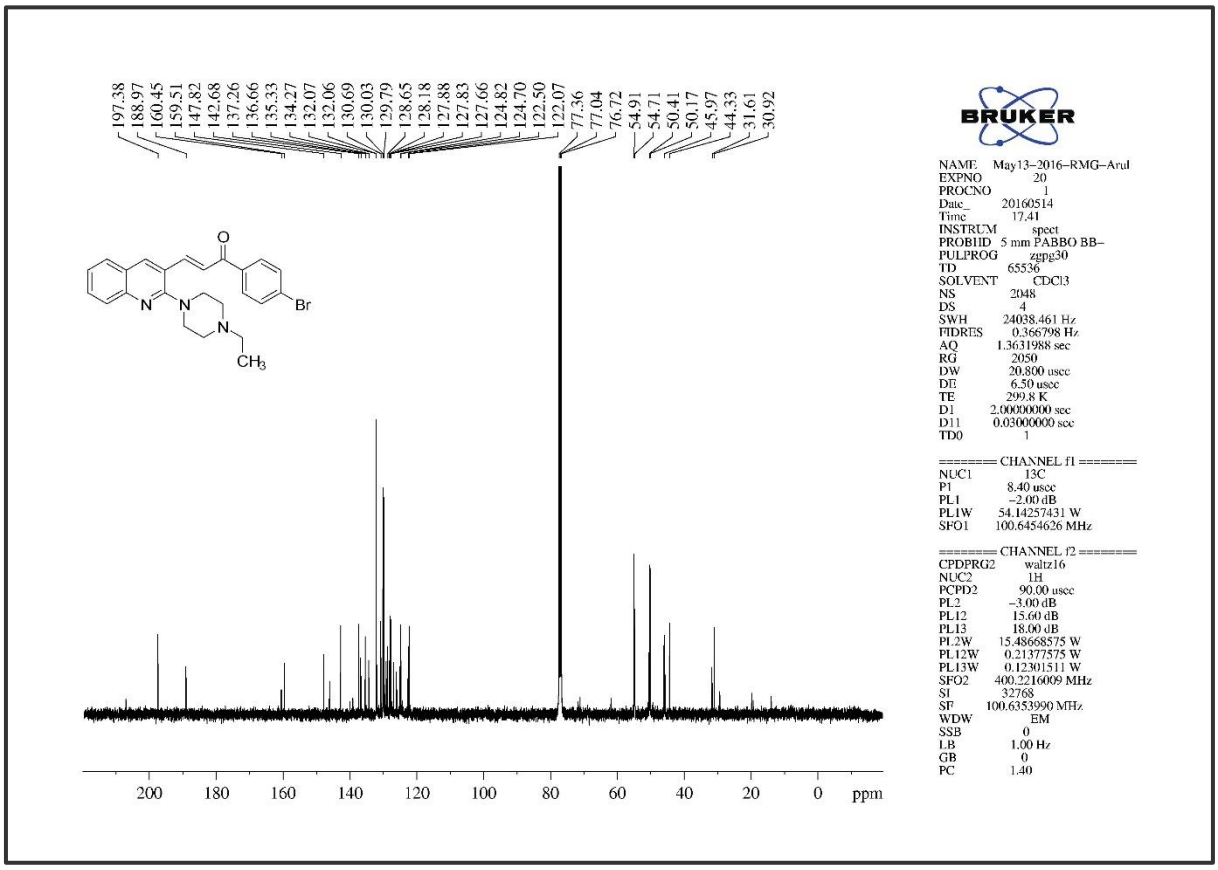

Figure 5B. S. 37. The ^{13}C NMR of compound 5j

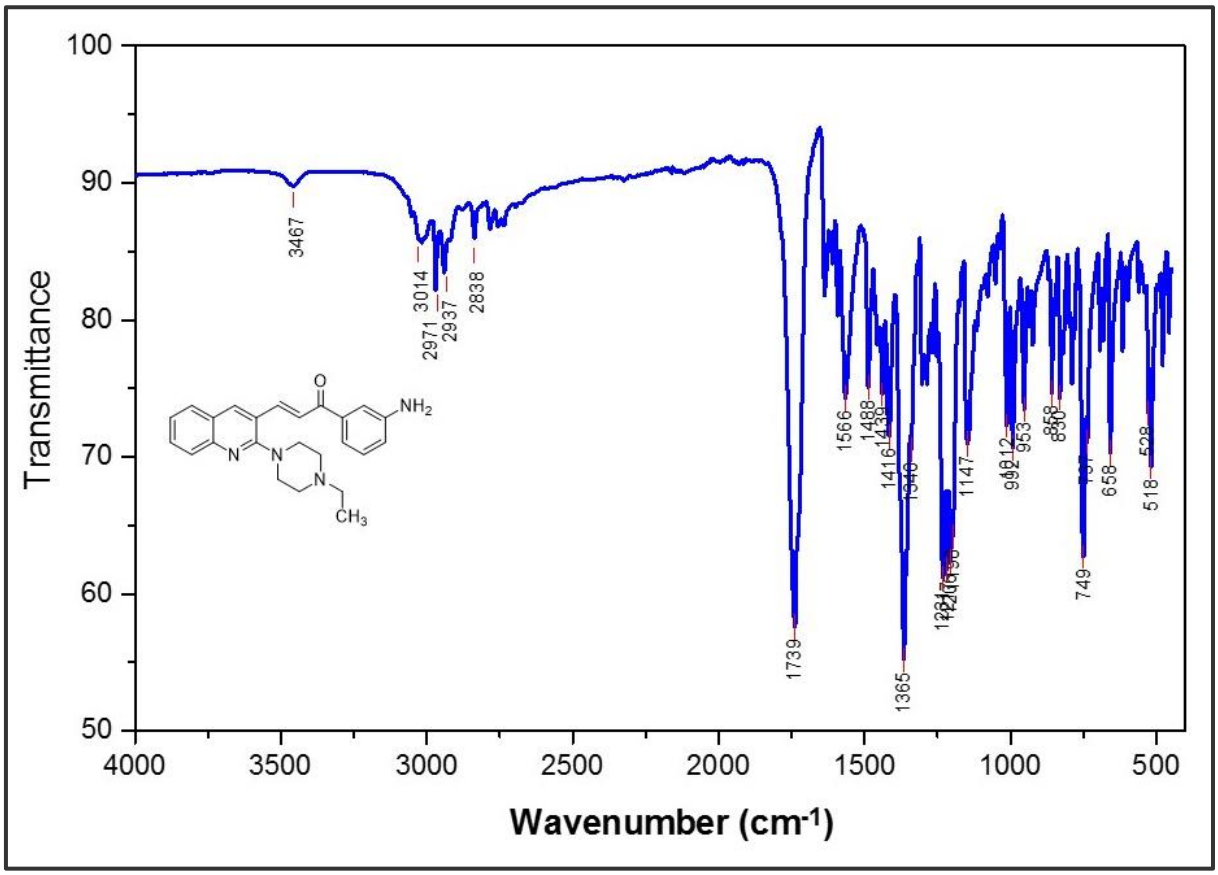

Figure 5B. S. 38. The Infra-Red Spectrum of compound 5k

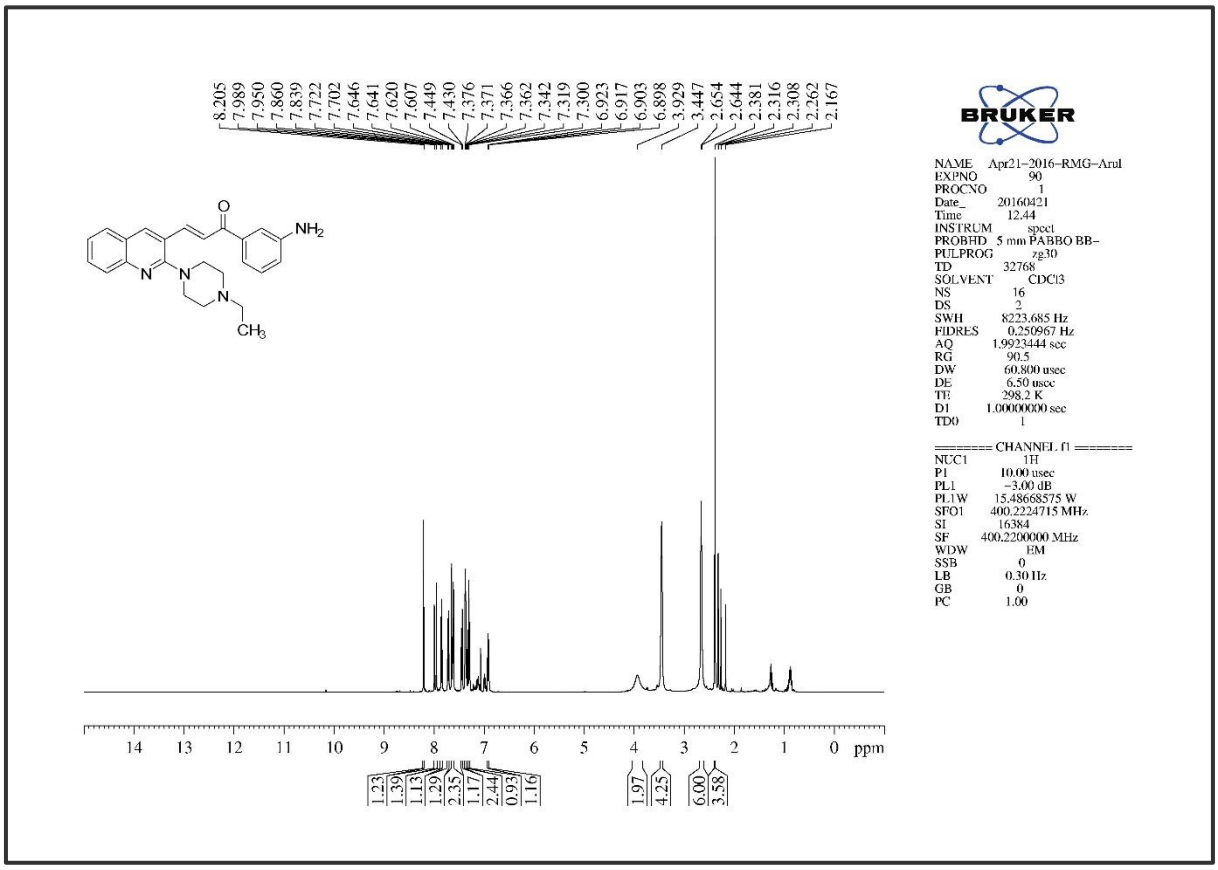

Figure 5B. S. 39. The ^{1}H NMR of compound 5k

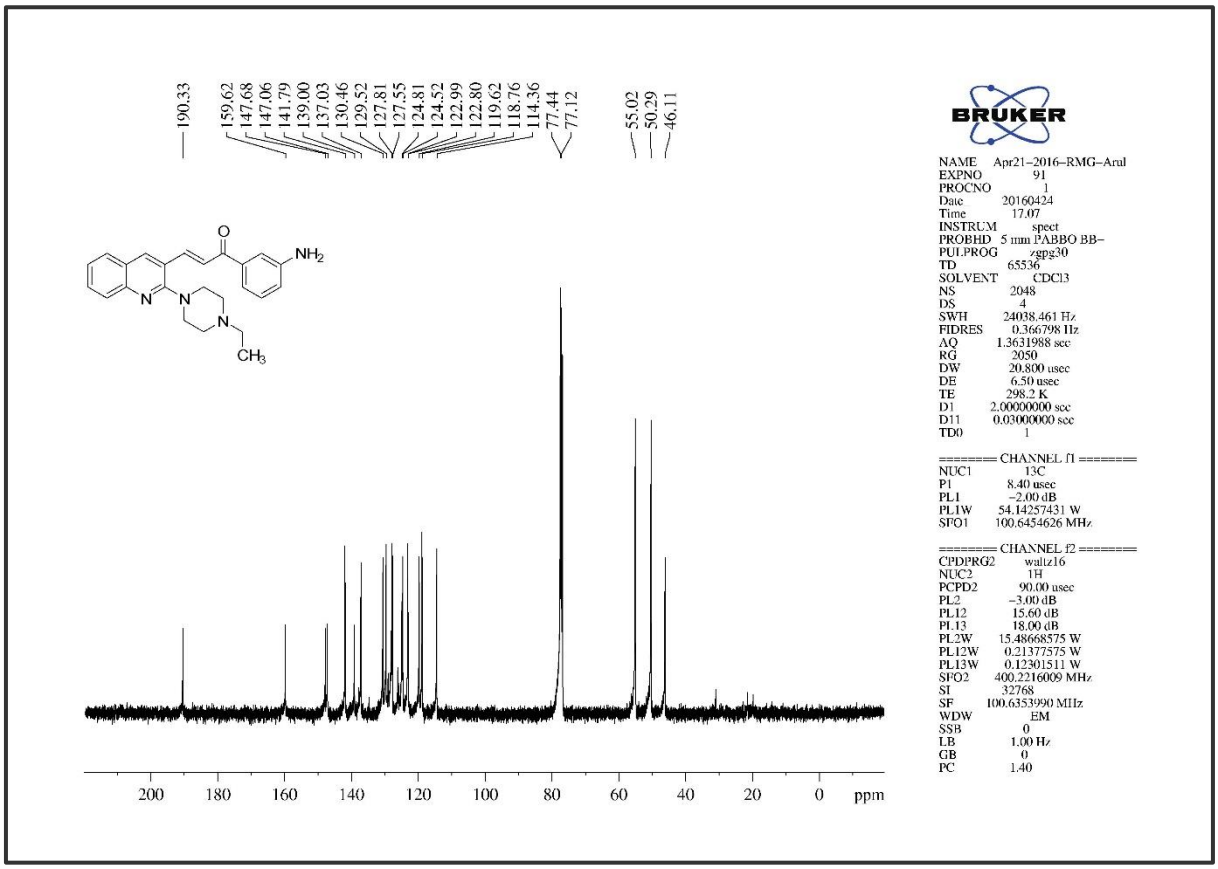

Figure 5B. S. 40. The ^{13}C NMR of compound 5k

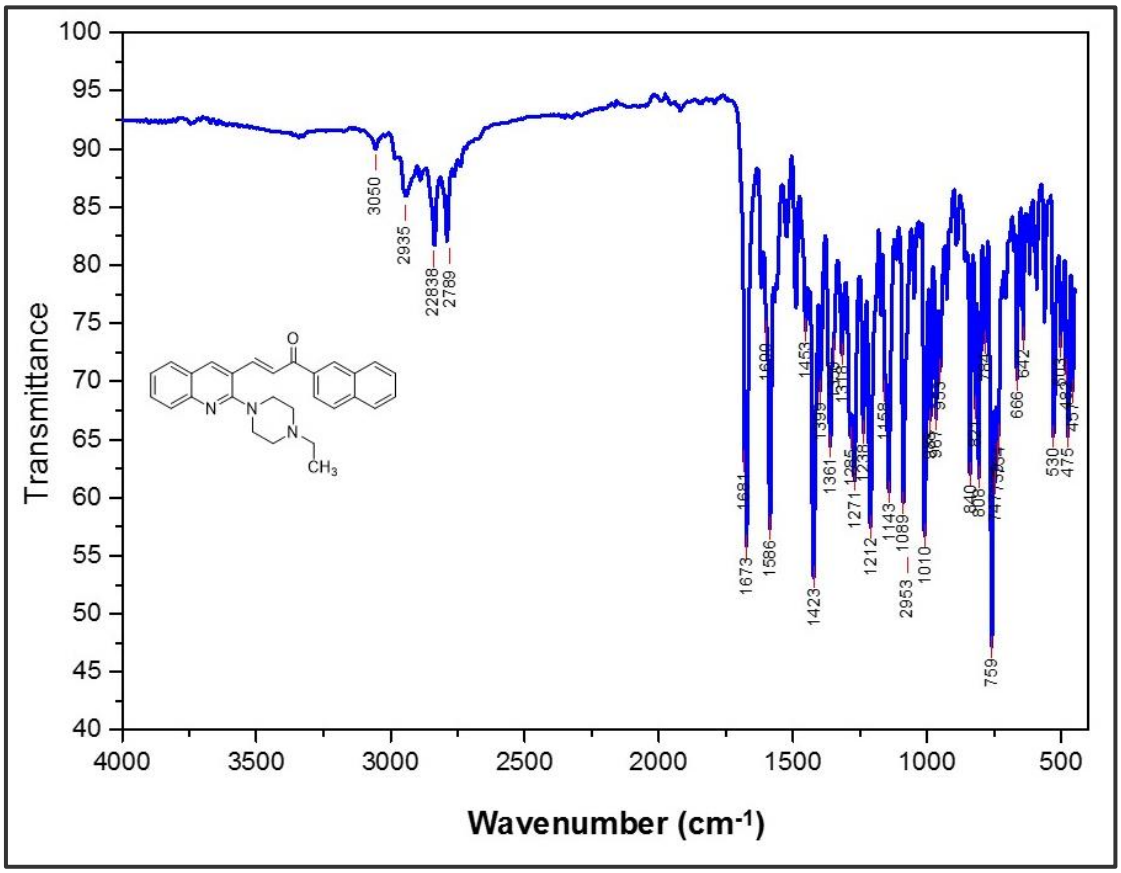

Figure 5B. S. 41. The Infra-Red Spectrum of compound 5l

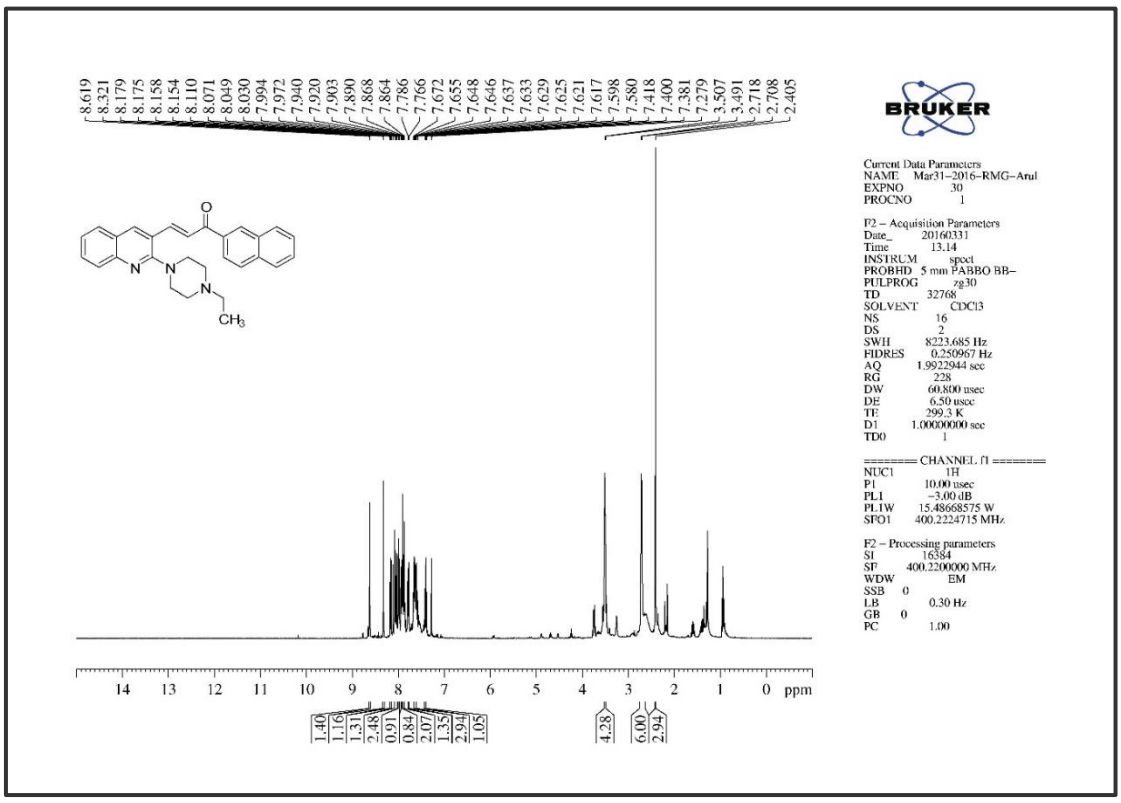

Figure 5B. S. 42. The ^{1}H NMR of compound 5l

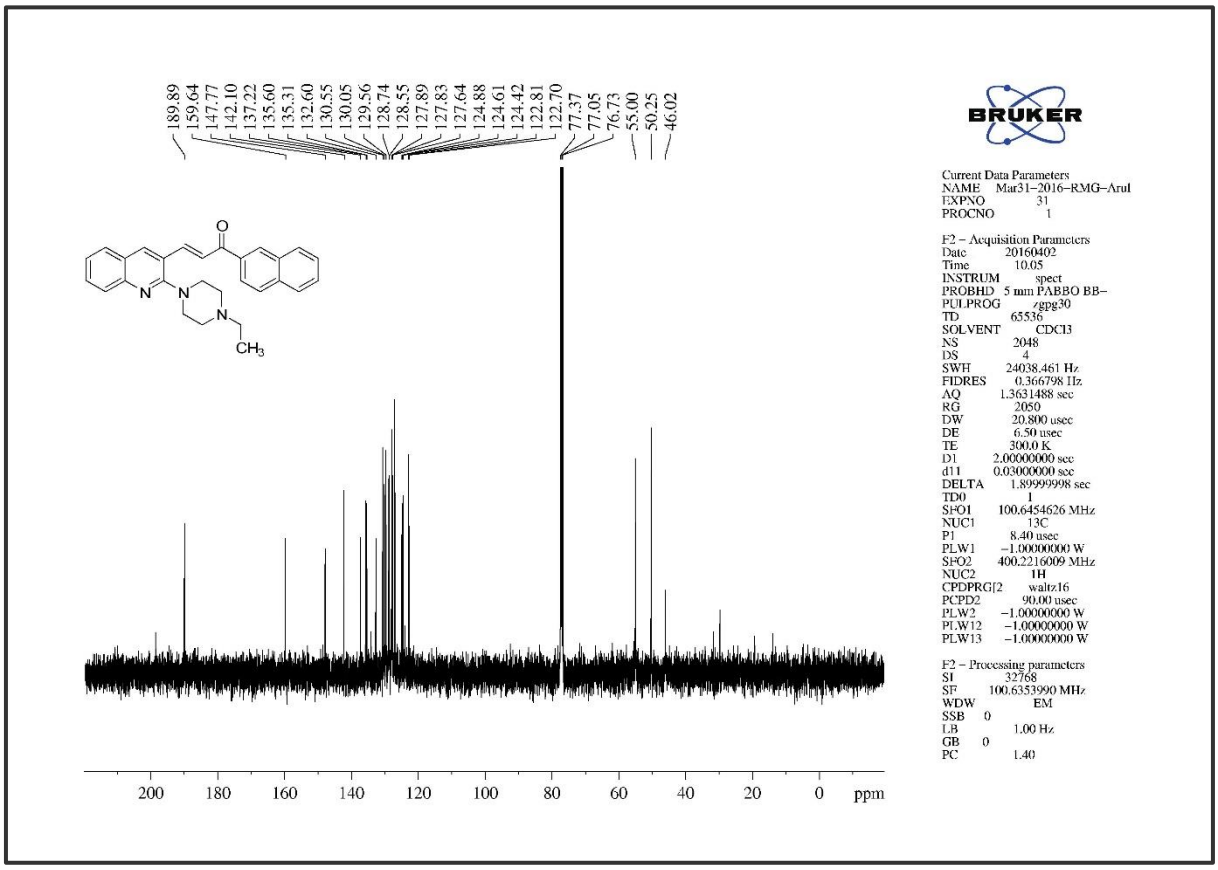

Figure 5B. S. 43. The ^{13}C NMR of compound 5l

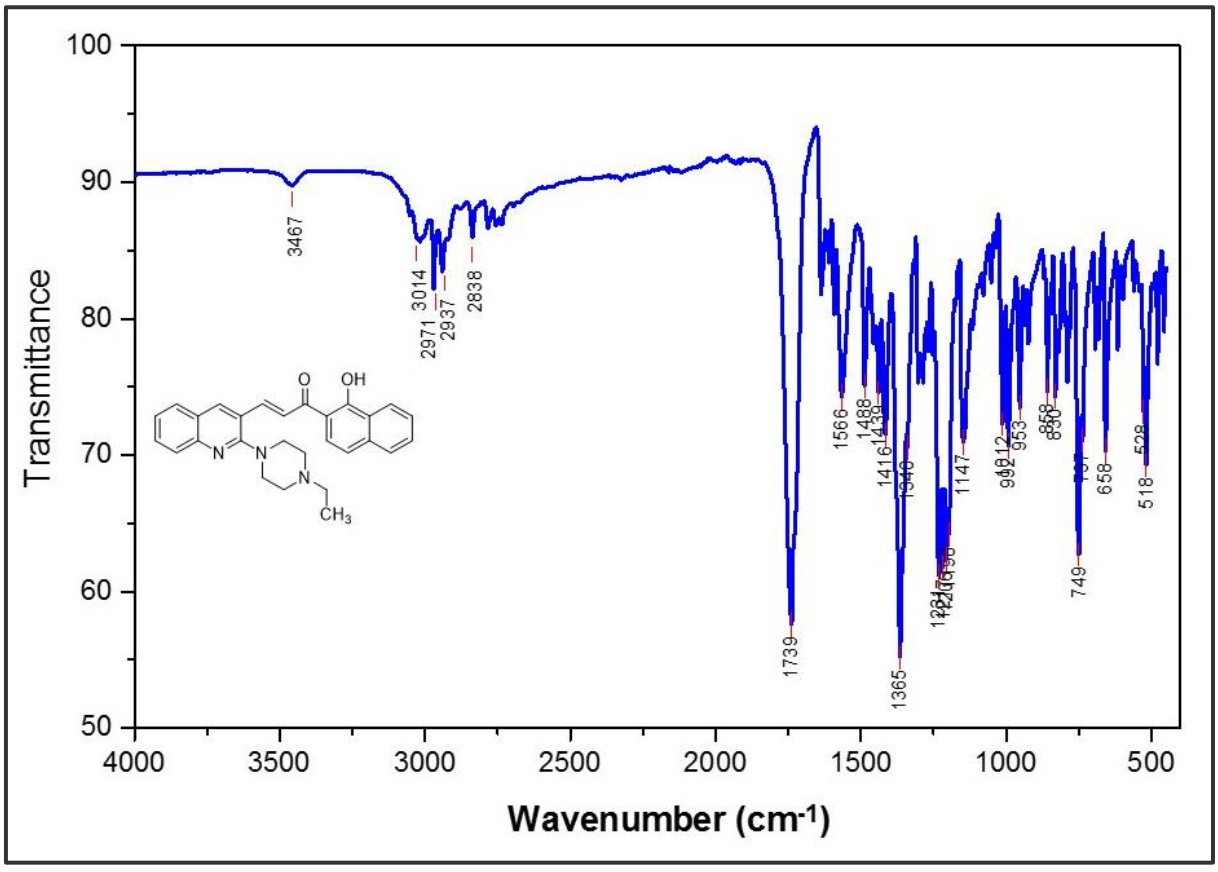

Figure 5B. S. 44. The Infra-Red Spectrum of compound 5m

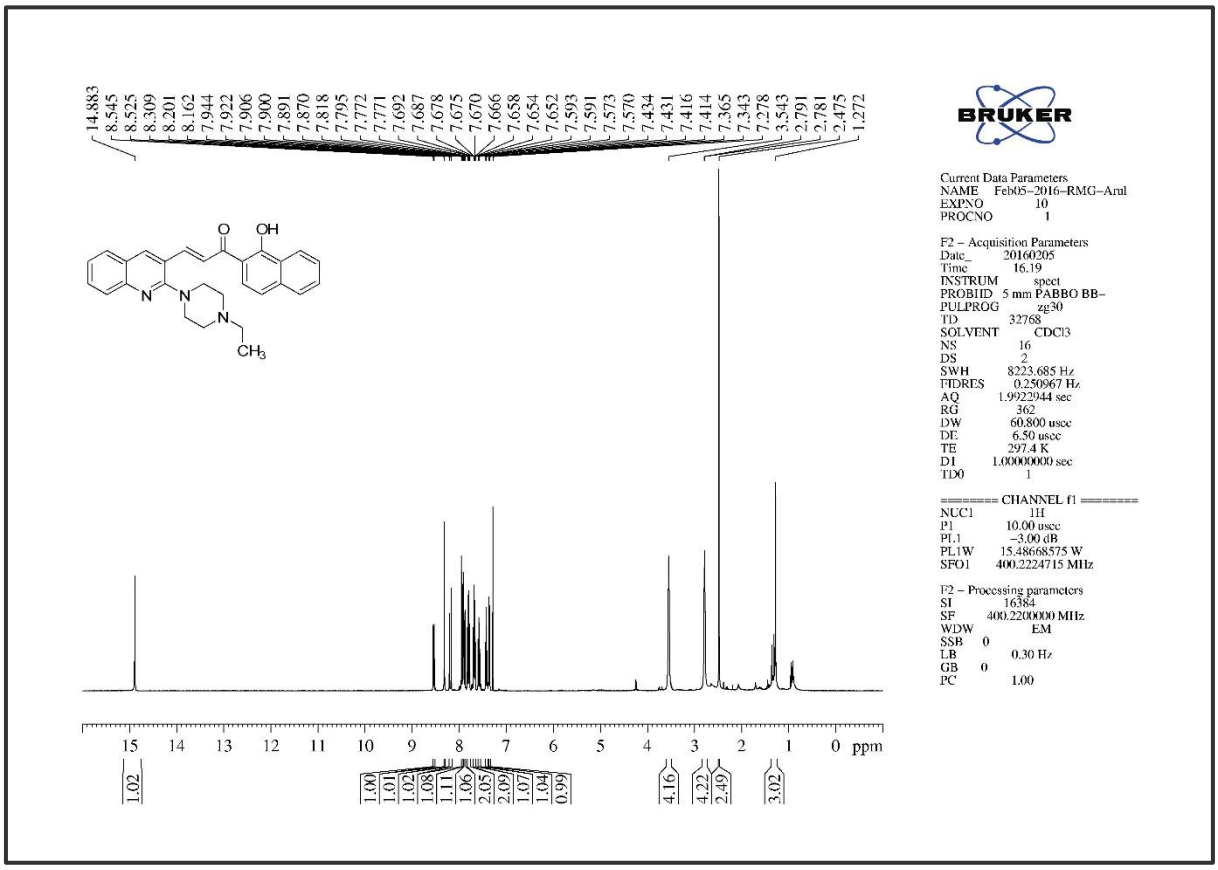

Figure 5B. S. 45. The ^{1}H NMR of compound 5m

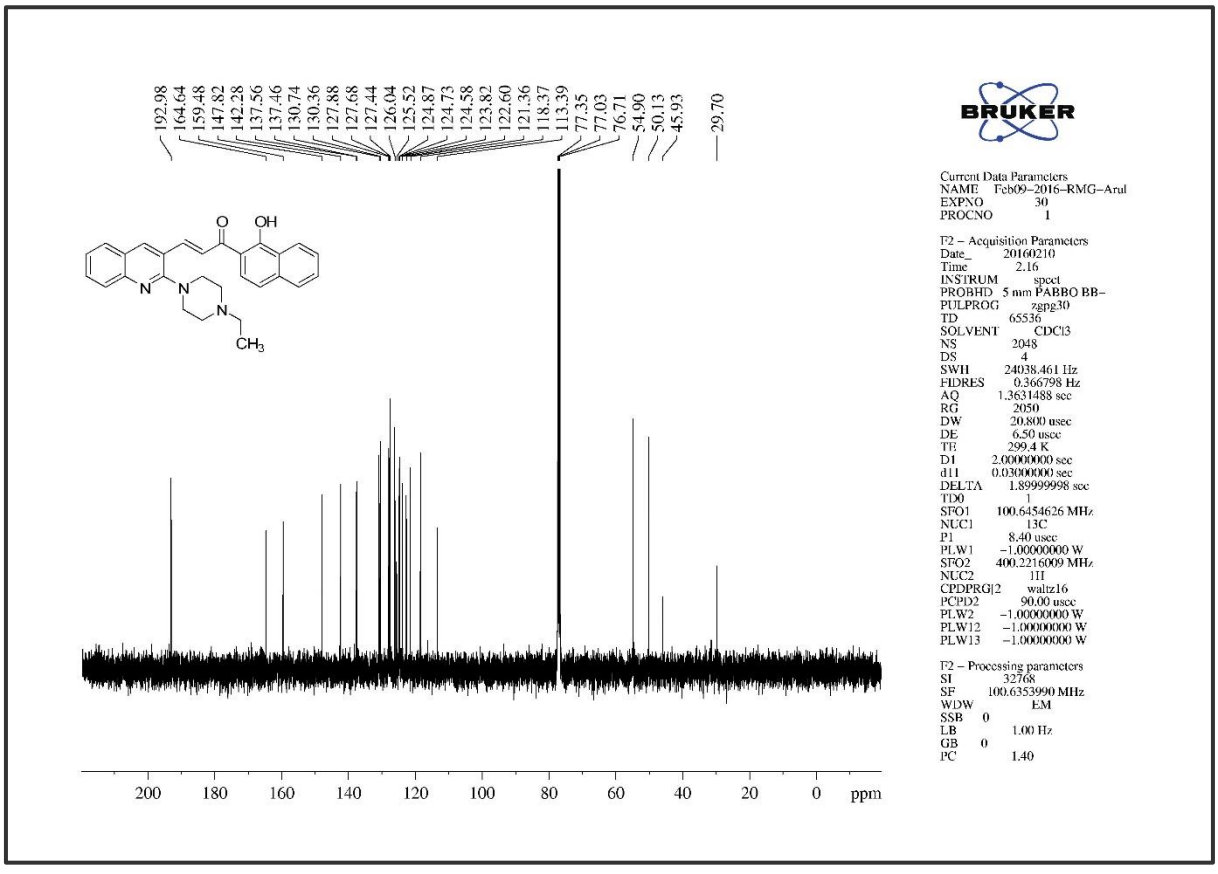

Figure 5B. S. 46. The ^{13}C NMR of compound 5m

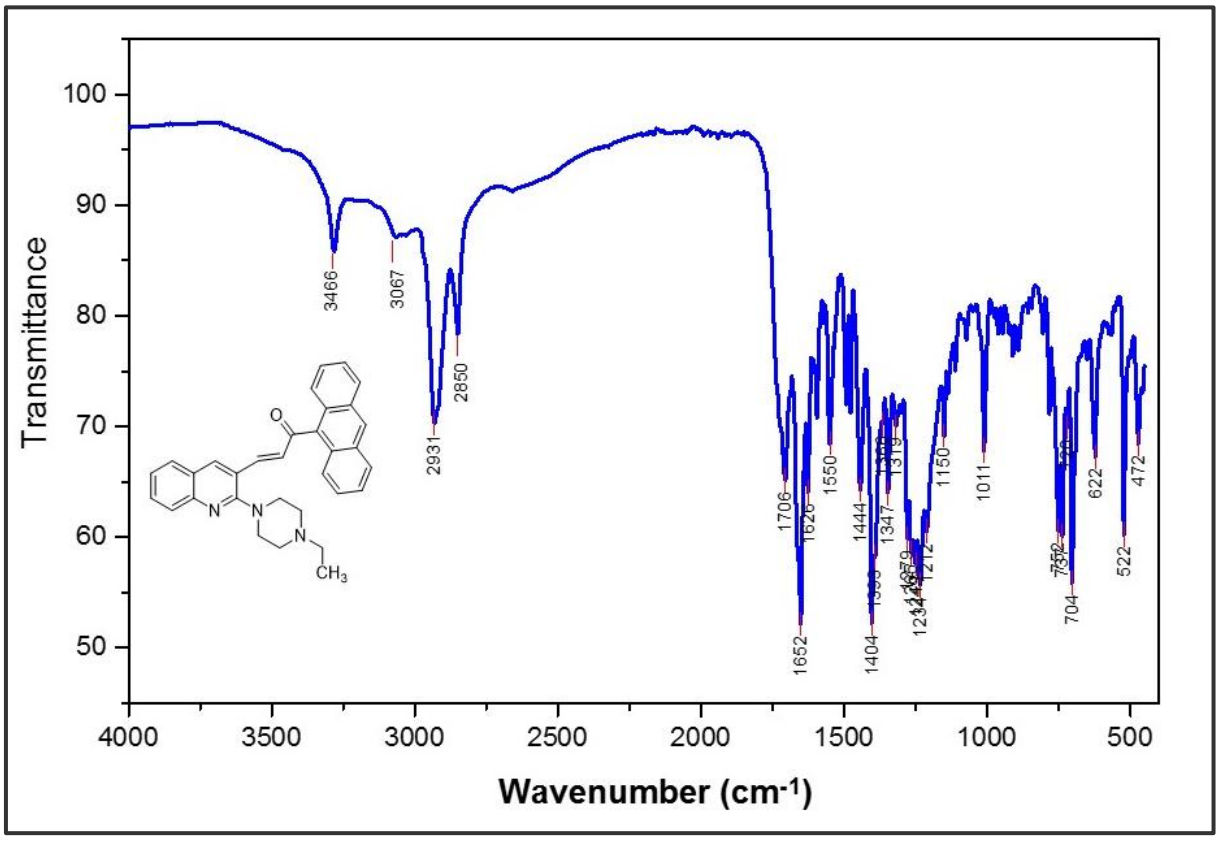

Figure 5B. S. 47. The Infra-Red Spectrum of compound 5n

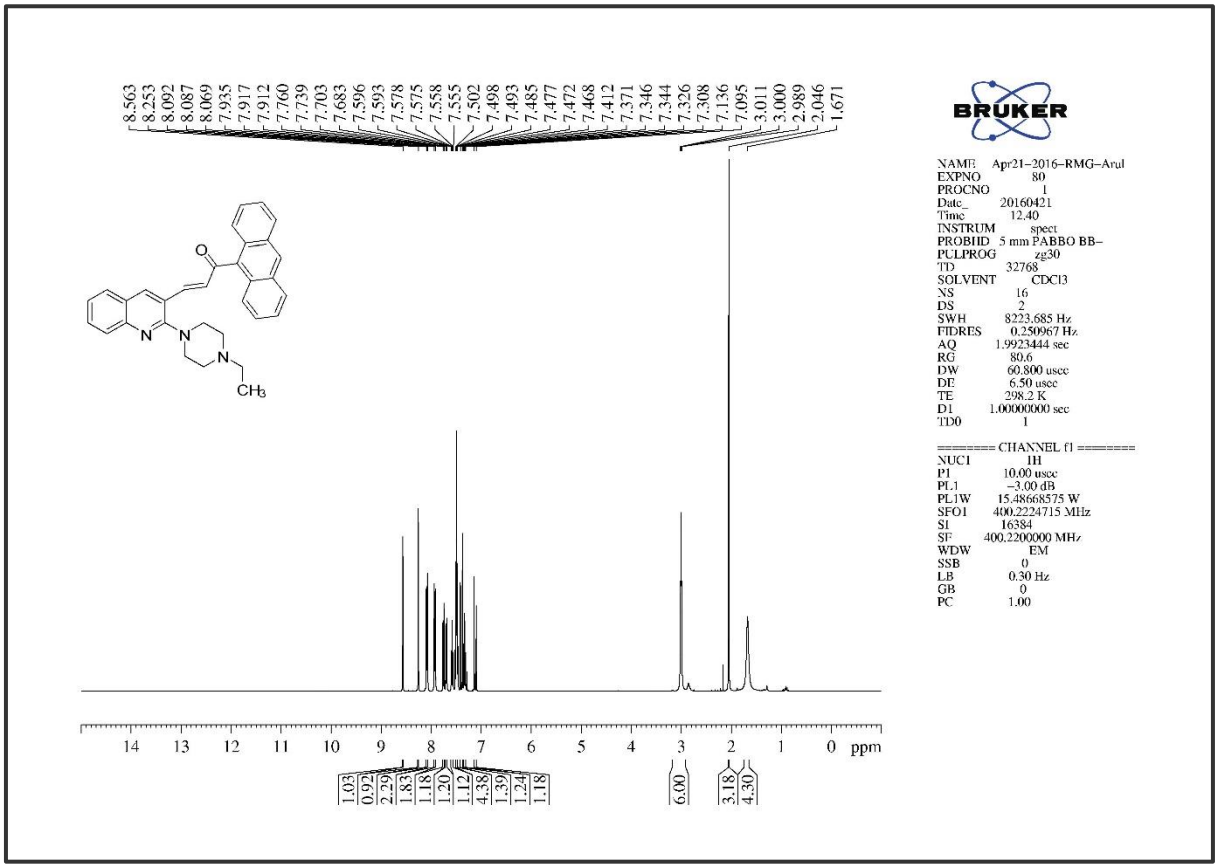

Figure 5B. S. 48. The ^{1}H NMR of compound 5n

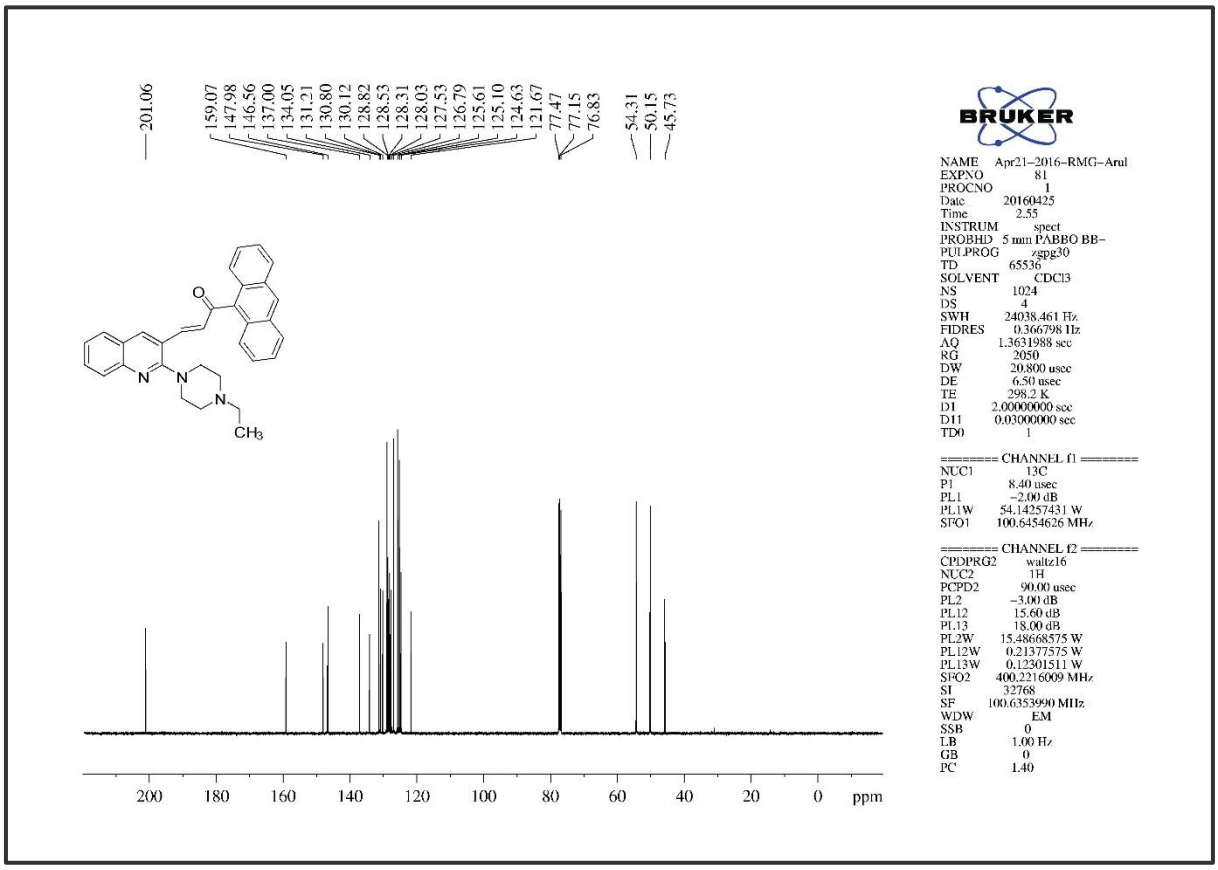

Figure 5B. S. 49. The ^{13}C NMR of compound 5n

Chapter Six

[1]One-pot synthesis of methyl piperazinyl-quinolinyl dispiro derivatives and spectrofluorometric and molecular docking studies

6. 1. Abstract

A series of novel dispiro heterocyclic systems, containing a piperazinyl-quinolinyl nucleus, were synthesized by azomethine ylides via a 1,3 dipolar cycloaddition reaction with a new synthesized (Z)-5-((2-(4-methylpiperazin-1-yl)quinolin-3-yl)methylene)-2-thioxothiazolidin-4-one chalcone as a dipolarophile. In this reaction, isatin and acenaphthalene-1,2-dione were reacted, separately, with sarcosine, thioproline and L-proline by microwave irradiation. The regio and stereochemistry of the synthesized compounds were established by FT-IR, ^{1}H NMR, ^{13}C NMR, 2D NMR and HRMS spectrometry techniques. Furthermore a representative compound 1'-(2-(4-methylpiperazin-1-yl)quinolin-3-yl)-2''-thioxo-5',6',7',7a'-tetrahydro 1'H,2Hdispiro[acenaphthylene-1,3'-pyrrolizine-2',5''-thiazolidine]-2,4''-dione was studied for its binding with human serum albumin (HSA) protein using the fluorescence quench titration method. Molecular docking was also performed to determine their interaction at the binding site of HSA. Addition of the compound to HSA produced slight fluorescence quenching and a red shift in the emission spectra. This was accounted for by considering some structural changes to HSA due to the ligand binding preferably at the tryptophan residue. The biomolecular quenching constant was estimated as 1.21×10^{12} dm^3 mol^{-1} s^{-1} whereas the maximum scatter collision quenching constant with the biopolymer is 2.00×10^{10} dm^3 mol^{-1} s^{-1}. Also, the free energy change for the complexation process of compound and HSA was evaluated as -29.98 kJ mol^{-1} thereby indicating a spontaneous and highly favourable reaction. The free energy changes acquired for HSA binding was -17.79 kJ mol^{-1} which was analogous with the experimental value obtained from emission data at room temperature. These observations support Tyr-263 as the moiety for binding between HSA and the compound.

[1]Arul Murugesan, R M Gengan* Ramar Rajamanikandan, Malaichamy Ilanchelian *"One-pot synthesis via 1, 3-dipolar cycloaddition reaction to piperazinyl-quinolinyl dispiro heterocyclic derivatives and spectrofluorometric and molecular docking studies on their binding with human serum albumin" Journal of molecular Structure,* ***2017, 1149, 439-451.***

6. 2. Introduction

Rhodanine-based molecules display good biological activities including anti-inflammatory and anti-hypertensive activities (Moulard *et al.* 1993:731) hence they are highly utilised in drug discovery strategies (Kim *et al.* 2008:2122). The pyrrolo-thiazoles are also endowed with a wide-range of biological activities, namely heptoprotective (Hasegawa *et al.* 1995:1125), antibiotic (Baldwin *et al.* 1989:4537), antidiabetic (Aicher *et al.* 1998:8579) and anticonvulsant actions (Trapani *et al.* 1994:197). The 2,3 dihydro-4-quinolone derivatives present in many alkaloids (Svoboda *et al.* 1966:758), is an important intermediate in organic synthesis (Nieman and Ennis 2000:1395) and exhibits a wide range of pharmacological properties such as antibacterial (Morrissey and Smith 1995:4), antimalarial (LaMontagne et al. 1989:1728), antitumor (Xia *et al.* 1998:1155), CRTH2 antagonist receptor (Liu *et al.* 2009:6840) and 5HT6 serotonin receptor (Park *et al.* 2011:698). When these functionalised scaffolds are fused into a single molecule, the biological potency of the new molecule was predicted to have increased activity.

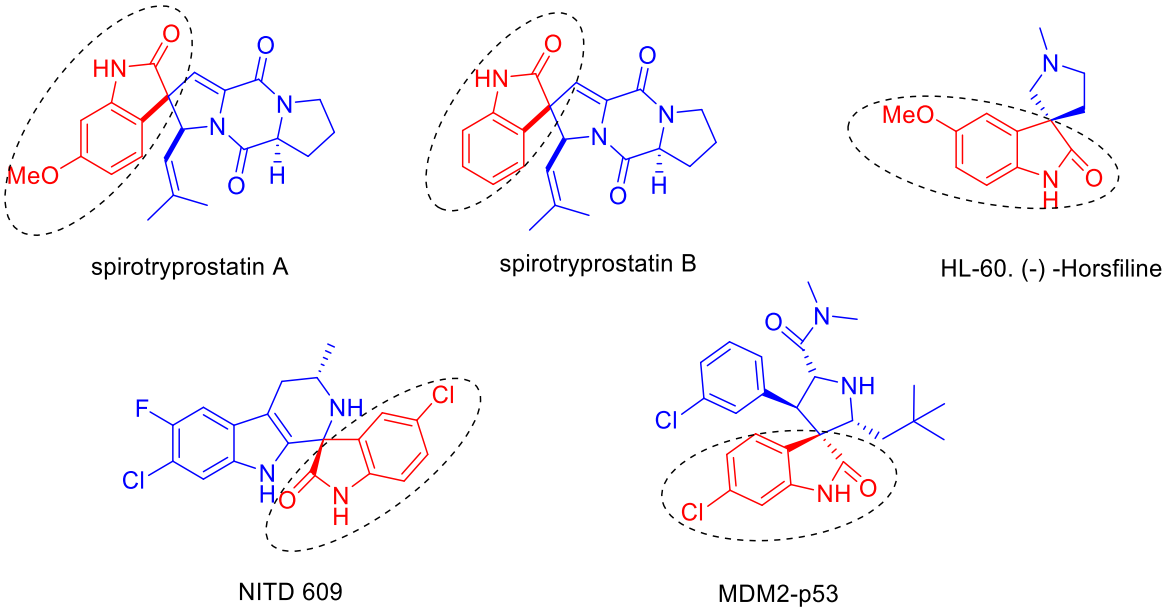

Figure 6. 1. Biologically active naturally occurring spiro compounds

The dispiro nitrogen containing heterocyclic compounds are usually prepared by a 1, 3 dipolar cycloaddition reaction (Padwa and Pearson 2013), (Sarotti *et al.* 2012:2556), (Maheswari *et al.* 2010:7278), (Yavuz *et al.* 2013:1437), (Alcaide *et al.* 2000:458) of dipolarophile azomethine ylides with a particular substrate especially with a five-membered heterocycles such as substituted pyrrolidine (Kawashima *et al.* 2007:1630). When this reaction

is performed in a multi-component system, the creation of chemical archives of potent drug-like compounds is possible which might be used in combinatorial chemistry for their profiling (Spandl *et al.* 3009:1148). These dispiro heterocycles containing two sp^3 carbon atoms, with different cyclic moieties, are biologically important (Van der Sar *et al.* 2006:2059) molecules. The spiro oxindoles are important pharmacological agents which display pronounced cell-type-specific anti-cancer properties (Kondoh *et al.* 1999:411). Typical examples are Horsfiline (Jossang *et al.* 1991:6527) which is a natural product, spirotryptostatine A and B (Cui *et al.* 1996:832) and NITD 609 which is a non-peptide inhibitor of MDM2-p53 (Van Pelt-Koops *et al.* 2012:3544), (Lu *et al.* 2006:3759) (Fig 6. 1).

The 1,3 cycloaddition of azomethine ylides with an acetylenic dipolarophile is one of the most effective approaches for the regio and stereo selective construction of a variety of complex spiro-oxindole derivatives (Albertshofer *et al.* 2012:1834) including quinoline based molecules (Chandraprakash *et al.* 2013:3896). Quinolines perfectly displayed potent biological activity hence the 1,3 cycloaddition reaction was selected for the synthesis of novel dispiro heterocyclic derivatives containing the quinoline moiety.

6. 3. Results and discussion

To synthesize new piperazinyl-quinolinyl dispiro heterocyclic derivatives, 2-(4-methylpiperazin-1-yl)quinoline-3-carbaldehyde **3** was employed (Chapter 3 described the synthesis and characterisation). The reaction plan was a combination of linear and MCRs. The first reaction was linear followed by MCRs. Firstly, the new chalcone (Z)-5-((2-(4-methylpiperazin-1-yl)quinolin-3-yl)methylene)-2-thioxothiazolidin-4-one **5** was synthesized by a condensation reaction of a mixture containing **3** and rhodanine **4** (Scheme 6. 1). This reaction occurred in a mixture of CH_3COOH/CH_3COONa in 6 h of reflux. The reaction was monitored by TLC. **5** was characterized by FT-IR, ^1H NMR, ^{13}C NMR, MS-TOF and elemental analysis.

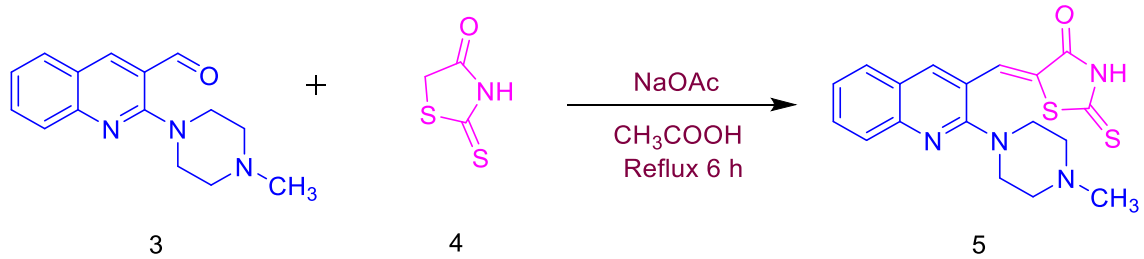

3 4 5

Scheme 6. 1. Synthesis of (Z)-5-((2-(4-methylpiperazin-1-yl)quinolin-3-yl)methylene)-2-thioxothiazolidin-4-one

The FT-IR spectrum of **5** showed N-H stretching at 3452 cm^{-1}, C=O stretching at 1641 cm^{-1} and C=S at 1232 cm^{-1}. The ^{1}H-NMR spectrum exhibited three singlet protons at δ 8.12 (Ar-H) whist the remaining aromatic protons were in the region of δ 7.42-7.85. The signals at δ 6.90 was assigned to C-H whist δ 6.73 was assigned to N-H. The carbon spectrum showed the carbonyl group C=O at δ 200.79 and thiaxothiazolidin group C=S at δ 178.43. The HRMS data: TOFMS ES *m/z* (rel. int.): m/z: 369.08 $[M]^{+}$and elemental analysis: Anal. Calc. for $C_{18}H_{18}N_4OS_2$: C, 58.35; H, 4.90; N, 15.12 %. Found: C, 58.37; H, 4.88; N, 15.14 %, confirmed the structure.

Secondly, MCRs was used. The dispiro heterocyclic derivatives (**10a-15l**) (Scheme 6. 2 and 6. 3) were synthesized by using **5** together with isatin **6** or acenaphthenequinone **6a** and secondary amino acids sarcosine **7**, L-thioproline **8** and L-proline **9,** separately. This is a 1,3-dipolar cycloaddition reaction. Herein the correct substrates were simply added and refluxed in methanol, under MW irradiation conditions.

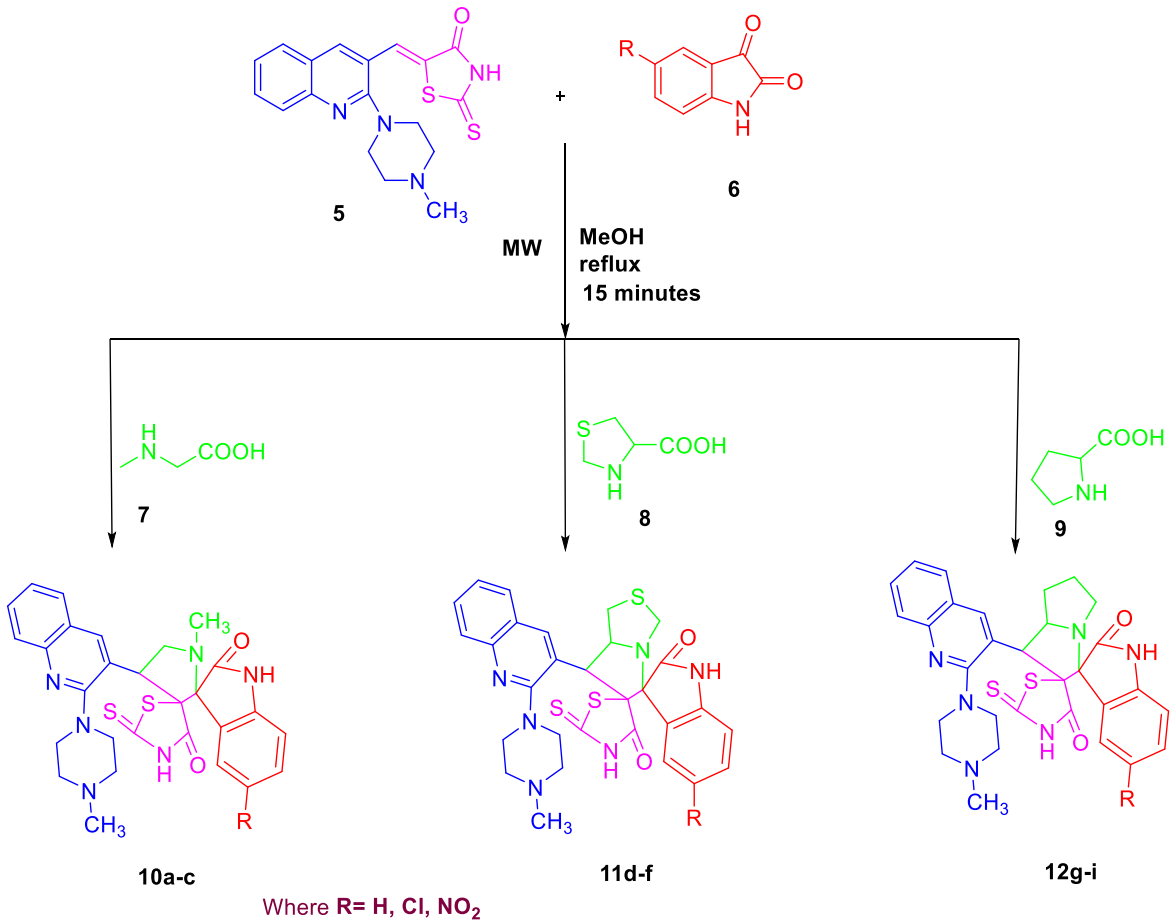

Scheme 6. 2. Synthesis of piperazinyl-quinolinyl dispiro heterocycle isatin derivatives

In a preliminary study to synthesize **10a** (Scheme 6. 2), various solvents (Table 6. 1) such as ethanol, methanol, acetonitrile, toluene, dioxane, isopropyl alcohol, t-butyl alcohol and DMF were compared. This reaction involved 6-12 h of reflux: the TLC profile was used to determine complete conversion to **10a**. Moderate yields were observed when solvents such as ethanol, methanol and acetonitrile were used (Table 6.1 entries 1-3). The yield decreased and a longer reaction time was required when the other solvents were used (Table 6.1 entries 4-8). The yield decreased and a longer reaction time was required in solvents such as iso-propanol, tert-butanol and DMF under reflux conditions for 8 h (Table 6. 1 entries 6-7). Since methanol gave the highest yield, it was selected for all subsequent reactions. When MW irradiation was used, the reaction went to completion in 15 minutes at 120 W (Table 6.1 entry 9) compared to conventional reflux which was 6 h. Furthermore, it was observed that at 100 ˚C some additional spots were present on the TLC plate which was taken as evidence formation of by-products. Also, a shorter reaction time showed the presence of starting materials thereby indicating an incomplete reaction.

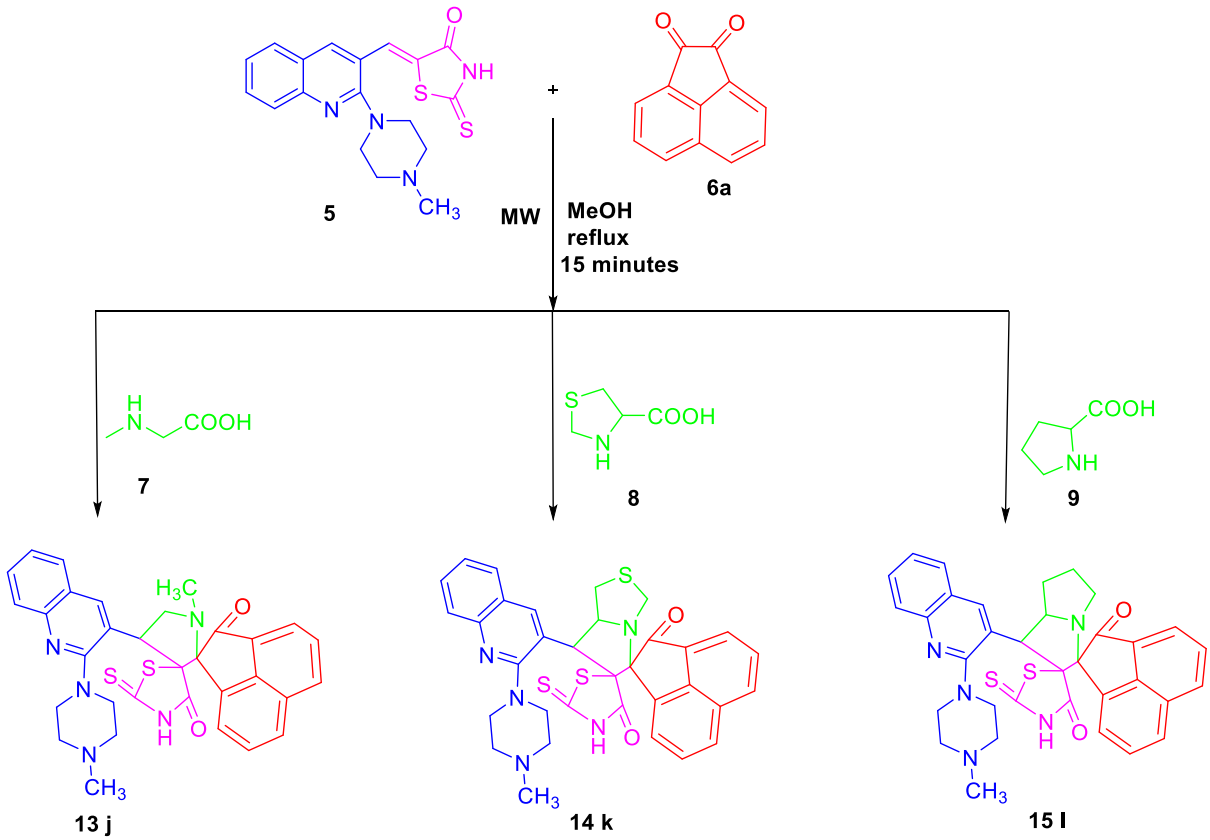

Scheme 6. 3. Synthesis of piperazinyl-quinolinyl dispiro heterocycle acenaphthalene derivatives

The synthesis of **10a-15l** was conducted in methanol in a MW irradiation reflux system for a reaction time of 15 min at 120W. The product yields (Table 6. 2) ranged from 75 to 90 %. The presence of electron withdrawing groups such as NO_2 and Cl on the aromatic ring for isatin led to good yields of product (5-nitroisatin 75 %, 77 %, and 80 % for entries 3, 6, and 9 respectively), (5-chloro isatin 80 %, 82 %, and 83 % for entries 2, 8, and 5 respectively). In the case of isatin and acenaphthenequinone, good yields of product were obtained: isatin (87 %, 90 %, and 90 % for entries 4, 1 and 7 respectively) and acenaphthalene (85 %, 87 % and 90 % for entries 11, 10 and 12, respectively).

All the compounds **10a-15l** were characterized by FT-IR, ^{1}H NMR, ^{13}C NMR, MS-TOF except **11d** which also included DEPT-90 and DEPT-135, COSY, NOSEY, HSQCE, HMBC whereas **10a**, **11d** and **14k** included ^{13}C and APT (all spectra are as presented in the Appendix).

Table 6. 1. The effect of solvents for the synthesis of 10a

Entry	Temp (^{o} C)	Solvent	Time(h/mins)	Isolated Yield (%)
1	Reflux	EtOH	6	80
2	Reflux	MeOH	6	85
3	Reflux	CH_3CN	6	80
4	Reflux	Toluene	12	65
5	Reflux	Dioxane	12	58
6	Reflux	i-PrOH	8	75
7	Reflux	t-BuOH	8	70
8	Reflux	DMF	8	60
9	MWI	MeOH	15 (mins)	90

Equimolar quantities (1 mmol) of reactants were used

As a typical analysis, **11d** showed FT-IR stretching frequency at 3454 and 3201 cm^{-1} for N-H , two C=O stretching at 1706 and 1672 cm^{-1} for the thioxothiazolidin and indole moieties, respectively whilst the C=S occurred at 1224 cm^{-1}. The ^{1}H NMR spectrum showed four singlets

at δ 10.52, 8.38, 5.22, and 2.08 corresponding to the 2-thioxothiazolidin-4-one N-H, quinoline C_4-H, indole N-H, and piperazinyl CH_3 group respectively. Eight aromatic protons were at δ 6.77-8. The specific regio-isomer was decided on the basis of a doublet at δ 4.49 (J= 9.32 Hz) for the $C_{7'}$-H proton and the C_{7a}'-H proton appeared as a triplet. Furthermore, the $_{1'}$-CH_2 thiazolidine ring proton appeared as a doublet at δ 3.41 (J= 5.4 Hz). The ^{13}C NMR spectrum showed the presence of two spiro carbon peaks at δ 74.52 and 109.82. The methyl and methylene carbon peaks were at δ 36.6, 31.4, 46.00 and 50.00 which were confirmed on the ^{13}C, ^{1}H-COSY correlation spectrum. The carbonyl and thio-carbonyl peaks were at δ 176.53 and 206.46, respectively. The two spiro carbons were confirmed by the DEPT-135 spectrum: peaks at δ 74.52 and δ 109.82. The selected HMBC correlation of compound **11d** is shown in Figure 6. 2.

Table 6. 2. The physical data for the synthesis of dispiro heterocycles

Entry	Amino acids	Product	6 or 6a	Yield (%)	M. p (˚C)
1	7	10a	$C_8H_5NO_2$	90	232-234
2	7	10b	5-$C_8H_4ClNO_2$	80	250-252
3	7	10c	5-$C_8H_4N_2O_4$	75	243-245
4	8	11a	$C_8H_5NO_2$	87	230-232
5	8	11b	5-$C_8H_4ClNO_2$	83	235-237
6	8	11f	5-$C_8H_4N_2O_4$	77	270-272
7	9	12g	$C_8H_5NO_2$	90	250-252
8	9	12h	5-$C_8H_4ClNO_2$	82	240-242
9	9	12i	5-$C_8H_4N_2O_4$	80	247-249
10	7	13j	$C_{12}H_6O_2$	87	220-224
11	8	14k	$C_{12}H_6O_2$	85	228-230
12	9	15l	$C_{12}H_6O_2$	90	218-220

Equimolar quantities (1 mmol) of reactants were used

The COSY spectrum revealed one doublet at δ 4. 49 (J= 9. 32 Hz), one singlet at δ 3. 89 and two diastereotopic methane protons as a triplet at δ 3. 41 (J= 5. 4 Hz). In the ^{13}C-COSY spectrum, the signal at δ 143. 54 was assigned to the C_4 quinolinyl carbon. The characteristic quinolinyl proton C_4-H of the quinoline ring showed HMBC correlation with C_2 at δ 145. 17

and C_5 at δ 127. 36. The C_5-H of the quinoline proton correlated with C_2 at δ 145. 17, C_7 at δ 129.39 whilst C_6-H correlated with C_2 at δ 145. 17. The $C_{4''}$-H proton for isatin ring correlated with $C_{5'}$ at δ 109. 82 and $C_{6''}$ at δ 126. 11. The $C_{7'}$-H proton for the pyrrolidine ring correlated with $C_{7a'}$at δ 31.45 and C_5 at δ 127. 36. The $C_{6''}$-H proton for the isatin ring correlated with $C_{4'}$ at δ 125. 42 whilst the $C_{7''}$-H proton showed HMBC correlation with $C_{6''}$ at δ 126. 11.

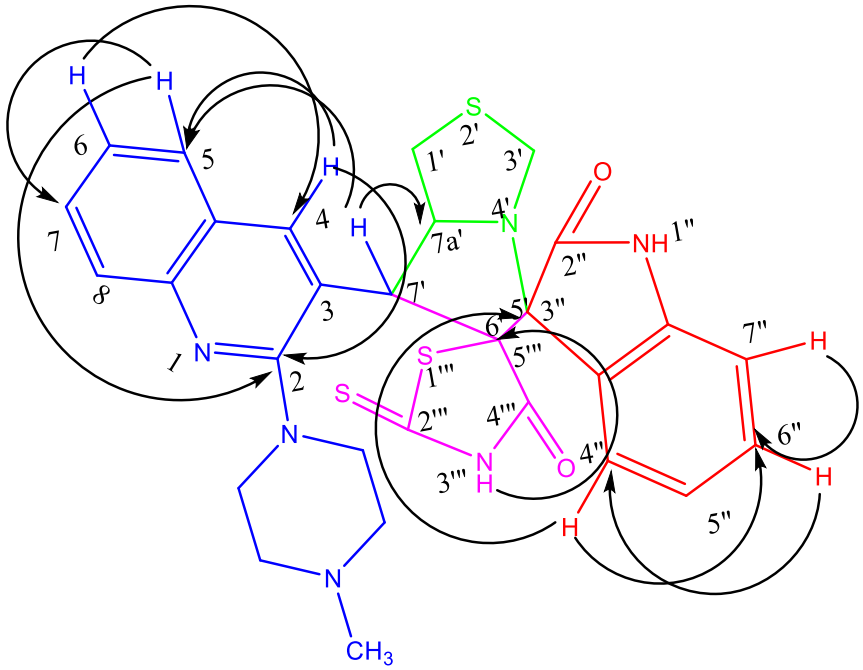

Figure 6. 2. Selected HMBC correlations of compound 11d.

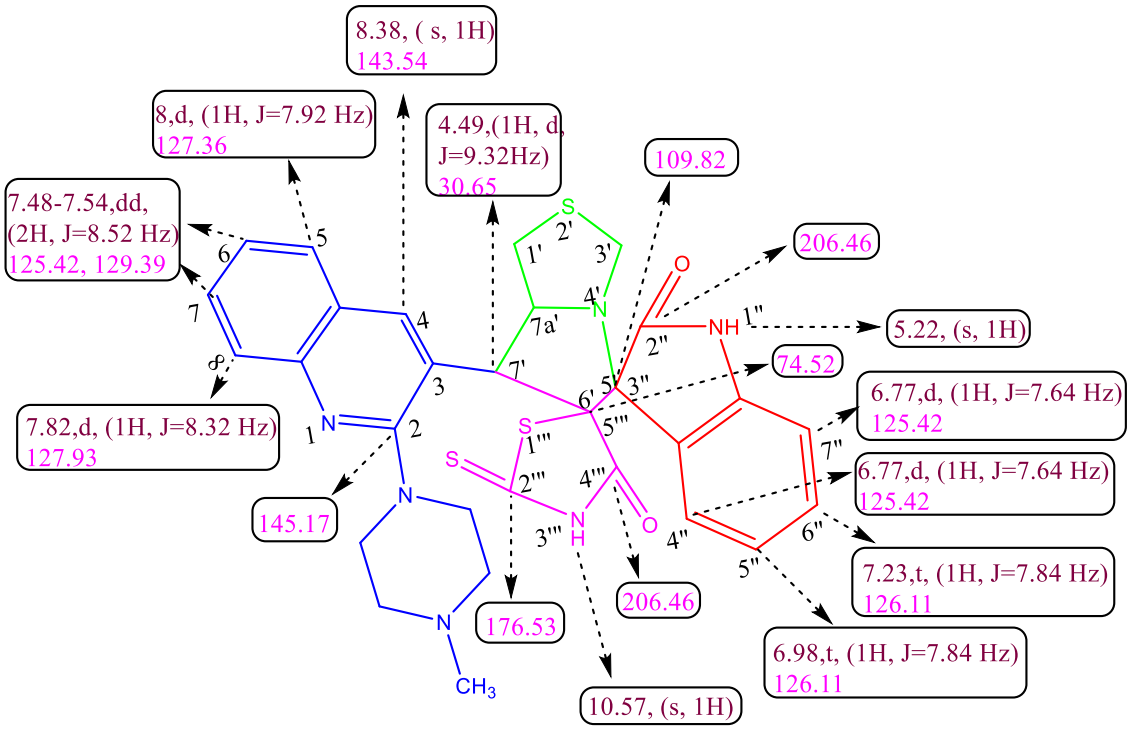

Figure 6. 3. Selected (^{1}H) and (^{13}C) NMR and HMBC chemical shifts of 11d.

Selected ^{1}H NMR, ^{13}C NMR and HMBC chemical shifts of **11d** are presented in Table 6. 3. Based on the above spectral details and its TOF-MS ES *m/z* (rel. int.): m/z: 588.13 $[M]^{+}$ and elemental analysis Anal. Calc. for $C_{29}H_{28}N_6O_2S_3$: C, 59.16; H, 4.79; N, 14.27 %. Found: C, 59.18; H, 4.81; N, 14. 29%, the structure was confirmed as 7'-(2-(4-methylpiperazin-1-yl)quinolin-3-yl)-2"-thioxo-7',7a'-dihydro-1'H,3'H-dispiro[indoline-3,5'-pyrrolo[1,2-c]thiazole-6',5"-thiazolidine]-2,4"-dione.

Table 6. 3. Selected HMBC correlations of compound 11d

S No	Proton	Correlated Carbons
1	C_4-H (s, 1H) at δ 8.38	C_2 at δ (145.17), C_5 at δ (127.36)
2	C_5-H (d,1H, *J*= 7.92 Hz) at δ 8	C_2 at δ (145.17), C_7 at δ (129.39)
3	$C_{4"}$-H (d, 1H, *J*= 7.64Hz) at δ 6.77	$C_{5'}$ at δ (109.82), $C_{6"}$ at δ (126.11)
4	C_6-H (dd,1H, *J*= 8.52 Hz) at δ 7.48-7.54	C_2 at δ (145.17)
5	$C_{7'}$-H (d,1H, *J*=9.32Hz) at δ 4.49	$C_{7a'}$ at δ (31.45), C_5 at δ (127.36).
6	$C_{6"}$-H (t, 1H, *J*= 7.84Hz) at δ. 7.23	$C_{4'}$ at δ (125.42).
7	$C_{7"}$-H (d, 1H, *J*= 7.64Hz) at δ 6.77	$C_{6"}$ at δ (126.11).

As a typical analysis, the FT-IR spectrum of **15l** showed stretching at 3454 cm^{-1} for N-H, 1637 and 1583 cm^{-1} for the 2-thioxothiazolidin-4-one and acenaphthalene pyrrolizidine C=O groups and 1231 cm^{-1} for the C=S groups. The ^{1}H NMR spectrum showed three singlets at δ 8.82, 8.30, and 1.07 corresponding to the 2-thioxothiazolidin-4-one N-H, quinolinyl C_4-H and piperazinyl CH_3 group, respectively. The ten aromatic protons appeared in the range of δ 7.26-7.91. The regio-specificity was established by two doublets at δ 4.05 (*J*= 12.68 Hz) and at δ 3.88 (*J*= 13.56 Hz) for the C_7-H and $C_{7a'}$-H protons, respectively. The $_{1'}$-CH_2 pyrrolizidine ring protons appeared at δ 3.39 (*J*= 12.8 Hz) as a triplet. The ^{13}C NMR spectrum showed the presence of two peaks at δ 110.4 and at δ 113.3 reflecting two spiro carbons. Finally, the sulphur with acenaphthalene carbonyl peaks was found at δ 195.5 and at δ 206, respectively. Base on the above spectral details and mass TOF-MS ES *m/z* (rel. int.): m/z: 591.96 $[M]^{+}$ and good

agreement for elemental analysis, the structure were confirmed as 1'-(2-(4-methylpiperazin-1-yl)quinolin-3-yl)-2"-thioxo-5',6',7',7a'-tetrahydro-1'H,2H-dispiro[acenaphthylene-1,3'-pyrrolizine-2',5"-thiazolidine]-2,4"-dione.

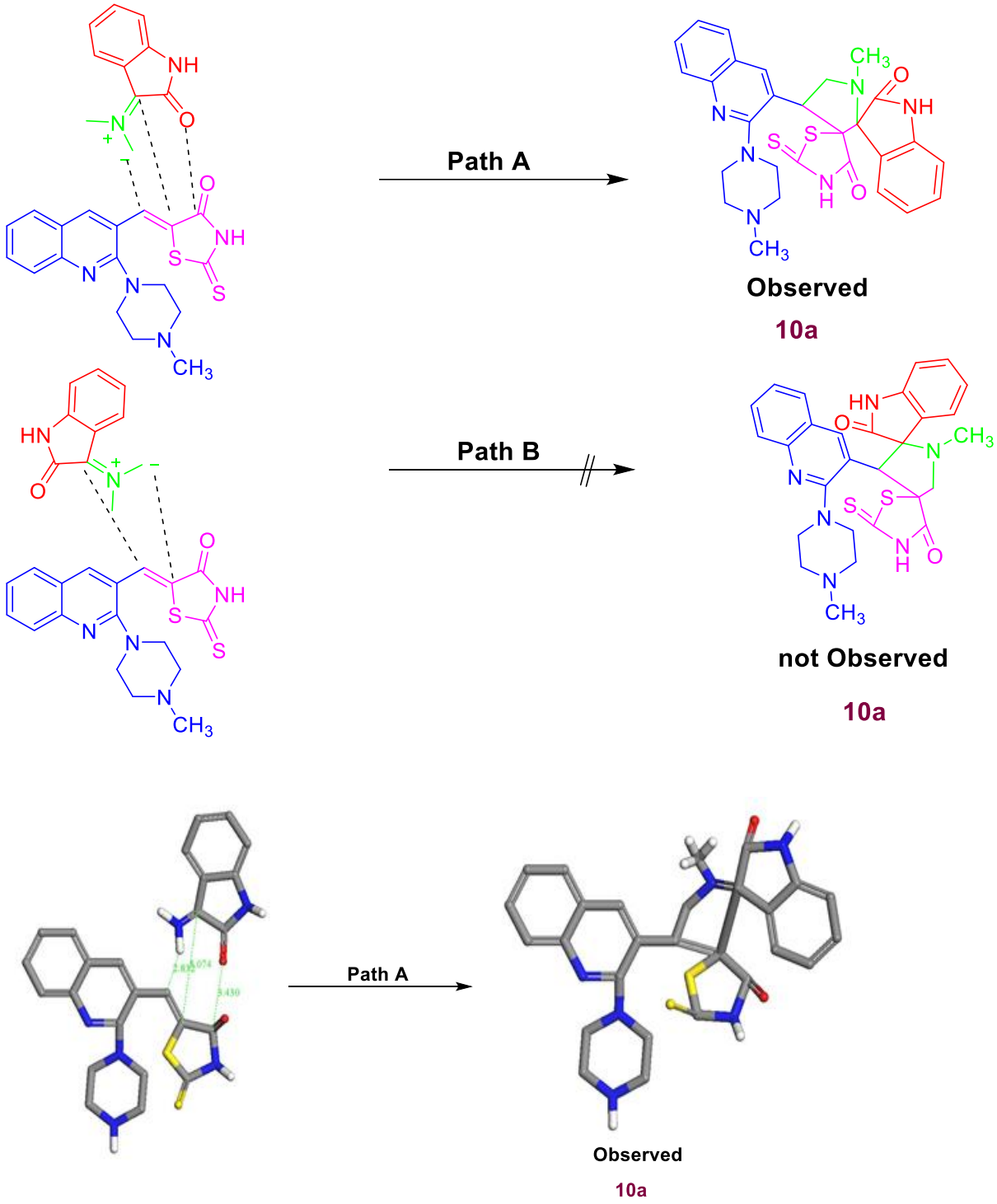

Scheme 6. 4. Secondary orbital interaction of compound 10a

The regio-isomer product **10a** was confirmed on the basis of its secondary orbital interactions. The orbital interaction was between the carbonyl group of **5** with azomethine ylides via endo selectivity. The regio-isomer observed via path A is more favourable because of the secondary orbital interactions whilst path B is not possible in the other isomer of **10a** as shown in Scheme 6. 4.

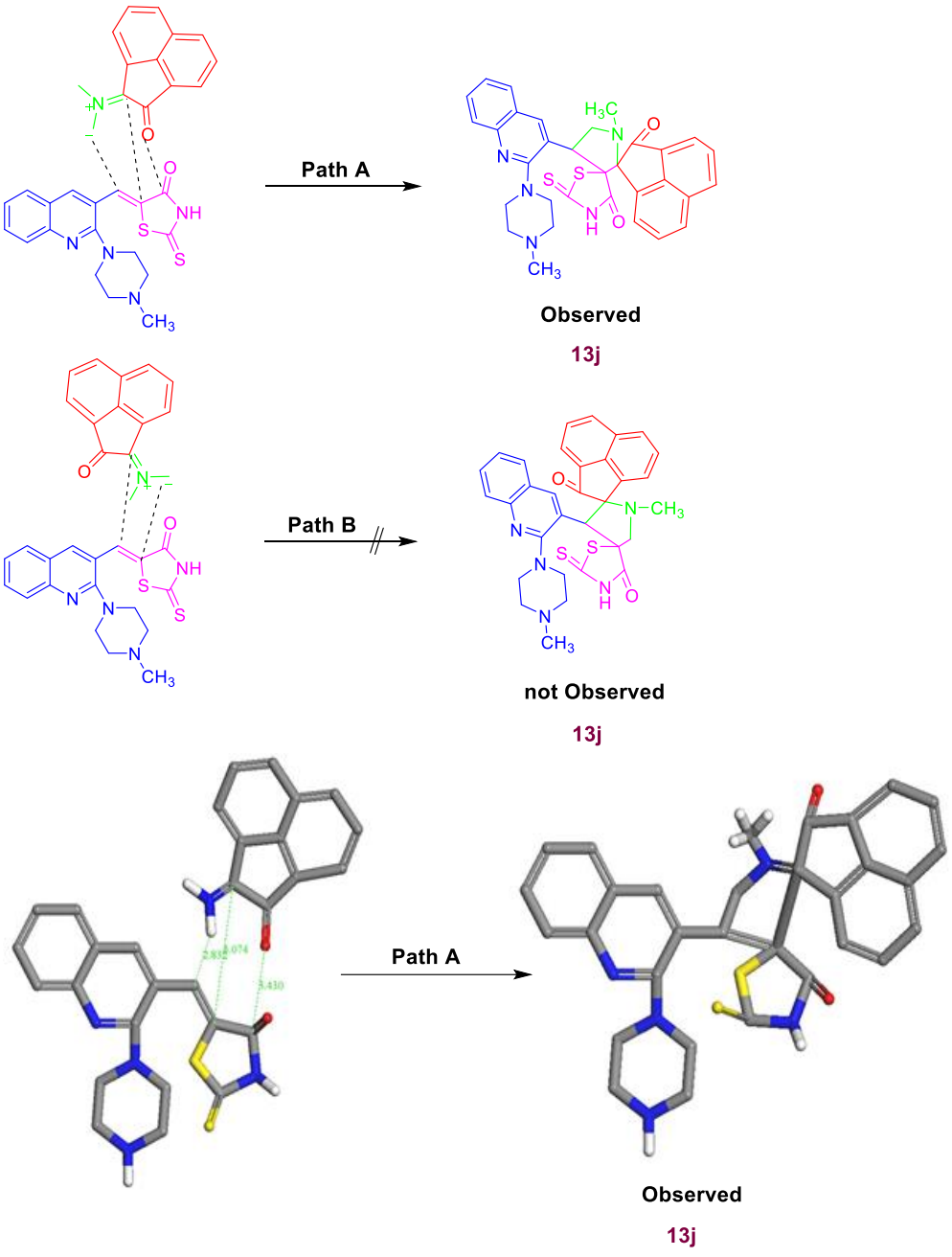

Scheme 6. 5. Secondary orbital interaction of compound 13j

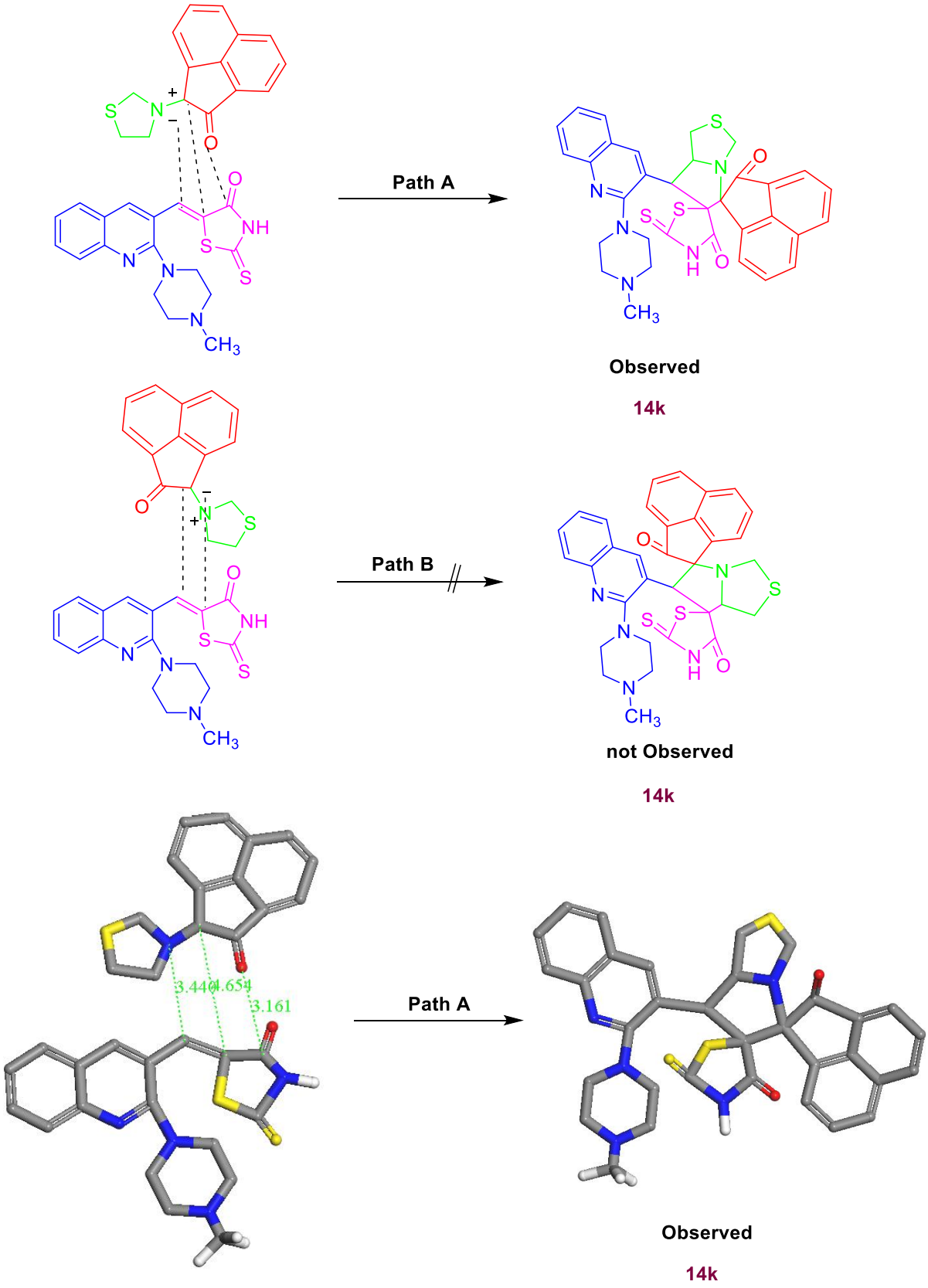

Scheme 6. 6. Secondary orbital interaction of compound 14k

Finally, the regio-isomer product **13j** and **14k** were confirmed by the secondary orbital interaction: the orbital interaction between the carbonyl group of **5** with azomethine ylides was via endo selectivity. The regio-isomer via path A was more favourable because of the secondary orbital interactions whilst path B was not possible for compound **13j** (Scheme 6. 5) and compound **14k** (Scheme 6. 6).

In order to acquire information on the conformational changes of protein and the extent of its local mobility (Zhang *et al.* 2013:14018), fluorescence spectroscopy was used. Since tryptophan, tyrosine and phenylalanine are ideal aromatic fluorophores for studying structural alterations on drug binding; tryptophan (Zaidi *et al.* 2013:2595) was selected to account for its intrinsic emission behaviour. The emissions spectra of HSA with increasing concentrations of compound **15l** and the collected spectral changes are as represented in Figure 6.4.

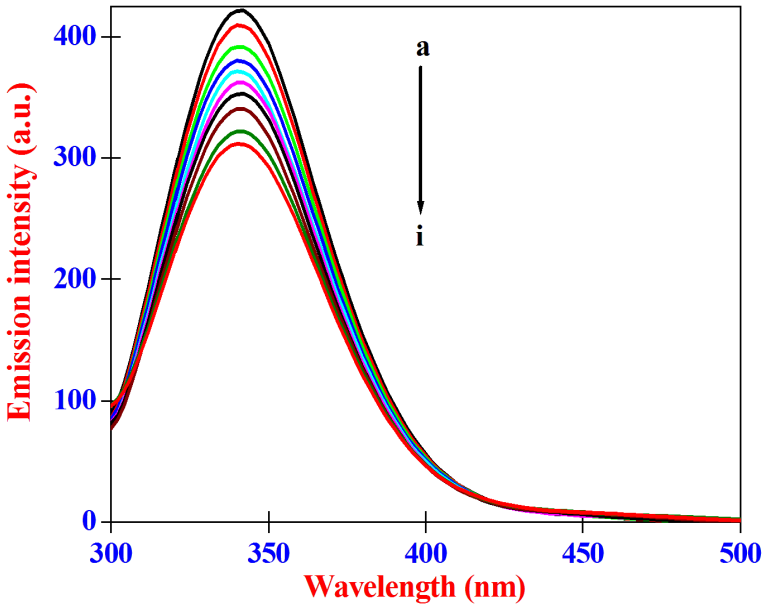

Figure 6. 4. Emission spectra of HSA (4.20×10^{-6} mol dm^{-3}) at various concentrations of compound 15l. [compound 15l]: [a] 0.00, [b] 3.00×10^{-6}, [c] 6.00×10^{-6}, [d] 9.00×10^{-6}, [e] 12.00×10^{-6}, [f] 15.00×10^{-6}, [g] 18.00×10^{-6}, [h] $21.00 \times 10^{-6}$and [i] 24.00×10^{-6} mol dm^{-3}; pH 7.40.

It was observed that the emission spectrum of HSA, in the absence of compound, demonstrated an emission maximum at 345 nm, when excited at 295 nm. However, with the regular addition with increasing concentration of **15l**, the emission intensity of HSA was faced with a red shift (346-349 nm) in the maximum emission wavelength. Similar behaviour was

reported in the case of HSA with some organic moieties (Bhattacharya *et al.* 2009:2143), (Khan *et al.* 2011:617), (Zhang *et al.* 2013:14018), (Sharma *et al.* 2014:206). Thus, in the present study it is suggested that the decreasing emission intensity is essentially owing to the binding interaction between HSA and the compound. This probably indicates that the micro environmental/ conformational changes occur in and around the tryptophan residue. These results inferred that the binding site of compound on HSA was neighbouring to the tryptophan residues of HSA.

To predict the possible quenching mechanism, the emission quenching data were analysed by conventional Stem-Volmer equation (Valeur Berberan-Santos 2012). (Eq. (6.1)).

$$\frac{F_0}{F} = 1 + k_{sv}[Q] = 1 + k_q \tau_0 [Q] \ldots\ldots\ldots (6.1)$$

F_0 and F are the emission intensities in the absence and presence of compound, respectively. K_{SV} is the Stern-Volmer quenching constant, which was computed by the linear plot of F_0/F against [compound], Kq is the bimolecular quenching rate constant, τ_0 is the average lifetime of the biomolecule without quencher ($\tau_0 = 10^{-8}$ s)[3] and [Q] is the concentration of quencher. Figure 6.5. Shows the Stern- Volmer plot for the quenching of HSA with **15l**.

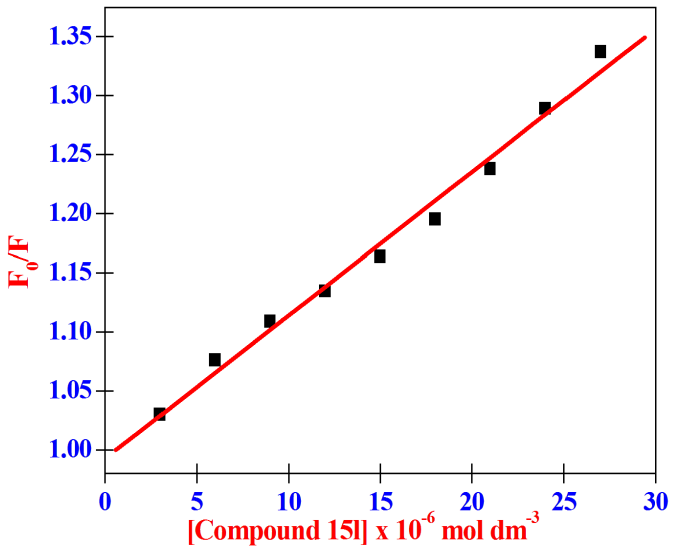

Figure 6. 5. Stern-Volmer plot of HSA by various ratio of compound. [HSA] = 4 × 10^{-6} mol dm^{-3}; [compound] = (3.00 to 27.00 × 10^{-6} mol dm^{-3}); pH 7.40

The Stern-Volmer plot demonstrated a good linear relationship with the experimental concentrations of quencher. The K_{SV} value was determined from the slope of the linear plot and

Ksv value (Table 6. 4**).** The biomolecular quenching constant *Kq* was calculated from the relation $Kq=Ksv/\tau_0$ and it was estimated as 1.21×10^{12} dm^3 mol^{-1} s^{-1}. However, the maximum scatter collision quenching constant, K_q of various quenchers with the biopolymer was 2.00×10^{10} dm^3 mol^{-1} s^{-1} (Shanmugaraj *et al.* 2014:43), (Thangavel *et al.* 2016:124).Thus, the rate constant calculated by protein quenching procedure was greater than K_q of scatter procedure which means that the quenching process was static quenching.

Table 6. 4. Binding parameters of HSA with synthesized compound system

Binding Parameters	K_{sv} (dm^3 mol^{-1})	K_q ($dm^3 mol^{-1} s^{-1}$)	K_b (dm^3 mol^{-1})	***n***
HSA -compound	1.21×10^4	1.21×10^{12}	1.81×10^4	1.04

For a system involving ground state complex formation, data from emission spectral studies was used to appraise the binding constant K_b and number of binding sites *n*. The emission quenching of HSA by **15l** was exploited to obtain binding parameters. The binding constant (K_b) and number of binding sites (*n*) were calculated using the double-logarithmic equation (Sharma *et al.* 2014:206), (Shanmugaraj *et al.* 2014:43), (Nithya *et al.* 2016:220) (Eq. (6. 2)).

$$\log\left[\frac{F_0-F}{F}\right] = \log K_b + n \log [Q] \ldots\ldots\ldots (6.\ 2)$$

Where F_0, F and [Q] are the same as per in Eq.1, *n* is the number of binding sites and binding constant K_b. According to Eq. (2), the plot of log [(F_0-F)/F] *vs* log [**15l**] (Figure 6. 6) yielded a straight line with a slope value of approximately 1 and the analogous results are given in Table 6. 4. The value of binding sites (n) close to unity indicated that there was only one independent class of binding site on HSA for **15l**. The correlation coefficients are closer to 0.9996 which clearly indicated that the interaction between HSA and **15l** is in good accordance with the binding site model obeyed the Eq. (6. 2).

In order to elucidate the complexation between 15l and HSA, the thermodynamic parameter free energy change (ΔG) was calculated using the following equation (Sharma *et al.* 2014:206), (Shanmugaraj *et al.* 2014:43), (Nithya *et al.* 2016:220) (Eq. (6. 3))

$$\Delta G = -2.303\ RT \log K \ldots \ldots \ldots (6.3)$$

where, ΔG is free energy change, R is universal gas constant and T is room temperature (298 K) and K is analogous to binding constant value obtained from the double logarithmic equation. The free energy (ΔG) change for the complexation process of **15l** and HSA was evaluated as -29.98 kJ mol^{-1}. The observed negative free energy change value indicated that the complexation process of **15l** with HSA was spontaneous and highly favourable.

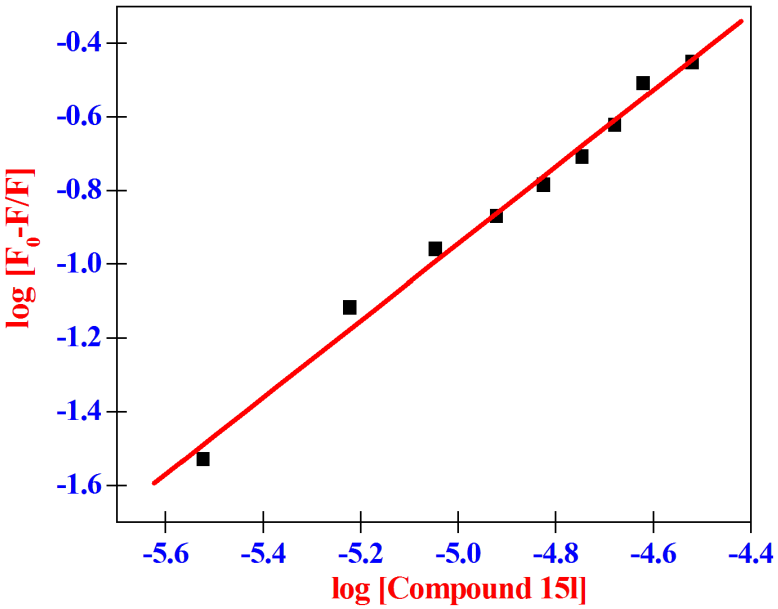

Figure 6. 6. Plot of log [(F_0-F)/F] *vs* log [compound] for the HSA-compound system; pH 7.40.

UV-visible absorption measurement was used as a simple and rapid technique to investigate the secondary structural changes of bio macromolecules while interacting with ligands and also to determine the complex formation (Sharma *et al.* 2014:206), (Shanmugaraj *et al.* 2014:43). To explore the structural changes of HSA and establish the quenching mechanism, UV-visible absorption spectra of HSA in different ratios of compounds were measured and observed (Figure 6.7). It was observed that in the absence of **15l**, HSA exhibited strong absorption band at 218 and 279 nm which mainly instigates from protein backbone peak and aromatic amino acid residues and disulphide bonds in the protein, respectively. Upon the successive addition of increasing concentrations of **15l** to HSA, the absorption at 218 and 279 nm intensified with an increase in a slight blue shift of both peaks. Thus, the changes observed by the absorption spectra of HSA suggested that a small structural change is probably due to an increased hydrophobicity of the Trip environment upon interaction of **15l** (Khan *et al.*

2011:617). These results can be re-organized by assuming minor secondary structural changes in HSA after binding to **15l** and also establishes the interaction between HSA and **15l**.

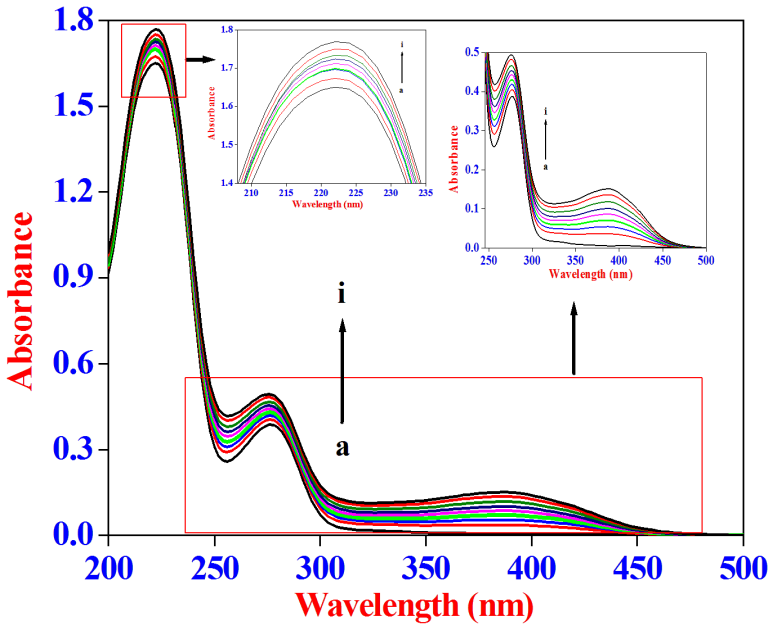

Figure 6. 7. Absorption spectra of HSA (8.00×10^{-6} mol dm^{-3}) at various compound 15l concentrations. [compound 15l]: [a] 0.00, [b] 3.00×10^{-6}, [c] 6.00×10^{-6}, [d] 9.00×10^{-6}, [e] 12.00×10^{-6}, [f] 15.00×10^{-6}, [g] 18.00×10^{-6}, [h] $21.00 \times 10^{-6}$and [i] 24.00×10^{-6} mol dm^{-3}; pH 7.40.

Circular dichroism (CD) spectroscopy is an important tool to investigate the secondary structure of a variety of bimolecular systems including proteins (Thangavel *et al.* 2016:124) (Nithya *et al.* 2016:220). The influence of **15l** binding interaction on the protein secondary structure was ascertained by monitoring the CD spectra of the protein in the presence of increasing concentration of **15l** and the results were displayed in Figure 6. 8. The CD spectra for HSA showed the two bands at 208 and 222 nm which are characteristic of the α-helical structure in proteins (Thangavel *et al.* 2016:124), (Nithya *et al.* 2016:220). **15l** displayed a small decrease in CD signals at all wavelengths for HSA without any shifting of the peak positions (Figure 6. 8**).** This indicated that the binding interaction of compound **15l** induces some modification in the secondary structural content of HSA. The lowering in the negative ellipticity points toward a decrease in the α-helical content which dictates unfolding of the peptide strand even more. To get more details from the spectra of HSA in the presence of

compound **15l**, the percentage α-helical content of HSA was calculated from Eq. 6. 4 and Eq. 6. 5 (Shanmugaraj *et al.* 2014:43), (Thangavel *et al.* 2016:124), (Nithya *et al.* 2016:220).

$$\text{MRE} = \frac{\text{ObservedCD(mdeg)}}{[\text{Cpnlx10}]} \ldots \ldots \ldots (6.4)$$

$$\alpha\text{-Hélix content (\%)} = \left[\frac{-\text{MRE}_{208} - 4000}{33000 - 4000}\right] \text{x } 100 \ldots \ldots \ldots (6.5)$$

where, C_P is the molar concentration of the protein, n is the number of amino acid residues (585 amino acids for HSA) and l is the path length of the cell, MRE_{208} is the observed MRE value at 208 nm, 4000 was the MRE of the β-form and random coil conformation cross at 208 nm and 33000 was the MRE value of a pure α-helix at 208 nm.

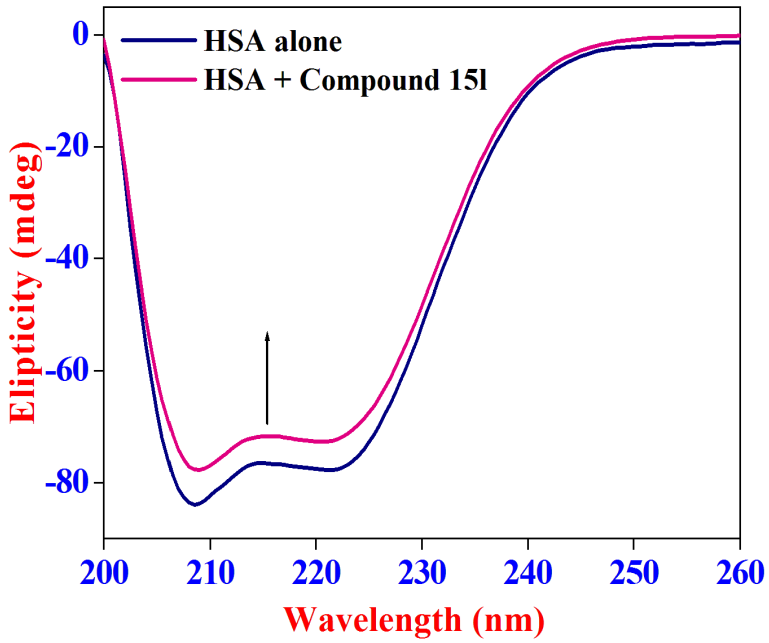

Figure 6. 8. CD spectral changes of HSA in the absence and presence of compound 15l. Conditions: [HAS] = 4.20 × 10^{-6} mol dm^{-3}; [compound 15l] = 25.00 × 10^{-6} mol $dm^{-3.}$

According to equations, the estimated α-helicity content of free HSA in PBS buffer (pH = 7.40 and T= 298 K) is 61.2 %, which is in reasonable accord with reported literature (Thangavel *et al.* 2016:124), (Nithya *et al.* 2016:220), (Anand et al. 2010:15839). The percentage α-Hélix content of HSA in the présence of **15l** showed a decrease from 61.2 % to 58.19 % (HSA + **15l**). The decrease in the α-hélix content suggested that **15l** altered the secondary structure of the protein thereby inducing changes in the atomic arrangement and their hydrogen bonding network. Similar results are reported in the literatures (Thangavel *et al.* 2016:124), (Nithya *et*

al. 2016:220), (Anand *et al.* 2010:15839). CD spectral observations are good and in accordance with absorption spectral studies.

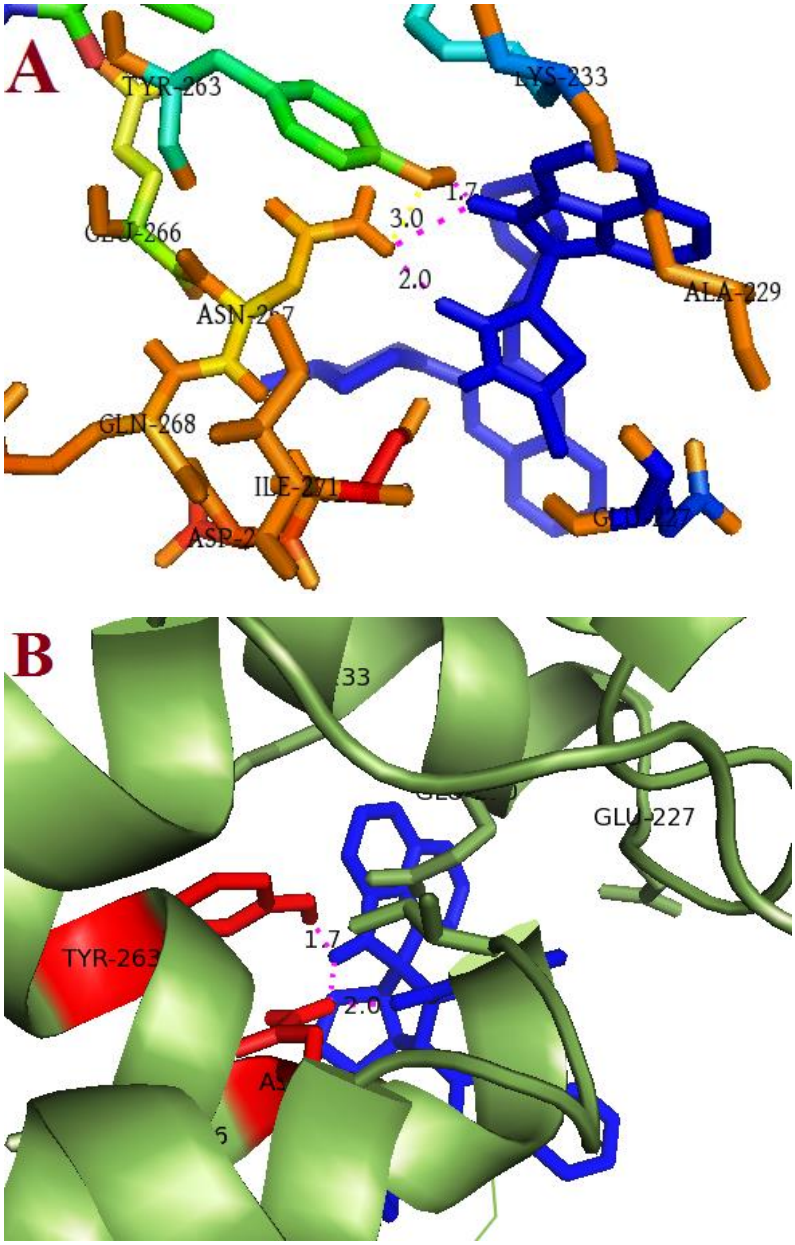

Figure 6. 9. (A-B). (A) Molecular docking of HSA-compound 15l complex. (B) Binding site of compound **15l** on HSA–**15l** and selected amino acid residues are represented by stick and ribbon sounds models. Hydrogen bond is shown in pink dotted line

In order to support the experimental results, computational docking analysis was performed to create a model for the HSA-**15l** complex. It has been stated earlier that each domain of the HSA protein contains two sub domains (IA and B, IIA and B, IIIA and B) that possess common structural motifs. Sudlow site I and Sudlow site II (subdomains IIA and IIIA, respectively) are the most probable binding sites of the ligands. Molecular docking analysis

was performed using the Auto Dock 4.2 program and the energetically most feasible HSA-**15l** complex as displayed in Figure 6.9 (A&B). Docking results clearly pointed out that **15l** binds inside the binding pocket located in subdomain II A of HSA (Anand *et al.* 2010:15839), (Neelam *et al.* 2010:3005). It can be seen from Figure 6. 9. (A-B**),** that **15l** was located adjacent to the amino acid residues Tyr-263, Lys-233, Ala-229, Asn-267, Gln-268, Ile-271, Asp-222 and Glu-227of subdomain IIA. Furthermore, **15l** forms a hydrogen bond with Tyr-263 and Asn-267 shows the bond length values of 1.7 Å and 2.0 Å respectively. It is imperative to note from the computational observations that **15l** was located at Tyr-263 amino acid residue of HSA. From the docking analyses, the free energy changes acquired for HSA binding is -20.79 kJ mol^{-1} which was close to the experimental value of -29.98 kJ mol^{-1} obtained from emission spectral data at room temperature. Furthermore, the difference between the calculated ΔG values and the experimental ΔG values can be accounted for based on the fact that X-ray structure of HSA from crystals is different from that of the aqueous system used in the study, which results in the difference of the microenvironment around the ligand. Similar results were observed in some organic molecules binding to HSA (Sharma *et al.* 2014:36267), (Neelam *et al.* 2010:3005), (Zhang *et al.* 2008:1). Therefore, the molecular docking study supports the emission spectral results regarding intrinsic emission quenching of Tyr-263 for binding interaction between HSA and **15l**. These values obtained just provide the probable geometry of the complexes however the binding has been established experimentally.

6. 4. Conclusion

The present study described a highly regio-selective reaction for novel dispiro heterocyclic compounds containing pyrrolidine, thiopyrrolizidine and pyrrolizidine-substituted piperazinyl-quinolinyl derivatives in high yields. The synthetic method involved the 1,3-dipolar cycloaddition reaction of azomethine ylides with various isatin, acenaphthalene and secondary amino acids with piperazinyl-quinoline dipolarophile in a multi-component reaction. The simple and effective strategy provided rapid entry to stereo chemically complex core structures common to a variety of bioactive molecules. Furthermore, HSA protein binding and molecular docking investigations were conducted and gave an indication of the binding sites. It was anticipated that the protocol described here could be explored further to have other interesting implications in the fields of combinatorial chemistry and chemistry-driven drug discovery.

6. 5. Experimental

6. 5. 1. General Procedure for the synthesis of substituted 2-(4-methylpiperazin-1-yl) quinoline-3-carbaldehyde (3)

The synthetic method is described in **Chapter 3. 5. 2.**

6. 5. 2. General Procedure for the synthesis of substituted (Z)-5-((2-(4-methylpiperazin-1-yl)quinolin-3-yl)methylene)-2-thioxothiazolidin-4-one (5)

An aliquot (0.001mol) of (**3**), rhodanine **(4)** (0.001mol) and sodium acetate (0.002 mol) was added to a round bottom flask and an excess of glacial acetic acid was added. The mixture was refluxed for 6 h at 120°C (Scheme 6.1) whilst the reaction was monitored by TLC. After completion, the reaction content was cooled to room temperature and poured into ice water. It was then filtered, washed with water and dried. The crude product was recrystallized from methanol to obtain a pure red solid product **5** of m.p 248-250 °C. Yield 90 %: FT-IR (KBr): 3452, 2964, 2963, 2731, 2611, 2364, 1641, 1506, 1419, 1332, 1232, 1027, 998, 762 cm^{-1}. ^{1}H NMR (400 MHz, $DMSOd_6$): δ 8.12 (1H, s, Ar-H), 7.85 (1H, d, *J*= 7.44 Hz, Ar-H), 7.75 (1H, d, *J*= 8.28 Hz, Ar-H), 7.67 (1H, dt, *J*= 1.36 Hz, Ar-H), 7.42 (1H, dd, *J*= 0.84 Hz, Ar-H), 6.90 (1H, s, C-H), 6.73 (1H, s, NH), 3.12 (4H, t, *J*= 4.48 Hz, CH_2), 2.49 (4H, m, *J*= 1.68 Hz, CH_2), 2.15 (3H, s, CH_3). ^{13}C NMR (100 MHz, $DMSOd_6$): δ 200.7, 178.4, 158.7, 146.4, 137.6, 135.1, 131, 128.6, 127.5, 125.4, 125.1, 122.7, 122.1, 53.6, 45.5, 44.1, 40.8, 31. TOFMS ES *m/z* (rel. int.): m/z: 369.08 $[M]^+$. Anal. Calc. for $C_{18}H_{18}N_4OS_2$: C, 58.35; H, 4.90; N, 15.12 %. Found: C, 58.37; H, 4.88; N, 15.14 %.This compound was fully characterized by FT-IR, ^{1}H NMR, ^{13}C NMR, TOF-MS and elemental analysis (Fig. 5-8 in Appendix).

6. 6. General procedure for the synthesis of piperazinyl-quinolinyl based spiropyrrolidines bearing oxindole system (10a-c; 11d-f; 12g-i)

An equimolar (1mmol) quantity containing **5** and isatin derivatives (**6**) followed by secondary amino acids sarcosine (**7**), thiaproline (**8**) and L-proline (**9**) were added separately. The reaction mixture was refluxed in methanol (25 mL) using MW irradiation for 15 minutes. After completion, monitored by TLC, the reaction mixture was cooled and the solvent removed under vacuum. The product was purified by column chromatography using silica gel mesh and a solvent system of n-hexane: acetone (80: 20) as eluent to produce a yellow solid which was further recrystallized from MeOH and DMF mixtures (8: 2).

6. 6. 1. 1'-methyl-4'-(2-(4-methylpiperazin-1-yl)quinolin-3-yl)-2''-thioxodispiro[indoline-3,2'-pyrrolidine-3',5''-thiazolidine]-2,4''-dione (10a)

Yellow colour solid: m.p 232-234 °C, yield 90 %: FT-IR (KBr): 3463, 3390, 3064, 2920, 2951, 2364, 2062, 1664, 1586, 1419, 1334, 2229, 1026, 909, 761 cm^{-1}. ^{1}H NMR (400 MHz, $DMSOd_6$): δ 10.43(1H, s, NH), 8.37 (1H, s, Ar-H), 7.94 (1H, d, *J*= 7.96 Hz, Ar-H), 7.81 (1H, d, *J*= 8.28 Hz, Ar-H), 7.68 (1H, t, *J*= 7.28 Hz, Ar-H), 7.52 (1H, t, *J*= 7.44 Hz, Ar-H), 7.35 (1H, d, *J*= 7.4 Hz, Ar-H), 7.24 (1H, t, *J*= 7.36 Hz, Ar-H), 6.98 (1H, t, *J*= 7.48Hz, Ar-H), 6.75 (1H, d, *J*= 7.68 Hz, Ar-H), 4.73 (1H, s, NH), 4.20 (1H, t, *J*= 8.64Hz, C-H), 3.47 (6H, t, *J*= 7.76 Hz, CH_2), 2.54 (4H, d, *J*= 8.48 Hz, CH_2), 2.08(6H, s, CH_3). ^{13}C NMR (100 MHz, $DMSOd_6$): δ 206.4, 176.9, 145.2, 143.8, 136.4, 129.8, 129.2, 127.8, 127.3, 126.9, 126, 125.4, 121.8, 109.5, 78.2, 54.3, 45, 40.1, 34.8, 30.6. TOFMS ES *m/z* (rel. int.): m/z: 545.07 $[M]^+$. Anal. Calc. for $C_{28}H_{28}N_6O_2S_2$: C, 61.74; H, 5.18; N, 15.43 %. Found: C, 61.76; H, 5.20; N, 15.43 %.

6. 6. 2. 5-chloro-1'-methyl-4'-(2-(4-methylpiperazin-1-yl)quinolin-3-yl)-2'' thioxodispiro[indoline-3,2'-pyrrolidine-3',5''-thiazolidine]-2,4''-dione (10b)

Yellow colour solid: m.p 250-252 °C, yield 80 %: FT-IR (KBr): 3463, 3390, 2963, 2602, 1637, 1583, 1419, 1330, 2231, 1026, 967, 762, 732 cm^{-1}. ^{1}H NMR (400 MHz, $DMSOd_6$): δ 9.90 (1H, s, NH), 8.35 (1H, s, Ar-H), 7.98 (2H, d, *J*= 7.72 Hz, Ar-H), 7.79 (2H, d, *J*= 8.36 Hz, Ar-H), 7.69-7.73 (2H, dd, *J*= 5.64 Hz, Ar-H), 7.54 (1H, s, Ar-H), 7.46 (1H, s, NH), 3.85 (1H, d, *J*= 11.32Hz, C-H), 3.51 (4H, d, *J*= 9.52 Hz, CH_2), 3.30 (6H, t, *J*= 11.08 Hz, CH_2), 2.88 (3H, s, CH_3), 2.03(3H, s, CH_3). ^{13}C NMR (100 MHz, $DMSOd_6$): δ 206.2, 197.6, 167.7, 166.9, 145.5, 138.3, 131.2, 128.4, 128.3, 126.6, 125.2, 124.1, 123.9, 120.6, 119.2, 116.4, 113.5, 110.7, 68.45, 67.28, 52, 46.8, 42.1, 31.7, 31.2, 31.1, 29.3, 26.7. Anal. Calc. for $C_{28}H_{27}ClN_6O_2S_2$: C, 58.07; H, 4.70; N, 14.51 %. Found: C, 58.05; H, 4.72; N, 14.50 %.

6. 6. 3. 1'-methyl-4'-(2-(4-methylpiperazin-1-yl)quinolin-3-yl)-5-nitro-2'' thioxodispiro[indoline-3,2'-pyrrolidine-3',5''-thiazolidine]-2,4''-dione (10c)

Yellow colour solid: m.p 243-245 °C, yield 75 %: FT-IR (KBr): 3463, 3306, 3064, 2920, 2961, 2364, 2062, 1664, 1586, 1434, 1229, 1026, 761cm^{-1}. ^{1}H NMR (400 MHz, $DMSOd_6$): δ 9.91 (1H, s, NH), 8.33 (1H, s, Ar-H), 7.93 (2H, d, *J*= 7.92 Hz, Ar-H), 7.80 (2H, d, *J*= 8.4 Hz, Ar-H), 7.67-7.69 (1H, dd, *J*= 1 Hz, Ar-H), 7.50 (1H, s, Ar-H), 7.44 (1H, t, *J*= 7.32 Hz, Ar-H), 6.95 (1H, s, NH), 3.88 (1H, d, *J*= 13.4 Hz, C-H), 3.49 (1H, d, *J*= 11.32 Hz, C-H), 3.36 (5H, t, *J*= 13.08 Hz, CH_2), 3.26 (5H, d, *J*= 10.68 Hz, CH_2), 2.16 (3H, s, CH_3), 1.98 (3H, s, CH_3). ^{13}C

NMR (100 MHz, $DMSOd_6$): δ 208.2, 197.6, 167.7, 166.9, 145.5, 138.3, 131.2, 128.4, 128.3, 126.6, 125.2, 124.1, 123.9, 120.6, 119.2, 116.4, 113.5, 110.7, 68.45, 67.28, 52, 46.8, 42.1, 31.7, 31.2, 31.1, 29.3, 26.7. Anal. Calc. for $C_{28}H_{27}N_7O_4S_2$: C, 57.03; H, 4.62; N, 16.63 %. Found: C, 57.06; H, 4.65; N, 16.60 %.

6. 6. 4. 7''-(2-(4-methylpiperazin-1-yl)quinolin-3-yl)-2''-thioxo-7',7a'-dihydro-1'H,3'H-dispiro[indoline-3,5'-pyrrolo[1,2-c]thiazole-6',5''-thiazolidine]-2,4''-dione (11d)

Yellow colour solid: m.p 230-232 °C, yield 87 %: FT-IR (KBr): 3454, 3201, 3076, 2929, 2834, 2366, 1706, 1672, 1664, 1618, 1336, 1224, 796 cm^{-1}. ^1H NMR (400 MHz, $DMSOd_6$): δ 10.52(1H, s, NH), 8.38 (1H, s, Ar-H), 8 (1H, d, *J*= 7.92 Hz, Ar-H), 7.82 (1H, d, *J*= 8.32 Hz, Ar-H), 7.70 (1H, t, *J*= 7.2 Hz, Ar-H), 7.48-7.54 (2H, dd, *J*= 8.54 Hz, Ar-H), 7.23 (1H, t, *J*= 7.84 Hz, Ar-H), 6.98 (1H, t, *J*= 7.56 Hz, Ar-H), 6.77 (1H, d, *J*= 7.64 Hz, Ar-H), 5.22 (1H, s, NH) 4.49 (1H, d, *J*= 9.32 Hz, C-H), 3.89 (1H, s, C-H), 3.41 (6H, t, *J*= 5.4 Hz, CH_2), 2.92 (2H, t, *J*= 8.4 Hz, CH_2), 2.49 (4H, t, *J*= 1.56 Hz, CH_2), 2.08(3H, s, CH_3). ^{13}C NMR (100 MHz, $DMSOd_6$): δ 206.4, 176.5, 145.1, 143.5, 130, 129.3, 126.1, 125.4, 109.8, 74.5, 50, 46, 40.1, 31.4, 36.6. TOFMS ES *m/z* (rel. int.): m/z: 588.13 $[M]^+$. Anal. Calc. for $C_{29}H_{28}N_6O_2S_3$: C, 59.16; H, 4.79; N, 14.27 %. Found: C, 59.18; H, 4.81; N, 14.29 %.

6. 6. 5. 5-chloro-7''-(2-(4-methylpiperazin-1-yl)quinolin-3-yl)-2''-thioxo-7',7a'-dihydro-1'H,3'H-dispiro[indoline-3,5'-pyrrolo[1,2-c]thiazole-6',5''-thiazolidine]-2,4''-dione (11e)

Yellow colour solid: m.p 235-237 °C, yield 83 %: FT-IR (KBr): 3454, 3201, 3076, 2929, 2834, 2366, 1706, 1672, 1664, 1618, 1336, 1224, 756 cm^{-1}. ^1H NMR (400 MHz, $DMSOd_6$): δ 9.91(1H, s, NH), 8.33 (1H, s, Ar-H), 7.93 (2H, d, *J*= 7.92 Hz, Ar-H), 7.80 (2H, d, *J*= 8.4 Hz, Ar-H), 7.68 (1H, dd, *J*= 3.25 Hz, Ar-H), 7.50 (1H, s, Ar-H), 7.42 (1H, t, *J*= 7.16 Hz, Ar-H), 6.95 (1H, s, NH), 3.88 (1H, d, *J*= 13.4 Hz, C-H), 3.49 (1H, d, *J*= 11.32 Hz, C-H), 3.36 (5H, t, *J*= 13.08 Hz, CH_2), 3.26 (5H, t, *J*= 10.68 Hz, CH_2), 2.16 (2H, t, *J*= 4.88 Hz, CH_2), 1.98 (3H, s, CH_3). ^{13}C NMR (100 MHz, $DMSOd_6$): δ 206.1, 195.8, 169, 166.6, 156.9, 145.6, 138.9, 131.4, 128.4, 128, 126.6, 126.4, 125.3, 124.3, 120.5, 116.3, 113.5, 110.6, 52, 46.9, 42.1, 30.2 Anal. Calc. for $C_{29}H_{27}ClN_6O_2S_3$: C, 55.89; H, 4.37; N, 13.49 %. Found: C, 55. 90; H, 4.39; N, 13.48 %.

6. 6. 6. 7'-(2-(4-methylpiperazin-1-yl)quinolin-3-yl)-5-nitro-2''-thioxo-7',7a'-dihydro 1'H,3'H-dispiro[indoline-3,5'-pyrrolo[1,2-c]thiazole-6',5''-thiazolidine]-2,4''-dione (11f)

Yellow colour solid: m.p 270-272 °C, yield 77 %: FT-IR (KBr): 3454, 3076, 2929, 2834, 2366, 1706, 1672, 1664, 1618, 1336, 1224, 756 cm^{-1}. ^{1}H NMR (400 MHz, $DMSOd_6$): δ 8.82 (1H, s, NH), 8.31 (1H, s, Ar-H), 7.92 (1H, t, *J*= 7.76 Hz, Ar-H), 7.86 (1H, d, *J*= 7.8 Hz, Ar-H), 7.80 (1H, d, *J*= 8.4 Hz, Ar-H), 7.66-7.70 (2H, d, *J*= 1.16 Hz, Ar-H), 7.49 (1H, s, Ar-H), 7.43 (1H, t, *J*= 7.76 Hz, Ar-H), 7.25 (1H, s, NH), 4.04 (1H, d, *J*= 13.12 Hz, C-H), 3.87 (1H, d, *J*= 13.44 Hz, C-H), 3.50 (4H, t, *J*= 11.4 Hz, CH_2), 3.39 (4H, t, *J*= 12.8 Hz, CH_2), 3.28 (4H, d, *J*= 10.64 Hz, CH_2), 1.97 (3H, s, CH_3). ^{13}C NMR (100 MHz, $DMSOd_6$): δ 201.5, 166.9, 158.2, 145.6, 136.7, 130.4, 128.1, 126.9, 125, 124.7, 122.5, 119.7, 71.9, 69.9, 68, 67, 60, 52,8, 47.8, 23.3, 18.7, 13.8, 13.7, 10.7 Anal. Calc. for $C_{29}H_{27}N_7O_4S_3$: C, 54.96; H, 4.29; N, 15.47 %. Found: C, 54. 94; H, 4.30; N, 15.49 %.

6. 6. 7. 1'-(2-(4-methylpiperazin-1-yl)quinolin-3-yl)-2''-thioxo-5',6',7',7a'-tetrahydro-1'H dispiro[indoline-3,3'-pyrrolizine-2',5''-thiazolidine]-2,4''-dione (12g)

Yellow colour solid: m.p 250-252 °C, yield 90 %: FT-IR (KBr): 3463, 3396, 3064, 2920, 2961, 2364, 2062, 1664, 1585, 1419, 1334, 2229, 1026, 909, 761, 732 cm^{-1}. ^{1}H NMR (400 MHz, $DMSOd_6$): δ 10.57 (1H, s, NH), 8.38 (1H, s, Ar-H), 8 (1H, d, *J*= 7.92 Hz, Ar-H), 7.82 (1H, d, *J*= 8.32 Hz, Ar-H), 7.70 (1H, t, *J*= 7.2 Hz, Ar-H), 7.48-7.54 (2H, dd, *J*= 8.52 Hz, Ar-H), 7.23 (1H, t, *J*= 7.84 Hz, Ar-H), 6.99 (1H, t, *J*= 7.56 Hz, Ar-H), 6.77 (1H, d, *J*= 7.64 Hz, Ar-H), 5.22 (1H, s, NH), 4.39 (1H, d, *J*= 9.32 Hz, C-H), 3.89 (1H, s, C-H), 3.40 (6H, t, *J*= 5.4 Hz, CH_2), 2.92 (2H, t, *J*= 8.4 Hz, CH_2), 2.49 (6H, t, *J*= 1.56 Hz, CH_2), 2.08 (3H, s, CH_3). ^{13}C NMR (100 MHz, $DMSOd_6$): δ 206.4, 176.5, 145.1, 143.5, 130, 129.3, 127.9, 127.3, 126.1, 125.4, 121.7, 109.8, 74.5, 50, 46. 3, 40.1, 38.8, 31.4, 30.6 TOFMS ES *m/z* (rel. int.): m/z: 564.97 $[M]^+$. Anal. Calc. for $C_{30}H_{30}N_6O_2S_2$: C, 63.13; H, 5.30; N, 14.75 %. Found: C, 63.15; H, 5.32; N, 14.75 %.

6. 6. 8. 5-chloro-1'-(2-(4-methylpiperazin-1-yl)quinolin-3-yl)-2''-thioxo-5',6',7',7a' tetrahydro-1'H-dispiro[indoline-3,3'-pyrrolizine-2',5''-thiazolidine]-2,4''-dione (12h)

Yellow colour solid: m.p 240-242 °C, yield 82 %: FT-IR (KBr): 3463, 3209, 2963, 2902, 1664, 1637, 1583, 1419, 1330, 1211, 1036, 967, 763, 737 cm^{-1}. ^{1}H NMR (400 MHz, $DMSOd_6$): δ 8.82 (1H, s, NH), 8.31 (1H, s, Ar-H), 7.92 (1H, t, *J*= 7.76 Hz, Ar-H), 7.86 (1H, d, *J*= 7.8 Hz, Ar-H), 7.80 (1H, d, *J*= 8.4 Hz, Ar-H), 7.66-7.70 (2H, dd, *J*= 1.16 Hz, Ar-H), 7.49 (1H, s, Ar-H), 7.43 (1H, t, *J*= 7.76 Hz, Ar-H), 7.25 (1H, s, NH), 4.04 (1H, d, *J*= 13.12 Hz, C-H), 3.87 (1H,

d, *J*= 13.44 Hz, C-H), 3.50 (4H, t, *J*= 11.4 Hz, CH_2), 3.39 (4H, t, *J*= 13.16 Hz, CH_2), 3.28 (4H, d, *J*= 10.64 Hz, CH_2), 1.97 (3H, s, CH_3). ^{13}C NMR (100 MHz, $DMSOd_6$): δ 201.5, 166.9, 158.2, 145.6, 136.4, 131.5, 130.4, 128.6, 128.1, 126.9, 125, 124.7, 122.5, 119.7, 71.9, 69.9, 60.2, 52.8, 47.8, 43.2, 31.3, 29.7, 28.3 Anal. Calc. for $C_{30}H_{29}ClN_6O_2S_2$: C, 59.54; H, 4.83; N, 13.89 %. Found: C, 59.56; H, 4.80; N, 13.87 %.

6. 6. 9. 1''-(2-(4-methylpiperazin-1-yl)quinolin-3-yl)-5-nitro-2''-thioxo-5',6',7',7a' tetrahydro 1'H-dispiro[indoline-3,3'-pyrrolizine-2',5''-thiazolidine]-2,4''-dione (12i)

Yellow colour solid: m.p 247-249 °C, yield 80 %: FT-IR (KBr): 3463, 3339, 2946, 2963, 2250, 1637, 1583, 1419, 1300, 1231, 1026, 967, 763, 737 cm^{-1}. ^{1}H NMR (400 MHz, $DMSOd_6$): δ 11.18 (1H, s, NH), 8.24 (1H, s, Ar-H), 7.96 (2H, d, *J*= 8.04 Hz, Ar-H), 7.76 (2H, d, *J*= 8.28 Hz, Ar-H), 7.65-7.69 (1H, m, *J*= 1.56 Hz, Ar-H), 7.45 (1H, t, *J*= 1.16 Hz, Ar-H), 7.26 (1H, s, Ar-H), 7.04 (1H, s, NH), 3.37 (2H, d, *J*= 2.52 Hz, Ar-H), 3.36 (1H, s, C-H), 3.17 (4H, s, CH_2), 2.72 (4H, s, CH_2) 2.49(4H, t, *J*= 8.4Hz, CH_2), 1.13 (3H, s, CH_3). ^{13}C NMR (100 MHz, $DMSOd_6$): δ 201.5, 166.9, 158.2, 145.6, 136.4, 131.5, 130.4, 128.6, 128.1, 126.9, 125, 124.7, 122.5, 119.7, 71.9, 69.9, 60.2, 52.8, 47.8, 43.2, 31.3, 29.7, 28.3 Anal. Calc. for $C_{30}H_{29}N_7O_4S_2$: C, 58.52; H, 4.75; N, 15.92 %. Found: C, 58.55; H, 4.73; N, 15.94 %.

6. 7. General Procedure for the synthesis of piperazinyl-quinolinyl grafted spiropyrrolidines bearing acenaphthalene ring system (13j, 14k, 15l)

An equimolar (1mmol) quantity containing **5** and acenaphthalene-1,2-dione (**6a**) followed by secondary amino acids **7**, **8** and **9** were added separately. The reaction mixture was refluxed in methanol (25 mL) using MW irradiation for 15 minutes. After completion of the reaction, monitored by TLC, the reaction mixture was cooled and the solvent was removed under vacuum. The product was purified by column chromatography using silica gel mesh and a solvent system of n-hexane: acetone (80:20) as eluent to produce a yellow solid which was further recrystallized from MeOH and DMF mixtures (8:2).

6. 7. 1. 1'-methyl-4'-(2-(4-methylpiperazin-1-yl)quinolin-3-yl)-2''-thioxo-2H dispiro[acenaphthylene-1,2'-pyrrolidine-3',5''-thiazolidine]-2,4''-dione (13j)

Yellow colour solid: m.p 220-224 °C, yield 87 %: FT-IR (KBr): 3463, 3329, 2963, 2946, 2602, 1637, 1583, 1419, 1330, 1231, 1026, 967, 763 cm^{-1}. ^{1}H NMR (400 MHz, $DMSOd_6$): δ 8.79 (1H, s, NH), 8.35 (1H, s, Ar-H), 7.98 (2H, d, *J*= 8.4 Hz, Ar-H), 7.85 (1H, t, *J*= 2.8 Hz, Ar-H), 7.79 (2H, d, *J*= 8.4 Hz, Ar-H), 7.71-7.74 (2H, m, *J*= 1.44 Hz, Ar-H), 7.54 (1H, d, *J*=

0.36 Hz, Ar-H), 7.44-7.48 (2H, dd, *J*= 1.08 Hz, Ar-H), 7.33 (1H, d, *J*= 0.8 Hz, C-H), 3.85 (2H, d, *J*= 11.44 Hz, CH_2), 3.50 (4H, d, *J*= 9.56 Hz, CH_2), 3.29 (4H, t, *J*= 11.16 Hz, CH_2), 2.88 (3H, s, CH_3), 2.03 (3H, s, CH_3). ^{13}C NMR (100 MHz, DMSOd_6): δ 206, 195.9, 168.8, 166.64, 156.28, 155, 144.3, 144, 140, 139.6, 132.5, 131.6, 130.9, 128.8, 128.4, 128.2, 128.1, 125.9, 125.4, 125, 123.9, 122.7, 119, 116.3, 113.3, 110.4, 51.9, 49.5, 47, 46.8, 42.1, 42, 40.1, 29.6 Anal. Calc. for $C_{32}H_{29}N_5O_2S_2$: C, 66.30; H, 5.04; N, 12.08 %. Found: C, 60.32; H, 5.06; N, 12.06 %.

6. 7. 2. (7'-(2-(4-methylpiperazin-1-yl)quinolin-3-yl)-2''-thioxo-7',7a'-dihydro-1'H,2H,3'H-dispiro[acenaphthylene-1,5'-pyrrolo[1,2-c]thiazole-6',5''-thiazolidine]-2,4''-dione (14k)

Yellow colour solid: m.p 228-230 °C, yield 85 %: FT-IR (KBr): 3464, 3301, 3076, 2929, 2634, 2366, 1706, 1672, 1664, 1618, 1336, 1224, 795 cm^{-1}. ^{1}H NMR (400 MHz, DMSOd_6): δ 9.88 (1H, s, N-H), 8.34 (1H, s, Ar-H), 7.96 (2H, d, *J*= 7.68 Hz, Ar-H), 7.79 (2H, d, *J*= 8.45 Hz, Ar-H), 7.68-7.72 (3H, t, *J*= 1.08 Hz, Ar-H), 7.53 (1H, d, *J*= 0.38 Hz, Ar-H), 7.43-7.47 (2H, t, *J*= 7.08 Hz, Ar-H), 3.86 (2H, d, *J*= 12.44 Hz, 2C-H), 3.50 (6H, d, *J*= 10.52 Hz, CH_2), 3.32 (6H, t, *J*= 14 Hz, CH_2), 2.01 (3H, s, CH_3). ^{13}C NMR (100 MHz, DMSOd_6): δ 206.1, 195.8, 169, 166.6, 156.9, 145.6, 138.9, 131.4, 128.4, 128, 126.6, 126.4, 125.3, 124.3, 120.5, 116.3, 113.5, 110.6, 52, 46.9, 42.1, 30.2 Anal. Calc. for $C_{33}H_{29}N_5O_2S_3$: C, 63.54; H, 4.69; N, 11.23 %. Found: C, 63.56; H, 4.71; N, 11.25 %.

6. 7. 3. 1'-(2-(4-methylpiperazin-1-yl)quinolin-3-yl)-2''-thioxo-5',6',7',7a'-tetrahydro 1'H,2H-dispiro[acenaphthylene-1,3'-pyrrolizine-2',5''-thiazolidine]-2,4''-dione (15l)

Yellow colour solid: m.p 218-220 °C, yield 90 %: FT-IR (KBr): 3463, 3389, 2963, 2602, 1637, 1583, 1419, 1330, 1231, 1026, 987, 763, 737 cm^{-1}. ^{1}H NMR (400 MHz, DMSOd_6): δ 8.82 (1H, s, N-H), 8.30 (1H, s, Ar-H), 7.84-7.91(2H, t, *J*= 9.96 Hz, Ar-H), 7.80 (2H, d, *J*= 8.36 Hz, Ar-H), 7.65-7.69 (2H, td, *J*= 7.12 Hz, Ar-H), 7.50 (1H, d, *J*= 4.56 Hz, Ar-H), 7.40-7.44 (2H, t, *J*= 7.2 Hz, Ar-H), 7.26 (1H, t, *J*= 8.32 Hz, Ar-H), 4.05 (1H, d, *J*= 12.68 Hz, C-H), 3.88 (1H, d, *J*= 13.56 Hz, C-H), 3.50 (6H, t, *J*= 11.36 Hz, CH_2), 3.39 (6H, t, *J*= 12.8 Hz, CH_2), 1.07 (3H, s, CH_3). ^{13}C NMR (100 MHz, DMSOd_6): δ 206, 195.5, 168.8, 166.6, 156.2, 155, 144.3, 144, 140, 139.6, 132.5, 131.6, 130.9, 128.8, 128.4, 128.2, 128.1, 125.9, 125.4, 125, 123.9, 122.7, 119, 116.3, 113.3, 110.4, 51.9, 49.5, 47, 46.8, 42.1, 42, 40.1, 29.6 TOFMS ES *m/z* (rel. int.): m/z: 591.96 [M]$^+$. Anal. Calc. for $C_{34}H_{31}N_5O_2S_2$: C, 67.41; H, 5.16; N, 11.56 %. Found: C, 67.43; H, 5.18; N, 11.55 %.

6. 8. Absorption and emission spectral measurements

Absorption spectral measurements were recorded using a JASCO V-630 UV-visible spectrophotometer. Quartz cuvettes of path length 1 cm were used. The emission spectral studies were carried out with JASCO FP-6600 spectrofluorometric equipped with a 1cm quartz cuvette. All the emission titration experiments were carried out by adding appropriate amounts of compound **15l** to 1 ml of HSA solution in a 5 ml standard flask in sequence and then phosphate buffer solution (PBS) was added. The solution was allowed to equilibrate for 15 min before recording the spectra and the homogeneous solution systems were transferred to a quartz (1 cm) cuvette. Circular dichroism measurements were executed by a JASCO-810 Spectropolarimeter using a 0.1 cm path length quartz cell. The CD spectral changes were recorded in the range of 200-260 nm with 0.1 nm step resolution and averaged over two scans at a speed of 50 nm min^{-1}. All observed spectra were baseline corrected for the buffer solution and the α-helical content was calculated on the basis of change of molar ellipticity value. The stock solution of HSA was prepared by using PBS of pH = 7.40. The concentration of HSA was measured spectrophotometrically by a reported procedure (Sharma *et al.* 2014:36267). All experiments were carried out at ambient temperature (28 °C).

6. 9. Molecular Docking Studies

AutoDock 4.2 program which operates the Lamarckian genetic algorithm (LGA) was used to dock compound **15l** with the 3D structure of HSA. The crystal structure HSA (PDB id: 1AO6) was obtained from the protein data bank and all water molecules were eliminated with successive addition of hydrogen atoms, followed by the computation of Gasteiger charges as required for LGA molecular docking procedure. The grid size along the x-, y- z- axes and grid space were set to 60 Å, 60 Å and 60 Å and 0.403 Å for HSA. To include the whole subdomain IIA of HSA during the docking process, the grid centre along the x-, y- z- axes was set as 34.016 Å, 42.121 Å, and 50.644 Å. The following docking parameters were used: Genetic Algorithm (GA) population=150; maximum number of energy evaluations=250,000 and GA crossover mode of two points. For each docking simulation, 20 different conformers were generated and the PyMOL package software was used for visualization of the interaction of docked protein−ligand complex. The conformation with the lowest binding free energy was used for further analysis.

Reference

Aicher, T. D., Knorr, D. C. and Smith, H. C., 1998. Synthesis of chiral tetrahydropyrrolo [2, 1-b] thiazol-5 (6H)-ones. Tetrahedron letters (39) 8579-8580.

Alcaide, B., Almendros, P., Alonso, J. M. and Aly, M. F., 2000. 1, 3-Dipolar cycloaddition of 2-azetidinone-tethered azomethine ylides. Application to the rapid, stereocontrolled synthesis of optically pure highly functionalised pyrrolizidine systems. Chemical Communications (6) 485-486.

Albertshofer, K., Tan, B. and Barbas III, C. F., 2012. Assembly of spirooxindole derivatives containing four consecutive stereocenters via organocatalytic Michael–Henry cascade reactions. Org. Lett (14) 1834-1837.

Anand, U., Jash, C. and Mukherjee, S., 2010. Spectroscopic probing of the microenvironment in a protein− surfactant assembly. The Journal of Physical Chemistry B (114) 15839-15845.

Baldwin, J. E., Freeman, R. T., Lowe, C., Schofield, C. J., Lee, E., 1989. A γ-lactam analogue of the penems possessing antibacterial activity. Tetrahedron **(**45) 4537-4550.

Bhattacharya, B., Nakka, S., Guruprasad, L. and Samanta, A., 2009. Interaction of bovine serum albumin with dipolar molecules: fluorescence and molecular docking studies. The Journal of Physical Chemistry B (113) 2143-2150.

Cui, C. B., Kakeya, H. and Osada, H., 1996. Spirotryprostatin B, a novel mammalian cell cycle inhibitor produced by Aspergillus fumigatus. The Journal of antibiotics (49) 832-835.

Chandraprakash, K., Sankaran, M., Uvarani, C., Shankar, R., Ata, A., Dallemer, F. and Mohan, P. S., 2013. A strategic approach to the synthesis of novel class of dispiroheterocyclic derivatives through 1, 3 dipolar cycloaddition of azomethine ylide with (E)-3-arylidene-2, 3-dihydro-8-nitro-4-quinolone. Tetrahedron Letters (54) 3896-3901.

Hasegawa, M., Nakayama, A., Yokohama, S., Hosokami, T., Kurebayashi, Y., Ikeda, T., Shimoto, Y., Ide, S., Honda, Y. and Suzuki, N., 1995. Synthesis and pharmacological activities of novel bicyclic thiazoline derivatives as hepatoprotective agents. II. (7-Alkoxycarbonyl-2, 3, 5, 6-tetrahydropyrrolo [2, 1-b] thiazol-3-ylidene) acetamide derivatives. Chemical and pharmaceutical bulletin (43) 1125-1131.

Jossang, A., Jossang, P., Hadi, H. A., Sevenet, T. and Bodo, B., 1991. Horsfiline, an oxindole alkaloid from Horsfieldia superba. The Journal of Organic Chemistry (56) 6527-6530.

Kim, D. K., Choi, J. H., An, Y. J. and Lee, H. S., 2008. Synthesis and biological evaluation of 5-(pyridin-2-yl) thiazoles as transforming growth factor-β type1 receptor kinase inhibitors. Bioorganic & medicinal chemistry letters (18) 2122-2127.

Kawashima, K., Kakehi, A. and Noguchi, M., 2007. Generation of functionalized azomethine ylides and their application to stereoselective heterocycle synthesis: An equivalent process of C-unsubstituted nitrile ylide cycloaddition reaction. Tetrahedron (63) 1630-1643.

Kondoh, M., Takeo, U. S. U. I., Nishikiori, T., Mayumi, T. and Osada, H., 1999. Apoptosis induction via microtubule disassembly by an antitumour compound, pironetin. Biochemical Journal (340) 411-416.

Khan, M. K., Rakotomanomana, N., Dufour, C. and Dangles, O., 2011. Binding of citrus flavanones and their glucuronides and chalcones to human serum albumin. Food & function (2) 617-626.

LaMontagne, M. P., Blumbergs, P. and Smith, D. C., 1989. Antimalarials. Synthesis of 2-substituted analogs of 8-[(4-amino-1-methylbutyl) amino]-6-methoxy-4-methyl-5-[3-(trifluoromethyl) phenoxy] quinoline as candidate antimalarials. Journal of medicinal chemistry (32) 1728-1732.

Liu, J., Wang, Y., Sun, Y., Marshall, D., Miao, S., Tonn, G., Anders, P., Tocker, J., Tang, H.L. and Medina, J., 2009. Tetrahydroquinoline derivatives as CRTH2 antagonists. Bioorganic & medicinal chemistry letters (19) 6840-6844.

Lu, Y., Nikolovska-Coleska, Z., Fang, X., Gao, W., Shangary, S., Qiu, S., Qin, D. and Wang, S., 2006. Discovery of a nanomolar inhibitor of the human murine double minute 2 (MDM2)− p53 interaction through an integrated, virtual database screening strategy. Journal of medicinal chemistry (49) 3759-3762.

Moulard, T., Lagorce, J. F., Thomes, J. C. and Raby, C., 1993. Biological Evaluation of Compounds with-NCS-Group or Derived from Thiazole and Imidazole. Activity on Prostaglandin Synthetase Complex. Journal of pharmacy and pharmacology (45) 731-735.

Morrissey, I. and Smith, J. T., 1995. Bactericidal activity of the new 4-quinolones DU-6859a and DV-7751a. Journal of medical microbiology (43) 4-8.

Maheswari, S.U., Balamurugan, K., Perumal, S., Yogeeswari, P. and Sriram, D., 2010. A facile 1, 3-dipolar cycloaddition of azomethine ylides to 2-arylidene-1, 3-indanediones: Synthesis of dispiro-oxindolylpyrrolothiazoles and their antimycobacterial evaluation. Bioorganic & medicinal chemistry letters (20) 7278-7282.

Nieman, J. A. and Ennis, M. D., 2000. Enantioselective synthesis of the pyrroloquinoline core of the martinellines. Organic letters (2) 1395-1397.

Nithya, P., Helena, S., Simpson, J., Ilanchelian, M., Muthusankar, A. and Govindarajan, S., 2016. New cobalt (II) and nickel (II) complexes of benzyl carbazate Schiff bases: Syntheses, crystal structures, in vitro DNA and HSA binding studies. Journal of Photochemistry and Photobiology B: Biology (165) 220-231.

Neelam, S., Gokara, M., Sudhamalla, B., Amooru, D. G. and Subramanyam, R., 2010. Interaction studies of coumaroyltyramine with human serum albumin and it's biological importance. The Journal of Physical Chemistry B (114) 3005-3012.

Park, C. M., Choi, J. I., Choi, J. H., Kim, S.Y., Park, W. K. and Seong, C. M., 2011. 1-(Arylsulfonyl)-2, 3-dihydro-1H-quinolin-4-one derivatives as 5-HT 6 serotonin receptor ligands. Bioorganic & medicinal chemistry letters (21) 698-703.

Padwa, A. and Pearson, W. H. eds., 2003. The Chemistry of Heterocyclic Compounds, Synthetic Applications of 1, 3-Dipolar Cycloaddition Chemistry toward Heterocycles and Natural Products (Vol. 59). John Wiley & Sons.

Svoboda, G. H., Poore, G. A., Simpson, P. J. and Boder, G. B., 1966. Alkaloids of Acronychia Baueri Schott I: Isolation of the alkaloids and a study of the antitumor and other biological properties of acronycine. Journal of pharmaceutical sciences (55) 758-768.

Sarotti, A. M., Spanevello, R. A., Suárez, A. G., Echeverría, G. A. and Piro, O. E., 2012. 1, 3-Dipolar Cycloaddition Reactions of Azomethine Ylides with a Cellulose-Derived Chiral Enone. A Novel Route for Organocatalysts Development. Organic letters (14) 2556-2559.

Spandl, R. J., Bender, A. and spring, D. R., 2008. Diversity-oriented synthesis; a spectrum of approaches and results. Organic & biomolecular chemistry (6) 1149-1158.

Sharma, A. S., Anandakumar, S. and Ilanchelian, M., 2014. A combined spectroscopic and molecular docking study on site selective binding interaction of Toluidine blue O with Human and Bovine serum albumins. Journal of Luminescence (151) 206-218.

Shanmugaraj, K., Anandakumar, S. and Ilanchelian, M., 2014. Exploring the biophysical aspects and binding mechanism of thionine with bovine hemoglobin by optical spectroscopic and molecular docking methods. Journal of Photochemistry and Photobiology B: Biology (131) 43-52.

Sharma, A. S., Anandakumar, S. and Ilanchelian, M., 2014. In vitro investigation of domain specific interactions of phenothiazine dye with serum proteins by spectroscopic and molecular docking approaches. RSC Advances (4) 36267-36281.

Trapani, G., Franco, M., Latrofa, A., Genchi, G., Brigiani, G. S., Mazzoccoli, M., Persichella, M., Serra, M., Biggio, G. and Liso, G., 1994. Synthesis and anticonvulsant activity of some 1, 2, 3, 3a-tetrahydropyrrolo [2, 1-b] benzothiazol-1-ones and pyrrolo [2, 1-b] thiazole analogues. European journal of medicinal chemistry (29) 197-204.

Thangavel, S., Rajamanikandan, R., Friedrich, H. B., Ilanchelian, M. and Omondi, B., 2016. Binding interaction, conformational change, and molecular docking study of N-(pyridin-2-ylmethylene) aniline derivatives and carbazole Ru (II) complexes with human serum albumins. Polyhedron (107) 124-135.

Van der Sar, S. A., Blunt, J. W. and Munro, M. H., 2006. Spiro-Mamakone A: a unique relative of the spirobisnaphthalene class of compounds. Organic letters (8) 2059-2061.

Van Pelt-Koops, J. C., Pett, H. E., Graumans, W., van der Vegte-Bolmer, M., Van Gemert, G. J., Rottmann, M., Yeung, B. K. S., Diagana, T. T. and Sauerwein, R.W., 2012. The spiroindolone drug candidate NITD609 potently inhibits gametocytogenesis and blocks Plasmodium falciparum transmission to anopheles mosquito vector. Antimicrobial agents and chemotherapy (56) 3544-3548.

Valeur, B. and Berberan-Santos, M. N., 2012. Molecular fluorescence: principles and applications. John Wiley & Sons.

Xia, Y., Yang, Z.Y., Xia, P., Bastow, K. F., Tachibana, Y., Kuo, S. C., Hamel, E., Hackl T. and Lee, K. H., 1998. Antitumor Agents. Synthesis and Biological Evaluation of 6, 7, 2 ‘, 3 ‘, 4 ‘-Substituted-1, 2, 3, 4-tetrahydro-2-phenyl-4-quinolones as a New Class of Antimitotic Antitumor Agents. Journal of medicinal chemistry (41) 1155-1162.

Yavuz, S., Özkan, H., Tok, G. and Dişli, A., 2013. Facile Method for 1, 3-Dipolar Cycloaddition Reaction of Azomethine Ylides: Highly Stereoselective Synthesis of Substituted Pyrrolidine Derivatives. Journal of Heterocyclic Chemistry (50) 1437-1440**.**

Zhang, J., Tian, Z., Liang, L., Subirade, M. and Chen, L., 2013. Binding interactions of β-conglycinin and glycinin with vitamin B12. The Journal of Physical Chemistry B (117) 14018-14028.

Zaidi, N., Ahmad, E., Rehan, M., Rabbani, G., Ajmal, M. R., Zaidi, Y., Subbarao, N. and Khan, R. H., 2013. Biophysical insight into furosemide binding to human serum albumin: a study to unveil its impaired albumin binding in uremia. The Journal of Physical Chemistry B (117) 2595-2604.

Zhang, Y., Li, Y., Dong, L., Li, J., He, W., Chen, X. and Hu, Z., 2008. Investigation of the interaction between naringin and human serum albumin. Journal of Molecular Structure (875) 1-8.

Chapter Six

Appendix

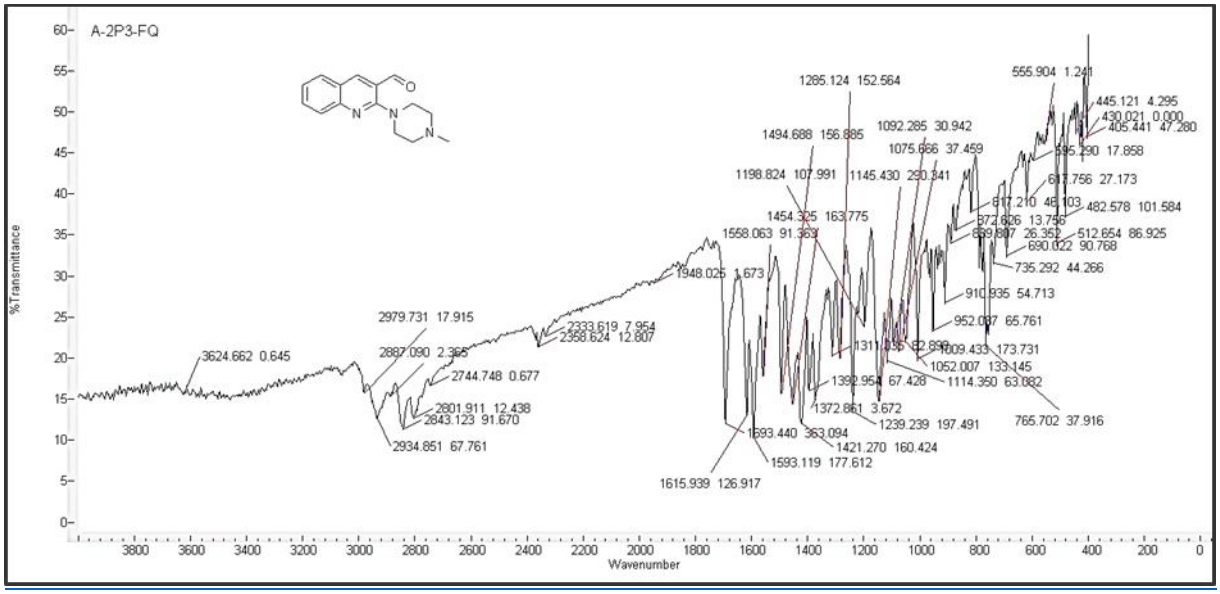

Figure 6. S. 1. The Infra-Red Spectrum of compound 3

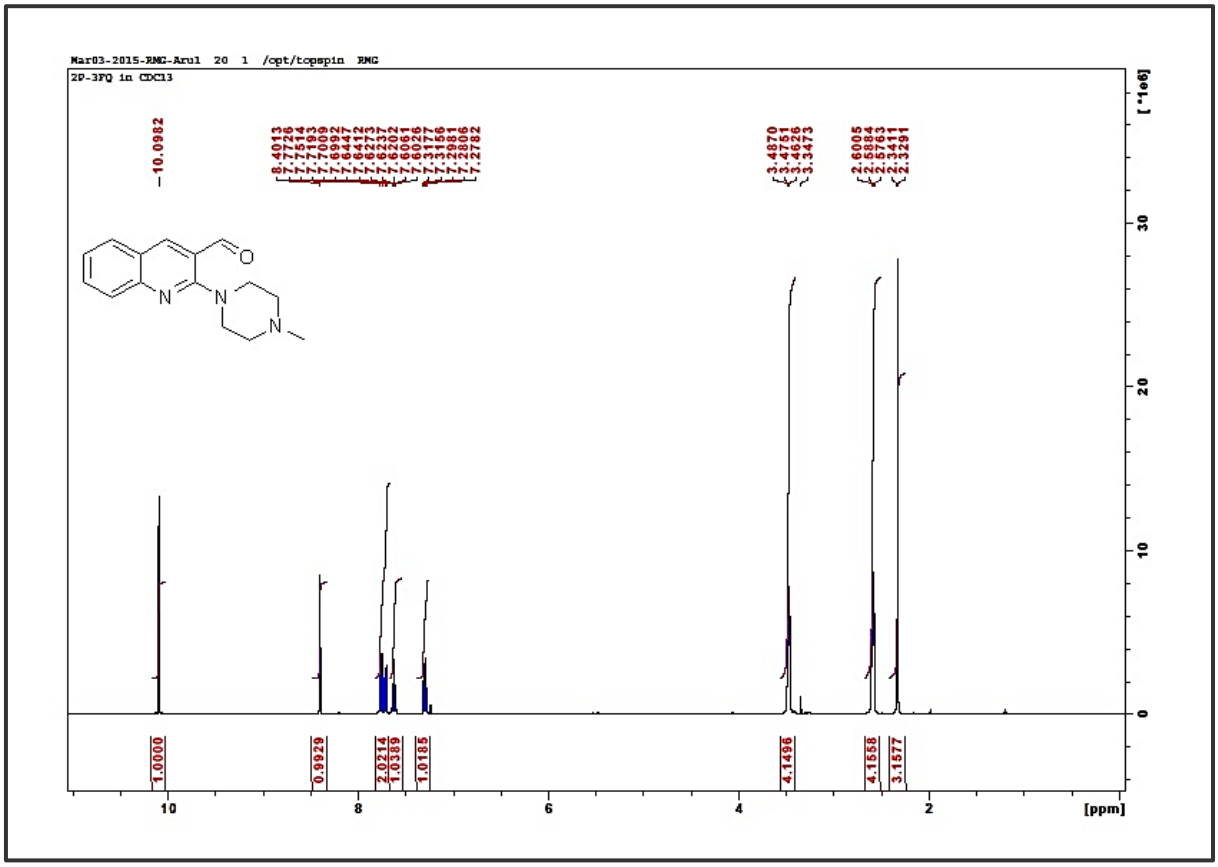

Figure 6. S. 2. The ^{1}H NMR of compound 3

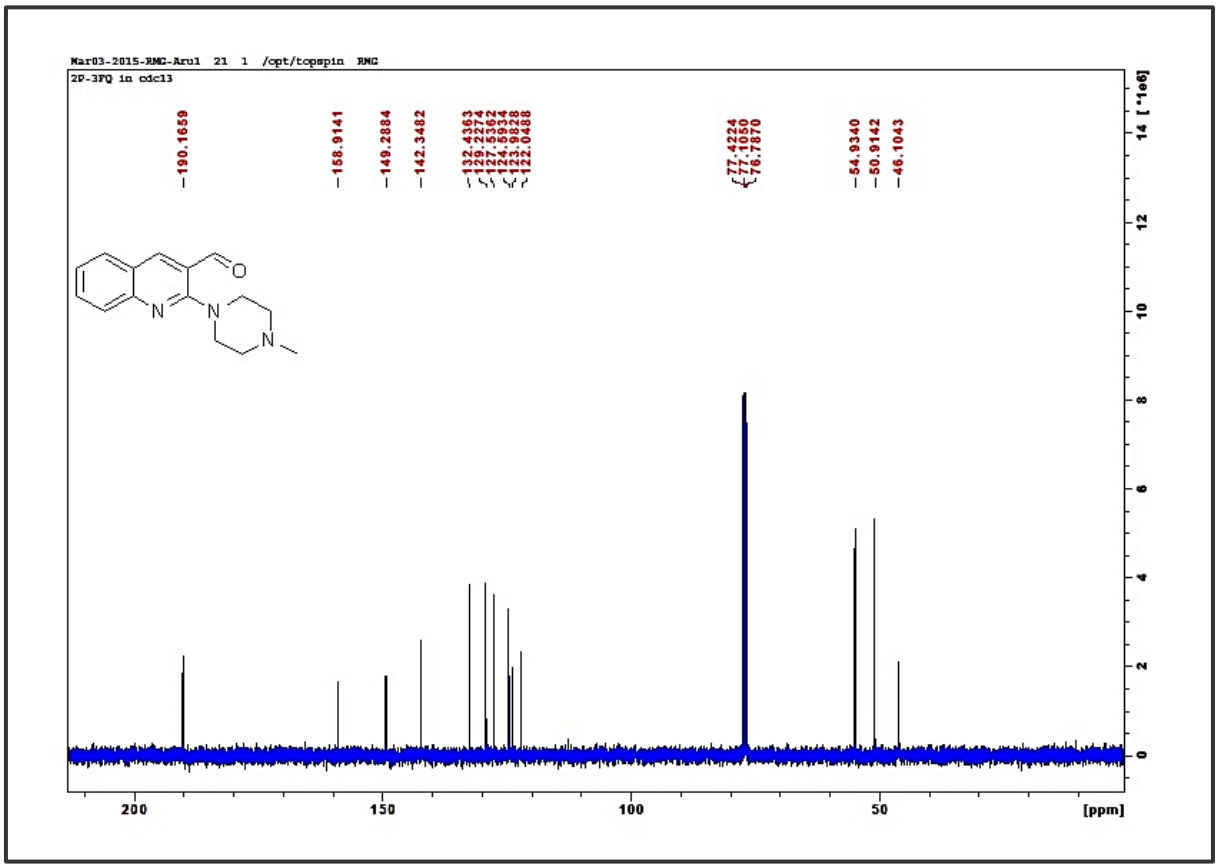

Figure 6. S. 3. The ^{13}C NMR of compound 3

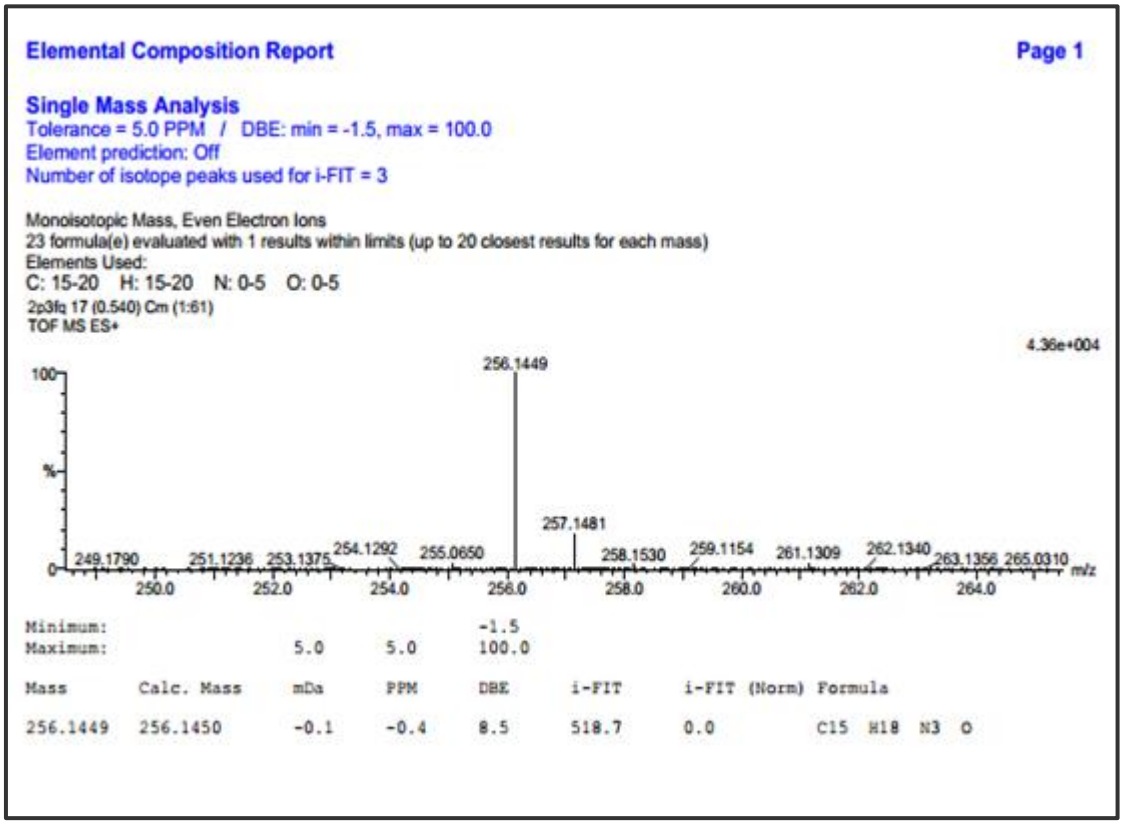

Figure 6. S. 4. The HRMS of compound 3

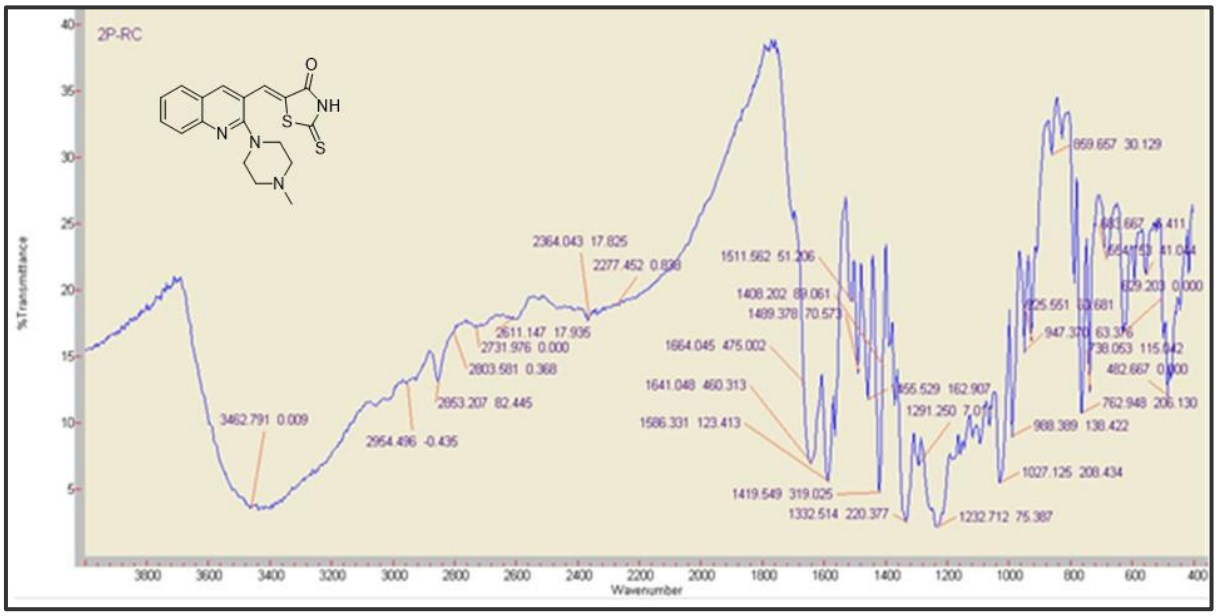

Figure 6. S. 5. The Infra-Red Spectrum of compound 5

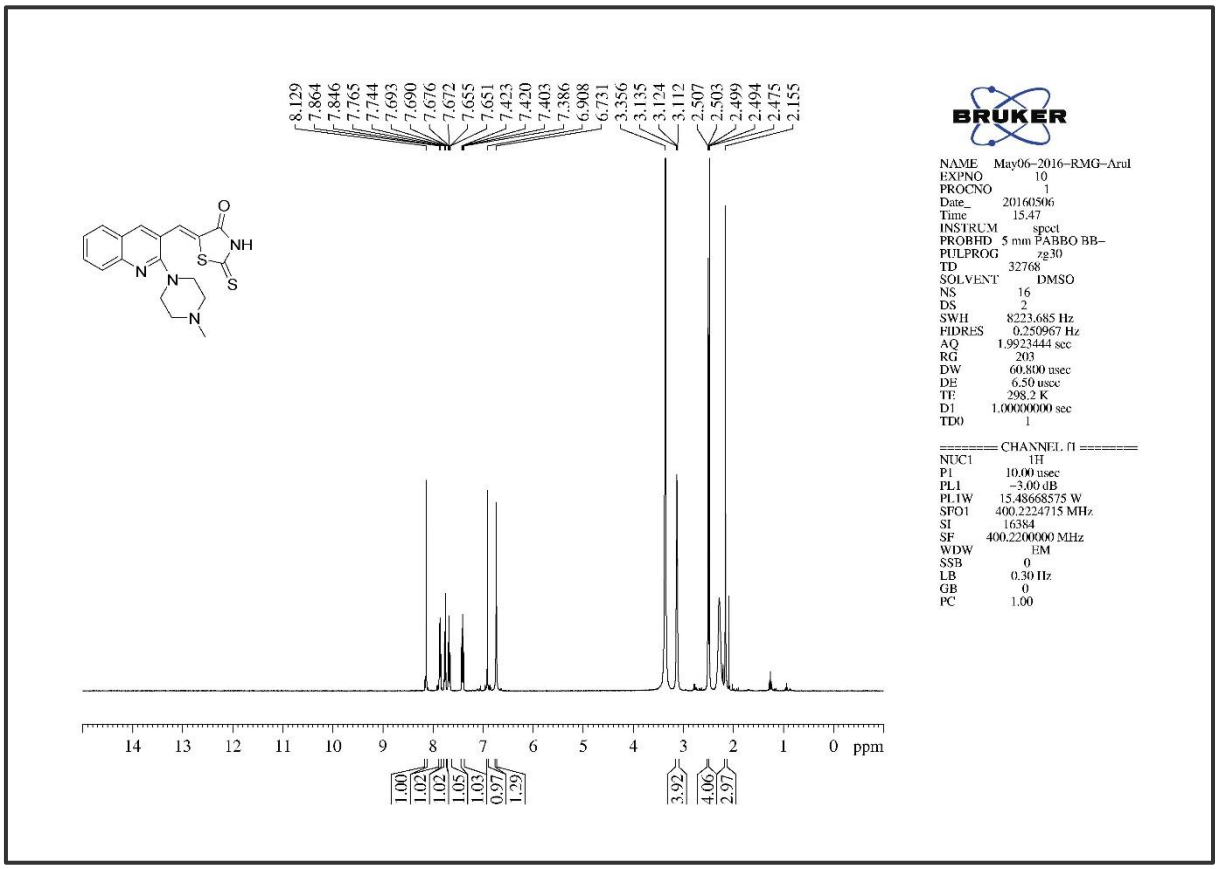

Figure 6. S. 6. The ^{1}H NMR of compound 5

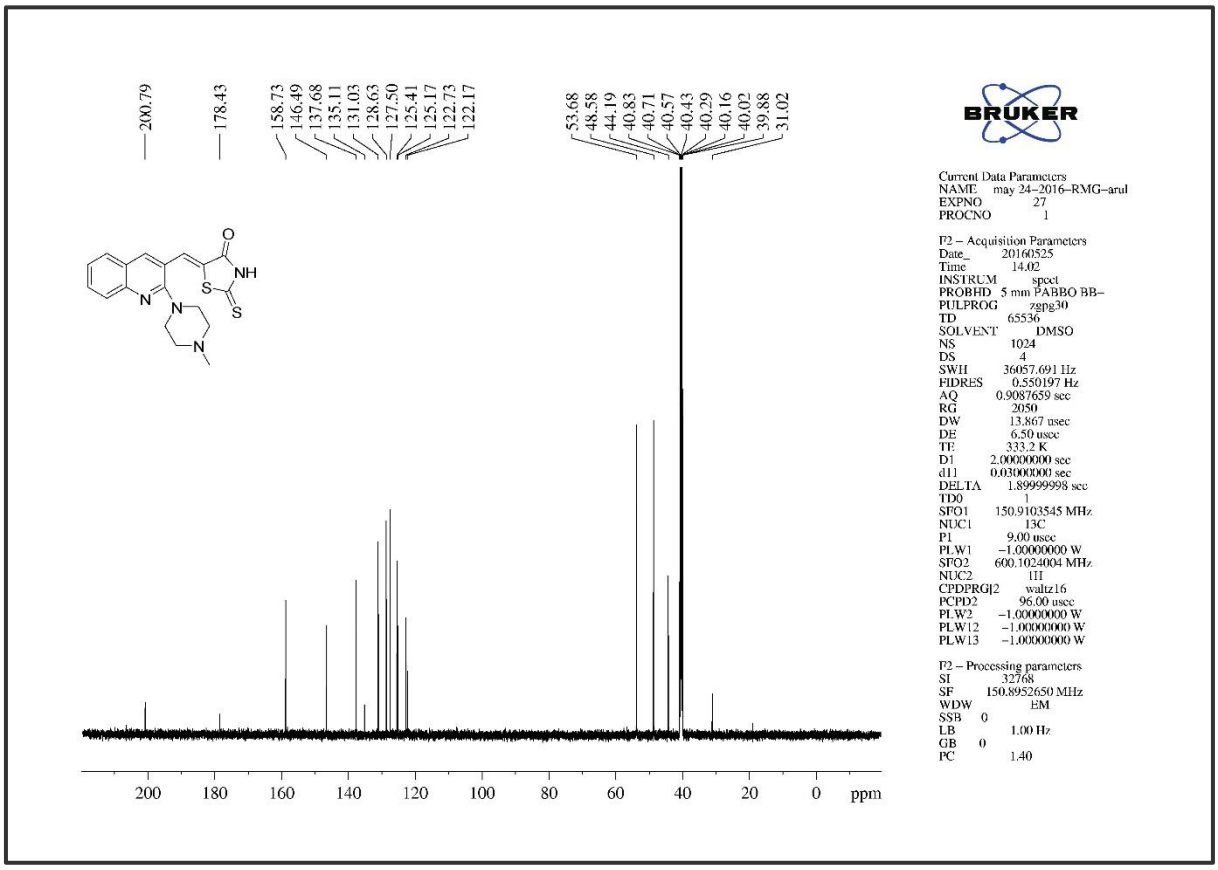

Figure 6. S. 7. The ^{13}C NMR of compound 5

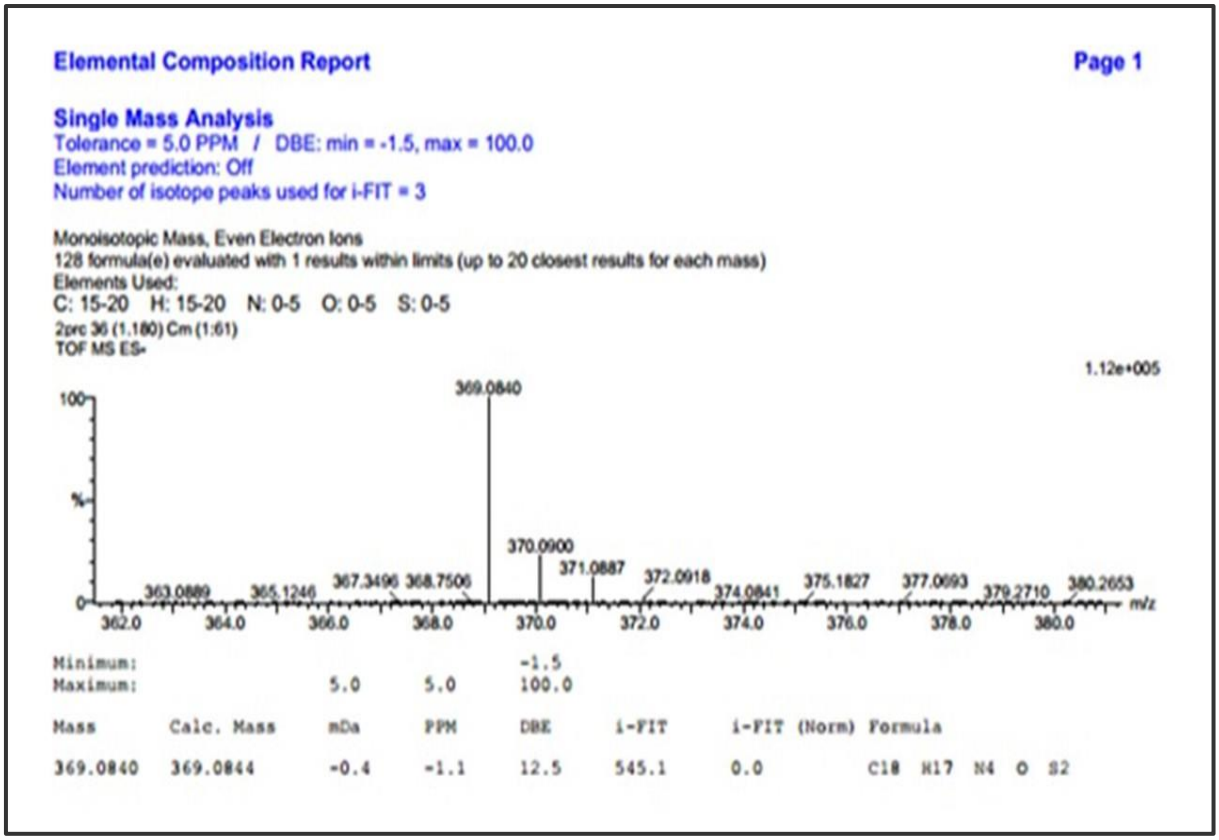

Figure 6. S. 8. The HRMS of compound 5

Figure 6. S. 9. The Infra-Red Spectrum of compound 10a

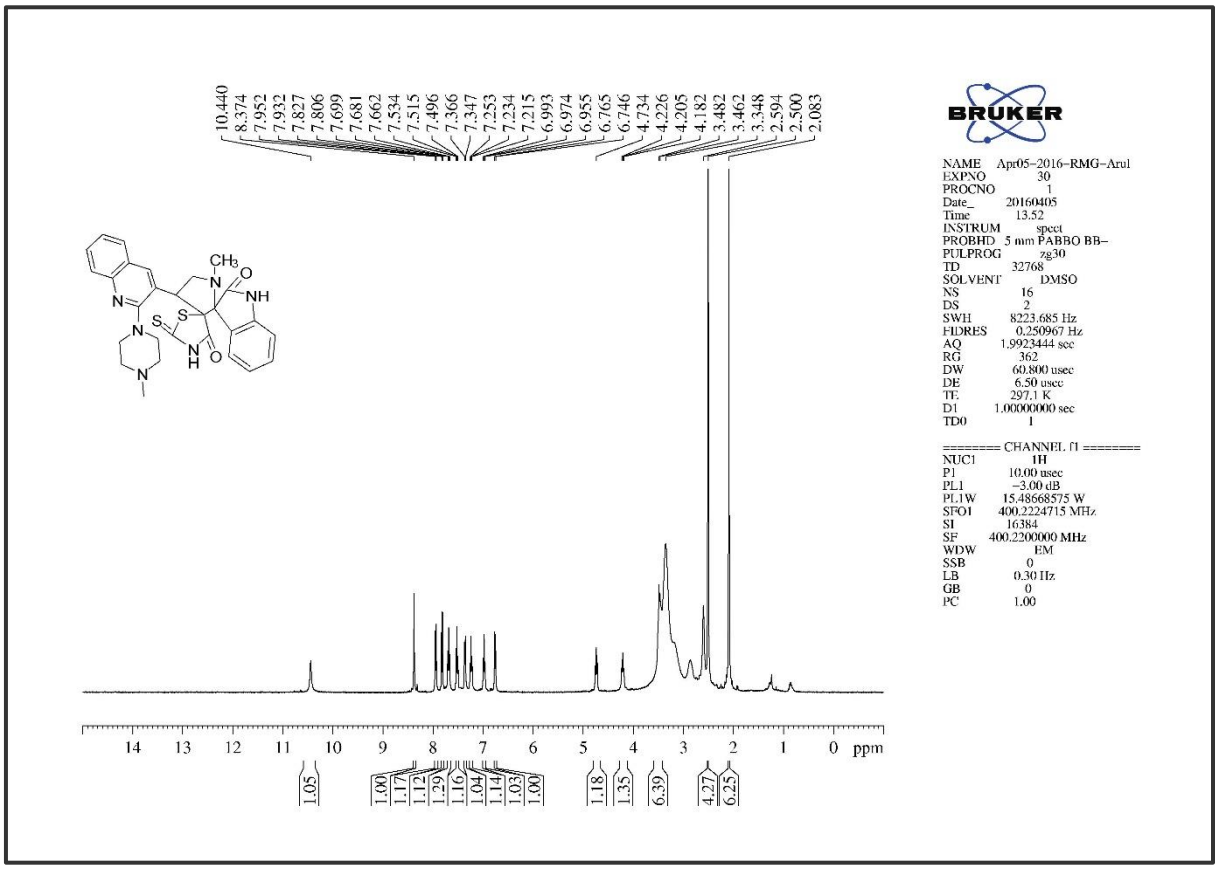

Figure 6. S. 10. The ^{1}H NMR of compound 10a

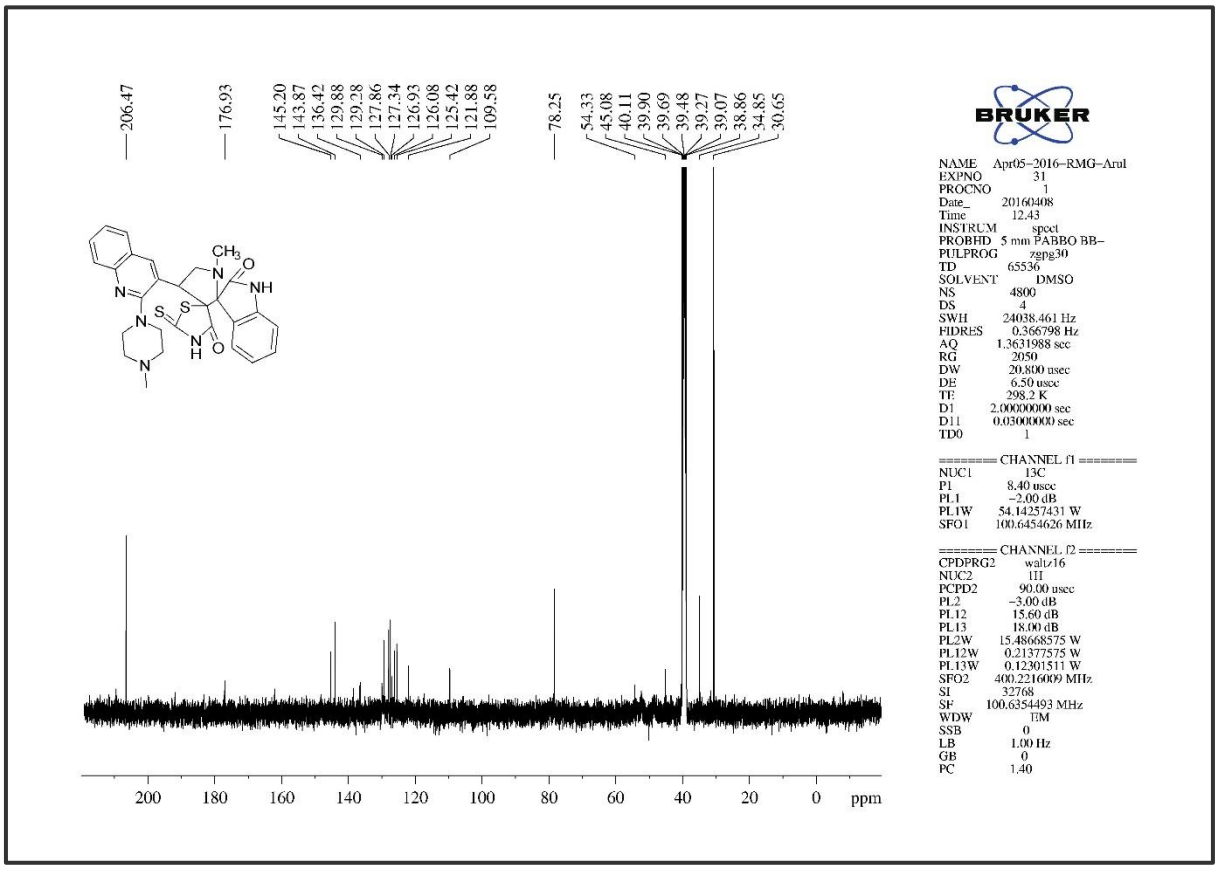

Figure 6. S. 11. The ^{13}C NMR of compound 10a

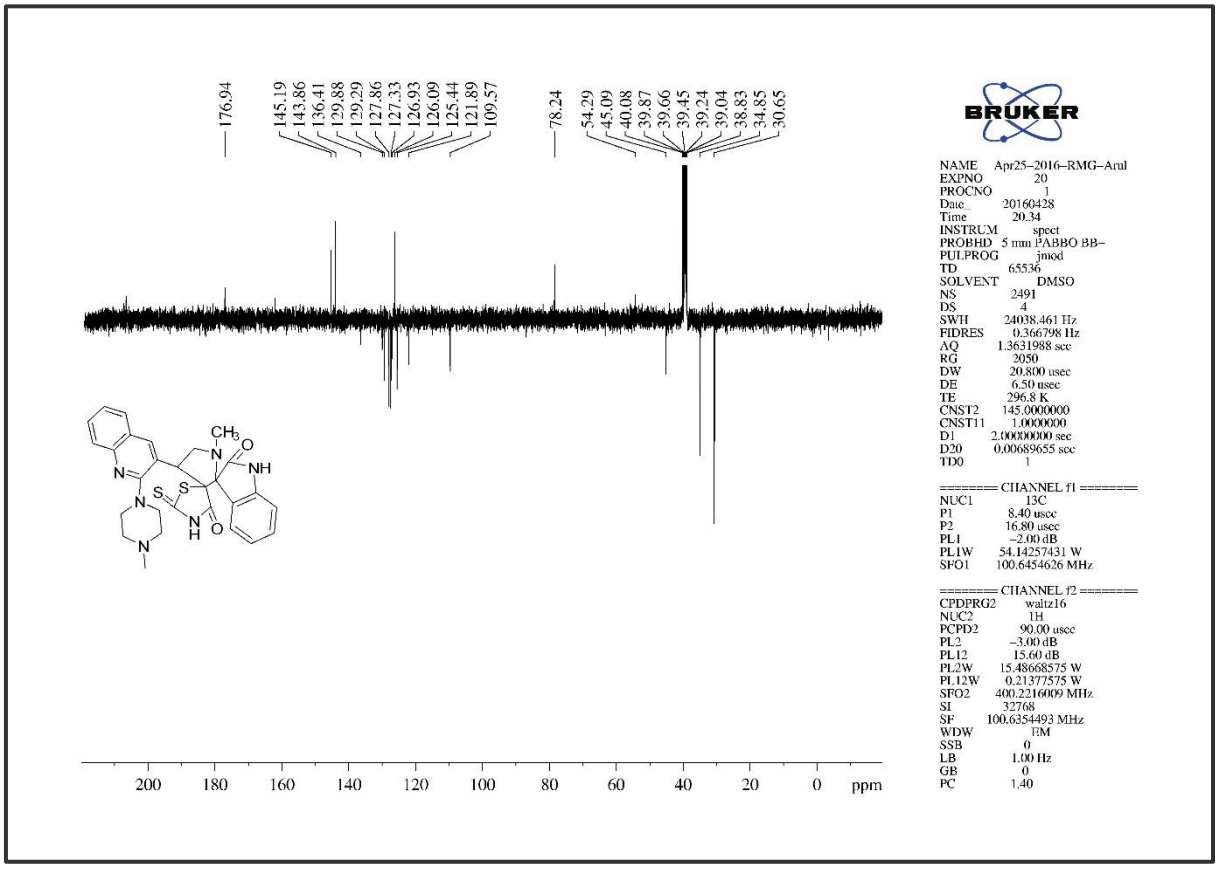

Figure 6. S. 12. The ^{13}C APT NMR Spectrum of compound 10a

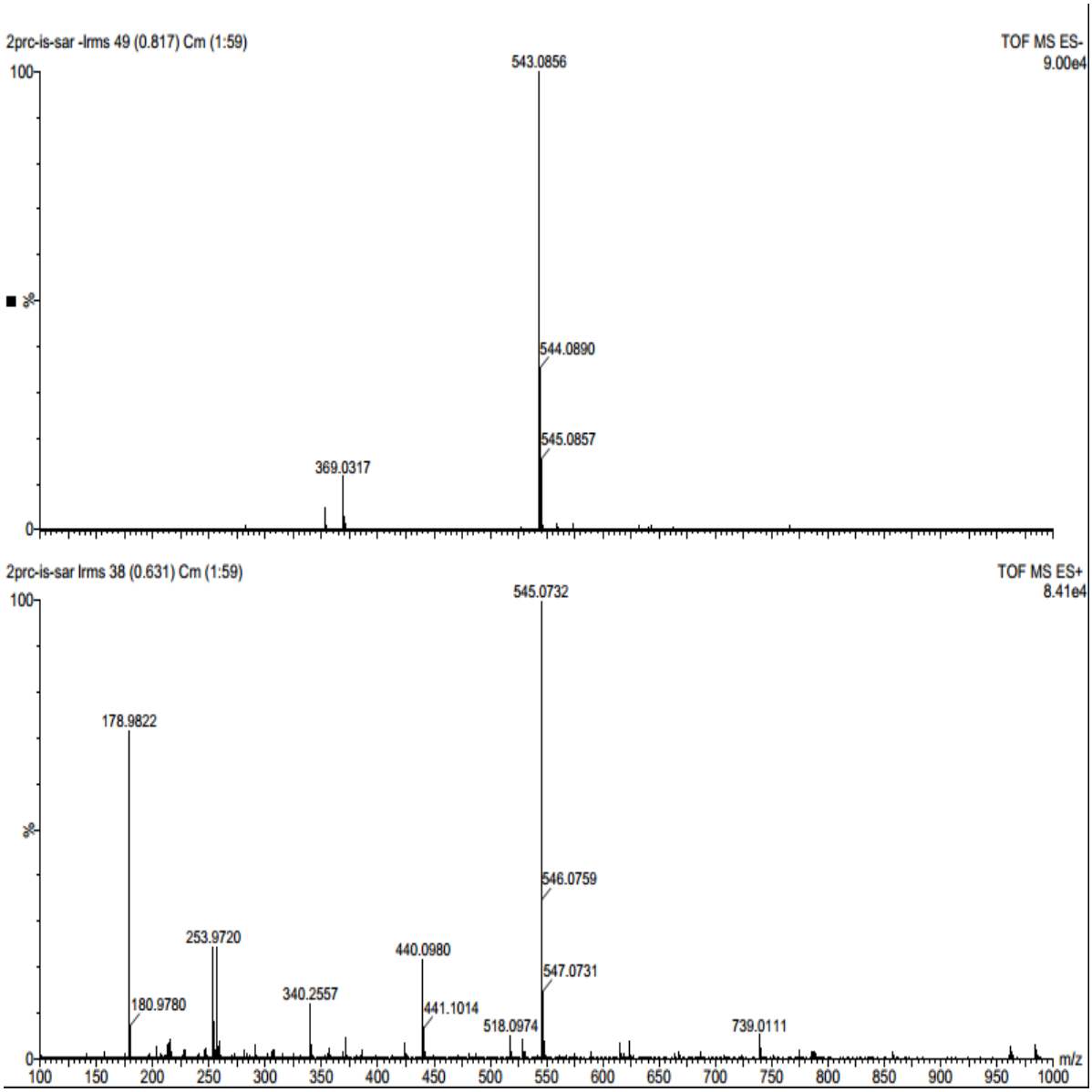

Figure 6. S. 13. The HRMS of compound 10a

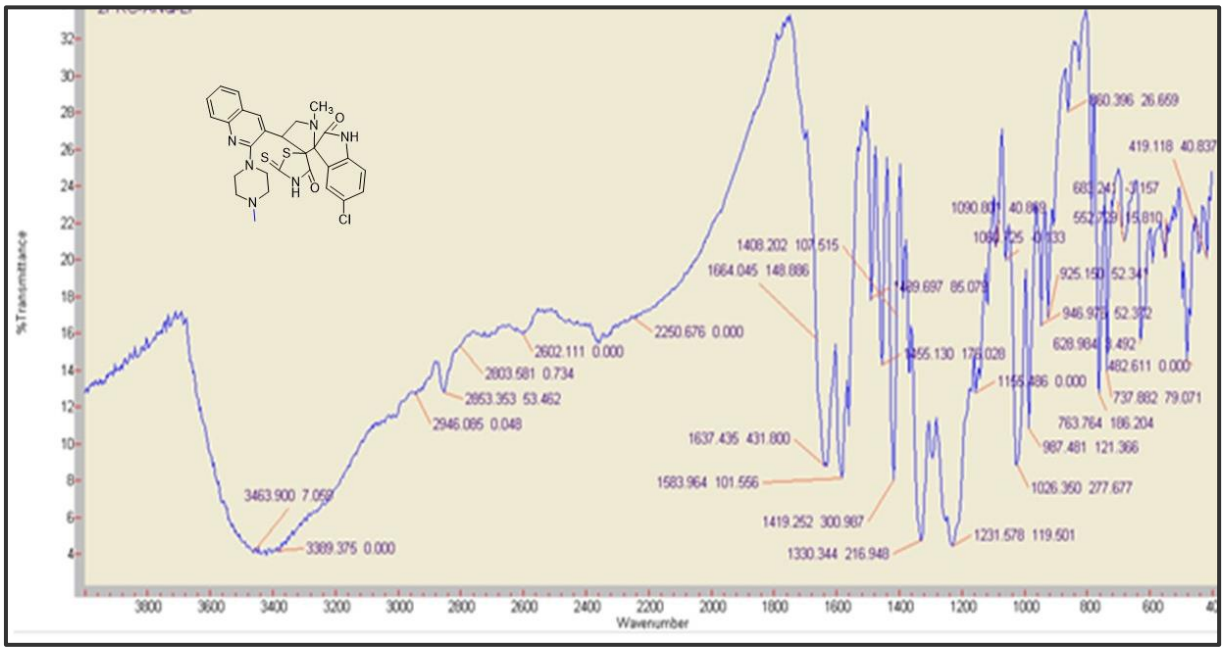

Figure 6. S. 14. The Infra-Red Spectrum of compound 10b

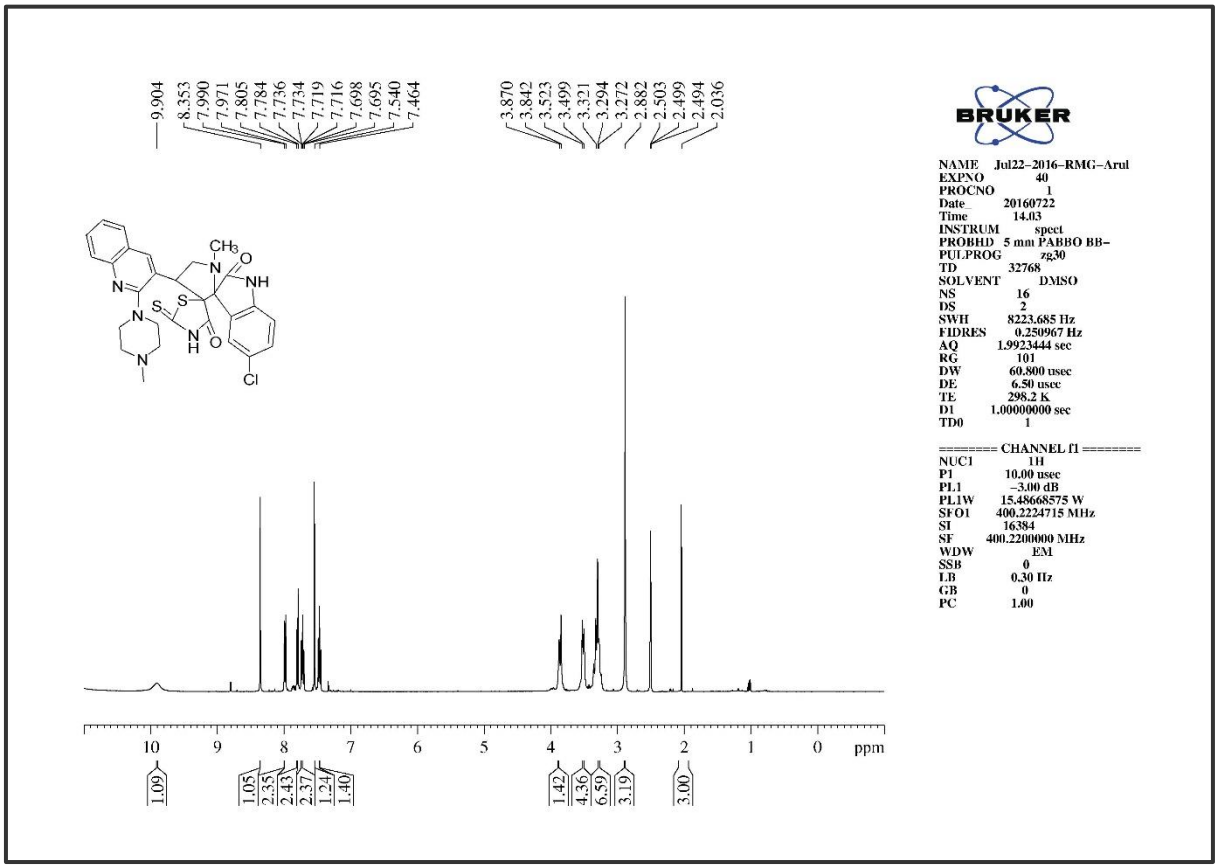

Figure 6. S. 15. The ^{1}H NMR of compound 10b

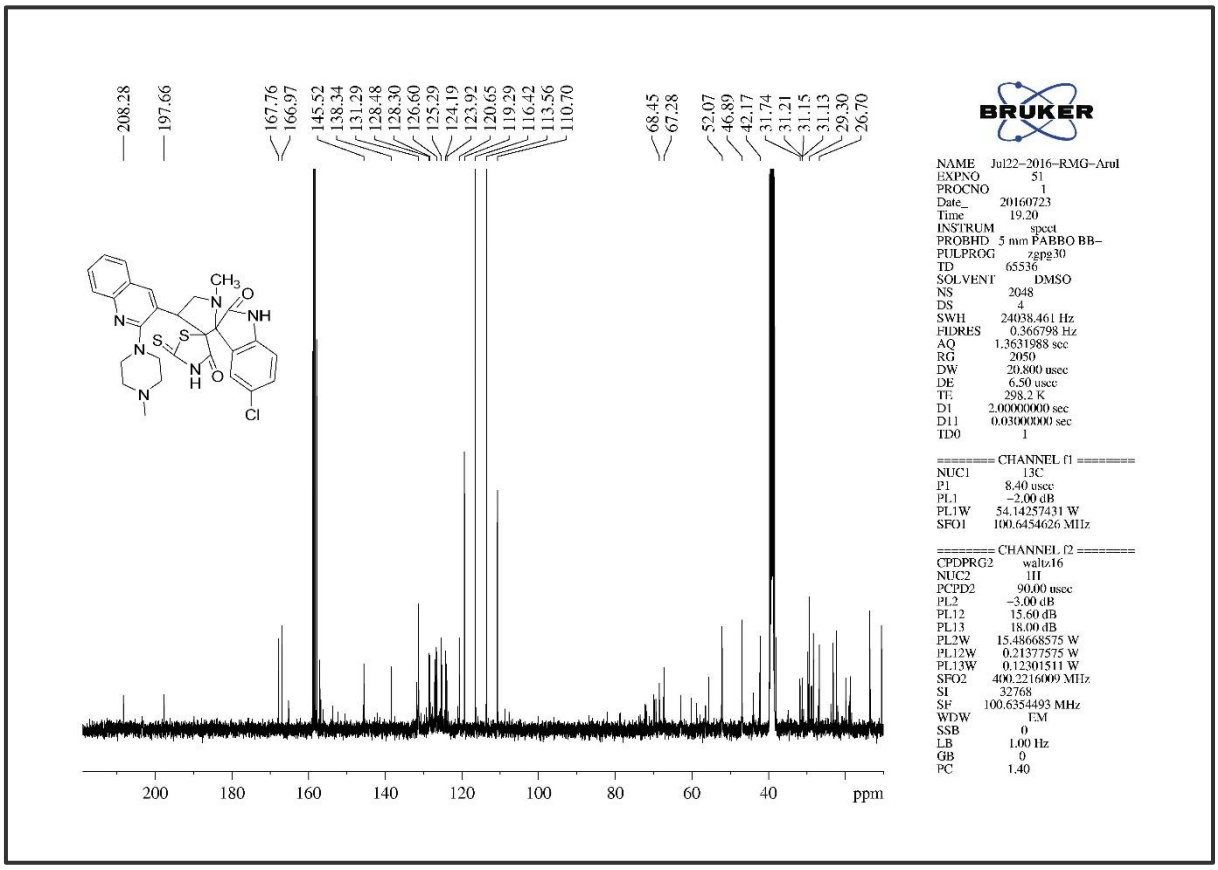

Figure 6. S. 16. The ^{13}C NMR of compound 10b

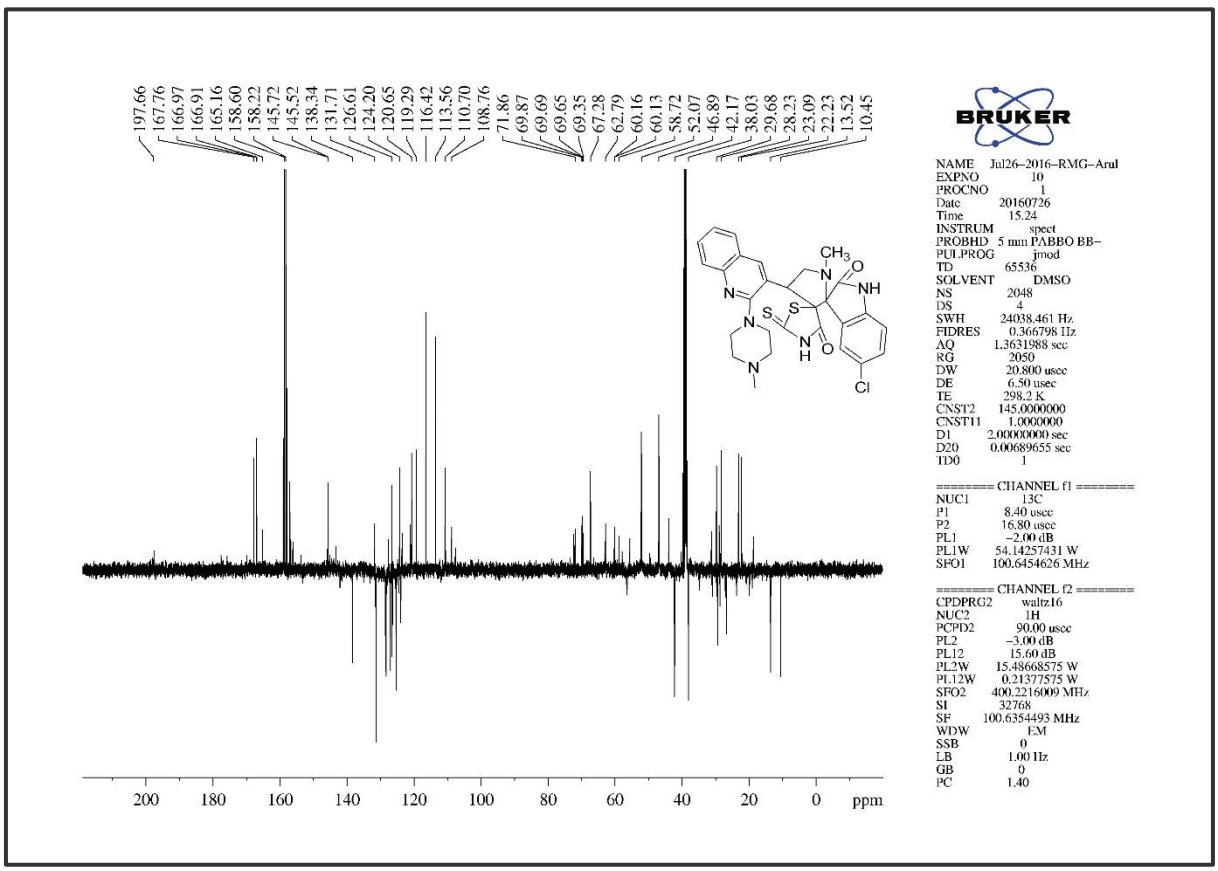

Figure 6. S. 17. The ^{13}C APT NMR Spectrum of compound 10b

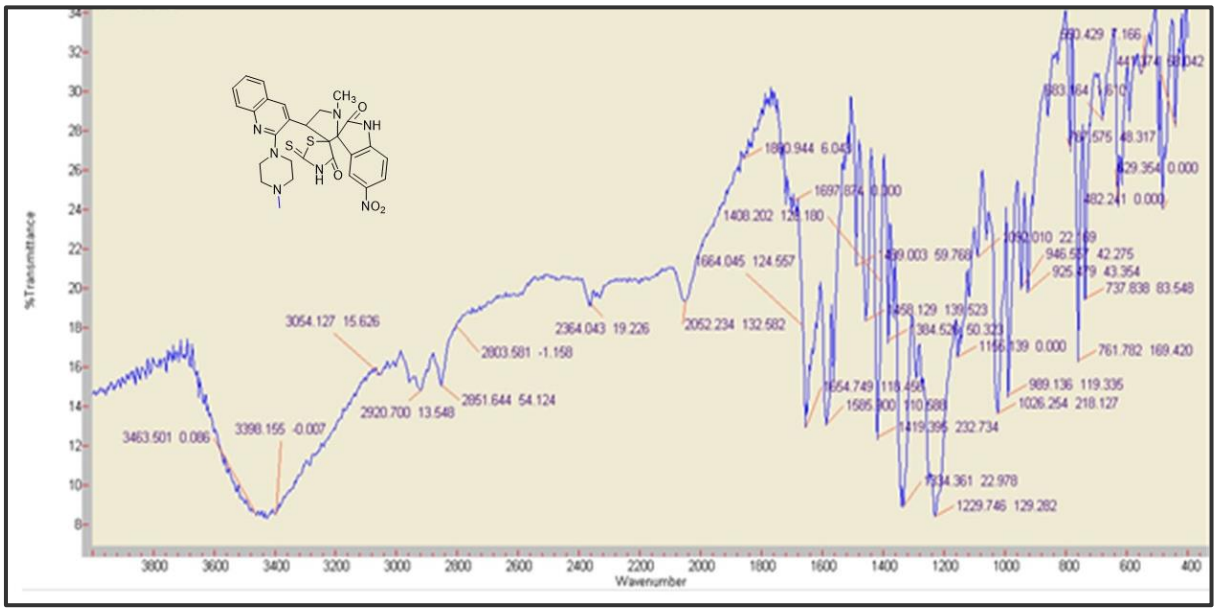

Figure 6. S. 18. The Infra-Red Spectrum of compound 10c

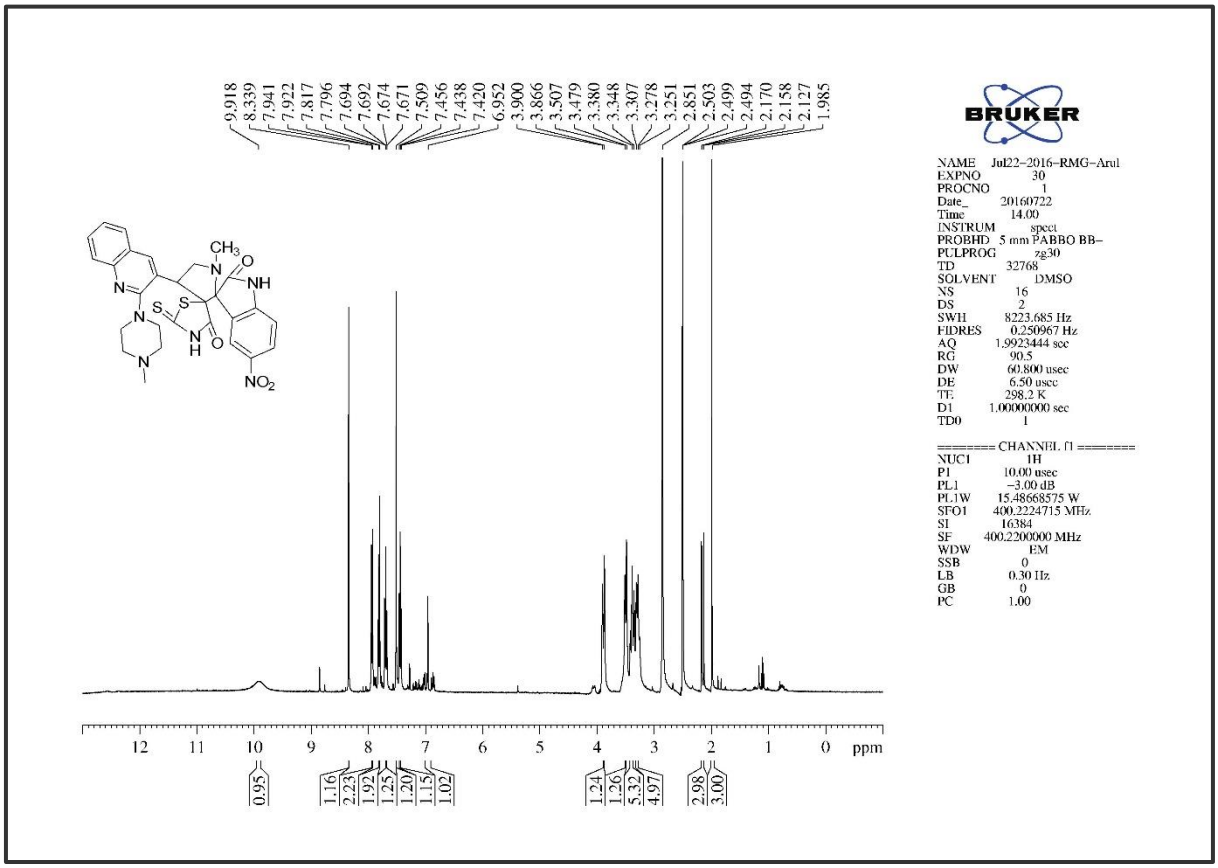

Figure 6. S. 19. The ^{1}H NMR of compound 10c

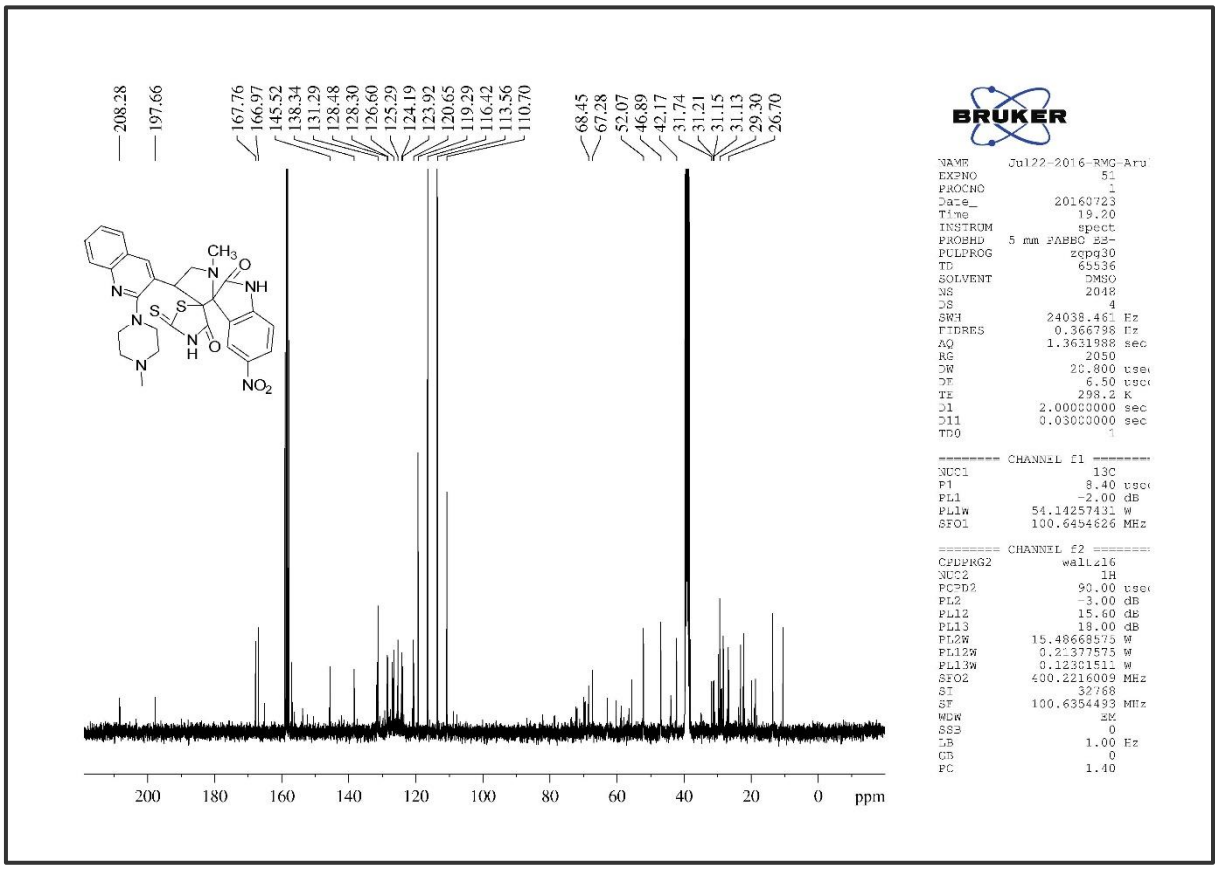

Figure 6. S. 20. The ^{13}C NMR of compound 10c

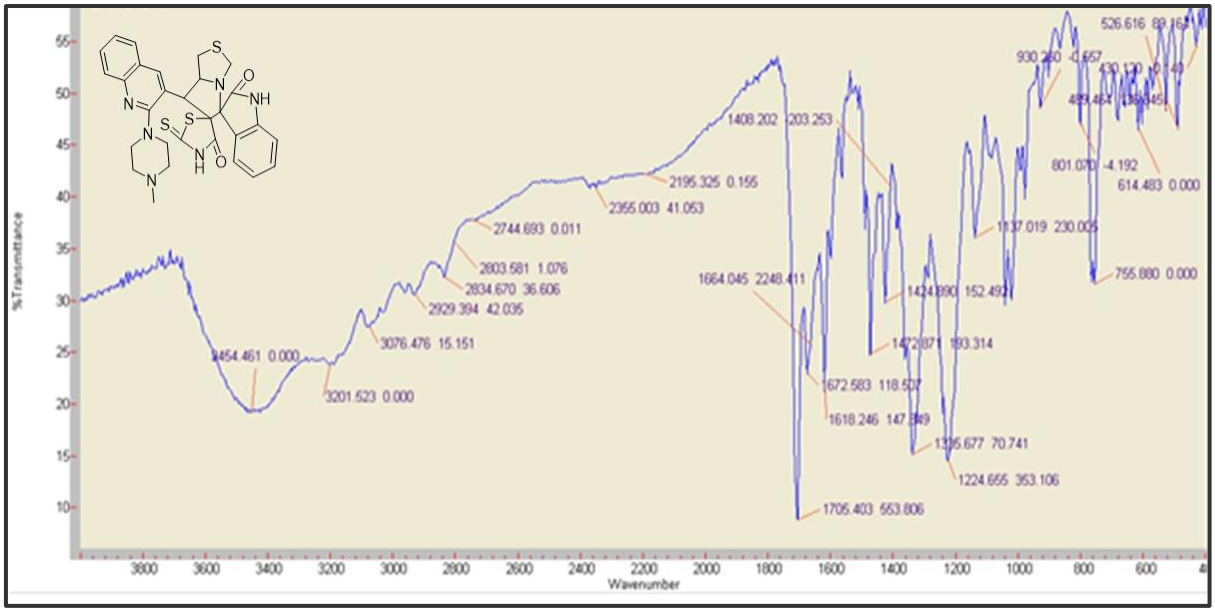

Figure 6. S. 21. The Infra-Red Spectrum of compound 11d

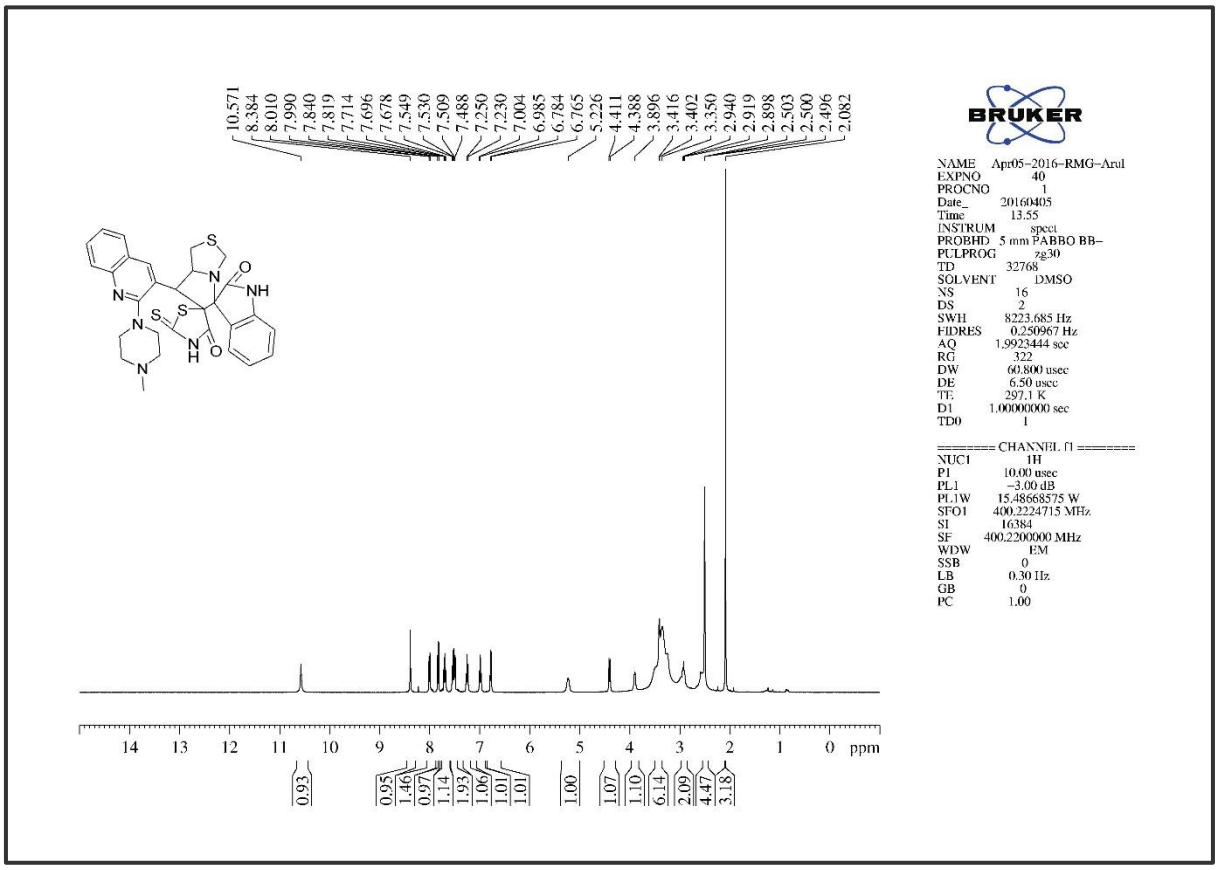

Figure 6. S. 22. The ^{1}H NMR of compound 11d

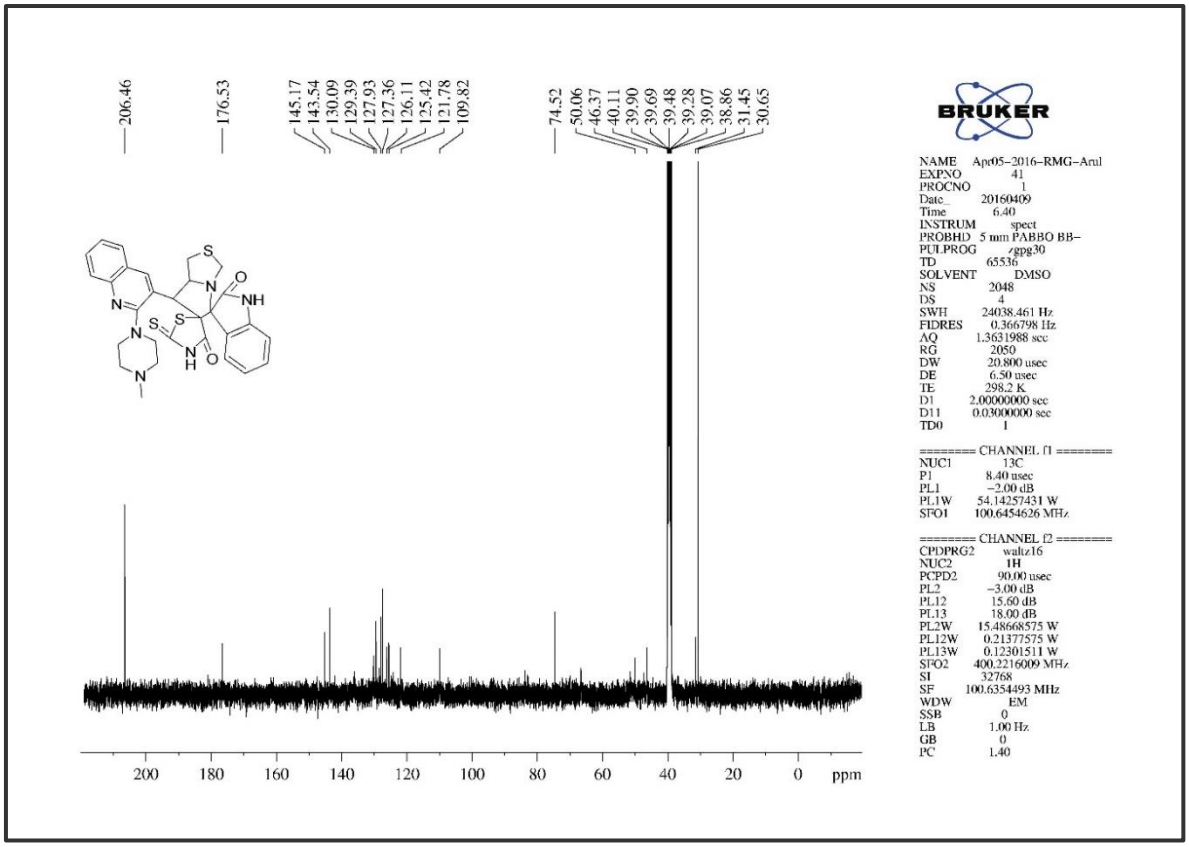

Figure 6. S. 27. The ^{13}C NMR of compound 11d

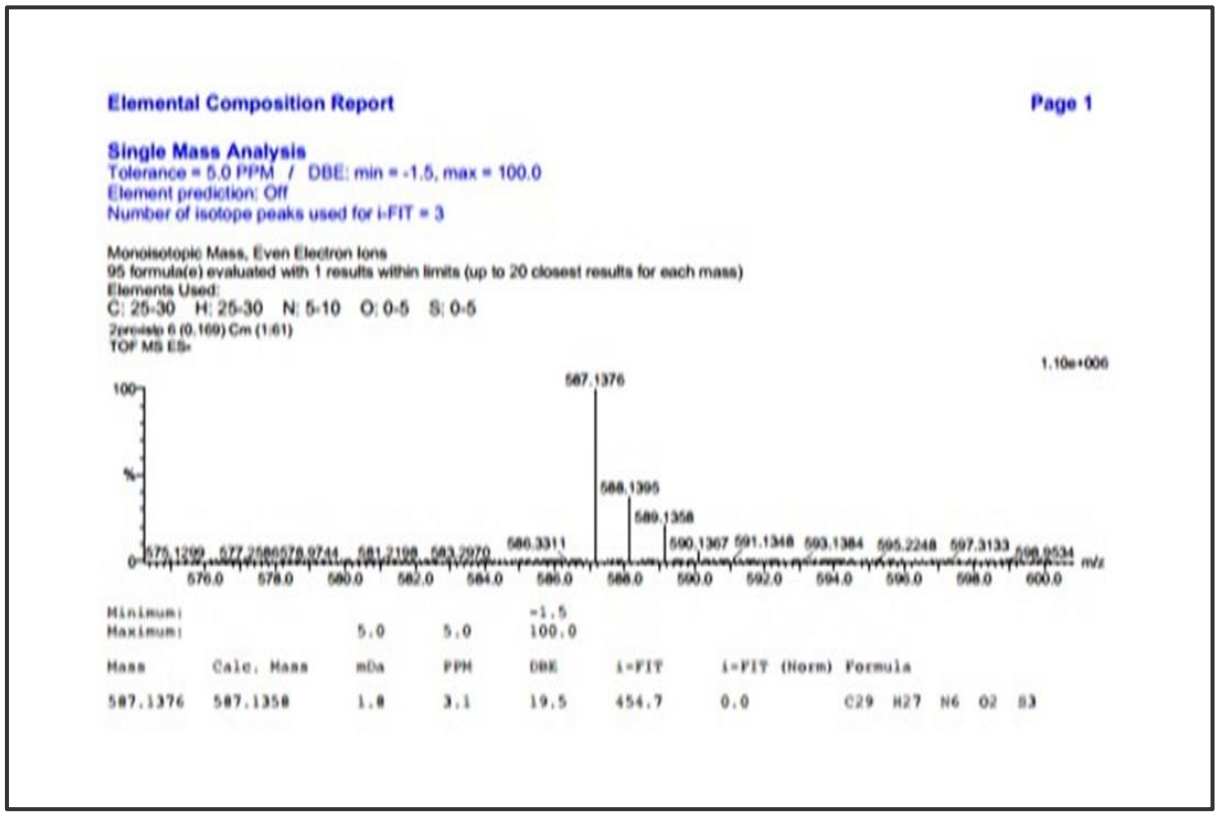

Figure 6. S. 28. The HRMS of compound 11d

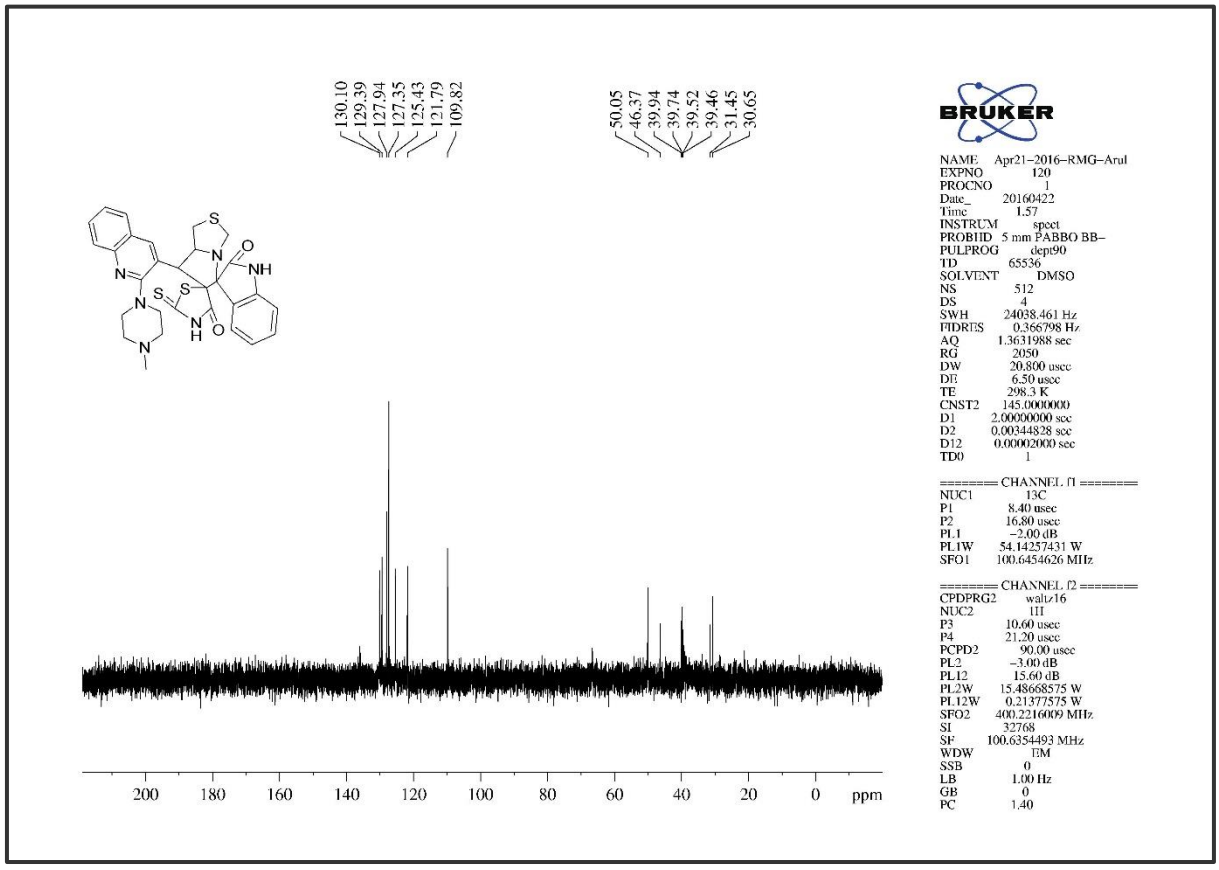

Figure 6. S. 29. The DEPT-90 NMR of compound 11d

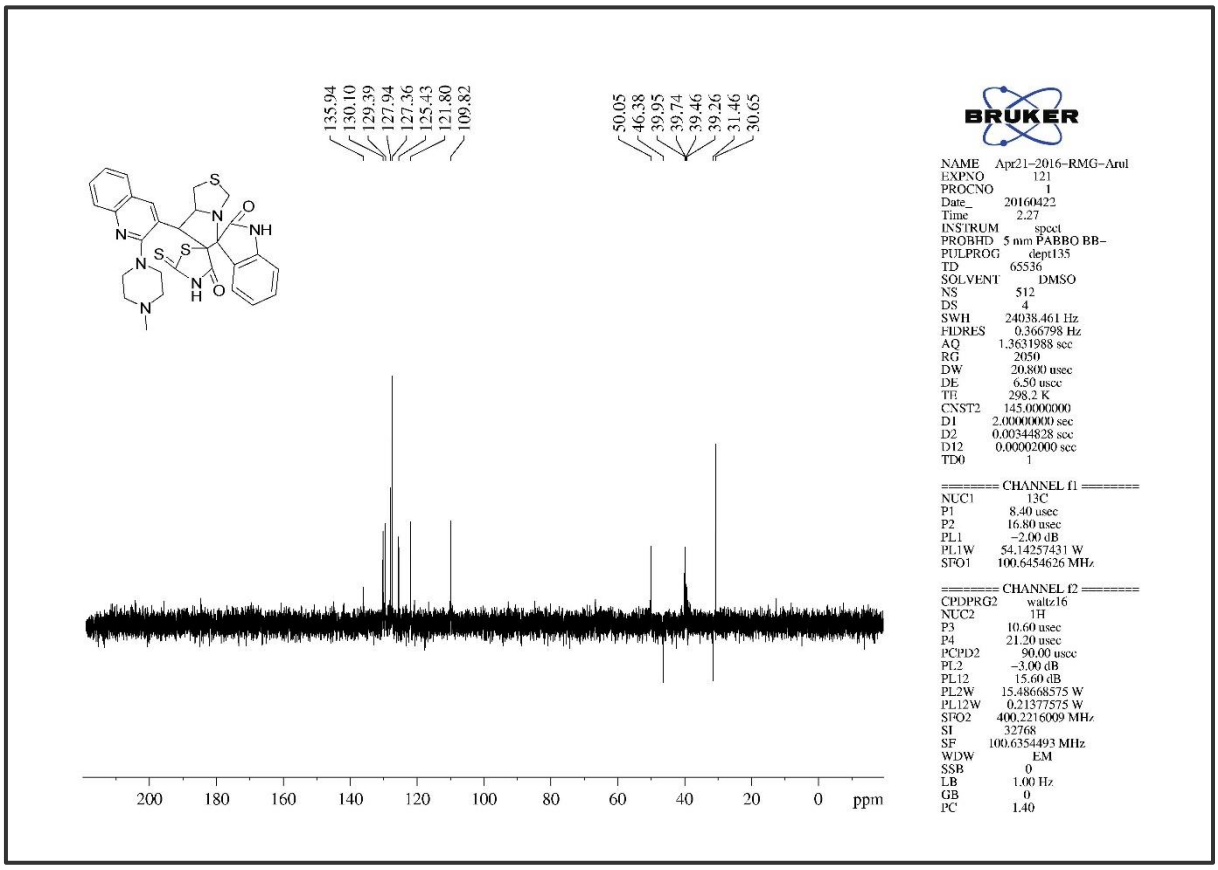

Figure 6. S. 30. DEPT-135 NMR of compound 11d

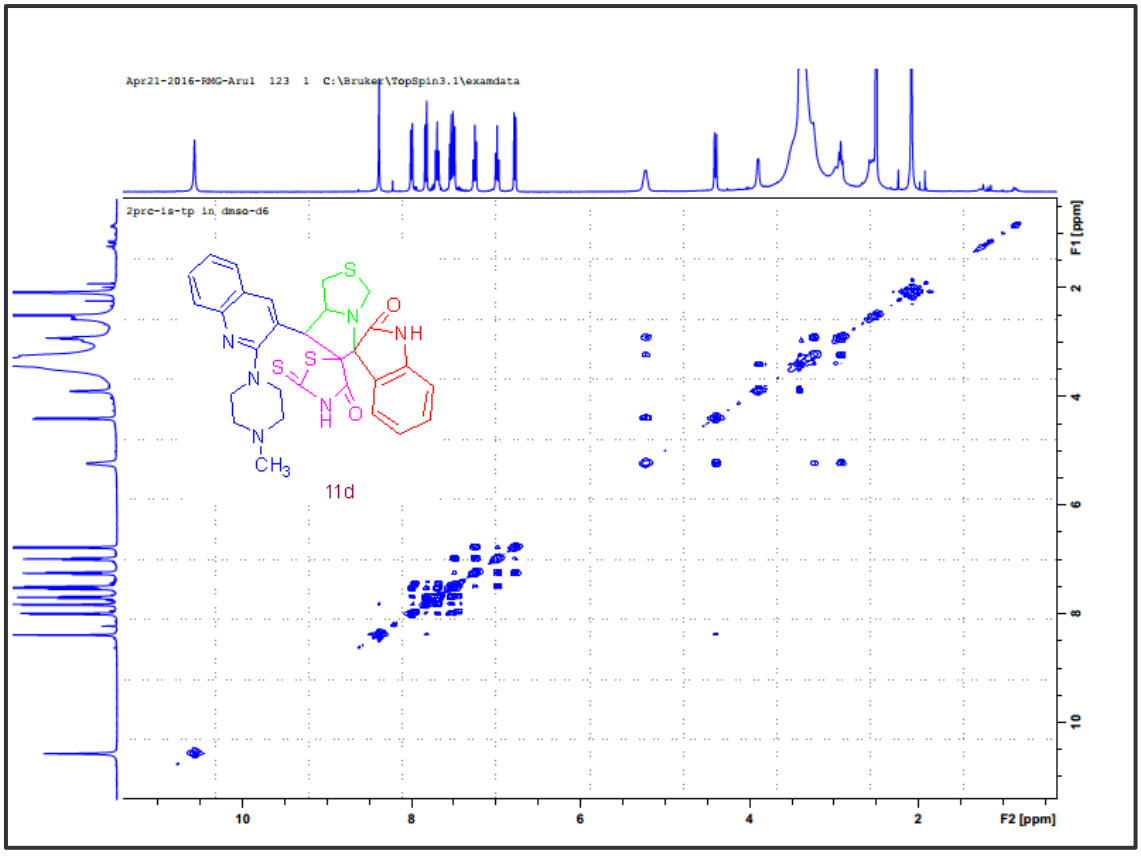

Figure 6. S. 31. COSY NMR of compound 11d

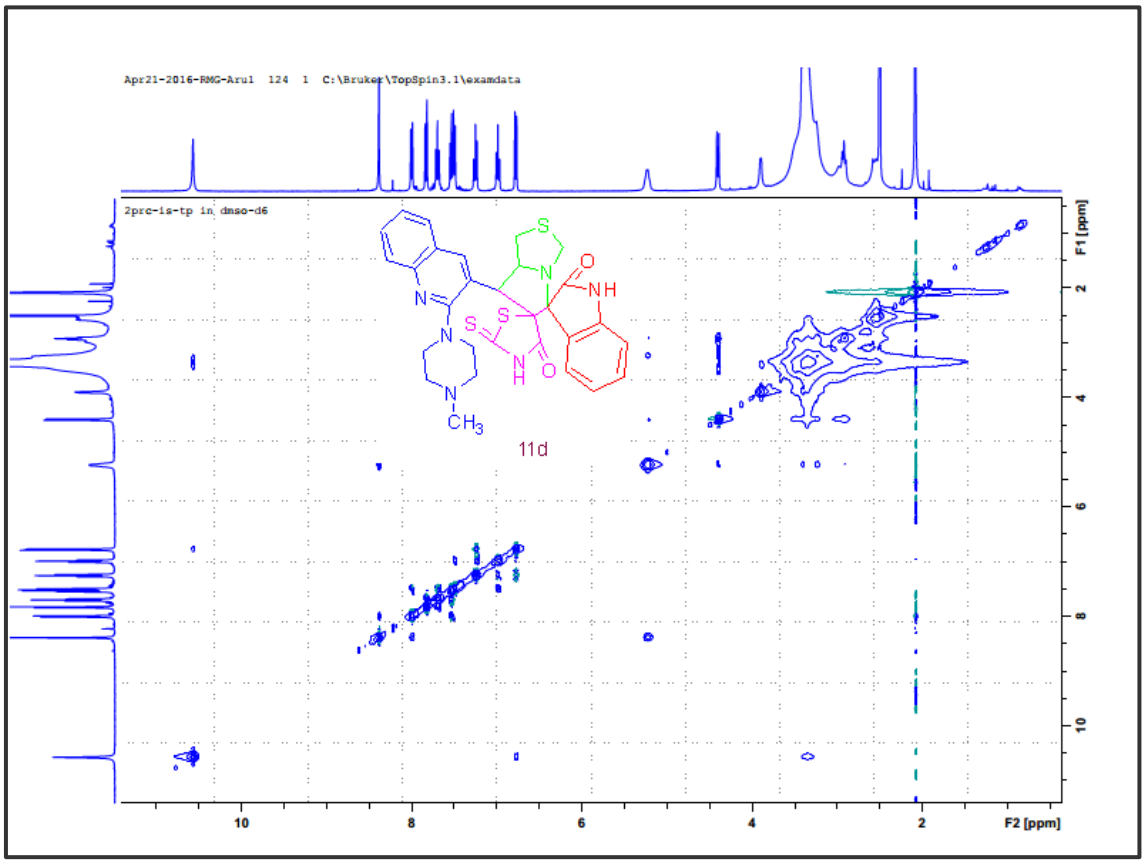

Figure 6. S. 32. NOESY NMR of compound 11d

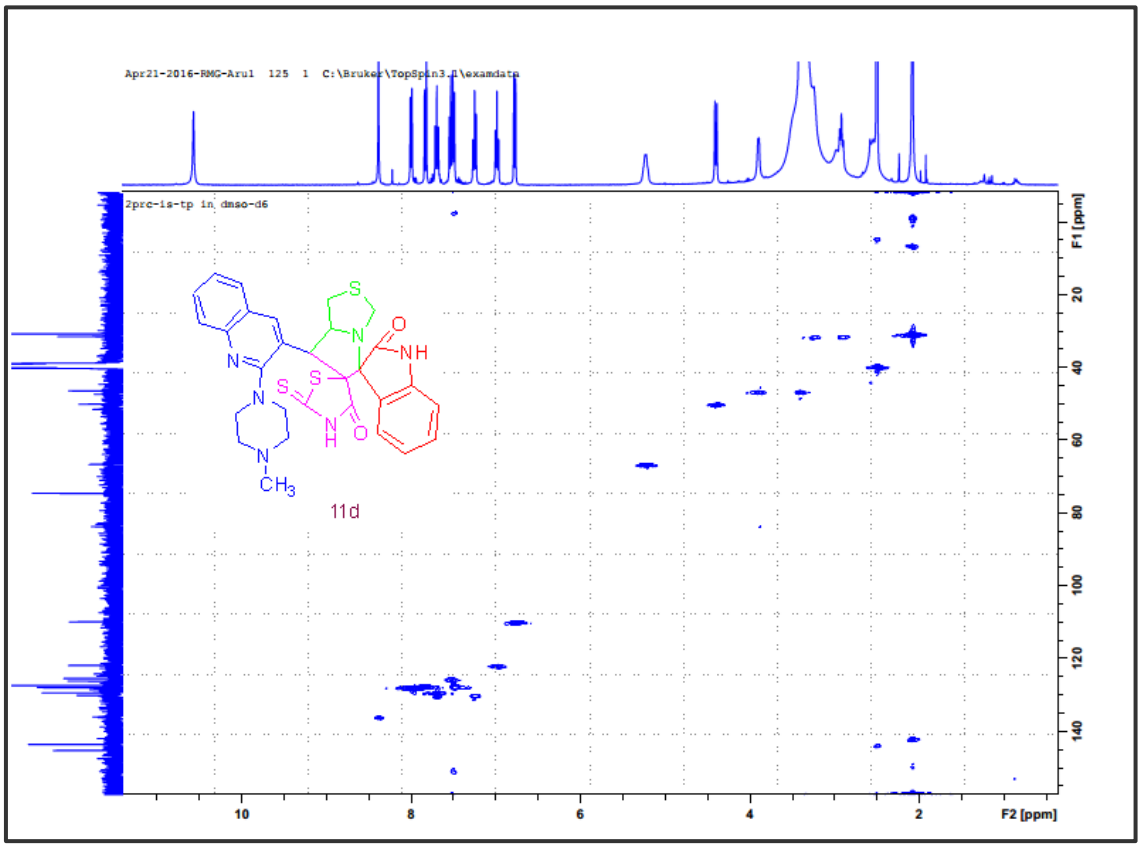

Figure 6. S. 33. HSQCE NMR of compound 11d

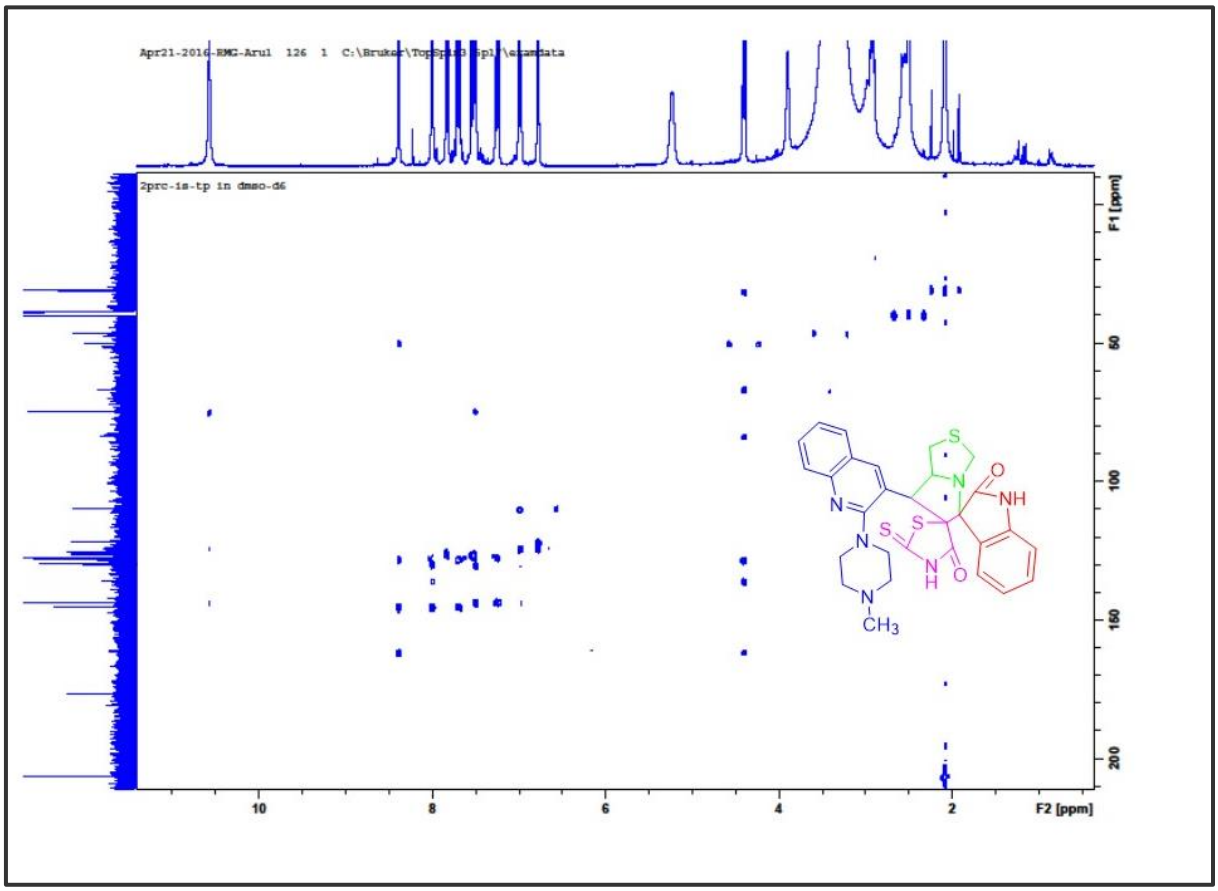

Figure 6. S. 34. HMBC NMR of compound 11d

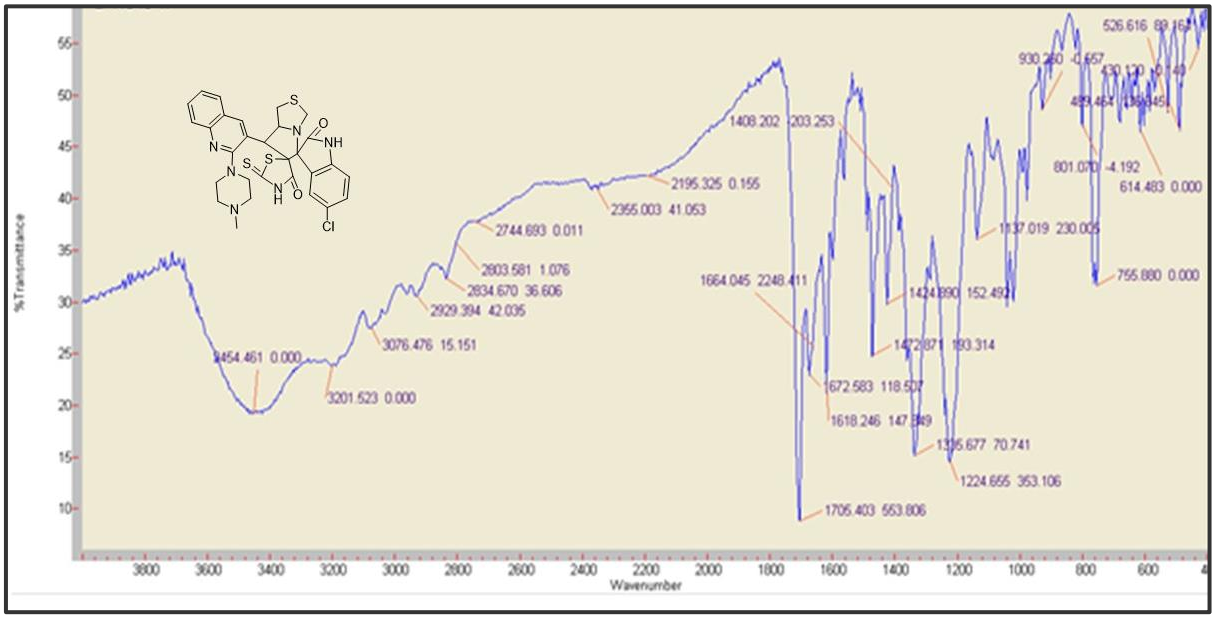

Figure 6. S. 35. The Infra-Red Spectrum of compound 11e

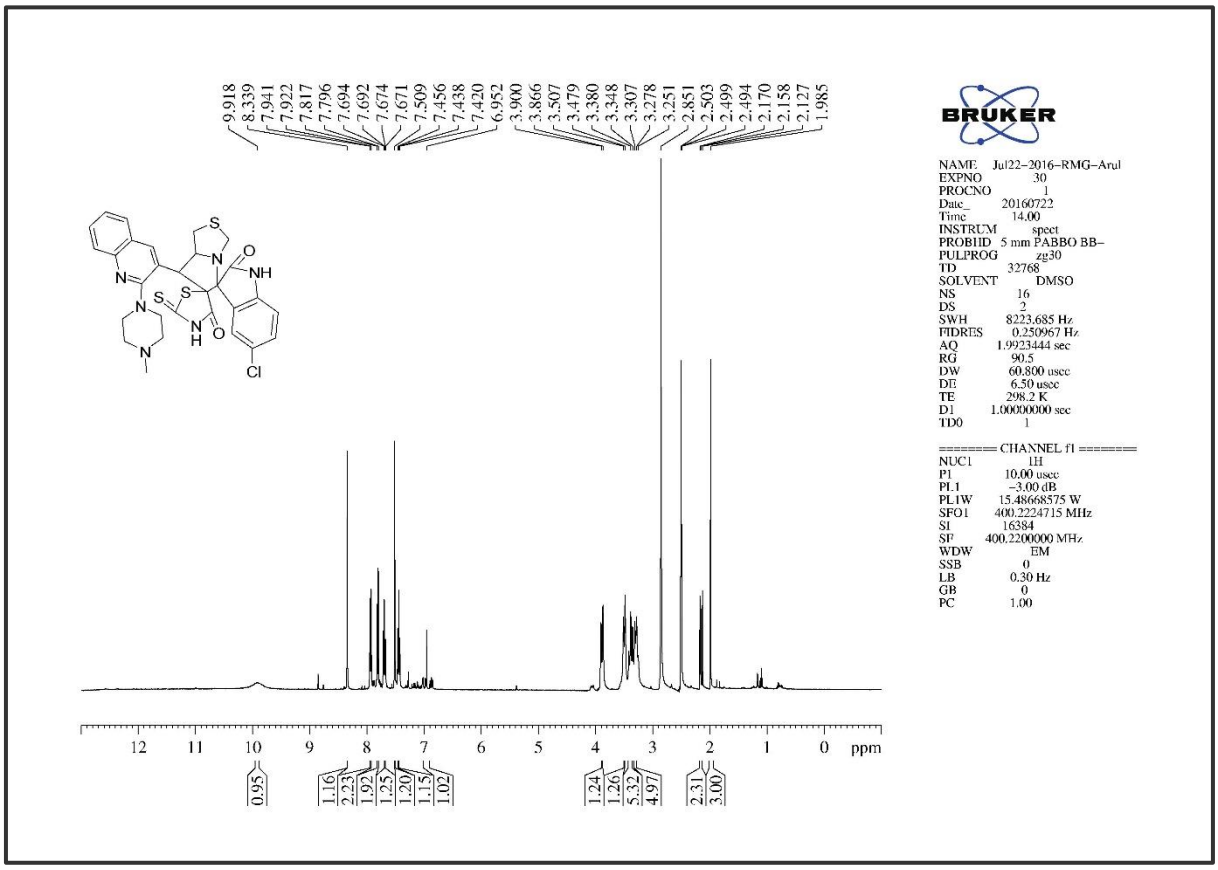

Figure 6. S. 36. The ^{1}H NMR of compound 11e

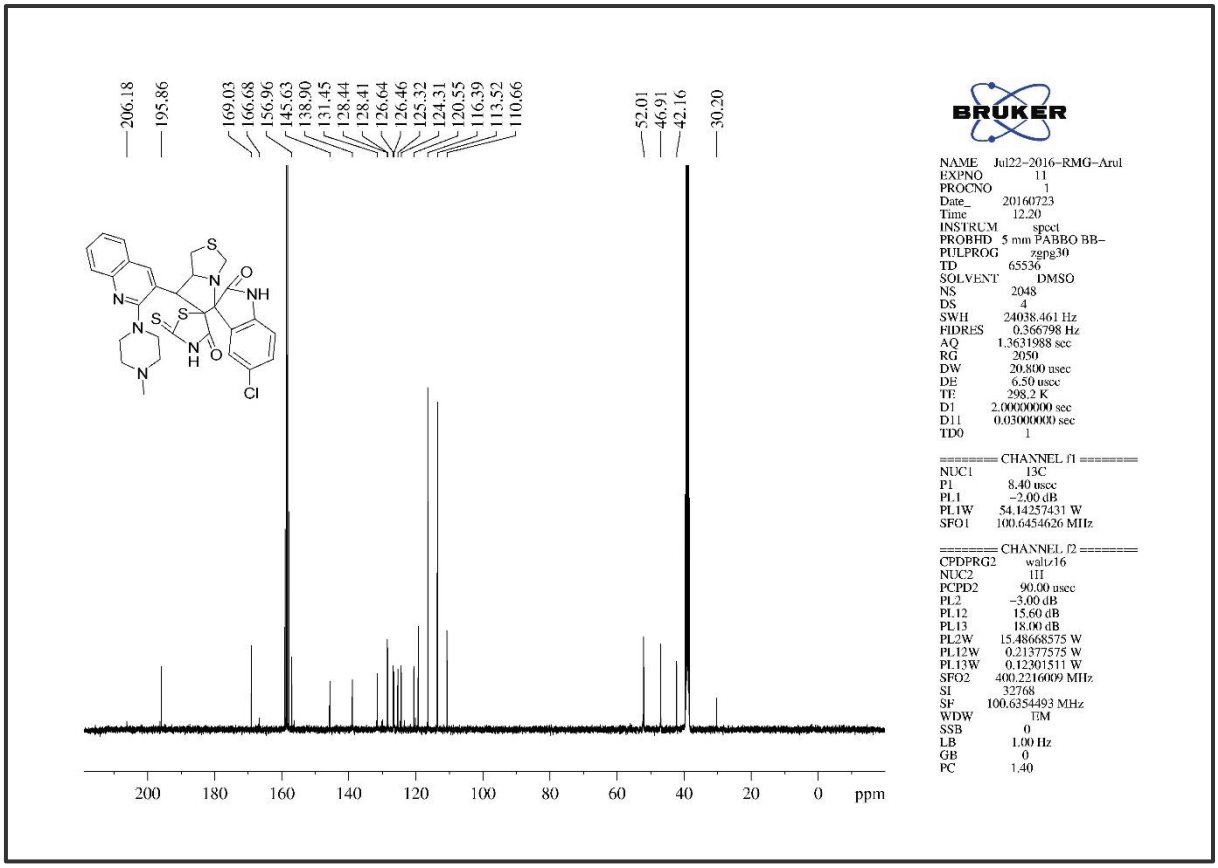

Figure 6. S. 37. The ^{13}C NMR of compound 11e

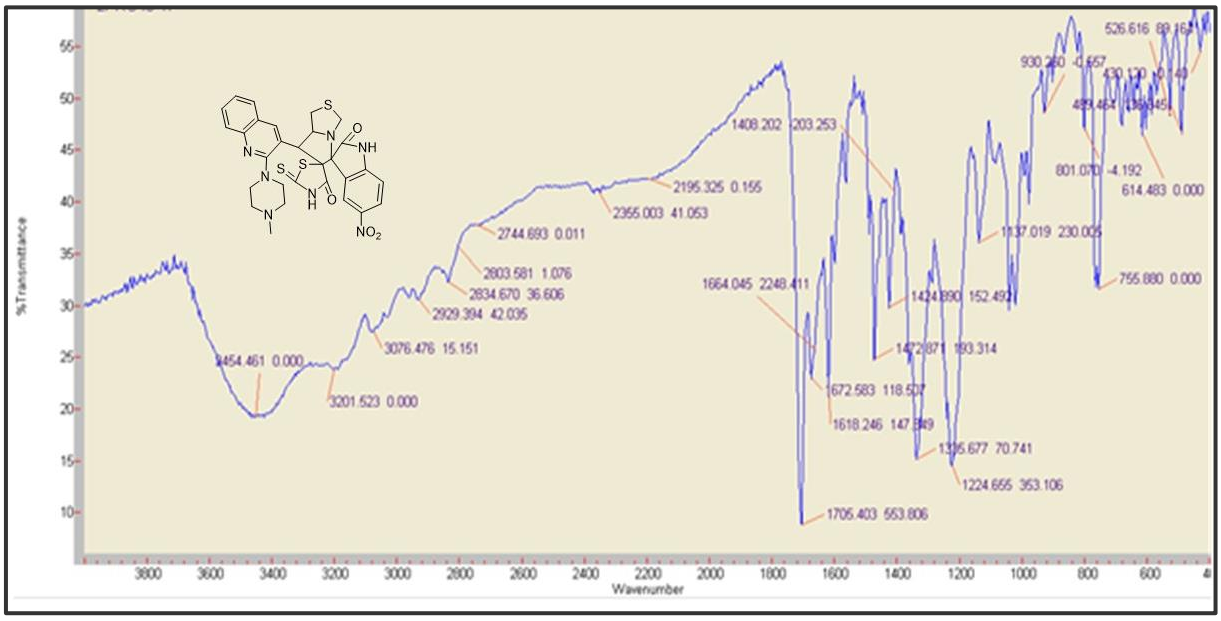

Figure 6. S. 38. The Infra-Red Spectrum of compound 11f

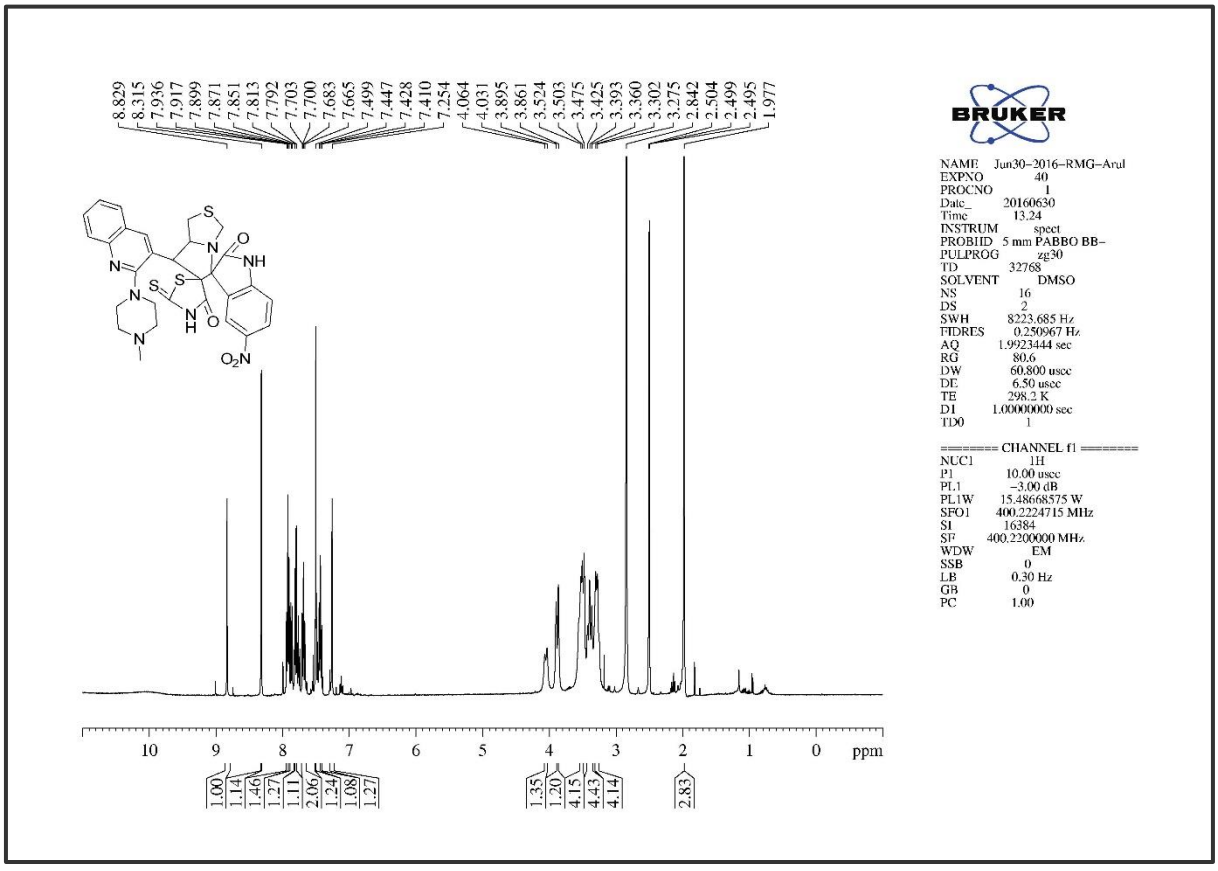

Figure 6. S. 39. The ^{1}H NMR of compound 11f

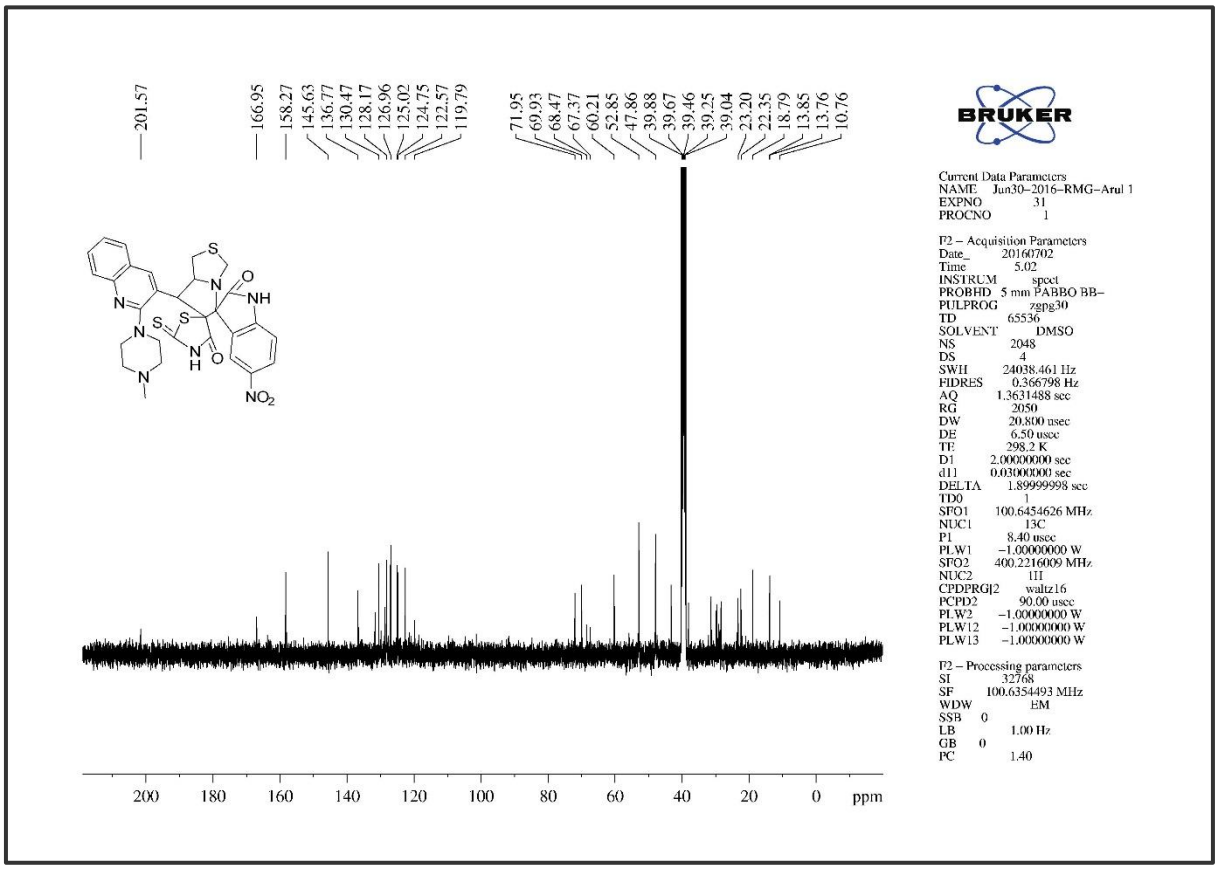

Figure 6. S. 40. The ^{13}C NMR of compound 11f

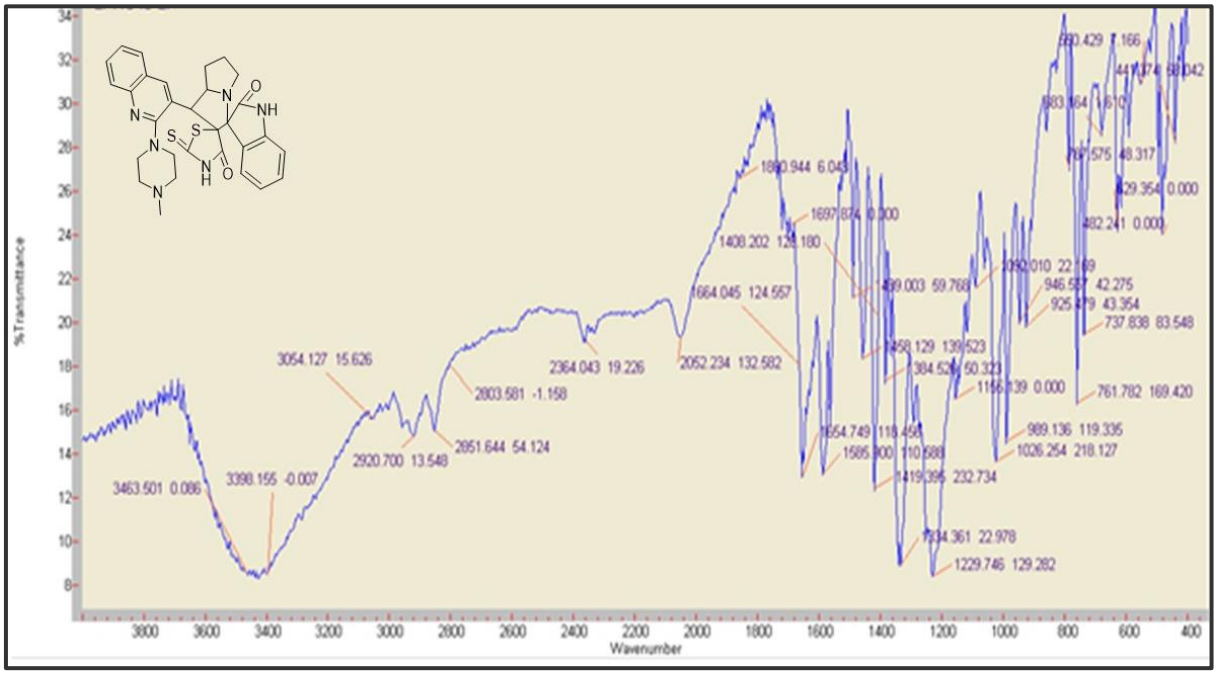

Figure 6. S. 41. The Infra-Red Spectrum of compound 12g

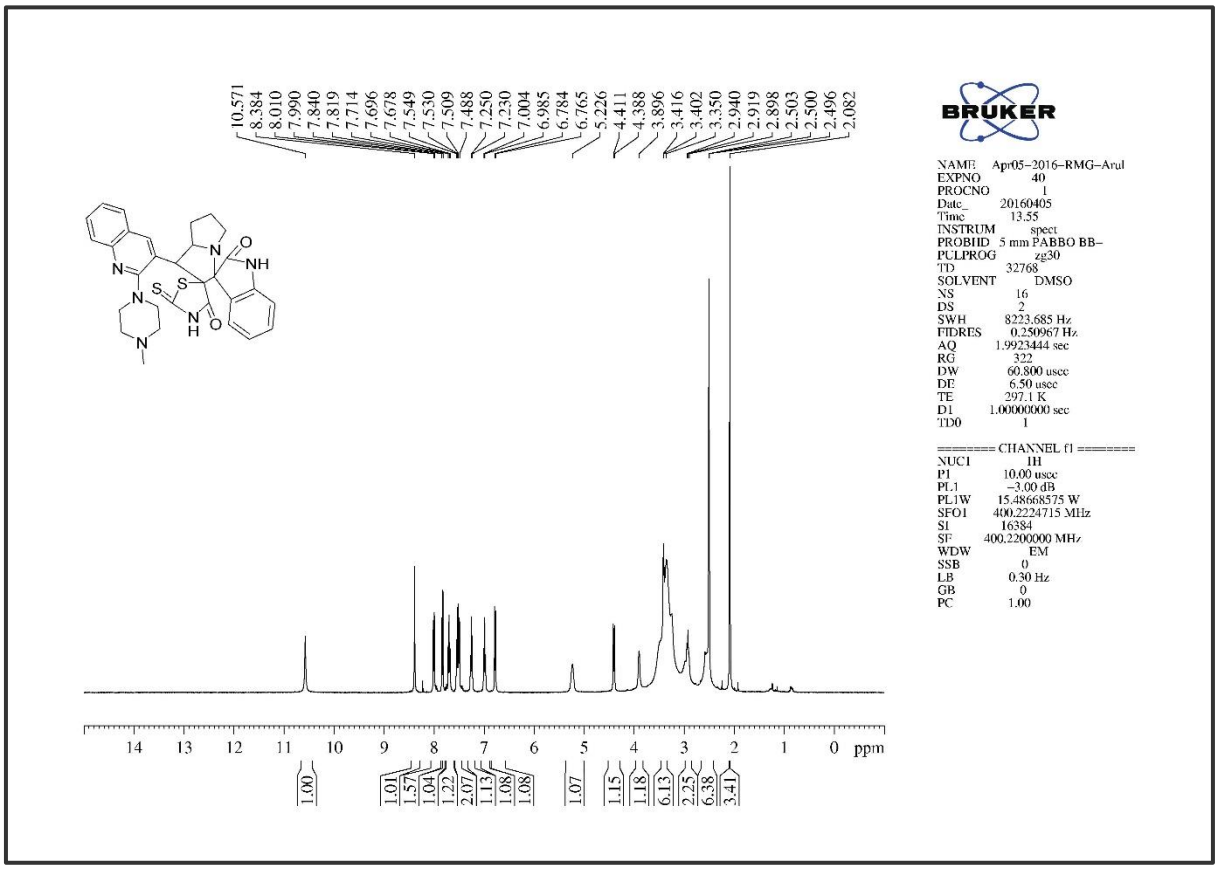

Figure 6. S. 42. The ^{1}H NMR of compound 12g

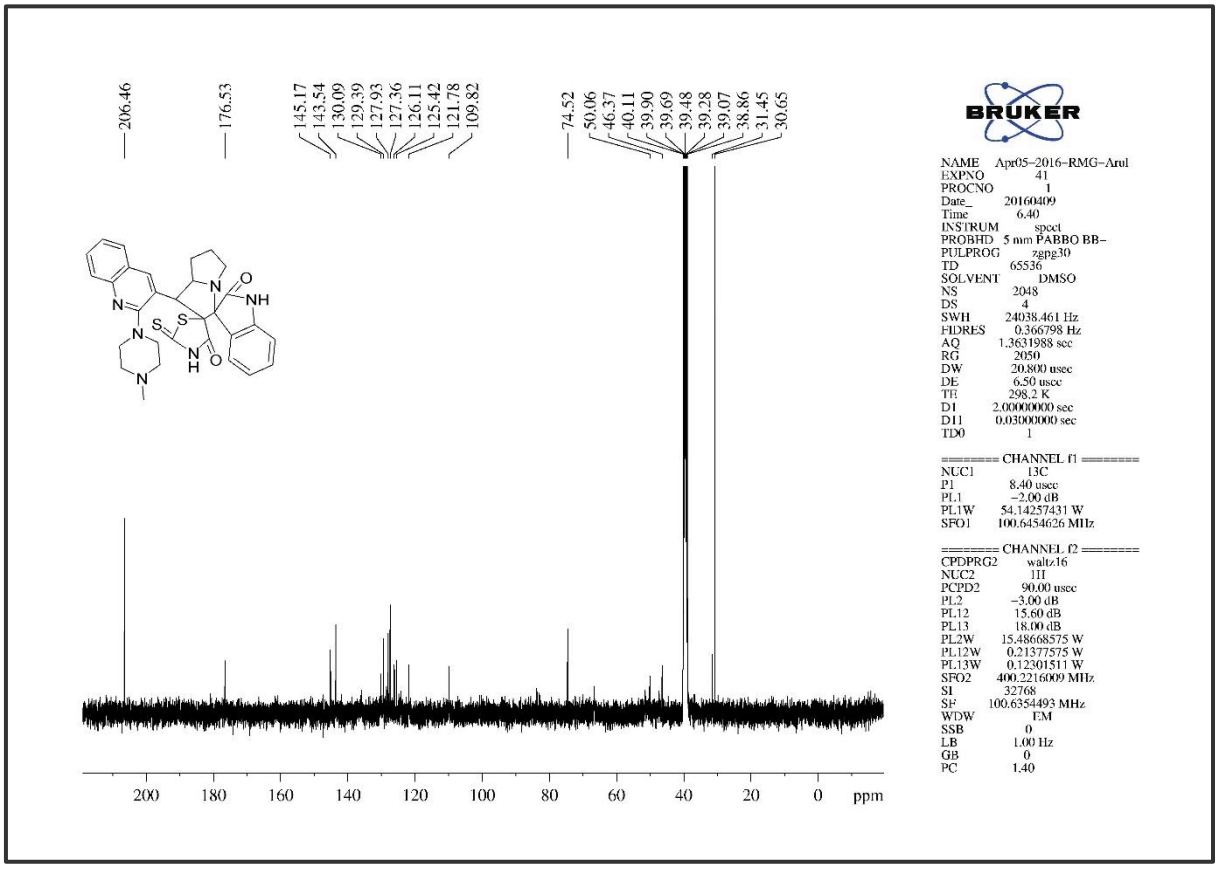

Figure 6. S. 43. The ^{13}C NMR of compound 12g

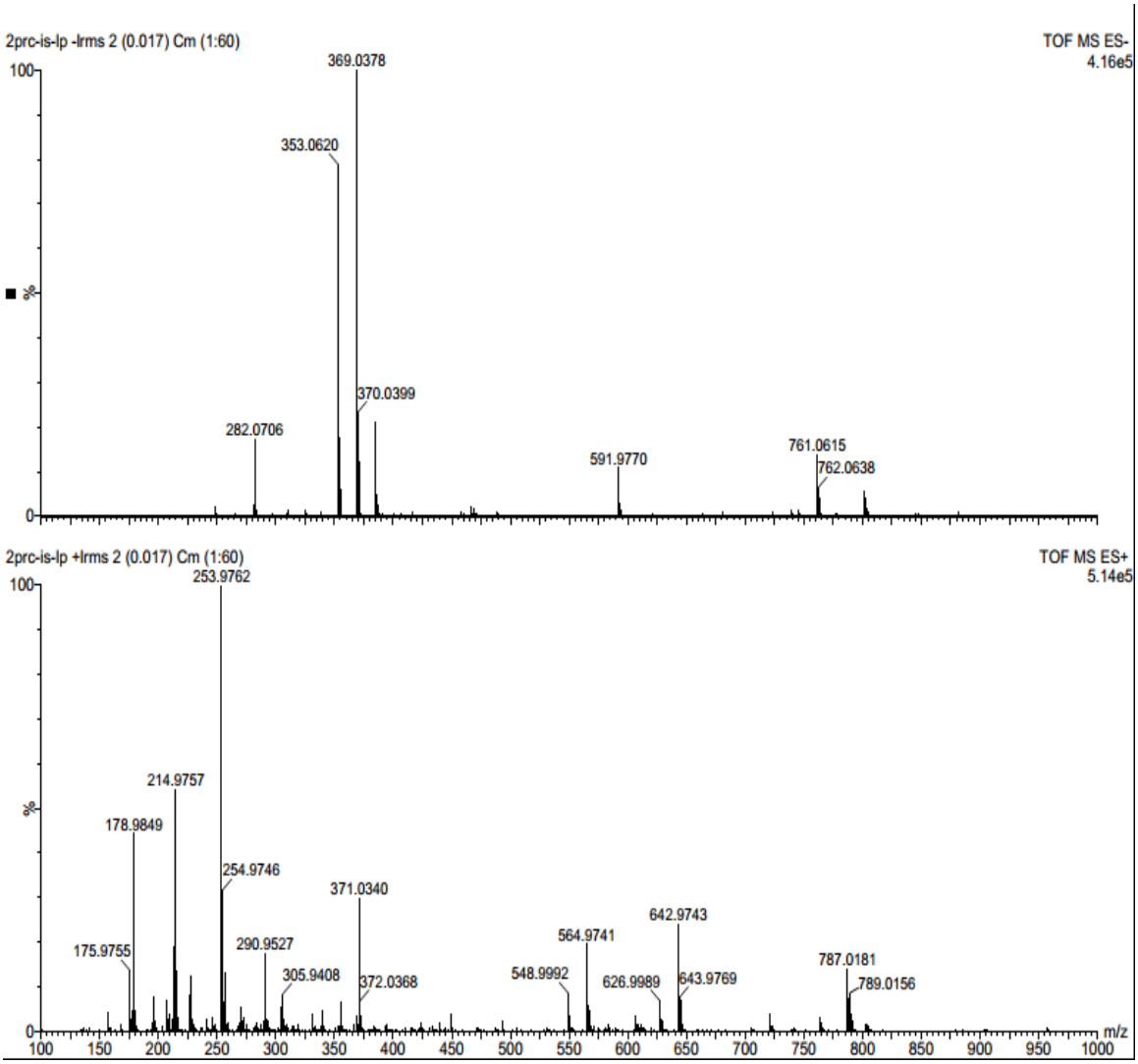

Figure 6. S. 44. The HRMS of compound 12g

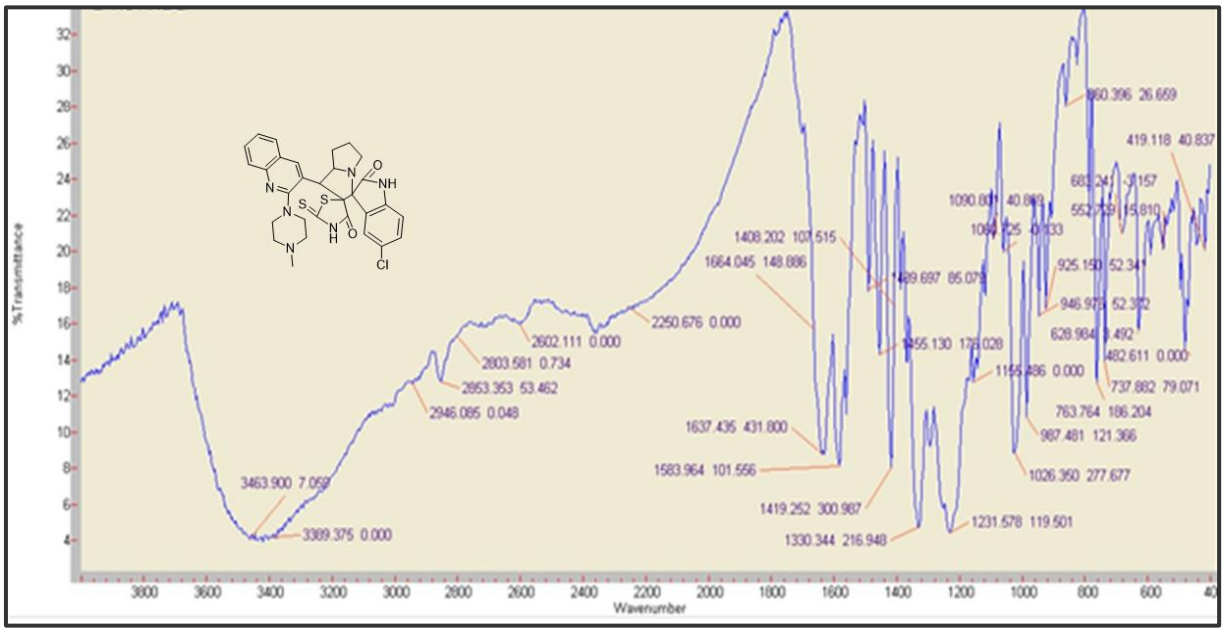

Figure 6. S. 45. The Infra-Red Spectrum of compound 12h

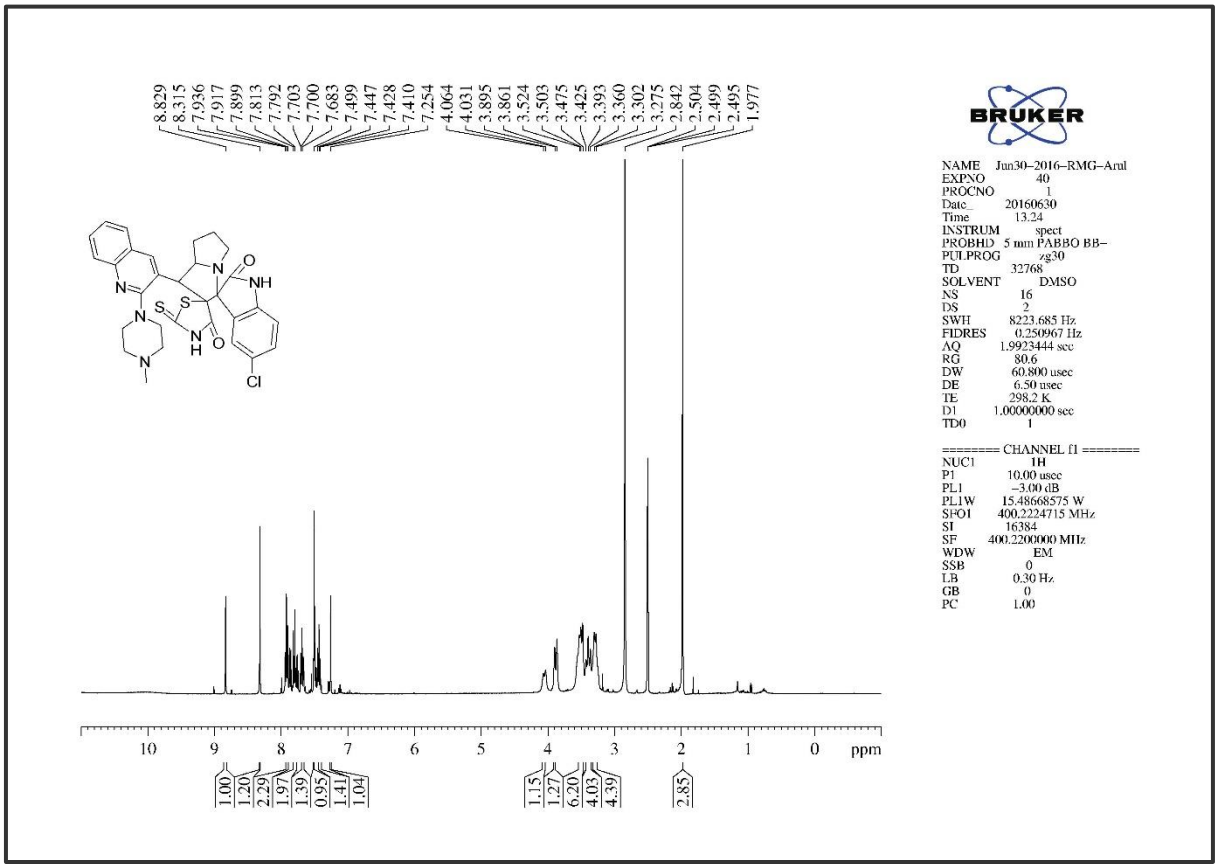

Figure 6. S. 46. The ^{1}H NMR of compound 12h

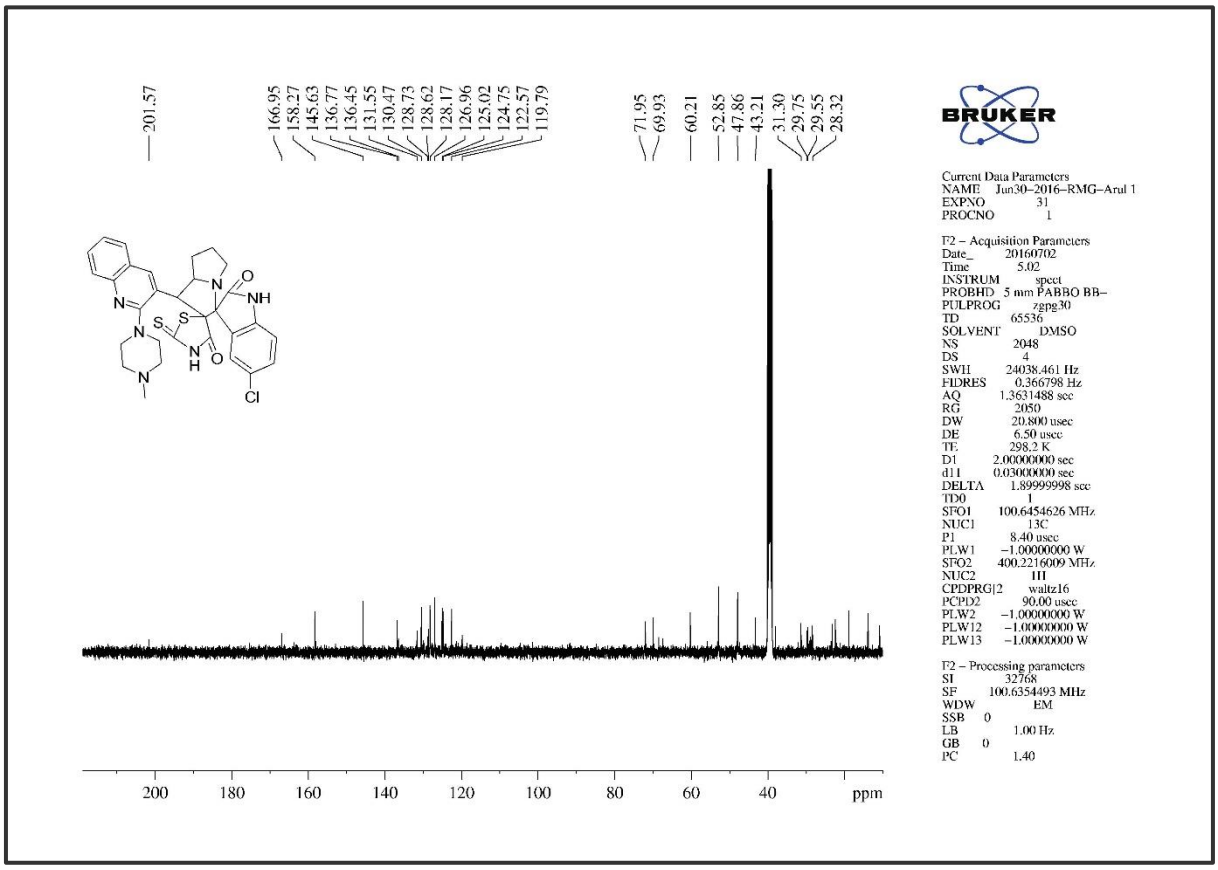

Figure 6. S. 47. The ^{13}C NMR of compound 12h

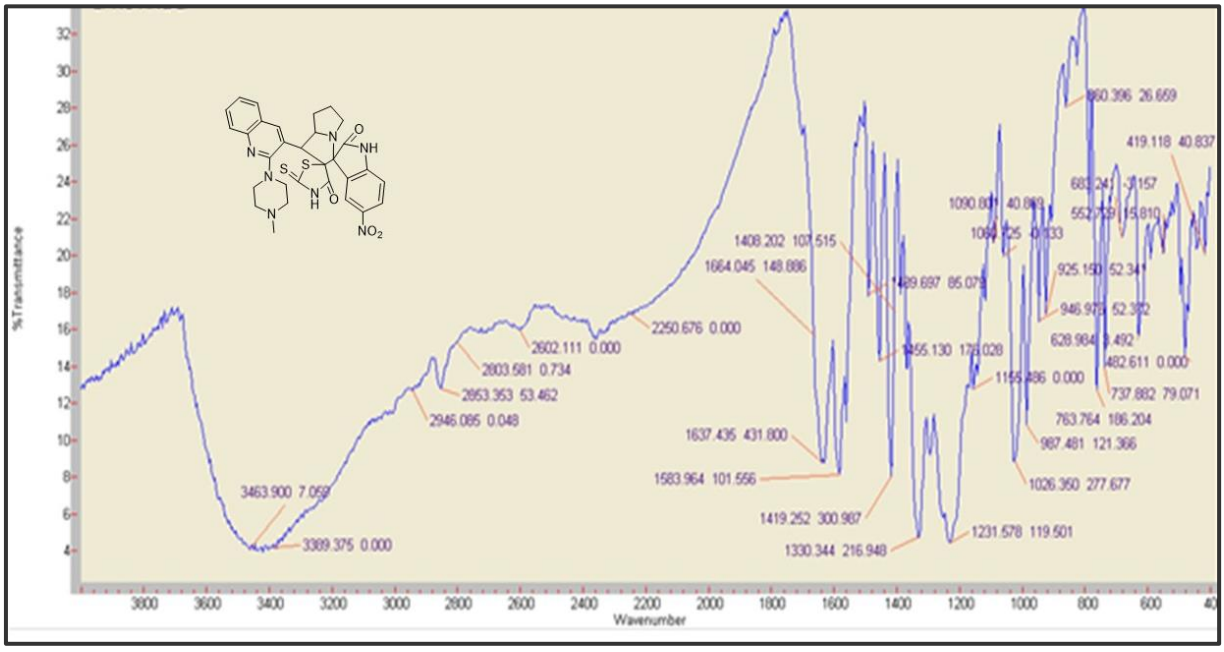

Figure 6. S. 48. The Infra-Red Spectrum of compound 12i

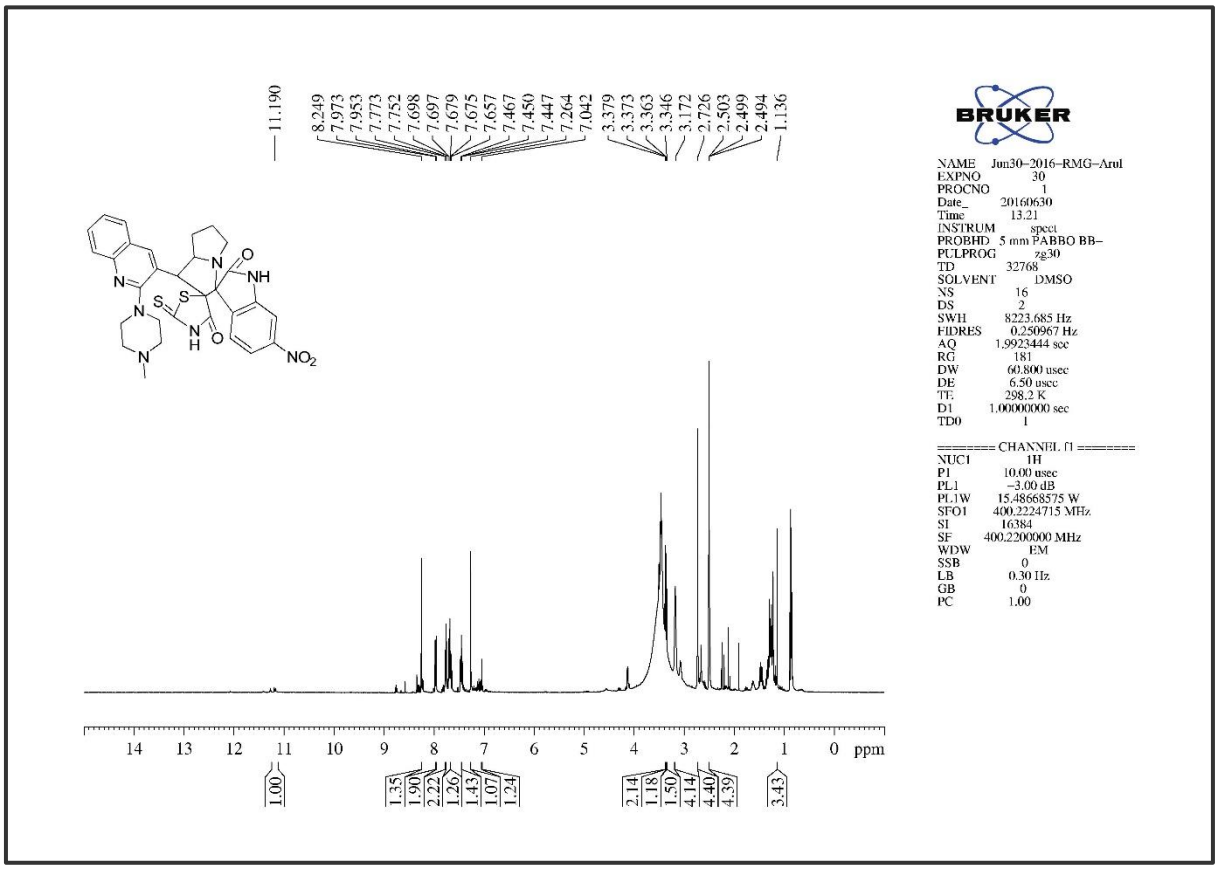

Figure 6. S. 49. The ^{1}H NMR of compound 12i

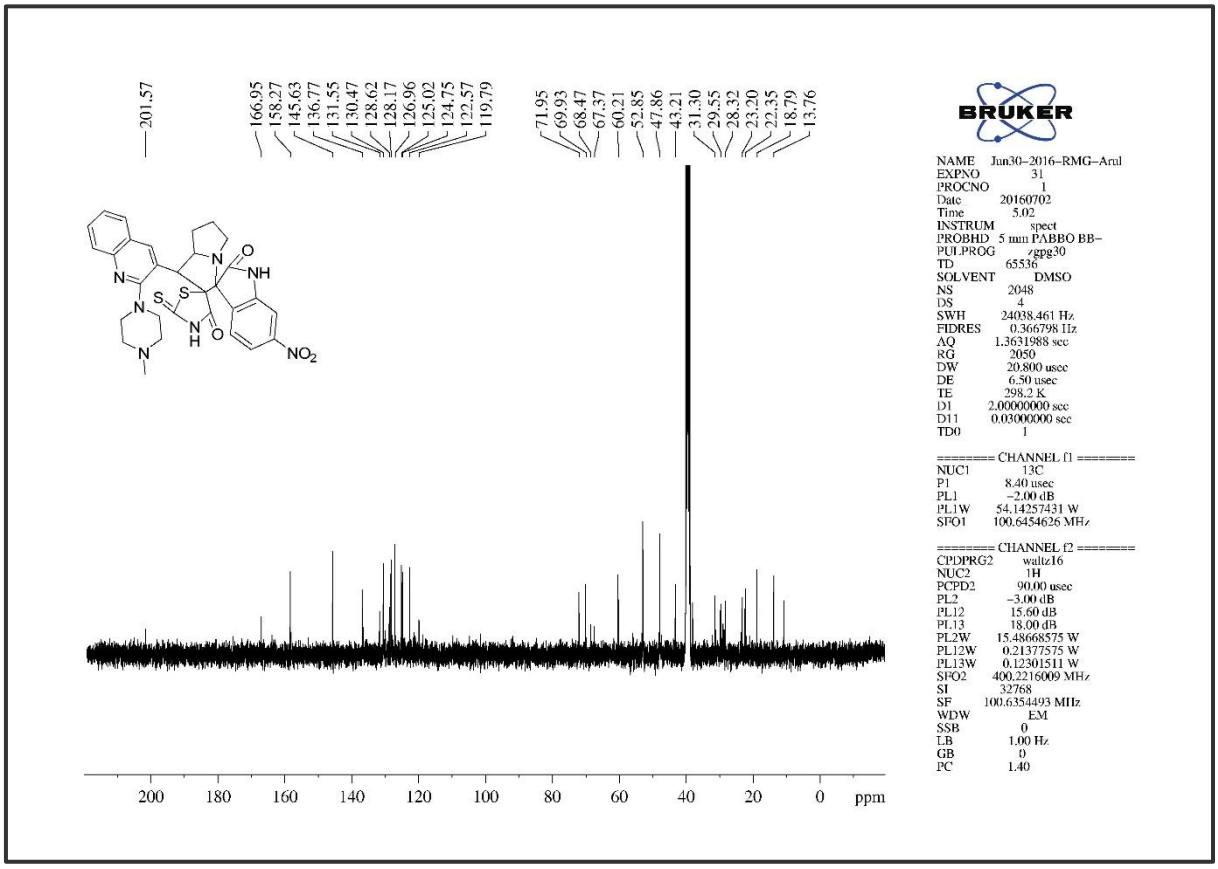

Figure 6. S. 50. The ^{13}C NMR of compound 12i

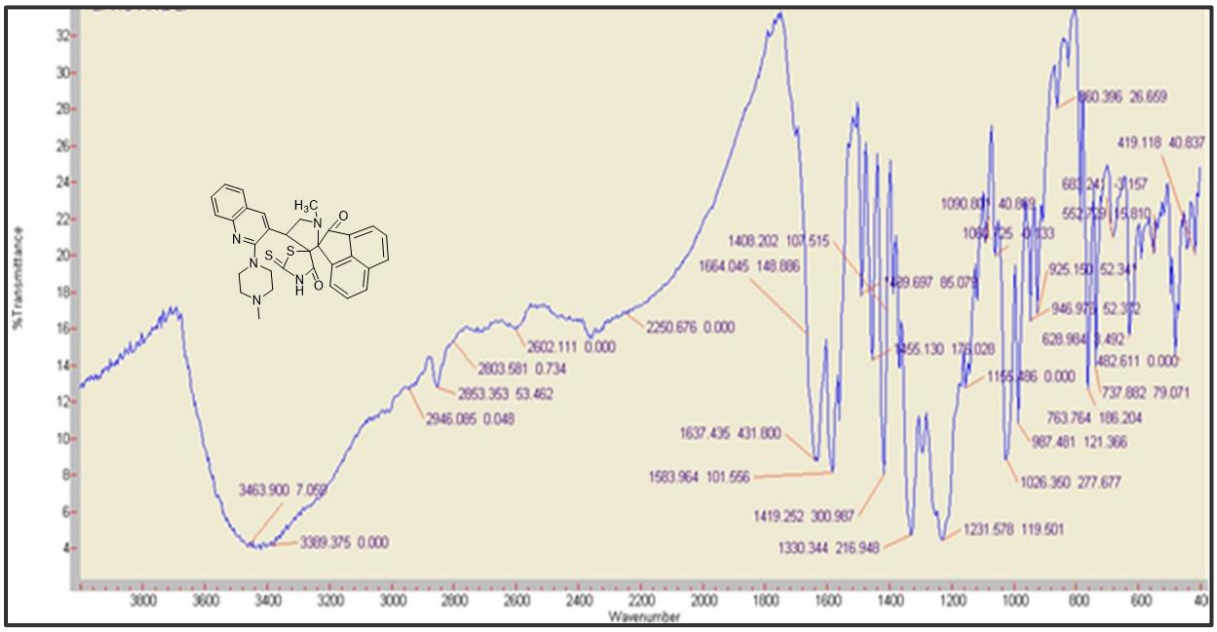

Figure 6. S. 51. The Infra-Red Spectrum of compound 13j

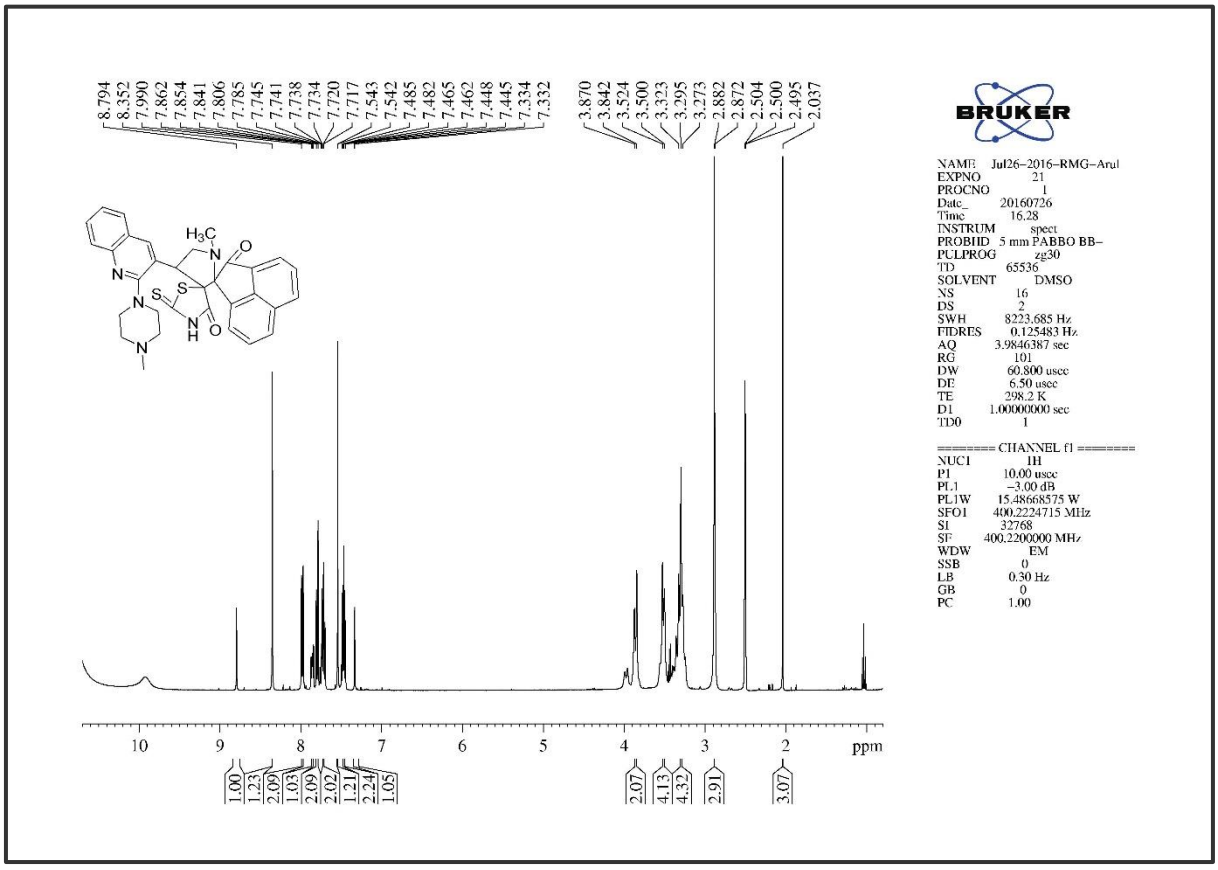

Figure 6. S. 52. The ^{1}H NMR of compound 13j

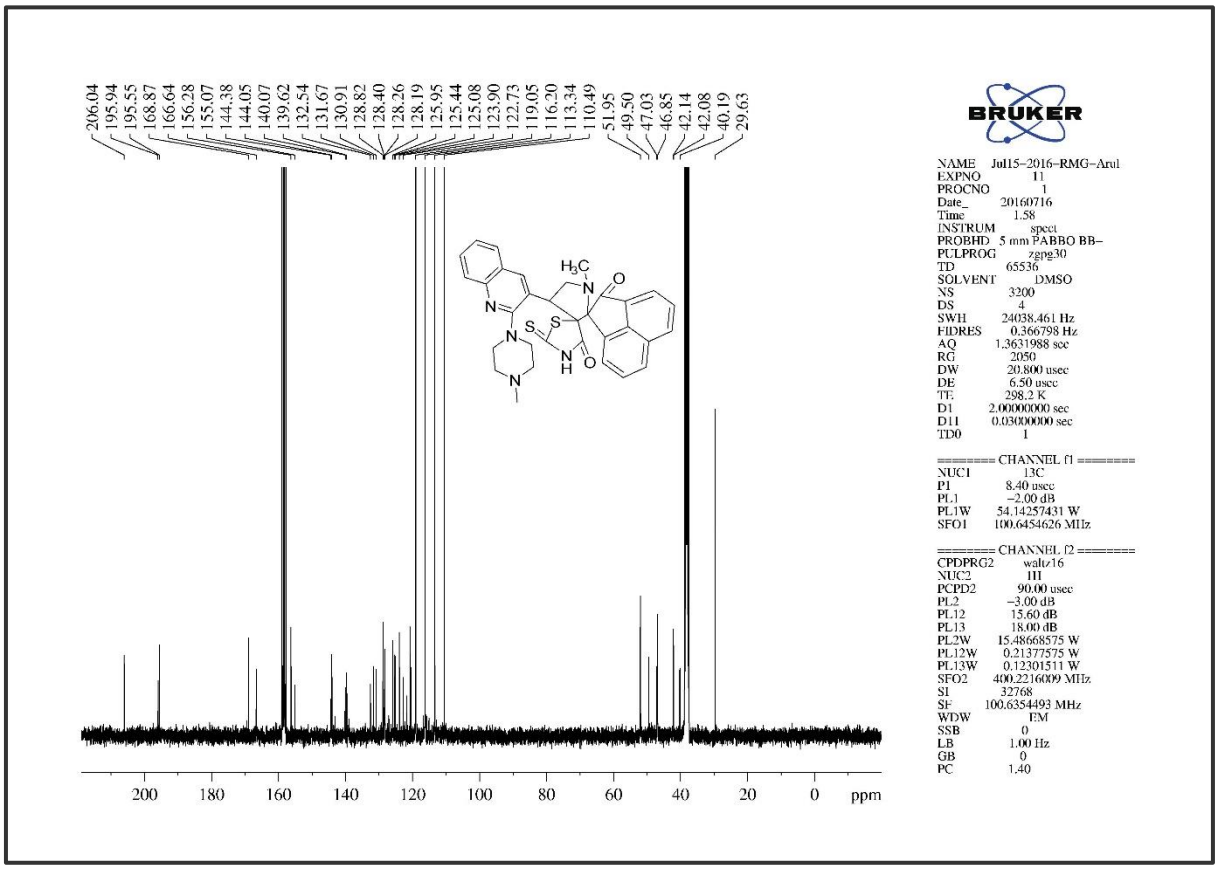

Figure 6. S. 53. The ^{13}C NMR of compound 13j

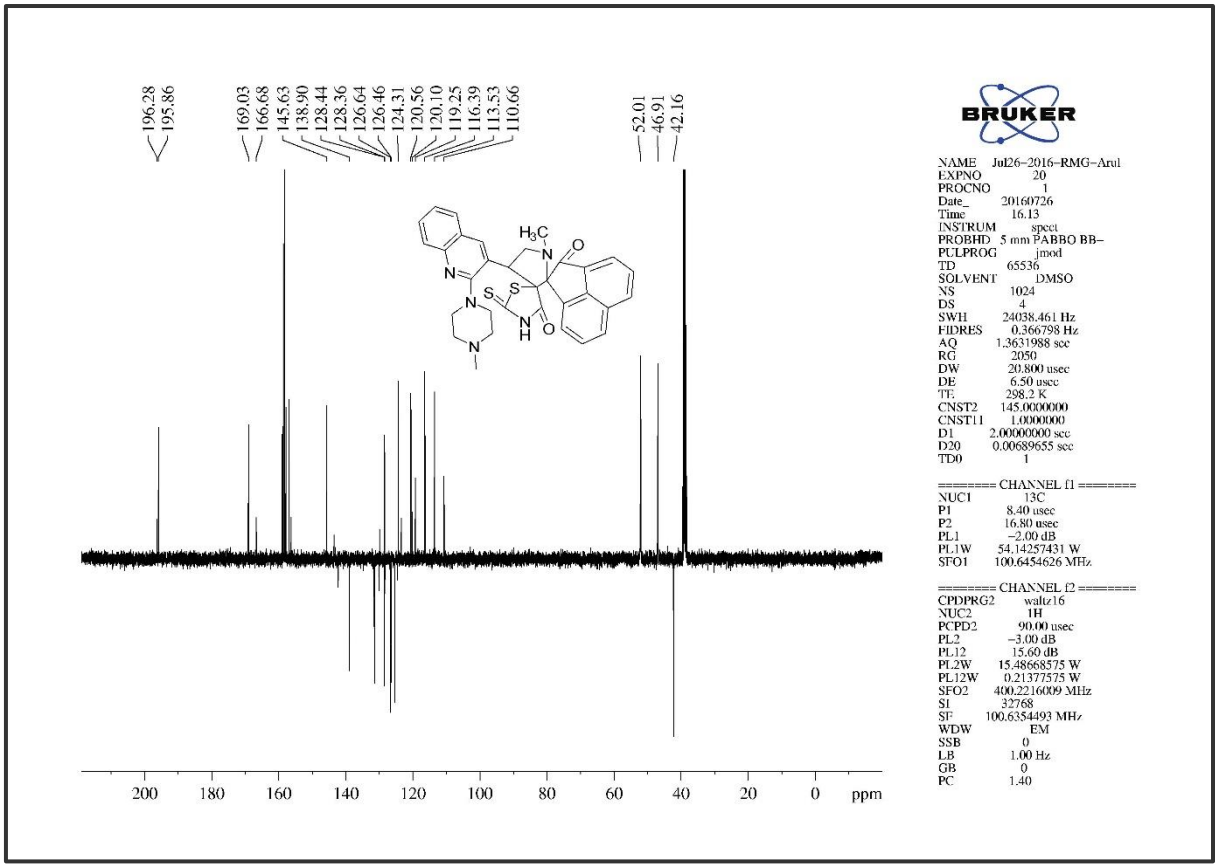

Figure 6. S. 54. The ^{13}C APT NMR Spectrum of compound 13j

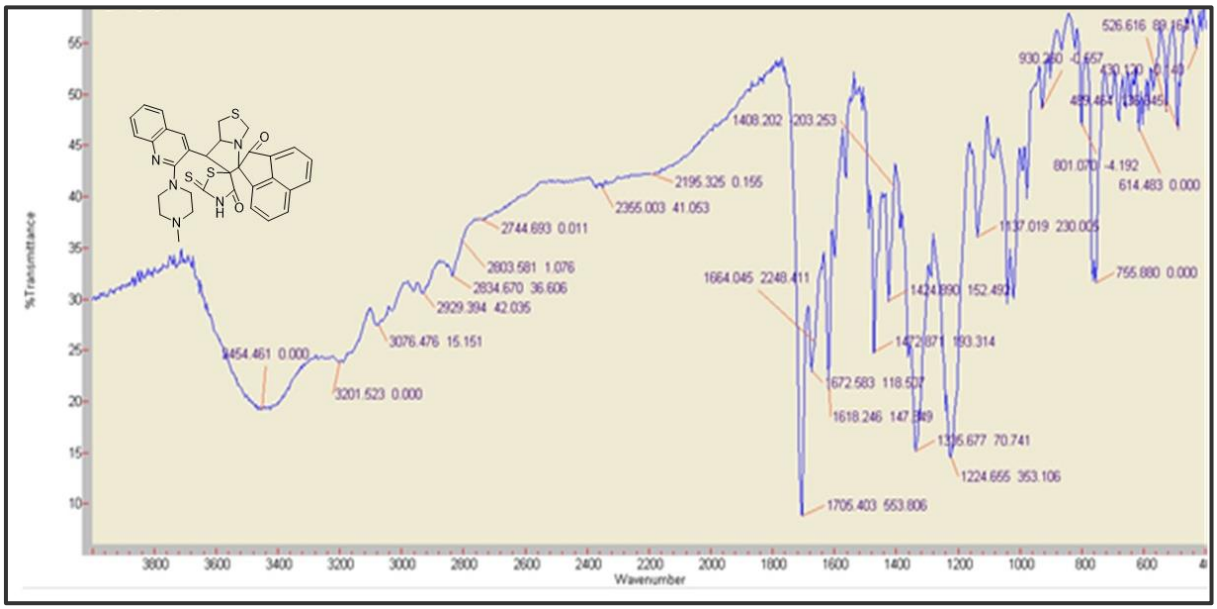

Figure 6. S. 55. The Infra-Red Spectrum of compound 14k

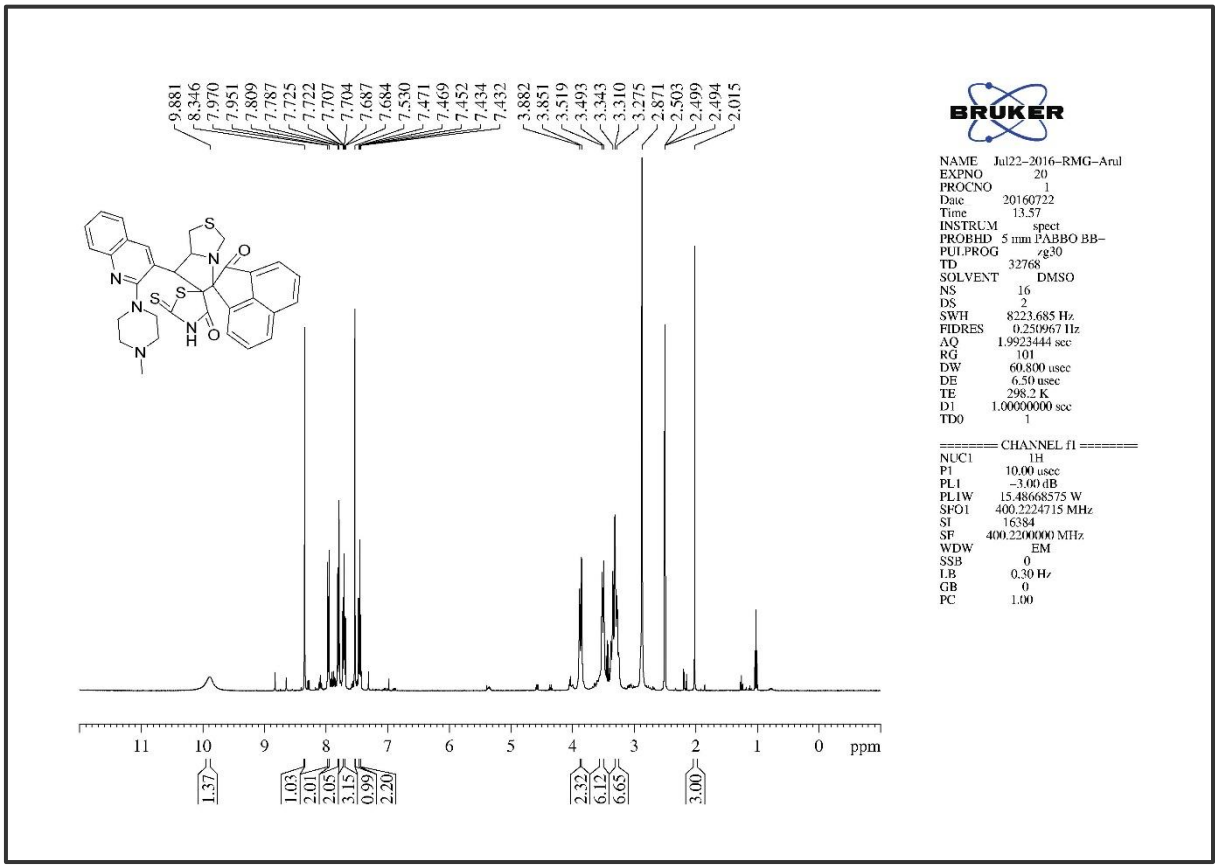

Figure 6. S. 56. The ^{1}H NMR of compound 14k

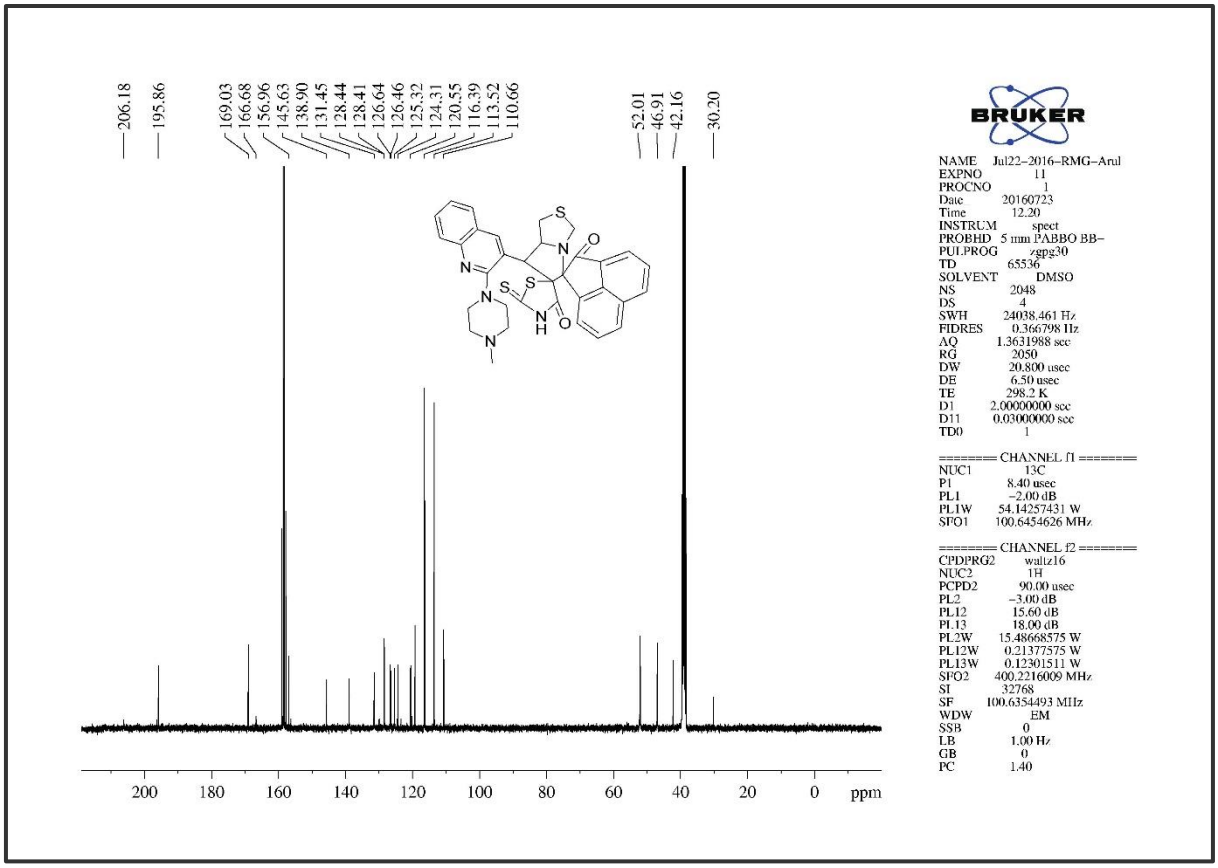

Figure 6. S. 57. The ^{13}C NMR of compound 14k

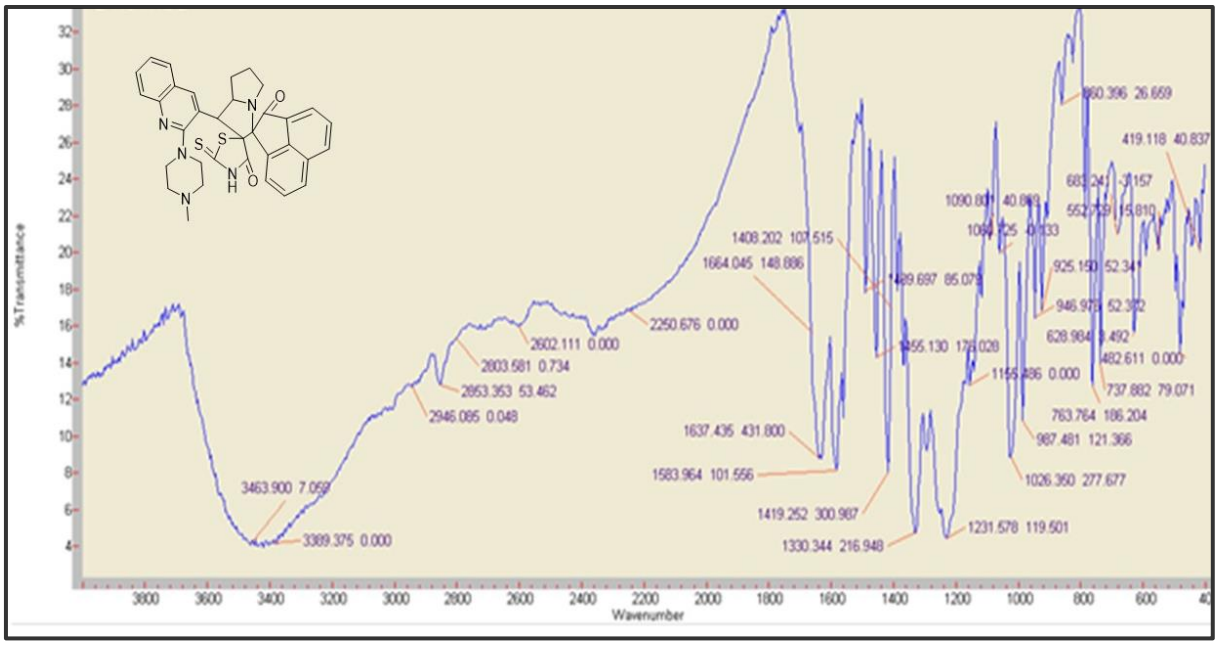

Figure 6. S. 58. The Infra-Red Spectrum of compound 15l

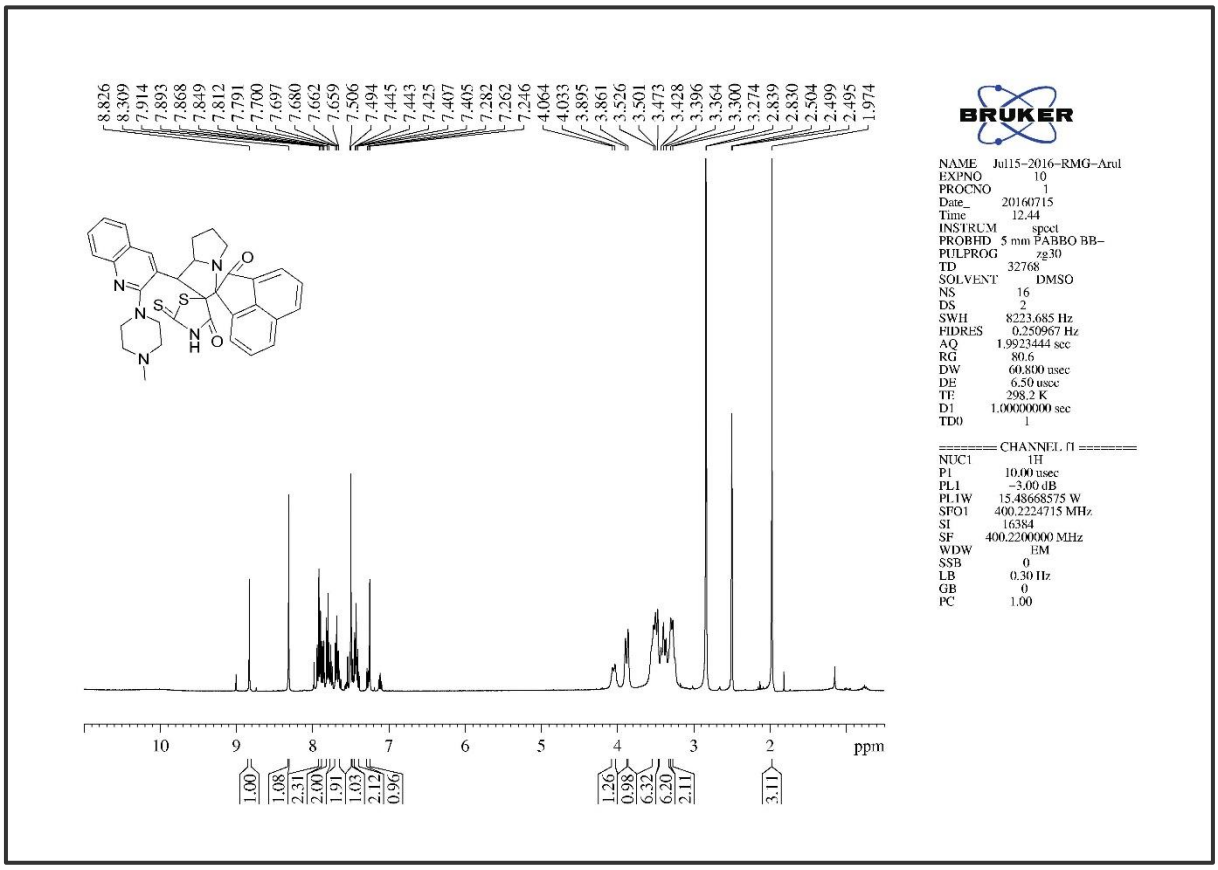

Figure 6. S. 59. The ^{1}H NMR of compound 15l

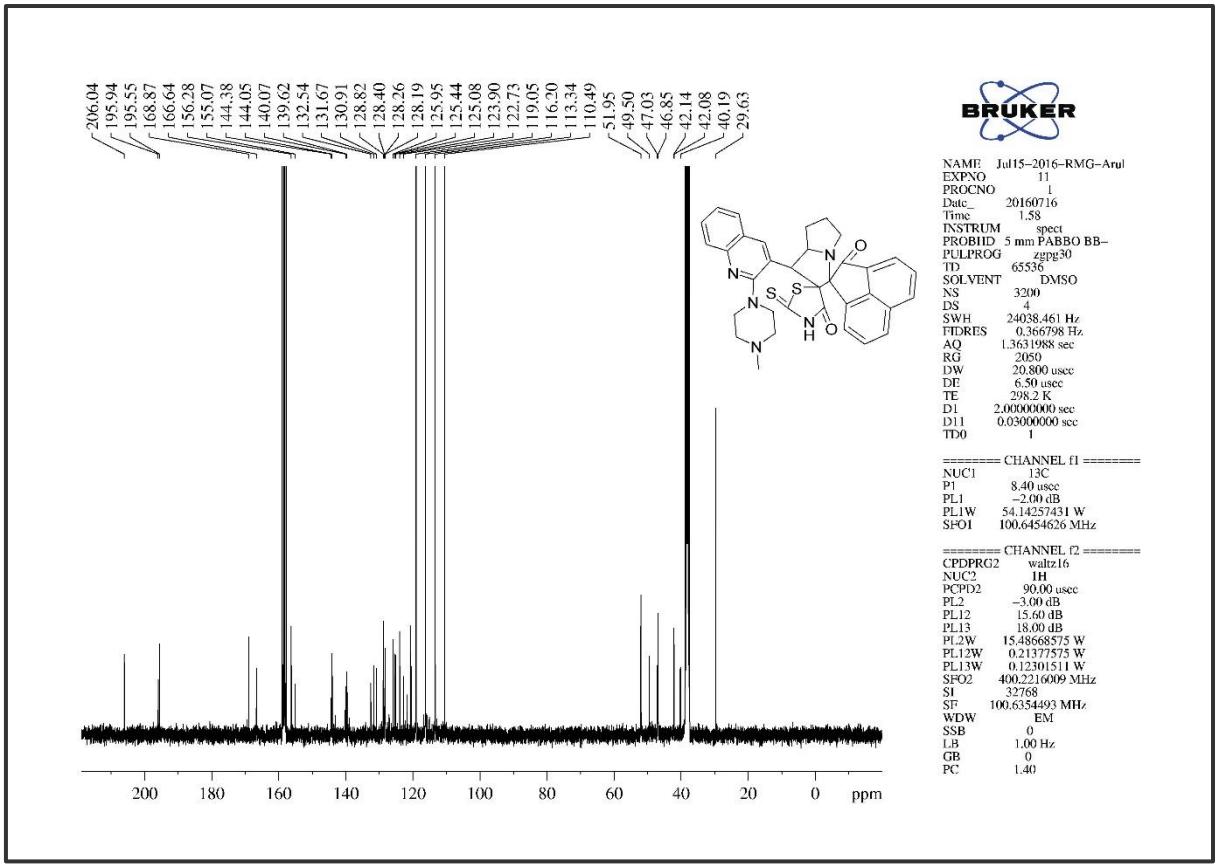

Figure 6. S. 60. The ^{13}C NMR of compound 15l

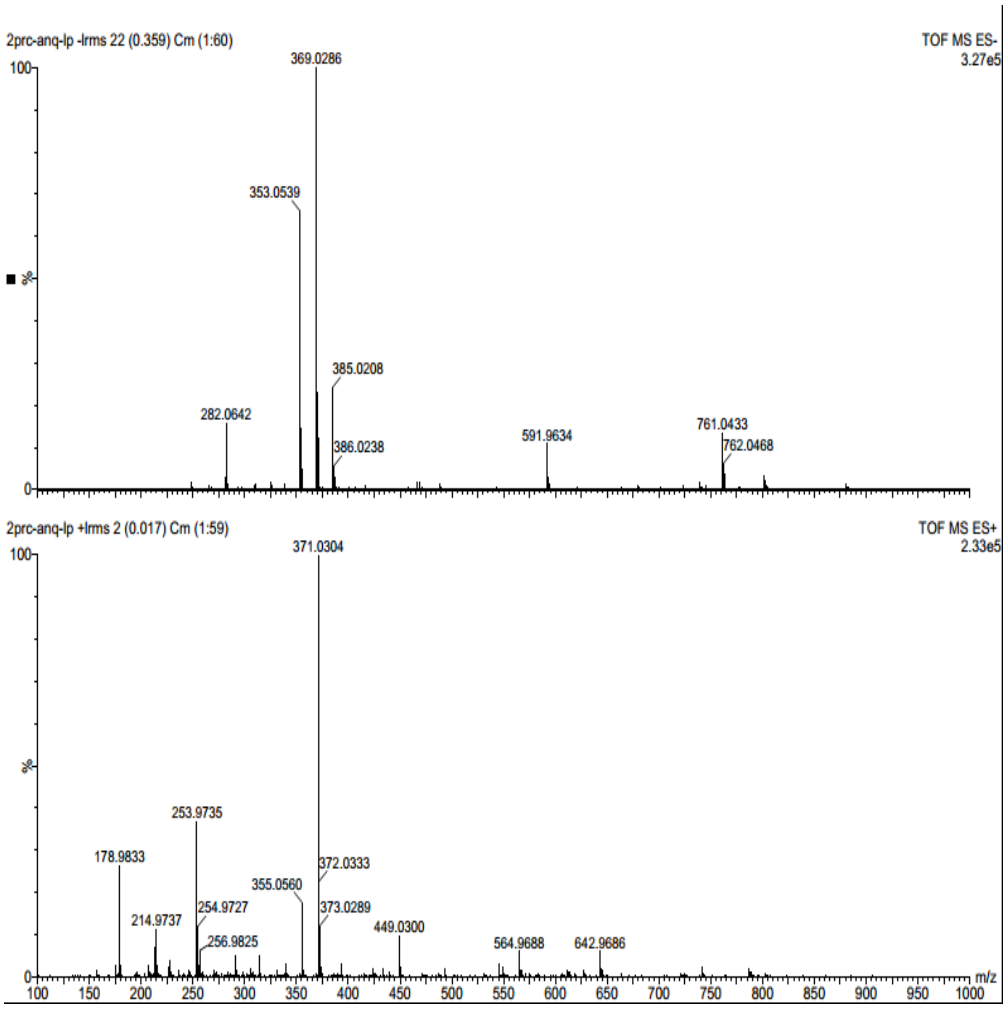

Figure 6. S. 61. The HRMS of compound 15l

PUBLICATIONS

1. **Arul Murugesan**, R M Gengan* and Anand Krishnan "Green approach: nanocrystalline titania-based sulfonic acid catalyst for the synthesis of piperazinyl-quinolinyl pyran derivatives" ***Advanced Materials Letters*, 2017,** 8, 128-135.

2. **Arul Murugesan**, R M Gengan* and Anand Krishnan "Sulfonic acid Functionalized Boron nitride nano materials as a Microwave-assisted efficient and highly biological active one-pot synthesis of piperazinyl-quinolinyl fused Benzo[c]acridine derivatives" ***Materials Chemistry and Physics,* 2017**, 188,154-167.

3. **Arul Murugesan**, R M Gengan*, Kandasamy G Moodley and Gerhard Gericke "Microwave-assisted: Boron nitride nano materials based sulfonic acid catalyst for the synthesis of biological active ethylpiperazinyl-quinolinyl fused acridine derivatives" ***Advanced Materials Letters, 2017,*** *8, 773-782.*

4. **Arul Murugesan,** R M Gengan*, Ramar Rajamanikandan, Malaichamy Ilanchelian, Chia-Her Lin "One-pot synthesis of Claisen–Schmidt reaction through (*E*)-chalcone derivatives: Spectral studies in human serum albumin protein binding and molecular docking investigation" **Synthetic Communications, 2017,** 47, 1884-1904.

5. **Arul Murugesan**, R M Gengan*, Ramar Rajamanikandan, Malaichamy Ilanchelian "One-pot synthesis via 1, 3-dipolar cycloaddition reaction to piperazinyl-quinolinyl dispiro heterocyclic derivatives and spectrofluorometric and molecular docking studies on their binding with human serum albumin" ***Journal of molecular Structure***, **2017,** 1149, 439-451

6. **Arul Murugesan**, R M Gengan*, Chia-Her Lin "Efficient synthesis of ethyl–piperazinyl quinolinyl-(E)-chalcone derivatives via Claisen–Schmidt reaction by using TiO2-BPTETSA catalyst" ***Journal of the Taiwan Institute of Chemical Engineers,* 2017**, 80, 852-866.

List of papers presented at international conferences

1. **Arul Murugesan** and R M Gengan, Synthesis and characterisations of boron nitride based propyl triethylenetetramine sulfonic acid catalyst, paper presented in "International Conference on Nanomaterials and Nanotechnology" held at Vinoba Bhave Research Institute, Allahabad, India, March, 01-03, 2017.

2. R M Gengan and **Arul Murugesan,** preparation and characterisations of boron nitride fused sulfonic acid catalyst for the synthesis of new active acridine derivatives paper presented in "5th Annual International Conference on chemistry" held at Athens, Greece, July, 17-20, 2017.

3. **Arul Murugesan** and R M Gengan, Investigation of HSA protein binding and molecular docking studies with methyl-piperazinyl-quinolinyl dispiro heterocyclic derivatives, paper presented in "national Conference 2018 SACI POSTGRADUATE COLLOQUIUM" held at Durban University of Technology, Durban, South Africa, and February, 02-02, 2018.

Research Article 2017, **8**(2), 128-135 Advanced Materials Letters

Green approach: Nanocrystalline titania-based sulfonic acid catalyst for the synthesis of piperazinyl-quinolinyl pyran derivatives

Arul Murugesan, Robert M Gengan*, Anand Krishnan

Department of Chemistry, Faculty of Applied Sciences, Durban University of Technology, Durban 4001, South Africa

*Corresponding author, Tel: (+27) 31 3732309; Fax: (+27) 866740441; E-mail: genganrm@dut.ac.za

Received: 23 August 2016, Revised: 29 September 2016 and Accepted: 22 November 2016

DOI: 10.5185/amlett.2017.7040
www.vbripress.com/aml

Abstract

A nanocrystalline titania-based sulfonic acid material was prepared, characterized and used as an effective, efficient and re-usable catalyst for the synthesis of 2-amino-4-(2-(4-methylpiperazin-1-yl) quinolin-3-yl)-6-phenyl-4H-pyran-3-carbonitriles and 2-amino-4-(2-(4-methylpiperazin-1-yl)quinolin-3-yl)-6-(pyridin-4-yl)-4H-pyran-3-carbonitrile derivatives under solvent-free conditions. This simple three component one-pot synthesis results in high yield products in 2 hours via conventional heating protocols. The catalyst was characterized by XRD, TEM, SEM, BET and Raman spectroscopy. The catalyst was recycled 5 times and recorded a decrease of 10 % in catalytic activity making it cost effective for large scale production.

Keywords: Sulfonic-acid catalyst, solvent-free, MCR, knoevenagel condensation.

Introduction

Heterocyclic compounds such as pyrans and pyranopyrans are important scaffolds since they amplify the bioactivity of compounds. These compounds exhibit a wide spectrum of pharmacological activities such as insecticidal [**1**], anti-viral [**2**], anti-tumor [**3**], inhibition of influenza virus [**4**] and phytotoxic activities [**5**]. Hence there has been a renewed interest in developing a general, versatile and more efficient method for the synthesis of pyrans and pyranopyran derivatives. A number of synthetic approaches to this class of compounds are documented [**6**] including the synthesis of 2-amino-4-aryl-3-cyano-4H-pyrans by the cyclization of arylidene malononitrile and other active methylene compounds in the presence of organic bases such as piperidine [**7**], pyridine [**8**] and trimethylamine [**9-10**]. Most of these methods are unsuitable as they utilise volatile solvents and require long reaction time (~ 12 h) whilst catalyst recovery is also sometimes problematic. Recently, a one-pot synthesis using Mg/La mixed oxide and MgO [**11-12**] as a basic catalyst as well as a multi-component synthesis of 2-amino-4H-pyran derivatives in aqueous medium [**13-14**] were reported. Most recently a new Brönsted acid, i.e., 4-(succinimido)-1-butane sulfonic acid (SBSA) was used for the synthesis of dihydropyrano **[4, 3-b]** pyran derivatives [**15**]. The recent years has witnessed gigantic advance in the catalysis of organic reactions by solid acid catalysts since they provide better opportunities for recovering and recycling from reaction mixtures. In particular, chemically bound adsorbed sulfonic acid on TiO_2 viz., TiO_2-Pr-SO_3H was synthesised, characterised then applied to the synthesis of quinoxalines [**16**], coumarins [**17**] and the promotion of the N-Boc protection of amines [**18**], however the scope of this catalyst is unlimited and needs further exploration. Green chemistry underlays twelve principles, and catalysis is one of the thumb principles which states using catalyst for a reaction instead of using a stoichiometric reagents which helps to increase selectivity, minimise waste and reduce reaction times and energy demands.

TiO_2, the most widely studied and used in many applications because of its strong oxidizing abilities and for the decomposition of organic pollutants and superhydrophilicity, chemical stability, long durability, nontoxicity, low cost, and transparency to visible light. The photocatalytic properties of TiO_2 are due to the formation of photogenerated charge carriers (hole and electron) which are formed upon the absorption of ultraviolet (UV) light corresponding to the band gap. The photogenerated holes in the valence band diffuses TiO_2 surface and react with adsorbed water molecules, forming hydroxyl radicals ($^{\bullet}OH$). The photogenerated holes and the hydroxyl radicals oxidize organic molecules on the TiO_2 surface in vicinity. In the meantime, electrons in the conduction band typically participate in reduction processes, which typically reacts with molecular oxygen in the air to produce superoxide radical anions ($O_2^{\bullet-}$). The development of new materials, however, is strongly required to provide enhanced performances with respect to the photocatalytic properties and to find new uses for TiO_2 photocatalysis. In this work, recent developments in the area of TiO_2photocatalysis research, in terms of new materials from a structural design perspective, have been

Materials Chemistry and Physics 188 (2017) 154–167

Contents lists available at ScienceDirect

Materials Chemistry and Physics

journal homepage: www.elsevier.com/locate/matchemphys

Sulfonic acid functionalized boron nitride nano materials as a microwave-assisted efficient and highly biologically active one-pot synthesis of piperazinyl-quinolinyl fused Benzo[*c*]acridine derivatives

Arul Murugesan, R.M. Gengan*, Anand Krishnan

Department of Chemistry, Faculty of Applied Sciences, Durban University of Technology, Durban, South Africa

HIGHLIGHTS

- One-pot Synthesis of Knoevenagel and Michel type reactions.
- Synthesis of Sulfonic acid Functionalized Boron nitride nano materials.
- Synthesis of piperazinyl-quinolinyl fused Benzo[*c*]acridine derivatives under Microwave irradiation.
- Molecular docking studies were performed on piperazinyl-quinolinyl acridine derivatives using DNA.

GRAPHICAL ABSTRACT

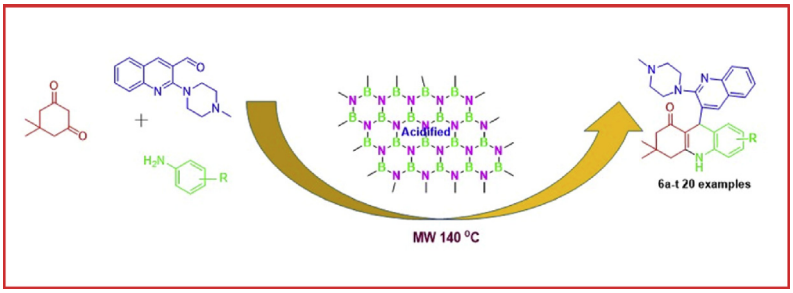

ARTICLE INFO

Article history:
Received 24 October 2016
Received in revised form
10 December 2016
Accepted 18 December 2016
Available online 21 December 2016

Keywords:
Boron nitride
Solid acid catalyst
Knoevenagel reactions
Microwave irradiation
Raman spectroscopy

ABSTRACT

Boron nitride nano material based solid acid catalyst was found to be an efficient and reusable sulfonic acid catalyst for the synthesis of one-pot Knoevenagel and Michael type reactions in 3, 3-dimethyl-9-(2-(4-methylpiperazin-1-yl) quinolin-3-yl)-3, 4, 9, 10-tetrahydroacridin-1(2H)-one derivatives under microwave irradiation conditions. The catalyst was prepared by mixing boron nitrile and (3-mercaptopropyl) trimethoxysilane. This is simple and safe method for the preparation of solid acid catalysts. The morphological properties of catalyst determined by using FT-IR, XRD, TEM, SEM and Raman spectroscopy. The synthesised catalyst was employed in Knoevenagel and Michael type reactions to synthesise novel piperazinyl-quinolinyl based acridine derivatives. Furthermore the newly-synthesised compounds have been used for molecular docking in DNA binding studies. The method developed in this study has the advantages of good yield, simplicity coupled with safety and short reaction time. Most importantly it was found that the solid acid catalyst can be recycled with only 5% loss of activity.

1. Introduction

Multicomponent reactions (MCRs) are one-pot processes which have powerful bond-forming efficiency. They are therefore generally utilized in combinatorial and medicinal chemistry [1]. Specifically, benzo acridine derivatives have been employed as antibacterial [2], cytotoxic [3], antifungal [4] and anti-malarial [5] agents on account of their biological activities. In the last few years, acridione and acridine frameworks have become the focus of much research in producing anti-cancer drugs. Whereas they were previously targeted as antimicrobials [6,7], acridone and acridine moieties are being exploited in anti-melanoma reagents [8] and DNA binding [9]. These moieties have also been used in the

* Corresponding author. Tel.: +27 31 3732309; fax: +27 866740441.
E-mail address: genganrm@dut.ac.za (R.M. Gengan).

http://dx.doi.org/10.1016/j.matchemphys.2016.12.039
0254-0584/

SYNTHETIC COMMUNICATIONS®
2017, VOL. 47, NO. 20, 1884–1904
https://doi.org/10.1080/00397911.2017.1355466

Taylor & Francis
Taylor & Francis Group

One-pot synthesis of Claisen–Schmidt reaction through (*E*)-chalcone derivatives: Spectral studies in human serum albumin protein binding and molecular docking investigation

Arul Murugesan[a], Robert Moonsamy Gengan[a], Ramar Rajamanikandan[b], Malaichamy Ilanchelian[a], and Chia-Her Lin[c]

[a]Department of Chemistry, Faculty of Applied Sciences, Durban University of Technology, Durban, South Africa; [b]Department of Chemistry, Bharathiar University, Coimbatore, India; [c]Department of Chemistry, Chung Yuan Christian University, Chungli, Taiwan

ABSTRACT

An efficient and environmentally benign one-pot multicomponent synthesis of *E*-chalcones was developed using a mild and reusable new boron nitride-sulphonic acid catalyst. The catalyst was prepared by activating the boron nitride surface with nitric acid, followed by a simple reaction with 3-mercaptopropyl trimethoxysilane. The catalyst was characterized and morphological properties were studied by Fourier transform infrared, X-ray diffraction, transmission electron spectroscopy, scanning electron microscopy, Brunauer–Emmett–Teller theory, and Raman spectroscopy techniques. The solid acid catalyst was recycled five times in a Claisen–Schmidt reaction to synthesize new chalcone derivatives, and X-ray crystallography was used to elucidate the structure of (*E*)-1-(anthracen-9-yl)-3-(2-(4-methylpiperazin-1-yl)quinolin-3-yl)prop-2-en-1-one. A fluorescence quench titration method was used to assess its binding ability with human serum albumin (HSA), while molecular docking was also performed to get a more detailed insight into their interaction at the binding site of HSA.

GRAPHICAL ABSTRACT

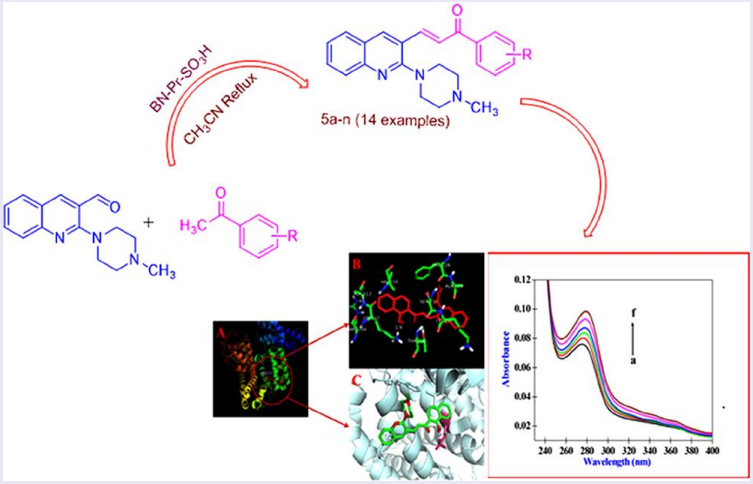

ARTICLE HISTORY

Received 16 June 2017

KEYWORDS

Boron nitride; Claisen–Schmidt reaction; HSA protein; molecular docking

CONTACT Robert Moonsamy Gengan genganrm@dut.ac.za Department of Chemistry, Faculty of Applied Sciences, Durban University of Technology, Durban 4001, South Africa.

Color versions of one or more of the figures in the article can be found online at www.tandfonline.com/lsyc.

Supplemental data (general procedure for the synthesis and spectral data of all the compounds) can be accessed on the publisher's website.

Journal of Molecular Structure 1149 (2017) 439–451

Contents lists available at ScienceDirect

Journal of Molecular Structure

journal homepage: http://www.elsevier.com/locate/molstruc

One-pot synthesis via 1, 3-dipolar cycloaddition reaction to piperazinyl-quinolinyl dispiro heterocyclic derivatives and spectrofluorometric and molecular docking studies on their binding with human serum albumin

Arul Murugesan [a], Robert Moonsamy Gengan [a, *], Ramar Rajamanikandan [b], Malaichamy Ilanchelian [b]

[a] Department of Chemistry, Faculty of Applied Sciences, Durban University of Technology, Durban, South Africa
[b] Department of Chemistry, Bharathiar University Coimbatore, India

ARTICLE INFO

Article history:
Received 4 February 2017
Received in revised form
4 August 2017
Accepted 5 August 2017
Available online 7 August 2017

Keywords:
1, 3 Dipolar cycloaddition
Microwave irradiation
HSA protein
Molecular docking

ABSTRACT

A series of novel dispiro piperazinyl-quinolinyl-thioxothiazolidin-2, 4-dione derivatives were synthesised and characterised by FT-IR ^{1}H, ^{13}C, 2D NMR and HRMS spectroscopic techniques. A representative compound 1'-(2-(4-methylpiperazin-1-yl)quinolin-3-yl)-2″-thioxo-5′,6′,7′,7a'-tetrahydro-1′H,2H-dispiro [acenaphthylene-1,3′-pyrrolizine-2′,5″-thiazolidine]-2,4″-dione was studied for its binding ability with human serum albumin (HSA) using the fluorescence quench titration method. Addition of the compound to HSA produced slight fluorescence quenching and red shift. The free energy change for the complexation process was evaluated as −29.98 kJ mol^{-1} thereby indicating a spontaneous and highly favourable reaction. Molecular docking analyses revealed the binding as −20.79 kJ mol^{-1} which was analogous with the experimental value obtained from emission data. It was concluded that TYR-263 is the moiety responsible for the binding in the complex.

1. Introduction

Rhodanine based molecules display good biological activities including anti-inflammatory and anti-hypertensive activities [1] hence they are highly utilised in drug discovery strategies [2]. The pyrrolo-thiazoles are also endowed with a wide-ranging of biological activities, namely for their heptoprotective [3], anti-biotic [4], anti-diabetic [5] and anti-convulsant actions [6]. The 2, 3 dihydro-4-quinolone derivatives, present in many alkaloids [7], is an important intermediate in organic synthesis [8] and exhibits a wide range of pharmacological properties such as anti-bacterial [9], anti-malarial [10], anti-tumor [11], CRTH2 antagonist receptor [12] and 5HT6 serotonin receptor [13]. When these functionalised scaffolds are fused into a single molecule, the biological potency of the new molecule is predicted to have increased activity.

The dispiro nitrogen containing heterocyclic compounds are usually prepared by a 1, 3 dipolar cycloaddition reaction [14–18] of an olefin dipolarophile azomethine ylide with a particular substrate especially with a five-membered heterocycles such as substituted pyrrolidines [19]. When this reaction is performed in a multi-component system, the creation of chemical archives of potent drug-like compounds is possible which might be used in combinatorial chemistry for their profiling [20]. These dispiro heterocycles containing two sp^{3} carbon atom, with different cyclic moieties, are biologically important [21] molecules. The spiro oxindole are important pharmacological agents which display pronounced cell-type-specific anti-cancer properties [22]. Typical examples are Horsfiline [23] which is a natural product, spirotryptostatine A and B [24] and NITD 609 which is a non-peptide inhibitor of MDM2-p53 [25,26] (Fig. 1).

Since the 1, 3 cycloaddition of azomethine ylide with an acetylenic dipolarophile is one of the most effective approaches for the regio- and stereo selective construction of a variety of complex spiro-oxindole derivatives [27] including a quinoline based molecule [28]. Quinolines display potent biological activity hence the 1, 3 cycloaddition reaction was selected for the synthesis of novel dispiro heterocyclic derivatives containing the quinoline moiety.

* Corresponding author.
E-mail address: genganrm@dut.ac.za (R.M. Gengan).

http://dx.doi.org/10.1016/j.molstruc.2017.08.017
0022-2860/

Research Article 2017, **8**(7), 773-782 Advanced Materials Letters

Microwave-assisted: Boron nitride nano materials based sulfonic acid catalyst for the synthesis of biologically active ethylpiperazinyl-quinolinyl fused acridine derivatives

Arul Murugesan[1], Robert M Gengan[1*], Kandasamy G Moodley[1*] and Gerhard Gericke[2]

[1]*Department of Chemistry, Faculty of Applied Sciences, Durban University of Technology, Durban 4001, South Africa*
[2]*Eskom RT&ND Laboratories, Rosherville, Gauteng, South Africa*

*Corresponding author. Tel: (+27) 31 3732309, (+27) 31 3735133; Fax: (+27)866740441, (+27)866740839;
E-mail: genganrm@dut.ac.za; moodlykg@dut.ac.za

Received: 16 November 2016, Revised: 09 December 2016 and Accepted: 20 December 2016

DOI: 10.5185/amlett.2017.1495
www.vbripress.com/aml

Abstract

Boron nitride nanomaterial based solid acid catalyst is an efficient and reusable sulfonic acid catalyst for the one-pot synthesis of 9-(2-(4-ethylpiperazin-1-yl)quinolin-3-yl)-3,3-dimethyl-3,4,9,10-tetrahydroacridin-1(2H)-one derivatives under microwave irradiation conditionsvia. The Knoevenagel and Michael type reactions. The catalyst was prepared by simply mixing boron nitride and 3-amino-4-methoxybenzenesulfonic acid in a safe method. The morphological properties of the catalyst was determined by using FT-IR, XRD, TEM, SEM and Raman spectroscopy. The synthesised catalyst was employed in a Knoevenagel and Michael type reaction to synthesise novel ethylpiperazinyl-quinolinyl based acridine derivatives. Furthermore, the newly-synthesised compounds was used for molecular docking in Hsp90 protein studies. The method developed in this study has the advantages of good yield, simplicity coupled with safety and short reaction time. Most importantly it was found that the solid acid catalyst can be recycled with minimal loss of activity over five cycles.

Keywords: Boron nitride, MW, MCRs, knoevenagel condensation.

Introduction

Multicomponent reactions (MCRs) are one-pot processes which have powerful bond-forming capability and henceutilized in combinatorial and medicinal chemistry [**1**]. One important class of compounds are benzo-acridine derivatives which have been employed as anti-bacterial [**2**], cytotoxic [**3**], anti-fungal [**4**] and anti-malarial [**5**] agents. In the last few years, acridone and acridine frameworks have become the focus of much research in producing anti-cancer drugs. Whereas they were previously targeted as antimicrobials [**6-7**], acridone and acridine moieties are being exploited in anti-melanoma reagents [**8**] and DNA binding [**9**]. These moieties have also been used in the synthesis of new acridine derivatives as polycyclics with five- or six-member ring systems. The new compounds have been studied as important DNA intercalating anticancer drugs [**10-11**]. Since cancer is considered to be the foremost cause of human death, a multitude of research groups have the goal of discovering affordable but effective anti-cancer formulations. The current treatment or therapies for cancer include surgery, radiotherapy and chemotherapy [**12-15**]. Among these therapies, chemotherapy is the most widely-used one. Unfortunately, most of the antineoplastic drugs used as therapeutic agents, have major drawbacks such as poor efficacy, increased risk of side effects and increased instances of multi-drug resistance. An additional major hurdle in cancer treatment is the non-selectivity of antineoplastic agents towards cancerous cells and normal cells [**16**]. Hence development of a potent, safe and selective antineoplastic is of prime importance to prevent cancer [**17-18**]. Benzo[*c*]acridine derivatives have been recently synthesized by a number of methods involving one-pot multi-component condensation reactions of naphthylamines, dimedone and aldehydes under various reaction conditions; for example, using triethylbenzylammonium chloride (TEBAC)/H2O [**19**], ionic liquid [**20**], under microwave irradiation (MWI) [**21-23**], or ultrasound irradiation (USI) [**24**]. Use of heterogeneous catalysts has recently received considerable interest in various organic syntheses. The SBA-15 is a nano-porous silica which has a hexagonal structure, large pore size, high surface area and good thermal constancy. It has denser aperture walls and higher aperture size. [**25**]. There are only a few reports on the applications of SBA-

Journal of the Taiwan Institute of Chemical Engineers 80 (2017) 852–866

Contents lists available at ScienceDirect

Journal of the Taiwan Institute of Chemical Engineers

journal homepage: www.elsevier.com/locate/jtice

Efficient synthesis of ethyl–piperazinyl quinolinyl-(*E*)-chalcone derivatives via Claisen–Schmidt reaction by using TiO_2-BPTETSA catalyst

Arul Murugesan[a], Robert Moonsamy Gengan[a,*], Chia-Her Lin[b]

[a] Department of Chemistry, Faculty of Applied sciences, Durban University of Technology, Durban, South Africa
[b] Department of Chemistry, Chung Yuan Christian University, Chungli 32023, Taiwan

ARTICLE INFO

Article history:
Received 18 February 2017
Revised 4 July 2017
Accepted 4 July 2017
Available online 29 July 2017

Keywords:
Titanium dioxide
Claisen–Schmidt reaction
BSA protein
Molecular docking

ABSTRACT

A new titanium nanomaterial based sulfonic acid catalyst was prepared and exhibited efficient catalytic activity for the synthesis of (*E*)-3-(2-(4-ethylpiperazin-1-yl)quinolin-3-yl)-1phenylprop-2-en-1-one derivatives under solvent free conditions. Briefly the catalyst was synthesized by refluxing a mixture of nitric acid activated titanium dioxide, 3-mercaptochloropropyl and triethylene tetramine followed by filtration. This is a facile and environmentally benign method for preparation of the catalyst. The morphological properties of the catalyst was characterized by FT-IR, XRD, TEM, SEM, BET and Raman spectroscopy. The starting substrate 2-(4-ethylpiperazin-1-yl) quinoline-3-carbaldehyde (**1**) was synthesised from 2-chloro-3-formyl quinoline and an excess of 1-ethylpiperazine. The X-ray structure showed that the ethyl–piperazinyl N atom is attached to the aromatic ring and the dihedral angle between the mean planes of ethyl–piperazinyl ring atoms N (3)-C-(3)-N (2) has a geometric parameter of 117.9 (4) Å thereby confirming the identity of the crystal structure. The one-pot Claisen–Schmidt reaction containing **1** and acetophenone derivatives were refluxed to produce chalcone derivative **3a-3n** of yield 85–97%. They were characterised by IR, ^{1}H NMR, ^{13}C NMR and MS-TOF whilst **3 m** included 90° DEPT, 135° DEPT, COSY, NOSEY, HSQCE and HMBC. High yield, simple methodology and short reaction time were some of the advantages of this methodology whilst a decrease of a mere 10% in catalytic activity, in five cycles, makes it cost effective for any possible large scale production. Furthermore (*E*)-1-(1-hydroxynaphthalen-2-yl)-3-(2-(4-ethylpiperazin-1-yl)quinolin-3-yl) prop-2-en-1-one was used in molecular docking studies with bovine serum albumin protein binding was located in subdomain II A of BSA containing the amino acid residues ARG-209, LYS-212, ALA-213, VAL-216, PHE-226, ALA-229, SER-232, LYS-233 and THR239.

1. Introduction

Chalcones are α-β unsaturated ketones found in abundance in edible plants and are considered to be precursors of flavonoids and isoflavonoids. The presence of the double bond in conjugation with a carbonyl functionality is proposed as one of the functionality that contributes to their important biological activities as compared to their saturated analogues. Chalcones have attracted much attention because of their various biological applications such as anti-cancer, anti-inflammatory and anti-hyperglycaemic [1–3] agents.

The most preferred method for the synthesis of chalcones is by the Claisen–Schmidt condensation of an aldehyde and ketone by either an acid or base catalysed reaction followed by *in situ* dehydration [4]. Different heterogeneous catalyst have been used such as Lewis acid [5,6], Brønsted acid [7], solid acid [8–10] and solid base [11–13]. The Claisen–Schmidt condensation reaction is also carried out in common ionic liquids [14–17]. The reaction ensures C–C bond formation between two carbonyl derivatives and is a modification of the well-known aldol condensation [18,19] which also provides the synthesis of various important molecules which is promoted under acidic and basic [20–22] catalytic conditions. Recently an ionic liquid catalyst was used for the aldol condensation [23,24] for C–C bond formation in an acid medium and further extended to the synthesis of chalcone derivatives via Claisen–Schmidt condensation [25]. Also new ionic liquid catalysts were used as a green approach [26,27] for new chalcones. Silica based nanomaterial solid acid catalyst such as MCM-4, SBA-15 and amino propyl based nano silica were used under solvent free conditions [28–30]. Protonated aluminate mesoporous silica nanomaterial was also used for biological active compounds [31].

* Corresponding author.
E-mail addresses: organicarul91@gmail.com, genganrm@dut.ac.za (Robert.M. Gengan).

http://dx.doi.org/10.1016/j.jtice.2017.07.014
1876-1070/